

**Total Synthesis of Peganumine A:
Journey towards drug discovery, organocatalyst
design and synthetic methodology development**

Inaugural-Dissertation

to obtain the academic degree

Doctor rerum naturalium (Dr. rer. nat.)

submitted to the Department of Biology, Chemistry, Pharmacy
Freie Universität Berlin

by

Guoli He

from Shaanxi, China

2021

Hereby, I declare that the submitted thesis is my own work and was prepared autonomously without the aid of other sources than the ones cited and acknowledged. The work was not submitted to any other prior doctoral procedure

Guoli He

The following doctoral work has been carried out within the research group of Prof. Dr. Mathias Christmann from October 2015 until March 2021 at the Department of Biology, Chemistry, Pharmacy of the Freie Universität Berlin.

1st Reviewer: Prof. Dr. Mathias Christmann

(Institut für Chemie und Biochemie, Freie Universität Berlin)

2nd Reviewer: Prof. Dr. Philipp Heretsch

(Institut für Organische Chemie, Leibniz Universität Hannover)

Date of disputation: 07.10.2021

Part of this dissertation have been published in:

Guoli He, Benjamin List, Mathias Christmann, “Unified Synthesis of Polycyclic Alkaloids by Complementary Carbonyl Activation” *Angew. Chem. Int. Ed.* **2021**, *60*, 13591–13596.

„Aber es ist mit dem Menschen wie mit dem Baume. Je mehr er hinauf in die Höhe und Helle will, um so stärker streben seine Wurzeln erdwärts, abwärts, in's Dunkle, Tiefe, ins Böse.“

Friedrich Nietzsche

Acknowledgement

I would like firstly to express my sincere gratitude to my Doktorvater Prof. Dr. Mathias Christmann for his kind acceptance to conduct my doctoral research on this marvelous topic in his group, for his professional guidance to explore the area of natural product total synthesis; for his heartening encouragement to overcome the challenging problems; for his solid support to realize my ideas in the projects; for his wise enlightenment to improve my understanding of the world.

I am grateful for Prof. Dr. Philipp Heretsch to be the second reviewer for the dissertation. Additionally, his brilliance and knowledge of organic synthesis inspired me a lot in my doctoral study. I also would like to thank him for his kind help and constructive suggestion at the crucial points of my doctoral research.

I also appreciate Prof. Dr. Benjamin List for giving me the opportunity to conduct the research of asymmetric total synthesis in his group, to learn how organocatalysis works, to experience how the top-ranking lab organizes.

I want to thank all the former and present members of the AG Christmann. I would like to extend deep thanks to Dr. Florian Bartels and Dr. Johannes Schwan for their kind help, great support and constructive discussion in all aspects. The chemistry, the happiness and the frustration experienced with them waives the unforgettable memory of room 22.14. Special thanks go to Bence Hartmayer for his “always there to help” for all my problems. I thank my “second lab” mates Merlin Kleoff and Lorenz Wiese for their organization of the lab facilities and peaceful working atmosphere. I am thankful to Dr. Reinhold Zimmer for his scientific support during these years. I acknowledge Christiane Groneberg for her kind assistance in my numerous compounds of HPLC and IR analyses and our former secretary, Katharine Machnik, and the current one, Regine Verena Blühdorn, for their assistance.

I also like to thank all members of the AK List for the generous donation of the organocatalysts. I am grateful to Sebastian Schwengers and Dr. Santanu Ghosh—my box-side-mates, and Stefanie Dehn—our “box leader” for their help and understanding to make my work efficient

in my visiting stay. I thank Dr. Monika Lindner, Alexandra Kaltsidis and Maximilian Jansen for their intensive and patient documentary assistance.

I am thankful for all the collaborators of my doctoral projects. Special regards go to Prof. Dr. Jinhua Wang and Dr. Wan Li (Institute of Materia Medica at Chinese Academy of Medical Sciences and Peking Union Medical College) for their professional cytotoxicity assay and further cellular mechanism investigation. I also appreciate Prof. Dr. Yong Liang, Dr. Yinghan Chen and Jun Chen (Nanjing University) for the intensive DFT calculation. I am grateful to Yogita Joshi, Max Branson (University of Bath) and Abdulrahman Radwan for their helps as interns.

The core facility BioSupraMol is acknowledged for NMR and MS analyses carried out during these years. Special thanks go to Gregor Drendel and Anja Peuker for their professional NMR measurement for numerous samples from me, Xuan Pham and Fabian Klautzsch for the MS measurement, and Manuela Weber for her patient measurement of X-ray crystal structures. I also want to thank Dr. Andreas Schäfer for the useful discussion on the NMR spectra and Dr. Richard Gorddard for the suggestion of crystallographic analysis.

I also would like to thank Dr. Yiming Cao, Dr. Robert Heinze, Stefan Leisering, Dr. Jian Li (The Scripps Research Institute, FL) and Dr. Xin Yue (Sun Yat-sen University Cancer Center) for the productive discussion and suggestion at the crucial points of my doctoral research.

I want to thank Bence Hartmayer, Mykhaylo Alekseychuk, Daniel Scutt (University of Nottingham) for proofreading this thesis.

I am grateful for China Scholarship Council and Dahlem Research School for doctoral scholarships.

A unique thanks goes to peganumine A. It is my natural product, my research target and my friend in these years. Fabulous is the journey towards peganumine A. I enjoy the training, the practice and the cultivation providing by it.

Doctoral study is a long and challenging journey, which is also a training of personality, like hard working, dedication and perseverance. I would like to thank my 20-year-old self for choosing organic synthesis as the career track. This guides me to the medicinal chemistry in my bachelor thesis, methodology development in my master thesis, and now a comprehensive

research of medicinal chemistry, methodology development and organocatalysis integrated by the crown of organic synthesis, the natural product total synthesis. It is joyful to learn all the chemistry these years, to experience all the challenging tasks, to explore the truth.

The support from people outside the work are important as well. Dr. Chenyu Wen (Uppsala University) needs special acknowledgement. We have known each other since kindergarten. Though our research is focused on different areas, he inspired me a lot on how to conduct scientific research. I also like to thank Dr. Xinghao Huang (Shanghai ChemPartner Co.) for his encouragement to overcome the challenging problems one by one in these years.

My family deserves so much credit for me getting here. To my parents, thank you very much for your endless support to keep me grounded and to be fearless to explore the unknown area of my life. Even though they never understand my research, they still provide me their unwavering support. To my wife, I sincerely appreciate her understanding and support throughout the past 7+ years, especially the past five years in Germany. I cannot imagine how my life would be, without your unswerving backing. I am also grateful to my grandparents and parents-in-law for their encouragement on the journey to graduation.

Guoli He

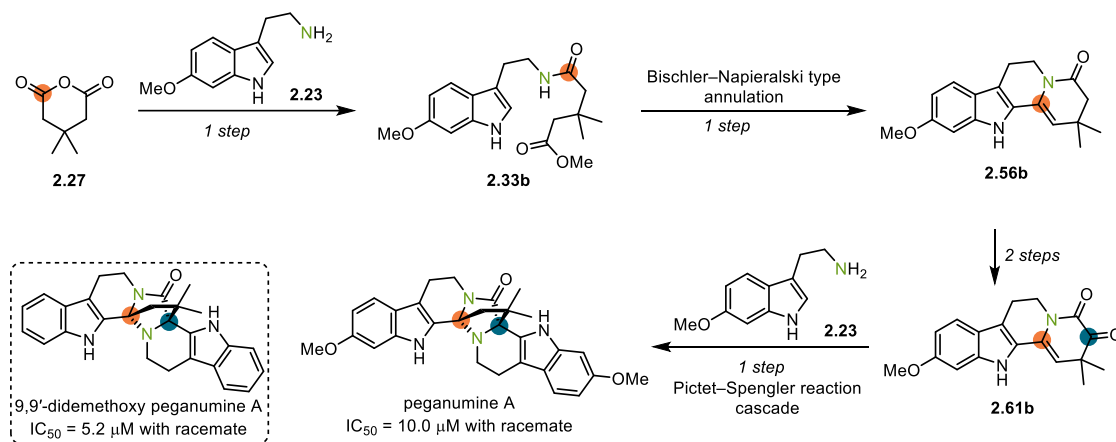
20.05.2021

at Düsseldorf

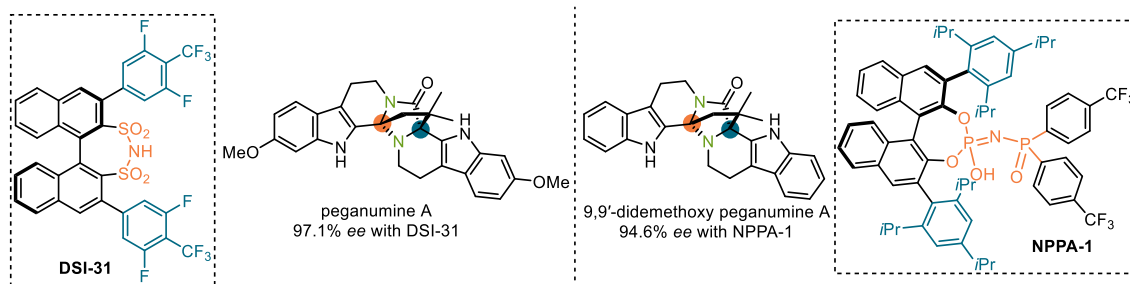
Abstract

The primary aim of this thesis was to develop an efficient synthetic route of peganumine A and its application to the discovery of potent analogues. Peganumine A was isolated from the seeds of *Peganum harmala* in 2014, and is distinguished from the classic tetrahydro- β -carboline alkaloids due to the unique 5,5-dimethyl-2,7-diazabicyclo[2.2.1]heptan-3-one ring system, as well as the excellent cytotoxicity.

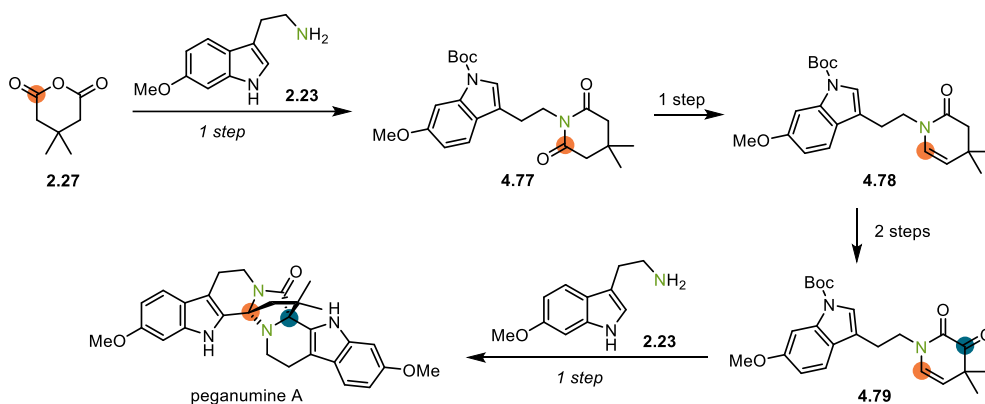
In the initial total synthesis of racemic peganumine A, three different strategies were investigated. One strategy could realize the total synthesis of peganumine A in a protection group free fashion, which relied on a Bischler–Napieralski type annulation and a Pictet–Spengler reaction cascade to construct the two tetrahydro- β -carboline cores. With the powerful synthetic route in hand, 11 analogues were designed and synthesized based on the function-oriented strategy. By further cytotoxic assay, not only the preliminary SAR was illustrated, but also a potent analogue was discovered.



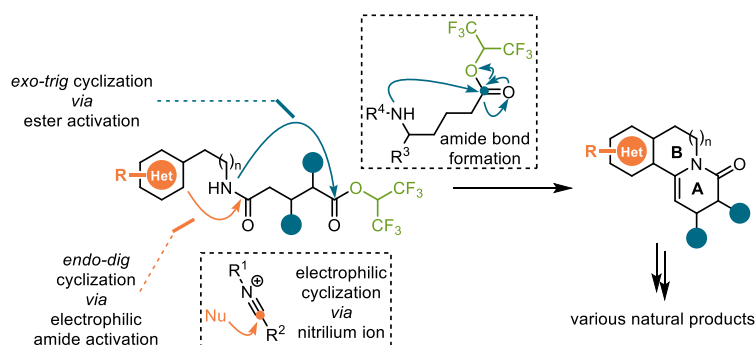
Based on the racemic synthetic route, organocatalysis was applied to the asymmetric syntheses of peganumine A and its analogues. The enantioselective synthesis of was realized by a chiral disulfonimide catalyzed Pictet–Spengler reaction cascade. However, the highly enantioenriched analogues could not be obtained by the chiral disulfonimide catalyzed Pictet–Spengler reaction cascade. Through design, synthesis and screening of chiral *N*-phosphinyl phosphoramides, a highly enantioselective synthesis of the potent analogue was achieved.



Besides the original three strategies, two new *N*-acyliminium ion cyclization strategies were further explored to improve the efficiency of the synthetic route. Another 5-step synthesis of peganumine A was realized and featured a Pictet–Spengler reaction–iminium ion cyclization–amination cascade to assemble the two tetrahydro- β -carboline motifs in a one-step synthesis.



In the protection group free total synthesis of peganumine A, an annulation reaction was discovered, which was then developed into a general methodology to construct the polycyclic fused quinolizidine scaffolds. This new approach was then applied to the total synthesis of harmalanine, harmalacanine, nortetoybyrine and ilicifoline B, and the formal total synthesis of deplancheine, 10-desbromoarborescidine A, hirsutine, rynchophylline and isorynchophylline.

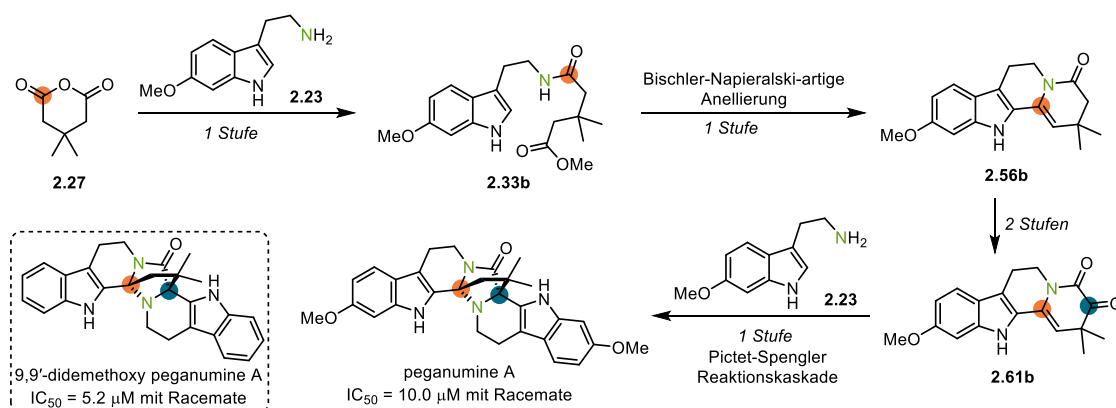


In summary, this thesis focused on the development of efficient synthetic routes towards peganumine A, which promoted the discovery of a potent analogue, design of new organocatalyst and investigation of new synthetic methodology.

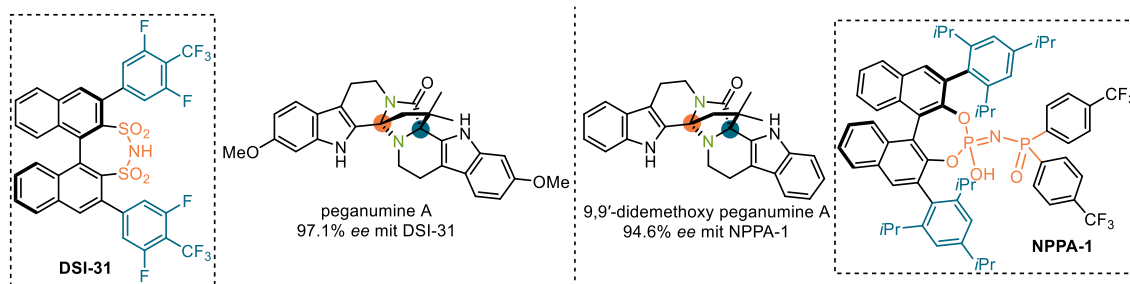
Zusammenfassung

Das primäre Ziel dieser Dissertation war die Entwicklung einer effizienten Route zur Synthese von Peganumin A und die Anwendung dieser Route zur Entdeckung potenter Analoga. Peganumin A wurde aus den Samen der Steppenraute *Peganum harmala* in 2014 isoliert und unterscheidet sich von den klassischen Tetrahydro- β -carbolin-Alkaloiden durch das einzigartige 5,5-Dimethyl-2,7-diazabicyclo[2.2.1]heptan-3-on-Ringsystem, sowie eine hohe Zytotoxizität.

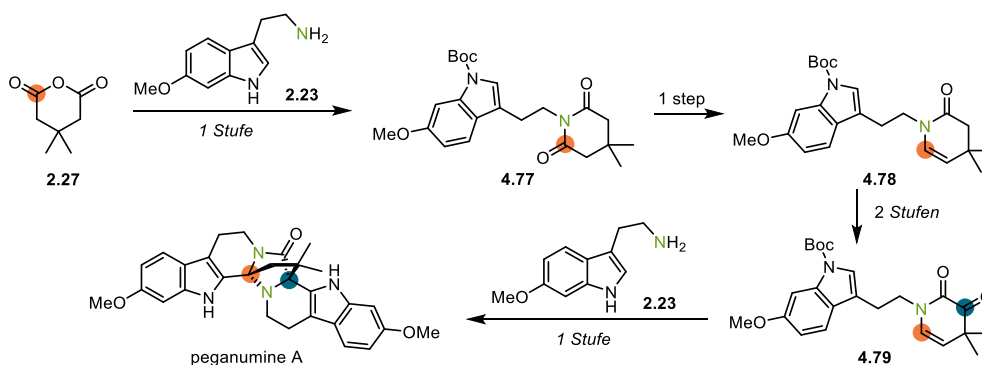
Bei der anfänglichen Totalsynthese von racemischem Peganumin A wurden drei verschiedene Strategien untersucht. Eine dieser Strategien lieferte schließlich den Naturstoff in einer schutzgruppenfreien Synthese. Dabei wurde das Tetrahydro- β -carbolin-Gerüst durch eine Bischler-Napieralski-artige Anellierung und einer Pictet-Spengler-Reaktionskaskade aufgebaut. Mit Hilfe dieser Syntheseroute wurden 11 weitere Analoga, basierend auf dieser funktionsorientierten Strategie, entworfen und synthetisiert. Durch zytotoxische Tests konnte nicht nur eine vorläufige SAR ermittelt, sondern ein potentes Analogon entdeckt werden.



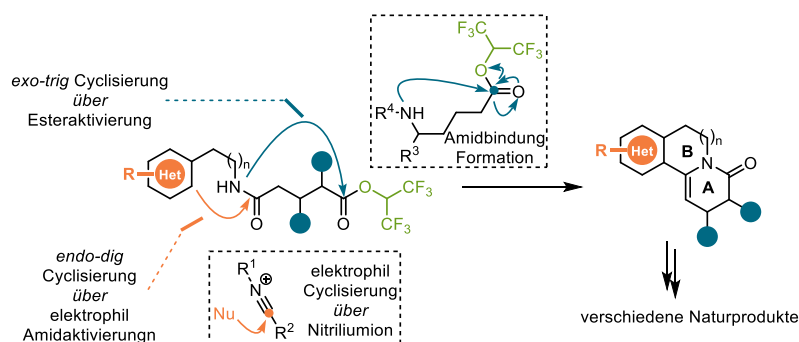
Die Verwendung von Organokatalyse erlaubte, basierend auf der Strategie für die Synthese des Racemats, eine asymmetrische Synthese von Peganumin A und dessen Analoga. Während die hohe Enantioselektivität für Peganumin A durch ein chirales Disulfonimid als Katalysator für die Pictet-Spengler-Reaktionskaskade erreicht werden konnte, war dieses für die entsprechenden Analoga nicht möglich. Durch Design, Synthese und Screening chiraler *N*-Phosphylnylphosphoramide gelang es schließlich einen geeigneten Katalysator für die hoch enantioselektive Synthese eines potenten Analogons zu finden.



Neben den ursprünglichen drei Strategien wurden zusätzlich zwei neue Strategien zur Zyklisierung von *N*-Acyliminiumionen untersucht, um die Effizienz der Syntheseroute zu verbessern. Dabei konnte eine fünfstufige Synthese von Peganumin A durch eine Kaskade, bestehend aus Pictet-Spengler-Reaktion, Iminiumionenzyklisierung und Amination, die es ermöglichte die Tetrahydro- β -carbolin-Motive in einer Stufe aufzubauen, realisiert werden.



Die Anellierungsreaktion aus der Synthese von Peganumin A wurde anschließend zu einer allgemeinen Methodik für den Aufbau von polyzyklischen, fusionierten Chinolizidingerüsten weiterentwickelt. Dieser neue Ansatz wurde schließlich auf die Totalsynthese von Harmalanin, Harmalacinin, Nortetoyobyrin und Illicifolin B, sowie die Formalsynthese von Deplanchein, 10-Desbromarborescidin A, Hirsutin, Rhynchophyllin und Isorhynchophyllin angewandt.



Zusammenfassend konnten mit dieser Arbeit effizienter Syntheserouten von Peganumin A realisiert werden, wodurch sich die Entdeckung eines potenten Analogons sowie das Design eines neuen Organokatalysators und Untersuchungen neuer Synthesemethoden ergaben.

Content

Acknowledgement	I
Abstract	IV
Zusammenfassung.....	VI
Content	VIII
List of Schemes	XIII
List of Figures	XIX
List of Tables	XXI
List of Abbreviations.....	XXIII
1. Motivation and Background.....	1
1.1. Introduction	2
1.2. Natural product and drug discovery	12
1.2.1. Natural product as drug	12
1.2.2. Strategies for natural product analogues synthesis in drug discovery	16
1.3. Natural product and organocatalyst.....	21
1.3.1. Organocatalysis.....	21
1.3.2. Organocatalytic asymmetric total synthesis	27
1.4. Natural product and synthetic methodology development.....	32
1.5. Brief summary.....	35
2. Total Synthesis of Racemic Peganumine A and Its Analogues.....	37
2.1. Introduction	38
2.1.1. β -Carboline alkaloids.....	38
2.1.2. Peganumine A.....	41
2.1.2.1. Background.....	41
2.1.2.2. Structure determination	42
2.1.2.3. Proposed biosynthesis hypothesis.....	43
2.2. 1 st generation synthetic approach towards peganumine A.....	44
2.2.1. 1 st generation retrosynthetic analysis	44

2.2.2. Synthesis of the 7C motif	44
2.2.3. Study of the double Pictet–Spengler reaction	46
2.3. 2 nd generation synthetic approach to peganumine A	47
2.3.1. 2 nd generation retrosynthetic analysis	47
2.3.2. Construction of the west β -carboline core	47
2.3.3. C–H oxidation to prepare the α -ketolactam	48
2.3.4. Mono Pictet–Spengler reaction.....	49
2.3.5. Zhu’s total synthesis of peganumine A	49
2.3.6. Comparison between the α -ketolactam and the α -ketoenamide	50
2.3.7. Selective benzylic oxidation attempt	53
2.4. 3 rd generation improved synthesis towards peganumine A	54
2.4.1. Discovery of an annulation reaction	54
2.4.2. 3 rd generation improved retrosynthetic analysis	54
2.4.3. Construction of the west β -carboline core	55
2.4.4. C–H oxidation to prepare the α -ketoenamide.....	56
2.4.5. Scalable and reliable synthesis to 6-methoxytryptamine.....	57
2.4.5.1. Indole synthesis strategy	57
2.4.5.2. Indole functionalization strategy	60
2.4.6. Improved protection group free synthesis of peganumine A	61
2.5. Analogues design, synthesis and bioactivity evaluation.....	62
2.5.1. Motivation and strategy of the study of the analogues of peganumine A.....	62
2.5.2. Synthesis of analogues.....	64
2.5.3. Cytotoxicity assay of analogues	66
2.5.4. Gram scale synthesis of PAA-2	67
2.6. Brief summary.....	70
3. Organocatalyst Design and Asymmetric Total Synthesis of Peganumine A and Its Analogues	71
3.1. Introduction for the asymmetric Pictet–Spengler reaction.....	72
3.2. Asymmetric total synthesis of peganumine A	78

3.2.1. Analysis of the key cascade reaction	78
3.2.2. Initial investigation of the asymmetric Pictet–Spengler reaction cascade	79
3.2.3. Study of the asymmetric Pictet–Spengler reaction cascade by ACDC	82
3.3. Asymmetric synthesis of the analogues of peganumine A	95
3.3.1. Asymmetric synthesis platform for the analogues with DSI	95
3.3.2. Asymmetric synthesis platform for the analogues with NPPA	97
3.3.3. Asymmetric synthesis of PAA-2	104
3.4. Brief summary	106
4. New Routes to the Total Synthesis of Peganumine A	107
4.1. Iminium ion and <i>N</i> -acyliminium ion	108
4.1.1. Iminium ion and its reactions	108
4.1.2. <i>N</i> -acyliminium ion and its application in total synthesis	111
4.2. 4 th generation synthetic approach to peganumine A	114
4.2.1. Retrosynthesis of peganumine A	114
4.2.2. 4 th generation synthesis of peganumine A	114
4.3. 5 th generation synthetic approach for peganumine A	115
4.3.1. Retrosynthesis of peganumine A	115
4.3.2. 5 th generation synthesis of peganumine A	116
4.3.2.1. Mono-ring α -ketoenamides preparation via oxidative pathway	116
4.3.2.2. Pictet–Spengler reaction of the mono-ring α -ketoenamide	121
4.3.2.3. Late-stage construction of the indole motif	122
4.3.2.4. Reduction of mono-ring α -ketoenamide and its Pictet–Spengler reaction ..	124
4.3.2.5. Study of the iminium ion cyclization	128
4.3.2.6. Pictet–Spengler reaction–iminium ion cyclization–amination cascade	131
4.3.2.7. Asymmetric Pictet–Spengler reaction–cyclization–amination cascade	134
4.3.2.7. Asymmetric Pictet–Spengler reaction of the mono-ring α -ketoenamide	136
4.4. Brief summary	141
5. Complementary Carbonyl Activation Annulation and Its Application to Natural Product Total Synthesis	143

5.1. Introduction	144
5.1.1. Polycyclic compound	144
5.1.2. Polycyclic natural products	144
5.2. Unified synthesis towards some polycyclic alkaloids	147
5.2.1. Consideration of some bioactive polycyclic alkaloids	147
5.2.2. Dual carbonyl activation.....	148
5.2.3. Generality of the annulation	157
5.2.4. Divergent application of the annulation in total synthesis.....	163
5.2.4. Total synthesis of ilicifoline B	167
5.3. Brief summary.....	170
6. Summary and Outlook	171
6.1. Summary	172
6.2. Outlook.....	175
7. Experimental Information	177
7.1. General information	178
7.2. Experimental procedures.....	180
7.2.1. Total synthesis of racemic peganumine A and its analogues	180
7.2.1.1. 1 st generation synthetic approach towards peganumine A.....	180
7.2.1.2. 2 nd generation synthetic approach towards peganumine A	183
7.2.1.3. 3 rd generation synthetic approach towards peganumine A	188
7.2.1.4. Analogues design, synthesis and bioactivity investigation	210
7.2.2. Organocatalyst design and asymmetric synthesis of analogues	237
7.2.2.1. Catalyst preparation	237
7.2.2.1.1. Chiral thiourea	237
7.2.2.1.2. Chiral phosphoric acid.....	237
7.2.2.1.3. Chiral CBSBA acid and pentamethyl ester of PCCP.....	237
7.2.2.1.4. Chiral disulfonimide	238
7.2.2.1.5. Chiral <i>N</i> -phosphinyl phosphoramidate	243
7.2.2.1.6. Other chiral Brønsted acids	258

7.2.2.2. Asymmetric synthesis of peganumine A and its analogues	258
7.2.3. New generation routes to the total synthesis of peganumine A	267
7.2.3.1. 4 th generation synthetic approach to peganumine A	267
7.2.3.2. 5 th generation synthetic approach to peganumine A	269
7.2.3.2.1. Mono-ring α -ketoenamides preparation via oxidative pathway and their Pictet–Spengler reactions	269
7.2.3.2.2. Mono-ring α -ketoenamides preparation via reductive pathway and their Pictet–Spengler reactions	283
7.2.3.2.3. 5 th generation synthetic route	296
7.2.3.2.4. Racemic Brønsted acids syntheses	300
7.2.4. Complementary carbonyl activation annulation and its application to polycyclic natural products total syntheses	304
7.2.4.1. Substrate preparation	304
7.2.4.1.1. Substrates for the reaction optimization	305
7.2.4.1.2. Substrates for the reaction scope	313
7.2.4.2. One-pot annulation reaction	341
7.2.4.2.1. Reaction optimization	341
7.2.4.2.2. Substrate scope	341
7.2.4.3. Oxidative pathway	364
7.2.4.4. Reductive pathway	367
7.2.4.5. β -formylation	370
7.2.4.6. Total synthesis of ilicifoline B	371
7.2.4.7. Preparation of amines for the substrates of the annulation	373
8. Reference	377
9. Appendix	395
9.1. NMR Spectra	396
9.2. HPLC Traces	672
9.3. Crystallographic Data	682

List of Schemes

Scheme 1–1: Remarkable total syntheses in the 19 th century.	2
Scheme 1–2: Landmark total syntheses in the pre-World War II stage.	3
Scheme 1–3: Representative total syntheses of Woodward.	3
Scheme 1–4: Vitamin B ₁₂ was traced back to cobalamin.	4
Scheme 1–5: Retrosynthetic analysis of prostaglandin F _{2α} and CBS reduction.	5
Scheme 1–6: Other breakthrough total syntheses in Woodward and Corey era.	6
Scheme 1–7: Total syntheses of Taxol in the 1990s.	7
Scheme 1–8: 6- π electrocyclization–rearomatization strategy in total synthesis.	9
Scheme 1–9: Two-phase strategy in total synthesis.	11
Scheme 1–10: Complexity to diversity of pleuromutilin.	18
Scheme 1–11: The diverted total synthesis of migrastatin.	19
Scheme 1–12: Function-oriented synthesis of bryostatins.	20
Scheme 1–13: Discovery of ATP1 inhibitor through biology-oriented synthesis.	20
Scheme 1–14: Dynamic strategic bond analysis of salvinorin A.	21
Scheme 1–15: Catalytic cycle of the Knoevenagel reaction.	22
Scheme 1–16: Organocatalytic Hajos–Parrish–Eder–Sauer–Wiechert reaction.	22
Scheme 1–17: Organocatalysis in the total synthesis of erythromycin A.	23
Scheme 1–18: Pioneering organocatalytic Michael additions.	23
Scheme 1–19: Landmark works of organocatalysis.	24
Scheme 1–20: Organocatalytic asymmetric total synthesis of (–)-huperzine A.	28
Scheme 1–21: Total synthesis of callipeltoside C by L-proline.	29
Scheme 1–22: Unified total synthesis of indole alkaloids.	29
Scheme 1–23: Organocatalyst in the total synthesis of diazonamide A.	30
Scheme 1–24: DSI catalyzed asymmetric total synthesis of estrone.	30
Scheme 1–25: Chiral imidodiphosphoric acid in total synthesis.	31
Scheme 1–26: Chiral organophosphine in the total synthesis of (+)-ibophyllidine.	31

Scheme 1–27: NHC catalyst in the total synthesis of bakkenolide S.	31
Scheme 1–28: Hydrogen bond catalysis in total synthesis.	32
Scheme 1–29: Modular synthesis of propellanes and their application in total synthesis.	32
Scheme 1–30: Total synthesis of axinellamines and development of Palau'chlor.	33
Scheme 1–31: Total synthesis of (+)-pancratistatin through dearomatization.	34
Scheme 2–1: Biosynthesis of β -carboline scaffolds.	40
Scheme 2–2: Chemosynthesis of β -carboline scaffolds.	41
Scheme 2–3: Biosynthetic hypothesis of peganumine A.	43
Scheme 2–4: 1 st generation retrosynthetic analysis.	44
Scheme 2–5: Preparation of 7C motif.	45
Scheme 2–6: Model study of double Pictet–Spengler reaction.	46
Scheme 2–7: Diverse C ₇ units.	46
Scheme 2–8: 2 nd generation retrosynthetic analysis.	47
Scheme 2–9: Construction of the west β -carboline core.	48
Scheme 2–10: Zhu's total synthesis of peganumine A.	50
Scheme 2–11: Updated mono Pictet–Spengler reaction.	50
Scheme 2–12: DFT calculation of Zhu's reaction pathway.	51
Scheme 2–13: DFT calculation of the mono Pictet–Spengler reaction.	52
Scheme 2–14: Concise annulation reaction.	54
Scheme 2–15: 3 rd generation improved retrosynthetic analysis.	55
Scheme 2–16: Construction of the west β -carboline core.	55
Scheme 2–17: Construction of 5,5-dimethyl-2,7-diazabicyclo[2.2.1]heptan-3-one.	57
Scheme 2–18: Protection group free Pictet–Spengler reaction cascade.	57
Scheme 2–19: Modified Fischer indole synthesis.	58
Scheme 2–20: Buchwald indole synthesis.	58
Scheme 2–21: Modified Fischer indole synthesis.	59
Scheme 2–22: Preparation of the precursors of Larock reaction.	59
Scheme 2–23: Global deprotection in the Larock indole synthesis.	60
Scheme 2–24: Synthesis of 6-methoxytryptamine.	61

Scheme 2–25: Protection group free total synthesis of peganumine A.....	61
Scheme 2–26: General synthetic route of the analogues.	65
Scheme 2–27: Attempt for the analogues with different heterocycles.....	65
Scheme 2–28: Alkylation and attempt of core modification.....	66
Scheme 2–29: Didemethylation screening.....	66
Scheme 2–30: Efficient gram scale synthesis.	70
Scheme 3–1: Asymmetric Pictet–Spengler reaction by amino acid derived auxiliaries.	72
Scheme 3–2: Asymmetric Pictet–Spengler reaction by other auxiliaries.	73
Scheme 3–3: The first catalytic asymmetric Pictet–Spengler reaction.....	73
Scheme 3–4: Catalytic asymmetric Pictet–Spengler reaction of aldehydes.	74
Scheme 3–5: Catalytic asymmetric Pictet–Spengler reaction of ketones.	75
Scheme 3–6: Thiourea catalyzed asymmetric Pictet–Spengler reactions.	76
Scheme 3–7: Thiourea–benzoic acid system in asymmetric Pictet–Spengler reactions.....	77
Scheme 3–8: CBSBA in asymmetric Pictet–Spengler reactions.	77
Scheme 3–9: Au(I) catalyzed asymmetric Pictet–Spengler reaction.	77
Scheme 3–10: Analysis of the key cascade reaction.	78
Scheme 3–11: Thiourea catalyzed asymmetric Pictet–Spengler reaction by Zhu et al.....	79
Scheme 3–12: PCCP catalyzed Mukaiyama–Mannich reaction and its preparation.	80
Scheme 3–13: Preparation of DSI and NPPA.....	90
Scheme 3–14: Scale-up reactions with DSI-31.	95
Scheme 3–15: 1 st round synthesis of NPPA.....	98
Scheme 3–16: Synthetic route of the phosphinic amides.	100
Scheme 3–17: Updated synthesis of the phosphinic amides.	100
Scheme 3–18: 2 nd round synthesis of NPPAs.	101
Scheme 3–19: Scale-up reactions for the asymmetric synthesis of PAA-2.	105
Scheme 4–1: Selected strategies for the preparation of isolatable iminium ions/salts.	109
Scheme 4–2: Iminium ions in organic reactions.....	110
Scheme 4–3: The iminium ions in total synthesis.	110
Scheme 4–4: Iminium ion vs <i>N</i> -acyliminium ion.	112

Scheme 4–5: Common disfavored equilibriums of <i>N</i> -acyliminium ion.	112
Scheme 4–6: <i>N</i> -acyliminium ions in total synthesis.	113
Scheme 4–7: Fourth generation retrosynthesis of peganumine A.	114
Scheme 4–8: 4 th generation synthetic attempt.	115
Scheme 4–9: 5 th generation retrosynthesis of peganumine A.	116
Scheme 4–10: Mono-ring enamide intermediate preparation.	117
Scheme 4–11: Potential side-reactions.	117
Scheme 4–12: Mono-oxidation with free indole.	118
Scheme 4–13: Mono-oxidation with phenyl group.	118
Scheme 4–14: Different strategies for the indole motif construction.	119
Scheme 4–15: Substrate preparation for the indole C3 alkylation strategy.	119
Scheme 4–16: Preparation of α -ketoenamide 4.55a	121
Scheme 4–17: Acid-free Pictet–Spengler reaction and structure determination.	121
Scheme 4–18: The acid-free Pictet–Spengler reaction with tryptamine.	122
Scheme 4–19: C3 alkylation strategy.	122
Scheme 4–20: Attempt for the alkyl halide preparation.	123
Scheme 4–21: Fischer indole synthesis and Larock indole synthesis strategies.	124
Scheme 4–22: Reanalysis of the preparation of mono-ring α -ketoenamide.	124
Scheme 4–23: Model study of the selective reduction–elimination.	125
Scheme 4–24: Preparation of diverse imides.	125
Scheme 4–25: Towards Pictet–Spengler reaction.	126
Scheme 4–26: One-pot synthesis of Boc-protected imide.	127
Scheme 4–27: Preparation of the key intermediate starting with 6-methoxytryptamine.	128
Scheme 4–28: Analysis of the iminium ion cyclization.	129
Scheme 4–29: Expected iminium ion cyclization.	130
Scheme 4–30: Proposed mechanism of peganumine A formation.	133
Scheme 4–31: Diphenyldisulfonimide promoted cascade reaction.	134
Scheme 4–32: 5 th generation total synthesis route of peganumine A.	134
Scheme 4–33: Analysis of the cascade.	136

Scheme 5–1: Versatile intermediate.....	148
Scheme 5–2: Mono-carbonyl activation.....	149
Scheme 5–3: Dual carbonyl activation by Lewis acids.....	150
Scheme 5–4: Classic activation in peptide synthesis.....	150
Scheme 5–5: Neighboring group participation strategy for amide synthesis.....	151
Scheme 5–6: Carboxylic alternatives strategy.....	151
Scheme 5–7: Amine alternatives strategy.....	152
Scheme 5–8: Thioester in biochemical reactions.....	153
Scheme 5–9: Consideration of active ester strategy.....	154
Scheme 5–10: Initial synthesis of active esters.....	155
Scheme 5–11: 1 st screening of cyclization with the active esters.....	155
Scheme 5–12: Fluorinated aliphatic active esters preparation.....	156
Scheme 5–13: Annulation with fluorinated aliphatic active esters.....	156
Scheme 5–14: HFIPE in synthesis.....	157
Scheme 5–15: Preparation of substrates.....	157
Scheme 5–16: Limitation of the annulation-1.....	161
Scheme 5–17: Limitation of the annulation-2.....	162
Scheme 5–18: Strategy of the divergent redox synthesis.....	163
Scheme 5–19: Oxidative diversification.....	164
Scheme 5–20: Synthesis attempt of demethoxypegaharmine J.....	165
Scheme 5–21: Reduction pathway for the divergent synthesis.....	165
Scheme 5–22: Desired model for the asymmetric reduction of enamide.....	166
Scheme 5–23: Synthetic plan of the β -formylation.....	167
Scheme 5–24: Retrosynthetic analysis of ilicifoline B.....	168
Scheme 5–25: Anhydride preparation.....	169
Scheme 5–26: Synthesis of 8-oxopseudopalmitine by the annulation reaction.....	169
Scheme 5–27: Dimerization by hypervalent iodine reagent.....	169
Scheme 6–1: The key Pictet–Spengler reactions in different strategies.....	172
Scheme 6–2: The complementary carbonyl activation annulation.....	174

Scheme 7-1: Synthesis of phthalimide derivatives.	193
Scheme 7-2: Indole functionalization.	200
Scheme 7-3: Synthesis of CBSBA.	238
Scheme 7-4: Synthesis of PCCP.	238
Scheme 7-5: Synthesis of DSIs.	238
Scheme 7-6: Screened the readily available DSIs.	239
Scheme 7-7: Synthetic strategy of NPPA.	243
Scheme 7-8: Noncommercially available amines synthesis by reported methods.	373

List of Figures

Figure 1–1: Structure and synthetic fragments of palytoxin.	8
Figure 1–2: Examples of natural products as drugs.	14
Figure 1–3: Structure of gentamicin.	15
Figure 1–4: PGH ₂ and 9,11-diazo-PGH ₂	16
Figure 1–5: Calicheamicin γ_1 and its analogues.	16
Figure 1–6: Hybrid in nature.	17
Figure 1–7: Hybrid with linker.	18
Figure 1–8: Organo-Lewis base catalysts.	24
Figure 1–9: Representative organo-Lewis base catalysts.	25
Figure 1–10: Representative scaffolds of chiral Brønsted acids.	26
Figure 1–11: Hydrogen bond catalysts.	27
Figure 1–12: The general activation modes of organocatalysts.	27
Figure 2–1: β -Carboline alkaloids.	39
Figure 2–2: Three types of β -carboline alkaloids.	39
Figure 2–3: Dimeric β -carboline alkaloids.	42
Figure 2–4: Structure of peganumine A.	42
Figure 2–5: Indole synthesis strategies.	58
Figure 2–6: Artificially designed drugs.	62
Figure 2–7: Consideration of analogues design.	63
Figure 2–8: Design of the analogues.	63
Figure 2–9: Cytotoxicity assay of the synthetic <i>rac</i> -peganumine A and its analogues.	67
Figure 2–10: Primary SAR.	67
Figure 3–1: Proposed activation modes of different catalysis systems.	84
Figure 3–2: pK_a trend of Brønsted acids in MeCN.	84
Figure 3–3: Typical backbones of chiral Brønsted acids.	85
Figure 3–4: The catalyst selection of the first round screening.	85
Figure 3–5: Proposed activation modes for asymmetric Pictet–Spengler reaction.	87

Figure 3–6: Additional catalysts selection for the screening.....	88
Figure 3–7: Analysis the screening result.....	90
Figure 3–8: The selection of DSIs.....	91
Figure 3–9: New DSIs preparation.....	93
Figure 3–10: Structural analysis of NPPA.....	98
Figure 3–11: Proposed stereochemical mode of the NPPA catalyzed system.	103
Figure 3–12: ECD spectra of (+)-peganumine A and (+)-PAA-2.....	105
Figure 3–13: Experimental and calculated ECD spectra of (+)-PAA-2.	106
Figure 4–1: Electrophilicity parameter of some iminium ions and related compounds.....	108
Figure 4–2: Design of racemic Brønsted acids.....	132
Figure 5–1: Representative polycyclic compounds.....	144
Figure 5–2: Selective drugs from polycyclic natural products.....	145
Figure 5–3: Selected drugs derived from polycyclic natural products.....	145
Figure 5–4: Different types of polycyclic natural products.....	146
Figure 5–5: Fused complex polycyclic natural products.....	147
Figure 5–6: A common scaffold of polycyclic alkaloids.....	148
Figure 5–7: Lewis acid activation mode of carbonyl group.....	149
Figure 5–8: The common active ester groups.	153
Figure 5–9: Substrate design-1.....	158
Figure 5–10: Substrate design-2.....	159
Figure 5–11: Representative benzylisoquinoline alkaloids.	168
Figure 6–1: The potent analogue and SAR.	173
Figure 6–2: Asymmetric synthesis of peganumine A and its analogues.....	174
Figure 6–3: Further investigation of analogues.....	175

List of Tables

Table 1–1: Minimum inhibitory concentration of platensimycin and its analogues.....	17
Table 2–1: C–H oxidation of tetracyclic lactam.....	48
Table 2–2: Screening for mono Pictet–Spengler reaction.	49
Table 2–3: Screening for selective benzylic oxidation.	53
Table 2–4: α -hydroxylation of the Boc-protected α -ketoamide.	56
Table 2–5: Optimization of Larock indole synthesis.	60
Table 2–6: Screening of the Brønsted acids for the annulation.	68
Table 2–7: Screening of the Lewis acids for the annulation.....	69
Table 2–8: Optimization of reaction condition with TFA.....	69
Table 3–1: Initial screening of asymmetric Pictet–Spengler reaction by chiral thioureas.....	79
Table 3–2: Screening of multi-binding-site catalysts.	81
Table 3–3: Screening of chiral phosphoric acids.	82
Table 3–4: Screening of novel chiral Brønsted acids by one-pot procedure.	86
Table 3–5: First screening of novel chiral Brønsted acids by cascade procedure.....	87
Table 3–6: 2 nd screening of novel chiral Brønsted acids by cascade procedure.	89
Table 3–7: First screening of DSIs.	92
Table 3–8: Reaction optimization by DSI-1.	93
Table 3–9: New DSIs screening.	94
Table 3–10: Screening with DSI-31	94
Table 3–11: Initial application of DSI-31 to asymmetric synthesis of analogues.	95
Table 3–12: Asymmetric synthesis of the analogues with DSI-31	96
Table 3–13: Asymmetric synthesis of PAA-2 with NPPA-1	97
Table 3–14: 1 st round screening of NPPAs.	99
Table 3–15: 2 nd round screening of NPPAs.	101
Table 3–16: 3 rd round screening of NPPA.	102
Table 3–17: Scale-up reactions of analogues.....	103
Table 3–18: Optimization of the asymmetric synthesis of PAA-2	104

Table 4–1: α -functionalization of mono-ring enamide.	120
Table 4–2: Screening of oxime hydrolysis.	120
Table 4–3: Screening of indole C3 alkylation by borrowing hydrogen strategy.	123
Table 4–4: Preparation of the enamides by selective reduction–elimination.....	126
Table 4–5: Optimization of imide synthesis.	127
Table 4–6: Iminium ion cyclization.	129
Table 4–7: Iminium ion cyclization with confined Brønsted acids.	131
Table 4–8: Screening of Boc cleavage with racemic Brønsted acids.	132
Table 4–9: Initial investigation of the asymmetric cascade reaction.	135
Table 4–10: 1 st screening of the Pictet–Spengler reaction.	137
Table 4–11: 2 nd screening of the Pictet–Spengler reaction.	138
Table 4–12: 3 rd screening of the Pictet–Spengler reaction.....	139
Table 4–13: 4 th screening of the Pictet–Spengler reaction.....	140
Table 4–14: 5 th screening of the Pictet–Spengler reaction.....	140
Table 5–1: Substrate scope.	160
Table 5–2: Screening for the regioselective dehydrogenation.	163
Table 5–3: Screening of Newhouse dehydrogenation.	164
Table 5–4: Asymmetric reduction of the enamide.	166
Table 7–1: Optimization of the annulation.	341

List of Abbreviations

Å	Angström	Ac	Acetyl
AD	Anno Domini	AIBN	Azobisisobutyronitrile
ATPase	Adenosine triphosphatase	BHT	Butylated hydroxytoluene
BINOL	1,1'-Bi-2-naphthol	Bn	Benzyl
B3LYP	Becke, 3-parameter, Lee–Yang–Parr	Boc	<i>tert</i> -Butyloxycarbonyl
BOP	Benzotriazol-1-yloxytris(dimethylamino)phosphonium hexafluorophosphate	BPO	Benzoyl peroxide
b.r.s.m.	Based on recovered starting material	BTMAC	Benzyltrimethylammonium chloride
Bu	Butyl	Bz	Benzoyl group
δ	Chemical shift	CD	Circular dichroism
CDI	Carbonyldiimidazole	CNS	Central nervous system
CoA	Coenzyme A	CPA	Chiral phosphoric acids
d	Doublet/ day	DBU	1,8-Diazabicyclo[5.4.0]-undecane
DCC	<i>N,N'</i> -Dicyclohexylcarbodiimide	DCE	1,2-Dichloroethane
DDQ	2,3-Dichloro-5,6-dicyano-1,4-benzoquinone	DFT	Density functional theory
DIPEA	<i>N,N</i> -Diisopropylethylamine	DMAP	<i>N,N</i> -Dimethylaminopyridine
DMF	Dimethylformamide	DMSO	Dimethyl sulfoxide
DMP	Dess–Martin periodinane	DNA	Deoxyribonucleic acid
DPPA	Diphenylphosphoryl azide	d.r.	Diastereomeric ratio
DTBMP	2,6-Di- <i>tert</i> -butyl-4-methyl-pyridine	ECD	Electronic circular dichroism
EDG	Electron donating group	ee	Enantiomeric excess
e.g.	exempli gratia	<i>ent</i>	Enantiomer
equiv.	Equivalentents	et al.	et alia
EWG	Electron withdrawing group	FDA	Food and Drug Administration
G	Gibbs free energy	GABA	γ -Aminobutyric acid
h	hour	HMBC	Heteronuclear multiple bond correlation
HMQC	Heteronuclear multiple quantum correlation	HMDS	Bis(trimethylsilyl)amine
HOBt	Hydroxybenzotriazole	HPLC	High performance liquid chromatography
Hsp	Heat shock protein	Hz	Hertz
IBX	2-Iodoxybenzoic acid	<i>i</i>	<i>iso</i> -

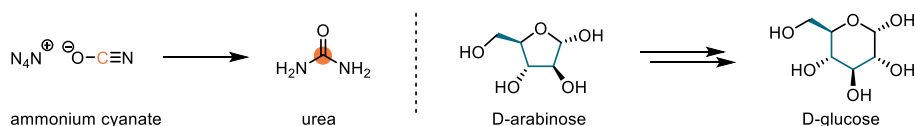
IC ₅₀	half maximal inhibitory concentration	ipc	diisopinocampheyl
LDA	Lithium diisopropylamide	LLS	Longest linear sequence
<i>m</i> CPBA	<i>meta</i> -Chloroperoxybenzoic acid	Me	methyl
NADP	Nicotinamide adenine dinucleotide phosphate	NCS	<i>N</i> -Chlorosuccinimide
NMI	<i>N</i> -methylimidazole	NMO	<i>N</i> -Methylmorpholine <i>N</i> -oxide
PAA	Peganumine A analogue	PCC	Pyridinium chlorochromate
Ph	Phenyl	PMP	<i>p</i> -Methoxyphenyl
PPTS	Pyridinium <i>p</i> -toluenesulfonate	Pr	Propyl
PROTAC	Proteolysis targeting chimera	py	Pyridine
rac	Racemic	RNA	Ribonucleic acid
SAR	Structure–activity relationship	SDS	Sodium dodecyl sulfate
SEM	2-(Trimethylsilyl)-ethoxymethyl	SM	Starting material
SMD	Solvation model based on density	<i>t</i>	<i>tert</i> -
<i>T</i>	Temperature	TBAF	Tetrabutylammonium fluoride
TBDPS	<i>tert</i> -Butyl diphenylsilyl	TBME	Methyl <i>tert</i> -butyl ether
TEA	Triethylamine	TEAC	Tetraethylammonium chloride
TES	Triethylsilyl	TEMPO	2,2,6,6-Tetramethylpiperidin-1-yl)oxidanyl
Tf	Trifluoromethanesulfonyl	TFA	Trifluoroacetic acid
TFAA	Trifluoroacetic anhydride	THF	Tetrahydrofuran
TMBE	Methyl <i>tert</i> -butyl ether	TMP	2,2,6,6-Tetramethylpiperidine
TMSE	2-(Trimethylsilyl)-ethanol	TPAP	Tetrapropylammonium perruthenate
Ts	Toluenesulfonyl	TS	Transition state

1. Motivation and Background

1.1. Introduction

As the science of matter, chemistry is considered by many as the center discipline standing between physics and biology.^[1] Besides analyzing existing molecules, the power of chemistry is rooted in its ability to create new chemical entities by synthesis. One of the most important subdisciplines of chemistry is organic synthesis, which addresses the construction of natural or artificial carbon-based molecules. Being the flagship of organic synthesis, total synthesis is regarded as not only an art, but also a science to endeavor the replication of the molecules of nature in laboratory.^[2]

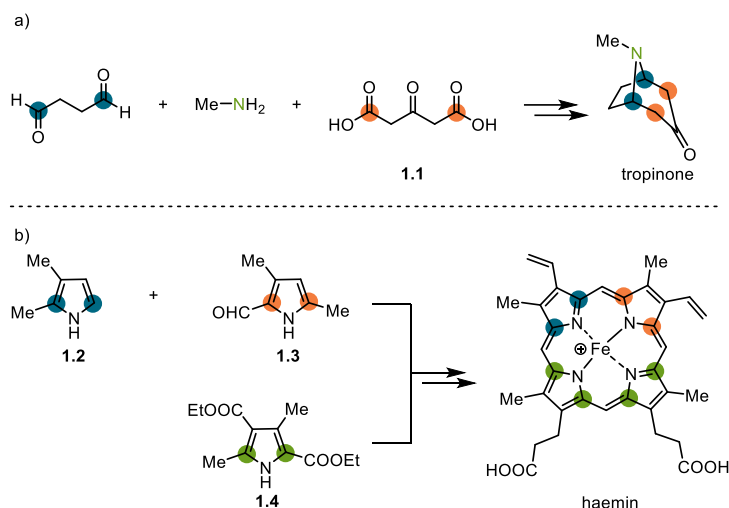
Total synthesis of natural products is a marvelous development in human history.^[3] The pioneering landmark, synthesis of urea, was accomplished by German chemist F. Wöhler in 1828, counting as the beginning of organic chemistry (Scheme 1–1).^[4] In the 19th century, many natural products were synthesized, such as alizarin^[5] and indigo.^[6] Another remarkable achievement was the total synthesis of (+)-glucose by E. Fischer^[7] which is regarded as the first total synthesis concerning stereochemistry.



Scheme 1–1: Remarkable total syntheses in the 19th century.

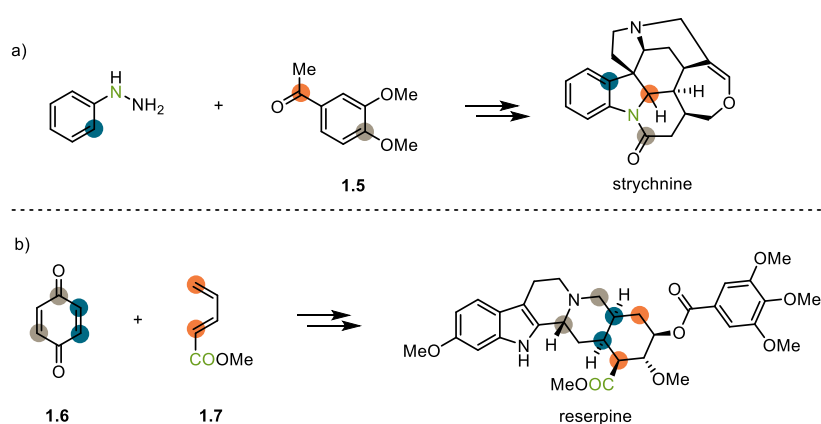
The 20th century has witnessed tremendous development of science and technology and has seen enormous achievements in total synthesis. According to the classification of Nicolaou et al., total synthesis in the 20th century could be divided into four eras, 1) the pre-World War II era; 2) the Woodward era; 3) the Corey era; 4) the 1990s era.^[3]

In the pre-World War II era, the significant change of total synthesis was in the complexity of the natural products. More complicated molecules were synthesized by using target-oriented strategy. The elegant biomimetic synthesis of (±)-tropinone by Sir Robinson, using succinaldehyde, methylamine and dicarboxylic acid **1.1**, is considered as the first alkaloid total synthesis (Scheme 1–2a).^[8] The total synthesis of Haemin by Fischer et al. is another landmark in this period, starting from diverse pyrrole building blocks (**1.2**, **1.3** and **1.4**) even without the assistance of modern structure elucidation methods (Scheme 1–2b).^[9]



Scheme 1–2: Landmark total syntheses in the pre-World War II stage.

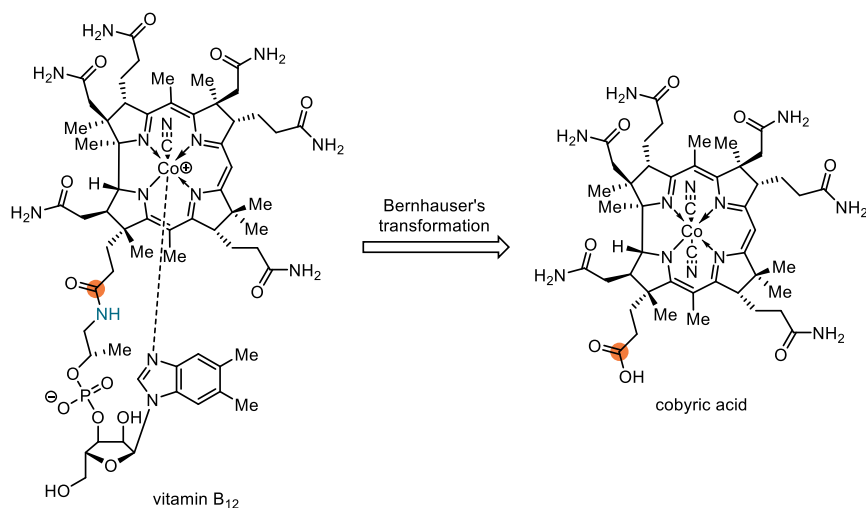
In the Woodward era, total synthesis was improved and became both a science and an art. Even till modern day, Woodward’s achievement is one of the peaks in total synthesis. In 1954, Woodward accomplished the total synthesis of strychnine by utilizing the Fischer indole synthesis^[10] with phenylhydrazine and acetophenone **1.5**, which established the foundation of Woodward’s contribution to total synthesis as a genius (Scheme 1–3a).^[11] This achievement also unveiled the golden age of total synthesis. Another milestone contribution of Woodward was the total synthesis of reserpine. His brilliant application of the Diels–Alder reaction^[12] between dienophile **1.6** and diene **1.7** realized a highly efficient construction of the reserpine scaffold (Scheme 1–3b).^[13]



Scheme 1–3: Representative total syntheses of Woodward.

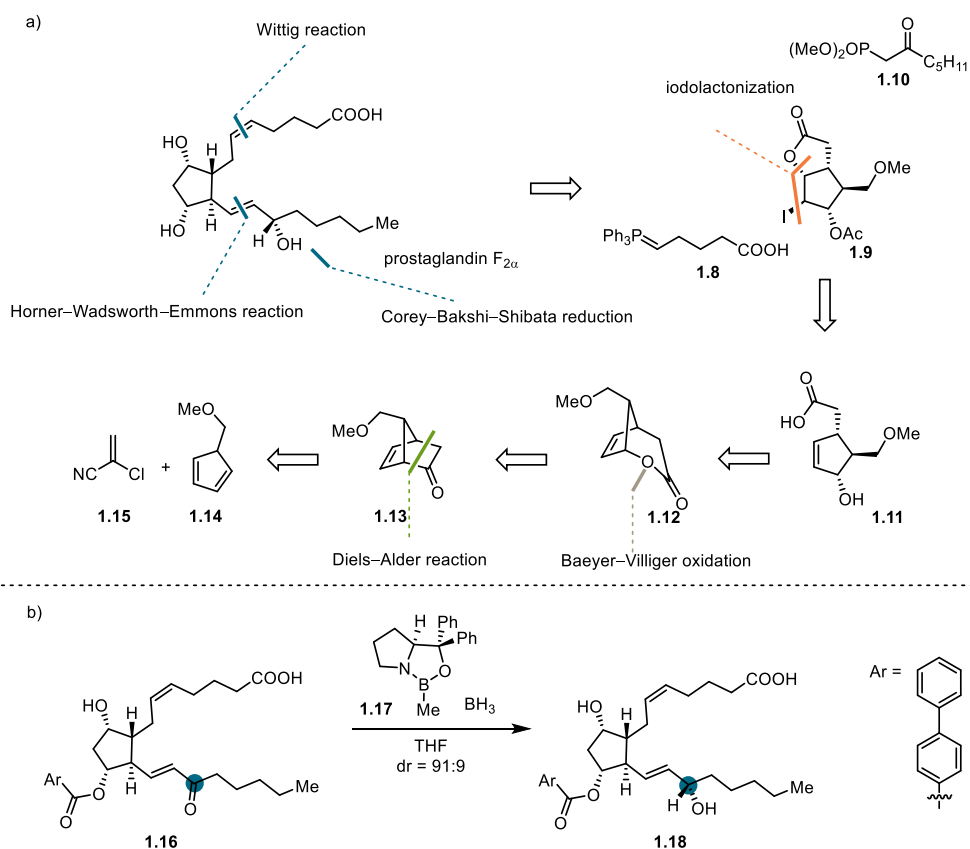
The total synthesis of vitamin B₁₂ was probably the most challenging synthetic problem in Woodward’s career.^[14] It was accomplished by the collaboration of the Woodward group and

the Eschenmoser group, with the participation of no less than 91 postdoctoral researchers and 12 Ph.D. students from 19 different nations over a period of almost 12 years.^[15] The monumental achievement of the total synthesis of vitamin B₁₂ is not only the construction of the molecule itself, but also expanding the margin of human knowledge and yielding novel methodologies and theories. The breakthrough theory, Woodward and Hoffmann rule, was developed during the total synthesis of vitamin B₁₂.^[16]



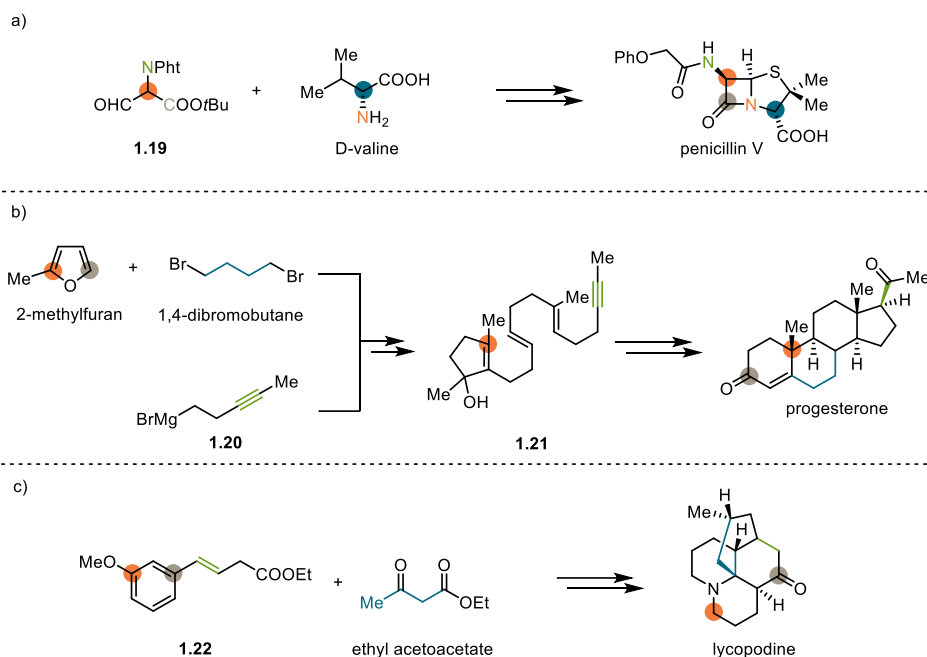
Scheme 1-4: Vitamin B₁₂ was traced back to cobyrinic acid.

During the Corey era, the two main characteristics were the increased emphasis of retrosynthetic analysis and an effort to develop new synthetic methodologies. In 1969, Corey et al. completed the total synthesis of racemic prostaglandin F_{2 α} , utilizing the concept of retrosynthetic analysis to simplify the target by several disconnections.^[17] The disconnections of the double bonds by Wittig reaction^[18] and Horner–Wadsworth–Emmons reaction^[19] led to phosphonium ylide **1.8**, phosphonate **1.10** and lactone **1.9**. The lactone **1.9** was traced back to carboxylic acid **1.11**, which could be constructed from bridged ketone **1.13** through a Baeyer–Villiger oxidation.^[20] The bridged ketone **1.13** was simplified to diene **1.15** and dienophile **1.14** by a Diels–Alder reaction (Scheme 1-5a).^[12] In 1987, Corey et al. achieved its enantioselective synthesis, using a Corey–Bakshi–Shibata (CBS) reduction.^[21] The CBS reduction relied on chiral oxazaborolidine **1.17**, realizing the reduction of ketone **1.16** to chiral secondary alcohol **1.18** (Scheme 1-5b).



Scheme 1-5: Retrosynthetic analysis of prostaglandin $F_{2\alpha}$ and CBS reduction.

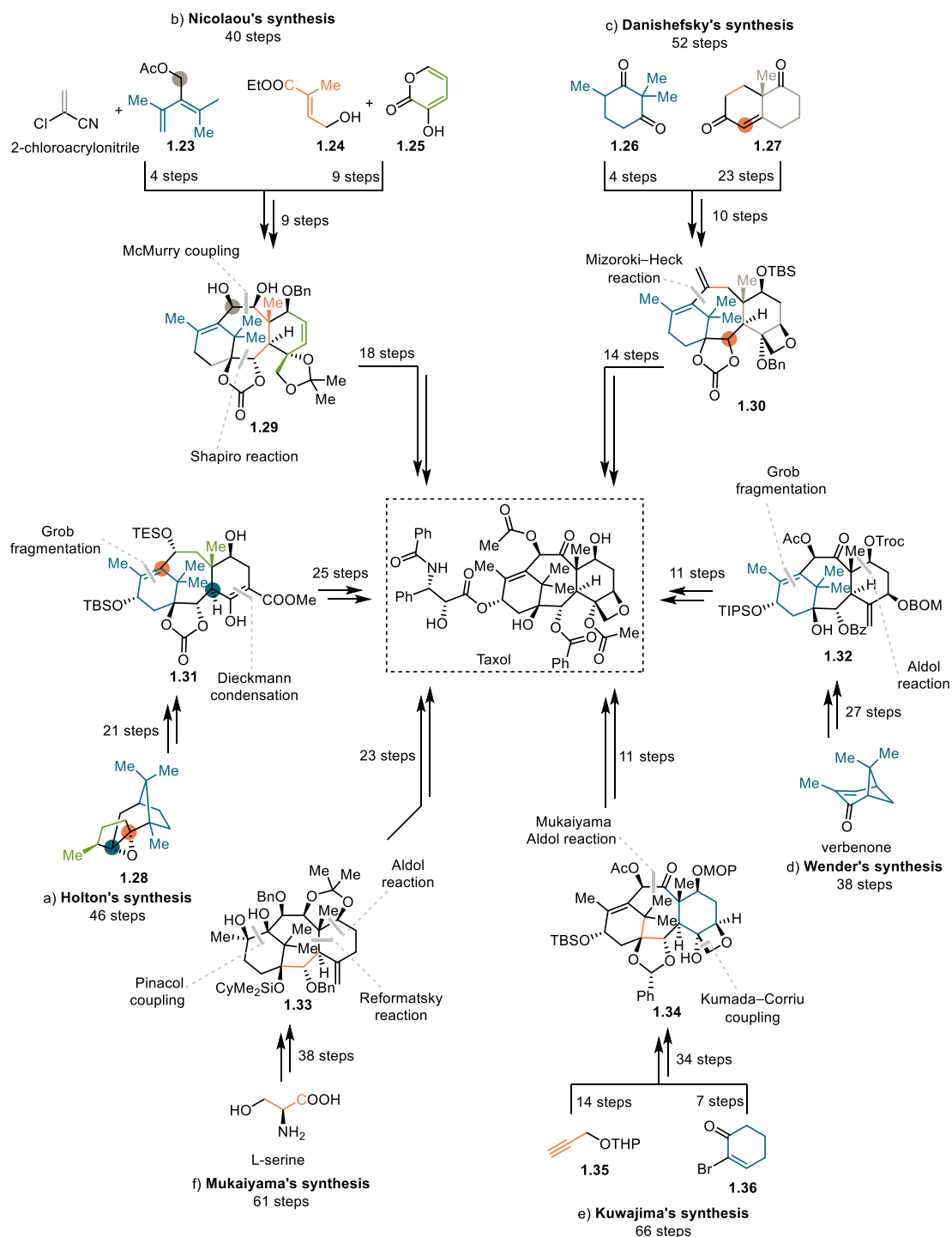
While Woodward and Corey are the two main representatives of that era, there were also lots of masters of total synthesis in the same period. The total synthesis of penicillin V from simple aldehyde **1.19** and D-valine by Sheehan et al. was a milestone to promote the development of diverse β -lactam antibiotics (Scheme 1-6a).^[22] The total synthesis of progesterone unlocked the area of steroidal molecules.^[23] Johnson et al. employed the polyene cyclization of **1.21** as the key step to complete the total synthesis of progesterone, demonstrating the profound power of biomimetic strategies in total synthesis, which were inspired by the biosynthetic pathway (Scheme 1-6b).^[24] Later in the era, Stork addressed the challenge to construct polycyclic lycopodium-type alkaloid from ester **1.22** and ethyl acetoacetate (Scheme 1-6c).^[25] Besides these breakthrough achievements, there are a multitude of brilliant chemists who also accomplished a variety of natural products to expand the knowledge of total synthesis.



Scheme 1–6: Other breakthrough total syntheses in Woodward and Corey era.

Since the 1990s, the total synthesis of natural products is frequently accompanied with the study of bioactivity, due to the increasing development of biology and medicine. In addition, with the progress of related areas, such as isolation methods, structure elucidation and synthetic methodologies, total synthesis encountered a blooming and competitive stage. The 6 concurring syntheses of Taxol in the 1990s is a good example of competition and development within the field of total synthesis. In 1994, Holton et al. reported their enantioselective total synthesis of Taxol from epoxide **1.28** in 46 linear steps, featuring a Grob fragmentation^[26] and a Dieckmann condensation^[27] (Scheme 1–7a).^[28] Simultaneously, Nicolaou et al. published their 40-step convergent total synthesis, employing two Diels–Alder reactions^[12] of dienophile 2-chloroacrylonitrile and diene **1.23**, as well as dienophile **1.24** and diene **1.25** (Scheme 1–7b).^[29] The key steps are a Shapiro reaction^[30] to integrate the two fragments and a McMurry coupling^[31] to close the eight-membered ring. Two years later, Danishefsky et al. provided another 52-step synthesis starting from diketone **1.26** and ketone **1.27** (Scheme 1–7c).^[32] The Mizoroki–Heck reaction^[33] was the key step in the synthesis. In 1997, another 38-step linear synthesis was accomplished by Wender et al (Scheme 1–7d).^[34] They commenced the synthesis from natural monoterpene verbenone and utilized a Grob fragmentation^[26] and an aldol reaction to construct **1.32**. Kuwajima et al. achieved the first total synthesis of Taxol using artificial small molecules **1.35** and **1.36** as starting material via a 66-step synthesis (Scheme 1–7e).^[35]

Through the key Mukaiyama aldol reaction,^[36] Reformatski reaction,^[37] and pinacol coupling,^[38] Mukaiyama et al. also completed the total synthesis of Taxol from L-serine in 61 steps in 1998 (Scheme 1–7f).^[39]



Scheme 1–7: Total syntheses of Taxol in the 1990s.

This is a unique example in the history of total synthesis that manifold total synthesis routes were published in such a short period (1994–1998) for such a complex molecule. The main

driving forces for the intensive research of its total synthesis was because of its extreme scarcity and extraordinary bioactivity with novel interaction with tubulin by stabilizing the microtubule polymer.^[40] Additionally, the bioactivity of natural product became a paramount consideration of total synthesis since then.

On the other hand, the structures of the natural products being synthesized were increasingly complex. Palytoxin was considered as “*the Mount Everest of organic synthesis, the largest molecule that anyone has ever even thought about making*”.^[41] The structure contains more than 100 stereocenters, which was elucidated by Uemura et al.^[42] After 12 years, Kishi et al. completed its total synthesis by subsequent connections of 9 fragments.^[43] It is undoubted that the completion of the total synthesis of palytoxin is a “pivotal moment” in the field of natural product synthesis. It is also an epitome of human’s development. Starting from the synthesis of urea, within 200 years exploration, humans could manipulate and construct such a giant and complex molecule (Figure 1–1).

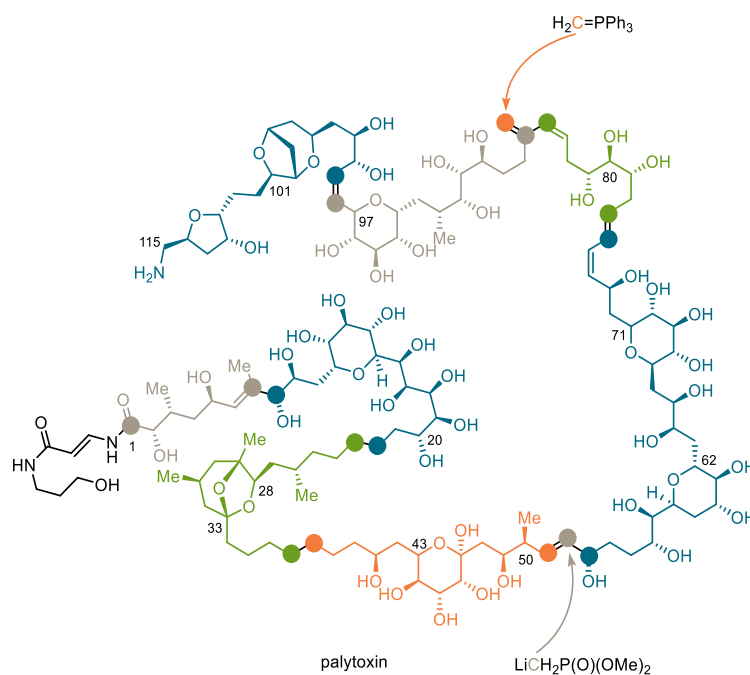
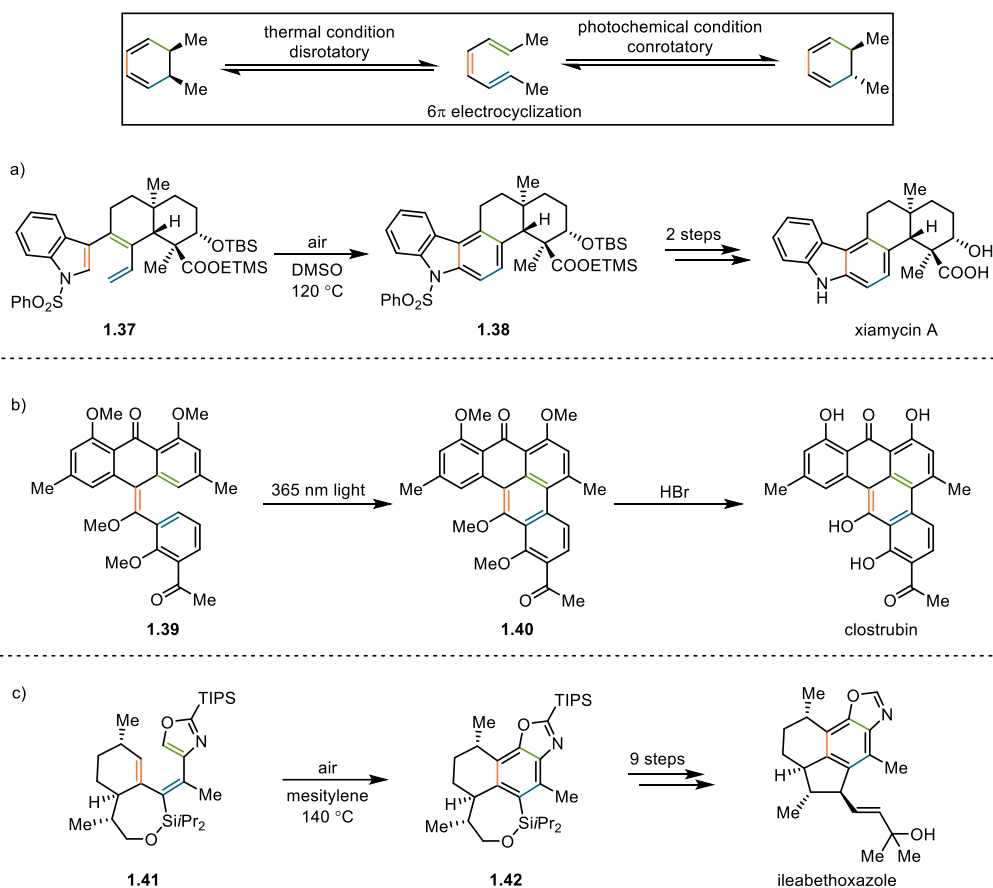


Figure 1–1: Structure and synthetic fragments of palytoxin.

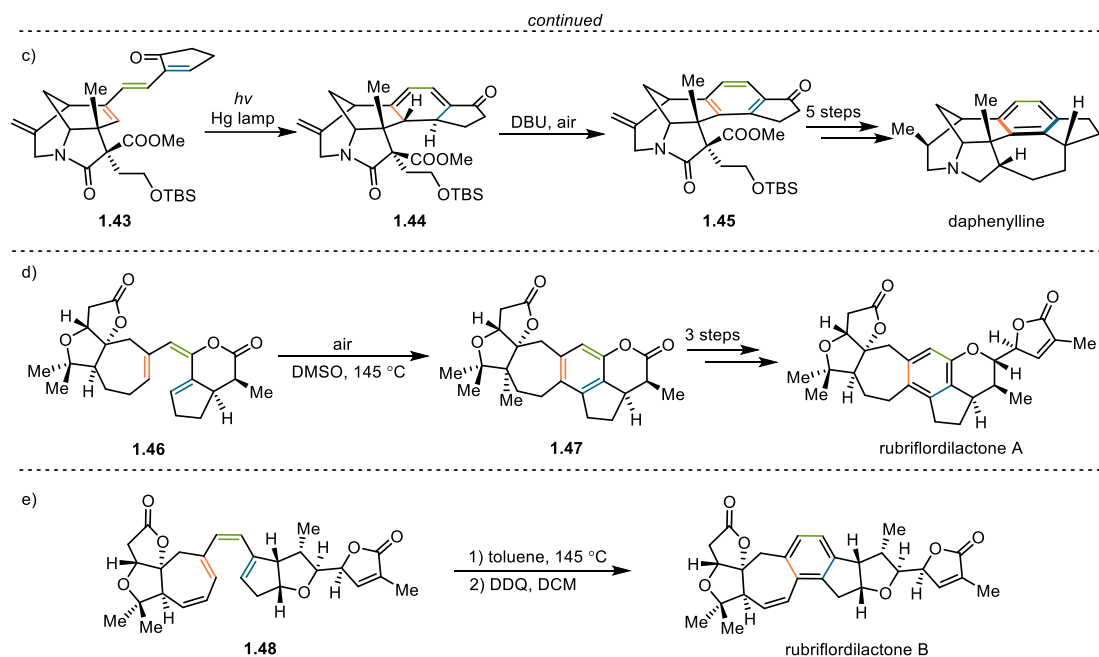
However, it was also a moment to discover potential new directions in the field of total synthesis. During the pre-World War II era, many methodologies and theories were undeveloped. This has altered vastly since then, going via the Woodward and Corey era and then into a time where high throughput screening and computer-aided technology played a more important role in the

drug discovery pathway. In the 21st century, the sustainability and efficiency of natural product synthesis underlay the precepts of modern chemistry.^[44] These developments have all contributed to the current era of natural product synthesis, based on the results and methodologies of the pioneers in the past to mold the field of modern drug discovery and organic synthesis to allow for simplified and strategic total synthesis towards natural products.^[45]

The 6- π electrocyclization–rearomatization strategy was proposed by Li et al., by which concise total syntheses of various complex natural products were achieved. In the total synthesis of xiamycin A, indole-based triene **1.37** underwent a 6- π electrocyclization–rearomatization cascade reaction to afford carbazole **1.38** (Scheme 1–8a).^[46] The polyphenol natural product clostrubin was also synthesized through a 6- π electrocyclization–rearomatization tandem reaction of highly conjugated triene **1.39** (Scheme 1–8b).^[47] Triene **1.41** was converted to arene **1.42**, which was the key intermediate of the total synthesis of ileabethoxazole (Scheme 1–8c).^[48]



Scheme 1–8: 6- π electrocyclization–rearomatization strategy in total synthesis.

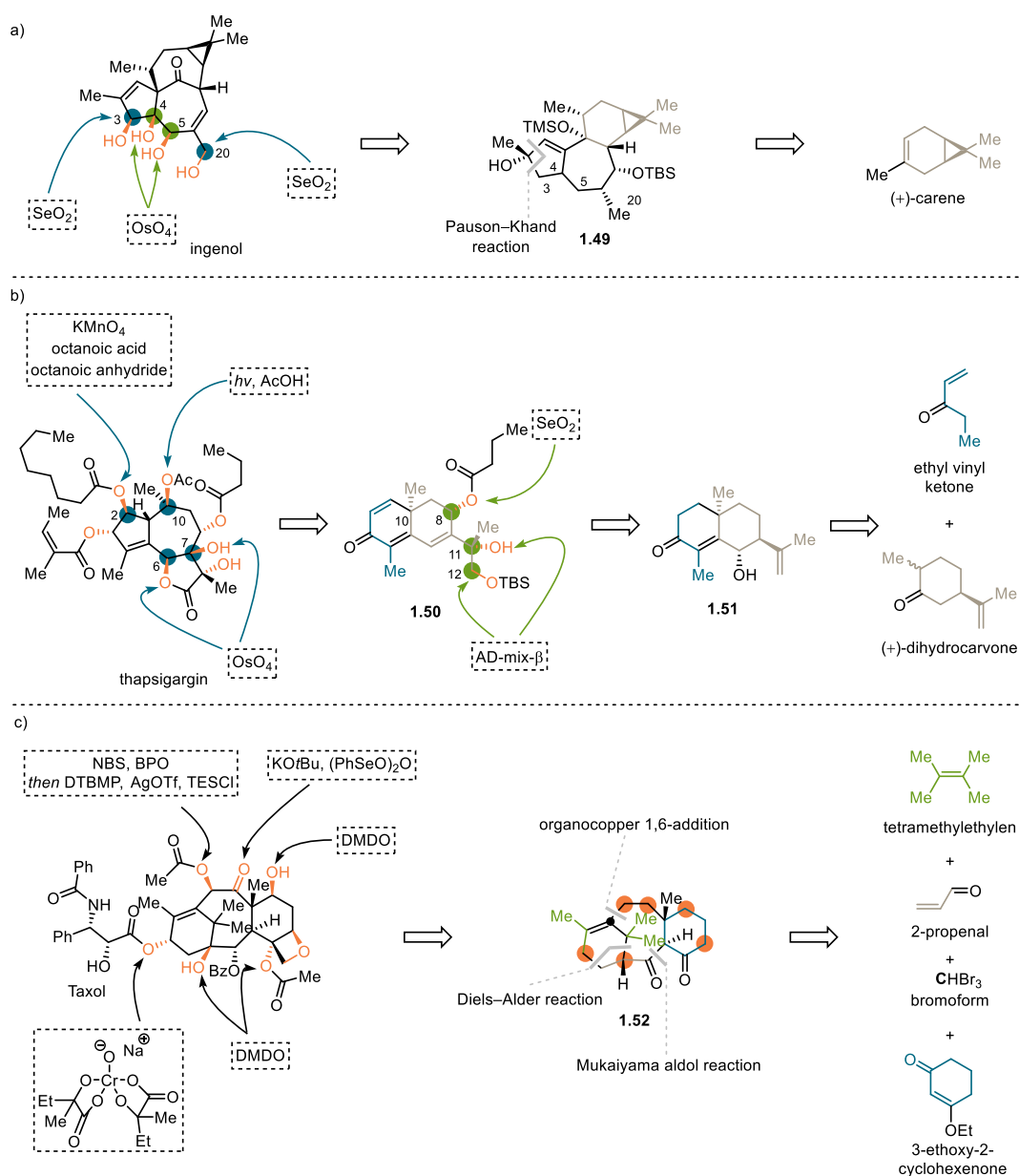


Scheme 1–8: 6- π electrocyclization–rearomatization strategy in total synthesis. (continued)

Besides those natural products with heterocycles, the 6- π electrocyclization–rearomatization strategy was also applied to the less activated triene system. In the total synthesis of daphenylline, the photochemically induced 6- π electrocyclization of triene **1.43** afforded conrotatory product **1.44**, which underwent rearomatization under DBU/air condition yielding arene **1.45** (Scheme 1–8c).^[49] The strategy was also used in the total synthesis of rubriflordilactone A^[50] and B,^[51] whereby trienes **1.46** and **1.48** were converted to arene **1.47** and rubriflordilactone B (Scheme 1–8d and e).

Inspired by the biosynthesis of terpenoids, Baran et al. proposed a two-phase synthesis strategy for highly oxidized terpenoids. In this strategy, the first cyclase phase is to construct the carbon skeleton, which can be realized by various C–C bond formation methodologies. The challenging second phase is to functionalize the hydrocarbon skeletons of the complex terpenes. In the total synthesis of ingenol,^[52] starting from (+)-carene, the cyclase phase end point **1.49** was synthesized through a 7-step sequence, featuring a Pauson–Khand reaction (Scheme 1–9a).^[53] In the oxidase phase, by utilizing the C–C double bonds, the four hydroxyl groups were successfully introduced by OsO₄ catalyzed dihydroxylation^[54] and SeO₂ mediated Riley oxidation^[55] respectively. The two-phase strategy was also applied to the total synthesis of the more oxidized terpenoid thapsigargin. The final product of cyclase phase **1.51** only needed a one-step Robinson annulation^[56] between ethyl vinyl ketone and (+)-dihydrocarvone (Scheme

1–9b). By exploiting the double bonds, five of the six hydroxyl groups were installed. It is noteworthy that the C10 hydroxyl group was introduced in the same process of the photochemical rearrangement.^[57] In 2020, after 13-year effort, Baran et al. accomplished the two-phase total synthesis of Taxol, which demonstrated that the two-phase logic could be a favorable guiding strategy to the terpenoid total synthesis (Scheme 1–9c). The unique 6/8/6 tricyclic taxane **1.52** was constructed by a six-step cyclase phase from simple building blocks.^[58] It is remarkable that in the oxidase phase, there was no skeleton rearrangement, which means all the C–H functionalization were achieved by direct manipulation of the 6/8/6 tricyclic carbon skeleton.^[59]



Scheme 1–9: Two-phase strategy in total synthesis.

This brief overview of the development of natural product total synthesis indicates that it has evolved to a mature scientific subject from an empirical technique. However, huge terra incognita still needs to be explored. It is anticipated that one day in the future, with the assistance of computational technology, the reactivity of every atom in any molecule could be predicted precisely. This would allow natural product total synthesis to become more efficient and environmentally friendly by avoiding the time-consuming optimization of reaction conditions. It is also envisioned that with the development of new theories, novel methods for bond formation can be discovered which will provide new concise strategies for natural product total synthesis. Moreover, being the flagship of organic synthesis, natural product total synthesis will certainly play an important role in the development of humans.

1.2. Natural product and drug discovery

1.2.1. Natural product as drug

The importance of natural products in the treatment of human disease is well documented throughout history. Sumerian cuneiform tablets (2400 BC) from Mesopotamia record prescriptions for medicine. The ancient Egyptian *Ebers Papyrus* recorded roughly 800 prescriptions using 700 drugs. Greek physician Pedanius Dioscorides wrote *De Materia Medica* covering over 600 medicinal plants. The earliest known Chinese manual on Materia medica is the *Shennong Bencao Jing* dating back to the 1st century AD. After the isolation of morphine from opium by Sertürner, humans have since started to investigate the active ingredient of medicinal plants.^[60] The isolation and total synthesis of natural product become more and more important in drug discovery, as it can provide the pure active ingredient. Additionally, the unique structure of natural product is a good starting point for drug discovery.

Natural products are usually classified into two major classes: primary and secondary metabolites. Primary metabolites are organic molecules of basic metabolic pathways that are required for life, such as nucleic acids, amino acids, sugars, and fatty acids, and the major macromolecules from these simple building blocks, for example DNA, RNA, proteins, carbohydrates, and lipids. In contrast, secondary metabolites are organic molecules that

typically have an extrinsic function and mainly affects other organisms rather than the one synthesizing them.^[61] Secondary metabolites are not essential for survival but increase the competitiveness of the organism within its environment. Since secondary metabolites have diverse structures and activities, they attract more attention of research. Based on their structures, natural products can be divided into four major classes: alkaloids, terpenoids, phenylpropanoids and polyketides. Alkaloids are a diverse group of nitrogen-containing basic compounds. Terpenoids are oxygenated hydrocarbons composed of isoprene units. Phenylpropanoids are chemical compounds characterized by the presence of aromatic ring structure bearing one or more hydroxyl groups. Polyketides contain alternating carbonyl groups (or hydroxyl groups) and methylene groups.

The discovery of the biologically active natural products has dramatically changed human life and society. Alkaloid contains diverse natural products with a wide range of pharmacological activities. Morphine was the first isolated natural product and exhibited excellent interaction with the central nervous system to decrease the feeling of pain. It is also on the World Health Organization's List of Essential Medicines. Although both cocaine and anisodamine contain a tropane scaffold, they show distinct medicinal effect. The activity of cocaine is related with the neurotransmitters, such as dopamine and serotonin.^[62] But anisodamine mainly interacts with α_1 adrenergic receptor to treat acute circulatory shock.^[63] Tetrahydroisoquinoline and isoquinoline alkaloids exhibit diverse bioactivities^[64] making them frequently used in clinic, such as noscapine,^[65] papaverine,^[66] emetine,^[67] tubocurarine^[68] and so on. The unique *Colchicum autumnale* has been used as early as 1500 BC to treat joint swelling. The active component is colchicine, which was approved by FDA in 1961 and is still a first line drug for gout.^[69] Caffeine is probably the most widely consumed psychoactive drug, as it is legal and unregulated in most parts of the world, and even appears in coffee and tea. Its prominent mechanism is believed to be through reversible blocking the action of adenosine on its receptors.^[70] The discovery of cinchona alkaloid quinine is a landmark in the treatment of malaria. It not only spurred the development of synthetic chemistry,^[71] but also inspired the invention of lots of low-toxic anti-malaria drugs, such as chloroquine (Figure 1–2).^[72]

Terpenoids is also an important type of natural product. *Andrographis paniculate* is a widely

used traditional Chinese medicinal herb. One of the active compounds was isolated as andrographolide,^[73] which is an anti-inflammatory terpenoid drug. The terpenoid digoxin is a representative of the cardiac glycosides, which usually applied to increase the output force of heart and decrease its rate of contractions through the interaction with the cellular sodium-potassium ATPase pump.^[74] Digoxin is on the World Health Organization's List of Essential Medicines with millions prescriptions per year (Figure 1–2).

The phenylpropanoids is a class of molecules that contains lots of excellent drug applications as well. Podophyllotoxin is usually the active ingredient of medicinal cream to treat external warts.^[75] Etoposide is a topoisomerase inhibitor, acting as a chemotherapeutic agent for the treatment of cancer. Polyketides are produced in bacteria, fungi, plants, and certain marine animals, exhibiting special bioactivities. Erythromycin is an antibiotic which usually is regarded safer than penicillin concerning the potential allergic effects (Figure 1–2).

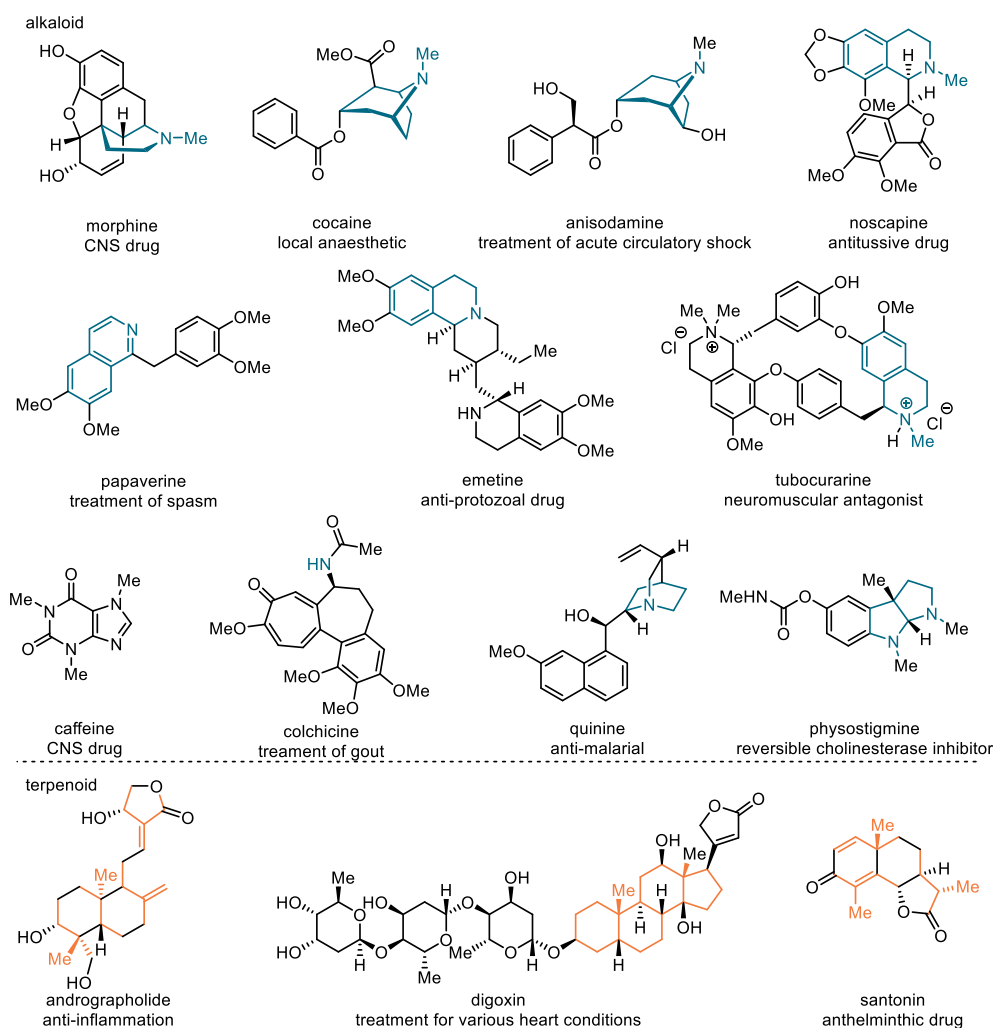


Figure 1–2: Examples of natural products as drugs.

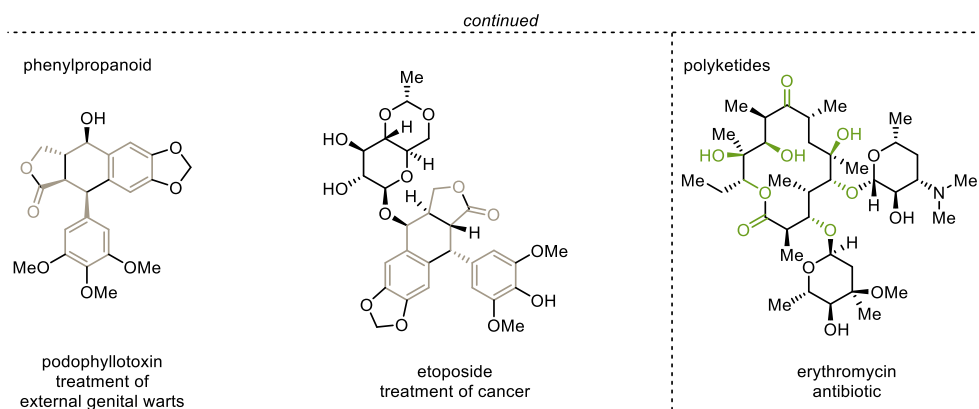


Figure 1–2: Examples of natural products as drugs. (continued)

In the history of mankind, natural products played a crucial role to conquer diseases. In ancient times, people were only able to use the herbs based on observational experience, which in most cases is not an effective way. With the development of isolation methods, people could utilize the pure active component of the natural remedies, which is more efficient due to the elimination of the other potential toxic compounds. For example, during World War II, the successful application of penicillin saved the lives of thousands of wounded people and attracted scientists' attention to discover more active antibiotics. With the blooming of pharmaceuticals, the strict safety criteria of drugs are also updated. Gentamicin is an aminoglycoside antibiotic, produced by the fermentation of *Micromonospora purpurea* and was widely used in the 1960s (Figure 1–3). However, it had serious side-effects, such as kidney damage and inner ear problem, which were discovered during the usage, thereby limiting its application in clinic.

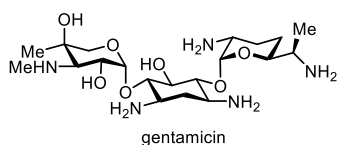


Figure 1–3: Structure of gentamicin.

Although the direct usage of natural product as drug is challenging to meet the modern standard of drug, natural products still play an important role in the drug discovery,^[76] due to their scaffold diversity, structural complexity and molecular rigidity.^[77] In the modern drug discovery, the research based on natural product and computer design are two of the most important methods to discover new druggable entities and they promote each other to hit the potent candidates of drugs indeed.^[78]

1.2.2. Strategies for natural product analogues synthesis in drug discovery

Historically, a natural product total synthesis was usually a target-oriented synthesis, which was mainly focused on the natural product itself before the Corey stage. The value of total synthesis for drug discovery was only to provide the rare natural products themselves. The design and synthesis of 9,11-diazo-prostaglandin H₂ by Corey et al. is an early natural product analogue design, synthesis and evaluation (Figure 1–4).^[79] It is not only more stable, but also about eight times faster to promote irreversible aggregation of platelets than prostaglandin H₂.

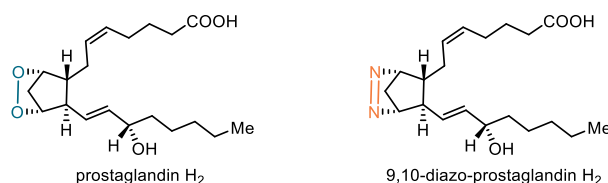


Figure 1–4: PGH₂ and 9,11-diazo-PGH₂.

Nicolaou as one of the masters of total synthesis in the post Woodward and Corey era, focused on total synthesis incorporating biological and medicinal consideration in his endeavors.^[80] After accomplishing the total synthesis of calicheamicin γ_1 , Nicolaou et al. designed calicheamicin θ_1 which exhibited one thousand times improvement of DNA cleaving property and apoptosis inducing activity.^[81]

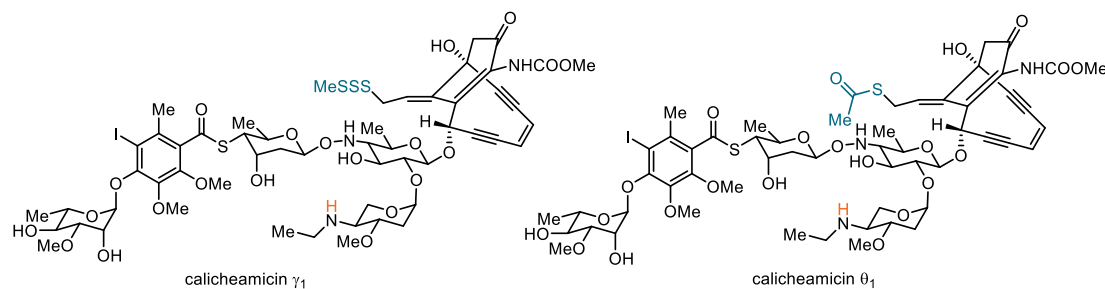
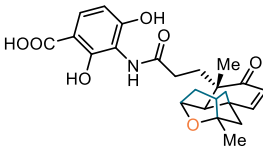
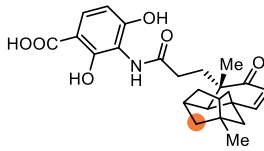
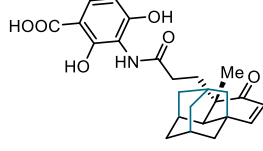
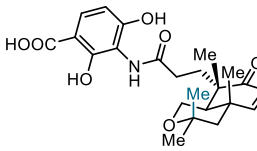


Figure 1–5: Calicheamicin γ_1 and its analogues.

Besides the strategy of changing the side chain, the modification of core carbon scaffold is also an important strategy for the design of natural product analogues. Platensimycin is a novel cage-like antibacterial natural product which inhibits bacterial fatty acid biosynthesis.^[82] In 2009, Nicolaou et al. completed the total synthesis of platensimycin,^[83] together with its analogues, such as carbaplatensimycin,^[84] adamantaplatensimycin^[85] and the bicyclic analogue.^[86] Although these attempts of structure simplification were not fruitful, the result showed the unique cage-like structure was crucial for the bioactivity and provided guidance for the further

design of analogues (Table 1–1).

Table 1–1: Minimum inhibitory concentration of platensimycin and its analogues.

	 platensimycin [$\mu\text{g/mL}$]	 carbaplatensimycin [$\mu\text{g/mL}$]	 adamantaplatensimycin [$\mu\text{g/mL}$]	 bicyclic analogue [$\mu\text{g/mL}$]
MRSA ^[a]	0.2–0.4	1.1–2.2	1.3–1.8	3.5–4.3
VREF ^[b]	0.4–0.8	1.1–2.2	1.3–1.8	6.5–8.5

[a] Methicillin-resistant *Staphylococcus aureus*. [b] Vancomycin-resistant *Enterococcus*

Since then, various strategies were developed to guide the design and synthesis of natural product analogues. The most popular strategies are hybrid synthesis (HS),^[87] complexity to diversity (CtD),^[88] diverted total synthesis (DTS),^[89] function-oriented synthesis (FOS)^[90] and biology-oriented synthesis (BIOS).^[91]

The hybrid synthesis is generally a way to integrate two active molecules to a single molecule. Compared to the combinatorial chemistry approach, the advantage of hybrid synthesis is the inherent biological activity of the hybrids. One interesting example exists in nature is the antimicrobial antibiotic thiomarinol, which is a hybrid of the pseudomonic acid C analogue and holothin (Figure 1–6).^[92]

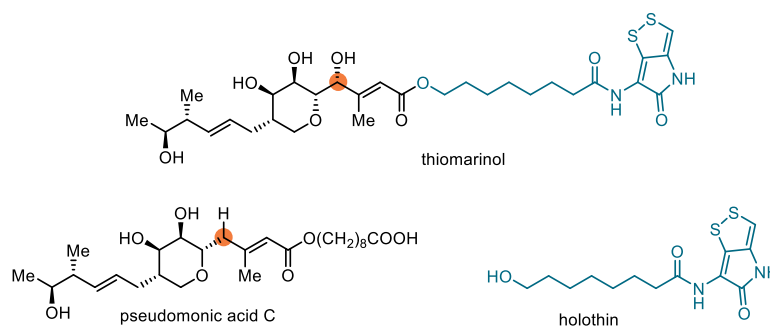


Figure 1–6: Hybrid in nature.

The most common hybrid strategy is a straightforward connection between two components by a linker. Geldanamycin is an ansamycin antibiotic, which could bind to the Hsp90 chaperone protein and lead to the degradation of several important proteins. The interaction is non-selective thereby compromising its applicability as a drug lead. Therefore, a hybrid with estradiol was anticipated to increase the affinity to estrogen receptor. The assay revealed that **1.53** targeted the estradiol receptor-Hsp90 interaction exclusively without affecting other Hsp90 associated proteins (Figure 1–7).^[93]

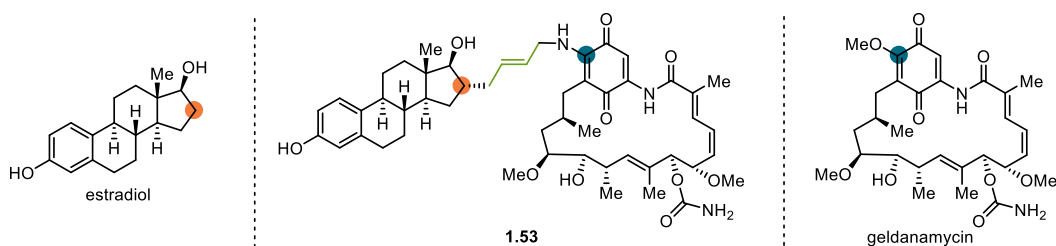
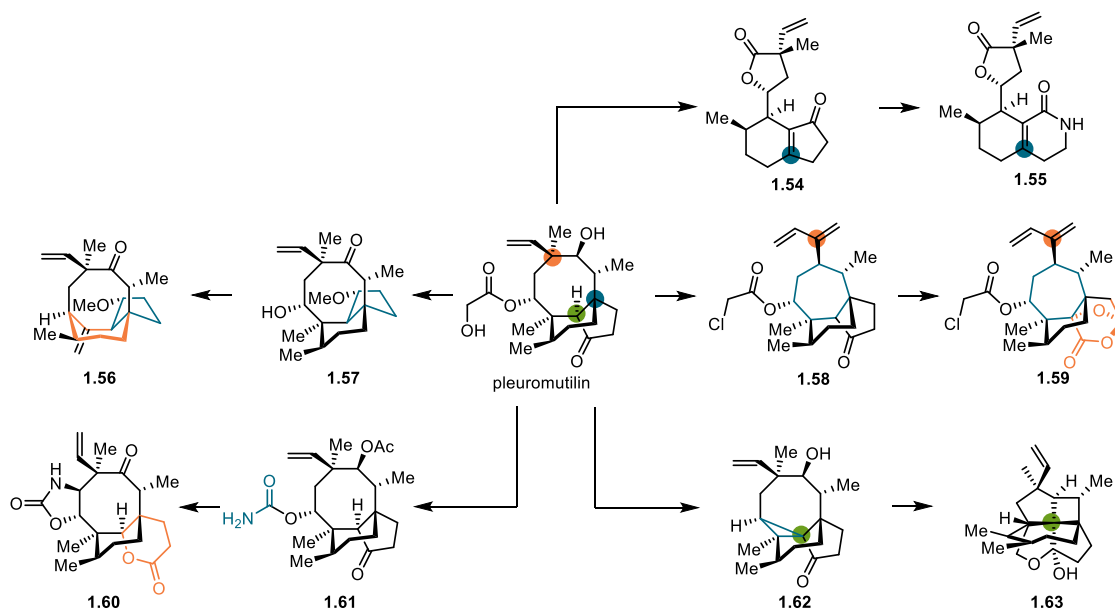


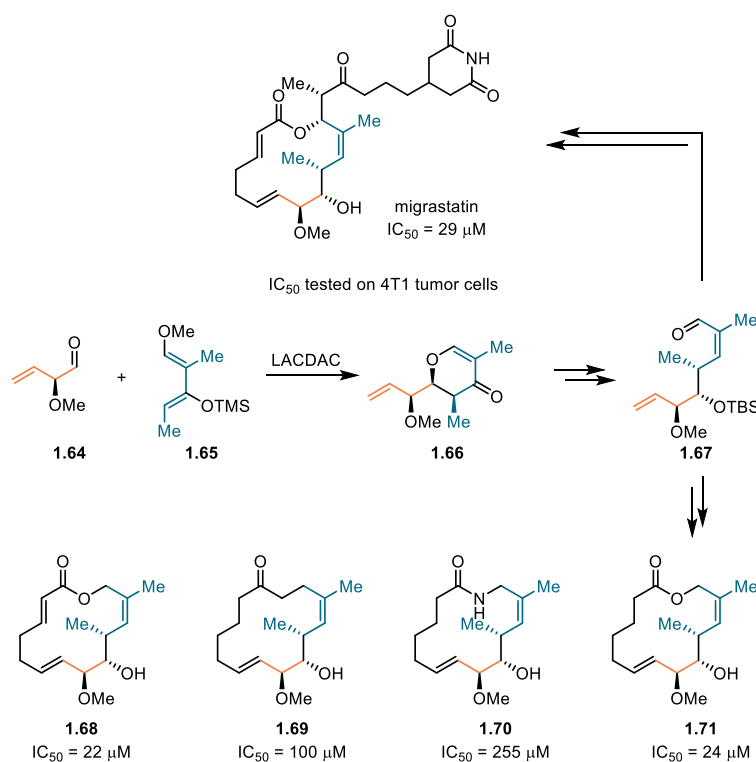
Figure 1-7: Hybrid with linker.

Complexity to diversity is another strategy to generate new chemical entities by utilizing the functional groups of natural products. The efficiency of this strategy was exhibited in the diversification of diterpene pleuromutilin, which transformed the tricyclic ring system of pleuromutilin into a variety of novel and complex polycyclic compounds in short synthetic sequences.^[94] Through a retro-Michael ring cleavage and oxidation sequence, pleuromutilin was converted to lactone **1.54**, which could undergo a Beckmann rearrangement^[95] yielding **1.55** (Scheme 1-10).^[96] The ring expansion product **1.56** was obtained by the carbocation rearrangement of **1.57**. An isomerization and subsequent 1,5-hydride shift afforded **1.57** from pleuromutilin.^[97] The 8-membered ring of pleuromutilin could also be contracted to a 7-membered ring resulting in diene **1.58**, which was able to be further transformed into **1.59**.^[98] The side chain could also be modified yielding **1.61**, which underwent autoxidation to afford lactone **1.60**.^[99] Tetracyclic **1.62** was obtained via an alkylation type reaction of pleuromutilin. Treating **1.62** with PCl_5 , triggered a carbocation rearrangement cascade leading to a complex pentacyclic compound **1.63**.^[100]



Scheme 1-10: Complexity to diversity of pleuromutilin.

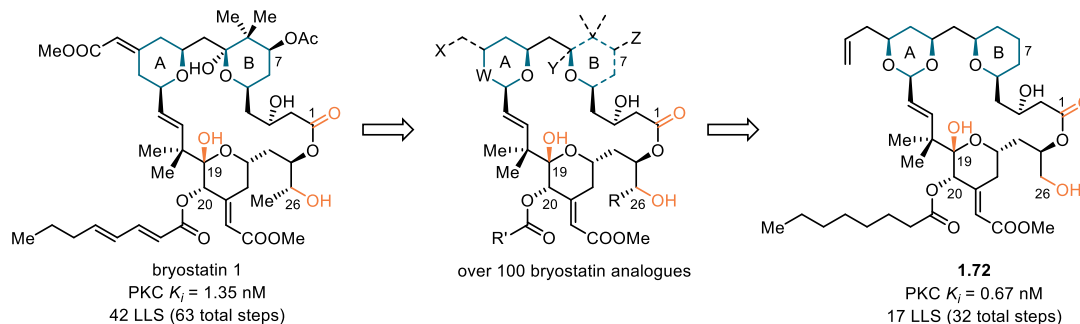
Diverted total synthesis is probably the most frequently used strategy for natural product analogues synthesis. This term was proposed by Danishefsky,^[89] holding the central consideration, that the natural products and analogues are equal concerning the properties sought after in the eventual drug. The key of diverted total synthesis is an advanced intermediate having access to both the natural product and the analogues. In the diverted total synthesis of migrastatin, the advanced intermediate **1.67** was constructed by a sequence featuring a Lewis acid-catalyzed diene aldehyde condensation (LACDAC) between **1.64** and **1.65** (Scheme 1–11).^[101] Utilizing a divergent synthesis route from **1.67**, both migrastatin and structure simplified analogues (**1.68–1.71**) were synthesized. Further assay showed the simplified analogues **1.68** and **1.71** have improved cytotoxicity against 4T1 cell.



Scheme 1–11: The diverted total synthesis of migrastatin.

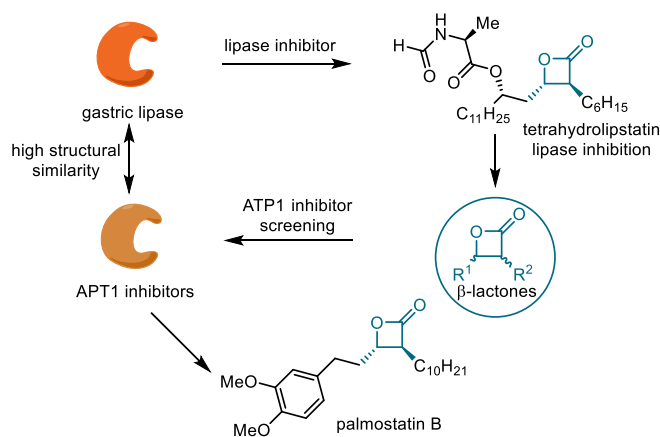
Function-oriented synthesis is another way to overcome the random design of analogues. This strategy is usually based on a preliminary SAR study. Wender et al. demonstrated this strategy in the analogue design and synthesis of bryostatin 1, which is a polyketide isolated from the marine organism *Bugula neritina* and exhibits remarkable biological activities.^[102] However, the poor natural abundance, low isolated yield (10^{-3} to 10^{-8} %) and long total synthesis steps limited its application in clinic. Based on the preliminary SAR study, the pharmacophoric

regions were identified; being the upper lipophilic A and B rings and the C1 carbonyl group and the C19 and C26 hydroxyl groups. After intensive investigation, Wender et al. discovered that analogue **1.72** exhibits better activity and can be prepared by a shorter and more simplistic synthetic route (Scheme 1–12).^[103]



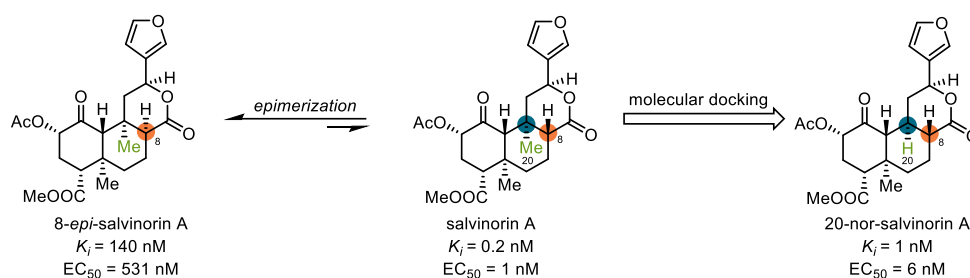
Scheme 1–12: Function-oriented synthesis of bryostatins.

As the primary SAR study with randomly designed analogues is required in the HS, DOS and FOS, Waldmann et al. proposed a biology-oriented synthesis. The BIOS is based on the understanding of structural conservatism of proteins and natural products in the evolution.^[104] Waldmann et al. considered that it could be an efficient way to design analogues by utilizing the conservatism of the binding between natural products and proteins.^[91] One example of such structural conservatism was discovered in ligand binding sites of APT1 and gastric lipase, by an analysis of the protein structure similarity clusters. Based on the structural and spatial arrangement similarities, Waldmann et al. hypothesized that lipase inhibitor might be a good starting point for the development of novel APT1 inhibitor (Scheme 1–13). Based on the marketed lipase inhibitor tetrahydrolipstatin, a variety of β -lactones were designed and synthesized. Finally palmostatin B was proven to be an efficient APT1 inhibitor.^[105]



Scheme 1–13: Discovery of ATP1 inhibitor through biology-oriented synthesis.

With the development of computational chemistry, the *in silico* techniques were utilized in the analogue design and synthesis of bioactive natural products. Shenvi et al. reported a stabilized analogue of salvininorin A, which overcome the epimerization problem at the C8 position (Scheme 1–14).^[106] By analyzing the epimerization mechanism, the C20 methyl group deleted 20-nor-salvinorin A was considered as a more stable analogue. The further docking with *kappa*-opioid receptor showed the binding model of 20-nor-salvinorin A was similar as salvininorin A. The investigation of the chemical reactivity and biological activity of 20-nor-salvinorin A demonstrated it was more stable than salvininorin A with comparable bioactivity.



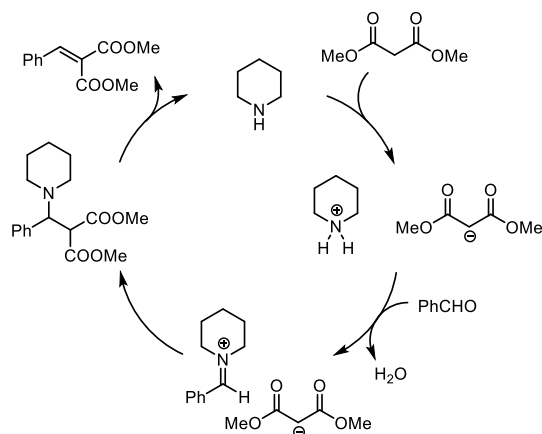
Scheme 1–14: Dynamic strategic bond analysis of salvininorin A.

1.3. Natural product and organocatalyst

1.3.1. Organocatalysis

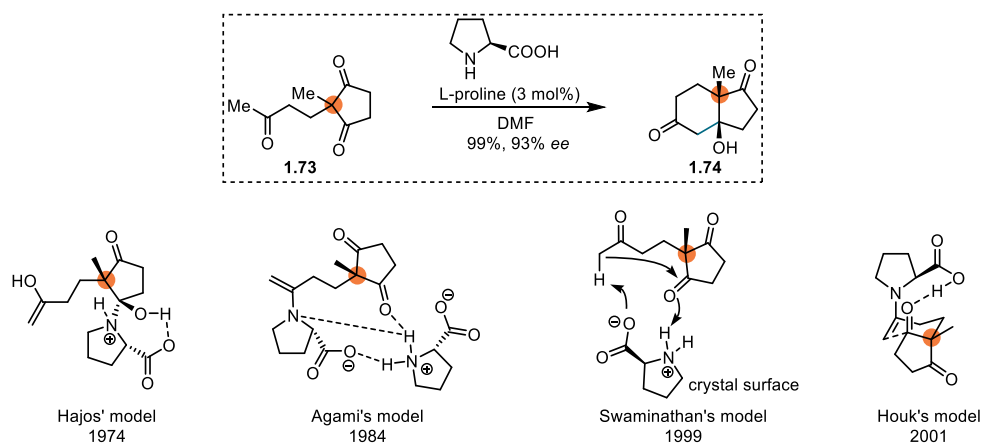
Catalysis is built on three pillars according to the modern classification, namely biocatalysis, metal catalysis and organocatalysis.^[107] Generally, organocatalysis could be further sub-divided into four types, Lewis bases, Lewis acids, Brønsted bases and Brønsted acids. The fundamental activation mode of these catalysts is either providing or removing electrons or protons from a substrate or a transition state. Lewis base catalysts, such as amines and carbenes, and Brønsted acid catalysts are the prominent types in organocatalysis.

Although the concept of organocatalysis was proposed in the late 1990s, the application of achiral organocatalyst can be trace back to the late 19th century. Knoevenagel found that amine could catalyze the aldol condensation between malonate with aldehyde (Scheme 1–15).^[108]



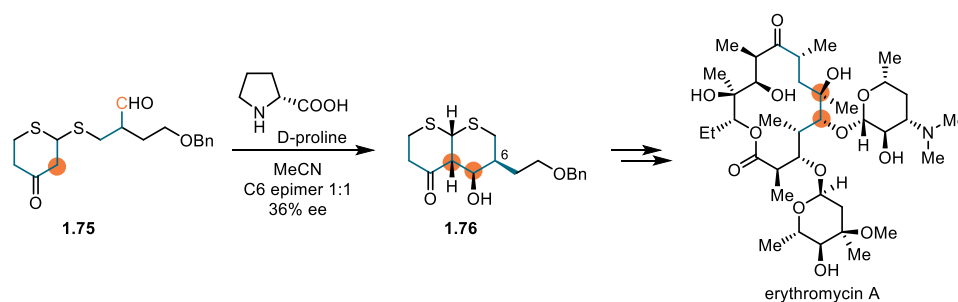
Scheme 1-15: Catalytic cycle of the Knoevenagel reaction.

The pioneering reaction in asymmetric organocatalysis was the proline catalyzed intramolecular aldol condensation of **1.73** in the 1970s, namely Hajos–Parrish–Eder–Sauer–Wiechert reaction, leading to bicyclic ketol **1.74** (Scheme 1-16).^[109] Unfortunately, in the following three decades, this type of catalytic reaction was not fully explored. In the following studies, different mechanisms were proposed for this reaction. Hajos et al. postulated the reaction was via a hemiaminal intermediate.^[109b] In contrast, Agami et al. hypothesized the transition state involved an enamine with two proline units.^[110] Swaminathan et al. suggested a heterogeneous mechanism on the surface of crystalline proline, despite the reaction was homogenous.^[111] Houk et al. proposed another enamine participated mechanism.^[112]



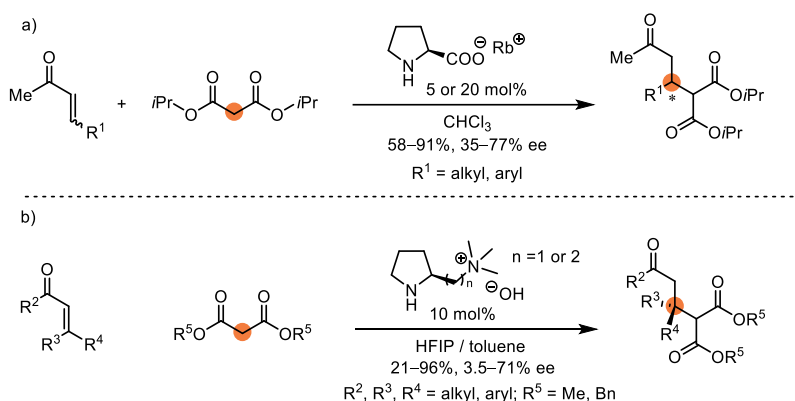
Scheme 1-16: Organocatalytic Hajos–Parrish–Eder–Sauer–Wiechert reaction.

It is noteworthy that in the total synthesis of erythromycin A, Woodward et al. employed a D-proline promoted intramolecular aldol condensation to construct **1.76** from aldehyde **1.75** (Scheme 1-17).^[113]



Scheme 1–17: Organocatalysis in the total synthesis of erythromycin A.

Finally, some less noticed but nonetheless important discoveries by Yamaguchi et al. and Taguchi et al. broke the silence of the organocatalysis field in the early 1990s. They independently reported enantioselective Michael additions using L-proline derivatives. Yamaguchi et al. employed the rubidium salt of proline to realize an asymmetric Michael addition to enones (Scheme 1–18a).^[114] Taguchi et al. discovered L-proline derived chiral ammonium hydroxides could also catalyze the enantioselective Michael addition (Scheme 1–18b).^[115]



Scheme 1–18: Pioneering organocatalytic Michael additions.

At the end of the 20th century and the beginning of the 21st century, the golden era of organocatalysis arrived. In the beginning, most of the investigations were focused on the organo-Lewis base catalysts.

In the late 1990s, Shi et al.,^[116] Denmark et al.^[117] and Yang et al.^[118] showed that the enantioselective epoxidation of simple alkenes could be achieved by a catalytic process with enantiomerically pure ketones (**1.77**–**1.79**). Hydrogen-bonding catalysts **CTU-1** and **1.80** were demonstrated to be efficient in an asymmetric Strecker reaction by Jacobsen et al.^[119] and Corey et al.^[120] Miller et al. mimicked enzyme-substrate interaction and introduced tripeptide **1.81** for

the enantioselective kinetic resolution of alcohols (Figure 1–8).^[121]

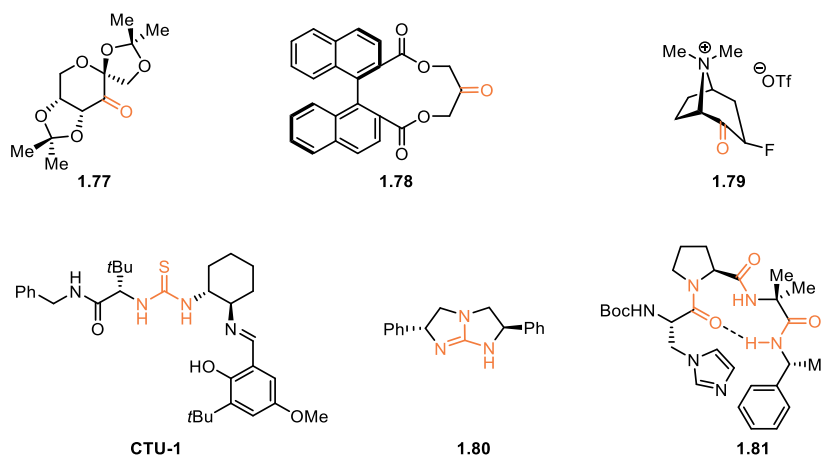
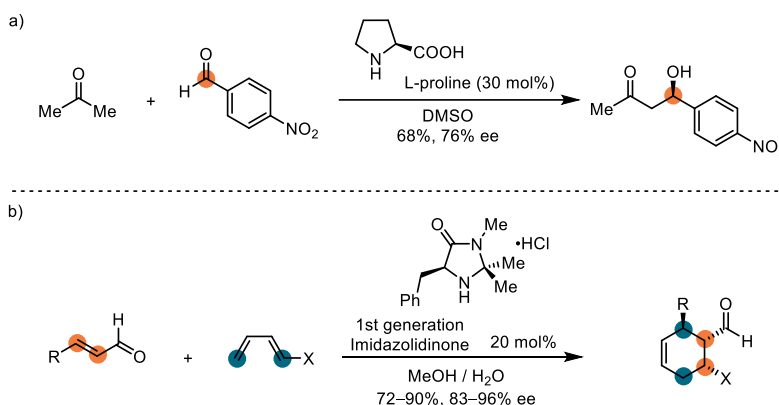


Figure 1–8: Organo-Lewis base catalysts.

The year 2000 is considered as the first year of the era of organocatalysis, as the systematic and extensive research started to bloom. Additionally, two landmark publications announced the concept of organocatalysis in 2000. One is from List et al. which illustrated the L-proline as an enamine catalysis for the direct asymmetric aldol reactions (Scheme 1–19a).^[122] The other from MacMillan et al. reported an organocatalyzed Diels–Alder reaction via iminium catalysis and conceptualized as “organocatalysis” (Scheme 1–19b).^[123]



Scheme 1–19: Landmark works of organocatalysis.

The field of organocatalysis grew very fast in the first decade of the 21st century. A variety of catalysts were developed.^[124] Many secondary amines were designed to achieve various asymmetric reactions by using prolines and imidazolidinones as templates (Figure 1–9a).^[125] The cinchona alkaloid was regarded as a privileged scaffold and frequently employed as organocatalyst. By introducing a primary amine moiety at C9 position, the multifunctional cinchona-based primary aminocatalysts were obtained, which have been utilized in the

activation of hindered carbonyl compounds (Figure 1–9b).^[126] The C9 alkoxy cinchona alkaloids could act as a tertiary amine catalyst to generate reactive ammonium enolates (Figure 1–9c).^[127] The chiral quaternary ammonium salts also exhibited the value in organocatalysis (Figure 1–9d).^[128] The bridge nitrogen alkylated cinchona motifs and *N*-spiro binary scaffold have catalyzed diverse asymmetric transformations. Inspired by the vitamin B₁ in nature, the chiral *N*-heterocyclic carbene as bivalent carbon based motif was also applied to organocatalysis (Figure 1–9e).^[129]

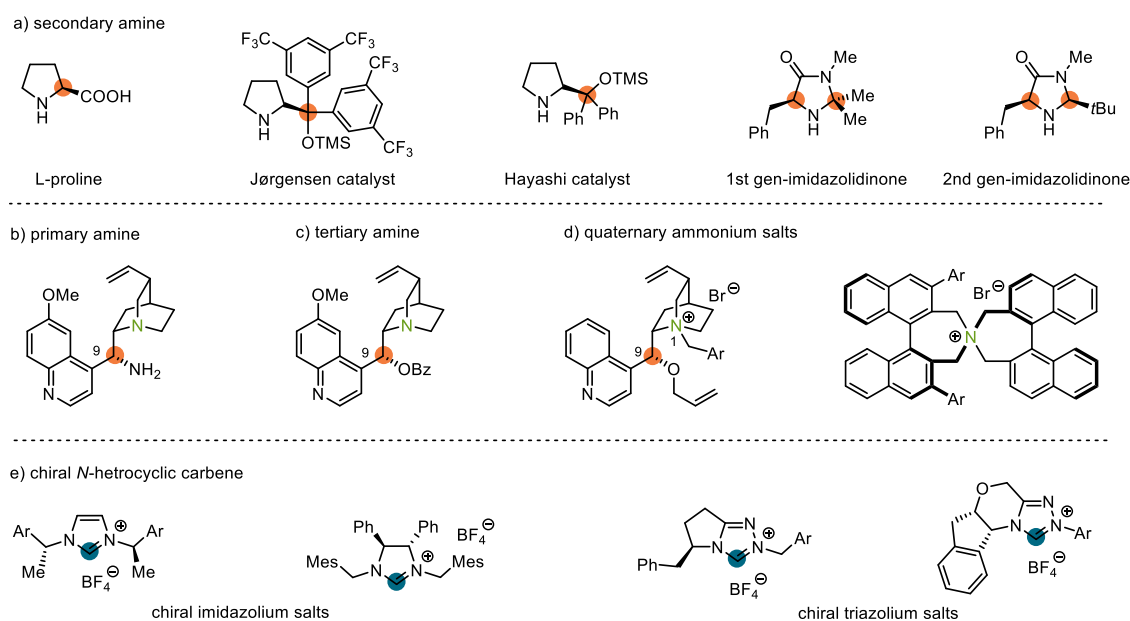


Figure 1–9: Representative organo-Lewis base catalysts.

Meanwhile, the chiral Brønsted acid catalysts were well-developed as another important branch of organocatalysis. Since Akiyama et al.^[130] and Terada et al.^[131] independently reported the pioneering utilization of the BINOL-derived chiral phosphoric acids to catalyze C–C bond formation reactions, a wide range of phosphoric acids with other chiral backbones were developed, such as *H*₈-BINOL, VAPOL, TADDOL, SPINOL. In addition, investigations also focused on the core of the chiral Brønsted acid, such as chiral phosphoric acids (CPA),^[132] chiral dicarboxylic acid (DCA),^[133] phosphorodiamidic acid (PDA),^[134] *N*-triflylphosphoramidate (NTPA),^[135] *N,N'*-bistriflylphosphoramidimidate (NBPI),^[136] *N,N'*-bistriflylphosphoramidimidate (NBPI),^[136] bis(sulfuryl)imide (JINGLE),^[137] disulfonimide (DSI),^[138] binaphthyl-allyl-tetrasulfone (BALT)^[139] as the mono-BINOL unit catalysts. The dual-BINOL units catalysts were developed by List et al., such as imidodiphosphate (IDP),^[140] imino-

imidodiphosphate (iIDP),^[141] imidodiphosphorimidate (IDPi) (Figure 1–10).^[142]

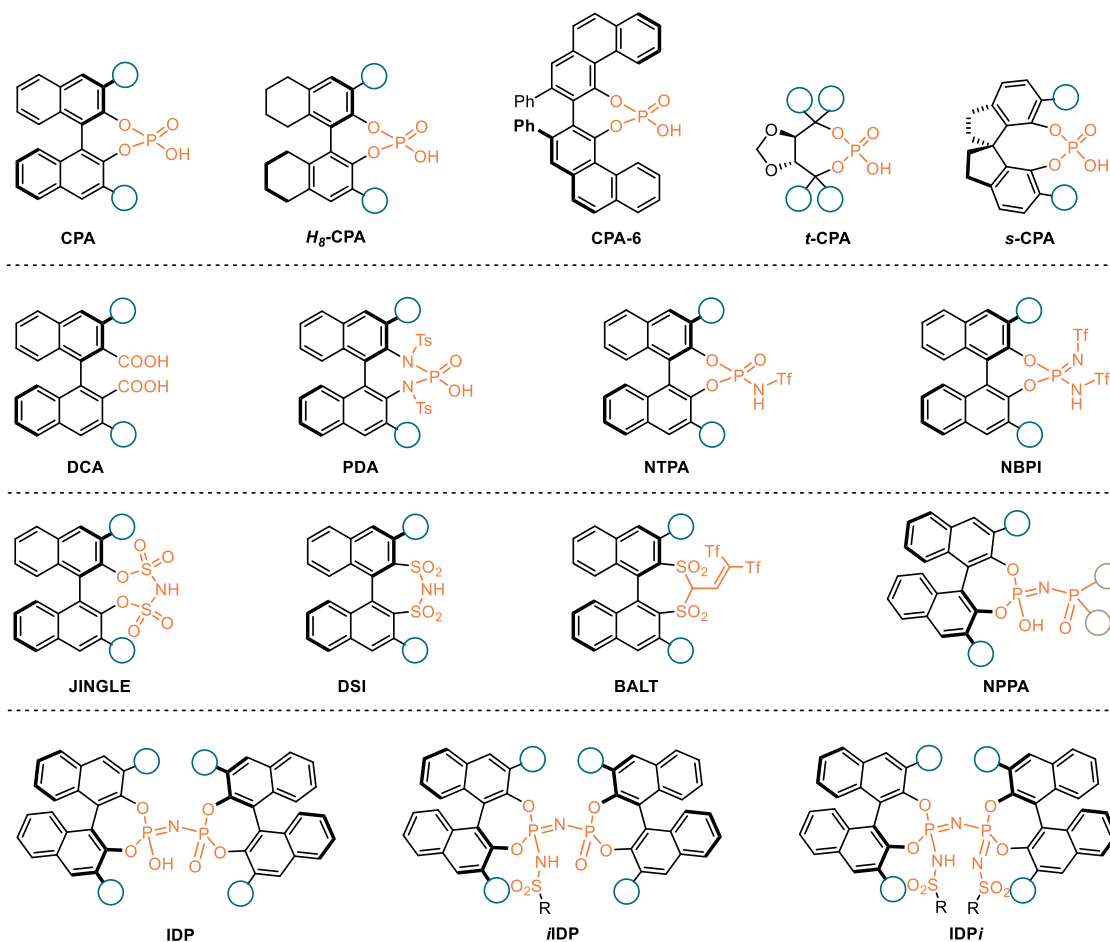
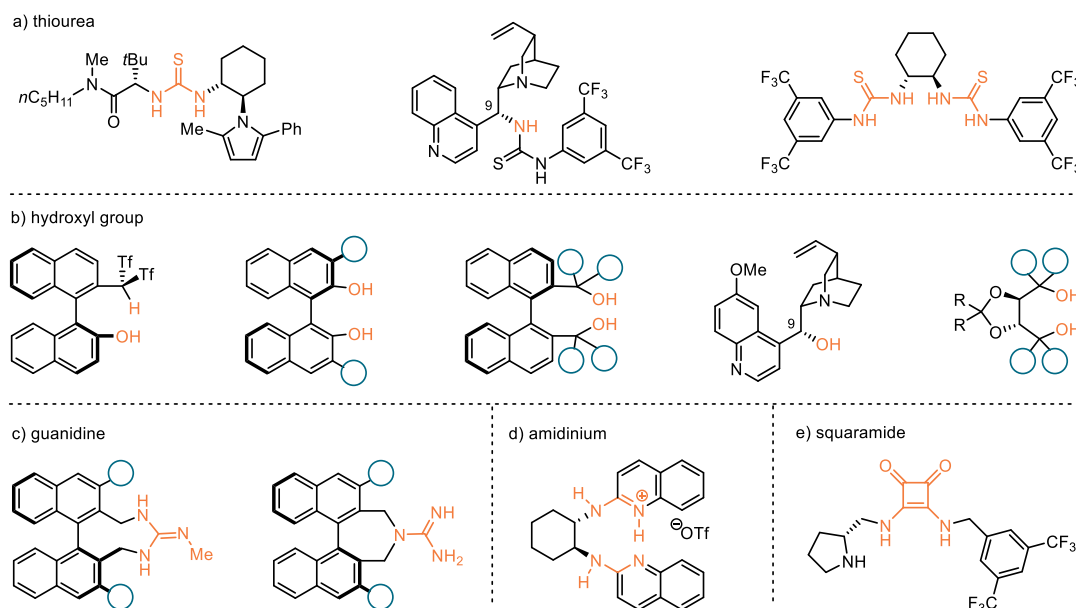
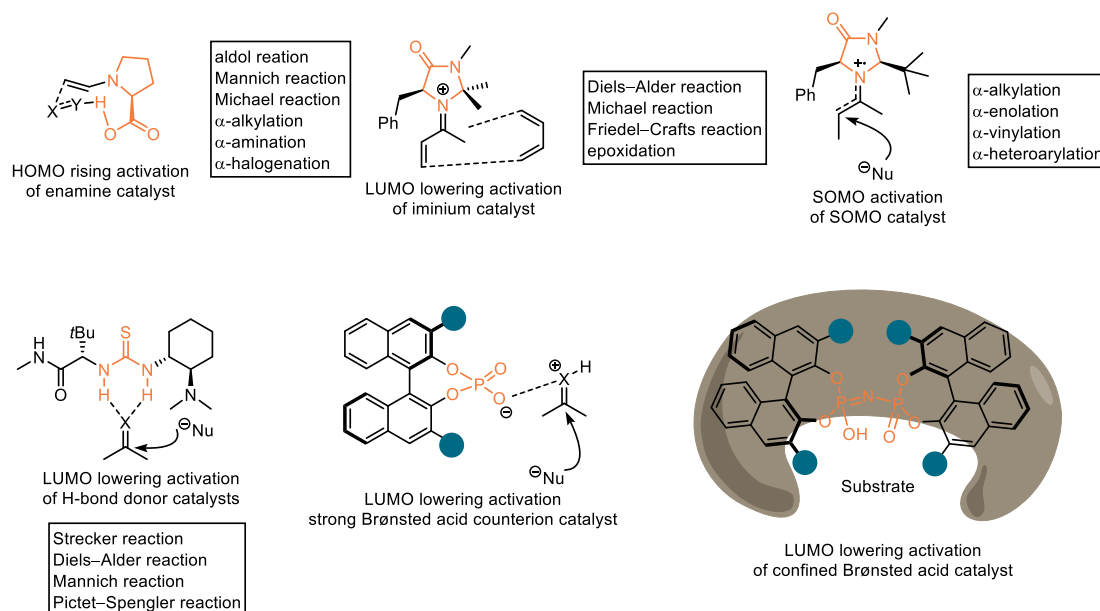


Figure 1–10: Representative scaffolds of chiral Brønsted acids.

Hydrogen bond is a relatively weaker noncovalent bond which can also be utilized in organocatalysis.^[143] Due to the two hydrogen bonds provided by coplanar amino substituents, thiourea is probably the most popular motif of hydrogen bond organocatalysts (Figure 1–11a).^[144] Hydroxyl group is also a good hydrogen bond donor, which can integrate with various chiral backbones to serve as the catalysts for many reactions (Figure 1–11b).^[145] As the conjugated acid of guanidine, guanidinium inherits the well-established electrostatic and hydrogen-bonding abilities, making it widely used in organocatalysis (Figure 1–11c).^[146] Similar as guanidine, amidine is also employed as hydrogen bond organocatalysis (Figure 1–11d).^[147] Due to the rigid planar structure, squaramide exhibits binding properties and catalytic capacities, which appears in some novel hydrogen bond organocatalysts (Figure 1–11e).^[148]


Figure 1–11: Hydrogen bond catalysts.

Besides the structure-based classification of these organocatalysts, the mode of activation is another criterion for categorization. With regards to the molecular orbits, they can be divided into HOMO activation, LUMO activation and SOMO activation.^[124b] The special dual-BINOL-unit catalysts increase the importance of confinement in the activation mode.

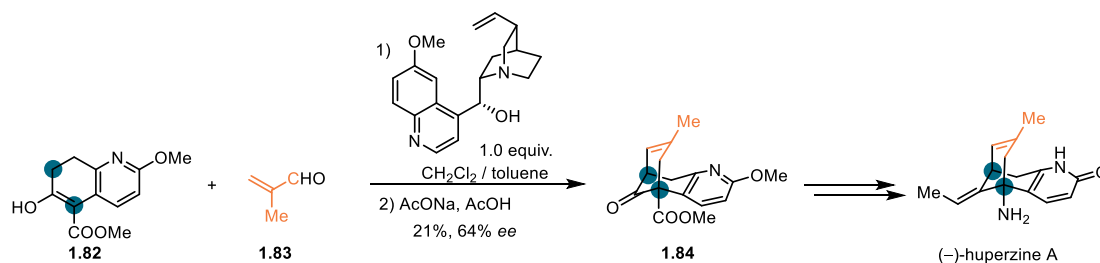

Figure 1–12: The general activation modes of organocatalysts.

1.3.2. Organocatalytic asymmetric total synthesis

In chemistry, chirality is a property of molecule or ion, whereby it cannot be superposed on its

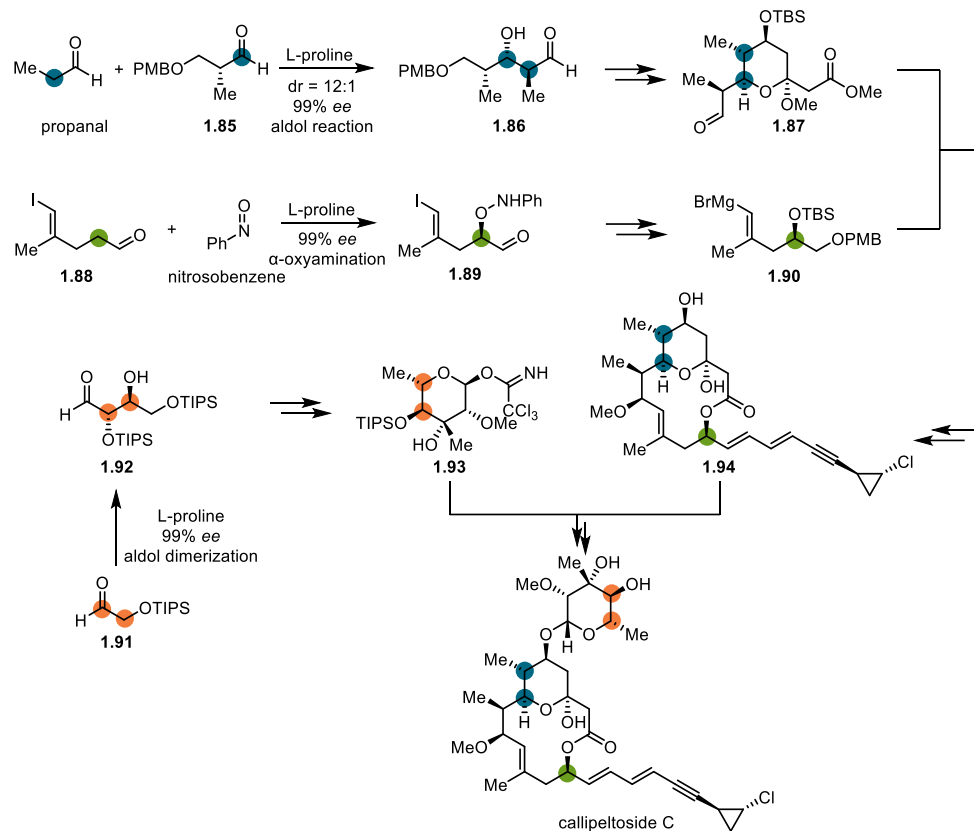
mirror image by any combination of rotations and translations.^[149] The natural products are often chiral and usually enantiomerically pure, as they are constructed by enzyme catalyzed reactions. The building block of enzymes, the amino acids are also chiral. This asymmetric property is crucial for the bioactivity of natural products in many cases. Therefore, realizing the total synthesis of natural products in an asymmetric fashion is significant. However, the chirality of a compound can only be generated in a chiral atmosphere. In the early time of synthesis, chemists used chiral resolution to separate the enantiomers. This method not only wasted half of the material, but also cannot be applied to every natural product, as not every compound had proper resolving agents. In modern times, the asymmetric total synthesis using a chiral catalyst is more practical and reliable. Organocatalysis as an important catalysis type was proven to be a powerful approach to achieve asymmetric total synthesis.

Even in the early stage of organocatalysis, Terashima completed the asymmetric total synthesis of (-)-huperzine A through a cinchona alkaloid promoted Michael–aldol cascade between achiral **1.82** and aldehyde **1.83** constructing enantioenriched tricyclic ester **1.84** (Scheme 1–20).^[150]



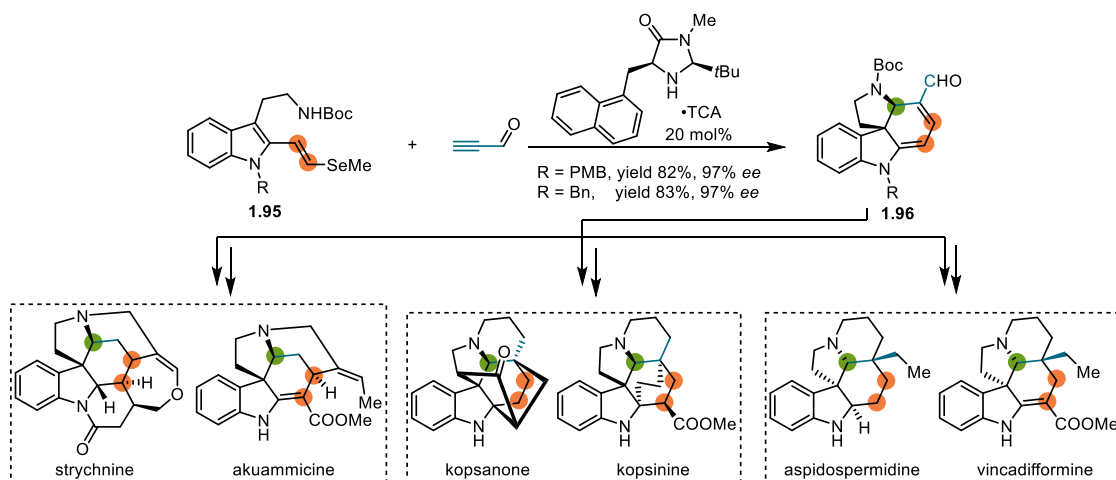
Scheme 1–20: Organocatalytic asymmetric total synthesis of (-)-huperzine A.

In the total synthesis and structure revision of callipeltoside C, MacMillan et al. demonstrated the power of organocatalysis. The L-proline catalyzed enantioselective aldol reaction between propanal and aldehyde **1.85** afforded **1.86** with 99% *ee*. The enantioselective α -oxyamination reaction of aldehyde **1.88** with nitrosobenzene yielded **1.89** with 99% *ee* catalyzed by L-proline. Aldehyde **1.92** was obtained with 99% *ee* through the L-proline catalyzed enantioselective aldol dimerization of aldehyde **1.91**.^[151] Through further transformations, the intermediates **1.87** and **1.90** led to **1.94**, which reacted with **1.93** affording callipeltoside C (Scheme 1–21).



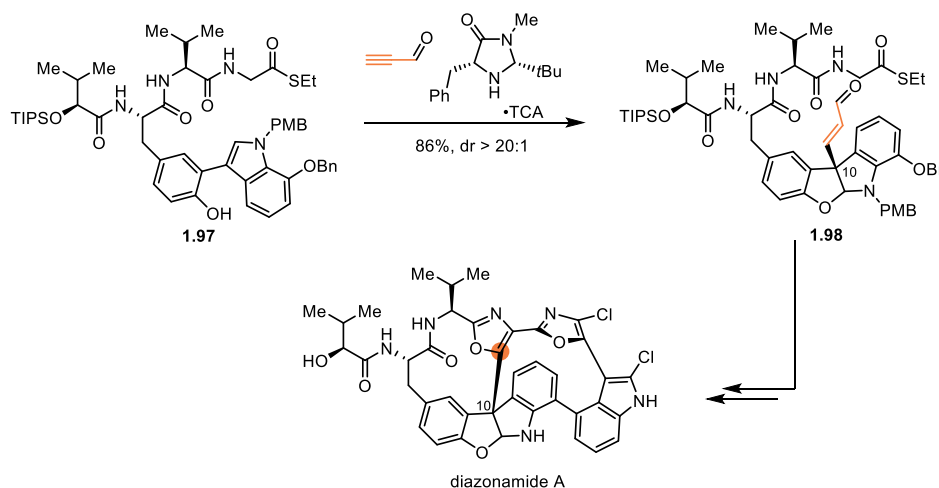
Scheme 1–21: Total synthesis of callipeltoside C by L-proline.

Enzyme-catalyzed cascade reactions play a crucial role in nature to construct the complex structures of natural products. By mimicking nature's strategies using organocatalysis, MacMillan et al. reported the landmark total synthesis of six complex alkaloids, akuammicine, strychnine, kopsanone, kopsinine, aspidospermidine and vincadifformine via an asymmetric Diels–Alder reaction–elimination–conjugate addition cascade catalyzed by imidazolidinone, transforming tryptamine derivative **1.95** to tetracyclic aldehyde **1.96** (Scheme 1–22).^[152]



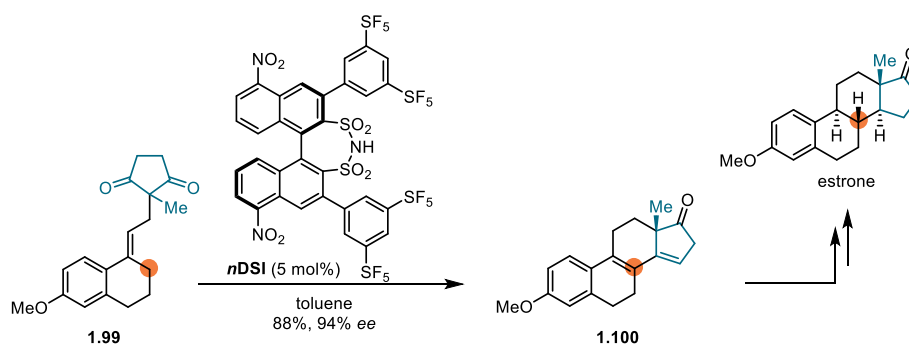
Scheme 1–22: Unified total synthesis of indole alkaloids.

Besides these total syntheses which usually utilized the organocatalysis in the early stage synthesis, MacMillan et al. demonstrated that organocatalysis could also be applied to an advanced complex system, by realizing the alkylation–cyclization cascade between the complex intermediate **1.97** and propynal (Scheme 1–23). This asymmetric transformation yielded **1.98** and achieved the installation of the challenging C10 stereocenter of diazonamide A with high enantioselectivity.^[153]



Scheme 1–23: Organocatalyst in the total synthesis of diazonamide A.

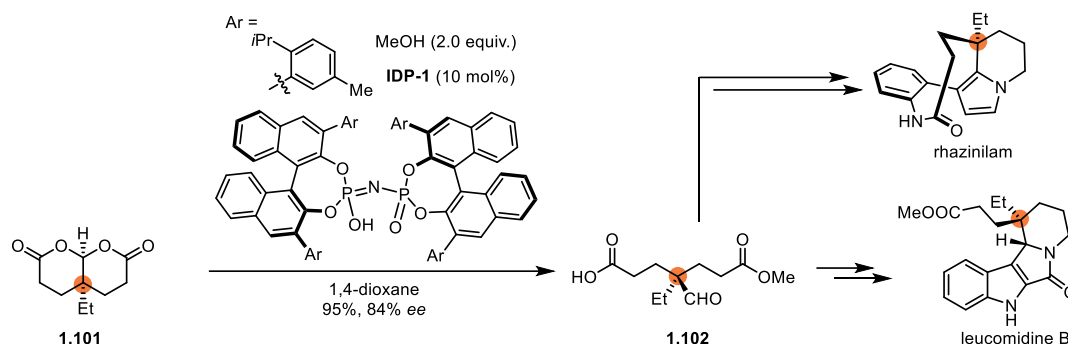
Chiral Brønsted acids also exhibited potential in asymmetric total synthesis. In the total synthesis of estrone, List et al. realized a chiral dinitro-disulfonimide (*dn*DSI) catalyzed enantioselective Torgov cyclization^[154] of **1.99** leading to the tetracyclic intermediate **1.100** with 94% *ee* (Scheme 1–24).^[155]



Scheme 1–24: DSI catalyzed asymmetric total synthesis of estrone.

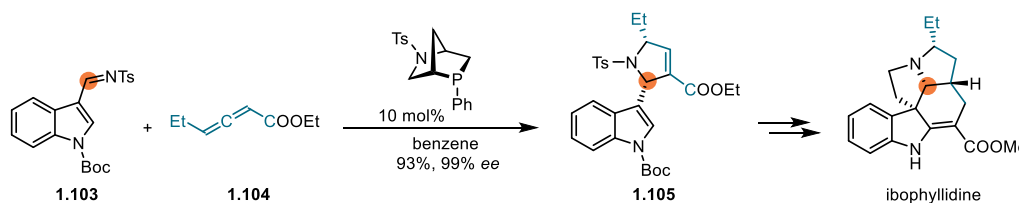
Another remarkable application of chiral Brønsted acid catalysis is the asymmetric total synthesis of (–)-rhazinilam and (–)-leucomidine B by Zhu et al. The enantioenriched intermediate **1.102** was provided by the dimeric imidodiphosphoric acid **IDP-1** catalyzed

desymmetrization of bicyclic bislactone **1.101** with 84% *ee* (Scheme 1–25).^[156]



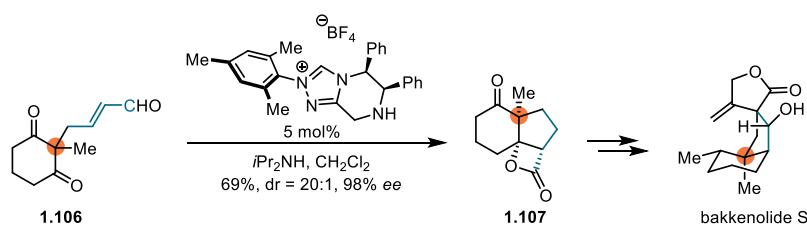
Scheme 1–25: Chiral imidodiphosphoric acid in total synthesis.

In 2012, Kwon et al. reported the first enantioselective total synthesis of (+)-ibophyllidine using a chiral phosphine catalyzed asymmetric [3 + 2] annulation between **1.103** and **1.104**, yielding all-*syn* pyrrolidine **1.105** with 99% *ee* (Scheme 1–26).^[157]



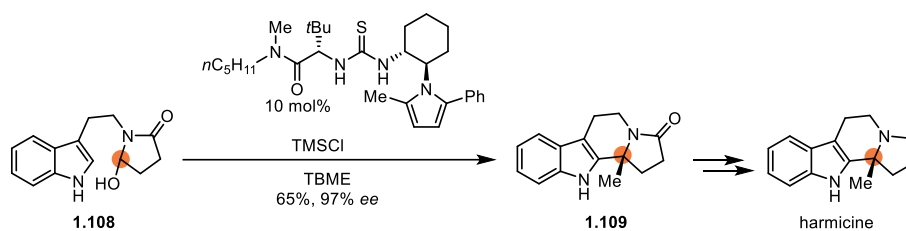
Scheme 1–26: Chiral organophosphine in the total synthesis of (+)-ibophyllidine.

Scheidt et al. utilized an asymmetric desymmetrization in the total synthesis of bakkenolide S. Lactone **1.107** was afforded with 98% *ee* from 1,3-diketones **1.106**, through a homoenolate protonation–intramolecular aldol addition–acylation tandem in the presence of chiral NHC catalyst (Scheme 1–27).^[158]



Scheme 1–27: NHC catalyst in the total synthesis of bakkenolide S.

Chiral thiourea as hydrogen bond catalyst also plays an important role in natural product total synthesis. In 2007, Jacobsen et al. developed a thiourea-catalyzed asymmetric Pictet–Spengler-type cyclization. This methodology was applied to the cyclization of **1.108**, yielding lactam **1.109** with 97% *ee*. The enantioselective synthesis of (+)-harmicine was completed by the reduction of lactam **1.109** (Scheme 1–28).^[159]



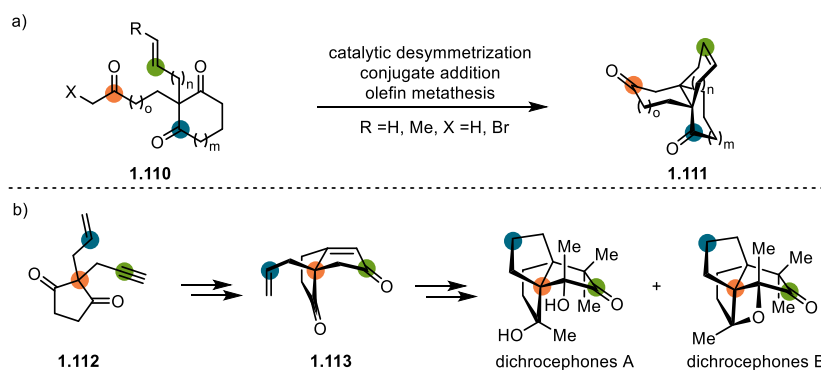
Scheme 1–28: Hydrogen bond catalysis in total synthesis.

Organocatalytic reactions generally involve mild and metal-free conditions with convenient procedure and are amenable to the construction of complex and diverse molecules in enantioselective manner. These virtues bestow them a crucial role in the total synthesis of natural products. With the various recently developed organocatalysts in hand, numerous efficient total syntheses can be envisaged. Meanwhile, exploration and application of new chiral scaffolds and activation modes are the developing directions of organocatalysis.

1.4. Natural product and synthetic methodology development

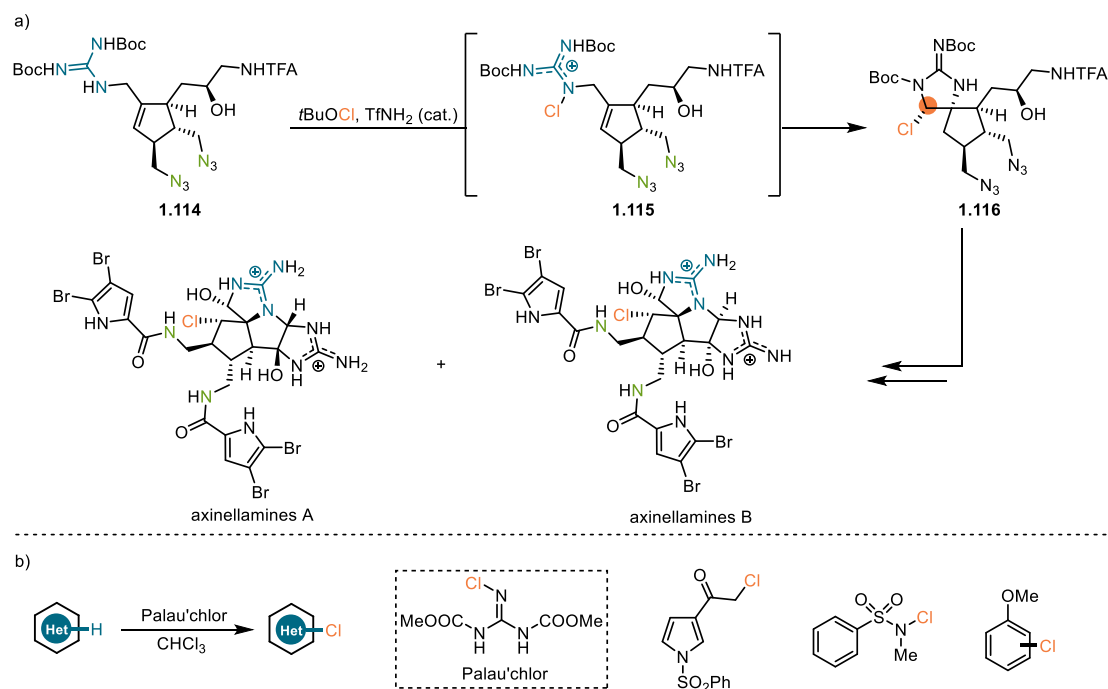
Natural product total synthesis and methodology development are not only two of the most important pillars in organic synthesis, but also promote each other. That means natural product total synthesis provides a complex platform to test new methodologies, while new methodologies can inspire natural product total synthesis with efficient strategies.

In 2017, Christmann et al. developed a modular synthesis of functionalized carbocyclic propellanes **1.111** from diketone **1.110**, providing a flexible strategy to a variety of polycyclic scaffolds (Scheme 1–29a).^[160] In 2018, Christmann et al. utilized this methodology in the total synthesis of dichrocephone A and B, by preparing [3.3.3]propellane **1.113** from diketone **1.112** (Scheme 1–29b).^[161]



Scheme 1–29: Modular synthesis of propellanes and their application in total synthesis.

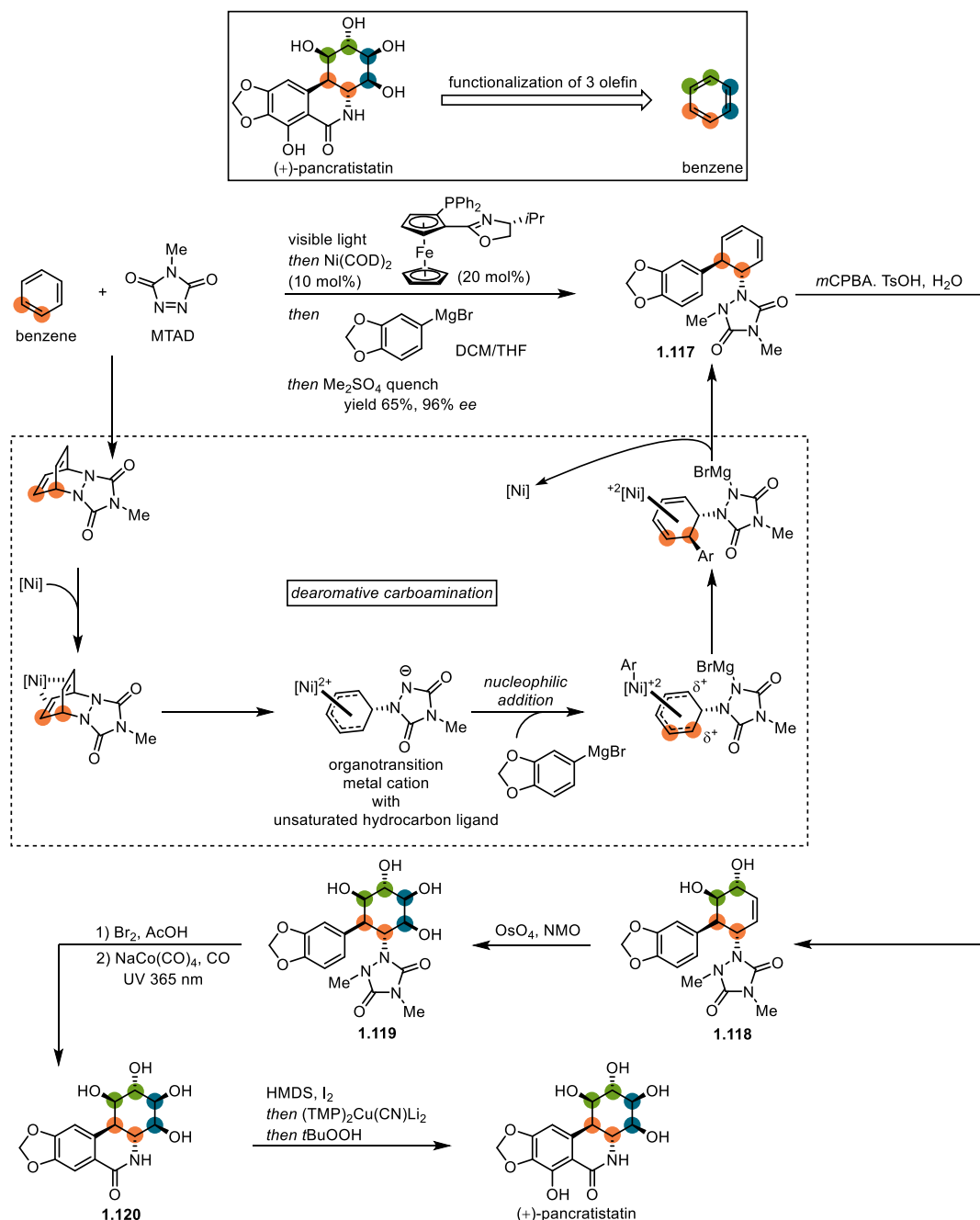
Total synthesis also promoted new reagent development. In the total synthesis of axinellamine A and B, Baran et al. discovered an intramolecular chlorospirocyclization of guanidine **1.114** affording **1.116**. *N*-chloroguanidine intermediate **1.115** was considered as the functioning chlorinating agent (Scheme 1–30a).^[162] This finding inspired further exploration of similar reagents for chlorination. A novel chlorinating reagent named Palau'chlor was invented, which exhibited excellent reactivity for various substrates (Scheme 1–30b).^[163]



Scheme 1–30: Total synthesis of axinellamines and development of Palau'chlor.

In fact, methodology development and natural product total synthesis are synergistic with each other, promoting the development of organic synthesis together. In the total synthesis of (+)-pancratistatin, Sarlah et al. designed a straightforward strategy via triple functionalization of benzene (Scheme 1–31).^[164] It is a creative and efficient strategy to employ the benzene as starting material, providing a platform to evaluate the existing methodology and discover new synthetic methodology. Although a methodology for dearomative dihydroxylation of arene was developed,^[165] it was still challenging to introduce the aryl group to realize the dearomative carboamination. By incorporating the nucleophilic addition to unsaturated hydrocarbon ligand of transition metal cations^[166] with the visible light-promoted *para*-cycloaddition, Sarlah et al. realized a dearomative *trans*-carboamination of benzene with high enantioselectivity. This carboamination installed the first two vicinal stereocenters, efficiently furnishing **1.117** with

96% *ee* in 65% yield. With diene **1.117** in hand, *trans*-diol **1.118** was prepared through a chemo- and diastereoselective epoxidation and subsequent epoxide hydrolysis. Under Upjohn dihydroxylation condition,^[167] alkene **1.118** was converted to tetraol **1.119**, completing the trifold olefin functionalization sequence. (+)-Pancratistatin was obtained by further transformation of **1.120**.



Scheme 1-31: Total synthesis of (+)-pancratistatin through dearomatization.

1.5. Brief summary

This chapter has given a brief overview of natural product total synthesis, and the related research areas, including drug discovery, asymmetric synthesis by organocatalysis and methodology development. In the early stage of natural product total synthesis, research focused on the construction of the carbon-based structure. Diverse synthetic methodologies were blooming in this time to realize efficient total synthesis. With the development of biology, the bioactivity information of natural product exhibited its importance in drug discovery. Many novel strategies were evolved to design and synthesize natural product analogues. Chirality is a crucial consideration of drug discovery.^[168] Therefore, the asymmetric total synthesis of natural product and its analogues is a lucrative goal. As one of the most important catalysis types, organocatalysis plays an essential role in asymmetric synthesis. Different activation modes include a variety of organocatalysts, which have applied frequently in natural product total synthesis. Additionally, natural product total synthesis and methodology development incorporates each other to promote organic synthesis. Therefore, as the flagship of organic synthesis, the study of natural product total synthesis can integrate the related areas to stimulate the progress of organic synthesis.

2. Total Synthesis of Racemic Peganumine A and Its Analogues

2.1. Introduction

2.1.1. β -Carboline alkaloids

β -Carboline alkaloids are an important group of natural products sharing a common tricyclic pyrido[3,4-*b*]indole ring motif. They are widely distributed in nature. Their numerous biological activities are attractive, such as intercalation with DNA, inhibition of cyclin-dependent kinases (CDK), topoisomerases, and monoamine oxidases (MAO), as well as interaction with benzodiazepine receptors and serotonin receptors.^[169]

Moreover, many β -carboline alkaloids are directly used as drugs, for example reserpine is an antipsychotic and antihypertensive drug for the regulation of high blood pressure and relief of psychotic symptoms for decades; ajmalicine is used for the treatment of high blood pressure; its analogue, yohimbine is used in veterinary medicine; vincamine is a peripheral vasodilator (Figure 2–1). Besides these well-known drugs, some β -carboline alkaloids are under preclinical investigation, such as lavendamycin (anti-proliferative activity).^[170] Additionally, synthetic analogues of β -carboline alkaloids also exhibit their potential in drug discovery. ET-736 is a natural product isolated from the ascidian species *Ecteinascidia turbinata*.^[171] Its synthetic analogue lurbinedin was approved by FDA for the treatment of metastatic small cell lung cancer in 2020. Vinpocetine is derived from vincamine as a treatment of cerebrovascular disorders.^[172]

As a privileged scaffold, β -carboline core is frequently applied in drug discovery. Tadalafil is a medication used to treat erectile dysfunction containing a β -carboline motif. Cipargamin was discovered as an antimalarial drug candidate.^[173] Abecarnil was proven to be a partial agonist acting selectively at the benzodiazepine site of the GABA_A receptor,^[174] which might overcome the tolerance problem of the nonselective benzodiazepine agonist.^[175] Eudistomin C is able to inhibit the process of protein translation by binding to the subunits of ribosomes.^[176] In addition, by hybridizing β -carboline scaffold with salicylic acid, **2.1** displayed potent anti-proliferative activity.^[177] Therefore, it is worthy to investigate not only the total synthesis of β -carboline alkaloids, but also utilizing the efficient synthetic route to discover potent natural product analogues.

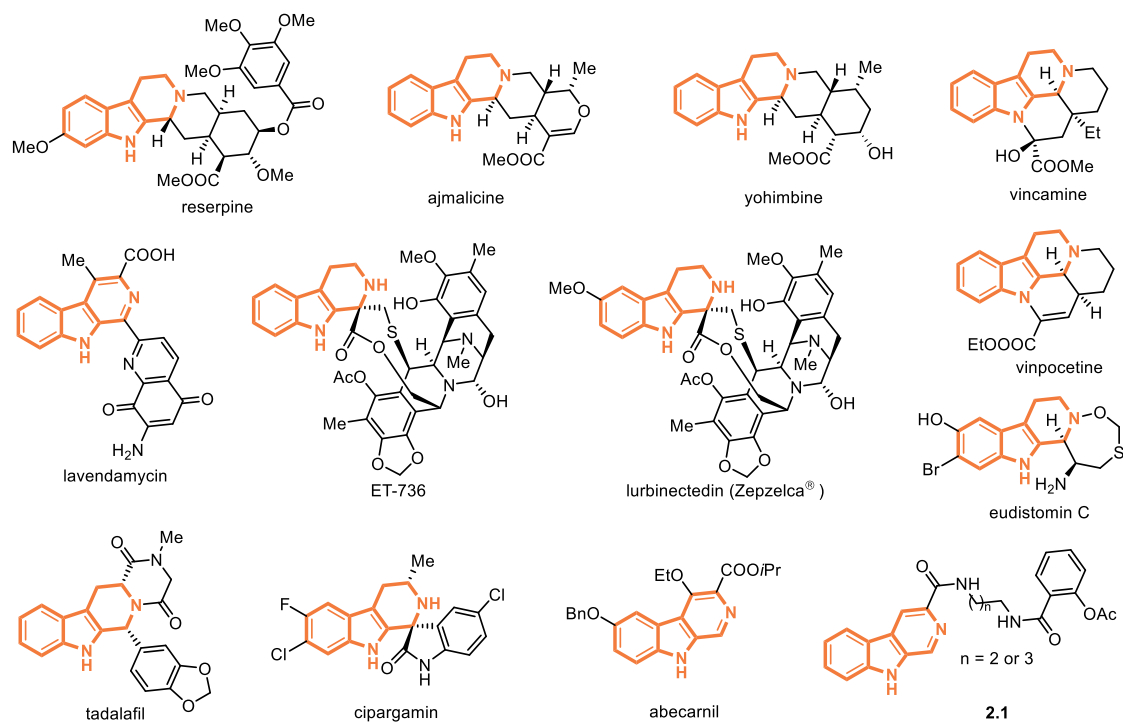


Figure 2-1: β -Carboline alkaloids.

β -Carboline alkaloids can be divided into three subtypes. The fully aromatic members are named β -carbolines (β Cs), whereas the members with partially saturated C-rings are known as 3,4-dihydro- β -carbolines (DH β Cs) and 1,2,3,4-tetrahydro- β -carbolines (TH β Cs) (Figure 2-2).

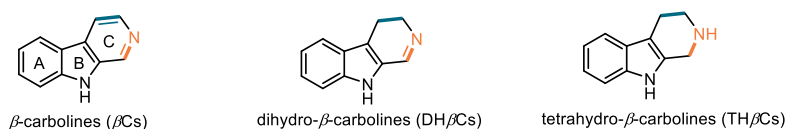
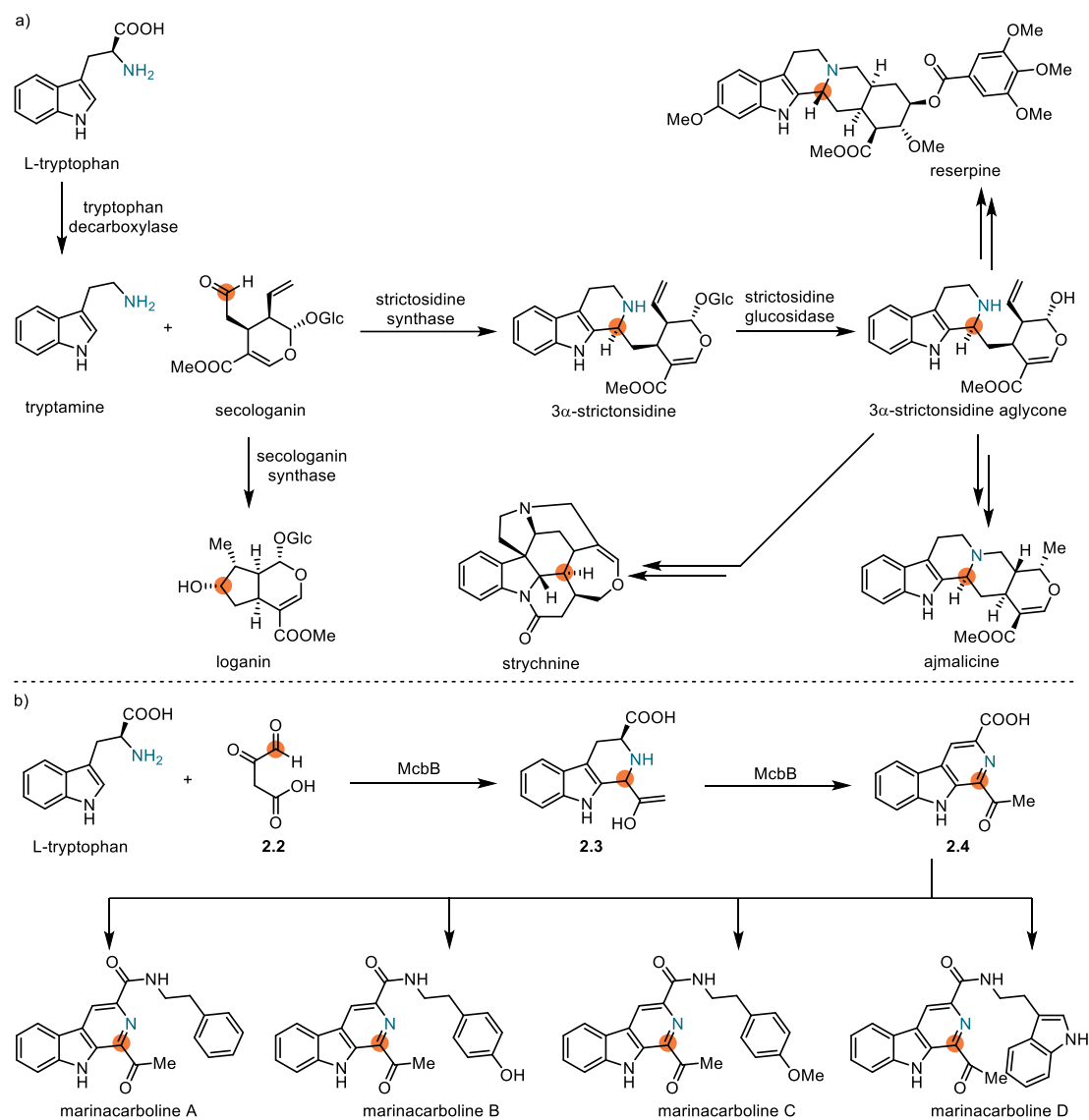


Figure 2-2: Three types of β -carboline alkaloids.

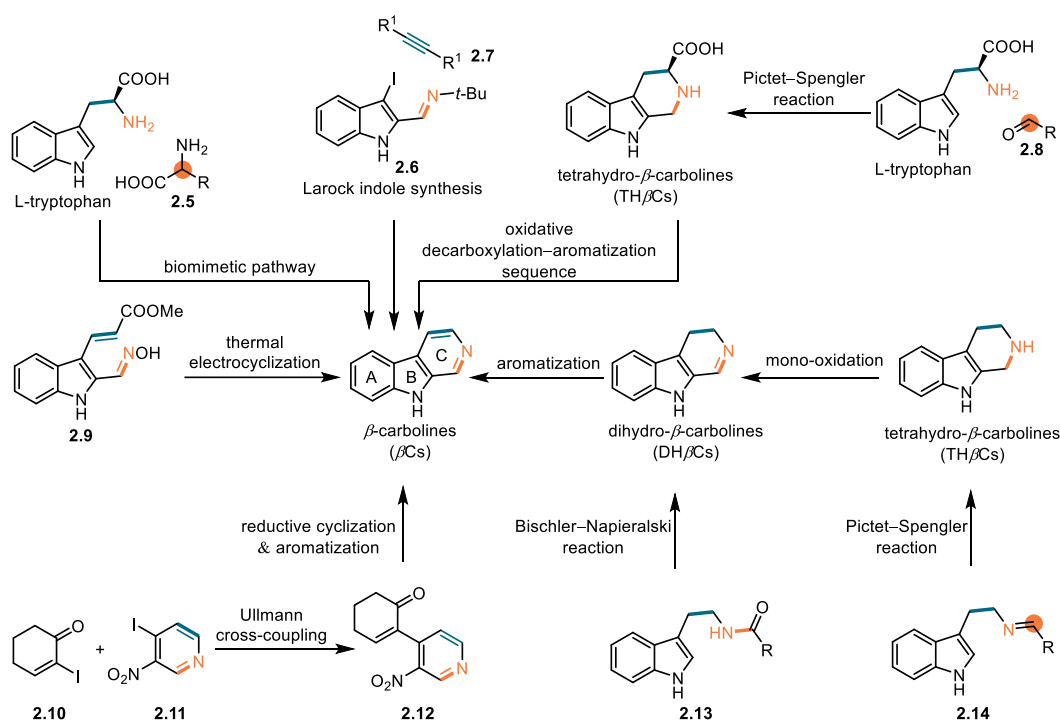
Some evidence indicates that the β -carboline scaffolds are synthesized from L-tryptophan by an enzymatic tandem process. Waldmann et al. considered that 3 α -strictosidine aglycone is the central linchpin of diverse monoterpene indole alkaloids,^[178] according to the results of isotope-labeled feeding experiments.^[179] The TH β C core of strictosidine is synthesized by the strictosidine synthase catalyzed Pictet–Spengler reaction between tryptamine and secologanin (Scheme 2–1a).^[180] After hydrolysis of 3 α -strictosidine, the 3 α -strictosidine aglycone is afforded, which can convert to various alkaloids. Recent research discovered that McbB is able to catalyze biosynthesis of DH β C **2.3** from L-tryptophan and aldehyde **2.2** via a Pictet–Spengler reaction–decarboxylation sequence. Through an oxidation reaction, **2.3** can be converted to β C **2.4**, which is the key intermediate to synthesize marinacarboline A–D (Scheme 2–1b).^[181]



Scheme 2–1: Biosynthesis of β -carboline scaffolds.

The artificial synthetic approaches of β -carboline motifs are more diverse, compared to the biosynthetic pathways. The classic ways to construct β Cs rely on a condensation, cyclization and oxidation–aromatization sequence. The condensation provides amides **2.13** for Bischler–Napieralski reactions^[182] or imines **2.14** for Pictet–Spengler reactions (Scheme 2–2).^[183] After these reactions the amides **2.13** can be transformed to DH β Cs, and the imines **2.14** are able to be converted to TH β Cs. From DH β Cs, preparation of β Cs can be achieved by aromatization. From TH β Cs, β Cs can be obtained either through a stepwise mono-oxidation^[184] and aromatization procedure or a direct oxidative decarboxylation–aromatization sequence.^[185] Meanwhile, some novel methods were developed to construct β C scaffolds. Larock indole synthesis was utilized in the preparation of β Cs by cross couplings between *tert*-butylimines

2.6 and acetylenes **2.7**.^[186] Banwell et al. utilized iodide **2.10** and enone **2.11** to synthesize β C scaffolds, through a Ullmann cross-coupling–reductive cyclization–aromatization sequence.^[187] Thermal electrocyclicization of oxime **2.9** was also used to the synthesis of β C backbones.^[188] Recently, Wu et al. established a biomimetic straightforward synthesis of β C motifs starting from L-tryptophan and amino acid **2.5**.^[189]



Scheme 2–2: Chemosynthesis of β -carboline scaffolds.

2.1.2. Peganumine A

2.1.2.1. Background

Besides the famous β -carboline alkaloids mentioned above (Figure 2–1), dimeric β -carboline alkaloids are a special class.^[190] In most cases, the dimerization patterns can be classified as a direct link (such as (–)-accedinisine),^[191] chain link (such as (+)-macralstonine)^[192] or ring-fused link (such as (+)-macralstonidine) (Figure 2–3).^[193] The synthesis of the first two classes mostly relies on the C–C bond formation with a linker to integrate two β -carboline motifs in the late-stage of the synthesis.^[194] For the synthesis of the polycyclic fused link, the fundamental idea is relatively similar as the direct link and chain link, which is based on the pre-construction of the two β -carboline motifs and late-stage connection.^[195] All these links can be regarded as

a “loose” link, which means the link did not make the connection between two β -carboline motifs constrained. This “loose” property makes the total synthesis of such dimeric β -carboline alkaloids unified, relying on a strategy to construct two fragments separately and integrated them later.

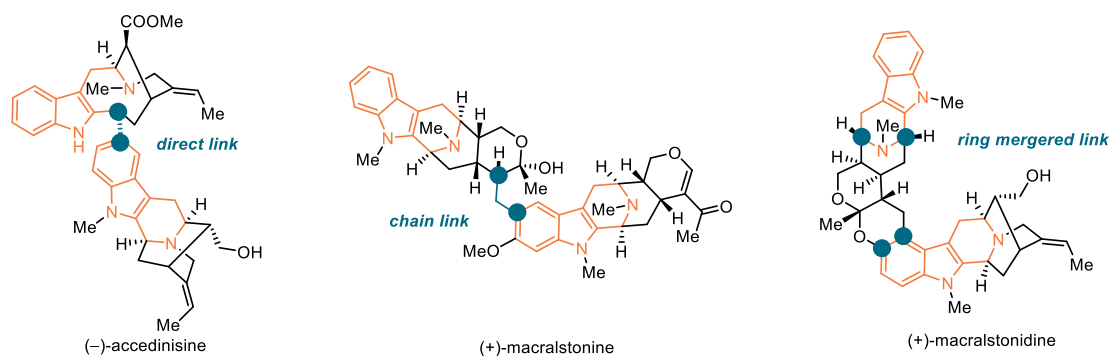


Figure 2-3: Dimeric β -carboline alkaloids.

Hua et al. isolated a novel tetrahydro- β -carboline alkaloid from the seeds of *Peganum harmala* in 2014, namely peganumine A (Figure 2-4).^[196] The unique 5,5-dimethyl-2,7-diazabicyclo[2.2.1]heptan-3-one ring system makes the dimeric β -carboline cores not only link with a bridged ring system, but also merged into the same ring system. In addition, it exhibits selective cytotoxic effects on HL-60 cell line (human leukemia) with an IC_{50} of 5.8 μ M and moderate cytotoxic activity against MCF-7 (human adenocarcinoma), PC-3 (prostate cancer), and Hep G2 (human liver cancer) cell lines. Unfortunately, the low isolation yield (3.5 mg peganumine A out of 15.4 kg seeds of *Peganum harmala*) not only limits the further research towards this unique alkaloid, but also demands total synthesis to prepare peganumine A and its analogues in greater quantities for further scientific analysis and potential future application.

5,5-dimethyl-2,7-diazabicyclo[2.2.1]heptan-3-one

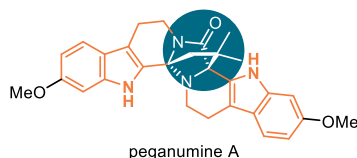


Figure 2-4: Structure of peganumine A.

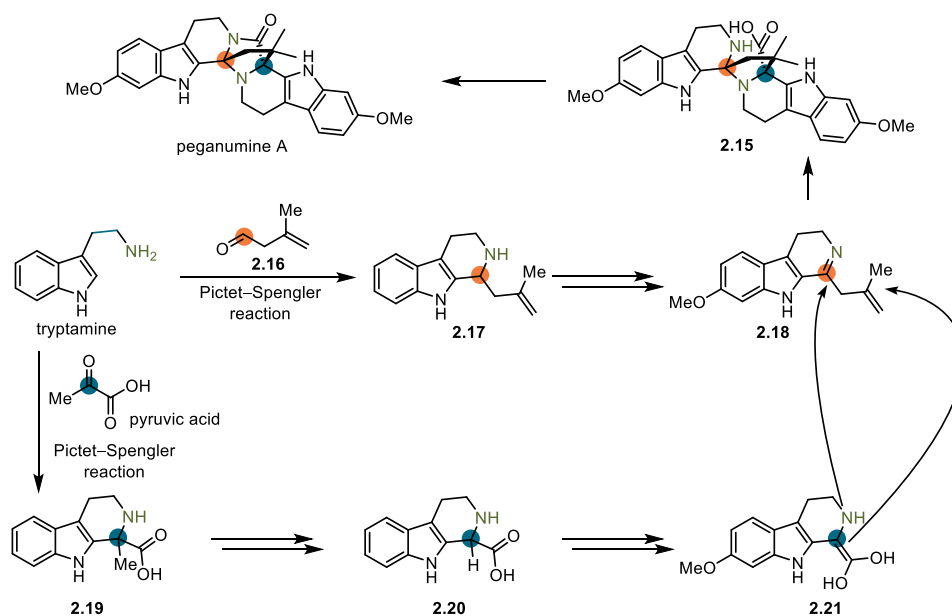
2.1.2.2. Structure determination

Since the structure of peganumine A is unique and there are no previous reports in literature for the 5,5-dimethyl-2,7-diazabicyclo[2.2.1]heptan-3-one scaffold, the determination of both

planar structure and absolute configuration is important before the total synthesis. According to the research by Hua et al., the molecular formula of $C_{29}H_{30}N_4O_3$ with 17 degrees of unsaturation was determined by HR-ESI-MS. The functional groups, such as amide carbonyl group, two methoxy groups and two methyl groups, were elucidated by the 1H NMR and ^{13}C NMR. With the assistance of 2D NMR, two β -carboline motifs were assigned. The relative configuration was unveiled by NOESY spectrum. Meanwhile, the planar structure was unambiguously confirmed by a single crystal X-ray diffraction study. With the assistance of CD exciton chirality method^[197] and additional comparison between the experimental and calculated ECD spectra, the absolute configuration of peganumine A was also established (*S,S*).

2.1.2.3. Proposed biosynthesis hypothesis

Hua et al. postulated a biosynthetic pathway of peganumine A (Scheme 2–3). This hypothesis is based on the classic dimeric β -carboline alkaloid synthesis route, which relies on constructing the two β -carboline motifs first and integrating them together later. Tryptamine could undergo Pictet–Spengler reactions with aldehyde **2.16** and pyruvic acid to afford two β -carboline motifs **2.17** and **2.19** respectively. With further transformations, β -carboline **2.18** and **2.21** are obtained, which can be coupled by a Claisen-type reaction, yielding dimeric β -carboline **2.15**. Through the lactamization of **2.15**, peganumine A could be synthesized.

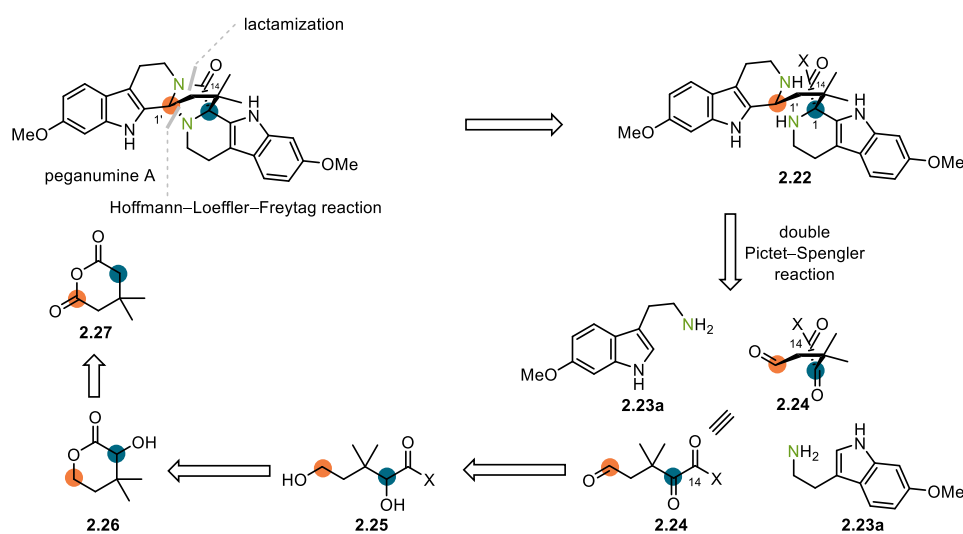


Scheme 2–3: Biosynthetic hypothesis of peganumine A.

2.2. 1st generation synthetic approach towards peganumine A

2.2.1. 1st generation retrosynthetic analysis

As the unique 5,5-dimethyl-2,7-diazabicyclo[2.2.1]heptan-3-one motif of peganumine A is merged into the dimeric β -carboline cores, it is efficient to incorporate the two β -carboline cores with the bridged linker simultaneously. Based on this fundamental consideration, the first disconnection was at C1' aminal and lactam motifs. The formation of the C–N bond of the aminal could be realized by a Hofmann–Loeffler–Freitag reaction (Scheme 2–4).^[198] The amide bond of **2.22** could be constructed through a carbonyl activation group promoted lactamization. Then peganumine A was simplified to the dimeric β -carboline **2.22** connected by a linear 7C linker. The two β -carboline cores of **2.22** could be constructed via a double Pictet–Spengler reaction of 7C-motif **2.24** with two-fold 6-methoxytryptamines. The highly oxidized 7C-motif **2.24** could be obtained from anhydride **2.27** via a redox–ring opening sequence.

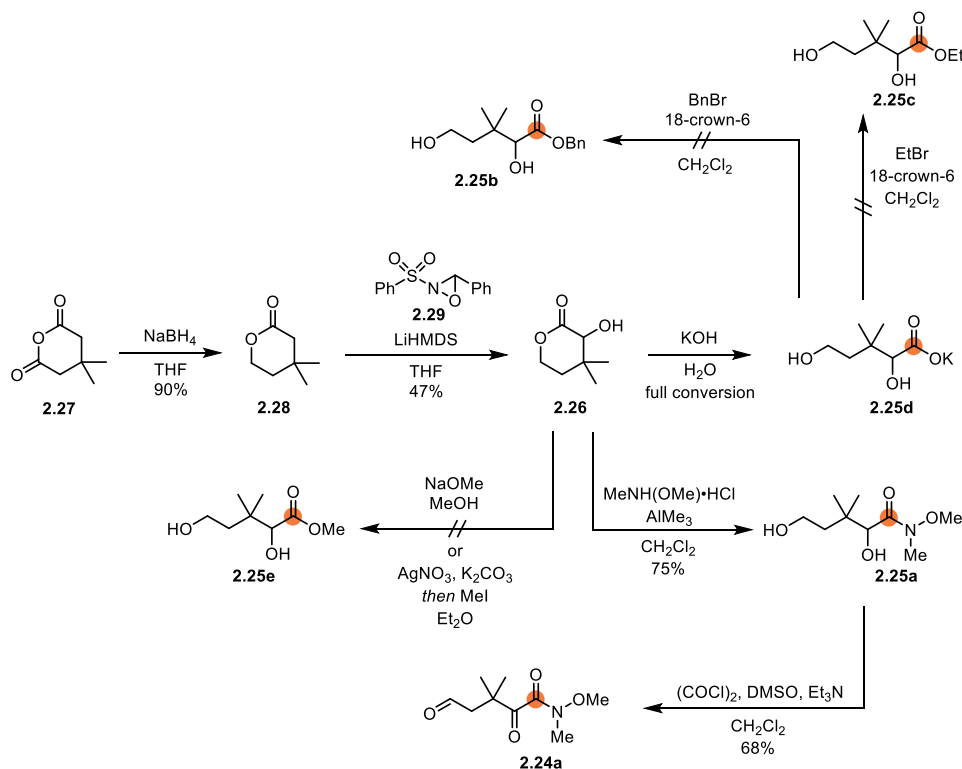


Scheme 2–4: 1st generation retrosynthetic analysis.

2.2.2. Synthesis of the 7C motif

The 1st generation total synthesis attempt was started with the preparation of the 7C motif. Since there were various activation groups for the terminal C14-carbonyl group, such as carboxylate acid, ester and amide, a flexible strategy to prepare these replacements was envisioned. A

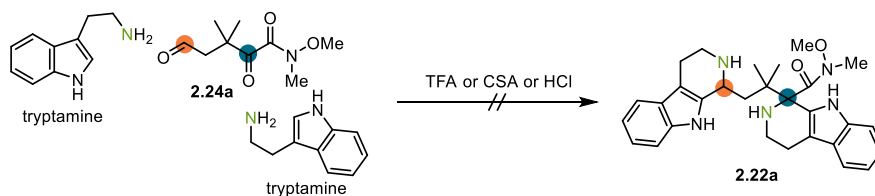
nucleophilic lactone opening strategy was proposed. Lactone **2.28** was prepared through the reduction of anhydride **2.27** in 90% yield (Scheme 2–5).^[199] After a hydroxylation by Davis oxaziridine **2.29**,^[200] the precursor of the nucleophilic lactone opening, α -hydroxylactone **2.26**, was obtained in 47% yield. The hydrolysis of the α -hydroxylactone **2.26**, using H₂O as nucleophile, was proceeded with full conversion, but the resulting potassium carboxylate salt **2.25d** was difficult to be isolated and purified.^[201] To overcome such problem, the in situ esterification was screened with EtBr and BnBr, but the corresponding esters **2.25b** and **2.25c** were not observed. Then the in situ MeI trapping approach^[202] was applied. There was still no formation of ester **2.25e**. It was hypothesized that these results could be attributed to the regeneration of the α -hydroxylactone **2.26** which was promoted by the Thorpe–Ingold effect^[203] of the *gem*-dimethyl group of those linear intermediates (**2.25b–e**). Based on this explanation, the formation of a more stable amide could be a solution. Therefore, by utilizing an aminolysis of the α -hydroxylactone **2.26**,^[204] Weinreb amide derivative **2.25a** was obtained, which was converted to amide **2.24a** by a Swern oxidation.^[205]



Scheme 2–5: Preparation of 7C motif.

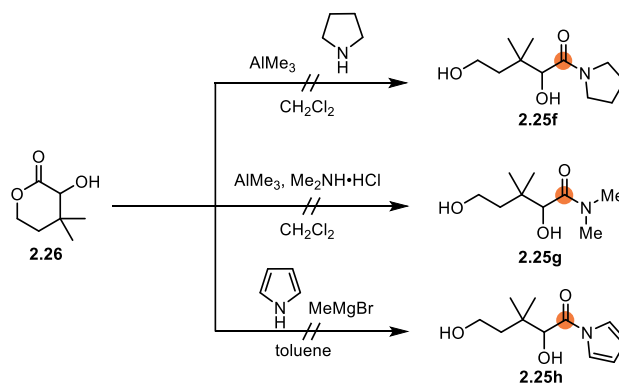
2.2.3. Study of the double Pictet–Spengler reaction

With the amide **2.24a** in hand, the investigation of the double Pictet–Spengler reaction was commenced. Due to the cost and availability of 6-methoxytryptamine, the screening was conducted with tryptamine. Although the Pictet–Spengler reaction^[183] is a classic reaction to construct TH β Cs and tetrahydroisoquinolines, there was still no report about the double Pictet–Spengler reaction with two different fragments of the same compound. It is even more challenging to control the enantioselectivity of such double Pictet–Spengler reaction, as the enantioselectivity of Pictet–Spengler reaction is still not fully solved for the unfunctionalized substrates. Thus, the double Pictet–Spengler reaction was initially screened with some racemic Brønsted acids,^[206] all the reactions led to decomposition (Scheme 2–6). It was rationalized that the ketoaldehyde **2.24a** was highly reactive to undergo complex condensation reactions and the Weinreb amide fragment might not be compatible with the reaction condition, leading to hydrolysis or substitution.



Scheme 2–6: Model study of double Pictet–Spengler reaction.

The next idea was to screen other amide 7C units, however the preparation of different alternatives **2.25f–h** was unsuccessful (Scheme 2–7). due to the complexity of the double Pictet–Spengler reaction, it was considered that it is reasonable to explore a mono-Pictet–Spengler reaction thoroughly, before the realization of this challenging strategy.

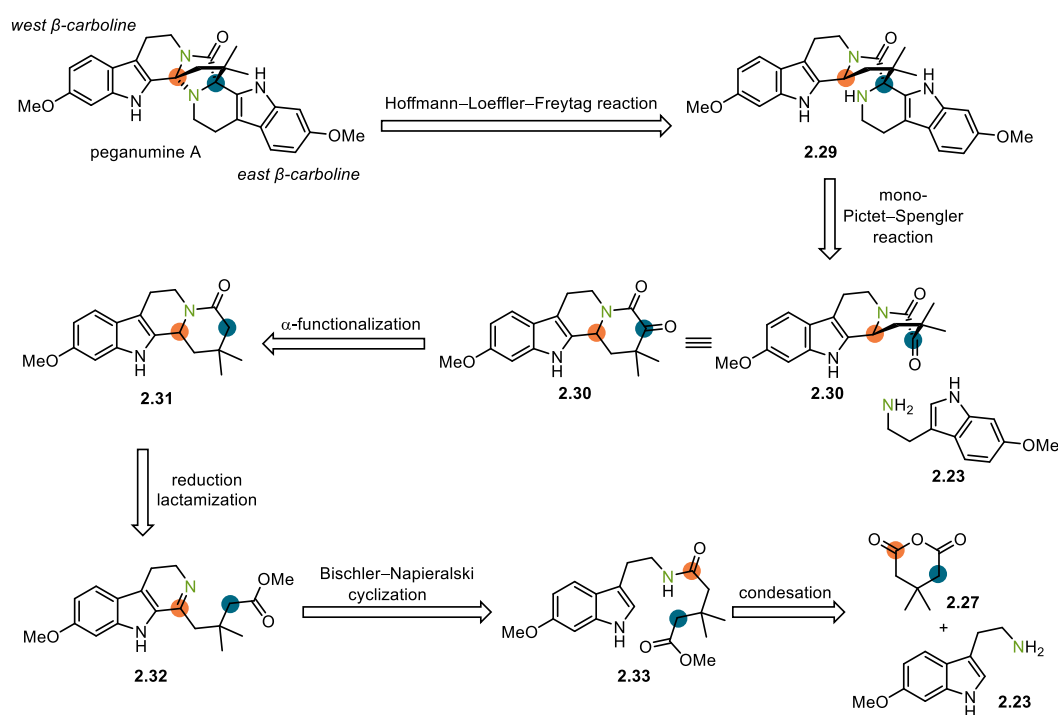


Scheme 2–7: Diverse C₇ units.

2.3. 2nd generation synthetic approach to peganumine A

2.3.1. 2nd generation retrosynthetic analysis

Based on the previous result, the double Pictet–Spengler reaction strategy was simplified to a mono-Pictet–Spengler reaction strategy (Scheme 2–8). Same as the previous retrosynthesis, the central 5,5-dimethyl-2,7-diazabicyclo[2.2.1]heptan-3-one unit was also disconnected by a Hofmann–Loeffler–Freitag reaction at the C1' aminal, tracing back to lactam **2.29**. The east β -carboline motif could be constructed by a mono-Pictet–Spengler reaction and the west β -carboline core was envisioned to install at early stage. The key intermediate, α -ketolactam **2.30**, would be prepared from tetracyclic lactam **2.31** through an oxidation sequence. The west β -carboline core could be synthesized by a Bischler–Napieralski reaction and lactamization sequence of **2.33**, which could be traced back to 6-methoxytryptamine and anhydride **2.27**.

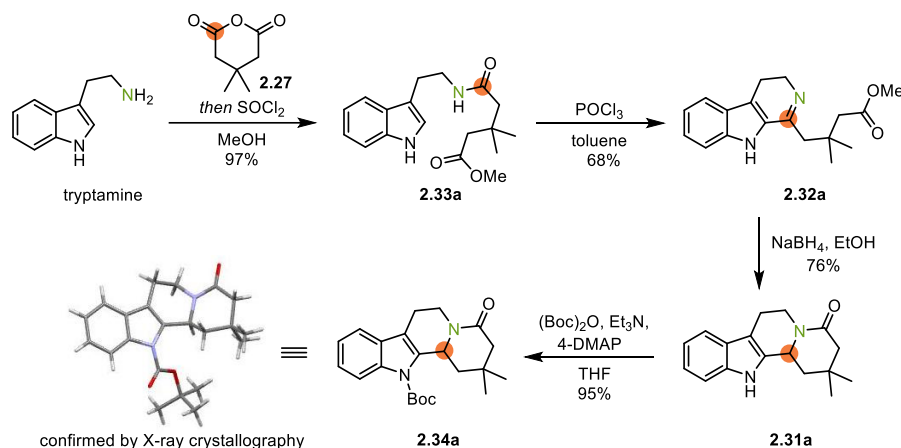


Scheme 2–8: 2nd generation retrosynthetic analysis.

2.3.2. Construction of the west β -carboline core

Due to the very high cost of 6-methoxytryptamine, an initial model study was conducted by using tryptamine, although the methoxy group could make a difference. Methyl ester **2.33a** was

obtained by the condensation between tryptamine and anhydride **2.27** in MeOH and subsequent SOCl_2 promoted esterification in 97% overall yield (Scheme 2–9). A Bischler–Napieralski cyclization furnished β -carboline **2.32a** in 68% yield. The reduction of **2.32a** by NaBH_4 and in situ cyclization afforded the tetracyclic lactam **2.31a** in 76% yield. The Boc protection of the indole nitrogen led to tetracyclic lactam **2.34a** in 95% yield.



Scheme 2–9: Construction of the west β -carboline core.

2.3.3. C–H oxidation to prepare the α -ketolactam

Before assembling the east β -carboline core, the oxidation state of C1 needed to be increased. A stepwise oxidation strategy was utilized to prepare α -ketolactam **2.36a**. The hydroxyl group was installed successfully in 70% yield under the optimized condition (Table 2–1, entry 6).^[50, 207] Subsequently, the α -hydroxyl lactam **2.36a** was converted to α -ketolactam **2.70a** by a Corey–Kim oxidation^[208] in 92% yield.

Table 2–1: C–H oxidation of tetracyclic lactam.

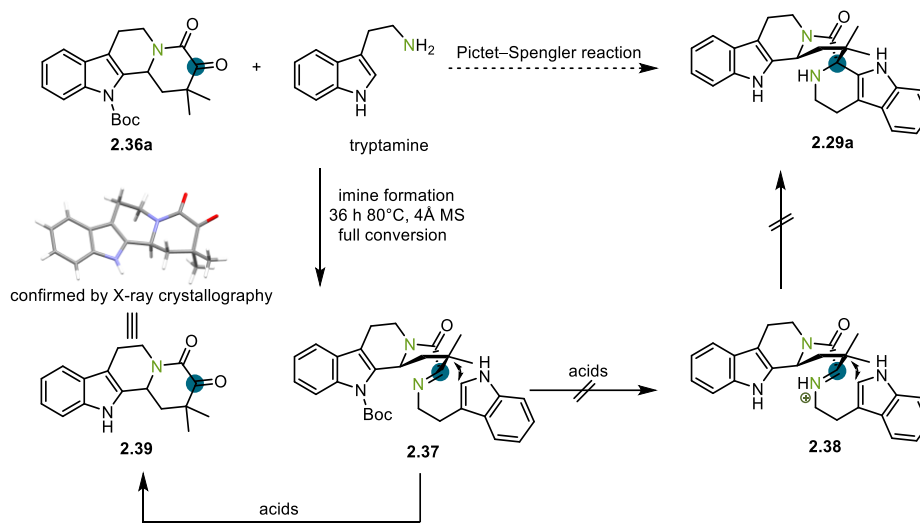
entry ^[a]	conditions	yield ^[b]
1	LDA, oxaziridine	decomposition
2	LDA, <i>m</i> CPBA	low conversion
3	LDA, <i>t</i> BuONO	no desired product
4	LDA, DMDO	no conversion
5	LDA, MeSSO ₂ Me	decomposition
6	LDA, O ₂ , P(OMe) ₃	70%, dr = 1.6:1

[a] Reactions were performed with lactam (15 mg, 41 μmol); [b] isolated yield; [c] dr was determined by ¹H NMR

2.3.4. Mono Pictet–Spengler reaction

With α -ketolactam **2.36a** in hand, the key Pictet–Spengler reaction was investigated (Table 2–2). Numerous Brønsted and Lewis acids failed to promote the mono Pictet–Spengler reaction. Most conditions led to the Boc cleavage compound **2.39**. The formation of imine **2.37** was detected, but the envisaged Friedel–Crafts type reaction did not take place, which was probably inhibited by steric hindrance between the indole ring with the lactam ring.

Table 2–2: Screening for mono Pictet–Spengler reaction.



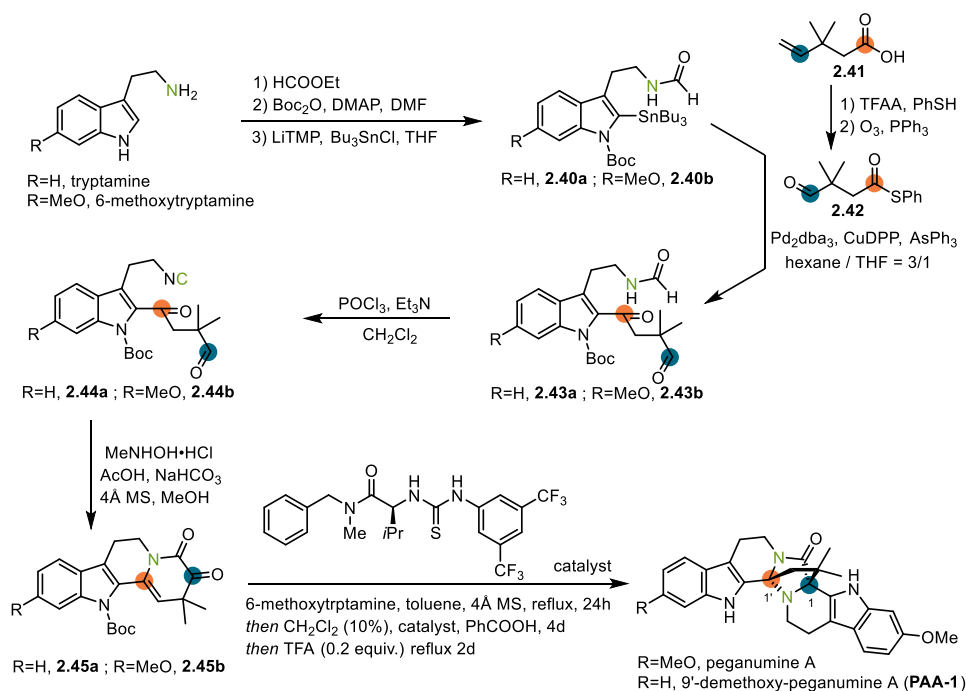
entry ^[a]	acid	solvent	T [°C]	yield
1	TFA (0.2 equiv.) ^[b]	toluene	110	de-Boc
2	TFA (0.2 equiv.)	toluene	110	de-Boc
3	TFA (1.0 equiv.)	toluene	110	de-Boc
4	TFA (5.0 equiv.)	toluene	110	decomposition
5	TfOH	toluene	23 to 110	de-Boc
6	PhCOOH	toluene	23 to 110	N.D. ^[c]
7	CSA	toluene	110	de-Boc
8	BF ₃ •Et ₂ O	CH ₂ Cl ₂	23	de-Boc
9	octadecylphosphonic acid	toluene	23 to 110	de-Boc
10	TMSOTf	CH ₂ Cl ₂	23	recovery of SM
11	bis(trifluoromethanesulfonyl)imide	toluene	23 to 110	de-Boc

[a] Reactions were performed with lactam (7.0 mg, 18 μ mol) and 4Å MS; [b] with NaSO₄; [c] N.D. = not determined

2.3.5. Zhu's total synthesis of peganumine A

At the same time of the mono-Pictet–Spengler reaction screening, Zhu et al. published their total synthesis of peganumine A (Scheme 2–10).^[209] They utilized a chiral thiourea catalyzed Pictet–Spengler reaction between α -ketoamide **2.45b** and 6-methoxytryptamine to install the east β -carboline core of peganumine A. Through a hydroxylamine-mediated intramolecular oxidative coupling of ω -isocyano aldehyde **2.44**, the α -ketoamide **2.45** was readily available.

The aldehyde **2.44** was obtained by the dehydration of *N*-formamide **2.43**. The Liebeskind–Srogl cross coupling^[210] between aldehyde **2.40** and thioate **2.42** delivered the *N*-formamide **2.43**. It is noteworthy that 9'-demethoxy-peganumine A as an analogue of peganumine A was also prepared in their synthesis.

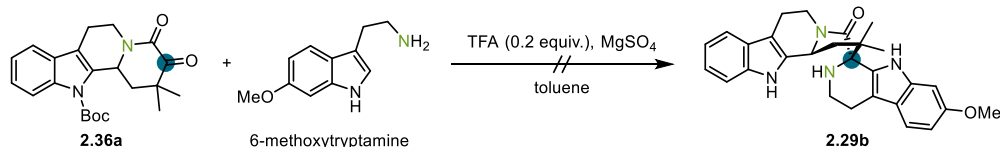


Scheme 2–10: Zhu's total synthesis of peganumine A.

2.3.6. Comparison between the α -ketolactam and the α -ketoenamide

In Zhu's reported results, the Pictet–Spengler reaction was achieved between α -ketoenamide **2.45** and 6-methoxytryptamine. However, in the 2nd generation total synthesis attempt, the α -ketolactam **2.36a** could not undergo the Pictet–Spengler reaction with tryptamine.

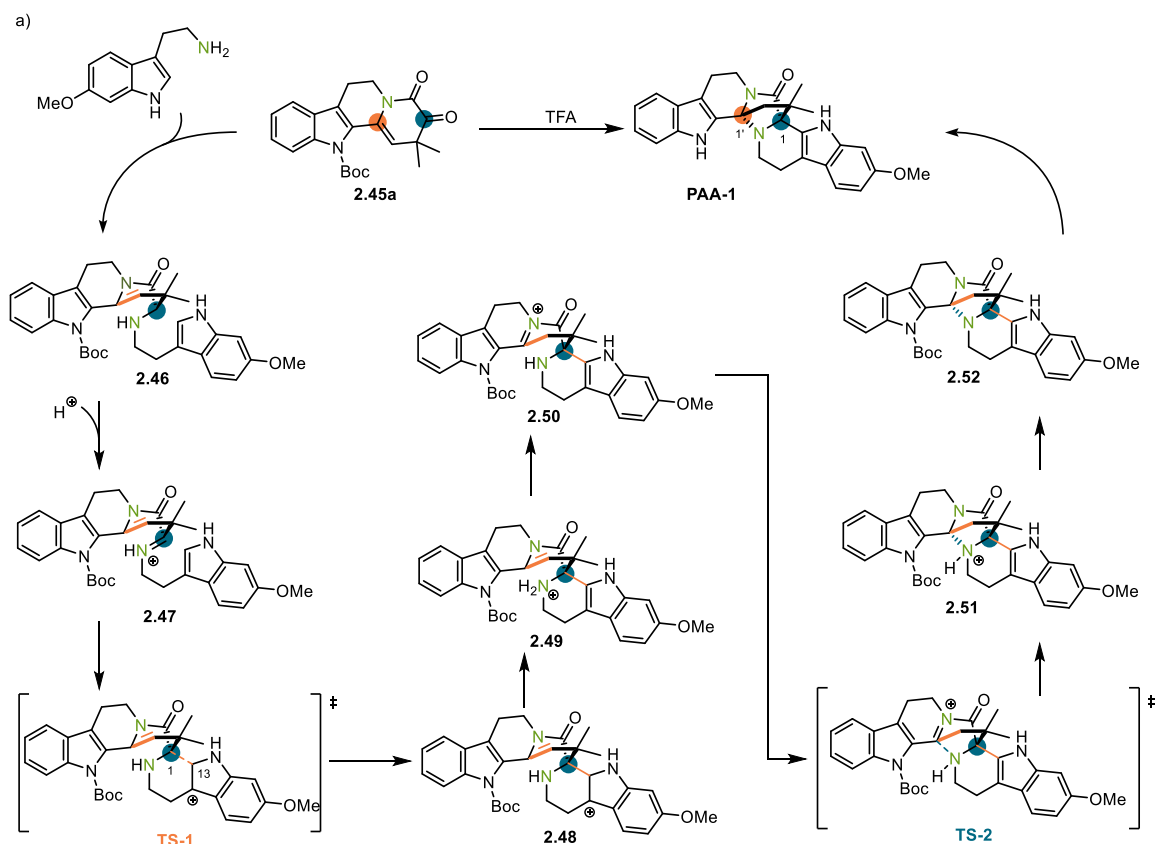
Initially, it was hypothesized that the difference of reactivity between 6-methoxytryptamine and tryptamine could be crucial for the Pictet–Spengler reactions (Scheme 2–11). Therefore, a mono Pictet–Spengler reaction was tested using α -ketolactam **2.36a** and 6-methoxytryptamine. Unfortunately, the desired mono Pictet–Spengler reaction product **2.29b** was still not detected.



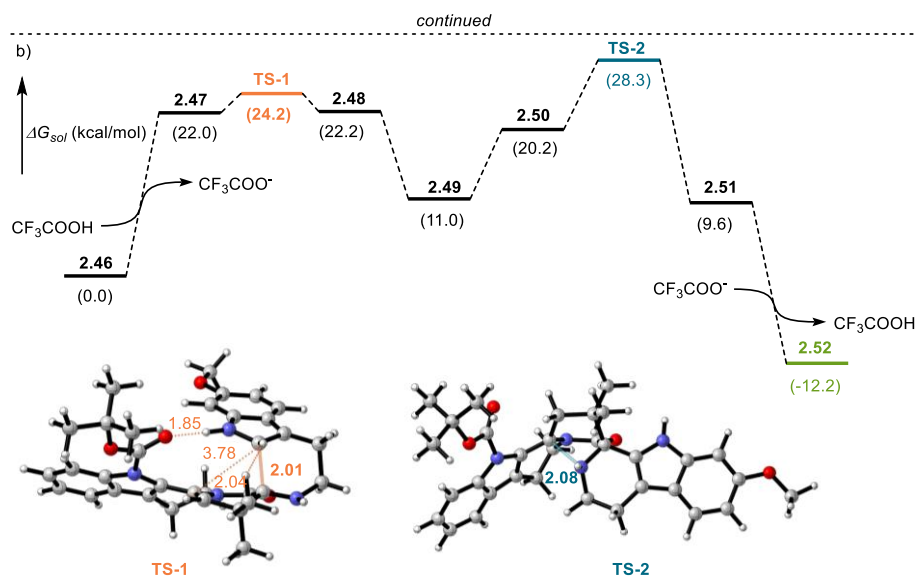
Scheme 2–11: Updated mono Pictet–Spengler reaction.

Excluding the influence of the amine, attention was paid to the difference between the α -ketolactam **2.36a** and the α -ketoenamide **2.45a**. The distinct results were rationalized by the assistance of DFT calculations performed by collaboration with Dr. Yinghan Chen and Professor Dr. Yong Liang at Nanjing University. Geometry optimizations were carried out at the B3LYP-D3/6-31G(d) level in toluene with the SMD model. Then the energy was computed at the more accurate B3LYP-D3/6-311+G(d,p) level in toluene with the SMD model. A quasiharmonic correction was applied during the entropy calculation.

Zhu's successful pathway is thermodynamically favorable ($\Delta G = -12.2$ kcal/mol) (Scheme 2-12b). The generation of iminium ion **2.47** was kinetically accessible ($\Delta G_{TS1}^\ddagger = +24.2$ kcal/mol) under toluene reflux condition from the α -ketoenamide **2.45a** and 6-methoxytryptamine via imine **2.46**. The **TS-1** showed the forming 6-membered ring was a chair conformation and the distance of the forming C–C bond between C1 and C13 is 2.01 Å. Additionally, there was a hydrogen bond interaction between the indole N–H and the Boc group to further stabilize the transition state.

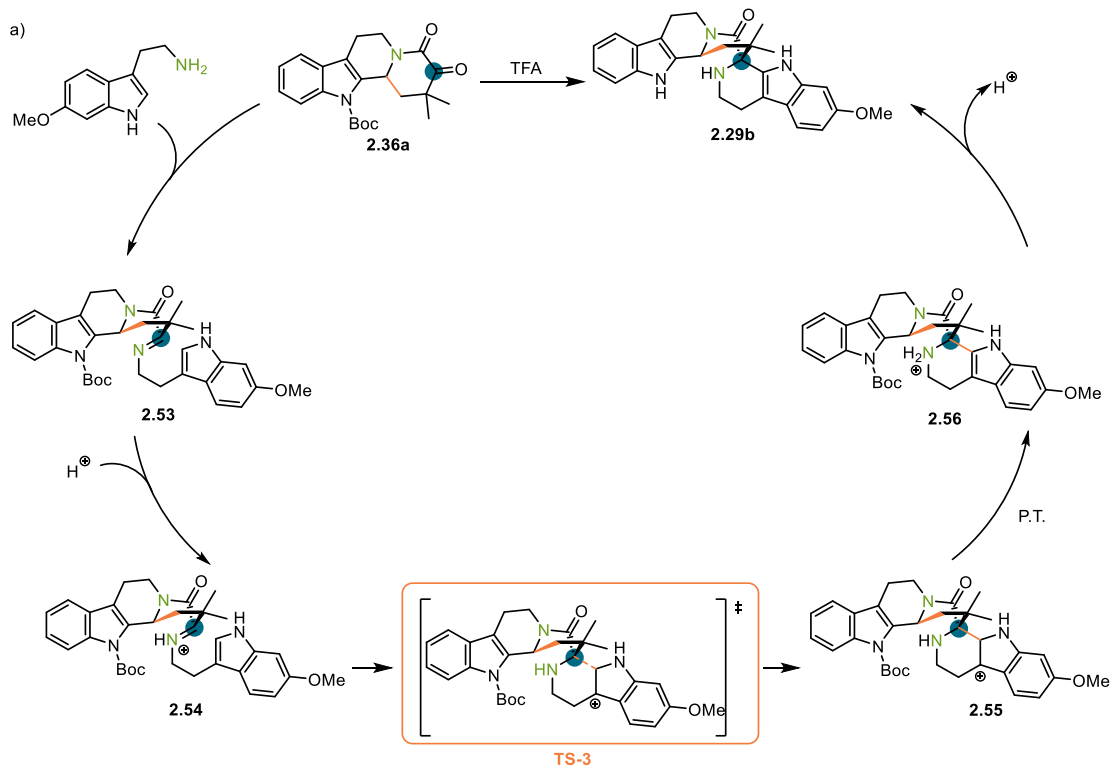


Scheme 2-12: DFT calculation of Zhu's reaction pathway.

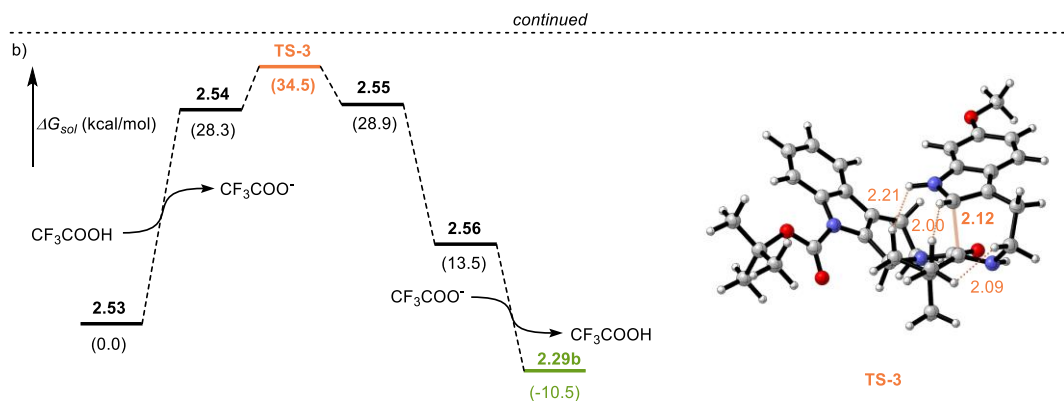


Scheme 2–12: DFT calculation of Zhu's reaction pathway. (continued)

Meanwhile, the reaction pathway with α -ketolactam **2.36a** was also thermodynamically favorable ($\Delta G = -10.5$ kcal/mol) (Scheme 2–13). However, the reaction pathway through **TS-3** was kinetically more disfavored by 10.3 kcal/mol (34.5 kcal/mol versus 24.2 kcal/mol). The remarkable difference between the energy barriers illustrated the distinct reaction outcomes. In addition, the forming 6-membered ring was shown to process a twist-boat conformation and under a more sterically hindered circumstance.



Scheme 2–13: DFT calculation of the mono Pictet–Spengler reaction.



Scheme 2–13: DFT calculation of the mono Pictet–Spengler reaction. (continued)

2.3.7. Selective benzylic oxidation attempt

Since the DFT calculations revealed the difficulty to realize the Pictet–Spengler reaction with α -ketolactam **2.36a**, it was proposed to convert α -ketolactam **2.36a** to α -ketoenamide **2.45a** achieving a formal total synthesis of 9'-demethoxy-peganumine A following Zhu's synthetic route. In order to accomplish this transformation, a two-step procedure was designed through the selective benzylic oxidation of **2.36a** at C1' position to obtain **2.57**, which could eliminate to **2.36a**. Although some traditional benzylic oxidation conditions were investigated, no promising result could be obtained. By careful analysis, it was speculated that a selective benzylic oxidation for this steric hindered tertiary carbon is difficult. Intriguingly, with a CoCl_2 and O_2 system, α -ketolactam **2.36a** was reduced to α -hydroxylactam **2.35a**.

Table 2–3: Screening for selective benzylic oxidation.

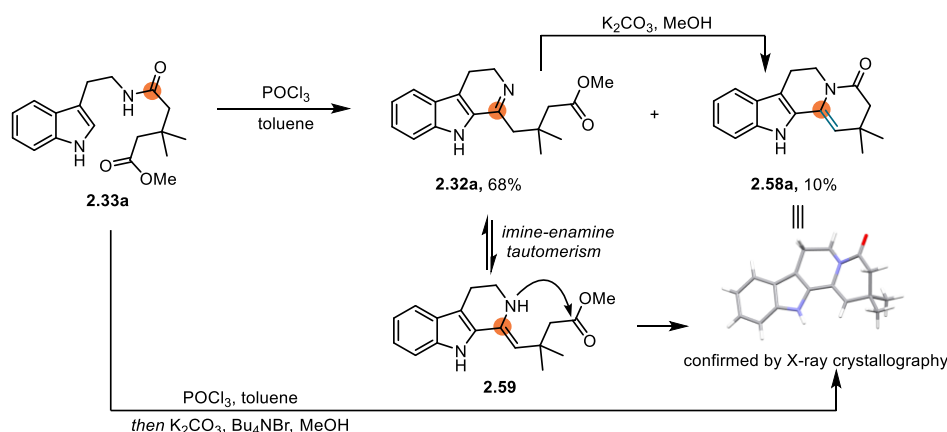
entry ^[a]	conditions	solvent	T [°C]	yield [%] ^[b]
1	K_2CO_3 , O_2	DMF	120	de-Boc
2	KOH , O_2	DMF	120	decomposition
3	KOH , O_2	MeOH	60	de-Boc
4	NBS, AIBN	MeCN	70	no conversion
5	NCS, BPO	CHCl_3	70	no conversion
6	CuCl_2 , pyridine, O_2	CHCl_3	120	no conversion
7	DDQ, <i>t</i> BuONO, O_2 , blue LED	toluene	23	no conversion
8	RuO_2 , NaClO	EtOAc	23	no conversion
9	$\text{Mn}(\text{OAc})_2 \cdot \text{H}_2\text{O}$, O_2	CH_2Cl_2	23	no conversion
10	CsCO_3 , O_2	DMF	23	no conversion
11	Pd/C , O_2	EtOH	23	no conversion
12	CoCl_2 , O_2	MeCN/ <i>i</i> PrOH	23	80 (2.35a)
13	<i>N</i> -hydroxyphthalimide, AIBN, O_2	MeCN	23	no conversion
14	$\text{Cr}(\text{CO})_6$, O_2	Pyridine	23	decomposition
15	Ru/C , MeCOOOME	EtOAc	23	no conversion
16	RuCl_3 , MeCOOOME	EtOAc	23	no conversion

[a] Reactions were performed with ketolactam (10 mg, 26 μmol); [b] isolated yield

2.4. 3rd generation improved synthesis towards peganumine A

2.4.1. Discovery of an annulation reaction

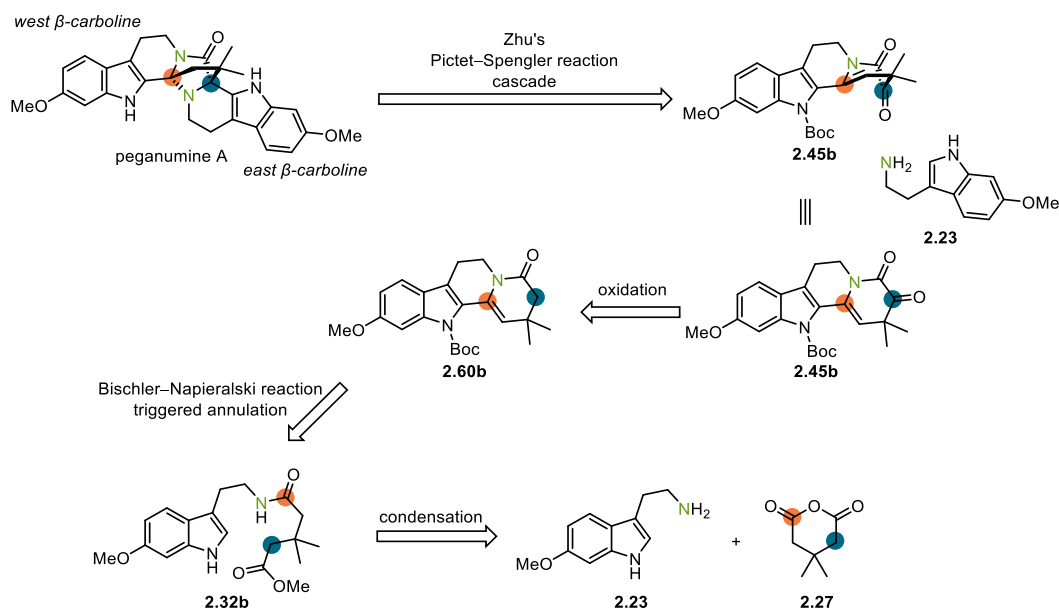
In the optimization of the Bischler–Napieralski reaction in the 2nd generation approach, a minor product **2.58a** with enamide motif was isolated in 10% yield. Treating imine **2.32a** with K_2CO_3 in MeOH, enamide **2.58a** was also obtained. It was proposed that imine **2.32a** was formed by a Bischler–Napieralski reaction, which underwent an imine–enamine tautomerization {Lammertsma, 1994 #996; Lammertsma, 2000 #995; Pérez, 2001 #994} and subsequent lactam formation to afford enamide **2.58a** (Scheme 2–14). Based on this consideration, the annulation reaction was optimized in a one-pot fashion.



Scheme 2–14: Concise annulation reaction.

2.4.2. 3rd generation improved retrosynthetic analysis

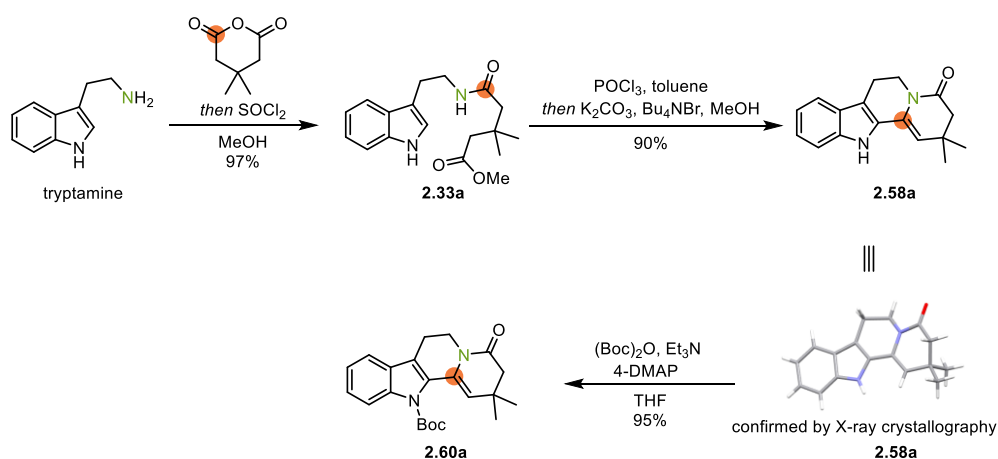
Inspired by the Bischler–Napieralski reaction triggered annulation and Zhu’s elegant total synthesis of peganumine A, an idea to realize a transition metal free formal total synthesis was proposed. Utilizing Zhu’s Pictet–Spengler reaction cascade, the synthesis was simplified to α -ketoenamide **2.45b** which could be functionalized from tetracyclic enamide **2.60b** (Scheme 2–15). With the Bischler–Napieralski reaction triggered annulation, tetracyclic enamide **2.60b** could be prepared from methyl ester **2.32b**, which can be traced back to a condensation between 6-methoxytryptamine and anhydride **2.27**.



Scheme 2-15: 3rd generation improved retrosynthetic analysis.

2.4.3. Construction of the west β -carboline core

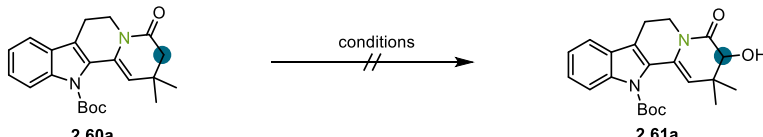
A model study was also conducted by using tryptamine due to the same reason mentioned before. Followed the same condensation as the 2nd generation synthetic approach afforded methyl ester **2.33a** in 97% yield (Scheme 2-16). With the Bischler-Napieralski reaction triggered annulation, enamide **2.58a** with west β -carboline core was obtained in 90% yield. The structure of tetracyclic enamide **2.58a** was unambiguously elucidated by X-ray crystallography. The Boc protection of the indole nitrogen led to **2.60a** in 95% yield.



Scheme 2-16: Construction of the west β -carboline core.

2.4.4. C–H oxidation to prepare the α -ketoenamide

With the tetracyclic enamide **2.60a** in hand, the same C–H oxidation condition which successfully delivered α -hydroxyl lactam **2.35a** in the 2nd generation synthetic approach, did not furnish the desired α -hydroxylation product **2.61a**. Firstly, following the enolate oxidation strategy, various bases and oxidants were investigated (Table 2–4, entries 1–15). It was proposed that the reactivity of tetracyclic lactam **2.34a** was different from that of tetracyclic enamide **2.60a**. Therefore, different oxidation strategies were tested. The direct oxidation of amides to α -keto amides developed by Maulide et. al.^[211] resulted in the recovery of starting material (Table 2–4, entry 16). Some classic oxidation mediated by TEMPO, Ruthenium, Selenium and Manganese also did not yield the desired α -hydroxylation product (Table 2–4, entries 17–22).

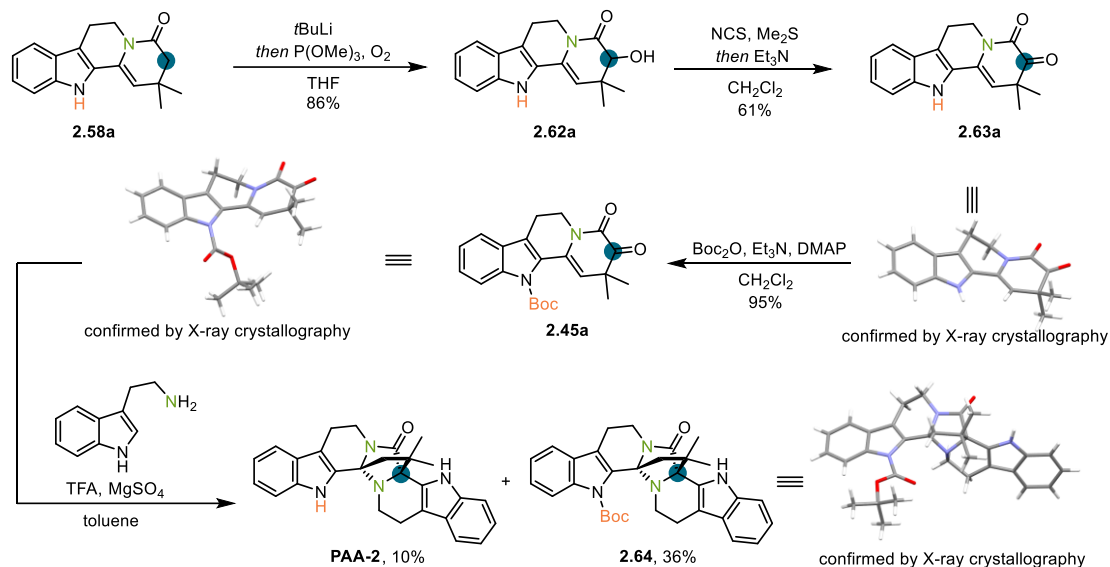
Table 2–4: α -hydroxylation of the Boc-protected α -ketoenamide.


entry ^[a]	condition	solvent	yield
1	LDA, O ₂ , P(OMe) ₃	THF	recovery of SM
2	LDA, TMSCl, O ₂ , P(OMe) ₃	THF	recovery of SM
3	LDA, (iPrO) ₃ TiCl, O ₂ , P(OMe) ₃	THF	recovery of SM
4	tBuLi, O ₂ , P(OMe) ₃	THF	recovery of SM
5	LDA, oxaziridine	THF	recovery of SM
6	LDA, TMSCl, oxaziridine	THF	de-Boc
7	LDA, (iPrO) ₃ TiCl, oxaziridine	THF	de-Boc
8	tBuLi, oxaziridine	THF	recovery of SM
9	LDA, TMSCl, mCPBA	THF	recovery of SM
10	LDA, MeSSMe	THF	recovery of SM
11	LDA, MeSSO ₂ Me	THF	recovery of SM
12	LDA, DMF-dimethyl sulfate adduct	THF	no product detected
13	tBuLi, PhCOOOtBu	THF	no conversion
14	tBuLi, tBuOOH	THF	no conversion
15	tBuLi, CeCl ₃ , oxaziridine	THF	no product detected
16	LNO, Tf ₂ O	THF	recovery of SM
17	TMSOTf, TEMPO	THF	no conversion
18	RuO ₂ , NaIO ₄	EtOAc	no product detected
19	SeO ₂	1,4-Dioxane	recovery of SM
20	MnO ₂	CH ₂ Cl ₂	no product detected

[a] Reactions were performed with ketoenamide (7.0 mg, 19 μ mol)

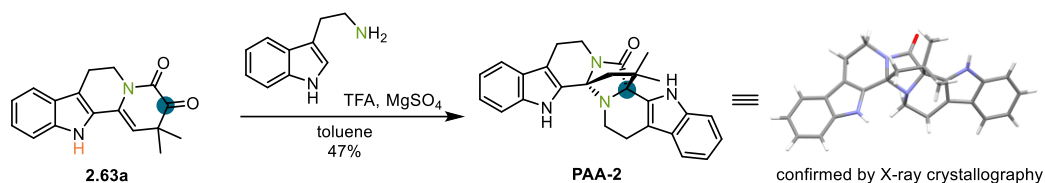
Since the Boc-group of **2.60a** could act as a directing group to promote the lithiation of the indole ring, the α -hydroxylation of the protection group free enamide **2.58a** was tested (Scheme 2–17). Surprisingly, α -hydroxyenamide **2.62a** was obtained in 80% yield. After a Corey–Kim reaction, α -ketoenamide **2.63a** was obtained in 90% yield. After a Boc protection, the key intermediate **2.45a** in Zhu's total synthesis was obtained. With **2.45a** in hand, a TFA promoted

Pictet–Spengler reaction cascade delivered both 9,9'-dididemethoxy peganumine A (**PAA-2**) and its analogue **2.64** successfully.



Scheme 2–17: Construction of 5,5-dimethyl-2,7-diazabicyclo[2.2.1]heptan-3-one.

Inspired by this Pictet–Spengler reaction cascade with less electrophilic tryptamine, rather than 6-methoxytryptamine in Zhu’s synthesis, the protection group free α -ketoamide **2.63a** was also anticipated to undergo the cascade reaction. Therefore, a protection group free Pictet–Spengler reaction cascade was conducted. Gratifyingly, this reaction afforded **PAA-2** in 47% yield (Scheme 2–18).



Scheme 2–18: Protection group free Pictet–Spengler reaction cascade.

2.4.5. Scalable and reliable synthesis to 6-methoxytryptamine

2.4.5.1. Indole synthesis strategy

With the successful model procedure in hand, the preparation of 6-methoxytryptamine was next challenge. There are numerous methods to construct indole scaffold.^[212] Considering the structural characteristic of 6-methoxytryptamine, Fischer,^[10] Hemtesberger–Buchwald^[213] and Sundberg–Larock^[214] strategies are plausible to be investigated (Figure 2–5).

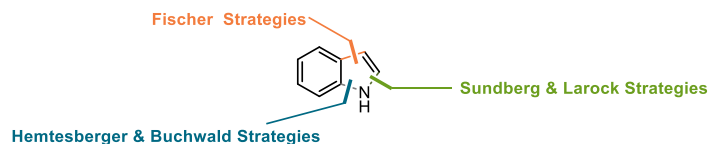
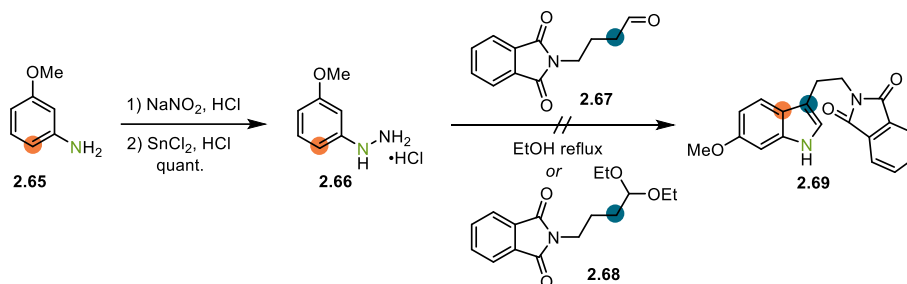


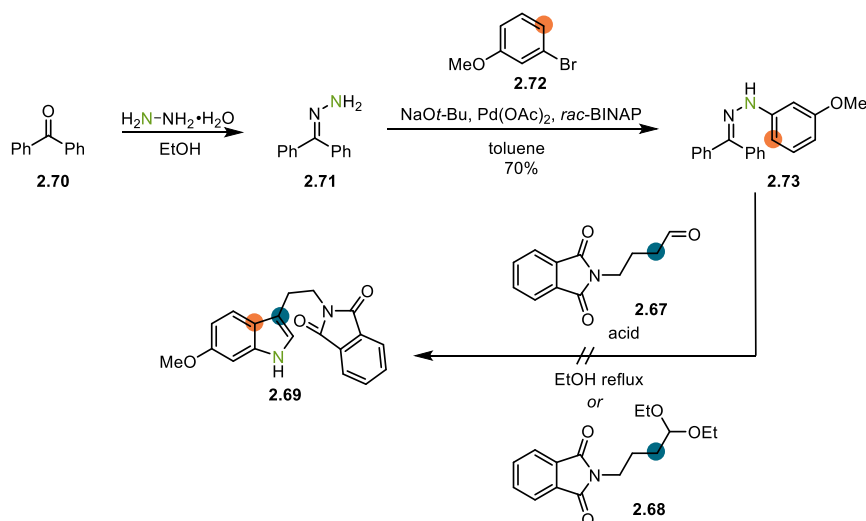
Figure 2-5: Indole synthesis strategies.

At first, the traditional Fischer indole synthesis was investigated (Scheme 2-19). Hydrazine hydrochloride salt **2.66** was prepared from *m*-anisidine **2.65** by diazotization in quantitative yield. However, the condensation with either aldehyde **2.67** or acetal **2.68** and the followed [3,3] sigmatropic rearrangement always led to a complex mixture of products.



Scheme 2-19: Modified Fischer indole synthesis.

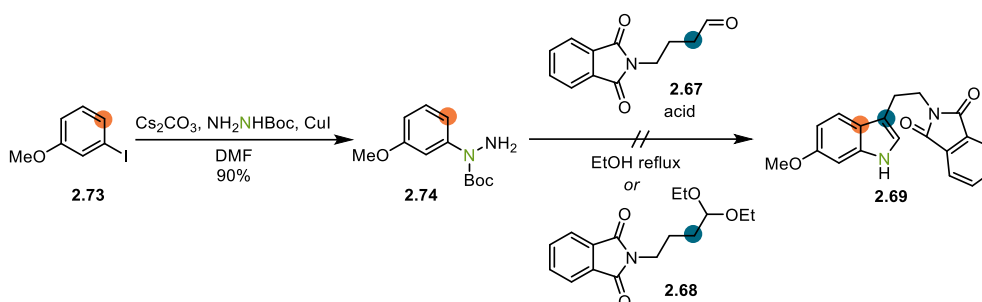
Since the high reactivity of the hydrazine hydrochloride salt **2.66** could be a reason for the formation of the side-products, Buchwald's modification^[213b] was tested, which utilized a hydrazone exchange reaction between **2.73** and aldehyde **2.67** or acetal **2.68** following a subsequent [3,3] sigmatropic rearrangement (Scheme 2-20). Unfortunately, no desired product **2.69** could be detected from the reaction mixture.



Scheme 2-20: Buchwald indole synthesis.

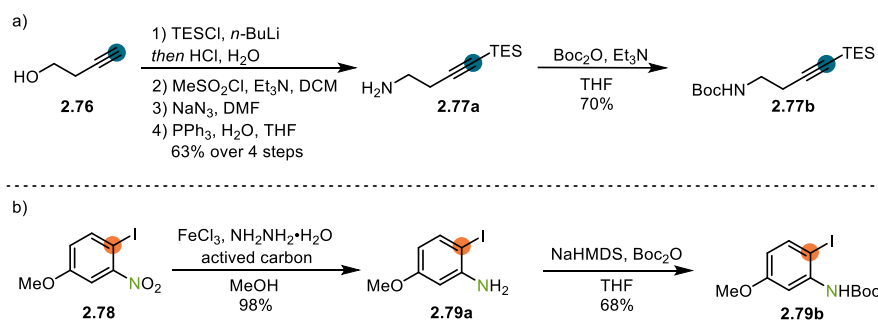
Analyzing the two failed cases, the activity of the hydrazones was suspected to be a key factor.

Thus, hydrazine **2.75** with moderate reactivity was synthesized (Scheme 2–21). However, the [3,3] sigmatropic rearrangement also proved to be difficult in this case. These failed experiments indicated that Fischer strategy which was normally used for 2,3-substituted indoles, is probably not suitable for the synthesis of 3-substituted indole such as 6-methoxytryptamine. In addition, regioselectivity of the [3,3] sigmatropic rearrangement was also a potential problem.



Scheme 2–21: Modified Fischer indole synthesis.

Following these initial investigations, Larock's indole synthesis^[214b] was explored, because of its high regioselectivity for 3-substituted indoles. For the butynylamine fragment synthesis, TES protected butynylamine **2.77a** was prepared from 3-butyn-1-ol **2.76** via a terminal alkyne protection with TES, following azide substitution and reduction (Scheme 2–22a). The Boc-protected butynylamine **2.77b** was also prepared. The iodoanisidine fragment **2.79a** was reduced from **2.78** (Scheme 2–22b). The Boc protected derivative **2.79b** was also prepared.



Scheme 2–22: Preparation of the precursors of Larock reaction.

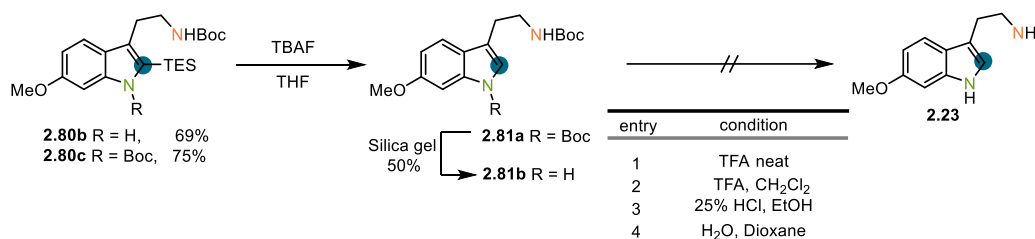
By extensive screening, the Larock reactions turned out to be a practical way to construct the scaffold of 6-methoxytryptamines. The results indicated that the Boc protection of the butynylamine was necessary, as the Larock reaction of amine **2.77a** could not afford the desired product (Table 2–5, entries 1–2). Additionally, the Boc protection of both reactants resulted in good yields (entries 5–6). With TEACl and DIPEA, the reaction between **2.77b** and **2.79b** afforded **2.80c** in 96% yield (entry 5).

Table 2–5: Optimization of Larock indole synthesis.

entry ^[a]	R ¹	R ²	Cl ⁻ source	base	yield ^[b]
1	H	H	TEACl	DIPEA	complex mixture
2	H	H	LiCl	K ₂ CO ₃	complex mixture
3	H	Boc	TEACl	DIPEA	11 (2.80b)
4	H	Boc	LiCl	K ₂ CO ₃	51 (2.80b)
5	Boc	Boc	TEACl	DIPEA	96 (2.80c)
6	Boc	Boc	LiCl	K ₂ CO ₃	74 (2.80c)

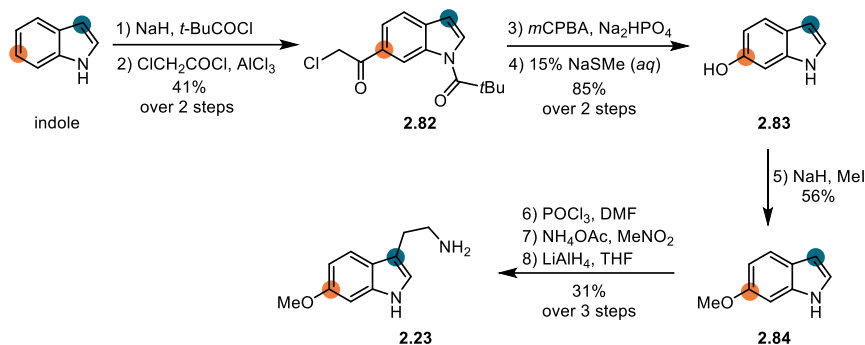
[a] Reactions were performed with iodoanisidine (92 μ mol, 1.0 equiv.), amine (184 μ mol, 2.0 equiv.), Cl⁻ source (92 μ mol, 1.0 equiv.), base (184 μ mol, 2.0 equiv.); [b] isolated yield

With these protected 6-methoxytryptamines in hand, the next aim was to cleave the protection groups. The TES removal reactions of **2.80b** and **2.80c** were successful by using TBAF (Scheme 2–23). The indole *N*-Boc deprotection of **2.81a** afforded **2.81b** in 50% yield. However, the aliphatic *N*-Boc removal of **2.81b** led to complex mixture under various conditions.

**Scheme 2–23:** Global deprotection in the Larock indole synthesis.

2.4.5.2. Indole functionalization strategy

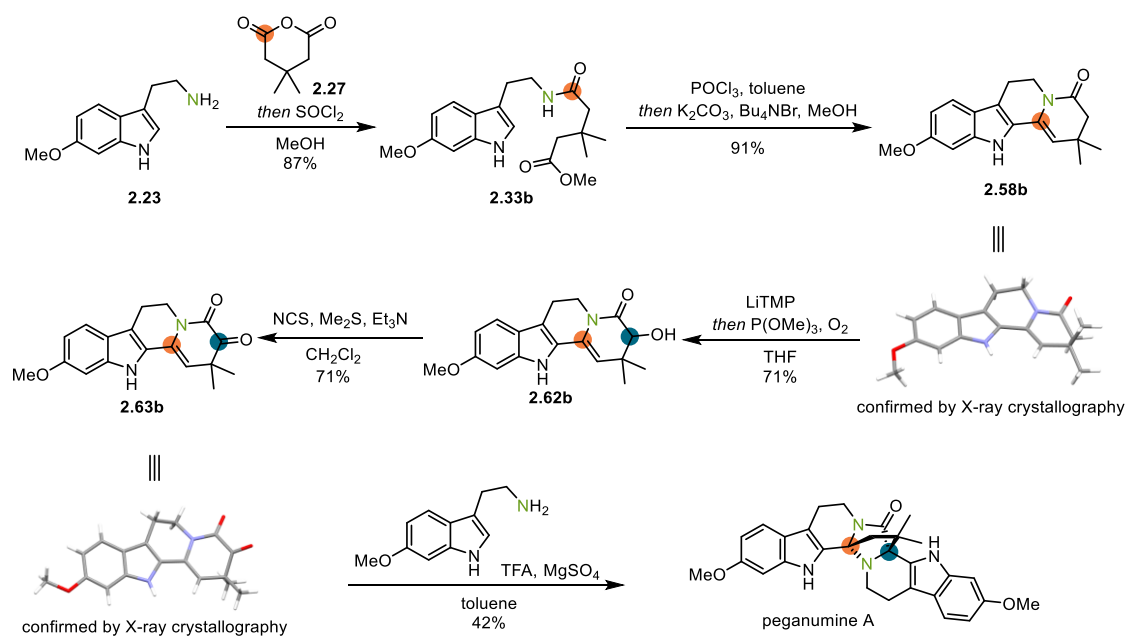
After investigation of the indole synthesis strategies, an indirect C–H functionalization was adapted to obtain 6-methoxytryptamine.^[215] Starting from indole, through a pivaloyl group protection and regioselective chloroacetylation, 6-acyl indole derivative **2.82** was prepared (Scheme 2–24). The following Baeyer–Villiger oxidation and subsequent deacylation afforded 6-hydroxyindole **2.83**, which was converted to 6-methoxyindole **2.84** by an *O*-methylation. 6-Methoxytryptamine was finally obtained by a Vilsmeier–Haack reaction, followed by nitromethane addition and reduction.



Scheme 2–24: Synthesis of 6-methoxytryptamine.

2.4.6. Improved protection group free synthesis of peganumine A

With the successful tryptamine model procedure and the scalable 6-methoxytryptamine synthesis in hand, the protection group free synthesis towards peganumine A was initiated. Starting with 6-methoxytryptamine, methyl ester **2.33b** was obtained in 87% yield through a condensation and esterification sequence (Scheme 2–25). The one-pot annulation furnished tetracyclic enamide **2.58b** in 91% yield. The α -hydroxylation of **2.58b** was realized by an enolate oxidation following a Corey–Kim oxidation,^[208] α -ketoenamide **2.63b** was obtained in 71% yield. Both structures of **2.58b** and **2.63b** were confirmed by X-ray crystallography. Racemic peganumine A was obtained in 42% yield by treating the α -ketoenamide **2.63b** with TFA.



Scheme 2–25: Protection group free total synthesis of peganumine A.

2.5. Analogues design, synthesis and bioactivity evaluation

2.5.1. Motivation and strategy of the study of the analogues of peganumine A

The examples in the section “1.2. Natural product and drug discovery” illustrate that natural products are undoubtedly important for drug discovery. It is still worthy to point out that the artificially designed drugs by medicinal chemists usually contain aromatic heterocycles and aliphatic linkers as the fundamental motifs, which make the molecules more flexible, while the natural products are usually more rigid with diverse functional groups, which usually interact with the targets in unique modes (Figure 2–6).

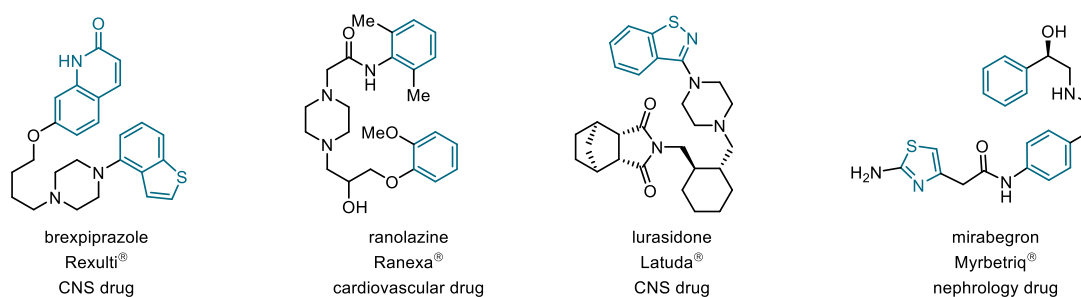


Figure 2–6: Artificially designed drugs.

Peganumine A exhibits selective effects on HL-60 cell line with an IC_{50} of 5.8 μ M, which was the motivation to identify the SAR and clarify the mechanism of the cytotoxicity. As the 5,5-dimethyl-2,7-diazabicyclo[2.2.1]heptan-3-one is a unique motif of peganumine A, it was proposed to retain this special scaffold in the initial analogue design. Relying on the strategies in the section “1.2.2. Strategies for natural product analogues synthesis in drug discovery”, different ideas for the analogue design were proposed. Based on the function-oriented synthesis, the pharmacophoric β -carboline cores were intended to be modified by changing the substitution of the indole rings and by switching to different heterocycles (Figure 2–7). Inspired by the hybrid synthesis, other fragment was envisioned to be installed to the β -carboline motifs to enhance the selectivity and activity of the analogues. With the idea of complexity to diversity, the lactam could also be modified by reduction or thionation, which will illustrate the role of the geometry of the unique ring system in bioactivity.

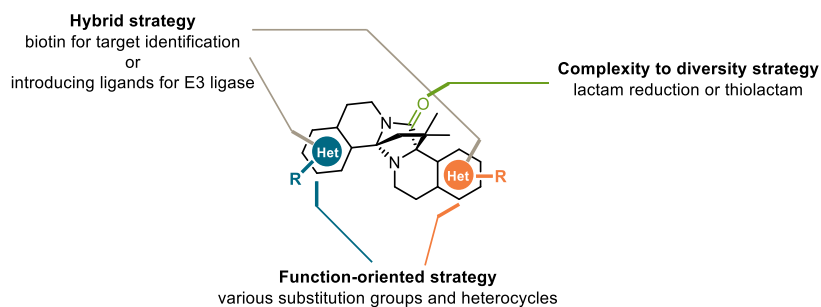


Figure 2–7: Consideration of analogues design.

The initial investigation was employing the function-oriented strategy, focusing on the introduction of new groups at C9 and C9'. Due to the special character of fluorine in small molecule drug discovery,^[216] such as small atom radius, great electronegativity and bond polarity, fluorine was selected. Deuterium, a stable isotope of hydrogen, was utilized in tracer studies of medicinal research.^[217] Compared to C–H bond, C–D bond is shorter, leading to reduced electronic polarizability, lesser hyper-conjugative stabilization of adjacent bonds and weaker van der Waals stabilization,^[218] which lead to difference in metabolism between deuterium and hydrogen. Therefore, the deuterated methoxy groups were introduced. Meanwhile, a bromo substitute was envisioned to install at the C9 and C9' positions, which could be a handle for introducing of various functional groups by cross coupling reactions (Figure 2–8a). The position of the methoxy groups is also worth exploring. (Figure 2–8b).

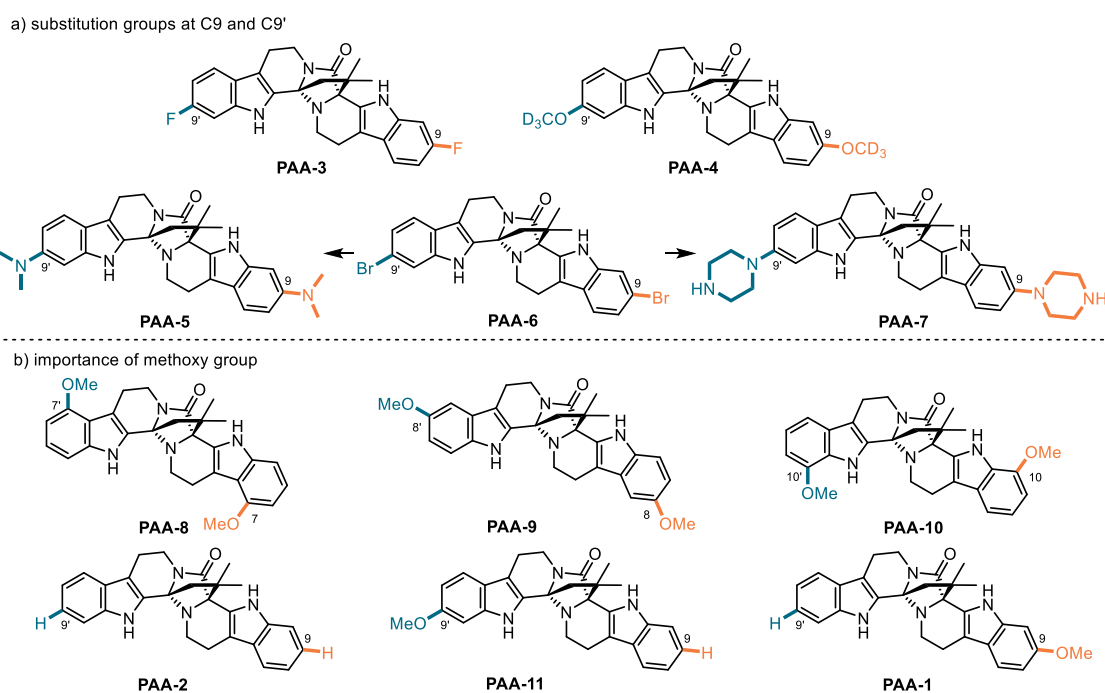
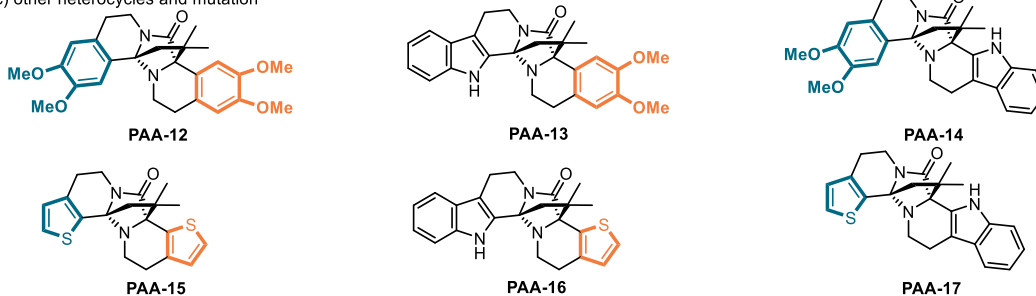
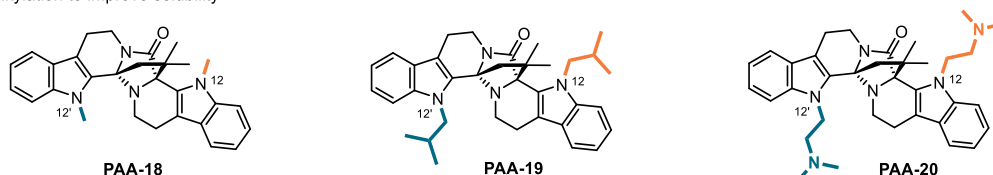


Figure 2–8: Design of the analogues.

c) other heterocycles and mutation



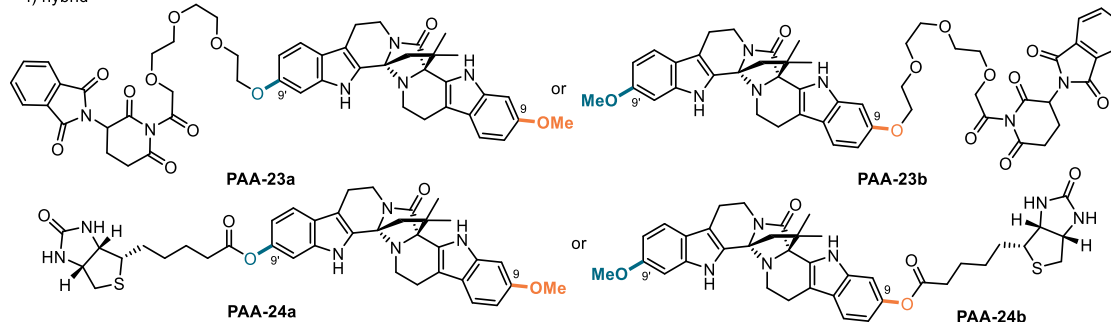
d) alkylation to improve solubility



e) core modification



f) hybrid

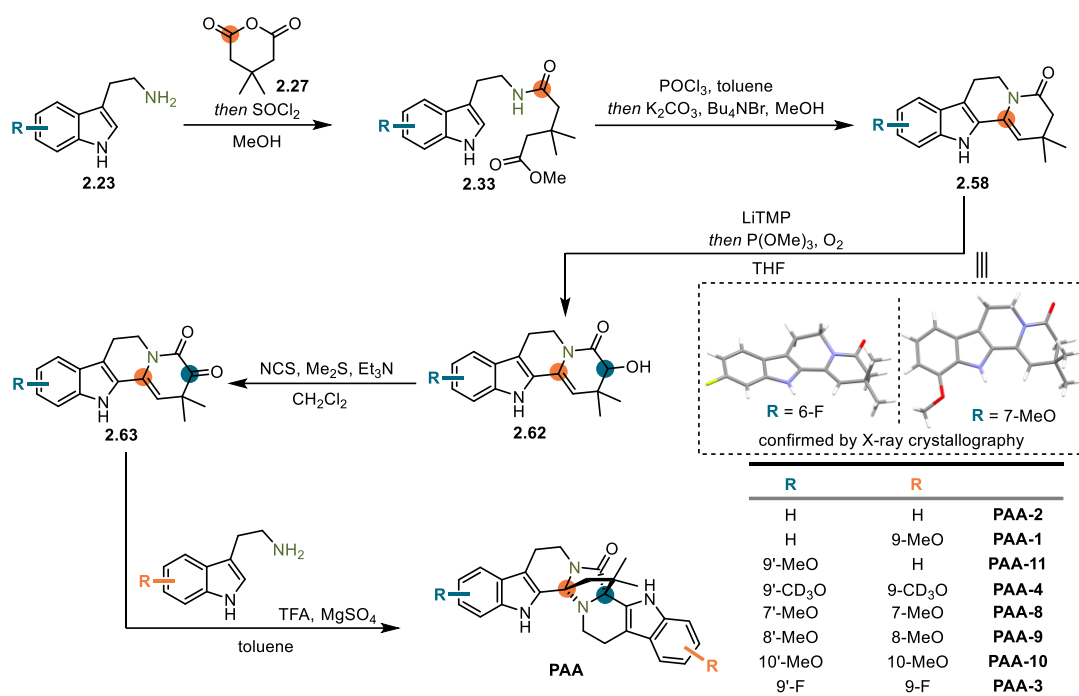


Furthermore, it was anticipated to introduce various new heterocycles or permutate among these heterocycles (Figure 2–8c). In addition, the N–H alkylation of peganumine A was also anticipated to increase the lipophilicity for the improvement of the membrane permeability (Figure 2–8d). Although the core of peganumine A is unique, slight changing of the spatial arrangement was also anticipated by the manipulation of the lactam group (Figure 2–8e). Inspired by the PROTAC technology,^[219] thalidomide as the ligand for E3 ligase was a proposed hybrid. The biotinylated analogue was designed for the target identification (Figure 2–8f).

2.5.2. Synthesis of analogues

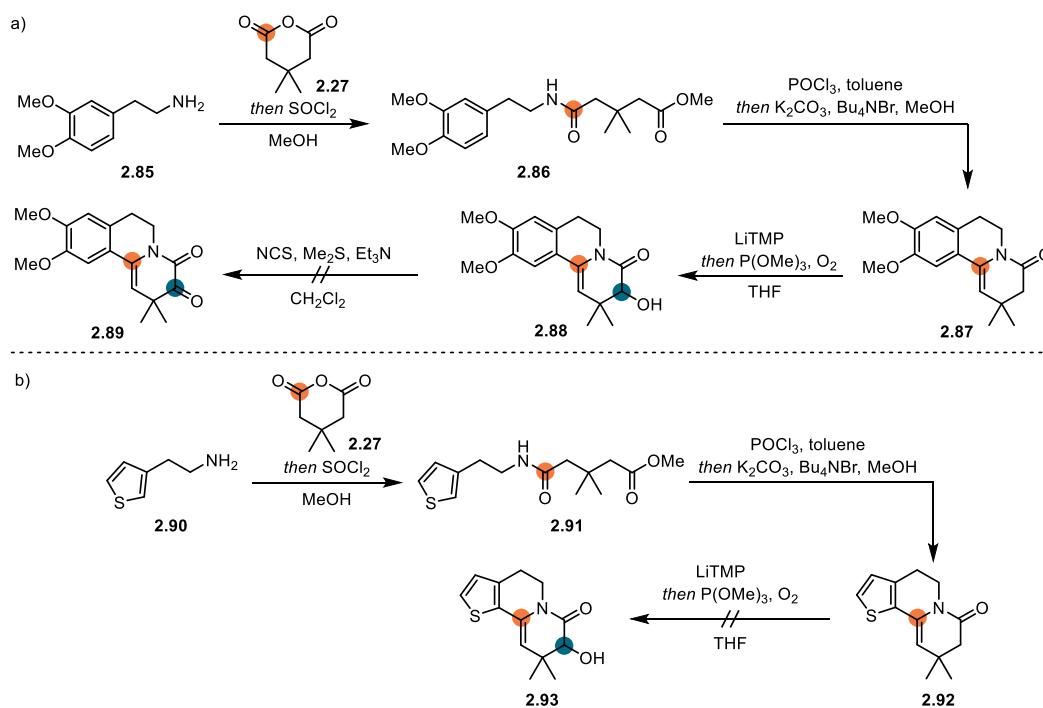
Following the same procedure as the synthesis of peganumine A, eight analogues with different indole substitutions were prepared (Scheme 2–26). However, **PPA-6** was not obtained, as the

α -hydroxylation might lead to lithiation of the indole ring.



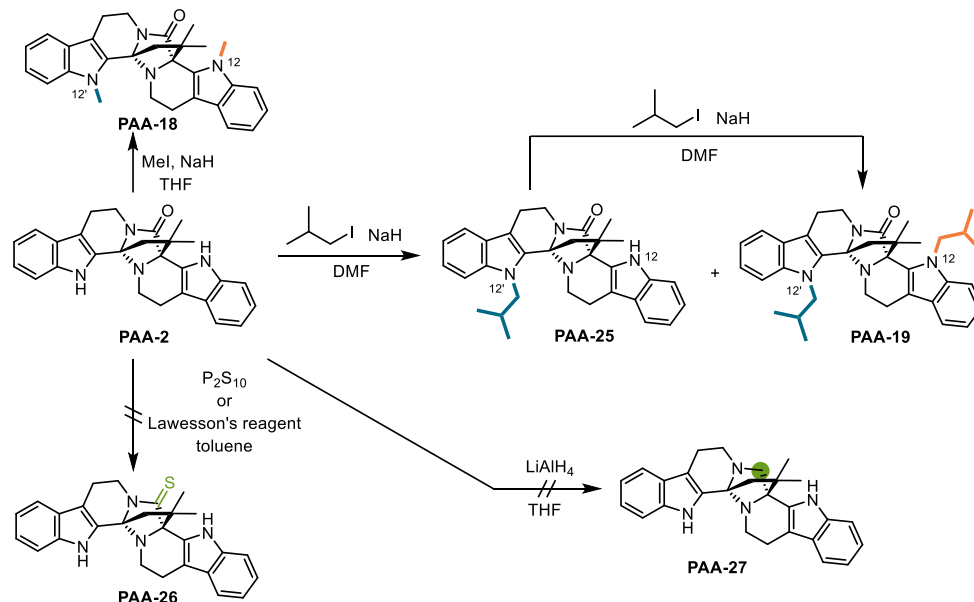
Scheme 2–26: General synthetic route of the analogues.

Next, the syntheses of the analogues with other heterocycles were commenced. Unfortunately, the benzene ring enamide **2.87** could not tolerate the Corey–Kim reaction (Scheme 2–27a). The α -hydroxylation of thiophene enamide **2.92** was unsuccessful (Scheme 2–27b). Due to the synthetic efficiency, the case-by-case optimization was not conducted initially.



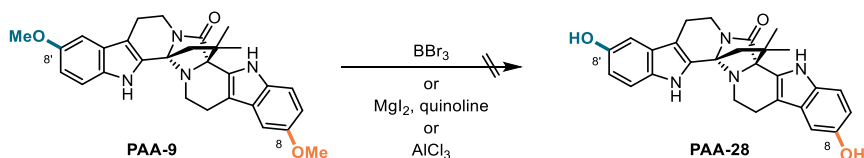
Scheme 2–27: Attempt for the analogues with different heterocycles.

Attention was also paid to the *N*-alkylation of indole and the core modification. The alkylation with methyl and *iso*-butyl groups were successful respectively (Scheme 2–28). However, as the lactam group is sterically hindered, the manipulation of it was still challenging.



Scheme 2–28: Alkylation and attempt of core modification.

In order to introduce the hybrids, a didemethylation was needed to liberate the hydroxyl groups. As the supply of 6-methoxytryptamine was limited, **PAA-9** was selected as the model substrate for the demethylation screening. Unfortunately, the classic demethylation conditions did not afford the desired product **PAA-28** (Scheme 2–29).



Scheme 2–29: Didemethylation screening.

2.5.3. Cytotoxicity assay of analogues

Hua et al. reported that the peganumine A has selective cytotoxicity on HL-60 cells with an IC₅₀ value of 5.8 μM.^[196] Based on this pioneering result, the cytotoxicity assay of the synthetic *rac*-peganumine A and its analogues was initiated by collaboration with Dr. Wan Li and Professor Dr. Jinhua Wang at the Institute of Materia Medica, Chinese Academy of Medical Sciences and Peking Union Medical College. **PAA-2** showed better cytotoxicity against HL-60 cells with an IC₅₀ value of 5.2 μM, compared to 10.0 μM of *rac*-peganumine A.

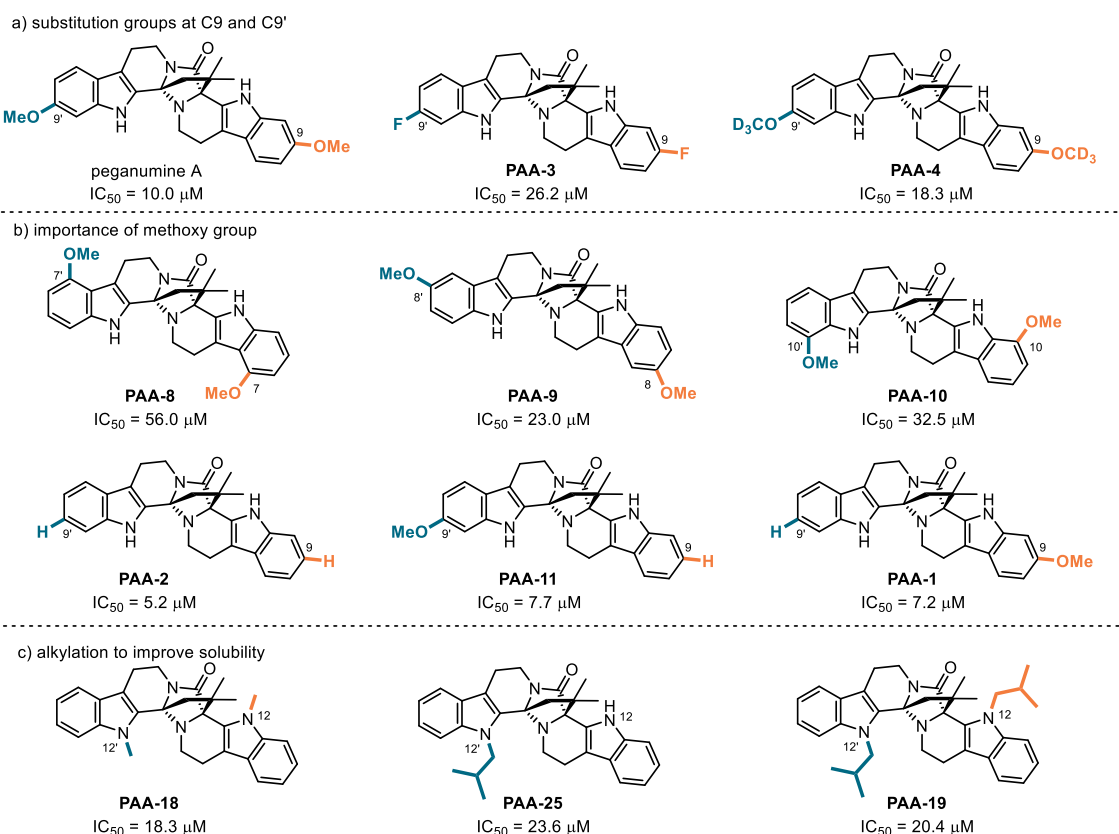


Figure 2–9: Cytotoxicity assay of the synthetic *rac*-peganumine A and its analogues.

Based on the cytotoxicity assay, the primary SAR was summarized. 1) The N–H is important for the activity, as alkylation of N–H led to activity decrease. 2) The unsubstituted β -carbolines analogue was the best (Figure 2–11).

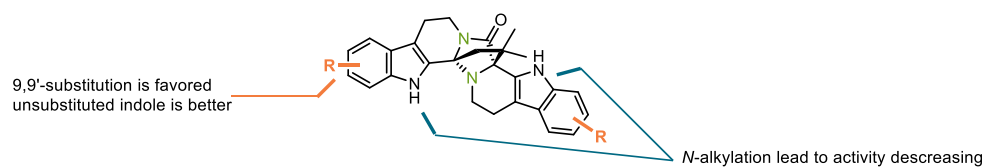


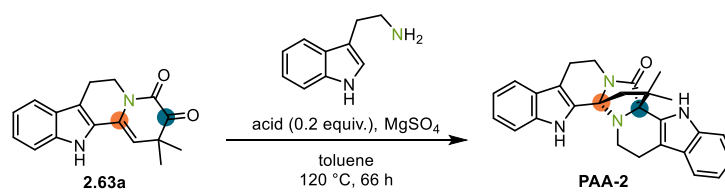
Figure 2–10: Primary SAR.

2.5.4. Gram scale synthesis of PAA-2

Since **PAA-2** was discovered as a potent analogue, the gram scale synthesis of it was required for further biological studies. Therefore, various Brønsted acids^[220] were screened for the Pictet–Spengler reaction, which showed that TFA was still the most efficient acid for the cascade reaction (Table 2–6, entries 1–10). Acids which are weaker than TFA resulted in lower yields (entries 3–10). However, Tf₂NH with stronger acidity also led to lower yield (entry 2). Interestingly the reaction with dodecylbenzene sulfonic acid afforded a comparable yield as

TFA, which indicated that the hydrophobic micro-atmosphere generated by the long aliphatic chain of dodecylbenzene sulfonic acid might be beneficial for the cascade reaction (entry 10). This hypothesis was supported by the lower yield with sulfonic acid (entries 11 and 12) and relatively high yield with octanoic acid (entry 13). Arachidic acid, with a longer aliphatic chain, did not furnish the desired product, indicating carboxylate acid might not be favored (entry 14). Based on these results, sulfonic acids with different chains were screened (entries 15–20). As the reactions with selected sulfonic acids did not afford improvement of yield, the attention was switched to the fluorinated acids (entries 21–24). Fortunately, with trifluoropropionic acid the reaction furnished a slightly improved yield (entry 21). Additionally, the hydrophobic effect was also shown with the fluorinated acids (entries 22–24). However, due to the cost of such fluorinated acids, TFA was still regarded as the most efficient Brønsted acid for this reaction.

Table 2–6: Screening of the Brønsted acids for the annulation.



entry ^[a]	acid	yield [%] ^[b]
1	TFA	42
2	Tf ₂ NH	13
3	CSA	16
4	<i>rac</i> -BINOL phosphoric acid	18
5	4 M HCl	trace
6	AcOH	trace
7	PhCOOH	trace
8	phenylpyruvic acid	recovery of SM
9	oxalic acid	16
10	4-dodecylbenzenesulfonic acid	34

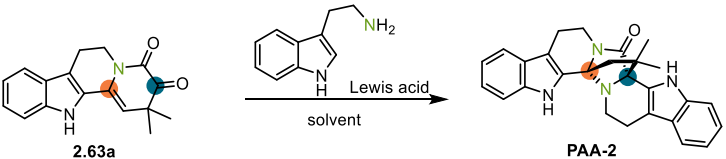
11	<i>p</i> TsOH	recovery of SM
12	MeSO ₃ H	trace
13	C ₇ H ₁₅ COOH	27
14	C ₁₉ H ₃₉ COOH	recovery of SM
15	MOPS ^[c]	recovery of SM
16	amidosulfonic acid	recovery of SM
17	hydroxylamine- <i>o</i> -sulfonic acid	recovery of SM
18	TfOH	trace
19	taurin	recovery of SM
20	sulfanilic acid	recovery of SM

21	CF ₃ CH ₂ COOH	45
22	C ₂ F ₅ COOH	26
23	C ₇ F ₁₅ COOH	34
24	C ₈ F ₁₇ COOH	28
25	TCA	recovery of SM
26	TBA	recovery of SM

[a] Reaction were performed with α -ketoenamide (10 mg, 36 μ mol), tryptamine (0.6 mg, 38 μ mol);

[b] isolated yield; [c] MOPS = 3-(*N*-morpholino)propanesulfonic acid

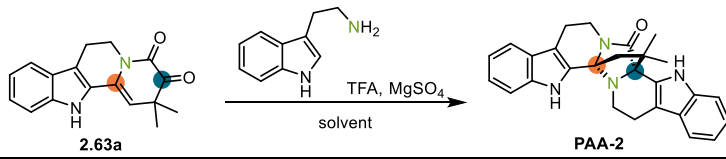
Since the reactions with those Brønsted acids did not afford an improved yield, Lewis acid was anticipated to promote the Pictet–Spengler reaction more efficiently.^[221] However, the preliminary screening of the Lewis acids did not obtain the desired product (Table 2–7).

Table 2–7: Screening of the Lewis acids for the annulation.


entry ^[a]	acid	solvent	T [°C]	t [h]	yield
1	Yb(OTf) ₃	toluene	23	24	complex mixture
2	AlCl ₃	toluene	23	24	complex mixture
3	Hg(OTf) ₂	toluene	23	24	complex mixture
4	Sc(OTf) ₃	toluene	23	24	complex mixture
5	In(OTf) ₃	toluene	23	24	complex mixture
6	Hg(OTf) ₂	toluene	23	24	complex mixture
7	AuCl ₃ , AgOTf	DCE	80	66	complex mixture
8	PPh ₃ AuCl, AgOTf	DCE	80	66	complex mixture
9	<i>t</i> Bu ₃ PAuCl, AgOTf	DCE	80	66	complex mixture
10	Yb(OTf) ₃	toluene	120	66	complex mixture
11	La(OTf) ₃	toluene	120	66	complex mixture

[a] Reaction were performed with α -ketoenamide (10 mg, 36 μ mol), tryptamine (0.6 mg, 38 μ mol).

Since the screening of both Brønsted acids and Lewis acids did not afford improvement in the cascade reaction, TFA was still selected for the further optimization of the reaction condition. The reaction time was investigated first, showing that the yield could not be increased after 66 h (Table 2–8, entries 1–6). Next, the screening of temperature indicated that high temperature is necessary for the cascade reaction (entries 7–9). The best stoichiometry of the TFA in the reaction was proven as 0.1 or 0.2 equivalent (entries 10–14). Although different solvents and mixtures of solvents were tested, the best option was still toluene (entries 15–20).

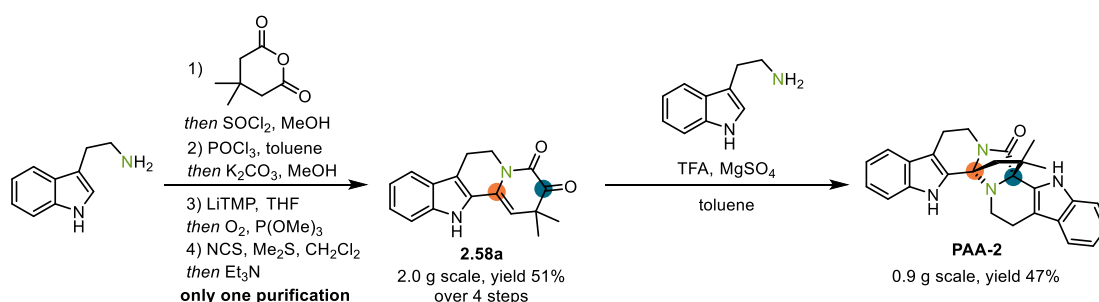
Table 2–8: Optimization of reaction condition with TFA.


entry ^[a]	equivalent	solvent	T [°C]	t [h]	yield [%] ^[b]
1	0.2	toluene	120	17	34
2	0.2	toluene	120	40	33
3	0.2	toluene	120	66	42
4	0.2	toluene	120	121	41
5	0.2	toluene	120	162	43
6	0.2	toluene	120	325	40
7	0.2	toluene	90	162	33
8	0.2	toluene	60	162	trace
9	0.2	toluene	23	162	trace
10	0.5	toluene	120	66	30
11	1.0	toluene	120	66	31
12	2.0	toluene	120	66	14
13	0.1	toluene	120	66	43
14	0.05	toluene	120	66	trace
15	0.2	toluene/hexane 1:1	120	66	30
16	0.2	toluene/perfluorohexane 1:1	120	66	24
17	0.2	toluene/perfluorotoluene 10:1	120	66	25
18	0.2	octane	120	66	27
19	0.2	DMF	120	66	16
20	0.2	1,4-dioxane	120	66	37

[a] Reaction were performed with α -ketoenamide (10 mg, 36 μ mol), tryptamine (0.6 mg, 38 μ mol);

[b] isolated yield

In order to further improve the efficiency of the synthetic route, the gram scale rapid preparation of α -ketoenamide **2.63a** was realized with only one purification in the last step (Scheme 2–30). With α -ketoenamide **2.63a** in hand a large-scale synthesis of **PAA-2** was achieved in 47% yield. This robust synthetic route could pave the avenue to further investigation of this potent analogue.



Scheme 2–30: Efficient gram scale synthesis.

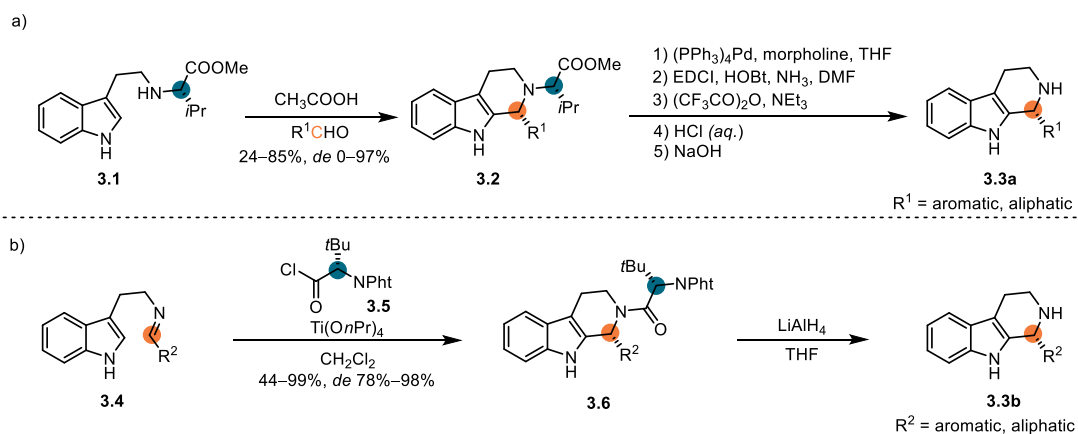
2.6. Brief summary

In this chapter, three strategies were investigated to discover an efficient synthetic route towards peganumine A. The 1st generation route relying on a challenging double Pictet–Spengler reaction turned out to be unfruitful with the Weinreb amide derivative. Based on this experience, the 2nd generation route was simplified to a mono-Pictet–Spengler reaction to construct east β -carboline motif. The west β -carboline fragment was assembled by a stepwise cyclization. Unfortunately, the mono-Pictet–Spengler reaction could not be realized, which was caused by the hindrance of the 1,3-interaction revealed by DFT calculations. By thorough analysis, a minor product of the cyclization with enamide motif was discovered. Inspired by Zhu's synthesis, an improved protection group free and transition metal free synthesis was realized. Utilizing this synthetic route, 11 analogues were successfully obtained. With the collaboration with Dr. Wan Li and Professor Jinhua Wang, a potent analogue was discovered and prepared in large scale, which could pave the avenue for further cellular mechanism study.

3. Organocatalyst Design and Asymmetric Total Synthesis of Peganumine A and Its Analogues

3.1. Introduction for the asymmetric Pictet–Spengler reaction

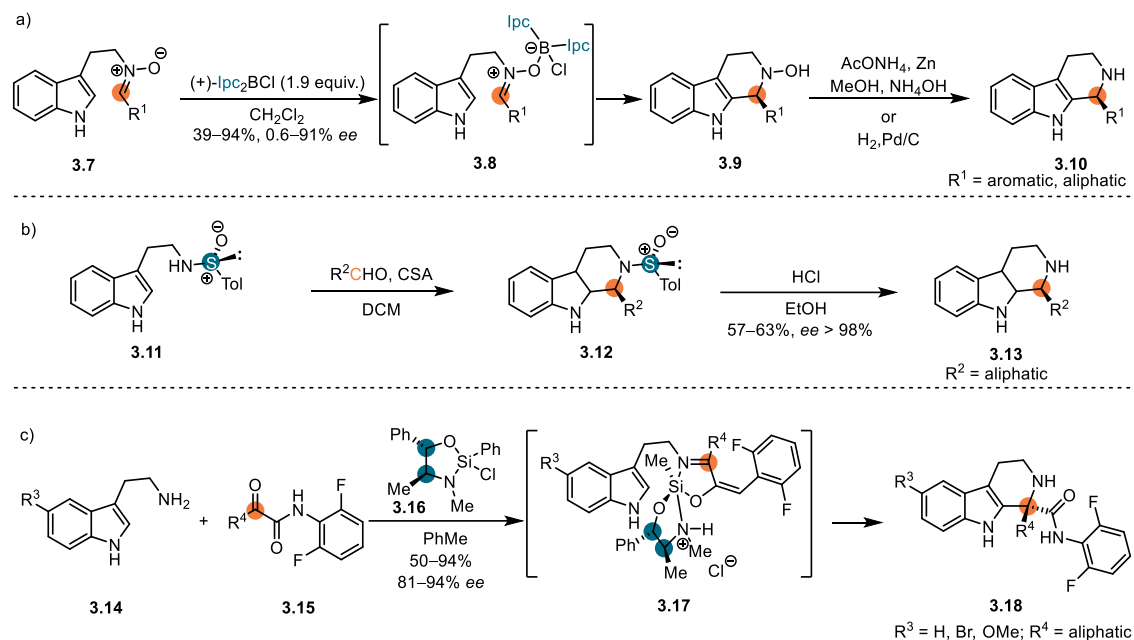
In order to realize the asymmetric protection group free total synthesis of peganumine A, an enantioselective catalytic system for the Pictet–Spengler reaction cascade needed to be discovered. The Pictet–Spengler reaction is a classic reaction to construct β -carboline core through an iminium ion. As β -carboline is an attractive motif in various bioactive molecules, the formulation of an asymmetric Pictet–Spengler reaction was a hot topic in the last decades. In the early stage of research, the enantioenriched β -carbolines were obtained by a chiral auxiliary group assisted Pictet–Spengler reaction.^[222] The pioneering work was reported in 1994 whereby Waldmann et al. prepared the enantioenriched tetrahydro- β -carboline **3.2** by using an L-valine derived methyl ester **3.1**.^[223] However, the L-valine derived chiral auxiliary group was very difficult to be cleaved, which needed a five-step procedure to afford the liberated tetrahydro- β -carboline **3.3a** (Scheme 3–1a). Later, Waldmann et al. improved a one-step reduction procedure to afford **3.3b** by employing *N,N*-phthaloyl amino acid derivative **3.5** as chiral auxiliary group (Scheme 3–1b).^[224]



Scheme 3–1: Asymmetric Pictet–Spengler reaction by amino acid derived auxiliaries.

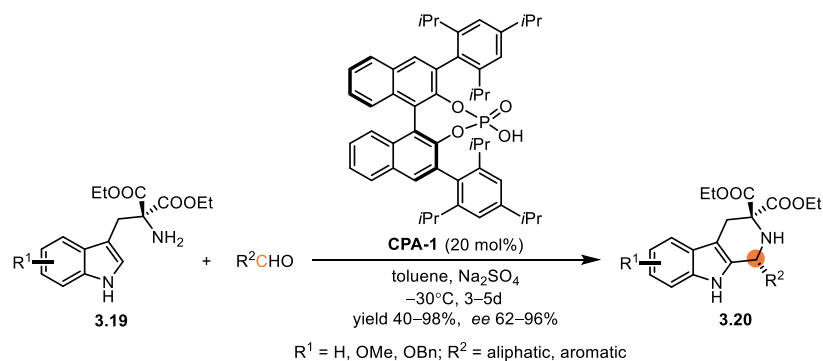
Besides these amino acids derived chiral auxiliary groups, borane-based, sulfur-based and silane-based chiral auxiliary groups were also applied in the asymmetric Pictet–Spengler reactions. In 1998 Nakagawa et al. utilized (+)-diisopinocampheylchloroborane to form the chiral iminium ion intermediate **3.8** in situ from nitron **3.7**, yielding the enantioenriched hydroxylamine **3.9** (Scheme 3–2a). A reduction reaction could afford tetrahydro- β -carboline **3.10**. Meanwhile, tetrahydro- β -carboline **3.13** could be constructed by the Pictet–Spengler

reaction of *p*-tolylsulfonamide **3.11** employing a *N*-sulfinyl chiral auxiliary group (Scheme 3–2b).^[225] Lewis acidic chiral chlorosilane **3.16** was also applied to the asymmetric ketimine Pictet–Spengler reaction by generating the chiral silane–amide complex **3.17** in situ (Scheme 3–2c).^[226]



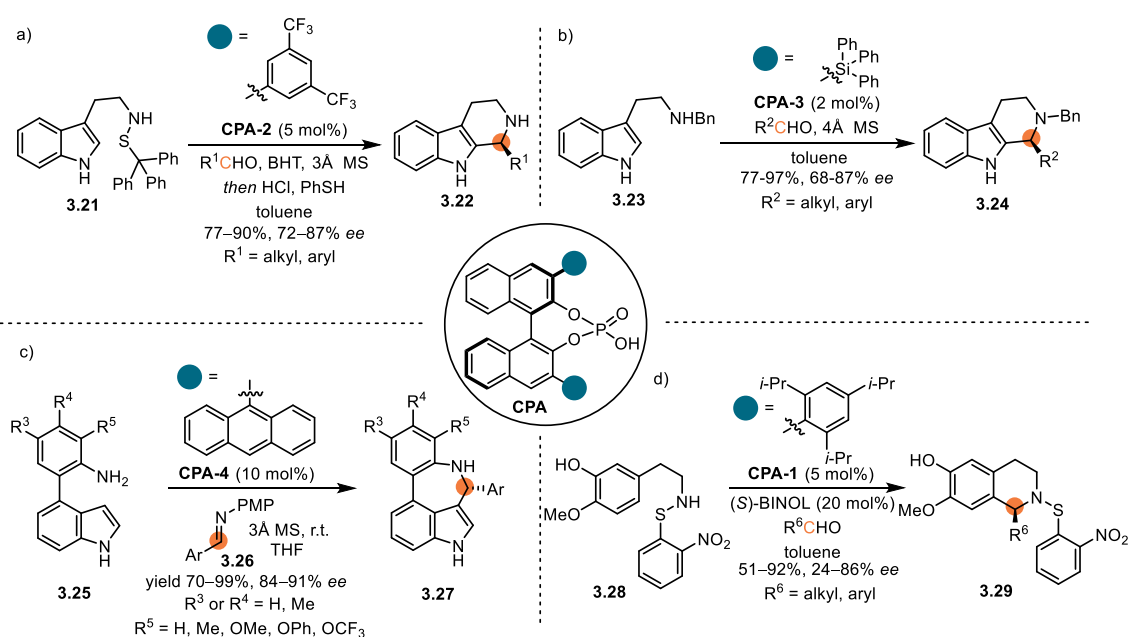
Scheme 3–2: Asymmetric Pictet–Spengler reaction by other auxiliaries.

Although the asymmetric Pictet–Spengler reaction could be achieved by the chiral auxiliary strategy, the large stoichiometric excess of the chiral auxiliaries was required. The catalytic asymmetric Pictet–Spengler reaction remained challenging until 2006, when List et al. made a huge progress in this area, achieving the first catalytic asymmetric Pictet–Spengler reaction.^[227] With a BINOL derived chiral phosphoric acid catalyst **CPA-1**, tryptamines **3.19** were converted to the corresponding tetrahydro- β -carbolines **3.20** in good yields and enantioselectivities (Scheme 3–3).

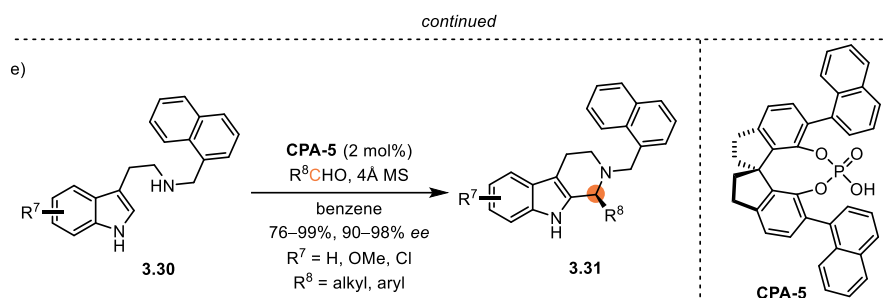


Scheme 3–3: The first catalytic asymmetric Pictet–Spengler reaction.

After the pioneering work of List et al., lots of different chiral phosphoric acid catalysts were applied to the catalytic asymmetric Pictet–Spengler reactions for both aldehyde^[228] and ketone^[229] substrates. For the reactions with aldehydes, Hiemstra et al. developed a catalytic asymmetric Pictet–Spengler reaction of *N*-sulfenytryptamine **3.21** with **CPA-2** as the catalyst (Scheme 3–4a).^[228a] An update of this system was studied, using *N*-benzyltryptamine **3.23** as starting material to construct benzyl tetrahydro- β -carbolines **3.24** (Scheme 3–4b).^[228b] Tian et al. realized the construction of chiral seven-membered ring scaffold **3.27** through a transamination triggered catalytic asymmetric Pictet–Spengler reaction with up to 91% *ee*. This transamination process of substrates **3.25** with PMP protected imines **3.26** could avoid the generation of water as byproduct of imine formation, which might be beneficial for the nonbonding interactions to enhance enantioselectivity (Scheme 3–4c).^[228c] Besides the construction of enantioenriched tetrahydro- β -carbolines, Hiemstra et al. achieved an enantioselective Pictet–Spengler reaction for the synthesis of tetrahydroisoquinolines **3.29** from *o*-nitrophenylsulfenamide **3.28** with **CPA-1** (Scheme 3–4d).^[228e] Besides these BINOL derived chiral phosphoric acid catalysts, **CPA-5** with a SPINOL backbone could also catalyze an enantioselective Pictet–Spengler reaction of *N*₆- α -naphthylmethyl tryptamines **3.30**, yielding tetrahydro- β -carbolines **3.31** with up to 98% *ee* (Scheme 3–4e).

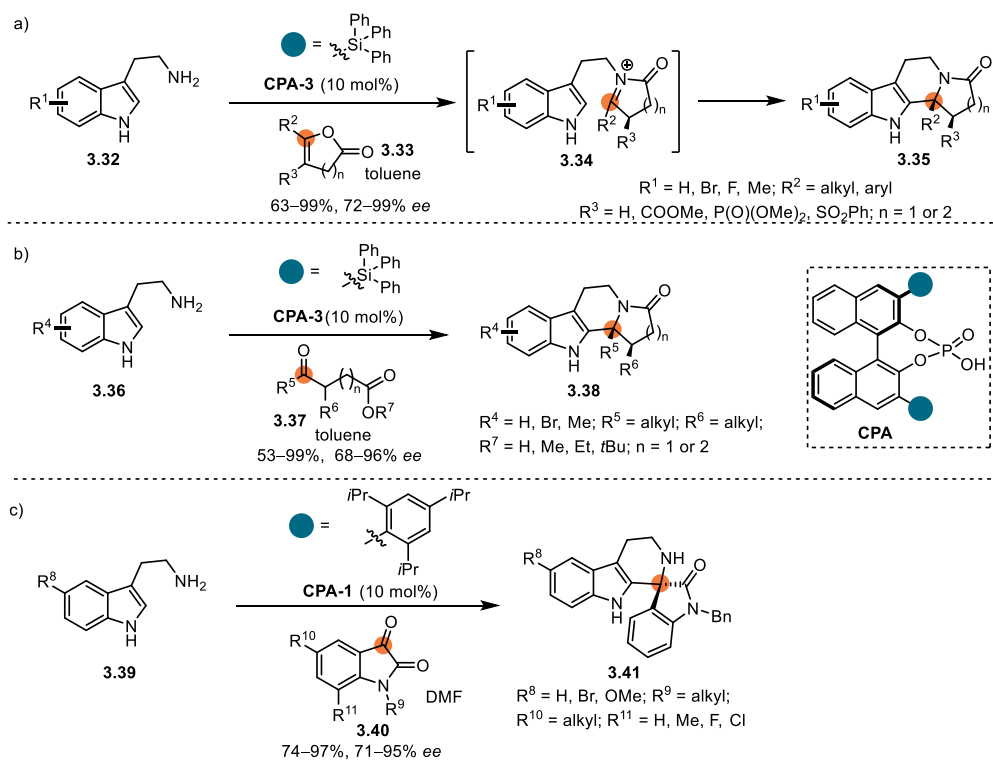


Scheme 3–4: Catalytic asymmetric Pictet–Spengler reaction of aldehydes.



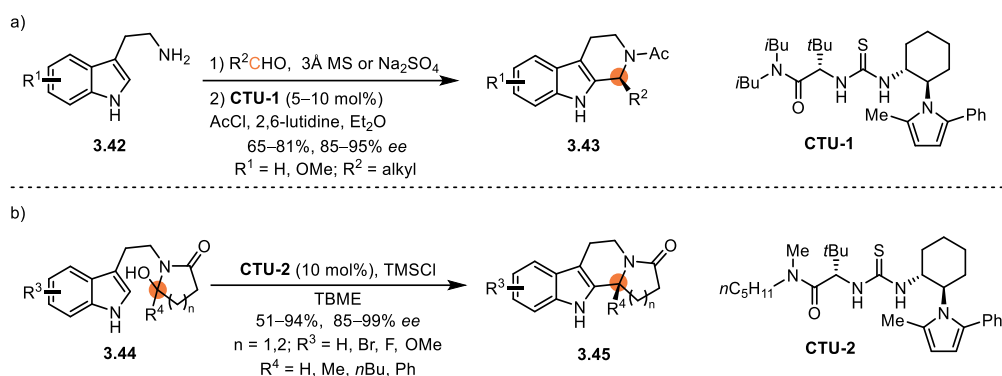
Scheme 3-4: Catalytic asymmetric Pictet–Spengler reaction of aldehydes. (continued)

Meanwhile, due to the hindrance, reactions using ketones are more challenging than those of aldehydes. Although the catalytic asymmetric Pictet–Spengler reaction of inactivated ketones is still an unexplored area, there are some examples with activated ketones. Dixon et al. utilized *N*-acyliminium ions **3.34** as highly reactive intermediates to realize **CPA-3** catalyzed asymmetric Pictet–Spengler reactions between tryptamines **3.32** and enol lactones **3.33** (Scheme 3–5a).^[229a] As a long preparation of the enol lactones **3.33** hampered the application, the use of keto esters/acids **3.37** circumvented such drawback later (Scheme 3–5b).^[229b] Both systems could achieve decent yields and enantioselectivities. Additionally, by employing tryptamines **3.39** and isatins **3.40**, diverse enantioenriched ispiroindolinones **3.41** with spirocyclic quaternary chiral center could be obtained with up to 95% *ee* (Scheme 3–5c).



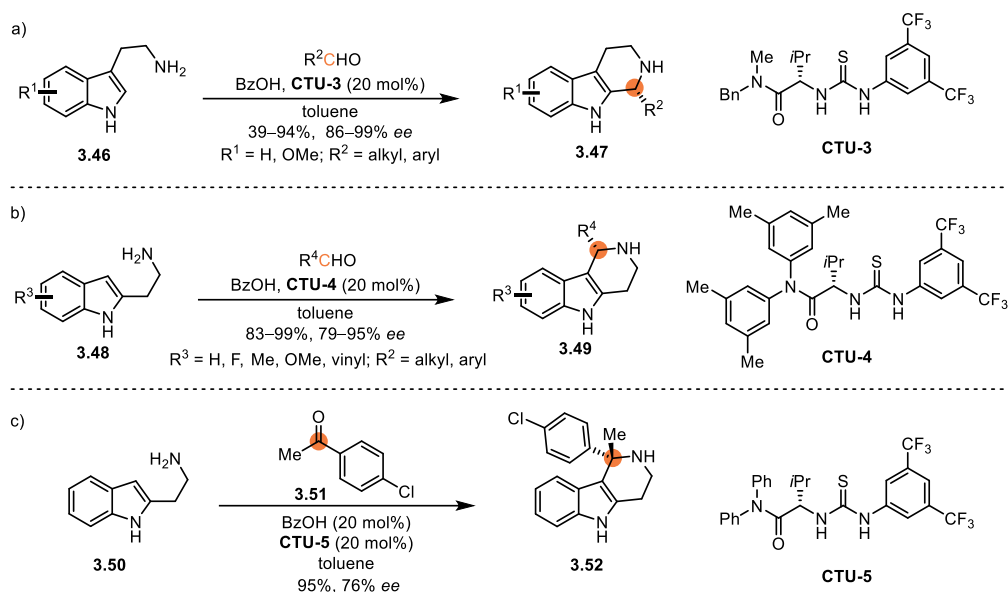
Scheme 3-5: Catalytic asymmetric Pictet–Spengler reaction of ketones.

According to the activation mode, all the examples mentioned above could be classified as the asymmetric counteranion directed catalysis (ACDC),^[230] which usually needed a stronger chiral acid, such as chiral phosphoric acid, to activate the imine. Besides the ACDC activation mode, the ion pair binding activation through weaker hydrogen bond was explored by Jacobsen et al. Since hydrogen bond is a weak non-covalent interaction, a highly reactive cationic reaction partner is demanded. *N*-acyliminium ion^[231] was a better choice, compared with the normal iminium ion. By utilizing *N*-acyliminium ions, chiral thiourea **CTU-1** and **CTU-2** could catalyze the corresponding asymmetric Pictet–Spengler reactions with up to 95% *ee*. The *N*-acyliminium ion was prepared either through an in situ fashion by treating the imine with acetic chloride or by the elimination of hydroxylactams **3.44** (Scheme 3–6).^[159, 232]



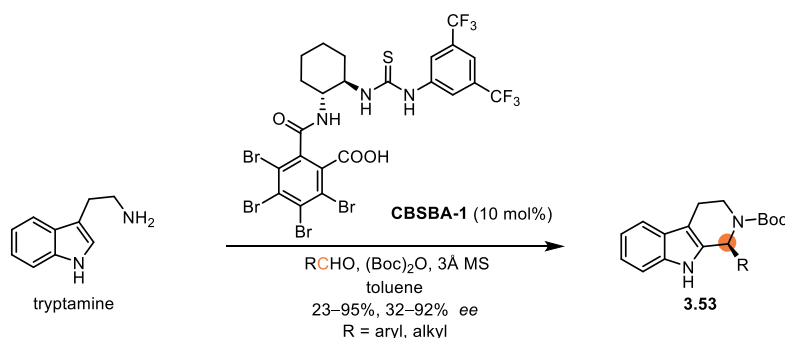
Scheme 3–6: Thiourea catalyzed asymmetric Pictet–Spengler reactions.

Although the reactions using *N*-acyliminium ions and chiral thioureas could construct the enantioenriched tetrahydro- β -carboline, cleavage of the *N*-acetyl group turned out to be difficult^[228b] and the preparation of hydroxylactams **3.44** needed a long synthetic procedure.^[159] To overcome such drawbacks, Jacobsen et al. developed a cocatalyst system using chiral thiourea and benzoic acid to realize an asymmetric Pictet–Spengler reaction catalyzed by **CTU-3** and an *iso*-Pictet–Spengler reaction catalyzed by **CTU-4** (Scheme 3–7a and b). It is noteworthy that the unfunctionalized aromatic ketone **3.51** could also undergo the *iso*-Pictet–Spengler reaction with good enantioselectivity (76% *ee*) (Scheme 3–7c).^[233] Recently, the detailed mechanism of such cocatalyst system was revealed.^[234] The key is the anion-binding interaction to stabilize the pentahydro- β -carbolinium ion intermediate, as well as multiple hydrogen-bonding interaction by differential π – π and C–H– π interactions to mediate enantio-induction.



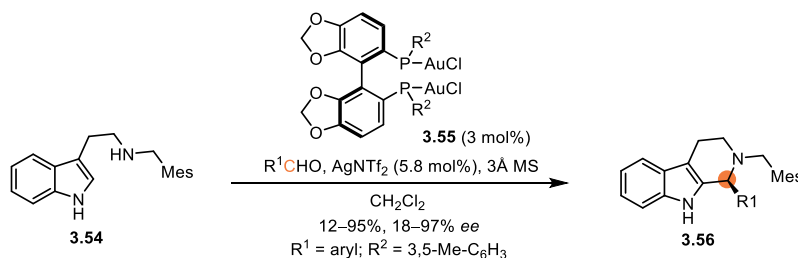
Scheme 3–7: Thiourea–benzoic acid system in asymmetric Pictet–Spengler reactions.

Beyond the ACDC and ion pair activation mode, Seidel et al. developed a conjugate base stabilized Brønsted acid strategy which also achieved catalytic enantioselective Pictet–Spengler reactions (Scheme 3–8).^[235]



Scheme 3–8: CBSBA in asymmetric Pictet–Spengler reactions.

The first organometallic asymmetric Pictet–Spengler reaction was reported in 2019. Guinchard et al. demonstrated that chiral Au(I) complex **3.55** could efficiently catalyze enantioselective Pictet–Spengler reaction of tryptamine derivative **3.54**.^[236]



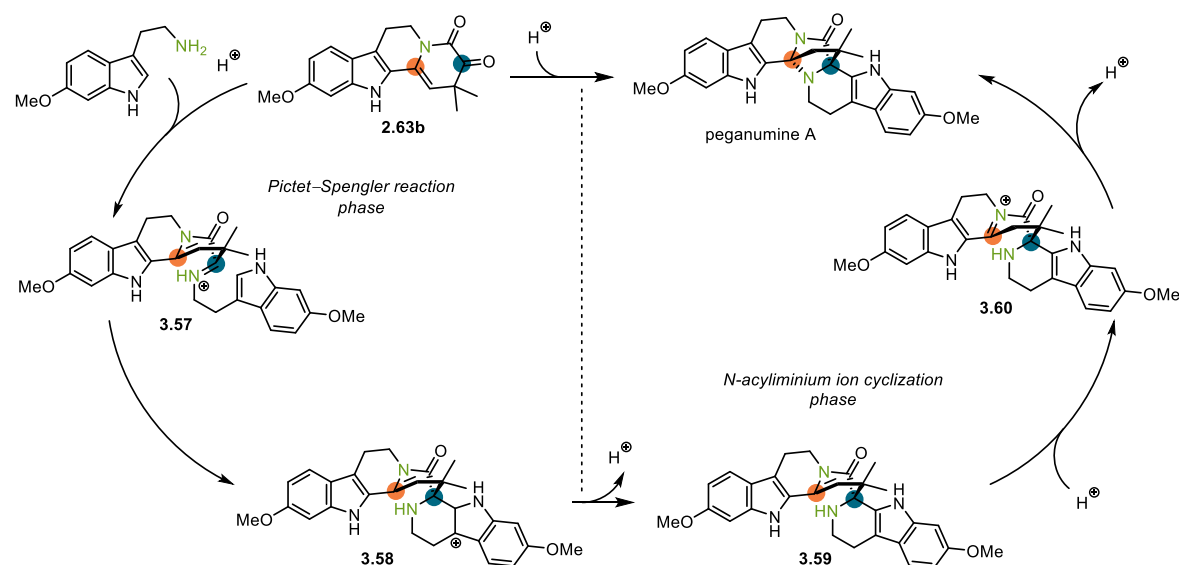
Scheme 3–9: Au(I) catalyzed asymmetric Pictet–Spengler reaction.

In summary, the asymmetric Pictet–Spengler reaction could be achieved in either auxiliary group assisted or catalytic fashion. The catalytic enantioselective reactions were realized by ACDC, ion pair and organometallic activation modes. To date, the asymmetric Pictet–Spengler reaction of aldehydes is fruitful through diverse activation mode with various catalysts. In contrast, the reaction of ketones, especially unfunctionalized ketones, is still less explored.

3.2. Asymmetric total synthesis of peganumine A

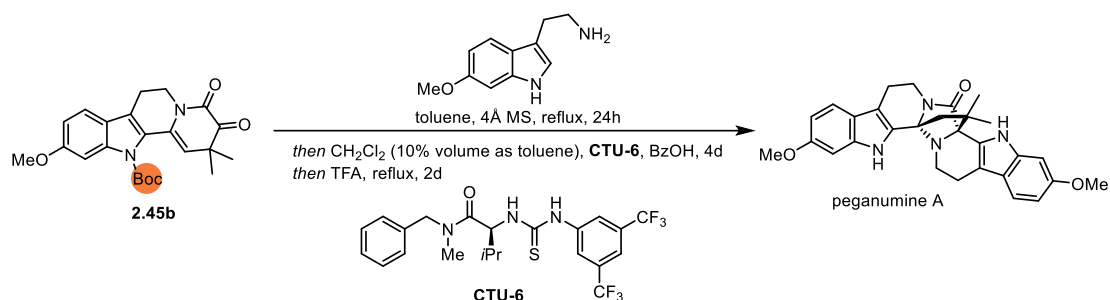
3.2.1. Analysis of the key cascade reaction

In the 3rd generation improved synthesis, both quaternary chiral centers of peganumine A were constructed through the Pictet–Spengler reaction and an *N*-acyliminium ion amination cascade of α -ketoenamide **2.63b** and 6-methoxytryptamine. The similar DFT calculation in section “2.2.2.6. Comparison between the α -ketolactam and the α -ketoenamide” indicated that the Pictet–Spengler reaction of iminium **3.57** followed a classic Friedel–Crafts electrophilic reaction mechanism. Since the facial selectivity of the *N*-acyliminium ion amination was fixed by the spiro C1 center of **3.59**, the chiral center of C1' was determined by the C1 quaternary chiral center generated by the Pictet–Spengler reaction. Therefore, the foundation of the asymmetric total synthesis of peganumine A was the enantioselective Pictet–Spengler reaction between α -ketoenamide **2.63b** and 6-methoxytryptamine.



Scheme 3–10: Analysis of the key cascade reaction.

According to the previous overview of asymmetric Pictet–Spengler reactions, generally three types of activation were developed. As the organometallic activation mode limited to simple aromatic aldehydes, the ion pair binding and ACDC activation modes were investigated first. In addition, Zhu et al. applied a thiourea and Brønsted acid cocatalyst system in their elegant total synthesis achieving 92% *ee* with Boc-protected substrate **2.45b**.^[209]



Scheme 3–11: Thiourea catalyzed asymmetric Pictet–Spengler reaction by Zhu et al.

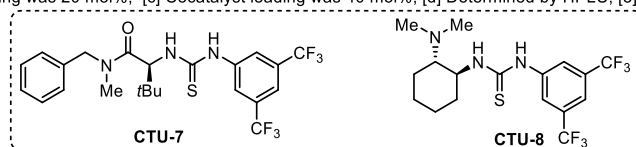
3.2.2. Initial investigation of the asymmetric Pictet–Spengler reaction cascade

Inspired by the elegant synthesis of Zhu et al., the thiourea system was initially investigated.^[233a] Surprisingly, with the chiral thiourea, the resulting enantioselectivity was only 9.2% *ee* for the protection group free substrate **2.63b** (Table 3–1, entry 2). Although the reaction parameters were optimized concerning cocatalyst loading (entry 4), cocatalyst (entries 6 and 7), solvent (entry 5) and temperature (entry 1), only slight increase of the enantioselectivity was achieved.

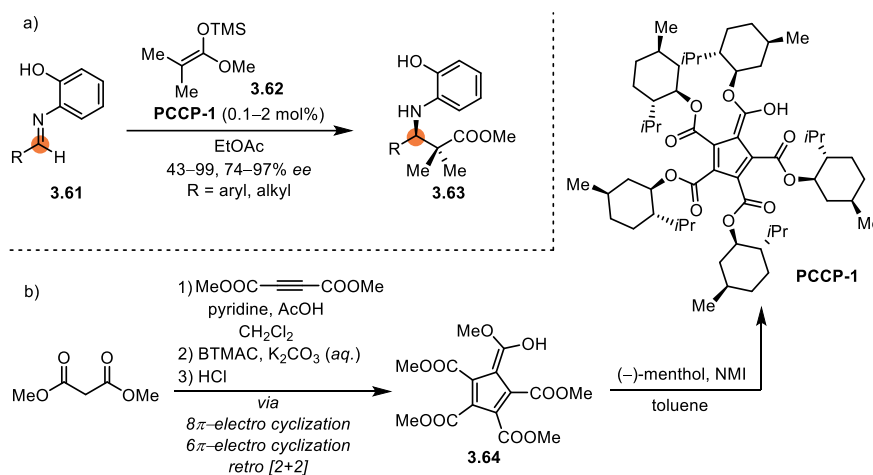
Table 3–1: Initial screening of asymmetric Pictet–Spengler reaction by chiral thioureas.

entry ^[a]	catalyst	cocatalyst ^[b]	additional solvent	T [°C]	<i>ee</i> [%] ^[d]	yield [%] ^[e]
1	CTU-7	BzOH	toluene	90	12.2	35
2	CTU-7	BzOH	CH ₂ Cl ₂	35	9.2	27
3	CTU-8	BzOH	CH ₂ Cl ₂	35	1.8	18
4	CTU-7	BzOH ^[c]	CH ₂ Cl ₂	35	1.2	33
5	CTU-7	BzOH	hexane	35	1.8	36
6	CTU-7	4-NO ₂ -BzOH	CH ₂ Cl ₂	35	2.8	33
7	CTU-7	TFA	CH ₂ Cl ₂	35	1.8	11

[a] Reactions were performed with ketolactam (1.0 mg, 3 μmol, 1.0 equiv.), 6-methoxytryptamine (0.75 mg, 4 μmol 1.2 equiv.); [b] Cocatalyst loading was 20 mol%; [c] Cocatalyst loading was 40 mol%; [d] Determined by HPLC; [e] Isolated yield

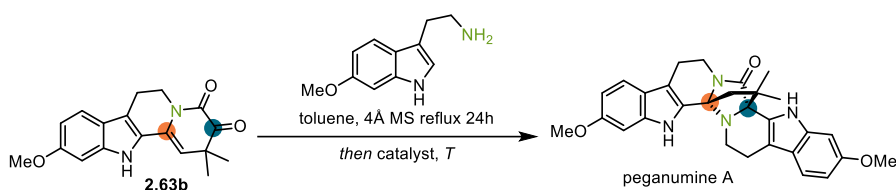


This difference could be attributed to the impaired recognition between the substrate and the catalyst which proposed the free indole N–H interrupted the substrate binding. Based on this consideration, it was anticipated that the multi-binding-site catalysts could enhance the stability of the transition state by anchoring the free N–H. Besides the conjugate-base-stabilized Brønsted acid (CBSBA) developed by Seidel et al.,^[237] Lambert et al. discovered a novel C–H acid, utilizing a 1,2,3,4,5-pentacarboxycyclopentadiene (PCCP) scaffold as the backbone and (–)-menthol as the chiral motif.^[238] **CBSBA-1** has already applied to catalytic enantioselective Pictet–Spengler reactions (Scheme 3–8). **PCCP-1** could catalyze enantioselective Mukaiyama–Mannich reaction of imines **3.60** and silyl enol ether **3.61** which was also through an iminium ion intermediate (Scheme 3–12a). **PCCP-1** could be prepared by a one-pot procedure from dimethyl malonate (Scheme 3–12b).^[239]



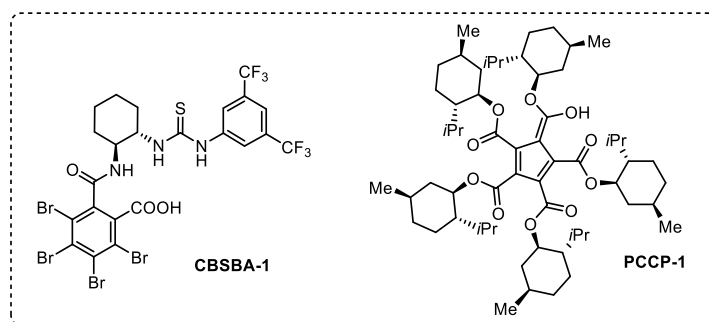
Scheme 3–12: PCCP catalyzed Mukaiyama–Mannich reaction and its preparation.

Inspired by these novel chiral Brønsted acids, the application of multi-binding-site catalyst in the Pictet–Spengler reaction cascade was investigated. The initial screening of these two catalysts showed that **PCCP-1** was able to catalyze the cascade reaction (Table 3–2, entry 3). Inspired by this result, the cascade reaction catalyzed by **PCCP-1** was optimized in the aspect of catalyst loading (entries 8–11). Although the reactions afforded moderate yields, the *ee* value of these reactions were less than 10%. Due to the importance of solvent for such non-covalent interaction, different types of solvent were also screened. Unfortunately, other solvents still turned out to be ineffective to the cascade reaction (entries 12–19).

Table 3-2: Screening of multi-binding-site catalysts.

entry ^[a]	catalyst [mol%]	solvent	T [°C]	time	yield ^[b]
1	PCCP-1 (10)	toluene	23	66h	recovery of SM ^[c]
2	PCCP-1 (10)	toluene	60	66h	recovery of SM
3	PCCP-1 (10)	toluene	110	66h	trace
4	PCCP-1 (20)	toluene	60	66h	recovery of SM
5	CBSBA-1 (20)	toluene	23	66h	recovery of SM
6	CBSBA-1 (20)	toluene	80	66h	recovery of SM
7	CBSBA-1 (20)	toluene	110	66h	recovery of SM
8	PCCP-1 (20)	toluene	110	6d	44%, 3.9% <i>ee</i>
9	PCCP-1 (50)	toluene	110	6d	40%, 3.7% <i>ee</i>
10	PCCP-1 (80)	toluene	110	6d	N.D. ^[d]
11	PCCP-1 (20), BzOH (20)	toluene	110	6d	41%, 6.4% <i>ee</i>
12	PCCP-1 (50)	toluene	80	4d	recovery of SM
13	PCCP-1 (50)	PhH	80	4d	recovery of SM
14	PCCP-1 (50)	dioxane	80	4d	recovery of SM
15	PCCP-1 (50)	EtOAc	80	4d	recovery of SM
16	PCCP-1 (50)	DCE	80	4d	recovery of SM
17	PCCP-1 (50)	PhCF ₃	80	4d	recovery of SM
18	PCCP-1 (50)	CHCl ₃	60	4d	recovery of SM
19	PCCP-1 (50)	C ₆ F ₁₄	60	4d	recovery of SM

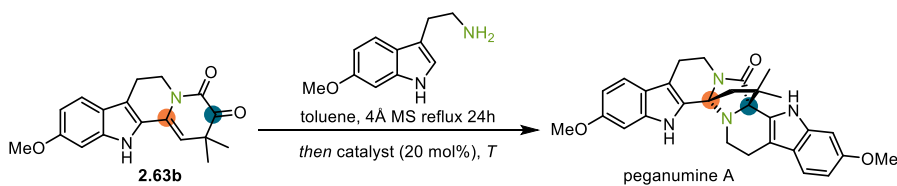
[a] Reactions were performed with ketolactam (1.0 mg, 3 μ mol, 1.0 equiv.), 6-methoxytryptamine (0.75 mg, 4 μ mol, 1.2 equiv.); [b] Isolated yield; [c] SM=starting material; [d] N.D. = not determined



As it was unsuccessful to utilize the ion pair binding activation mode by thiourea and multi-binding-site catalysts, the attention was switched to the ADAC strategy. The optimization was started with chiral phosphoric acids due to their wide utilization. The screening of different CPAs showed that BINOL was a better backbone compared to VAPOL (Table 3-3, entries 1–8). Since the BINOL derived CPAs afforded relatively same results, **CPA-1** was selected for further optimization due to its wide applications. After screening the reaction temperature (entries 9–13), an improved enantioselectivity was obtained with 31.0% *ee* (entry 9), which proved that the ADAC strategy was a promising direction for the catalytic enantioselective Pictet–Spengler reaction cascade. Next, the solvent was also screened, but it turned out to be no remarkable improvement (entries 9–15).

3.2. Asymmetric total synthesis of peganumine A

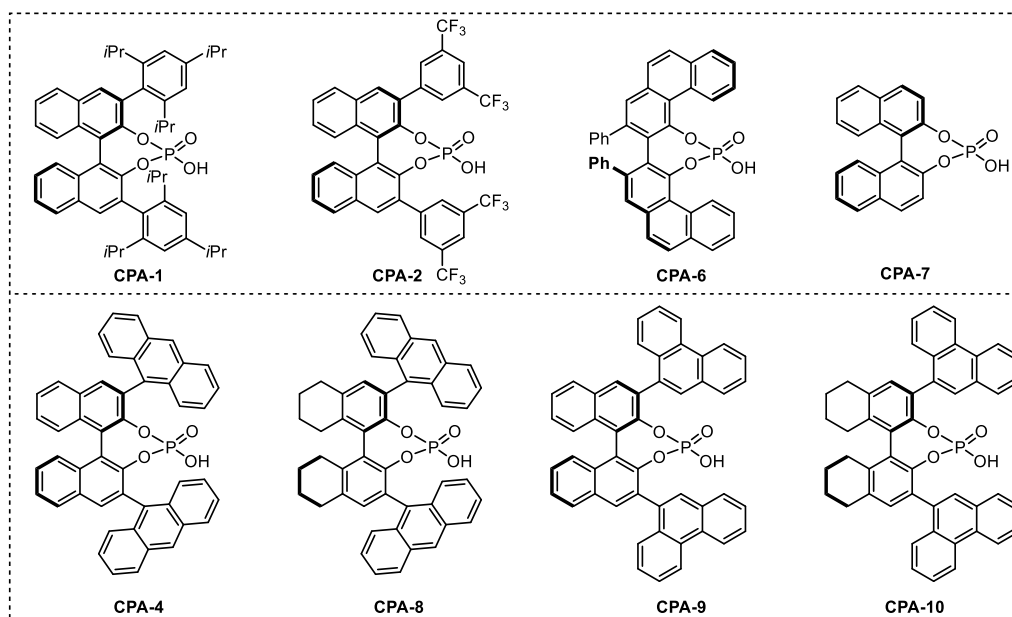
Table 3–3: Screening of chiral phosphoric acids.



entry ^[a]	catalyst	solvent	T [°C]	ee [%] ^[b]	yield [%] ^[c]
1	CPA-1	toluene	110	10.0	32
2	CPA-2	toluene	110	9.8	33
3	CPA-4	toluene	110	10.0	33
4	CPA-6	toluene	110	4.2	42
5	CPA-7	toluene	110	0.8	0.8
6	CPA-8	toluene	110	9.8	26
7	CPA-9	toluene	110	9.4	18
8	CPA-10	toluene	110	9.6	37

9	CPA-1	toluene	90	31.0	60
10	CPA-1	toluene	70	19.6	50
11	CPA-1	toluene	50	11.6	40
12	CPA-1	toluene	-26	3.0	46
13	CPA-1	toluene	23	2.7	59
14	CPA-1	DMF	23	4.4	24
15	CPA-1	CH ₂ Cl ₂	23	7.3	51
16	CPA-1	THF	23	3.0	64
17	CPA-1	1,4-dioxane	23	3.4	41

[a] Reactions were performed with ketolactam (1.0 mg, 3 μmol, 1.0 equiv.), 6-methoxytryptamine (0.75 mg, 4 μmol, 1.2 equiv.); [b] ee was determined by HPLC; [c] Isolated yield;



3.2.3. Study of the asymmetric Pictet–Spengler reaction cascade by ACDC

Asymmetric counteranion directed catalysis (ACDC) is a useful strategy for organic synthesis.^[230] Based on this concept, catalytic reactions that proceed via cationic intermediates can be conducted asymmetrically by using a chiral counteranion. List et al. proposed and utilized this strategy in organocatalysis and achieved remarkable enantioselectivities in many asymmetric transformations.^[230e-g, 230i] The enantioselectivity of these reactions are derived from

the confined chiral pocket of the corresponding counteranion.^[240] Such pocket contains spatially distributed reactive functional groups over nanometer dimensions within the catalyst framework enabling excellent stabilizing of transition state and reaction selectivity.^[241] Meanwhile, high acidity is also a pivotal element in asymmetric catalysis, rendering the catalyst robust for the activation of basic electrophiles.^[242] Therefore, the enantioselectivity and yield of the ACDC based catalytic asymmetric reaction are mainly determined by the confinement and acidity of the chiral Brønsted acid.

Based on these considerations, the promising improvement achieved by **CPA-1** could be attributed to the proper acidity and confinement (Figure 3–1a). The phosphoric acid core could interact with the iminium ion through ACDC. The BINOL scaffold could provide a proper confinement, and the π – π stackings were able to stabilize the favored transition state, which all led to good enantioselectivity.

In contrast, it was proposed that the active pocket of the multi-binding-site catalyst **PCCP-1** was too crowded, as the PCCP motif was based on a five-membered ring (Figure 3–1b). In addition, the lack of aromatic ring system made the corresponding transition state of **PCCP-1** catalyzed reaction less stable. The extra ester groups could also interrupt the favored hydrogen bonding interactions (Figure 3–1b). For the thiourea–benzoic acid system and **CBSBA-1**, the acidity was based on the benzoic acid or the carboxyl group, which turned out to be insufficient to promote the cascade reaction. Meanwhile, as the chiral confined sites of the thiourea–benzoic acid system and **CBSBA-1** were all flexible, the favored conformation of the transition states could not be stabilized leading to low enantioselectivities (Figure 3–1c and d).

Therefore, it was proposed that stronger acidity was needed to activate the imine of the Pictet–Spengler reaction cascade and proper chiral confinement was also demanded for the enantioselectivity of the Friedel–Crafts type reaction of the iminium ion. Although the acidity and confinement of **CPA-1** led to the promising yield, the enantioselectivity still needed to be improved. According to these hypotheses, proper acidity and confinement were the key factors to discover a catalyst to afford increased the yield and enantioselectivity.

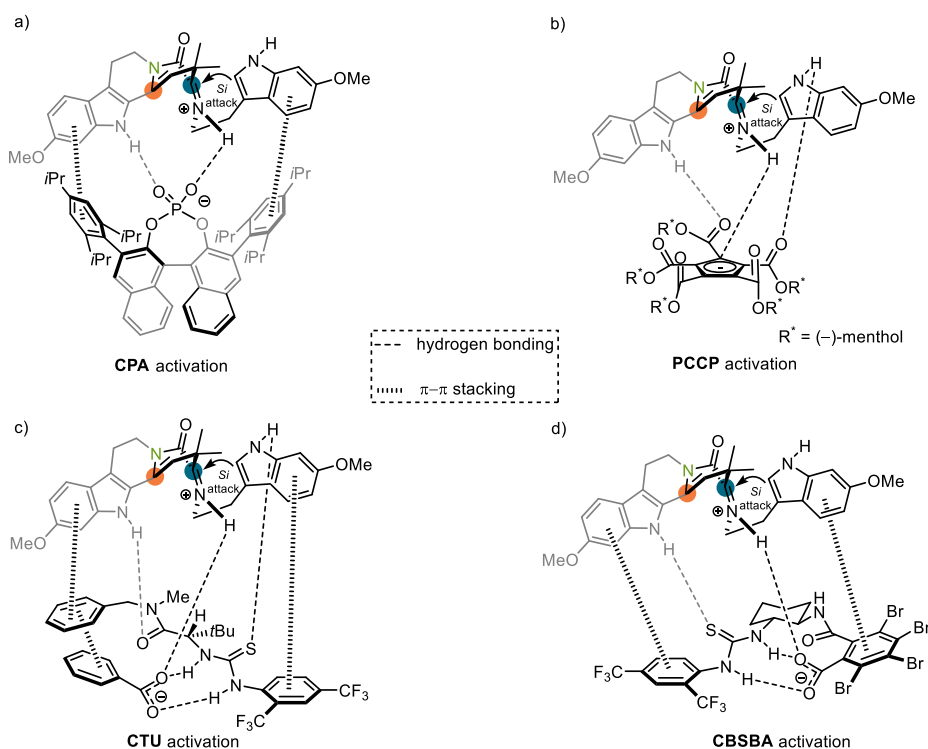


Figure 3–1: Proposed activation modes of different catalysis systems.

A variety of chiral Brønsted acids were developed, since Akiyama et al.^[130] and Terada et al.^[131] independently reported the pioneering applications of the chiral phosphoric acids to catalyze C–C bond forming reactions. Besides diverse chiral phosphoric acids,^[132] chiral dicarboxylic acids (DCAs),^[133] *N*-triflylphosphoramides (NTPAs)^[135] and bis(sulfuryl)imides (JINGLES)^[137] were invented (Figure 3–2). In addition, List et al. made a great contribution to this area. They developed chiral disulfonimides (DSIs),^[138] *N,N'*-bistriflylphosphoramidimidates (NBPIs),^[136] binaphthyl-allyl-tetrasulfones (BALTs)^[139] and *N*-phosphinyl phosphoramides (NPPAs)^[243] as the mono-BINOL unit catalysts. For the dual-BINOL units catalysts, they designed imidodiphosphates (IDPs),^[140] imino-imidodiphosphate (iIDPs),^[141] imidodiphosphorimidates (IDPis).^[142]

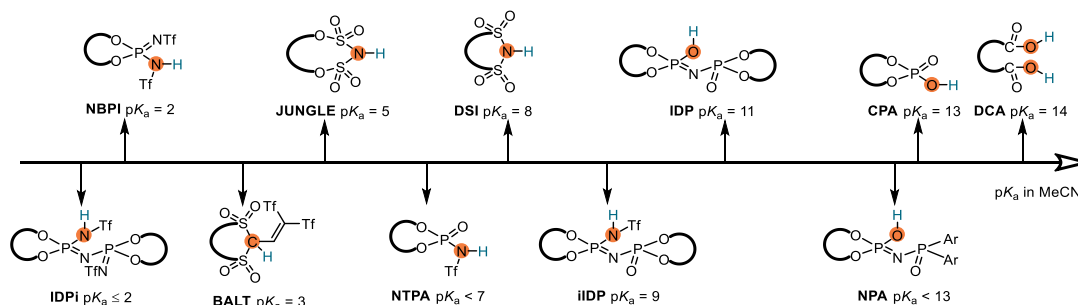


Figure 3–2: pK_a trend of Brønsted acids in MeCN.

Meanwhile, the chirality of the catalysts is derived from the chiral backbones, which could be classified as 1,1'-bi-2-naphthol (BINOL), octahydro-1,1'-bi-2-naphthol (H₈-BINOL), 1,1'-spirobiindane-7,7'-diol (SPINOL), vaulted 3,3'-biphenanthrol (VAPOL) and biphenyl (BP) (Figure 3–3). Due to the advantages, such as easier to functionalize and control the conformation, BINOL is the most frequently used chiral backbone.

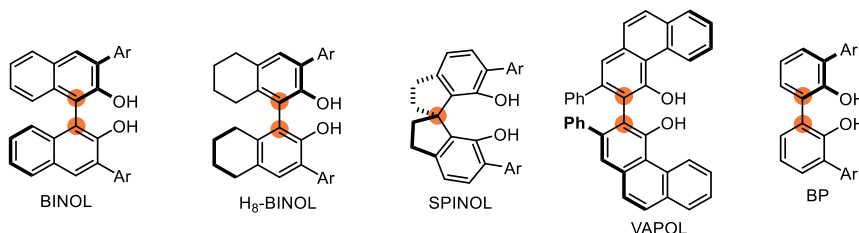


Figure 3–3: Typical backbones of chiral Brønsted acids.

The initial selection of diverse Brønsted acid catalysts included an acidic mono-BINOL unit catalyst—DSI^[138] and two types of dual-BINOL units catalysts—IDP^[140] and IDP_i^[142] with various substitutes (Figure 3–4). A special of type mono-BINOL unit catalyst, namely NPPA,^[243] was also chosen. The NPPA contains a same core as IDP but with one side BINOL unit and bisaryl substitutes at the other side. This unique characteristic contributed the confinement of NPPA in the middle of mono-BINOL unit catalyst and dual-BINOL unit catalyst.

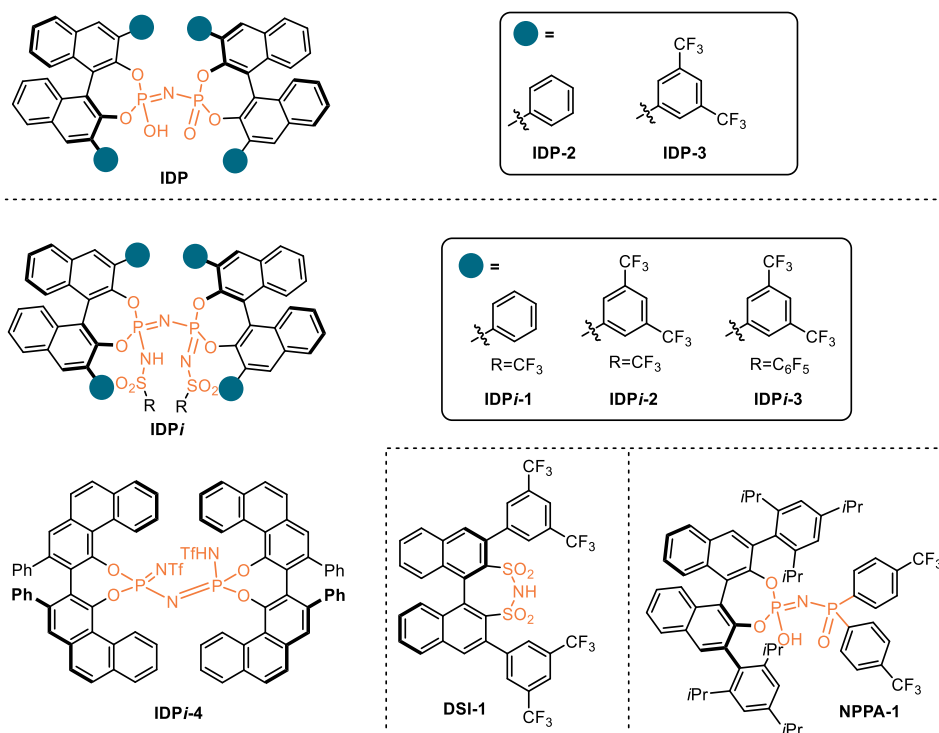
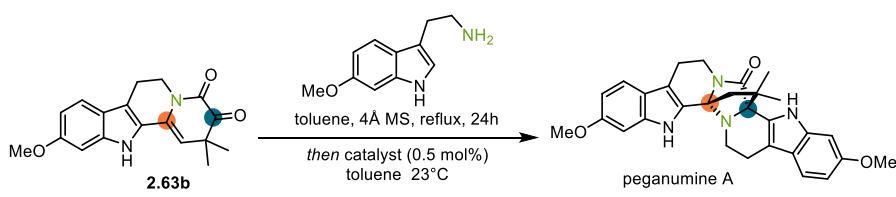


Figure 3–4: The catalyst selection of the first round screening.

Initially, the experiment was followed the same one-pot procedure as before, which was conducted in the sequence: the imine formation at neutral condition, then the addition of the corresponding chiral Brønsted acid to the reaction mixture. Surprisingly, the reactions furnished no enantioselectivity, but resulted in relatively good yields even at room temperature with 0.5 mol% catalyst loading (Table 3–4). This could be attributed to the strong acidity of these catalysts, which promoted the reaction too efficiently to decimate the enantioselectivity.

Table 3–4: Screening of novel chiral Brønsted acids by one-pot procedure.



entry ^[a]	catalyst	ee [%] ^[b]	yield [%] ^[c]
1	IDPi-1	0	82
2	IDPi-2	0	30
3	IDPi-3	0	33
4	IDPi-4	0.4	19
5	IDP-2	0.4	35
6	IDP-3	1	26
7	NTPA-1	0.6	19
8	NTPA-2	0.6	14
9	NPPA-1	0.8	100
10	DSI-1	0	20

[a] Reactions were performed with ketolactam (1.0 mg, 3 μ mol, 1.0 equiv.), 6-methoxytryptamine (0.75 mg, 4 μ mol, 1.2 equiv.); [b] ee was determined by HPLC; [c] Isolated yield;

It seemed to be a dilemma that the less acidic chiral thiourea could not promote the reaction efficiently, moderate acidic chiral phosphoric acids could afford improved enantioselectivity and yield, but more acidic chiral Brønsted acid devastated the enantioselectivity in high yield. It was hypothesized, the enantioselectivity of the reaction following one-pot imine preformation procedure should be determined by the ion pair between the iminium ion and the counteranion of the chiral Brønsted acid (Figure 3–5a). But it was considered that such complex tended to be separated by the increasing of acidity, as a more stable anion led to a less tight ion pair.^[230h-k] Meanwhile, it was envisioned that the reaction could undergo through a bifunctional activation mode leading to an amine–ketone–chiral Brønsted acid complex, if a cascade procedure was utilized (Figure 3–5b). Such complex could pre-organize the favored position of the substrates spatially, which would be beneficial for the enantioselectivity. In addition, compared to the one-

pot procedure, the cascade procedure^[244] precludes the addition of new reagents making the reaction easier to manipulate.

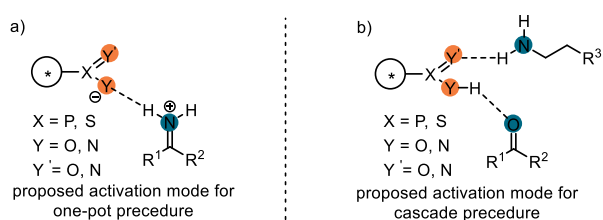
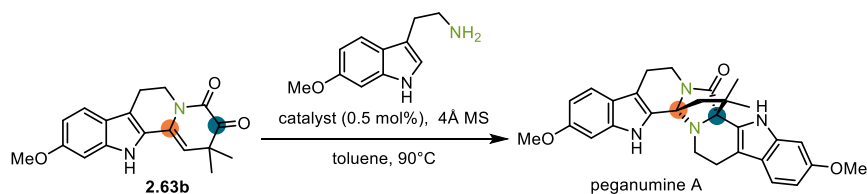


Figure 3–5: Proposed activation modes for asymmetric Pictet–Spengler reaction.

Based on this hypothesis, the exploration of the asymmetric Pictet–Spengler reaction in a cascade fashion was commenced. Indeed, a remarkable improvement of the enantioselectivity was obtained with 50.4% *ee* (Table 3–5, entry 9). It is noteworthy that the reaction needed higher temperature by the cascade procedure.

Table 3–5: First screening of novel chiral Brønsted acids by cascade procedure.



entry ^[a]	catalyst	<i>ee</i> [%] ^[b]	yield [%] ^[c]
1	IDPi-1	N.D. ^[d]	trace
2	IDPi-2	3	15
3	IDPi-3	0.6	62
4	IDPi-4	0.2	18
5	IDP-2	2	10
6	IDP-3	5	6
7	NTPA-1	1.6	10
8	NTPA-2	0	8
9	NPPA-1	50.4	18
10	DSI-1	3	29

[a] Reactions were performed with ketolactam (1.0 mg, 3 μmol , 1.0 equiv.), 6-methoxytryptamine (0.75 mg, 4 μmol , 1.2 equiv.); [b] *ee* was determined by HPLC; [c] Isolated yield; [d] not determined

Additional catalysts were selected for the 2nd round screening (Figure 3–6). **iIDP** is a dual-BINOL-unit catalyst, which can be considered as a hybrid of IDP and IDPi, regarding the acidity and confinement. It has been demonstrated more acidic than IDP.^[141] Considering the diversity of the chiral backbone, the dual-VAPOL-unit IDPis were also chosen. **IDP-5** was also selected, containing a less confined active site. In order to cover a large pK_a range, the highly acidic *N,N'*-bistriflylphosphoramidimidates (NBPIs)^[136] and binaphthyl-allyl-tetrasulfone (BALT)^[139] were also selected. Since **NPPA-1** showed an improved result, a less acidic **NPPA-2** was also planned to test.

3.2. Asymmetric total synthesis of peganumine A

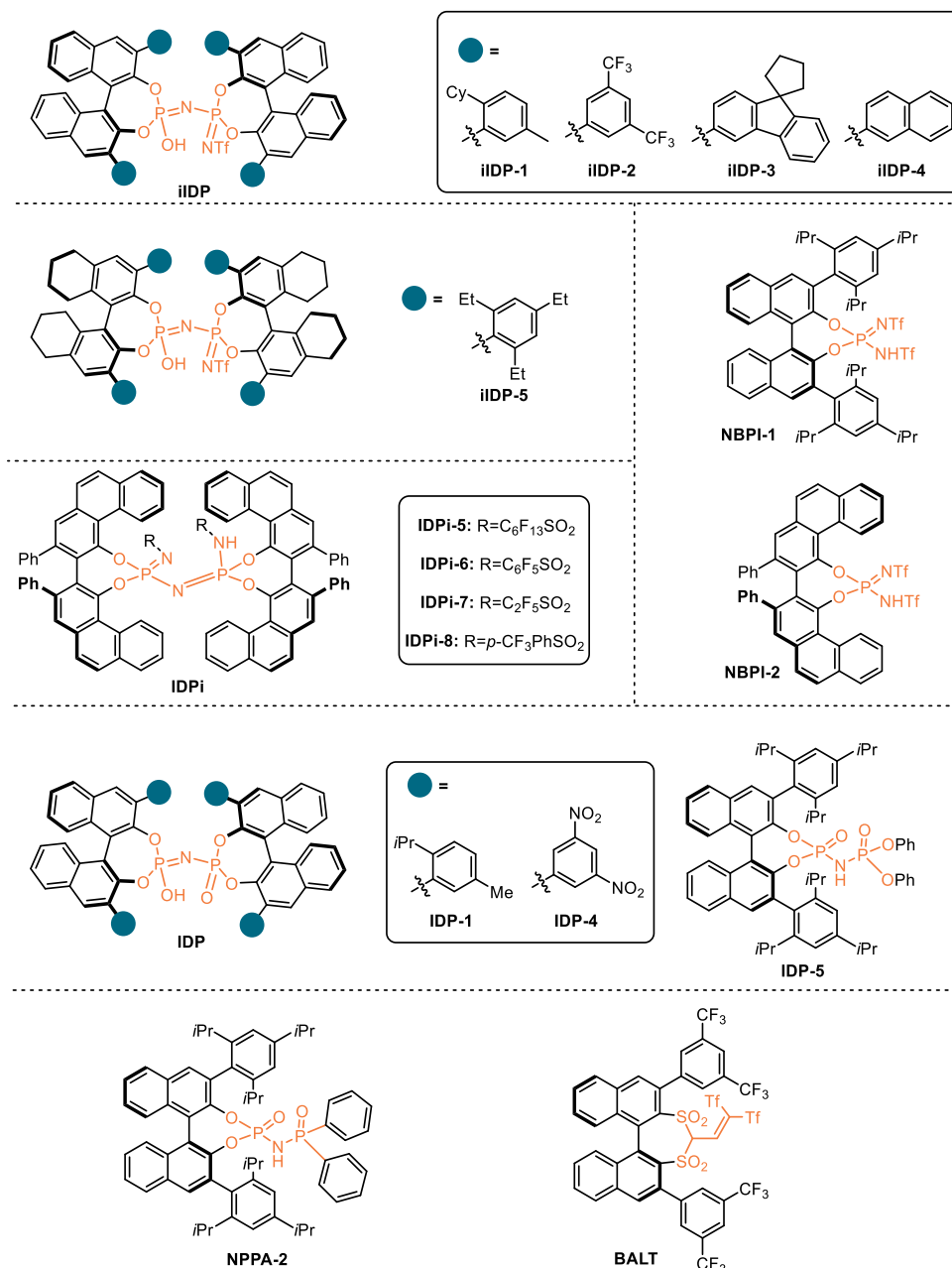
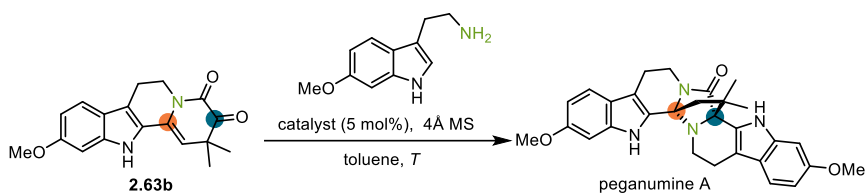


Figure 3–6: Additional catalysts selection for the screening.

The 2nd round screening was launched with 5 mol% catalyst loading. With the iIDPs (Table 3–6, entries 14–18), the reactions furnished the enantioselectivity up to 39.2% *ee*, which was obtained by iIDP-3 (entry 16). For the more acidic IDPis (entries 1–7) and less acidic IDPs (entries 9–13), the results were not as satisfying as iIDPs. It was hypothesized that a balance existed between the acidity and confinement. The mono-BINOL-unit catalysts afforded an acidity-dependent result. The more acidic NPBIs (entries 19–20) and BALT (entry 21) yielded nearly racemic product. In contrast, relatively less acidic NPPAs (entries 22–23) and DSI (entry 24) achieved the promising enantioselectivities (75.2–85.2% *ee*).

Table 3–6: 2nd screening of novel chiral Brønsted acids by cascade procedure.

entry ^[a]	catalyst	T [°C]	ee [%] ^[b]	yield [%] ^[c]
1	IDPi-1	90	N.D. ^[d]	trace
2	IDPi-2	90	3.0	8
3	IDPi-3	90	1.0	52
4	IDPi-4	90	22.8	26
5	IDPi-5	90	7.6	21
6	IDPi-6	90	N.D.	trace
7	IDPi-7	90	1.2	21
8	IDPi-8	90	5.6	18
9	IDP-1	90	20.6	19
10	IDP-2	90	0.2	26
11	IDP-3	90	0.2	53
12	IDP-4	70	12.8	15
13	IDP-5	90	35.8	60
14	iIDP-1	90	16.4	14
15	iIDP-2	90	10.8	30
16	iIDP-3	90	39.2	19
17	iIDP-4	90	0	77
18	iIDP-5	70	6.6	10
19	NBPI-1	70	0.6	19
20	NBPI-2	70	4.6	46
21	BALT	70	0.6	19
22	NPPA-2	70	85.2	86
23	NPPA-1	70	75.2	41
24	DSI-1	70	79.1	60
25	CPA-1	90	45.0	61

[a] Reactions were performed with ketolactam (1.0 mg, 3 μ mol, 1.0 equiv.), 6-methoxytryptamine (0.75 mg, 4 μ mol, 1.2 equiv.); [b] ee was determined by HPLC; [c] Isolated yield; [d] not determined

For all the mono-BINOL-unit catalysts, the best result was obtained by **DSI-1** with moderate acidity ($pK_a = 8$) (Figure 3–7). The NBPI, BALT and CPA cores resulted in low enantioselectivity, especially reactions with the highly acidic NBPI and BALT afforded racemic product. For the other catalysts, it was interesting that the best result was furnished by **NPPA-2** with less acidity ($pK_a = 13$), which is eclectic among these catalysts concerning confinement and acidity. It was hypothesized that the confinement and acidity were not independent but synergistic to influence the yield and enantioselectivity of the catalytic asymmetric Pictet–Spengler reaction cascade. If the catalyst was too confined like the IDP, iIDP and IDPi, the ion pair tended to separate, and the interaction might be inefficient between the catalyst and the substrate. Therefore, it was envisioned that the cascade reaction required moderate acidity to activate the iminium ion and proper confinement to arrange the transition state in the chiral pocket of the catalyst.

3.2. Asymmetric total synthesis of peganumine A

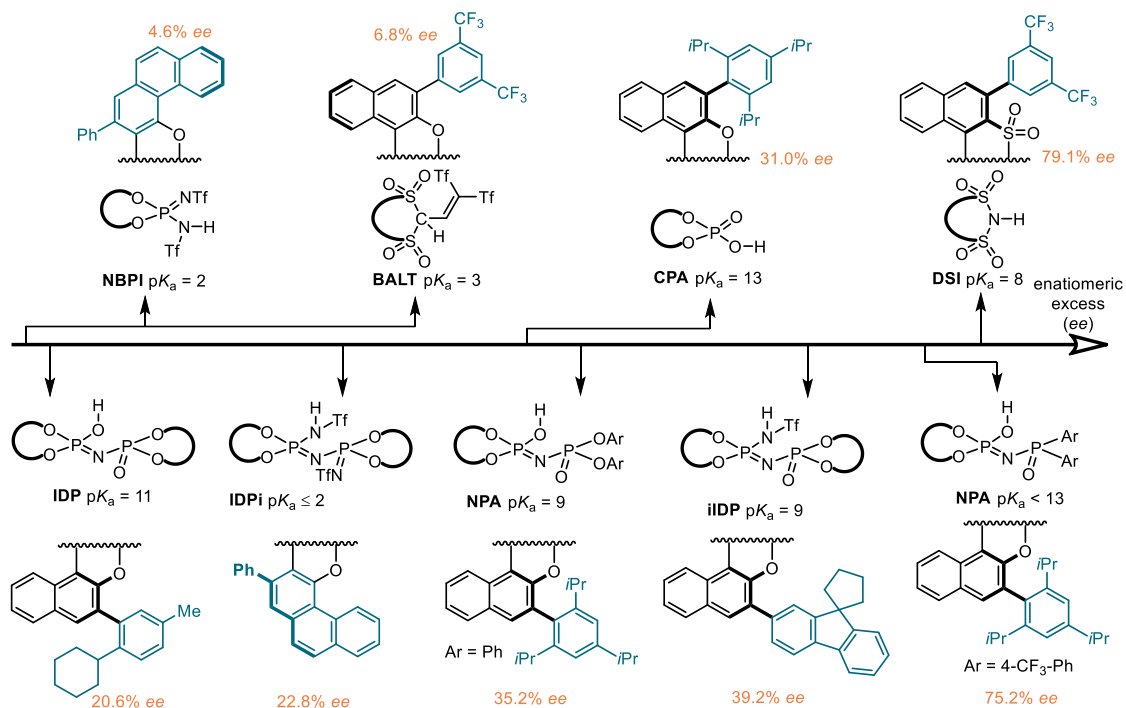
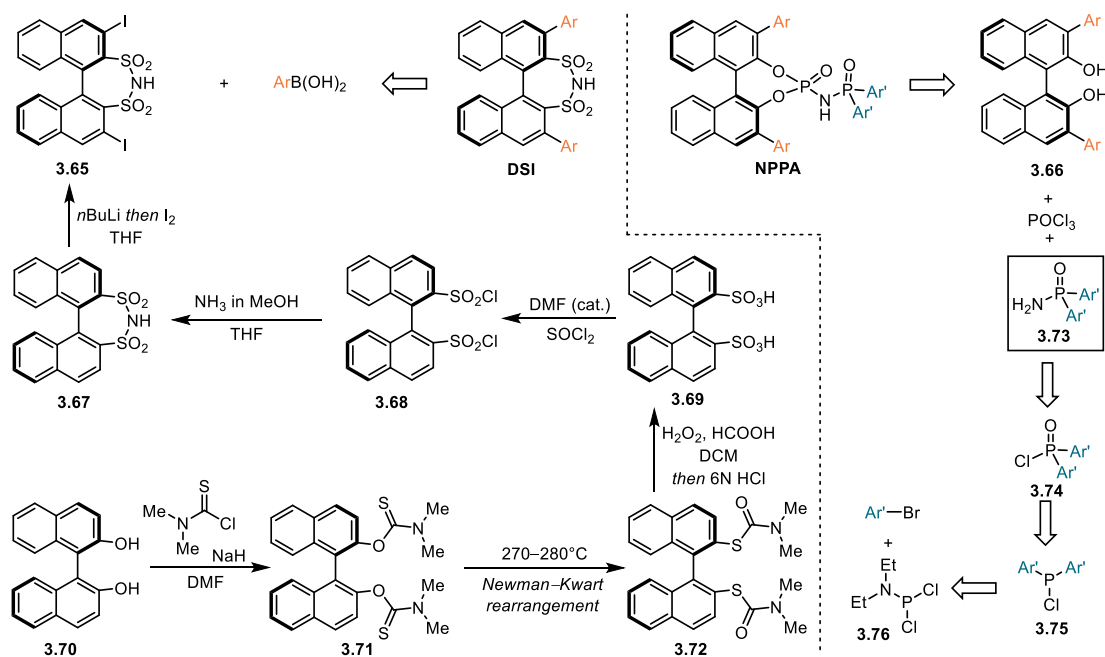


Figure 3-7: Analysis the screening result.

The selection between NPPA and DSI was needed for the further screening, due to the promising result achieved by them. Although the preparation of DSI needs 7 steps (LLS) from BINOL, and NPPA needs 5 steps (LLS), DSIs have been applied to a variety of transformations,^[138a-e, 138g-j] which renders DSI more practical for the further screening (Scheme 3-13).



Scheme 3-13: Preparation of DSI and NPPA.

To discover the best DSI for the reaction, diverse DSIs were selected, including large π system substitutes, various phenyl substitutes and long linear triple bond substitutes (Figure 3–8).

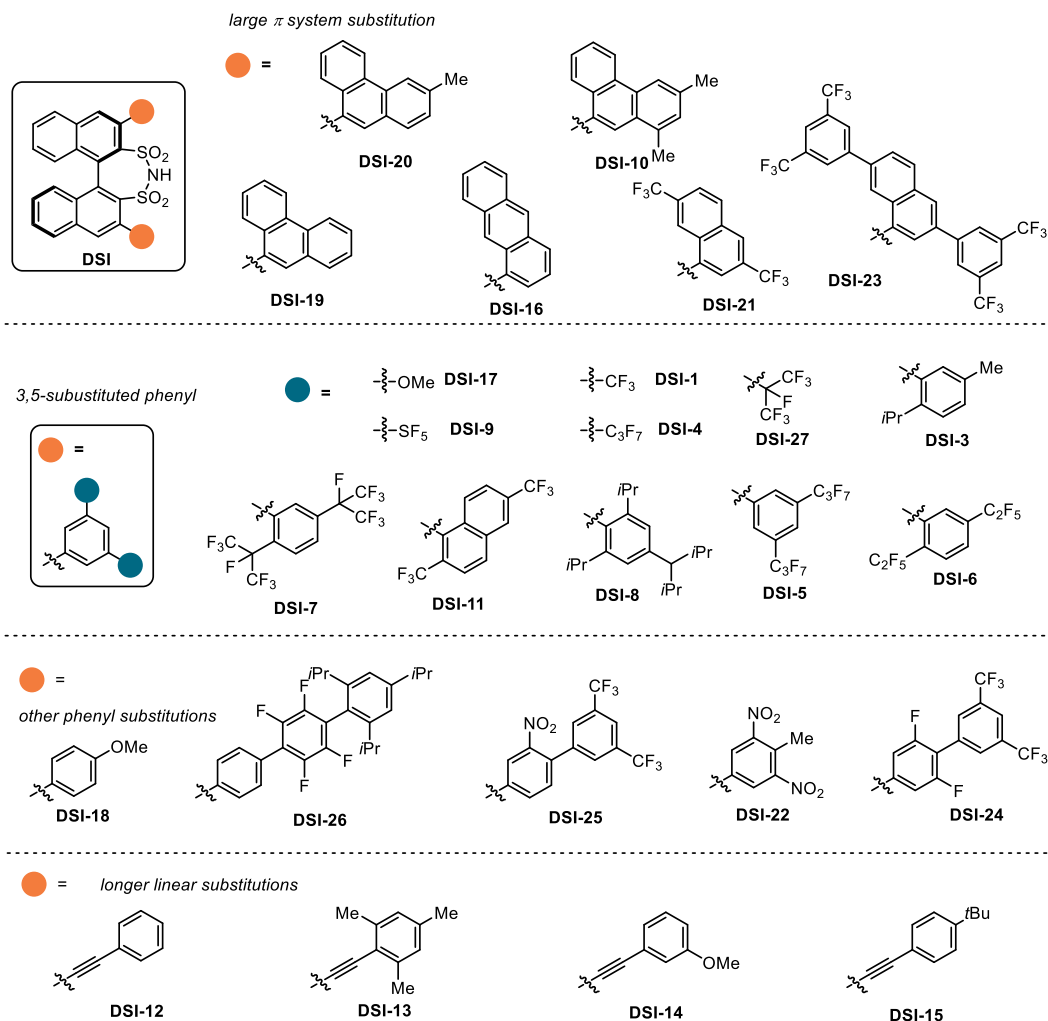


Figure 3–8: The selection of DSIs.

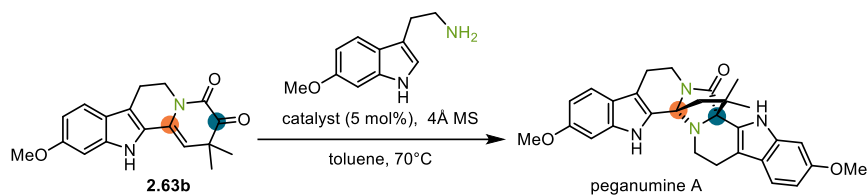
Although no better result was obtained in this screening, some tendency could be rationalized:

- 1) EWG was favored (Table 3–7, entries 3, 8, 21 and 23), and EDG was disfavored (entries 16–17), which showed the reaction was acidity demanding.
- 2) Polycyclic aromatic groups resulted in decreased enantioselectivity (entries 9, 15, 18, 19, 24 and 25), which illustrated steric π -substituents might weaken the substrate–catalyst interaction.
- 3) Long linear substitutes with carbon–carbon triple bond (entries 11–14) led to poor enantioselectivity, which also indicated the substrate was sensitive to steric hindrance.
- 4) Large functionalized phenyl group at 3,5-position could be tolerated at some degree (entries 1–2, 4–7, and 10), also EWG group was favored.
- 5) For the functionalized 1-naphthyl group, neither 4,7-substitution (entry 1) nor 3,7-

substitution (entry 22) could achieve a good result.

6) The 4-position of phenyl group was tolerated with small substitutes (entry 21), but as the size increasing, both enantioselectivity and yield were decreased (entries 24, 25 and 26).

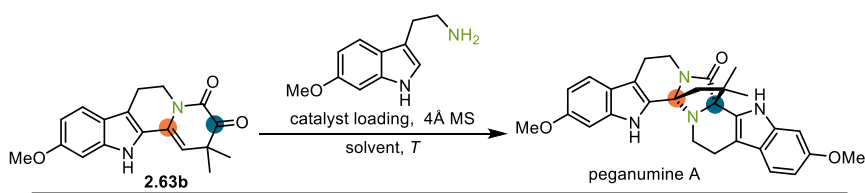
Table 3–7: First screening of DSIs.



entry ^[a]	catalyst	ee [%] ^[b]	yield [%] ^[c]
1	DSI-2	4.2	60
2	DSI-3	63.4	17
3	DSI-4	73.0	24
4	DSI-5	4.2	25
5	DSI-6	39.4	41
6	DSI-7	2.6	29
7	DSI-8	16.8	37
8	DSI-9	63.0	30
9	DSI-10	37.8	14
10	DSI-11	66.4	40
11	DSI-12	8.6	50
12	DSI-13	21.8	9
13	DSI-14	33.8	31
14	DSI-15	7.0	17
15	DSI-16	2.2	20
16	DSI-17	14	33
17	DSI-18	20.6	10
18	DSI-19	22.0	21
19	DSI-20	20.6	96
20	DSI-21	26.6	17
21	DSI-22	75.6	28
22	DSI-23	52.0	6
23	DSI-24	61.2	21
24	DSI-25	14.2	44
25	DSI-26	2.6	29
26	DSI-27	8.2	33

[a] Reactions were performed with ketolactam (1.0 mg, 3 μ mol, 1.0 equiv.), 6-methoxytryptamine (0.75 mg, 4 μ mol, 1.2 equiv.); [b] ee was determined by HPLC; [c] Isolated yield;

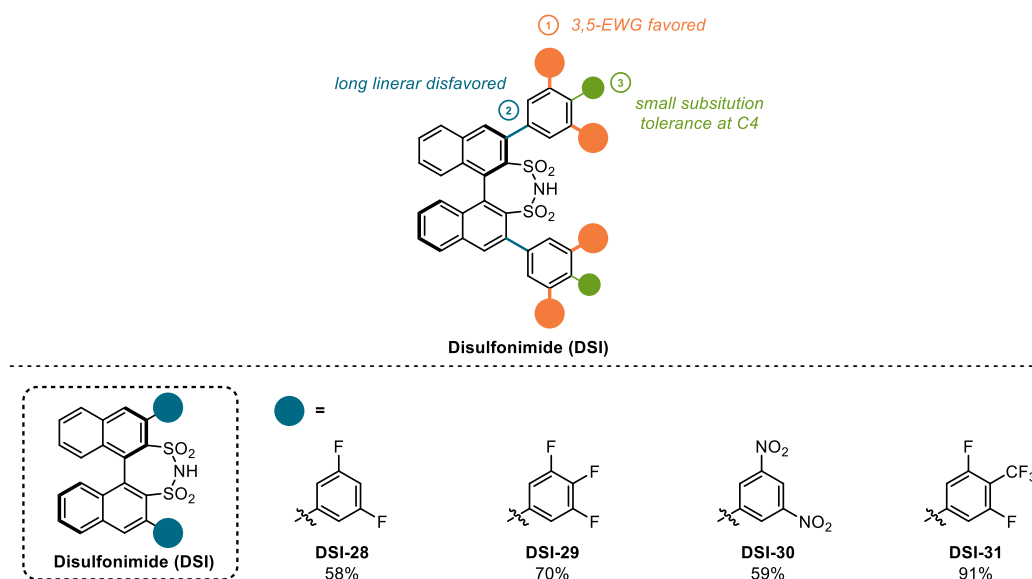
To improve the enantioselectivity and yield, the reaction parameters with **DSI-1** were optimized, such as catalyst loading, solvent and temperature. For the catalyst loading, 5 mol% was the best at 70 °C (Table 3–8, entries 1–3), and lower temperatures required higher catalyst loading (entries 14–15 and 19–20). Reactions with polar solvents could hardly afford the desired product (entries 6–9), indicating that the compact ion pair was crucial for the yield and enantioselectivity. Aliphatic non-polar solvents resulted in low yield, which could be caused by the poor solubility of both substrates and catalyst (entries 4–5). In contrast, aromatic non-polar solvent was preferable for the reaction, which could enhance the ion pair interaction. As the temperature decreased, the reactivity was also reduced (entries 14–23), showing the **DSI-1** catalyzed reaction still had a relatively high energy barrier.

Table 3–8: Reaction optimization by DSI-1.


entry ^[a]	cat. loading [mol%]	solvent	T [°C]	ee [%] ^[b]	yield [%] ^[c]
1	2.5	toluene	70	46.0	28
2	5.0	toluene	70	79.1	53
3	10.0	toluene	70	67.4	19
4	5.0	hexane	70	19.4	10
5	5.0	cyclohexane	70	64.4	12
6	5.0	EtOAc	70	N.D. ^[d]	trace
7	5.0	MeCN	70	N.D.	trace
8	5.0	THF	70	N.D.	trace
9	5.0	1,4-dioxane	70	N.D.	trace
10	5.0	<i>p</i> -xylene	70	64.4	14
11	5.0	<i>m</i> -xylene	70	72.0	48
12	5.0	<i>o</i> -xylene	70	N.D.	trace
13	5.0	benzene	70	54.2	23
14	5.0	toluene	50	N.D.	trace
15	10.0	toluene	50	64.8	5
16	5.0	<i>p</i> -xylene	50	58.4	13
17	5.0	<i>m</i> -xylene	50	N.D.	trace
18	5.0	benzene	50	N.D.	trace
19	5.0	toluene	60	N.D.	trace
20	10.0	toluene	60	68.8	24
21	5.0	<i>p</i> -xylene	60	71.6	32
22	5.0	<i>m</i> -xylene	60	34.8	13
23	5.0	benzene	60	47.4	20

[a] Reactions were performed with ketolactam (1.0 mg, 3 μ mol, 1.0 equiv.), 6-methoxytryptamine (0.75 mg, 4 μ mol, 1.2 equiv.); [b] ee was determined by HPLC; [c] Isolated yield; [d] not determined

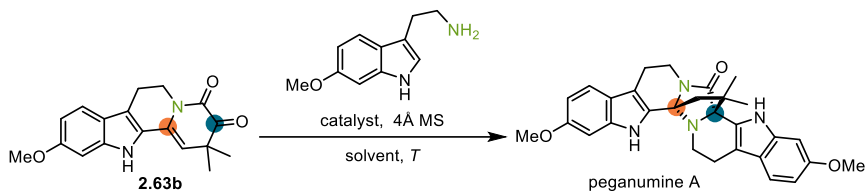
Since the enantioselectivity could not be improved with **DSI-1** by changing the reaction parameters. Four new DSIs were synthesized based on the SAR which showed that 3,5-EWG substitution was favored, and small group could be tolerated at 4-position (Figure 3–9).

**Figure 3–9:** New DSIs preparation.

With **DSI-28**, **DSI-29**, **DSI-30** and **DSI-31** in hand, the investigation of the cascade reaction

was initiated. The improved enantioselectivity was achieved with **DSI-28**, **DSI-29** and **DSI-31** (Table 3–9, entries 5, 9, 10 and 14–16). The yield was higher with **DSI-31** than those with **DSI-28** and **DSI-29**, indicating the reaction was acidity demanding. The reactions with **DSI-30** resulted in low enantioselectivity (entries 11–13).

Table 3–9: New DSIs screening.



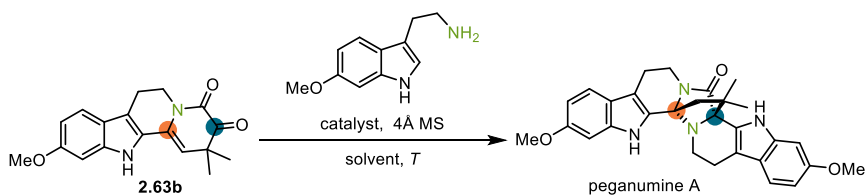
entry ^[a]	catalyst [mol%]	solvent	T [°C]	ee [%] ^[b]	yield [%] ^[c]
1	DSI-28 (5)	toluene	60	41.0	57
2	DSI-28 (5)	fluorobenzene	60	32.2	26
3	DSI-28 (5)	<i>p</i> -xylene	60	7.7	42
4	DSI-28 (5)	toluene	70	38.6	35
5	DSI-28 (10)	toluene	60	83.8	48
6	DSI-29 (5)	toluene	60	47.4	20
7	DSI-29 (5)	fluorobenzene	60	48.2	30
8	DSI-29 (5)	<i>p</i> -xylene	60	52.0	27
9	DSI-29 (5)	toluene	70	80.8	23
10	DSI-29 (10)	toluene	60	83.8	58
11	DSI-30 (5)	toluene	60	10.8	48
12	DSI-30 (5)	toluene	70	4.4	44
13	DSI-30 (10)	toluene	60	48.2	39
14	DSI-31 (5)	toluene	60	83.0	66
15	DSI-31 (5)	toluene	70	83.0	27
16	DSI-31 (10)	toluene	60	92.4	62

[a] Reactions were performed with ketolactam (1.0 mg, 3 μ mol, 1.0 equiv.), 6-methoxytryptamine (0.75 mg, 4 μ mol, 1.2 equiv.); [b] ee was determined by HPLC; [c] Isolated yield;

Inspired by the improved results, the reaction conditions were further optimized with **DSI-31**.

Finally, the enantioselectivity was improved to 93.6% ee (Table 3–10, entry 7).

Table 3–10: Screening with DSI-31.

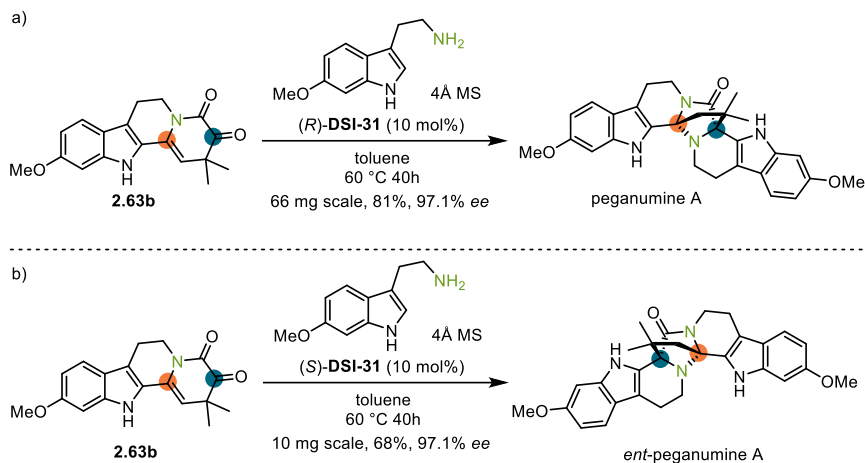


entry ^[a]	catalyst [mol%]	solvent	T [°C]	ee [%] ^[b]	yield [%] ^[c]
1	DSI-31 (5)	toluene	50	N.D. ^[d]	trace
2	DSI-31 (10)	toluene	50	87.4	39
3	DSI-31 (5)	<i>p</i> -xylene	50	89.4	26
4	DSI-31 (5)	<i>m</i> -xylene	50	75.2	6
5	DSI-31 (5)	<i>p</i> -xylene	60	91.0	62
6	DSI-31 (5)	<i>m</i> -xylene	60	90.2	47
7	DSI-31 (10)	toluene	70	93.6	34
8	DSI-31 (5)	<i>p</i> -xylene	70	91.0	62
9	DSI-31 (5)	<i>m</i> -xylene	70	90.2	47

[a] Reactions were performed with ketolactam (1.0 mg, 3 μ mol, 1.0 equiv.), 6-methoxytryptamine (0.75 mg, 4 μ mol, 1.2 equiv.); [b] ee was determined by HPLC; [c] Isolated yield; [d] not determined

Based on the previous results, the reaction condition with 10 mol% catalyst loading, toluene as

solvent at 60 °C was utilized. The result was confirmed by a scale-up reaction (Scheme 3–14a). Additionally, (*S*)-**DSI-31** was also prepared to synthesize the enantiomer of peganumine A, which was obtained with the same enantioselectivity (Scheme 3–14b).



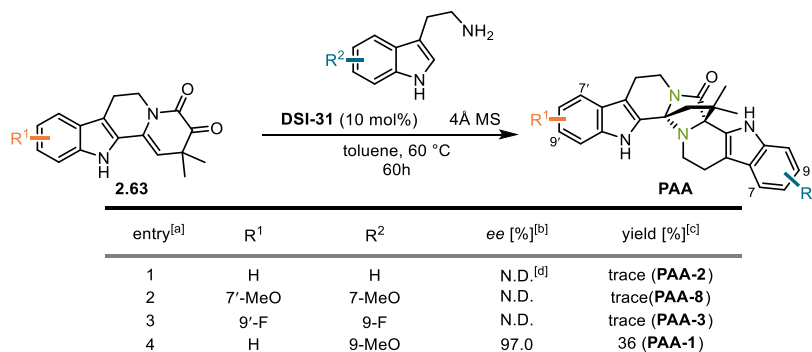
Scheme 3–14: Scale-up reactions with DSI-31.

3.3. Asymmetric synthesis of the analogues of peganumine A

3.3.1. Asymmetric synthesis platform for the analogues with DSI

With the optimized conditions in hand, it was anticipated to realize the asymmetric synthesis for the analogues of peganumine A. Surprisingly, the application of the optimized reaction condition furnished remarkable different results. Only the asymmetric synthesis of **PAA-11** achieved 97% *ee*, which also used 6-methoxytryptamine (Table 3–11, entry 4).

Table 3–11: Initial application of **DSI-31** to asymmetric synthesis of analogues.

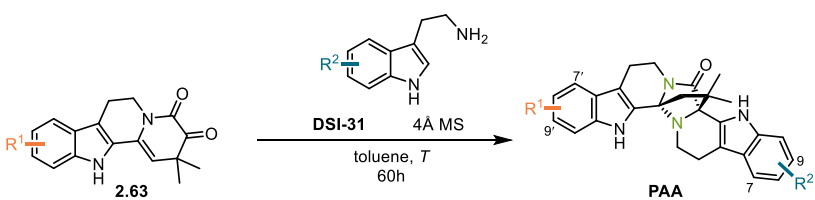


[a] Reactions were performed with ketolactam (15 μmol, 1.0 equiv.), amine (20 μmol, 1.2 equiv.); [b] *ee* was determined by HPLC; [c] Isolated yield; [d] not determined

In order to overcome the problems in the asymmetric synthesis of the analogues, specific

reaction conditions need to be optimized case by case. For the asymmetric synthesis of **PAA-2**, the reaction could not afford full conversion below 90 °C with less than 10 mol% catalyst loading (Table 3–12, entries 1–4). The best enantioselectivity was 78.9% *ee* (entry 5). By further increasing the reaction temperature and catalyst loading, the enantioselectivity started to decrease (entries 6–11). In the asymmetric synthesis of **PAA-8**, 4-methoxytryptamine was used. Surprisingly, the result was even worse. While the enantioselectivity remained in the same range as **PAA-2**, the yield dropped to less than 25% (entries 12–19). Additionally, the asymmetric synthesis of **PAA-3** was investigated (entries 20–25). The results were still comparable with those of **PAA-2** and **PAA-8**. Taken these results into consideration, it was proposed that the DSI might not be a unified catalyst to realize the asymmetric synthesis of the analogues.

Table 3–12: Asymmetric synthesis of the analogues with **DSI-31**.



entry ^[a]	cat. loading [mol%]	R ¹	R ²	T [°C]	ee [%] ^[b]	yield [%] ^[c]
1	10	H	H	60	N.D. ^[d]	trace
2	10	H	H	70	N.D.	64% (conv.) ^[e]
3	20	H	H	70	N.D.	61% (conv.)
4	10	H	H	90	N.D.	64% (conv.)
5	20	H	H	90	78.9	56
6	10	H	H	110	61.9	20
7	20	H	H	110	63.7	24

8	30	H	H	90	67.4	55
9	40	H	H	90	57.5	72
10	30	H	H	80	62.8	38
11	40	H	H	80	62.2	71

12	10	7'-MeO	7'-MeO	50	N.D.	trace
13	20	7'-MeO	7'-MeO	50	N.D.	trace
14	10	7'-MeO	7'-MeO	60	N.D.	trace
15	20	7'-MeO	7'-MeO	60	58.4	24
16	20	7'-MeO	7'-MeO	80	67.0	22
17	5	7'-MeO	7'-MeO	90	30.0	10
18	10	7'-MeO	7'-MeO	90	34.6	16
19	20	7'-MeO	7'-MeO	90	77.8	22

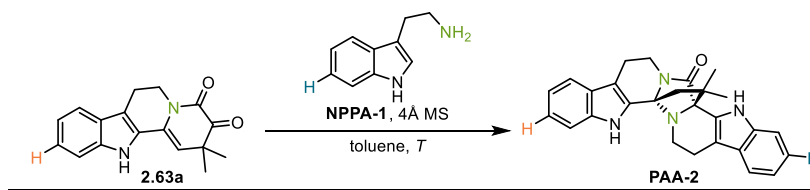
20	10	9'-F	9'-F	60	N.D.	trace
21	20	9'-F	9'-F	60	N.D.	trace
22	10	9'-F	9'-F	80	N.D.	trace
23	20	9'-F	9'-F	80	65.6	37
24	10	9'-F	9'-F	90	51.6	11
25	20	9'-F	9'-F	90	68.2	78

[a] Reactions were performed with ketolactam (3 μmol, 1.0 equiv.), amine (4 μmol, 1.2 equiv.); [b] *ee* was determined by HPLC; [c] Isolated yield; [d] not determined; [e] conversion was determined by ¹H-NMR

Since the NPPAs also achieved high enantioselectivity in the asymmetric synthesis of peganumine A, it was anticipated that the NPPAs could catalyze the enantioselective cascade

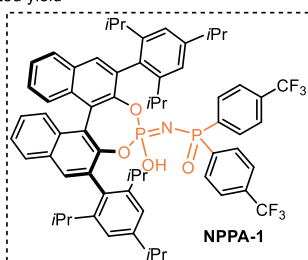
reaction in the asymmetric synthesis of the analogues. Initially the asymmetric synthesis of **PAA-2** was investigated using **NPPA-1** as the catalyst. Gratifyingly, all the screening conditions resulted in over 90% *ee* (Table 3–13, entries 1–4). Due to the low acidity of NPPA, the yields with 10 mol% catalyst loading were remarkably less than those with 20 mol% catalyst loading.

Table 3–13: Asymmetric synthesis of **PAA-2** with **NPPA-1**.



entry ^[a]	cat. loading [mol%]	T [°C]	<i>ee</i> [%] ^[b]	yield [%] ^[c]
1	10	80	90.4	31
2	20	80	91.8	75
3	10	90	93.4	38
4	20	90	96.0	64

[a] Reactions were performed with ketolactam (3 μmol, 1.0 equiv.), amine (4 μmol, 1.2 equiv.); [b] *ee* was determined by HPLC; [c] Isolated yield



3.3.2. Asymmetric synthesis platform for the analogues with NPPA

Inspired by the promising results of the asymmetric synthesis of **PAA-2** with **NPPA-1**, it was proposed that NPPA could be a general catalyst for the asymmetric synthesis of the analogues. Therefore, a thorough design and synthesis of NPPAs were commenced to prepare a catalyst pool for the asymmetric synthesis of the analogues. It was considered that the NPPA could be divided into two parts structurally, one was a phosphoric amide fragment, defining both chirality and acidity; the other was a phosphinic amide fragment, which mainly influenced the acidity (Figure 3–10). As the enantioselectivity was the primary goal, the initial design of NPPA was focus on the phosphoric amide fragment and kept the phosphinic amide fragment as the simple and commercially available phenyl group.

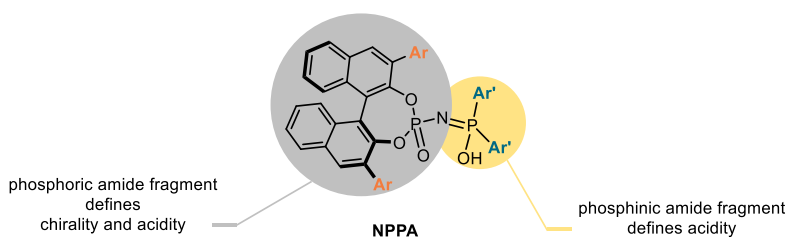
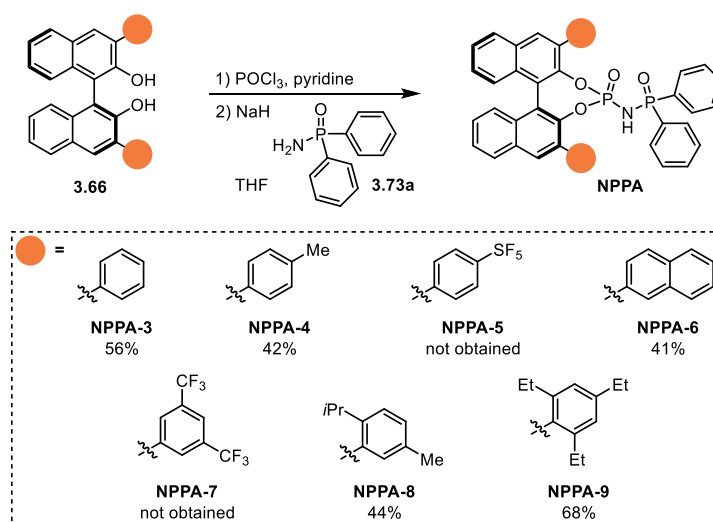


Figure 3–10: Structural analysis of NPPA.

With the diphenyl phosphinic amide (**3.73a**) in hand, the NPPAs could be synthesized through a two-step sequence from the corresponding 3,3'-substituted-BINOL **3.66**. Except **NPPA-5** and **NPPA-7** with EWGs, all the rest designed NPPAs were successfully obtained in moderate yield (Table 3–15).

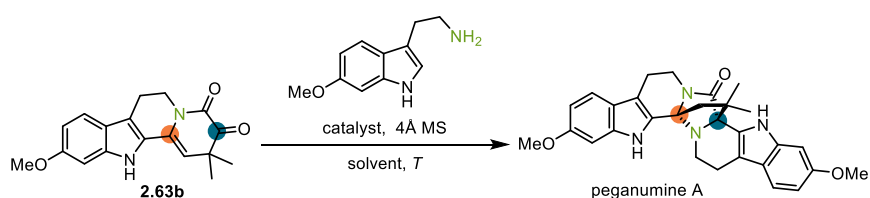


Scheme 3–15: 1st round synthesis of NPPA

Since peganumine A was the targeted natural product, which was a reasonable starting point for the catalyst screening of the analogues, the asymmetric synthesis of peganumine A was selected as a model to investigate the NPPA catalyzed cascade reaction. The results showed some interesting discoveries. **NPPA-3** was regarded as a control catalyst, as the phenyl group is the smallest substitute (Table 3–14, entries 4–7). The catalysts with 4-substituted phenyl group, such as **NPPA-3** and **NPPA-10**, could improve the enantioselectivity (entries 8–11 and 24–26). However, the enantioselectivity of the reaction with **NPPA-3** was found to be better than that with **NPPA-10**, indicating a larger substitution group was disfavored. The results with **NPPA-6** showed that a large π system could enhance the interaction between the substrate and catalyst leading to an improved enantioselectivity (entries 12–15). The catalysts with 2,4,6-trisubstituted phenyl group, such as **NPPA-2** and **NPPA-9**, exhibited good enantioselectivity

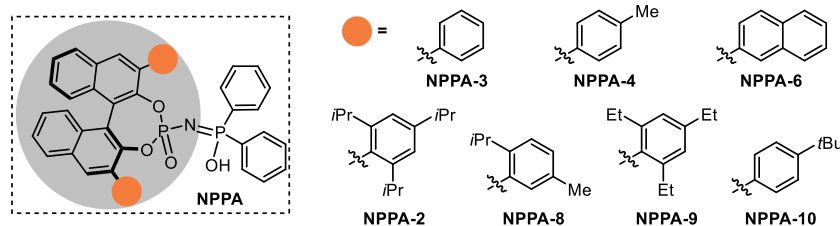
(entries 1–3 and 20–23). The enantioselectivity of the reaction with **NPPA-2** was better than that with **NPPA-9**, which could be explained as a larger *i*Pr group provided a proper confined catalytic site. In this round of screening, it could be concluded that the 2,4,6-triisopropyl-phenyl group was the best substitute for the chirality control of NPPA.

Table 3–14: 1st round screening of NPPAs.



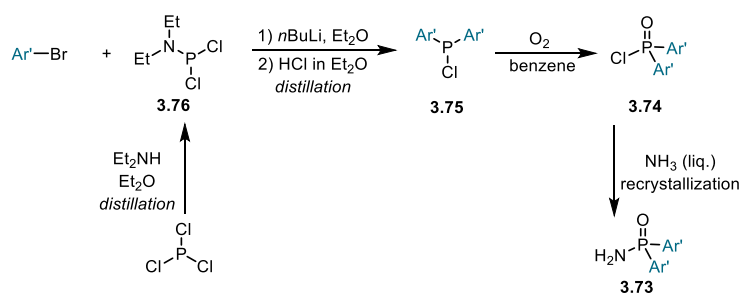
entry ^[a]	catalyst [mol%]	<i>T</i> [°C]	ee [%] ^[b]	yield [%] ^[c]
1	NPPA-2 (10)	90	27.2	27
2	NPPA-2 (20)	90	50.4	48
3	NPPA-2 (5)	70	83.8	86
4	NPPA-3 (10)	60	9.2	32
5	NPPA-3 (20)	60	31.4	24
6	NPPA-3 (10)	90	10.8	49
7	NPPA-3 (20)	90	24.0	51
8	NPPA-4 (10)	60	6.8	46
9	NPPA-4 (20)	60	51.6	69
10	NPPA-4 (10)	90	68.0	33
11	NPPA-4 (20)	90	46.6	23
12	NPPA-6 (10)	60	51.6	20
13	NPPA-6 (20)	60	70.0	20
14	NPPA-6 (10)	90	63.0	19
15	NPPA-6 (20)	90	53.4	48
16	NPPA-8 (10)	60	12.2	31
17	NPPA-8 (20)	60	3.2	31
18	NPPA-8 (10)	90	39.2	31
19	NPPA-8 (20)	90	6.0	42
20	NPPA-9 (10)	60	42.0	30
21	NPPA-9 (20)	60	52.8	41
22	NPPA-9 (10)	90	44.6	4
23	NPPA-9 (20)	90	47.8	15
24	NPPA-10 (5)	60	4.5	5
25	NPPA-10 (10)	60	24.6	18
26	NPPA-10 (20)	90	40.0	12

[a] Reactions were performed with ketoenamide (1.0 mg, 3 μmol, 1.0 equiv.), 6-methoxytryptamine (0.75 mg, 4 μmol, 1.2 equiv.); [b] ee was determined by HPLC; [c] Isolated yield;



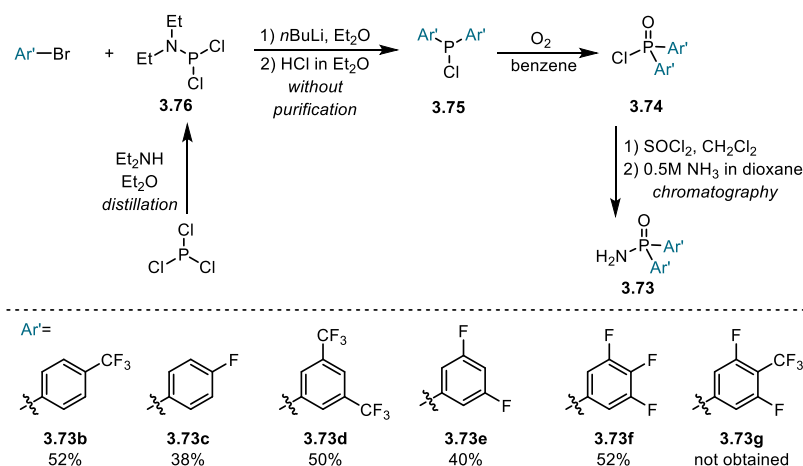
As 2,4,6-triisopropyl-phenyl group was discovered as the best substitution group for phosphoric amide fragment, the next issue was to clarify the best phosphinic amide fragment. Since most of the substituted phosphinic amides were not commercially available, a practical synthetic route was necessary for the further investigation. According to the related literatures, phosphinic amides **3.73** were usually prepared from the corresponding aryl bromides and

diethylamino phosphinous dichloride **3.76** which was synthesized from PCl_3 and diethylamine (Scheme 3–16). In the classic synthetic route, the key intermediate chlorophosphine **3.75** was prepared through lithiation of aryl bromide, reacting with diethylamino phosphinous dichloride **3.76** and hydrolysis with HCl. After oxidation of diethylamino phosphinous dichloride **3.76** with oxygen following amidation by liquid ammonia, the phosphinic amide could be obtained. However, there were some practical problems for this synthetic route, especially for small-scale preparation. The purification of crude chlorophosphine **3.75** required distillation at high temperature, but **3.75** was not thermally stable and prone to be oxidized. In addition, phosphinyl chloride **3.74** was sensitive to moisture leading to the corresponding phosphinic acid.



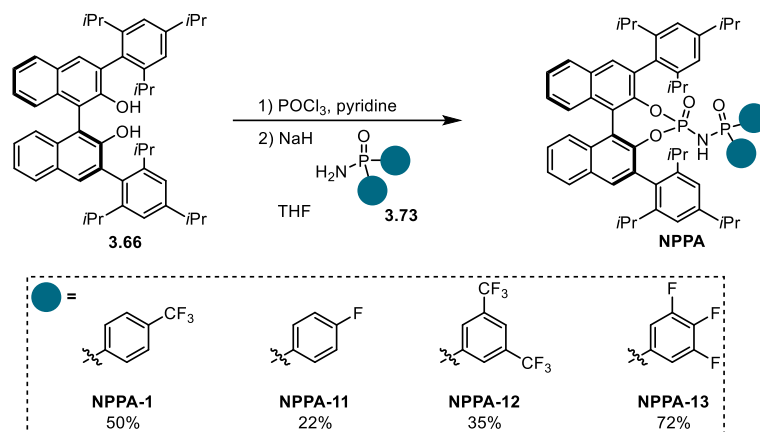
Scheme 3–16: Synthetic route of the phosphinic amides.

Due to such drawbacks, a modified route was implemented (Scheme 3–17). By using the crude chlorophosphine **3.75**, the decomposition caused by the high temperature of distillation was avoided. The partly hydrolyzed phosphinic acid could be converted to phosphinyl chloride **3.74** by using SOCl_2 . Utilization of ammonia solution simplified the amidation procedure. With this updated route, phosphinic amides were successfully prepared.



Scheme 3–17: Updated synthesis of the phosphinic amides.

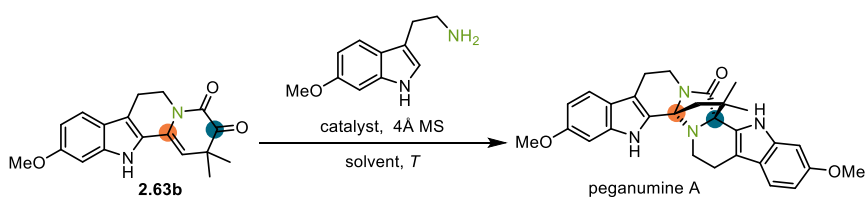
Following the same procedure, the synthesis of the NPPAs with privileged phosphoric amide motif was commenced. Since the reactivity was needed to be improved, phosphinic amides with EWGs were introduced to increase the acidity (Scheme 3–18).



Scheme 3–18: 2nd round synthesis of NPPAs.

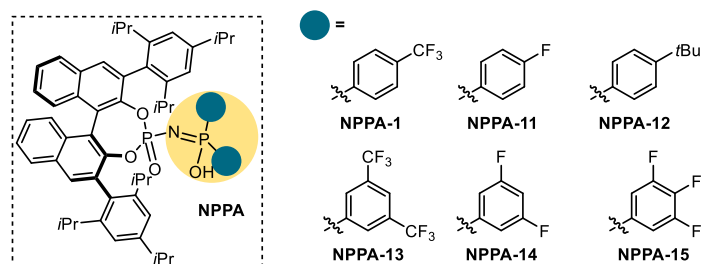
Unfortunately, the enantioselectivity was not improved as expected in the 2nd round screening (Table 3–15).

Table 3–15: 2nd round screening of NPPAs.



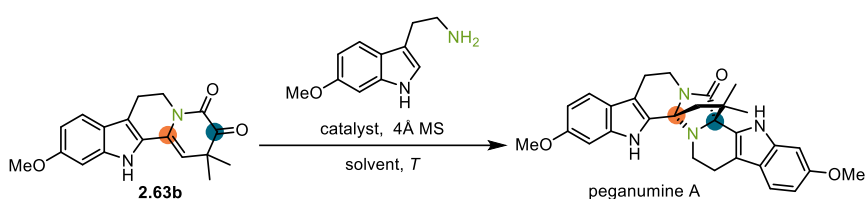
entry ^[a]	catalyst [mol%]	T [°C]	ee [%] ^[b]	yield [%] ^[c]
1	NPPA-1 (5)	60	35.0	42
2	NPPA-1 (10)	60	62.2	37
3	NPPA-1 (20)	60	71.2	25
4	NPPA-1 (10)	50	58.6	55
5	NPPA-1 (20)	50	70.4	38
6	NPPA-11 (10)	60	52.0	36
7	NPPA-11 (10)	50	66.2	27
8	NPPA-12 (5)	60	49.8	61
9	NPPA-12 (10)	60	66.6	51
10	NPPA-12 (20)	60	44.4	43
11	NPPA-13 (10)	60	52.0	17
12	NPPA-14 (10)	60	60.4	64
13	NPPA-14 (20)	60	45.6	22
14	NPPA-15 (10)	60	32.4	31

[a] Reactions were performed with ketoenamide (1.0 mg, 3 μmol, 1.0 equiv.), 6-methoxytryptamine (0.75 mg, 4 μmol, 1.2 equiv.); [b] ee was determined by HPLC; [c] Isolated yield;



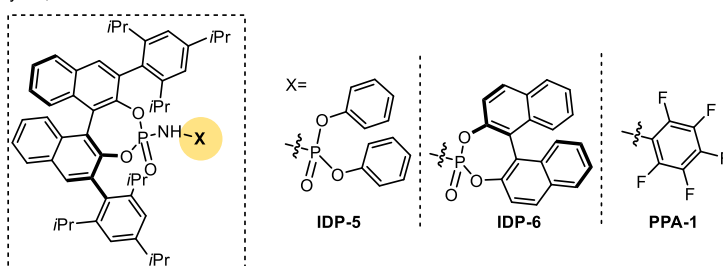
In addition, some related catalysts with different cores were also screened. However, there was no further improvement for the enantioselectivity. **IDP-5** and **IDP-6** resulted in remarkable decrease of enantioselectivity, indicating the NPPA core was a privileged motif for the cascade reaction (Table 3–16, entries 1–4). Meanwhile, the enantioselectivity of the reaction catalyzed by **PPA-1** was also low, which was evidence that the phosphinic amide motif of NPPA played a crucial role in the substrate–catalyst recognition. Although the 3rd round screening did not furnish an improvement of enantioselectivity, the catalysts with related structure clarified that the achiral phosphinic amide fragment was also critical for the cascade reaction.

Table 3–16: 3rd round screening of NPPA.

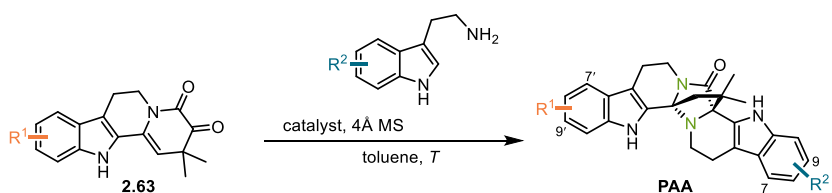


entry ^[a]	catalyst [mol%]	T [°C]	ee [%] ^[b]	yield [%] ^[c]
1	IDP-5 (5)	70	35.8	60
2	IDP-6 (5)	60	0	50
3	IDP-6 (10)	60	17.8	54
4	IDP-6 (20)	60	18.2	57
5	PPA-16 (5)	60	6.2	32
6	PPA-16 (10)	60	3.8	26
7	PPA-16 (20)	60	16.8	26

[a] Reactions were performed with ketoenamide (1.0 mg, 3 μ mol, 1.0 equiv.), 6-methoxytryptamine (0.75 mg, 4 μ mol, 1.2 equiv.); [b] ee was determined by HPLC; [c] Isolated yield;



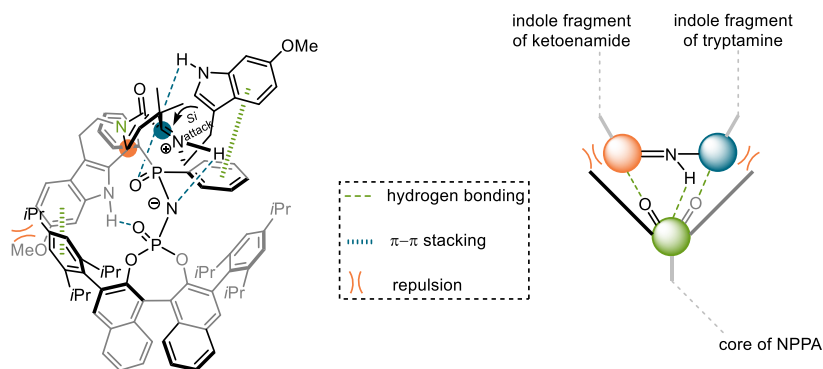
Based on these results, **NPPA-1** and **NPPA-2** were considered as the promising catalysts for the asymmetric synthesis platform of the analogues. Therefore, scale-up reactions of asymmetric synthesis of the analogues were commenced. For the dimethoxy substituted substrates, such as **PAA-8** and peganumine A, the enantioselectivities were not satisfying (Table 3–17, entries 1–2). However, the mono-methoxy and fluoro substituted analogues furnished over 90% ee (entries 3–5).

Table 3–17: Scale-up reactions of analogues.


entry ^[a]	catalyst [mol%]	scale [mg]	R ¹	R ²	T [°C]	ee [%] ^[b]	yield [%] ^[c]
1	NPPA-1 (20)	17	7'-MeO	7-MeO	60	69.0	40 (PAA-8)
2	NPPA-2 (7.5)	15	9'-MeO	9-MeO	60	71.0	31
3	NPPA-1 (10)	21	9'-F	9-F	90	98.6	72 (PAA-3)
4	NPPA-2 (10)	18	H	9-MeO	60	97.8	30 (PAA-1)
5	NPPA-1 (10)	15	9'-MeO	H	90	93.2	24 (PAA-11)

[a] Reactions were performed with ketoenamide (1.0 mg, 3 μmol , 1.0 equiv.), 6-methoxytryptamine (0.75 mg, 4 μmol , 1.2 equiv.); [b] ee was determined by HPLC; [c] Isolated yield;

It was proposed that in the transition state of the Pictet–Spengler reaction, the ketoenamide was constrained in the chiral catalytic pocket of the catalyst and stabilized by hydrogen bonding and π – π stacking (Figure 3–11). Additionally, the two separated phenyl groups of the phosphinic amide motif were relatively flexible, which could be induced the substrate to get a proper alignment for the interaction.^[245] It was also speculated that the dimension of the pocket was probably not fit for the ketoenamide with large substitution group, such as the methoxy group. The methoxytryptamine could interrupt the affinity with phosphoric amide motif. Therefore, the enantioselectivities of the dimethoxy analogues, such as **PAA-8** and peganumine A, are relatively low. Since the van der Waals radius of fluorine is similar with that of hydrogen,^[246] the asymmetric synthesis of **PAA-2** and **PAA-3** achieved over 90% ee. For the mono-methoxy substituted analogues, **PAA-1** and **PAA-10**, the high enantioselectivity could be explained as the flexibility of the phosphinic amide motif enables the tolerance of the mismatching with the chiral pocket.

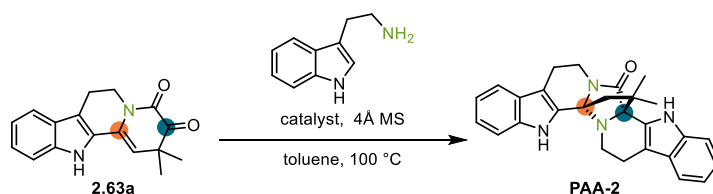
**Figure 3–11:** Proposed stereochemical mode of the NPPA catalyzed system.

3.3.3. Asymmetric synthesis of PAA-2

Inspired by the proposed model of the NPPA catalytic system, it was envisioned that this type of catalyst was ideal for the asymmetric synthesis of **PAA-2**, which was regarded as a potent analogue of peganumine A. Realizing the asymmetric synthesis of it would clarify the difference of the cytotoxicity and target affinity between the two enantiomers.

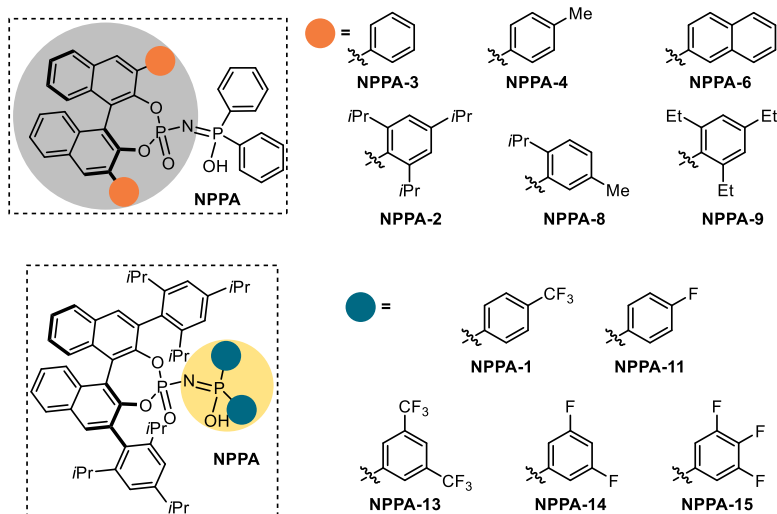
Based on the previous results, the catalyst screening was started with 20 mol% catalyst loading at 100 °C. The screening of the phosphoric amide part showed that the 2,4,6-triisopropyl-phenyl group was also the privileged chirality determining group (Table 3–18, entries 1–6). Further optimization indicated that **NPPA-1** was the best catalyst (entries 7–11).

Table 3–18: Optimization of the asymmetric synthesis of **PAA-2**.

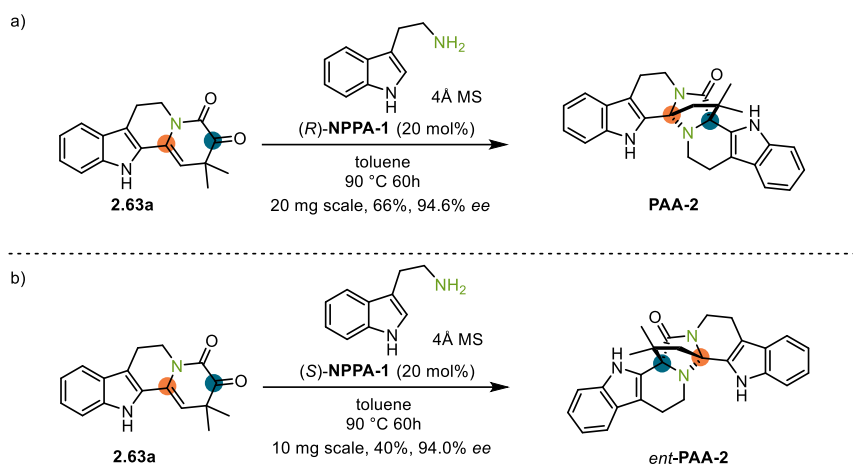


entry ^[a]	catalyst [mol%]	ee [%] ^[b]	yield [%] ^[c]
1	NPPA-2 (20)	86.4	75
2	NPPA-3 (20)	7.2	53
3	NPPA-4 (20)	21.0	30
4	NPPA-6 (20)	8.8	63
5	NPPA-8 (20)	39.2	44
6	NPPA-9 (20)	51.6	53
7	NPPA-1 (20)	91.0	81
8	NPPA-11 (20)	78.0	35
9	NPPA-13 (20)	34.8	59
10	NPPA-14 (20)	57.0	46
11	NPPA-15 (20)	66.2	33

[a] Reactions were performed with ketoenamide (0.9 mg, 2.9 μmol, 1.0 equiv.), tryptamine (0.67 mg, 3.5 μmol, 1.2 equiv.); [b] ee was determined by HPLC; [c] Isolated yield;



With the optimized condition in hand, the scale-up reactions were investigated. Both enantiomers of **PAA-2** were obtained with high enantioselectivity (Scheme 3–19).



Scheme 3–19: Scale-up reactions for the asymmetric synthesis of **PAA-2**.

Since the crystal structure of either of the two enantiomers of **PAA-2** was difficult to obtain, the absolute configuration of the stereocenters were initially determined by the comparison of the ECD spectra of the synthetic (+)-peganumine A and (+)-**PAA-2**. The result showed that the curves matched well with each other, indicating both compounds had the same absolute configuration (Figure 3–12). As the absolute configuration of (+)-peganumine A was determined by Hua et al. as (*S,S*) configuration,^[196] (+)-**PAA-2** was assigned also as (*S,S*) configuration.

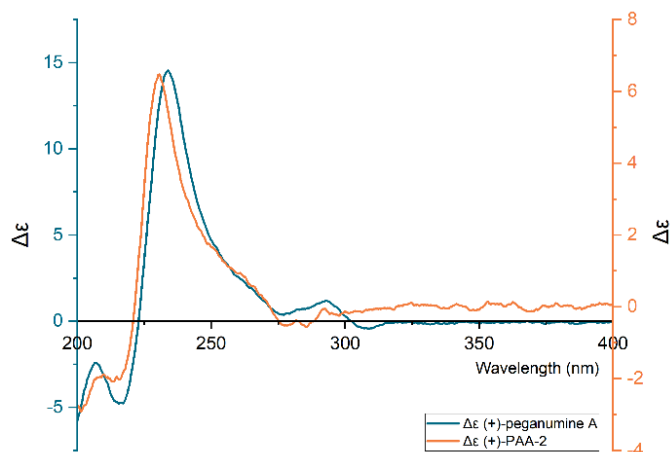


Figure 3–12: ECD spectra of (+)-peganumine A and (+)-**PAA-2**.

Additionally, comparisons were later made between the experimental and calculated ECD spectra with the assistance of DFT calculations performed by collaboration with Yu Chen and

Professor Dr. Yong Liang at Nanjing University. The calculated ECD curve matched well with the experimental one, unambiguously confirming the absolute configuration of (+)-**PAA-2** as (*S,S*) configuration.

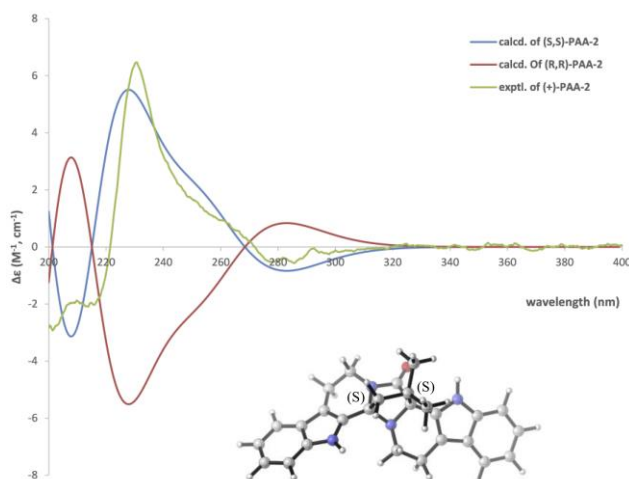


Figure 3–13: Experimental and calculated ECD spectra of (+)-**PAA-2**.

3.4. Brief summary

In this part, a variety of chiral organocatalysts were screened to achieve the asymmetric total synthesis of peganumine A based on the 3rd generation improved synthetic route. With a chiral DSI, the asymmetric synthesis of peganumine A was accomplished with high enantioselectivity (97% *ee*). However, the application of the chiral DSI to the asymmetric synthesis of the analogues of peganumine A was fruitless. After further investigation, the chiral NPPA was selected to perform the asymmetric synthesis of the analogues. With the chiral NPPA, four analogues were achieved over 90% *ee* synthesis, including the potent analogue **PAA-2**. And the absolute configuration of the enantioenriched **PAA-2** was determined by ECD.

4. New Routes to the Total Synthesis of Peganumine A

4.1. Iminium ion and *N*-acyliminium ion

4.1.1. Iminium ion and its reactions

In 1864, Schiff discovered a condensation reaction between primary amines and aldehydes or ketones, resulting in an equilibrium presenting imines.^[247] The imines are also named as Schiff bases, which exist as iminium ions in acidic solution. Secondary amines can condense with aldehydes and ketones to form iminium ions. These iminium ions can be isolated as salts of strong acids. Iminium ions/salts are more electrophilic than the corresponding aldehydes or ketones. Kinetic studies of the reactions of benzaldehyde-derived iminium ions in acetonitrile revealed the electrophilic reactivities (*E*) of some iminium substrates (Figure 4–1).^[248]

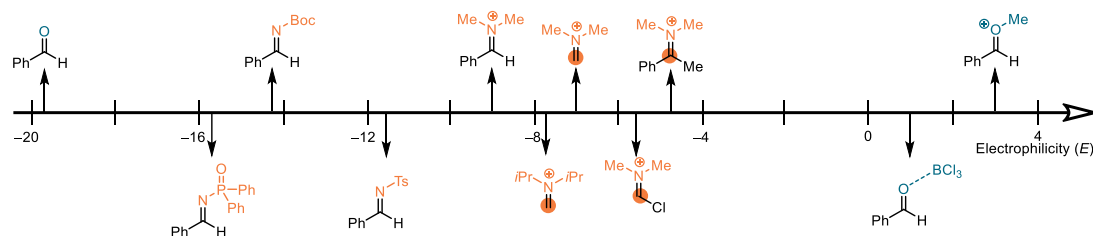
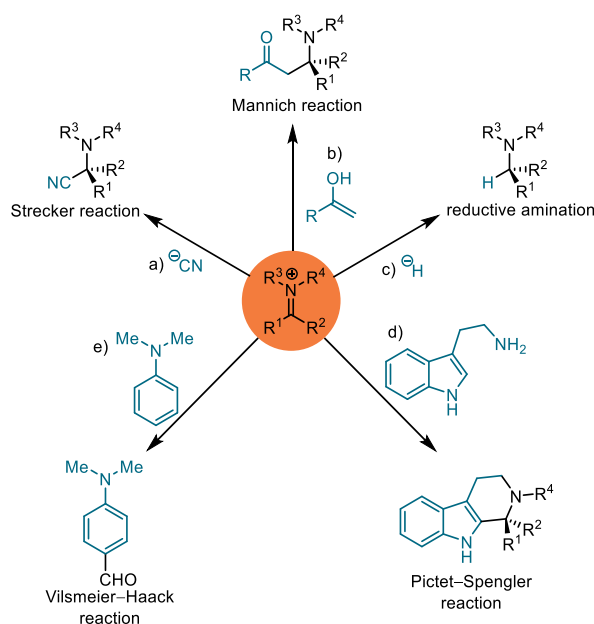


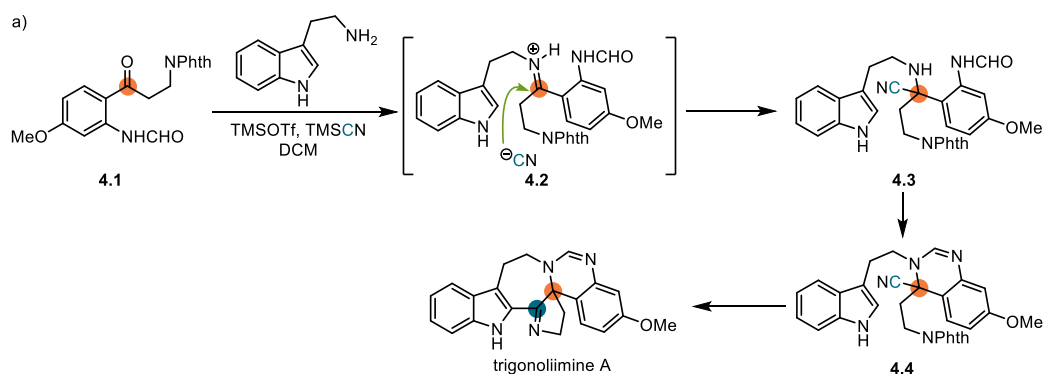
Figure 4–1: Electrophilicity parameter of some iminium ions and related compounds.

Due to the high reactivity of iminium ions/salts, the preparation of them has attracted attention from the scientific community. While iminium ions/salts are usually generated in situ, it is also possible to synthesize the isolatable iminium ions/salts. In principle, the most straightforward way to prepare iminium ions/salts is direct condensation of amines with aldehydes or ketones under acidic conditions (Scheme 4–1a). Selective alkoxy group cleavage of hemiaminals also furnishes iminium ions/salts (Scheme 4–1b).^[249] Iminium ions/salts can be obtained through hydride abstractions of tertiary amines by Mercury(II) acetate (Scheme 4–1c).^[250] In some special cases, iminium ions/salts are obtained from *N*-methylproline derivatives by decarbonylation of α -tertiary amino acids (Scheme 4–1d).^[251] In addition, imines and enamines are able to convert to iminium ions/salts by *N*-alkylation or protonation (Scheme 4–1e and f).^[252]

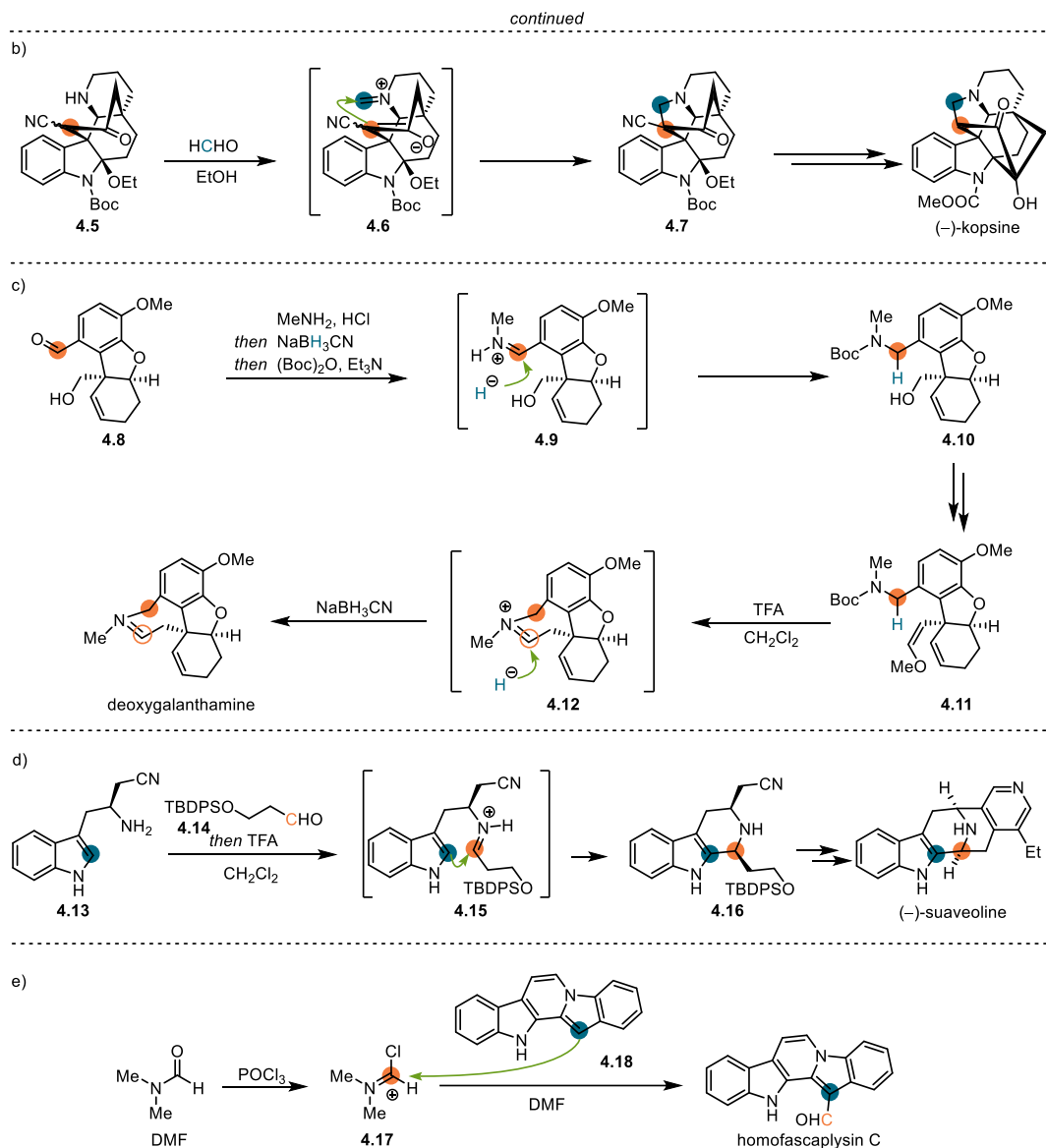


Scheme 4-2: Iminium ions in organic reactions.

Iminium ions have been widely applied in natural product total synthesis. A Strecker reaction was employed to construct the fused ring system of indole alkaloid trigonoliimine A via the attack of cyanide anion to iminium ion **4.2** (Scheme 4-3a).^[258] Qin et al. accomplished the total synthesis of *Kopsia* indole alkaloid (–)-kopsine by using an intramolecular Mannich reaction via iminium ion **4.6** (Scheme 4-3b).^[259] In the synthesis of deoxygalanthamine, Trost et al. used two reductive aminations for the construction of the azepine ring (Scheme 4-3c).^[260] The hydride attacked iminium ions **4.9** and **4.12**, leading to the corresponding tertiary amine **4.10** and deoxygalanthamine. The Pictet–Spengler reaction of amine **4.13** and aldehyde **4.14** was utilized to construct the β -carboline scaffold of suaveoline through iminium ion **4.15** (Scheme 4-3d).^[261] The chloroiminium ion **4.17** was applied to the total synthesis of homofascaplysin C through a selective formylation of **4.18** (Scheme 4-3e).^[262]



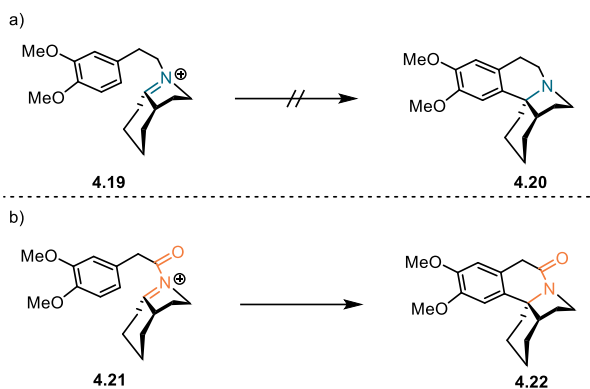
Scheme 4-3: The iminium ions in total synthesis.



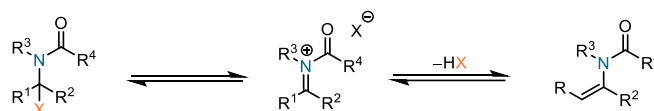
Scheme 4-3: The iminium ions in total synthesis. (continued)

4.1.2. *N*-acyliminium ion and its application in total synthesis

The iminium ion is a highly reactive species, which plays an important role in the construction of C–C and C–N bonds. However, in the synthesis of isoquinoline alkaloid erythrinane, Belleau et al. found iminium ion **4.19** was ineffective to undergo the designed reaction, and in contrast, the *N*-acyliminium ion **4.21** could undergo the electrophilic cyclization. It was attributed to extra activation of the electron-withdrawing of the carbonyl group (Scheme 4-4).^[263]

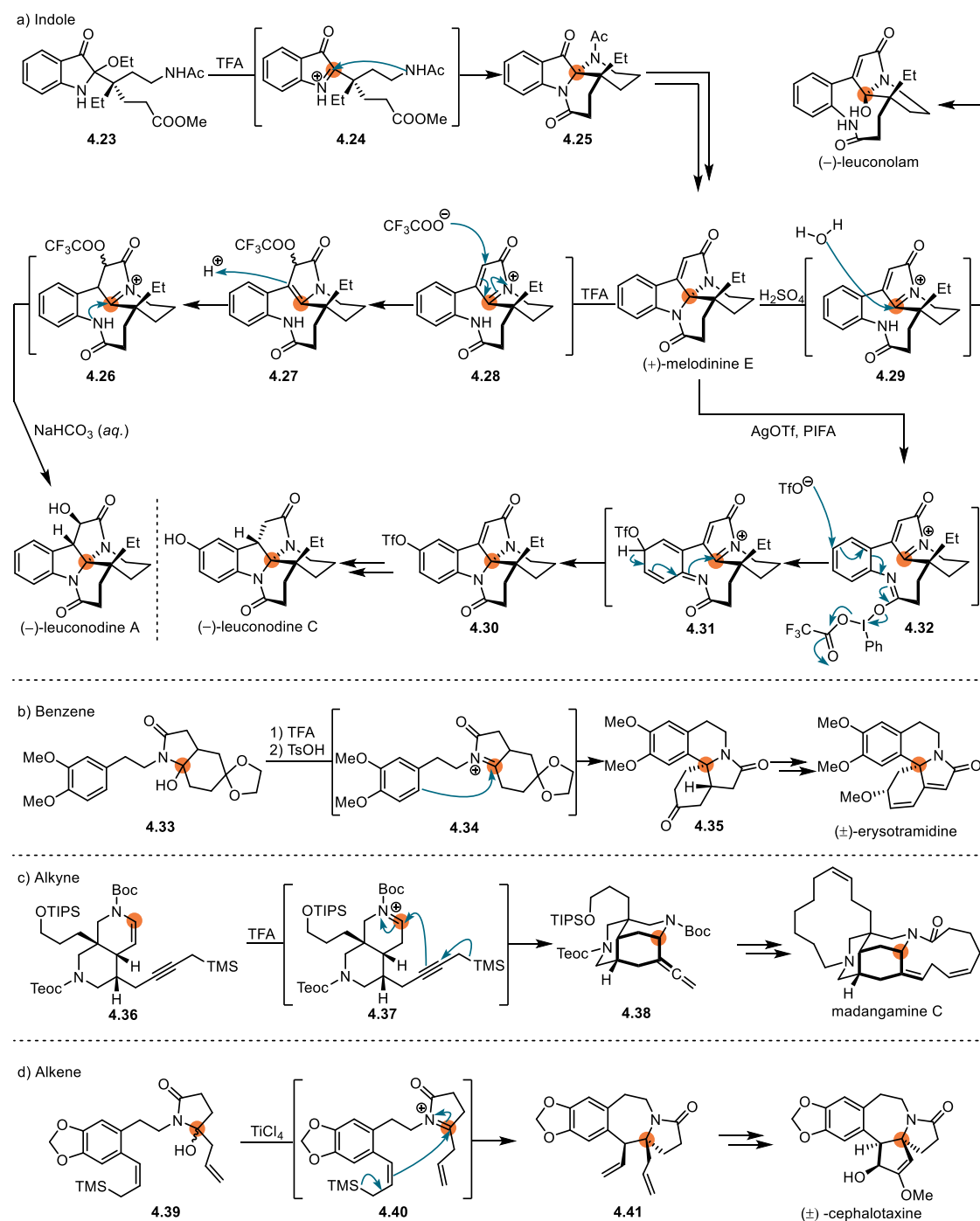
**Scheme 4-4:** Iminium ion vs *N*-acyliminium ion.

In principle, most of the characteristics of *N*-acyliminium ion are similar with that of iminium ion, such as the electrophilicity, preparation and reactivity. But one distinct property of *N*-acyliminium ion is that it is likely to not generate stoichiometrically in the reaction but exists in an equilibrium (Scheme 4-5).^[264] As a cationic species, *N*-acyliminium ion can undergo an elimination process yielding enamide. This process depends on the acidic reagent, the solvent and the structure of the *N*-acyliminium ion.^[265] As the subsequent electrophilic reaction of cyclic *N*-acyliminium ion is usually more difficult, the equilibrium tends to accumulate the cyclic enamide. In addition, the regeneration of *N*-acyliminium ion from cyclic enamide is hard in some cases leading to dimerization.^[266]

**Scheme 4-5:** Common disfavored equilibria of *N*-acyliminium ion.

As an important and highly reactive species, *N*-acyliminium ions have applied to various natural product total syntheses. In the divergent total synthesis of monoterpene indole alkaloids, Zhu et al. showed the power of *N*-acyliminium ions (Scheme 4-6a). The linchpin intermediate (+)-melodinine E was prepared by amination via *N*-acyliminium ion **4.24**. Treating (+)-melodinine E with sulphuric acid, (–)-leuconolam could be obtained via an intermolecular addition of H₂O to *N*-acyliminium ion **4.29**. Vinylogous addition of trifluoroacetate anion to *N*-acyliminium ion **4.28** afforded **4.27**, which could convert to (–)-leuconodine A by hydrolysis and amination through *N*-acyliminium ion **4.26**. Meanwhile, under oxidative acidic condition, synthesis of (–)-leuconodine C could be furnished from (+)-melodinine E via *N*-acyliminium ions **4.31** and **4.32**.^[267] In the total synthesis of alkaloid erysotramidine (±)-

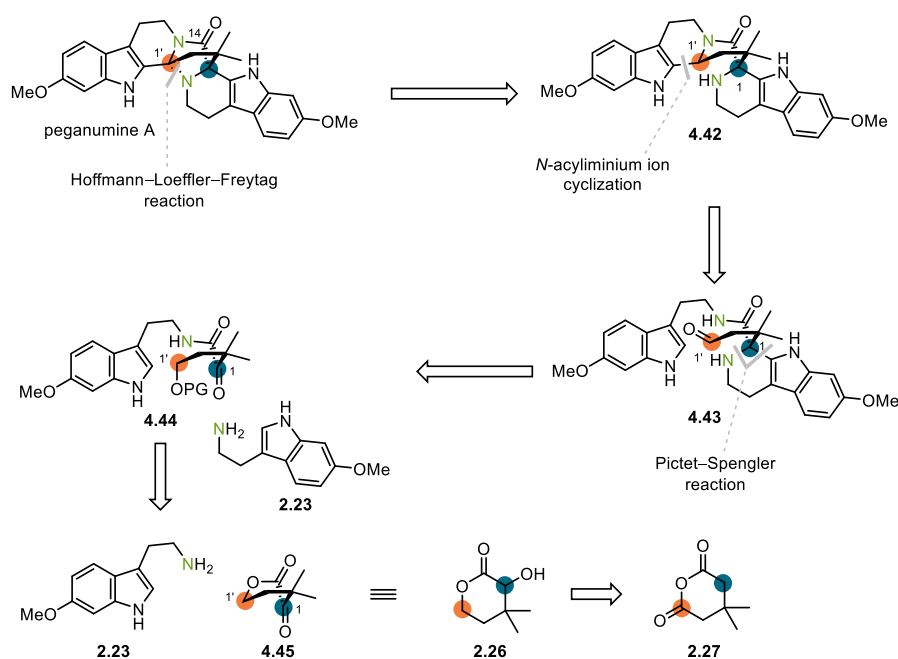
erythrinan, Tu et al. utilized *N*-acyliminium ion **4.34** to react with electro-rich arene yielding the tetracyclic compound **4.35** (Scheme 4–6b).^[268] Besides the aromatic rings, *N*-acyliminium ions are also able to react with alkynes and alkenes. Sato et al. disclosed the unified total synthesis of the madangamine alkaloids using the cyclization of *N*-acyliminium ion **4.37** to construct the caged tetracyclic **4.38** (Scheme 4–6c).^[269] In the synthesis of (±)-cephalotaxine, Hong et al. achieved the cyclization of *N*-acyliminium ion **4.40** with alkene (Scheme 4–6d).^[270]

Scheme 4–6: *N*-acyliminium ions in total synthesis.

4.2. 4th generation synthetic approach to peganumine A

4.2.1. Retrosynthesis of peganumine A

In the section “2.3.6. Comparison between the α -ketolactam and the α -ketoenamide”, the remarkably different reactivity between the α -ketolactam **2.36a** and the α -ketoenamide **2.45a** was clarified by the DFT calculations performed by collaboration with Dr. Yinghan Chen and Professor Dr. Yong Liang. Steric hindrance was considered as a crucial factor for the Pictet–Spengler reaction, therefore a linear intermediate **4.44** was envisioned to be the substrate of the Pictet–Spengler reaction (Scheme 4–7). Based on this idea, the 4th generation retrosynthesis of peganumine A was proposed. The C1' quaternary carbon center could also be constructed by a Hoffmann–Loeffler–Freitag reaction^[198] and a *N*-acyliminium ion cyclization. The construction of C1 quaternary carbon center relied on the Pictet–Spengler reaction of the linear α -ketolactam **4.44** which could be synthesized from α -ketolactone **4.45**. Anhydride **2.27** was considered as the starting material to prepare the α -ketolactone **4.45** via redox reactions.

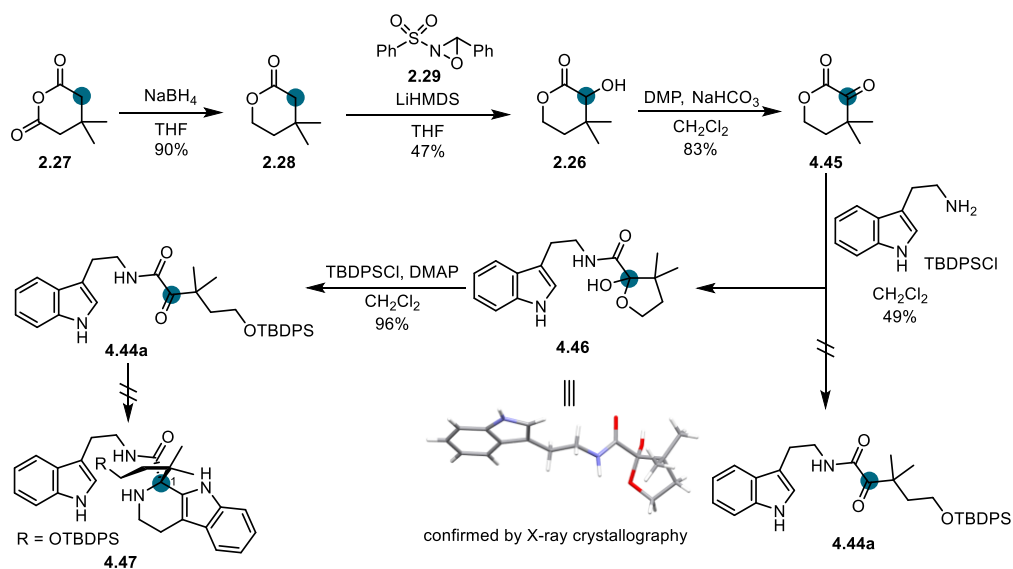


Scheme 4–7: Fourth generation retrosynthesis of peganumine A.

4.2.2. 4th generation synthesis of peganumine A

α -ketolactone **4.45** was obtained from the α -hydroxylactone **2.26** which was prepared according

to the procedure in the section “2.2.2. *Synthesis of the 7C motif*”. It was initially anticipated that a ring opening reaction would occur, resulting in lactone **4.45** and followed an in situ protection of the free hydroxyl group by TBDPSCI. Unfortunately, this sequence yielded hemiacetal **4.46**. The TBDPS protected linear α -ketoamide **4.44a** was afforded by a hemiacetal ring opening and in situ protection sequence. However, neither the Pictet–Spengler reaction of α -ketoamide **4.44a** nor the formation of the corresponding imine was turned out to be successful (Scheme 4–8).



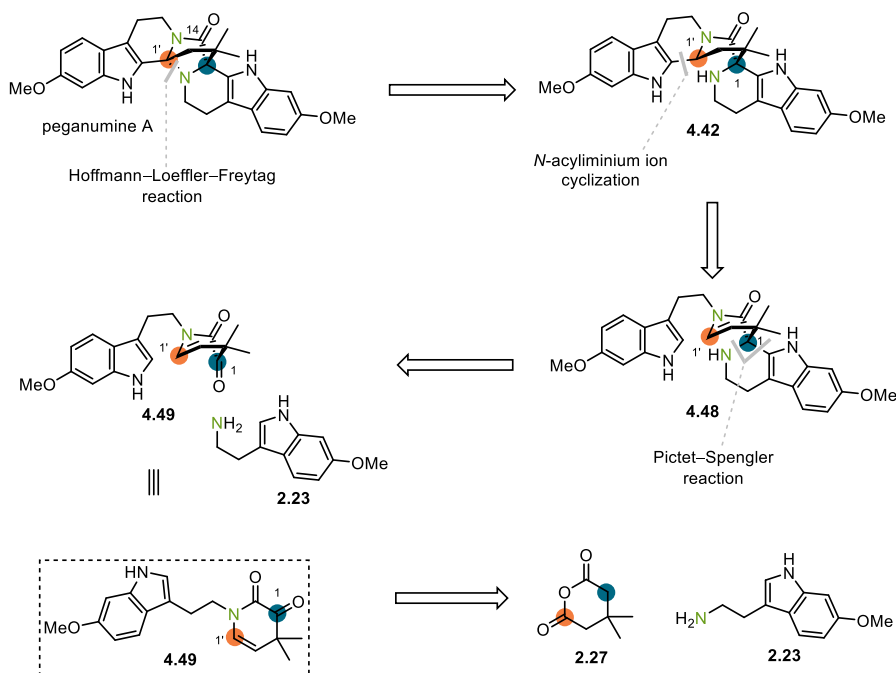
Scheme 4–8: 4th generation synthetic attempt.

4.3. 5th generation synthetic approach for peganumine A

4.3.1. Retrosynthesis of peganumine A

Based on the unfruitful attempt of the total synthesis of peganumine A, a 5th generation synthetic route was proposed. In the 1st generation approach, the Pictet–Spengler reaction of the highly functionalized intermediate **2.24a** was challenging in an intermolecular fashion. According to the 2nd generation attempt and the 3rd generation improved synthesis, it was demonstrated that the Pictet–Spengler reaction of the tetracyclic ring system was sensitive to steric hindrance. The 4th generation attempt indicated that the Pictet–Spengler reaction also required a relatively fixed conformation, as the linear intermediate **4.44a** with the freely rotated bonds could not realize the cyclization. Therefore, it was envisioned that using a mono-ring

system to “lock” the conformation could avoid the steric problems in previous syntheses (Scheme 4–9). In this strategy, the key reactions are the intramolecular *N*-acyliminium ion cyclization of **4.42** and the Pictet–Spengler reaction of monocyclic α -ketolactam **4.49**. The key intermediate **4.49** can be prepared from the anhydride **2.27** and 6-methoxytryptamine.

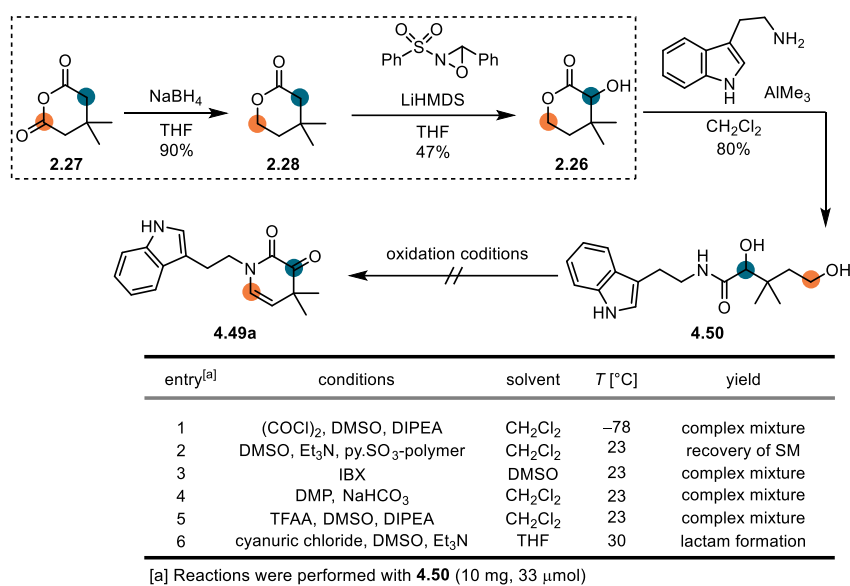


Scheme 4–9: 5th generation retrosynthesis of peganumine A.

4.3.2. 5th generation synthesis of peganumine A

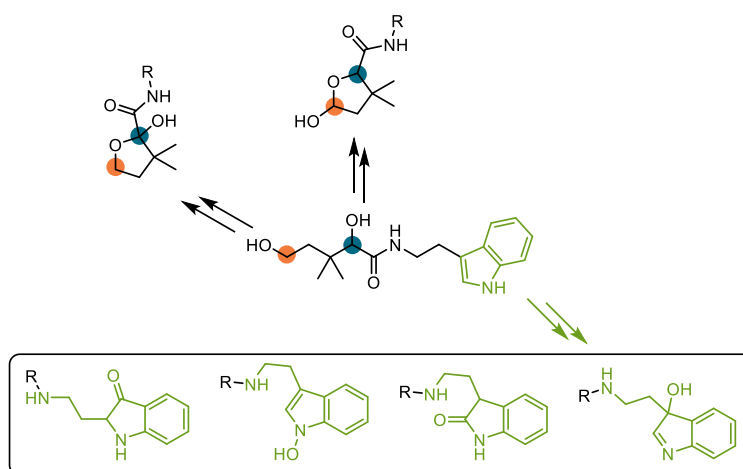
4.3.2.1. Mono-ring α -ketoenamides preparation via oxidative pathway

Starting from the α -hydroxylactone **2.26** which was synthesized in the section “2.2.2. *Synthesis of the 7C motif*”, dihydroxyamide **4.50** was prepared through an AlMe_3 promoted aminolysis in 80% yield.^[204] The synthetic attempt to mono-ring enamide **4.49a** was carried out by a global hydroxyl groups oxidation of dihydroxyamide **4.50** following a hemiaminal formation–elimination sequence (Scheme 4–10). Unfortunately, that oxidation sequence could not be realized through various classic oxidation reactions.



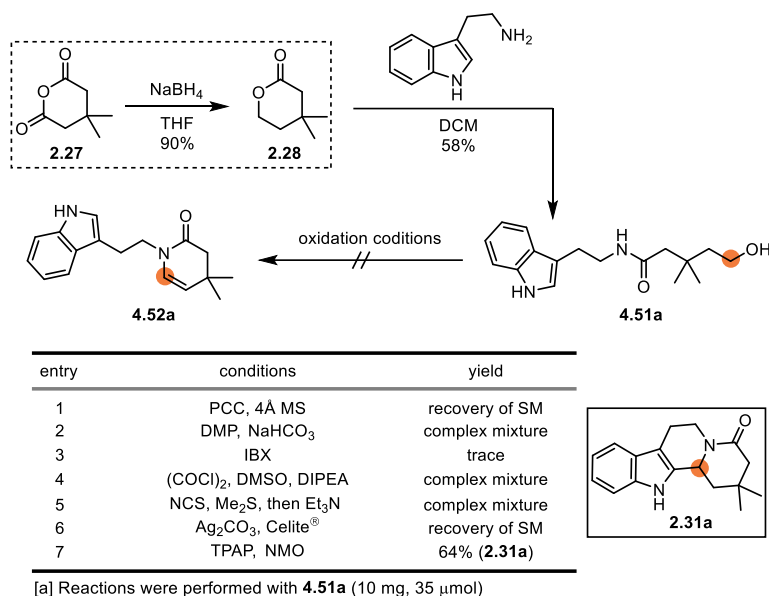
Scheme 4–10: Mono-ring enamide intermediate preparation.

Analysis of the oxidation reaction showed the indole fragment, especially the free C₂ position of indole, could lead to various side reactions (Scheme 4–11).^[271] Meanwhile, the stepwise oxidation of the two hydroxyl groups could afford hemiacetal or hemiketal, which might suspend the desired reaction pathway.



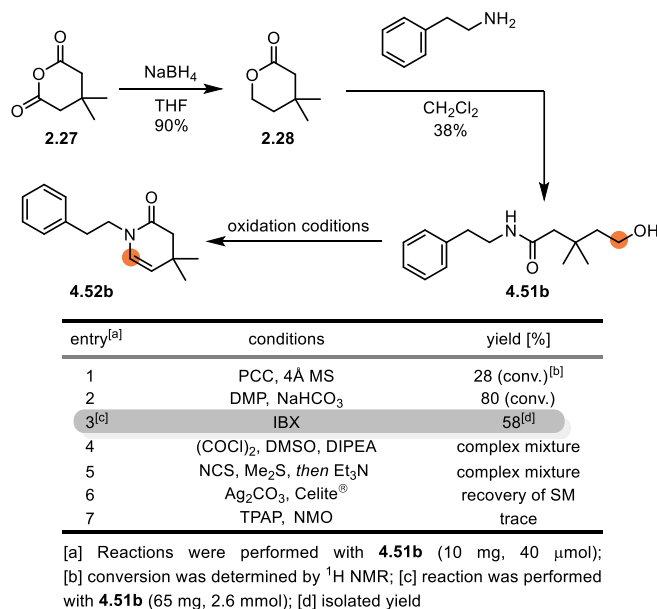
Scheme 4–11: Potential side-reactions.

In order to avoid these possible side reactions, the removal of the secondary hydroxyl group of **4.50** was proposed, simplifying the oxidation with the amide **4.51a**. Although the desired enamide **4.52a** was not obtained, the cyclization product **2.31a** was afforded under classic Ley oxidation^[272] condition, which indicated that the proposed iminium ion could be generated and underwent a cyclization reaction (Scheme 4–12).



Scheme 4–12: Mono-oxidation with free indole.

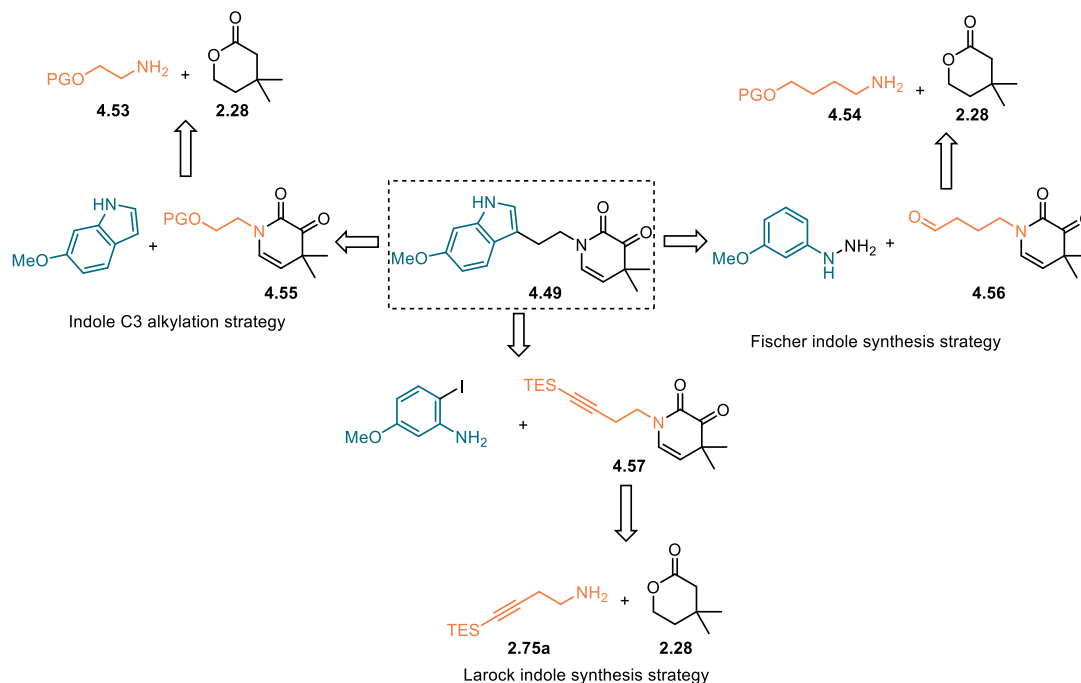
To further investigate the oxidation–elimination sequence, alcohol **4.51b** with a phenyl group was utilized as a model to circumvent the indole initiated side reactions. The preparation of **4.51b** worked successfully from anhydride **2.27** following the same procedure. Satisfyingly, the desired enamide **4.52b** was afforded with IBX^[273] in 58% yield (Scheme 4–13). This result indicated that the oxidation–elimination sequence could construct the core of the mono-ring α -ketoenamide motifs without the indole fragment.



Scheme 4–13: Mono-oxidation with phenyl group.

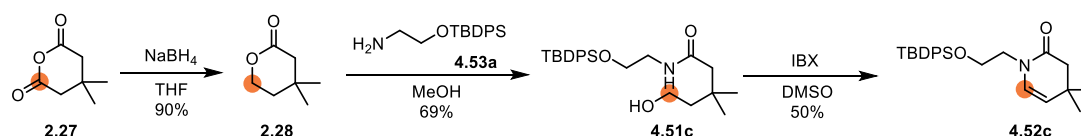
Inspired by the successful synthesis of **4.52b**, it was considered to introduce the secondary

hydroxyl group and indole fragment to the mono-ring enamide in late-stage synthesis. The secondary hydroxyl group could be installed by an α -functionalization. The indole fragment could be installed by diverse indole synthesis strategies (Scheme 4–14).



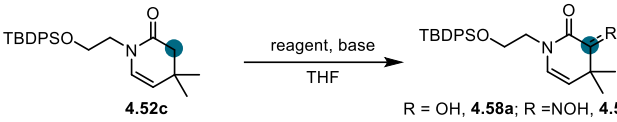
Scheme 4–14: Different strategies for the indole motif construction.

The indole C3 alkylation strategy was investigated first. Amide **4.51c** was obtained in 69% yield by using the TBDPS-protected ethanolamine **4.53a** to open lactone **2.28** (Scheme 4–15). The oxidation–hemiaminal formation–elimination cascade of **4.51c** yielded mono-ring enamide **4.52c** in 50% yield.



Scheme 4–15: Substrate preparation for the indole C3 alkylation strategy.

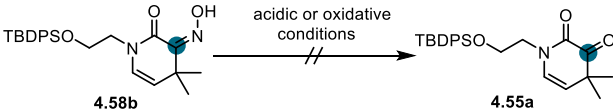
Based on previous experience, the α -functionalization of the enamide **4.52c** was commenced before the introduction of the indole fragment. Following the similar α -hydroxylation strategy in the chapter “2. Total Synthesis of Racemic Peganumine A and Its Analogues”, the α -hydroxylation^[50, 207] product **4.58a** was obtained in 61% yield by using LiTMP as base and O₂ as oxidant (Table 4–1, entry 4). Additionally, the α -oximization^[274] was also realized with *tert*-butyl nitrite yielding oxime **4.58b** (entry 9).

Table 4–1: α -functionalization of mono-ring enamide.


entry ^[a]	reagent	base [equiv.]	R	yield ^[b]
1	P(O <i>t</i> Pr) ₃ , O ₂	LDA (3.0)	OH (hydroxy)	recovery of SM
2	P(O <i>t</i> Pr) ₃ , O ₂	<i>t</i> BuLi (3.0)	OH (hydroxy)	70% (conv.) ^[c]
3	P(O <i>t</i> Pr) ₃ , O ₂	LiTMP (3.0)	OH (hydroxy)	64% (conv.)
4 ^[d]	P(O <i>t</i> Pr) ₃ , O ₂	LiTMP (8.0)	OH (hydroxy)	61%
5	P(O <i>t</i> Pr) ₃ , O ₂	<i>t</i> BuLi (8.0)	OH (hydroxy)	17%
6	<i>t</i> BuONO	LDA (3.0)	NOH (oxime)	60% (conv.)
7	<i>t</i> BuONO	<i>t</i> BuLi (3.0)	NOH (oxime)	67% (conv.)
8	<i>t</i> BuONO	LiTMP (3.0)	NOH (oxime)	96% (conv.)
9 ^[e]	<i>t</i> BuONO	LiTMP (6.0)	NOH (oxime)	54%

[a] Reactions were performed with enamide (5.0 mg, 12 μ mol); [b] Isolated yield; [c] conversion was determined by ¹H NMR; [d] reaction was performed with enamide (25 mg, 60 μ mol); [e] reaction was performed with enamide (115 mg, 269 μ mol)

It was anticipated that enamide **4.52c** could convert to α -ketoenamide **4.55a** through a one-pot procedure by the α -oximization of **4.52c** and subsequent hydrolysis of oxime **4.58b**. Unfortunately, the hydrolysis of oxime **4.58b** under acidic conditions was unsuccessful (Table 4–2, entries 1–4). The oxidative cleavage of oxime **4.58b** was also screening with various oxidants, most of the oxidants resulted in the recovery of starting material (entries 5–9). Interestingly, the IBX with β -cyclodextrin condition afforded the corresponding α -nitroenamide (entries 11–14).

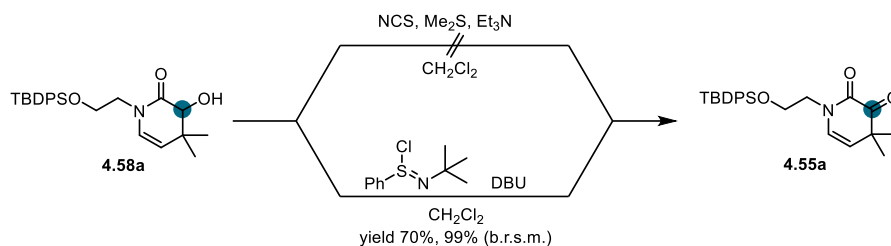
Table 4–2: Screening of oxime hydrolysis.


entry	conditions	solvent	T [°C]	yield
1	CuCl ₂ , H ₂ O	MeCN	70	complex mixture
2	SnCl ₂ , HCl (aq.)	MeCN	23	complex mixture
3	15% HCl	H ₂ O	70	complex mixture
4	levulinic acid, 1N HCl	H ₂ O	23	complex mixture
5	Na ₂ S ₂ O ₃	H ₂ O	23	recovery of SM
6	SDS, I ₂	CH ₂ Cl ₂	23	recovery of SM
7	Mn(OAc) ₃	PhH	80	recovery of SM
8	PCC	CH ₂ Cl ₂ /H ₂ O	23	recovery of SM
9	DMP	CH ₂ Cl ₂ /H ₂ O	23	recovery of SM
10	NBS, β -cyclodextrin	acetone/H ₂ O	23	complex mixture
11 ^[b]	IBX, β -cyclodextrin	acetone/H ₂ O	23	28% (conv.) ^[c]
12 ^[d]	IBX, β -cyclodextrin	acetone/H ₂ O	23	83% (conv.)
13 ^[e]	IBX, β -cyclodextrin	acetone/H ₂ O	23	91% (conv.)
14 ^[b]	IBX, β -cyclodextrin	acetone/H ₂ O	23	61% ^[f]
15	O ₂ , Fe(NO ₃) ₃	toluene	40	complex mixture
16	O ₂ , NaNO ₂ , Amberlyst-15	CH ₂ Cl ₂ /H ₂ O	23	recovery of SM

[a] Reactions were performed with oxime (4.0 mg, 9 μ mol); [b] IBX (3.0 equiv.), β -cyclodextrin (0.3 equiv.); [c] conversion was determined by ¹H NMR; [d] IBX (1.0 eq), β -cyclodextrin (0.1 eq); [e] IBX (2.0 eq), β -cyclodextrin (0.2 eq); [f] Isolated yield, with oxime (25.0 mg, 56 μ mol), IBX, β -cyclodextrin condition afforded α -nitro enamide;

Next, a stepwise α -hydroxylation–oxidation procedure was explored. Corey–Kim oxidation^[208] did not afford α -ketoenamide **4.55a**, which could be caused by the chlorination of the enamide

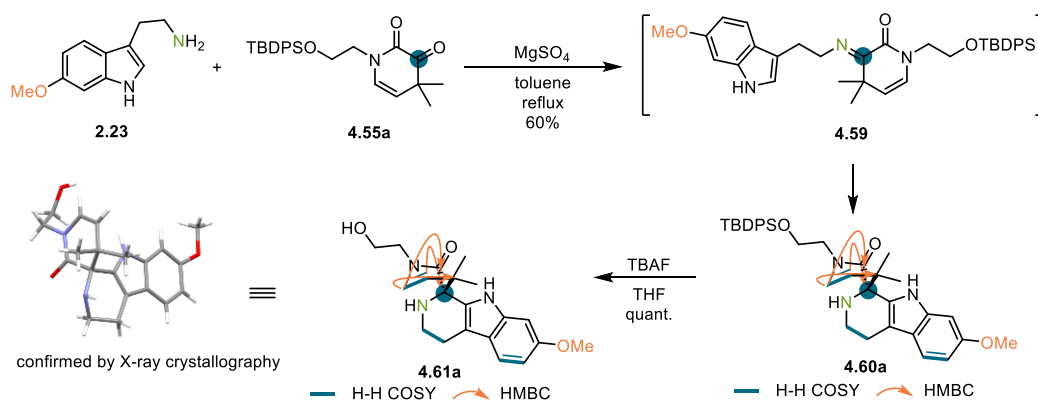
motif. With the milder Mukaiyama oxidation,^[275] α -ketoenamide **4.55a** was obtained successfully from **4.58a** in 70% yield (Scheme 4–16).



Scheme 4–16: Preparation of α -ketoenamide **4.55a**.

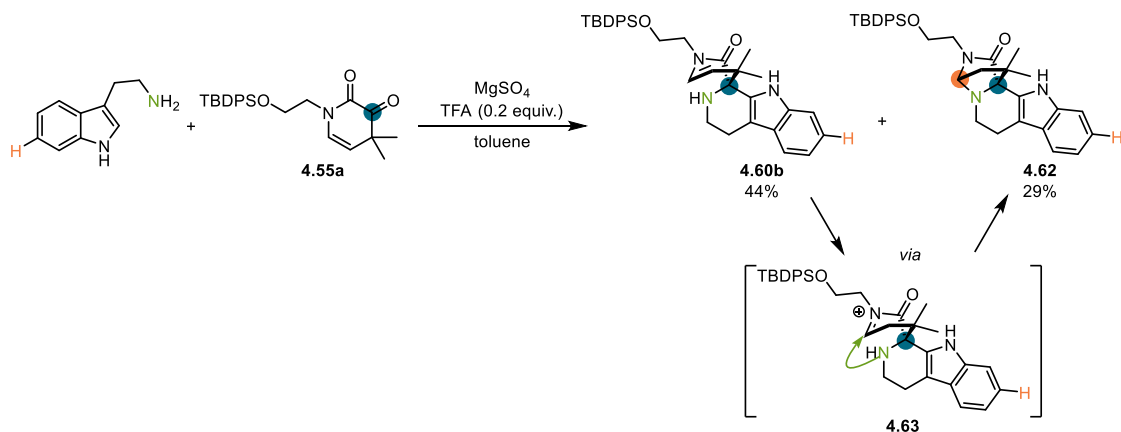
4.3.2.2. Pictet–Spengler reaction of the mono-ring α -ketoenamide

With the α -ketoenamide **4.55a** in hand, the Pictet–Spengler reaction of the mono-ring system was investigated (Scheme 4–17). Surprisingly, the Pictet–Spengler reaction product **4.60a** was formed in 60% yield under an acid-free condition, which was planned to prepare imine **4.59**. The structure of **4.60a** was confirmed by 2D NMR. Furthermore, by the TBDPS group cleavage of **4.60a**, the terminal hydroxyl group was liberated yielding **4.61a**. The 2D NMR and X-ray crystallography of **4.61a** confirmed the successful construction of the β -carboline scaffold in this acid-free condition.



Scheme 4–17: Acid-free Pictet–Spengler reaction and structure determination.

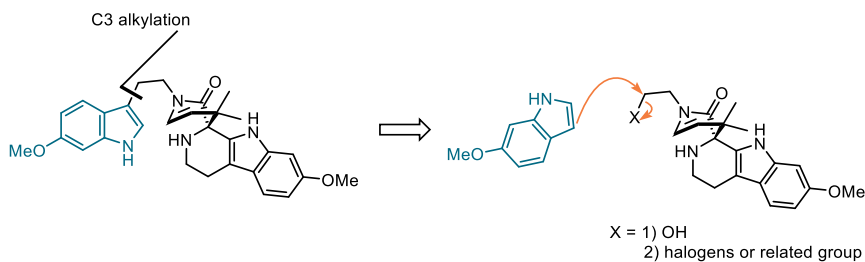
Inspired by the acid-free Pictet–Spengler reaction, the Pictet–Spengler reaction with tryptamine and α -ketoenamide **4.55a** was also explored (Scheme 4–18). However, the β -carboline scaffold was not formed under the acid-free condition. By the addition of TFA, the Pictet–Spengler reaction afforded **4.60b** in 44% yield. In addition, ainal **4.62** was also obtained via a proposed *N*-acyliminium ion **4.63** in 29% yield.



Scheme 4–18: The acid-free Pictet–Spengler reaction with tryptamine.

4.3.2.3. Late-stage construction of the indole motif

As the Pictet–Spengler reaction of mono-ring system was successfully achieved and the formation of *N*-acyliminium ion **4.63** was indicated. Installation of the indole motif was commenced by indole C3 alkylation strategy (Scheme 4–19). The selective C3 alkylation of indole was realized by various methods. The classic strategy relied on the activation of alkyl halides or related alkyl agents mediated by Lewis acid^[276] or catalyzed by palladium.^[277] The major drawback of the transformations using alkyl halides or related reagents was the generation of by-products, which usually caused some side-reactions. Borrowing hydrogen strategy^[278] realized the C3 alkylation of indole with alcohols. Grigg et al. developed a $[\text{Cp}^*\text{IrCl}_2]_2$ catalyzed C3 alkylation of indoles with benzyl alcohols.^[279] Since then, other noble metals were utilized, such as Pt,^[280] Ru^[281] and Pd.^[282] Lately, earth-abundant metals could be employed, such as Fe and Co.^[283] It was envisioned to install the indole motif by borrowing hydrogen strategy with primary alcohol first.

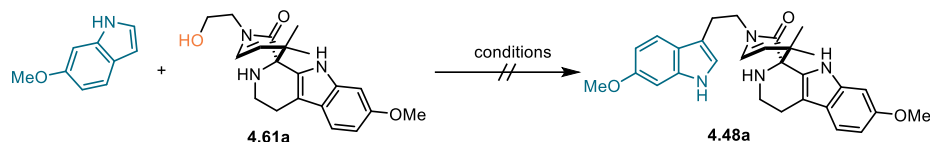


Scheme 4–19: C3 alkylation strategy.

Different metals were screened in the investigation of the borrowing hydrogen strategy (Table

4–3). However, the introduction of an indole motif was not achieved. It could be explained that the high reaction temperature required by the borrowing hydrogen strategy leading to side-reactions. Additionally, the borrowing hydrogen strategy usually needed special ligands for the hydrogen auto-transfer process.

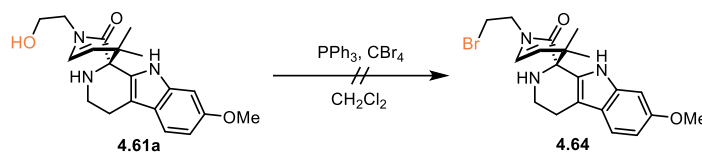
Table 4–3: Screening of indole C3 alkylation by borrowing hydrogen strategy.



entry ^[a]	catalyst [mol%]	solvent	T [°C]	yield
1	Pt on Al ₂ O ₃ (5)	xylene	135	decomposed
2	RuCl ₃ (10)	toluene	110	complex mixture
3	[(IrCp*Cl) ₂] ₂ (10)	toluene	110	complex mixture
4	RhCl ₃ (10)	toluene	110	complex mixture
5	FeCl ₃ (50)	MeNO ₂	23	recovery of SM
6	FeCl ₂ (50)	xylene	135	complex mixture
7	Iron(II) phthalocyanin (10)	xylene	135	complex mixture

[a] Reactions were performed with alcohol (2.0 mg, 6 μmol) and indole (0.7 mg, 6 μmol)

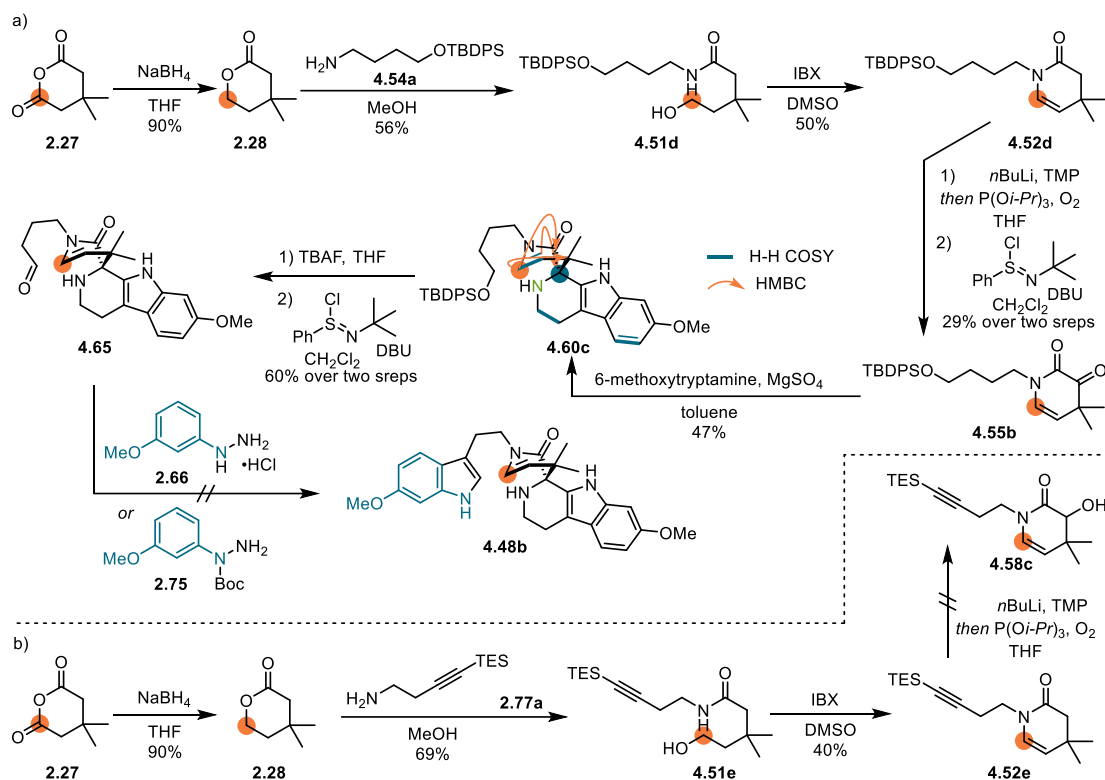
Due to the challenges of the borrowing hydrogen strategy, it was envisioned to utilize an alkyl halide to realize a direct alkylation. Unfortunately alcohol **4.61a** could not be transformed to the corresponding alkyl bromide **4.64** through an Appel reaction (Scheme 4–20).^[284]



Scheme 4–20: Attempt for the alkyl halide preparation.

Next, Fischer indole synthesis and Larock indole synthesis strategies were investigated to introduce the indole motif. These two strategies relied on the β-carboline scaffolds with different chains. The same lactone opening–oxidation procedure as before afforded enamides **4.52d** and **4.52e** (Scheme 4–21). Unfortunately, the α-hydroxylation of enamide **4.52e** led to decomposition (Scheme 4–21b). **4.55b** was prepared through the α-hydroxylation–oxidation sequence of enamide **4.52d**. The acid-free Pictet–Spengler reaction yielded β-carboline **4.60c**, which was confirmed by 2D NMR. The precursor of Fischer indole synthesis, aldehyde **4.65**, was obtained by a deprotection and Mukaiyama oxidation.^[275] Based on the previous experience of Fischer indole synthesis in the section “2.2.3.5. Scalable and reliable synthesis to 6-methoxytryptamine”, the hydrazine **2.66** and **2.75** were employed. However, the Fischer indole synthesis led to decomposition, indicating the highly functionalized enamides were not

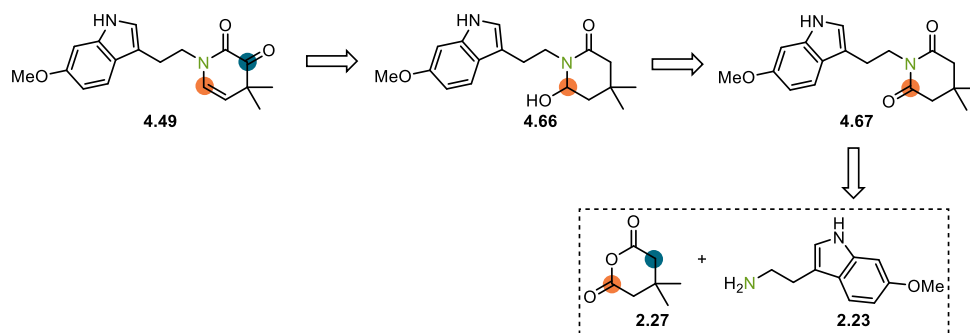
compactible to the late-stage indole assemble strategy.



Scheme 4–21: Fischer indole synthesis and Larock indole synthesis strategies.

4.3.2.4. Reduction of mono-ring α -ketoenamide and its Pictet–Spengler reaction

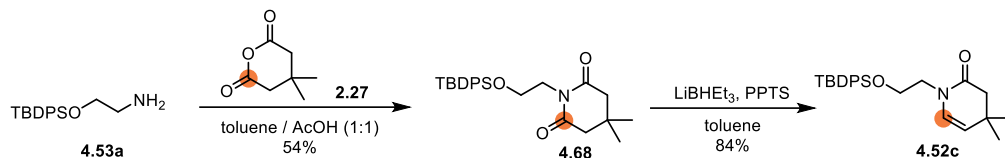
Next, it was anticipated to introduce the indole scaffold in the early-stage synthesis. Since it was shown ineffective to prepare the mono-ring α -ketoenamide with indole fragment by oxidation in the section “4.3.2.1. Mono-ring α -ketoenamide preparation via oxidative pathway”, a reductive pathway was envisaged to obtain α -ketoenamide **4.49**, which relied on the selective reduction of imide **4.67** and in situ elimination of hemiaminal **4.66** (Scheme 4–22).



Scheme 4–22: Reanalysis of the preparation of mono-ring α -ketoenamide.

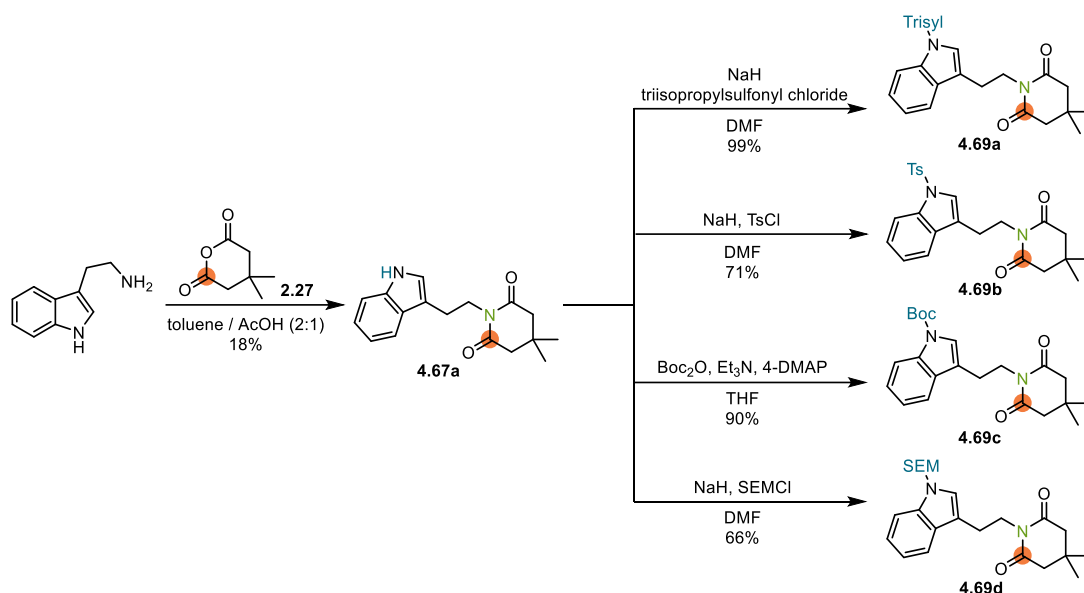
Initially the investigation of the reduction–elimination sequence was conducted with the model

imide **4.68**, which was prepared by a condensation reaction between anhydride **2.27** and amine **4.53a** (Scheme 4–23). After the reduction of imide **4.68** by LiBHET₃, the elimination was triggered by the addition of PPTS. Enamide **4.52c** was afforded in 45% yield over two steps.



Scheme 4–23: Model study of the selective reduction–elimination.

Inspired by the model study with imide **4.68**, the reduction–elimination sequence was investigated with the tryptamine derived imides. Using the same condensation reaction, imide **4.67a** was prepared in 18% yield (Scheme 4–24). Additionally, imides with various protection groups were also synthesized.

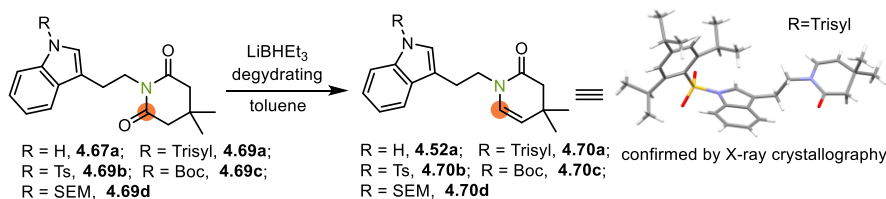


Scheme 4–24: Preparation of diverse imides.

With these imides in hand, the selective reduction–elimination sequence was investigated. The protection group free imide **4.67a** resulted in decomposition in all the tested reaction conditions (Table 4–4, entries 1–3). Next, the Ts-protected imide **4.69b** was selected for the dehydration screening (entries 4–8). It was discovered that after the reduction by LiBHET₃, the corresponding hemiacetal intermediate was liable to decompose by the dehydration reagent (entries 4–6). Surprisingly, the desired enamide **4.70b** was obtained by heating the concentrated hemiacetal intermediate (entries 7–8). This condition was applied to prepare the Boc (entry 9) and Trisyl (entry 10) protected mono-ring enamides **4.70a** and **4.70c**. In addition, the SEM-

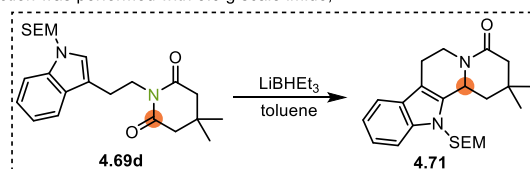
protected imide **4.69d** furnished the cyclization product **4.71** (entry 11).

Table 4–4: Preparation of the enamides by selective reduction–elimination.

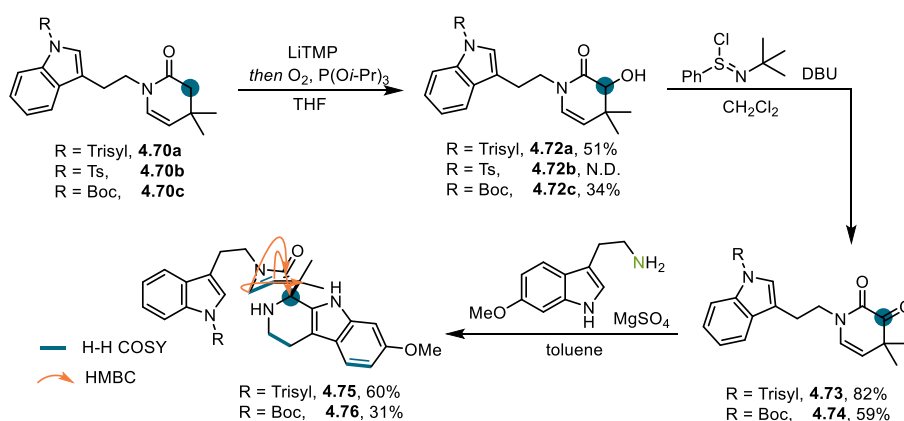


entry ^[a]	dehydration reagent	R	yield [%] ^[b]
1	PPTS	H	complex mixture
2	MeSO ₂ Cl, Et ₃ N	H	complex mixture
3	-	H	complex mixture
4	PPTS	Ts	47
5	MeSO ₂ Cl, Et ₃ N	Ts	59
6	TFAA, DMAP, DIPEA	Ts	trace
7	40 °C heating ^[c]	Ts	55
8 ^[d]	60 °C heating ^[c]	Ts	80
9 ^[e]	60 °C heating ^[c]	Boc	97
10 ^[f]	110 °C in toluene with PPTS ^[c]	Trisyl	78
11	-	SEM	70 (4.71)

[a] Reactions were performed with imide (30 μmol); [b] isolated yield; [c] after quenching and concentration; [d] reaction was performed with 2.6 g scale imide; [e] reaction was performed with 1.6 g scale imide; [f] reaction was performed with 3.3 g scale imide;



Following the previous α -hydroxylation–oxidation sequence, the corresponding mono-ring enamides **4.70a** and **4.70c** were converted to α -ketoenamides **4.73** and **4.74**, except the Ts-protected substrate **4.70b** (Scheme 4–25). The Pictet–Spengler reactions furnished the desired Boc and Trisyl protected β -carboline products **4.75** and **4.76**.

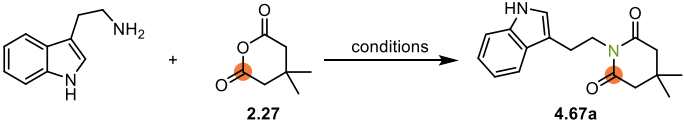


Scheme 4–25: Towards Pictet–Spengler reaction.

With the discovery of a successful route to construct the dimeric β -carboline model substrate, the investigation with 6-methoxytryptamine was initiated. Before that, the inefficient

condensation for the imide preparation needed to be optimized due to the limited supply of 6-methoxytryptamine. The yield was not improved by increasing the amount of AcOH to promote the formation of the mixture anhydride (Table 4–5, entries 1–2). Later, different combinations of activation esters and coupling reagents were screened (entries 3–10). The condensation yield was improved to 39% by using HOBT, EDC and DMAP (entry 4). However, through further optimization of this combination, there was no improvement of the yield (entries 11–14). Interestingly, with the Lewis acid and HMDS-promoted imide synthesis developed by Toru et al.,^[285] a remarkably increased yield was achieved, although the major product was the TMS-protected imide (entry 15). By screening the one-pot procedure of imide formation–desilylation (entries 16 and 17), the yield of the desired imide **4.67a** was finally increased to 74%.

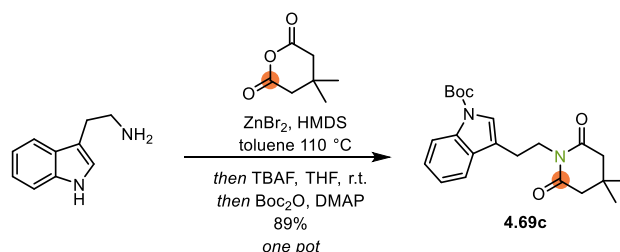
Table 4–5: Optimization of imide synthesis.



entry ^[a]	conditions	solvent	T [°C]	yield [%] ^[b]
1	toluene / AcOH (2:1)	toluene / AcOH (2:1)	120	13
2	toluene / AcOH (1:2)	toluene / AcOH (1:2)	120	18
3	BOP, Et ₃ N	THF	60	22
4	HOBT, EDC, DMAP	DMF	23	39
5	CDI	THF	23	trace
6	DPPA, Et ₃ N	DMF	23	14
7	<i>N</i> -hydroxysuccinimide, EDC, DMAP	CH ₂ Cl ₂	23	trace
8	pentafluorophenol, EDC, DMAP	CH ₂ Cl ₂	23	trace
9	cyanuric chloride, Et ₃ N	MeCN	23	30
10	Mukaiyama's reagent ^[c] , Et ₃ N	DMF	23	28
11	HOBT, EDC, DMAP	DCE	70	24
12	HOBT, EDC, DIPEA	DCE	70	27
13	HOBT, EDC, DMAP	DMF	23	27
14	HOBT, DCC, DMAP	DMF	23	31
15	ZnBr ₂ , HMDS	toluene	110	14 (85) ^[d]
16	ZnBr ₂ , HMDS, then CsF	toluene	110 to 23 ^[e]	52
17	ZnBr ₂ , HMDS, then TBAF	toluene	110 to 23	74

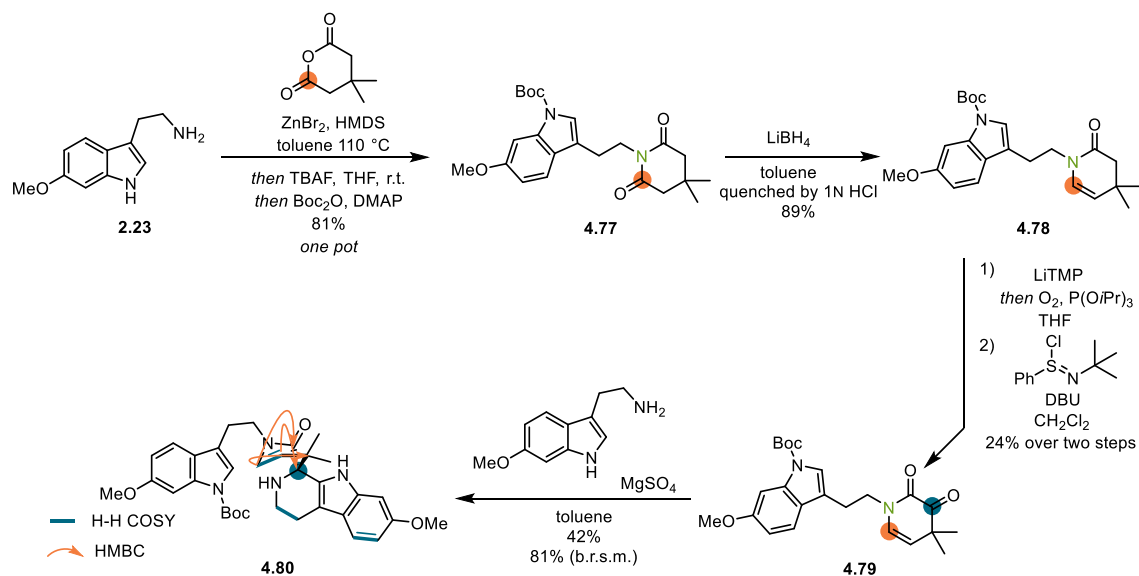
[a] Reactions were performed with typtamine (150 mg, 0.938 mmol), anhydride (133 mg, 0.938 mmol); [b] isolated yield; [c] Mukaiyama's reagent = 2-chloro-1-methylpyridinium iodide; [d] 85% yield is for the total yield of imide and TMS-imide; [e] the desilylation was performed at 23 °C

Next, the one-pot synthesis of the Boc-protected imide **4.69c** was realized in 89% yield, through the imide formation–desilylation sequence incorporating a Boc protection (Scheme 4–26).



Scheme 4–26: One-pot synthesis of Boc-protected imide.

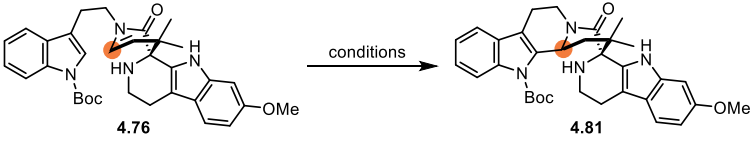
With the efficient preparation of the Boc-protected imide in hand, the synthesis starting with 6-methoxytryptamine was commenced. Following the one-pot procedure, the Boc-protected imide **4.77** was prepared in 81% yield (Scheme 4–27). After the selective reduction–elimination, enamide **4.78** was afforded in 89% yield. Through the two-step α -oxidation, the α -ketoenamide **4.79** was obtained in 24% yield. The acid-free Pictet–Spengler reaction of α -ketoenamide **4.79** worked smoothly leading to dimeric β -carboline **4.80**.



Scheme 4–27: Preparation of the key intermediate starting with 6-methoxytryptamine.

4.3.2.5. Study of the iminium ion cyclization

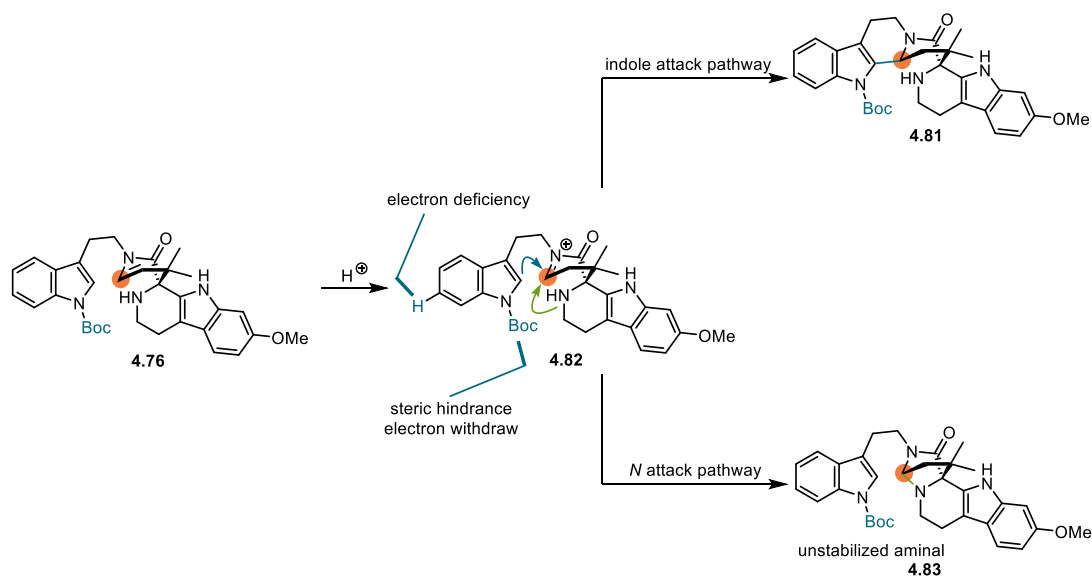
Since the Trisyl is a very robust protection group and very difficult to be removed, it was used to provide a strong protection of the indole fragment to avoid false negative results. The further exploration of the iminium ion cyclization was commenced with the Boc-protected substrate **4.76**. Although both classic Brønsted acids (Table 4–6, entries 1–5) and Lewis acids (entries 6–8) were screened, most conditions led to a complex mixture of products (entries 4–8). With relatively weaker Brønsted acids, the iminium ion cyclization resulted in recovery of starting material (entries 1–3). Based on this result, the reaction was further optimized under increased temperature with weaker Brønsted acids conditions (entries 9–14) or decreased temperature with stronger acids conditions (entries 15–17). However, the formation of the desired cyclization product was not observed under these reaction conditions.

Table 4–6: Iminium ion cyclization.


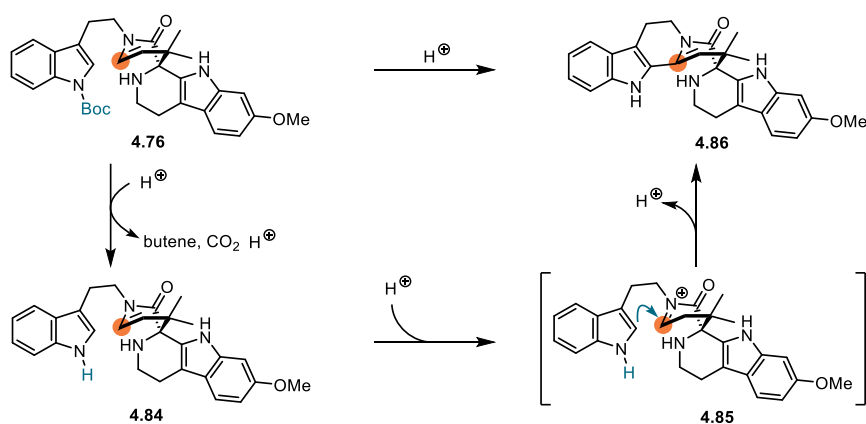
entry ^[a]	acid	solvent	T [°C]	yield
1	TFA	CH ₂ Cl ₂	23	recovery of SM
2	CSA	CH ₂ Cl ₂	23	recovery of SM
3	hydroxysulfamic acid	CH ₂ Cl ₂	23	recovery of SM
4	TfOH	CH ₂ Cl ₂	23	complex mixture
5	MeSO ₃ H	CH ₂ Cl ₂	23	complex mixture
6	TMSOTf	CH ₂ Cl ₂	23	complex mixture
7	BF ₃ ·OEt ₂	CH ₂ Cl ₂	23	complex mixture
8	BF ₃ ·AcOH	CH ₂ Cl ₂	23	complex mixture
9	TFA	DCE	60	recovery of SM
10	CSA	DCE	60	recovery of SM
11	hydroxysulfamic acid	DCE	60	recovery of SM
12	TFA	toluene	80	complex mixture
13	CSA	toluene	80	complex mixture
14	hydroxysulfamic acid	toluene	80	complex mixture
15	TfOH	CH ₂ Cl ₂	0	recovery of SM
16	MeSO ₃ H	CH ₂ Cl ₂	0	recovery of SM
17	TMSOTf	CH ₂ Cl ₂	0	recovery of SM

[a] Reactions were performed with substrate (1.0 mg, 2.2 μmol)

Based on these results, a hypothesis of the iminium ion cyclization was proposed. There were competitive pathways concerning the attack to iminium ion **4.82** (Scheme 4–28). It was considered that the indole attack pathway yielding **4.81** might be disfavored, as the Boc group caused the steric hindrance and electron withdrawing, accompanying the electron deficiency of the model substrate lacking the methoxy group. Therefore, the iminium ion cyclization probably underwent the *N* attack pathway to afford amination **4.83**, which was prone to be decomposed under acidic condition.^[286]

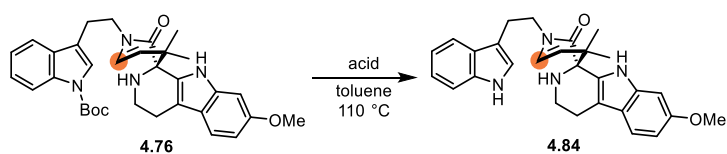
**Scheme 4–28:** Analysis of the iminium ion cyclization.

Compared to the absence of the indole methoxy group, it was envisioned that the Boc group might be more crucial for the reactivity, as it was closer to the reaction center. Therefore, in order to afford the cyclization product **4.86**, a tactic sequence need be followed (Scheme 4–29). The Boc group should be cleaved selectively first, and then generate iminium ion **4.85** to receive the attack from the indole fragment.



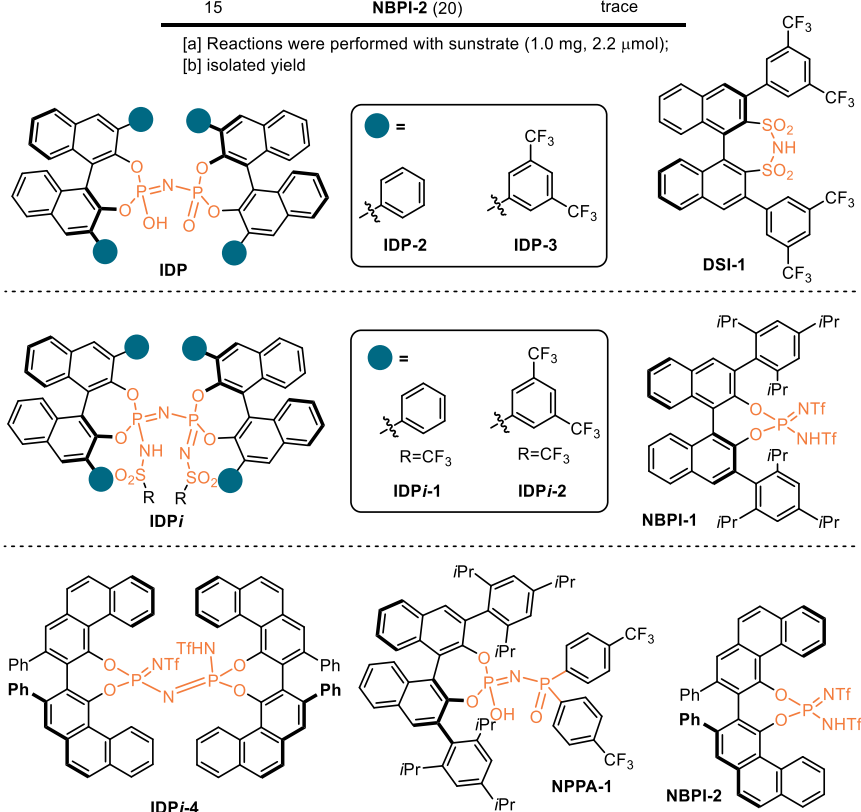
Scheme 4–29: Expected iminium ion cyclization.

Based on this hypothesis, it was important to discover an acid which could promote the iminium ion cyclization in the expected reaction order. The novel confined Brønsted acids developed by List et al.,^[140-142] were anticipated to realize the expected reaction sequence through a different activation mode. Although the desired cyclization product **4.86** was not obtained, the Boc group cleavage was achieved by some novel confined Brønsted acids to afford **4.84** (Table 4–7, entries 1, 3, 5, 9 and 10). By further increasing the catalyst loading, neither the improved yield of **4.84** nor the formation of **4.86** was achieved (Table 4–7, entries 11–15). Compared with the results of the classic Brønsted acids (Table 4–6), it was proposed that the novel confined Brønsted acids could selectively interact with the Boc group through molecular recognition in the catalytic pocket. Additionally, the large substitution groups of the confined Brønsted acids could inhibit the further iminium ion cyclization. The increased acid loading resulted in a decrease of the yield of **4.84**, indicating that **4.84** might be unstable in acidic condition. Therefore, it was considered that this reaction needed a proper acid which could provide selective recognition of Boc group and had a relatively small counterion.

Table 4–7: Iminium ion cyclization with confined Brønsted acids.

entry ^[a]	acid [mol%] ^[b]	yield [%] ^[b]
1	DSI-1 (5)	58
2	NPPA-1 (5)	66
3	IDP-2 (5)	21
4	IDP-3 (5)	trace
5	IDPi-1 (5)	30
6	IDPi-2 (5)	trace
7	IDPi-4 (5)	trace
8	IDPi-10 (5)	trace
9	NBPI-1 (5)	66
10	NBPI-2 (5)	57
11	DSI-1 (20)	trace
12	IDP-2 (20)	trace
13	IDP-1 (20)	trace
14	NBPI-1 (20)	trace
15	NBPI-2 (20)	trace

[a] Reactions were performed with substrate (1.0 mg, 2.2 μ mol);
 [b] isolated yield



4.3.2.6. Pictet–Spengler reaction–iminium ion cyclization–amination cascade

Those reactions with the confined Brønsted acids showed that **DSI-1**, **NPPA-1**, **IDP-2** and **IDPi-1** could catalyze the Boc group cleavage efficiently, but the following iminium ion cyclization was unsuccessful probably due to the large size of the corresponding counterions.

It was hypothesized that racemic Brønsted acids with similar acidic cores, but smaller

substitution groups could overcome the problems. DSI, IDP, NPPA and permutation of these cores were selected to design the racemic Brønsted acids. Initially, phenyl group was chosen as the substitution groups. These racemic Brønsted acids with different cores were obtained in moderate to good yields (Figure 4–2).

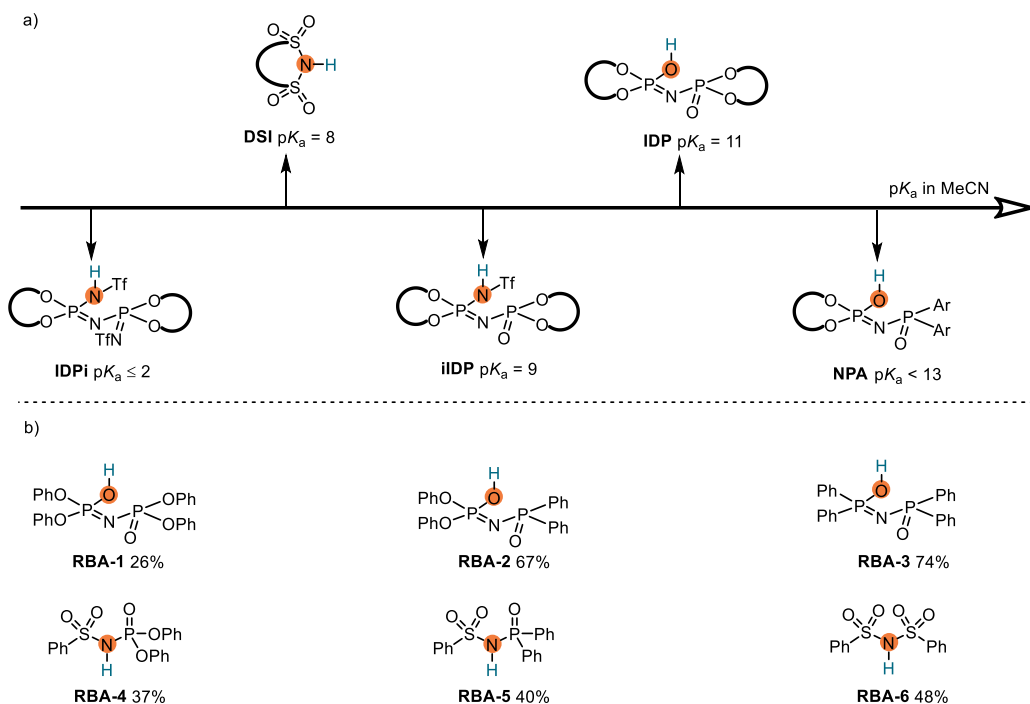
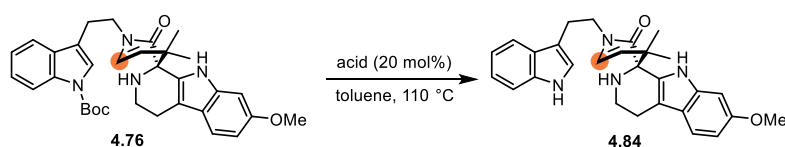


Figure 4–2: Design of racemic Brønsted acids.

All of the above Brønsted acids could remove the Boc group with different conversion, but the iminium ion cyclization was still not realized. The screening showed that the combination between phosphinyl and phosphonyl groups resulted in low conversion (Table 4–8, entries 1–3). Introduction of the sulfonyl group furnished remarkable improvement of the conversion (entries 4–6), especially the diphenyldisulfonimide (entry 6).

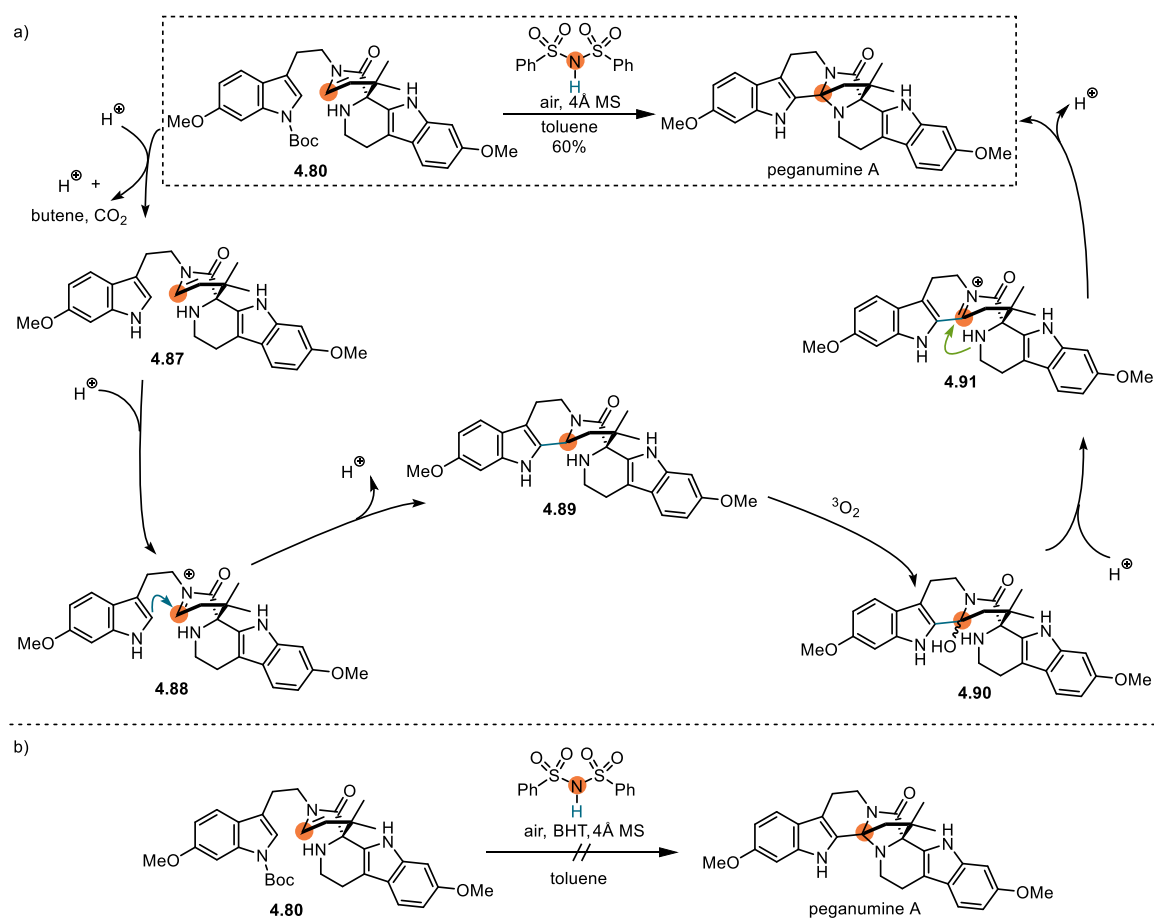
Table 4–8: Screening of Boc cleavage with racemic Brønsted acids.



entry ^[a]	acid	conversion [%] ^[b]
1	RBA-1	8
2	RBA-2	11
3	RBA-3	8
4	RBA-4	20
5	RBA-5	22
6	RBA-6	50

[a] Reactions were performed with substrate (1.0 mg, 2.2 μ mol);
[b] conversion was determined by ^1H NMR

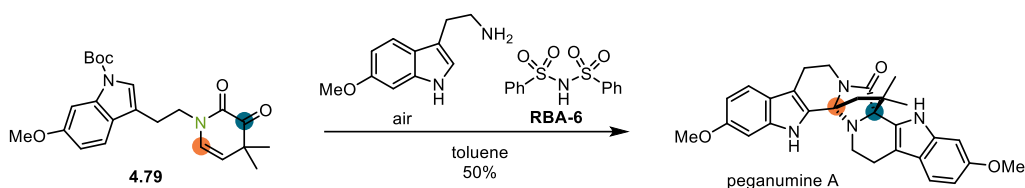
Since neither the novel confined Brønsted acids nor the newly designed racemic Brønsted acids could realize the iminium ion cyclization of **4.76**, it was speculated that the absence of the *o*-indole methoxy group could cause the unsuccessful iminium ion cyclization. Therefore, the iminium ion cyclization of substrate **4.80** was investigated. Surprisingly, this reaction afforded peganumine A. The proposed mechanism showed that the reaction was initiated by the Boc group cleavage (Scheme 4–30a). The subsequent cyclization of **4.87** yielded **4.89** through iminium ion **4.88**. Dimeric β -carboline **4.89** was autoxidized by the triplet oxygen in the air affording **4.90**, which could generate *N*-acyliminium ion **4.91**. Iminium ion **4.91** was attacked by the *N* atom leading to peganumine A. The hypothesis of the autoxidation was supported by a control experiment with the addition of BHT as antioxidant (Scheme 4–30b).



Scheme 4–30: Proposed mechanism of peganumine A formation.

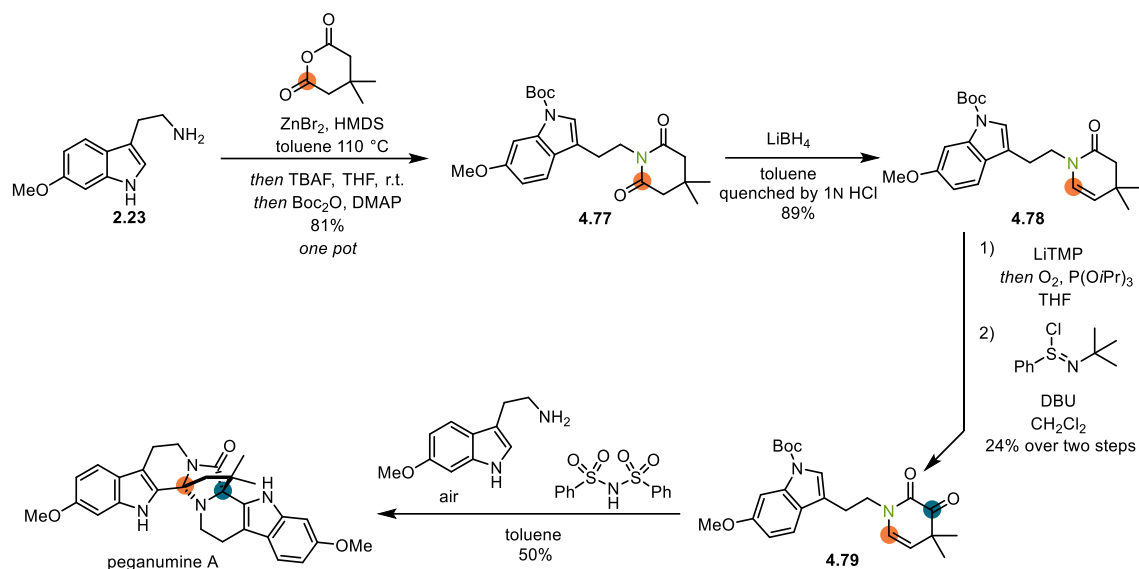
Since the Pictet–Spengler reaction could also be promoted by acid, the cascade reaction incorporated with Pictet–Spengler reaction, iminium ion cyclization and amination was envisioned. Starting with α -ketoamide **4.79**, the cascade reaction underwent successfully, leading to peganumine A in 50% yield (Scheme 4–31).

4.3. 5th generation synthetic approach for peganumine A



Scheme 4-31: Diphenyldisulfonimide promoted cascade reaction.

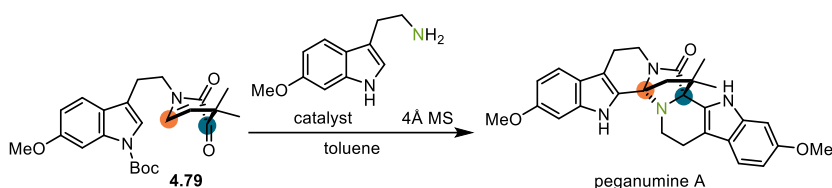
Till this point, the total synthesis of the racemic peganumine A was realized in a five-step concise synthesis. The synthetic route can be divided into three stages. The first stage is monocyclic enamide **4.78** preparation through a one-pot condensation–Boc protection reaction and reduction–elimination sequence. The second stage is the α -functionalization by an α -oxidation sequence afforded α -ketoenamide **4.79**. The last stage is cyclization stage via a Pictet–Spengler reaction–*N*-acyliminium ion cyclization–amination cascade (Scheme 4–32).



Scheme 4-32: 5th generation total synthesis route of peganumine A.

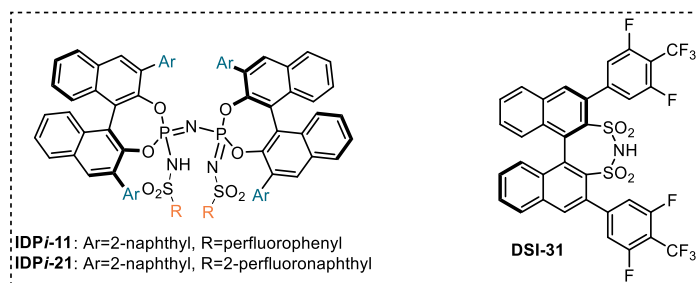
4.3.2.7. Asymmetric Pictet–Spengler reaction–cyclization–amination cascade

After the accomplishment of the total synthesis of the racemic peganumine A, the asymmetric version of the cascade reaction was anticipated. **DSI-31** was selected to catalyze the asymmetric cascade reaction initially, resulting in only 10% yield and 52.8% *ee* (Table 4–9, entry 1). By increasing the catalyst loading to 60 mol%, the yield was improved to 40%, but the enantioselectivity was dropped to 37.6% *ee* (entry 2). The novel confined dual-core Brønsted acids **IDPi-11** and **IDPi-21** were also screened (entries 3–8). However, no improvement was afforded.

Table 4-9: Initial investigation of the asymmetric cascade reaction.

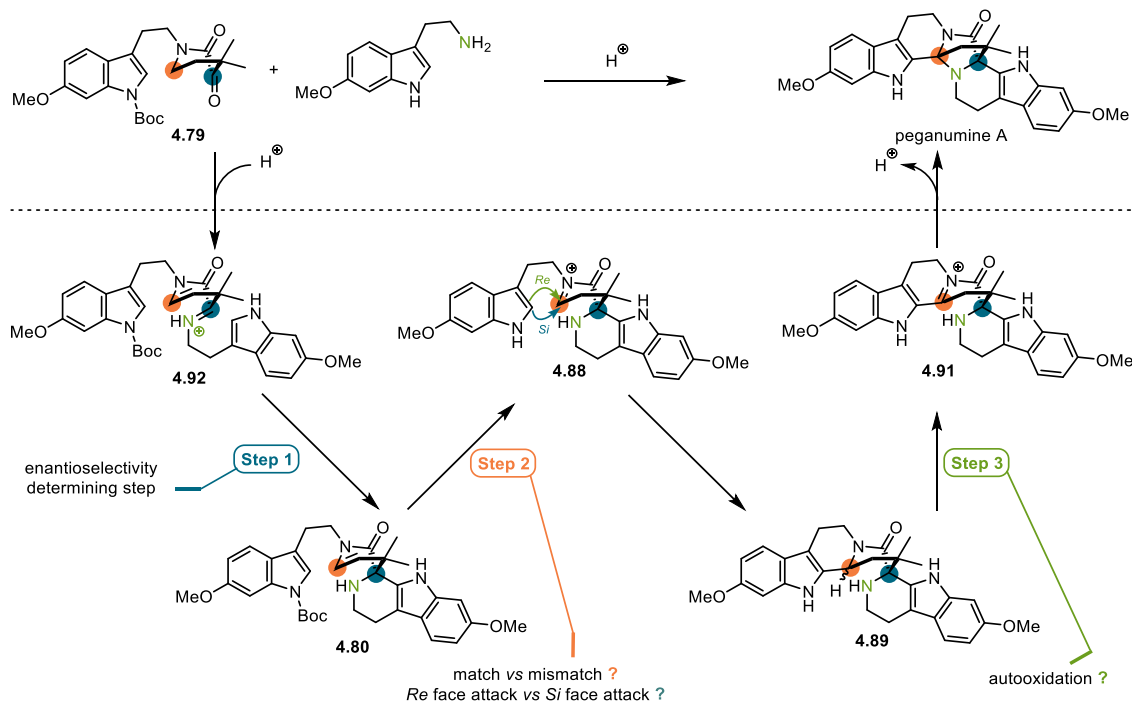
entry ^[a]	catalyst [mol%]	T [°C]	ee [%] ^[b]	yield [%] ^[c]
1	DSI-31 (20)	110	52.8	10
2	DSI-31 (60)	110	37.6	40
3	IDP<i>i</i>-11 (20)	110	8.7	trace
4	IDP<i>i</i>-21 (20)	110	N.D.	trace
5	IDP<i>i</i>-11 (60)	110	50.5	trace
6	IDP<i>i</i>-11 (100)	23 to 110	16.7	20
7	IDP<i>i</i>-21 (60)	110	39.7	10
8	IDP<i>i</i>-21 (100)	23 to 110	27.6	30

[a] Reactions were performed with ketoenamide (1.0 mg, 2.4 μ mol), 6-methoxytryptamine (0.55 mg, 2.9 μ mol) [b] enantiomeric excess (ee) was measured by HPLC. [c] yield was determined by ¹H NMR.



In order to investigate the asymmetric cascade reaction thoroughly, the mechanism and origin of the enantioselectivity were analyzed. The cascade reaction contained three main steps: 1, Pictet–Spengler reaction; 2, *N*-acyliminium ion cyclization triggered by the Boc group cleavage; 3, C–N bond formation through an in situ benzylic autoxidation (Scheme 4–33). Each single step contained unresolved problems. Firstly, the Pictet–Spengler reaction was the enantioselectivity determining step. It was necessary to discover a proper catalyst for this asymmetric Pictet–Spengler reaction. Secondly, the *N*-acyliminium ion cyclization was proposed to be triggered by the Boc group cleavage in the total synthesis of racemic peganumine A. Thus, the catalyst should also be able to promote the selective Boc group cleavage and subsequent *N*-acyliminium ion cyclization. Additionally, the *N*-acyliminium ion cyclization had not only a facial selectivity issue, but also a potential mismatch issue between *N*-acyliminium ion **4.88** and the chiral catalyst. Thirdly, in the C–N bond formation step, the stereocenter could influence the efficiency of the autoxidation and the chiral catalyst needed to promote the generation of *N*-acyliminium ion **4.91**. Due to the complexity of this cascade reaction, it was envisioned to solve the problems step by step.

4.3. 5th generation synthetic approach for peganumine A



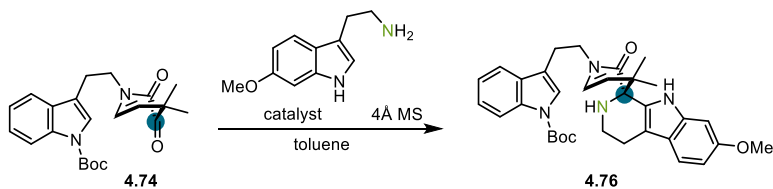
Scheme 4-33: Analysis of the cascade.

4.3.2.7. Asymmetric Pictet–Spengler reaction of the mono-ring α -ketoenamide

The Pictet–Spengler reaction was investigated initially. In order to simplify and focus on the Pictet–Spengler reaction, the modal system that without the west indole methoxy group was selected for the screening, as the absence of that methoxy group cannot trigger the iminium ion cyclization making the reaction suspension after the Pictet–Spengler reaction. The control experiments revealed that there was no reaction under 60 °C without catalyst (Table 4–10, entries 1 and 2), and substrates could partially convert to product at temperature over 80 °C (entries 3 and 4). The reactions catalyzed by **DSI-31** and **IDPi-11** with high catalyst loading and temperature resulted in low enantioselectivity (entries 7–9 and 12–14). With high catalyst loading of **IDPi-11** at room temperature, the enantioselectivity was not improved (entries 5–6). Meanwhile, with lower catalyst loading of **IDPis** at room temperature, the reaction cannot undergo successfully (entries 15–17 and 21–23). With high catalyst loading of **DSI-31** at room temperature, there was slight improvement of enantioselectivity (entries 10–11). Interestingly, with lower catalyst loading of **DSI-31** at room temperature, the reaction worked well and the enantioselectivity was slight increased (entries 18–20). Analyzing the results afforded by **IDPis** and **DSI-31**, it was hypothesized that the dimeric BINOL backbone like **IDPis** was too

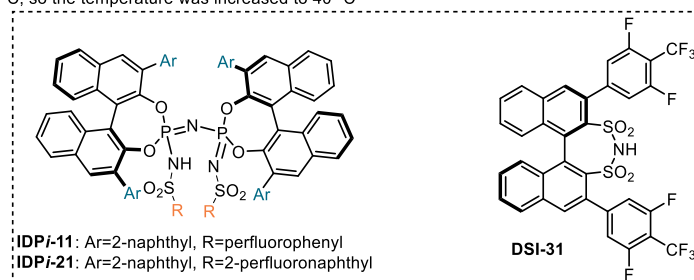
sterically hindered to interact with the substrates, which indicated that the open-site catalysts, like **DSI**, could be favored for the reaction.

Table 4–10: 1st screening of the Pictet–Spengler reaction.

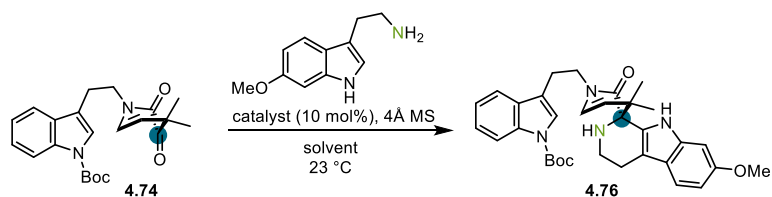


entry ^[a]	catalyst [mol%]	T [°C]	ee [%] ^[b]	yield [%] ^[c]
1	--	23	N.D. ^[d]	full recovery of SM
2	--	60	N.D.	full recovery of SM
3	--	80	N.D.	17 (conv.) ^[e]
4	--	100	N.D.	50 (conv.)
5	IDP<i>i</i>-11 (20)	23	2.6	30
6	IDP<i>i</i>-11 (40)	23	11.0	17
7	IDP<i>i</i>-11 (20)	60	2.6	47
8	IDP<i>i</i>-11 (40)	60	3.0	25
9	IDP<i>i</i>-11 (20)	80	0.4	28 (4.84) ^[f]
10	DSI-31 (20)	23	19.4	27
11	DSI-31 (40)	23	23.5	52
12	DSI-31 (20)	60	14.6	31
13	DSI-31 (40)	60	9.6	50
14	DSI-31 (20)	80	11.0	35 (4.84) ^[f]
15	IDP<i>i</i>-11 (10)	23 to 40 ^[g]	0.6	40
16	IDP<i>i</i>-11 (5)	23 to 40 ^[g]	1.0	14
17	IDP<i>i</i>-11 (2.5)	23 to 40 ^[g]	1.4	17
18	DSI-31 (10)	23	26.6	15
19	DSI-31 (5)	23	7.0	19
20	DSI-31 (2.5)	23	6.0	11
21	IDP<i>i</i>-21 (10)	23 to 40 ^[g]	1.0	13
22	IDP<i>i</i>-21 (5)	23 to 40 ^[g]	0.8	20
23	IDP<i>i</i>-21 (2.5)	23 to 40 ^[g]	0.4	18

[a] Reactions were performed with ketoenamide (1.0 mg, 2.6 μ mol), 6-methoxytryptamine (0.60 mg, 3.1 μ mol) [b] enantiomeric excess (ee) was measured by HPLC. [c] isolated yield; [d] N.D. = not determined; [e] conversion was determined by ¹H NMR; [f] the Boc group was cleaved; [g] product was not formed at 23 °C, so the temperature was increased to 40 °C

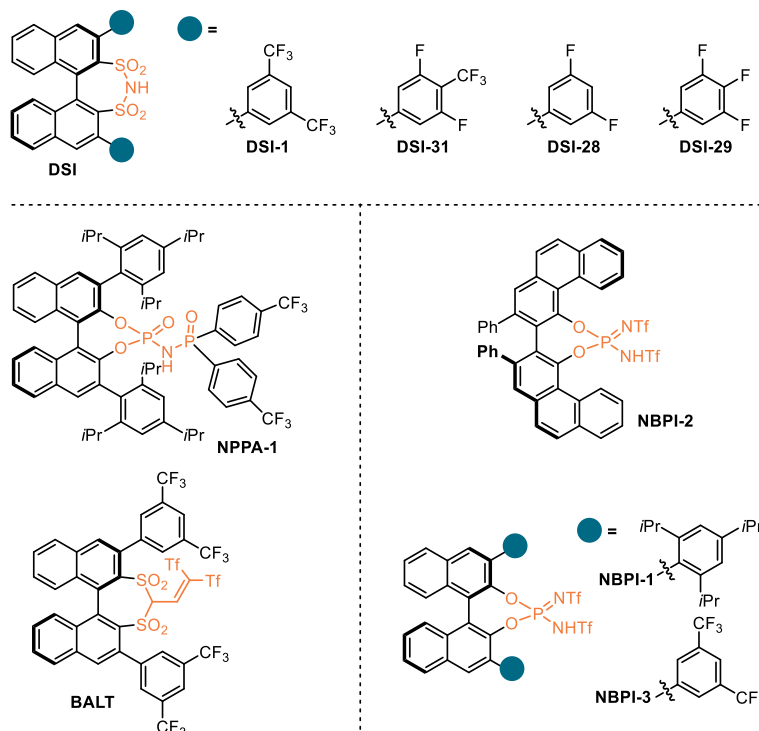


Next, open-site catalysts were screened. With the more acidic **NBPIs** and **BALT**, the enantioselectivity was not as good as **DSI** (Table 4–11, entries 5–7 and 9). **DSIs** with different substitutes resulted in various enantioselectivities and yields (entries 1–4). The result of **NPPA** also supported this reaction system needed open-site catalyst (entry 8). The screening of the solvents indicated that only aromatic solvents could promote the reaction (entries 10–17).

Table 4–11: 2nd screening of the Pictet–Spengler reaction.

entry ^[a]	catalyst	solvent	ee [%] ^[b]	yield [%] ^[c]
1	DSI-31	toluene	26.6	15
2	DSI-28	toluene	10.8	22
3	DSI-29	toluene	20	29
4	DSI-1	toluene	4.0	10
5	NBPI-1	toluene	2.0	13
6	NBPI-2	toluene	2.4	13
7	NBPI-3	toluene	4.4	7
8	NPPA-1	toluene	1.0	30
9	BALT	toluene	3.6	37
<hr/>				
10	DSI-31	CHCl ₃	N.D. ^[d]	trace
11	DSI-31	Et ₂ O	N.D.	trace
12	DSI-31	<i>p</i> -xylene	33.0	11
13	DSI-31	benzene	22.4	11
14	DSI-31	PhCF ₃	29.0	16
15	DSI-31	PhF	21.8	33
16	DSI-31	octafluorotoluene	N.D.	trace
17	DSI-31	CH ₃ CN	N.D.	trace

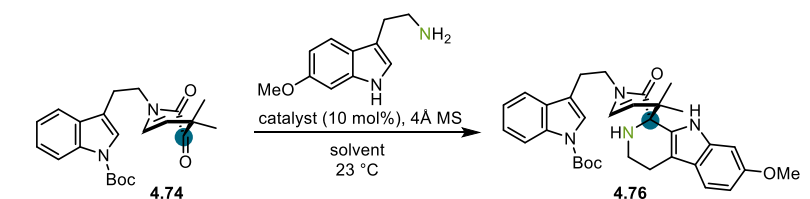
[a] Reactions were performed with ketoenamide (1.0 mg, 2.6 μmol), 6-methoxytryptamine (0.60 mg, 3.1 μmol) [b] enantiomeric excess (*ee*) was measured by HPLC. [c] isolated yield; [d] N.D. = not determined;



The reason for the low enantioselectivities with these strong Brønsted acids could be rationalized by the over-acidity, so the next attempt was to utilize weaker Brønsted acids to increase the enantioselectivity. Fortunately, with **CPA-1** and **CPA-14**, the enantioselectivities were remarkably increased (Table 4–12, entries 1 and 2). **CPA-1** was chosen to screen different

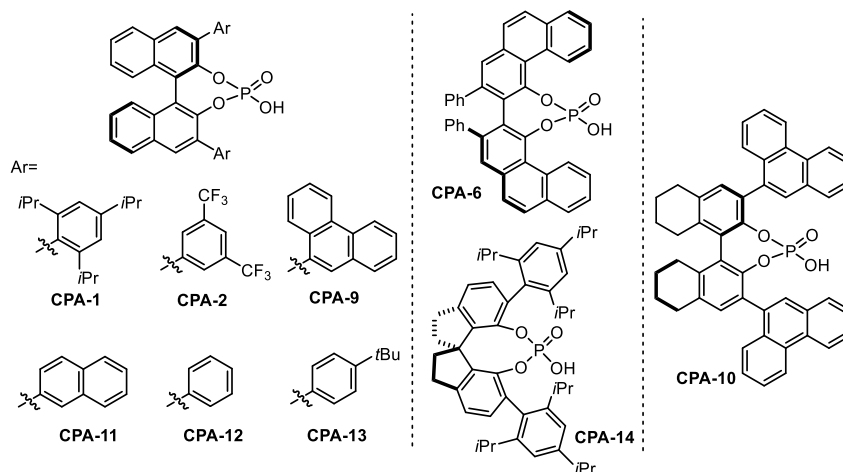
solvents. For the ethereal solvents, only Et₂O furnished 10% *ee* (entry 10). There was no conversion in THF and 1,4-dioxane (entries 11 and 12). Other aromatic solvent (entries 13 and 14), such as PhCF₃ and PhF, afforded slightly improved enantioselectivity. Surprisingly, using chloroform (entry 16) led to an increased enantioselectivity (63.8% *ee*), although other halogenated solvents afforded no such benefit (entries 18 and 19).

Table 4–12: 3rd screening of the Pictet–Spengler reaction.



entry	catalyst	solvent	<i>ee</i>	yield
1	CPA-1	toluene	48.0%	18%
2	CPA-2	toluene	16.2%	64%
3	CPA-6	toluene	N.D.	N.D.
4	CPA-9	toluene	7.6%	18%
5	CPA-10	toluene	0%	31%
6	CPA-11	toluene	6.2%	40%
7	CPA-12	toluene	1.6%	22%
8	CPA-13	toluene	1.8%	13%
9	CPA-14	toluene	-45.6%	23%
10	CPA-1	Et ₂ O	10.0%	20%
11	CPA-1	THF	N.D.	N.D.
12	CPA-1	1,4-dioxane	N.D.	N.D.
13	CPA-1	PhCF ₃	53.4%	52%
14	CPA-1	PhF	50.6%	6.9%
15	CPA-1	CH ₂ Cl ₂	18.4%	54%
16	CPA-1	CHCl ₃	63.8%	43%
17	CPA-1	CH ₃ CN	N.D.	N.D.
18	CPA-1	CHBr ₃	4.2%	28%
19	CPA-1	CH ₂ Br ₂	13.6%	49%

[a] Reactions were performed with ketoamide (1.0 mg, 2.6 μmol), 6-methoxytryptamine (0.60 mg, 3.1 μmol) [b] enantiomeric excess (*ee*) was measured by HPLC. [c] isolated yield; [d] N.D. = not determined;



With such promising results, further optimization was conducted. Taking the catalyst loading and reaction temperature into consideration (Table 4–13, entries 1–10), 70.2% *ee* and 85% isolated yield was afforded with 20 mol% catalyst at 45 °C (entry 7). Through amine equivalent

screening, 1.2 equiv. amine was found to be the best (entries 11–15).

Table 4–13: 4th screening of the Pictet–Spengler reaction.

entry ^[a]	CPA-2 [mol%]	amine [equiv.]	T [°C]	ee [%] ^[b]	yield [%] ^[c]
1	5	1.2	23	8.4	35
2	10	1.2	23	16.2	64
3	20	1.2	23	61.4	18
4	20	1.2	23	70.6	57
5	5	1.2	45	36.8	30
6	10	1.2	45	51.6	30
7	20	1.2	45	70.2	85
8	5	1.2	60	19.0	95
9	10	1.2	60	44.0	38
10	20	1.2	60	61.6	49
11	30	1.2	45	67.6	33
12	20	1.8	45	65.2	58
13	20	2.4	45	54.0	70
14	20	3.0	45	46.4	45
15	20	3.6	45	51.0	40

[a] Reactions were performed with ketoenamide (1.0 mg, 2.6 μ mol), 6-methoxytryptamine (0.60 mg, 3.1 μ mol) [b] enantiomeric excess (ee) was measured by HPLC. [c] isolated yield

Simultaneously, the preform-imine procedure was also tested, which could allow low catalyst loading and low temperature. With low catalyst loading and low temperature, the enantioselectivities improved slightly (entries 4 and 14). But the yields dropped, although the reaction times were extended.

Table 4–14: 5th screening of the Pictet–Spengler reaction.

entry ^[a]	CPA-2 [mol%]	amine [equiv.]	T [°C]	ee [%] ^[b]	yield [%] ^[c]
1	20	1.8	23 to 45 ^[d]	47.4	37
2	20	1.8	45	29.6	30
3	10	1.8	23	72.8	34
4	5	1.8	23	17.2	trace
5	2.5	1.8	23	N.D. ^[e]	N.D.
6	10	1.2	23	31.4	38
7	5	1.2	23	44.2	28
8	2.5	1.2	23	45.6	25
9	10	1.8	–20	N.D.	N.D.
10	20	1.8	–20	15.6	9
11	10	1.2	–20	56.2	3
12	20	1.2	–20	65.8	39
13	10	1.8	0	64.8	14
14	20	1.8	0	76.8	35
15	10	1.2	0	55.6	17
16	20	1.2	0	60.4	14

[a] Reactions were performed with ketoenamide (1.0 mg, 2.6 μ mol), 6-methoxytryptamine (0.60 mg, 3.1 μ mol) [b] enantiomeric excess (ee) was measured by HPLC. [c] isolated yield; [d] after CPA addition, the mixture was stirred at 23 °C for 1d and 45 °C for 1d; [e] N.D. = not determined

4.4. Brief summary

In this chapter, two new synthetic strategies of peganumine A were explored, which were based on a *N*-acyliminium ion cyclization to construct the west β -carboline motif and a Pictet–Spengler reaction to install the east one. In the 4th generation route, the Pictet–Spengler reaction with the acyclic substrate was unsuccessful, which probably caused by the free rotation of the C–C bond leading to steric hindrance. Therefore, the Pictet–Spengler reaction of a mono-cyclic enamide was employed in the 5th generation route. Various mono-cyclic enamides were prepared either by the oxidation pathway or the reduction pathway. The Pictet–Spengler reaction of the mono-cyclic enamide underwent successfully even in the acid free condition. However, the *N*-acyl iminium ion cyclization turned out to be challenging. After some screenings, the racemic disulfimide was able to promote the reaction in a cascade fashion.

**5. Complementary Carbonyl Activation Annulation and Its
Application to Natural Product Total Synthesis**

5.1. Introduction

5.1.1. Polycyclic compound

Polycyclic compound is a special type of organic molecule featuring several closed rings, primarily including cycloalkanes and aromatics, e.g. tricyclic sesquiterpene longifolene^[287] and pentacyclic aromatic hydrocarbon benzo[*a*]pyrene (Figure 5–1). Polycyclic aromatic hydrocarbons (PAH) can be divided into planar PAHs and curved PAHs. Some PAHs are related to carcinogenic pollutants. The others are highly useful in materials science, as they possess special optical and electrochemical properties.^[288] The research of PAHs is mainly focused on the physical properties and applications.

The scaffolds of other polycyclic compounds are more diverse. Tetracyclic terpene cholesterol is one of the most essential compounds for all animals' life, serving as a precursor for the biosynthesis of steroid hormones, bile acids and vitamin D (Figure 5–1).^[289] Humans have also created many artificial polycyclic compounds, such as pagodane.^[290] In the aspect of organic synthesis and drug discovery, the polycyclic natural product is an invaluable treasure.

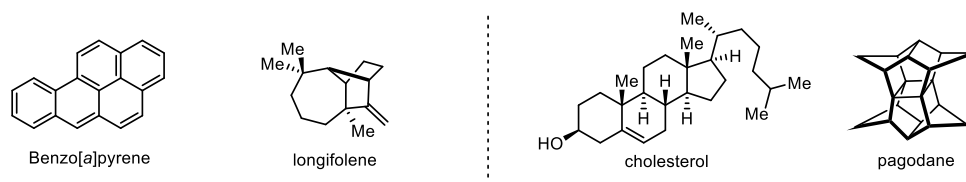


Figure 5–1: Representative polycyclic compounds.

5.1.2. Polycyclic natural products

Compared to the PAHs and artificial polycyclic compounds, polycyclic natural products (PNPs) are particularly attractive for their superb complexity of scaffold with well-arranged functional group, as well as unique responses and diverse interactions with biological systems.^[291] The relative rigidity of PNPs generates unique 3D structures which would provide useful chemical resources to explore the unknown biological space. PNPs are not only an important source for the treatment of various diseases, but also provide leads for drug discovery. Morphine was discovered as the first active alkaloid extracted from the opium poppy plant in 1804 by

Sertürner (Figure 5–2). It is still widely used to treat both acute and chronic severe pains.^[292] Artemisinin is a standard treatment worldwide for malaria isolated from *Artemisia annua*, which has been used by Chinese herbalists for more than 2000 years.^[293] Homoharringtonine is an alkaloid derived from *Cephalotaxus fortune* and was approved by FDA in 2012 for the treatment of adult patients with chronic myeloid leukemia.^[294] Paclitaxel targets tubulin through a novel interaction mode and is applied to treat cancer.^[295]

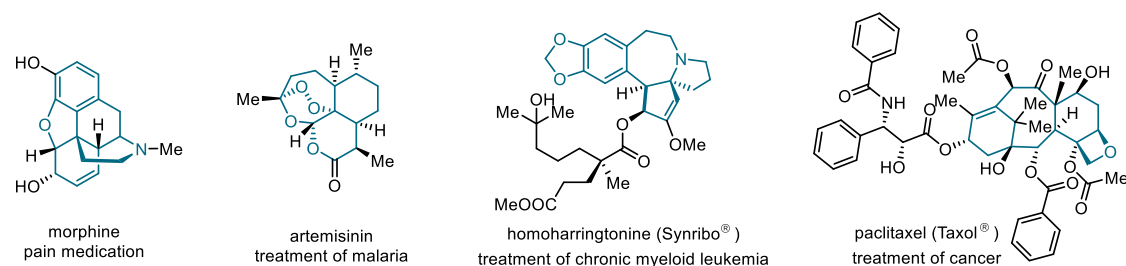


Figure 5–2: Selective drugs from polycyclic natural products.

Besides these PNP drugs, PNPs also inspire drug development. Eribulin is a simplified synthetic analogue of the sponge-derived tubulin inhibitor halichondrin B,^[296] approving for the treatment of metastatic breast cancer (Figure 5–3).^[297] It is noteworthy that eribulin was discovered based on the total synthesis of halichondrin B.^[298] Lefamulin is derived from pleuromutilin (isolated from the fungus *Omphalina mutila*)^[299], which has been approved by the FDA in 2019 for the treatment of bacterial pneumonia.

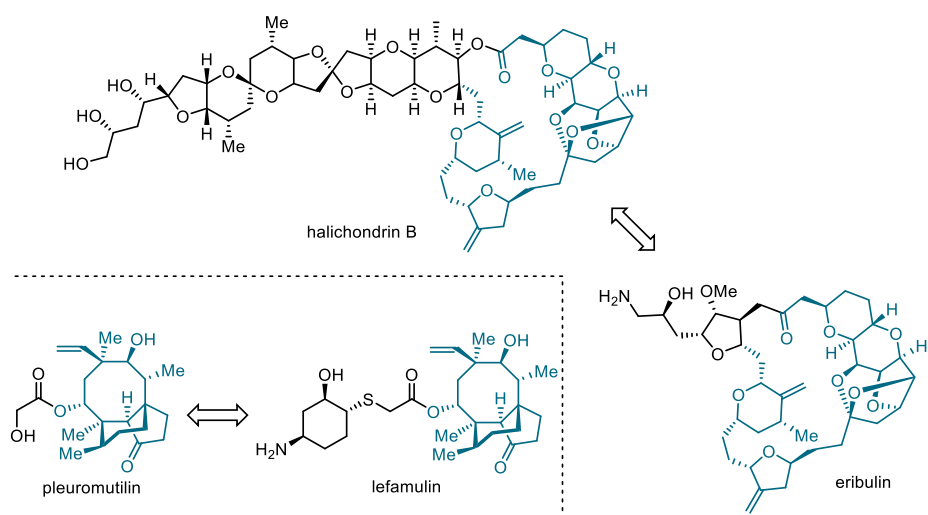


Figure 5–3: Selected drugs derived from polycyclic natural products.

Polycyclic natural products could be classified by their linking patterns, including four elements, fusing, tethering, bridging and twisting. Fusing is an edge-to-edge linking which is a common

type, pentacyclic natural product malagashanine is an example,^[300] tethering is two rings linked with each other directly, like mastigophorenes A;^[301] bridging is rings share three or more atoms by a bridge, e.g. hyperforin.^[302] Twisting is rings with only one common atom at the connection point, like the spiro compounds, such as pathylactone (Figure 5–4a).^[303]

Besides these PNPs with single-element-linking types above, two-element-linking types are more common. The well-known *Daphniphyllum* alkaloid daphenylline is consist of a fused-bridged type hexacyclic ring system (Figure 5–4b).^[304] The heptacyclic *Schisandraceae* triterpenoid rubriflordilactone A has a fused-tethered type ring system.^[305] The structurally unusual 9,11-secosteroid aplysiasecoesterol A contains a unique tethered-bridged tetracyclic ring system.^[306] Purpurolide B is sesquiterpene lactone encountering a bridged-twisted skeleton.^[307]

In addition, some PAHs contain a combination of three elements. Complanadine A is a dimeric lycopodium alkaloid, having the fused-tethered-bridged type ring system (Figure 5–4c).^[308] Acutumine features a tetracyclic fused-bridged-twisted type ring system.^[309] Rubialatins A also belongs to the fused-bridged-twisted type involving a naphthohydroquinone dimeric scaffold.^[310]

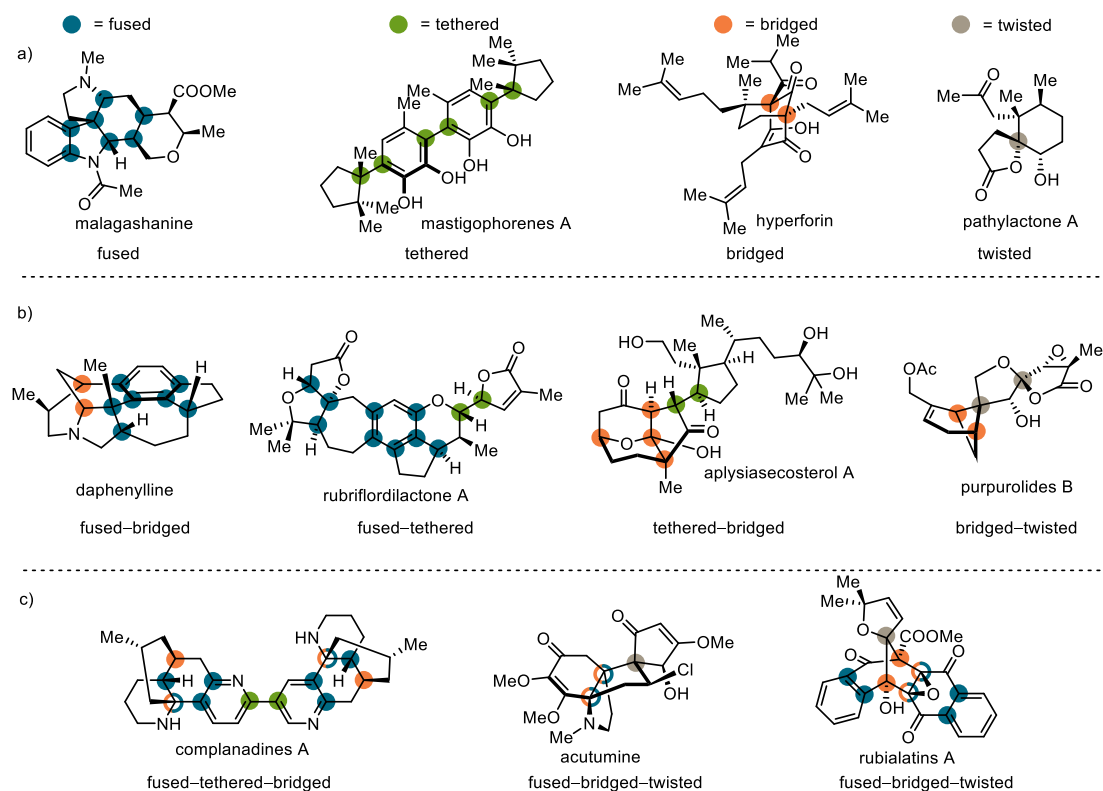


Figure 5–4: Different types of polycyclic natural products.

By reviewing these PNPs, fusing was considered as the fundamental linking element, which indicated in most cases the other elements usually accompanying fusing. Even only by fusing, a variety of complex skeletons could be generated. Rearranged *Aspidosperma* alkaloid (–)-leuconoxine contains a fused tetracyclic 6/5/6/7 ring system (Figure 5–5).^[311] *Bis*-indole alkaloid (–)-methylenebismehranine was isolated from *Tabernaemontana bovina*, owning a ten-ring scaffold which was constituted by ring fusing.^[312] Brevetoxin is a complex cyclic polyether neurotoxin produced by *Karenia brevis*, featuring a ten-ring fused scaffold.^[313] Therefore, it is significant to develop a unified methodology to construct fused polycyclic rings for the total synthesis of PNPs and drug discovery.

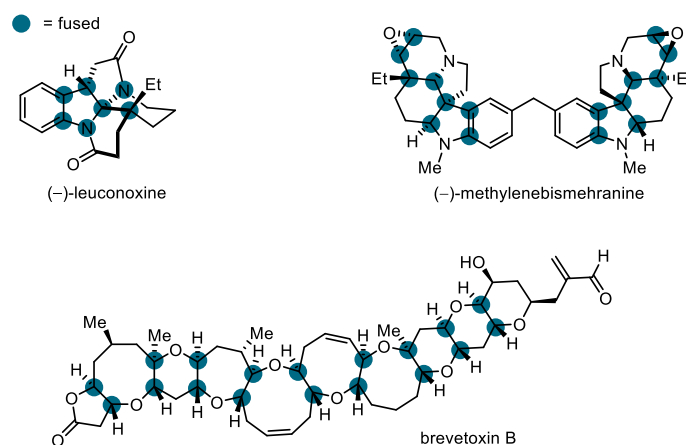


Figure 5–5: Fused complex polycyclic natural products.

5.2. Unified synthesis towards some polycyclic alkaloids

5.2.1. Consideration of some bioactive polycyclic alkaloids

A common scaffold was found to frequently appear in numerous bioactive polycyclic natural products, such as yohimibine, hirsutine, deplancheine, eburnamonine, ilicifoline B, peganumine A, and reserpine (Figure 5–6). The scaffold **I** comprises of a quinolizidine core fused with different heterocyclic rings. Developing a straightforward annulation method for the efficient construction of such scaffolds would be beneficial for the total synthesis of polycyclic natural products and their analogues.

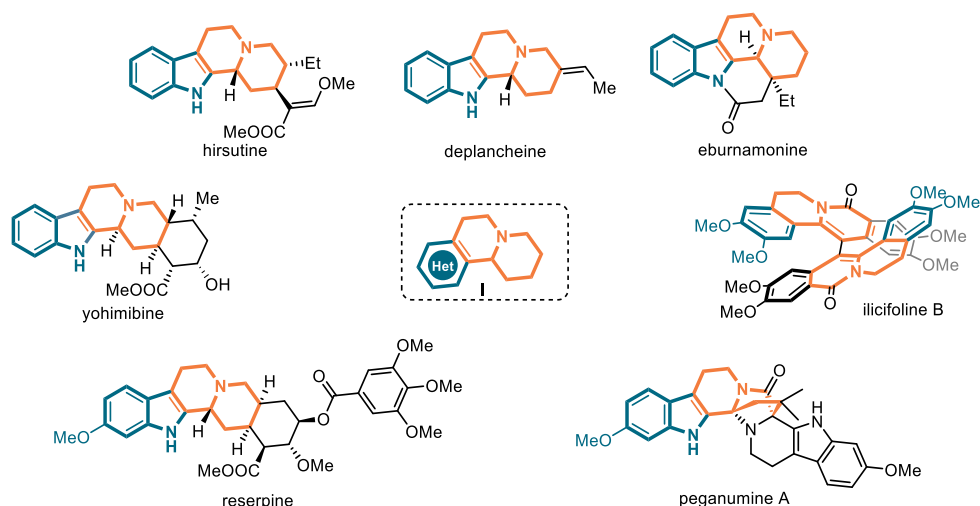
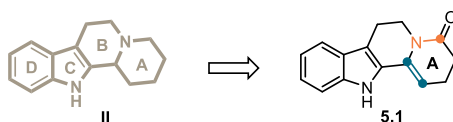


Figure 5-6: A common scaffold of polycyclic alkaloids.

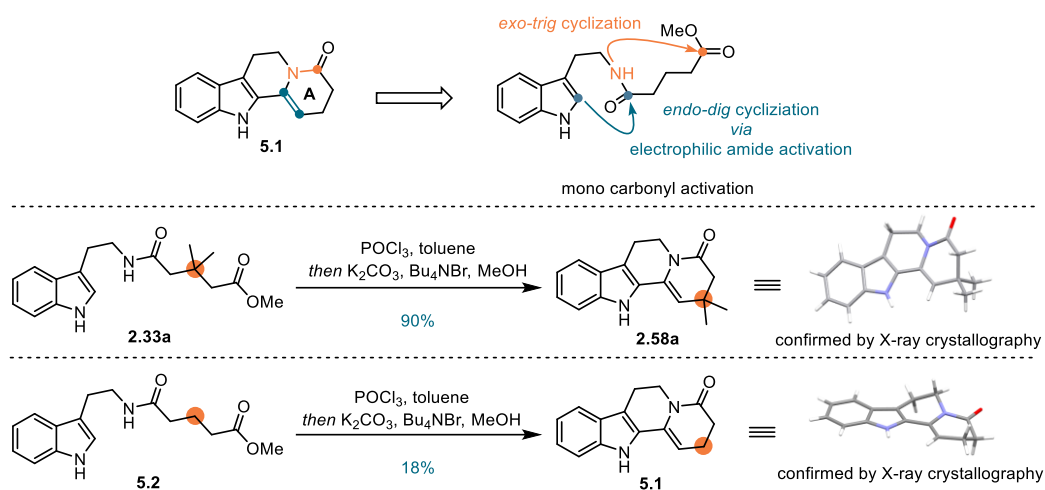
5.2.2. Dual carbonyl activation

Since indole is one of the most prevalent heterocycles in these polycyclic natural products, indole fused with quinolizidine core **II** was selected as starting point (Scheme 5-1). Incorporating an enamide motif in the A ring of **II** will provide a handle for subsequent transformation. Therefore, intermediate **5.1** was considered as the central linchpin for the divergent total synthesis routes of polycyclic alkaloids.



Scheme 5-1: Versatile intermediate.

Based on the investigation in the section “2.4.1. Discovery of an annulation reaction”, the construction of **5.1** was proposed to utilize the same annulation sequence via a mono-carbonyl activation, involving an intramolecular electrophilic cyclization and subsequent lactamization. However, the reactions resulted in significant differences, which could be attributed to the Thorpe–Ingold effect^[203] caused by the *gem*-dimethyl group to promote the cyclization (Scheme 5-2).^[314] On the other hand, this initial attempt indicated that the intramolecular electrophilic cyclization^[315] was realized by the selective activation of the amide carbonyl group.



Scheme 5-2: Mono-carbonyl activation.

It was considered that the terminal carbonyl group also needed an activation. The carbonyl group could be polarized by coordinating to a Lewis acid, leading to effectively enhancing its electrophilicity (Figure 5-7).^[316] Multiple modes of coordination could occur between Lewis acids and carbonyl groups, which resulted in different reactivities. σ bonding occurred when carbonyl groups interacted with main-group Lewis acids through one of the oxygen atom lone pairs coordinating with the metal. The coordination with transition metals was realized through donating of the carbonyl π orbital and back-bonding to the carbonyl π^* orbital.^[317]

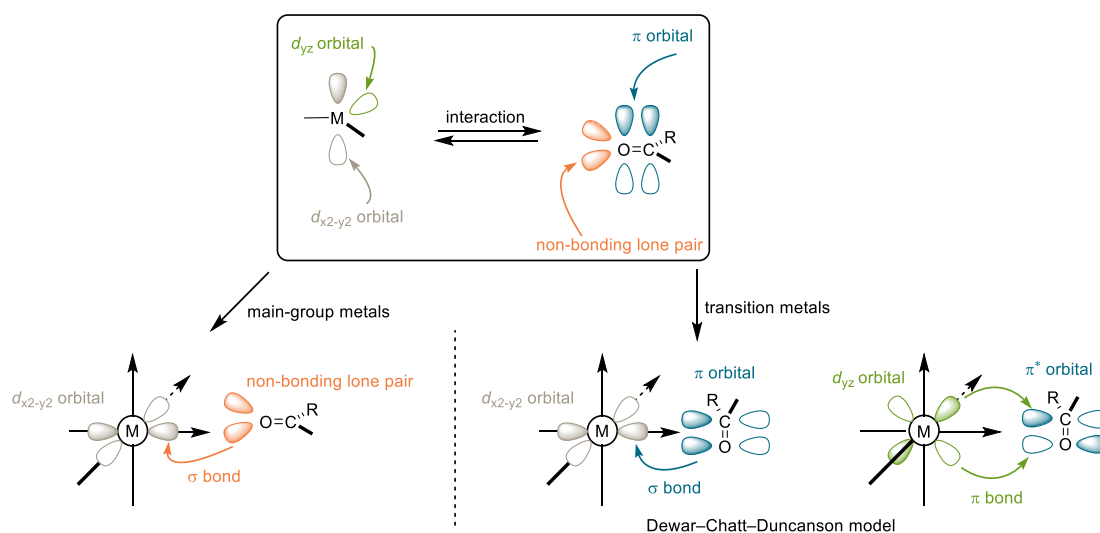
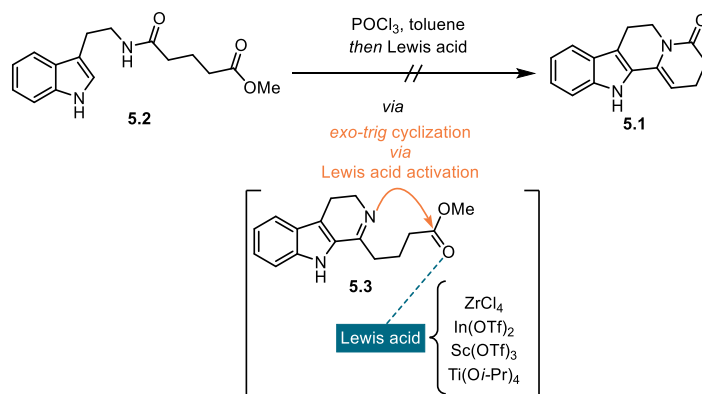


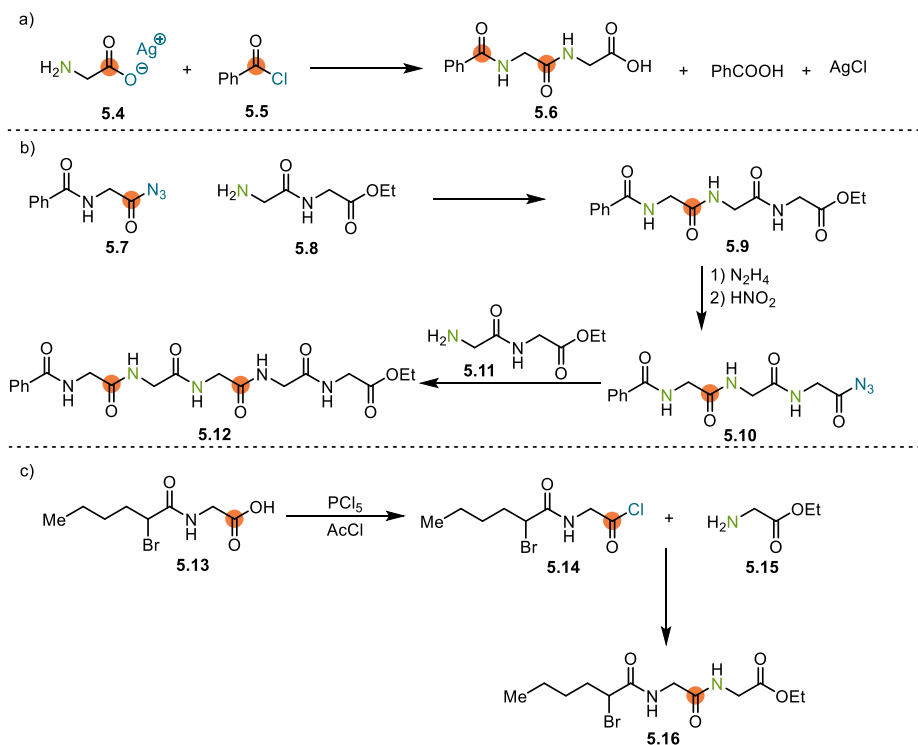
Figure 5-7: Lewis acid activation mode of carbonyl group.

Lewis acids was envisioned to promote the lactamization by activating the terminal carbonyl group. Unfortunately, the reactions with Lewis acids resulted in decomposition, which indicated that the coordination with the substrate was unselective and could activate other positions of the substrate leading to side-reactions (Scheme 5-3).



Scheme 5-3: Dual carbonyl activation by Lewis acids.

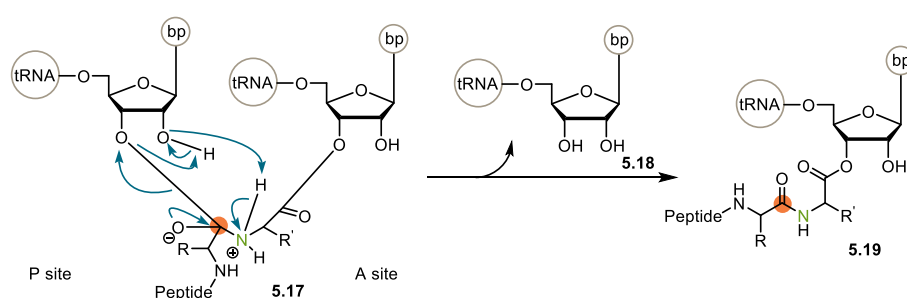
During the past centuries, many carbonyl activation strategies for amide bond formation were developed in the field of peptide synthesis. The first peptide synthesis was accomplished by Curtius in 1882 using silver salt **5.4** and benzoylchloride (Scheme 5-4a).^[318] Later, Curtius developed a new coupling approach by utilizing acyl azide (Scheme 5-4b).^[319] Fischer applied acyl chloride **5.14** to the peptide synthesis (Scheme 5-4c).^[320]



Scheme 5-4: Classic activation in peptide synthesis.

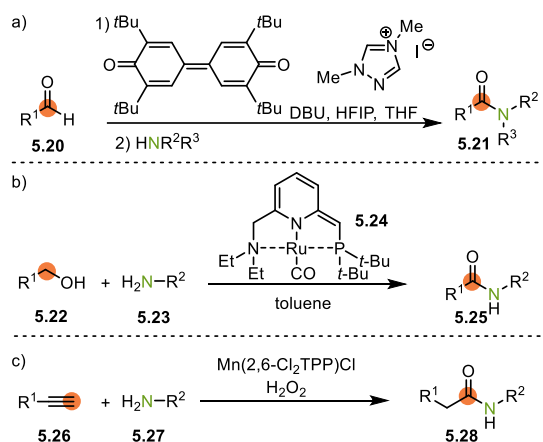
However, it was difficult to introduce such chloride or azide activation groups to the substrate, as the indole ring is sensitive to acids and oxidants. Additionally, the indole nitrogen and the enamide motif were also sensitive to such acidic conditions. Therefore, some mild peptide synthesis strategies were reviewed.^[321] In nature, the amide bond is formed between the α -

amino group of the amino acyl-tRNA and ester carbon of the peptidyl-tRNA by a nucleophilic reaction (Scheme 5–5). Ribosomes play an important role in this transformation by binding and orienting the substrates in the active site. Chemically, this bonding formation relies on the 2'-OH of the peptidyl-tRNA, which is well positioned to abstract and donate proton from the nucleophile and leaving group.^[322] This neighboring group participation^[323] is the key driving force to promote the elongation of the peptide.^[324] Although this neighboring group participation could be an efficient method, it was challenging to development a proper directing group to mimic such biological process in small molecule synthesis.



Scheme 5–5: Neighboring group participation strategy for amide synthesis.

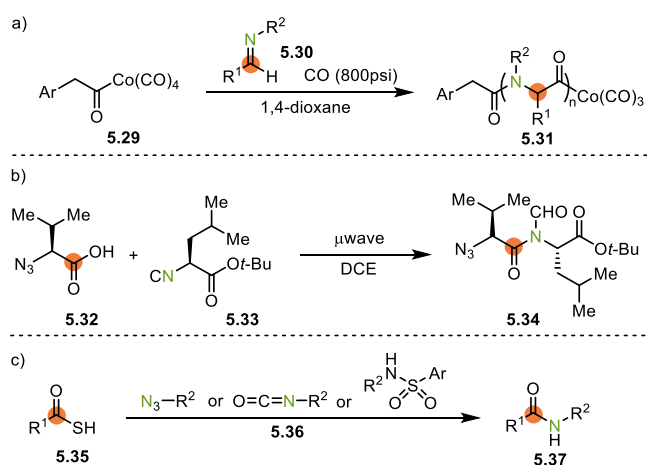
Another activation strategy was to utilize carboxylic equivalents. Studer et al. discovered a *N*-heterocyclic carbene catalyzed oxidative amidation between aldehydes and amines (Scheme 5–6a).^[325] Milstein et al. disclosed a novel ruthenium catalyzed oxidative amidation of alcohols with amines (Scheme 5–6b).^[326] In the investigation of oxidative amide formation by Che et al., aromatic and aliphatic alkynes were proved to be another alternative for the carboxylic equivalents (Scheme 5–6c).^[327]



Scheme 5–6: Carboxylic alternatives strategy.

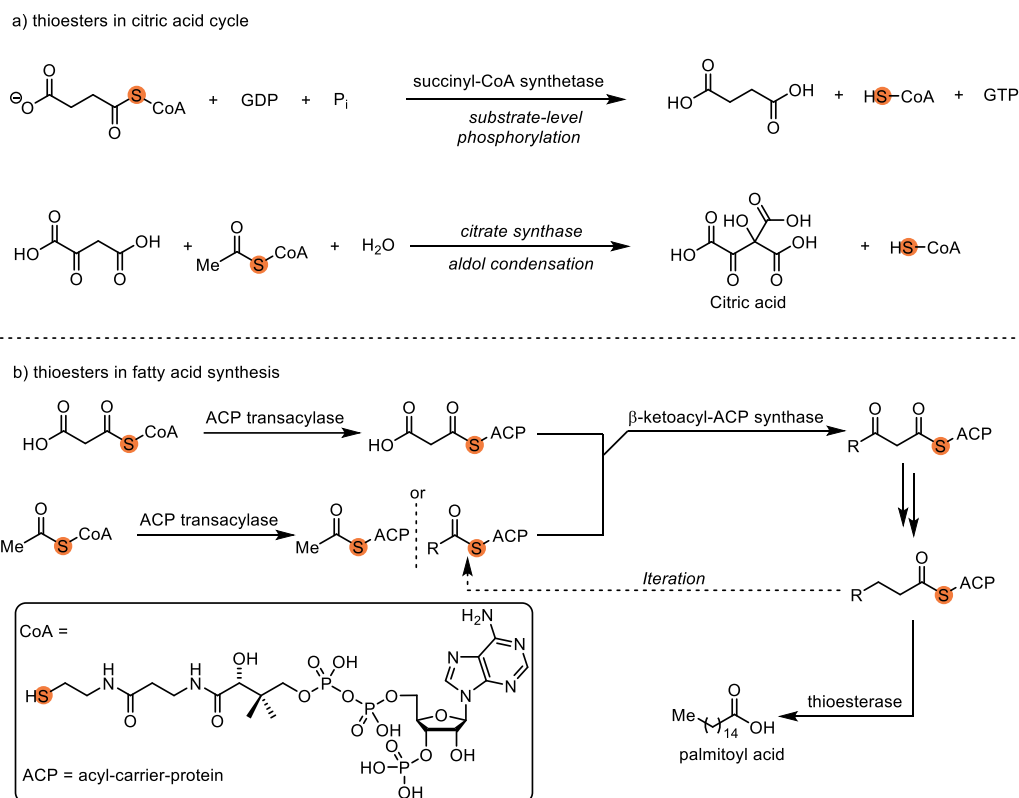
Besides these strategies by the activation of carboxylic equivalents, amidation of the amine

equivalents was also studied. Sun et al. disclosed a direct polypeptides synthesis employing readily available imines **5.30** and carbon monoxide as monomers to undergo a metal-catalyzed polymerization (Scheme 5–7a).^[328] In the synthesis of the cyclic peptide cyclosporine A, Danishefsky et al. utilized a isonitrile-mediated coupling with carboxylic acid to construct the amide bond (Scheme 5–7b).^[329] Thioacids **5.35** could also be applied to the peptide synthesis (Scheme 5–7c). Williams et al. reported a thioacetic acid-induced nucleophilic acyl substitution reaction with azides,^[330] electron-deficient sulphonamides^[331] and isocyanates^[332].



Scheme 5–7: Amine alternatives strategy.

Besides these novel strategies, the carbonyl group activation by activated esters was a classic but well-developed strategy. The activated esters were usually prone to react with a wide range of nucleophiles under mild conditions. Moreover, activated ester chemistry was also applied to post-polymerization modification, which could potentially synthesize many biostructures.^[333] Since thiolates (RS^-) are weaker bases and better leaving groups than alkoxides (RO^-), the thioester was utilized as the active ester for amide synthesis by nature in many biochemical reactions.^[334] The citric acid cycle is a series of reactions which releases stored energy through the oxidation of acetyl-CoA derived from carbohydrates, fats, and proteins, accompanying the generation of nicotinamide adenine dinucleotide (NADH), flavin adenine dinucleotide (FADH_2), and guanosine triphosphate (GTP).^[335] The thioesters, acetyl-CoA and succinyl-CoA, play crucial roles in the citric acid cycle (Scheme 5–8a). In addition, thioesters participate in the fatty acid synthesis to promote the elongation process (Scheme 5–8b).^[336]



Scheme 5–8: Thioester in biochemical reactions.

Besides the thioesters, some EWGs were also introduced to the active esters (Figure 5–8).^[337] A variety of active ester groups have been developed in the past decades.^[338] They are normally designed to render the carbonyl of the acyl moiety susceptible to nucleophilic attack by an amine at mild conditions. For most of these groups, the electron-withdrawing property played an important role in promoting the amide bond formation. In some aza derivatives, such as HOAt, HODhAd and HODhAt, additional assistance of neighboring atoms could also involve.

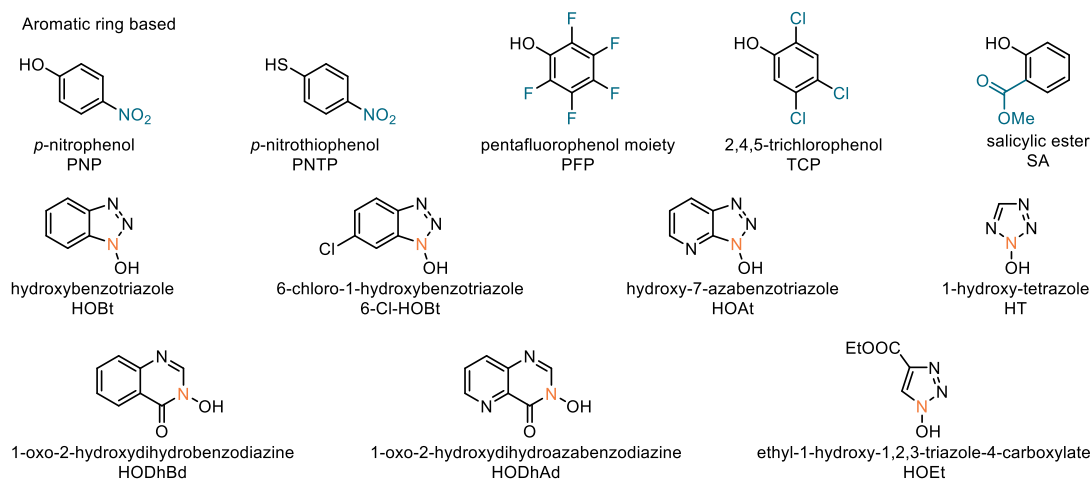


Figure 5–8: The common active ester groups.

5.2. Unified synthesis towards some polycyclic alkaloids

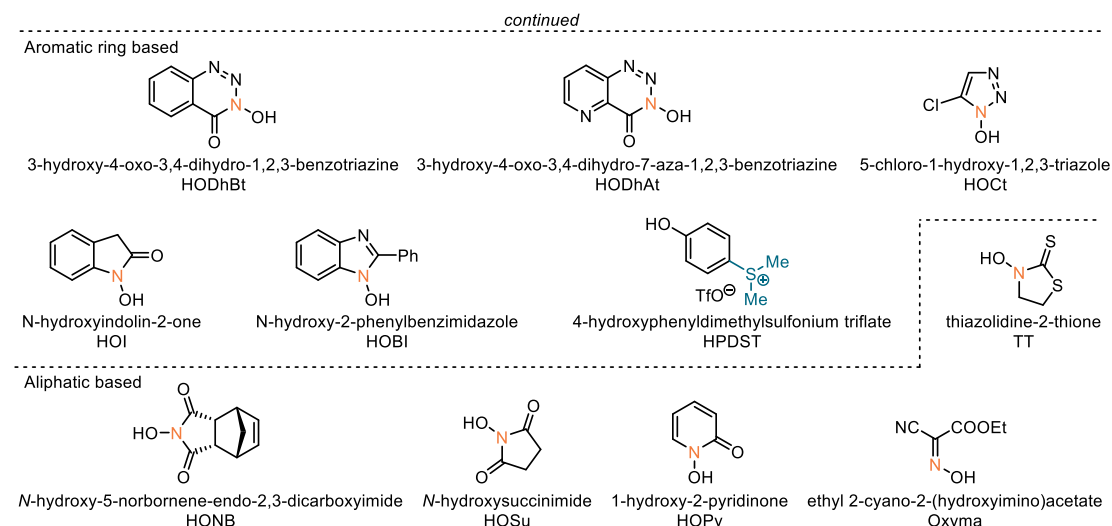
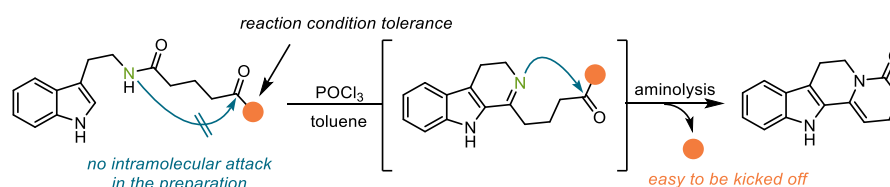


Figure 5–8: The common active ester groups. (continued)

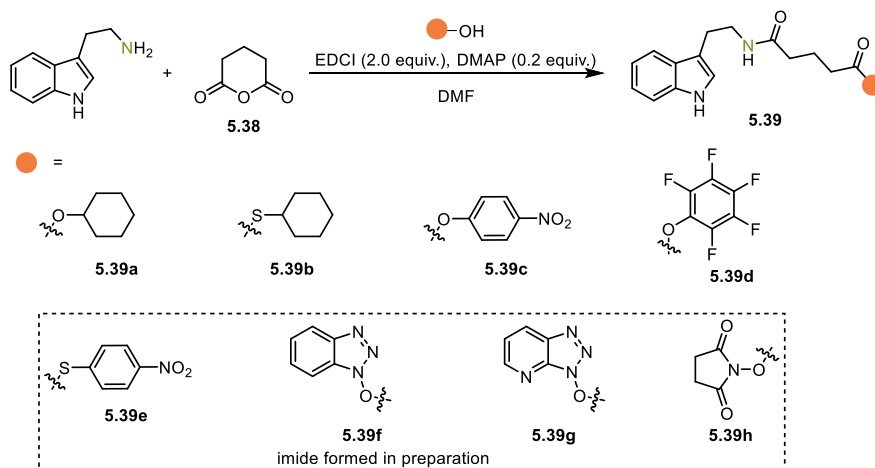
Inspired by this strategy, an active ester promoted lactamization was hypothesized (Scheme 5–9). Three challenges were proposed in this strategy:

- 1) The substrate preparation could lead to the imide formation, if the activated terminal carbonyl group is too liable to be attacked by the amide nitrogen.
- 2) The active ester should be robust to survive from the first cyclization promoted by an amide activation reagent.
- 3) The active ester group needed to be susceptible enough to be attacked nucleophilically by the imine.



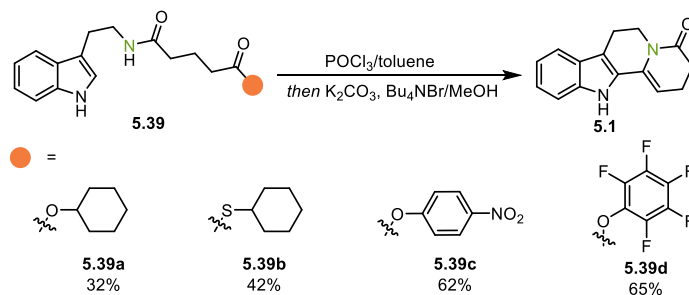
Scheme 5–9: Consideration of active ester strategy.

Inspired by many diverse active esters, the selection included both aromatic and aliphatic active thioesters, the aromatic active esters with different substitution groups and some classic benzotriazoles (Scheme 5–10). However, during the mild preparation condition, the active esters, such as HOBt, HOAt, HOSu and *p*-nitrothiophenol, underwent the intramolecular attack leading to the imide. Nevertheless, some other active esters were successfully obtained, including the thioesters and EWG substituted aromatic esters.

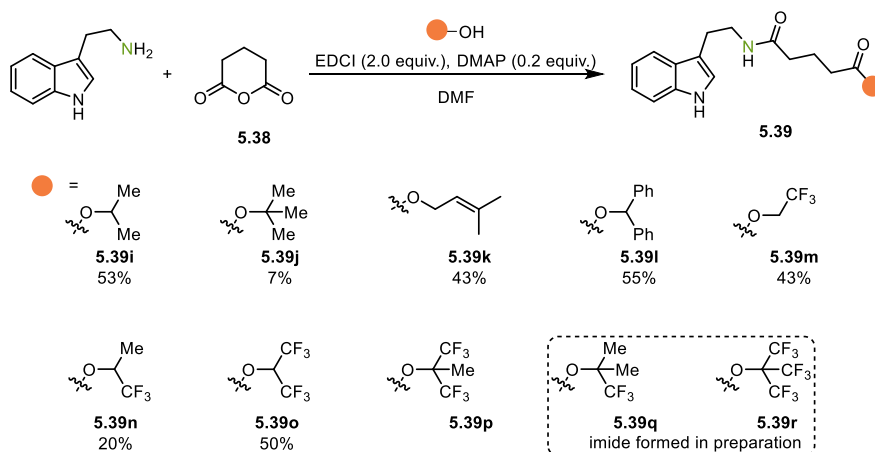


Scheme 5–10: Initial synthesis of active esters.

Rewardingly, the active esters furnished an improved yield of the annulation product **5.1** (Scheme 5–11). The result showed that thioester **5.39b** was a better activation group than ester **5.39a**, and the aromatic ester was generally better than aliphatic ester.

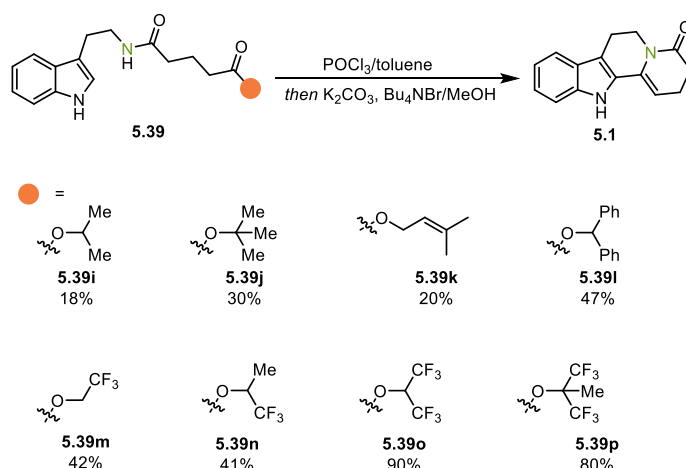
Scheme 5–11: 1st screening of cyclization with the active esters.

However, the promising result of the ester with pentafluorophenol as activating group created a dilemma. The pentafluorophenol was one of the most electro-deficient phenol. And the thioesters with EWGs were liable to form the imide. Although introducing more nitro groups could improve the electro-deficiency, the 2,4-dinitrophenol (DNP) was considered to have high acute toxicity (ingest fatal dose 4.3 mg/kg) which was comparable with cyanide.^[339] and the 2,4,6-trinitrophenol (TNP) had relatively the same explosive ability as 2,4,6-trinitrotoluene (TNT). Therefore, it was decided to suspend the idea due to the inherent dangers of these molecules which made them incompatible for their contribution to a pharmaceutical application. As the pentafluorophenol achieved slightly better result than that of *p*-nitrothiophenol, introducing the fluorine to aliphatic esters was expected to be a solution (Scheme 5–12).



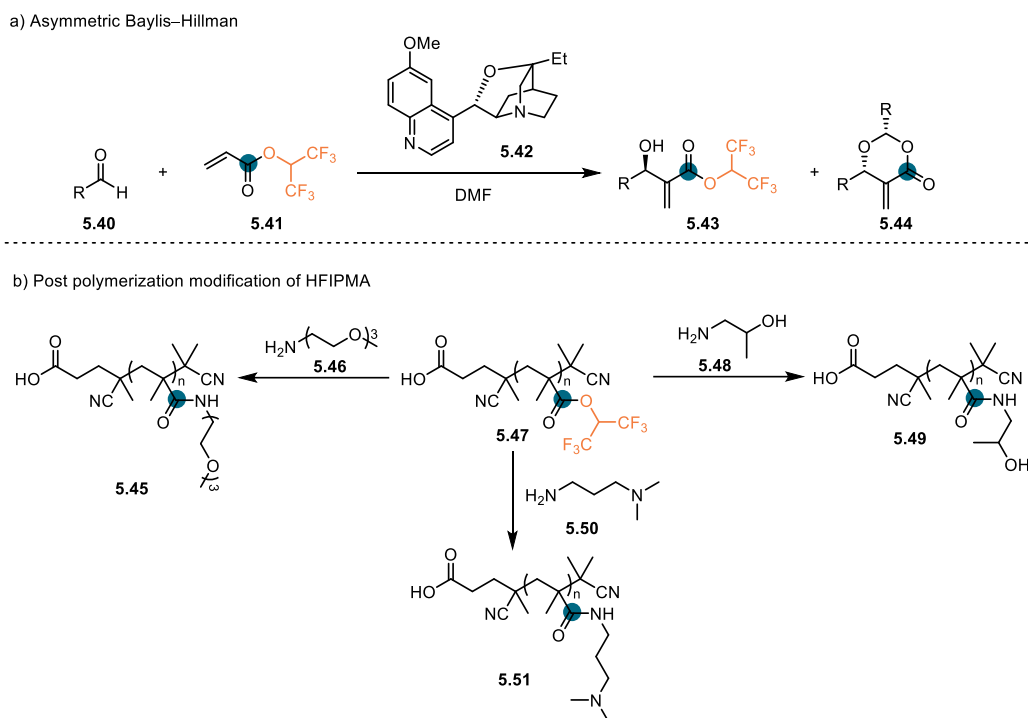
Scheme 5–12: Fluorinated aliphatic active esters preparation.

The annulations of the fluorinated aliphatic active esters were tested and resulted in a remarkable improvement (Scheme 5–13). It was noteworthy that the difference of the yields was distinct between the fluorinated aliphatic ester and corresponding aliphatic ester.



Scheme 5–13: Annulation with fluorinated aliphatic active esters.

The results of the fluorinated aliphatic esters were promising, especially the hexafluoroisopropylester (HFIPE). In order to understand the mechanism of such activation, some related literatures were reviewed. Interestingly, HFIPE was applied to the asymmetric Baylis–Hillman reactions to promote the lactonization (Scheme 5–14a).^[340] In polymer science, the 1,1,1,3,3,3-hexafluoroisopropyl methacrylate (HFIPMA) was used as a precursor for the post polymerization modification to synthesize multifunctional water-soluble polymers, which realized the amide bond formation by utilizing the primary amines as nucleophiles to attack the activated HFIPE (Scheme 5–14b).^[341]

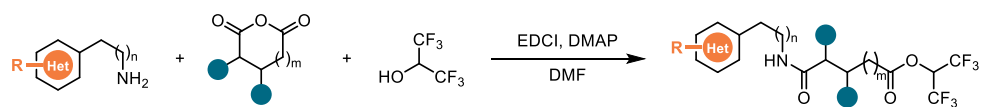


Scheme 5–14: HFIPe in synthesis.

Although the HFIPe has been applied in some transformations, the utilization of HFIPe in the synthesis of polycyclic ring system was not reported. Therefore, further investigation of the generality to construct different polycyclic ring system was commenced.

5.2.3. Generality of the annulation

Before the exploration of the annulation, a general and mild condensation reaction was proposed to realize the preparation of the substrates with the assistance of the coupling reagent EDCI (Scheme 5–15).



Scheme 5–15: Preparation of substrates.

Firstly, in order to investigate the tolerance of the selective amide activation, both EDGs and EWGs were introduced to the indole ring of **5.52**. (Figure 5–9a). Next, diverse substitution groups, including methyl group, ester groups and aromatic groups, were installed to the chain of the motif **5.53**. This design was to examine the substituted effect of the active ester activation (Figure 5–9b). By modifying the indole fragment and the chain of **5.54** simultaneously, a

variety of substrates were prepared to explore the combination of these two factors (Figure 5–9c).

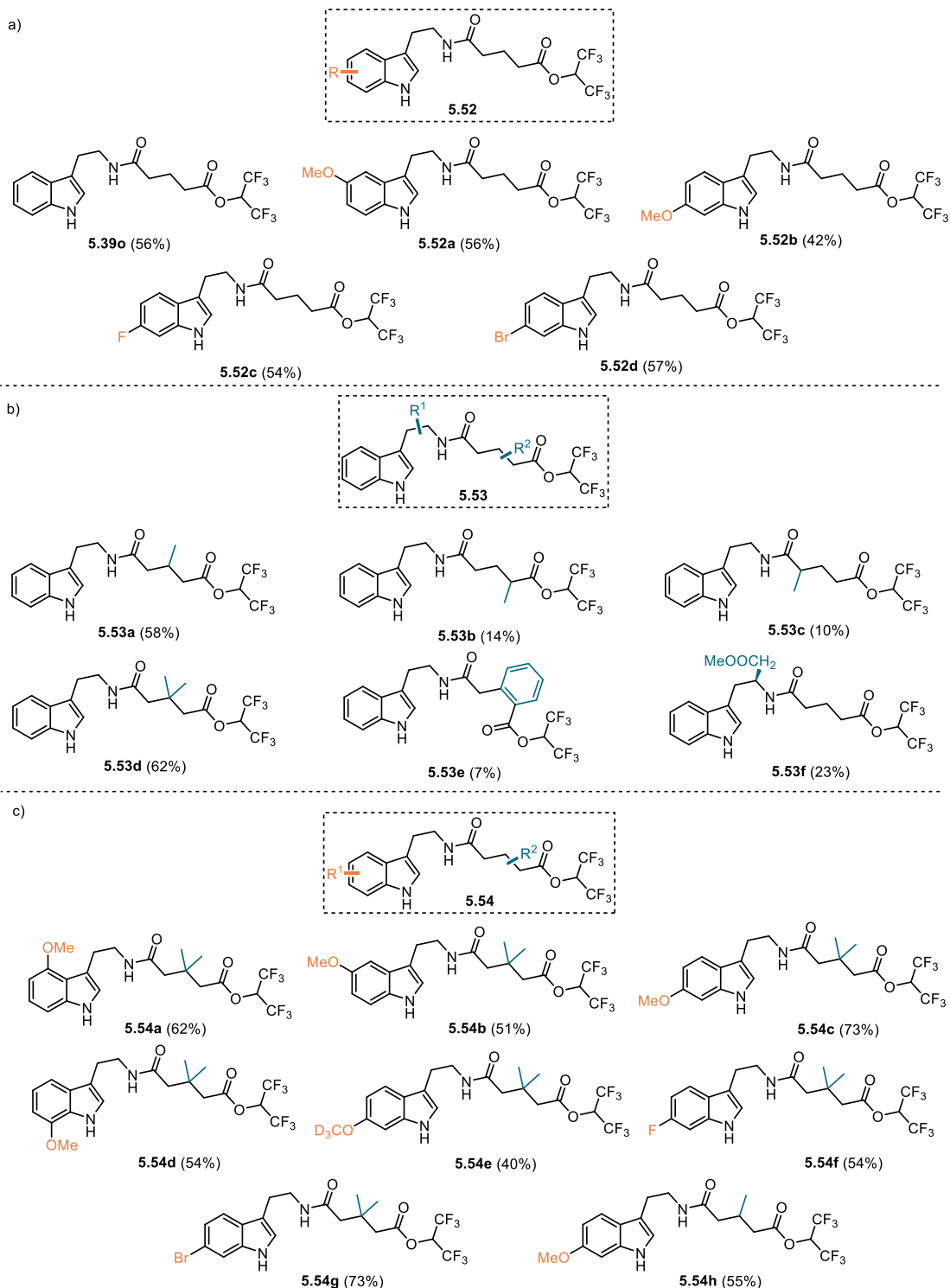


Figure 5–9: Substrate design-1.

Besides the 6/6 fused ring system, construction of the 5/6, 7/6, 8/6, 6/5, 6/7, 6/8 and 6/11 fused ring patterns were anticipated. Therefore, substrates with various length of the chain were

prepared (Figure 5–10a). Meanwhile, the generality about the aromatic ring was also considered by introducing various heterocycles, such as benzene, furan, thiophene and benzothiophene (Figure 5–10b).

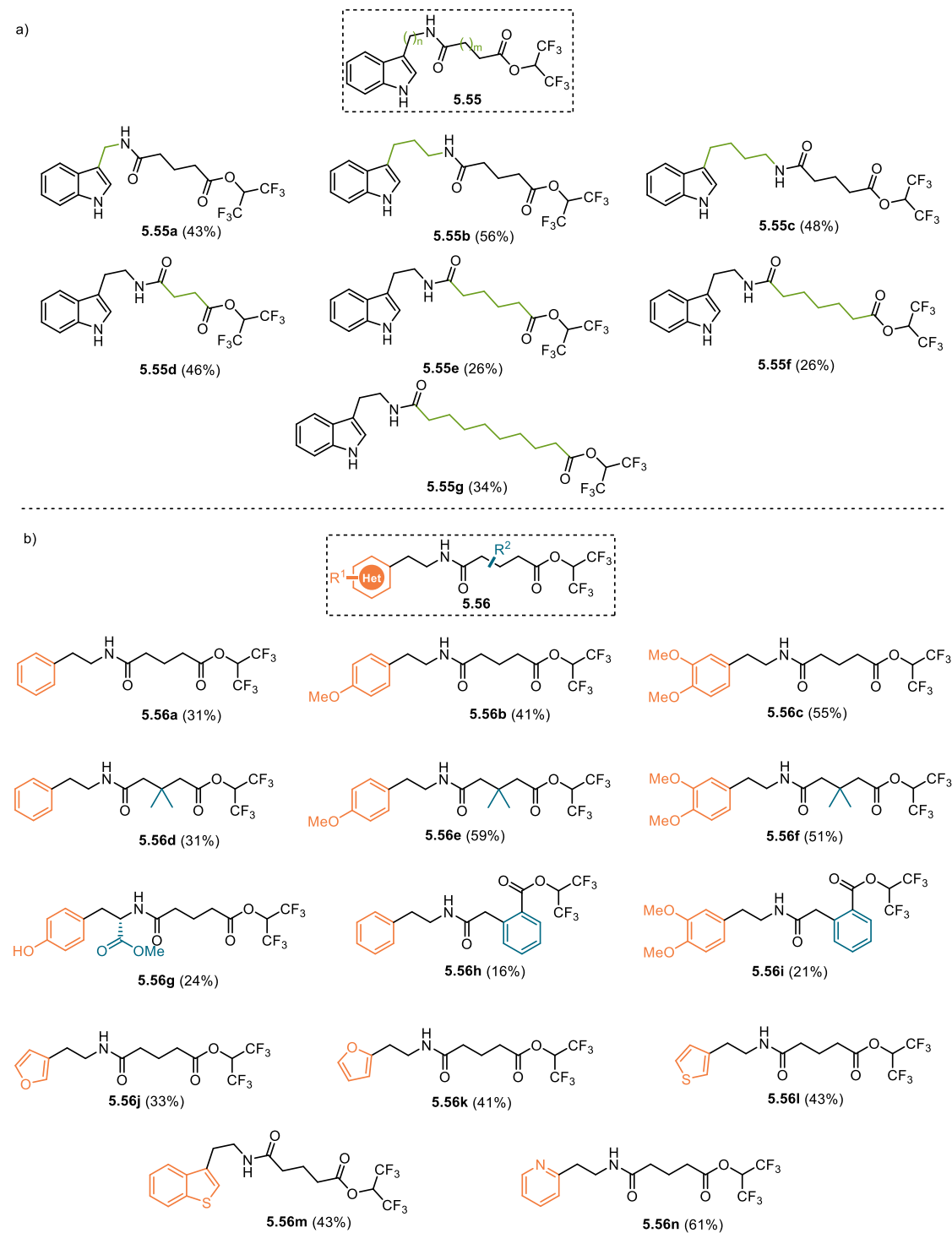


Figure 5–10: Substrate design-2.

With these substrates in hand, the generality of the one-pot annulation was investigated.

Substitution at indole ring with EDG and EWG were well-tolerated, providing the corresponding tetracyclic scaffold (**5.57a–5.57d**) in good yields (76%–86%) (Table 5–1a). Encouraged by these results, the different substitution patterns and ring systems were further investigated. The substituents at the quinolizidine core were tested (**5.57e–5.57j**) with good yield (64%–83%) (Table 5–1b). Notably, that indoloquinolizidine-type alkaloid nortetoybyrine (**5.57j**) could be obtained in a single step in 83% yield. The exploration of the combination of indole substitutions and chain substitutions also afforded the corresponding scaffolds (**5.57k–5.57r**) in good yield (75%–85%) (Table 5–1c). The 7/6, 8/6, 6/7 and 6/8 fused ring systems (**5.57s–5.57v**) could be obtained in moderate yield (26%–52%) (Table 5–1d). The annulation also showed generality to different heteroaromatics, such as unfunctionalized and electron-rich benzene, furan, thiophene and benzothiophene (**5.58a–5.58j**, 33%–91%) (Table 5–1e).

Table 5–1: Substrate scope.

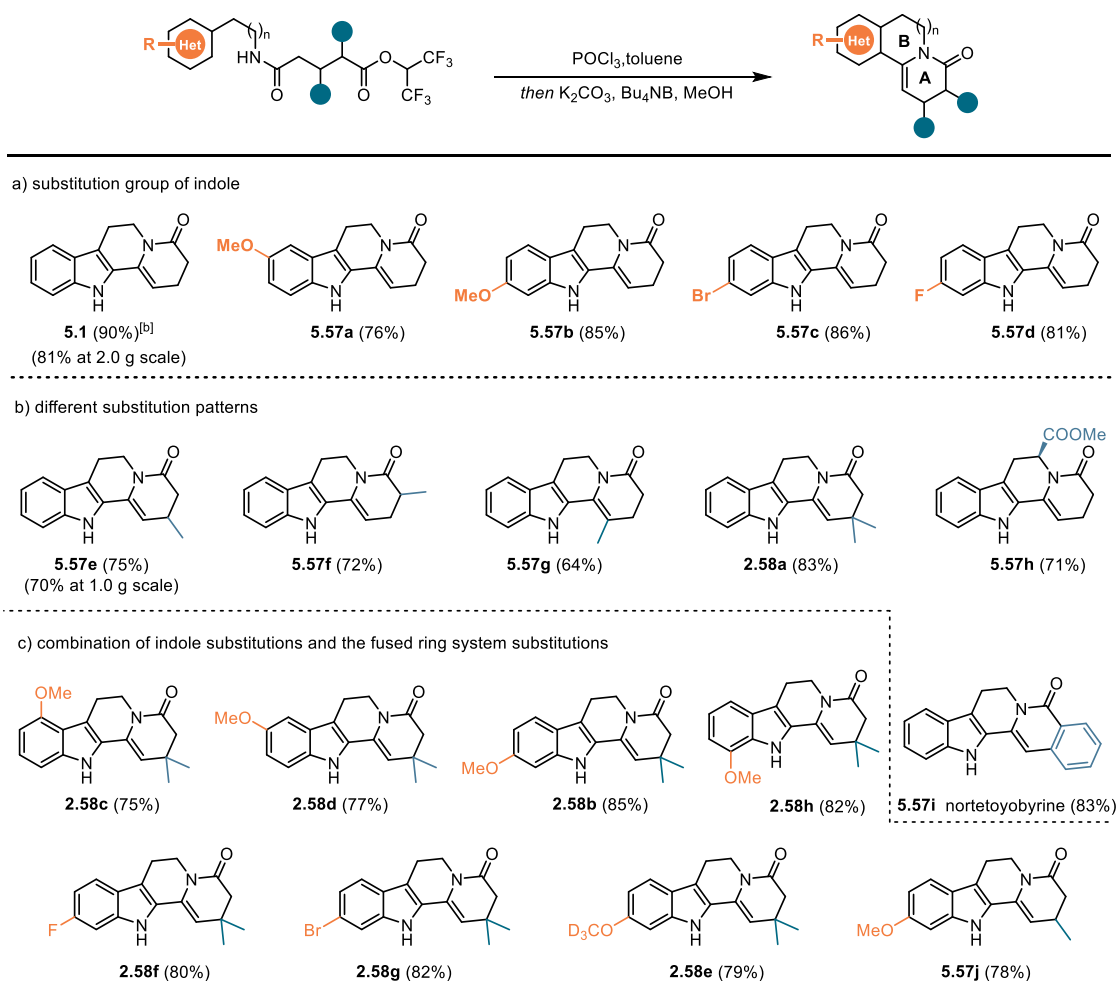
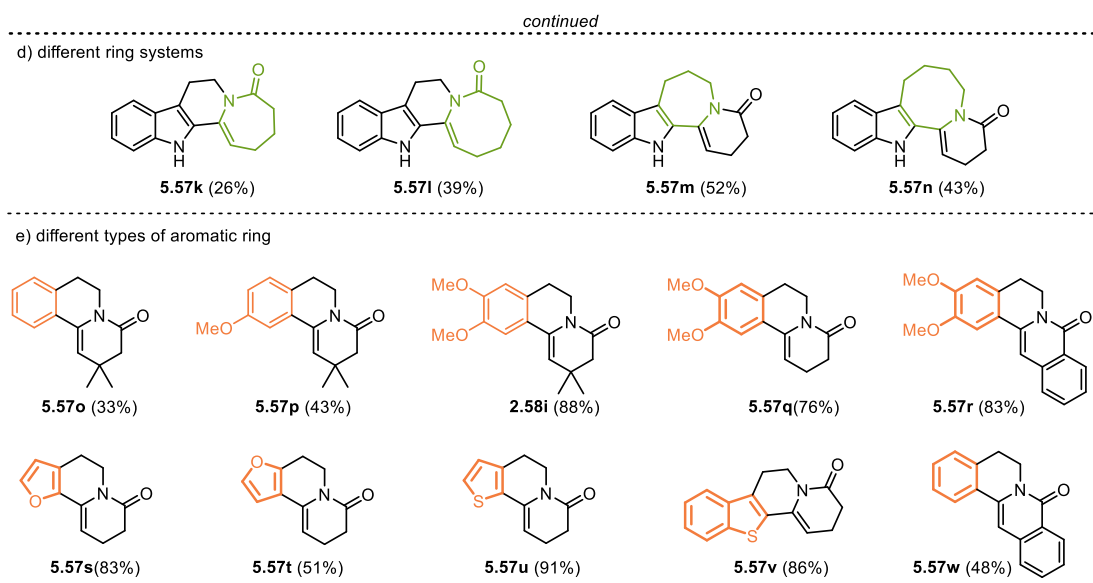
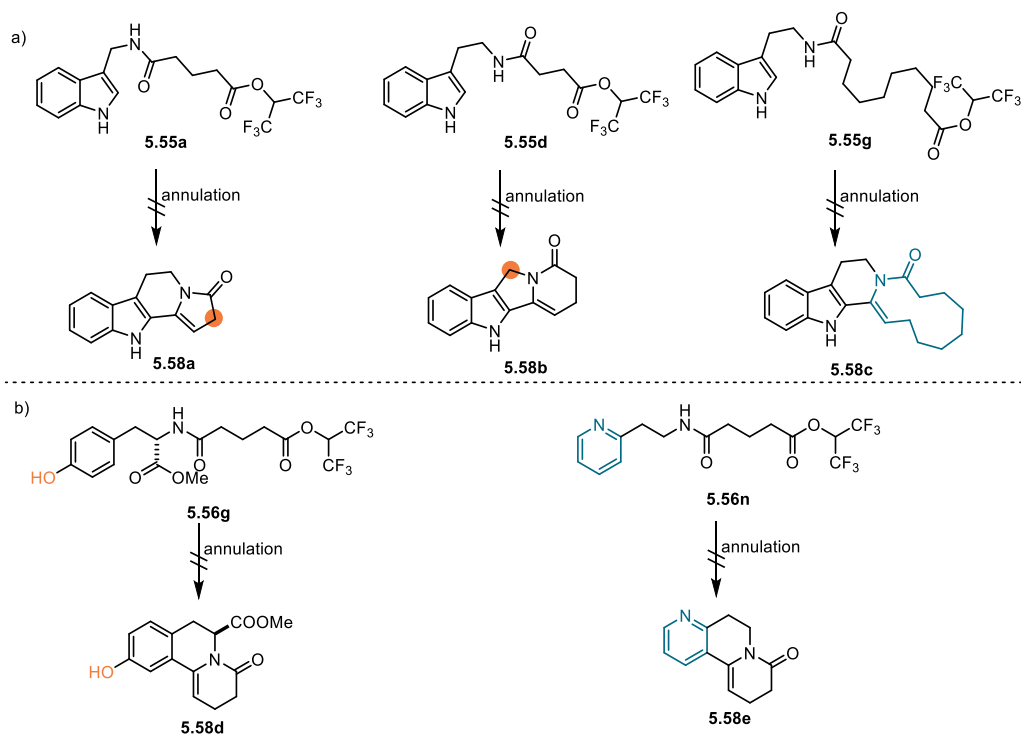


Table 5–1: Substrate scope. (continued)

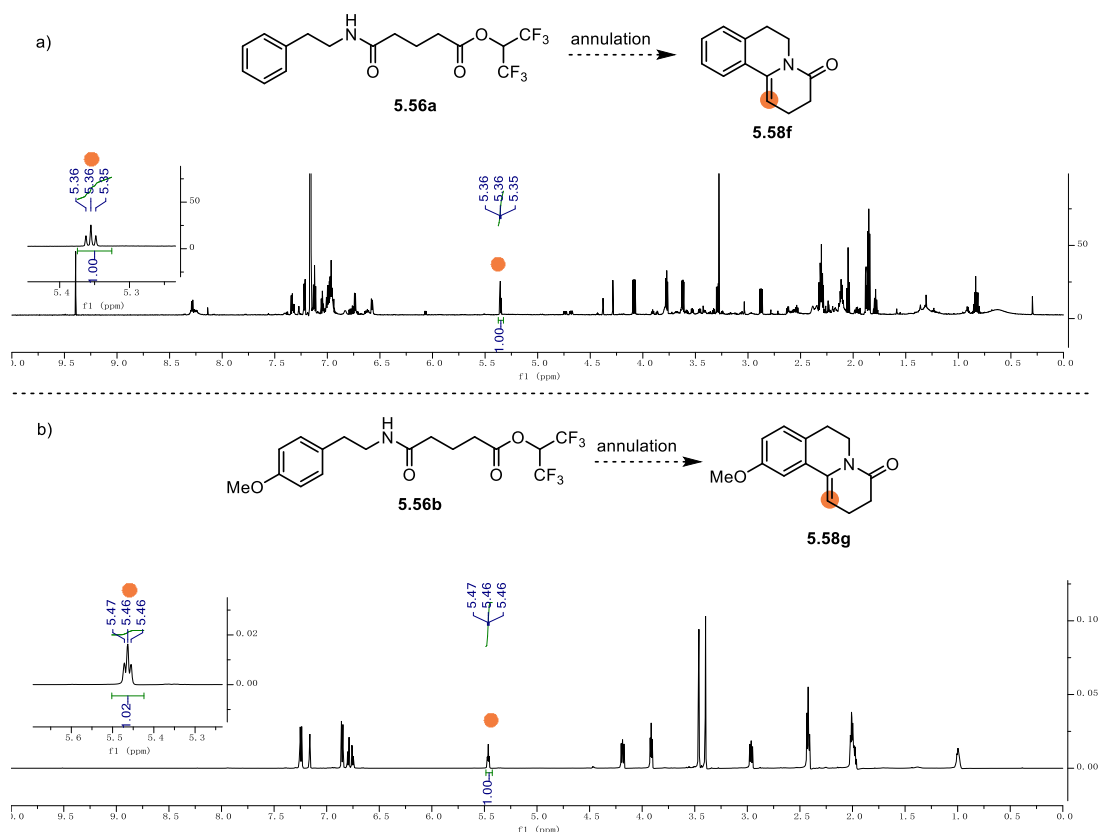
However, there were still some limitations of this annulation, as some examples were not fruitful. The results of these examples could be divided into two parts. One showed no observation of the desired product by the NMR; the other could find the identical NMR signal but with impurities.

**Scheme 5–16:** Limitation of the annulation-1.

The reactions with **5.55a**, **5.55d**, **5.55g**, **5.56g** and **5.56n** had no proof that the corresponding

products were formed. It was proposed that the reactive methylene groups of **5.58a** and **5.58b** might be unstable at the reaction condition (Scheme 5–16a). The unsuccessful result of **5.55g** could be attributed to the difficulty of the macrolactamization or the geometry of the C–C double bond (Scheme 5–16a). Failed annulation of **5.56g** could be caused by the reaction between the free hydroxyl group and the phosphorus(V) reagent (Scheme 5–16b). **5.56n** indicates that the reaction relied on the electrophilicity of the heterocycles.

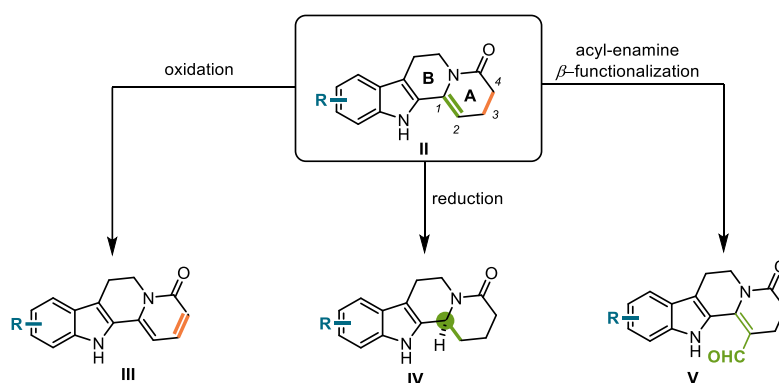
The identical peaks of the desired products **5.58f** and **5.58g** were shown on the NMR, but there were some impurities which could be the side products during the reaction period or in the isolation (Scheme 5–17). It was hypothesized that the electrophilicity of the benzene ring influenced the reaction rate of the *endo-dig* cyclization. If the rate of the *endo-dig* cyclization was slow, some competition reactions could undergo, leading to side products. In the *exo-trig* cyclization stage, the absence of the Thorpe–Ingold effect could decrease the rate and driving-force of the whole reaction equilibrium.



Scheme 5–17: Limitation of the annulation-2.

5.2.4. Divergent application of the annulation in total synthesis

With the efficient annulation in hand, a divergent natural product synthesis strategy was investigated by manipulating the A ring (Scheme 5–18). Another double bond could be easily introduced to the 3,4-position by oxidation. Additionally, both racemic and enantioenriched 1,2-position double bond reduced products could be afforded. Moreover, by utilizing the enamine fragment, a β -formylation could also be achieved.



Scheme 5–18: Strategy of the divergent redox synthesis.

Starting with the oxidation pathway, various classic dehydrogenation were explored, such as DDQ,^[342] selenium-^[343] and sulfur-^[275a]based dehydrogenations (Table 5–2). Only the reaction with *N-tert*-butyl phenylsulfinimidoyl chloride afforded the regioselective dehydrogenation product **5.59a**.

Table 5–2: Screening for the regioselective dehydrogenation.

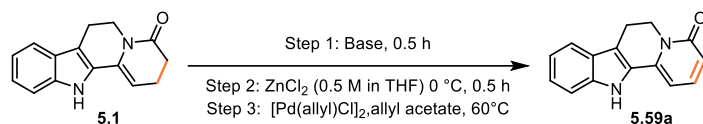
entry ^[a]	conditions	solvent	yield ^[b]
1	MnO ₂	CH ₂ Cl ₂	trace
2	γ -MnO ₂	CH ₂ Cl ₂	trace
3	NBS, BPO	CDCl ₃	recovery of SM
4	S, Dowtherm [®] A	--	complex mixture
5	DDQ	Dioxane	complex mixture
6	Cu(OAc) ₂ , Na ₂ CO ₃ , py, O ₂	toluene	recovery of SM
7	CuBr ₂	MeCN	recovery of SM
8	Pd(OAc) ₂ , O ₂	DMSO	trace
9	V(acac) ₂ , TFA, Bu ₄ NBr, O ₂	Dioxane	complex mixture
10	LiTMP, Sulfinimidoyl chloride	THF	complex mixture
11	NaHMDS, Sulfinimidoyl chloride	THF	trace
12	MeLi, Sulfinimidoyl chloride	THF	14%
13	LDA, PhSeCl	THF	trace
14	LDA, PhSOOMe	THF	complex mixture
15	LDA, Sulfinimidoyl chloride	THF	33%

[a] Reactions were performed with enamide (10 mg, 42 μ mol); [b] Isolated yield

With the allyl-palladium catalyzed amide α,β -dehydrogenation developed by Newhouse et

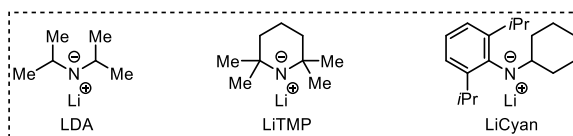
al.,^[344] an improved conversion was obtained (Table 5–3). By further optimization of the reaction conditions, the LDA, rather than the LiCyan, was proven to be the best base for the reaction, due to the steric hindrance of the tetracyclic substrate.

Table 5–3: Screening of Newhouse dehydrogenation.

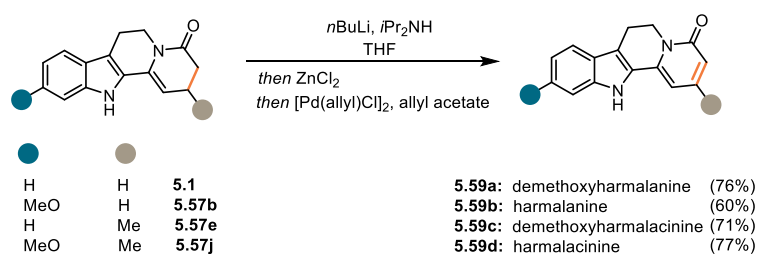


entry ^[a]	Step 1	Step 2	Step 3	conversion [%] ^[b]
1	LiCyan (2.5 eq.), –40 °C	ZnCl ₂ (3.5 eq.)	[Pd] (2.5 mol%), 14h	9
2	LiCyan (2.5 eq.), –40 °C	ZnCl ₂ (3.5 eq.)	[Pd] (2.5 mol%), 38h	16
3	LiCyan (2.5 eq.), –40 °C	ZnCl ₂ (3.5 eq.)	[Pd] (2.5 mol%), 62h	13
4	LiCyan (2.5 eq.), –40 °C	ZnCl ₂ (3.5 eq.)	[Pd] (2.5 mol%), 86h	32
5	LiCyan (5.0 eq.), –40 °C	ZnCl ₂ (7.0 eq.)	[Pd] (5.0 mol%), 14h	20
6	LiCyan (5.0 eq.), –40 °C	ZnCl ₂ (7.0 eq.)	[Pd] (5.0 mol%), 38h	21
7	LiCyan (5.0 eq.), –40 °C	ZnCl ₂ (7.0 eq.)	[Pd] (5.0 mol%), 62h	23
8	LiCyan (5.0 eq.), –40 °C	ZnCl ₂ (7.0 eq.)	[Pd] (5.0 mol%), 86h	30
9	LiCyan (2.5 eq.), 0 °C	ZnCl ₂ (3.5 eq.)	[Pd] (2.5 mol%), 14h	3
10	LiCyan (2.5 eq.), 0 °C	ZnCl ₂ (3.5 eq.)	[Pd] (2.5 mol%), 75h	10
11	LiCyan (2.5 eq.), 0 °C	ZnCl ₂ (3.5 eq.)	[Pd] (2.5 mol%), 96h	10
12	LiTMP (2.5 eq.), 0 °C	ZnCl ₂ (3.5 eq.)	[Pd] (2.5 mol%), 14h	20
13	LiTMP (2.5 eq.), 0 °C	ZnCl ₂ (3.5 eq.)	[Pd] (2.5 mol%), 75h	30
14	LiTMP (2.5 eq.), 0 °C	ZnCl ₂ (3.5 eq.)	[Pd] (2.5 mol%), 96h	29
15	LiCyan (10 eq.), –40 °C	ZnCl ₂ (3.5 eq.)	[Pd] (2.5 mol%), 21h	25
16	LiCyan (10 eq.), –40 °C	ZnCl ₂ (3.5 eq.)	[Pd] (2.5 mol%), 51h	26
17	LiCyan (10 eq.), –40 °C	ZnCl ₂ (3.5 eq.)	[Pd] (2.5 mol%), 88h	40
18	LiTMP (10 eq.), 0 °C	ZnCl ₂ (3.5 eq.)	[Pd] (2.5 mol%), 21h	37
19	LiTMP (10 eq.), 0 °C	ZnCl ₂ (3.5 eq.)	[Pd] (2.5 mol%), 51h	33
20	LiTMP (10 eq.), 0 °C	ZnCl ₂ (3.5 eq.)	[Pd] (2.5 mol%), 88h	66
21	LDA (10 eq.), 0 °C	ZnCl ₂ (3.5 eq.)	[Pd] (2.5 mol%), 88h	76 ^[c]

[a] Reactions were performed with enamide (10 mg, 42 μmol); [b] conversion was determined by ¹H NMR; [c] Isolated yield



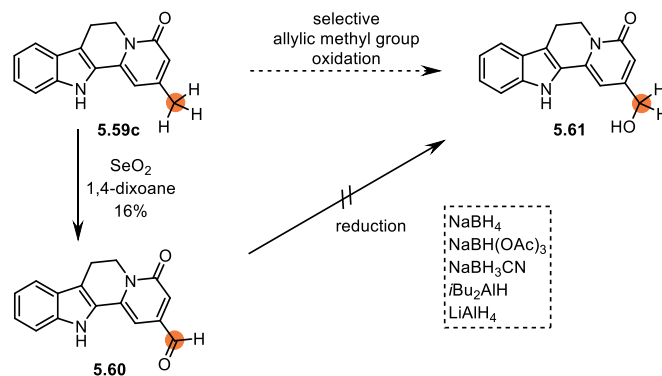
With the optimized dehydrogenation condition, demethoxyharmalanine, harmalanine, demethoxyharmalacinine and harmalacinine,^[345] were successfully obtained in excellent yields (60%–77%) (Scheme 5–19).



Scheme 5–19: Oxidative diversification.

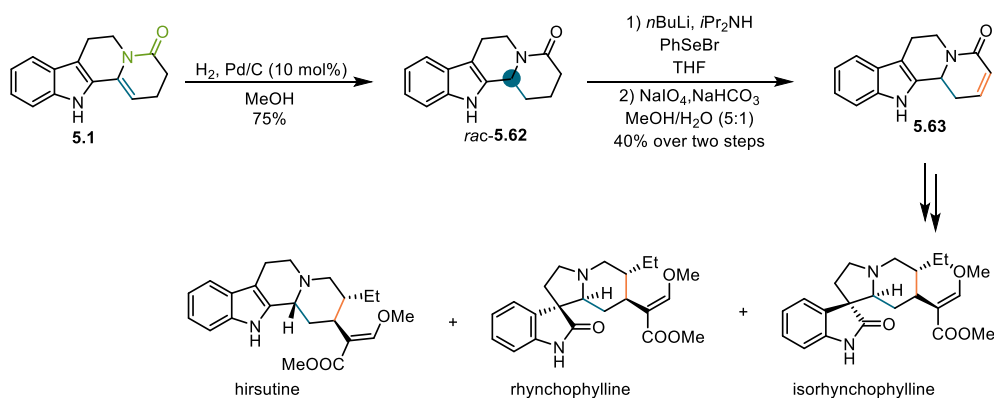
With the demethoxyharmalacinine (**5.59c**) in hand, demethoxypegaharmine J (**5.61**)^[346] was envisioned to be synthesized through a selective allylic methyl group oxidation (Scheme 5–20).

By the SeO₂-mediated Riley oxidation of the allylic methyl group,^[55] aldehyde **5.60** was obtained in 16% yield. However, the selective reduction of **5.60** to alcohol **5.61** turned out to be challenging.



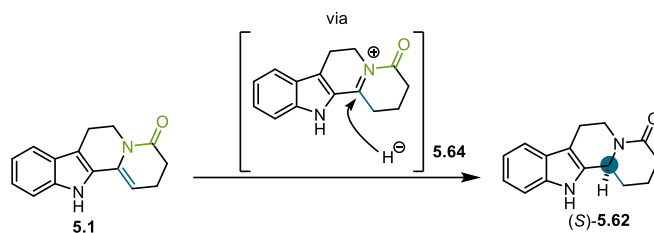
Scheme 5–20: Synthesis attempt of demethoxypegaharmine J.

Next, the reductive pathway was explored. Through a selective catalytic hydrogenation of the C–C double bond, racemate of **5.62** was successfully obtained in 75% yield (Scheme 5–21). From this racemic intermediate, selenoxide elimination afforded **5.63**, a key intermediate in the total synthesis of hirsutine, rhynchophylline and isorhynchophylline. {Deiters, 2006 #993}



Scheme 5–21: Reduction pathway for the divergent synthesis.

The asymmetric reduction of the C–C double bond was also envisioned. Although the asymmetric hydrogenation was an efficient method to reduce double bonds,^[347] the asymmetric hydrogenation of an enamide scaffold was still challenging, which usually needed special ligands and high pressure.^[348] Therefore, utilizing the enamide motif to generate a reactive *N*-acyliminium ion would be a practical strategy. The enantioselectivity could be controlled by the ion pair between the *N*-acyliminium ion and a chiral counterion (Scheme 5–22).



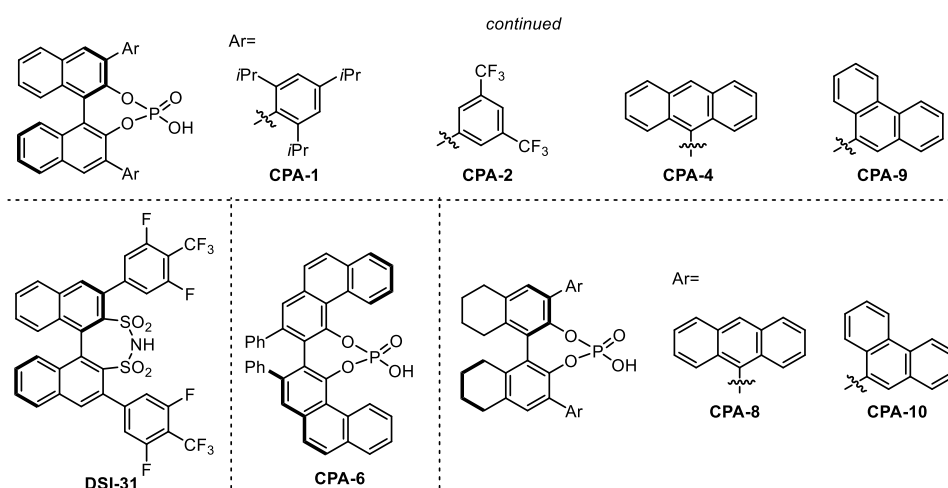
Scheme 5-22: Desired model for the asymmetric reduction of enamide.

Asymmetric transfer hydrogenation^[349] employing chiral phosphoric acid and Hantzsch ester has been applied to the reduction of various unsaturated functional groups.^[230e, 350] Inspired by the branched enamide reduction developed by Antilla et al.,^[350e] the investigation of the asymmetric transfer hydrogenation of enamide **5.1** was initiated. Starting with different catalyst cores and backbones (Table 5-4, entries 1-3), the BINOL derived phosphoric acid showed a promising result (53.3% *ee* and 40% yield). Following this hint, the substitution group of BINOL was screened (entries 4-8), and **CPA-2** turned out to be the best catalyst. After reaction condition optimization with **CPA-2** (entries 9-13), the best result was shown as 80% *ee* and 61% yield (99% (b.r.s.m.)). From the enantioenriched **5.62**, both (*S*)-deplancheine and (*S*)-10-desbromoarborescidine A could be obtained by the reported way.^{da Silva, 2009 #992}

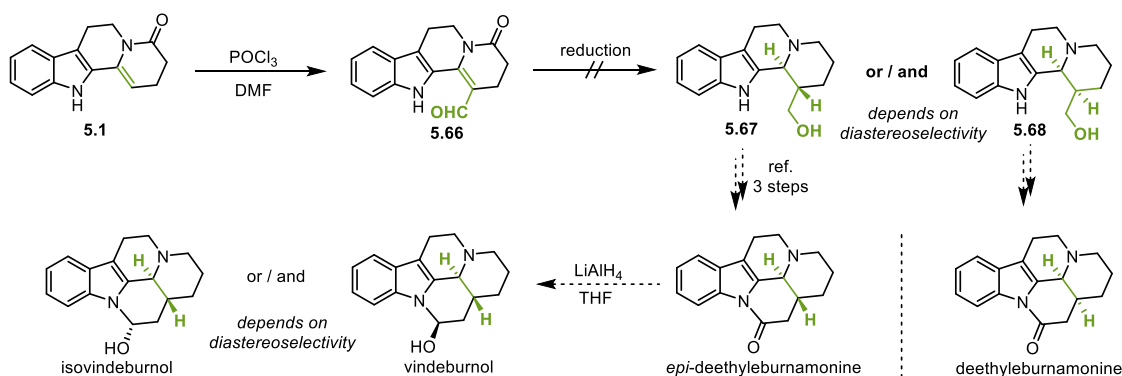
Table 5-4: Asymmetric reduction of the enamide.

entry ^[a]	catalyst [mol%]	T [°C]	<i>ee</i> [%] ^[b]	yield [%] ^[c]
1	DSI-31 (10)	60	7.6	79
2	CPA-1 (10)	60	53.3	40
3	CPA-6 (10)	60	20.2	30
4	CPA-2 (10)	60	80	61
5	CPA-4 (10)	60	9.8	48
6	CPA-8 (10)	60	0.1	36
7	CPA-9 (10)	60	20.8	42
8	CPA-10 (10)	60	5.0	20
9	CPA-2 (10)	50	71.3	36
10	CPA-2 (10)	30	68.8	20
11	CPA-2 (5)	30	63.1	10
12	CPA-2 (10)	0	65.4	6
13	CPA-2 (10)	-20	N.D. ^[d]	trace

[a] Reactions were performed with enamide (5.0 mg, 21 μmol); [b] *ee* was determined by HPLC; [c] Isolated yield; [d] N.D. = not determined

Table 5–4: Asymmetric reduction of the enamide. (continued)

Inspired by the efficient oxidation and reduction, the investigation of β -formylation of **5.1** was commenced. The β -formylation underwent successfully by a Vilsmeier–Haack type reaction. However, the reduction of **5.66** was unsuccessful, resulting in neither the selective aldehyde reduction nor the global reduction products.

**Scheme 5–23:** Synthetic plan of the β -formylation.

5.2.4. Total synthesis of ilicifoline B

Benzylisoquinoline alkaloids (BIAs) are plant specialized metabolites with structural diversity and long history of investigation. Many BIAs possess excellent potent pharmacological properties, including the antimicrobial berberine, the muscle relaxants tubocurarine and papaverine, the histamine H1 receptor inhibitor protopine, the narcotic analgesic codeine and the anticancer noscapine (Figure 5–11).^[351] These prominent examples of BIAs belong to different subtypes based on the type of their scaffolds.

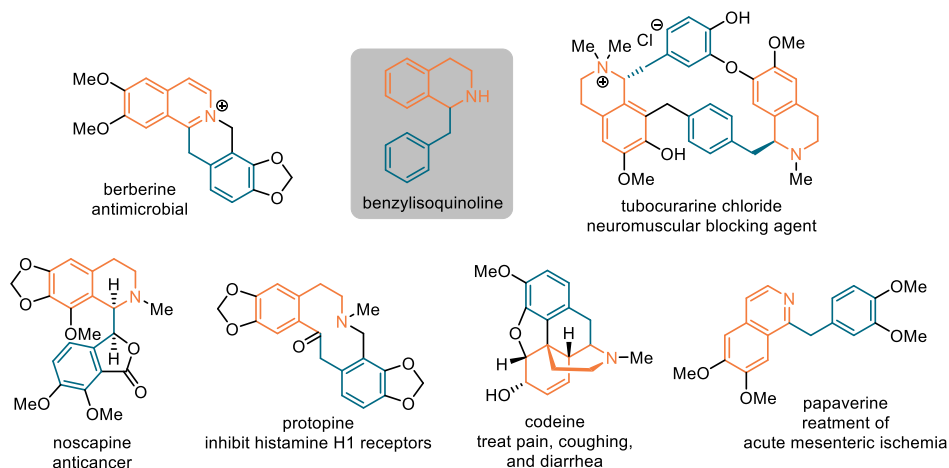
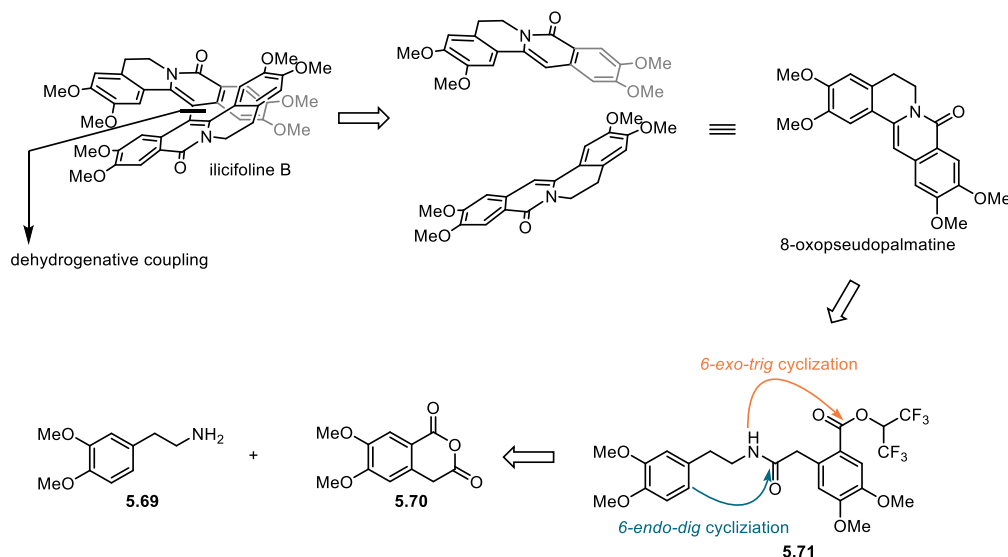


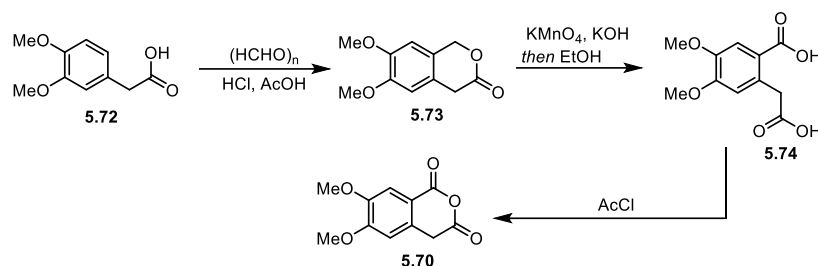
Figure 5–11: Representative benzyloquinoline alkaloids.

As the polycyclic alkaloids are attractive, especially the fused ring system, the annulation was anticipated to be applied to the total synthesis of protoberberine-type BIAs. The fascinating structure of ilicifoline B was selected as the target, as it featured a unique dimeric ring system. The dimerization of 8-oxopseudopalmatine could be achieved by a dehydrogenative coupling (Scheme 5–24). The annulation reaction was proposed to prepare 8-oxopseudopalmatine. The starting material was traced back to amine **5.69** and anhydride **5.70**.



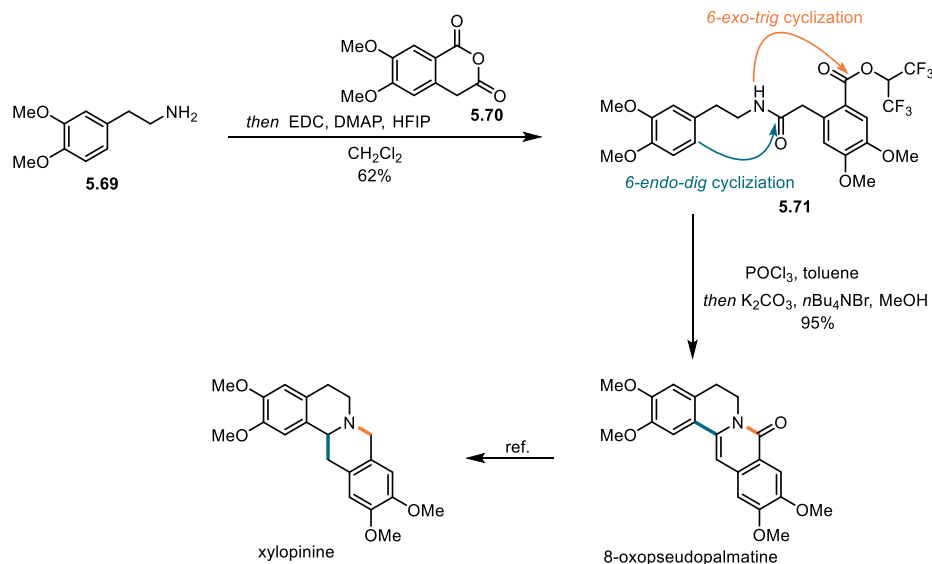
Scheme 5–24: Retrosynthetic analysis of ilicifoline B.

Anhydride **5.70** was commercially available, but taking the cost into consideration, it was prepared by a three-step procedure from acid **5.72** (Scheme 5–25).^[352]



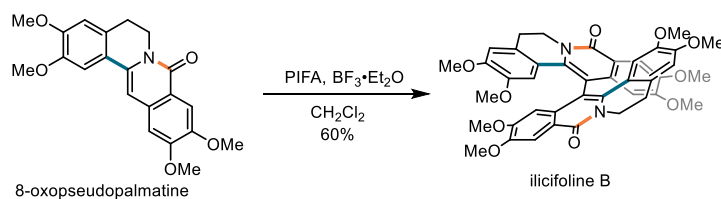
Scheme 5–25: Anhydride preparation.

With the anhydride and amine in hand, the synthesis of 8-oxopseudopalmatine was commenced through the annulation reaction. HFIPE **5.71** was obtained in 62% yield through the condensation (Scheme 5–26). The annulation reaction underwent successfully to afford 8-oxopseudopalmatine in 95% yield. According to the reported reduction, 8-oxopseudopalmatine could be converted to tetracyclic protoberberine alkaloid xylopinine.^[353]



Scheme 5–26: Synthesis of 8-oxopseudopalmatine by the annulation reaction

The dimerization was realized by a hypervalent iodine promoted oxidative biaryl coupling,^[354] which has proven to be efficient in Opatz's novel total synthesis of ilicifoline B by xylochemistry (Scheme 5–27).^[355]



Scheme 5–27: Dimerization by hypervalent iodine reagent.

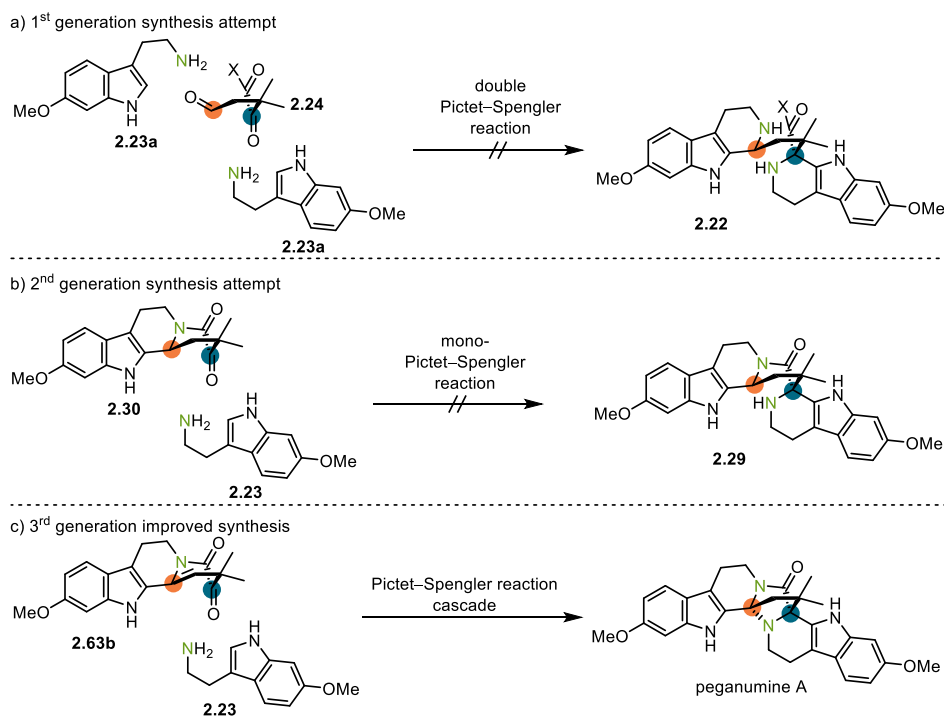
5.3. Brief summary

This chapter aimed at the investigation of an annulation methodology. Started from the annulation discovered in the 2nd generation synthesis attempt, the complementary carbonyl activation annulation was developed after an intensive screening of different activation modes. This updated annulation was applied to the total synthesis of harmalanine, harmalacine, nortetoybyrine and ilicifoline B, as well as the formal total synthesis of deplancheine, 10-desbromoarborescidine A, hirsutine, rhynchophylline and isorhynchophylline.

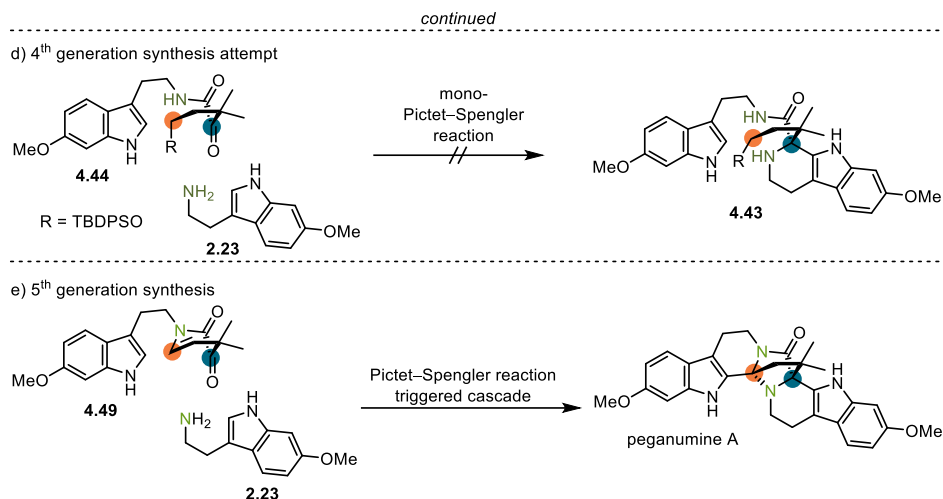
6. Summary and Outlook

6.1. Summary

The primary aim of the research in this thesis was the total synthesis of peganumine A. By analyzing the characteristic dimeric β -carboline motifs, five retrosynthetic strategies were proposed relying on different types of Pictet–Spengler reaction. In the 1st generation synthetic attempt, the ambitious double Pictet–Spengler reaction turned out to be challenging (Scheme 6–1a). The simplified mono-Pictet–Spengler reaction was proposed in the 2nd generation synthetic attempt. Unfortunately, such reaction with α -ketolactam **2.30** was difficult to be realized, as DFT calculation performed by Dr. Yinghan Chen and Professor Dr. Yong Liang at Nanjing University indicated this transformation is kinetically unfavorable ($\Delta G_{TS1}^\ddagger = +34.5$ kcal/mol) (Scheme 6–1b). Inspired by Zhu’s synthesis of peganumine A, the protection group free 3rd generation improved synthesis was realized with α -ketoamide **2.63b** (Scheme 6–1c). Based on the experience of these strategies, a Pictet–Spengler reaction of linear α -ketoamide **4.44** was anticipated in the 4th generation synthetic strategy. However, such reaction was still challenging (Scheme 6–1d). Finally, by employing α -ketoamide **4.49**, the 5th generation synthesis afforded peganumine A through a Pictet–Spengler reaction, which triggered an iminium ion cyclization cascade (Scheme 6–1e).



Scheme 6–1: The key Pictet–Spengler reactions in different strategies.



Scheme 6–1: The key Pictet–Spengler reactions in different strategies. (continued)

With the efficient 3rd generation improved protection group free synthetic route, 11 racemic analogues were successfully synthesized through utilizing the function-oriented synthesis strategy. A potent analogue was discovered with an IC₅₀ value of 5.2 μM against HL-60 cells, by the collaboration with Dr. Wan Li and Professor Dr. Jinhua Wang at the Institute of Materia Medica, Chinese Academy of Medical Sciences and Peking Union Medical College (Figure 6–1). Additionally, the preliminary SAR was also proposed to guide the further analogue design.

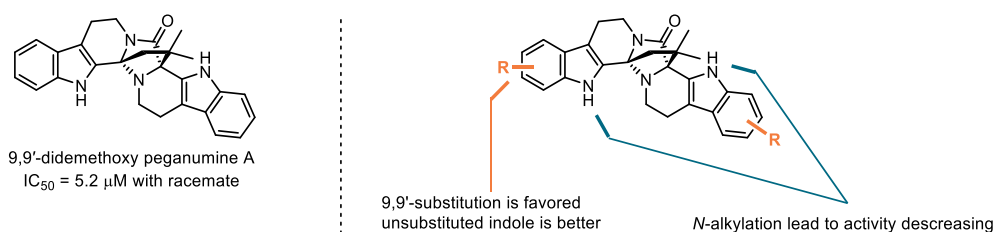


Figure 6–1: The potent analogue and SAR.

Next, the asymmetric total synthesis of peganumine A and its analogues was realized by organocatalysis. The asymmetric total synthesis of peganumine A was achieved by the DSI catalyzed cascade with 97.1% *ee* (Figure 6–2). However, the DSI could not catalyze the asymmetric synthesis of the analogues of peganumine A with high enantioselectivity. After the design, synthesis and screening, the NPPA was discovered as a better catalyst for the asymmetric synthesis of the analogues, which yielded over 90% *ee* syntheses of 4 analogues including the potent 9,9'-didemethoxy peganumine A.

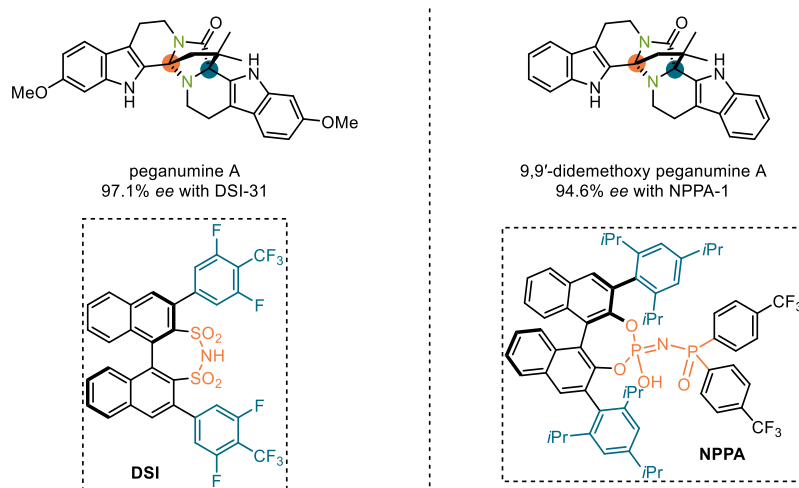
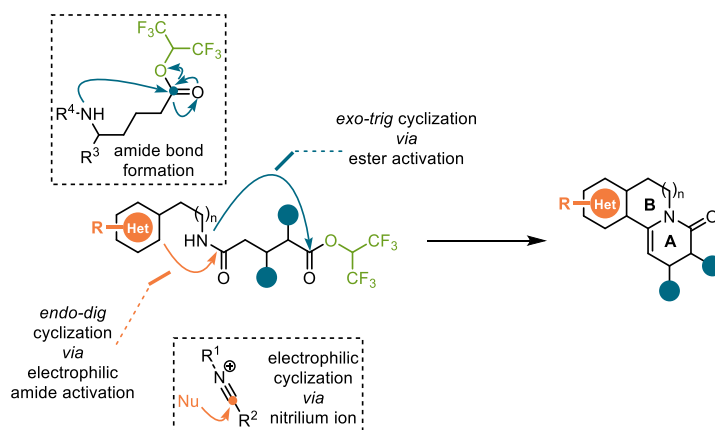


Figure 6–2: Asymmetric synthesis of peganumine A and its analogues.

The last chapter focused on the development of an annulation, which was initially discovered in the 2nd generation synthetic attempt. By analyzing the results caused by the Thorpe–Ingold effect of the *gem*-dimethyl group, the complementary carbonyl activation annulation was developed (Scheme 6–2). With this efficient annulation in hand, various polycyclic fused quinolizidine scaffolds were obtained. In addition, the annulation was applied to the total synthesis of harmalanine, harmalacine, nortetoyobyrine and ilicifoline B, and the formal total synthesis of deplancheine, 10-desbromoarborescidine A, hirsutine, rhynchophylline and isorhynchophylline.



Scheme 6–2: The complementary carbonyl activation annulation.

6.2. Outlook

Although a potent analogue was discovered, the cytotoxicity probably can be improved by further analogue design and synthesis. The 5,5-dimethyl-2,7-diazabicyclo[2.2.1]heptan-3-one core can be modified to show the importance of this unique scaffold. Other heterocycles can also be introduced. A cellular mechanism study is also anticipated.

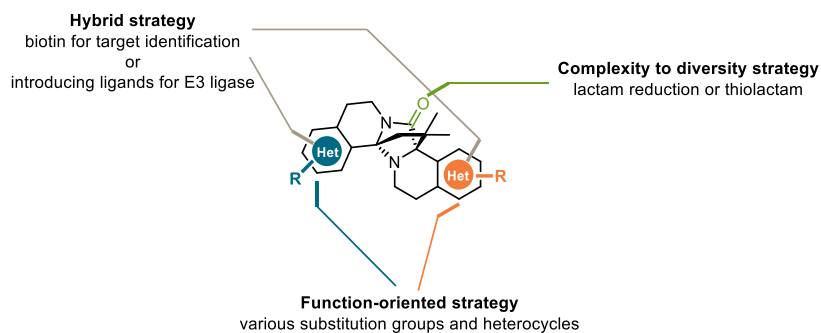


Figure 6–3: Further investigation of analogues.

In the 5th generation synthesis, a Pictet–Spengler reaction–iminium ion cyclization–amination cascade was realized yielding the peganumine A (Scheme 6–1e). DFT calculation of the efficient cascade reaction is envisioned to clarify the mechanism of such reaction. Meanwhile, the asymmetric version of this cascade reaction is also an interesting topic to explore the proper catalyst and activation mode.

7. Experimental Information

7.1. General information

Unless otherwise stated, all reactions were magnetically stirred and conducted in anhydrous solvents under argon, applying standard Schlenk techniques. Solvents and liquid reagents, as well as solutions of solid or liquid reagents were added via syringes, stainless steel cannulas through rubber septa or micropipettes in a weak stream of argon. Solid reagents were added through a weak argon counter-flow. Cooling baths were prepared in Dewar vessels, filled with ice/water (0 °C), dry ice/acetonitrile (−40 °C) or dry ice/acetone (−78 °C). Heated oil baths were used for reactions requiring elevated temperatures. Solvents were removed under reduced pressure at 40 °C using a rotary evaporator. All given yields are isolated yields of NMR spectroscopically pure materials, unless otherwise stated.

Chemicals

Chemicals (Abcr, Alfa Aesar, Apollo Scientific, Fisher Scientific, Fluorochem, Sigma-Aldrich, TCI) were purchased as reagent grade and used without further purification unless otherwise stated. Molecular sieves (MS) 4 Å were dried at 150 °C under vacuum and stored in Schlenk flask.

Solvents

Solvents (toluene, tetrahydrofuran (THF), dichloromethane (DCM)) were purified with the solvent purification system Braun MB-SPS-800 (Institut für Chemie und Biochemie, Freie Universität Berlin) or dried by distillation from an appropriate drying agent and stored in Schlenk flasks under argon (Max-Planck-Institut für Kohlenforschung). Additional solvents (dimethylformamide (DMF) and methanol) were purchased from Fisher Scientific in AcroSeal[®]-bottles under argon atmosphere with MS 4 Å.

Thin-layer chromatography (TLC)

TLC was performed using silica gel coated aluminum plates (ALUGRAM[®] Xtra SIL G/UV254, Macherey-Nagel) or pre-coated silica gel plastic sheets (Polygram SIL G/UV254, 0.20 mm, with fluorescent indicator; Macherey-Nagel) which were visualized under irradiation with UV light ($\lambda = 254$) or vanillin stain (500 mg vanillin, 5 mL H₂SO₄ (conc.), 10 mL HOAc, 100 mL MeOH).

Column Chromatography

Column chromatography was carried out using silica gel from Merck or Macherey & Nagel (60 Å, 230–400 mesh, particle size 40–63 µm) or neutral aluminium oxide from Fisher Scientific (Brockmann I, 60 Å, 50–200 µm) using technical grade solvents. Fractions containing a desired substance were combined and concentrated in vacuo. Solvent mixtures (mobile phase) are reported in terms of volume ratios (v/v).

Nomenclature

Nomenclature follows the suggestions proposed by the computer program ChemDraw Professional (17.1.0.105) of PerkinElmer.

Nuclear Magnetic Resonance (NMR) Spectroscopy

¹H and ¹³C NMR spectra were recorded on a JEOL ECX 400 (400 MHz), JEOL ECP 500 (500 MHz), Bruker Avance 500 (500 MHz), JEOL ECZ600 S (600 MHz) and Bruker Avance 700 (700 MHz) spectrometers in reported deuterated solvent. All spectra were processed with MestReNova 12.0.3. The residual deuterated solvent signal relative to tetramethylsilane (TMS) was used as the internal reference in ¹H NMR spectra (DMSO δ [ppm] = 2.50; CD₂Cl₂ δ [ppm] = 5.32; CD₃OD δ [ppm] = 3.31; C₆D₆ δ [ppm] = 7.16; CDCl₃ δ [ppm] = 7.26). Data are reported as follows: chemical shift, multiplicity (s = singlet, bs = broad singlet, d = doublet, t = triplet, q = quartet, m = multiplet), coupling constants (Hz) and integration. ¹³C NMR spectra reported in ppm from tetramethylsilane (TMS) with the solvent resonance as the internal standard (DMSO δ [ppm] = 39.5; CD₂Cl₂ δ [ppm] = 53.8; CD₃OD δ [ppm] = 49.0, CDCl₃ δ [ppm] = 72.16; C₆D₆ δ [ppm] = 128.0).

Mass Spectrometry

High resolution mass spectrometry (HRMS) was performed on a Finnigan MAT 95 (EI), Bruker APEX III FTMS (ESI) or Agilent 6210 (ESI). The ionization method and mode of detection employed is indicated for the respective experiment and all masses are reported in atomic units per elementary charge (m/z).

IR Spectroscopy

IR Spectra were recorded on a JASCO FT/IR-4100 spectrometer. Characteristic absorption bands are reported in wavenumbers ν in cm⁻¹ and were analyzed with the software from JASCO.

Specific Rotations

Specific rotations $[\alpha]_D^T$ were measured on a Rudolph RA Autopol IV Automatic Polarimeter or JASCO P-2000 Polarimeter at the indicated temperature with a sodium lamp (sodium D line, $\lambda = 589$ nm). Measurements were performed in an acid resistant 50 mm cell (Rudolph) or 100 mm (JASCO) with concentrations (g/100 mL) reported in the corresponding solvent.

Circular Dichroism (CD) Spectroscopy

CD were recorded on a Jasco J-810 spectropolarimeter equipped with a temperature-controlled quartz cell of 0.1 cm path length. The recorded spectra were evaluated with the Jasco software package. The spectra were the averaged from three scans obtained by collecting data from 190 to 400 nm at 0.2 nm intervals, 2 nm bandwidth, and 1 sec response time.

High Performance Liquid Chromatography (HPLC)

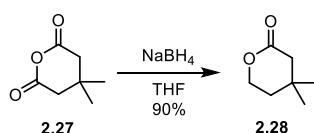
HPLC was performed on Shimadzu LC-20AD liquid chromatograph (SIL-20AC auto sampler, CMB-20A communication bus module, DGU-20A5 degasser, CTO-20AC column oven, SPD-M20A diode array detector), Shimadzu LC-20AB liquid chromatograph (SIL-20ACHT auto sampler, DGU-20A5 degasser, CTO-20AC column oven, SPD-M20A diode array detector), or Agilent Technologies 1200 series with CHIRALPAK[®] IA. All solvents used were HPLC-grade solvents purchased from Sigma-Aldrich or VWR. The column employed and respective solvent mixture are indicated for each experiment.

7.2. Experimental procedures

7.2.1. Total synthesis of racemic peganumine A and its analogues

7.2.1.1. 1st generation synthetic approach towards peganumine A

4,4-Dimethyltetrahydro-2H-pyran-2-one (2.28)



To suspension of 3,3-dimethyl glutaric anhydride (5.00 g, 35.1 mmol, 1.0 equiv.) in THF (100 mL) was added NaBH₄ (3.98 g, 105 mmol, 3.0 equiv.) by portions at 0 °C. The reaction

mixture was stirred at room temperature for 3 d, before it was quenched by careful addition of H₂O at 0 °C and extracted with DCM. The combined organic phase was dried over MgSO₄ and concentrated under reduced pressure. The crude product was filtered through a short pad of Celite[®] to afford the lactone **2.28** (4.05 g, 31,6 mmol, 90%) as a colorless liquid.

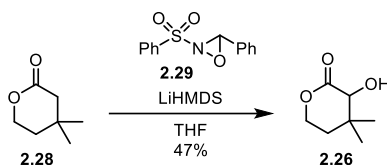
¹H NMR (500 MHz, CDCl₃) δ [ppm] = 4.13–4.00 (m, 2H), 2.10–1.96 (m, 2H), 1.42 (q, *J* = 6.2 Hz, 2H), 0.80 (dt, *J* = 5.6, 1.5 Hz, 6H).

¹³C NMR (126 MHz, CDCl₃) δ [ppm] = 171.2, 66.2, 43.8, 35.5, 29.4, 28.5.

HRMS-ESI: calcd. for C₇H₁₂O₂Na [M + Na]⁺: 151.0729; found: 151.0737.

FT-IR: ν [cm⁻¹] = 2957, 2930, 2872, 1731, 1403, 1268, 1254, 1173, 1076, 1068, 992, 797.

3-Hydroxy-4,4-dimethyltetrahydro-2H-pyran-2-one (**2.26**)



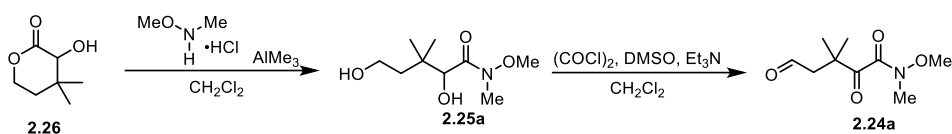
A solution of HMDS (480 μL, 2.34 mmol, 1.5 equiv.) in THF (5.0 mL) was added *n*BuLi (2.5 M in hexane, 930 μL, 2.34 mmol, 1.5 equiv.) at –78 °C. The mixture was stirred for 1 h, before a solution of lactone **2.28** (200 mg, 1.56 mmol, 1.0 equiv.) in THF (2.0 mL) was added dropwise. The resulting mixture was stirred at –78 °C for 1 h. A solution of Davis reagent **2.29** (533 mg, 2.04 mmol, 1.3 equiv.) in THF (2.0 mL) was added dropwise at –78 °C over a period of 30 min, and then reaction mixture was stirred for 3 h at –40 °C. The reaction was quenched with NH₄Cl (sat. aq.) and extracted with DCM. The combined organic phases were washed with brine, dried over MgSO₄, filtered and concentrated under reduced pressure. The crude product was purified by silica gel column chromatography (pentane/EtOAc = 5:1) to afford the α-hydroxylactone **2.26** (105 mg, 0.729 mmol, 47%) as a colorless liquid.

¹H NMR (600 MHz, CDCl₃) δ [ppm] = 4.21 (ddd, *J* = 6.7, 5.7, 2.1 Hz, 2H), 3.87 (s, 1H), 3.21 (s, 1H), 1.81–1.76 (m, 1H), 1.76–1.63 (m, 1H), 1.05 (s, 3H), 0.86 (s, 3H).

¹³C NMR (151 MHz, CDCl₃) δ [ppm] = 175.2, 75.0, 65.9, 36.4, 34.7, 27.7, 21.2.

HRMS-ESI: calcd. for C₇H₁₂O₃Na [M + Na]⁺: 167.0678; found: 167.0671.

FT-IR: ν [cm⁻¹] = 3473, 2960, 2930, 1733, 1368, 1258, 1165, 1108, 1065, 883, 730.

***N*-methoxy-3,3-trimethyl-2,5-dioxopentamide (2.24a)**

To a solution of α -hydroxylactone **2.26** (150 mg, 1.04 mmol, 1.0 equiv.) in DCM (5.0 mL) was added *N,O*-dimethylhydroxylamine hydrochloride (304 mg, 3.12 mmol, 3.0 equiv.). AlMe_3 (2.0 M in toluene, 1.56 mL, 3.12 mmol, 3.0 equiv.) was added to the reaction mixture dropwise carefully at 0 °C. After the addition, the resulting mixture was moved to room temperature to stir overnight. The reaction was quenched with potassium sodium tartrate (sat. aq.) carefully and extracted with DCM. The combined organic phases were washed with brine, dried over MgSO_4 , filtered and concentrated under reduced pressure. The crude diol **2.25a** was used without further purification.

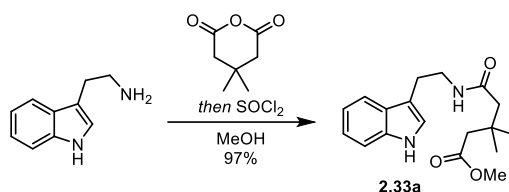
To a solution of DMSO (133 μL , 1.87 mmol, 4.8 equiv.) in DCM (4.0 mL) was added oxalyl chloride (79.2 μL , 0.936 mmol, 2.4 equiv.) at -78 °C. After the mixture was stirred for 30 min, a solution of the crude diol **2.25a** (80 mg, 0.390 mmol, 1.0 equiv.) in DCM (2.0 mL) was added at -78 °C. The resulting mixture was stirred for 30 min, before the addition of Et_3N (541 μL , 3.90 mmol, 10 equiv.). The reaction mixture was stirred for another 20 min and quenched with NaHCO_3 (sat. aq.). The mixture was extracted with DCM. The combined organic phases were washed with brine, dried over MgSO_4 , filtered and concentrated under reduced pressure. The crude product was purified by silica gel column chromatography (pentane/ EtOAc = 5:1) to afford **2.24a** (105 mg, 0.522 mmol, 50% over two steps) as a light yellow liquid.

$^1\text{H NMR}$ (400 MHz, CDCl_3) δ [ppm] = 9.71 (t, J = 2.2 Hz, 1H), 3.63 (s, 3H), 3.20 (s, 3H), 2.63 (d, J = 2.2 Hz, 2H), 1.35 (s, 6H).

$^{13}\text{C NMR}$ (101 MHz, CDCl_3) δ [ppm] = 205.2, 200.5, 167.4, 62.0, 51.7, 44.6, 31.3, 24.5.

HRMS-ESI: calcd. for $\text{C}_9\text{H}_{15}\text{NO}_4\text{Na}$ $[\text{M} + \text{Na}]^+$: 224.0893; found: 224.0894.

FT-IR: ν [cm^{-1}] = 2925, 1713, 1658, 1462, 1386, 966.

7.2.1.2. 2nd generation synthetic approach towards peganumine A**Methyl 5-((2-(1*H*-indol-3-yl)ethyl)amino)-3,3-dimethyl-5-oxopentanoate (2.33a)**

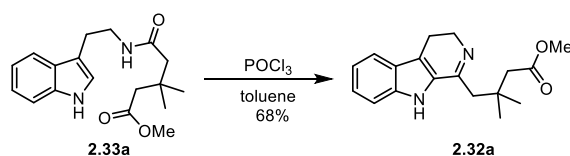
Tryptamine (2.00 g, 12.3 mmol, 1.0 equiv.) and 3,3-dimethylglutaric anhydride (1.75 g, 12.3 mmol, 1.0 equiv.) were dissolved in MeOH (25 mL). The mixture was stirred overnight, before SOCl₂ (880 μL, 12.3 mmol, 1.0 equiv.) was added dropwise at 0 °C. The reaction mixture was allowed to warm to room temperature for 3 h and quenched with NaHCO₃ (sat. aq.). The mixture was extracted with DCM. The combined organic phases were washed with brine, dried over MgSO₄, filtered and concentrated under reduced pressure. The crude product was purified by silica gel column chromatography (pentane/EtOAc = 2:1) to afford the methyl ester **2.33a** (3.83 g, 12.1 mmol, 97%) as a light yellow solid.

¹H NMR (700 MHz, CDCl₃) δ [ppm] = 8.13 (s, 1H), 7.62–7.60 (m, 1H), 7.37–7.35 (m, 1H), 7.19 (ddd, *J* = 8.1, 7.0, 1.2 Hz, 1H), 7.12 (ddd, *J* = 7.9, 7.0, 1.0 Hz, 1H), 7.05 (dd, *J* = 2.3, 1.1 Hz, 1H), 6.41 (s, 1H), 3.63 (td, *J* = 7.0, 5.7 Hz, 2H), 3.60 (s, 3H), 2.98 (td, *J* = 7.0, 1.0 Hz, 2H), 2.24 (s, 2H), 2.20 (s, 2H), 1.04 (s, 6H).

¹³C NMR (176 MHz, CDCl₃) δ [ppm] = 173.5, 171.2, 136.5, 127.5, 122.3, 122.1, 119.5, 118.9, 113.3, 111.3, 51.5, 47.4, 44.7, 39.6, 33.5, 28.7, 25.6.

HRMS-ESI: calcd. for C₁₈H₂₄N₂O₃Na [M + Na]⁺: 339.1679; found: 339.1683.

FT-IR: ν [cm⁻¹] = 3401, 3293, 2952, 1735, 1728, 1644, 1525, 1435, 1354, 1227, 1218, 740.

Methyl 4-(4,9-dihydro-3*H*-pyrido[3,4-*b*]indol-1-yl)-3,3-dimethylbutanoate (2.32a)

To a solution of methyl ester **2.33a** (1.2 g, 4.02 mmol, 1.0 equiv.) in toluene (50 mL) was added POCl₃ (364 μL, 4.02 mmol, 1.0 equiv.) at room temperature. The reaction mixture was heated to 110 °C till the methyl ester **2.33a** was fully consumed (TLC monitoring). After the reaction

mixture was cooled down to room temperature, the solvent was removed under reduced pressure. The crude product was purified by silica gel column chromatography (DCM/MeOH = 10:1) to afford imine **2.32a** (770 mg, 2.58 mmol, 68%) as a dark yellow solid.

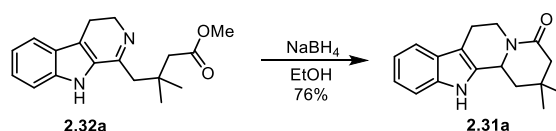
¹H NMR (700 MHz, *d*₆-DMSO) δ [ppm] = 11.36 (s, 1H), 7.55–7.51 (m, 1H), 7.42 (dt, *J* = 8.2, 1.0 Hz, 1H), 7.18 (ddd, *J* = 8.2, 6.9, 1.2 Hz, 1H), 7.03 (ddd, *J* = 7.9, 6.9, 1.0 Hz, 1H), 3.76–3.69 (m, 2H), 3.54 (s, 3H), 2.75–2.70 (m, 2H), 2.67 (s, 2H), 2.42 (s, 2H), 1.02 (s, 6H).

¹³C NMR (176 MHz, *d*₆-DMSO) δ [ppm] = 172.0, 158.8, 136.4, 129.9, 124.9, 123.4, 119.5, 119.3, 114.1, 112.3, 50.9, 47.9, 44.9, 44.8, 33.8, 27.0, 18.9.

HRMS-ESI: calcd. for C₁₈H₂₃N₂O₂ [M + H]⁺: 299.1754; found: 299.1752.

FT-IR: ν [cm⁻¹] = 3392, 2969, 2879, 1735, 1626, 1552, 1431, 1339, 1227, 1217, 751.

2,2-Dimethyl-2,3,6,7,12,12b-hexahydroindolo[2,3-*a*]quinolizin-4(1*H*)-one (2.31a)



To a solution of imine **2.32a** (750 mg, 1.68 mmol, 1.0 equiv.) in EtOH (15 mL) was added NaBH₄ (189 mg, 3.36 mmol, 2.0 equiv.) at 0 °C by portions. The resulting mixture was allowed to warm to room temperature and stirred for another 5 h, before the reaction mixture was quenched with HOAc (1% aq.). The mixture was extracted with DCM. The combined organic phases were washed with brine, dried over MgSO₄, filtered and concentrated under reduced pressure. The crude product was purified by silica gel column chromatography (pentane/EtOAc = 5:1) to afford lactam **2.31a** (515 mg, 1.92 mmol, 76%) as a white solid.

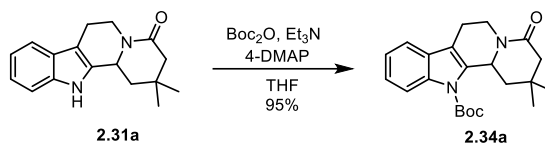
¹H NMR (500 MHz, CD₂Cl₂) δ [ppm] = 8.97 (s, 1H), 7.49 (d, *J* = 7.8 Hz, 1H), 7.38–7.38 (m, 1H), 7.17–7.14 (m, 1H), 7.12–7.05 (m, 1H), 5.22–5.11 (m, 1H), 4.92–4.81 (m, 1H), 2.96–2.86 (m, 1H), 2.85–2.81 (m, 1H), 2.81–2.74 (m, 1H), 2.40–2.30 (m, 1H), 2.26 (q, *J* = 11.2, 10.0 Hz, 2H), 1.70 (dd, *J* = 13.1, 11.4 Hz, 1H), 1.16 (s, 3H), 1.07 (s, 3H).

¹³C NMR (126 MHz, CD₂Cl₂) δ [ppm] = 168.8, 136.9, 134.4, 127.4, 122.0, 119.8, 118.4, 111.4, 109.1, 52.0, 46.4, 41.4, 40.3, 30.7, 29.4, 25.5, 21.6.

HRMS-ESI: calcd. for C₁₇H₂₁N₂O [M + H]⁺: 269.1649; found: 269.1647.

FT-IR: ν [cm⁻¹] = 3375, 3177, 2955, 2931, 2369, 2317, 2269, 1704, 1624, 1415, 1156, 741.

Tert-butyl 2,2-dimethyl-4-oxo-1,3,4,6,7,12b-hexahydroindolo[2,3-*a*]quinolizine-12(2*H*)-carboxylate (2.34a)



To a solution of lactam **2.31a** (350 mg, 1.30 mmol, 1.0 equiv.) in THF (10 mL) was added Et₃N (450 μL, 1.95 mmol, 2.5 equiv.), 4-DMAP (39.7 mg, 325 μmol, 0.25 equiv.) and Boc₂O (425 mg, 1.95 mmol, 1.5 equiv.) subsequently. The resulting mixture was stirred at room temperature overnight before the reaction mixture was quenched with NaHCO₃ (sat. aq.). The mixture was extracted with DCM. The combined organic phases were washed with brine, dried over MgSO₄, filtered and concentrated under reduced pressure. The crude product was purified by silica gel column chromatography (pentane/EtOAc = 10:1) to afford lactam **2.34a** (455 mg, 1.24 mmol, 95%) as a white solid.

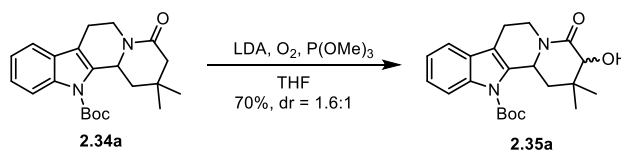
¹H NMR (500 MHz, CDCl₃) δ [ppm] = 7.98 (dt, *J* = 8.3, 0.9 Hz, 1H), 7.43 (ddd, *J* = 7.6, 1.5, 0.7 Hz, 1H), 7.29 (ddd, *J* = 8.4, 7.2, 1.4 Hz, 1H), 7.24 (td, *J* = 7.4, 1.1 Hz, 1H), 5.26–5.19 (m, 1H), 5.13 (ddd, *J* = 12.0, 4.4, 1.6 Hz, 1H), 2.83 (td, *J* = 11.7, 3.6 Hz, 1H), 2.75 (dddd, *J* = 15.7, 11.2, 4.4, 2.5 Hz, 1H), 2.71–2.65 (m, 1H), 2.39–2.32 (m, 2H), 2.21 (d, *J* = 17.5 Hz, 1H), 1.70 (s, 9H), 1.38 (dd, *J* = 12.9, 11.1 Hz, 1H), 1.18 (s, 3H), 1.01 (s, 3H).

¹³C NMR (126 MHz, CDCl₃) δ [ppm] = 169.4, 150.4, 136.9, 135.9, 128.8, 124.6, 123.0, 118.5, 118.3, 115.4, 84.4, 53.2, 46.2, 42.1, 39.2, 31.2, 28.8, 28.3, 25.9, 21.9.

HRMS-ESI: calcd. for C₂₂H₂₈N₂O₃Na [M + Na]⁺: 391.1992; found: 391.1978.

FT-IR: ν [cm⁻¹] = 2958, 2927, 1726, 1620, 1455, 1310, 1158, 1137, 748.

Tert-butyl 3-hydroxy-2,2-dimethyl-4-oxo-1,3,4,6,7,12b-hexahydroindolo[2,3-*a*]quinolizine-12(2*H*)-carboxylate (2.35a)



A solution of *i*Pr₂NH (249 μL, 1.76 mmol, 4.0 equiv.) in THF (3.0 mL) was added *n*BuLi (2.5 M in hexane, 700 μL, 1.76 mmol, 4.0 equiv.) at 0 °C. The mixture was stirred for 1 h at 0 °C,

before a solution of lactam **2.34a** (162 mg, 440 μ mol, 1.0 equiv.) in THF (2.0 mL) was added dropwise at -78 °C. After the resultant mixture was stirred at -78 °C for 1 h, $\text{P}(\text{OMe})_3$ (104 μ L, 880 μ mol, 2.0 equiv.) was added. O_2 (balloon pressure) was bubbled through the mixture for 20 min, and the mixture was stirred for additional 2 h under O_2 atmosphere (the generation of the product was monitored by TLC). Then reaction was quenched with NaHCO_3 (sat. aq.). The aqueous phase was extracted with DCM. The combined organic phases were washed with brine, dried over MgSO_4 , filtered and the solvent was removed under reduced pressure. The crude product was purified by silica gel column chromatography (pentane/EtOAc = 5:1) to afford α -hydroxylactam **2.35a** (118 mg, 0.307 mmol, 70%, dr = 1.6:1) as a yellow solid.

^1H NMR (500 MHz, CDCl_3) δ [ppm] = 8.05 (dt, J = 8.3, 0.9 Hz, 2H), 7.98 (dt, J = 8.4, 0.9 Hz, 1H), 7.47–7.41 (m, 3H), 7.31 (dddd, J = 8.4, 7.2, 3.8, 1.4 Hz, 3H), 7.28–7.23 (m, 3H), 5.36–5.30 (m, 2H), 5.16 (ddd, J = 11.3, 4.4, 2.3 Hz, 1H), 5.03 (ddd, J = 12.6, 4.8, 1.5 Hz, 1H), 4.89 (ddd, J = 12.6, 5.0, 1.7 Hz, 2H), 4.00 (d, J = 2.2 Hz, 2H), 3.94 (d, J = 3.1 Hz, 2H), 3.75 (s, 1H), 3.70 (s, 1H), 3.64 (d, J = 7.7 Hz, 1H), 3.05–2.97 (m, 2H), 2.93 (ddd, J = 12.6, 11.1, 4.2 Hz, 1H), 2.86–2.79 (m, 2H), 2.79–2.70 (m, 3H), 2.50 (dd, J = 13.6, 4.3 Hz, 1H), 2.37 (dd, J = 13.9, 5.8 Hz, 2H), 1.71 (s, 13H), 1.70 (s, 11H), 1.58–1.50 (m, 3H), 1.24 (s, 5H), 1.14 (d, J = 1.9 Hz, 6H), 0.78 (s, 5H).

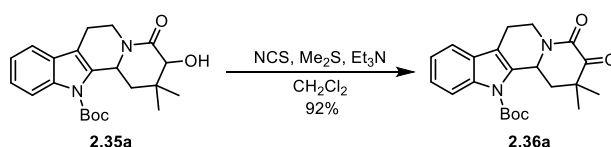
^{13}C NMR (126 MHz, CDCl_3) δ [ppm] = 172.7, 171.5, 150.4, 150.1, 137.0, 136.5, 135.3, 134.9, 128.7, 128.5, 124.8, 124.8, 123.2, 123.2, 118.4, 118.3, 116.9, 115.8, 115.4, 84.7, 84.6, 76.2, 74.7, 53.4, 49.9, 43.9, 40.1, 40.1, 39.7, 34.6, 33.3, 28.4, 28.3, 28.1, 23.2, 22.1, 20.8, 18.4.

(Note: The diastereomers were not to be separated. Therefore, the NMRs showed peaks of the two diastereomers.)

HRMS-ESI: calcd. for $\text{C}_{22}\text{H}_{28}\text{N}_2\text{O}_4\text{Na}$ [$\text{M} + \text{Na}$] $^+$: 407.1941; found: 407.1923.

FT-IR: ν [cm^{-1}] = 2971, 2927, 2869, 1728, 1638, 1455, 1366, 1251, 1145, 1139, 1069, 754.

***Tert*-butyl 2,2-dimethyl-3,4-dioxo-1,3,4,6,7,12b-hexahydroindolo[2,3-*a*]quinolizine-12-(2*H*)-carboxylate (**2.36a**)**



To a solution of NCS (260 mg, 1.95 mmol, 5.0 equiv.) in DCM (10 mL) at 0 °C was added Me₂S (716 μL, 9.75 mmol, 25 equiv.) and the mixture was stirred at –78 °C for 1 h. The solution of α-hydroxylactam **2.35a** (130 mg, 0.390 mmol, 1.0 equiv.) in DCM (5.0 mL) was added dropwise. The resulting mixture was stirred at –78 °C for another 2 h before Et₃N (1.08 mL, 7.80 mmol, 20 equiv.) was added. Then the mixture was stirred at –78 °C for 2 h before quenched with NH₄Cl (sat. aq.) and extracted with DCM. The combined organic phases were washed with brine, dried over MgSO₄, filtered and concentrated under reduced pressure. The crude product was purified by silica gel column chromatography (pentane/EtOAc = 5:2) to afford the α-ketolactam **2.36a** (120 mg, 0.312 mmol, 92%) as a yellow solid.

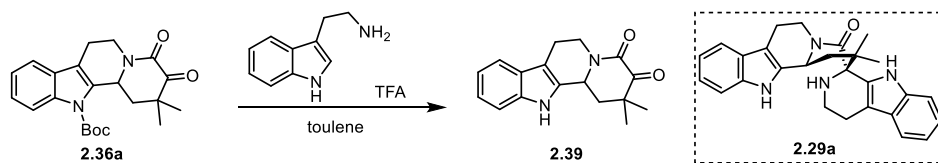
¹H NMR (500 MHz, CDCl₃) δ [ppm] = 7.96 (dt, *J* = 8.4, 0.9 Hz, 1H), 7.48–7.42 (m, 1H), 7.32 (ddd, *J* = 8.5, 7.3, 1.5 Hz, 1H), 7.26 (td, *J* = 7.3, 1.1 Hz, 1H), 5.63–5.59 (m, 1H), 5.08 (dt, *J* = 12.5, 3.5 Hz, 1H), 3.01 (ddd, *J* = 12.6, 8.7, 6.8 Hz, 1H), 2.82 (ddd, *J* = 8.9, 4.8, 2.5 Hz, 2H), 2.56 (dd, *J* = 13.7, 2.9 Hz, 1H), 1.86 (dd, *J* = 13.7, 10.9 Hz, 1H), 1.71 (s, 9H), 1.40 (s, 3H), 1.21 (s, 3H).

¹³C NMR (126 MHz, CDCl₃) δ [ppm] = 195.7, 157.3, 150.4, 136.5, 134.1, 128.5, 125.0, 123.3, 118.5, 118.4, 115.7, 84.9, 52.0, 42.3, 42.1, 40.2, 28.3, 25.2, 22.3, 21.5.

HRMS-ESI: calcd. for C₂₂H₂₆N₂O₄Na [M + Na]⁺: 405.1785; found: 405.1786.

FT-IR: ν [cm⁻¹] = 2920, 2851, 1726, 1669, 1456, 1367, 1307, 1223, 1138, 771, 754.

2,2-Dimethyl-1,2,6,7,12,12b-hexahydroindolo[2,3-a]quinolizine-3,4-dione (**2.39**)



A mixture of α-ketolactam **2.36a** (20.0 mg, 52.0 μmol, 1.0 equiv.), tryptamine (8.4 mg, 52.0 μmol, 1.0 equiv.) and 4Å MS in toluene (3.0 mL) was heated to 115 °C (oil bath temperature) overnight. The reaction mixture was cooled to room temperature and TFA (7.0 μL, 10 μmol, 0.2 equiv.) were added. The mixture was then heated to reflux for 2 d, before the reaction was quenched with NaHCO₃ (sat. aq.). The aqueous phase was extracted with DCM. The combined organic phases were washed with brine, dried over MgSO₄, filtered and concentrated under reduced pressure. The crude product was purified by silica gel column

chromatography (pentane/EtOAc = 2:1) to afford the α -ketolactam **2.39** (10.0 mg, 35.5 μ mol, 68%) as a light yellow solid.

$^1\text{H NMR}$ (700 MHz, d_6 -DMSO) δ [ppm] = 10.98 (s, 1H), 7.43 (dd, J = 7.8, 1.0 Hz, 1H), 7.34 (dt, J = 8.0, 0.9 Hz, 1H), 7.08 (ddd, J = 8.1, 7.0, 1.2 Hz, 1H), 6.99 (ddd, J = 7.9, 7.0, 1.0 Hz, 1H), 5.26–5.24 (m, 1H), 4.82 (ddd, J = 12.7, 5.3, 1.3 Hz, 1H), 3.08 (td, J = 12.4, 4.3 Hz, 1H), 2.83–2.80 (m, 1H), 2.70 (dddd, J = 14.9, 12.0, 5.3, 2.3 Hz, 1H), 2.59 (dd, J = 13.9, 4.1 Hz, 1H), 2.09 (dd, J = 13.9, 11.4 Hz, 1H), 1.28 (s, 3H), 1.13 (s, 3H).

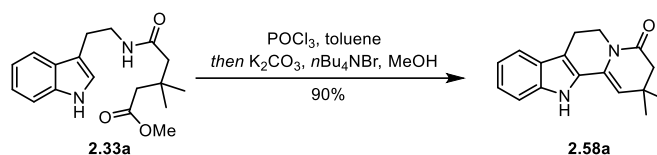
$^{13}\text{C NMR}$ (176 MHz, d_6 -DMSO) δ [ppm] = 195.3, 156.2, 136.2, 133.3, 126.2, 121.2, 118.7, 117.8, 111.2, 107.1, 49.1, 41.7, 40.3, 38.9, 24.1, 21.8, 20.5.

HRMS-ESI: calcd. for $\text{C}_{17}\text{H}_{18}\text{N}_2\text{O}_2\text{K}$ $[\text{M} + \text{K}]^+$: 321.1000; found: 321.0988.

FT-IR: ν [cm^{-1}] = 3253, 2922, 1728, 1651, 1427, 1303, 1009, 744.

7.2.1.3. 3rd generation synthetic approach towards peganumine A

2,2-Dimethyl-2,6,7,12-tetrahydroindolo[2,3-*a*]quinolizin-4(3*H*)-one (**2.58a**)



To a solution of the methyl ester **2.33a** (3.80 g, 12.0 mmol, 1.0 equiv.) in toluene (150 mL) was added POCl_3 (1.10 mL, 12.0 mmol, 1.0 equiv.) dropwise. Then the mixture was heated to 115 $^\circ\text{C}$ (oil bath temperature) until the starting material was fully consumed. After allowing the mixture to cool down to 80 $^\circ\text{C}$ (oil bath temperature), the MeOH (150 mL), K_2CO_3 (16.6 g, 120 mmol, 10.0 equiv.) and $n\text{Bu}_4\text{NBr}$ (388 mg, 1.20 mmol, 0.1 equiv.) were added subsequently. Afterwards the resulting mixture was stirred overnight at 80 $^\circ\text{C}$, cooled to room temperature, filtered through Celite[®], concentrated under reduced pressure. The crude product was purified by silica gel column chromatography (pentane/EtOAc = 5:3) to afford enamide **2.58a** (2.59 g, 10.9 mmol, 90%) as a light yellow solid. (Note: It is not necessary to perform the reaction under argon.)

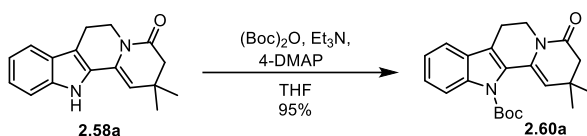
$^1\text{H NMR}$ (500 MHz, CDCl_3) δ [ppm] = 8.32 (s, 1H), 7.51 (d, J = 8.8 Hz, 1H), 7.33 (d, J = 8.1 Hz, 1H), 7.22 (dd, J = 8.4, 6.9 Hz, 1H), 7.15–7.09 (m, 1H), 5.39 (s, 1H), 4.12 (t, J = 6.0 Hz, 2H), 2.92 (t, J = 6.0 Hz, 2H), 2.50 (s, 2H), 1.18 (s, 6H).

$^{13}\text{C NMR}$ (126 MHz, CDCl_3) δ [ppm] = 169.6, 137.4, 128.9, 128.0, 126.8, 123.6, 120.1, 119.0, 112.3, 111.1, 110.6, 46.5, 39.4, 30.8, 28.3, 20.8.

HRMS-ESI: calcd. for $\text{C}_{17}\text{H}_{18}\text{N}_2\text{OK}$ $[\text{M} + \text{K}]^+$: 305.1051; found: 305.1039.

FT-IR: ν [cm^{-1}] = 3361, 2959, 2927, 1720, 1664, 1591, 1523, 1345, 1198, 1046, 943, 859, 743.

Tert-butyl 2,2-dimethyl-4-oxo-3,4,6,7-tetrahydroindolo[2,3-*a*]quinolizine-12(2*H*)-carboxylate (2.60a)



To a solution of enamide **2.58a** (92.0 mg, 0.346 mmol, 1.0 equiv.) in THF (10 mL) was added Et_3N (120 μL , 87.3 mmol, 2.5 equiv.), 4-DMAP (10.6 mg, 86.0 μmol , 0.25 equiv.) and Boc_2O (113 mg, 0.519 mmol, 1.5 equiv.) subsequently. The resulting mixture was stirred at room temperature overnight, before the reaction mixture was quenched with NaHCO_3 (sat. aq.). The mixture was extracted with DCM. The combined organic phases were washed with brine, dried over MgSO_4 , filtered and concentrated under reduced pressure. The crude product was purified by silica gel column chromatography (pentane/ EtOAc = 10:1) to afford the enamide **2.60a** (120 mg, 0.328 mmol, 95%) as a white solid.

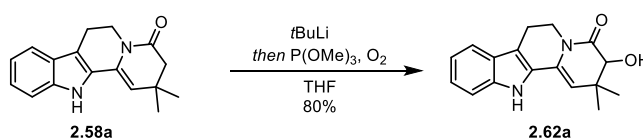
$^1\text{H NMR}$ (600 MHz, CDCl_3) δ [ppm] = 7.99 (dt, J = 8.4, 0.9 Hz, 1H), 7.45 (dt, J = 7.7, 1.0 Hz, 1H), 7.33 (ddd, J = 8.4, 7.2, 1.3 Hz, 1H), 7.24 (td, J = 7.5, 1.0 Hz, 1H), 5.29 (s, 1H), 4.09 (t, J = 5.8 Hz, 2H), 2.84 (t, J = 5.8 Hz, 2H), 2.45 (s, 2H), 1.65 (s, 9H), 1.17 (s, 6H).

$^{13}\text{C NMR}$ (151 MHz, CDCl_3) δ [ppm] = 168.5, 149.7, 138.4, 128.9, 126.7, 126.6, 124.8, 122.2, 120.8, 118.0, 114.7, 113.8, 83.2, 45.0, 37.2, 29.8, 27.2, 27.1, 20.4.

HRMS-ESI: calcd. for $\text{C}_{22}\text{H}_{26}\text{N}_2\text{O}_3\text{Na}$ $[\text{M} + \text{Na}]^+$: 389.1835; found: 389.1842.

FT-IR: ν [cm^{-1}] = 2969, 2933, 1732, 1672, 1451, 1369, 1307, 1149, 748.

3-Hydroxy-2,2-dimethyl-2,6,7,12-tetrahydroindolo[2,3-*a*]quinolizine-4(3*H*)-one (2.62a)



To a solution of enamide **2.58a** (136 mg, 0.511 mmol, 1.0 equiv.) in THF (5.0 mL) was added *t*BuLi (1.9 M in hexane, 1.08 mL, 2.04 mmol, 4.0 equiv.) dropwise at $-78\text{ }^{\circ}\text{C}$. After the resultant mixture was stirred at $-78\text{ }^{\circ}\text{C}$ for 1 h, P(OMe)₃ (44.8 μL , 0.379 mmol, 1.0 equiv.) was added. O₂ (balloon pressure) was bubbled through the mixture for 20 min, and the mixture was stirred for additional 2 h under O₂ atmosphere (the generation of the product was monitored by TLC). Then the reaction was quenched with NaHCO₃ (sat. aq.). The aqueous phase was extracted with DCM. The combined organic phases were washed with brine, dried over MgSO₄, filtered and the solvent was removed under reduced pressure. The crude product was purified by silica gel column chromatography (pentane/EtOAc = 5:1) to afford α -hydroxyenamide **2.62a** (120 mg, 0.439 mmol, 86%) as a light yellow solid.

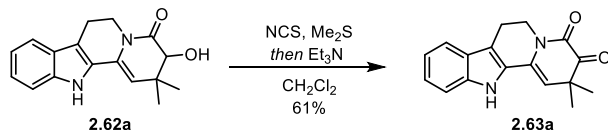
¹H NMR (700 MHz, *d*₆-acetone) δ [ppm] = 10.37 (s, 1H), 7.52–7.50 (m, 1H), 7.36 (dt, *J* = 8.1, 0.9 Hz, 1H), 7.16 (ddd, *J* = 8.2, 7.0, 1.1 Hz, 1H), 7.04 (ddd, *J* = 7.9, 7.0, 1.0 Hz, 1H), 5.67 (s, 1H), 4.80 (dddd, *J* = 12.7, 5.5, 1.9, 0.6 Hz, 1H), 4.05 (d, *J* = 2.8 Hz, 1H), 4.01 (td, *J* = 3.1, 0.9 Hz, 1H), 3.28 (dddd, *J* = 12.9, 12.2, 4.4, 1.0 Hz, 1H), 3.00 (ddd, *J* = 15.8, 4.5, 1.9 Hz, 1H), 2.90–2.85 (m, 1H), 1.24 (s, 3H), 0.95 (s, 3H).

¹³C NMR (176 MHz, *d*₆-acetone) δ [ppm] = 172.1, 138.7, 129.0, 128.7, 127.5, 124.1, 120.4, 119.7, 112.2, 112.1, 111.1, 75.5, 41.1, 35.9, 26.7, 21.2, 20.2.

HRMS-ESI: calcd. for C₁₇H₁₈N₂O₂Na [M + Na]⁺: 305.1260; found: 305.1275.

FT-IR: ν [cm⁻¹] = 3322, 2963, 2926, 1649, 1450, 1392, 1359, 1229, 1154, 1040, 919, 742.

2,2-Dimethyl-2,6,7,12-tetrahydroindolo[2,3-*a*]quinolizine-3,4-dione (**2.63a**)



To a solution of NCS (218 mg, 1.63 mmol, 5.0 equiv.) in DCM (5.0 mL) at 0 $^{\circ}\text{C}$ was added Me₂S (599 μL , 8.15 mmol, 25 equiv.) and the mixture was stirred at $-78\text{ }^{\circ}\text{C}$ for 1 h. The solution of α -hydroxyenamide **2.62a** (92.0 mg, 0.326 mmol, 1.0 equiv.) in DCM (5.0 mL) was added dropwise. The resulting mixture was stirred at $-78\text{ }^{\circ}\text{C}$ for another 2 h before Et₃N (905 μL , 6.52 mmol, 20 equiv.) was added. Then the mixture was stirred at $-78\text{ }^{\circ}\text{C}$ for 2 h. The mixture was quenched with NH₄Cl (sat. aq.) and extracted with DCM. The combined organic phases

were washed with brine, dried over MgSO₄, filtered and concentrated under reduced pressure. The crude product was purified by silica gel column chromatography (pentane/EtOAc = 3:2) to afford α -ketoenamide **2.63a** (56.0 mg, 0.200 mmol, 61%) as a yellow solid.

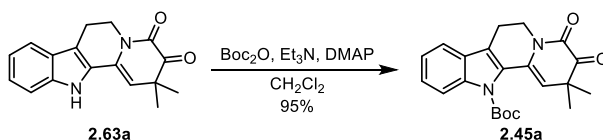
¹H NMR (700 MHz, CDCl₃) δ [ppm] = 8.08 (s, 1H), 7.55–7.53 (m, 1H), 7.36 (dt, J = 8.2, 0.9 Hz, 1H), 7.28–7.26 (m, 1H), 7.15 (ddd, J = 7.9, 7.0, 1.0 Hz, 1H), 5.38 (s, 1H), 4.22 (t, J = 6.0 Hz, 2H), 3.03 (t, J = 6.1 Hz, 2H), 1.40 (s, 6H).

¹³C NMR (176 MHz, CDCl₃) δ [ppm] = 195.8, 157.3, 137.6, 127.0, 126.9, 126.6, 124.4, 120.6, 119.4, 113.1, 111.3, 107.0, 45.0, 40.5, 25.0, 20.4.

HRMS-ESI: calcd. for C₁₇H₁₆N₂O₂Na [M + Na]⁺: 303.1104; found: 303.1116.

FT-IR: ν [cm⁻¹] = 3332, 3319, 2974, 2925, 1732, 1656, 1453, 1402, 1381, 1237, 1064, 745.

***Tert*-butyl 2,2-dimethyl-3,4-dioxo-3,4,6,7-tetrahydroindolo[2,3-*a*]quinolizine-12(2H)-carboxylate (2.45a)**



To a solution of α -ketoenamide **2.63a** (46.0 mg, 0.164 mmol, 1.0 equiv.) in THF (5.0 mL) was added Et₃N (57.0 μ L, 0.411 mmol, 2.5 equiv.), 4-DMAP (5.0 mg, 41.0 μ mol, 0.25 equiv.) and Boc₂O (53.7 mg, 0.245 mmol, 1.5 equiv.) subsequently. The resulting mixture was stirred at room temperature overnight before the reaction mixture was quenched with NaHCO₃ (sat. aq.). The mixture was extracted with DCM. The combined organic phases were washed with brine, dried over MgSO₄, filtered and concentrated under reduced pressure. The crude product was purified by silica gel column chromatography (pentane/EtOAc = 10:1) to afford α -ketoenamide **2.45a** (55.0 mg, 0.156 mmol, 95%) as a white solid.

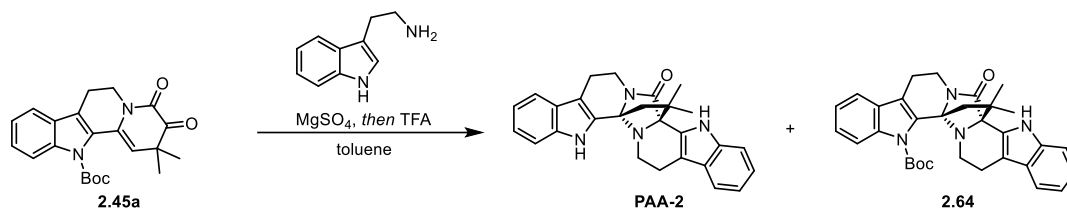
¹H NMR (500 MHz, CDCl₃) δ [ppm] = 7.98 (dt, J = 8.5, 0.8 Hz, 1H), 7.51–7.46 (m, 1H), 7.37 (ddd, J = 8.4, 7.2, 1.3 Hz, 1H), 7.28 (dd, J = 7.5, 1.0 Hz, 1H), 5.34 (s, 1H), 4.21 (t, J = 5.7 Hz, 2H), 2.95 (t, J = 5.7 Hz, 2H), 1.66 (s, 9H), 1.39 (s, 6H).

¹³C NMR (126 MHz, CDCl₃) δ [ppm] = 195.6, 156.5, 150.4, 139.6, 129.1, 127.4, 126.5, 125.6, 123.5, 122.7, 119.3, 115.2, 113.0, 84.7, 45.3, 39.6, 28.2, 25.0, 21.1.

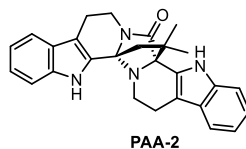
HRMS-ESI: calcd. for C₂₂H₂₄N₂O₄Na [M + Na]⁺: 403.1628; found: 403.1647.

FT-IR: ν [cm^{-1}] = 2977, 2929, 1726, 1668, 1456, 1414, 1368, 1307, 1224, 1158, 1050, 751.

9,9'-Didemethoxy-peganumine A (PAA-2) and 12'-tert-butyl 9,9'-didemethoxy-peganumine A (2.64)



A mixture of α -ketoamide **2.45a** (33.0 mg, 86.0 μmol , 1.0 equiv.), tryptamine (13.8 mg, 86.0 μmol , 1.0 equiv.) and MgSO_4 (104 mg, 0.864 mmol, 10 equiv.) in toluene (5.0 mL) was heated to 115 $^\circ\text{C}$ (oil bath temperature) overnight. The reaction mixture was cooled to room temperature and TFA (1.3 μL , 17 μmol , 0.2 equiv.) were added. The mixture was then heated to reflux for 2 d, before the reaction was quenched with NaHCO_3 (sat. aq.). The aqueous phase was extracted with DCM. The combined organic phases were washed with brine, dried over MgSO_4 , filtered and concentrated under reduced pressure. The crude product was purified by silica gel column chromatography (pentane/EtOAc = 2:1) to afford **PAA-2** (3.6 mg, 8.5 μmol , 10%) as a light yellow solid and **2.64** (16.0 mg, 31.4 μmol , 36%) as a white solid.

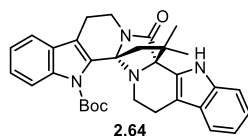


^1H NMR (500 MHz, d_6 -DMSO) δ [ppm] = 11.44 (s, 1H), 10.97 (s, 1H), 7.52 (d, J = 7.9 Hz, 1H), 7.44–7.35 (m, 3H), 7.15 (ddd, J = 8.2, 7.0, 1.2 Hz, 1H), 7.10–7.02 (m, 2H), 6.99–6.94 (m, 1H), 4.04 (dd, J = 12.9, 5.8 Hz, 1H), 3.16–3.10 (m, 1H), 2.96 (dd, J = 15.2, 4.3 Hz, 1H), 2.81–2.68 (m, 3H), 2.48–2.46 (m, 1H), 2.41–2.32 (m, 2H), 1.93 (d, J = 11.2 Hz, 1H), 1.41 (s, 3H), 1.16 (s, 3H).

^{13}C NMR (126 MHz, d_6 -DMSO) δ [ppm] = 171.7, 137.3, 137.3, 129.2, 127.7, 126.5, 126.4, 122.5, 121.3, 119.7, 119.4, 118.9, 118.2, 112.1, 112.0, 111.7, 110.1, 79.3, 78.0, 50.9, 40.6, 40.4, 36.1, 27.3, 26.5, 21.5, 21.4.

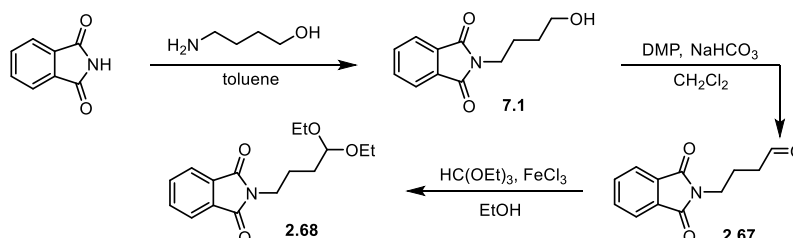
HRMS-ESI: calcd. for $\text{C}_{27}\text{H}_{26}\text{N}_4\text{ONa}$ [$\text{M} + \text{Na}$] $^+$: 445.1999; found: 445.2000.

FT-IR: ν [cm^{-1}] = 3307, 3267, 2922, 2857, 1704, 1451, 1410, 1320, 1270, 1146, 1039, 742.



¹H NMR (700 MHz, CDCl₃) δ [ppm] = 8.20 (s, 1H), 7.93 (dt, *J* = 8.5, 0.9 Hz, 1H), 7.51 (ddd, *J* = 7.8, 1.3, 0.7 Hz, 1H), 7.47–7.45 (m, 1H), 7.39 (dt, *J* = 8.2, 0.9 Hz, 1H), 7.37 (ddd, *J* = 8.5, 7.2, 1.3 Hz, 1H), 7.16 (ddd, *J* = 8.2, 7.1, 1.2 Hz, 1H), 7.08 (ddd, *J* = 8.0, 7.1, 1.0 Hz, 1H), 4.21 (ddd, *J* = 13.0, 6.5, 1.0 Hz, 1H), 3.14 (ddd, *J* = 13.0, 11.7, 4.8 Hz, 1H), 3.09 (d, *J* = 11.2 Hz, 1H), 2.99 (ddd, *J* = 15.9, 4.8, 1.0 Hz, 1H), 2.93–2.84 (m, 2H), 2.72 (ddd, *J* = 14.8, 3.8, 1.5 Hz, 1H), 2.64 (ddd, *J* = 10.6, 5.5, 1.5 Hz, 1H), 2.53 (ddd, *J* = 11.5, 10.7, 3.8 Hz, 1H), 1.72 (d, *J* = 11.1 Hz, 1H), 1.71 (s, 9H), 1.41 (s, 3H), 1.26 (s, 3H).

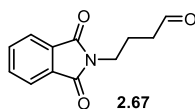
HRMS-ESI: calcd. for C₃₂H₃₄N₄O₃K [M + K]⁺: 561.2263; found: 561.2289.



Scheme 7-1: Synthesis of phthalimide derivatives.

The alcohol **7.1** was prepared according to the procedure of Walczyński et al.^[356]

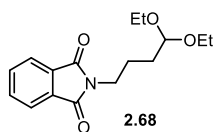
4-(1,3-Dioxisoindolin-2-yl)butanal (**2.67**)



To a solution of the alcohol **7.1** (2.6 g, 11.9 mmol, 1.0 equiv.) in DCM (100 mL) was added NaHCO₃ (4.98 g, 59.4 mmol, 5.0 equiv.) and DMP (7.50 g, 17.8 mmol, 1.5 equiv.) at 0 °C. The mixture was allowed to warm to room temperature and stirred for 3 h, before the reaction was quenched with Na₂S₂O₃ (sat. aq.). The aqueous phase was extracted with DCM. The combined organic phases were washed with brine, dried over MgSO₄, filtered and concentrated under reduced pressure. The crude product was purified by silica gel column chromatography (pentane/EtOAc = 10:1) to afford aldehyde **2.67** (2.3 g, 10.7 mmol, 90%) as a light yellow solid.

¹H NMR (400 MHz, CDCl₃) δ [ppm] = 9.77 (s, 1H), 7.85 (dd, *J* = 5.4, 3.1 Hz, 2H), 7.72 (dd, *J* = 5.5, 3.0 Hz, 2H), 3.74 (t, *J* = 6.8 Hz, 2H), 2.54 (td, *J* = 7.3, 1.2 Hz, 2H), 2.05–1.98 (m, 2H).

FT-IR: ν [cm⁻¹] = 2941, 1769, 1701, 1395, 1362, 1188, 1170, 1116, 1031, 880, 718.

2-(4,4-Diethoxybutyl)isoindoline-1,3-dione (2.68)

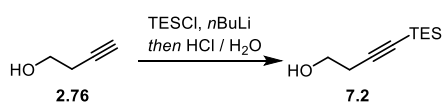
To a solution of aldehyde **2.67** (200 mg, 0.920 mmol, 1.0 equiv.) in EtOH (2.0 mL) was added FeCl₃ (5.0 mg, 31 μmol, 3.3 mol%) and ethyl orthoformate (180 μL, 1.06 mmol, 1.2 equiv.) dropwise. The mixture was heated to reflux for 2.5 h, before concentrated under reduced pressure. The crude product was purified by silica gel column chromatography (pentane/EtOAc = 20:1) to afford acetal **2.68** (112 mg, 0.386 mmol, 42%) as a light yellow solid.

¹H NMR (400 MHz, CDCl₃) δ [ppm] = 7.83 (ddd, *J* = 5.5, 3.0, 1.4 Hz, 2H), 7.74–7.67 (m, 2H), 4.50 (td, *J* = 5.6, 1.3 Hz, 1H), 3.70 (td, *J* = 7.1, 1.4 Hz, 2H), 3.67–3.56 (m, 2H), 3.51–3.43 (m, 2H), 1.84–1.71 (m, 2H), 1.65 (dddd, *J* = 9.9, 5.6, 4.0, 1.5 Hz, 2H), 1.18 (td, *J* = 7.1, 1.3 Hz, 6H).

¹³C NMR (101 MHz, CDCl₃) δ [ppm] = 168.5, 134.0, 132.3, 123.3, 102.5, 61.4, 37.9, 31.1, 24.1, 15.4.

HRMS-ESI: calcd. for C₁₆H₂₁NO₄Na [M + Na]⁺: 314.1363; found: 314.1370.

FT-IR: ν [cm⁻¹] = 2974, 2932, 1770, 1706, 1439, 1395, 1370, 1362, 1115, 1044, 719.

4-(Triethylsilyl)but-3-yn-1-ol (7.2)

To a solution of 3-butyn-1-ol (2.00 g, 28.5 mmol, 1.0 equiv.) in THF (50 mL) was added *n*BuLi (2.5 M in hexane, 25.0 mL, 62.7 mmol, 2.2 equiv.) at –78 °C. The mixture was stirred for 30 min, before the addition of TESCl (14.3 mL, 85.5 mmol, 3.0 equiv.) at –78 °C. The resulting mixture was allowed to warm to room temperature and stirred for 1 d. Then HCl (1 M aq. 50 mL) was added dropwise and the reaction mixture was stirred for another 2 d. The aqueous phase was extracted with DCM. The combined organic phases were washed with brine, dried over MgSO₄, filtered and concentrated under reduced pressure. The crude product was purified by silica gel column chromatography (pentane/EtOAc = 10:1) to afford **7.2** (2.65 g, 10.7 mmol, 90%) as a colorless liquid.

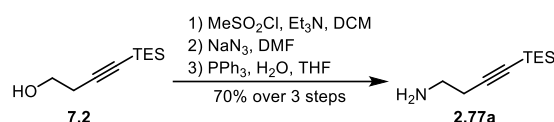
¹H NMR (400 MHz, CDCl₃) δ [ppm] = 3.72 (td, *J* = 6.2, 0.5 Hz, 2H), 2.52 (t, *J* = 6.2 Hz, 2H), 1.74 (s, 1H), 1.03–0.94 (m, 9H), 0.61–0.57(m, 6H).

¹³C NMR (101 MHz, CDCl₃) δ [ppm] = 104.5, 83.9, 61.0, 24.2, 7.4, 4.4.

HRMS-ESI: calcd. for C₁₀H₂₁OSi [M + H]⁺: 185.1356; found: 185.1547.

FT-IR: ν [cm⁻¹] = 3321, 2954, 2875, 2174, 1459, 1414, 1237, 1052, 1029, 1016, 973, 722.

4-(Triethylsilyl)but-3-yn-1-amine (**2.77a**)



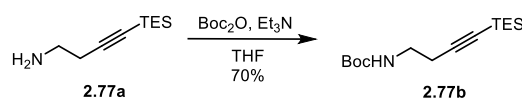
To a solution of **7.2** (1.50 g, 8.15 mmol, 1.0 equiv.) in DCM (25 mL) was added Et₃N (2.26 mL, 16.3 mmol, 2.0 equiv.). After the addition of MeSO₂Cl (630 μL, 8.15 mmol, 1.0 equiv.) at 0 °C, the resulting mixture was stirred at room temperature overnight. The mixture was quenched with NH₄Cl (sat. aq.) and extracted with DCM. The combined organic phases were washed with brine, dried over MgSO₄, filtered and concentrated under reduced pressure. The crude product was dissolved in DMF (50 mL). Then NaN₃ (596 mg, 9.18 mmol, 1.1 equiv.) was added to that solution by portions at 0 °C. The resulting mixture was stirred at room temperature overnight. The mixture was quenched with NH₄Cl (sat. aq.) and extracted with DCM. The combined organic phases were washed with brine, dried over MgSO₄, filtered and concentrated under reduced pressure. The crude product was dissolved in THF (35 mL). The solution was added H₂O (0.710 mL) and Ph₃P (2.35 g, 8.96 mmol, 1.1 equiv.). The resulting mixture was stirred at room temperature overnight. After removing the solvent, the crude product was purified by Kugelrohr distillation to afford **2.77a** (1.05 g, 5.70 mmol, 70% over 3 steps) as a colorless liquid.

¹H NMR (400 MHz, CDCl₃) δ [ppm] = 2.83 (t, *J* = 6.3 Hz, 2H), 2.38 (t, *J* = 6.3 Hz, 2H), 1.41 (s, 2H), 0.98 (t, *J* = 7.9 Hz, 9H), 0.58 (q, *J* = 8.0 Hz, 6H).

¹³C NMR (101 MHz, CDCl₃) δ [ppm] = 106.4, 83.7, 41.5, 25.4, 7.8, 4.8.

HRMS-ESI: calcd. for C₁₀H₂₂NSi [M + H]⁺: 184.1516; found: 184.1524.

FT-IR: ν [cm⁻¹] = 2953, 2874, 2169, 1459, 1236, 1016, 722.

Tert-butyl (4-(triethylsilyl)but-3-yn-1-yl)carbamate (2.77b)

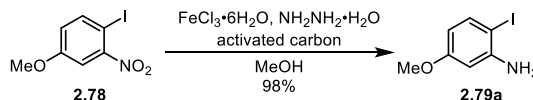
To a solution of amine **2.77a** (200 mg, 1.37 mmol, 1.0 equiv.) in THF (5.0 mL) was added Et_3N (340 μL , 2.47 mmol, 1.8 equiv.) and Boc_2O (328 mg, 1.50 mmol, 1.1 equiv.) subsequently. The resulting mixture was stirred at room temperature overnight, before the reaction mixture was quenched with NaHCO_3 (sat. aq.). The mixture was extracted with DCM. The combined organic phases were washed with brine, dried over MgSO_4 , filtered and concentrated under reduced pressure. The crude product was purified by silica gel column chromatography (pentane/ EtOAc = 10:1) to afford amine **2.77b** (271 mg, 0.959 mmol, 70%) as a colorless liquid.

$^1\text{H NMR}$ (500 MHz, CDCl_3) δ [ppm] = 4.82 (s, 1H), 3.25 (q, J = 6.5 Hz, 2H), 2.42 (t, J = 6.6 Hz, 2H), 1.43 (s, 9H), 0.97 (t, J = 7.9 Hz, 9H), 0.56 (q, J = 7.9 Hz, 6H).

$^{13}\text{C NMR}$ (126 MHz, CDCl_3) δ [ppm] = 155.8, 105.3, 83.7, 79.4, 39.6, 28.5, 21.4, 7.6, 4.6.

HRMS-ESI: calcd. for $\text{C}_{15}\text{H}_{29}\text{NO}_2\text{SiNa}$ [$\text{M} + \text{Na}$] $^+$: 306.1860; found: 306.1852.

FT-IR: ν [cm^{-1}] = 2954, 2875, 2173, 1695, 1506, 1365, 1249, 1168, 723.

2-Iodo-5-methoxyaniline (2.79a)

To a solution of 1-iodo-4-methoxy-2-nitrobenzene **2.78** (500 mg, 1.79 mmol, 1.0 equiv.) in MeOH (8.0 mL) was added $\text{FeCl}_3 \cdot 6\text{H}_2\text{O}$ (23.0 mg, 85.2 μmol , 5 mol%), activated carbon (20 mg, 1.67 mmol, 0.9 equiv.) and $\text{NH}_2\text{NH}_2 \cdot \text{H}_2\text{O}$ (180 μL , 3.58 mmol, 2.0 equiv.) subsequently. The resulting mixture was heated to reflux for 3 h, before the reaction mixture was cooled to room temperature and filtered through a silica gel pad. The solvent was removed under reduced pressure to afford **2.79a** (435 mg, 1.75 mmol, 98%) as a colorless liquid.

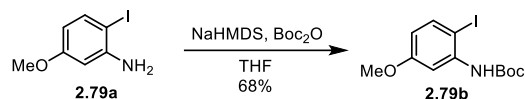
$^1\text{H NMR}$ (400 MHz, CDCl_3) δ [ppm] = 7.48 (d, J = 8.7 Hz, 1H), 6.33 (d, J = 2.8 Hz, 1H), 6.14 (dd, J = 8.7, 2.8 Hz, 1H), 4.07 (s, 2H), 3.74 (s, 3H).

$^{13}\text{C NMR}$ (101 MHz, CDCl_3) δ [ppm] = 161.2, 147.7, 139.3, 106.7, 100.6, 73.6, 55.4.

HRMS-ESI: calcd. for $\text{C}_7\text{H}_9\text{INO}$ [$\text{M} + \text{H}$] $^+$: 249.9724; found: 249.9714.

FT-IR: ν [cm^{-1}] = 3442, 3359, 2928, 1608, 1463, 1295, 1258, 1039, 1002, 823.

***Tert*-butyl (2-iodo-5-methoxyphenyl)carbamate (**2.79b**)**



To a solution of **2.79a** (150 mg, 600 μmol , 1.0 equiv.) in THF (5.0 mL) was added NaHMDS (2.0 M in THF, 660 μL , 1.32 mmol, 2.2 equiv.) at 0 °C. The mixture was stirred at 0 °C for 30 min, before the addition of Boc_2O (124 mg, 570 μmol , 0.95 equiv.) subsequently. The resulting mixture was stirred at room temperature for 2 h, before the reaction mixture was quenched with NaHCO_3 (sat. aq.). The mixture was extracted with DCM. The combined organic phases were washed with brine, dried over MgSO_4 , filtered and concentrated under reduced pressure. The crude product was purified by silica gel column chromatography (pentane/EtOAc = 50:1) to afford **2.79b** (141 mg, 0.408 mmol, 68%) as a colorless liquid.

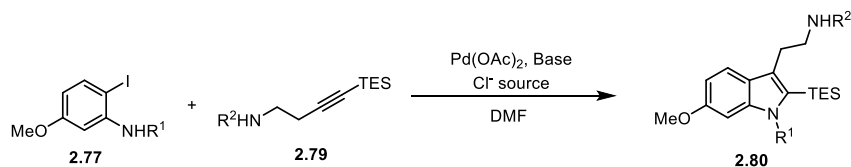
^1H NMR (500 MHz, CDCl_3) δ [ppm] = 7.77 (d, J = 3.0 Hz, 1H), 7.52 (d, J = 8.7 Hz, 1H), 6.82 (s, 1H), 6.36 (dd, J = 8.7, 2.9 Hz, 1H), 3.76 (s, 3H), 1.52 (s, 9H).

^{13}C NMR (126 MHz, CDCl_3) δ [ppm] = 160.6, 152.3, 139.6, 138.6, 111.5, 105.3, 80.9, 76.7, 55.3, 28.3.

HRMS-ESI: calcd. for $\text{C}_{12}\text{H}_{16}\text{INO}_3\text{Na}$ [$\text{M} + \text{Na}$] $^+$: 372.0067; found: 372.0065.

FT-IR: ν [cm^{-1}] = 3392, 2976, 1731, 1578, 1514, 1452, 1151, 1047, 867.

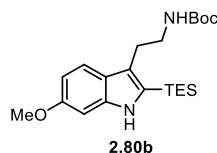
General procedure A



To a solution of $\text{Pd}(\text{OAc})_2$ (20 mol%), Cl^- salt (1.0 equiv.) in DMF was added base (3.0 equiv.) and Ph_3P (0.4 equiv.). Then a solution of iodide **2.77** (1.0 equiv.) in DMF and a solution of amine (2.0 equiv.) in DMF were added to the mixture subsequently. The resulting mixture was degassed before putting to a pre-heated 80 °C oil bath. After stirring at 80 °C for 3 d, the reaction mixture was diluted with H_2O and EtOAc. After washing by brine for three times, the organic

phase was dried over MgSO_4 , and concentrated under reduced pressure. The crude product was purified by silica gel column chromatography.

***Tert*-butyl (2-(6-methoxy-2-(triethylsilyl)-1*H*-indol-3-yl)ethyl)carbamate (**2.80b**)**



2.80b was prepared according to **General procedure A**, starting from $\text{Pd}(\text{OAc})_2$ (4.0 mg, 18 μmol , 20 mol%), TEACl (30.5 mg, 0.184 mmol, 1.0 equiv.) in DMF (1.0 mL) was added DIPEA (46 μL , 0.276 mmol, 3.0 equiv.) and Ph_3P (9.6 mg, 37 μmol , 0.4 equiv.). Then a solution of iodide **2.77a** (23 mg, 92 μmol , 1.0 equiv.) in DMF (0.5 mL) and a solution of amine **2.79b** (46 μL , 0.276 mmol, 2.0 equiv.) in DMF (0.5 mL). Purification by silica gel column chromatography (pentane/EtOAc = 10:1) afforded **2.80b** (18.9 mg, 46.9 μmol , 51%) as a light brown liquid.

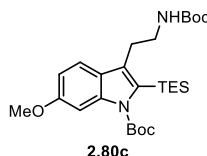
^1H NMR (400 MHz, CDCl_3) δ [ppm] = 7.81 (s, 1H), 7.50 (d, J = 8.7 Hz, 1H), 6.86 (d, J = 2.2 Hz, 1H), 6.80–6.74 (m, 1H), 4.57 (s, 1H), 3.84 (s, 3H), 3.44 (d, J = 6.3 Hz, 2H), 2.97 (t, J = 6.9 Hz, 2H), 1.44 (s, 9H), 1.02–0.97 (m, 9H), 0.88 (td, J = 7.4, 1.2 Hz, 6H).

^{13}C NMR (126 MHz, CDCl_3) δ [ppm] = 156.7, 156.1, 137.2, 121.9, 120.8, 119.5, 113.2, 109.5, 94.8, 79.2, 55.8, 40.9, 28.5, 25.9, 22.8, 14.2.

HRMS-ESI: calcd. for $\text{C}_{22}\text{H}_{36}\text{N}_2\text{O}_3\text{SiNa}$ $[\text{M} + \text{Na}]^+$: 427.2387; found: 427.2367.

FT-IR: ν [cm^{-1}] = 3402, 3342, 2924, 2852, 1687, 1628, 1503, 1457, 1256, 1159, 1028.

***Tert*-butyl 3-(2-((*tert*-butoxycarbonyl)amino)ethyl)-6-methoxy-2-(triethylsilyl)-1*H*-indole-1-carboxylate (**2.80c**)**



2.80c was prepared according to **General procedure A**, starting from $\text{Pd}(\text{OAc})_2$ (55.8 mg, 0.248 mmol, 20 mol%), TEACl (206 mg, 1.24 mmol, 1.0 equiv.) in DMF (10 mL) was added DIPEA (610 μL , 3.68 mmol, 3.0 equiv.) and Ph_3P (130 mg, 0.490 mmol, 0.4 equiv.). Then a solution of iodide **2.77b** (432 mg, 1.24 mmol, 1.0 equiv.) in DMF (5.0 mL) and a solution of

amine **2.79b** (700 mg, 2.45 mmol, 2.0 equiv.) in DMF (5.0 mL). Purification by silica gel column chromatography (pentane/EtOAc = 10:1) afforded **2.80c** (391 mg, 0.777 mmol, 96%) as a brown liquid.

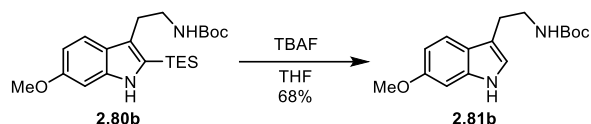
¹H NMR (500 MHz, CDCl₃) δ [ppm] = 7.54 (d, *J* = 2.3 Hz, 1H), 7.48 (d, *J* = 8.7 Hz, 1H), 6.86 (dd, *J* = 8.6, 2.3 Hz, 1H), 4.61 (s, 1H), 3.86 (s, 3H), 3.37 (d, *J* = 6.8 Hz, 2H), 3.00 (t, *J* = 7.1 Hz, 2H), 1.71 (s, 9H), 1.45 (s, 9H), 0.97–0.91 (m, 15H).

¹³C NMR (126 MHz, CDCl₃) δ [ppm] = 158.2, 155.9, 151.5, 138.6, 133.3, 130.8, 125.8, 119.7, 111.4, 99.8, 83.5, 79.2, 55.6, 41.6, 28.5, 28.3, 26.2, 8.2, 5.7.

HRMS-ESI: calcd. for C₂₇H₄₄N₂O₅SiNa [M + Na]⁺: 527.2911; found: 527.2894.

FT-IR: ν [cm⁻¹] = 3014, 2924, 1737, 1437, 1365, 1228, 1217, 770, 701.

***Tert*-butyl (2-(6-methoxy-1*H*-indol-3-yl)ethyl)carbamate (**2.81b**)**



To a solution of **2.80b** (20.0 mg, 49.5 μmol, 1.0 equiv.) in THF (2.0 mL) was added TBAF (1.0 M in THF, 495 μL, 495 μmol, 10 equiv.) and stirred at room temperature for 5 h. After removing the solvent, the crude product was purified by silica gel column chromatography (pentane/EtOAc = 5:1) to afford **2.81b** (9.8 mg, 34 μmol, 68%) as a yellow solid.

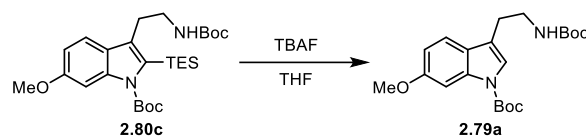
¹H NMR (500 MHz, CDCl₃) δ [ppm] = 8.00 (s, 1H), 7.46 (d, *J* = 8.6 Hz, 1H), 6.91 (s, 1H), 6.86 (d, *J* = 2.2 Hz, 1H), 6.79 (dd, *J* = 8.6, 2.1 Hz, 1H), 4.63 (s, 1H), 3.84 (s, 3H), 3.45 (d, *J* = 6.6 Hz, 2H), 2.91 (t, *J* = 6.9 Hz, 2H), 1.44 (s, 9H).

¹³C NMR (126 MHz, CDCl₃) δ [ppm] = 156.7, 156.1, 137.2, 121.9, 120.8, 119.5, 113.2, 109.5, 94.8, 79.2, 55.8, 40.9, 28.5, 25.9.

HRMS-ESI: calcd. for C₁₆H₂₂N₂O₃Na [M + Na]⁺: 313.1522; found: 313.1518.

FT-IR: ν [cm⁻¹] = 3168, 2976, 2933, 1728, 1618, 1489, 1444, 1384, 1368, 1253, 1161, 1091, 852, 811, 768.

***Tert*-butyl 3-(2-((*tert*-butoxycarbonyl)amino)ethyl)-6-methoxy-1*H*-indole-1-carboxylate (2.79a)**



To a solution of **2.80c** (300 mg, 0.595 mmol, 1.0 equiv.) in THF (50 mL) was added TBAF (1.0 M in THF, 5.95 mL, 5.95 mmol, 10 equiv.) and stirred at room temperature for 5 h. After removing the solvent, the crude product was purified by silica gel column chromatography (pentane/EtOAc = 5:1) to afford **2.79a** (174 mg, 0.446 mmol, 75%) as a yellow solid.

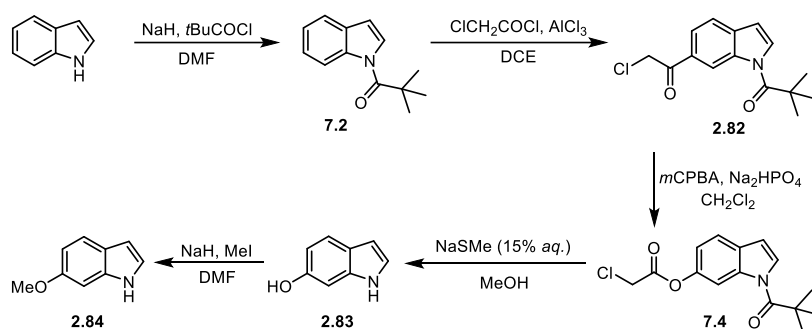
¹H NMR (700 MHz, CDCl₃) δ [ppm] = 7.73 (s, 1H), 7.39 (d, *J* = 8.5 Hz, 1H), 7.29 (s, 1H), 6.87 (dd, *J* = 8.6, 2.4 Hz, 1H), 4.63 (s, 1H), 3.87 (s, 3H), 3.44 (q, *J* = 6.6 Hz, 2H), 2.96–2.76 (m, 2H), 1.66 (s, 9H), 1.44 (s, 9H).

¹³C NMR (176 MHz, CDCl₃) δ [ppm] = 158.1, 156.0, 149.9, 136.7, 124.3, 121.9, 119.6, 117.9, 112.0, 99.6, 83.5, 79.4, 55.8, 40.4, 28.6, 28.4, 25.8.

HRMS-ESI: calcd. for C₂₁H₃₀N₂O₅Na [M + Na]⁺: 413.2047; found: 413.2047.

FT-IR: ν [cm⁻¹] = 2976, 2930, 1711, 1382, 1366, 1251, 1226, 1157, 1092, 755.

6-Methoxyindole (2.84)

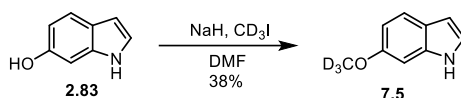


Scheme 7-2: Indole functionalization.

The preparation was according to the procedure of Teranishi et al.^[215] The pivaloylation was started from indole (30.0 g, 256 mmol) to afford **7.2** (45.0 g, 224 mmol, 87%). The chloroacetylation was from **7.2** (20.0 g, 99.4 mmol) to yield **2.82** (13.0 g, 46.9 mmol, 47%). The Baeyer–Villiger oxidation of **2.82** (13.0 g, 46.9 mmol, 47%) resulted in **7.4** (8.60 g, 29.4 mmol, 62%). The deprotection of **7.4** (8.60 g, 29.4 mmol) afforded 6-hydroxyindole (3.7 g,

27.8 mmol, 95%). The methylation was started from 6-hydroxyindole (520 mg, 3.91 mmol) to yield 6-methoxyindole (320 mg, 2.18 mmol, 56%). The spectroscopic data are in agreement with the literature.

6-(methoxy-*d*₃)-indole (7.5)



The 6-(methoxy-*d*₃)-indole was prepared from 6-hydroxyindole (200 mg, 1.50 mmol) to afford **7.5** (86.0 mg, 0.573 mmol, 38%).

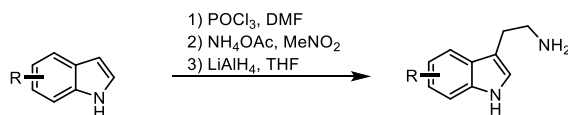
¹H NMR (500 MHz, CDCl₃) δ [ppm] = 7.99 (s, 1H), 7.57 (d, *J* = 8.6 Hz, 1H), 7.08 (t, *J* = 2.8 Hz, 1H), 6.87 (dd, *J* = 8.6, 2.3 Hz, 1H), 6.83 (d, *J* = 2.3 Hz, 1H), 6.53 (t, *J* = 2.7 Hz, 1H).

¹³C NMR (176 MHz, CDCl₃) δ [ppm] = 156.5, 136.7, 123.3, 122.3, 121.4, 110.1, 102.5, 94.7, 55.4–54.6 (m).

HRMS-ESI: calcd. for C₉H₆D₃NO [M + Na]⁺: 173.0764; found: 173.0766.

FT-IR: ν [cm⁻¹] = 3393, 3006, 2833, 1620, 1503, 1454, 1244, 1160, 1025, 811.

General procedure B

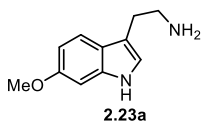


Vilsmeier–Haack reaction: To a dried Schlenk flask with DMF, was added POCl₃ (3.0 equiv.) dropwise at 0 °C. After the mixture was stirred for 30 min, a solution of corresponding indole (1.0 equiv.) in DMF was added to the reaction mixture dropwise. The resulting mixture was allowed to stir at room temperature for another 2 h. Then the reaction mixture was poured to a flask with ice, and carefully neutralized by NaHCO₃ (sat. aq.) until pH = 7–8. The suspension was left to rest overnight at room temperature, filtered, collected the solid and dried under reduced pressure. This crude product was used without further purification.

Henry reaction: A flask with NH₄OAc (3.0 equiv.) and corresponding aldehyde (1.0 equiv.) was added MeNO₂ (75 equiv.) and the reaction mixture was stirred at 115 °C for 2 h. After allowing the mixture to cool down to room temperature, the reaction mixture was diluted with water and DCM, and the organic phase was separated. The aqueous phase was extracted with DCM. The combined organic layers were washed with brine, dried over MgSO₄, filtered and concentrated

under reduced pressure to afford the crude product which was used directly without purification. Reduction: To a Schlenk flash charged with solid LiAlH₄ (6.0 equiv.) was added THF carefully at 0 °C. Then a solution of the crude product of the Henry reaction in THF was added dropwise. The resulting reaction mixture was replaced with an oil bath and heated to 65 °C for 3 h, then cooled down to 0 °C. Excess LiAlH₄ was quenched with the drop-wise addition of NaOH (sat. aq.) and H₂O. The suspension was allowed to warm to room temperature overnight and then filtered through a plug of Celite[®]. The organic phase was separated. The aqueous phase was extracted with DCM and the combined organic layers were washed with brine, dried over MgSO₄, filtered and concentrated under reduced pressure. The crude product was purified by silica gel column chromatography.

2-(6-Methoxy-1*H*-indol-3-yl)ethan-1-amine (**2.23a**)



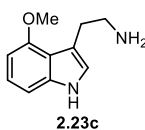
2.23a was prepared according to **General procedure B**, starting from 6-methoxy-1*H*-indole (530 mg, 3.60 mmol, 1.0 equiv.) and POCl₃ (1.01 mL, 10.8 mmol, 3.0 equiv.) in DMF (3.0 mL). The reaction mixture was subsequently treated with NH₄OAc (833 mg, 10.8 mmol, 3.0 equiv.), MeNO₂ (14.5 mL, 270 mmol, 75 equiv.) and LiAlH₄ (821 mg, 10.8 mmol, 6.0 equiv.) in THF (25 mL). Purification by silica gel column chromatography (DCM/MeOH/TEA = 80:20:5) afforded **2.23a** (270 mg, 1.42 mmol, 39%) as a light brown solid.

¹H NMR (500 MHz, CD₃OD) δ [ppm] = 7.37 (d, *J* = 8.6 Hz, 1H), 6.91 (s, 1H), 6.87 (d, *J* = 2.3 Hz, 1H), 6.67 (dd, *J* = 8.6, 2.3 Hz, 1H), 3.76 (s, 3H), 2.87 (t, *J* = 6.8 Hz, 2H), 2.81 (t, *J* = 6.7 Hz, 2H).

¹³C NMR (126 MHz, CD₃OD) δ [ppm] = 157.6, 138.9, 123.2, 122.3, 119.9, 113.3, 109.9, 95.6, 56.0, 42.9, 29.4.

HRMS-ESI: calcd. for C₁₁H₁₅N₂O [M + H]⁺: 191.1179; found: 191.1179.

FT-IR: ν [cm⁻¹] = 3401, 2924, 2834, 1627, 1456, 1305, 1262, 1200, 1160, 1026, 800, 753.

2-(4-Methoxy-1*H*-indol-3-yl)ethan-1-amine (2.23c)

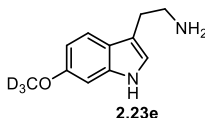
2.23c was prepared according to **General procedure B**, starting from 4-methoxy-1*H*-indole (2.00 g, 13.6 mmol, 1.0 equiv.) and POCl₃ (3.81 mL, 40.8 mmol, 3.0 equiv.) in DMF (25.0 mL). The reaction mixture was subsequently treated with NH₄OAc (3.15 g, 40.8 mmol, 3.0 equiv.), MeNO₂ (54.6 mL, 1.02 mol, 75 equiv.) and LiAlH₄ (3.10 g, 10.8 mmol, 6.0 equiv.) in THF (125 mL). Purification by silica gel column chromatography (DCM/MeOH/TEA = 80:20:5) afforded **2.23c** (950 mg, 5.00 mmol, 37%) as a light brown solid.

¹H NMR (700 MHz, CD₃OD) δ [ppm] = 6.98 (dd, *J* = 8.1, 7.6 Hz, 1H), 6.94 – 6.93 (m, 1H), 6.90 (d, *J* = 0.9 Hz, 1H), 6.44 (dd, *J* = 7.7, 0.8 Hz, 1H), 3.87 (s, 3H), 2.99 (t, *J* = 6.7 Hz, 2H), 2.92 (t, *J* = 6.8 Hz, 2H).

¹³C NMR (176 MHz, CD₃OD) δ [ppm] = 155.9, 140.1, 123.2, 122.6, 118.4, 113.6, 105.8, 105.8, 99.8, 55.4, 43.9, 31.0.

HRMS-ESI: calcd. for C₁₁H₁₅N₂O [M + H]⁺: 191.1179; found: 191.1179.

FT-IR: ν [cm⁻¹] = 3158, 2932, 2871, 1584, 1507, 1360, 1253, 1007, 733.

2-(6-(Methoxy-*d*₃)-1*H*-indol-3-yl)ethan-1-amine (2.23e)

2.23e was prepared according to **General procedure B**, starting from 6-(methoxy-*d*₃)-1*H*-indole (80.0 mg, 0.533 mmol, 1.0 equiv.) and POCl₃ (0.150 mL, 1.60 mmol, 3.0 equiv.) in DMF (3.0 mL). The reaction mixture was subsequently treated with NH₄OAc (123 mg, 1.60 mmol, 3.0 equiv.), MeNO₂ (2.14 mL, 40.0 mmol, 75 equiv.) and LiAlH₄ (121 mg, 3.20 mmol, 6.0 equiv.) in THF (5.0 mL). Purification by silica gel column chromatography (DCM/MeOH/TEA = 80:20:5) afforded **2.23c** (15.0 mg, 77.7 μmol, 15%) as a light brown solid.

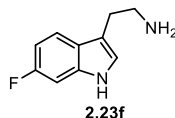
¹H NMR (600 MHz, CD₃OD) δ [ppm] = 7.42 (d, *J* = 8.6 Hz, 1H), 7.04 (d, *J* = 0.9 Hz, 1H), 6.90 (d, *J* = 2.2 Hz, 1H), 6.71 (dd, *J* = 8.6, 2.3 Hz, 1H), 3.20 (dd, *J* = 7.8, 6.9 Hz, 2H), 3.07 (t, *J* = 7.4 Hz, 2H).

^{13}C NMR (151 MHz, CD_3OD) δ [ppm] = 179.0 (impurity), 156.5, 137.8, 121.5, 121.3, 118.2, 109.4, 109.0, 94.3, 40.1, 23.9, 22.8 (impurity). (The impurity was determined by the comparison with 6-methoxyindole. Due to the intensity, the resonance of CD_3 was not found.)

HRMS-ESI: calcd. for $\text{C}_{11}\text{H}_{11}\text{D}_3\text{NO}$ $[\text{M} + \text{H}]^+$: 194.1367; found: 194.1364.

FT-IR: ν [cm^{-1}] = 3408, 2917, 2834, 1626, 1457, 1305, 1161, 1026, 800.

2-(6-fluoro-1*H*-indol-3-yl)ethan-1-amine (2.23f)



2.23f was prepared according to **General procedure B**, starting from 6-fluoro-1*H*-indole (1.70 g, 12.6 mmol, 1.0 equiv.) and POCl_3 (3.53 mL, 37.8 mmol, 3.0 equiv.) in DMF (25.0 mL). The reaction mixture was subsequently treated with NH_4OAc (2.91 g, 37.8 mmol, 3.0 equiv.), MeNO_2 (50.5 mL, 944 mmol, 75 equiv.) and LiAlH_4 (2.87 g, 75.5 mmol, 6.0 equiv.) in THF (50.0 mL). Purification by silica gel column chromatography ($\text{DCM}/\text{MeOH}/\text{TEA} = 80:20:5$) afforded **2.23f** (580 mg, 3.26 mmol, 26%) as a light brown solid.

^1H NMR (500 MHz, CD_3OD) δ [ppm] = 7.50 (dd, $J = 8.7, 5.3$ Hz, 1H), 7.13 (s, 1H), 7.06 (dd, $J = 9.9, 2.3$ Hz, 1H), 6.86–6.77 (m, 1H), 3.11 (dd, $J = 7.9, 6.4$ Hz, 2H), 3.02 (t, $J = 7.2$ Hz, 2H).

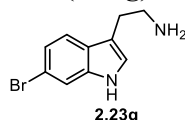
^{13}C NMR (126 MHz, CD_3OD) δ [ppm] = 161.3 (d, $J = 235.3$ Hz), 138.2 (d, $J = 12.4$ Hz), 125.1, 124.5 (d, $J = 3.3$ Hz), 119.9 (d, $J = 10.2$ Hz), 111.7, 108.3 (d, $J = 24.9$ Hz), 98.3 (d, $J = 26.0$ Hz), 41.8, 26.2.

^{19}F NMR (471 MHz, CD_3OD) δ [ppm] = -124.28.

HRMS-ESI: calcd. for $\text{C}_{10}\text{H}_{12}\text{N}_2\text{F}$ $[\text{M} + \text{H}]^+$: 179.0979; found: 179.0979.

FT-IR: ν [cm^{-1}] = 3147, 2991, 2918, 2840, 1456, 1345, 1143, 951, 835, 799.

2-(6-Bromo-1*H*-indol-3-yl)ethan-1-amine (2.23g)



2.23g was prepared according to **General procedure B**, starting from 6-bromo-1*H*-indole (1.00 g, 5.16 mmol, 1.0 equiv.) and POCl_3 (1.44 mL, 15.5 mmol, 3.0 equiv.) in DMF (15.0 mL). The reaction mixture was subsequently treated with NH_4OAc (1.19 g, 15.5 mmol, 3.0 equiv.),

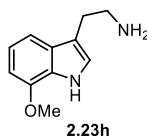
MeNO₂ (20.7 mL, 386 mmol, 75 equiv.) and LiAlH₄ (1.17 g, 30.9 mmol, 6.0 equiv.) in THF (20.0 mL). Purification by silica gel column chromatography (DCM/MeOH/TEA = 80:20:5) afforded **2.23g** (580 mg, 3.26 mmol, 47%) as a light brown solid.

¹H NMR (500 MHz, CD₃OD) δ [ppm] = 7.50 (d, *J* = 1.7 Hz, 1H), 7.45 (d, *J* = 8.4 Hz, 1H), 7.10 (dd, *J* = 8.4, 1.8 Hz, 1H), 7.08 (d, *J* = 0.8 Hz, 1H), 2.95–2.90 (m, 2H), 2.90–2.85 (m, 2H).
¹³C NMR (126 MHz, CD₃OD) δ [ppm] = 139.0, 127.7, 124.5, 122.7, 120.7, 115.8, 115.1, 113.7, 43.0, 29.1.

HRMS-ESI: calcd. for C₁₀H₁₂N₂Br [M + H]⁺: 239.0179; found: 239.0191.

FT-IR: ν [cm⁻¹] = 3423, 3126, 2935, 1578, 1456, 1334, 1048, 894, 852, 802, 771.

2-(7-Methoxy-1H-indol-3-yl)ethan-1-amine (**2.23h**)



2.23h was prepared according to **General procedure B**, starting from 7-methoxy-1*H*-indole (1.50 g, 10.2 mmol, 1.0 equiv.) and POCl₃ (2.86 mL, 30.6 mmol, 3.0 equiv.) in DMF (15.0 mL). The reaction mixture was subsequently treated with NH₄OAc (2.36 g, 30.6 mmol, 3.0 equiv.), MeNO₂ (41.0 mL, 765 mmol, 75 equiv.) and LiAlH₄ (2.32 g, 61.2 mmol, 6.0 equiv.) in THF (50.0 mL). Purification by silica gel column chromatography (DCM/MeOH/TEA = 80:20:5) afforded **2.23g** (1.30 g, 6.84 mmol, 67%) as a light brown solid.

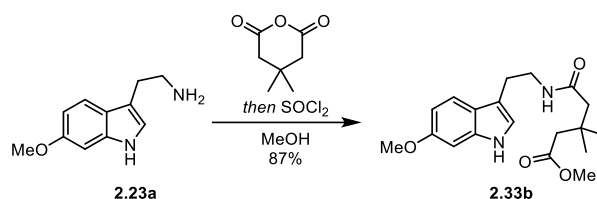
¹H NMR (500 MHz, CD₃OD) δ [ppm] = 7.14 (d, *J* = 8.0 Hz, 1H), 7.01 (s, 1H), 6.93 (t, *J* = 7.8 Hz, 1H), 6.61 (d, *J* = 7.6 Hz, 1H), 3.92 (s, 3H), 2.95–2.90 (m, 2H), 2.87 (dd, *J* = 7.5, 4.8 Hz, 2H).

¹³C NMR (126 MHz, CD₃OD) δ [ppm] = 147.9, 130.2, 128.5, 123.2, 120.2, 113.6, 112.2, 102.5, 55.7, 43.0, 29.3.

HRMS-ESI: calcd. for C₁₁H₁₅N₂O [M + H]⁺: 191.1179; found: 191.1179.

FT-IR: ν [cm⁻¹] = 3411, 2933, 2838, 1576, 1258, 1238, 1053, 782, 750, 729.

Methyl 5-((2-(6-methoxy-1*H*-indol-3-yl)ethyl)amino)-3,3-dimethyl-5-oxopentanoate (2.33b)



6-Methoxytryptamine (1.30 g, 6.84 mmol, 1.0 equiv.) and 3,3-dimethylglutaric anhydride (972 mg, 6.84 mmol, 1.0 equiv.) were dissolved in MeOH (20 mL). The mixture was stirred overnight, before SOCl₂ (496 μL, 6.84 mmol, 1.0 equiv.) was added dropwise at 0 °C. The reaction mixture was allowed to warm to room temperature for 3 h and quenched with NaHCO₃ (sat. aq.). The mixture was extracted with DCM. The combined organic phases were washed with brine, dried over MgSO₄, filtered and concentrated under reduced pressure. The crude product was purified by silica gel column chromatography (pentane/EtOAc = 2:1) to afford methyl ester **2.33b** (2.05 g, 5.92 mmol, 87%) as a light brown solid.

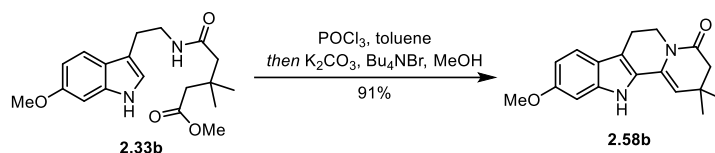
¹H NMR (500 MHz, CD₂Cl₂) δ [ppm] = 8.18 (s, 1H), 7.44 (d, *J* = 8.6 Hz, 1H), 6.92 (dd, *J* = 2.1, 1.0 Hz, 1H), 6.85 (d, *J* = 2.2 Hz, 1H), 6.73 (dd, *J* = 8.6, 2.3 Hz, 1H), 6.28 (s, 1H), 3.80 (s, 3H), 3.58 (s, 3H), 3.56–3.51 (m, 2H), 2.89 (td, *J* = 7.0, 1.0 Hz, 2H), 2.25 (s, 2H), 2.15 (s, 2H), 1.01 (s, 6H).

¹³C NMR (126 MHz, CD₂Cl₂) δ [ppm] = 173.5, 171.2, 157.0, 137.6, 122.2, 121.2, 119.7, 113.4, 109.6, 94.9, 55.9, 51.6, 47.6, 44.9, 39.8, 33.5, 28.5, 25.9.

HRMS-ESI: calcd. for C₁₉H₂₆N₂O₄Na [M + Na]⁺: 369.1785; found: 369.1789.

FT-IR: ν [cm⁻¹] = 3317, 2953, 2935, 1732, 1643, 1540, 1511, 1438, 1244, 1176, 1033, 752.

10-Methoxy-2,2-dimethyl-2,6,7,12-tetrahydroindolo[2,3-*a*]quinolizin-4(3*H*)-one (2.58b)



To a solution of methyl ester **2.33b** (1.80 g, 5.20 mmol, 1.0 equiv.) in toluene (100 mL) was added POCl₃ (0.475 mL, 5.20 mmol, 1.0 equiv.) dropwise. Then the mixture was heated to 115 °C (oil bath temperature) until the starting material was fully consumed. After allowing the

mixture to cool down to 80 °C (oil bath temperature), the MeOH (100 mL), K₂CO₃ (7.19 g, 52.0 mmol, 10.0 equiv.) and *n*Bu₄NBr (168 mg, 0.520 mmol, 0.1 equiv.) were added subsequently. Afterwards the resulting mixture was stirred overnight at 80 °C, cooled to room temperature, filtered through Celite[®], concentrated under reduced pressure. The crude product was purified by silica gel column chromatography (pentane/EtOAc = 5:3) to afford **2.58b** (1.40 g, 4.73 mmol, 91%) as a light yellow solid.

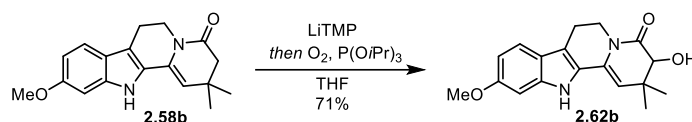
¹H NMR (700 MHz, CDCl₃) δ [ppm] = 8.09 (s, 1H), 7.37 (d, *J* = 8.5 Hz, 1H), 6.83 (s, 1H), 6.78 (d, *J* = 8.5 Hz, 1H), 5.27 (s, 1H), 4.09 (t, *J* = 5.9 Hz, 2H), 3.85 (s, 3H), 2.88 (t, *J* = 5.9 Hz, 2H), 2.48 (s, 2H), 1.16 (s, 6H).

¹³C NMR (176 MHz, CDCl₃) δ [ppm] = 169.6, 157.6, 138.3, 128.9, 126.9, 121.3, 119.7, 112.4, 109.7, 109.5, 95.0, 55.8, 46.6, 39.3, 30.8, 28.3, 20.8.

HRMS-EI: calcd. for C₁₈H₂₀N₂O₂ [M]⁺: 296.1519; found: 296.1520.

FT-IR: ν [cm⁻¹] = 2954, 2919, 2850, 1736, 1663, 1628, 1461, 1365, 1230, 1174, 1149.

3-Hydroxy-10-methoxy-2,2-dimethyl-2,6,7,12-tetrahydroindolo[2,3-*a*]quinolizin-4(3*H*)-one (**2.62b**)



To a solution of tetracyclic enamide **2.58b** (100 mg, 0.34 mmol, 1.0 equiv.) in THF, was added LiTMP (1.0 M solution in THF, 3.40 mL, 3.38 mmol, 10.0 equiv.) at -78 °C. The resulting mixture was stirred at that temperature for 1 h before P(OMe)₃ (250 μL, 1.01 mmol, 2.5 equiv.) was added. O₂ was bubbled through the mixture for 20 min, and the mixture was stirred for additional 2 h under O₂ atmosphere. Then the reaction mixture was quenched with NaHCO₃ (sat. aq.). The aqueous phase was extracted with DCM. The combined organic phases were washed with brine, dried over MgSO₄, filtered and concentrated under reduced pressure. The crude product was purified by silica gel column chromatography (pentane/EtOAc = 3:2) to afford **2.62b** (75.0 mg, 0.240 mmol, 71%) as a yellow solid.

¹H NMR (500 MHz, CDCl₃) δ [ppm] = 8.09 (s, 1H), 7.37 (d, *J* = 8.6 Hz, 1H), 6.82 (d, *J* = 2.2 Hz, 1H), 6.79 (dd, *J* = 8.6, 2.2 Hz, 1H), 5.27 (s, 1H), 4.86 (ddd, *J* = 12.7, 5.2, 2.1 Hz, 1H),

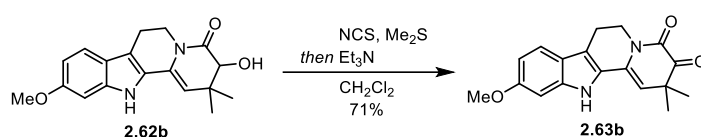
4.08 (d, $J = 2.5$ Hz, 1H), 3.89 (d, $J = 2.6$ Hz, 1H), 3.85 (s, 3H), 3.28 (td, $J = 12.1, 5.4$ Hz, 1H), 2.96–2.83 (m, 2H), 1.30 (s, 3H), 1.00 (s, 3H).

^{13}C NMR (126 MHz, CDCl_3) δ [ppm] = 171.7, 157.9, 138.4, 127.8, 126.1, 121.2, 119.8, 112.4, 110.1, 109.3, 94.9, 75.0, 55.8, 40.7, 35.2, 26.5, 20.6, 19.9.

HRMS-ESI: calcd. for $\text{C}_{18}\text{H}_{20}\text{N}_2\text{O}_3\text{Na}$ [$\text{M} + \text{Na}$] $^+$: 335.1366; found: 335.1367.

FT-IR: ν [cm^{-1}] = 3343, 2958, 2924, 1653, 1393, 1360, 1328, 1231, 1151, 1027, 920, 743.

10-Methoxy-2,2-dimethyl-2,6,7,12-tetrahydroindolo[2,3-*a*]quinolizine-3,4-dione (2.63b)



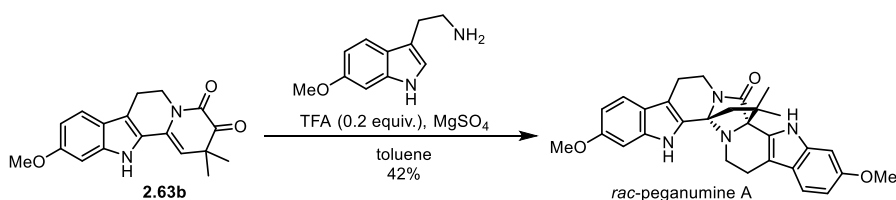
To a solution of NCS (171 mg, 1.28 mmol, 5.0 equiv.) in DCM (5.0 mL) at 0 °C was added Me_2S (471 μL , 6.41 mmol, 25 equiv.) and the mixture was stirred at -78 °C for 1 h. The solution of α -hydroxyenamide **2.62b** (80 mg, 0.256 mmol, 1.0 equiv.) in DCM (2.0 mL) was added dropwise. The resulting mixture was stirred at -78 °C for another 2 h before Et_3N (712 μL , 5.13 mmol, 20 equiv.) was added. Then the mixture was stirred at -78 °C for 2 h. The mixture was quenched with NH_4Cl (sat. aq.) and extracted with DCM. The combined organic phases were washed with brine, dried over MgSO_4 , filtered and concentrated under reduced pressure. The crude product was purified by silica gel column chromatography (pentane/ EtOAc = 3:2) to afford α -ketoenamide **2.63b** (57.0 mg, 0.184 mmol, 71%) as an orange solid.

^1H NMR (700 MHz, CDCl_3) δ [ppm] = 8.08 (s, 1H), 7.42–7.37 (m, 1H), 6.87–6.84 (m, 1H), 6.80 (dd, $J = 8.6, 2.2$ Hz, 1H), 5.31 (s, 1H), 4.20 (t, $J = 6.0$ Hz, 2H), 3.86 (s, 3H), 2.98 (t, $J = 6.0$ Hz, 2H), 1.39 (s, 6H).

^{13}C NMR (176 MHz, CDCl_3) δ [ppm] = 196.1, 158.1, 157.4, 138.7, 127.0, 125.9, 121.0, 120.0, 113.0, 110.3, 106.0, 95.1, 55.9, 44.9, 40.5, 25.0, 20.4.

HRMS-EI: calcd. for $\text{C}_{18}\text{H}_{18}\text{N}_2\text{O}_3$ [M] $^+$: 310.1312; found: 310.1314.

FT-IR: ν [cm^{-1}] = 3284, 2956, 2925, 1642, 1392, 1305, 1184, 1143, 1047, 799, 756.

***rac*-Peganumine A**

To a mixture of α -ketoenamide **2.63b** (35.0 mg, 0.113 mmol, 1.0 equiv.), 6-methoxytryptamine (25.7 mg, 0.135 mmol, 1.2 equiv.) and MgSO₄ (136 mg, 1.13 mmol, 10.0 equiv.) in toluene (10 mL) under argon atmosphere, was added TFA (1.7 μ L, 23 μ mol, 0.2 equiv.). The resulting reaction mixture was heated to 115 °C (oil bath temperature) for 2 days. Then the reaction was quenched with NaHCO₃ (sat. aq.). The aqueous phase was extracted with DCM. The combined organic phases were washed with brine, dried over MgSO₄, filtered and concentrated under reduced pressure. The crude product was purified by silica gel column chromatography (pentane/EtOAc = 3:2) to afford *rac*-peganumine A (23.0 mg, 47.7 μ mol, 42%) as a light yellow solid.

¹H NMR (700 MHz, CD₃OD) δ [ppm] = 7.38 (d, J = 8.7 Hz, 1H), 7.26 (d, J = 8.6 Hz, 1H), 6.99 (d, J = 2.2 Hz, 1H), 6.93 (d, J = 2.2 Hz, 1H), 6.73 (dd, J = 8.7, 2.2 Hz, 1H), 6.67 (dd, J = 8.6, 2.3 Hz, 1H), 4.14 (dd, J = 13.0, 5.8 Hz, 1H), 3.83 (s, 3H), 3.82 (s, 3H), 3.21–3.16 (m, 1H), 2.98 (dd, J = 15.4, 4.4 Hz, 1H), 2.90–2.76 (m, 2H), 2.69 (dd, J = 15.5, 3.5 Hz, 1H), 2.59 (dd, J = 10.8, 5.3 Hz, 1H), 2.48–2.41 (m, 1H), 2.39 (d, J = 11.5 Hz, 1H), 1.94 (d, J = 11.5 Hz, 1H), 1.44 (s, 3H), 1.24 (s, 3H).

¹³C NMR (176 MHz, CD₃OD) δ [ppm] = 175.2, 158.3, 157.6, 139.5, 139.4, 127.8, 126.4, 122.3, 122.2, 119.9, 119.2, 112.9, 112.2, 110.5, 109.8, 96.0, 95.7, 81.2, 79.7, 56.0, 55.9, 51.9, 41.7, 41.6, 37.3, 27.3, 26.3, 22.5, 22.1.

¹H NMR (500 MHz, *d*₆-DMSO) δ [ppm] = 11.24 (s, 1H), 10.77 (s, 1H), 7.38 (d, J = 8.6 Hz, 1H), 7.25 (d, J = 8.6 Hz, 1H), 6.93 (d, J = 2.3 Hz, 1H), 6.88 (d, J = 2.3 Hz, 1H), 6.70 (dd, J = 8.6, 2.3 Hz, 1H), 6.63 (dd, J = 8.6, 2.3 Hz, 1H), 4.00 (dd, J = 12.9, 5.8 Hz, 1H), 3.78 (s, 3H), 3.77 (s, 3H), 3.10 (td, J = 12.6, 4.5 Hz, 1H), 2.90 (dd, J = 15.3, 4.2 Hz, 1H), 2.76–2.69 (m, 1H), 2.69–2.65 (m, 1H), 2.64–2.60 (m, 1H), 2.48–2.43 (m, 1H), 2.34 (dd, J = 10.8, 4.9 Hz, 1H), 2.30 (d, J = 11.3 Hz, 1H), 1.88 (d, J = 11.2 Hz, 1H), 1.38 (s, 3H), 1.15 (s, 3H).

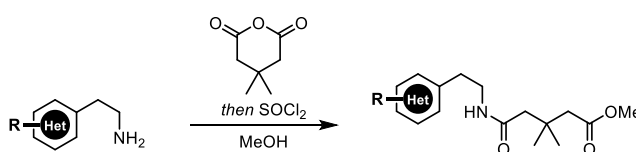
^{13}C NMR (126 MHz, d_6 -DMSO) δ [ppm] = 171.3, 156.1, 155.4, 137.6, 137.5, 127.3, 125.7, 120.5, 120.4, 119.0, 118.2, 111.2, 109.5, 109.0, 108.3, 94.9, 94.7, 78.8, 77.4, 55.23, 55.18, 50.4, 40.1, 39.9, 35.6, 26.8, 26.0, 21.0, 20.9.

HRMS-ESI: calcd. for $\text{C}_{29}\text{H}_{31}\text{N}_4\text{O}_3$ $[\text{M} + \text{H}]^+$: 483.2391; found: 483.2384.

FT-IR: ν [cm^{-1}] = 2954, 2923, 2857, 1736, 1457, 1366, 1217, 820.

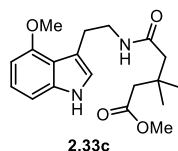
7.2.1.4. Analogues design, synthesis and bioactivity investigation

General procedure C



Amine (1.0 equiv.) and 3,3-dimethylglutaric anhydride (1.0 equiv.) were dissolved in MeOH. The mixture was stirred overnight at room temperature, before SOCl_2 (1.0 equiv.) was added dropwise at 0 °C. The reaction mixture was allowed to warm to room temperature for 3 h and quenched with NaHCO_3 (sat. aq.). The mixture was extracted with DCM. The combined organic phases were washed with brine, dried over MgSO_4 , filtered and concentrated under reduced pressure. The crude product was purified by silica gel column chromatography to afford the corresponding methyl ester.

Methyl 5-((2-(4-methoxy-1*H*-indol-3-yl)ethyl)amino)-3,3-dimethyl-5-oxopentanoate (2.33c)



2.33c was prepared according to the **General procedure C** starting from 4-methoxytryptamine (440 mg, 2.32 mmol, 1.0 equiv.) and 3,3-dimethylglutaric anhydride (329 mg, 2.32 mmol, 1.0 equiv.) in MeOH (10 mL). The reaction mixture was subsequently treated with SOCl_2 (168 μL , 2.32 mmol, 1.0 equiv.). Purification by silica gel column chromatography (pentane/EtOAc = 3:2) afforded **2.33c** (570 mg, 1.63 mmol, 71%) as a light brown solid.

^1H NMR (500 MHz, CDCl_3) δ [ppm] = 8.38 (s, 1H), 7.09–7.05 (m, 1H), 6.96 (d, J = 8.2 Hz,

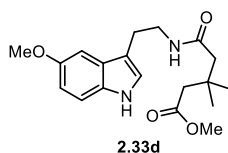
1H), 6.86 (s, 1H), 6.48 (d, $J = 8.2$ Hz, 1H), 6.44 (s, 1H), 3.93 (s, 3H), 3.60 (s, 5H), 3.06 (d, $J = 0.7$ Hz, 2H), 2.29 (s, 2H), 2.17 (d, $J = 2.9$ Hz, 2H), 1.03 (s, 6H).

^{13}C NMR (126 MHz, CDCl_3) δ [ppm] = 173.3, 171.2, 154.6, 138.3, 122.8, 121.3, 117.4, 113.5, 104.8, 99.4, 55.2, 51.4, 47.5, 44.8, 41.0, 33.3, 28.4, 26.8.

HRMS-ESI: calcd. for $\text{C}_{19}\text{H}_{26}\text{N}_2\text{O}_4\text{K}$ $[\text{M} + \text{K}]^+$: 385.1525; found: 385.1542.

FT-IR: ν [cm^{-1}] = 3390, 3285, 2953, 2838, 1733, 1649, 1508, 1436, 1360, 1255, 1086, 736.

Methyl 5-((2-(5-methoxy-1*H*-indol-3-yl)ethyl)amino)-3,3-dimethyl-5-oxopentanoate (2.33d)



2.33d was prepared according to the **General procedure C** starting from 5-methoxytryptamine (2.00 g, 10.5 mmol, 1.0 equiv.) and 3,3-dimethylglutaric anhydride (1.49 g, 10.5 mmol, 1.0 equiv.) in MeOH (30 mL). The reaction mixture was subsequently treated with SOCl_2 (763 μL , 10.5 mmol, 1.0 equiv.). Purification by silica gel column chromatography (pentane/EtOAc = 3:2) afforded **2.33d** (3.40 g, 9.83 mmol, 93%) as a light brown solid.

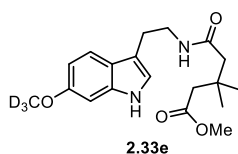
^1H NMR (500 MHz, CDCl_3) δ [ppm] = 8.25 (s, 1H), 7.24 (dd, $J = 8.8, 0.7$ Hz, 1H), 7.03 (d, $J = 2.4$ Hz, 1H), 7.00 (d, $J = 2.1$ Hz, 1H), 6.85 (dd, $J = 8.8, 2.4$ Hz, 1H), 6.45 (s, 1H), 3.85 (s, 3H), 3.60 (d, $J = 0.6$ Hz, 5H), 2.93 (t, $J = 7.0$ Hz, 2H), 2.24 (s, 2H), 2.20 (s, 2H), 1.04 (s, 6H).

^{13}C NMR (126 MHz, CDCl_3) δ [ppm] = 173.5, 171.2, 154.1, 131.7, 127.9, 122.9, 112.8, 112.4, 112.0, 100.6, 56.1, 51.5, 47.4, 44.6, 39.5, 33.4, 28.6, 25.5.

HRMS-ESI: calcd. for $\text{C}_{19}\text{H}_{26}\text{N}_2\text{O}_4\text{K}$ $[\text{M} + \text{K}]^+$: 385.1525; found: 385.1543.

FT-IR: ν [cm^{-1}] = 3340, 3311, 2954, 1733, 1650, 1539, 1487, 1439, 1217, 1173, 1033, 795.

Methyl 5-((2-(6-(methoxy- d_3)-1*H*-indol-3-yl)ethyl)amino)-3,3-dimethyl-5-oxopentanoate (2.33e)



2.33e was prepared according to the **General procedure C** starting from 2-(6-(methoxy- d_3)-1*H*-indol-3-yl)ethan-1-amine (100 mg, 0.518 mmol, 1.0 equiv.) and 3,3-dimethylglutaric anhydride (73.6 mg, 0.518 mmol, 1.0 equiv.) in MeOH (5.0 mL). The reaction mixture was subsequently treated with SOCl₂ (37.6 μ L, 0.518 mmol, 1.0 equiv.). Purification by silica gel column chromatography (pentane/EtOAc = 3:2) afforded **2.33e** (120 mg, 0.344 mmol, 66%) as a light brown solid.

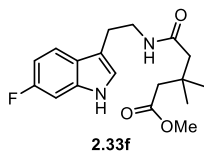
¹H NMR (500 MHz, CDCl₃) δ [ppm] = 8.47 (s, 1H), 7.44 (d, J = 8.6 Hz, 1H), 6.87 (dd, J = 2.2, 1.1 Hz, 1H), 6.82 (dd, J = 2.3, 0.5 Hz, 1H), 6.76 (dd, J = 8.6, 2.2 Hz, 1H), 6.45 (s, 1H), 3.60 (s, 3H), 3.59–3.56 (m, 2H), 2.91 (td, J = 7.0, 0.9 Hz, 2H), 2.26 (s, 2H), 2.19 (s, 2H), 1.04 (s, 6H).

¹³C NMR (176 MHz, CDCl₃) δ [ppm] = 173.4, 171.3, 156.5, 137.3, 121.9, 120.9, 119.3, 112.8, 109.3, 94.8, 55.2–54.5 (m), 51.4, 47.3, 44.6, 39.6, 33.4, 28.5, 25.6.

HRMS-ESI: calcd. for C₁₉H₂₄D₃N₂O [M + H]⁺: 350.2154; found: 350.2163.

FT-IR: ν [cm⁻¹] = 3315, 2945, 2935, 1733, 1642, 1511, 1438, 1244, 1176, 1152, 1033, 822.

Methyl 5-((2-(6-fluoro-1*H*-indol-3-yl)ethyl)amino)-3,3-dimethyl-5-oxopentanoate (**2.33f**)



2.33f was prepared according to the **General procedure C** starting from 6-fluorotryptamine (650 mg, 3.65 mmol, 1.0 equiv.) and 3,3-dimethylglutaric anhydride (518 mg, 3.65 mmol, 1.0 equiv.) in MeOH (10 mL). The reaction mixture was subsequently treated with SOCl₂ (265 μ L, 3.65 mmol, 1.0 equiv.). Purification by silica gel column chromatography (pentane/EtOAc = 3:2) afforded **2.33f** (660 mg, 1.98 mmol, 54%) as a light brown solid.

¹H NMR (500 MHz, CDCl₃) δ [ppm] = 8.41 (s, 1H), 7.54–7.44 (m, 1H), 7.09–6.96 (m, 2H), 6.86 (t, J = 8.8 Hz, 1H), 6.50 (s, 1H), 3.61 (s, 5H), 2.95 (s, 2H), 2.24 (s, 2H), 2.21 (s, 2H), 1.04 (s, 6H).

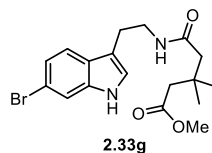
¹³C NMR (126 MHz, CDCl₃) δ [ppm] = 173.6, 171.5, 160.1 (d, J = 237.3 Hz), 136.4 (d, J = 12.1 Hz), 124.2, 122.4, 119.6 (d, J = 10.1 Hz), 113.23, 108.2 (d, J = 24.6 Hz), 97.6 (d, J = 25.8 Hz), 51.57, 47.4, 44.6, 39.6, 33.5, 28.7, 25.5.

¹⁹F NMR (376 MHz, CDCl₃) δ [ppm] = -121.2.

HRMS-ESI: calcd. for $C_{18}H_{23}FN_2O_3$ $[M + H]^+$: 335.1766; found: 335.1782.

FT-IR: ν [cm^{-1}] = 3306, 2957, 2874, 1717, 1647, 1628, 1540, 1455, 1226, 1142, 802.

Methyl 5-((2-(6-bromo-1H-indol-3-yl)ethyl)amino)-3,3-dimethyl-5-oxopentanoate (2.33g)



2.33g was prepared according to the **General procedure C** starting from 6-bromotryptamine (335 mg, 1.41 mmol, 1.0 equiv.) and 3,3-dimethylglutaric anhydride (200 mg, 1.41 mmol, 1.0 equiv.) in MeOH (10 mL). The reaction mixture was subsequently treated with $SOCl_2$ (102 μ L, 1.41 mmol, 1.0 equiv.). Purification by silica gel column chromatography (pentane/EtOAc = 3:2) afforded **2.33g** (400 mg, 1.02 mmol, 72%) as a light brown solid.

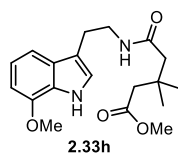
1H NMR (500 MHz, $CDCl_3$) δ [ppm] = 8.57 (s, 1H), 7.50 (d, J = 1.7 Hz, 1H), 7.44 (d, J = 8.5 Hz, 1H), 7.20–7.17 (m, 1H), 6.99 (dd, J = 2.2, 1.0 Hz, 1H), 6.53 (s, 1H), 3.59 (q, J = 7.1 Hz, 5H), 2.93 (t, J = 7.1 Hz, 2H), 2.23 (s, 2H), 2.21 (s, 2H), 1.04 (s, 6H).

^{13}C NMR (126 MHz, $CDCl_3$) δ [ppm] = 173.6, 171.4, 137.3, 126.5, 122.8, 122.7, 120.1, 115.7, 114.3, 113.3, 51.6, 47.3, 44.6, 39.6, 33.5, 28.7, 25.4.

HRMS-ESI: calcd. for $C_{18}H_{24}BrN_2O_3$ $[M + H]^+$: 395.0965; found: 395.0949.

FT-IR: ν [cm^{-1}] = 3306, 3270, 2961, 1716, 1647, 1541, 1456, 1334, 1223, 1168, 802, 775.

Methyl 5-((2-(7-methoxy-1H-indol-3-yl)ethyl)amino)-3,3-dimethyl-5-oxopentanoate (2.33h)



2.33h was prepared according to the **General procedure C** starting from 7-methoxytryptamine (400 mg, 2.10 mmol, 1.0 equiv.) and 3,3-dimethylglutaric anhydride (299 mg, 2.10 mmol, 1.0 equiv.) in MeOH (10 mL). The reaction mixture was subsequently treated with $SOCl_2$ (153 μ L, 2.10 mmol, 1.0 equiv.). Purification by silica gel column chromatography (pentane/EtOAc = 3:2) afforded **2.33h** (580 mg, 1.67 mmol, 80%) as a light brown solid.

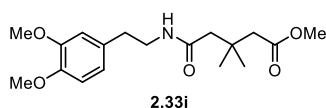
¹H NMR (500 MHz, CDCl₃) δ [ppm] = 8.29 (s, 1H), 7.21 (d, *J* = 8.0 Hz, 1H), 7.06–6.99 (m, 2H), 6.64 (d, *J* = 7.7 Hz, 1H), 6.36 (s, 1H), 3.95 (s, 3H), 3.60 (s, 5H), 2.96 (s, 2H), 2.25 (s, 2H), 2.20 (s, 2H), 1.04 (s, 6H).

¹³C NMR (176 MHz, CDCl₃) δ [ppm] = 173.4, 171.2, 146.3, 128.8, 127.0, 121.7, 119.9, 113.6, 111.7, 102.0, 55.5, 51.5, 47.4, 44.7, 39.6, 33.4, 28.6, 25.7.

HRMS-ESI: calcd. for C₁₉H₂₇N₂O₄ [M + H]⁺: 347.1966; found: 347.1967.

FT-IR: ν [cm⁻¹] = 3382, 3306, 2953, 2936, 2873, 1732, 1647, 1577, 1450, 1436, 1371, 1344, 1258, 1230, 1173, 1058, 782, 830.

Methyl 5-((3,4-dimethoxyphenethyl)amino)-3,3-dimethyl-5-oxopentanoate (**2.33i**)



2.33i was prepared according to the **General procedure C** starting from amine (2.00 g, 11.0 mmol, 1.0 equiv.) and 3,3-dimethylglutaric anhydride (1.57 g, 11.0 mmol, 1.0 equiv.) in MeOH (50 mL). The reaction mixture was subsequently treated with SOCl₂ (801 μL, 11.0 mmol, 1.0 equiv.). Purification by silica gel column chromatography (pentane/EtOAc = 5:2) afforded **2.33i** (3.25 g, 9.64 mmol, 87%) as a white solid.

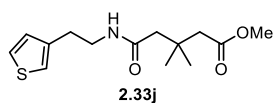
¹H NMR (500 MHz, CDCl₃) δ [ppm] = 6.79–6.75 (m, 1H), 6.73–6.69 (m, 2H), 6.46 (s, 1H), 3.85 (d, *J* = 0.9 Hz, 3H), 3.83 (d, *J* = 0.9 Hz, 3H), 3.63 (d, *J* = 0.9 Hz, 3H), 3.52–3.48 (m, 2H), 2.75 (t, *J* = 7.1 Hz, 2H), 2.20 (d, *J* = 0.7 Hz, 2H), 2.18 (d, *J* = 0.9 Hz, 2H), 1.02 (s, 6H).

¹³C NMR (126 MHz, CDCl₃) δ [ppm] = 173.6, 171.1, 149.1, 147.7, 131.6, 120.7, 112.0, 111.4, 56.0, 55.9, 51.5, 47.3, 44.6, 40.5, 35.3, 33.5, 28.7.

HRMS-ESI: calcd. for C₁₈H₂₇NO₅Na [M + Na]⁺: 360.1781; found: 360.1786.

FT-IR: ν [cm⁻¹] = 3307, 2953, 2935, 1733, 1642, 1612, 1511, 1438, 1244, 1176, 1033, 754.

Methyl 3,3-dimethyl-5-oxo-5-((2-(thiophen-3-yl)ethyl)amino)pentanoate (**2.33j**)



2.33j was prepared according to the **General procedure C** starting from amine (250 mg,

1.97 mmol, 1.0 equiv.) and 3,3-dimethylglutaric anhydride (280 mg, 1.97 mmol, 1.0 equiv.) in MeOH (10 mL). The reaction mixture was subsequently treated with SOCl₂ (143 μL, 1.97 mmol, 1.0 equiv.). Purification by silica gel column chromatography (pentane/EtOAc = 5:2) afforded **2.33j** (333 mg, 1.18 mmol, 60%) as a light brown solid.

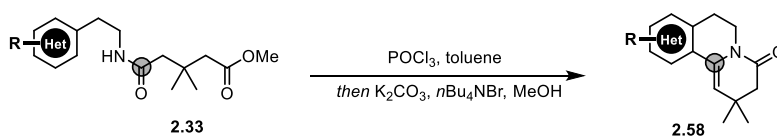
¹H NMR (500 MHz, CDCl₃) δ [ppm] = 7.24 (ddd, *J* = 4.9, 2.9, 0.9 Hz, 1H), 6.99–6.97 (m, 1H), 6.94 (dt, *J* = 4.9, 1.1 Hz, 1H), 6.51 (s, 1H), 3.63 (d, *J* = 0.9 Hz, 3H), 3.54–3.50 (m, 2H), 2.87–2.80 (m, 2H), 2.21–2.16 (m, 4H), 1.02 (s, 6H).

¹³C NMR (126 MHz, CDCl₃) δ [ppm] = 173.6, 171.1, 139.4, 128.1, 125.9, 121.4, 51.6, 47.2, 44.5, 39.7, 33.4, 30.3, 28.7.

HRMS-ESI: calcd. for C₁₄H₂₁NO₃SNa [M + Na]⁺: 306.1134; found: 3306.1140.

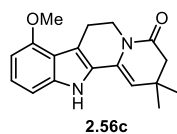
FT-IR: ν [cm⁻¹] = 3312, 2953, 2934, 1732, 1643, 1536, 1436, 1366, 1226, 1152, 856, 778.

General procedure D



To a solution of the methyl ester (1.0 equiv.) in toluene was added POCl₃ (1.0 equiv.) dropwise. Then the mixture was heated to 115 °C (oil bath temperature) until the starting material was fully consumed. After the mixture was cooled down to 80 °C (oil bath temperature), the MeOH, K₂CO₃ (10.0 equiv.) and *n*Bu₄NBr (0.1 equiv.) were added subsequently. Afterwards the resulting mixture was stirred overnight at 80 °C, cooled to room temperature, filtered through Celite[®], concentrated under reduced pressure. The crude product was purified by silica gel column chromatography. (Note: It is not necessary to perform the reaction under argon.)

8-Methoxy-2,2-dimethyl-2,6,7,12-tetrahydroindolo[2,3-*a*]quinolizin-4(3*H*)-one (2.58c)



2.58c was prepared according to the **General procedure D** starting from methyl ester **2.33c** (275 mg, 0.795 mmol, 1.0 equiv.) and POCl₃ (72.5 μL, 0.795 mmol, 1.0 equiv.) in toluene

(10 mL). The reaction mixture was subsequently treated with MeOH (10 mL), K₂CO₃ (1.10 g, 7.95 mmol, 10 equiv.) and *n*Bu₄NBr (25.6 mg, 79.0 μmol, 0.1 equiv.). Purification by silica gel column chromatography (pentane/EtOAc = 3:2) afforded **2.58c** (180 mg, 0.608 mmol, 77%) as a yellow solid.

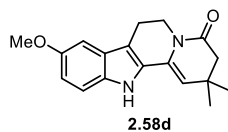
¹H NMR (500 MHz, CDCl₃) δ [ppm] = 8.22 (s, 1H), 7.10 (t, *J* = 8.0 Hz, 1H), 6.92 (dd, *J* = 8.2, 0.6 Hz, 1H), 6.51–6.45 (m, 1H), 5.28 (s, 1H), 4.07 (t, *J* = 6.0 Hz, 2H), 3.90 (s, 3H), 3.14 (t, *J* = 6.0 Hz, 2H), 2.49–2.46 (m, 2H), 1.16 (s, 6H).

¹³C NMR (126 MHz, CDCl₃) δ [ppm] = 169.6, 155.0, 138.7, 128.9, 126.4, 124.4, 117.2, 112.4, 109.6, 104.4, 100.2, 55.3, 46.6, 39.6, 30.8, 28.3, 22.6.

HRMS-ESI: calcd. for C₁₈H₁₉N₂O₂ [M – H][–]: 295.1452; found: 295.1452.

FT-IR: ν [cm^{–1}] = 3305, 3286, 2955, 2921, 1662, 1641, 1514, 1397, 1361, 1252, 1106, 742.

9-Methoxy-2,2-dimethyl-2,6,7,12-tetrahydroindolo[2,3-*a*]quinolizin-4(3*H*)-one (**2.58d**)



2.58d was prepared according to the **General procedure D** starting from methyl ester **2.33d** (2.40 g, 6.94 mmol, 1.0 equiv.) and POCl₃ (253 μL, 6.94 mmol, 1.0 equiv.) in toluene (80 mL). The reaction mixture was subsequently treated with MeOH (80 mL), K₂CO₃ (9.59 g, 69.4 mmol, 10 equiv.) and *n*Bu₄NBr (224 mg, 694 μmol, 0.1 equiv.). Purification by silica gel column chromatography (pentane/EtOAc = 3:2) afforded **2.58d** (2.00 g, 6.76 mmol, 97%) as a yellow solid.

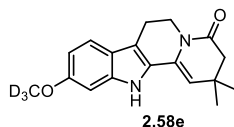
¹H NMR (500 MHz, CDCl₃) δ [ppm] = 7.82 (s, 1H), 7.21 (dd, *J* = 8.8, 0.7 Hz, 1H), 6.94 (d, *J* = 2.4 Hz, 1H), 6.90–6.85 (m, 1H), 5.29 (s, 1H), 4.09 (t, *J* = 6.0 Hz, 2H), 3.86 (s, 3H), 2.89 (t, *J* = 6.0 Hz, 2H), 2.47 (s, 2H), 1.16 (s, 6H).

¹³C NMR (176 MHz, CDCl₃) δ [ppm] = 169.6, 154.5, 132.4, 128.9, 128.7, 127.2, 113.7, 112.1, 111.9, 110.4, 100.8, 56.0, 46.6, 39.4, 30.8, 28.3, 20.8.

HRMS-ESI: calcd. for C₁₈H₂₁N₂O₂ [M + H]⁺: 297.1598; found: 297.1611.

FT-IR: ν [cm^{–1}] = 3287, 3272, 2955, 2924, 1663, 1642, 1488, 1457, 1393, 1289, 1217, 1113, 1028, 810, 753.

10-(methoxy-*d*₃)-2,2-dimethyl-2,6,7,12-tetrahydroindolo[2,3-*a*]quinolizin-4(3*H*)-one (2.58e)



2.58e was prepared according to the **General procedure D** starting from methyl ester **2.33e** (120 mg, 0.344 mmol, 1.0 equiv.) and POCl₃ (31.4 μL, 0.344 mmol, 1.0 equiv.) in toluene (5.0 mL). The reaction mixture was subsequently treated with MeOH (5.0 mL), K₂CO₃ (475 mg, 3.43 mmol, 10 equiv.) and *n*Bu₄NBr (11.1 mg, 34.0 μmol, 0.1 equiv.). Purification by silica gel column chromatography (pentane/EtOAc = 3:2) afforded **2.58e** (62.0 mg, 0.210 mmol, 61%) as a yellow solid.

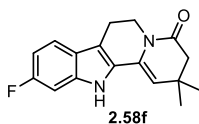
¹H NMR (700 MHz, CDCl₃) δ [ppm] = 8.11 (s, 1H), 7.37 (d, *J* = 8.6 Hz, 1H), 6.81 (d, *J* = 2.1 Hz, 1H), 6.77 (ddd, *J* = 8.6, 2.2, 0.8 Hz, 1H), 5.26 (s, 1H), 4.09 (t, *J* = 6.0 Hz, 2H), 2.87 (t, *J* = 6.0 Hz, 2H), 2.47 (s, 2H), 1.16 (s, 6H).

¹³C NMR (176 MHz, CDCl₃) δ [ppm] = 169.6, 157.6, 138.4, 128.9, 126.9, 121.3, 119.7, 112.4, 109.8, 109.4, 94.9, 55.2–54.7 (m), 46.6, 39.3, 30.8, 28.3, 20.8.

HRMS-EI: calcd. for C₁₈H₁₇D₃N₂O₂Na [M+Na]⁺: 322.1605; found: 322.1612.

FT-IR: ν [cm⁻¹] = 3311, 2955, 2924, 1738, 1662, 1640, 1623, 1557, 1456, 1391, 1364, 1269, 1178, 1110, 753.

10-Fluoro-2,2-dimethyl-2,6,7,12-tetrahydroindolo[2,3-*a*]quinolizin-4(3*H*)-one (2.58f)



2.58f was prepared according to the **General procedure D** starting from methyl ester **2.33f** (140 mg, 0.419 mmol, 1.0 equiv.) and POCl₃ (38.2 μL, 0.419 mmol, 1.0 equiv.) in toluene (5.0 mL). The reaction mixture was subsequently treated with MeOH (5.0 mL), K₂CO₃ (579 mg, 4.19 mmol, 10 equiv.) and *n*Bu₄NBr (13.5 mg, 42.0 μmol, 0.1 equiv.). Purification by silica gel column chromatography (pentane/EtOAc = 3:2) afforded **2.58f** (120 mg, 0.426 mmol, 99%) as a yellow solid.

¹H NMR (500 MHz, CDCl₃) δ [ppm] = 8.54 (s, 1H), 7.40 (dd, *J* = 8.6, 5.3 Hz, 1H), 7.01 (dd, *J* = 9.5, 2.3 Hz, 1H), 6.91–6.84 (m, 1H), 5.38 (s, 1H), 4.11 (t, *J* = 6.0 Hz, 2H), 2.94–2.87 (m, 2H), 2.49 (s, 2H), 1.17 (s, 6H).

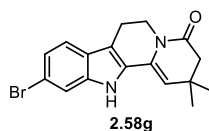
¹³C NMR (126 MHz, CDCl₃) δ [ppm] = 169.7, 160.8 (d, *J* = 239.3 Hz), 137.5 (d, *J* = 12.5 Hz), 128.7, 128.4 (d, *J* = 3.8 Hz), 123.5, 119.8 (d, *J* = 10.3 Hz), 112.1, 110.6, 108.8 (d, *J* = 24.6 Hz), 97.7 (d, *J* = 26.5 Hz), 46.5, 39.3, 30.8, 28.2, 20.7.

¹⁹F NMR (566 MHz, CDCl₃) δ [ppm] = -118.57.

HRMS-ESI: calcd. for C₁₇H₁₇FN₂ONa [M + Na]⁺: 307.1217; found: 307.1203.

FT-IR: ν [cm⁻¹] = 3294, 2956, 2923, 1663, 1642, 1393, 1360, 1265, 1223, 1134, 796.

10-Bromo-2,2-dimethyl-2,6,7,12-tetrahydroindolo[2,3-*a*]quinolizin-4(3*H*)-one (2.58g)



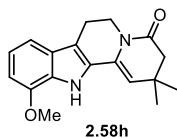
2.58g was prepared according to the **General procedure D** starting from methyl ester **2.33g** (200 mg, 0.508 mmol, 1.0 equiv.) and POCl₃ (46.3 μL, 0.508 mmol, 1.0 equiv.) in toluene (5.0 mL). The reaction mixture was subsequently treated with MeOH (5.0 mL), K₂CO₃ (702 mg, 5.08 mmol, 10 equiv.) and *n*Bu₄NBr (16.4 mg, 51.0 μmol, 0.1 equiv.). Purification by silica gel column chromatography (pentane/EtOAc = 3:2) afforded **2.58g** (140 mg, 0.398 mmol, 78%) as a yellow solid.

¹H NMR (500 MHz, CDCl₃) δ [ppm] = 7.93 (s, 1H), 7.49–7.45 (m, 1H), 7.38–7.33 (m, 1H), 7.22 (ddd, *J* = 8.4, 1.7, 0.8 Hz, 1H), 5.32 (s, 1H), 4.09 (t, *J* = 6.0 Hz, 2H), 2.89 (t, *J* = 6.0 Hz, 2H), 2.48 (s, 2H), 1.17 (s, 6H).

¹³C NMR (126 MHz, CDCl₃) δ [ppm] = 169.6, 138.1, 128.6, 128.6, 125.8, 123.4, 120.2, 117.0, 114.0, 112.2, 111.2, 46.4, 39.2, 30.9, 28.2, 20.6.

HRMS-ESI: calcd. for C₁₇H₁₇N₂OBrNa [M + Na]⁺: 367.0416; found: 367.0423.

FT-IR: ν [cm⁻¹] = 3282, 2955, 1663, 1638, 1452, 1394, 1294, 1233, 1186, 1136, 741.

11-Methoxy-2,2-dimethyl-2,6,7,12-tetrahydroindolo[2,3-*a*]quinolizin-4(3*H*)-one (2.58h)

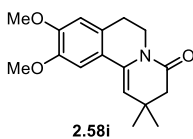
2.58h was prepared according to the **General procedure D** starting from methyl ester **2.33h** (400 mg, 1.16 mmol, 1.0 equiv.) and POCl₃ (106 μL, 1.16 mmol, 1.0 equiv.) in toluene (10 mL). The reaction mixture was subsequently treated with MeOH (10 mL), K₂CO₃ (1.60 mg, 11.6 mmol, 10 equiv.) and *n*Bu₄NBr (37.3 mg, 116 μmol, 0.1 equiv.). Purification by silica gel column chromatography (pentane/EtOAc = 3:2) afforded **2.58h** (334 mg, 1.13 mmol, 98%) as a yellow solid.

¹H NMR (500 MHz, CDCl₃) δ [ppm] = 8.31 (s, 1H), 7.15–7.11 (m, 1H), 7.04 (t, *J* = 7.8 Hz, 1H), 6.69 (d, *J* = 7.7 Hz, 1H), 5.38 (s, 1H), 4.09 (t, *J* = 6.0 Hz, 2H), 3.97 (s, 3H), 2.90 (d, *J* = 12.0 Hz, 2H), 2.48 (s, 2H), 1.16 (s, 6H).

¹³C NMR (126 MHz, CDCl₃) δ [ppm] = 169.6, 146.0, 128.9, 128.0, 127.6, 120.6, 120.0, 112.7, 111.8, 110.3, 103.6, 55.5, 46.5, 39.3, 30.8, 28.2, 20.9.

HRMS-ESI: calcd. for C₁₈H₂₀N₂O₂K [M + K]⁺: 335.1157; found: 335.1141.

FT-IR: ν [cm⁻¹] = 3312, 2957, 2928, 1662, 1644, 1452, 1394, 1359, 1294, 1233, 1219, 1135, 1040, 743.

9,10-Dimethoxy-2,2-dimethyl-2,3,6,7-tetrahydro-4*H*-pyrido[2,1-*a*]isoquinolin-4-one (2.58i)

2.58i was prepared according to the **General procedure D** starting from methyl ester **2.33i** (2.5 g, 7.42 mmol, 1.0 equiv.) and POCl₃ (677 μL, 7.42 mmol, 1.0 equiv.) in toluene (80 mL). The reaction mixture was subsequently treated with MeOH (80 mL), K₂CO₃ (10.3 mg, 74.2 mmol, 10 equiv.) and *n*Bu₄NBr (239 mg, 742 μmol, 0.1 equiv.). Purification by silica gel column chromatography (pentane/EtOAc = 3:2) afforded **2.58i** (1.65 g, 5.75 mmol, 78%) as a white solid.

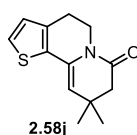
¹H NMR (500 MHz, CDCl₃) δ [ppm] = 7.02 (s, 1H), 6.61 (s, 1H), 5.47 (s, 1H), 3.91–3.89 (m, 5H), 3.88 (s, 3H), 2.77 (t, *J* = 5.9 Hz, 2H), 2.42 (s, 2H), 1.14 (s, 6H).

¹³C NMR (126 MHz, CDCl₃) δ [ppm] = 169.7, 149.3, 148.2, 133.2, 127.6, 122.3, 112.0, 110.8, 106.8, 56.2, 56.1, 46.0, 38.5, 30.5, 28.9, 28.2.

HRMS-ESI: calcd. for C₁₇H₂₁NO₃Na [M + Na]⁺: 310.1413; found: 310.1428.

FT-IR: ν [cm⁻¹] = 2964, 2934, 1775, 1645, 1516, 1388, 1358, 1287, 1263, 1234, 1198, 937.

9,9-Dimethyl-4,5,8,9-tetrahydro-7*H*-thieno[2,3-*a*]quinolizin-7-one (**2.58j**)



2.58j was prepared according to the **General procedure D** starting from methyl ester (270 mg, 0.954 mmol, 1.0 equiv.) and POCl₃ (87.1 μ L, 0.954 mmol, 1.0 equiv.) in toluene (10 mL). The reaction mixture was subsequently treated with MeOH (10 mL), K₂CO₃ (1.32 g, 9.54 mmol, 10 equiv.) and *n*Bu₄NBr (30.8 mg, 95.0 μ mol, 0.1 equiv.). Purification by silica gel column chromatography (pentane/EtOAc = 3:2) afforded **2.58j** (70.0 mg, 0.300 mmol, 31%) as a light brown solid.

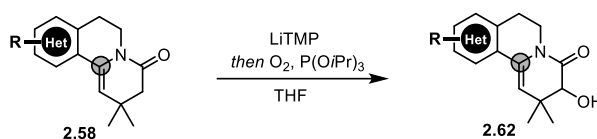
¹H NMR (500 MHz, CDCl₃) δ [ppm] = 7.10 (d, *J* = 5.1 Hz, 1H), 6.78 (dd, *J* = 5.1, 0.5 Hz, 1H), 5.35 (s, 1H), 3.97 (t, *J* = 6.0 Hz, 2H), 2.76 (t, *J* = 6.0 Hz, 2H), 2.41 (s, 2H), 1.11 (s, 6H).

¹³C NMR (126 MHz, CDCl₃) δ [ppm] = 169.3, 136.2, 131.2, 130.5, 127.4, 124.4, 112.1, 46.3, 38.6, 30.8, 28.0, 25.1.

HRMS-ESI: calcd. for C₁₃H₁₅NOSNa [M + Na]⁺: 256.0766; found: 256.0769.

FT-IR: ν [cm⁻¹] = 3286, 2956, 1664, 1641, 1452, 1395, 1295, 1233, 742.

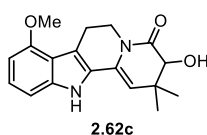
General procedure E



To a solution of tetracyclic lactam **2.58** (1.0 equiv.) in THF, was added LiTMP (10.0 equiv.) at -78 °C. The resulting mixture was stirred at that temperature for 1 h before P(O*i*Pr)₃ or P(OMe)₃

(2.5 equiv.) was added. O₂ was bubbled through the mixture for 20 min, and the mixture was stirred for additional 2 h under O₂ atmosphere. Then the reaction mixture was quenched with saturated NaHCO₃ (sat. aq.). The aqueous phase was extracted with DCM. The combined organic phases were washed with brine, dried over MgSO₄, filtered and concentrated under reduced pressure. The crude product was purified by silica gel column chromatography.

3-Hydroxy-8-methoxy-2,2-dimethyl-2,6,7,12-tetrahydroindolo[2,3-*a*]quinolizin-4(3*H*)-one (2.62c)



2.62c was prepared according to the **General procedure E** starting from enamide **2.58c** (100 mg, 0.338 mmol, 1.0 equiv.) and LiTMP (1.0 M in THF, 3.38 mL, 3.38 mmol, 10 equiv.) in THF (5.0 mL). After bubbled O₂, the reaction mixture was treated with P(O*i*Pr)₃ (209 μL, 0.845 mmol, 2.5 equiv.). Purification by silica gel column chromatography (pentane/EtOAc = 3:2) afforded **2.62c** (50.0 mg, 0.173 mmol, 51%) as a light yellow solid.

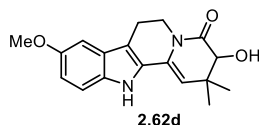
¹H NMR (500 MHz, CDCl₃) δ [ppm] = 7.96 (s, 1H), 7.12 (t, *J* = 8.0 Hz, 1H), 6.92 (d, *J* = 8.1 Hz, 1H), 6.49 (d, *J* = 7.8 Hz, 1H), 5.25 (s, 1H), 4.85–4.77 (m, 1H), 4.07 (s, 1H), 3.90 (s, 3H), 3.85 (s, 1H), 3.35–3.24 (m, 2H), 3.08–2.99 (m, 1H), 1.30 (s, 3H), 0.99 (s, 3H).

¹³C NMR (126 MHz, CDCl₃) δ [ppm] = 171.6, 155.1, 138.7, 127.7, 125.6, 124.9, 117.1, 112.6, 109.5, 104.3, 100.4, 75.0, 55.4, 41.0, 35.3, 26.5, 22.4, 19.9.

HRMS-ESI: calcd. for C₁₈H₂₀N₂O₃Na [M + Na]⁺: 335.1366; found: 335.1370.

FT-IR: ν [cm⁻¹] = 3321, 2969, 2926, 1738, 1654, 1454, 1364, 1229, 1217, 1150, 746.

3-Hydroxy-9-methoxy-2,2-dimethyl-2,6,7,12-tetrahydroindolo[2,3-*a*]quinolizin-4(3*H*)-one (2.62d)



2.62d was prepared according to the **General procedure E** starting from enamide **2.58d**

(400 mg, 1.35 mmol, 1.0 equiv.) and LiTMP (1.0 M in THF, 13.5 mL, 13.52 mmol, 10 equiv.) in THF (30 mL). After bubbled O₂, the reaction mixture was treated with P(OMe)₃ (1.00 mL, 4.05 mmol, 2.5 equiv.). Purification by silica gel column chromatography (pentane/EtOAc = 3:2) afforded **2.62d** (298 mg, 0.955 mmol, 71%) as a light yellow solid.

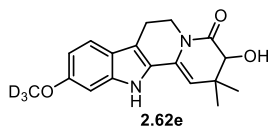
¹H NMR (500 MHz, CDCl₃) δ [ppm] = 8.06 (s, 1H), 7.22 (dd, *J* = 8.8, 0.6 Hz, 1H), 6.94 (d, *J* = 2.4 Hz, 1H), 6.89 (dd, *J* = 8.8, 2.5 Hz, 1H), 5.34 (s, 1H), 4.88 (ddd, *J* = 12.7, 5.1, 2.2 Hz, 1H), 4.11–4.06 (m, 1H), 3.87 (d, *J* = 2.5 Hz, 1H), 3.86 (s, 3H), 3.29 (dddd, *J* = 12.6, 11.4, 5.2, 1.0 Hz, 1H), 2.98–2.86 (m, 2H), 1.30 (s, 3H), 1.00 (s, 3H).

¹³C NMR (126 MHz, CDCl₃) δ [ppm] = 171.6, 154.6, 132.4, 127.9, 127.8, 127.1, 114.2, 112.1, 112.0, 110.3, 100.8, 74.9, 56.0, 40.7, 35.3, 26.4, 20.7, 19.8.

HRMS-ESI: calcd. for C₁₈H₂₀N₂O₃Na [M + Na]⁺: 335.1366; found: 335.1375.

FT-IR: ν [cm⁻¹] = 3322, 2959, 2923, 1652, 1536, 1456, 1217, 1173, 1034, 920, 752.

3-Hydroxy-10-(methoxy-*d*₃)-2,2-dimethyl-2,6,7,12-tetrahydroindolo[2,3-*a*]quinolizin-4(3*H*)-one (**2.62e**)



2.62e was prepared according to the **General procedure E** starting from enamide **2.58e** (35.0 mg, 0.117 mmol, 1.0 equiv.) and LiTMP (1.0 M in THF, 1.17 mL, 1.17 mmol, 10 equiv.) in THF (3.0 mL). After bubbled O₂, the reaction mixture was treated with P(O*i*Pr)₃ (72.5 μL, 0.293 mmol, 2.5 equiv.). Purification by silica gel column chromatography (pentane/EtOAc = 3:2) afforded **2.62e** (17.0 mg, 54.0 μmol, 46%) as a light yellow solid.

¹H NMR (700 MHz, CDCl₃) δ [ppm] = 7.96 (s, 1H), 7.37 (d, *J* = 8.6 Hz, 1H), 6.81 (d, *J* = 2.2 Hz, 1H), 6.78 (dd, *J* = 8.6, 2.2 Hz, 1H), 5.25 (s, 1H), 4.86 (ddd, *J* = 12.7, 5.4, 2.0 Hz, 1H), 4.07 (s, 1H), 3.85 (s, 1H), 3.28 (tdd, *J* = 12.7, 4.9, 1.0 Hz, 1H), 2.96–2.86 (m, 2H), 1.92–1.86 (m, 1H, impurity), 1.59 (s, 3H), 1.48–1.43 (m, 1H, impurity), 1.37–1.32 (m, 1H, impurity), 1.30 (s, 3H, impurity), 1.21 (s, 3H), 0.99 (s, 3H, impurity).

$^{13}\text{C NMR}$ (176 MHz, CDCl_3) δ [ppm] = 171.6, 157.9, 138.4, 127.8, 126.1, 121.2, 119.8, 112.5, 110.1, 109.3, 94.9, 88.4 (impurity), 75.0, 70.9 (impurity), 55.2–54.7 (m), 43.6 (impurity), 41.5 (impurity), 40.7, 35.3, 29.5 (impurity), 26.5, 26.0 (impurity), 20.7, 19.9, 19.2 (impurity).

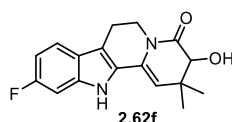
(Note: The impurity could not be removed after several purification by column chromatography. Because of the limited amount of the material, this material was used for next step reaction.

The resonances of the impurities were determined by the comparison with **2.62b**)

HRMS-ESI: calcd. for $\text{C}_{18}\text{H}_{17}\text{D}_3\text{N}_2\text{O}_3\text{Na}$ $[\text{M} + \text{Na}]^+$: 338.1554; found: 338.1566.

FT-IR: ν [cm^{-1}] = 3311, 2961, 2926, 1651, 1452, 1393, 1360, 1303, 1231, 1045, 920, 743.

10-Fluoro-3-hydroxy-2,2-dimethyl-2,6,7,12-tetrahydroindolo[2,3-*a*]quinolizin-4(3*H*)-one (2.62f)



2.62f was prepared according to the **General procedure E** starting from enamide **2.58f** (80.0 mg, 0.282 mmol, 1.0 equiv.) and LiTMP (1.0 M in THF, 2.82 mL, 2.82 mmol, 10 equiv.) in THF (10 mL). After bubbled O_2 , the reaction mixture was treated with $\text{P}(\text{O}i\text{Pr})_3$ (174 μL , 0.704 mmol, 2.5 equiv.). Purification by silica gel column chromatography (pentane/EtOAc = 3:2) afforded **2.62f** (53.0 mg, 0.177 mmol, 63%) as a light yellow solid.

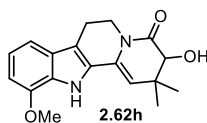
$^1\text{H NMR}$ (500 MHz, CDCl_3) δ [ppm] = 8.09 (s, 1H), 7.41 (dd, J = 8.6, 5.3 Hz, 1H), 7.01 (dd, J = 9.4, 2.2 Hz, 1H), 6.89 (td, J = 9.1, 2.3 Hz, 1H), 5.32 (s, 1H), 4.87 (ddd, J = 12.8, 5.2, 2.2 Hz, 1H), 4.08 (s, 1H), 3.84 (d, J = 2.3 Hz, 1H), 3.29 (td, J = 12.2, 5.0 Hz, 1H), 3.00–2.86 (m, 2H), 1.31 (s, 3H), 1.00 (s, 3H).

$^{13}\text{C NMR}$ (176 MHz, CDCl_3) δ [ppm] = 171.6, 161.1 (d, J = 240.5 Hz), 137.5 (d, J = 12.5 Hz), 127.6 (d, J = 3.7 Hz), 127.5, 123.4, 120.0 (d, J = 10.1 Hz), 112.3, 110.4, 109.2 (d, J = 24.6 Hz), 97.8 (d, J = 26.4 Hz), 74.9, 40.6, 35.4, 26.5, 20.6, 19.9.

$^{19}\text{F NMR}$ (565 MHz, CDCl_3) δ [ppm] = -117.86 (dd, J = 14.8, 9.1 Hz).

HRMS-ESI: calcd. for $\text{C}_{17}\text{H}_{17}\text{N}_2\text{O}_2\text{FNa}$ $[\text{M} + \text{Na}]^+$: 323.1166; found: 323.1176.

FT-IR: ν [cm^{-1}] = 3283, 2961, 2928, 1652, 1625, 1537, 1388, 1360, 1224, 1131, 1027, 754.

3-Hydroxy-11-methoxy-2,2-dimethyl-2,6,7,12-tetrahydroindolo[2,3-a]quinolizin-4(3H)-one (2.62h)

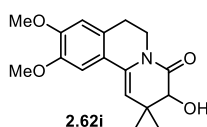
2.62h was prepared according to the **General procedure E** starting from enamide **2.58h** (99.0 mg, 0.334 mmol, 1.0 equiv.) and LiTMP (1.0 M in THF, 1.48 mL, 1.48 mmol, 10 equiv.) in THF (10 mL). After bubbled O₂, the reaction mixture was treated with P(O*i*Pr)₃ (207 μL, 0.836 mmol, 2.5 equiv.). Purification by silica gel column chromatography (pentane/EtOAc = 3:2) afforded **2.62h** (55.0 mg, 0.176 mmol, 53%) as a light yellow solid.

¹H NMR (500 MHz, CDCl₃) δ [ppm] = 8.23 (s, 1H), 7.12 (dd, *J* = 7.9, 1.6 Hz, 1H), 7.09–7.01 (m, 1H), 6.70 (dt, *J* = 7.7, 1.2 Hz, 1H), 5.38 (d, *J* = 2.4 Hz, 1H), 4.92–4.81 (m, 1H), 4.08 (d, *J* = 2.3 Hz, 1H), 4.01–3.93 (m, 3H), 3.85 (d, *J* = 2.7 Hz, 1H), 3.29 (dt, *J* = 5.0, 1.3 Hz, 1H), 3.03–2.86 (m, 2H), 1.31 (d, *J* = 1.8 Hz, 3H), 1.04–0.95 (m, 3H).

¹³C NMR (176 MHz, CDCl₃) δ [ppm] = 171.6, 146.0, 127.9, 127.7, 127.7, 126.8, 120.8, 112.7, 111.8, 110.3, 103.8, 74.9, 55.6, 40.8, 35.3, 26.5, 20.8, 19.9.

HRMS-ESI: calcd. for C₁₈H₂₁N₂O₃ [M + H]⁺: 313.1547; found: 313.1538.

FT-IR: ν [cm⁻¹] = 3313, 2961, 2926, 1653, 1452, 1360, 1231, 1150, 1045, 1027, 920, 744.

3-Hydroxy-11-methoxy-2,2-dimethyl-2,6,7,12-tetrahydroindolo[2,3-a]quinolizin-4(3H)-one (2.62i)

2.62i was prepared according to the **General procedure E** starting from enamide **2.58i** (1.10 g, 3.83 mmol, 1.0 equiv.) and LiTMP (1.0 M in THF, 38.3 mL, 38.3 mmol, 10 equiv.) in THF (50 mL). After bubbled O₂, the reaction mixture was treated with P(O*i*Pr)₃ (2.37 mL, 9.58 mmol, 2.5 equiv.). Purification by silica gel column chromatography (pentane/EtOAc = 3:2) afforded **2.62i** (490 mg, 1.60 mmol, 42%) as a yellow solid.

¹H NMR (700 MHz, CDCl₃) δ [ppm] = 7.03 (s, 1H), 6.61 (s, 1H), 5.53 (s, 1H), 4.36 (dt, *J* = 12.6, 4.8 Hz, 1H), 4.02 (d, *J* = 2.2 Hz, 1H), 3.92 (s, 3H), 3.89 (s, 3H), 3.76 (d, *J* = 2.4 Hz, 1H),

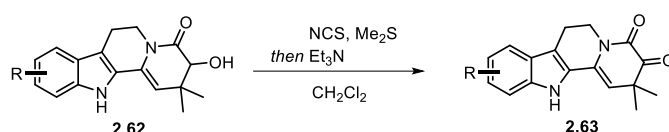
3.46 (dddd, $J = 12.6, 10.2, 4.0, 0.8$ Hz, 1H), 2.91–2.85 (m, 1H), 2.75 (dt, $J = 15.7, 4.4$ Hz, 1H), 1.31 (s, 3H), 0.97 (s, 3H).

^{13}C NMR (176 MHz, CDCl_3) δ [ppm] = 171.5, 149.7, 148.4, 132.0, 127.2, 121.5, 112.1, 111.0, 106.6, 74.8, 56.3, 56.1, 39.6, 35.2, 28.7, 26.6, 19.4.

HRMS-ESI: calcd. for $\text{C}_{17}\text{H}_{21}\text{NO}_4\text{Na}$ $[\text{M} + \text{Na}]^+$: 326.1363; found: 326.1379.

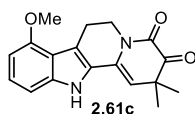
FT-IR: ν [cm^{-1}] = 2957, 2925, 2870, 1725, 1664, 1608, 1512, 1464, 1378, 1271, 1101, 764.

General procedure F



To a solution of NCS (5.0 equiv.) in DCM at 0 °C was added Me_2S (25 equiv.) and the mixture was stirred at -78 °C for 1 h. The solution of α -hydroxylenamide (1.0 equiv.) in DCM was added dropwise. The resulting mixture was stirred at -78 °C for another 2 h before Et_3N (20 equiv.) was added. Then the mixture was stirred at -78 °C for 2 h. The mixture was quenched with NH_4Cl (sat. aq.) and extracted with DCM. The combined organic phases were washed with brine, dried over MgSO_4 , filtered and concentrated under reduced pressure. The crude product was purified by silica gel column chromatography.

8-Methoxy-2,2-dimethyl-2,6,7,12-tetrahydroindolo[2,3-*a*]quinolizine-3,4-dione (2.63c)



2.63c was prepared according to the **General procedure F** starting from NCS (214 mg, 1.60 mmol, 5.0 equiv.) and Me_2S (588 μL , 8.01 mmol, 25 equiv.). After the addition of **2.62c** (100 mg, 0.321 mmol, 1.0 equiv.), the reaction mixture was treated with Et_3N (889 μL , 6.41 mmol, 20 equiv.). Purification by silica gel column chromatography (pentane/ $\text{EtOAc} = 3:2$) afforded **2.63c** (60.0 mg, 0.194 mmol, 60%) as a yellow solid.

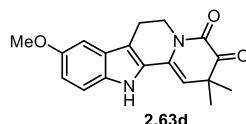
^1H NMR (500 MHz, CDCl_3) δ [ppm] = 8.00 (s, 1H), 7.14 (t, $J = 8.0$ Hz, 1H), 6.94 (dd, $J = 8.2, 0.6$ Hz, 1H), 6.50 (d, $J = 7.8$ Hz, 1H), 5.29 (s, 1H), 4.17 (t, $J = 6.0$ Hz, 2H), 3.92 (s, 3H), 3.24 (t, $J = 6.0$ Hz, 2H), 1.39 (s, 6H).

^{13}C NMR (176 MHz, CDCl_3) δ [ppm] = 196.0, 157.3, 155.2, 138.9, 127.0, 125.3, 125.3, 117.0, 113.2, 106.1, 104.4, 100.5, 55.4, 44.9, 40.7, 25.0, 22.1.

HRMS-ESI: calcd. for $\text{C}_{18}\text{H}_{18}\text{N}_2\text{O}_3\text{Na}$ [$\text{M} + \text{Na}$] $^+$: 333.1210; found: 333.1210.

FT-IR: ν [cm^{-1}] = 3340, 2968, 2924, 1726, 1656, 1452, 1403, 1304, 1235, 1065, 750.

9-Methoxy-2,2-dimethyl-2,6,7,12-tetrahydroindolo[2,3-*a*]quinolizine-3,4-dione (2.63d)



2.63d was prepared according to the **General procedure F** starting from NCS (214 mg, 1.60 mmol, 5.0 equiv.) and Me_2S (588 μL , 8.01 mmol, 25 equiv.). After the addition of **2.62d** (100 mg, 0.321 mmol, 1.0 equiv.), the reaction mixture was treated with Et_3N (889 μL , 6.41 mmol, 20 equiv.). Purification by silica gel column chromatography (pentane/ EtOAc = 3:2) afforded **2.63d** (65.0 mg, 0.210 mmol, 65%) as a yellow solid.

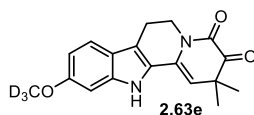
^1H NMR (700 MHz, CDCl_3) δ [ppm] = 7.85 (s, 1H), 7.24 (dt, J = 8.9, 0.9 Hz, 1H), 6.95 (d, J = 2.5 Hz, 1H), 6.93–6.91 (m, 1H), 5.32 (s, 1H), 4.25–4.19 (m, 2H), 3.86 (s, 3H), 2.99 (t, J = 6.0 Hz, 2H), 1.39 (s, 6H).

^{13}C NMR (126 MHz, CDCl_3) δ [ppm] = 195.9, 157.3, 154.8, 132.6, 127.6, 127.1, 127.0, 114.7, 112.8, 112.2, 106.9, 100.8, 56.0, 44.9, 40.6, 25.0, 20.4.

HRMS-ESI: calcd. for $\text{C}_{18}\text{H}_{18}\text{N}_2\text{O}_3\text{Na}$ [$\text{M} + \text{Na}$] $^+$: 333.1210; found: 333.1208.

FT-IR: ν [cm^{-1}] = 2955, 2922, 2869, 1725, 1677, 1491, 1458, 1378, 1263, 1217, 1099, 730.

10-(Methoxy-*d*₃)-2,2-dimethyl-2,6,7,12-tetrahydroindolo[2,3-*a*]quinolizine-3,4-dione (2.63e)



2.63e was prepared according to the **General procedure F** starting from NCS (35.7 mg, 0.268 mmol, 5.0 equiv.) and Me_2S (98.2 μL , 1.34 mmol, 25 equiv.). After the addition of **2.62e** (16.0 mg, 54.0 μmol , 1.0 equiv.), the reaction mixture was treated with Et_3N (148 μL , 1.07 mmol, 20 equiv.). Purification by silica gel column chromatography (pentane/ EtOAc = 3:2)

afforded **2.63e** (12.0 mg, 40.4 μmol , 76%) as a yellow solid.

^1H NMR (700 MHz, CDCl_3) δ [ppm] = 7.96 (s, 1H), 7.40 (dt, $J = 8.6, 0.6$ Hz, 1H), 6.83 (dd, $J = 2.2, 0.6$ Hz, 1H), 6.80 (dd, $J = 8.6, 2.2$ Hz, 1H), 5.27 (s, 1H), 4.55 (s, 1H, impurity), 4.20 (t, $J = 6.0$ Hz, 2H), 2.98 (t, $J = 6.0$ Hz, 2H), 2.75 (s, 1H, impurity), 2.25 (s, 1H, impurity), 2.17 (s, 3H, impurity), 1.39 (s, 6H).

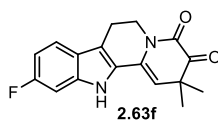
^{13}C NMR (176 MHz, CDCl_3) δ [ppm] = 207.1 (impurity), 196.0, 176.5 (impurity), 158.2, 157.4, 138.7, 127.1, 125.8, 121.0, 120.1, 113.2, 110.4, 105.8, 94.9, 44.9, 41.7 (impurity), 40.4, 31.1 (impurity), 28.3 (impurity), 25.0, 20.4, 16.5(impurity).

(Note: The impurity could not be removed after several purification by column chromatography. Because of the limitation of material, we used this material for next step. The resonances of the impurities were determined by the comparison with **2.63b**. Additionally, the carbon resonance of CD_3 was not detected, probably due to the signal intensity.)

HRMS-EI: calcd. for $\text{C}_{18}\text{H}_{15}\text{D}_3\text{N}_2\text{O}_3\text{Na}$ $[\text{M} + \text{Na}]^+$: 336.1398; found: 336.1412.

FT-IR: ν [cm^{-1}] = 2954, 2920, 2850, 1721, 1461, 1377, 1278, 1264, 1122, 1098, 972, 729.

10-Fluoro-2,2-dimethyl-2,6,7,12-tetrahydroindolo[2,3-*a*]quinolizine-3,4-dione (**2.63f**)



2.63f was prepared according to the **General procedure F** starting from NCS (84.6 mg, 0.633 mmol, 5.0 equiv.) and Me_2S (233 μL , 3.17 mmol, 25 equiv.). After the addition of **2.62f** (38.0 mg, 127 μmol , 1.0 equiv.), the reaction mixture was treated with Et_3N (352 μL , 2.53 mmol, 20 equiv.). Purification by silica gel column chromatography (pentane/ $\text{EtOAc} = 3:2$) afforded **2.63f** (37.0 mg, 124 μmol , 98%) as a yellow solid.

^1H NMR (600 MHz, d_6 -DMSO) δ [ppm] = 11.49 (s, 1H), 7.52 (dd, $J = 8.7, 5.5$ Hz, 1H), 7.12 (dd, $J = 10.0, 2.3$ Hz, 1H), 6.89 (ddd, $J = 9.8, 8.6, 2.3$ Hz, 1H), 5.77 (s, 1H), 4.06 (t, $J = 6.0$ Hz, 2H), 2.94 (t, $J = 6.1$ Hz, 2H), 1.30 (s, 6H).

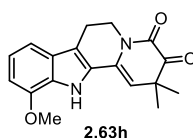
^{13}C NMR (151 MHz, d_6 -DMSO) δ [ppm] = 196.5, 160.4 (d, $J = 237.0$ Hz), 157.1, 138.0 (d, $J = 13.2$ Hz), 128.5, 126.9, 123.2, 120.6 (d, $J = 10.3$ Hz), 111.5, 108.3 (d, $J = 24.6$ Hz), 107.9, 98.0 (d, $J = 25.7$ Hz), 55.5, 44.9, 24.8, 20.1.

^{19}F NMR (565 MHz, d_6 -DMSO) δ [ppm] = -118.96 (td, J = 10.5, 5.5 Hz).

HRMS-ESI: calcd. for $\text{C}_{17}\text{H}_{15}\text{FN}_2\text{O}_4\text{K}$ [$\text{M} + \text{K}$] $^+$: 337.0750; found: 337.0766.

FT-IR: ν [cm^{-1}] = 3339, 2929, 1731, 1655, 1403, 1255, 1228, 1131, 956, 754.

11-Methoxy-2,2-dimethyl-2,6,7,12-tetrahydroindolo[2,3-*a*]quinolizine-3,4-dione (**2.63h**)



2.63h was prepared according to the **General procedure F** starting from NCS (188 mg, 1.41 mmol, 5.0 equiv.) and Me_2S (518 μL , 7.05 mmol, 25 equiv.). After the addition of **2.62h** (88.0 mg, 282 μmol , 1.0 equiv.), the reaction mixture was treated with Et_3N (783 μL , 5.64 mmol, 20 equiv.). Purification by silica gel column chromatography (pentane/ EtOAc = 3:2) afforded **2.63h** (70.0 mg, 226 μmol , 80%) as a yellow solid.

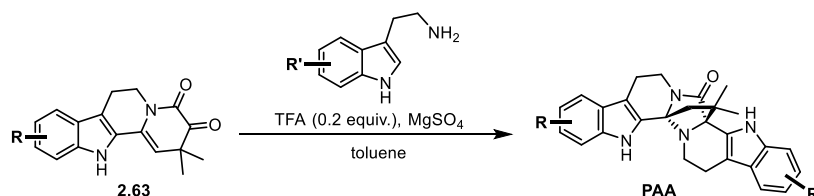
^1H NMR (700 MHz, CDCl_3) δ [ppm] = 8.21 (s, 1H), 7.14 (dt, J = 8.0, 0.7 Hz, 1H), 7.07 (t, J = 7.8 Hz, 1H), 6.72 (dd, J = 7.8, 0.8 Hz, 1H), 5.39 (s, 1H), 4.20 (t, J = 6.0 Hz, 2H), 3.97 (s, 3H), 3.00 (t, J = 6.0 Hz, 2H), 1.39 (s, 6H).

^{13}C NMR (176 MHz, CDCl_3) δ [ppm] = 195.9, 157.3, 146.1, 128.0, 127.7, 127.0, 126.6, 121.0, 113.3, 112.0, 106.9, 104.1, 55.6, 44.9, 40.6, 24.9, 20.5.

HRMS-ESI: calcd. for $\text{C}_{18}\text{H}_{19}\text{N}_2\text{O}_3$ [$\text{M} + \text{H}$] $^+$: 311.1390; found: 311.1389.

FT-IR: ν [cm^{-1}] = 3708, 2924, 2853, 1736, 1365, 1227, 1217, 743.

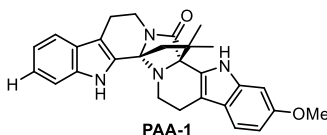
General procedure G



To a mixture of α -ketoamide **2.63** (1.0 equiv.), amine (1.2 equiv.) and MgSO_4 (10.0 equiv.) in toluene under argon atmosphere, was added TFA (0.2 equiv.). The resulting reaction mixture was heated to 115 $^\circ\text{C}$ (oil bath temperature) for 2 days. Then the reaction was cooled down to room temperature and quenched with NaHCO_3 (sat. aq.). The aqueous phase was extracted with

DCM. The combined organic phases were washed with brine, dried over MgSO_4 , filtered and concentrated under reduced pressure. The crude product was purified by silica gel column chromatography.

PAA-1



PAA-1 was prepared according to the **General procedure G** starting from α -ketoenamide **2.63a** (23.0 mg, 82.0 μmol , 1.0 equiv.) 6-methoxytryptamine (18.7 mg, 99.0 μmol , 1.2 equiv.) and MgSO_4 (98.9 mg, 821 μmol , 10.0 equiv.). The reaction mixture was treated with TFA (1.3 μL , 16 μmol , 0.2 equiv.). Purification by silica gel column chromatography (pentane/EtOAc = 3:2) afforded **PAA-1** (8.3 mg, 18.4 μmol , 22%) as a light yellow solid.

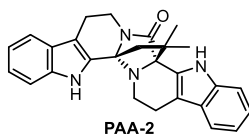
$^1\text{H NMR}$ (500 MHz, CD_3OD) δ [ppm] = 7.51 (dt, $J = 7.9, 1.1$ Hz, 1H), 7.42–7.36 (m, 1H), 7.25 (d, $J = 8.6$ Hz, 1H), 7.16 (ddd, $J = 8.2, 7.1, 1.2$ Hz, 1H), 7.05 (ddd, $J = 8.1, 7.1, 1.0$ Hz, 1H), 6.97 (d, $J = 2.3$ Hz, 1H), 6.66 (dd, $J = 8.6, 2.3$ Hz, 1H), 4.18–4.10 (m, 1H), 3.81 (s, 3H), 3.18 (ddd, $J = 13.0, 11.7, 4.7$ Hz, 1H), 3.01 (ddd, $J = 15.4, 4.7, 1.1$ Hz, 1H), 2.90–2.76 (m, 2H), 2.66 (ddd, $J = 15.2, 4.1, 1.5$ Hz, 1H), 2.55 (ddd, $J = 10.8, 5.6, 1.5$ Hz, 1H), 2.44 (dd, $J = 11.2, 4.1$ Hz, 1H), 2.40 (d, $J = 11.4$ Hz, 1H), 1.94 (d, $J = 11.5$ Hz, 1H), 1.43 (s, 3H), 1.24 (s, 3H).

$^{13}\text{C NMR}$ (126 MHz, CD_3OD) δ [ppm] = 175.2, 157.6, 139.4, 138.8, 127.9, 127.741, 127.737, 123.5, 122.3, 120.3, 119.4, 119.2, 112.9, 112.5, 112.2, 109.8, 96.0, 81.2, 79.7, 56.0, 52.0, 41.7, 41.6, 37.3, 27.3, 26.3, 22.5, 22.1.

HRMS-ESI: calcd. for $\text{C}_{28}\text{H}_{28}\text{N}_4\text{O}_2\text{Na}$ [$\text{M} + \text{Na}$] $^+$: 475.2104; found: 475.2106.

FT-IR: ν [cm^{-1}] = 2926, 2863, 1738, 1456, 1367, 1228, 1216, 750.

PAA-2



PAA-2 was prepared according to the **General procedure G** starting from α -ketoenamide **2.63a** (900 mg, 3.21 mmol, 1.0 equiv.) tryptamine (617 mg, 3.86 mmol, 1.2 equiv.) and MgSO_4

(3.87 g, 32.1 mmol, 10.0 equiv.). The reaction mixture was treated with TFA (49.2 μL , 643 μmol , 0.2 equiv.). Purification by silica gel column chromatography (pentane/EtOAc = 3:2) afforded **PAA-2** (640 mg, 1.52 mmol, 47%) as a light yellow solid.

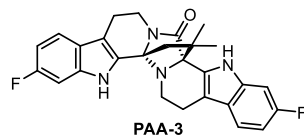
$^1\text{H NMR}$ (500 MHz, d_6 -DMSO) δ [ppm] = 11.44 (s, 1H), 10.97 (s, 1H), 7.52 (d, J = 7.9 Hz, 1H), 7.44–7.35 (m, 3H), 7.15 (ddd, J = 8.2, 7.0, 1.2 Hz, 1H), 7.10–7.02 (m, 2H), 6.99–6.94 (m, 1H), 4.04 (dd, J = 12.9, 5.8 Hz, 1H), 3.16–3.10 (m, 1H), 2.96 (dd, J = 15.2, 4.3 Hz, 1H), 2.81–2.68 (m, 3H), 2.48–2.46 (m, 1H), 2.41–2.32 (m, 2H), 1.93 (d, J = 11.2 Hz, 1H), 1.41 (s, 3H), 1.16 (s, 3H).

$^{13}\text{C NMR}$ (126 MHz, d_6 -DMSO) δ [ppm] = 171.7, 137.3, 137.3, 129.2, 127.7, 126.5, 126.4, 122.5, 121.3, 119.7, 119.4, 118.9, 118.2, 112.1, 112.0, 111.7, 110.1, 79.3, 78.0, 50.9, 40.6, 40.4, 36.1, 27.3, 26.5, 21.5, 21.4.

HRMS-ESI: calcd. for $\text{C}_{27}\text{H}_{26}\text{N}_4\text{ONa}$ [$\text{M} + \text{Na}$] $^+$: 445.1999; found: 445.2000.

FT-IR: ν [cm^{-1}] = 3307, 3267, 2922, 2857, 1704, 1451, 1410, 1320, 1302, 1270, 1168, 1146, 1039, 742.

PAA-3



PAA-3 was prepared according to the **General procedure G** starting from α -ketoamide **2.63f** (26.0 mg, 87.0 μmol , 1.0 equiv.) 6-fluorotryptamine (18.6 mg, 105 μmol , 1.2 equiv.) and MgSO_4 (105 mg, 872 μmol , 10.0 equiv.). The reaction mixture was treated with TFA (1.3 μL , 17 μmol , 0.2 equiv.). Purification by silica gel column chromatography (pentane/EtOAc = 3:2) afforded **PAA-3** (12.0 mg, 26.2 μmol , 30%) as a light yellow solid.

$^1\text{H NMR}$ (500 MHz, CD_3OD) δ [ppm] = 7.48 (dd, J = 8.7, 5.3 Hz, 1H), 7.33 (dd, J = 8.6, 5.3 Hz, 1H), 7.10 (td, J = 10.1, 2.3 Hz, 2H), 6.85 (ddd, J = 9.7, 8.6, 2.3 Hz, 1H), 6.77 (ddd, J = 9.8, 8.6, 2.4 Hz, 1H), 4.15 (ddd, J = 13.1, 6.0, 1.1 Hz, 1H), 3.19 (ddd, J = 13.0, 11.6, 4.6 Hz, 1H), 3.01 (ddd, J = 15.5, 4.6, 1.1 Hz, 1H), 2.92–2.78 (m, 2H), 2.75–2.68 (m, 1H), 2.57 (ddd, J = 10.8, 5.6, 1.6 Hz, 1H), 2.48–2.41 (m, 1H), 2.39 (d, J = 11.5 Hz, 1H), 1.96 (d, J = 11.5 Hz, 1H), 1.44 (s, 3H), 1.23 (s, 3H).

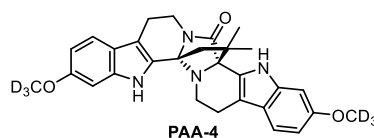
^{13}C NMR (126 MHz, CD_3OD) δ [ppm] = 174.9, 162.4 (d, $J = 66.7$ Hz), 160.5 (d, $J = 65.0$ Hz), 138.7, 138.6, 129.5, 128.4, 124.5, 124.5, 120.4 (d, $J = 10.3$ Hz), 119.5 (d, $J = 10.4$ Hz), 113.2, 112.4, 108.8 (d, $J = 24.9$ Hz), 108.2 (d, $J = 24.8$ Hz), 98.6, 98.4, 81.1, 79.7, 51.9, 41.7, 41.6, 37.2, 27.3, 26.2, 22.4, 22.0.

^{19}F NMR (471 MHz, CD_3OD) δ [ppm] = -122.69, -124.36.

HRMS-ESI: calcd. for $\text{C}_{27}\text{H}_{24}\text{F}_2\text{N}_4\text{ONa}$ [$\text{M} + \text{Na}$] $^+$: 481.1810; found: 481.1813.

FT-IR: ν [cm^{-1}] = 3427, 3297, 2953, 2922, 1684, 1450, 1410, 1347, 1319, 1301, 1269, 736.

PAA-4



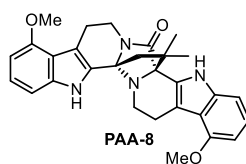
PAA-4 was prepared according to the **General procedure G** starting from α -ketoenamide **2.63e** (7.0 mg, 22 μmol , 1.0 equiv.) 2-(6-(methoxy- d_3)-1*H*-indol-3-yl)ethan-1-amine (5.2 mg, 27 μmol , 1.2 equiv.) and MgSO_4 (31.8 mg, 224 μmol , 10.0 equiv.). The reaction mixture was treated with TFA (0.3 μL , 4 μmol , 0.2 equiv.). Purification by silica gel column chromatography (pentane/EtOAc = 3:2) afforded **PAA-4** (3.0 mg, 6.1 μmol , 27%) as a light yellow solid.

^1H NMR (600 MHz, d_6 -DMSO) δ [ppm] = 11.24 (s, 1H), 10.77 (s, 1H), 7.38 (d, $J = 8.6$ Hz, 1H), 7.25 (d, $J = 8.5$ Hz, 1H), 6.92 (d, $J = 2.3$ Hz, 1H), 6.87 (d, $J = 2.2$ Hz, 1H), 6.69 (dd, $J = 8.6, 2.3$ Hz, 1H), 6.63 (dd, $J = 8.5, 2.3$ Hz, 1H), 4.04–3.96 (m, 1H), 3.14 – 3.05 (m, 1H), 2.94–2.86 (m, 1H), 2.72 (ddd, $J = 14.9, 11.5, 5.9$ Hz, 1H), 2.67 (dd, $J = 10.2, 5.1$ Hz, 1H), 2.66–2.60 (m, 1H), 2.45 (ddd, $J = 10.7, 5.3, 1.8$ Hz, 1H), 2.34 (dt, $J = 11.2, 5.6$ Hz, 1H), 2.30 (d, $J = 11.2$ Hz, 1H), 1.88 (d, $J = 11.2$ Hz, 1H), 1.38 (s, 3H), 1.15 (s, 3H).

^{13}C NMR (151 MHz, d_6 -DMSO) δ [ppm] = 171.4, 156.1, 155.4, 137.6, 137.5, 133.5, 129.6, 127.3, 125.7, 120.5, 120.4, 119.0, 118.2, 111.2, 109.5, 109.0, 108.3, 94.9, 94.7, 78.8, 77.4, 54.4, 50.4, 40.1, 35.6, 26.8, 26.0, 21.0, 20.9.

HRMS-ESI: calcd. for $\text{C}_{29}\text{H}_{24}\text{D}_6\text{N}_4\text{O}_3\text{Na}$ [$\text{M} + \text{Na}$] $^+$: 511.2587; found: 511.2563.

FT-IR: ν [cm^{-1}] = 3300, 3292, 2918, 2849, 1683, 1451, 1410, 1320, 1302, 1217, 1168, 739.

PAA-8

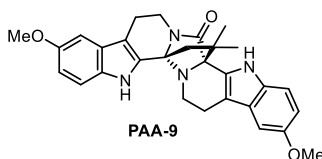
PAA-8 was prepared according to the **General procedure G** starting from α -ketoenamide **2.63c** (25.0 mg, 81.0 μ mol, 1.0 equiv.) 4-methoxytryptamine (15.5 mg, 97.0 μ mol, 1.2 equiv.) and MgSO_4 (97.1 mg, 806 μ mol, 10.0 equiv.). The reaction mixture was treated with TFA (1.2 μ L, 16 μ mol, 0.2 equiv.). Purification by silica gel column chromatography (pentane/EtOAc = 3:2) afforded **PAA-8** (15.0 mg, 33.2 μ mol, 41%) as a light yellow solid.

$^1\text{H NMR}$ (600 MHz, d_6 -DMSO) δ [ppm] = 11.40 (s, 1H), 10.89 (s, 1H), 7.05–7.00 (m, 2H), 6.99–6.93 (m, 2H), 6.49 (dd, J = 7.8, 0.8 Hz, 1H), 6.43 (dd, J = 7.9, 0.8 Hz, 1H), 4.00–3.94 (m, 1H), 3.84 (s, 3H), 3.78 (s, 3H), 3.24–3.18 (m, 1H), 3.09 (td, J = 12.5, 4.4 Hz, 1H), 2.96–2.91 (m, 1H), 2.90–2.79 (m, 2H), 2.44–2.40 (m, 1H), 2.33 (dd, J = 11.4, 4.2 Hz, 1H), 2.30 (d, J = 11.2 Hz, 1H), 1.88 (d, J = 11.2 Hz, 1H), 1.38 (s, 3H), 1.14 (s, 3H).

$^{13}\text{C NMR}$ (151 MHz, d_6 -DMSO) δ [ppm] = 171.4, 154.1, 153.7, 138.1, 129.6, 128.9, 128.2, 126.8, 125.3, 122.8, 121.6, 116.1, 110.9, 109.3, 105.0, 99.3, 98.8, 78.6, 77.3, 55.1, 54.9, 50.5, 40.5, 35.7, 28.0, 26.8, 26.0, 23.2, 23.1.

HRMS-ESI: calcd. for $\text{C}_{29}\text{H}_{30}\text{N}_4\text{O}_3\text{Na}$ [$\text{M} + \text{Na}$] $^+$: 505.2210; found: 505.2203.

FT-IR: ν [cm^{-1}] = 3302, 3285, 2969, 2953, 1739, 1684, 1450, 1410, 1364, 1228, 1217, 741.

PAA-9

PAA-9 was prepared according to the **General procedure G** starting from ketoenamide **2.63d** (35.0 mg, 113 μ mol, 1.0 equiv.) 5-methoxytryptamine (25.7 mg, 135 μ mol, 1.2 equiv.) and MgSO_4 (136 mg, 1.13 μ mol, 10.0 equiv.). The reaction mixture was treated with TFA (1.7 μ L, 23 μ mol, 0.2 equiv.). Purification by silica gel column chromatography (pentane/EtOAc = 3:2) afforded **PAA-9** (33.0 mg, 86.4 μ mol, 76%) as a light yellow solid.

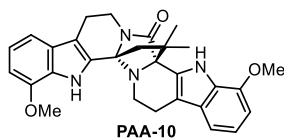
$^1\text{H NMR}$ (700 MHz, d_6 -DMSO) δ [ppm] = 11.25 (s, 1H), 10.78 (s, 1H), 7.29 (t, J = 9.0 Hz, 2H), 7.01 (d, J = 2.5 Hz, 1H), 6.88 (d, J = 2.4 Hz, 1H), 6.79 (dd, J = 8.7, 2.5 Hz, 1H), 6.72 (dd, J = 8.8, 2.4 Hz, 1H), 4.06–4.00 (m, 1H), 3.77 (s, 3H), 3.73 (s, 3H), 3.16–3.08 (m, 1H), 2.98–2.89 (m, 1H), 2.74 (ddd, J = 15.2, 11.7, 6.0 Hz, 1H), 2.70–2.63 (m, 2H), 2.46 (ddd, J = 10.8, 5.1, 2.0 Hz, 1H), 2.35 (td, J = 10.8, 5.1 Hz, 1H), 2.31 (d, J = 11.2 Hz, 1H), 1.91 (d, J = 11.3 Hz, 1H), 1.39 (s, 3H), 1.15 (s, 3H).

$^{13}\text{C NMR}$ (176 MHz, d_6 -DMSO) δ [ppm] = 171.2, 153.4, 153.1, 131.9, 129.3, 127.8, 126.3, 126.2, 112.3, 112.2, 112.1, 111.0, 110.8, 109.5, 100.3, 99.7, 78.8, 77.5, 55.4, 55.3, 50.4, 40.01, 39.97, 35.6, 26.8, 26.0, 21.1, 21.0. (A carbon resonance is missing, probably due to overlapping.)

HRMS-ESI: calcd. for $\text{C}_{29}\text{H}_{30}\text{N}_4\text{O}_3\text{Na}$ [$\text{M} + \text{Na}$] $^+$: 505.2210; found: 505.2225.

FT-IR: ν [cm^{-1}] = 3432, 3308, 3298, 1686, 1453, 1412, 1320, 1169, 760, 739.

PAA-10



PAA-10 was prepared according to the **General procedure G** starting from α -ketoenamide **2.63h** (27.0 mg, 87.0 μmol , 1.0 equiv.) 7-methoxytryptamine (19.9 mg, 105 μmol , 1.2 equiv.) and MgSO_4 (105 mg, 871 μmol , 10.0 equiv.). The reaction mixture was treated with TFA (1.3 μL , 17 μmol , 0.2 equiv.). Purification by silica gel column chromatography (pentane/EtOAc = 3:2) afforded **PAA-10** (23.0 mg, 47.7 μmol , 55%) as a light yellow solid.

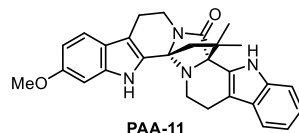
$^1\text{H NMR}$ (700 MHz, CD_3OD) δ [ppm] = 7.10 (d, J = 7.9 Hz, 1H), 7.02–6.96 (m, 2H), 6.93 (t, J = 7.8 Hz, 1H), 6.70 (d, J = 7.8 Hz, 1H), 6.66 (d, J = 7.7 Hz, 1H), 4.12 (dd, J = 13.0, 5.9 Hz, 1H), 3.97 (s, 3H), 3.96 (s, 3H), 3.19–3.14 (m, 1H), 2.97 (dt, J = 15.2, 4.7 Hz, 1H), 2.87–2.78 (m, 2H), 2.71–2.65 (m, 1H), 2.55 (dd, J = 10.8, 5.6 Hz, 1H), 2.47 (dd, J = 11.6, 3.6 Hz, 1H), 2.40 (td, J = 11.6, 11.1, 4.7 Hz, 1H), 1.90 (d, J = 11.0 Hz, 1H), 1.42 (s, 3H), 1.22 (s, 3H).

$^{13}\text{C NMR}$ (176 MHz, CD_3OD) δ [ppm] = 175.0, 148.0, 147.7, 129.3, 129.0, 128.9, 128.8, 128.6, 127.4, 120.9, 120.7, 113.39, 113.36, 112.1, 111.8, 103.7, 103.1, 81.4, 79.7, 55.82, 55.77, 51.7, 41.9, 41.5, 37.3, 27.2, 26.5, 22.6, 22.2.

HRMS-ESI: calcd. for $\text{C}_{29}\text{H}_{30}\text{N}_4\text{O}_3\text{K}$ [$\text{M} + \text{K}$] $^+$: 521.1950; found: 521.1966.

FT-IR: ν [cm^{-1}] = 3370, 3359, 2924, 2853, 1773, 1697, 1409, 1381, 1320, 1284, 1159, 748.

PAA-11



PAA-11 was prepared according to the **General procedure G** starting from α -ketoenamide **2.63b** (25.0 mg, 81.0 μmol , 1.0 equiv.) tryptamine (15.5 mg, 97.0 μmol , 1.2 equiv.) and MgSO_4 (97.1 mg, 806 μmol , 10.0 equiv.). The reaction mixture was treated with TFA (1.2 μL , 16 μmol , 0.2 equiv.). Purification by silica gel column chromatography (pentane/EtOAc = 3:2) afforded **PAA-11** (15.0 mg, 33.2 μmol , 41%) as a light yellow solid.

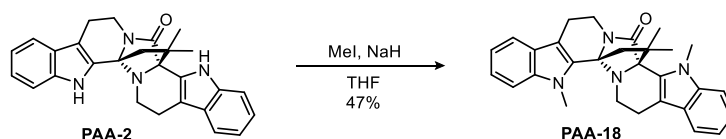
^1H NMR (500 MHz, CD_3OD) δ [ppm] = 7.43 (dt, J = 8.2, 0.9 Hz, 1H), 7.41–7.36 (m, 2H), 7.09 (ddd, J = 8.2, 7.1, 1.1 Hz, 1H), 6.99 (ddd, J = 8.0, 7.0, 1.0 Hz, 1H), 6.93 (d, J = 2.2 Hz, 1H), 6.73 (dd, J = 8.6, 2.3 Hz, 1H), 4.17–4.10 (m, 1H), 3.83 (s, 3H), 3.24–3.14 (m, 1H), 2.98 (dd, J = 15.7, 4.1 Hz, 1H), 2.90–2.79 (m, 2H), 2.78–2.70 (m, 1H), 2.61 (ddd, J = 9.6, 5.6, 1.7 Hz, 1H), 2.45 (td, J = 11.3, 4.1 Hz, 1H), 2.40 (dd, J = 11.5, 1.8 Hz, 1H), 1.95 (d, J = 11.5 Hz, 1H), 1.45 (s, 3H), 1.24 (s, 3H).

^{13}C NMR (126 MHz, CD_3OD) δ [ppm] = 175.1, 158.4, 139.6, 138.7, 129.1, 127.7, 126.4, 122.4, 122.2, 120.0, 119.9, 118.7, 113.0, 112.4, 112.3, 110.5, 95.7, 81.3, 79.7, 56.0, 51.9, 41.8, 41.6, 37.3, 27.3, 26.3, 22.5, 22.1.

HRMS-ESI: calcd. for $\text{C}_{28}\text{H}_{28}\text{N}_4\text{O}_2\text{Na}$ [$\text{M} + \text{Na}$] $^+$: 475.2104; found: 475.2106.

FT-IR: ν [cm^{-1}] = 3278, 2953, 2924, 2853, 1707, 1602, 1455, 1396, 1386, 1267, 1100, 754.

PAA-18



To a solution of **PAA-18** (30.0 mg, 71.0 μmol , 1.0 equiv.) in DMF (5.0 mL) was added NaH (60% dispersion mineral oil, 1.2 mg, 178 μmol , 2.5 equiv.) at 0 $^\circ\text{C}$. The reaction mixture was stirred for 30 min, before the addition of MeI (11.0 μl , 178 mmol, 2.5 equiv.) The resulting

mixture was stirred overnight and then quenched with NaHCO_3 (sat. aq.). The mixture was extracted with DCM. The combined organic phases were washed with brine, dried over MgSO_4 , filtered and concentrated under reduced pressure. The crude product was purified by silica gel column chromatography (pentane/EtOAc = 15:1) to afford **PAA-18** (15.0 mg, 33.3 μmol , 47%) as a white solid.

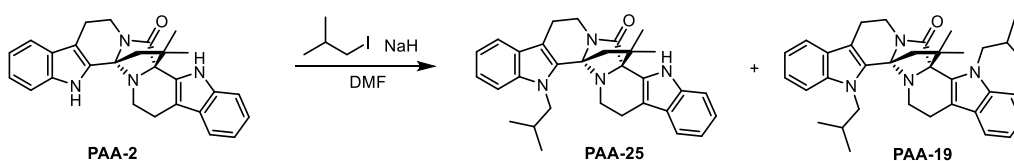
$^1\text{H NMR}$ (700 MHz, CDCl_3) δ [ppm] = 7.57 (dt, $J = 7.8, 1.0$ Hz, 1H), 7.48 (dt, $J = 7.8, 1.0$ Hz, 1H), 7.38 (dt, $J = 8.3, 0.9$ Hz, 1H), 7.35 (dt, $J = 8.3, 0.9$ Hz, 1H), 7.31 (ddd, $J = 8.3, 7.1, 1.2$ Hz, 1H), 7.24 (ddd, $J = 8.3, 7.0, 1.2$ Hz, 1H), 7.18 (ddd, $J = 7.9, 7.1, 1.0$ Hz, 1H), 7.10 (ddd, $J = 7.9, 7.0, 0.9$ Hz, 1H), 4.25 (ddd, $J = 13.0, 6.2, 1.2$ Hz, 1H), 4.08 (s, 3H), 3.93 (s, 3H), 3.16 (ddd, $J = 12.9, 11.6, 4.9$ Hz, 1H), 3.02 (ddd, $J = 15.4, 4.9, 1.2$ Hz, 1H), 2.97–2.90 (m, 2H), 2.78 (ddd, $J = 14.8, 3.6, 1.6$ Hz, 1H), 2.61 (ddd, $J = 10.9, 5.4, 1.6$ Hz, 1H), 2.52 (ddd, $J = 11.7, 10.9, 3.6$ Hz, 1H), 2.44 (d, $J = 11.7$ Hz, 1H), 1.92 (d, $J = 11.7$ Hz, 1H), 1.55 (s, 3H), 1.26 (s, 3H).

$^{13}\text{C NMR}$ (176 MHz, CDCl_3) δ [ppm] = 172.0, 138.7, 138.1, 130.9, 127.7, 126.7, 126.3, 122.8, 121.8, 119.8, 119.1, 119.0, 118.4, 113.2, 111.9, 109.6, 109.4, 79.3, 79.1, 52.3, 43.2, 40.9, 35.8, 34.1, 30.6, 27.9, 27.6, 22.4, 21.3.

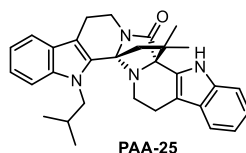
HRMS-ESI: calcd. for $\text{C}_{29}\text{H}_{30}\text{N}_4\text{ONa}$ $[\text{M} + \text{Na}]^+$: 473.2312; found: 473.2294.

FT-IR: ν [cm^{-1}] = 3299, 2970, 2922, 1739, 1684, 1365, 1228, 1217, 742.

PAA-19 and PAA-25



To a solution of **PAA-2** (100 mg, 209 μmol , 1.0 equiv.) in DMF (15 mL) was added NaH (60% dispersion mineral oil, 83.7 mg, 2.09 mmol, 10 equiv.) at 0 $^\circ\text{C}$. The reaction mixture was stirred for 30 min, before the addition of isobutyl iodide (242 μl , 2.09 mmol, 10 equiv.). The resulting mixture was stirred overnight and then quenched with NaHCO_3 (sat. aq.). The mixture was extracted with DCM. The combined organic phases were washed with brine, dried over MgSO_4 , filtered and concentrated under reduced pressure. The crude product was purified by silica gel column chromatography (pentane/EtOAc = 15:1) to afford **PAA-25** (60.0 mg, 126 μmol , 60%) as a white solid and **PAA-19** (35.0 mg, 65.5 μmol , 31%) as a white solid.

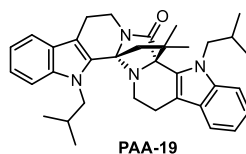


¹H NMR (700 MHz, CD₂Cl₂) δ [ppm] = 8.43 (s, 1H), 7.55 (dt, *J* = 7.8, 1.1 Hz, 1H), 7.47–7.45 (m, 1H), 7.43 (dt, *J* = 8.4, 0.8 Hz, 1H), 7.39 (dt, *J* = 8.2, 0.9 Hz, 1H), 7.24 (ddd, *J* = 8.3, 7.1, 1.2 Hz, 1H), 7.15 (ddd, *J* = 8.2, 7.0, 1.2 Hz, 1H), 7.12 (ddd, *J* = 7.9, 7.1, 0.9 Hz, 1H), 7.07 (ddd, *J* = 7.9, 7.0, 1.0 Hz, 1H), 4.24–4.17 (m, 2H), 4.06 (dd, *J* = 14.8, 7.1 Hz, 1H), 3.17 (ddd, *J* = 13.0, 11.8, 4.7 Hz, 1H), 3.03 (ddd, *J* = 15.4, 4.7, 1.1 Hz, 1H), 2.93 (ddd, *J* = 15.4, 11.8, 6.3 Hz, 1H), 2.86 (ddd, *J* = 15.0, 11.6, 5.5 Hz, 1H), 2.76–2.71 (m, 1H), 2.57–2.47 (m, 4H), 1.95 (d, *J* = 11.9 Hz, 1H), 1.43 (s, 3H), 1.25 (s, 3H), 1.05 (d, *J* = 6.7 Hz, 3H), 0.95 (d, *J* = 6.7 Hz, 3H).

¹³C NMR (176 MHz, CD₂Cl₂) δ [ppm] = 172.3, 138.9, 137.3, 129.3, 128.1, 127.2, 126.8, 123.0, 122.3, 120.0, 119.9, 119.2, 118.7, 113.4, 112.6, 111.8, 111.2, 80.5, 77.7, 52.4, 51.4, 41.4, 41.2, 35.9, 30.4, 27.4, 26.4, 22.0, 21.9, 21.3, 20.7.

HRMS-ESI: calcd. for C₃₁H₃₄N₄ONa [M + Na]⁺: 501.2625; found: 501.2608.

FT-IR: ν [cm⁻¹] = 3303, 2954, 2918, 2847, 1724, 1686, 1453, 1406, 1265, 970, 715.



¹H NMR (600 MHz, CDCl₃) δ [ppm] = 7.55 (dt, *J* = 7.9, 0.9 Hz, 1H), 7.47–7.40 (m, 3H), 7.29–7.26 (m, 1H), 7.20–7.14 (m, 2H), 7.09–7.04 (m, 1H), 4.31–4.24 (m, 3H), 4.20 (dd, *J* = 14.7, 8.3 Hz, 1H), 4.02 (dd, *J* = 14.7, 7.0 Hz, 1H), 3.15 (ddd, *J* = 12.9, 11.8, 4.7 Hz, 1H), 3.07–3.00 (m, 1H), 2.98–2.91 (m, 1H), 2.86 (dt, *J* = 14.9, 8.7 Hz, 1H), 2.74–2.70 (m, 2H), 2.55 (d, *J* = 11.6 Hz, 1H), 2.52–2.49 (m, 2H), 1.92 (d, *J* = 11.7 Hz, 1H), 1.51 (s, 3H), 1.21 (s, 3H), 1.05 (d, *J* = 6.6 Hz, 3H), 1.02 (d, *J* = 6.6 Hz, 3H), 0.96 (d, *J* = 6.7 Hz, 3H), 0.77 (d, *J* = 6.7 Hz, 3H).

¹³C NMR (151 MHz, CDCl₃) δ [ppm] = 171.7, 138.6, 138.4, 131.5, 129.9, 127.9, 127.3, 126.3, 122.8, 121.5, 119.7, 119.0, 118.3, 114.0, 113.0, 111.8, 110.9, 80.0, 79.2, 53.5, 52.8, 52.0, 43.0, 40.7, 35.5, 30.0, 28.8, 27.6, 27.2, 22.3, 21.6, 21.3, 20.6, 20.5, 19.2.

HRMS-ESI: calcd. for C₃₅H₄₂N₄ONa [M + Na]⁺: 557.3251; found: 557.3274.

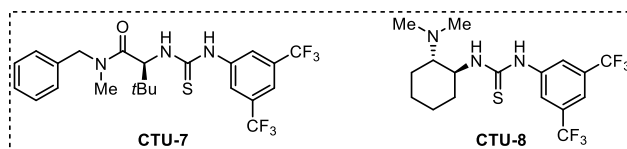
FT-IR: ν [cm⁻¹] = 2958, 2924, 2869, 1698, 1463, 1400, 1305, 1215, 1193, 1096, 740.

7.2.2. Organocatalyst design and asymmetric synthesis of analogues

7.2.2.1. Catalyst preparation

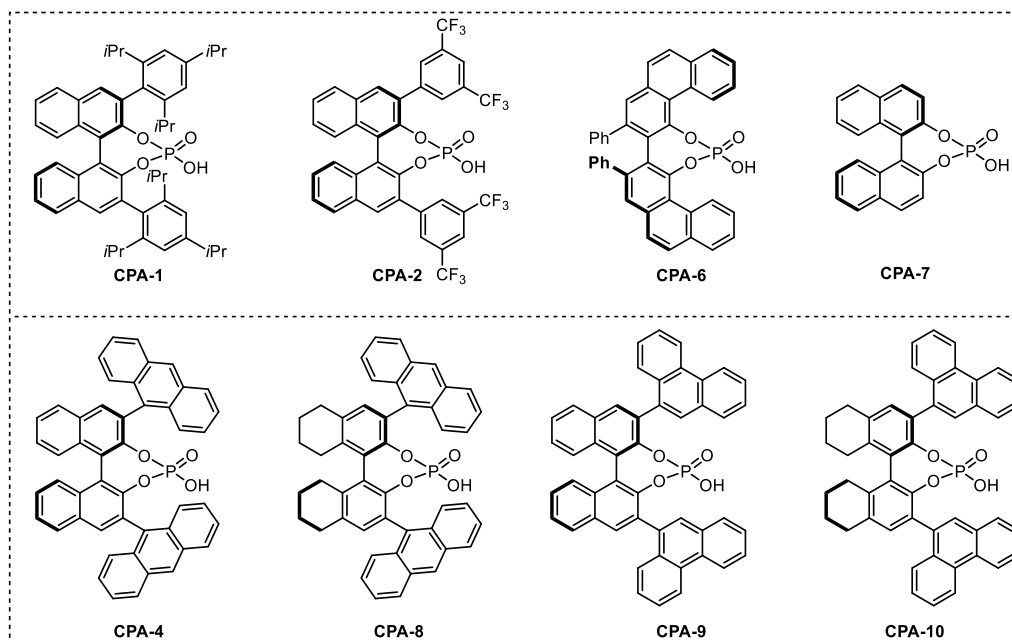
7.2.2.1.1. Chiral thiourea

The two chiral thiourea were purchased from Sigma-Aldrich and used directly.



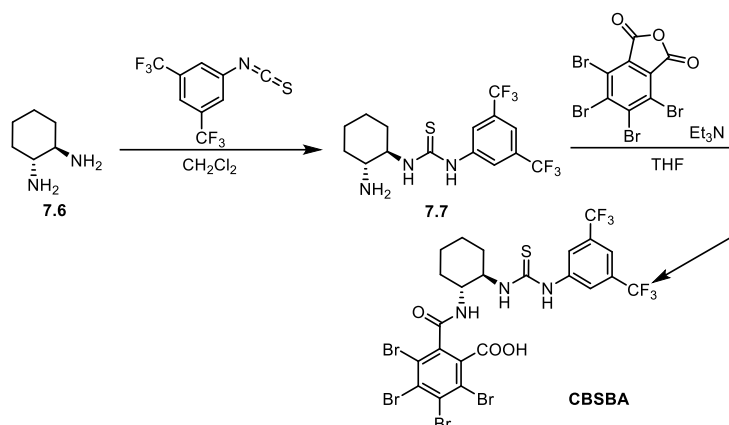
7.2.2.1.2. Chiral phosphoric acid

The chiral phosphoric acid **CPA-2**, **CPA-6** and **CPA-7** were purchased from Sigma-Aldrich and used directly. The rest were synthesized by the former group member Dr. Yiming Cao. I am grateful for his donation.



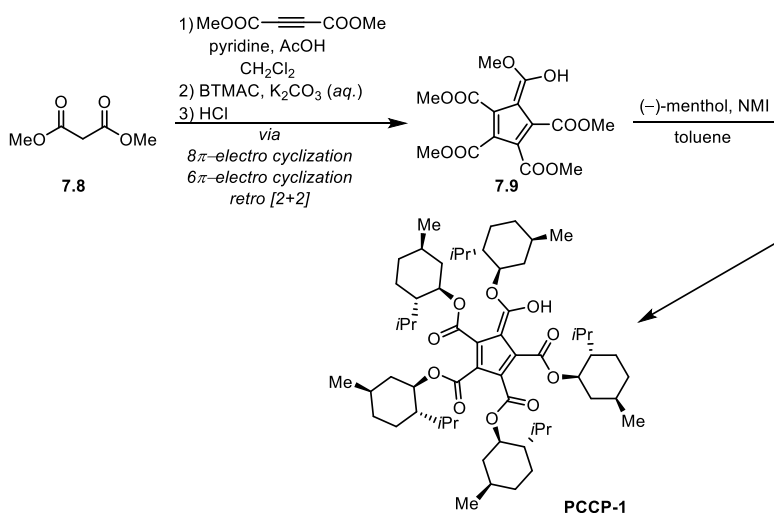
7.2.2.1.3. Chiral CBSBA acid and pentamethyl ester of PCCP

7.7 was prepared from **7.6** by a procedure of Lee et al.^[357] The spectroscopic data are in agreement with literature. **CBSBA** was synthesized from **7.7** following the procedure of Seidel et al.^[237] The spectroscopic data are in agreement with literature.



Scheme 7-3: Synthesis of CBSBA.

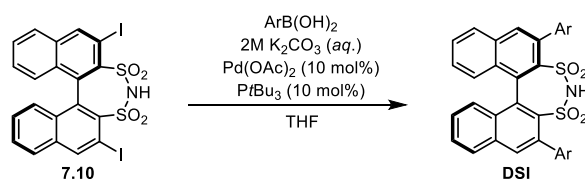
1,2,3,4,5-pentacarboxycyclopentadiene (PCCP) derived pentamethyl ester was synthesized from 7.8 according to a procedure by Lambert et al.^[239b] The spectroscopic data are in agreement with literature.



Scheme 7-4: Synthesis of PCCP.

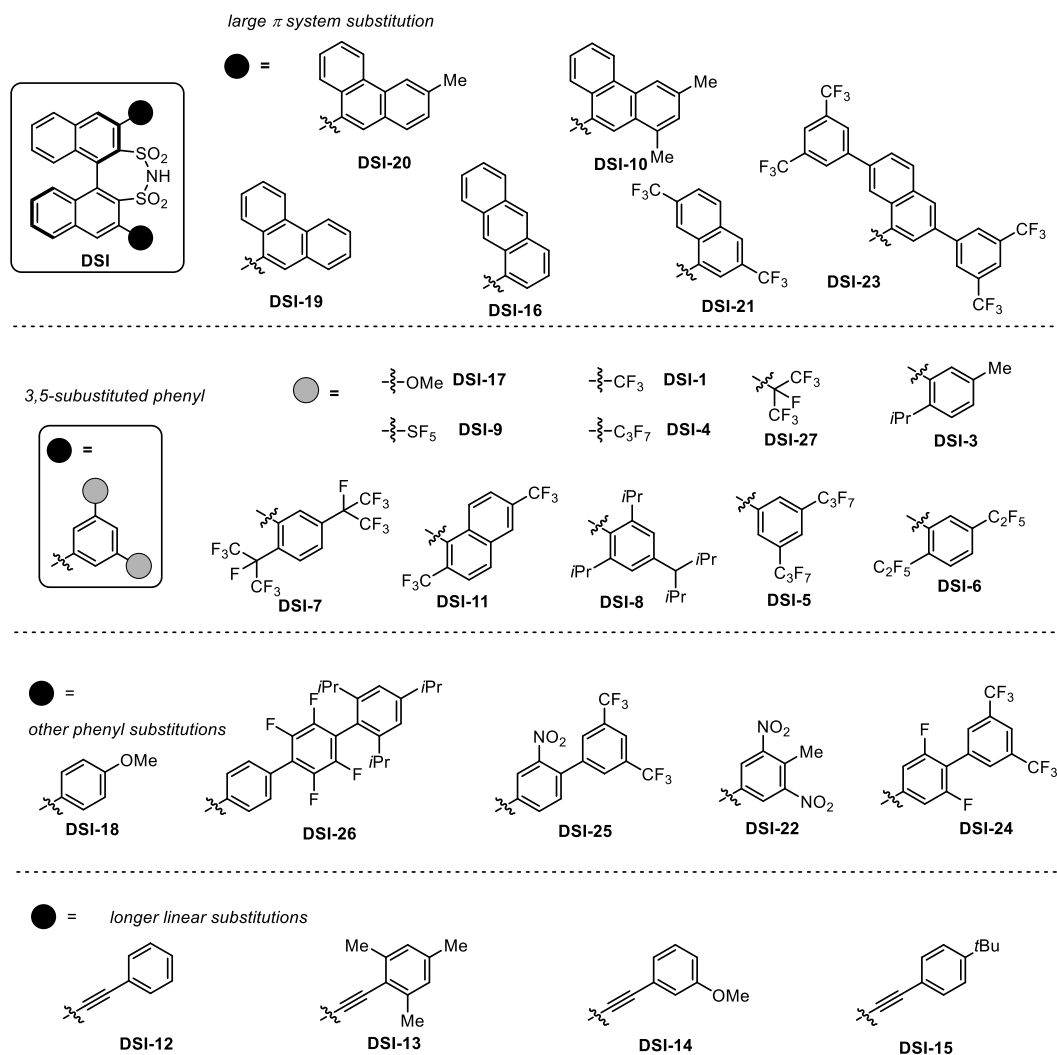
7.2.2.1.4. Chiral disulfonimide

The iodide 7.10 was synthesized by the technician team of AK List. I am grateful for their preparation. With 7.10 in hand, DSIs could be obtained by Suzuki coupling with boronic acid.



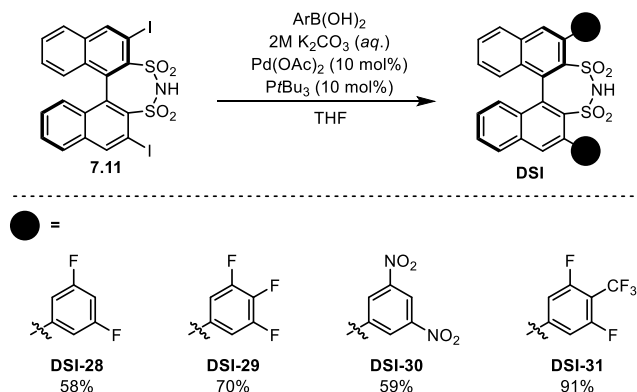
Scheme 7-5: Synthesis of DSIs.

The DSIs in Scheme 7–6 were donated from the group members of AK List. I appreciate for their generous help.



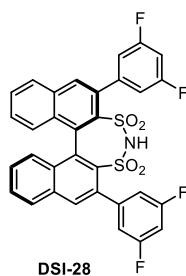
Scheme 7–6: Screened the readily available DSIs.

General procedure H



2M K₂CO₃ was added to a solution of (*R*)-DSI iodide **7.11** (1.0 equiv.), boronic acid (3.0 equiv.), Pd(OAc)₂ (0.1 equiv.) in THF at room temperature. The reaction flask was degassed and filled with argon three times before PtBu₃ (1.0 M in toluene, 0.1 equiv.) was added. The reaction mixture was then put to a preheated 85 °C oil bath for 24 h, before quenched with HCl (10% aq.). was added and the reaction mixture was extracted three times with DCM. The mixture was extracted with DCM. The combined organic phases were washed with brine, dried over MgSO₄, filtered and concentrated under reduced pressure. The crude product was purified by column chromatography on silica gel and dissolved in DCM to stir with 6 N HCl for 1 h. The organic layer was then separated, dried over MgSO₄ and concentrated under reduced pressure to yield the desired compound.

(*R*)-2,6-Bis(3,5-difluorophenyl)-4*H*-dinaphtho[2,1-*d*:1',2'-*f*][1,3,2]dithiazepine 3,3,5,5-tetraoxide (DSI-28)



DSI-28 was prepared according to **General procedure H**, starting from **7.9** (50 mg, 77 μmol, 1.0 equiv.), (3,5-difluorophenyl)boronic acid (38 mg, 0.23 mmol, 3.0 equiv.) and Pd(OAc)₂ (1.7 mg, 8.0 μmol, 0.1 equiv.) in THF (3.0 mL). After degassing, the mixture was treated with PtBu₃ (1.0 M in toluene, 7.7 μL, 8.0 μmol, 0.1 equiv.). Purification by silica gel column chromatography (pentane/EtOAc = 2:1) afforded **DSI-28** (28 mg, 45 μmol, 58%) as a white solid.

¹H NMR (500 MHz, CDCl₃) δ [ppm] = 8.02 (d, *J* = 9.0 Hz, 4H), 7.72 (ddd, *J* = 8.2, 6.8, 1.1 Hz, 2H), 7.45 (ddd, *J* = 8.4, 6.9, 1.2 Hz, 2H), 7.16 (d, *J* = 8.6 Hz, 2H), 7.08 (d, *J* = 8.6 Hz, 2H), 6.99 (d, *J* = 8.6 Hz, 2H), 6.90–6.85 (m, 2H), 5.76 (s, 1H).

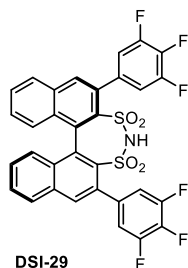
¹³C NMR (126 MHz, CDCl₃) δ [ppm] = 162.6, 162.5, 162.1, 162.0, 160.6, 160.5, 160.1, 160.0, 141.2, 141.1, 141.0, 137.5, 133.6, 133.4, 132.6, 131.1, 130.8, 129.4, 128.0, 127.7, 127.2, 113.1, 112.9, 111.3, 111.1, 102.8, 102.6, 102.4. (Due to the complexity of the F–C coupling, the coupling constants were not calculated.)

^{19}F NMR (471 MHz, CDCl_3) δ [ppm] = $-109.97, -110.59$.

HRMS-ESI: calcd. for $\text{C}_{32}\text{H}_{16}\text{F}_4\text{NO}_4\text{S}_2$ $[\text{M} - \text{H}]^-$: 618.0462; found: 618.0472.

FT-IR: ν [cm^{-1}] = 3158(br), 2927, 1617, 1529, 1439, 1423, 1362, 1340, 1319, 1044, 845, 751.

(*R*)-2,6-Bis(3,4,5-trifluorophenyl)-4*H*-dinaphtho[2,1-*d*:1',2'-*f*][1,3,2]dithiazepine 3,3,5,5-tetraoxide (DSI-29)



DSI-29 was prepared according to **General procedure H**, starting from **7.9** (50 mg, 77 μmol , 1.0 equiv.), (3,4,5-trifluorophenyl)boronic acid (41 mg, 0.23 mmol, 3.0 equiv.) and $\text{Pd}(\text{OAc})_2$ (1.7 mg, 8.0 μmol , 0.1 equiv.) in THF (3.0 mL). After degassing, the mixture was treated with PtBu_3 (1.0 M in toluene, 7.7 μL , 8.0 μmol , 0.1 equiv.). Purification by silica gel column chromatography (pentane/EtOAc = 2:1) afforded **DSI-29** (36 mg, 54 μmol , 70%) as a white solid.

^1H NMR (500 MHz, CDCl_3) δ [ppm] = 8.02 (d, $J = 8.7$ Hz, 4H), 7.74 (ddd, $J = 8.2, 6.9, 1.1$ Hz, 2H), 7.46 (ddd, $J = 8.4, 6.9, 1.3$ Hz, 2H), 7.20–7.01 (m, 6H).

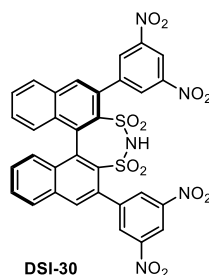
^{13}C NMR (126 MHz, CDCl_3) δ [ppm] = 151.8, 151.5, 149.9, 149.8, 149.5, 149.5, 138.7, 135.0, 134.9, 134.9, 134.9, 134.8, 134.8, 134.5, 134.0, 133.9, 132.3, 131.9, 130.7, 129.3, 128.8, 128.3, 115.3, 115.1, 113.6, 113.5. (Due to the complexity of the F–C coupling, the coupling constants were not calculated.)

^{19}F NMR (471 MHz, CDCl_3) δ [ppm] = (-138.15) – (-140.64) (m), -167.04 (t, $J = 19.9$ Hz).

HRMS-ESI: calcd. for $\text{C}_{32}\text{H}_{14}\text{F}_6\text{NO}_4\text{S}_2$ $[\text{M} - \text{H}]^-$: 654.0274; found: 654.0282.

FT-IR: ν [cm^{-1}] = 3161(br), 2924, 1738, 1618, 1529, 1424, 1362, 1217, 1045, 848, 750.

(*R*)-2,6-Bis(3,5-dinitrophenyl)-4*H*-dinaphtho[2,1-*d*:1',2'-*f*][1,3,2]dithiazepine 3,3,5,5-tetraoxide (DSI-30)



DSI-30 was prepared according to **General procedure H**, starting from **7.9** (15 mg, 23 μ mol, 1.0 equiv.), (3,5-dinitrophenyl)boronic acid (15 mg, 0.70 mmol, 3.0 equiv.) and Pd(OAc)₂ (0.50 mg, 2.0 μ mol, 0.1 equiv.) in THF (1.0 mL). After degassing, the mixture was treated with *Pt*-Bu₃ (1.0 M in toluene, 2.3 μ L, 2.0 μ mol, 0.1 equiv.). Purification by silica gel column chromatography (pentane/EtOAc = 2:1) afforded **DSI-30** (10 mg, 14 μ mol, 59%) as a white solid.

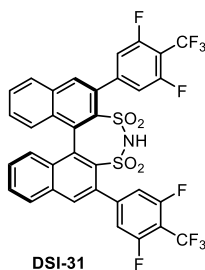
¹H NMR (500 MHz, CD₂Cl₂) δ [ppm] = 9.05 (t, *J* = 2.1 Hz, 2H), 8.76–8.61 (m, 4H), 8.12 (d, *J* = 6.6 Hz, 4H), 7.82 (t, *J* = 7.6 Hz, 2H), 7.55 (dd, *J* = 8.8, 6.8 Hz, 2H), 7.25 (d, *J* = 8.6 Hz, 2H).

¹³C NMR (126 MHz, CD₂Cl₂) δ [ppm] = 148.2, 147.6, 142.7, 138.9, 134.6, 134.5, 132.5, 132.1, 131.8, 131.2, 130.9, 130.0, 129.3, 129.2, 128.4, 118.5.

HRMS-ESI: calcd. for C₃₂H₁₆N₅O₁₂S₂ [M – H][–]: 726.0256; found: 726.0242.

FT-IR: ν [cm^{–1}] = 2924, 1738, 1541, 1343, 1175, 831, 750.

(*R*)-2,6-Bis(3,5-difluoro-4-(trifluoromethyl)phenyl)-4*H*-dinaphtho[2,1-*d*:1',2'-*f*][1,3,2]dithiazepine 3,3,5,5-tetraoxide (DSI-31)



DSI-31 was prepared according to **General procedure H**, starting from **7.9** (300 mg, 0.464 mmol, 1.0 equiv.), (3,5-difluoro-4-(trifluoromethyl)phenyl)boronic acid (315 mg, 1.39 mmol, 3.0 equiv.) and Pd(OAc)₂ (10.4 mg, 46.4 μ mol, 0.1 equiv.) in THF (15 mL). After

degassing, the mixture was treated with $PtBu_3$ (1.0 M in toluene, 46.4 μ L, 46.4 μ mol, 0.1 equiv.). Purification by silica gel column chromatography (pentane/EtOAc = 2:1) afforded **DSI-31** (320 mg, 0.424 mmol, 91%) as a white solid.

1H NMR (500 MHz, $CDCl_3$) δ [ppm] = 8.07–7.97 (m, 4H), 7.76 (t, J = 7.6 Hz, 2H), 7.54–7.46 (m, 2H), 7.24–7.07 (m, 6H).

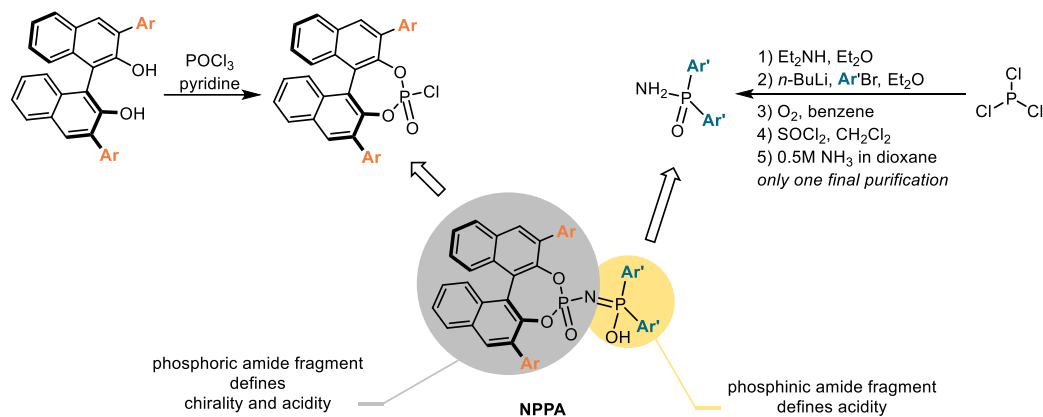
^{13}C NMR (126 MHz, $CDCl_3$) δ [ppm] = 160.4, 159.9, 158.3, 157.8, 145.6, 138.5, 134.2, 133.5, 133.1, 132.1, 131.4, 130.8, 129.5, 128.9, 128.2, 122.8, 120.7, 115.2, 115.0, 113.6, 113.5. (Due to the complexity of the F–C coupling, the coupling constants were not calculated.)

^{19}F NMR (471 MHz, $CDCl_3$) δ [ppm] = –56.16 (t, J = 21.7 Hz), –111.17 (dq, J = 329.9, 22.4, 21.7 Hz).

HRMS-ESI: calcd. for $C_{34}H_{14}F_{10}NO_4S_2$ $[M - H]^-$: 754.0219; found: 754.0210.

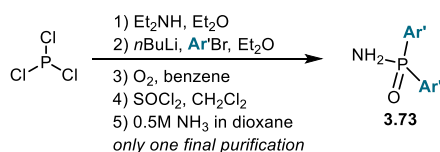
FT-IR: ν [cm^{-1}] = 3075, 1641, 1493, 1429, 1352, 1306, 1137, 1046, 856, 753.

7.2.2.1.5. Chiral *N*-phosphinyl phosphoramidate



Scheme 7–7: Synthetic strategy of NPPA.

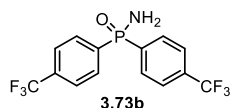
General procedure I



Diethylamino phosphinous dichloride was prepared from PCl_3 by a procedure of Charette et al.^[358] The spectroscopic data are in agreement with literatures.

To a solution of aryl bromide (1.0 equiv.) in Et₂O was added *n*BuLi (2.5 M in hexane, 1.0 equiv.) at -78 °C slowly. The mixture was stirred at 0 °C before the addition of diethylamino phosphinous dichloride (0.5 equiv.). The resulting mixture was allowed to warm to room temperature and stirred overnight. After cooling to -78 °C again, HCl (2.0 M in Et₂O, 1.5 equiv.) was added to the reaction mixture. The mixture was allowed to warm to room temperature and the solvent was removed under reduced pressure. The residue was dissolved in hexanes and filtered. The filtrate was concentrated.^[359] The crude diarylphosphine chloride was dissolved in benzene. After bubbling O₂ through the mixture for 20 min, the reaction mixture was stirred under O₂ atmosphere overnight. Then the solvent was removed under reduced pressure to afford the crude product. The mixture of diarylphosphinic chloride and diarylphosphinic acid was dissolved in a mixture of SOCl₂/DCM (v/v = 1:1). The resulting mixture was stirred at room temperature overnight. Then the solvent was removed under reduced pressure to afford the crude product. The crude diarylphosphinic chloride was added NH₃ (0.5 M in dioxane). The resulting mixture was stirred at room temperature overnight. Then the solvent was removed under reduced pressure and purified by silica gel column chromatography.

***P,P*-Bis(4-(trifluoromethyl)phenyl)phosphinic amide (3.73b)**



3.73b was prepared according to **General procedure I**, starting from 1-bromo-4-(trifluoromethyl)benzene (1.00 g, 4.44 mmol, 1.0 equiv.), *n*BuLi (2.5 M in hexane, 1.78 mL, 4.44 mmol, 1.0 equiv.) and diethylamino phosphinous dichloride (322 mg, 2.22 mmol, 0.5 equiv.). After the oxidation with O₂ in benzene, the crude product was dissolved in a mixture of SOCl₂/DCM (v/v = 1:1, 10 mL). NH₃ (0.5 M in dioxane, 10 mL) was used. Purification by silica gel column chromatography (DCM/MeOH = 20:1) afforded **3.73b** (400 mg, 1.13 mmol, 52% over 4 steps) as a light yellow solid.

¹H NMR (500 MHz, CD₃OD) δ [ppm] = 8.09 (dd, *J* = 12.0, 8.0 Hz, 4H), 7.80 (dd, *J* = 8.4, 2.7 Hz, 4H).

¹³C NMR (126 MHz, CD₃OD) δ [ppm] = 139.8 (d, *J* = 130.0 Hz), 135.9 (dd, *J* = 32.5, 3.0 Hz), 134.6 (d, *J* = 10.4 Hz), 127.4 (dd, *J* = 12.9, 3.8 Hz), 126.0 (q, *J* = 271.9 Hz).

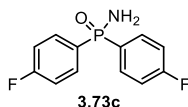
^{31}P NMR (203 MHz, CD_3OD) δ [ppm] = 22.02.

^{19}F NMR (471 MHz, CD_3OD) δ [ppm] = -64.68.

HRMS-ESI: calcd. for $\text{C}_{14}\text{H}_9\text{F}_6\text{NOP}$ $[\text{M} - \text{H}]^-$: 352.0331; found: 352.0334.

FT-IR: ν [cm^{-1}] = 3097, 1399, 1324, 1170, 1129, 1105, 1063, 836.

***P,P*-Bis(4-fluorophenyl)phosphinic amide (3.73c)**



3.73c was prepared according to **General procedure I**, starting from chlorobis(4-fluorophenyl)phosphane (500 mg, 1.89 mmol, 1.0 equiv.). After the oxidation with O_2 in benzene, the crude product was dissolved in SOCl_2/DCM ($v/v = 1:1$, 10 mL). NH_3 (0.5 M in dioxane, 10 mL) was used. Purification by silica gel column chromatography ($\text{DCM}/\text{MeOH} = 20:1$) afforded **3.73c** (180 mg, 0.712 mmol, 38% over 3 steps) as a light yellow solid.

^1H NMR (500 MHz, CD_3OD) δ [ppm] = 7.95–7.90 (m, 4H), 7.23 (td, $J = 8.8, 2.4$ Hz, 4H).

^{13}C NMR (126 MHz, CD_3OD) δ [ppm] = 167.4 (dd, $J = 251.6, 3.3$ Hz), 136.4 (dd, $J = 11.4, 8.8$ Hz), 131.8 (dd, $J = 135.4, 3.4$ Hz), 117.6 (dd, $J = 21.7, 13.8$ Hz).

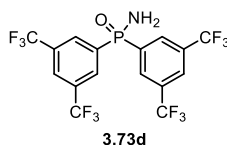
^{31}P NMR (203 MHz, CD_3OD) δ [ppm] = 23.34.

^{19}F NMR (471 MHz, CD_3OD) δ [ppm] = -109.42.

HRMS-ESI: calcd. for $\text{C}_{12}\text{H}_{11}\text{F}_2\text{NOP}$ $[\text{M} + \text{H}]^+$: 254.0541; found: 254.0540.

FT-IR: ν [cm^{-1}] = 3243, 3124, 1592, 1497, 1225, 1175, 1159, 1124, 1111, 1093, 909, 829.

***P,P*-Bis(3,5-bis(trifluoromethyl)phenyl)phosphinic amide (3.73d)**



3.73d was prepared according to **General procedure I**, starting from bis(3,5-bis(trifluoromethyl)phenyl)chlorophosphane (500 mg, 1.02 mmol, 1.0 equiv.). After the oxidation with O_2 in benzene, the crude product was dissolved in a mixture of SOCl_2/DCM ($v/v = 1:1$, 10 mL). NH_3 (0.5 M in dioxane, 10 mL) was used. Purification by silica gel column chromatography ($\text{DCM}/\text{MeOH} = 20:1$) afforded **3.73d** (250 mg, 0.511 mmol, 50% over 3 steps)

as a light yellow solid.

¹H NMR (500 MHz, CD₃OD) δ [ppm] = 8.50 (dd, *J* = 12.0, 1.7 Hz, 4H), 8.22 (s, 2H).

¹³C NMR (126 MHz, CD₃OD) δ [ppm] = 137.7 (d, *J* = 133.1 Hz), 133.5 (td, *J* = 33.8, 13.1 Hz), 135.6–133.4 (m), 127.3–127.2 (m). 124.40 (q, *J* = 271.5 Hz).

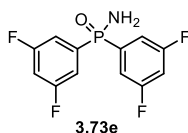
³¹P NMR (203 MHz, CD₃OD) δ [ppm] = 18.00.

¹⁹F NMR (471 MHz, CD₃OD) δ [ppm] = –64.54.

HRMS-EI: calcd. for C₁₆H₈F₁₂NOP [M]⁺: 489.0146; found: 489.0152.

FT-IR: ν [cm⁻¹] = 1699, 1619, 1362, 1278, 1127, 1051, 904, 757.

***P,P*-Bis(3,5-difluorophenyl)phosphinic amide (3.73e)**



3.73e was prepared according to **General procedure I**, starting from 1-bromo-3,5-difluorobenzene (500 mg, 2.62 mmol, 1.0 equiv.), *n*BuLi (2.5 M in hexane, 1.04 mL, 2.62 mmol, 1.0 equiv.) and diethylamino phosphinous dichloride (228 mg, 1.31 mmol, 0.5 equiv.). After the oxidation with O₂ in benzene, the crude product was dissolved in a mixture of SOCl₂/DCM (v/v = 1:1, 10 mL). NH₃ (0.5 M in dioxane, 10 mL) was used. Purification by silica gel column chromatography (DCM/MeOH = 20:1) afforded **3.73e** (150 mg, 0.519 mmol, 40% over 4 steps) as a light yellow solid.

¹H NMR (500 MHz, CD₃OD) δ [ppm] = 7.50–7.43 (m, 4H), 7.18–7.14 (m, 2H).

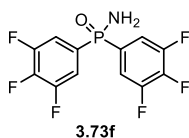
¹³C NMR (126 MHz, CD₃OD) δ [ppm] = 165.3 (ddd, *J* = 252.0, 21.5, 11.5 Hz), 139.5 (dt, *J* = 132.6, 7.3 Hz), 116.6 (ddd, *J* = 20.1, 10.3, 6.5 Hz), 109.5 (td, *J* = 25.6, 2.2 Hz).

³¹P NMR (203 MHz, CD₃OD) δ [ppm] = 20.06 (td, *J* = 14.3, 13.3, 7.0 Hz).

¹⁹F NMR (471 MHz, CD₃OD) δ [ppm] = –109.22 (d, *J* = 8.1 Hz).

HRMS-ESI: calcd. for C₁₂H₇F₄NOP [M – H]⁻: 288.0207; found: 288.0209.

FT-IR: ν [cm⁻¹] = 3248, 3099, 1593, 1425, 1291, 1178, 1122, 1096, 985, 862.

***P,P*-Bis(3,4,5-trifluorophenyl)phosphinic amide (3.73f)**

3.73f was prepared according to **General procedure I**, starting from 5-bromo-1,2,3-trifluorobenzene (500 mg, 2.39 mmol, 1.0 equiv.), *n*BuLi (2.5 M in hexane, 957 μ L, 2.39 mmol, 1.0 equiv.) and diethylamino phosphinous dichloride (208 mg, 1.20 mmol, 0.5 equiv.). After the oxidation with O₂ in benzene, the crude product was dissolved in a mixture of SOCl₂/DCM (v/v = 1:1, 10 mL). NH₃ (0.5 M in dioxane, 10 mL) was used. Purification by silica gel column chromatography (DCM/MeOH = 20:1) afforded **3.73f** (200 mg, 0.615 mmol, 52% over 4 steps) as a light yellow solid.

¹H NMR (500 MHz, CD₃OD) δ [ppm] = 7.71–7.61 (m, 4H).

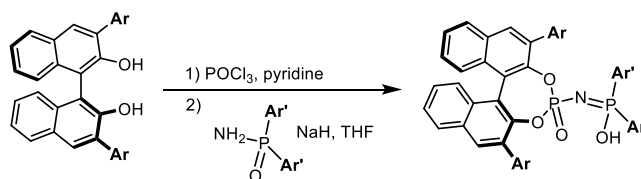
¹³C NMR (126 MHz, CD₃OD) δ [ppm] = 153.4 (dddd, J = 253.2, 21.7, 10.0, 3.0 Hz), 147.1–140.7 (m), 132.1 (dd, J = 136.1, 5.3 Hz), 118.6 (ddd, J = 16.4, 10.9, 5.4 Hz).

³¹P NMR (203 MHz, CD₃OD) δ [ppm] = 18.71.

¹⁹F NMR (471 MHz, CD₃OD) δ [ppm] = –134.52 (dd, J = 19.3, 6.5 Hz), –157.24 (td, J = 20.1, 19.6, 3.2 Hz).

HRMS-ESI: calcd. for C₁₂H₅F₆NOP [M – H][–]: 324.0018; found: 324.0020.

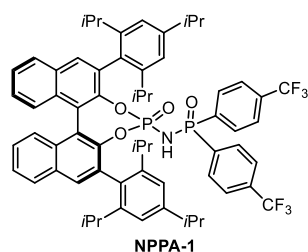
FT-IR: ν [cm^{–1}] = 3228, 3124, 1617, 1523, 1419, 1327, 1214, 1185, 1086, 1047, 761.

General procedure J

To a solution of (*S*)-3,3'-substituted-[1,1'-binaphthalene]-2,2'-diol (1.0 equiv.) in pyridine was added POCl₃ (3.0 equiv.) at room temperature. After being stirred for 12 hours at 60 °C, pyridine was removed in vacuo and the crude mixture was filtered through a short pad of silica to afford the corresponding phosphoric chloride. It was then dissolved in THF and added to a solution (for 30 min) of diaryl phosphoramidate (2.0 equiv.) and NaH (60% dispersion in mineral oil,

3.0 equiv.) in THF. The resulting mixture was stirred for 12 h at room temperature. The reaction mixture was then quenched with H₂O, extracted with DCM, dried over MgSO₄ and concentrated. The crude product was purified by column chromatography on silica gel. The pure product was re-dissolved in DCM was washed with 6 N HCl, dried over MgSO₄, and concentrated under reduced pressure to afford the final product. (Note: The corresponding diols was synthesized by the technician team of AK List. I am grateful for their preparation.)

***N*-((4*S*)-4-oxido-2,6-bis(2,4,6-triisopropylphenyl)dinaphtho[2,1-*d*:1',2'-*f*][1,3,2]dioxaphosphepin-4-yl)-*P,P*-bis(4-(trifluoromethyl)phenyl)phosphinic amide (NPPA-1)**



NPPA-1 was prepared according to **General procedure J**, starting from (*S*)-3,3'-bis(2,4,6-triisopropylphenyl)-[1,1'-binaphthalene]-2,2'-diol (100 mg, 145 μmol, 1.0 equiv.) and POCl₃ (66.5 μL, 0.435 mmol, 3.0 equiv.) in pyridine (2.0 mL). Then crude phosphoric chloride was added to the mixture of *P,P*-bis(4-(trifluoromethyl)phenyl)phosphinic amide **3.73b** (61.4 mg, 174 μmol, 1.2 equiv.) and NaH (60% dispersion in mineral oil, 17.4 mg, 0.435 mmol, 3.0 equiv.) in THF (2.0 mL). Purification by silica gel column chromatography (pentane/EtOAc = 10:1) and acidification with 6 N HCl afforded **NPPA-1** (88.0 mg, 72.0 μmol, 50%) as a white solid.

¹H NMR (600 MHz, CDCl₃) δ [ppm] = 7.95 (s, 1H), 7.94 (d, *J* = 8.1 Hz, 1H), 7.90 (d, *J* = 8.2 Hz, 1H), 7.86 (s, 1H), 7.56–7.47 (m, 4H), 7.45–7.38 (m, 4H), 7.31 (dddd, *J* = 15.4, 8.3, 6.7, 1.3 Hz, 2H), 7.25 (t, *J* = 2.2 Hz, 2H), 7.23–7.18 (m, 3H), 7.14 (d, *J* = 1.8 Hz, 1H), 7.13–7.06 (m, 2H), 4.18 (br, 1H), 3.15–3.11 (m, 1H), 3.07–3.03 (m, 1H), 2.83–2.79 (m, 1H), 2.76–2.69 (m, 3H), 1.41–1.36 (m, 12H), 1.32–1.31 (m, 6H), 1.24 (d, *J* = 6.8 Hz, 3H), 1.12 (d, *J* = 6.8 Hz, 3H), 1.04 (d, *J* = 6.8 Hz, 3H), 0.97 (d, *J* = 6.7 Hz, 3H), 0.94 (d, *J* = 6.7 Hz, 3H), 0.90 (d, *J* = 6.7 Hz, 3H).

¹³C NMR (151 MHz, CDCl₃) δ [ppm] = 149.1, 148.7, 148.4, 148.0, 147.5, 147.3, 146.1, 144.7, 135.6, 135.1, 134.7, 134.2, 133.7, 132.6, 132.5, 132.4, 132.3, 132.2, 131.5, 131.3, 130.9, 128.34,

128.29, 127.5, 127.4, 126.8, 126.7, 126.3, 126.2, 125.5, 125.2, 124.6, 122.8, 122.6, 122.4, 122.0, 121.6, 121.4, 120.2, 34.3, 34.0, 31.3, 31.2, 31.1, 27.3, 26.4, 25.3, 24.8, 24.7, 24.5, 23.81, 23.76, 23.44, 23.39, 23.3.

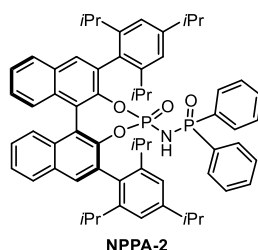
^{31}P NMR (243 MHz, CDCl_3) δ [ppm] = 27.0, 0.9.

^{19}F NMR (565 MHz, CDCl_3) δ [ppm] = -62.8, -63.2.

HRMS-ESI: calcd. for $\text{C}_{64}\text{H}_{65}\text{F}_6\text{NO}_4\text{P}_2\text{Na}$ $[\text{M} + \text{Na}]^+$: 1110.4185; found: 1110.4229.

FT-IR: ν [cm^{-1}] = 2961, 2929, 2870, 1399, 1322, 1172, 1135, 1063, 938, 895, 795, 750.

***N*-((4*S*)-4-oxido-2,6-bis(2,4,6-triisopropylphenyl)dinaphtho[2,1-*d*:1',2'-*f*][1,3,2]dioxaphosphepin-4-yl)-*P,P*-diphenylphosphinic amide (NPPA-2)**



NPPA-2 was prepared according to **General procedure J**, starting from (*S*)-3,3'-bis(2,4,6-triisopropylphenyl)-[1,1'-binaphthalene]-2,2'-diol (213 mg, 0.309 mmol, 1.0 equiv.) and POCl_3 (86.4 μL , 0.926 mmol, 3.0 equiv.) in pyridine (3.0 mL). Then crude phosphoric chloride was added to the mixture of diphenyl phosphoramidate (134 mg, 0.617 mmol, 2.0 equiv.) and NaH (60% dispersion in mineral oil, 37.0 mg, 0.926 mmol, 3.0 equiv.) in THF (4.0 mL). Purification by silica gel column chromatography (pentane/EtOAc = 10:1) and acidification with 6 N HCl afforded **NPPA-2** (150 mg, 158 μmol , 51%) as a white solid.

^1H NMR (500 MHz, CD_2Cl_2) δ [ppm] = 7.95 (d, J = 7.9 Hz, 2H), 7.89 (d, J = 8.2 Hz, 1H), 7.77 (s, 1H), 7.49 (dt, J = 17.5, 7.6 Hz, 2H), 7.42–7.35 (m, 4H), 7.31–7.23 (m, 3H), 7.20–7.12 (m, 6H), 7.12–7.01 (m, 5H), 5.07 (br, 1H), 3.11–3.05 (m, 1H), 3.03–2.98 (m, 1H), 2.89–2.79 (m, 2H), 2.78–2.70 (m, 1H), 2.70–2.59 (m, 1H), 1.44–1.38 (m, 6H), 1.36 (dd, J = 6.9, 1.7 Hz, 3H), 1.33–1.26 (m, 6H), 1.20 (d, J = 6.9 Hz, 6H), 1.08–1.05 (m, 6H), 0.96 (d, J = 6.8 Hz, 3H), 0.92 (d, J = 6.8 Hz, 6H).

^{13}C NMR (126 MHz, CD_2Cl_2) δ [ppm] = 149.2, 148.6, 148.5, 148.3, 147.69, 147.67, 146.5, 146.4, 145.6, 145.5, 133.8, 133.7, 133.1, 133.0, 132.80, 132.78, 132.76, 132.28, 132.26, 132.21,

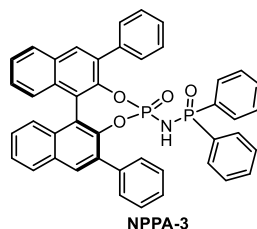
132.17, 132.10, 132.05, 132.0, 131.80, 131.76, 131.71, 131.66, 131.42, 131.38, 131.24, 131.16, 130.8, 128.7, 128.61, 128.58, 128.52, 127.6, 127.51, 127.47, 126.8, 126.7, 126.6, 126.3, 126.2, 126.1, 122.7, 122.6, 122.3, 122.1, 121.5, 120.8, 120.7, 34.7, 34.6, 31.7, 31.5, 31.41, 31.35, 31.3, 30.1, 27.3, 26.7, 26.4, 25.3, 25.0, 24.8, 24.4, 24.3, 24.12, 24.06, 24.0, 23.8, 23.6, 23.5, 23.4, 23.1.

^{31}P NMR (203 MHz, CD_2Cl_2) δ [ppm] = 28.86, 1.90.

HRMS-ESI: calcd. for $\text{C}_{62}\text{H}_{67}\text{NO}_4\text{P}_2$ $[\text{M} - \text{H}]^-$: 950.4473; found: 950.4484

FT-IR: ν [cm^{-1}] = 2960, 2925, 2866, 1738, 1460, 1439, 1361, 1198, 1148, 968, 938, 889, 749.

***N*-((4*S*)-4-oxido-2,6-diphenyldinaphtho[2,1-*d*:1',2'-*f*][1,3,2]dioxaphosphepin-4-yl)-*P,P*-diphenylphosphinic amide (NPPA-3)**



NPPA-3 was prepared according to **General procedure J**, starting from (*S*)-3,3'-diphenyl-[1,1'-binaphthalene]-2,2'-diol (50.0 mg, 0.114 mmol, 1.0 equiv.) and POCl_3 (31.9 μL , 0.342 mmol, 3.0 equiv.) in pyridine (1.0 mL). Then crude phosphoric chloride was added to the mixture of diphenyl phosphoramidate (49.5 mg, 0.342 mmol, 2.0 equiv.) and NaH (60% dispersion in mineral oil, 13.7 mg, 0.342 mmol, 3.0 equiv.) in THF (2.0 mL). Purification by silica gel column chromatography (pentane/EtOAc = 10:1) and acidification with 6 N HCl afforded **NPPA-3** (45.0 mg, 64.4 μmol , 56%) as a white solid.

^1H NMR (500 MHz, CDCl_3) δ [ppm] = 7.96 (s, 1H), 7.94–7.87 (m, 2H), 7.82 (d, J = 8.2 Hz, 1H), 7.67 (d, J = 7.4 Hz, 2H), 7.56 (d, J = 7.5 Hz, 2H), 7.48 (t, J = 7.4 Hz, 1H), 7.37–7.10 (m, 15H), 7.10–6.89 (m, 8H).

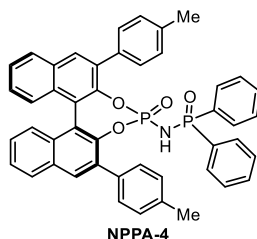
^{13}C NMR (126 MHz, CDCl_3) δ [ppm] = 145.2, 144.7, 137.6, 137.4, 134.6, 134.4, 132.6, 132.3, 132.2, 131.8, 131.7, 131.64, 131.59, 131.52, 131.50, 131.2, 130.4, 130.2, 128.6, 128.45, 128.37, 128.24, 128.18, 128.16, 128.1, 128.0, 127.7, 127.5, 127.3, 127.0, 126.4, 126.2, 125.9, 125.6, 123.0, 122.9.

^{31}P NMR (203 MHz, CDCl_3) δ [ppm] = 24.73, 3.05.

HRMS-ESI: calcd. for $\text{C}_{44}\text{H}_{31}\text{NO}_4\text{P}_2$ $[\text{M} - \text{H}]^-$: 698.1656; found: 698.1666.

FT-IR: ν [cm^{-1}] = 2926, 2853, 1738, 1438, 1364, 1188, 1149, 970, 890, 766, 751.

***N*-((4*S*)-4-oxido-2,6-di-*p*-tolylidnaphtho[2,1-*d*:1',2'-*f*][1,3,2]dioxaphosphepin-4-yl)-*P,P*-diphenylphosphinic amide (NPPA-4)**



NPPA-4 was prepared according to **General procedure J**, starting from (*S*)-3,3'-di-*p*-tolyl-[1,1'-binaphthalene]-2,2'-diol (53.0 mg, 0.114 mmol, 1.0 equiv.) and POCl_3 (31.9 μL , 0.342 mmol, 3.0 equiv.) in pyridine (1.0 mL). Then crude phosphoric chloride was added to the mixture of diphenyl phosphoramidate (49.5 mg, 0.342 mmol, 2.0 equiv.) and NaH (60% dispersion in mineral oil, 13.7 mg, 0.342 mmol, 3.0 equiv.) in THF (2.0 mL). Purification by silica gel column chromatography (pentane/EtOAc = 10:1) and acidification with 6 N HCl afforded **NPPA-4** (35.0 mg, 48.1 μmol , 42%) as a white solid.

^1H NMR (500 MHz, CD_2Cl_2) δ [ppm] = 8.00 (s, 1H), 7.96–7.91 (m, 2H), 7.90–7.83 (m, 1H), 7.62–7.57 (m, 2H), 7.49 (td, $J = 7.9, 1.7$ Hz, 3H), 7.43–7.34 (m, 2H), 7.33–7.21 (m, 5H), 7.21–7.16 (m, 2H), 7.12 (tt, $J = 16.6, 5.6$ Hz, 10H), 5.05 (br, 1H), 2.38 (d, $J = 13.5$ Hz, 6H).

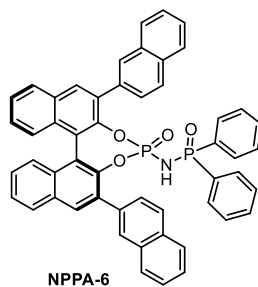
^{13}C NMR (126 MHz, CD_2Cl_2) δ [ppm] = 145.3, 145.2, 144.74, 144.67, 144.66, 137.9, 137.8, 137.39, 137.35, 134.9, 134.6, 134.4, 132.8, 132.3, 132.1, 132.0, 131.91, 131.87, 131.78, 131.73, 131.6, 131.5, 130.4, 130.2, 129.6, 129.3, 128.7, 128.6, 128.5, 128.4, 128.3, 127.4, 127.1, 126.7, 126.5, 126.2, 126.1, 123.2, 123.1, 21.50, 21.46.

^{31}P NMR (203 MHz, CD_2Cl_2) δ [ppm] = 24.39, 3.48.

HRMS-ESI: calcd. for $\text{C}_{46}\text{H}_{35}\text{NO}_4\text{P}_2\text{Na}$ $[\text{M} + \text{Na}]^+$: 750.1933; found: 750.1969.

FT-IR: ν [cm^{-1}] = 2960, 2926, 2867, 1644, 1593, 1461, 1426, 1295, 1196, 1124, 986, 862, 751.

***N*-((4*S*)-2,6-di(naphthalen-2-yl)-4-oxidodiphospho[2,1-*d*:1',2'-*f*][1,3,2]dioxaphosphepin-4-yl)-*P,P*-diphenylphosphinic amide (NPPA-6)**



NPPA-6 was prepared according to **General procedure J**, starting from (*S*)-[2,2':4',1'':3'',2'''-quaternaphthalene]-2'',3'-diol (81.0 mg, 0.151 mmol, 1.0 equiv.) and POCl₃ (42.1 μL, 0.452 mmol, 3.0 equiv.) in pyridine (1.0 mL). Then crude phosphoric chloride was added to the mixture of diphenyl phosphoramidate (65.3 mg, 0.301 mmol, 2.0 equiv.) and NaH (60% dispersion in mineral oil, 18.1 mg, 0.452 mmol, 3.0 equiv.) in THF (2.0 mL). Purification by silica gel column chromatography (pentane/EtOAc = 10:1) and acidification with 6 N HCl afforded **NPPA-6** (49.0 mg, 61.3 μmol, 41%) as a white solid.

¹H NMR (500 MHz, CD₂Cl₂) δ [ppm] = 8.17 (s, 1H), 8.11 (s, 1H), 8.07 (s, 2H), 8.02 (d, *J* = 8.3 Hz, 1H), 7.95 (d, *J* = 8.2 Hz, 1H), 7.88 (d, *J* = 8.5 Hz, 1H), 7.80 (d, *J* = 8.1 Hz, 1H), 7.78–7.67 (m, 5H), 7.62 (d, *J* = 8.7 Hz, 1H), 7.58–7.27 (m, 8H), 7.22 (d, *J* = 8.5 Hz, 1H), 7.17–7.09 (m, 2H), 7.06 (t, *J* = 7.5 Hz, 1H), 7.01 (dd, *J* = 13.3, 7.6 Hz, 2H), 6.85 (dd, *J* = 13.3, 7.7 Hz, 2H), 6.72–6.59 (m, 4H).

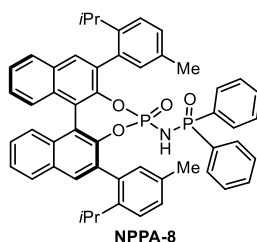
¹³C NMR (126 MHz, CD₂Cl₂) δ [ppm] = 145.55, 145.45, 145.0, 144.9, 135.6, 135.4, 134.57, 134.55, 134.53, 134.51, 133.8, 133.7, 133.2, 133.0, 132.6, 132.5, 132.1, 131.92, 131.87, 131.5, 131.4, 131.3, 131.2, 129.4, 129.2, 128.9, 128.8, 128.7, 128.6, 128.4, 128.3, 128.1, 128.1, 128.0, 128.0, 127.9, 127.8, 127.6, 127.1, 126.8, 126.6, 126.41, 126.39, 126.35, 126.33, 126.1, 123.2.

³¹P NMR (203 MHz, CD₂Cl₂) δ [ppm] = 24.13, 3.48.

HRMS-ESI: calcd. for C₅₂H₃₅NO₄O₂ [M – H][–]: 798.1969; found: 798.1984.

FT-IR: ν [cm^{–1}] = 3049, 2924, 2854, 1739, 1438, 1366, 1200, 1179, 1122, 983, 747.

***N*-((4*S*)-2,6-bis(2-isopropyl-5-methylphenyl)-4-oxidodinaphtho[2,1-*d*:1',2'-*f*][1,3,2]dioxaphosphepin-4-yl)-*P,P*-diphenylphosphinic amide (NPPA-8)**



NPPA-8 was prepared according to **General procedure J**, starting from (*S*)-3,3'-bis(2-isopropyl-5-methylphenyl)-[1,1'-binaphthalene]-2,2'-diol (130 mg, 0.236 mmol, 1.0 equiv.) and POCl₃ (66.2 μL, 0.709 mmol, 3.0 equiv.) in pyridine (2.0 mL). Then crude phosphoric chloride was added to the mixture of diphenyl phosphoramidate (103 mg, 0.473 mmol, 2.0 equiv.) and NaH (60% dispersion in mineral oil, 28.4 mg, 0.709 mmol, 3.0 equiv.) in THF (3.0 mL). Purification by silica gel column chromatography (pentane/EtOAc = 10:1) and acidification with 6 N HCl afforded **NPPA-8** (84.0 mg, 104 μmol, 44%) as a white solid.

¹H NMR (500 MHz, CD₂Cl₂) δ [ppm] = 8.03–7.93 (m, 3H), 7.89–7.83 (m, 1H), 7.57–7.48 (m, 2H), 7.44–7.37 (m, 5H), 7.36–7.31 (m, 3H), 7.30–7.25 (m, 3H), 7.22–7.11 (m, 6H), 7.08 (td, *J* = 7.8, 3.6 Hz, 1H), 7.05–6.97 (m, 2H), 6.09 (br, 1H), 2.95–2.86 (m, 1H), 2.76 (t, *J* = 6.8 Hz, 1H), 2.31–2.30 (m, 3H), 2.13 (d, *J* = 2.9 Hz, 3H), 1.26–1.23 (m, H), 1.02–0.98 (m, 6H), 0.90 (dd, *J* = 6.9, 2.2 Hz, 3H).

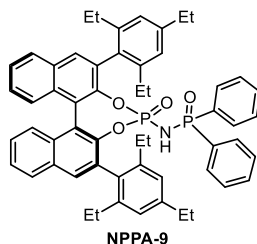
¹³C NMR (126 MHz, CD₂Cl₂) δ [ppm] = 145.19, 145.18, 145.10, 145.09, 144.9, 144.84, 144.82, 144.7, 144.6, 144.3, 135.8, 135.74, 135.69, 135.5, 134.6, 134.3, 134.19, 134.16, 133.9, 132.5, 132.2, 132.12, 132.08, 132.06, 132.03, 131.95, 131.92, 131.89, 131.87, 131.83, 131.76, 131.70, 131.53, 131.49, 131.4, 131.32, 131.27, 131.22, 131.18, 131.1, 130.9, 129.7, 129.14, 129.12, 128.6, 128.35, 128.30, 128.24, 128.19, 128.12, 128.08, 128.01, 127.2, 127.05, 127.00, 126.44, 126.41, 126.1, 126.0, 125.97, 125.92, 125.2, 125.1, 124.9, 122.10, 122.05, 122.04, 30.6, 30.3, 30.1, 24.8, 24.6, 24.5, 22.9, 22.8, 20.6, 20.4.

³¹P NMR (203 MHz, CD₂Cl₂) δ [ppm] = 27.73, 3.84.

HRMS-ESI: calcd. for C₅₂H₄₇NO₄P₂ [*M* – H][–]: 810.2908; found: 810.2919.

FT-IR: ν [cm^{–1}] = 2960, 2924, 2869, 2854, 1438, 1296, 1179, 1099, 977, 924, 861, 748.

***N*-((4*S*)-4-oxido-2,6-bis(2,4,6-triethylphenyl)dinaphtho[2,1-*d*:1',2'-*f*][1,3,2]dioxaphosphepin-4-yl)-*P,P*-diphenylphosphinic amide (NPPA-9)**



NPPA-9 was prepared according to **General procedure J**, starting from (*S*)-3,3'-bis(2,4,6-triethylphenyl)-[1,1'-binaphthalene]-2,2'-diol (70.0 mg, 0.116 mmol, 1.0 equiv.) and POCl₃ (32.3 μL, 0.347 mmol, 3.0 equiv.) in pyridine (1.0 mL). Then crude phosphoric chloride was added to the mixture of diphenyl phosphoramidate (50.1 mg, 0.231 mmol, 2.0 equiv.) and NaH (60% dispersion in mineral oil, 13.9 mg, 0.347 mmol, 3.0 equiv.) in THF (2.0 mL). Purification by silica gel column chromatography (pentane/EtOAc = 10:1) and acidification with 6 N HCl afforded **NPPA-9** (68.0 mg, 78.4 μmol, 68%) as a white solid.

¹H NMR (500 MHz, CD₂Cl₂) δ [ppm] = 7.96 (d, *J* = 8.2 Hz, 1H), 7.91 (t, *J* = 4.2 Hz, 2H), 7.77 (s, 1H), 7.51 (dddd, *J* = 15.1, 8.1, 6.5, 1.3 Hz, 2H), 7.45–7.35 (m, 4H), 7.34–7.23 (m, 4H), 7.21–7.10 (m, 5H), 7.06 (d, *J* = 1.8 Hz, 1H), 6.98–6.88 (m, 4H), 2.76 (q, *J* = 7.6 Hz, 2H), 2.69–2.60 (m, 2H), 2.55–2.47 (m, 2H), 2.46–2.29 (m, 4H), 2.23 (q, *J* = 7.5 Hz, 2H), 1.34 (t, *J* = 7.6 Hz, 3H), 1.27–1.24 (m, 3H), 1.19 (t, *J* = 7.4 Hz, 3H), 1.08 (t, *J* = 7.5 Hz, 3H), 1.01 (t, *J* = 7.5 Hz, 3H), 0.88 (t, *J* = 7.6 Hz, 3H).

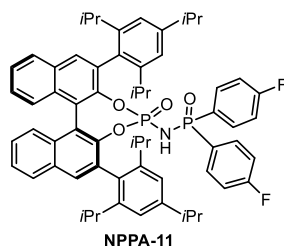
¹³C NMR (126 MHz, CD₂Cl₂) δ [ppm] = 146.2, 146.1, 145.5, 145.4, 144.6, 143.9, 143.8, 143.6, 143.1, 143.0, 133.1, 133.03, 133.01, 132.94, 132.89, 132.87, 132.78, 132.54, 132.51, 132.34, 132.32, 132.26, 132.23, 132.21, 132.18, 132.10, 132.0, 131.8, 131.7, 131.62, 131.56, 131.5, 131.1, 128.68, 128.66, 128.64, 128.58, 128.57, 128.47, 128.43, 127.5, 127.3, 126.9, 126.8, 126.6, 126.3, 126.2, 125.5, 125.4, 125.0, 122.77, 122.75, 122.67, 122.65, 29.3, 29.1, 27.8, 27.3, 27.2, 27.1, 16.7, 15.6, 15.5, 15.4, 15.1, 15.0.

³¹P NMR (203 MHz, CD₂Cl₂) δ [ppm] = 26.73, 2.53.

HRMS-ESI: calcd. for C₅₆H₅₅NO₄P₂ [M – H][–]: 866.3534; found: 866.3541.

FT-IR: ν [cm^{–1}] = 2963, 2928, 2871, 1738, 1461, 1438, 1295, 1186, 1127, 967, 904, 870, 750.

***P,P*-bis(4-fluorophenyl)-*N*-((4*S*)-4-oxido-2,6-bis(2,4,6-triisopropylphenyl)dinaphtho[2,1-*d*:1',2'-*f*][1,3,2]dioxaphosphepin-4-yl)phosphinic amide (NPPA-11)**



NPPA-11 was prepared according to **General procedure J**, starting from (*S*)-3,3'-bis(2,4,6-triisopropylphenyl)-[1,1'-binaphthalene]-2,2'-diol (70.0 mg, 0.101 mmol, 1.0 equiv.) and POCl_3 (28.4 μL , 0.304 mmol, 3.0 equiv.) in pyridine (2.0 mL). Then crude phosphoric chloride was added to the mixture of *P,P*-bis(4-fluorophenyl)phosphinic amide **3.73c** (30.8 mg, 0.122 mmol, 1.2 equiv.) and NaH (60% dispersion in mineral oil, 12.2 mg, 0.304 mmol, 3.0 equiv.) in THF (3.0 mL). Purification by silica gel column chromatography (pentane/EtOAc = 10:1) and acidification with 6 N HCl afforded **NPPA-11** (22.0 mg, 22.3 μmol , 22%) as a white solid.

^1H NMR (500 MHz, CD_2Cl_2) δ [ppm] = 7.85 (d, J = 9.2 Hz, 2H), 7.80 (d, J = 8.2 Hz, 1H), 7.67 (s, 1H), 7.40 (dddd, J = 16.5, 8.1, 6.7, 1.1 Hz, 2H), 7.29 (ddd, J = 12.8, 8.6, 5.6 Hz, 2H), 7.22–7.12 (m, 3H), 7.11–7.01 (m, 4H), 7.00–6.91 (m, 3H), 6.74 (td, J = 8.9, 2.5 Hz, 2H), 6.67 (td, J = 8.9, 2.6 Hz, 2H), 3.05–2.98 (m, 1H), 2.95–2.86 (m, 1H), 2.76–2.67 (m, 2H), 2.66–2.53 (m, 2H), 1.30 (dd, J = 6.9, 5.7 Hz, 6H), 1.25 (d, J = 6.8 Hz, 3H), 1.21 (dd, J = 6.7, 3.2 Hz, 6H), 1.10 (dd, J = 10.0, 6.8 Hz, 6H), 1.05 (d, J = 6.9 Hz, 3H), 0.97 (d, J = 6.8 Hz, 3H), 0.85 (d, J = 6.8 Hz, 3H), 0.82 (dd, J = 6.8, 2.7 Hz, 6H).

^{13}C NMR (126 MHz, CD_2Cl_2) δ [ppm] = 149.3, 148.7, 148.5, 148.3, 147.8, 146.3, 146.2, 145.3, 145.2, 134.8, 134.73, 134.70, 134.6, 134.5, 134.5, 134.44, 134.37, 133.9, 133.8, 133.0, 132.7, 132.6, 132.0, 131.72, 131.66, 131.3, 131.2, 128.5, 127.6, 127.5, 126.9, 126.8, 126.4, 122.6, 122.4, 122.3, 122.1, 121.5, 120.7, 116.1, 116.0, 116.0, 115.93, 115.92, 115.87, 115.81, 115.7, 34.5, 34.3, 31.6, 31.5, 31.4, 31.3, 30.1, 27.4, 26.3, 25.2, 24.8, 24.4, 24.3, 23.9, 23.85, 23.76, 23.69, 23.54, 23.47.

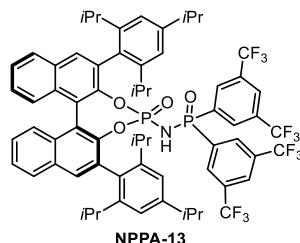
^{31}P NMR (203 MHz, CD_2Cl_2) δ [ppm] = 27.34, 1.43.

^{19}F NMR (471 MHz, CD_2Cl_2) δ [ppm] = –106.88, –106.98.

HRMS-ESI: calcd. for $C_{62}H_{65}NO_4P_2F_2$ $[M - H]^-$: 986.4284; found: 986.4294.

FT-IR: ν [cm^{-1}] = 2957, 2922, 2853, 1594, 1457, 1124, 818, 752.

***P,P*-bis(3,5-bis(trifluoromethyl)phenyl)-*N*-((4*S*)-4-oxido-2,6-bis(2,4,6-triisopropylphenyl)dinaphtho[2,1-*d*:1',2'-*f*][1,3,2]dioxaphosphepin-4-yl)phosphinic amide (NPPA-13)**



NPPA-13 was prepared according to **General procedure J**, starting from (*S*)-3,3'-bis(2,4,6-triisopropylphenyl)-[1,1'-binaphthalene]-2,2'-diol (70.0 mg, 101 μ mol, 1.0 equiv.) and $POCl_3$ (28.4 μ L, 0.304 mmol, 3.0 equiv.) in pyridine (1.0 mL). Then crude phosphoric chloride was added to the mixture of *P,P*-bis(3,5-bis(trifluoromethyl)phenyl)phosphinic amide **3.73d** (59.5 mg, 122 μ mol, 1.2 equiv.) and NaH (60% dispersion in mineral oil, 12.2 mg, 0.304 mmol, 3.0 equiv.) in THF (1.0 mL). Purification by silica gel column chromatography (pentane/EtOAc = 10:1) and acidification with 4N HCl afforded **NPPA-13** (44.0 mg, 36.0 μ mol, 35%) as a white solid.

1H NMR (500 MHz, CD_2Cl_2) δ [ppm] = 8.03–7.79 (m, 10H), 7.51 (ddd, J = 8.0, 6.7, 1.2 Hz, 1H), 7.47 (t, J = 7.5 Hz, 1H), 7.31–7.18 (m, 3H), 7.11–7.03 (m, 3H), 6.96 (dd, J = 23.0, 1.8 Hz, 2H), 2.95–2.83 (m, 3H), 2.68–2.59 (m, 3H), 1.29–1.27 (m, 6H), 1.25–1.24 (m, 6H), 1.22–1.18 (m, 6H), 1.18–1.14 (m, 3H), 1.07 (d, J = 6.8 Hz, 3H), 0.86 (dd, J = 12.9, 7.6 Hz, 9H), 0.64 (d, J = 6.9 Hz, 3H).

^{13}C NMR (126 MHz, CD_2Cl_2) δ [ppm] = 149.2, 148.9, 148.1, 146.8, 133.4, 132.9, 132.7, 132.1, 132.0, 131.6, 131.4, 131.3, 128.62, 128.56, 127.6, 127.3, 126.8, 126.4, 126.22, 126.18, 121.7, 121.23, 121.19, 120.9, 34.4, 32.3, 31.4, 31.3, 31.0, 30.1, 29.8, 26.6, 26.5, 25.2, 25.1, 24.2, 24.1, 23.9, 23.7, 23.0, 22.5.

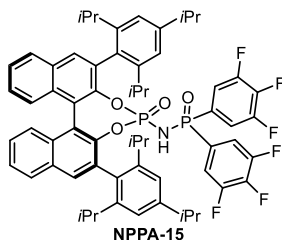
^{31}P NMR (203 MHz, CD_2Cl_2) δ [ppm] = 17.05, 6.55.

^{19}F NMR (471 MHz, CD_2Cl_2) δ [ppm] = –63.20, –63.54.

HRMS-ESI: calcd. for $C_{66}H_{62}NO_4P_2F_{12}$ $[M - H]^-$: 1222.3968; found: 1222.3984.

FT-IR: ν [cm^{-1}] = 2960, 2926, 2856, 1458, 1362, 1279, 1181, 1141, 971, 819, 749.

***N*-((4*S*)-4-oxido-2,6-bis(2,4,6-triisopropylphenyl)dinaphtho[2,1-*d*:1',2'-*f*][1,3,2]dioxaphosphepin-4-yl)-*P,P*-bis(3,4,5-trifluorophenyl)phosphinic amide (NPPA-15)**



NPPA-15 was prepared according to **General procedure J**, starting from (*S*)-3,3'-bis(2,4,6-triisopropylphenyl)-[1,1'-binaphthalene]-2,2'-diol (30.0 mg, 43.0 μmol , 1.0 equiv.) and POCl_3 (12.2 μL , 0.130 mmol, 3.0 equiv.) in pyridine (1.0 mL). Then crude phosphoric chloride was added to the mixture of *P,P*-bis(3,4,5-trifluorophenyl)phosphinic amide **3.73f** (17.0 mg, 52.0 μmol , 1.2 equiv.) and NaH (60% dispersion in mineral oil, 5.2 mg, 0.130 mmol, 3.0 equiv.) in THF (1.0 mL). Purification by silica gel column chromatography (pentane/EtOAc = 10:1) and acidification with 4N HCl afforded **NPPA-15** (33.0 mg, 31.2 μmol , 72%) as a white solid.

^1H NMR (500 MHz, CD_2Cl_2) δ [ppm] = 7.96 (t, $J = 4.2$ Hz, 2H), 7.90 (d, $J = 8.2$ Hz, 1H), 7.77 (s, 1H), 7.51 (dddd, $J = 16.3, 8.1, 6.7, 1.2$ Hz, 2H), 7.28 (dddd, $J = 12.9, 8.3, 6.9, 1.4$ Hz, 2H), 7.21 (d, $J = 1.8$ Hz, 1H), 7.16 (dd, $J = 13.4, 8.6$ Hz, 2H), 7.09–6.98 (m, 5H), 6.92 (dt, $J = 13.7, 6.5$ Hz, 2H), 3.07–3.01 (m, 1H), 2.95–2.88 (m, 1H), 2.84–2.77 (m, 2H), 2.69–2.63 (m, 1H), 2.58–2.53 (m, 1H), 1.31 (d, $J = 7.0$ Hz, 6H), 1.29 (d, $J = 6.6$ Hz, 3H), 1.27–1.25 (m, 6H), 1.22 (d, $J = 7.0$ Hz, 3H), 1.18 (d, $J = 6.8$ Hz, 3H), 1.05 (d, $J = 6.8$ Hz, 3H), 1.01 (d, $J = 6.8$ Hz, 3H), 0.97 (dd, $J = 12.3, 6.7$ Hz, 6H), 0.90 (d, $J = 6.8$ Hz, 3H).

^{13}C NMR (126 MHz, CD_2Cl_2) δ [ppm] = 149.5, 149.0, 148.14, 148.05, 147.2, 147.1, 145.9, 145.8, 145.2, 145.1, 134.0, 133.9, 133.2, 132.9, 132.6, 132.54, 132.51, 131.8, 131.4, 131.2, 131.1, 131.0, 128.6, 127.6, 127.51, 127.49, 127.1, 126.9, 126.8, 126.6, 126.5, 126.2, 122.3, 122.2, 122.1, 121.92, 121.87, 121.6, 120.8, 120.3, 117.0, 116.8, 116.6, 116.5, 34.3, 33.8, 31.7, 31.5, 31.3, 31.2, 30.1, 27.3, 26.3, 25.4, 24.8, 24.3, 24.2, 24.1, 24.0, 23.7, 23.6, 23.5, 23.4, 23.2.

^{31}P NMR (203 MHz, CD_2Cl_2) δ [ppm] = 21.56, 0.78.

^{19}F NMR (471 MHz, CD_2Cl_2) δ [ppm] = -130.56, -130.57, -130.61, -130.62, -131.28, -131.34,

-131.35, -131.38, -131.40, -131.46, -152.62, -152.67, -152.73, -153.15, -153.20, -153.25.

HRMS-ESI: calcd. for $C_{62}H_{60}NO_4P_2F_6$ $[M - H]^-$: 1058.3907; found: 1058.3922.

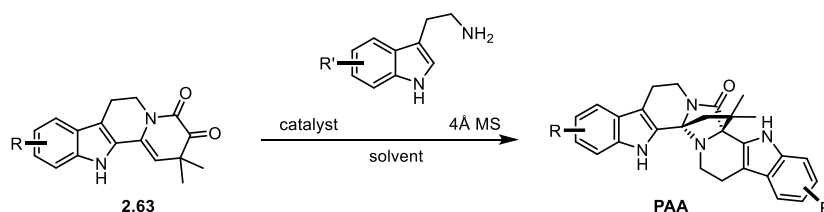
FT-IR: ν [cm^{-1}] = 2961, 2926, 2868, 1616, 1523, 1418, 1326, 1046, 969, 864, 750.

7.2.2.1.6. Other chiral Brønsted acids

All the other chiral Brønsted acids were synthesized and provided by the technician team and group members of AK List. I appreciated their generous donation.

7.2.2.2. Asymmetric synthesis of peganumine A and its analogues

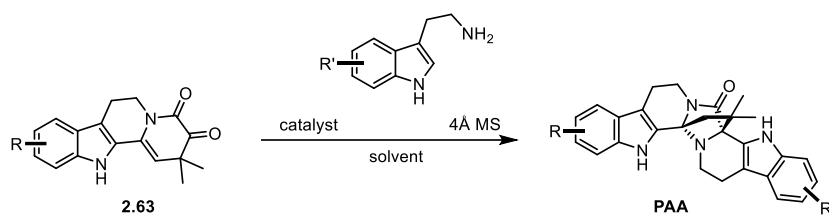
General Procedure for the small scale ($\cong 1.00$ mg) screening reactions



A mixture of α -ketoamide **2.63** (1.00 mg, 3.00 μ mol, 1.0 equiv.), tryptamine derivatives (0.75 mg, 3.60 μ mol, 1.2 equiv.) and 4 Å MS in corresponding solvent (0.5 mL) was stirred at room temperature under argon in sealed vial. A solution of corresponding catalyst in the same solvent was added to the reaction mixture and the reaction mixture was heated up to the corresponding temperature for the set duration. The reaction mixture was cooled to room temperature and purified by silica gel column chromatography (pentane/EtOAc = 3:2) to yield the pure product as solid.

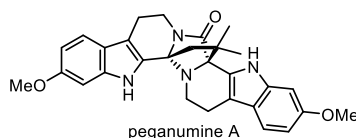
(Note: since the ketoamide is not a fine powder and cannot dissolve in toluene (the frequently used solvent), the practical way to prepare the 1.00 mg or 0.50 mg ketoamide was that, using fine balance to take 10.00 mg ketoamide which was then dissolved in 5.0 mL DCM (10.0 mL for 0.50 mg preparation), then adding 0.5 mL of such solvent to the 1.5 mL glass reaction vials, finally removing the DCM by rotary evaporator. And the catalyst was prepared in the corresponding solvent to load into the reaction.)

General procedure K



A mixture of α -ketoamide **2.63** (1.0 equiv.), tryptamine derivatives (1.2 equiv.) and 4Å molecular sieves in toluene was stirred at room temperature. A solution of catalyst in toluene was added to the reaction mixture and the reaction mixture was stirred at set temperature. After the reaction mixture was cooled to room temperature, filtered through Celite[®], washed by NaHCO₃ (sat. aq.), dried over MgSO₄ and concentrated under reduced pressure. The crude product was purified by silica gel column chromatography to afforded **PAA**.

Peganumine A



Peganumine A was prepared according to **General procedure K**, starting from α -ketoamide **2.63b** (66.0 mg, 0.213 mmol, 1.0 equiv.), 6-methoxytryptamine (48.5 mg, 0.255 mmol, 1.2 equiv.) and 4 Å molecular sieves (50.0 mg) in toluene (50 mL). Then a solution of (*R*)-**DSI-31** (16.1 mg, 21.3 μ mol, 0.1 equiv.) in toluene (5.0 mL) was added to the reaction mixture and the reaction mixture was stirred at 60 °C for 60 h. Purification by silica gel column chromatography (pentane/EtOAc = 3:2) afforded peganumine A (83.3 mg, 0.173 mmol, 81%) as a white solid.

¹H NMR (700 MHz, CD₃OD) δ [ppm] = 7.38 (d, *J* = 8.7 Hz, 1H), 7.26 (d, *J* = 8.6 Hz, 1H), 6.99 (d, *J* = 2.2 Hz, 1H), 6.93 (d, *J* = 2.2 Hz, 1H), 6.73 (dd, *J* = 8.7, 2.2 Hz, 1H), 6.67 (dd, *J* = 8.6, 2.3 Hz, 1H), 4.14 (dd, *J* = 13.0, 5.8 Hz, 1H), 3.83 (s, 3H), 3.82 (s, 3H), 3.21–3.16 (m, 1H), 2.98 (dd, *J* = 15.4, 4.4 Hz, 1H), 2.90–2.76 (m, 2H), 2.69 (dd, *J* = 15.5, 3.5 Hz, 1H), 2.59 (dd, *J* = 10.8, 5.3 Hz, 1H), 2.48–2.41 (m, 1H), 2.39 (d, *J* = 11.5 Hz, 1H), 1.94 (d, *J* = 11.5 Hz, 1H), 1.44 (s, 3H), 1.24 (s, 3H).

^{13}C NMR (176 MHz, CD_3OD) δ [ppm] = 175.2, 158.3, 157.6, 139.5, 139.4, 127.8, 126.4, 122.3, 122.2, 119.9, 119.2, 112.9, 112.2, 110.5, 109.8, 96.0, 95.7, 81.2, 79.7, 56.0, 55.9, 51.9, 41.7, 41.6, 37.3, 27.3, 26.3, 22.5, 22.1.

^1H NMR (500 MHz, d_6 -DMSO) δ [ppm] = 11.24 (s, 1H), 10.77 (s, 1H), 7.38 (d, J = 8.6 Hz, 1H), 7.25 (d, J = 8.6 Hz, 1H), 6.93 (d, J = 2.3 Hz, 1H), 6.88 (d, J = 2.3 Hz, 1H), 6.70 (dd, J = 8.6, 2.3 Hz, 1H), 6.63 (dd, J = 8.6, 2.3 Hz, 1H), 4.00 (dd, J = 12.9, 5.8 Hz, 1H), 3.78 (s, 3H), 3.77 (s, 3H), 3.10 (td, J = 12.6, 4.5 Hz, 1H), 2.90 (dd, J = 15.3, 4.2 Hz, 1H), 2.76–2.69 (m, 1H), 2.69–2.65 (m, 1H), 2.64–2.60 (m, 1H), 2.48–2.43 (m, 1H), 2.34 (dd, J = 10.8, 4.9 Hz, 1H), 2.30 (d, J = 11.3 Hz, 1H), 1.88 (d, J = 11.2 Hz, 1H), 1.38 (s, 3H), 1.15 (s, 3H).

^{13}C NMR (126 MHz, d_6 -DMSO) δ [ppm] = 171.3, 156.1, 155.4, 137.6, 137.5, 127.3, 125.7, 120.5, 120.4, 119.0, 118.2, 111.2, 109.5, 109.0, 108.3, 94.9, 94.7, 78.8, 77.4, 55.23, 55.18, 50.4, 40.1, 39.9, 35.6, 26.8, 26.0, 21.0, 20.9.

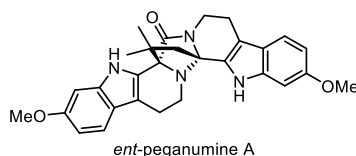
HRMS-ESI: calcd. for $\text{C}_{29}\text{H}_{31}\text{N}_4\text{O}_3$ $[\text{M} + \text{H}]^+$: 483.2391; found: 483.2384.

FT-IR: ν [cm^{-1}] = 2954, 2923, 2857, 1736, 1457, 1366, 1217, 820.

$[\alpha]_{\text{D}}^{26} = +92$ (c = 0.1, MeOH).

HPLC: 40% *i*PrOH/Heptane, IA, 1.0 mL/min, 97.1% *ee*.

ent-Peganumine A



ent-Peganumine A was prepared according to **General procedure K**, starting from α -ketoamide **2.63b** (10.0 mg, 32.0 μmol , 1.0 equiv.), 6-methoxytryptamine (7.35 mg, 39.0 μmol , 1.2 equiv.) and 4 Å molecular sieves (10.0 mg) in toluene (7.5 mL). Then a solution of (*S*)-**DSI-31** (2.44 mg, 3.20 μmol , 0.1 equiv.) in toluene (1.0 mL) was added to the reaction mixture and the reaction mixture was stirred at 60 °C for 60 h. Purification by silica gel column chromatography (pentane/EtOAc = 3:2) afforded *ent*-peganumine A (10.5 mg, 21.8 μmol , 68%) as a white solid.

^1H NMR (700 MHz, CD_3OD) δ [ppm] = 7.38 (d, J = 8.7 Hz, 1H), 7.26 (d, J = 8.6 Hz, 1H), 6.99 (d, J = 2.2 Hz, 1H), 6.93 (d, J = 2.2 Hz, 1H), 6.73 (dd, J = 8.7, 2.2 Hz, 1H), 6.67 (dd, J = 8.6, 2.3 Hz, 1H), 4.14 (dd, J = 13.0, 5.8 Hz, 1H), 3.83 (s, 3H), 3.82 (s, 3H), 3.21–3.16 (m, 1H),

2.98 (dd, $J = 15.4, 4.4$ Hz, 1H), 2.90–2.76 (m, 2H), 2.69 (dd, $J = 15.5, 3.5$ Hz, 1H), 2.59 (dd, $J = 10.8, 5.3$ Hz, 1H), 2.48–2.41 (m, 1H), 2.39 (d, $J = 11.5$ Hz, 1H), 1.94 (d, $J = 11.5$ Hz, 1H), 1.44 (s, 3H), 1.24 (s, 3H).

^{13}C NMR (176 MHz, CD_3OD) δ [ppm] = 175.2, 158.3, 157.6, 139.5, 139.4, 127.8, 126.4, 122.3, 122.2, 119.9, 119.2, 112.9, 112.2, 110.5, 109.8, 96.0, 95.7, 81.2, 79.7, 56.0, 55.9, 51.9, 41.7, 41.6, 37.3, 27.3, 26.3, 22.5, 22.1.

^1H NMR (500 MHz, d_6 -DMSO) δ [ppm] = 11.24 (s, 1H), 10.77 (s, 1H), 7.38 (d, $J = 8.6$ Hz, 1H), 7.25 (d, $J = 8.6$ Hz, 1H), 6.93 (d, $J = 2.3$ Hz, 1H), 6.88 (d, $J = 2.3$ Hz, 1H), 6.70 (dd, $J = 8.6, 2.3$ Hz, 1H), 6.63 (dd, $J = 8.6, 2.3$ Hz, 1H), 4.00 (dd, $J = 12.9, 5.8$ Hz, 1H), 3.78 (s, 3H), 3.77 (s, 3H), 3.10 (td, $J = 12.6, 4.5$ Hz, 1H), 2.90 (dd, $J = 15.3, 4.2$ Hz, 1H), 2.76–2.69 (m, 1H), 2.69–2.65 (m, 1H), 2.64–2.60 (m, 1H), 2.48–2.43 (m, 1H), 2.34 (dd, $J = 10.8, 4.9$ Hz, 1H), 2.30 (d, $J = 11.3$ Hz, 1H), 1.88 (d, $J = 11.2$ Hz, 1H), 1.38 (s, 3H), 1.15 (s, 3H).

^{13}C NMR (126 MHz, d_6 -DMSO) δ [ppm] = 171.3, 156.1, 155.4, 137.6, 137.5, 127.3, 125.7, 120.5, 120.4, 119.0, 118.2, 111.2, 109.5, 109.0, 108.3, 94.9, 94.7, 78.8, 77.4, 55.23, 55.18, 50.4, 40.1, 39.9, 35.6, 26.8, 26.0, 21.0, 20.9.

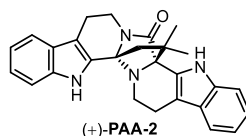
HRMS-ESI: calcd. for $\text{C}_{29}\text{H}_{31}\text{N}_4\text{O}_3$ $[\text{M} + \text{H}]^+$: 483.2391; found: 483.2384.

FT-IR: ν [cm^{-1}] = 2954, 2923, 2857, 1736, 1457, 1366, 1217, 820.

$[\alpha]_{\text{D}}^{26} = -90$ ($c = 0.1$, MeOH).

HPLC: 40% *i*PrOH/Heptane, IA, 1.0 mL/min, 97.1% *ee*.

(+)-PAA-2



(+)-PAA-2 was prepared according to the **General procedure K** starting from α -ketoamide **2.63a** (20.0 mg, 71.0 μmol , 1.0 equiv.), tryptamine (13.7 mg, 8.60 mmol, 1.2 equiv.) and 4 Å molecular sieves (20.0 mg) in toluene (15 mL). Then a solution of (*R*)-NPPA-1 (15.5 mg, 14.0 μmol , 0.2 equiv.) in toluene (2.0 mL) was added to the reaction mixture and the reaction mixture was stirred at 90 °C for 60 h. Purification by silica gel column chromatography (pentane/EtOAc = 3:2) afforded (+)-PAA-2 (20.0 mg, 47.4 μmol , 66%) as a white solid.

¹H NMR (500 MHz, *d*₆-DMSO) δ [ppm] = 11.44 (s, 1H), 10.97 (s, 1H), 7.52 (d, *J* = 7.9 Hz, 1H), 7.44–7.35 (m, 3H), 7.15 (ddd, *J* = 8.2, 7.0, 1.2 Hz, 1H), 7.10–7.02 (m, 2H), 6.99–6.94 (m, 1H), 4.04 (dd, *J* = 12.9, 5.8 Hz, 1H), 3.16–3.10 (m, 1H), 2.96 (dd, *J* = 15.2, 4.3 Hz, 1H), 2.81–2.68 (m, 3H), 2.48–2.46 (m, 1H), 2.41–2.32 (m, 2H), 1.93 (d, *J* = 11.2 Hz, 1H), 1.41 (s, 3H), 1.16 (s, 3H).

¹³C NMR (126 MHz, *d*₆-DMSO) δ [ppm] = 171.7, 137.3, 137.3, 129.2, 127.7, 126.5, 126.4, 122.5, 121.3, 119.7, 119.4, 118.9, 118.2, 112.1, 112.0, 111.7, 110.1, 79.3, 78.0, 50.9, 40.6, 40.4, 36.1, 27.3, 26.5, 21.5, 21.4.

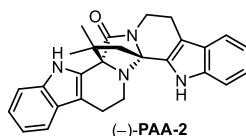
HRMS-ESI: calcd. for C₂₇H₂₆N₄ONa [M + Na]⁺: 445.1999; found: 445.2000.

FT-IR: ν [cm⁻¹] = 3307, 3267, 2922, 2857, 1704, 1451, 1410, 1320, 1302, 1270, 1168, 1146, 1039, 752, 742.

[α]_D²⁶ = +86 (*c* = 0.1, MeOH).

HPLC: 30% *i*PrOH/Hexane, IA, 1.0 mL/min, 94.6% *ee*.

(-)-PAA-2



(-)-PAA-2 was prepared according to the **General procedure K** starting from α -ketoamide **2.63a** (10.0 mg, 36.0 μ mol, 1.0 equiv.), tryptamine (6.9 mg, 4.3 mmol, 1.2 equiv.) and 4 Å molecular sieves (10.0 mg) in toluene (7.5 mL). Then a solution of (*S*)-NPPA-1 (7.8 mg, 7.0 μ mol, 0.2 equiv.) in toluene (1.0 mL) was added to the reaction mixture and the reaction mixture was stirred at 90 °C for 60 h. Purification by silica gel column chromatography (pentane/EtOAc = 3:2) afforded (-)-PAA-2 (6.1 mg, 14.4 μ mol, 40%) as a white solid.

¹H NMR (500 MHz, *d*₆-DMSO) δ [ppm] = 11.44 (s, 1H), 10.97 (s, 1H), 7.52 (d, *J* = 7.9 Hz, 1H), 7.44–7.35 (m, 3H), 7.15 (ddd, *J* = 8.2, 7.0, 1.2 Hz, 1H), 7.10–7.02 (m, 2H), 6.99–6.94 (m, 1H), 4.04 (dd, *J* = 12.9, 5.8 Hz, 1H), 3.16–3.10 (m, 1H), 2.96 (dd, *J* = 15.2, 4.3 Hz, 1H), 2.81–2.68 (m, 3H), 2.48–2.46 (m, 1H), 2.41–2.32 (m, 2H), 1.93 (d, *J* = 11.2 Hz, 1H), 1.41 (s, 3H), 1.16 (s, 3H).

^{13}C NMR (126 MHz, d_6 -DMSO) δ [ppm] = 171.7, 137.3, 137.3, 129.2, 127.7, 126.5, 126.4, 122.5, 121.3, 119.7, 119.4, 118.9, 118.2, 112.1, 112.0, 111.7, 110.1, 79.3, 78.0, 50.9, 40.6, 40.4, 36.1, 27.3, 26.5, 21.5, 21.4.

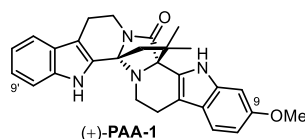
HRMS-ESI: calcd. for $\text{C}_{27}\text{H}_{26}\text{N}_4\text{ONa}$ $[\text{M} + \text{Na}]^+$: 445.1999; found: 445.2000.

FT-IR: ν [cm^{-1}] = 3307, 3267, 2922, 2857, 1704, 1451, 1410, 1320, 1302, 1270, 1168, 1146, 1039, 752, 742.

$[\alpha]_{\text{D}}^{26} = -80$ ($c = 0.1$, MeOH).

HPLC: 30% *i*PrOH/Hexane, IA, 1.0 mL/min, 94.0% *ee*.

(+)-PAA-1



(+)-**PAA-1** was prepared according to the **General procedure K** starting from α -ketoenamide **2.63a** (21.0 mg, 75.0 μmol , 1.0 equiv.), tryptamine (17.1 mg, 90.0 μmol , 1.2 equiv.) and 4Å molecular sieves (20.0 mg) in toluene (15 mL). Then a solution of (*R*)-**NPPA-2** (7.1 mg, 7.5 μmol , 0.1 equiv.) in toluene (2.0 mL) was added to the reaction mixture and the reaction mixture was stirred at 60 °C for 60 h. Purification by silica gel column chromatography (pentane/EtOAc = 3:2) afforded (+)-**PAA-1** (10.0 mg, 22.3 μmol , 30%) as a white solid.

^1H NMR (500 MHz, CD_3OD) δ [ppm] = 7.51 (dt, $J = 7.9, 1.1$ Hz, 1H), 7.42–7.36 (m, 1H), 7.25 (d, $J = 8.6$ Hz, 1H), 7.16 (ddd, $J = 8.2, 7.1, 1.2$ Hz, 1H), 7.05 (ddd, $J = 8.1, 7.1, 1.0$ Hz, 1H), 6.97 (d, $J = 2.3$ Hz, 1H), 6.66 (dd, $J = 8.6, 2.3$ Hz, 1H), 4.18–4.10 (m, 1H), 3.81 (s, 3H), 3.18 (ddd, $J = 13.0, 11.7, 4.7$ Hz, 1H), 3.01 (ddd, $J = 15.4, 4.7, 1.1$ Hz, 1H), 2.83 (dddd, $J = 34.5, 15.1, 11.7, 5.8$ Hz, 2H), 2.66 (ddd, $J = 15.2, 4.1, 1.5$ Hz, 1H), 2.55 (ddd, $J = 10.8, 5.6, 1.5$ Hz, 1H), 2.44 (dd, $J = 11.2, 4.1$ Hz, 1H), 2.40 (d, $J = 11.4$ Hz, 1H), 1.94 (d, $J = 11.5$ Hz, 1H), 1.43 (s, 3H), 1.24 (s, 3H).

^{13}C NMR (126 MHz, CD_3OD) δ [ppm] = 175.2, 157.6, 139.4, 138.8, 127.9, 127.7, 127.7, 123.5, 122.3, 120.3, 119.4, 119.2, 112.9, 112.5, 112.2, 109.8, 96.0, 81.2, 79.7, 56.0, 52.0, 41.7, 41.6, 37.3, 27.3, 26.3, 22.5, 22.1.

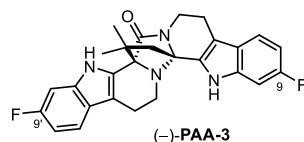
HRMS-ESI: calcd. for $\text{C}_{28}\text{H}_{28}\text{N}_4\text{O}_2\text{Na}$ $[\text{M} + \text{Na}]^+$: 475.2104; found: 475.2106.

FT-IR: ν [cm^{-1}] = 2926, 2863, 1738, 1456, 1367, 1228, 1216, 750.

$[\alpha]_{\text{D}}^{26} = +84$ ($c = 0.1$, MeOH).

HPLC: 40% *i*PrOH/Heptane, IA, 1.0 mL/min, 97.8% *ee*.

(-)-PAA-3



(-)-PAA-3 was prepared according to the **General procedure K** starting from α -ketoenamide **2.63f** (21.0 mg, 70.0 μmol , 1.0 equiv.), 6-fluorotryptamine (15.1 mg, 85.0 μmol , 1.2 equiv.) and 4 Å molecular sieves (20.0 mg) in toluene (15 mL). Then a solution of (*S*)-**NPPA-1** (7.7 mg, 7.0 μmol , 0.1 equiv.) in toluene (2.0 mL) was added to the reaction mixture and the reaction mixture was stirred at 90 °C for 60 h. Purification by silica gel column chromatography (pentane/EtOAc = 3:2) afforded **(-)-PAA-3** (23.2 mg, 50.8 μmol , 72%) as a white solid.

^1H NMR (500 MHz, CD_3OD) δ [ppm] = 7.48 (dd, $J = 8.7, 5.3$ Hz, 1H), 7.33 (dd, $J = 8.6, 5.3$ Hz, 1H), 7.10 (td, $J = 10.1, 2.3$ Hz, 2H), 6.85 (ddd, $J = 9.7, 8.6, 2.3$ Hz, 1H), 6.77 (ddd, $J = 9.8, 8.6, 2.4$ Hz, 1H), 4.15 (ddd, $J = 13.1, 6.0, 1.1$ Hz, 1H), 3.19 (ddd, $J = 13.0, 11.6, 4.6$ Hz, 1H), 3.01 (ddd, $J = 15.5, 4.6, 1.1$ Hz, 1H), 2.92–2.78 (m, 2H), 2.75–2.68 (m, 1H), 2.57 (ddd, $J = 10.8, 5.6, 1.6$ Hz, 1H), 2.48–2.41 (m, 1H), 2.39 (d, $J = 11.5$ Hz, 1H), 1.96 (d, $J = 11.5$ Hz, 1H), 1.44 (s, 3H), 1.23 (s, 3H).

^{13}C NMR (126 MHz, CD_3OD) δ [ppm] = 174.9, 162.4 (d, $J = 66.7$ Hz), 160.5 (d, $J = 65.0$ Hz), 138.7, 129.5, 128.4, 124.5, 124.5, 120.4 (d, $J = 10.3$ Hz), 119.5 (d, $J = 10.4$ Hz), 113.2, 112.4, 108.8 (d, $J = 24.9$ Hz), 108.2 (d, $J = 24.8$ Hz), 98.6, 98.4, 81.1, 79.7, 51.9, 41.7, 41.6, 37.2, 27.3, 26.2, 22.4, 22.0.

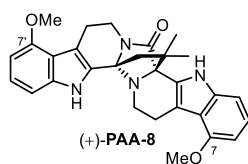
^{19}F NMR (471 MHz, CD_3OD) δ [ppm] = -122.69, -124.36.

HRMS-ESI: calcd. for $\text{C}_{27}\text{H}_{24}\text{F}_2\text{N}_4\text{ONa}$ [$\text{M} + \text{Na}$] $^+$: 481.1810; found: 481.1813.

FT-IR: ν [cm^{-1}] = 3427, 3297, 2953, 2922, 1684, 1450, 1410, 1347, 1319, 1301, 1269, 736.

$[\alpha]_{\text{D}}^{26} = -52$ ($c = 0.1$, MeOH).

HPLC: 15% *i*PrOH/Heptane, AD-3, 1.0 mL/min, 98.6% *ee*.

(+)-PAA-8

(+)-PAA-8 was prepared according to the **General procedure K** starting from α -ketoenamide **2.63c** (17.4 mg, 56.0 μ mol, 1.0 equiv.), 4-methoxytryptamine (12.8 mg, 67.0 μ mol, 1.2 equiv.) and 4 Å molecular sieves (20.0 mg) in toluene (15 mL). Then a solution of (*R*)-NPPA-1 (12.2 mg, 11.0 μ mol, 0.2 equiv.) in toluene (2.0 mL) was added to the reaction mixture and the reaction mixture was stirred at 90 °C for 60 h. Purification by silica gel column chromatography (pentane/EtOAc = 3:2) afforded (+)-PAA-8 (11.0 mg, 22.8 μ mol, 41%) as a white solid.

¹H NMR (600 MHz, *d*₆-DMSO) δ [ppm] = 11.40 (s, 1H), 10.89 (s, 1H), 7.05–7.00 (m, 2H), 6.99–6.93 (m, 2H), 6.49 (dd, *J* = 7.8, 0.8 Hz, 1H), 6.43 (dd, *J* = 7.9, 0.8 Hz, 1H), 4.00–3.94 (m, 1H), 3.84 (s, 3H), 3.78 (s, 3H), 3.24–3.18 (m, 1H), 3.09 (td, *J* = 12.5, 4.4 Hz, 1H), 2.96–2.91 (m, 1H), 2.90–2.79 (m, 2H), 2.44–2.40 (m, 1H), 2.33 (dd, *J* = 11.4, 4.2 Hz, 1H), 2.30 (d, *J* = 11.2 Hz, 1H), 1.88 (d, *J* = 11.2 Hz, 1H), 1.38 (s, 3H), 1.14 (s, 3H).

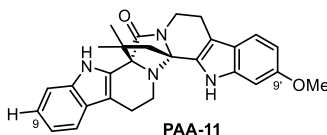
¹³C NMR (151 MHz, *d*₆-DMSO) δ [ppm] = 171.4, 154.1, 153.7, 138.1, 129.6, 128.9, 128.2, 126.8, 125.3, 122.8, 121.6, 116.1, 110.9, 109.3, 105.0, 99.3, 98.8, 78.6, 77.3, 55.1, 54.9, 50.5, 40.5, 35.7, 28.0, 26.8, 26.0, 23.2, 23.1.

HRMS-ESI: calcd. for C₂₉H₃₀N₄O₃Na [M + Na]⁺: 505.2210; found: 505.2203.

FT-IR: ν [cm⁻¹] = 3302, 3285, 2969, 2953, 1739, 1684, 1450, 1410, 1364, 1228, 1217, 741.

$[\alpha]_D^{26}$ = +60 (*c* = 0.1, MeOH).

HPLC: 5% *i*PrOH/Heptane, AD-3, 1.0 mL/min, 69.0% *ee*.

(-)-PAA-11

(-)-PAA-11 was prepared according to the **General procedure K** starting from α -ketoenamide **2.63b** (15.0 mg, 48.0 μ mol, 1.0 equiv.), tryptamine (9.3 mg, 58 μ mol, 1.2 equiv.) and 4 Å molecular sieves (20.0 mg) in toluene (10 mL). Then a solution of (*S*)-NPPA-1 (5.3 mg,

5.0 μmol , 0.1 equiv.) in toluene (1.0 mL) was added to the reaction mixture and the reaction mixture was stirred at 90 °C for 60 h. Purification by silica gel column chromatography (pentane/EtOAc = 3:2) afforded (–)-**PAA-11** (5.3 mg, 11.7 μmol , 24%) as a white solid.

$^1\text{H NMR}$ (500 MHz, CD_3OD) δ [ppm] = 7.43 (dt, $J = 8.2, 0.9$ Hz, 1H), 7.41–7.36 (m, 2H), 7.09 (ddd, $J = 8.2, 7.1, 1.1$ Hz, 1H), 6.99 (ddd, $J = 8.0, 7.0, 1.0$ Hz, 1H), 6.93 (d, $J = 2.2$ Hz, 1H), 6.73 (dd, $J = 8.6, 2.3$ Hz, 1H), 4.17–4.10 (m, 1H), 3.83 (s, 3H), 3.24–3.14 (m, 1H), 2.98 (dd, $J = 15.7, 4.1$ Hz, 1H), 2.90–2.79 (m, 2H), 2.78–2.70 (m, 1H), 2.61 (ddd, $J = 9.6, 5.6, 1.7$ Hz, 1H), 2.45 (td, $J = 11.3, 4.1$ Hz, 1H), 2.40 (dd, $J = 11.5, 1.8$ Hz, 1H), 1.95 (d, $J = 11.5$ Hz, 1H), 1.45 (s, 3H), 1.24 (s, 3H).

$^{13}\text{C NMR}$ (126 MHz, CD_3OD) δ [ppm] = 175.1, 158.4, 139.6, 138.7, 129.1, 127.7, 126.4, 122.4, 122.2, 120.0, 119.9, 118.7, 113.0, 112.4, 112.3, 110.5, 95.7, 81.3, 79.7, 56.0, 51.9, 41.8, 41.6, 37.3, 27.3, 26.3, 22.5, 22.1.

HRMS-ESI: calcd. for $\text{C}_{28}\text{H}_{28}\text{N}_4\text{O}_2\text{Na}$ [$\text{M} + \text{Na}$] $^+$: 475.2104; found: 475.2106.

FT-IR: ν [cm^{-1}] = 3278, 2953, 2924, 2853, 1707, 1602, 1455, 1396, 1386, 1267, 1214, 1100, 1029, 754.

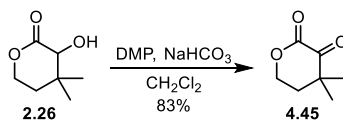
$[\alpha]_{\text{D}}^{26} = -112$ ($c = 0.1$, MeOH).

HPLC: 10% *i*PrOH/Heptane, AD-3, 1.0 mL/min, 93.2% *ee*.

7.2.3. New generation routes to the total synthesis of peganumine A

7.2.3.1. 4th generation synthetic approach to peganumine A

4,4-Dimethyldihydro-2H-pyran-2,3(4H)-dione (4.45)



To a solution of α -hydroxylactone **2.26** (300 mg, 2.08 mmol, 1.0 equiv.) in DCM (10 mL) was added added NaHCO_3 (875 mg, 10.4 mmol, 5.0 equiv.) and DMP (1.32 g, 3.12 mmol, 1.5 equiv.) at 0 °C. The mixture was allowed to warm to room temperature and stirred overnight, before the reaction was quenched with $\text{Na}_2\text{S}_2\text{O}_3$ (sat. aq.). The aqueous phase was extracted with DCM. The combined organic phases were washed with brine, dried over MgSO_4 , filtered and concentrated under reduced pressure. The crude product was purified by silica gel column chromatography (pentane/EtOAc = 20:1) to afford α -ketolactone **4.45** (496 mg, 1.73 mmol, 83%) as light yellow solid.

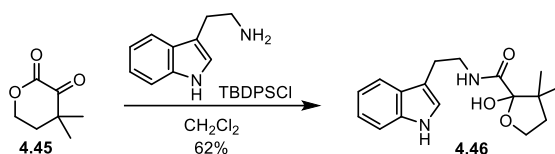
^1H NMR (600 MHz, CDCl_3) δ [ppm] = 4.58–4.53 (m, 2H), 2.18–2.14 (m, 2H), 1.29 (s, 6H).

^{13}C NMR (151 MHz, CDCl_3) δ [ppm] = 193.6, 157.5, 65.9, 44.1, 36.5, 23.7.

HRMS-ESI: calcd. for $\text{C}_7\text{H}_{10}\text{O}_3\text{Na}$ $[\text{M} + \text{Na}]^+$: 165.0522; found: 165.0525.

FT-IR: ν [cm^{-1}] = 2969, 2917, 1733, 1469, 1297, 1187, 965, 763.

N-(2-(1*H*-indol-3-yl)ethyl)-2-hydroxy-3,3-dimethyltetrahydrofuran-2-carboxamide (4.46)



To a solution of α -ketolactone **4.45** (77.0 mg, 0.542 mmol, 1.0 equiv.) in DCM (5.0 mL) was added tryptamine (104 mg, 0.651 mmol, 1.2 equiv.) and TBDPSCI (164 mg, 0.596 mmol, 1.1 equiv.). The mixture was stirred at room temperature overnight, before quenching with NaHCO_3 (sat. aq.). The aqueous phase was extracted with DCM. The combined organic phases were washed with brine, dried over MgSO_4 , filtered and concentrated under reduced pressure.

The crude product was purified by silica gel column chromatography (pentane/EtOAc = 10:1) to afford **4.46** (102 mg, 0.338 mmol, 62%) as a white solid.

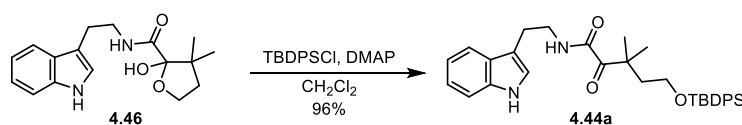
¹H NMR (500 MHz, CDCl₃) δ [ppm] = 8.16 (s, 1H), 7.63–7.61 (m, 1H), 7.37 (dt, *J* = 8.2, 0.9 Hz, 1H), 7.21 (ddd, *J* = 8.1, 7.0, 1.2 Hz, 1H), 7.13 (ddd, *J* = 8.0, 7.1, 1.0 Hz, 1H), 7.02 (d, *J* = 2.1 Hz, 1H), 6.80 (d, *J* = 6.7 Hz, 1H), 4.06 (ddd, *J* = 9.5, 8.3, 2.2 Hz, 1H), 3.91 (ddd, *J* = 10.1, 8.3, 7.0 Hz, 1H), 3.75 (s, 1H), 3.64–3.59 (m, 2H), 2.99 (td, *J* = 7.0, 0.8 Hz, 2H), 2.18–2.09 (m, 1H), 1.67 (ddd, *J* = 12.0, 7.0, 2.2 Hz, 1H), 1.22 (s, 3H), 0.86 (s, 3H).

¹³C NMR (126 MHz, CDCl₃) δ [ppm] = 170.8, 136.5, 127.4, 122.3, 122.2, 119.6, 118.8, 112.8, 111.4, 105.1, 66.6, 45.5, 39.6, 38.0, 25.4, 23.9, 22.0.

HRMS-ESI: calcd. for C₁₇H₂₂N₂O₃Na [M + Na]⁺: 325.1522; found: 325.1537.

FT-IR: ν [cm⁻¹] = 3369, 3330, 2957, 2925, 1660, 1529, 1458, 1079, 746.

***N*-(2-(1*H*-indol-3-yl)ethyl)-5-((*tert*-butyldiphenylsilyl)oxy)-3,3-dimethyl-2-oxopentanamide (4.44a)**



To a solution of hemiacetal **4.46** (55.0 mg, 0.182 mmol, 1.0 equiv.) in DCM (5.0 mL) was added TBDPSCI (237 mg, 0.910 mmol, 5.0 equiv.) and DMAP (111 mg, 0.910 mmol, 5.0 equiv.). The mixture was stirred at room temperature overnight, before quenching with NaHCO₃ (sat. aq.). The aqueous phase was extracted with DCM. The combined organic phases were washed with brine, dried over MgSO₄, filtered and concentrated under reduced pressure. The crude product was purified by silica gel column chromatography (pentane/EtOAc = 10:1) to afford **4.44a** (96.0 mg, 0.178 mmol, 96%) as a light yellow liquid.

¹H NMR (500 MHz, CDCl₃) δ [ppm] = 7.96 (s, 1H), 7.62–7.56 (m, 4H), 7.51 (dd, *J* = 7.9, 1.0 Hz, 1H), 7.46–7.28 (m, 7H), 7.19 (ddd, *J* = 8.1, 6.9, 1.2 Hz, 1H), 7.11 (ddd, *J* = 7.9, 6.9, 1.0 Hz, 1H), 6.92 (d, *J* = 2.3 Hz, 1H), 6.85 (t, *J* = 5.9 Hz, 1H), 3.66 (t, *J* = 6.0 Hz, 2H), 3.36 (td, *J* = 7.1, 5.9 Hz, 2H), 2.83–2.74 (m, 2H), 2.38 (t, *J* = 6.0 Hz, 2H), 1.32 (s, 6H), 0.97 (s, 9H).

¹³C NMR (126 MHz, CDCl₃) δ [ppm] = 202.4, 160.0, 136.5, 135.6, 133.7, 129.8, 127.8, 127.3, 122.3, 122.0, 119.6, 118.9, 112.9, 111.3, 61.0, 45.0, 42.0, 39.2, 27.0, 25.0, 25.0, 19.3.

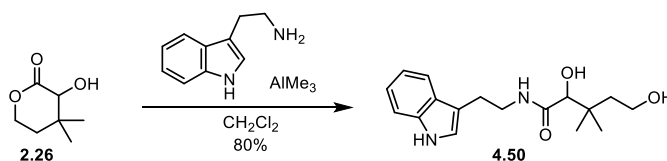
HRMS-ESI: calcd. for $C_{33}H_{40}N_2O_3SiK$ $[M + K]^+$: 579.2440; found: 579.2465.

FT-IR: ν [cm^{-1}] = 3386, 3360, 2955, 2927, 2856, 1674, 1516, 1362, 1252, 1097, 833, 740.

7.2.3.2. 5th generation synthetic approach to peganumine A

7.2.3.2.1. Mono-ring α -ketoenamides preparation via oxidative pathway and their Pictet–Spengler reactions

N-(2-(1*H*-indol-3-yl)ethyl)-2,5-dihydroxy-3,3-dimethylpentanamide (**4.50**)



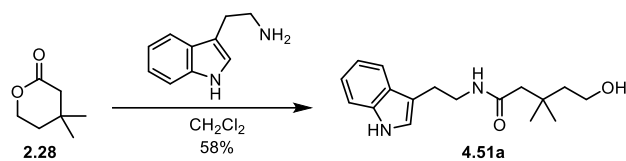
To a solution of α -hydroxylactone **2.26** (50.0 mg, 0.347 mmol, 1.0 equiv.) in DCM (10 mL) was added tryptamine (167 mg, 1.04 mmol, 3.0 equiv.) and $AlMe_3$ (2.0 M in toluene, 520 μ L, 1.04 mmol, 3.0 equiv.) was added to the reaction mixture dropwise carefully at 0 °C. After the addition, the resulting mixture was moved to room temperature to stir overnight. The reaction was quenched with potassium sodium tartrate (sat. aq.) carefully and extracted with DCM. The combined organic phases were washed with brine, dried over $MgSO_4$, filtered and concentrated under reduced pressure. The crude product was purified by silica gel column chromatography (pentane/EtOAc = 2:1) to afford the diol **4.50** (85.0 mg, 0.280 mmol, 80%) as a light yellow liquid.

1H NMR (500 MHz, $CDCl_3$) δ [ppm] = 8.54 (s, 1H), 7.58 (d, J = 7.8 Hz, 1H), 7.32 (d, J = 8.1 Hz, 1H), 7.20–7.15 (m, 1H), 7.14–7.08 (m, 2H), 6.95 (d, J = 2.3 Hz, 1H), 4.76 (s, 1H), 4.33 (s, 1H), 3.98 (s, 1H), 3.67 (dt, J = 5.9, 2.9 Hz, 2H), 3.63–3.52 (m, 2H), 2.93 (d, J = 1.0 Hz, 2H), 1.66–1.48 (m, 2H), 0.95 (s, 3H), 0.92 (s, 3H).

^{13}C NMR (126 MHz, $CDCl_3$) δ [ppm] = 173.7, 136.5, 127.3, 122.4, 122.1, 119.3, 118.7, 112.5, 111.5, 77.2, 58.9, 41.8, 39.3, 25.3, 24.3, 24.2.

HRMS-ESI: calcd. for $C_{17}H_{24}N_2O_3Na$ $[M + Na]^+$: 327.1679; found: 327.1681.

FT-IR: ν [cm^{-1}] = 3378, 3303, 2927, 1643, 1530, 1457, 1076.

***N*-(2-(1*H*-indol-3-yl)ethyl)-5-hydroxy-3,3-dimethylpentanamide (4.51a)**

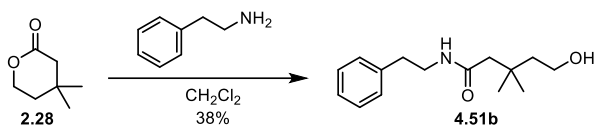
To a solution of lactone **2.28** (335 mg, 2.62 mmol, 1.0 equiv.) in DCM (10 mL) was added tryptamine (461 mg, 2.88 mmol, 1.1 equiv.) and stirred at room temperature overnight. After removing the solvent, the crude product was purified by silica gel column chromatography (pentane/EtOAc = 3:1) to afford **4.51a** (436 mg, 1.51 mmol, 58%) as a colorless liquid.

¹H NMR (700 MHz, CDCl_3) δ [ppm] = 8.12–8.04 (m, 1H), 7.62–7.61 (m, 1H), 7.38 (dt, J = 8.1, 0.9 Hz, 1H), 7.22 (ddd, J = 8.1, 6.9, 1.1 Hz, 1H), 7.14 (ddd, J = 8.0, 7.0, 1.0 Hz, 1H), 7.05 (dd, J = 2.3, 1.1 Hz, 1H), 5.85 (s, 1H), 3.72 (q, J = 5.4 Hz, 2H), 3.63 (td, J = 6.8, 5.8 Hz, 2H), 3.42 (s, 1H), 2.99 (td, J = 6.8, 0.9 Hz, 2H), 2.17 (s, 2H), 1.62–1.60 (m, 2H), 0.96 (s, 6H).

¹³C NMR (176 MHz, CDCl_3) δ [ppm] = 172.6, 136.6, 127.5, 122.4, 122.2, 119.7, 118.9, 113.2, 111.4, 59.5, 48.3, 42.6, 39.7, 32.8, 29.1, 25.5.

HRMS-ESI: calcd. for $\text{C}_{17}\text{H}_{24}\text{N}_2\text{O}_2\text{Na}$ [$\text{M} + \text{Na}$]⁺: 311.1730; found: 311.1732.

FT-IR: ν [cm^{-1}] = 3402, 3285, 2957, 2928, 1632, 1528, 1457, 1338, 1252, 1028, 741.

5-Hydroxy-3,3-dimethyl-*N*-phenethylpentanamide (4.51b)

To a solution of lactone **2.28** (335 mg, 2.62 mmol, 1.0 equiv.) in DCM (10 mL) was added 2-phenylethan-1-amine (348 mg, 2.88 mmol, 1.1 equiv.) and stirred at room temperature overnight. After removing the solvent, the crude product was purified by silica gel column chromatography (pentane/EtOAc = 5:1) to afford **4.51b** (250 mg, 1.00 mmol, 38%) as a colorless liquid.

¹H NMR (500 MHz, CDCl_3) δ [ppm] = 7.29 (d, J = 7.8 Hz, 2H), 7.23–7.17 (m, 3H), 6.20 (s, 1H), 3.72 (t, J = 5.5 Hz, 2H), 3.55–3.49 (m, 2H), 2.82 (t, J = 7.0 Hz, 2H), 2.18 (s, 2H), 1.59 (t, J = 5.5 Hz, 2H), 0.96 (s, 6H).

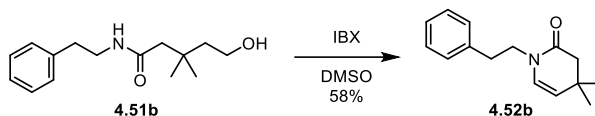
¹³C NMR (126 MHz, CDCl_3) δ [ppm] = 172.7, 139.0, 128.9, 128.7, 126.6, 59.4, 48.1, 42.5,

40.6, 35.8, 32.8, 29.1.

HRMS-ESI: calcd. for $C_{15}H_{23}NO_2Na$ $[M + Na]^+$: 272.1621; found: 272.1612.

FT-IR: ν $[cm^{-1}]$ = 3289, 2956, 2928, 2870, 1640, 1551, 1454, 1367, 1254, 1030, 747.

4,4-Dimethyl-1-phenethyl-3,4-dihydropyridin-2(1H)-one (4.52b)



To a solution of **4.51b** (65.0 mg, 2.62 mmol, 1.0 equiv.) in DMSO (5.0 mL) was added IBX (218 mg, 0.783 mmol, 3.0 equiv.). The resulting mixture was stirred for 24 h at room temperature, before the reaction mixture was diluted with H_2O and EtOAc. After washing by brine for three times, the organic phase was dried over $MgSO_4$, and concentrated under reduced pressure. The crude product was purified by silica gel column chromatography (pentane/EtOAc = 10:1) to afford **4.52b** (35.0 mg, 0.153 mmol, 58%) as a colorless liquid.

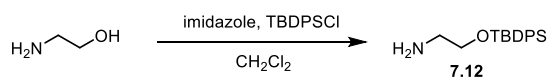
1H NMR (600 MHz, $CDCl_3$) δ [ppm] = 7.29 (ddd, J = 7.4, 6.4, 1.8 Hz, 2H), 7.23–7.19 (m, 3H), 5.77 (d, J = 7.7 Hz, 1H), 4.88 (dt, J = 7.7, 0.8 Hz, 1H), 3.77–3.64 (m, 2H), 2.86 (dd, J = 8.4, 6.7 Hz, 2H), 2.33 (s, 2H), 1.02 (s, 6H).

^{13}C NMR (151 MHz, $CDCl_3$) δ [ppm] = 169.2, 138.7, 129.1, 128.6, 127.4, 126.6, 117.4, 47.8, 46.3, 35.0, 31.8, 27.9.

HRMS-ESI: calcd. for $C_{15}H_{19}NONa$ $[M + Na]^+$: 250.1359; found: 250.1360.

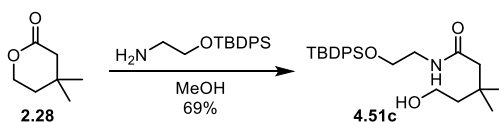
FT-IR: ν $[cm^{-1}]$ = 2955, 2924, 1730, 1670, 1385, 1363, 1310, 1286, 1151, 1095, 845, 742.

2-((*Tert*-butyldiphenylsilyl)oxy)ethan-1-amine (7.12)



The 2-((*tert*-butyldiphenylsilyl)oxy)ethan-1-amine (**7.12**) was synthesized from 2-aminoethan-1-ol according to a procedure by Moody et al.^[360] The spectroscopic data are in agreement with literature.

N-(2-((*tert*-butyldiphenylsilyl)oxy)ethyl)-5-hydroxy-3,3-dimethylpentanamide (4.51c)



To a solution of lactone **2.28** (300 mg, 2.34 mmol, 1.0 equiv.) in MeOH (10 mL) was added 2-((*tert*-butyldiphenylsilyl)oxy)ethan-1-amine (771 mg, 2.58 mmol, 1.1 equiv.) and stirred at room temperature overnight. After removing the solvent, the crude product was purified by silica gel column chromatography (pentane/EtOAc = 3:1) to afford **4.51c** (695 mg, 1.63 mmol, 69%) as a colorless liquid.

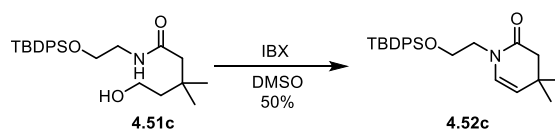
¹H NMR (500 MHz, CDCl₃) δ [ppm] = 7.57–7.52 (m, 4H), 7.38–7.32 (m, 2H), 7.31–7.25 (m, 4H), 6.10 (s, 1H), 3.66 (t, *J* = 5.1 Hz, 4H), 3.46 (s, 1H), 3.30 (q, *J* = 5.3 Hz, 2H), 2.11 (s, 2H), 1.56 (t, *J* = 5.5 Hz, 2H), 0.97 (s, 9H), 0.92 (s, 6H).

¹³C NMR (126 MHz, CDCl₃) δ [ppm] = 172.7, 135.6, 133.4, 130.0, 128.0, 62.9, 59.5, 48.2, 42.7, 41.8, 32.8, 29.1, 27.0, 19.3.

HRMS-ESI: calcd. for C₂₅H₃₇NO₃SiNa [M + Na]⁺: 450.2435; found: 450.2414.

FT-IR: ν [cm⁻¹] = 3285, 2957, 2930, 2857, 1644, 1557, 1471, 1428, 1112, 822, 739.

1-(2-((*Tert*-butyldiphenylsilyl)oxy)ethyl)-4,4-dimethyl-3,4-dihydropyridin-2(1*H*)-one (4.52c)



To a solution of **4.51c** (3.20 g, 7.49 mmol, 1.0 equiv.) in DMSO (50 mL) was added IBX (6.30 g, 22.5 mmol, 3.0 equiv.). The resulting mixture was stirred for 24 h at room temperature, before the reaction mixture was diluted with H₂O and EtOAc. After washing by brine for three times, the organic phase was dried over MgSO₄, and concentrated under reduced pressure. The crude product was purified by silica gel column chromatography (pentane/EtOAc = 10:1) to afford **4.52c** (1.68 g, 4.13 mmol, 55%) as a colorless liquid.

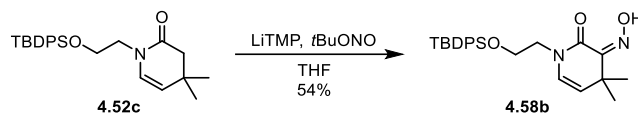
¹H NMR (500 MHz, CDCl₃) δ [ppm] = 7.71–7.61 (m, 4H), 7.45–7.40 (m, 2H), 7.40–7.35 (m, 4H), 6.06 (d, *J* = 7.7 Hz, 1H), 4.93 (dt, *J* = 7.7, 0.8 Hz, 1H), 3.78 (t, *J* = 5.3 Hz, 2H), 3.62 (t, *J* = 5.3 Hz, 2H), 2.34 (s, 2H), 1.07 (s, 6H), 1.04 (s, 9H).

¹³C NMR (151 MHz, CDCl₃) δ [ppm] = 169.3, 135.7, 133.4, 129.9, 128.9, 127.8, 116.3, 62.7, 48.4, 46.4, 31.7, 28.0, 26.9, 19.2.

HRMS-ESI: calcd. for C₂₅H₃₃NO₂SiNa [M + Na]⁺: 430.2173; found: 430.2194.

FT-IR: ν [cm^{-1}] = 2958, 2925, 2868, 1738, 1672, 1600, 1449, 1384, 1345, 1170, 972, 743.

1-(2-((*Tert*-butyldiphenylsilyl)oxy)ethyl)-3-(hydroxyimino)-4,4-dimethyl-3,4-dihydropyridin-2(1*H*)-one (4.58b)



To a solution of tetracyclic lactam **4.52c** (115 mg, 0.283 mmol, 1.0 equiv.) in THF (5.0 mL), was added LiTMP (1.0 M in THF, 1.41 mL, 1.41 mmol, 5.0 equiv.) at -78 °C. The resulting mixture was stirred at -78 °C for 1 h before *t*BuONO (116 mg, 1.13 mmol, 4.0 equiv.) was added. The mixture was stirred at -78 °C for additional 2 h. Then the reaction mixture was quenched with NaHCO_3 (sat. aq.). The aqueous phase was extracted with DCM. The combined organic phases were washed with brine, dried over MgSO_4 , filtered and concentrated under reduced pressure. The crude product was purified by silica gel column chromatography (pentane/EtOAc = 10:1) to afford **4.58b** (66.0 mg, 0.151 mmol, 54%) as a light yellow liquid.

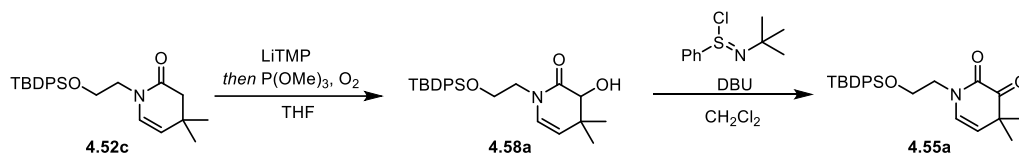
^1H NMR (500 MHz, CDCl_3) δ [ppm] = 7.65–7.62 (m, 4H), 7.45 (d, J = 7.3 Hz, 2H), 7.40 (t, J = 7.3 Hz, 5H), 6.01 (d, J = 7.8 Hz, 1H), 5.08 (d, J = 7.8 Hz, 1H), 3.84 (t, J = 4.8 Hz, 2H), 3.69 (t, J = 5.0 Hz, 2H), 1.36 (s, 6H), 1.06 (s, 9H).

^{13}C NMR (126 MHz, CDCl_3) δ [ppm] = 159.8, 148.8, 135.4, 132.8, 129.9, 127.8, 125.2, 117.9, 61.5, 48.7, 38.7, 28.9, 26.7, 19.0.

HRMS-ESI: calcd. for $\text{C}_{25}\text{H}_{33}\text{N}_2\text{O}_3\text{Si}$ [$\text{M} + \text{H}$] $^+$: 437.2255; found: 437.2243.

FT-IR: ν [cm^{-1}] = 2957, 2932, 2871, 1465, 1346, 1160, 1027, 974, 809, 747.

1-(2-((*Tert*-butyldiphenylsilyl)oxy)ethyl)-4,4-dimethyl-1,4-dihydropyridine-2,3-dione (4.55a)



To a solution of enamide **4.52c** (300 mg, 0.737 mmol, 1.0 equiv.) in THF (25 mL) was added LiTMP (1.0 M in THF, 5.90 mL, 5.90 mmol, 8.0 equiv.) dropwise at -78 °C. After the resultant mixture was stirred at -78 °C for 1 h, $\text{P}(\text{OMe})_3$ (365 μL , 1.47 mmol, 1.0 equiv.) was added. O_2

was bubbled through the mixture for 20 min, and the mixture was stirred for additional 2 h under O₂ atmosphere. Then reaction was quenched with NaHCO₃ (sat. aq.). The aqueous phase was extracted with DCM. The combined organic phases were washed with brine, dried over MgSO₄, filtered and the solvent was removed under reduced pressure. The crude product was dissolved in DCM (10 mL). The DBU (211 μL, 1.42 mmol, 5.0 equiv.) and phenylsulfonimidoyl chloride (122 mg, 0.567 mmol, 2.0 equiv.) was added subsequently. The reaction mixture was stirred at room temperature overnight, before quenching with NaHCO₃ (sat. aq.). The aqueous phase was extracted with DCM. The combined organic phases were washed with brine, dried over MgSO₄, filtered and concentrated under reduced pressure. The crude product was purified by silica gel column chromatography (pentane/EtOAc = 10:1) to afford **4.55a** (120 mg, 0.285 mmol, 39% over 2 steps) as a light yellow liquid.

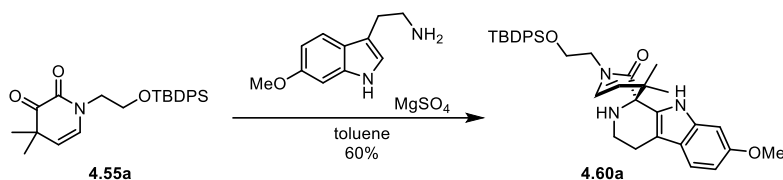
¹H NMR (700 MHz, CDCl₃) δ [ppm] = 7.63–7.60 (m, 4H), 7.45–7.41 (m, 2H), 7.39–7.35 (m, 4H), 6.17 (d, *J* = 8.2 Hz, 1H), 5.09 (d, *J* = 8.2 Hz, 1H), 3.87 (dd, *J* = 5.7, 4.6 Hz, 2H), 3.73 (dd, *J* = 5.6, 4.7 Hz, 2H), 1.30 (s, 6H), 1.04 (s, 9H).

¹³C NMR (176 MHz, CDCl₃) δ [ppm] = 196.9, 156.2, 135.6, 133.1, 130.0, 127.9, 127.1, 114.8, 62.1, 50.0, 46.3, 26.9, 25.0, 19.3.

HRMS-ESI: calcd. for C₂₅H₃₁NO₃SiK [M + K]⁺: 460.1705; found: 460.1726.

FT-IR: ν [cm⁻¹] = 2956, 2926, 2856, 1730, 1682, 1464, 1428, 1394, 1111, 1044, 822, 735, 703.

1-(2-((*Tert*-butyldiphenylsilyl)oxy)ethyl)-7'-methoxy-4,4-dimethyl-1,2',3',4,4',9'-hexahydro-2*H*-spiro[pyridine-3,1'-pyrido[3,4-*b*]indol]-2-one (4.60a**)**



To a solution of **4.55a** (45.0 mg, 0.107 mmol, 1.0 equiv.) in toluene (5.0 mL) was added 6-methoxytryptamine (19.2 mg, 0.107 mmol, 1.0 equiv.) and MgSO₄ (128 mg, 1.07 mmol, 10 equiv.). The mixture was heated to reflux and stirred for 2 d. After filtering through Celite[®] and removing the solvent, the crude product was purified by silica gel column chromatography (pentane/EtOAc = 3:2) afforded **4.60a** (38.0 mg, 64.1 μmol, 60%) as a white solid.

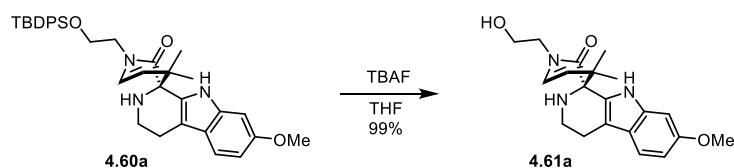
¹H NMR (700 MHz, CD₃CN) δ [ppm] = 8.95 (s, 1H), 7.65 (dt, *J* = 6.8, 1.5 Hz, 2H), 7.61–7.57 (m, 2H), 7.48–7.36 (m, 5H), 7.33 (t, *J* = 7.5 Hz, 2H), 7.31 (d, *J* = 8.6 Hz, 1H), 6.80 (d, *J* = 2.3 Hz, 1H), 6.66 (dd, *J* = 8.6, 2.3 Hz, 1H), 6.38 (d, *J* = 7.9 Hz, 1H), 5.19 (d, *J* = 7.9 Hz, 1H), 3.82–3.75 (m, 1H), 3.74–3.69 (m, 5H), 3.60–3.54 (m, 1H), 3.53–3.48 (m, 1H), 3.16–3.07 (m, 1H), 2.69–2.62 (m, 1H), 2.60 (dt, *J* = 10.0, 4.9 Hz, 1H), 1.14 (s, 3H), 1.00 (s, 9H), 0.89 (s, 3H).

¹³C NMR (176 MHz, CD₃CN) δ [ppm] = 172.7, 157.5, 137.5, 136.4, 134.3, 134.2, 130.9, 129.8, 128.8, 121.8, 119.4, 113.3, 110.0, 104.3, 95.7, 64.8, 63.1, 56.0, 50.2, 43.1, 41.2, 27.2, 23.8, 23.4, 22.8, 19.7.

HRMS-ESI: calcd. for C₃₆H₄₄N₃O₃Si [M + H]⁺: 594.3147; found: 594.3150.

FT-IR: ν [cm⁻¹] = 2957, 2930, 2857, 1670, 1627, 1460, 1428, 1389, 1258, 1222, 1111, 822, 703.

1-(2-Hydroxyethyl)-7'-methoxy-4,4-dimethyl-1,2',3',4,4',9'-hexahydro-2H-spiro[pyridine-3,1'-pyrido[3,4-*b*]indol]-2-one (4.61a)



To a solution of **4.60a** (10.0 mg, 17.0 μmol, 1.0 equiv.) in THF (2.0 mL) was added TBAF (1.0 M in THF, 50.6 μl, 50.6 μmol, 3.0 equiv.). The mixture was stirred at room temperature overnight. After removing the solvent, the crude product was purified by silica gel column chromatography (pentane/EtOAc = 1:2) to afford **4.61a** (6.0 mg, 16.9 μmol, 99%) as a white solid.

¹H NMR (700 MHz, CD₃OD) δ [ppm] = 7.31 (d, *J* = 8.6 Hz, 1H), 6.97 (d, *J* = 2.2 Hz, 1H), 6.69 (dd, *J* = 8.6, 2.3 Hz, 1H), 6.36 (dd, *J* = 7.9, 1.0 Hz, 1H), 5.20 (dd, *J* = 8.0, 1.2 Hz, 1H), 3.83 (s, 3H), 3.76–3.65 (m, 3H), 3.62–3.54 (m, 2H), 3.35–3.34 (m, 2H), 3.26 (d, *J* = 12.3 Hz, 1H), 2.70 (dd, *J* = 7.0, 4.5 Hz, 2H), 1.19 (s, 2H), 0.94 (s, 2H).

¹³C NMR (176 MHz, CD₃OD) δ [ppm] = 173.2, 158.0, 138.2, 130.3, 129.4, 122.0, 119.3, 118.7, 113.2, 110.1, 95.9, 65.5, 60.9, 55.9, 50.4, 43.5, 41.3, 23.5, 23.1, 22.7.

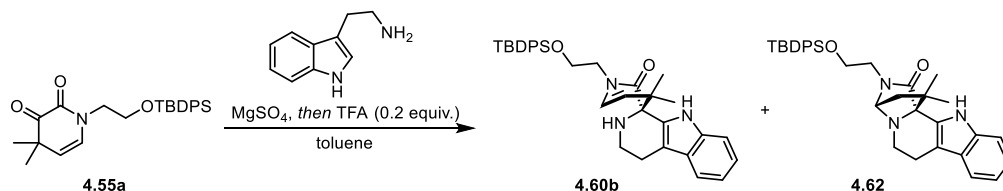
HRMS-ESI: calcd. for C₂₀H₂₆N₃O₃ [M + H]⁺: 356.1969; found: 356.1985.

FT-IR: ν [cm⁻¹] = 3470, 3441, 2856, 1740, 1428, 1363, 1229, 1217, 1113, 822, 741.

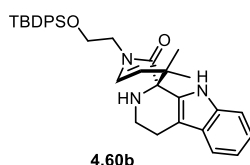
1-(2-((*Tert*-butyldiphenylsilyl)oxy)ethyl)-4,4-dimethyl-1,2',3',4,4',9'-hexa-hydro-2*H*-spiro[pyridine-3,1'-pyrido[3,4-*b*]indol]-2-one (4.60b)

and

13-(2-((*tert*-butyldiphenyl-silyl)oxy)ethyl)-1,1-dimethyl-2,3,6,11-tetrahydro-1*H*,5*H*-3,11*b*-(epiminomethano)indolizino[8,7-*b*]indol-12-one (4.62)



To a solution of **4.55a** (16.8 mg, 40.0 μmol , 1.0 equiv.) in toluene (5.0 mL) was added tryptamine (9.6 mg, 60.0 μmol , 1.0 equiv.) and MgSO_4 (47.9 mg, 0.399 mmol, 10 equiv.). The mixture was heated to reflux and stirred for 2 d. After cooling down to room temperature, TFA (0.6 μL , 8 μmol , 0.2 equiv.) was added to the reaction mixture and stirred at 110 $^\circ\text{C}$ for 2 d. Then the mixture was filtered through Celite[®] and concentrated under reduced pressure. The crude product was purified by silica gel column chromatography (pentane/EtOAc = 3:2) to afford **4.60b** (10.0 mg, 17.8 μmol , 44%) as a white solid and **4.62** (7.0 mg, 11.5 μmol , 29%) as a white solid.

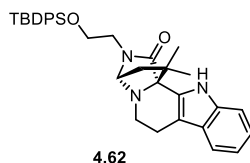


¹H NMR (700 MHz, CDCl_3) δ [ppm] = 8.73 (s, 1H), 7.64–7.60 (m, 2H), 7.59–7.56 (m, 2H), 7.50–7.48 (m, 1H), 7.44–7.40 (m, 1H), 7.40–7.37 (m, 1H), 7.37–7.33 (m, 2H), 7.30–7.27 (m, 2H), 7.14 (dt, J = 8.0, 1.0 Hz, 1H), 7.12–7.09 (m, 1H), 7.07 (ddd, J = 8.0, 6.9, 1.2 Hz, 1H), 6.41 (d, J = 7.9 Hz, 1H), 5.23 (d, J = 7.9 Hz, 1H), 3.80 (ddd, J = 10.4, 6.7, 3.5 Hz, 1H), 3.76–3.72 (m, 1H), 3.68 (ddd, J = 14.0, 6.0, 3.5 Hz, 1H), 3.63 (dt, J = 12.5, 6.5 Hz, 1H), 3.56 (ddd, J = 13.9, 6.7, 3.5 Hz, 1H), 3.21 (t, J = 6.3 Hz, 1H), 2.71–2.75 (m, 2H), 1.22 (s, 3H), 1.21 (s, 3H), 1.07 (s, 9H). (Note: the resonance of the tertiary N–H was missing.)

¹³C NMR (176 MHz, CDCl_3) δ [ppm] = 172.3, 135.7, 133.2, 131.5, 129.9, 129.1, 127.9, 126.6, 122.3, 119.4, 118.4, 118.1, 113.4, 111.1, 64.6, 63.9, 62.9, 50.0, 42.7, 40.9, 27.0, 25.5, 23.4, 23.0, 19.3.

HRMS-ESI: calcd. for C₃₅H₄₂N₃O₂Si [M + H]⁺: 564.3041; found: 564.3069.

FT-IR: ν [cm⁻¹] = 2929, 2856, 1670, 1627, 1459, 1428, 1389, 1258, 1222, 1156, 1111, 823, 702.



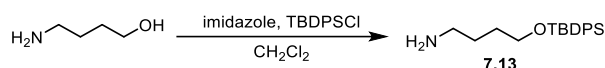
¹H NMR (700 MHz, CDCl₃) δ [ppm] = 8.17 (s, 1H), 7.67–7.64 (m, 4H), 7.50–7.49 (m, 1H), 7.47–7.43 (m, 2H), 7.42–7.36 (m, 5H), 7.16 (ddd, J = 8.1, 7.1, 1.2 Hz, 1H), 7.10 (ddd, J = 8.0, 7.1, 1.0 Hz, 1H), 4.84 (d, J = 2.8 Hz, 1H), 3.79 (dd, J = 5.7, 4.4 Hz, 2H), 3.56–3.49 (m, 1H), 3.23–3.16 (m, 1H), 3.14–3.09 (m, 1H), 2.96 (ddd, J = 16.6, 12.7, 5.4 Hz, 1H), 2.87–2.79 (m, 2H), 1.97 (dd, J = 11.5, 2.9 Hz, 1H), 1.74 (d, J = 11.5 Hz, 1H), 1.32 (s, 3H), 1.11 (s, 3H), 1.08 (s, 9H).

¹³C NMR (176 MHz, CDCl₃) δ [ppm] = 174.2, 137.0, 135.7, 133.2, 130.1, 128.8, 128.0, 127.0, 121.9, 119.6, 118.4, 112.0, 111.5, 78.1, 76.0, 63.5, 46.1, 43.4, 43.3, 39.5, 27.2, 27.0, 26.7, 22.1, 19.3.

HRMS-ESI: calcd. for C₃₅H₄₂N₃O₂Si [M + H]⁺: 564.3041; found: 564.3063.

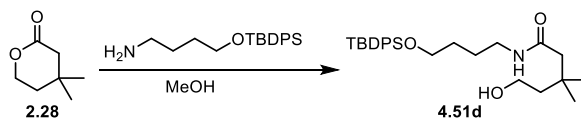
FT-IR: ν [cm⁻¹] = 2960, 2928, 2854, 1686, 1458, 1428, 1111, 824, 773, 739.

4-((*Tert*-butyldiphenylsilyl)oxy)butan-1-amine (7.13)



The amine **7.13** was synthesized from 4-aminobutan-1-ol according to a procedure by Gilbert et al.^[361] The spectroscopic data are in agreement with literature.

N-(4-((*tert*-butyldiphenylsilyl)oxy)butyl)-5-hydroxy-3,3-dimethylpentanamide (4.51d)



To a solution of lactone **2.28** (250 mg, 1.95 mmol, 1.0 equiv.) in MeOH (10 mL) was amine **7.13** (702 mg, 2.15 mmol, 1.1 equiv.) and stirred at room temperature overnight. After removing the solvent, the crude product was purified by silica gel column chromatography (pentane/EtOAc = 3:1) to afford **4.51d** (695 mg, 1.09 mmol, 56%) as a colorless liquid.

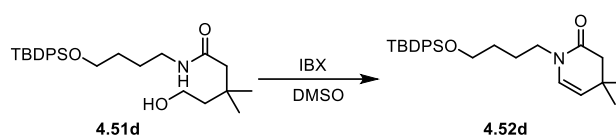
¹H NMR (600 MHz, CDCl₃) δ [ppm] = 7.69–7.62 (m, 4H), 7.47–7.40 (m, 2H), 7.38 (dd, *J* = 8.0, 6.6 Hz, 4H), 6.11 (t, *J* = 5.9 Hz, 1H), 3.87 (s, 1H), 3.76 (t, *J* = 5.8 Hz, 2H), 3.73–3.65 (m, 2H), 3.24 (q, *J* = 6.2 Hz, 2H), 2.20 (s, 2H), 1.65 (t, *J* = 5.6 Hz, 2H), 1.60 (dt, *J* = 6.3, 3.4 Hz, 4H), 1.05 (s, 9H), 1.00 (s, 6H).

¹³C NMR (151 MHz, CDCl₃) δ [ppm] = 172.6, 135.7, 134.0, 129.8, 127.8, 63.6, 59.4, 48.1, 42.5, 39.4, 32.8, 30.1, 29.2, 27.0, 26.2, 19.3.

HRMS-ESI: calcd. for C₂₇H₄₁NO₃SiNa [M + Na]⁺: 478.2748; found: 478.2771.

FT-IR: ν [cm⁻¹] = 2954, 2930, 2857, 1639, 1557, 1471, 1428, 1110, 822, 701.

1-(2-((*Tert*-butyldiphenylsilyl)oxy)ethyl)-4,4-dimethyl-3,4-dihydropyridin-2(1*H*)-one (4.52d)



To a solution of **4.51d** (300 mg, 0.659 mmol, 1.0 equiv.) in DMSO (10 mL) was added IBX (554 mg, 1.98 mmol, 3.0 equiv.). The resulting mixture was stirred for 24 h at room temperature, before the reaction mixture was diluted with H₂O and EtOAc. After washing by brine for three times, the organic phase was dried over MgSO₄, and concentrated under reduced pressure. The crude product was purified by silica gel column chromatography (pentane/EtOAc = 10:1) to afford **4.52d** (145 mg, 3.33 mmol, 50%) as a colorless liquid.

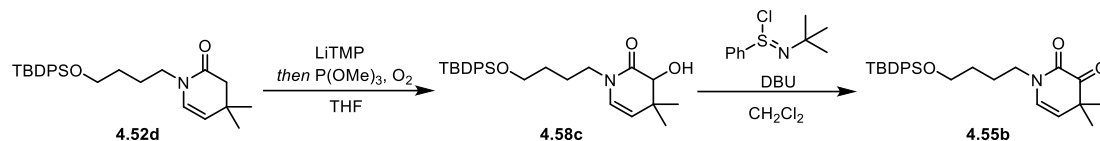
¹H NMR (500 MHz, CDCl₃) δ [ppm] = 7.68–7.63 (m, 4H), 7.44–7.37 (m, 6H), 5.88 (d, *J* = 8.0 Hz, 1H), 4.96 (d, *J* = 7.7 Hz, 1H), 3.69–3.64 (m, 2H), 3.50–3.44 (m, 2H), 2.33 (s, 2H), 1.65 (dd, *J* = 8.7, 7.0 Hz, 2H), 1.61–1.52 (m, 2H), 1.05 (s, 6H), 1.04 (s, 9H).

¹³C NMR (126 MHz, CDCl₃) δ [ppm] = 169.2, 135.7, 134.1, 129.7, 127.8, 127.3, 117.6, 63.6, 46.4, 45.7, 31.8, 29.9, 28.0, 27.0, 25.3, 19.4.

HRMS-ESI: calcd. for C₂₇H₃₇NO₂SiNa [M + Na]⁺: 458.2486; found: 458.2508.

FT-IR: ν [cm⁻¹] = 3070, 3051, 2955, 2929, 2857, 1672, 1427, 1386, 1109, 822, 738.

1-(2-((*Tert*-butyldiphenylsilyl)oxy)ethyl)-4,4-dimethyl-1,4-dihydropyridine-2,3-dione
(4.55b)



To a solution of lactam **4.52d** (100 mg, 0.230 mmol, 1.0 equiv.) in THF (10 mL) was added LiTMP (1.0 M in THF, 2.29 mL, 2.29 mmol, 10 equiv.) dropwise at $-78\text{ }^{\circ}\text{C}$. After the resultant mixture was stirred at $-78\text{ }^{\circ}\text{C}$ for 1 h, $\text{P}(\text{OMe})_3$ (114 μL , 0.460 mmol, 1.0 equiv.) was added. O_2 was bubbled through the mixture for 20 min, and the mixture was stirred for additional 2 h under O_2 atmosphere. Then reaction was quenched with NaHCO_3 (sat. aq.). The aqueous phase was extracted with DCM. The combined organic phases were washed with brine, dried over MgSO_4 , filtered and the solvent was removed under reduced pressure. The crude product was dissolved in DCM (10 mL). The DBU (59.5 μL , 0.399 mmol, 5.0 equiv.) and phenylsulfinimidoyl chloride (57.2 mg, 0.266 mmol, 2.0 equiv.) was added subsequently. The reaction mixture was stirred at room temperature overnight, before quenching with NaHCO_3 (sat. aq.). The aqueous phase was extracted with DCM. The combined organic phases were washed with brine, dried over MgSO_4 , filtered and concentrated under reduced pressure. The crude product was purified by silica gel column chromatography (pentane/EtOAc = 10:1) to afford **4.55b** (50.0 mg, 0.111 mmol, 29% over 2 steps) as a light yellow liquid.

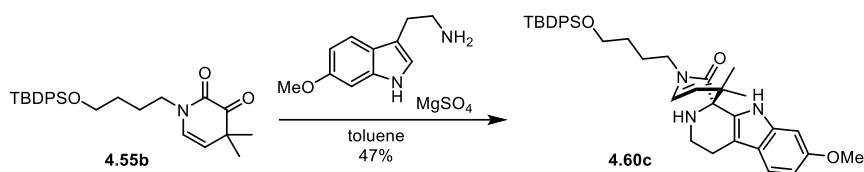
$^1\text{H NMR}$ (500 MHz, CDCl_3) δ [ppm] = 7.65 (d, J = 9.4 Hz, 4H), 7.43–7.36 (m, 6H), 5.97 (d, J = 8.8 Hz, 1H), 5.13 (d, J = 8.7 Hz, 1H), 3.69 (d, J = 5.4 Hz, 2H), 3.61–3.57 (m, 2H), 1.76 (dd, J = 8.5, 6.6 Hz, 2H), 1.63–1.55 (m, 2H), 1.28 (s, 6H), 1.05 (s, 9H).

$^{13}\text{C NMR}$ (126 MHz, CDCl_3) δ [ppm] = 197.0, 156.1, 135.7, 133.9, 129.8, 127.8, 125.3, 116.1, 63.4, 47.3, 46.2, 29.7, 27.0, 24.9, 24.8, 19.3.

HRMS-ESI: calcd. for $\text{C}_{27}\text{H}_{35}\text{NO}_3\text{SiNa}$ $[\text{M} + \text{Na}]^+$: 472.2278; found: 472.2298.

FT-IR: ν [cm^{-1}] = 2955, 2930, 2858, 1732, 1678, 1427, 1394, 1110, 823, 740, 702.

1-(4-((*Tert*-butyldiphenylsilyl)oxy)butyl)-7'-methoxy-4,4-dimethyl-1,2',3',4,4',9'-hexahydro-2*H*-spiro[pyridine-3,1'-pyrido[3,4-*b*]indol]-2-one (4.60c)



To a solution of **4.55b** (69.0 mg, 0.154 mmol, 1.0 equiv.) in toluene (5.0 mL) was added 6-methoxytryptamine (32.1 mg, 0.169 mmol, 1.0 equiv.) and MgSO_4 (184 mg, 1.54 mmol, 10 equiv.). The mixture was heated to reflux and stirred for 2 d. After filtering through Celite[®] and removing the solvent, the crude product was purified by silica gel column chromatography (pentane/EtOAc = 3:2) to afford **4.60c** (45.0 mg, 72.6 μmol , 47%) as a white solid.

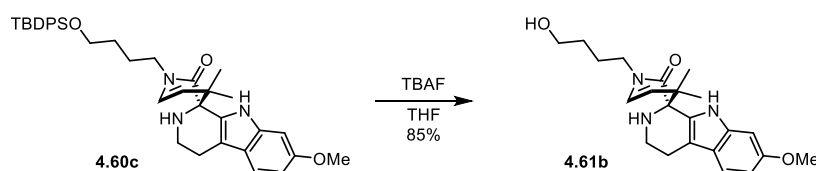
¹H NMR (700 MHz, CDCl_3) δ [ppm] = 8.52 (s, 1H), 7.65 (dt, J = 8.2, 1.6 Hz, 4H), 7.44–7.40 (m, 2H), 7.39–7.34 (m, 5H), 6.79–6.77 (m, 1H), 6.75 (dd, J = 8.6, 2.2 Hz, 1H), 6.14 (d, J = 8.0 Hz, 1H), 5.24 (d, J = 7.9 Hz, 1H), 3.81 (s, 3H), 3.71–3.67 (m, 1H), 3.65 (t, J = 6.2 Hz, 2H), 3.64–3.59 (m, 1H), 3.27 (ddd, J = 13.9, 8.1, 6.1 Hz, 1H), 3.16 (dt, J = 12.2, 5.0 Hz, 1H), 2.72–2.64 (m, 2H), 1.75–1.62 (m, 2H), 1.61–1.51 (m, 2H), 1.14 (s, 3H), 1.05 (s, 9H), 0.92 (s, 3H). (Note: the resonance of the indole N–H was missing, probably due to overlapping.)

¹³C NMR (176 MHz, CDCl_3) δ [ppm] = 172.3, 156.8, 136.1, 135.7, 134.0, 130.3, 129.7, 127.8, 127.4, 121.2, 119.6, 119.0, 113.4, 109.1, 94.8, 63.7, 63.5, 55.8, 47.4, 42.6, 40.9, 29.9, 27.0, 25.2, 23.3, 23.0, 22.4, 19.4.

HRMS-ESI: calcd. for $\text{C}_{38}\text{H}_{48}\text{N}_3\text{O}_3\text{Si}$ [$\text{M} + \text{H}$]⁺: 622.3460; found: 622.3476.

FT-IR: ν [cm^{-1}] = 2949, 2931, 2857, 1731, 1671, 1627, 1459, 1390, 1220, 1111, 823, 740, 706.

1-(4-Hydroxybutyl)-7'-methoxy-4,4-dimethyl-1,2',3',4,4',9'-hexahydro-2*H*-spiro[pyridine-3,1'-pyrido[3,4-*b*]indol]-2-one (4.61b)



To a solution of **4.60c** (72.0 mg, 116 μmol , 1.0 equiv.) in THF (5.0 mL) was added TBAF (1.0 M in THF, 174 μL , 174 μmol , 1.5 equiv.). The mixture was stirred at room temperature overnight before removing the solvent. The crude product was purified by silica gel column

chromatography (pentane/EtOAc = 1:2) to afford **4.61b** (56.0 mg, 99.5 μmol , 85%).

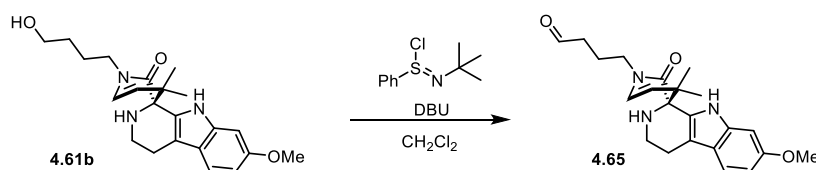
$^1\text{H NMR}$ (600 MHz, CDCl_3) δ [ppm] = 8.53 (s, 1H), 7.37–7.33 (m, 1H), 6.80 (d, $J = 2.2$ Hz, 1H), 6.74 (dd, $J = 8.5, 2.2$ Hz, 1H), 6.17 (d, $J = 7.9$ Hz, 1H), 5.25 (d, $J = 7.9$ Hz, 1H), 3.82 (s, 3H), 3.71–3.63 (m, 1H), 3.61 (td, $J = 6.3, 1.3$ Hz, 3H), 3.35 (ddd, $J = 14.0, 7.9, 6.4$ Hz, 1H), 3.15 (dt, $J = 12.2, 5.0$ Hz, 1H), 2.72–2.63 (m, 2H), 1.71–1.63 (m, 2H), 1.55–1.47 (m, 2H), 1.14 (s, 3H), 0.92 (s, 3H). (Note: the resonances of the O–H and tertiary N–H were missing.)

$^{13}\text{C NMR}$ (151 MHz, CDCl_3) δ [ppm] = 172.5, 156.8, 136.1, 130.2, 129.9, 127.3, 121.2, 119.7, 119.1, 109.1, 94.8, 63.8, 62.5, 55.9, 47.3, 42.6, 40.9, 29.6, 25.2, 23.4, 23.0, 22.4.

HRMS-ESI: calcd. for $\text{C}_{22}\text{H}_{29}\text{N}_3\text{O}_3\text{Na}$ [$\text{M} + \text{Na}$] $^+$: 406.2101; found: 406.2098.

FT-IR: ν [cm^{-1}] = 3437, 3400, 3379, 2925, 2867, 1654, 1626, 1457, 1390, 1257, 1221, 1154, 1028, 937, 816, 736.

4-(7'-Methoxy-4,4-dimethyl-2-oxo-2',3',4',9'-tetrahydro-2H-spiro[pyridine-3,1'-pyrido[3,4-b]indol]-1(4H)-yl)butanal (4.65**)**



To a solution of **4.61b** (50.0 mg, 131 μmol , 1.0 equiv.) in in DCM (5.0 mL) was added DBU (58.4 μL , 261 μmol , 3.0 equiv.) and phenylsulfinimidoyl chloride (56.1 mg, 261 μmol , 2.0 equiv.) was added subsequently. The reaction mixture was stirred at room temperature overnight, before quenching with NaHCO_3 (sat. aq.). The aqueous phase was extracted with DCM. The combined organic phases were washed with brine, dried over MgSO_4 , filtered and concentrated under reduced pressure. The crude product was purified by silica gel column chromatography (pentane/EtOAc = 10:1) afforded **4.65** (30.0 mg, 78.7 μmol , 60%) as a light yellow solid.

$^1\text{H NMR}$ (600 MHz, CDCl_3) δ [ppm] = 9.69 (d, $J = 1.1$ Hz, 1H), 8.50 (s, 1H), 7.35 (d, $J = 8.6$ Hz, 1H), 6.80 (d, $J = 2.2$ Hz, 1H), 6.74 (dd, $J = 8.6, 2.2$ Hz, 1H), 6.18 (d, $J = 7.9$ Hz, 1H), 5.27 (d, $J = 7.9$ Hz, 1H), 4.69 (s, 1H), 3.83 (s, 3H), 3.63–3.55 (m, 2H), 3.45 (dt, $J = 13.8, 7.0$ Hz,

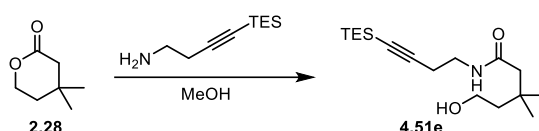
1H), 3.15 (dt, $J = 12.2, 5.0$ Hz, 1H), 2.73–2.62 (m, 2H), 2.49–2.36 (m, 2H), 1.96–1.86 (m, 2H), 1.14 (s, 3H), 0.92 (s, 3H).

^{13}C NMR (151 MHz, CDCl_3) δ [ppm] = 201.5, 156.9, 136.2, 133.9, 129.9, 127.2, 121.2, 119.9, 119.1, 113.6, 109.3, 94.8, 63.8, 55.9, 46.5, 42.6, 40.9, 40.9, 23.4, 22.9, 22.3, 20.9.

HRMS-ESI: calcd. for $\text{C}_{22}\text{H}_{28}\text{N}_3\text{O}_3\text{Si}$ [$\text{M} + \text{H}$] $^+$: 382.2125; found: 382.2120.

FT-IR: ν [cm^{-1}] = 3427, 3404, 2954, 2924, 2870, 1720, 1658, 1626, 1458, 1389, 1260, 1221, 1155, 1098, 1024, 828, 730.

5-Hydroxy-3,3-dimethyl-*N*-(4-(triethylsilyl)but-3-yn-1-yl)pentanamide (4.51e)



To a solution of lactone **2.28** (60.0 mg, 0.469 mmol, 1.0 equiv.) in MeOH (5.0 mL) was added 4-(triethylsilyl)but-3-yn-1-amine (94.4 mg, 0.516 mmol, 1.1 equiv.) and stirred at room temperature overnight. After removing the solvent, the crude product was purified by silica gel column chromatography (pentane/EtOAc = 3:1) to afford **4.51e** (100 mg, 0.322 mmol, 69%) as a colorless liquid.

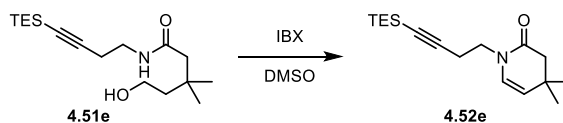
^1H NMR (600 MHz, CDCl_3) δ [ppm] = 6.27 (s, 1H), 3.77 (t, $J = 5.7$ Hz, 2H), 3.53 (s, 1H), 3.39 (q, $J = 6.3$ Hz, 2H), 2.46 (t, $J = 6.4$ Hz, 2H), 2.24 (s, 2H), 1.70–1.62 (m, 2H), 1.02 (s, 6H), 0.97 (t, $J = 7.9$ Hz, 9H), 0.57 (q, $J = 7.9$ Hz, 6H).

^{13}C NMR (151 MHz, CDCl_3) δ [ppm] = 172.7, 105.2, 83.9, 59.5, 48.2, 42.6, 38.4, 32.8, 29.2, 20.9, 7.6, 4.5.

HRMS-ESI: calcd. for $\text{C}_{17}\text{H}_{33}\text{NO}_2\text{SiK}$ [$\text{M} + \text{K}$] $^+$: 350.1913; found: 350.1924.

FT-IR: ν [cm^{-1}] = 3282, 2954, 2874, 2174, 1644, 1556, 1459, 1367, 1254, 1018, 725.

4,4-Dimethyl-1-(4-(triethylsilyl)but-3-yn-1-yl)-3,4-dihydropyridin-2(1H)-one (4.52e)



To a solution of **4.51e** (150 mg, 0.482 mmol, 1.0 equiv.) in DMSO (5.0 mL) was added IBX (405 mg, 1.45 mmol, 3.0 equiv.). The resulting mixture was stirred for 24 h at room temperature,

before the reaction mixture was diluted with H₂O and EtOAc. After washing by brine for three times, the organic phase was dried over MgSO₄, and concentrated under reduced pressure. The crude product was purified by silica gel column chromatography (pentane/EtOAc = 10:1) to afford **4.52e** (56.0 mg, 0.192 mmol, 40%) as a colorless liquid.

¹H NMR (500 MHz, CDCl₃) δ [ppm] = 6.00 (dd, *J* = 7.7, 1.1 Hz, 1H), 4.90 (dd, *J* = 7.7, 1.0 Hz, 1H), 3.58 (td, *J* = 6.7, 1.2 Hz, 2H), 2.51 (td, *J* = 6.6, 1.2 Hz, 2H), 2.32 (t, *J* = 1.0 Hz, 2H), 1.04 (s, 6H), 0.94 (td, *J* = 7.9, 1.2 Hz, 9H), 0.56–0.51 (m, 6H).

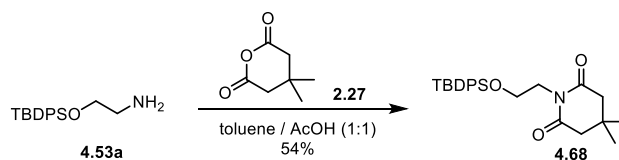
¹³C NMR (126 MHz, CDCl₃) δ [ppm] = 169.2, 128.1, 117.1, 104.9, 84.0, 46.3, 45.6, 31.7, 27.9, 20.0, 7.5, 4.5.

HRMS-ESI: calcd. for C₁₇H₂₉NOSiNa [M + Na]⁺: 330.1860; found: 330.1873.

FT-IR: ν [cm⁻¹] = 2954, 2911, 2874, 2173, 1676, 1655, 1459, 1385, 1232, 1008, 700.

7.2.3.2.2. Mono-ring α-ketoenamides preparation via reductive pathway and their Pictet–Spengler reactions

1-((*Tert*-butyldiphenylsilyl)oxy)ethyl-4,4-dimethylpiperidine-2,6-dione (**4.68**)



To a mixture of amine (500 mg, 1.67 mmol, 1.0 equiv.) and 3,3-glutaric anhydride (238 mg, 1.67 mmol, 1.0 equiv.) was added toluene (5.0 mL) and AcOH (5.0 mL). The resulting mixture was heated to reflux for 2 d. After cooling to room temperature, the mixture was basified by NaOH (1 M, aq.). The aqueous phase was extracted with DCM. The combined organic phases were washed with brine, dried over MgSO₄, filtered and concentrated under reduced pressure. The crude product was purified by silica gel column chromatography (pentane/EtOAc = 10:1) to afford **4.68** (380 mg, 0.898 mmol, 54%) as a colorless liquid.

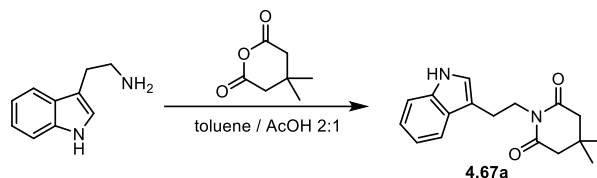
¹H NMR (500 MHz, CDCl₃) δ [ppm] = 7.74–7.66 (m, 4H), 7.46–7.35 (m, 6H), 4.05 (t, *J* = 5.9 Hz, 2H), 3.82 (t, *J* = 5.9 Hz, 2H), 2.46 (s, 4H), 1.07 (s, 6H), 1.04 (s, 9H).

¹³C NMR (126 MHz, CDCl₃) δ [ppm] = 171.8, 135.6, 133.5, 129.7, 127.7, 60.7, 46.4, 40.9, 29.0, 27.7, 26.7, 19.1.

HRMS-ESI: calcd. for C₂₅H₃₃NO₃SiNa [M + Na]⁺: 446.2122; found: 446.2125.

FT-IR: ν [cm^{-1}] = 2958, 1673, 1336, 1220, 1109, 910, 751, 701.

1-(2-(1*H*-indol-3-yl)ethyl)amino-4,4-dimethylpiperidine-2,6-dione (4.67a)



To a mixture of tryptamine (3.00 g, 18.8 mmol, 1.0 equiv.) and 3,3-glutaric anhydride (2.66 g, 18.8 mmol, 1.0 equiv.) was added toluene (100 mL) and AcOH (50 mL). The resulting mixture was heated to reflux for 2 d. After cooling to room temperature, the mixture was basified by NaOH (1 M, aq.). The aqueous phase was extracted with DCM. The combined organic phases were washed with brine, dried over MgSO_4 , filtered and concentrated under reduced pressure. The crude product was purified by silica gel column chromatography (pentane/EtOAc = 10:1) to afford **4.67a** (950 mg, 3.35 μmol , 18%) as a light yellow solid.

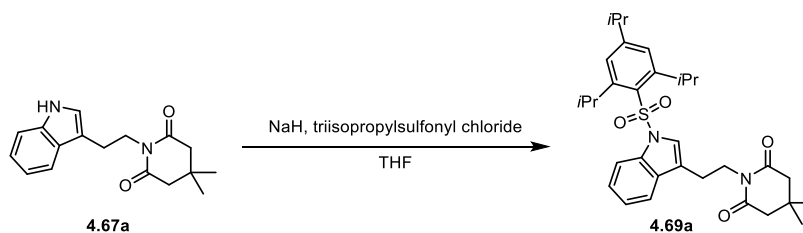
^1H NMR (500 MHz, CDCl_3) δ [ppm] = 7.98 (s, 1H), 7.80 (d, $J = 7.9$ Hz, 1H), 7.35 (ddd, $J = 8.0, 2.4, 1.3$ Hz, 1H), 7.23–7.17 (m, 1H), 7.16–7.12 (m, 1H), 7.09–7.05 (m, 1H), 4.14–4.01 (m, 2H), 3.00–2.96 (m, 2H), 2.49 (s, 4H), 1.06 (s, 6H).

^{13}C NMR (126 MHz, CDCl_3) δ [ppm] = 172.1, 136.3, 127.6, 122.3, 121.9, 119.4, 119.1, 112.6, 111.2, 46.4, 40.2, 29.1, 27.6, 23.8.

HRMS-ESI: calcd. for $\text{C}_{17}\text{H}_{20}\text{N}_2\text{O}_2\text{K}$ [$\text{M} + \text{K}$] $^+$: 323.1157; found: 323.1143.

FT-IR: ν [cm^{-1}] = 3373, 2958, 2929, 1720, 1661, 1392, 1348, 1274, 1199, 1134, 934, 743.

4,4-Dimethyl-1-(2-(1-((2,4,6-triisopropylphenyl)sulfonyl)-1*H*-indol-3-yl)ethyl)piperidine-2,6-dione (4.69a)



To a solution of **4.67a** (1.00 g, 3.52 mmol, 1.0 equiv.) in THF (50 mL) was added NaH (60% dispersion in mineral oil, 282 mg, 7.04 mmol, 2.0 equiv.) and triisopropylsulfonyl chloride

(2.13 g, 7.04 mmol, 2.0 equiv.). The mixture was stirred at room temperature overnight, before quenching with NaHCO_3 (sat. aq.). The aqueous phase was extracted with DCM. The combined organic phases were washed with brine, dried over MgSO_4 , filtered and concentrated under reduced pressure. The crude product was purified by silica gel column chromatography (pentane/EtOAc = 10:1) to afford **4.69a** (1.92 g, 3.49 mmol, 99%) as a light yellow solid.

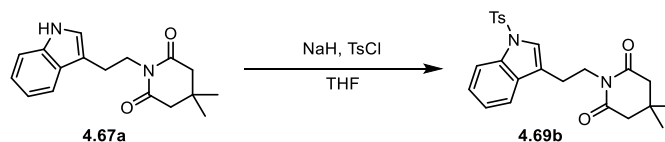
^1H NMR (500 MHz, CDCl_3) δ [ppm] = 7.79–7.74 (m, 1H), 7.47 (d, J = 8.0 Hz, 1H), 7.30 (s, 1H), 7.21 (ddd, J = 11.8, 7.7, 1.3 Hz, 2H), 7.17 (s, 2H), 4.20–4.15 (m, 2H), 4.06–3.97 (m, 2H), 2.94–2.85 (m, 3H), 2.52 (s, 4H), 1.25 (d, J = 6.9 Hz, 6H), 1.10 (s, 6H), 1.08 (d, J = 1.7 Hz, 12H).

^{13}C NMR (126 MHz, CDCl_3) δ [ppm] = 171.9, 154.5, 151.4, 135.4, 131.9, 130.0, 124.4, 124.3, 122.9, 122.6, 120.0, 117.6, 112.8, 46.5, 39.4, 34.3, 29.5, 29.3, 27.8, 24.6, 23.7, 23.6.

HRMS-ESI: calcd. for $\text{C}_{32}\text{H}_{42}\text{N}_2\text{O}_4\text{SK}$ [$\text{M} + \text{K}$] $^+$: 589.2497; found: 589.2522.

FT-IR: ν [cm^{-1}] = 2959, 2930, 1725, 1673, 1448, 1371, 1345, 1269, 1169, 1122, 967, 737.

4,4-Dimethyl-1-(2-(1-tosyl-1*H*-indol-3-yl)ethyl)piperidine-2,6-dione (**4.69b**)



To a solution of **4.67a** (100 mg, 0.352 mmol, 1.0 equiv.) in THF (10 mL) was added NaH (60% dispersion in mineral oil, 201 mg, 1.06 mmol, 3.0 equiv.) and TsCl (28.2 mg, 0.704 mmol, 2.0 equiv.). The mixture was stirred at room temperature overnight, before quenching with NaHCO_3 (sat. aq.). The aqueous phase was extracted with DCM. The combined organic phases were washed with brine, dried over MgSO_4 , filtered and concentrated under reduced pressure. The crude product was purified by silica gel column chromatography (pentane/EtOAc = 10:1) to afford **4.69b** (110 mg, 0.251 mmol, 71%) as a light yellow solid.

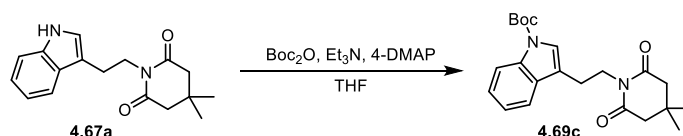
^1H NMR (500 MHz, CDCl_3) δ [ppm] = 7.97 (d, J = 8.1 Hz, 1H), 7.75 (d, J = 7.9 Hz, 2H), 7.69 (d, J = 7.7 Hz, 1H), 7.40 (s, 1H), 7.31 (t, J = 7.6 Hz, 1H), 7.21 (d, J = 8.0 Hz, 3H), 4.10–3.93 (m, 2H), 2.95–2.81 (m, 2H), 2.48 (s, 4H), 2.33 (s, 3H), 1.04 (s, 6H).

^{13}C NMR (126 MHz, CDCl_3) δ [ppm] = 171.9, 144.8, 135.4, 135.2, 130.9, 129.9, 126.9, 124.8, 123.6, 123.2, 119.9, 119.4, 113.7, 46.4, 39.1, 29.1, 27.7, 23.5, 21.6.

HRMS-ESI: calcd. for $C_{24}H_{26}N_2O_4SbA$ $[M + Na]^+$: 461.1505; found: 461.1519.

FT-IR: ν [cm^{-1}] = 2960, 2930, 1725, 1676, 1599, 1449, 1347, 1170, 1125, 744.

Tert-butyl 3-(2-(4,4-dimethyl-2,6-dioxopiperidin-1-yl)ethyl)-1H-indole-1-carboxylate (4.69c)



To a solution of **4.67a** (2.00 g, 7.04 mmol, 1.0 equiv.) in THF (100 mL) was added Et_3N (2.44 mL, 17.6 mmol, 2.5 equiv.) DMAP (215 mg, 1.76 mmol, 0.25 equiv.) and Boc_2O (1.69 g, 7.75 mmol, 1.1 equiv.). The mixture was stirred at room temperature overnight, before quenching with $NaHCO_3$ (sat. aq.). The aqueous phase was extracted with DCM. The combined organic phases were washed with brine, dried over $MgSO_4$, filtered and concentrated under reduced pressure. The crude product was purified by silica gel column chromatography (pentane/ $EtOAc$ = 10:1) to afford **4.69c** (2.50 g, 6.51 mmol, 92%) as a light yellow solid.

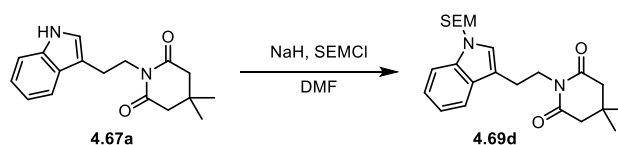
1H NMR (500 MHz, $CDCl_3$) δ [ppm] = 8.04 (d, J = 7.4 Hz, 1H), 7.69–7.62 (m, 1H), 7.35 (s, 1H), 7.22 (td, J = 7.7, 1.4 Hz, 1H), 7.17 (td, J = 7.5, 1.1 Hz, 1H), 4.04–3.91 (m, 2H), 2.88–2.73 (m, 2H), 2.41 (s, 4H), 1.57 (s, 9H), 0.98 (s, 6H).

^{13}C NMR (126 MHz, $CDCl_3$) δ [ppm] = 171.9, 149.7, 135.6, 130.5, 124.4, 123.4, 122.6, 119.4, 117.4, 115.2, 83.4, 46.4, 39.4, 29.2, 28.3, 27.7, 23.6.

HRMS-ESI: calcd. for $C_{22}H_{28}N_2O_4Na$ $[M + Na]^+$: 407.1941; found: 407.1958.

FT-IR: ν [cm^{-1}] = 2959, 1726, 1672, 1454, 1359, 1274, 1252, 1156, 1131, 1092, 1064, 747.

4,4-Dimethyl-1-(2-(1-((2-(trimethylsilyl)ethoxy)methyl)-1H-indol-3-yl)ethyl)piperidine-2,6-dione (4.69d)



To a solution of **4.67a** (500 mg, 1.76 mmol, 1.0 equiv.) in THF (50 mL) was added NaH (60% dispersion in mineral oil, 106 mg, 2.64 mmol, 1.5 equiv.) and SEMCl (618 μ L, 3.52 mmol, 2.0 equiv.). The mixture was stirred at room temperature overnight, before quenching with

NaHCO₃ (sat. aq.). The aqueous phase was extracted with DCM. The combined organic phases were washed with brine, dried over MgSO₄, filtered and concentrated under reduced pressure. The crude product was purified by silica gel column chromatography (pentane/EtOAc = 10:1) to afford **4.69d** (480 mg, 1.17 μmol, 66%) as a light yellow solid.

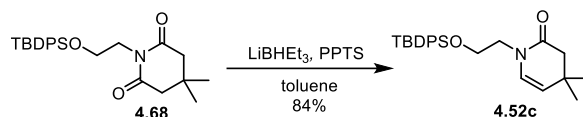
¹H NMR (500 MHz, CDCl₃) δ [ppm] = 7.79 (ddd, *J* = 7.8, 1.3, 0.7 Hz, 1H), 7.45 (dt, *J* = 8.2, 0.9 Hz, 1H), 7.23 (ddd, *J* = 8.2, 7.0, 1.2 Hz, 1H), 7.20–7.15 (m, 1H), 7.04 (s, 1H), 5.43 (s, 2H), 4.12–4.01 (m, 2H), 3.50–3.41 (m, 2H), 3.02–2.91 (m, 2H), 2.50 (s, 4H), 1.07 (s, 6H), 0.91–0.85 (m, 2H), –0.05 (s, 9H).

¹³C NMR (126 MHz, CDCl₃) δ [ppm] = 172.0, 136.8, 128.8, 126.1, 122.3, 119.9, 119.5, 112.8, 110.0, 75.6, 65.8, 46.6, 40.2, 29.3, 27.8, 23.8, 17.8, –1.3.

HRMS-ESI: calcd. for C₂₃H₃₄N₂O₃SiNa [M + Na]⁺: 437.2231; found: 437.2210.

FT-IR: ν [cm⁻¹] = 2954, 2895, 1725, 1673, 1466, 1351, 1248, 1248, 1132, 1073, 858, 834, 742.

1-(2-((*Tert*-butyldiphenylsilyl)oxy)ethyl)-4,4-dimethyl-3,4-dihydropyridin-2(1*H*)-one
(4.52c)



To a solution of imide **4.68** (150 mg, 0.355 mmol, 1.0 equiv.) in toluene (5.0 mL) was added LiBHET₃ (1.0 M in THF, 0.603 mL, 0.355 mmol, 1.7 equiv.) at –78 °C. The mixture was allowed to warm to room temperature and stirred overnight, before quenching with NaHCO₃ (sat. aq.). The aqueous phase was extracted with DCM. The combined organic phases were washed with brine, dried over MgSO₄, filtered and concentrated under reduced pressure. The crude product was dissolved in toluene (5.0 mL). PPTS (8.9 mg, 35 μmol, 0.1 equiv.) was added to the mixture and stirred at room temperature for 2 h. Then the resulting mixture was quenched with NaHCO₃ (sat. aq.). The aqueous phase was extracted with DCM. The combined organic phases were washed with brine, dried over MgSO₄, filtered and concentrated under reduced pressure. The crude product was purified by silica gel column chromatography (pentane/EtOAc = 10:1) to afford **4.52c** (121 mg, 0.297 mmol, 84%) as a colorless liquid.

¹H NMR (500 MHz, CDCl₃) δ [ppm] = 7.71–7.61 (m, 4H), 7.45–7.40 (m, 2H), 7.40–7.35 (m,

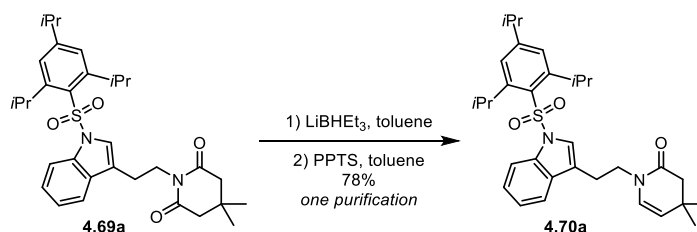
4H), 6.06 (d, $J = 7.7$ Hz, 1H), 4.93 (dt, $J = 7.7, 0.8$ Hz, 1H), 3.78 (t, $J = 5.3$ Hz, 2H), 3.62 (t, $J = 5.3$ Hz, 2H), 2.34 (s, 2H), 1.07 (s, 6H), 1.04 (s, 9H).

^{13}C NMR (151 MHz, CDCl_3) δ [ppm] = 169.3, 135.7, 133.4, 129.9, 128.9, 127.8, 116.3, 62.7, 48.4, 46.4, 31.7, 28.0, 26.9, 19.2.

HRMS-ESI: calcd. for $\text{C}_{25}\text{H}_{33}\text{NO}_2\text{SiNa}$ $[\text{M} + \text{Na}]^+$: 430.2173; found: 430.2194.

FT-IR: ν [cm^{-1}] = 2958, 2925, 2868, 1738, 1672, 1600, 1449, 1384, 1345, 1170, 972, 743.

4,4-Dimethyl-1-(2-(1-((2,4,6-triisopropylphenyl)sulfonyl)-1H-indol-3-yl)ethyl)-3,4-dihydropyridin-2(1H)-one (4.70a)



To a solution of imide **4.69a** (3.30 g, 6.00 mmol, 1.0 equiv.) in toluene (50 mL) was added LiBHEt_3 (1.0 M in THF, 10.2 mL, 10.2 mmol, 1.7 equiv.) at -78 °C. The mixture was allowed to warm to room temperature and stirred overnight, before quenching with NaHCO_3 (sat. aq.). The aqueous phase was extracted with DCM. The combined organic phases were washed with brine, dried over MgSO_4 , filtered and concentrated under reduced pressure. The crude product was dissolved in toluene (30 mL). PPTS (150 mg, 0.600 mmol, 0.1 equiv.) was added to the mixture and stirred at room temperature for 2 h. Then the resulting mixture was quenched with NaHCO_3 (sat. aq.). The aqueous phase was extracted with DCM. The combined organic phases were washed with brine, dried over MgSO_4 , filtered and concentrated under reduced pressure. The crude product was purified by silica gel column chromatography (pentane/EtOAc = 5:1) to afford **4.70a** (2.50 g, 4.68 mmol, 78%) as a yellow solid.

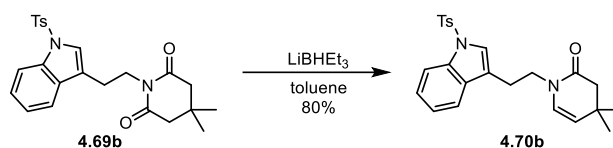
^1H NMR (500 MHz, CDCl_3) δ [ppm] = 7.64–7.60 (m, 1H), 7.47–7.44 (m, 1H), 7.27 (s, 1H), 7.24–7.19 (m, 2H), 7.18–7.15 (m, 2H), 5.84 (d, $J = 7.7$ Hz, 1H), 4.91 (d, $J = 7.7$ Hz, 1H), 4.24–4.09 (m, 2H), 3.79–3.67 (m, 2H), 2.96 (t, $J = 7.7$ Hz, 2H), 2.90 (dt, $J = 13.8, 6.9$ Hz, 1H), 2.35 (s, 2H), 1.25 (s, 3H), 1.24 (s, 3H), 1.09 (s, 6H), 1.08 (s, 6H), 1.05 (s, 6H).

$^{13}\text{C NMR}$ (176 MHz, CDCl_3) δ [ppm] = 169.3, 154.6, 151.5, 135.5, 131.9, 129.9, 127.4, 124.5, 124.4, 122.9, 122.6, 119.6, 117.7, 117.6, 112.9, 46.5, 46.4, 34.4, 31.9, 29.6, 28.0, 24.6, 24.4, 23.6.

HRMS-ESI: calcd. for $\text{C}_{32}\text{H}_{42}\text{N}_2\text{O}_3\text{SNa}$ $[\text{M} + \text{Na}]^+$: 557.2808; found: 557.2800.

FT-IR: ν [cm^{-1}] = 2957, 2927, 2869, 1668, 1600, 1448, 1386, 1344, 1170, 1119, 971, 742.

4,4-Dimethyl-1-(2-(1-tosyl-1*H*-indol-3-yl)ethyl)-3,4-dihydropyridin-2(1*H*)-one (4.70b)



To a solution of imide **4.69b** (2.60 g, 5.94 mmol, 1.0 equiv.) in toluene (80 mL) was added LiBHET₃ (1.0 M in THF, 10.1 mL, 10.1 mmol, 1.7 equiv.) at -78 °C. The mixture was allowed to warm to room temperature and stirred overnight, before quenching with NaHCO₃ (sat. aq.). The aqueous phase was extracted with DCM. The combined organic phases were washed with brine, dried over MgSO₄, filtered and concentrated under reduced pressure. The crude product was dissolved in toluene (30 mL) and heated to 60 °C for 2 h. Then the resulting mixture was quenched with NaHCO₃ (sat. aq.). The aqueous phase was extracted with DCM. The combined organic phases were washed with brine, dried over MgSO₄, filtered and concentrated under reduced pressure. The crude product was purified by silica gel column chromatography (pentane/EtOAc = 5:1) to afford **4.70b** (2.00 g, 4.74 mmol, 80%) as a light yellow solid.

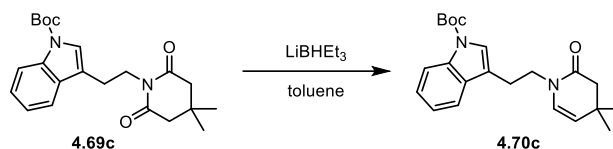
$^1\text{H NMR}$ (600 MHz, CDCl_3) δ [ppm] = 7.97 (dt, J = 8.4, 0.9 Hz, 1H), 7.77–7.72 (m, 2H), 7.57 (dt, J = 7.7, 1.0 Hz, 1H), 7.36 (d, J = 1.0 Hz, 1H), 7.31 (ddd, J = 8.4, 7.2, 1.2 Hz, 1H), 7.26–7.22 (m, 1H), 7.22–7.18 (m, 2H), 5.74 (d, J = 7.7 Hz, 1H), 4.85 (dd, J = 7.7, 0.8 Hz, 1H), 3.77–3.68 (m, 2H), 2.93 (ddd, J = 8.5, 6.5, 1.0 Hz, 2H), 2.33 (s, 5H), 1.02 (s, 6H).

$^{13}\text{C NMR}$ (151 MHz, CDCl_3) δ [ppm] = 169.3, 144.9, 135.5, 135.3, 130.8, 130.0, 127.3, 126.9, 124.9, 123.7, 123.3, 119.6, 119.5, 117.6, 113.9, 46.3, 46.0, 31.8, 27.9, 24.3, 21.7.

HRMS-ESI: calcd. for $\text{C}_{24}\text{H}_{25}\text{N}_2\text{O}_3$ $[\text{M} - \text{H}]^-$: 421.1597 found: 421.1606.

FT-IR: ν [cm^{-1}] = 2958, 2925, 2868, 1738, 1672, 1600, 1449, 1384, 1345, 1170, 972, 743.

Tert-butyl-3-(2-(4,4-dimethyl-2-oxo-3,4-dihydropyridin-1(2H)-yl)ethyl)-1H-indole-1-carboxylate (4.70c)



To a solution of imide **4.69c** (1.60 g, 4.17 mmol, 1.0 equiv.) in toluene (50 mL) was added LiBHEt₃ (1.0 M in THF, 6.25 mL, 6.25 mmol, 1.5 equiv.) at -78 °C. The mixture was allowed to warm to room temperature and stirred overnight, before quenching with NaHCO₃ (sat. aq.). The aqueous phase was extracted with DCM. The combined organic phases were washed with brine, dried over MgSO₄, filtered and concentrated under reduced pressure at 60 °C overnight. The crude product was purified by silica gel column chromatography (pentane/EtOAc = 5:1) to afford **4.70c** (1.50 g, 4.08 mmol, 97%) as a light yellow solid.

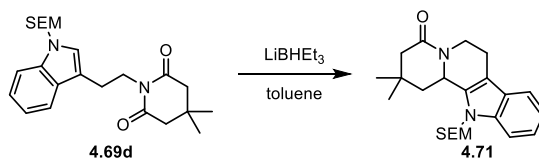
¹H NMR (500 MHz, CD₂Cl₂) δ [ppm] = 8.13 (d, J = 8.3 Hz, 1H), 7.61 (dt, J = 7.7, 1.0 Hz, 1H), 7.42 (s, 1H), 7.32 (ddd, J = 8.3, 7.1, 1.3 Hz, 1H), 7.26 (td, J = 7.5, 1.1 Hz, 1H), 5.86 (d, J = 7.7 Hz, 1H), 4.94–4.87 (m, 1H), 3.79–3.70 (m, 2H), 2.95 (ddd, J = 8.3, 6.9, 1.0 Hz, 2H), 2.31 (s, 2H), 1.65 (s, 9H), 1.04 (s, 6H).

¹³C NMR (126 MHz, CD₂Cl₂) δ [ppm] = 169.1, 150.0, 136.0, 130.8, 127.7, 124.7, 123.9, 122.8, 119.3, 117.7, 117.3, 115.6, 83.8, 46.6, 46.2, 32.0, 28.3, 28.0, 24.5.

HRMS-ESI: calcd. for C₂₂H₂₈N₂O₃Na [M + Na]⁺: 391.1992 found: 391.2011.

FT-IR: ν [cm⁻¹] = 2956, 2934, 1731, 1671, 1454, 1380, 1255, 1157, 1096, 1018, 748.

2,2-Dimethyl-12-((2-(trimethylsilyl)ethoxy)methyl)-2,3,6,7,12,12b-hexahydroindolo[2,3-a]quinolizin-4(1H)-one (4.71)



To a solution of imide **4.69d** (195 mg, 0.417 mmol, 1.0 equiv.) in toluene (10 mL) was added LiBHEt₃ (1.0 M in THF, 0.942 mL, 0.942 mmol, 2.0 equiv.) at -78 °C. The mixture was allowed to warm to room temperature and stirred overnight, before quenching with NaHCO₃ (sat. aq.). The aqueous phase was extracted with DCM. The combined organic phases were washed with

brine, dried over MgSO₄, filtered and concentrated under reduced pressure at 60 °C overnight. The crude product was purified by silica gel column chromatography (pentane/EtOAc = 5:1) to afford **4.71** (70.0 mg, 0.176 mmol, 37%) as a light yellow solid.

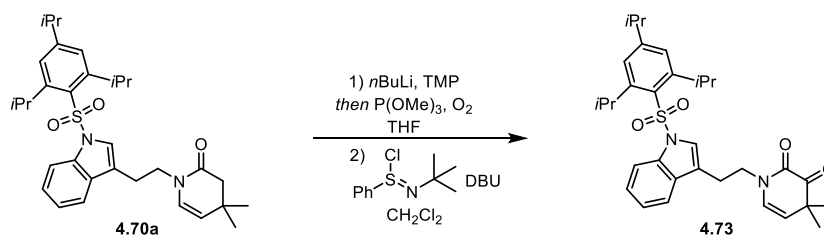
¹H NMR (700 MHz, CDCl₃) δ [ppm] = 7.49 (d, *J* = 7.8 Hz, 1H), 7.38 (d, *J* = 8.2 Hz, 1H), 7.23 (ddd, *J* = 8.2, 7.0, 1.2 Hz, 1H), 7.16–7.12 (m, 1H), 5.45 (d, *J* = 4.2 Hz, 2H), 5.16 (ddd, *J* = 12.3, 4.6, 1.6 Hz, 1H), 4.96–4.93 (m, 1H), 3.53 (td, *J* = 9.5, 6.6 Hz, 1H), 3.47 (td, *J* = 9.5, 6.7 Hz, 1H), 2.83 (dddd, *J* = 15.0, 12.3, 4.8, 2.5 Hz, 1H), 2.78–2.71 (m, 2H), 2.44 (ddd, *J* = 13.4, 4.7, 2.5 Hz, 1H), 2.37 (dd, *J* = 17.2, 2.5 Hz, 1H), 2.26 (d, *J* = 17.2 Hz, 1H), 1.65 (dd, *J* = 13.4, 11.5 Hz, 1H), 1.16 (s, 3H), 1.07 (s, 3H), 0.90 (ddd, *J* = 9.5, 6.5, 5.2 Hz, 2H), –0.04 (s, 9H).

¹³C NMR (176 MHz, CDCl₃) δ [ppm] = 169.4, 138.4, 134.9, 126.9, 122.5, 120.3, 118.6, 112.4, 109.4, 73.4, 66.0, 52.2, 46.0, 42.2, 40.2, 31.1, 28.9, 25.9, 21.7, 18.0, –1.3.

HRMS-ESI: calcd. for C₂₃H₃₄N₂O₂SiNa [M + Na]⁺: 421.2282; found: 421.2262.

FT-IR: ν [cm⁻¹] = 2955, 2927, 1672, 1639, 1462, 1348, 1288, 1090, 1070, 836, 743.

4,4-Dimethyl-1-(2-(1-((2,4,6-triisopropylphenyl)sulfonyl)-1*H*-indol-3-yl)ethyl)-1,4-dihydropyridine-2,3-dione (**4.73**)



To a solution of enamide **4.70a** (500 mg, 0.936 mmol, 1.0 equiv.) in THF (50 mL) was added LiTMP (1.0 M in THF, 7.49 mL, 7.49 mmol, 10 equiv.) dropwise at –78 °C. After the resultant mixture was stirred at –78 °C for 1 h, P(OMe)₃ (464 μL, 1.87 mmol, 2.0 equiv.) was added. O₂ was bubbled through the mixture for 20 min, and the mixture was stirred for additional 2 h under O₂ atmosphere. Then reaction was quenched with NaHCO₃ (sat. aq.). The aqueous phase was extracted with DCM. The combined organic phases were washed with brine, dried over MgSO₄, filtered and the solvent was removed under reduced pressure. The crude product was dissolved in DCM (10 mL). The DBU (216 μL, 1.42 mmol, 3.0 equiv.) and phenylsulfonimidoyl chloride (305 mg, 1.42 mmol, 3.0 equiv.) was added subsequently. The reaction mixture was

stirred at room temperature overnight, before quenching with NaHCO_3 (sat. aq.). The aqueous phase was extracted with DCM. The combined organic phases were washed with brine, dried over MgSO_4 , filtered and concentrated under reduced pressure. The crude product was purified by silica gel column chromatography (pentane/EtOAc = 5:1) to afford **4.73** (212 mg, 0.387 mmol, 41% over 2 steps) as a light yellow solid.

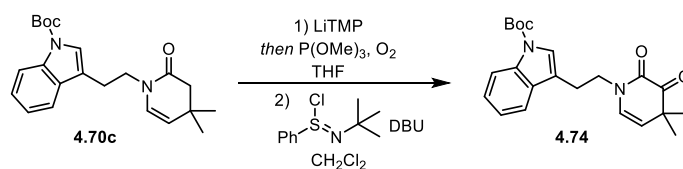
$^1\text{H NMR}$ (500 MHz, CDCl_3) δ [ppm] = 7.61 (d, J = 5.8 Hz, 1H), 7.46–7.40 (m, 1H), 7.31 (s, 1H), 7.25–7.20 (m, 2H), 7.17 (s, 2H), 5.90–5.72 (m, 1H), 5.09–4.92 (m, 1H), 4.18–4.13 (m, 2H), 3.85 (s, 2H), 3.09 (s, 2H), 2.93–2.87 (m, 1H), 1.25 (s, 9H), 1.23 (s, 3H), 1.09 (d, J = 6.6 Hz, 12H).

$^{13}\text{C NMR}$ (126 MHz, CDCl_3) δ [ppm] = 196.8, 156.1, 154.7, 151.4, 135.5, 131.6, 129.7, 125.6, 124.7, 124.4, 123.1, 122.8, 119.5, 116.9, 116.0, 112.9, 48.3, 46.3, 34.3, 29.6, 25.0, 24.6, 23.8, 23.5.

HRMS-ESI: calcd. for $\text{C}_{32}\text{H}_{40}\text{N}_2\text{O}_4\text{SNa}$ $[\text{M} + \text{Na}]^+$: 571.2601; found: 571.2597.

FT-IR: ν [cm^{-1}] = 2961, 2928, 1731, 1676, 1599, 1448, 1343, 1169, 1120, 970, 743.

***Tert*-butyl-3-(2-(4,4-dimethyl-2,3-dioxo-3,4-dihydropyridin-1(2*H*)-yl)ethyl)-1*H*-indole-1-carboxylate (**4.74**)**



To a solution of enamide **4.70c** (500 mg, 1.36 mmol, 1.0 equiv.) in THF (50 mL) was added LiTMP (1.0 M in THF, 10.9 mL, 10.9 mmol, 10 equiv.) dropwise at -78 °C. After the resultant mixture was stirred at -78 °C for 1 h, $\text{P}(\text{OMe})_3$ (1.01 mL, 4.08 mmol, 2.0 equiv.) was added. O_2 was bubbled through the mixture for 20 min, and the mixture was stirred for additional 2 h under O_2 atmosphere. Then reaction was quenched with NaHCO_3 (sat. aq.). The aqueous phase was extracted with DCM. The combined organic phases were washed with brine, dried over MgSO_4 , filtered and the solvent was removed under reduced pressure. Part of the crude product (182 mg, 0.3474 mmol, 1.0 equiv.) was dissolved in DCM (10 mL). The DBU (212 μL , 1.42 mmol, 3.0 equiv.) and phenylsulfonimidoyl chloride (204 mg, 0.948 mmol, 3.0 equiv.) was

added subsequently. The reaction mixture was stirred at room temperature overnight, before quenching with NaHCO₃ (sat. aq.). The aqueous phase was extracted with DCM. The combined organic phases were washed with brine, dried over MgSO₄, filtered and concentrated under reduced pressure. The crude product was purified by silica gel column chromatography (pentane/EtOAc = 5:1) to afford **4.74** (80.0 mg, 0.209 mmol, 20% over 2 steps) as a light yellow solid.

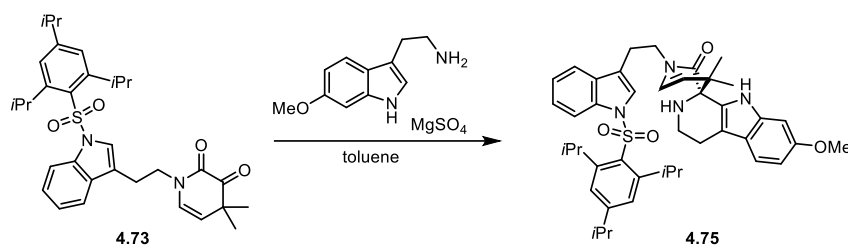
¹H NMR (500 MHz, CDCl₃) δ [ppm] = 8.14 (s, 1H), 7.59 (dt, *J* = 7.7, 0.9 Hz, 1H), 7.41 (s, 1H), 7.35–7.30 (m, 1H), 7.26–7.23 (m, 1H), 5.82 (d, *J* = 8.2 Hz, 1H), 4.99 (d, *J* = 8.2 Hz, 1H), 3.94–3.77 (m, 2H), 3.07 (td, *J* = 7.2, 0.9 Hz, 2H), 1.65 (s, 9H), 1.24 (s, 6H).

¹³C NMR (126 MHz, CDCl₃) δ [ppm] = 196.8, 156.0, 149.7, 135.7, 130.2, 125.6, 124.7, 123.7, 122.8, 118.9, 116.7, 115.8, 115.5, 83.8, 48.1, 46.2, 28.3, 24.9, 23.7.

HRMS-ESI: calcd. for C₂₂H₂₆N₂O₄Na [M + Na]⁺: 405.1785; found: 405.1786.

FT-IR: ν [cm⁻¹] = 2972, 2929, 1731, 1679, 1454, 1372, 1255, 1158, 1089, 766, 748.

7'-methoxy-4,4-dimethyl-1-(2-(1-((2,4,6-triisopropylphenyl)sulfonyl)-1*H*-indol-3-yl)-ethyl)-1,2',3',4,4',9'-hexahydro-2*H*-spiro[pyridine-3,1'-pyrido[3,4-*b*]indol]-2-one (4.75)



To a solution of **4.73** (36.0 mg, 66.0 μmol, 1.0 equiv.) in toluene (5.0 mL) was added 6-methoxytryptamine (25.0 mg, 0.131 mmol, 2.0 equiv.) and MgSO₄ (78.8 mg, 0.657 mmol, 10 equiv.). The mixture was heated to reflux and stirred for 2 d. After filtering through Celite[®] and removing the solvent, the crude product was purified by silica gel column chromatography (pentane/EtOAc = 3:2) to afford **4.75** (23.5 mg, 39.6 μmol, 60%) as a white solid.

¹H NMR (700 MHz, CD₂Cl₂) δ [ppm] = 8.45 (s, 1H), 7.55 (ddd, *J* = 7.7, 1.6, 0.8 Hz, 1H), 7.29 (ddd, *J* = 7.8, 1.4, 0.7 Hz, 1H), 7.26 (d, *J* = 1.0 Hz, 1H), 7.25–7.23 (m, 1H), 7.15–7.09 (m, 4H), 6.73 (dd, *J* = 2.2, 0.5 Hz, 1H), 6.61 (dd, *J* = 8.6, 2.2 Hz, 1H), 6.04 (d, *J* = 7.9 Hz, 1H), 5.12 (d, *J* = 7.9 Hz, 1H), 4.09–4.03 (m, 2H), 3.87 (ddd, *J* = 13.5, 9.6, 5.7 Hz, 1H), 3.72 (s, 3H), 3.51–

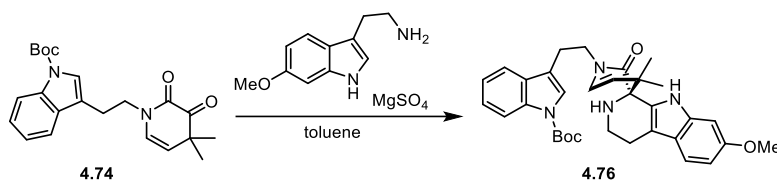
3.40 (m, 2H), 3.04 (dt, $J = 12.2, 5.1$ Hz, 1H), 2.96–2.91 (m, 1H), 2.87–2.78 (m, 2H), 2.61–2.51 (m, 2H), 1.15 (s, 3H), 1.14 (s, 3H), 1.03 (s, 3H), 1.00 (d, $J = 3.0$ Hz, 6H), 0.99 (d, $J = 2.9$ Hz, 6H), 0.81 (s, 3H).

$^{13}\text{C NMR}$ (176 MHz, CD_2Cl_2) δ [ppm] = 173.4, 158.0, 157.1, 156.0, 152.5, 137.4, 136.5, 132.8, 131.4, 131.1, 128.6, 125.6, 124.2, 123.8, 122.2, 120.8, 120.6, 120.0, 118.7, 114.4, 113.8, 110.2, 95.8, 64.9, 56.8, 48.8, 43.6, 42.0, 35.5, 31.9, 30.7, 25.4, 24.4, 24.2, 23.9, 23.6.

HRMS-ESI: calcd. for $\text{C}_{43}\text{H}_{53}\text{N}_4\text{O}_4\text{S}$ $[\text{M} + \text{H}]^+$: 721.3782; found: 721.3807.

FT-IR: ν [cm^{-1}] = 3446, 2959, 2930, 2870, 1736, 1662, 1627, 1600, 1497, 1452, 1386, 1374, 1343, 1257, 1219, 1169, 1122, 1036, 969, 884, 802, 769, 745.

***Tert*-butyl-3-(2-(7'-methoxy-4,4-dimethyl-2-oxo-2',3',4',9'-tetrahydro-2*H*-spiro[pyridine-3,1'-pyrido[3,4-*b*]indol]-1(4*H*)-yl)ethyl)-1*H*-indole-1-carboxylate (4.76)**



To a solution of **4.74** (86.0 mg, 225 μmol , 1.0 equiv.) in toluene (5.0 mL) was added 6-methoxytryptamine (42.8 mg, 225 μmol , 2.0 equiv.) and MgSO_4 (270 mg, 2.25 mmol, 10 equiv.). The mixture was heated to reflux and stirred for 2 d. After filtering through Celite[®] and removing the solvent, the crude product was purified by silica gel column chromatography (pentane/EtOAc = 3:2) to afford **4.76** (39.0 mg, 70.4 μmol , 31%) as a white solid.

$^1\text{H NMR}$ (700 MHz, CDCl_3) δ [ppm] = 8.45 (s, 1H), 8.12 (s, 1H), 7.59 (d, $J = 7.7$ Hz, 1H), 7.39 (s, 1H), 7.35 (d, $J = 8.6$ Hz, 1H), 7.32 (ddd, $J = 8.2, 7.1, 1.2$ Hz, 1H), 7.24 (td, $J = 7.5, 1.0$ Hz, 1H), 6.77 (d, $J = 2.0$ Hz, 1H), 6.74 (dd, $J = 8.6, 2.2$ Hz, 1H), 6.05 (d, $J = 7.9$ Hz, 1H), 5.15 (d, $J = 7.9$ Hz, 1H), 4.00–3.95 (m, 1H), 3.83 (s, 3H), 3.67–3.58 (m, 2H), 3.19 (dt, $J = 12.2, 4.9$ Hz, 1H), 3.04–2.93 (m, 2H), 2.69 (td, $J = 5.3, 2.2$ Hz, 2H), 1.65 (s, 9H), 1.15 (s, 3H), 0.90 (s, 3H).

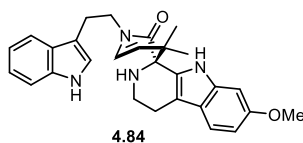
$^{13}\text{C NMR}$ (176 MHz, CDCl_3) δ [ppm] = 172.5, 156.8, 149.8, 136.2, 135.7, 130.3, 130.0, 127.5, 124.6, 123.7, 122.7, 121.1, 119.4, 119.0, 117.1, 115.5, 113.5, 109.2, 94.8, 83.7, 63.8, 55.8, 47.6,

42.6, 40.9, 28.4, 24.5, 23.3, 23.0, 22.4. (Note: one resonance of a sp^2 carbon was missing, probably due to overlapping.)

HRMS-ESI: calcd. for $C_{33}H_{39}N_4O_4$ $[M + H]^+$: 555.2966; found: 555.2944.

FT-IR: ν [cm^{-1}] = 3443, 2977, 2930, 2868, 1731, 1659, 1627, 1454, 1379, 1371, 1308, 1255, 1220, 1155, 1090, 1021, 856, 748.

1-(2-(1*H*-indol-3-yl)ethyl)-7'-methoxy-4,4-dimethyl-1,2',3',4,4',9'-hexahydro-2*H*-spiro-[pyridine-3,1'-pyrido[3,4-*b*]indol]-2-one (4.84)

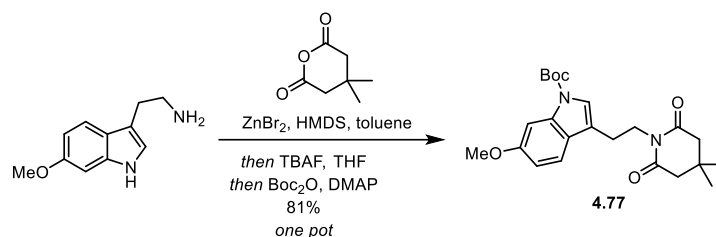


1H NMR (700 MHz, d_6 -DMSO) δ [ppm] = 10.82 (s, 1H), 9.75 (s, 1H), 7.61 (dt, J = 8.0, 1.0 Hz, 1H), 7.33 (dt, J = 8.1, 0.9 Hz, 1H), 7.24 (d, J = 8.7 Hz, 1H), 7.14 (d, J = 2.3 Hz, 1H), 7.07 (ddd, J = 8.1, 7.0, 1.2 Hz, 1H), 7.01–6.98 (m, 2H), 6.60 (dd, J = 8.6, 2.3 Hz, 1H), 6.29 (d, J = 7.9 Hz, 1H), 5.07 (d, J = 7.8 Hz, 1H), 3.92–3.85 (m, 1H), 3.73 (s, 3H), 3.56–3.46 (m, 1H), 3.38 (s, 1H), 3.02 (t, J = 7.1 Hz, 1H), 2.96 (ddd, J = 14.8, 10.0, 5.4 Hz, 1H), 2.86 (ddd, J = 14.1, 10.0, 6.0 Hz, 1H), 2.59–2.52 (m, 2H), 1.04 (s, 3H), 0.84 (s, 3H).

^{13}C NMR (176 MHz, d_6 -DMSO) δ [ppm] = 171.4, 155.5, 136.5, 136.3, 130.1, 129.6, 127.7, 127.0, 123.0, 121.0, 120.3, 118.3, 118.0, 117.0, 111.5, 111.4, 110.8, 108.4, 95.1, 79.2, 63.3, 55.0, 47.2, 41.5, 24.1, 23.1, 23.0, 22.1.

HRMS-ESI: calcd. for $C_{28}H_{30}N_4O_2Na$ $[M + Na]^+$: 477.2261; found: 477.2283.

FT-IR: ν [cm^{-1}] = 3443, 2978, 2930, 1731, 1659, 1627, 1454, 1379, 1371, 1255, 1220, 1155, 1089, 1021, 748.

7.2.3.2.3. 5th generation synthetic route***Tert*-butyl-3-(2-(4,4-dimethyl-2,6-dioxopiperidin-1-yl)ethyl)-6-methoxy-1*H*-indole-1-carboxylate (4.77)**

To a solution of 6-methoxytryptamine (218 mg, 1.15 mmol, 1.0 equiv.) in toluene (30 mL) was added 3,3-dimethylglutaric anhydride (163 mg, 1.15 mmol, 1.0 equiv.). The reaction mixture was stirred at room temperature for 2 h, before the addition of ZnBr_2 (353 mg, 1.15 mmol, 1.0 equiv.). Then the mixture was heated to 80 °C and HMDS (360 μL , 1.72 mmol, 1.5 equiv.) was added to the mixture dropwise at 80 °C. The resulting mixture was heated to 110 °C and stirred overnight. After cooling to room temperature, the THF (30 mL) and TBAF (1.0 M in THF, 2.29 mL, 2.29 mmol, 2.0 equiv.) was added to the mixture and stirred for 5 h. Then DMAP (420 mg, 3.44 mmol, 3.0 equiv.) and Boc_2O (3.00 g, 13.8 mmol, 12 equiv.) was added to the mixture and stirred overnight. The reaction mixture was then quenched with NaHCO_3 (sat. aq.). The aqueous phase was extracted with DCM. The combined organic phases were washed with brine, dried over MgSO_4 , filtered and concentrated under reduced pressure. The crude product was purified by silica gel column chromatography (pentane/EtOAc = 15:1) to afford **4.77** (387 mg, 0.935 mmol, 81%) as a light yellow solid.

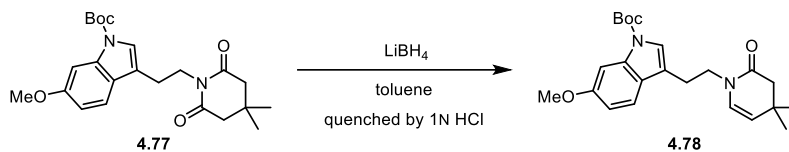
¹H NMR (500 MHz, CD_2Cl_2) δ [ppm] = 7.70 (s, 1H), 7.57 (d, J = 8.6 Hz, 1H), 7.32 (s, 1H), 6.88 (dd, J = 8.5, 2.4 Hz, 1H), 4.06–3.97 (m, 2H), 3.85 (s, 3H), 2.89–2.80 (m, 2H), 2.48 (s, 4H), 1.64 (s, 9H), 1.05 (s, 6H).

¹³C NMR (126 MHz, CD_2Cl_2) δ [ppm] = 172.1, 158.3, 150.1, 137.0, 124.6, 122.4, 120.1, 117.8, 111.9, 99.7, 83.6, 55.9, 46.7, 39.6, 29.4, 28.3, 27.8, 24.0.

HRMS-ESI: calcd. for $\text{C}_{23}\text{H}_{30}\text{N}_2\text{O}_5\text{Na}$ [$\text{M} + \text{Na}$]⁺: 437.2047; found: 437.2044.

FT-IR: ν [cm^{-1}] = 2960, 2931, 1727, 1673, 1451, 1361, 1275, 1253, 1158, 1132, 1093, 749.

***Tert*-butyl-3-(2-(4,4-dimethyl-2-oxo-3,4-dihydropyridin-1(2*H*)-yl)ethyl)-6-methoxy-1*H*-indole-1-carboxylate (**4.78**)**



To a solution of imide **4.77** (100 mg, 0.242 mmol, 1.0 equiv.) in toluene (10 mL) was added LiBH_4 (1.0 M in THF, 411 μL , 0.411 mmol, 2.0 equiv.) at $-78\text{ }^\circ\text{C}$. The mixture was allowed to warm to room temperature and stirred overnight, before carefully quenching with HCl (1 N, aq.). The aqueous phase was extracted with DCM. The combined organic phases were washed with brine, dried over MgSO_4 , filtered and concentrated under reduced pressure. The crude product was purified by silica gel column chromatography (pentane/EtOAc = 5:1) to afford **4.78** (86.0 mg, 0.216 mmol, 89%) as a light yellow solid. (Note: the quenching with HCl (1 N, aq.) should be very careful and monitor by TLC frequently.)

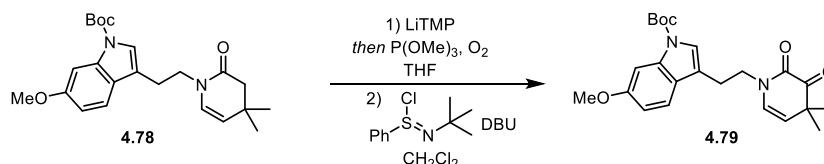
$^1\text{H NMR}$ (700 MHz, C_6D_6) δ [ppm] = 8.13 (s, 1H), 7.48 (d, $J = 8.5$ Hz, 1H), 7.38 (s, 1H), 7.01 (dd, $J = 8.5, 2.3$ Hz, 1H), 5.40 (d, $J = 7.7$ Hz, 1H), 4.50 (dt, $J = 7.7, 0.9$ Hz, 1H), 3.65–3.58 (m, 2H), 3.49 (s, 3H), 2.82 (ddd, $J = 8.5, 6.6, 1.1$ Hz, 2H), 2.25 (s, 2H), 1.41 (s, 9H), 0.81 (s, 6H).

$^{13}\text{C NMR}$ (176 MHz, C_6D_6) δ [ppm] = 168.1, 158.8, 150.0, 137.4, 128.3, 124.7, 122.3, 120.1, 118.0, 116.0, 112.4, 100.2, 82.7, 55.2, 46.6, 46.3, 31.7, 28.0, 27.8, 24.8.

HRMS-ESI: calcd. for $\text{C}_{23}\text{H}_{30}\text{N}_2\text{O}_4\text{Na}$ [$\text{M} + \text{Na}$] $^+$: 421.2098; found: 421.2095.

FT-IR: ν [cm^{-1}] = 2955, 2936, 2869, 1727, 1670, 1619, 1488, 1444, 1383, 1227, 1155, 1096, 1041, 848, 768.

***Tert*-butyl-3-(2-(4,4-dimethyl-2,3-dioxo-3,4-dihydropyridin-1(2*H*)-yl)ethyl)-6-methoxy-1*H*-indole-1-carboxylate (**4.79**)**



To a solution of enamide **4.78** (107 mg, 0.269 mmol, 1.0 equiv.) in THF (15 mL) was added LiTMP (1.0 M in THF, 215 μL , 2.15 mmol, 8.0 equiv.) dropwise at $-78\text{ }^\circ\text{C}$. After the resultant

mixture was stirred at $-78\text{ }^{\circ}\text{C}$ for 1 h, $\text{P}(\text{OMe})_3$ (200 μL , 0.807 mmol, 3.0 equiv.) was added. O_2 was bubbled through the mixture for 20 min, and the mixture was stirred for additional 2 h under O_2 atmosphere. Then reaction was quenched with NaHCO_3 (sat. aq.). The aqueous phase was extracted with DCM. The combined organic phases were washed with brine, dried over MgSO_4 , filtered and the solvent was removed under reduced pressure. The crude product was dissolved in DCM (10 mL). The DBU (47.5 μL , 0.319 mmol, 3.0 equiv.) and phenylsulfonimidoyl chloride (45.7 mg, 0.213 mmol, 2.0 equiv.) was added subsequently. The reaction mixture was stirred at room temperature overnight, before quenching with NaHCO_3 (sat. aq.). The aqueous phase was extracted with DCM. The combined organic phases were washed with brine, dried over MgSO_4 , filtered and concentrated under reduced pressure. The crude product was purified by silica gel column chromatography (pentane/EtOAc = 5:1) to afford **4.79** (25.0 mg, 59.5 μmol , 24% over 2 steps) as a light yellow solid.

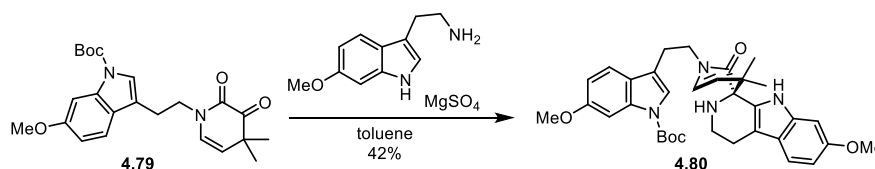
$^1\text{H NMR}$ (600 MHz, CD_2Cl_2) δ [ppm] = 7.72 (s, 1H), 7.45 (d, J = 8.6 Hz, 1H), 7.31 (s, 1H), 6.88 (dd, J = 8.6, 2.4 Hz, 1H), 5.86 (d, J = 8.2 Hz, 1H), 5.02 (d, J = 8.2 Hz, 1H), 3.87–3.82 (m, 5H), 3.01 (td, J = 7.2, 1.0 Hz, 2H), 1.64 (s, 9H), 1.22 (s, 6H).

$^{13}\text{C NMR}$ (151 MHz, CD_2Cl_2) δ [ppm] = 197.4, 158.4, 156.2, 150.0, 129.1, 125.9, 124.3, 122.7, 119.6, 117.0, 115.8, 112.1, 99.9, 83.8, 55.9, 48.0, 46.5, 28.3, 25.0, 24.0.

HRMS-ESI: calcd. for $\text{C}_{23}\text{H}_{28}\text{N}_2\text{O}_5\text{Na}$ [$\text{M} + \text{Na}$] $^+$: 435.1890; found: 435.1894.

FT-IR: ν [cm^{-1}] = 2966, 1676, 1488, 1443, 1381, 1274, 1256, 1158, 1089, 850, 768.

***Tert*-butyl-6-methoxy-3-(2-(7'-methoxy-4,4-dimethyl-2-oxo-2',3',4',9'-tetrahydro-2*H*-spiro[pyridine-3,1'-pyrido[3,4-*b*]indol]-1(4*H*)-yl)ethyl)-1*H*-indole-1-carboxylate (**4.80**)**



To a solution of **4.79** (41.0 mg, 100 μmol , 1.0 equiv.) in toluene (5.0 mL) was added 6-methoxytryptamine (22.7 mg, 119 μmol , 1.2 equiv.) and MgSO_4 (119 mg, 995 μmol , 10 equiv.). The mixture was heated to reflux and stirred for 2 d. After filtering through Celite[®] and removing the solvent, the crude product was purified by silica gel column chromatography

(pentane/EtOAc = 3:2) to afford **4.80** (24.5 mg, 42.0 μmol , 42%) as a white solid.

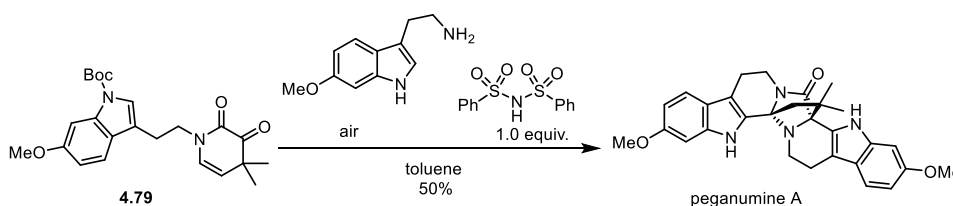
^1H NMR (700 MHz, d_6 -DMSO) δ [ppm] = 9.72 (s, 1H), 7.61 (s, 1H), 7.58 (dd, J = 8.6, 0.5 Hz, 1H), 7.34 (s, 1H), 7.23 (d, J = 8.5 Hz, 1H), 6.96 (dd, J = 2.3, 0.5 Hz, 1H), 6.89 (dd, J = 8.6, 2.4 Hz, 1H), 6.59 (dd, J = 8.5, 2.3 Hz, 1H), 6.26 (d, J = 7.9 Hz, 1H), 5.06 (d, J = 7.9 Hz, 1H), 3.95–3.88 (m, 1H), 3.80 (s, 3H), 3.73 (s, 3H), 3.51 (ddd, J = 13.3, 8.9, 6.5 Hz, 1H), 3.40–3.33 (m, 1H), 3.02 (dt, J = 11.2, 4.3 Hz, 1H), 2.94–2.82 (m, 2H), 2.54–2.51 (m, 2H), 1.61 (s, 9H), 1.02 (s, 3H), 0.83 (s, 3H).

^{13}C NMR (176 MHz, d_6 -DMSO) δ [ppm] = 171.5, 157.4, 155.5, 149.0, 136.5, 135.8, 130.0, 128.6, 127.5, 125.6, 123.7, 122.0, 120.3, 119.8, 118.0, 117.1, 117.0, 111.4, 108.4, 99.1, 95.1, 83.3, 63.3, 55.2, 55.0, 46.1, 41.5, 30.6, 27.7, 23.6, 23.0, 22.1.

HRMS-ESI: calcd. for $\text{C}_{34}\text{H}_{40}\text{N}_4\text{O}_5$ $[\text{M} + \text{H}]^+$: 585.3072; found: 585.3087.

FT-IR: ν [cm^{-1}] = 2954, 2924, 2853, 1720, 1456, 1374, 1261, 1097, 728.

rac-Peganumine A



To a mixture of ketoenamide **4.79** (20.0mg, 49.0 μmol , 1.0 equiv.), 6-methoxytryptamine (11.1 mg, 58.0 μmol , 1.2 equiv.) and MS 4 Å in toluene (10.0 mL) in a reaction vial with air inside, was added *N*-(phenylsulfonyl)benzenesulfonamide (11.1 mg, 49.0 μmol , 1.0 equiv.). The resulting reaction mixture was heated to 115 °C (oil bath temperature) for 2 d. Then the reaction was quenched with NaHCO_3 (sat. aq.). The aqueous phase was extracted with DCM. The combined organic phases were washed with brine, dried over MgSO_4 , filtered and concentrated under reduced pressure. The crude product was purified by silica gel column chromatography (pentane/EtOAc = 3:2) to afford *rac*-Peganumine A (11.8 mg, 24.5 μmol , 50%) as a light yellow solid.

^1H NMR (700 MHz, CD_3OD) δ [ppm] = 7.38 (d, J = 8.7 Hz, 1H), 7.26 (d, J = 8.6 Hz, 1H), 6.99 (d, J = 2.2 Hz, 1H), 6.93 (d, J = 2.2 Hz, 1H), 6.73 (dd, J = 8.7, 2.2 Hz, 1H), 6.67 (dd, J = 8.6, 2.3 Hz, 1H), 4.14 (dd, J = 13.0, 5.8 Hz, 1H), 3.83 (s, 3H), 3.82 (s, 3H), 3.21–3.16 (m, 1H),

2.98 (dd, $J = 15.4, 4.4$ Hz, 1H), 2.90–2.76 (m, 2H), 2.69 (dd, $J = 15.5, 3.5$ Hz, 1H), 2.59 (dd, $J = 10.8, 5.3$ Hz, 1H), 2.48–2.41 (m, 1H), 2.39 (d, $J = 11.5$ Hz, 1H), 1.94 (d, $J = 11.5$ Hz, 1H), 1.44 (s, 3H), 1.24 (s, 3H).

^{13}C NMR (176 MHz, CD_3OD) δ [ppm] = 175.2, 158.3, 157.6, 139.5, 139.4, 127.8, 126.4, 122.3, 122.2, 119.9, 119.2, 112.9, 112.2, 110.5, 109.8, 96.0, 95.7, 81.2, 79.7, 56.0, 55.9, 51.9, 41.7, 41.6, 37.3, 27.3, 26.3, 22.5, 22.1.

^1H NMR (500 MHz, $d_6\text{-DMSO}$) δ [ppm] = 11.24 (s, 1H), 10.77 (s, 1H), 7.38 (d, $J = 8.6$ Hz, 1H), 7.25 (d, $J = 8.6$ Hz, 1H), 6.93 (d, $J = 2.3$ Hz, 1H), 6.88 (d, $J = 2.3$ Hz, 1H), 6.70 (dd, $J = 8.6, 2.3$ Hz, 1H), 6.63 (dd, $J = 8.6, 2.3$ Hz, 1H), 4.00 (dd, $J = 12.9, 5.8$ Hz, 1H), 3.78 (s, 3H), 3.77 (s, 3H), 3.10 (td, $J = 12.6, 4.5$ Hz, 1H), 2.90 (dd, $J = 15.3, 4.2$ Hz, 1H), 2.76–2.69 (m, 1H), 2.69–2.65 (m, 1H), 2.64–2.60 (m, 1H), 2.48–2.43 (m, 1H), 2.34 (dd, $J = 10.8, 4.9$ Hz, 1H), 2.30 (d, $J = 11.3$ Hz, 1H), 1.88 (d, $J = 11.2$ Hz, 1H), 1.38 (s, 3H), 1.15 (s, 3H).

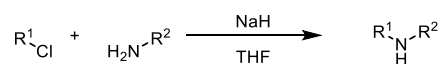
^{13}C NMR (126 MHz, $d_6\text{-DMSO}$) δ [ppm] = 171.3, 156.1, 155.4, 137.6, 137.5, 127.3, 125.7, 120.5, 120.4, 119.0, 118.2, 111.2, 109.5, 109.0, 108.3, 94.9, 94.7, 78.8, 77.4, 55.23, 55.18, 50.4, 40.1, 39.9, 35.6, 26.8, 26.0, 21.0, 20.9.

HRMS-ESI: calcd. for $\text{C}_{29}\text{H}_{31}\text{N}_4\text{O}_3$ $[\text{M} + \text{H}]^+$: 483.2391; found: 483.2384.

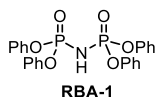
FT-IR: ν [cm^{-1}] = 2954, 2923, 2857, 1736, 1457, 1366, 1217, 820.

7.2.3.2.4. Racemic Brønsted acids syntheses

General procedure L



To a solution of the amide (1.0 equiv.) was added the chloride (1.0 equiv.) The mixture was stirred at room temperature overnight, before quenching with NaHCO_3 (sat. aq.). The aqueous phase was extracted with DCM. The combined organic phases were washed with brine, dried over MgSO_4 , filtered and concentrated under reduced pressure. The crude product was purified by silica gel column chromatography. The pure product was re-dissolved in DCM was washed with 6 N HCl, dried over MgSO_4 , and concentrated under reduced pressure to afford the final product.

Tetraphenyl iminodiphosphate (RBA-1)

RBA-1 was prepared according to **General procedure L**, starting from diphenyl phosphoramidate (100 mg, 0.402 mmol, 1.0 equiv.) and NaH (60% dispersion in mineral oil, 24.1 mg, 0.603 mmol, 1.5 equiv.) in THF (2.0 mL). The mixture was added diphenyl phosphorochloridate (115 mg, 0.402 mmol, 1.0 equiv.) Purification by silica gel column chromatography (DCM/MeOH = 20:1) and acidification with 6 N HCl afforded **RBA-1** (50.0 mg, 0.104 mmol, 26%) as a white solid.

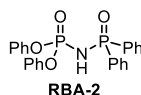
$^1\text{H NMR}$ (600 MHz, CDCl_3) δ [ppm] = 7.35–7.32 (m, 8H), 7.24–7.19 (m, 12H).

$^{13}\text{C NMR}$ (151 MHz, CDCl_3) δ [ppm] = 150.6, 130.0, 125.8, 120.3.

$^{31}\text{P NMR}$ (243 MHz, CDCl_3) δ [ppm] = –17.1.

HRMS-ESI: calcd. for $\text{C}_{24}\text{H}_{21}\text{NO}_6\text{P}_2\text{Na}$ $[\text{M} + \text{Na}]^+$: 504.0736; found: 504.0753.

FT-IR: ν [cm^{-1}] = 3056, 2928, 1737, 1438, 1393, 1327, 1200, 1169, 1126, 900, 748, 730.

Diphenyl (diphenylphosphoryl)phosphoramidate (RBA-2)

RBA-2 was prepared according to **General procedure L**, starting from *P,P*-diphenylphosphinic amide (87.3 mg, 0.402 mmol, 1.0 equiv.) and NaH (60% dispersion in mineral oil, 24.1 mg, 0.603 mmol, 1.5 equiv.) in THF (2.0 mL). The mixture was added diphenyl phosphorochloridate (115 mg, 0.402 mmol, 1.0 equiv.) Purification by silica gel column chromatography (DCM/MeOH = 20:1) and acidification with 6 N HCl afforded **RBA-2** (120 mg, 0.268 mmol, 67%) as a white solid.

$^1\text{H NMR}$ (600 MHz, CDCl_3) δ [ppm] = 7.70 (ddd, J = 13.2, 8.2, 1.4 Hz, 4H), 7.46 (td, J = 7.5, 1.5 Hz, 2H), 7.30 (td, J = 7.7, 3.3 Hz, 4H), 7.16 (t, J = 7.7 Hz, 4H), 7.11–7.03 (m, 6H).

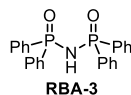
$^{13}\text{C NMR}$ (151 MHz, CDCl_3) δ [ppm] = 150.7, 150.7, 132.2, 132.0, 131.9, 129.5, 128.3, 128.3, 125.0, 120.9, 120.8.

$^{31}\text{P NMR}$ (243 MHz, CDCl_3) δ [ppm] = 23.8, –7.9.

HRMS-ESI: calcd. for $C_{24}H_{21}NO_4P_2Na$ $[M + Na]^+$: 472.0838; found: 472.0854.

FT-IR: ν [cm^{-1}] = 3058, 2924, 1591, 1489, 1188, 1126, 936, 751.

N-(diphenylphosphoryl)-*P,P*-diphenylphosphinic amide (**RBA-3**)



RBA-3 was prepared according to **General procedure L**, starting from *P,P*-diphenylphosphinic amide (106 mg, 0.487 mmol, 1.0 equiv.) and NaH (60% dispersion in mineral oil, 29.2 mg, 0.731 mmol, 1.5 equiv.) in THF (2.0 mL). The mixture was added diphenylphosphinic chloride (115 mg, 0.487 mmol, 1.0 equiv.) Purification by silica gel column chromatography (DCM/MeOH = 20:1) and acidification with 6 N HCl afforded **RBA-3** (150 mg, 0.360 mmol, 74%) as a white solid.

¹H NMR (600 MHz, *d*₆-DMSO) δ [ppm] = 7.77–7.66 (m, 8H), 7.55–7.50 (m, 4H), 7.49–7.45 (m, 4H), 7.43 (td, *J* = 7.7, 2.6 Hz, 4H).

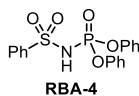
¹³C NMR (151 MHz, *d*₆-DMSO) δ [ppm] = 131.6, 131.5, 131.4, 130.9, 128.5, 128.4, 128.2.

³¹P NMR (243 MHz, *d*₆-DMSO) δ [ppm] = 24.0.

HRMS-ESI: calcd. for $C_{24}H_{21}NO_2P_2Na$ $[M + Na]^+$: 440.0940; found: 440.0955.

FT-IR: ν [cm^{-1}] = 3056, 2922, 1437, 1179, 1126, 964, 727.

Diphenyl (phenylsulfonyl)phosphoramidate (**RBA-4**)



RBA-4 was prepared according to **General procedure L**, starting from benzenesulfonamide (274 mg, 1.75 mmol, 1.0 equiv.) and NaH (60% dispersion in mineral oil, 105 mg, 2.62 mmol, 1.5 equiv.) in THF (2.0 mL). The mixture was added diphenyl phosphorochloridate (500 mg, 1.75 mmol, 1.0 equiv.) Purification by silica gel column chromatography (DCM/MeOH = 20:1) and acidification with 6 N HCl afforded **RBA-4** (250 mg, 0.643 mmol, 38%) as a white solid.

¹H NMR (600 MHz, *d*₆-DMSO) δ [ppm] = 7.85–7.79 (m, 2H), 7.60–7.55 (m, 1H), 7.53–7.48 (m, 2H), 7.37–7.30 (m, 4H), 7.20–7.15 (m, 2H), 7.12 (dt, *J* = 8.6, 1.2 Hz, 4H).

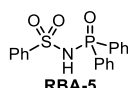
^{13}C NMR (151 MHz, d_6 -DMSO) δ [ppm] = 150.6, 150.6, 143.3, 132.1, 129.7, 128.7, 126.2, 124.8, 120.14, 120.11.

^{31}P NMR (243 MHz, d_6 -DMSO) δ [ppm] = -13.60.

HRMS-ESI: calcd. for $\text{C}_{18}\text{H}_{16}\text{NO}_5\text{PSNa}$ $[\text{M} + \text{Na}]^+$: 412.0397; found: 412.0397.

FT-IR: ν [cm^{-1}] = 2921, 2677, 1438, 1397, 1324, 1187, 1169, 1104, 915, 749.

N-(diphenylphosphoryl)benzenesulfonamide (**RBA-5**)



RBA-5 was prepared according to **General procedure L**, starting from benzenesulfonamide (333 mg, 2.12 mmol, 1.0 equiv.) and NaH (60% dispersion in mineral oil, 127 mg, 3.18 mmol, 1.5 equiv.) in THF (2.0 mL). The mixture was added diphenylphosphinic chloride (500 mg, 2.12 mmol, 1.0 equiv.) Purification by silica gel column chromatography (DCM/MeOH = 20:1) and acidification with 6 N HCl afforded **RBA-5** (302 mg, 0.846 mmol, 40%) as a white solid.

^1H NMR (600 MHz, d_6 -DMSO) δ [ppm] = 7.88 (dd, J = 8.3, 1.4 Hz, 2H), 7.72 (ddd, J = 12.7, 8.2, 1.4 Hz, 4H), 7.66–7.60 (m, 1H), 7.60–7.53 (m, 4H), 7.50 (td, J = 7.7, 3.5 Hz, 4H).

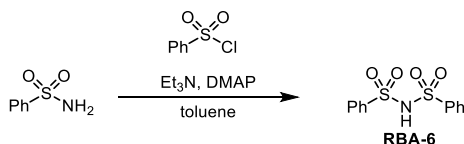
^{13}C NMR (151 MHz, d_6 -DMSO) δ [ppm] = 142.9, 132.5, 132.2, 131.7, 131.4, 131.3, 128.9, 128.6, 128.5, 126.4.

^{31}P NMR (243 MHz, d_6 -DMSO) δ [ppm] = 17.11.

HRMS-ESI: calcd. for $\text{C}_{18}\text{H}_{16}\text{NO}_3\text{PSNa}$ $[\text{M} + \text{Na}]^+$: 380.0481; found: 380.0492.

FT-IR: ν [cm^{-1}] = 2983, 2728, 1589, 1489, 1338, 1181, 960, 753.

N-(phenylsulfonyl)benzenesulfonamide (**RBA-6**)



To a solution of benzenesulfonamide (1.00 g, 6.37 mmol, 1.0 equiv.) in toluene (50 mL) was added Et_3N (1.77 mL, 12.7 mmol, 2.0 equiv.) and DMAP (155 mg, 1.27 mmol, 0.2 equiv.). The mixture was stirred at room temperature for 1h, before the addition of benzenesulfonyl chloride (772 μL , 6.05 mmol, 1.0 equiv.). The resulting mixture was heated to reflux for 2 d. After

cooling to room temperature, the mixture was quenched with HCl (1N, aq.) and acidified with 6 N HCl. The aqueous phase was extracted with EtOAc. The combined organic phases were washed with brine, dried over MgSO₄, filtered and concentrated under reduced pressure. The crude product was purified by recrystallization (hexane/CHCl₃ = 1:1) afforded **RBA-6** (886 mg, 2.98 mmol, 47%) as a white solid.

¹H NMR (600 MHz, CD₃OD) δ [ppm] = 7.85–7.81 (m, 4H), 7.64–7.60 (m, 2H), 7.52–7.47 (m, 4H).

¹³C NMR (151 MHz, CD₃OD) δ [ppm] = 141.7, 134.6, 130.1, 128.4.

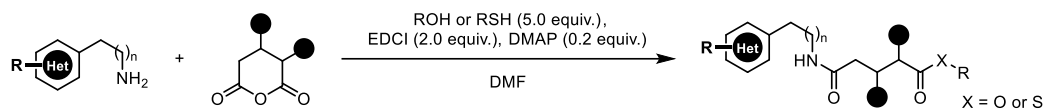
HRMS-ESI: calcd. for C₁₂H₁₁NO₄S₂Na [M + Na]⁺: 320.0021; found: 320.0033.

FT-IR: ν [cm⁻¹] = 3120, 3072, 1449, 1359, 1560, 1084, 878, 756, 724.

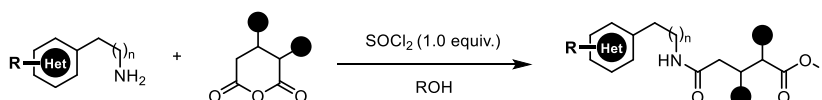
7.2.4. Complementary carbonyl activation annulation and its application to polycyclic natural products total syntheses

7.2.4.1. Substrate preparation

General procedure M

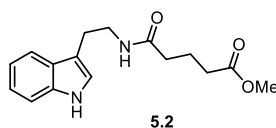


A mixture of the amine (1.0 equiv.) and the anhydride (1.0 equiv.) in DMF, was stirred overnight at room temperature. Then *N*-(3-dimethylaminopropyl)-*N'*-ethylcarbodiimide hydrochloride (EDCI) (2.0 equiv.), 4-dimethylaminopyridine (DMAP) (0.2 equiv.) and corresponding alcohol (5.0 equiv.) were added to the reaction mixture subsequently. The resulting mixture was stirred for 24 h at room temperature, before the reaction mixture was diluted with H₂O and EtOAc. After washing by brine for three times, the organic phase was dried over MgSO₄, and concentrated under reduced pressure. The crude product was purified by silica gel column chromatography. (Note: It is not necessary to perform the reaction under argon.)

General procedure N

A mixture of the amine (1.0 equiv.) and the anhydride (1.0 equiv.) in corresponding alcohol was stirred overnight at room temperature. The mixture was then cooled to 0 °C and SOCl₂ (1.0 equiv.) was added dropwise. Immediately after the addition, the reaction mixture was allowed to warm to room temperature and stirred for 2 h. The reaction was quenched with NaHCO₃ (sat. aq.) and extracted with DCM. The combined organic phases were washed with brine, dried over MgSO₄ and concentrated under reduced pressure. The crude product was purified by silica gel column chromatography. (Note: It is not necessary to perform the reaction under argon.)

7.2.4.1.1. Substrates for the reaction optimization

Methyl 5-((2-(1*H*-indol-3-yl)ethyl)amino)-5-oxopentanoate (5.2)

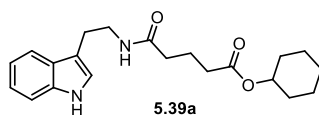
5.2 was prepared according to **General procedure N**, starting from tryptamine (1.50 g, 9.38 mmol, 1.0 equiv.) and glutaric anhydride (1.07 g, 9.38 mmol, 1.0 equiv.) in MeOH (30 mL). The reaction mixture was subsequently treated with SOCl₂ (680 μL, 9.38 mmol, 1.0 equiv.). Purification by silica gel column chromatography (pentane/EtOAc = 3:2) afforded **5.2** (2.39 g, 8.33 mmol, 88%) as a white solid.

¹H NMR (500 MHz, CDCl₃) δ [ppm] = 8.51 (s, 1H), 7.36 (dt, *J* = 8.1, 1.0 Hz, 1H), 7.36 (dt, *J* = 8.1, 1.0 Hz, 1H), 7.19 (ddd, *J* = 8.2, 7.0, 1.2 Hz, 1H), 7.11 (ddd, *J* = 8.0, 7.0, 1.0 Hz, 1H), 6.99 (d, *J* = 2.3 Hz, 1H), 5.72 (s, 1H), 3.64 (s, 3H), 3.58 (td, *J* = 6.8, 5.7 Hz, 2H), 2.95 (td, *J* = 6.8, 0.8 Hz, 2H), 2.33 (t, *J* = 7.3 Hz, 2H), 2.14 (t, *J* = 7.4 Hz, 2H), 1.94–1.89 (m, 2H).

¹³C NMR (126 MHz, CDCl₃) δ [ppm] = 173.8, 172.3, 136.6, 127.4, 122.3, 122.2, 119.4, 118.7, 112.8, 111.4, 51.7, 39.8, 35.6, 33.2, 25.4, 20.9.

HRMS-ESI: calcd. for C₁₆H₂₀N₂O₃Na [M + Na]⁺: 311.1366; found: 311.1371.

FT-IR: ν [cm⁻¹] = 3394, 3297, 2949, 1731, 1647, 1533, 1457, 1436, 1226, 1152, 743.

Cyclohexyl 5-((2-(1*H*-indol-3-yl)ethyl)amino)-5-oxopentanoate (5.39a)

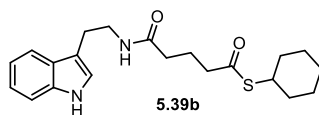
5.39a was prepared according to **General procedure M**, starting from tryptamine (509 mg, 3.18 mmol, 1.0 equiv.) and glutaric anhydride (363 mg, 3.18 mmol, 1.0 equiv.) in DMF (18.0 mL). The reaction mixture was subsequently treated with EDCI (1.21 g, 6.36 mmol, 2.0 equiv.), DMAP (77.7 mg, 0.636 mmol, 0.2 equiv.) and cyclohexanol (1.65 mL, 15.9 mmol, 5.0 equiv.). Purification by silica gel column chromatography (pentane/EtOAc = 3:2) afforded **5.39a** (362 mg, 1.02 mmol, 32%) as a white solid.

¹H NMR (700 MHz, CDCl₃) δ [ppm] = 8.28 (s, 1H), 7.59 (dt, *J* = 7.8, 1.0 Hz, 1H), 7.37 (dt, *J* = 8.1, 0.9 Hz, 1H), 7.20 (ddd, *J* = 8.2, 7.0, 1.2 Hz, 1H), 7.12 (ddd, *J* = 8.0, 7.0, 1.0 Hz, 1H), 7.03–7.00 (m, 1H), 5.65 (s, 1H), 3.60 (td, *J* = 6.8, 5.8 Hz, 2H), 3.49 (td, *J* = 10.3, 4.0 Hz, 1H), 2.97 (td, *J* = 6.8, 0.9 Hz, 2H), 2.52 (t, *J* = 7.2 Hz, 2H), 2.14 (t, *J* = 7.4 Hz, 2H), 1.96–1.92 (m, 2H), 1.91–1.85 (m, 2H), 1.72–1.65 (m, 2H), 1.62–1.55 (m, 1H), 1.45–1.35 (m, 4H), 1.29–1.23 (m, 1H).

¹³C NMR (126 MHz, CDCl₃) δ [ppm] = 172.8, 172.4, 136.6, 127.4, 122.24, 122.17, 119.5, 118.7, 112.8, 111.4, 72.8, 39.9, 35.7, 33.9, 31.7, 25.4, 23.8, 21.2. (One sp³ carbon is missing, probably due to the resonance overlap.)

HRMS-ESI: calcd. for C₂₁H₂₈N₂O₃Na [M + Na]⁺: 379.1992; found: 379.2006.

FT-IR: ν [cm⁻¹] = 3357, 3325, 2948, 2920, 2853, 1707, 1635, 1539, 1386, 1189, 1011, 748, 727.

Cyclohexyl 5-((2-(1*H*-indol-3-yl)ethyl)amino)-5-oxopentanethioate (5.39b)

5.39b was prepared according to **General procedure M**, starting from tryptamine (506 mg, 3.16 mmol, 1.0 equiv.) and glutaric anhydride (360 mg, 3.16 mmol, 1.0 equiv.) in DMF (18.0 mL). The reaction mixture was subsequently treated with EDCI (1.21 g, 6.36 mmol, 2.0 equiv.), DMAP (77.2 mg, 0.632 mmol, 0.2 equiv.) and cyclohexanethiol (1.93 mL, 15.8 mmol, 5.0 equiv.). Purification by silica gel column chromatography (pentane/EtOAc = 3:2) afforded **5.39b** (401 mg, 1.08 mmol, 34%) as a white solid.

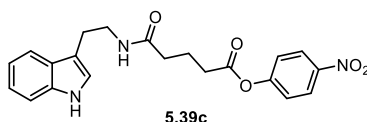
¹H NMR (500 MHz, CDCl₃) δ [ppm] = 8.23 (s, 1H), 7.62 (dd, *J* = 7.9, 1.0 Hz, 1H), 7.39 (dt, *J* = 8.1, 1.0 Hz, 1H), 7.23 (ddd, *J* = 8.2, 7.0, 1.2 Hz, 1H), 7.15 (ddd, *J* = 8.0, 7.0, 1.1 Hz, 1H), 7.05 (d, *J* = 2.3 Hz, 1H), 5.62 (s, 1H), 3.62 (td, *J* = 6.8, 5.7 Hz, 2H), 3.51 (ddt, *J* = 10.3, 6.2, 3.6 Hz, 1H), 2.99 (td, *J* = 6.8, 0.8 Hz, 2H), 2.55 (t, *J* = 7.2 Hz, 2H), 2.16 (t, *J* = 7.4 Hz, 2H), 1.99–1.94 (m, 2H), 1.93–1.87 (m, 2H), 1.75–1.68 (m, 2H), 1.65–1.56 (m, 1H), 1.49–1.36 (m, 4H), 1.34–1.23 (m, 1H).

¹³C NMR (176 MHz, CDCl₃) δ [ppm] = 199.2, 172.1, 136.6, 127.4, 122.3, 122.2, 119.6, 118.8, 113.0, 111.4, 43.1, 42.4, 39.8, 35.4, 33.1, 26.0, 25.6, 25.5, 21.7.

HRMS-ESI: calcd. for C₂₁H₂₈N₂O₂SNa [M + Na]⁺: 395.1763; found: 395.1782.

FT-IR: ν [cm⁻¹] = 3399, 3285, 2929, 2852, 1652, 1530, 1448, 1341, 998, 741.

4-Nitrophenyl 5-((2-(1*H*-indol-3-yl)ethyl)amino)-5-oxopentanoat (**5.39c**)



5.39c was prepared according to **General procedure M**, starting from tryptamine (300 mg, 1.87 mmol, 1.0 equiv.) and glutaric anhydride (214 mg, 1.87 mmol, 1.0 equiv.) in DMF (10.0 mL). The reaction mixture was subsequently treated with EDCI (718 mg, 3.74 mmol, 2.0 equiv.), DMAP (45.8 mg, 0.374 mmol, 0.2 equiv.) and *p*-nitrophenol (1.30 g, 9.36 mmol, 5.0 equiv.). Purification by silica gel column chromatography (DCM/MeOH = 10:1) afforded **5.39c** (318 mg, 0.806 mmol, 43%) as a yellow solid.

¹H NMR (500 MHz, CD₃OD: CDCl₃ (v/v = 1:1)) δ [ppm] = 8.27–8.21 (m, 2H), 7.57–7.53 (m, 1H), 7.35–7.31 (m, 1H), 7.29–7.25 (m, 2H), 7.09 (ddd, *J* = 8.2, 6.9, 1.2 Hz, 1H), 7.05–6.98 (m, 2H), 3.51 (t, *J* = 7.2 Hz, 2H), 2.95 (t, *J* = 7.3 Hz, 2H), 2.60 (t, *J* = 7.4 Hz, 2H), 2.26 (t, *J* = 7.3 Hz, 2H), 2.03–1.97 (m, 2H).

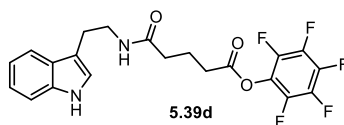
¹³C NMR (176 MHz, CD₃OD: CDCl₃ (v/v = 1:1)) δ [ppm] = 173.0, 170.7, 155.2, 144.9, 136.3, 127.0, 124.7, 124.6, 122.1, 121.9, 121.0, 118.2, 117.8, 117.8, 111.6, 110.9, 39.7, 34.4, 32.7, 24.7, 20.2.

(Due the poor solubility of this compound, the mixture of CD₃OD: CDCl₃ (v/v = 1:1) was used for ¹H NMR and ¹³C NMR spectroscopies.)

HRMS-ESI: calcd. for $C_{21}H_{21}N_3O_5K$ $[M + K]^+$: 434.1113; found: 434.1125.

FT-IR: ν [cm^{-1}] = 2925, 1591, 1522, 1336, 1290, 1208, 1109.

Perfluorophenyl 5-((2-(1*H*-indol-3-yl)ethyl)amino)-5-oxopentanoate (5.39d)



5.39d was prepared according to **General procedure M**, starting from tryptamine (300 mg, 1.87 mmol, 1.0 equiv.) and glutaric anhydride (214 mg, 1.87 mmol, 1.0 equiv.) in DMF (10.0 mL). The reaction mixture was subsequently treated with EDCI (715 mg, 3.74 mmol, 2.0 equiv.), DMAP (45.8 mg, 0.374 mmol, 0.2 equiv.) and pentafluorophenol (1.71 g, 9.36 mmol, 5.0 equiv.). Purification by silica gel column chromatography (DCM/MeOH = 10:1) afforded **5.39d** (382 mg, 0.867 mmol, 46%) as a yellow solid.

1H NMR (500 MHz, CD_3OD) δ [ppm] = 7.54 (dd, J = 7.9, 1.0 Hz, 1H), 7.30 (d, J = 8.1 Hz, 1H), 7.10–7.01 (m, 2H), 7.01–6.93 (m, 1H), 3.49 (t, J = 7.3 Hz, 2H), 2.94 (t, J = 7.3 Hz, 2H), 2.66 (t, J = 7.4 Hz, 2H), 2.26 (t, J = 7.4 Hz, 2H), 2.00–1.94 (m, 2H).

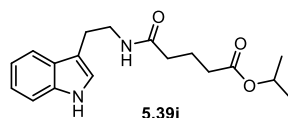
^{13}C NMR (126 MHz, CD_3OD) δ [ppm] = 174.7, 170.4, 143.4, 141.5, 140.2, 139.6, 138.1, 128.8, 126.4, 123.6, 123.4, 122.3, 119.6, 119.5, 119.3, 113.2, 112.2, 41.3, 35.6, 33.0, 26.2, 21.9. (Due to the complexity of the F–C coupling, the coupling constants were not calculated.)

^{19}F NMR (471 MHz, CD_3OD) δ [ppm] = –155.3 (d, J = 17.7 Hz), –161.3 (t, J = 20.7 Hz), –165.5 (m).

HRMS-ESI: calcd. for $C_{21}H_{17}F_5N_2O_3Na$ $[M + Na]^+$: 463.1051; found: 463.1067.

FT-IR: ν [cm^{-1}] = 3289, 2933, 1787, 1652, 1457, 1107, 1101, 743.

Isopropyl 5-((2-(1*H*-indol-3-yl)ethyl)amino)-5-oxopentanoate (5.39i)



5.39i was prepared according to **General procedure M**, starting from tryptamine (500 mg, 3.12 mmol, 1.0 equiv.) and glutaric anhydride (356 mg, 3.12 mmol, 1.0 equiv.) in *i*PrOH (10.0 mL). The reaction mixture was subsequently treated with $SOCl_2$ (221 μ L, 3.12 mmol,

1.0 equiv.). Purification by silica gel column chromatography (pentane/EtOAc = 3:2) afforded **5.39i** (524 mg, 1.66 mmol, 53%) as a white solid.

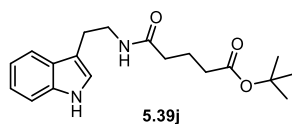
¹H NMR (500 MHz, CDCl₃) δ [ppm] = 8.44 (s, 1H), 7.59 (d, *J* = 7.9 Hz, 1H), 7.36 (d, *J* = 8.1 Hz, 1H), 7.19 (t, *J* = 7.6 Hz, 1H), 7.11 (t, *J* = 7.5 Hz, 1H), 7.00 (s, 1H), 5.69 (s, 1H), 5.06–4.90 (m, 1H), 3.59 (q, *J* = 6.4 Hz, 2H), 2.96 (t, *J* = 6.8 Hz, 2H), 2.28 (t, *J* = 7.2 Hz, 2H), 2.14 (t, *J* = 7.4 Hz, 2H), 1.91 (t, *J* = 7.3 Hz, 2H), 1.22 (d, *J* = 1.9 Hz, 3H), 1.20 (d, *J* = 1.8 Hz, 3H).

¹³C NMR (126 MHz, CDCl₃) δ [ppm] = 172.9, 172.4, 136.6, 127.4, 122.3, 122.2, 119.5, 118.8, 112.9, 111.4, 67.8, 39.8, 35.7, 33.8, 25.4, 21.9, 21.1.

HRMS-ESI: calcd. for C₁₈H₂₄N₂O₃Na [M + Na]⁺: 339.1679; found: 339.1692.

FT-IR: ν [cm⁻¹] = 3287, 2978, 1724, 1646, 1531, 1456, 1373, 1226, 1105, 740.

***Tert*-butyl 5-((2-(1*H*-indol-3-yl)ethyl)amino)-5-oxopentanoate (**5.39j**)**



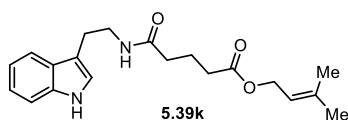
5.39j was prepared according to **General procedure L**, starting from tryptamine (150 mg, 0.938 mmol, 1.0 equiv.) and glutaric anhydride (107 mg, 0.938 mmol, 1.0 equiv.) in DMF (5.0 mL). The reaction mixture was subsequently treated with EDCI (358 mg, 1.88 mmol, 2.0 equiv.), DMAP (22.9 mg, 0.188 mmol, 0.2 equiv.) and *t*BuOH (445 μL, 4.69 mmol, 5.0 equiv.). Purification by silica gel column chromatography (pentane/EtOAc = 3:2) afforded **5.39j** (21.0 mg, 636 μmol, 7%) as a white solid.

¹H NMR (600 MHz, CDCl₃) δ [ppm] = 8.28 (s, 1H), 7.63–7.58 (m, 1H), 7.37 (dd, *J* = 8.1, 1.0 Hz, 1H), 7.20 (ddd, *J* = 8.1, 7.1, 1.2 Hz, 1H), 7.12 (ddd, *J* = 8.0, 7.0, 1.0 Hz, 1H), 7.04–7.00 (m, 1H), 5.65 (s, 1H), 3.64–3.56 (m, 2H), 2.97 (t, *J* = 6.8 Hz, 2H), 2.23 (t, *J* = 7.2 Hz, 2H), 2.14 (t, *J* = 7.4 Hz, 2H), 1.90–1.86 (m, 2H), 1.43 (s, 9H).

¹³C NMR (151 MHz, CDCl₃) δ [ppm] = 172.8, 172.4, 136.6, 127.4, 122.3, 122.2, 119.6, 118.8, 113.0, 111.4, 80.5, 39.8, 35.8, 34.8, 28.2, 25.5, 21.2.

HRMS-ESI: calcd. for C₁₉H₂₆N₂O₃Na [M + Na]⁺: 353.1835; found: 353.1852.

FT-IR: ν [cm⁻¹] = 3398, 3296, 2965, 2930, 1702, 1649, 1531, 1457, 1367, 1236, 1164, 1143, 741.

3-Methylbut-2-en-1-yl 5-((2-(1*H*-indol-3-yl)ethyl)amino)-5-oxopentanoate (5.39k).

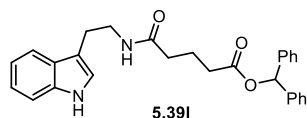
5.39k was prepared according to **General procedure M**, starting from tryptamine (509 mg, 3.18 mmol, 1.0 equiv.) and glutaric anhydride (363 mg, 3.18 mmol, 1.0 equiv.) in DMF (15.0 mL). The reaction mixture was subsequently treated with EDCI (1.21 g, 6.36 mmol, 2.0 equiv.), DMAP (77.7 mg, 0.636 mmol, 0.2 equiv.) and 3-methyl-2-buten-1-ol (1.61 mL, 15.9 mmol, 5.0 equiv.). Purification by silica gel column chromatography (pentane/EtOAc = 5:2) afforded **5.39k** (468 mg, 1.37 mmol, 43%) as a light yellow solid.

¹H NMR (500 MHz, CDCl₃) δ [ppm] = 8.20 (s, 1H), 7.63–7.57 (m, 1H), 7.37 (dt, *J* = 8.2, 0.9 Hz, 1H), 7.21 (ddd, *J* = 8.2, 7.0, 1.2 Hz, 1H), 7.13 (ddd, *J* = 8.0, 7.0, 1.0 Hz, 1H), 7.03 (d, *J* = 2.4 Hz, 1H), 5.59 (s, 1H), 5.34–5.30 (m, 1H), 4.55 (d, *J* = 7.3 Hz, 2H), 3.60 (td, *J* = 6.7, 5.7 Hz, 2H), 2.97 (td, *J* = 6.8, 0.9 Hz, 2H), 2.33 (t, *J* = 7.2 Hz, 2H), 2.16 (t, *J* = 7.4 Hz, 2H), 1.95–1.89 (m, 2H), 1.75 (d, *J* = 1.4 Hz, 3H), 1.70 (d, *J* = 1.4 Hz, 3H).

¹³C NMR (126 MHz, CDCl₃) δ [ppm] = 173.4, 172.3, 139.2, 136.6, 127.4, 122.24, 122.22, 119.5, 118.8, 118.6, 112.9, 111.4, 61.5, 39.8, 35.7, 33.5, 25.8, 25.4, 21.0, 18.1.

HRMS-ESI: calcd. for C₂₀H₂₆N₂O₃Na [M + Na]⁺: 365.1835; found: 365.1846.

FT-IR: ν [cm⁻¹] = 3398, 3293, 2969, 2932, 1728, 1650, 1537, 1457, 1378, 1339, 1229, 1151, 956, 742.

Benzhydryl 5-((2-(1*H*-indol-3-yl)ethyl)amino)-5-oxopentanoate (5.39l)

5.39l was prepared according to **General procedure M**, starting from tryptamine (513 mg, 3.20 mmol, 1.0 equiv.) and glutaric anhydride (366 mg, 3.20 mmol, 1.0 equiv.) in DMF (18.0 mL). The reaction mixture was subsequently treated with EDCI (1.22 g, 6.41 mmol, 2.0 equiv.), DMAP (78.3 mg, 0.641 mmol, 0.2 equiv.) and diphenylmethanol (2.95 g, 16.0 mmol, 5.0 equiv.). Purification by silica gel column chromatography (pentane/EtOAc = 5:2) afforded **5.39l** (772 mg, 1.75 mmol, 55%) as a white solid.

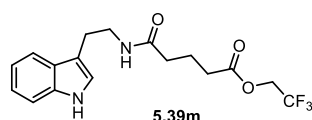
¹H NMR (500 MHz, CD₂Cl₂) δ [ppm] = 8.30 (s, 1H), 7.55 (dd, *J* = 7.9, 2.7 Hz, 1H), 7.36–7.28 (m, 9H), 7.27–7.23 (m, 2H), 7.18–7.11 (m, 1H), 7.06 (dd, *J* = 8.6, 6.0 Hz, 1H), 6.97 (d, *J* = 2.7 Hz, 1H), 6.80 (d, *J* = 3.0 Hz, 1H), 5.55 (s, 1H), 3.52–3.48 (m, 2H), 2.89 (td, *J* = 7.0, 2.8 Hz, 2H), 2.47–2.37 (m, 2H), 2.06 (td, *J* = 7.5, 2.8 Hz, 2H), 1.95–1.84 (m, 2H).

¹³C NMR (126 MHz, CD₂Cl₂) δ [ppm] = 172.2, 171.8, 140.6, 136.5, 128.6, 127.9, 127.4, 126.9, 122.2, 122.0, 119.3, 118.6, 112.9, 111.3, 76.9, 39.7, 35.4, 33.6, 25.4, 21.0.

HRMS-ESI: calcd. for C₂₈H₂₈N₂O₃Na [M + Na]⁺: 463.1992; found: 463.2008.

FT-IR: ν [cm⁻¹] = 3407, 3297, 2930, 1733, 1651, 1529, 1455, 1231, 1148, 743.

2,2,2-Trifluoroethyl 5-((2-(1*H*-indol-3-yl)ethyl)amino)-5-oxopentanoate (**5.39m**)



5.39m was prepared according to **General procedure M**, starting from tryptamine (285 mg, 1.78 mmol, 1.0 equiv.) and glutaric anhydride (203 mg, 1.78 mmol, 1.0 equiv.) in DMF (10.0 mL). The reaction mixture was subsequently treated with EDCI (680 mg, 3.56 mmol, 2.0 equiv.), DMAP (43.5 mg, 0.356 mmol, 0.2 equiv.) and 2,2,2-trifluoroethanol (675 μL, 8.91 mmol, 5.0 equiv.). Purification by silica gel column chromatography (pentane/EtOAc = 3:2) afforded **5.39m** (275 mg, 0.772 mmol, 43%) as a white solid.

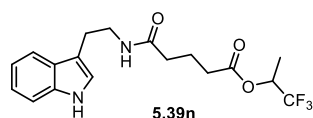
¹H NMR (500 MHz, CDCl₃) δ [ppm] = 8.13 (s, 1H), 7.60 (dd, *J* = 7.9, 1.1 Hz, 1H), 7.38 (dt, *J* = 8.1, 1.0 Hz, 1H), 7.21 (ddd, *J* = 8.2, 7.0, 1.2 Hz, 1H), 7.13 (ddd, *J* = 7.9, 7.0, 1.1 Hz, 1H), 7.04 (d, *J* = 2.3 Hz, 1H), 5.54 (s, 1H), 4.44 (q, *J* = 8.5 Hz, 2H), 3.61 (q, *J* = 6.5 Hz, 2H), 2.98 (td, *J* = 6.7, 0.8 Hz, 2H), 2.44 (t, *J* = 7.2 Hz, 2H), 2.16 (t, *J* = 7.3 Hz, 2H), 1.99–1.93 (m, 2H).

¹³C NMR (126 MHz, CDCl₃) δ [ppm] = 171.8, 171.7, 136.6, 127.5, 123.1 (q, *J* = 277.0 Hz), 122.4, 122.2, 119.7, 118.8, 113.1, 111.4, 60.7–59.9 (m), 39.8, 35.3, 32.8, 25.4, 20.6.

¹⁹F NMR (471 MHz, CDCl₃) δ [ppm] = -73.65 (t, *J* = 8.6 Hz).

HRMS-ESI: calcd. for C₁₇H₁₉F₃N₂O₃Na [M + Na]⁺: 379.1240; found: 379.1244.

FT-IR: ν [cm⁻¹] = 3388, 3322, 2927, 1736, 1630, 1545, 1411, 1275, 1261, 1179, 740.

1,1,1-Trifluoropropan-2-yl 5-((2-(1*H*-indol-3-yl)ethyl)amino)-5-oxopentanoate(5.39n).

5.39n was prepared according to **General procedure M**, starting from tryptamine (150 mg, 0.938 mmol, 1.0 equiv.) and glutaric anhydride (107 mg, 0.938 mmol, 1.0 equiv.) in DMF (5.0 mL). The reaction mixture was subsequently treated with EDCI (358 mg, 1.88 mmol, 2.0 equiv.), DMAP (22.9 mg, 0.188 mmol, 0.2 equiv.) and 1,1,1-trifluoro-2-propanol (424 μ L, 4.69 mmol, 5.0 equiv.). Purification by silica gel column chromatography (pentane/EtOAc = 3:2) afforded **5.39n** (70.0 mg, 0.189 mmol, 20%) as a white solid.

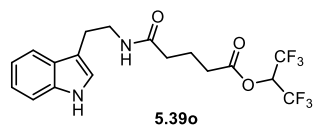
¹H NMR (500 MHz, CD₃OD) δ [ppm] = 7.55 (dt, J = 7.9, 1.0 Hz, 1H), 7.32 (dt, J = 8.2, 0.9 Hz, 1H), 7.08 (ddd, J = 8.2, 6.9, 1.2 Hz, 1H), 7.04 (s, 1H), 7.00 (ddd, J = 7.9, 7.0, 1.0 Hz, 1H), 5.41–5.33 (m, 1H), 3.47 (t, J = 7.3 Hz, 2H), 2.98–2.88 (m, 2H), 2.35 (t, J = 7.5 Hz, 2H), 2.18 (t, J = 7.4 Hz, 2H), 1.90–1.84 (m, 2H), 1.36 (d, J = 6.6 Hz, 3H).

¹³C NMR (126 MHz, CD₃OD) δ [ppm] = 174.9, 172.6, 138.1, 128.8, 125.6 (q, J = 279.1 Hz), 123.4, 119.6, 119.3, 113.2, 112.2, 68.2–67.4 (m), 41.4, 35.8, 33.7, 26.2, 21.9, 13.7, 13.7.

¹⁹F NMR (471 MHz, CD₃OD) δ [ppm] = –80.2. (Due to resolution, coupling was not observed.)

HRMS-ESI: calcd. for C₁₈H₂₁F₃N₂O₃Na [M + Na]⁺: 393.1396; found: 393.1410.

FT-IR: ν [cm⁻¹] = 3396, 3324, 2932, 1749, 1730, 1631, 1542, 1458, 1386, 1278, 1187, 1165, 1118, 1092, 1017, 741.

1,1,1,3,3,3-Hexafluoropropan-2-yl 5-((2-(1*H*-indol-3-yl)ethyl)amino)-5-oxopentanoate (5.39o)

5.39o was prepared according to **General procedure L**, starting from tryptamine (3.60 g, 22.5 mmol, 1.0 equiv.) and glutaric anhydride (2.56 g, 22.5 mmol, 1.0 equiv.) in DMF (80 mL). The reaction mixture was subsequently treated with EDCI (8.59 g, 45.0 mmol, 2.0 equiv.), DMAP (550 mg, 4.50 mmol, 0.2 equiv.) and hexafluoroisopropano (HFIP) (11.9 mL, 112 mmol, 5.0 equiv.). Purification by silica gel column chromatography (pentane/EtOAc = 3:2) afforded

5.39o (4.80 g, 11.3 mmol, 50%) as a white solid.

¹H NMR (600 MHz, CDCl₃) δ [ppm] = 8.21 (s, 1H), 7.60 (d, *J* = 7.9 Hz, 1H), 7.37 (dd, *J* = 8.1, 1.0 Hz, 1H), 7.24–7.18 (m, 1H), 7.13 (ddd, *J* = 8.0, 7.0, 1.1 Hz, 1H), 7.01 (d, *J* = 2.3 Hz, 1H), 5.79–5.73 (m, 1H), 5.56 (t, *J* = 5.8 Hz, 1H), 3.62–3.59 (m, 2H), 2.98 (t, *J* = 6.8 Hz, 2H), 2.54 (t, *J* = 7.3 Hz, 2H), 2.15 (t, *J* = 7.2 Hz, 2H), 2.01–1.97 (m, 2H).

¹³C NMR (151 MHz, CDCl₃) δ [ppm] = 171.5, 170.1, 136.6, 127.5, 122.4, 122.2, 120.5 (q, *J* = 282.2 Hz), 119.7, 118.8, 113.0, 111.4, 67.0–66.1 (m), 39.9, 34.9, 32.4, 25.4, 20.4.

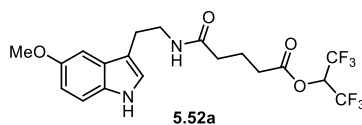
¹⁹F NMR (565 MHz, CDCl₃) δ [ppm] = –73.19 (d, *J* = 5.9 Hz).

HRMS-ESI: calcd. for C₁₈H₁₈F₆N₂O₃Na [M + Na]⁺: 447.1114; found: 447.1113.

FT-IR: ν [cm⁻¹] = 3418, 3328, 1777, 1753, 1633, 1540, 1384, 1359, 1286, 1201, 1108, 740.

7.2.4.1.2. Substrates for the reaction scope

1,1,1,3,3,3-Hexafluoropropan-2-yl-5-((2-(5-methoxy-1*H*-indol-3-yl)ethyl)amino)-5-oxopentanoate (5.52a)



5.52a was prepared according to **General procedure M**, starting from 5-methoxytryptamine (200 mg, 1.05 mmol, 1.0 equiv.) and glutaric anhydride (120 mg, 1.05 mmol, 1.0 equiv.) in DMF (5.0 mL). The reaction mixture was subsequently treated with EDCI (402 mg, 2.10 mmol, 2.0 equiv.), DMAP (25.7 mg, 0.211 mmol, 0.2 equiv.) and HFIP (556 μL, 5.26 mmol, 5.0 equiv.). Purification by silica gel column chromatography (pentane/EtOAc = 3:2) afforded **5.52a** (270 mg, 0.595 mmol, 56%) as a white solid.

¹H NMR (500 MHz, CDCl₃) δ [ppm] = 8.15 (s, 1H), 7.28–7.24 (m, 1H), 7.03 (d, *J* = 2.4 Hz, 1H), 7.00 (t, *J* = 2.4 Hz, 1H), 6.88 (dd, *J* = 8.8, 2.4 Hz, 1H), 5.82–5.71 (m, 1H), 5.60 (s, 1H), 3.86 (s, 3H), 3.65–3.57 (m, 2H), 2.97–2.91 (m, 2H), 2.56 (td, *J* = 7.3, 1.0 Hz, 2H), 2.17 (t, *J* = 7.2 Hz, 2H), 2.03–1.97 (m, 2H).

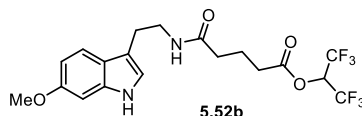
¹³C NMR (126 MHz, CDCl₃) δ [ppm] = 171.6, 170.1, 154.2, 131.7, 127.8, 123.0, 120.5 (q, *J* = 285.6 Hz), 112.7, 112.5, 112.2, 100.7, 66.8–66.2 (m), 56.1, 39.7, 34.9, 32.4, 25.4, 20.4.

¹⁹F NMR (565 MHz, CDCl₃) δ [ppm] = –73.18 (d, *J* = 5.8 Hz).

HRMS-ESI: calcd. for $C_{19}H_{21}F_6N_2O_4$ $[M + H]^+$: 455.1400; found: 455.1408.

FT-IR: ν [cm^{-1}] = 3432, 3325, 2928, 1779, 1759, 1635, 1541, 1487, 1218, 1195, 1108, 927, 794.

1,1,1,3,3,3-Hexafluoropropan-2-yl 5-((2-(6-methoxy-1*H*-indol-3-yl)ethyl)amino)-5-oxopentanoate (5.52b)



5.52b was prepared according to **General procedure M**, starting from 6-methoxytryptamine (100 mg, 0.526 mmol, 1.0 equiv.) and glutaric anhydride (60.0 mg, 0.526 mmol, 1.0 equiv.) in DMF (3.0 mL). The reaction mixture was subsequently treated with EDCI (201 mg, 1.05 mmol, 2.0 equiv.), DMAP (12.9 mg, 0.105 mmol, 0.2 equiv.) and HFIP (278 μ L, 2.63 mmol, 5.0 equiv.). Purification by silica gel column chromatography (pentane/EtOAc = 3:2) afforded **5.52b** (100 mg, 0.220 mmol, 42%) as a white solid.

1H NMR (500 MHz, CD_2Cl_2) δ [ppm] = 8.14 (s, 1H), 7.44 (d, J = 8.6 Hz, 1H), 6.93 (dd, J = 2.2, 1.1 Hz, 1H), 6.87 (d, J = 2.3 Hz, 1H), 6.75 (dd, J = 8.7, 2.3 Hz, 1H), 5.86–5.79 (m, 1H), 5.59 (s, 1H), 3.82 (s, 3H), 3.54 (td, J = 6.9, 5.8 Hz, 2H), 2.90 (td, J = 6.9, 0.9 Hz, 2H), 2.56 (t, J = 7.4 Hz, 2H), 2.15 (t, J = 7.3 Hz, 2H), 2.00–1.90 (m, 2H).

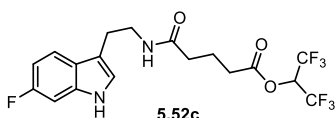
^{13}C NMR (126 MHz, CD_2Cl_2) δ [ppm] = 171.5, 170.5, 157.1, 137.6, 122.2, 121.2, 120.9 (q, J = 282.4 Hz), 119.6, 113.3, 109.8, 94.9, 67.3–66.2 (m), 55.9, 40.1, 35.1, 32.7, 25.8, 20.7.

^{19}F NMR (471 MHz, CD_2Cl_2) δ [ppm] = –73.66. (Due to resolution, coupling was not observed.)

HRMS-ESI: calcd. for $C_{19}H_{20}F_6N_2O_4Na$ $[M + Na]^+$: 477.1219 found: 477.1222.

FT-IR: ν [cm^{-1}] = 3302, 2965, 2937, 1764, 1635, 1384, 1281, 1257, 1107, 824.

1,1,1,3,3,3-Hexafluoropropan-2-yl 5-((2-(6-fluoro-1*H*-indol-3-yl)ethyl)amino)-5-oxopentanoate (5.52c)



5.52c was prepared according to **General procedure M**, starting from 6-fluorotryptamine (260 mg, 1.46 mmol, 1.0 equiv.) and glutaric anhydride (166 mg, 1.46 mmol, 1.0 equiv.) in

DMF (6.0 mL). The reaction mixture was subsequently treated with EDCI (558 mg, 2.92 mmol, 2.0 equiv.), DMAP (35.7 mg, 0.292 mmol, 0.2 equiv.) and HFIP (772 μ L, 7.30 mmol, 5.0 equiv.). Purification by silica gel column chromatography (pentane/EtOAc = 3:2) afforded **5.52c** (350 mg, 0.792 mmol, 54%) as a white solid.

¹H NMR (400 MHz, CDCl₃) δ [ppm] = 8.07 (s, 1H), 7.50 (dd, J = 8.7, 5.3 Hz, 1H), 7.05 (dd, J = 9.7, 2.3 Hz, 1H), 7.01 (s, 1H), 6.90 (td, J = 9.1, 2.3 Hz, 1H), 5.78–5.72 (m, 1H), 5.51 (s, 1H), 3.59 (q, J = 6.5 Hz, 2H), 2.95 (t, J = 6.8 Hz, 2H), 2.56 (t, J = 7.2 Hz, 2H), 2.18 (t, J = 7.2 Hz, 2H), 2.04–1.97 (m, 2H).

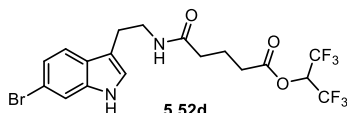
¹³C NMR (176 MHz, CDCl₃) δ [ppm] = 171.5, 170.1, 160.3 (d, J = 238.1 Hz), 136.5 (d, J = 12.6 Hz), 124.1, 122.3 (d, J = 2.9 Hz), 120.5 (d, J = 278.8 Hz), 119.6 (d, J = 10.1 Hz), 113.3, 108.6 (d, J = 24.5 Hz), 97.7 (d, J = 25.6 Hz), 66.9–66.1 (m), 39.8, 34.9, 32.4, 25.5, 20.4.

¹⁹F NMR (376 MHz, CDCl₃) δ [ppm] = –73.17 (d, J = 10.2 Hz), (–120.71)–(–120.78) (m).

HRMS-ESI: calcd. for C₁₈H₁₈F₇N₂O₃ [M + H]⁺: 443.1200; found: 443.1217.

FT-IR: ν [cm⁻¹] = 3411, 3397, 3277, 1778, 1653, 1543, 1522, 1290, 1239, 1199, 1110.

1,1,1,3,3,3-Hexafluoropropan-2-yl 5-((2-(6-bromo-1H-indol-3-yl)ethyl)amino)-5-oxopentanoate (5.52d)



5.52d was prepared according to **General procedure M**, starting from 6-bromotryptamine (100 mg, 0.420 mmol, 1.0 equiv.) and glutaric anhydride (47.9 mg, 0.420 mmol, 1.0 equiv.) in DMF (3.0 mL). The reaction mixture was subsequently treated with EDCI (160 mg, 0.840 mmol, 2.0 equiv.), DMAP (10.3 mg, 84.0 μ mol, 0.2 equiv.) and HFIP (222 μ L, 2.10 mmol, 5.0 equiv.). Purification by silica gel column chromatography (pentane/EtOAc = 3:2) afforded **5.52d** (120 mg, 0.239 mmol, 57%) as a white solid.

¹H NMR (700 MHz, CDCl₃) δ [ppm] = 8.23 (s, 1H), 7.52 (dd, J = 1.7, 0.6 Hz, 1H), 7.44 (dd, J = 8.4, 0.7 Hz, 1H), 7.22 (dd, J = 8.4, 1.7 Hz, 1H), 7.00 (dd, J = 2.3, 0.9 Hz, 1H), 5.77–5.74 (m, 1H), 5.53 (d, J = 6.2 Hz, 1H), 3.58 (td, J = 6.9, 5.8 Hz, 2H), 2.94 (td, J = 6.9, 0.9 Hz, 2H), 2.56 (t, J = 7.3 Hz, 2H), 2.18 (t, J = 7.3 Hz, 2H), 2.02–1.98 (m, 2H).

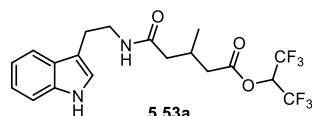
^{13}C NMR (176 MHz, CDCl_3) δ [ppm] = 171.6, 170.0, 137.3, 126.4, 123.0, 122.7, 121.3, 120.5 (q, $J = 281.7$ Hz), 120.0, 116.0, 114.4, 113.3, 66.9–66.1 (m), 39.9, 34.9, 32.4, 25.4, 20.4.

^{19}F NMR (471 MHz, CDCl_3) δ [ppm] = -73.17 (d, $J = 6.4$ Hz).

HRMS-ESI: calcd. for $\text{C}_{18}\text{H}_{17}\text{BrF}_6\text{N}_2\text{O}_3\text{Na}$ [$\text{M} + \text{Na}$] $^+$: 525.0219; found: 525.0244.

FT-IR: ν [cm^{-1}] 3396, 3326, 2930, 1779, 1749, 1638, 1385, 1287, 1231, 1201, 1110, 803, 746.

1,1,1,3,3,3-Hexafluoropropan-2-yl 5-((2-(1H-indol-3-yl)ethyl)amino)-3-methyl-5-oxopentanoate (5.53a)



5.53a was prepared according to **General procedure M**, starting from tryptamine (2.00 g, 12.5 mmol, 1.0 equiv.) and 3-methylglutaric anhydride (1.60 g, 12.5 mmol, 1.0 equiv.) in DMF (50 mL). The reaction mixture was subsequently treated with EDCI (4.78 g, 25.0 mmol, 2.0 equiv.), DMAP (305 mg, 2.50 mmol, 0.2 equiv.) and HFIP (6.60 mL, 62.5 mmol, 5.0 equiv.). Purification by silica gel column chromatography (pentane/EtOAc = 3:2) afforded **5.53a** (3.21 g, 7.33 mmol, 58%) as a white solid.

^1H NMR (500 MHz, CD_2Cl_2) δ [ppm] = 8.33 (s, 1H), 7.61–7.59 (m, 1H), 7.38 (dt, $J = 8.2, 1.0$ Hz, 1H), 7.18 (ddd, $J = 8.2, 7.0, 1.2$ Hz, 1H), 7.10 (ddd, $J = 7.9, 7.0, 1.0$ Hz, 1H), 7.06–7.02 (m, 1H), 5.87–5.82 (m, 1H), 5.64 (s, 1H), 3.57 (td, $J = 6.8, 5.7$ Hz, 2H), 2.96 (td, $J = 6.9, 0.9$ Hz, 2H), 2.64 (dd, $J = 15.3, 5.3$ Hz, 1H), 2.51–2.43 (m, 1H), 2.38 (dd, $J = 15.4, 8.0$ Hz, 1H), 2.13 (dd, $J = 14.4, 6.8$ Hz, 1H), 2.04 (dd, $J = 14.4, 7.1$ Hz, 1H), 0.99 (d, $J = 6.7$ Hz, 3H).

^{13}C NMR (126 MHz, CD_2Cl_2) δ [ppm] = 171.1, 169.8, 136.9, 127.8, 122.6, 122.4, 120.5 (q, $J = 282.1$ Hz), 119.7, 119.0, 113.3, 111.6, 67.2–66.1 (m), 43.0, 40.1, 39.9, 28.2, 25.8, 19.5.

^{19}F NMR (471 MHz, CD_2Cl_2) δ [ppm] = -73.59 (d, $J = 12.9$ Hz).

HRMS-ESI: calcd. for $\text{C}_{19}\text{H}_{20}\text{F}_6\text{N}_2\text{O}_3\text{Na}$ [$\text{M} + \text{Na}$] $^+$: 461.1270; found: 461.1269.

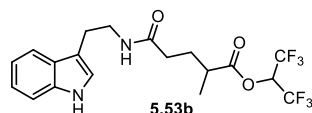
FT-IR: ν [cm^{-1}] = 3328, 1780, 1649, 1288, 1244, 1198, 1110, 933, 745.

1,1,1,3,3,3-Hexafluoropropan-2-yl 5-((2-(1*H*-indol-3-yl)ethyl)amino)-2-methyl-5-oxopentanoate (5.53b)

and

1,1,1,3,3,3-hexafluoropropan-2-yl 5-((2-(1*H*-indol-3-yl)ethyl)amino)-4-methyl-5-oxopentanoate (5.53c)

5.53b and **5.53c** were prepared according to **General procedure M**, starting from tryptamine (500 mg, 3.12 mmol, 1.0 equiv.) and 2-methylglutaric anhydride (400 mg, 3.12 mmol, 1.0 equiv.) in DMF (10.0 mL). The reaction mixture was subsequently treated with EDCI (1.19 g, 6.25 mmol, 2.0 equiv.), DMAP (76.4 mg, 0.625 mmol, 0.2 equiv.) and HFIP (1.65 mL, 15.6 mmol, 5.0 equiv.). Purification by silica gel column chromatography (pentane/EtOAc = 3:2) afforded **5.53b** (190 mg, 0.434 mmol, 14%) as a light brown solid and **5.53c** (135 mg, 0.308 mmol, 10%) as a light brown solid.



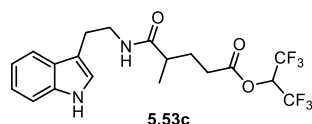
¹H NMR (500 MHz, CD₂Cl₂) δ [ppm] = 8.23 (s, 1H), 7.62–7.57 (m, 1H), 7.38 (dd, *J* = 8.1, 1.0 Hz, 1H), 7.18 (ddd, *J* = 8.1, 7.0, 1.2 Hz, 1H), 7.10 (ddd, *J* = 8.0, 7.0, 1.0 Hz, 1H), 7.06 (d, *J* = 2.4 Hz, 1H), 5.85–5.80 (m, 1H), 5.55 (s, 1H), 3.55 (td, *J* = 6.8, 5.7 Hz, 2H), 2.99–2.93 (m, 2H), 2.75–2.65 (m, 1H), 2.19–2.06 (m, 2H), 2.00–1.93 (m, 1H), 1.88–1.80 (m, 1H), 1.22 (d, *J* = 7.0 Hz, 3H).

¹³C NMR (126 MHz, CD₂Cl₂) δ [ppm] = 173.3, 171.6, 136.9, 127.8, 122.5, 122.4, 121.0 (d, *J* = 279.2 Hz), 119.7, 119.0, 113.4, 111.6, 67.2–66.1 (m), 40.1, 38.8, 33.8, 29.1, 25.7, 16.9.

¹⁹F NMR (471 MHz, CD₂Cl₂) δ [ppm] = –73.64 (d, *J* = 28.6 Hz).

HRMS-ESI: calcd. for C₁₉H₂₀F₆N₂O₃Na [M + Na]⁺: 461.1270; found: 461.1270.

FT-IR: *v* [cm⁻¹] = 3328, 1781, 1635, 1457, 1388, 1288, 1241, 1200, 1109, 932, 741.



¹H NMR (600 MHz, CDCl₃) δ [ppm] = 8.44 (s, 1H), 7.61 (dt, *J* = 7.9, 0.9 Hz, 1H), 7.36 (dt, *J* = 8.2, 0.9 Hz, 1H), 7.21 (ddd, *J* = 8.2, 7.0, 1.2 Hz, 1H), 7.13 (ddd, *J* = 8.0, 7.0, 1.0 Hz, 1H), 6.99 (d, *J* = 2.2 Hz, 1H), 5.79–5.68 (m, 1H), 5.69 (t, *J* = 5.9 Hz, 1H), 3.61 (td, *J* = 6.8, 5.8 Hz,

2H), 2.99–2.96 (m, 2H), 2.50 (ddd, $J = 16.6, 8.7, 6.0$ Hz, 1H), 2.41 (ddd, $J = 16.6, 8.5, 7.0$ Hz, 1H), 2.15–2.09 (m, 1H), 2.01–1.95 (m, 1H), 1.76–1.70 (m, 1H), 1.12 (d, $J = 6.9$ Hz, 3H).

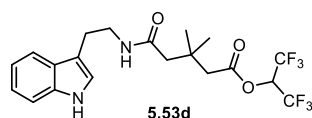
^{13}C NMR (151 MHz, CDCl_3) δ [ppm] = 175.2, 170.2, 136.6, 127.4, 122.3, 122.2, 120.5 (d, $J = 274.1$ Hz), 119.5, 118.7, 112.7, 111.5, 66.9–66.0 (m), 40.2, 39.8, 31.0, 28.6, 25.4, 17.9.

^{19}F NMR (565 MHz, CDCl_3) δ [ppm] = -73.18 (d, $J = 6.5$ Hz).

HRMS-ESI: calcd. for $\text{C}_{19}\text{H}_{20}\text{F}_6\text{N}_2\text{O}_3\text{Na}$ [$\text{M} + \text{Na}$] $^+$: 461.1270; found: 461.1271.

FT-IR: ν [cm^{-1}] = 3275, 2925, 2844, 1638, 1398, 1328, 1303, 1213, 1180, 742.

1,1,1,3,3,3-Hexafluoropropan-2-yl 5-((2-(1*H*-indol-3-yl)ethyl)amino)-3,3-dimethyl-5-oxopentanoate (5.53d)



5.53d was prepared according to **General procedure M**, starting from tryptamine (400 mg, 2.50 mmol, 1.0 equiv.) and 3,3-dimethylglutaric anhydride (355 mg, 2.50 mmol, 1.0 equiv.) in DMF (10.0 mL). The reaction mixture was subsequently treated with EDCI (955 mg, 5.00 mmol, 2.0 equiv.), DMAP (61.1 mg, 500 μmol , 0.2 equiv.) and HFIP (1.32 mL, 12.5 mmol, 5.0 equiv.). Purification by silica gel column chromatography (pentane/EtOAc = 3:2) afforded **5.53d** (697 mg, 1.54 mmol, 62%) as a white solid.

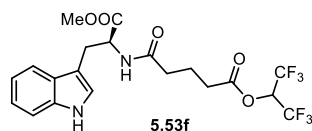
^1H NMR (500 MHz, CDCl_3) δ [ppm] = 8.21 (s, 1H), 7.60 (dt, $J = 7.9, 0.9$ Hz, 1H), 7.37 (dt, $J = 8.1, 0.9$ Hz, 1H), 7.21 (ddd, $J = 8.2, 7.0, 1.2$ Hz, 1H), 7.12 (ddd, $J = 8.0, 7.0, 1.0$ Hz, 1H), 7.01 (d, $J = 2.4$ Hz, 1H), 5.81 (s, 1H), 5.80–5.72 (m, 1H), 3.61 (td, $J = 6.8, 5.7$ Hz, 2H), 2.97 (td, $J = 6.9, 0.9$ Hz, 2H), 2.56 (s, 2H), 2.16 (s, 2H), 1.08 (s, 6H).

^{13}C NMR (126 MHz, CDCl_3) δ [ppm] = 170.7, 169.3, 136.6, 127.4, 122.3, 122.1, 120.6 (q, $J = 283.3$ Hz), 119.6, 118.8, 113.0, 111.4, 66.8–65.7 (m), 47.3, 43.8, 39.7, 33.5, 28.0, 25.4.

^{19}F NMR (565 MHz, CDCl_3) δ [ppm] = -72.98 (d, $J = 6.4$ Hz).

HRMS-ESI: calcd. for $\text{C}_{20}\text{H}_{23}\text{F}_6\text{N}_2\text{O}_3$ [$\text{M} + \text{H}$] $^+$: 453.1608; found: 453.1611.

FT-IR: ν [cm^{-1}] = 3238, 2963, 1779, 1647, 1522, 1388, 1289, 1236, 1198, 1109, 746.

(S)-1,1,1,3,3,3-Hexafluoropropan-2-yl-5-((3-(1*H*-indol-3-yl)-1-methoxy-1-oxopropan-2-yl)amino)-5-oxopentanoate (5.53f)

5.53f was prepared according to **General procedure M**, starting from (*S*)-tryptophan methyl ester (300 mg, 1.38 mmol, 1.0 equiv.) and glutaric anhydride (157 mg, 1.38 mmol, 1.0 equiv.) in DMF (10.0 mL). The reaction mixture was subsequently treated with EDCI (526 mg, 2.75 mmol, 2.0 equiv.), DMAP (33.6 mg, 0.275 mmol, 0.2 equiv.) and HFIP (727 μ L, 6.88 mmol, 5.0 equiv.). Purification by silica gel column chromatography (pentane/EtOAc = 3:2) afforded **5.53f** (150 mg, 0.311 mmol, 23%) as a white solid.

¹H NMR (500 MHz, CDCl₃) δ [ppm] = 8.32 (s, 1H), 7.53–7.50 (m, 1H), 7.34 (dt, J = 8.1, 0.9 Hz, 1H), 7.19 (ddd, J = 8.2, 7.0, 1.2 Hz, 1H), 7.11 (ddd, J = 8.0, 7.0, 1.0 Hz, 1H), 6.95 (d, J = 2.4 Hz, 1H), 6.05 (d, J = 8.0 Hz, 1H), 5.78–5.73 (m, 1H), 4.95 (dt, J = 7.9, 5.5 Hz, 1H), 3.70 (s, 3H), 3.36–3.26 (m, 2H), 2.49 (t, J = 7.4 Hz, 2H), 2.18 (t, J = 7.4 Hz, 2H), 1.98–1.92 (m, 2H).

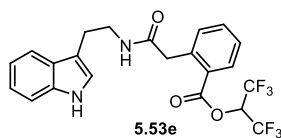
¹³C NMR (126 MHz, CDCl₃) δ [ppm] = 172.5, 171.4, 170.0, 136.3, 127.8, 122.8, 122.4, 120.5 (q, J = 278.7 Hz), 119.8, 118.5, 111.5, 110.0, 67.0–65.9 (m), 53.1, 52.5, 34.6, 32.2, 27.7, 20.1.

¹⁹F NMR (471 MHz, CDCl₃) δ [ppm] = –73.19 (d, J = 6.4 Hz).

HRMS-ESI: calcd. for C₂₀H₂₀F₆N₂O₅Na [M + Na]⁺: 505.1168; found: 505.1191.

FT-IR: ν [cm⁻¹] 3624, 3376, 2953, 1779, 1736, 1661, 1518, 1440, 1289, 1228, 1110, 781, 753.

$[\alpha]_{\text{D}}^{26}$ = +9.2 (c = 0.7, CHCl₃).

1,1,1,3,3,3-Hexafluoropropan-2-yl 2-(2-((2-(1*H*-indol-3-yl)ethyl)amino)-2-oxoethyl)benzoate (5.53e)

5.53e was prepared according to **General procedure M**, starting from tryptamine (150 mg, 0.938 mmol, 1.0 equiv.) and homophthalic anhydride (152 mg, 0.938 mmol, 1.0 equiv.) in DMF (5.0 mL). The reaction mixture was subsequently treated with EDCI (197 mg, 1.03 mmol,

2.0 equiv.), DMAP (22.9 mg, 0.188 mmol, 0.2 equiv.) and HFIP (495 μ L, 4.69 mmol, 5.0 equiv.). Purification by silica gel column chromatography (pentane/EtOAc = 5:2) afforded **5.53e** (32.0 mg, 678 μ mol, 7%) as a white solid.

$^1\text{H NMR}$ (500 MHz, CDCl_3) δ [ppm] = 8.06 (s, 1H), 8.02 (dd, J = 7.9, 1.5 Hz, 1H), 7.60–7.54 (m, 2H), 7.43 (dd, J = 7.8, 1.3 Hz, 1H), 7.40 (td, J = 7.7, 1.3 Hz, 1H), 7.34 (dd, J = 8.2, 1.0 Hz, 1H), 7.19 (ddd, J = 8.1, 7.0, 1.2 Hz, 1H), 7.10 (ddd, J = 8.1, 7.0, 1.0 Hz, 1H), 6.90 (d, J = 2.3 Hz, 1H), 5.96 (s, 1H), 5.90–5.68 (m, 1H), 3.83 (s, 2H), 3.56 (td, J = 6.9, 5.7 Hz, 2H), 2.98–2.86 (m, 2H).

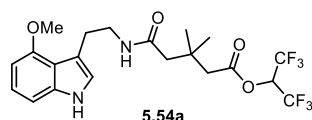
$^{13}\text{C NMR}$ (126 MHz, CDCl_3) δ [ppm] = 170.0, 163.8, 138.8, 136.5, 134.6, 132.9, 131.6, 127.8, 127.5, 125.9, 122.3, 122.1, 120.6 (q, J = 282.9 Hz), 119.6, 118.8, 113.1, 111.3, 67.5–66.4 (m), 42.2, 40.1, 25.2.

$^{19}\text{F NMR}$ (471 MHz, CDCl_3) δ [ppm] = –72.97. (It should be a doublet peak, but due to the resolution, only singlet peak was observed.)

HRMS-ESI: calcd. for $\text{C}_{22}\text{H}_{18}\text{F}_6\text{N}_2\text{O}_3\text{Na}$ [$\text{M} + \text{Na}$] $^+$: 495.1114; found: 495.1118.

FT-IR: ν [cm^{-1}] = 3306, 1755, 1651, 1551, 1360, 1242, 1193, 1104, 1019, 915, 715.

1,1,1,3,3,3-Hexafluoropropan-2-yl 5-((2-(4-methoxy-1H-indol-3-yl)ethyl)amino)-3,3-dimethyl-5-oxopentanoate (5.54a)



5.54a was prepared according to **General procedure M**, starting from 4-methoxytryptamine (50.0 mg, 0.263 mmol, 1.0 equiv.) and 3,3-dimethyl glutaric anhydride (37.4 mg, 0.263 mmol, 1.0 equiv.) in DMF (3.0 mL). The reaction mixture was subsequently treated with EDCI (100 mg, 0.526 mmol, 2.0 equiv.), DMAP (6.4 mg, 53 μ mol, 0.2 equiv.) and HFIP (139 μ L, 1.32 mmol, 5.0 equiv.). Purification by silica gel column chromatography (pentane/EtOAc = 5:2) afforded **5.54a** (79.0 mg, 164 μ mol, 62%) as a white solid.

$^1\text{H NMR}$ (700 MHz, CDCl_3) δ [ppm] = 8.26 (s, 1H), 7.09 (t, J = 7.9 Hz, 1H), 6.97 (dd, J = 8.1, 0.7 Hz, 1H), 6.85 (d, J = 2.4 Hz, 1H), 6.51 (dd, J = 7.8, 0.7 Hz, 1H), 6.09 (t, J = 5.5 Hz, 1H), 3.94 (s, 3H), 3.58 (td, J = 6.6, 5.3 Hz, 2H), 3.07 (td, J = 6.6, 0.8 Hz, 2H), 2.57 (s, 2H), 2.13 (s,

2H), 1.05 (s, 6H).

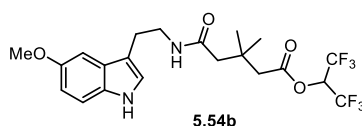
^{13}C NMR (176 MHz, CDCl_3) δ [ppm] = 170.7, 169.1, 154.5, 138.3, 123.0, 121.4, 119.8, 118.2, 117.4, 113.5, 104.9, 99.6, 66.6–65.8 (m), 55.3, 47.5, 43.8, 41.3, 33.3, 27.8, 26.5. (δ [ppm] = 119.8 and 118.2 belong to the q peaks of CF_3 , the other two peaks are missing, probably due to the overlap.)

^{19}F NMR (376 MHz, CDCl_3) δ [ppm] = -73.01 (d, J = 9.2 Hz).

HRMS-ESI: calcd. for $\text{C}_{21}\text{H}_{24}\text{F}_6\text{N}_2\text{O}_4\text{Na}$ [$\text{M} + \text{Na}$] $^+$: 505.1532; found: 505.1550.

FT-IR: ν [cm^{-1}] = 3291, 2962, 1774, 1648, 1508, 1356, 1287, 1226, 1198, 1107, 735.

1,1,1,3,3,3-Hexafluoropropan-2-yl 5-((2-(5-methoxy-1H-indol-3-yl)ethyl)amino)-3,3-dimethyl-5-oxopentanoate (5.54b)



5.54b was prepared according to **General procedure M**, starting from 5-methoxytryptamine (250 mg, 1.32 mmol, 1.0 equiv.) and 3,3-dimethyl glutaric anhydride (187 mg, 1.32 mmol, 1.0 equiv.) in DMF (3.0 mL). The reaction mixture was subsequently treated with EDCI (503 mg, 2.63 mmol, 2.0 equiv.), DMAP (32.2 mg, 263 μmol , 0.2 equiv.) and HFIP (695 μL , 6.58 mmol, 5.0 equiv.). Purification by silica gel column chromatography (pentane/EtOAc = 5:2) afforded **5.54b** (325 mg, 674 μmol , 51%) as a white solid.

^1H NMR (700 MHz, CDCl_3) δ [ppm] = 8.08 (s, 1H), 7.25 (dd, J = 8.7, 0.6 Hz, 1H), 7.03 (d, J = 2.4 Hz, 1H), 7.00–6.97 (m, 1H), 6.87 (ddd, J = 8.8, 2.4, 0.4 Hz, 1H), 5.79 (t, J = 5.7 Hz, 1H), 5.74 (p, J = 6.1 Hz, 1H), 3.86 (s, 3H), 3.60 (td, J = 6.9, 5.7 Hz, 2H), 2.94 (td, J = 6.9, 0.9 Hz, 2H), 2.57 (s, 2H), 2.17 (s, 2H), 1.09 (s, 6H).

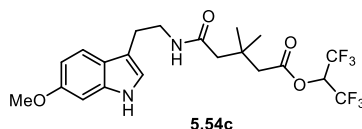
^{13}C NMR (176 MHz, CDCl_3) δ [ppm] = 170.7, 169.3, 154.2, 131.7, 127.8, 122.9, 120.6 (d, J = 282.5 Hz), 112.7, 112.6, 112.1, 100.7, 66.6–65.9 (m), 56.1, 47.3, 43.8, 39.5, 33.5, 28.0, 25.4.

^{19}F NMR (376 MHz, CDCl_3) δ [ppm] = -73.00 (d, J = 10.8 Hz).

HRMS-ESI: calcd. for $\text{C}_{21}\text{H}_{24}\text{F}_6\text{N}_2\text{O}_4\text{Na}$ [$\text{M} + \text{Na}$] $^+$: 505.1532; found: 505.1549.

FT-IR: ν [cm^{-1}] = 3301, 2969, 1741, 1649, 1364, 1289, 1217, 1202, 1109, 936, 728.

1,1,1,3,3,3-Hexafluoropropan-2-yl 5-((2-(6-methoxy-1H-indol-3-yl)ethyl)amino)-3,3-dimethyl-5-oxopentanoate (5.54c)



5.54c was prepared according to **General procedure M**, starting from 6-methoxytryptamine (200 mg, 1.05 mmol, 1.0 equiv.) and 3,3-dimethylglutaric anhydride (150 mg, 1.05 mmol, 1.0 equiv.) in DMF (5.0 mL). The reaction mixture was subsequently treated with EDCI (402 mg, 2.11 mmol, 2.0 equiv.), DMAP (25.7 mg, 0.211 mmol, 0.2 equiv.) and HFIP (556 μ L, 5.26 mmol, 5.0 equiv.). Purification by silica gel column chromatography (pentane/EtOAc = 3:2) afforded **5.54c** (370 mg, 0.768 mmol, 73%) as a yellow solid.

¹H NMR (500 MHz, CD₂Cl₂) δ [ppm] = 8.13 (s, 1H), 7.45 (d, J = 8.6 Hz, 1H), 6.92 (dt, J = 2.1, 1.0 Hz, 1H), 6.86 (d, J = 2.2 Hz, 1H), 6.75 (dd, J = 8.6, 2.3 Hz, 1H), 5.86–5.78 (m, 1H), 5.75 (s, 1H), 3.82 (s, 3H), 3.54 (td, J = 6.9, 5.7 Hz, 2H), 2.94–2.87 (m, 2H), 2.62 (s, 2H), 2.15 (s, 2H), 1.08 (s, 6H).

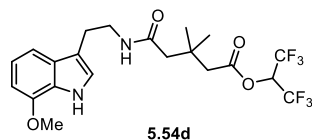
¹³C NMR (126 MHz, CD₂Cl₂) δ [ppm] = 170.7, 169.5, 157.1, 137.7, 122.2, 121.2, 119.6, 113.3, 109.8, 94.9, 66.7–66.2 (m), 55.9, 47.5, 44.0, 39.9, 33.5, 27.9, 25.8. (Due to the resolution or/and overlapping, the resonance of CF₃ is missing.)

¹⁹F NMR (471 MHz, CD₂Cl₂) δ [ppm] = –73.47.

HRMS-EI: calcd. for C₂₁H₂₄F₆N₂O₄Na [M + Na]⁺: 505.1532; found: 505.1533.

FT-IR: ν [cm⁻¹] = 2969, 2941, 1766, 1737, 1649, 1456, 1360, 1289, 1200, 1109, 771.

1,1,1,3,3,3-Hexafluoropropan-2-yl 5-((2-(7-methoxy-1H-indol-3-yl)ethyl)amino)-3,3-dimethyl-5-oxopentanoate (5.54d)



5.54d was prepared according to **General procedure M**, starting from 4-methoxytryptamine (50.0 mg, 0.263 mmol, 1.0 equiv.) and 3,3-dimethyl glutaric anhydride (37.4 mg, 0.263 mmol, 1.0 equiv.) in DMF (3.0 mL). The reaction mixture was subsequently treated with EDCI

(100 mg, 0.526 mmol, 2.0 equiv.), DMAP (6.4 mg, 53 μ mol, 0.2 equiv.) and HFIP (139 μ L, 1.32 mmol, 5.0 equiv.). Purification by silica gel column chromatography (pentane/EtOAc = 5:2) afforded **5.54d** (69.0 mg, 143 μ mol, 54%) as a white solid.

^1H NMR (700 MHz, CDCl_3) δ [ppm] = 8.34 (s, 1H), 7.20 (dd, J = 8.0, 0.8 Hz, 1H), 7.04 (t, J = 7.8 Hz, 1H), 7.00 – 6.96 (m, 1H), 6.66 (dd, J = 7.7, 0.8 Hz, 1H), 3.95 (s, 3H), 3.60 (td, J = 6.8, 5.7 Hz, 2H), 2.95 (td, J = 6.8, 0.9 Hz, 2H), 2.58 (s, 2H), 2.15 (s, 2H), 1.08 (s, 6H).

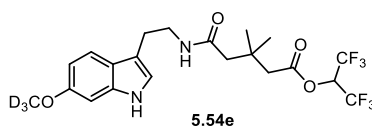
^{13}C NMR (176 MHz, CDCl_3) δ [ppm] = 170.7, 169.2, 146.4, 128.8, 127.1, 121.7, 120.5 (q, J = 282.4 Hz), 120.1, 113.4, 111.6, 102.1, 66.6–65.8 (m), 55.4, 47.3, 43.8, 39.7, 33.4, 27.9, 25.6.

^{19}F NMR (376 MHz, CDCl_3) δ [ppm] = –73.00 (d, J = 9.3 Hz).

HRMS-ESI: calcd. for $\text{C}_{21}\text{H}_{24}\text{F}_6\text{N}_2\text{O}_4\text{Na}$ [$\text{M} + \text{Na}$] $^+$: 505.1532; found: 505.1547.

FT-IR: ν [cm^{-1}] = 3407, 2964, 1774, 1650, 1578, 1357, 1288, 1230, 1200, 1108, 731.

1,1,1,3,3,3-Hexafluoropropan-2-yl 5-((2-(6-(methoxy- d_3)-1H-indol-3-yl)ethyl)amino)-3,3-dimethyl-5-oxopentanoate



5.54e was prepared according to **General procedure L**, starting from 6-(methoxy- d_3)-tryptamine (20.0 mg, 0.104 mmol, 1.0 equiv.) and 3,3-dimethylglutaric anhydride (14.7 mg, 0.104 mmol, 1.0 equiv.) in DMF (2.0 mL). The reaction mixture was subsequently treated with EDCI (39.6 mg, 0.207 mmol, 2.0 equiv.), DMAP (2.5 mg, 21 μ mol, 0.2 equiv.) and HFIP (54.7 μ L, 0.518 mmol, 5.0 equiv.). Purification by silica gel column chromatography (pentane/EtOAc = 3:2) afforded **5.54e** (20.0 mg, 41.2 μ mol, 40%) as a yellow solid.

^1H NMR (600 MHz, CDCl_3) δ [ppm] = 7.88 (s, 1H), 7.46 (d, J = 8.6 Hz, 1H), 6.91 (dd, J = 2.1, 1.0 Hz, 1H), 6.85 (d, J = 2.1 Hz, 1H), 6.79 (dd, J = 8.6, 2.3 Hz, 1H), 5.73 (p, J = 6.1 Hz, 2H), 3.60 (td, J = 6.8, 5.7 Hz, 2H), 2.93 (td, J = 6.8, 0.9 Hz, 2H), 2.57 (s, 2H), 2.16 (s, 2H), 1.08 (s, 6H).

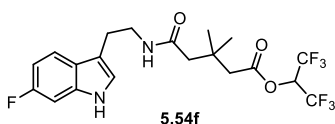
^{13}C NMR (151 MHz, CDCl_3) δ [ppm] = 170.6, 169.3, 137.3, 129.9, 121.9, 120.8, 119.5, 113.1, 109.7, 94.8, 47.3, 43.8, 39.6, 33.5, 28.0, 25.5.

^{19}F NMR (565 MHz, CDCl_3) δ [ppm] = –72.98, –73.00.

HRMS-ESI: calcd. for $C_{21}H_{21}D_3F_6N_2O_4Na$ $[M + Na]^+$: 508.1721; found: 508.1737.

FT-IR: ν [cm^{-1}] = 3408, 2959, 2924, 1774, 1646, 1628, 1288, 1265, 1199, 1109, 804, 732.

1,1,1,3,3,3-Hexafluoropropan-2-yl 5-((2-(6-fluoro-1H-indol-3-yl)ethyl)amino)-3,3-dimethyl-5-oxopentanoate (5.54f)



5.54f was prepared according to **General procedure M**, starting from 6-fluorotryptamine (50.0 mg, 0.281 mmol, 1.0 equiv.) and 3,3-dimethylglutaric anhydride (39.9 mg, 0.281 mmol, 1.0 equiv.) in DMF (2.0 mL). The reaction mixture was subsequently treated with EDCI (107 mg, 0.562 mmol, 2.0 equiv.), DMAP (6.9 mg, 56 μ mol, 0.2 equiv.) and HFIP (148 μ L, 1.40 mmol, 5.0 equiv.). Purification by silica gel column chromatography (pentane/EtOAc = 3:2) afforded **5.54f** (72.0 mg, 153 μ mol, 54%) as a yellow solid.

1H NMR (700 MHz, $CDCl_3$) δ [ppm] = 8.27 (s, 1H), 7.49 (dd, J = 8.7, 5.3 Hz, 1H), 7.03 (dd, J = 9.6, 2.3 Hz, 1H), 6.98 (dt, J = 2.1, 0.9 Hz, 1H), 6.88 (ddd, J = 9.6, 8.6, 2.3 Hz, 1H), 5.82 (t, J = 6.0 Hz, 1H), 5.74 (p, J = 6.1 Hz, 1H), 3.59 (td, J = 6.9, 5.8 Hz, 2H), 2.94 (td, J = 6.9, 0.9 Hz, 2H), 2.56 (s, 2H), 2.18 (s, 2H), 1.09 (s, 6H).

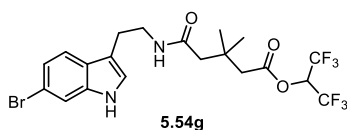
^{13}C NMR (176 MHz, $CDCl_3$) δ [ppm] = 170.8, 169.3, 160.2 (d, J = 237.6 Hz), 136.5 (d, J = 12.6 Hz), 124.1, 122.3, 120.5 (d, J = 283.1 Hz), 119.5 (d, J = 10.4 Hz), 113.1, 108.4 (d, J = 24.5 Hz), 97.7 (d, J = 26.2 Hz), 66.3 (m), 47.2, 43.8, 39.7, 33.5, 28.0, 25.4.

^{19}F NMR (376 MHz, $CDCl_3$) δ [ppm] = -73.00 (d, J = 9.0 Hz), -120.97 (q, J = 9.4 Hz).

HRMS-ESI: calcd. for $C_{20}H_{21}F_7N_2O_3Na$ $[M + Na]^+$: 493.1332; found: 493.1344.

FT-IR: ν [cm^{-1}] = 3406, 3315, 2964, 1774, 1650, 1386, 1357, 1288, 1230, 1200, 1108, 731.

1,1,1,3,3,3-Hexafluoropropan-2-yl 5-((2-(6-bromo-1H-indol-3-yl)ethyl)amino)-3,3-dimethyl-5-oxopentanoate (5.54g)



5.54g was prepared according to **General procedure M**, starting from 6-bromotryptamine (50.0 mg, 0.210 mmol, 1.0 equiv.) and 3,3-dimethylglutaric anhydride (29.8 mg, 0.210 mmol, 1.0 equiv.) in DMF (2.0 mL). The reaction mixture was subsequently treated with EDCI (80.3 mg, 0.420 mmol, 2.0 equiv.), DMAP (5.1 mg, 42 μ mol, 0.2 equiv.) and HFIP (176 μ L, 1.05 mmol, 5.0 equiv.). Purification by silica gel column chromatography (pentane/EtOAc = 3:2) afforded **5.54g** (75.0 mg, 141 μ mol, 67%) as a yellow solid.

¹H NMR (700 MHz, CDCl₃) δ [ppm] = 8.41 (s, 1H), 7.50 (d, J = 1.7 Hz, 1H), 7.43 (d, J = 8.4 Hz, 1H), 7.20 (dd, J = 8.4, 1.7 Hz, 1H), 6.97 (dd, J = 2.3, 1.1 Hz, 1H), 5.84 (t, J = 5.8 Hz, 1H), 5.75 (p, J = 6.1 Hz, 1H), 3.57 (td, J = 7.0, 5.8 Hz, 2H), 2.93 (td, J = 7.0, 1.0 Hz, 2H), 2.57 (s, 2H), 2.18 (s, 2H), 1.09 (s, 6H).

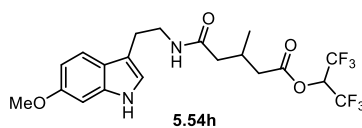
¹³C NMR (176 MHz, CDCl₃) δ [ppm] = 170.8, 169.3, 137.3, 126.4, 122.8, 122.7, 120.52 (d, J = 282.8 Hz), 120.0, 115.8, 114.3, 113.2, 66.7, 66.5, 66.3, 66.1, 65.9, 47.2, 43.8, 39.7, 33.5, 28.0, 25.4.

¹⁹F NMR (376 MHz, CDCl₃) δ [ppm] = -72.98 (d, J = 5.9 Hz).

HRMS-ESI: calcd. for C₂₀H₂₁BrF₆N₂O₃Na [M + Na]⁺: 553.0532; found: 553.0549.

FT-IR: ν [cm⁻¹] = 3300, 2965, 1772, 1650, 1288, 1225, 1198, 1107, 936, 735.

1,1,1,3,3,3-Hexafluoropropan-2-yl 5-((2-(6-methoxy-1H-indol-3-yl)ethyl)amino)-3-methyl-5-oxopentanoate (5.54h)



5.54h was prepared according to **General procedure M**, starting from 6-methoxytryptamine (100 mg, 0.526 mmol, 1.0 equiv.) and glutaric anhydride (67.4 mg, 0.526 mmol, 1.0 equiv.) in DMF (3.0 mL). The reaction mixture was subsequently treated with EDCI (201 mg, 1.05 mmol, 2.0 equiv.), DMAP (12.9 mg, 0.105 mmol, 0.2 equiv.) and HFIP (278 μ L, 2.63 mmol, 5.0 equiv.). Purification by silica gel column chromatography (pentane/EtOAc = 3:2) afforded **5.54h** (150 mg, 0.320 mmol, 61%) as a white solid.

¹H NMR (700 MHz, CDCl₃) δ [ppm] = 8.19 (s, 1H), 7.44 (d, J = 8.6 Hz, 1H), 6.89–6.87 (m, 1H), 6.84 (d, J = 2.3 Hz, 1H), 6.79 (dd, J = 8.6, 2.3 Hz, 1H), 5.79–5.75 (m, 1H), 5.66 (s, 1H),

3.83 (d, $J = 0.7$ Hz, 3H), 3.58 (dt, $J = 8.5, 6.8$ Hz, 2H), 2.95–2.89 (m, 2H), 2.65–2.59 (m, 1H), 2.52–2.48 (m, 1H), 2.48–2.34 (m, 1H), 2.13 (dd, $J = 14.3, 6.9$ Hz, 1H), 2.03 (ddd, $J = 14.5, 7.4, 1.7$ Hz, 1H), 0.99 (d, $J = 6.8$ Hz, 3H).

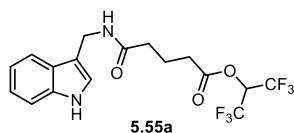
^{13}C NMR (176 MHz, CDCl_3) δ [ppm] = 171.1, 169.4, 156.8, 137.3, 121.9, 120.9, 120.5 (q, $J = 282.4$ Hz), 119.3, 112.9, 109.6, 94.9, 66.8–66.0 (m), 55.8, 42.8, 39.8, 39.5, 27.9, 25.5, 19.4.

^{19}F NMR (565 MHz, CDCl_3) δ [ppm] = -73.11 (d, $J = 7.7$ Hz).

HRMS-ESI: calcd. for $\text{C}_{20}\text{H}_{22}\text{F}_6\text{N}_2\text{O}_4\text{Na}$ [$\text{M} + \text{Na}$] $^+$: 491.1374; found: 491.1376.

FT-IR: ν [cm^{-1}] 2958, 1776, 1648, 1386, 1288, 1200, 1110, 937, 812.

1,1,1,3,3,3-Hexafluoropropan-2-yl 5-(((1H-indol-3-yl)methyl)amino)-5-oxopentanoate (5.55a)



5.55a was prepared according to **General procedure M**, starting from 1H-indole-3-methanamine (310 mg, 2.12 mmol, 1.0 equiv.) and glutaric anhydride (242 mg, 2.12 mmol, 1.0 equiv.) in DMF (10.0 mL). The reaction mixture was subsequently treated with EDCI (811 mg, 4.25 mmol, 2.0 equiv.), DMAP (51.9 mg, 0.425 mmol, 0.2 equiv.) and HFIP (1.12 mL, 10.6 mmol, 5.0 equiv.). Purification by silica gel column chromatography (pentane/EtOAc = 3:2) afforded **5.55a** (300 mg, 0.732 mmol, 34%) as a white solid.

^1H NMR (700 MHz, CDCl_3) δ [ppm] = 8.28 (s, 1H), 7.62–7.60 (m, 1H), 7.39 (dt, $J = 8.1, 0.9$ Hz, 1H), 7.23 (ddd, $J = 8.1, 7.0, 1.2$ Hz, 1H), 7.18–7.12 (m, 2H), 5.79–5.72 (m, 1H), 5.70 (s, 1H), 4.62 (dd, $J = 5.2, 0.8$ Hz, 2H), 2.60 (t, $J = 7.3$ Hz, 2H), 2.23 (t, $J = 7.2$ Hz, 2H), 2.07–2.03 (m, 2H).

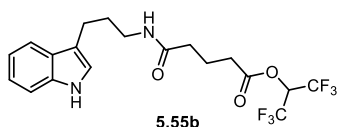
^{13}C NMR (176 MHz, CDCl_3) δ [ppm] = 171.3, 170.1, 136.5, 126.6, 123.4, 122.7, 120.5 (d, $J = 286.2$ Hz), 120.1, 118.8, 112.7, 111.5, 66.9–66.1 (m), 35.3, 34.9, 32.5, 20.5.

^{19}F NMR (565 MHz, CDCl_3) δ [ppm] = -73.20 (d, $J = 6.3$ Hz).

HRMS-ESI: calcd. for $\text{C}_{17}\text{H}_{16}\text{F}_6\text{N}_2\text{O}_3\text{Na}$ [$\text{M} + \text{Na}$] $^+$: 433.0957; found: 433.0972.

FT-IR: ν [cm^{-1}] = 3259, 1738, 1660, 1364, 1204, 1108, 744.

1,1,1,3,3,3-Hexafluoropropan-2-yl 5-((3-(1*H*-indol-3-yl)propyl)amino)-5-oxopentanoate (5.55b)



5.55b was prepared according to **General procedure M**, starting from 1*H*-indole-3-propanamine (85.0 mg, 0.489 mmol, 1.0 equiv.) and glutaric anhydride (55.7 mg, 0.489 mmol, 1.0 equiv.) in DMF (2.0 mL). The reaction mixture was subsequently treated with EDCI (187 mg, 0.977 mmol, 2.0 equiv.), DMAP (11.9 mg, 98.0 μ mol, 0.2 equiv.) and HFIP (258 μ L, 2.44 mmol, 5.0 equiv.). Purification by silica gel column chromatography (pentane/EtOAc = 3:2) afforded **5.55b** (120 mg, 0.274 mmol, 56%) as a white solid.

¹H NMR (500 MHz, CDCl₃) δ [ppm] = 8.11 (s, 1H), 7.59–7.57 (m, 1H), 7.36–7.34 (m, 1H), 7.19 (ddd, J = 8.2, 7.0, 1.2 Hz, 1H), 7.14–7.10 (m, 1H), 6.98 (dd, J = 2.3, 1.2 Hz, 1H), 5.80–5.75 (m, 1H), 5.46 (s, 1H), 3.32 (td, J = 7.1, 5.9 Hz, 2H), 2.80 (td, J = 7.3, 0.9 Hz, 2H), 2.55 (t, J = 7.2 Hz, 2H), 2.12 (t, J = 7.3 Hz, 2H), 2.00–1.89 (m, 4H).

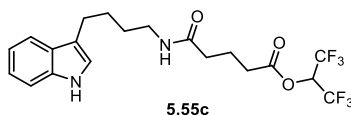
¹³C NMR (126 MHz, CDCl₃) δ [ppm] = 171.5, 170.1, 136.6, 127.4, 122.2, 121.6, 119.4, 118.8, 115.5, 111.3, 66.8–66.3 (m), 39.6, 34.9, 32.4, 29.8, 22.8, 20.4. (Due to the resolution or/and overlapping, the resonance of CF₃ was not observed.)

¹⁹F NMR (471 MHz, CDCl₃) δ [ppm] = –73.18 (d, J = 6.4 Hz).

HRMS-ESI: calcd. for C₁₉H₂₀F₆N₂O₃Na [M + Na]⁺: 461.1270; found: 461.1287.

FT-IR: ν [cm⁻¹] = 3404, 3295, 2925, 1780, 1649, 1385, 1356, 1288, 1228, 1200, 1110, 744.

1,1,1,3,3,3-Hexafluoropropan-2-yl 5-((4-(1*H*-indol-3-yl)butyl)amino)-5-oxopentanoate (5.55c)



5.55c was prepared according to **General procedure M**, starting from 1*H*-indole-3-butanamine (120 mg, 0.638 mmol, 1.0 equiv.) and glutaric anhydride (72.8 mg, 0.638 mmol, 1.0 equiv.) in DMF (2.0 mL). The reaction mixture was subsequently treated with EDCI (244 mg, 1.28 mmol, 2.0 equiv.), DMAP (15.6 mg, 0.128 mmol, 0.2 equiv.) and HFIP (337 μ L, 3.19 mmol,

5.0 equiv.). Purification by silica gel column chromatography (pentane/EtOAc = 3:2) afforded **5.55c** (140 mg, 0.310 mmol, 48%) as a white solid.

¹H NMR (500 MHz, CDCl₃) δ [ppm] = 8.06 (s, 1H), 7.62–7.56 (m, 1H), 7.35 (dt, *J* = 8.2, 0.9 Hz, 1H), 7.19 (ddd, *J* = 8.1, 7.0, 1.2 Hz, 1H), 7.11 (ddd, *J* = 8.0, 7.0, 1.0 Hz, 1H), 6.96 (dd, *J* = 2.3, 1.0 Hz, 1H), 5.80–5.75 (m, 1H), 5.43 (s, 1H), 3.26 (td, *J* = 7.2, 5.7 Hz, 2H), 2.78 (td, *J* = 7.4, 0.9 Hz, 2H), 2.57 (t, *J* = 7.2 Hz, 2H), 2.16 (t, *J* = 7.3 Hz, 2H), 2.01 (q, *J* = 7.3 Hz, 2H), 1.80–1.69 (m, 2H), 1.60–1.54 (m, 2H).

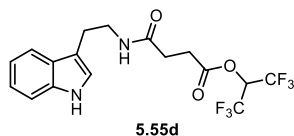
¹³C NMR (126 MHz, CDCl₃) δ [ppm] = 171.5, 170.1, 136.5, 127.5, 122.0, 121.5, 120.5 (d, *J* = 282.6 Hz), 119.2, 119.0, 116.3, 111.3, 66.7–66.2 (m), 39.6, 34.9, 32.4, 29.4, 27.4, 24.81, 20.4.

¹⁹F NMR (471 MHz, CDCl₃) δ [ppm] = –73.17 (d, *J* = 6.3 Hz).

HRMS-ESI: calcd. for C₂₀H₂₂F₆N₂O₃Na [M + Na]⁺: 475.1427; found: 475.1436.

FT-IR: ν [cm⁻¹] = 3401, 2924, 2854, 1781, 1651, 1288, 1228, 1200, 1110, 927, 906, 744.

1,1,1,3,3,3-Hexafluoropropan-2-yl 4-((2-(1*H*-indol-3-yl)ethyl)amino)-4-oxobutanoate (5.55d)



5.55d was prepared according to **General procedure M**, starting from tryptamine (250 mg, 1.56 mmol, 1.0 equiv.) and succinic anhydride (156 mg, 1.56 mmol, 1.0 equiv.) in DMF (5.0 mL). The reaction mixture was subsequently treated with EDCI (328 mg, 1.72 mmol, 2.0 equiv.), DMAP (38.2 mg, 0.313 mmol, 0.2 equiv.) and HFIP (825 μL, 7.81 mmol, 5.0 equiv.). Purification by silica gel column chromatography (pentane/EtOAc = 3:2) afforded **5.55d** (286 mg, 0.698 mmol, 45%) as a white solid.

¹H NMR (600 MHz, CDCl₃) δ [ppm] = 8.22 (s, 1H), 7.59 (dd, *J* = 7.9, 1.1 Hz, 1H), 7.37 (dt, *J* = 8.1, 0.9 Hz, 1H), 7.22 (ddd, *J* = 8.2, 7.0, 1.2 Hz, 1H), 7.13 (ddd, *J* = 8.0, 7.0, 1.0 Hz, 1H), 7.01 (d, *J* = 2.3 Hz, 1H), 5.79–5.75 (m, 1H), 5.63 (d, *J* = 5.6 Hz, 1H), 3.60 (q, *J* = 6.5 Hz, 2H), 2.96 (td, *J* = 6.8, 0.9 Hz, 2H), 2.84 (t, *J* = 6.9 Hz, 2H), 2.44 (t, *J* = 6.9 Hz, 2H).

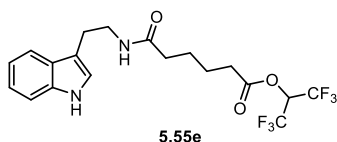
¹³C NMR (151 MHz, CDCl₃) δ [ppm] = 170.2, 170.0, 136.6, 127.4, 122.4, 122.2, 120.5 (d, *J* = 283.0 Hz), 119.6, 118.8, 112.9, 111.4, 67.2–66.3 (m), 40.1, 30.4, 28.7, 25.3.

^{19}F NMR (565 MHz, CDCl_3) δ [ppm] = -73.14 (d, $J = 6.6$ Hz).

HRMS-ESI: calcd. for $\text{C}_{17}\text{H}_{16}\text{F}_6\text{N}_2\text{O}_3\text{Na}$ [$\text{M} + \text{Na}$] $^+$: 433.0957; found: 433.0974.

FT-IR: ν [cm^{-1}] = 3422, 3328, 1754, 1633, 1384, 1286, 1201, 1108, 905, 738.

1,1,1,3,3,3-Hexafluoropropan-2-yl 6-((2-(1*H*-indol-3-yl)ethyl)amino)-6-oxohexanoate (5.55e)



5.55e was prepared according to **General procedure M**, starting from tryptamine (400 mg, 2.50 mmol, 1.0 equiv.) and oxepane-2,7-dione (320 mg, 2.50 mmol, 1.0 equiv.) in DMF (10.0 mL). The reaction mixture was subsequently treated with EDCI (955 mg, 5.00 mmol, 2.0 equiv.), DMAP (61.1 mg, 0.500 mmol, 0.2 equiv.) and HFIP (1.32 mL, 12.5 mmol, 5.0 equiv.). Purification by silica gel column chromatography (pentane/EtOAc = 3:2) afforded **5.55e** (289 mg, 0.660 mmol, 26%) as a white solid.

^1H NMR (500 MHz, CDCl_3) δ [ppm] = 8.73 (s, 1H), 7.59 (d, $J = 7.9$ Hz, 1H), 7.35 (d, $J = 8.1$ Hz, 1H), 7.21 (ddd, $J = 8.1, 7.0, 1.2$ Hz, 1H), 7.15–7.08 (m, 1H), 6.96 (d, $J = 2.3$ Hz, 1H), 5.87–5.75 (m, 2H), 3.61–3.57 (m, 2H), 2.96 (t, $J = 6.8$ Hz, 2H), 2.46 (t, $J = 6.7$ Hz, 2H), 2.15–2.01 (m, 2H), 1.67–1.62 (m, 4H).

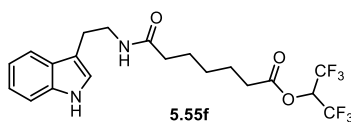
^{13}C NMR (126 MHz, CDCl_3) δ [ppm] = 172.6, 170.3, 136.6, 127.5, 123.9, 122.2, 120.6 (q, $J = 284.4$ Hz), 119.4, 118.7, 112.7, 111.5, 67.0–65.9 (m), 40.0, 36.0, 33.0, 25.4, 24.8, 24.1.

^{19}F NMR (565 MHz, CDCl_3) δ [ppm] = -73.24 (d, $J = 6.3$ Hz).

HRMS-ESI: calcd. for $\text{C}_{19}\text{H}_{20}\text{F}_6\text{N}_2\text{O}_3\text{Na}$ [$\text{M} + \text{Na}$] $^+$: 461.1270; found: 461.1285.

FT-IR: ν [cm^{-1}] = 2928, 2855, 1713, 1659, 1626, 1442, 1329, 1230, 745.

***N*-((2-(1*H*-indol-3-yl)ethyl)amino)-8-((1,1,1,3,3,3-hexafluoropropan-2-yl)oxy)-7-oxooctanamide (5.55f)**



5.55f was prepared according to **General procedure M**, starting from tryptamine (400 mg,

2.50 mmol, 1.0 equiv.) and oxocane-2,8-dione (355 mg, 2.50 mmol, 1.0 equiv.) in DMF (10.0 mL). The reaction mixture was subsequently treated with EDCI (955 mg, 5.00 mmol, 2.0 equiv.), DMAP (61.1 mg, 0.500 mmol, 0.2 equiv.) and HFIP (1.32 mL, 12.5 mmol, 5.0 equiv.). Purification by silica gel column chromatography (pentane/EtOAc = 3:2) afforded **5.55f** (300 mg, 0.644 mmol, 26%) as a white solid.

¹H NMR (500 MHz, CDCl₃) δ [ppm] = 8.62 (s, 1H), 7.60–7.58 (m, 1H), 7.36 (dt, *J* = 8.1, 0.9 Hz, 1H), 7.20 (ddd, *J* = 8.2, 7.0, 1.2 Hz, 1H), 7.11 (ddd, *J* = 8.0, 7.0, 1.1 Hz, 1H), 6.98 (d, *J* = 2.3 Hz, 1H), 5.80–5.75 (m, 1H), 5.70 (t, *J* = 5.8 Hz, 1H), 3.59 (td, *J* = 6.8, 5.7 Hz, 2H), 2.96 (td, *J* = 6.8, 0.9 Hz, 2H), 2.44 (t, *J* = 7.5 Hz, 2H), 2.08 (t, *J* = 7.5 Hz, 2H), 1.71–1.52 (m, 4H), 1.34–1.20 (m, 2H).

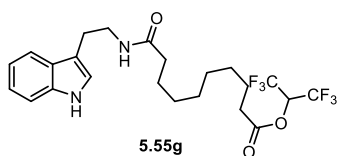
¹³C NMR (126 MHz, CDCl₃) δ [ppm] = 172.9, 170.4, 136.6, 127.5, 122.3, 122.2, 120.6 (q, *J* = 281.4 Hz), 119.5, 118.7, 112.8, 111.5, 67.0–65.9 (m), 39.9, 36.4, 33.1, 28.4, 25.4, 25.2, 24.3.

¹⁹F NMR (565 MHz, CDCl₃) δ [ppm] = –73.23 (d, *J* = 6.4 Hz).

HRMS-ESI: calcd. for C₂₀H₂₂F₆N₂O₃Na [M + Na]⁺: 475.1427; found: 475.1442.

FT-IR: *v* [cm⁻¹] = 3286, 2934, 2870, 1778, 1648, 1532, 1387, 1288, 1236, 1199, 1110, 745.

1,1,1,3,3,3-Hexafluoropropan-2-yl 10-((2-(1H-indol-3-yl)ethyl)amino)-10-oxodecanoate (5.55g)



5.55g was prepared according to **General procedure M**, starting from tryptamine (200 mg, 1.25 mmol, 1.0 equiv.) and oxacycloundecane-2,11-dione (230 mg, 1.25 mmol, 1.0 equiv.) in DMF (5.0 mL). The reaction mixture was subsequently treated with EDCI (477 mg, 2.50 mmol, 2.0 equiv.), DMAP (30.5 mg, 0.250 mmol, 0.2 equiv.) and HFIP (660 μL, 6.25 mmol, 5.0 equiv.). Purification by silica gel column chromatography (pentane/EtOAc = 3:2) afforded **5.55g** (150 mg, 0.304 mmol, 24%) as a white solid.

¹H NMR (500 MHz, CDCl₃) δ [ppm] = 8.72 (s, 1H), 7.60 (dd, *J* = 8.0, 1.1 Hz, 1H), 7.39–7.34 (m, 1H), 7.20 (ddd, *J* = 8.1, 7.0, 1.2 Hz, 1H), 7.11 (ddd, *J* = 8.0, 7.0, 1.0 Hz, 1H), 6.98 (d, *J* = 2.0 Hz, 1H), 5.85–5.67 (m, 2H), 3.62–3.58 (m, 2H), 2.97 (t, *J* = 6.8 Hz, 2H), 2.49 (t, *J* = 7.4 Hz,

2H), 2.10 (t, $J = 7.6$ Hz, 2H), 1.69–1.65 (m, 2H), 1.62–1.56 (m, 2H), 1.32–1.25 (m, 8H).

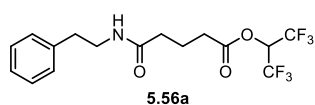
^{13}C NMR (126 MHz, CDCl_3) δ [ppm] = 173.4, 170.5, 136.6, 127.5, 122.3, 122.1, 120.5 (q, $J = 282.5$ Hz), 119.4, 118.7, 112.8, 111.5, 66.9–65.8 (m), 39.9, 36.8, 33.3, 29.2, 29.1, 28.9, 28.7, 25.7, 25.4, 24.5.

^{19}F NMR (471 MHz, CDCl_3) δ [ppm] = -73.26 (d, $J = 5.7$ Hz).

HRMS-ESI: calcd. for $\text{C}_{23}\text{H}_{28}\text{F}_6\text{N}_2\text{O}_3\text{Na}$ [$\text{M} + \text{Na}$] $^+$: 517.1896; found: 517.1921.

FT-IR: ν [cm^{-1}] = 2939, 2921, 2146, 2042, 1779, 1649, 1289, 1228, 1202, 1111, 760.

1,1,1,3,3,3-Hexafluoropropan-2-yl 5-oxo-5-(phenethylamino)pentanoate (5.56a)



5.56a was prepared according to **General procedure M**, starting from phenethylamine (200 mg, 1.65 mmol, 1.0 equiv.) and glutaric anhydride (188 mg, 1.65 mmol, 1.0 equiv.) in DMF (5.0 mL). The reaction mixture was subsequently treated with EDCI (631 mg, 3.31 mmol, 2.0 equiv.), DMAP (40.4 mg, 0.331 mmol, 0.2 equiv.) and HFIP (873 μL , 8.26 mmol, 5.0 equiv.). Purification by silica gel column chromatography (pentane/EtOAc = 5:2) afforded **5.56a** (200 mg, 0.519 mmol, 31%) as a white solid.

^1H NMR (500 MHz, CDCl_3) δ [ppm] = 7.33–7.28 (m, 2H), 7.26–7.21 (m, 1H), 7.18 (dt, $J = 7.9, 1.7$ Hz, 2H), 7.79–7.73 (m, 1H), 5.54 (s, 1H), 3.58–3.48 (m, 2H), 2.81 (td, $J = 7.0, 1.7$ Hz, 2H), 2.54 (td, $J = 7.3, 1.8$ Hz, 2H), 2.18 (td, $J = 7.2, 1.8$ Hz, 2H), 2.02–1.97 (m, 2H).

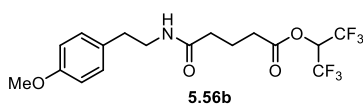
^{13}C NMR (126 MHz, CDCl_3) δ [ppm] = 171.5, 170.1, 138.8, 128.84, 128.78, 126.7, 120.5 (d, $J = 282.0$ Hz), 67.0–65.9 (m), 40.6, 35.7, 34.8, 32.4, 20.4.

^{19}F NMR (471 MHz, CDCl_3) δ [ppm] = -73.22 (d, $J = 6.3$ Hz).

HRMS-ESI: calcd. for $\text{C}_{16}\text{H}_{17}\text{F}_6\text{NO}_3\text{Na}$ [$\text{M} + \text{Na}$] $^+$: 408.1005; found: 408.1007.

FT-IR: ν [cm^{-1}] = 3309, 1967, 1645, 1543, 1282, 1268, 1107.

1,1,1,3,3,3-Hexafluoropropan-2-yl 5-((4-methoxyphenethyl)amino)-5-oxopentanoate (5.56b)



5.56b was prepared according to **General procedure M**, starting from 4-methoxyphenethylamine (200 mg, 1.32 mmol, 1.0 equiv.) and glutaric anhydride (151 mg, 1.32 mmol, 1.0 equiv.) in DMF (5.0 mL). The reaction mixture was subsequently treated with EDCI (506 mg, 2.65 mmol, 2.0 equiv.), DMAP (32.4 mg, 0.365 mmol, 0.2 equiv.) and HFIP (699 μ L, 6.62 mmol, 5.0 equiv.). Purification by silica gel column chromatography (pentane/EtOAc = 5:2) afforded **5.56b** (225 mg, 0.542 mmol, 41%) as a white solid.

$^1\text{H NMR}$ (500 MHz, CDCl_3) δ [ppm] = 7.08 (d, J = 8.6 Hz, 2H), 6.83 (d, J = 8.6 Hz, 2H), 5.78–5.73 (m, 1H), 5.63 (s, 1H), 3.77 (s, 3H), 3.46 (td, J = 7.0, 5.8 Hz, 2H), 2.74 (t, J = 7.0 Hz, 2H), 2.55 (t, J = 7.3 Hz, 2H), 2.18 (t, J = 7.2 Hz, 2H), 2.01–1.97 (m, 2H).

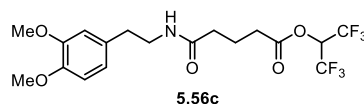
$^{13}\text{C NMR}$ (126 MHz, CDCl_3) δ [ppm] = 171.5, 170.0, 158.4, 130.8, 129.8, 120.5 (q, J = 279.4 Hz), 114.1, 67.0–65.9 (m), 55.30, 55.28, 40.8, 34.8, 32.4, 20.4.

$^{19}\text{F NMR}$ (471 MHz, CDCl_3) δ [ppm] = –73.25 (d, J = 8.6 Hz).

HRMS-ESI: calcd. for $\text{C}_{17}\text{H}_{19}\text{F}_6\text{NO}_4\text{Na}$ $[\text{M} + \text{Na}]^+$: 438.1110; found: 438.1109.

FT-IR: ν [cm^{-1}] 3299, 1767, 1636, 1542, 1282, 1257, 1202, 1107, 1038.

1,1,1,3,3,3-Hexafluoropropan-2-yl 5-((3,4-dimethoxyphenethyl)amino)-5-oxopentanoate (5.56c)



5.56c was prepared according to **General procedure M**, starting from 3,4-dimethoxyphenethylamine (500 mg, 2.76 mmol, 1.0 equiv.) and glutaric anhydride (315 mg, 2.76 mmol, 1.0 equiv.) in DMF (15.0 mL). The reaction mixture was subsequently treated with EDCI (1.05 g, 5.52 mmol, 2.0 equiv.), DMAP (67.5 mg, 0.552 mmol, 0.2 equiv.) and HFIP (1.46 mL, 13.8 mmol, 5.0 equiv.). Purification by silica gel column chromatography (pentane/EtOAc = 5:2) afforded **5.56c** (670 mg, 1.42 mmol, 55%) as a white solid.

$^1\text{H NMR}$ (500 MHz, CDCl_3) δ [ppm] = 6.79 (d, J = 8.7 Hz, 1H), 6.72–6.67 (m, 2H), 5.77–5.72 (m, 1H), 5.54 (s, 1H), 3.85 (d, J = 3.5 Hz, 6H), 3.49 (td, J = 7.0, 5.9 Hz, 2H), 2.74 (t, J = 7.0 Hz, 2H), 2.57 (t, J = 7.2 Hz, 2H), 2.18 (t, J = 7.2 Hz, 2H), 2.04–1.94 (m, 2H).

$^{13}\text{C NMR}$ (126 MHz, CDCl_3) δ [ppm] = 171.5, 170.0, 149.2, 147.9, 131.3, 120.7, 120.5 (q, J =

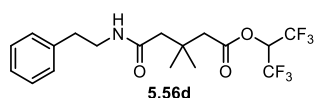
279.6 Hz), 111.9, 111.5, 67.0–65.9 (m), 56.0, 55.9, 40.8, 35.3, 34.8, 32.4, 20.4.

^{19}F NMR (565 MHz, CDCl_3) δ [ppm] = -73.22 (d, $J = 6.4$ Hz).

HRMS-ESI: calcd. for $\text{C}_{18}\text{H}_{21}\text{F}_6\text{NO}_5\text{Na}$ $[\text{M} + \text{Na}]^+$: 468.1216; found: 468.1217.

FT-IR: ν [cm^{-1}] = 2942, 1682, 1602, 1513, 1377, 1341, 1272, 1162, 752.

1,1,1,3,3,3-Hexafluoropropan-2-yl 3,3-dimethyl-5-oxo-5-(phenethylamino)pentanoate (5.56d)



5.56d was prepared according to **General procedure M**, starting from phenethylamine (300 mg, 2.48 mmol, 1.0 equiv.) and 3,3-dimethylglutaric anhydride (352 mg, 2.48 mmol, 1.0 equiv.) in DMF (10.0 mL). The reaction mixture was subsequently treated with EDCI (947 mg, 4.96 mmol, 2.0 equiv.), DMAP (60.6 mg, 0.496 mmol, 0.2 equiv.) and HFIP (1.31 mL, 12.4 mmol, 5.0 equiv.). Purification by silica gel column chromatography (pentane/EtOAc = 5:2) afforded **5.56d** (452 mg, 1.09 mmol, 44%) as a white solid.

^1H NMR (500 MHz, CDCl_3) δ [ppm] = 7.31–7.27 (m, 2H), 7.24–7.17 (m, 3H), 5.80–5.71 (m, 2H), 3.54 (td, $J = 7.0, 5.8$ Hz, 2H), 2.82 (t, $J = 6.9$ Hz, 2H), 2.50 (s, 2H), 2.17 (s, 2H), 1.08 (s, 6H).

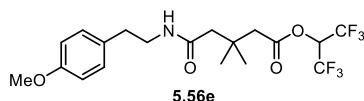
^{13}C NMR (126 MHz, CDCl_3) δ [ppm] = 170.6, 169.4, 138.9, 128.8, 128.8, 126.7, 120.5 (q, $J = 279.6$ Hz), 66.8–65.7 (m), 47.2, 43.7, 40.4, 35.7, 33.5, 28.0.

^{19}F NMR (471 MHz, CDCl_3) δ [ppm] = -73.02 (d, $J = 6.3$ Hz).

HRMS-ESI: calcd. for $\text{C}_{18}\text{H}_{21}\text{F}_6\text{NO}_3\text{Na}$ $[\text{M} + \text{Na}]^+$: 436.1318; found: 436.1335.

FT-IR: ν [cm^{-1}] = 3309, 1967, 1645, 1543, 1282, 1268, 1200, 1107.

1,1,1,3,3,3-Hexafluoropropan-2-yl 5-((4-methoxyphenethyl)amino)-3,3-dimethyl-5-oxopentanoate (5.56e)



5.56e was prepared according to **General procedure M**, starting from 4-

methoxyphenethylamine (300 mg, 1.99 mmol, 1.0 equiv.) and 3,3-dimethylglutaric anhydride (282 mg, 1.99 mmol, 1.0 equiv.) in DMF (10.0 mL). The reaction mixture was subsequently treated with EDCI (759 mg, 3.97 mmol, 2.0 equiv.), DMAP (48.5 mg, 0.397 mmol, 0.2 equiv.) and HFIP (1.05 mL, 9.93 mmol, 5.0 equiv.). Purification by silica gel column chromatography (pentane/EtOAc = 5:2) afforded **5.56e** (523 mg, 1.18 mmol, 59%) as a white solid.

¹H NMR (500 MHz, CDCl₃) δ [ppm] = 7.13–7.06 (m, 2H), 6.85–6.79 (m, 2H), 5.72–5.70 (m, 2H), 3.78 (s, 3H), 3.49 (td, *J* = 7.0, 5.8 Hz, 2H), 2.75 (t, *J* = 7.0 Hz, 2H), 2.53 (s, 2H), 2.17 (s, 2H), 1.08 (s, 6H).

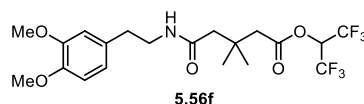
¹³C NMR (126 MHz, CDCl₃) δ [ppm] = 170.6, 169.4, 158.5, 130.8, 129.8, 120.6 (q, *J* = 291.0 Hz), 114.2, 66.6–66.0 (m), 55.3, 47.2, 43.7, 40.6, 34.8, 33.5, 28.0.

¹⁹F NMR (471 MHz, CDCl₃) δ [ppm] = –73.03 (d, *J* = 6.3 Hz).

HRMS-ESI: calcd. for C₁₉H₂₃F₆NO₄Na [M + Na]⁺: 466.1423; found: 466.1442.

FT-IR: ν [cm⁻¹] = 2970, 1738, 1515, 1440, 1366, 1217, 1105.

1,1,1,3,3,3-Hexafluoropropan-2-yl 5-((3,4-dimethoxyphenethyl)amino)-3,3-dimethyl-5-oxopentanoate (5.56f)



5.56f was prepared according to **General procedure M**, starting from 3,4-dimethoxyphenethylamine (500 mg, 2.76 mmol, 1.0 equiv.) and 3,3-dimethylglutaric anhydride (392 mg, 2.76 mmol, 1.0 equiv.) in DMF (15.0 mL). The reaction mixture was subsequently treated with EDCI (1.05 g, 5.52 mmol, 2.0 equiv.), DMAP (67.5 mg, 0.552 mmol, 0.2 equiv.) and HFIP (1.46 mL, 13.8 mmol, 5.0 equiv.). Purification by silica gel column chromatography (pentane/EtOAc = 5:2) afforded **5.56f** (670 mg, 1.42 mmol, 51%) as a white solid.

¹H NMR (500 MHz, CDCl₃) δ [ppm] = 6.80–6.77 (m, 1H), 6.71 (d, *J* = 7.6 Hz, 2H), 5.80–5.70 (m, 2H), 3.86 (s, 3H), 3.85 (s, 3H), 3.51 (td, *J* = 7.0, 5.8 Hz, 2H), 2.75 (t, *J* = 7.0 Hz, 2H), 2.54 (s, 2H), 2.18 (s, 2H), 1.08 (s, 6H).

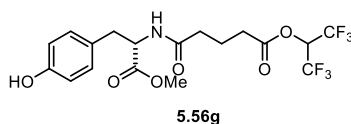
¹³C NMR (126 MHz, CDCl₃) δ [ppm] = 170.6, 169.4, 149.2, 147.8, 131.3, 120.7, 120.5 (q, *J* = 280.8 Hz), 111.8, 111.4, 66.5–65.7 (m), 56.0, 55.9, 47.2, 43.7, 40.5, 35.3, 33.5, 28.1.

^{19}F NMR (471 MHz, CDCl_3) δ [ppm] = -73.01 (d, $J = 6.5$ Hz).

HRMS-ESI: calcd. for $\text{C}_{20}\text{H}_{25}\text{F}_6\text{NO}_5\text{Na}$ $[\text{M} + \text{Na}]^+$: 496.1529; found: 496.1518.

FT-IR: ν [cm^{-1}] = 2371, 2354, 1649, 1518, 1288, 1243, 1107.

1,1,1,3,3,3-Hexafluoropropan-2-yl (*S*)-5-((3-(4-hydroxyphenyl)-1-methoxy-1-oxo-propan-2-yl)amino)-5-oxopentanoate (5.56g)



5.56g was prepared according to **General procedure M**, starting from (*S*)-tyrosine methyl ester (300 mg, 1.54 mmol, 1.0 equiv.) and glutaric anhydride (175 mg, 1.54 mmol, 1.0 equiv.) in DMF (10.0 mL). The reaction mixture was subsequently treated with EDCI (588 mg, 3.01 mmol, 2.0 equiv.), DMAP (37.6 mg, 0.308 mmol, 0.2 equiv.) and HFIP (813 μL , 7.69 mmol, 5.0 equiv.). Purification by silica gel column chromatography (pentane/EtOAc = 3:2) afforded **5.56g** (170 mg, 0.370 mmol, 24%) as a white solid.

^1H NMR (500 MHz, CDCl_3) δ [ppm] = 7.04 (s, 1H), 6.95–6.89 (m, 2H), 6.75–6.69 (m, 2H), 6.15 (d, $J = 8.1$ Hz, 1H), 5.79–5.74 (m, 1H), 4.85 (ddd, $J = 8.1, 6.4, 5.6$ Hz, 1H), 3.73 (s, 3H), 3.07 (dd, $J = 14.1, 5.5$ Hz, 1H), 2.95 (dd, $J = 14.1, 6.5$ Hz, 1H), 2.51 (td, $J = 7.3, 1.3$ Hz, 2H), 2.25 (t, $J = 7.5$ Hz, 2H), 1.99–1.93 (m, 2H).

^{13}C NMR (126 MHz, CDCl_3) δ [ppm] = 172.5, 172.0, 170.0, 155.7, 130.3, 127.0, 120.5 (q, $J = 284.3$ Hz), 115.7, 67.1–66.0 (m), 53.4, 52.6, 37.2, 34.7, 32.2, 20.2.

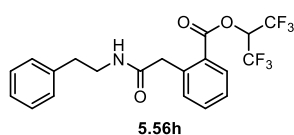
^{19}F NMR (471 MHz, CDCl_3) δ [ppm] = -73.24 (d, $J = 6.7$ Hz).

HRMS-ESI: calcd. for $\text{C}_{18}\text{H}_{19}\text{F}_6\text{NO}_6\text{K}$ $[\text{M} + \text{K}]^+$: 498.0749; found: 498.0774.

FT-IR: ν [cm^{-1}] = 2960, 1780, 1740, 1651, 1516, 1286, 1223, 1198, 1108, 905, 733.

$[\alpha]_{\text{D}}^{26} = +19.0$ ($c = 0.4$, CHCl_3).

1,1,1,3,3,3-Hexafluoropropan-2-yl 2-(2-oxo-2-(phenethylamino)ethyl)benzoate (5.56h)



5.56h was prepared according to **General procedure L**, starting from phenethylamine (250 mg,

2.07 mmol, 1.0 equiv.) and homophthalic anhydride (335 mg, 2.07 mmol, 1.0 equiv.) in DMF (10.0 mL). The reaction mixture was subsequently treated with EDCI (789 mg, 4.13 mmol, 2.0 equiv.), DMAP (50.5 mg, 0.413 mmol, 0.2 equiv.) and HFIP (1.09 mL, 10.3 mmol, 5.0 equiv.). Purification by silica gel column chromatography (pentane/EtOAc = 5:2) afforded **5.56h** (189 mg, 0.436 mmol, 21%) as a white solid.

¹H NMR (700 MHz, CDCl₃) δ [ppm] = 8.05 (dd, *J* = 8.0, 1.5 Hz, 1H), 7.59 (td, *J* = 7.6, 1.5 Hz, 1H), 7.45 (dd, *J* = 7.8, 1.3 Hz, 1H), 7.41 (td, *J* = 7.7, 1.3 Hz, 1H), 7.25–7.20 (m, 2H), 7.20–7.16 (m, 1H), 7.09–7.03 (m, 2H), 6.11 (t, *J* = 5.9 Hz, 1H), 5.96–5.92 (m, 1H), 3.84 (s, 2H), 3.47 (td, *J* = 7.0, 5.8 Hz, 2H), 2.75 (t, *J* = 7.0 Hz, 2H).

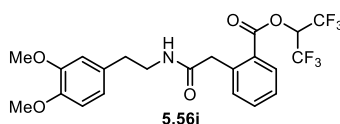
¹³C NMR (176 MHz, CDCl₃) δ [ppm] = 169.9, 163.8, 138.85, 138.78, 134.5, 132.8, 131.5, 128.7, 128.5, 127.7, 126.4, 125.8, 120.6 (q, *J* = 282.8 Hz), 67.5–66.3 (m), 42.0, 40.8, 35.5.

¹⁹F NMR (376 MHz, CDCl₃) δ [ppm] = –72.94 (d, *J* = 12.5 Hz).

HRMS-ESI: calcd. for C₂₀H₁₇F₆NO₃Na [M + Na]⁺: 456.1005; found: 456.1012.

FT-IR: *v* [cm⁻¹] = 3305, 1754, 1651, 1549, 1359, 1239, 1190, 1099, 1018, 914, 899, 714.

1,1,1,3,3,3-Hexafluoropropan-2-yl 2-(2-((3,4-dimethoxyphenethyl)amino)-2-oxoethyl)benzoate (5.56i)



5.56i was prepared according to **General procedure M**, starting from 3,4-dimethoxyphenethylamine (300 mg, 1.66 mmol, 1.0 equiv.) and homophthalic anhydride (268mg, 1.66 mmol, 1.0 equiv.) in DMF (10.0 mL). The reaction mixture was subsequently treated with EDCI (633 mg, 3.31 mmol, 2.0 equiv.), DMAP (40.5 mg, 0.331 mmol, 0.2 equiv.) and HFIP (1.39 mL, 8.29 mmol, 5.0 equiv.). Purification by silica gel column chromatography (pentane/EtOAc = 5:2) afforded **5.56i** (189 mg, 0.383 mmol, 23%) as a white solid.

¹H NMR (600 MHz, CDCl₃) δ [ppm] = 8.00 (dd, *J* = 7.9, 1.4 Hz, 1H), 7.55 (td, *J* = 7.6, 1.4 Hz, 1H), 7.40 (dd, *J* = 7.8, 1.3 Hz, 1H), 7.37 (td, *J* = 7.7, 1.3 Hz, 1H), 6.69 (d, *J* = 8.1 Hz, 1H), 6.63 (d, *J* = 2.0 Hz, 1H), 6.58 (dd, *J* = 8.1, 2.0 Hz, 1H), 6.07 (t, *J* = 5.8 Hz, 1H), 5.96–5.90 (m, 1H), 3.81 (s, 2H), 3.80 (s, 3H), 3.79 (s, 3H), 3.42 (td, *J* = 7.1, 5.7 Hz, 2H), 2.67 (t, *J* = 7.1 Hz, 2H).

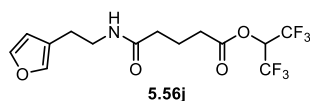
^{13}C NMR (151 MHz, CDCl_3) δ [ppm] = 169.8, 163.7, 148.9, 147.6, 138.7, 134.4, 132.7, 131.4, 131.3, 127.6, 125.7, 120.6, 120.5 (q, $J = 286.3$ Hz), 111.9, 111.2, 67.3–66.4 (m), 55.8, 55.7, 41.9, 40.8, 35.0.

^{19}F NMR (565 MHz, CDCl_3) δ [ppm] = -72.99 (d, $J = 6.9$ Hz).

HRMS-ESI: calcd. for $\text{C}_{22}\text{H}_{21}\text{F}_6\text{NO}_5\text{Na}$ $[\text{M} + \text{Na}]^+$: 516.1216; found: 516.1201.

FT-IR: ν [cm^{-1}] = 2937, 1755, 1652, 1515, 1237, 1194, 1109, 1096, 1025, 913, 715.

1,1,1,3,3,3-Hexafluoropropan-2-yl 5-((2-(furan-3-yl)ethyl)amino)-5-oxopentanoate (**5.56j**)



5.56j was prepared according to **General procedure M**, starting from 2-(furan-3-yl)ethan-1-amine (180 mg, 1.62 mmol, 1.0 equiv.) and glutaric anhydride (185 mg, 1.62 mmol, 1.0 equiv.) in DMF (5.0 mL). The reaction mixture was subsequently treated with EDCI (620 mg, 3.24 mmol, 2.0 equiv.), DMAP (39.6 mg, 0.324 mmol, 0.2 equiv.) and HFIP (857 μL , 8.11 mmol, 5.0 equiv.). Purification by silica gel column chromatography (pentane/EtOAc = 5:2) afforded **5.56j** (200 mg, 0.533 mmol, 33%) as a light yellow solid.

^1H NMR (700 MHz, CDCl_3) δ [ppm] = 7.36 (t, $J = 1.7$ Hz, 1H), 7.25–7.24 (m, 1H), 6.27 (dd, $J = 1.9, 0.9$ Hz, 1H), 5.77–5.73 (m, 1H), 5.63 (s, 1H), 3.44 (td, $J = 6.9, 5.8$ Hz, 2H), 2.62 (td, $J = 6.9, 1.0$ Hz, 2H), 2.56 (t, $J = 7.3$ Hz, 2H), 2.20 (t, $J = 7.3$ Hz, 2H), 2.01–1.97 (m, 2H).

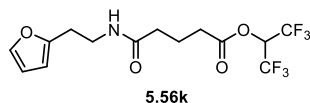
^{13}C NMR (176 MHz, CDCl_3) δ [ppm] = 171.5, 170.0, 143.4, 139.7, 121.8, 120.5 (q, $J = 282.0$ Hz), 110.8, 66.9–66.1 (m), 39.5, 34.8, 32.4, 25.0, 20.4.

^{19}F NMR (565 MHz, CDCl_3) δ [ppm] = -73.29 (d, $J = 6.5$ Hz).

HRMS-ESI: calcd. for $\text{C}_{14}\text{H}_{15}\text{F}_6\text{NO}_4\text{Na}$ $[\text{M} + \text{Na}]^+$: 398.0797; found: 398.0811.

FT-IR: ν [cm^{-1}] = 2920, 2850, 1780, 1659, 1447, 1386, 1288, 1227, 1198, 1110, 924, 789.

1,1,1,3,3,3-Hexafluoropropan-2-yl 5-((2-(furan-2-yl)ethyl)amino)-5-oxopentanoate (**5.56k**)



5.56k was prepared according to **General procedure M**, starting from 2-(furan-2-yl)ethan-1-

amine (180 mg, 1.62 mmol, 1.0 equiv.) and glutaric anhydride (185 mg, 1.62 mmol, 1.0 equiv.) in DMF (5.0 mL). The reaction mixture was subsequently treated with EDCI (620 mg, 3.24 mmol, 2.0 equiv.), DMAP (39.6 mg, 0.324 mmol, 0.2 equiv.) and HFIP (857 μ L, 8.11 mmol, 5.0 equiv.). Purification by silica gel column chromatography (pentane/EtOAc = 3:2) afforded **5.56k** (250 mg, 0.667 mmol, 41%) as a light yellow solid.

¹H NMR (700 MHz, CDCl₃) δ [ppm] = 7.33 (dd, J = 1.9, 0.8 Hz, 1H), 6.32–6.28 (m, 1H), 6.07–6.06 (m, 1H), 5.78–5.74 (m, 1H), 5.58 (s, 1H), 3.59–3.49 (m, 2H), 2.85 (td, J = 6.5, 0.8 Hz, 2H), 2.58 (t, J = 7.3 Hz, 2H), 2.22 (t, J = 7.2 Hz, 2H), 2.06–1.97 (m, 2H).

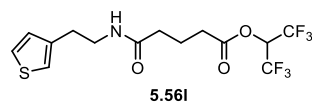
¹³C NMR (176 MHz, CDCl₃) δ [ppm] = 171.5, 170.1, 153.1, 141.8, 120.6 (d, J = 281.9 Hz), 110.5, 106.6, 66.7–66.3 (m), 38.3, 34.9, 32.4, 28.2, 20.4.

¹⁹F NMR (376 MHz, CDCl₃) δ [ppm] = –73.19 (d, J = 6.0 Hz).

HRMS-ESI: calcd. for C₁₄H₁₅F₆NO₄Na [M + Na]⁺: 398.0797; found: 398.0786.

FT-IR: ν [cm⁻¹] = 3314, 2930, 1781, 1647, 1551, 1386, 1288, 1232, 1200, 1111, 907, 780.

1,1,1,3,3,3-Hexafluoropropan-2-yl 5-oxo-5-((2-(thiophen-3-yl)ethyl)amino)pentanoate (5.56l)



5.56l was prepared according to **General procedure M**, starting from 2-(thiophen-3-yl)ethan-1-amine (150 mg, 1.18 mmol, 1.0 equiv.) and glutaric anhydride (135 mg, 1.18 mmol, 1.0 equiv.) in DMF (5.0 mL). The reaction mixture was subsequently treated with EDCI (451 mg, 2.36 mmol, 2.0 equiv.), DMAP (28.9 mg, 0.236 mmol, 0.2 equiv.) and HFIP (624 μ L, 5.91 mmol, 5.0 equiv.). Purification by silica gel column chromatography (pentane/EtOAc = 3:2) afforded **5.56l** (200 mg, 0.512 mmol, 43%) as a white solid.

¹H NMR (500 MHz, CDCl₃) δ [ppm] = 7.29–7.24 (m, 1H), 6.97–6.98 (m, 1H), 6.93 (dd, J = 4.9, 1.3 Hz, 1H), 5.77–5.71 (m, 1H), 5.63 (s, 1H), 3.53–3.48 (m, 2H), 2.83 (t, J = 6.9 Hz, 2H), 2.54 (td, J = 7.2, 0.8 Hz, 2H), 2.18 (t, J = 7.2 Hz, 2H), 2.05–1.93 (m, 2H).

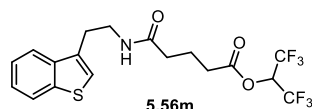
¹³C NMR (126 MHz, CDCl₃) δ [ppm] = 171.5, 170.0, 139.1, 128.1, 126.2, 121.5, 120.5 (q, J = 282.0 Hz), 67.0–65.9 (m), 39.9, 34.8, 32.3, 30.3, 20.4.

^{19}F NMR (471 MHz, CDCl_3) δ [ppm] = -73.24 (d, $J = 6.4$ Hz).

HRMS-ESI: calcd. for $\text{C}_{14}\text{H}_{15}\text{F}_6\text{NO}_3\text{SK}$ $[\text{M} + \text{K}]^+$: 430.0309; found: 430.0328.

FT-IR: ν [cm^{-1}] = 3319, 1770, 1638, 1534, 1385, 1281, 1201, 1106, 720.

1,1,1,3,3,3-Hexafluoropropan-2-yl 5-((2-(benzo[*b*]thiophen-3-yl)ethyl)amino)-5-oxopentanoate (5.56m)



5.56m was prepared according to **General procedure M**, starting from 2-(benzo[*b*]thiophen-3-yl)ethan-1-amine (140 mg, 0.791 mmol, 1.0 equiv.) and glutaric anhydride (90.2 mg, 0.791 mmol, 1.0 equiv.) in DMF (3.0 mL). The reaction mixture was subsequently treated with EDCI (302 mg, 1.58 mmol, 2.0 equiv.), DMAP (19.3 mg, 0.158 mmol, 0.2 equiv.) and HFIP (418 μL , 3.95 mmol, 5.0 equiv.). Purification by silica gel column chromatography (pentane/EtOAc = 2:1) afforded **5.56m** (183 mg, 0.415 mmol, 52%) as a white solid.

^1H NMR (700 MHz, CDCl_3) δ [ppm] = 7.86 (dt, $J = 7.8, 1.0$ Hz, 1H), 7.77 (dt, $J = 8.0, 1.0$ Hz, 1H), 7.39 (ddd, $J = 8.0, 7.0, 1.2$ Hz, 1H), 7.35 (ddd, $J = 8.2, 7.0, 1.3$ Hz, 1H), 7.14 (s, 1H), 5.80–5.73 (m, 2H), 3.60 (td, $J = 7.0, 5.9$ Hz, 2H), 3.05 (td, $J = 6.9, 1.0$ Hz, 2H), 2.55 (t, $J = 7.3$ Hz, 2H), 2.17 (t, $J = 7.3$ Hz, 2H), 2.01–1.97 (m, 2H).

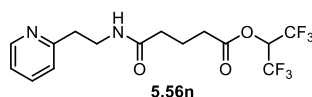
^{13}C NMR (176 MHz, CDCl_3) δ [ppm] = 171.6, 170.0, 140.6, 138.8, 133.4, 124.5, 124.2, 123.0, 122.5, 121.6, 120.5 (q, $J = 282.7$ Hz), 66.9–66.1 (m), 39.1, 34.8, 32.4, 28.7, 20.3.

^{19}F NMR (376 MHz, CDCl_3) δ [ppm] = -73.20 . (It should be a doublet peak, but due to the resolution, only singlet peak was observed.)

HRMS-ESI: calcd. for $\text{C}_{18}\text{H}_{17}\text{F}_6\text{NO}_3\text{SNa}$ $[\text{M} + \text{Na}]^+$: 464.0725; found: 464.0745.

FT-IR: ν [cm^{-1}] = 2928, 2850, 1736, 1698, 1215, 747.

1,1,1,3,3,3-Hexafluoropropan-2-yl 5-oxo-5-((2-(pyridin-2-yl)ethyl)amino)pentanoate (5.56n)



5.56n was prepared according to **General procedure M**, starting from 2-(pyridin-2-yl)ethan-1-amine (300 mg, 2.46 mmol, 1.0 equiv.) and glutaric anhydride (280 mg, 2.46 mmol, 1.0 equiv.) in DMF (10.0 mL). The reaction mixture was subsequently treated with EDCI (939 mg, 4.92 mmol, 2.0 equiv.), DMAP (60.1 mg, 0.492 mmol, 0.2 equiv.) and HFIP (1.30 mL, 12.3 mmol, 5.0 equiv.). Purification by silica gel column chromatography (pentane/EtOAc = 3:2) afforded **5.56n** (670 mg, 1.51 mmol, 61%) as a colorless oil.

¹H NMR (500 MHz, CDCl₃) δ [ppm] = 8.44 (ddd, J = 4.9, 1.9, 0.9 Hz, 1H), 7.56 (td, J = 7.7, 1.9 Hz, 1H), 7.14–7.06 (m, 2H), 6.75 (s, 1H), 5.74–5.69 (m, 1H), 3.60 (dt, J = 6.6, 5.7 Hz, 2H), 2.98–2.89 (m, 2H), 2.50 (t, J = 7.4 Hz, 2H), 2.17 (t, J = 7.2 Hz, 2H), 2.02–1.88 (m, 2H).

¹³C NMR (126 MHz, CDCl₃) δ [ppm] = 171.5, 170.0, 159.6, 149.1, 136.7, 123.5, 121.6, 120.4 (q, J = 279.4 Hz), 66.9–65.8 (m), 38.7, 36.9, 34.9, 32.4, 20.4.

¹⁹F NMR (471 MHz, CDCl₃) δ [ppm] = –73.19 (d, J = 6.5 Hz).

HRMS-ESI: calcd. for C₁₅H₁₆F₆N₂O₃Na [M + Na]⁺: 409.0957; found: 409.0972.

FT-IR: ν [cm⁻¹] = 2950, 1781, 1652, 1288, 1230, 1199, 1110, 747.

7.2.4.2. One-pot annulation reaction

7.2.4.2.1. Reaction optimization

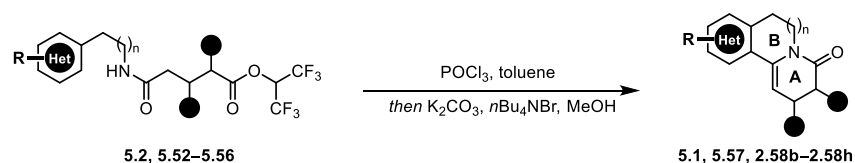
Table 7–1: Optimization of the annulation.

8a: R = methoxy
8b: R = 4-nitrophenoxy
8c: R = 2-propoxy
8d: R = 2-hexafluoropropoxy
8e: R = 2,2,2-trifluoroethoxy
8f: R = 2,2,2-trifluoro-1-methylethoxy
8g: R = pentafluorophenoxy
8h: R = prenyloxy
8i: R = diphenylmethoxy
8j: R = cyclohexyloxy
8k: R = cyclohexylthio
8l: R = *t*-butoxy

entry	substrate	base or acid	yield
1	8a	K ₂ CO ₃	18
2	8a	Cs ₂ CO ₃	4
3	8a	KOH	6
4	8a	TMSOK	6
5	8a	KOt-Bu	15
6	8a	ZrCl ₄	N.D. ^[a]
7	8a	In(OTf) ₂	N.D.
8	8a	Sc(OTf) ₃	N.D.
9	8a	Ti(O <i>i</i> -Pr) ₄	N.D.
10	8a	<i>p</i> -TsOH	N.D.
11	8b	K ₂ CO ₃ , Bu ₄ NBr	62
12	8c	K ₂ CO ₃ , Bu ₄ NBr	18
13	8d	K ₂ CO ₃ , Bu ₄ NBr	90
14	8e	K ₂ CO ₃ , Bu ₄ NBr	42
15	8f	K ₂ CO ₃ , Bu ₄ NBr	41
16	8g	K ₂ CO ₃ , Bu ₄ NBr	65
17	8h	K ₂ CO ₃ , Bu ₄ NBr	20
18	8i	K ₂ CO ₃ , Bu ₄ NBr	47
19	8j	K ₂ CO ₃ , Bu ₄ NBr	32
20	8k	K ₂ CO ₃ , Bu ₄ NBr	42
21	8l	K ₂ CO ₃ , Bu ₄ NBr	30

[a] Not determined

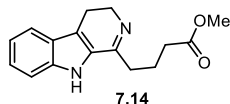
7.2.4.2.2. Substrate scope

General procedure O


To a solution of the substrate (1.0 equiv.) in toluene was added POCl₃ (1.0 equiv.) dropwise. Then the mixture was heated to 115 °C (oil bath temperature) until the starting material was fully consumed. After allowing the mixture to cool down to 80 °C (oil bath temperature), the same volume of MeOH, K₂CO₃ (10.0 equiv.) and *n*Bu₄NBr (0.1 equiv.) were added subsequently. Afterwards the resulting mixture was stirred overnight at 80 °C, cooled to room temperature, filtered through Celite[®], concentrated under reduced pressure, and purified by

silica gel or neutral aluminium oxide column chromatography. (Note: It is not necessary to perform the reaction under argon.)

Methyl 4-(4,9-dihydro-3*H*-pyrido[3,4-*b*]indol-1-yl)butanoate (**7.14**)



To a solution of the substrate **5.2** (100 mg, 0.347 mmol, 1.0 equiv.) in toluene (3.0 mL), was added POCl₃ (31.7 μL, 0.347 mmol, 1.0 equiv.). The mixture was heated to 115 °C (oil bath temperature) until the starting material was fully consumed. Then the mixture was concentrated under reduced pressure and purified by silica gel flash column chromatography (DCM/MeOH=10:1). **7.14** (79.0 mg, 0.293 mmol, 84%) was afforded as a dark yellow solid.

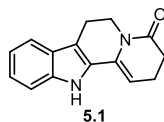
¹H NMR (500 MHz, CDCl₃) δ [ppm] = 11.39 (s, 1H), 7.63 (d, *J* = 8.2 Hz, 1H), 7.59 (dd, *J* = 8.5, 0.9 Hz, 1H), 7.46 (ddd, *J* = 8.4, 6.9, 1.2 Hz, 1H), 7.22 (ddd, *J* = 8.1, 6.9, 1.4 Hz, 1H), 4.02 (t, *J* = 8.8 Hz, 2H), 3.76 (s, 3H), 3.36–3.28 (m, 2H), 3.26–3.19 (m, 2H), 2.66–2.57 (m, 2H), 2.24–2.10 (m, 2H).

¹³C NMR (126 MHz, CDCl₃) δ [ppm] = 173.9, 169.3, 141.7, 129.1, 125.7, 124.3, 124.0, 122.0, 121.4, 114.1, 52.0, 42.4, 32.8, 31.7, 23.4, 19.5.

HRMS-ESI: calcd. for C₁₆H₁₉N₂O₂ [M + H]⁺: 271.1441; found: 271.1455.

FT-IR: ν [cm⁻¹] = 2925, 1733, 1630, 1554, 1434, 1336, 1229, 747.

2,6,7,12-Tetrahydroindolo[2,3-*a*]quinolizin-4(3*H*)-one (**5.1**)



5.1 was prepared according to **General procedure O**, starting from **5.39o** (100 mg, 0.236 mmol, 1.0 equiv.) and POCl₃ (21.5 μL, 0.236 mmol, 1.0 equiv.) in toluene (3.0 mL). The reaction mixture was subsequently treated with MeOH (3.0 mL), K₂CO₃ (326 mg, 2.36 mmol, 10 equiv.) and *n*Bu₄NBr (7.6 mg, 24.0 μmol, 0.1 equiv.). Purification by silica gel column chromatography (pentane/EtOAc = 2:1) afforded **5.1** (51.0 mg, 0.214 mmol, 90%) as a yellow solid.

Scale-up reaction starting from **5.39o** (2.00 g, 4.72 mmol, 1.0 equiv.) and POCl₃ (430 μL,

4.72 mmol, 1.0 equiv.) in toluene (80 mL). The reaction mixture was subsequently treated with MeOH (80 mL), K₂CO₃ (6.52 g, 47.2 mmol, 10 equiv.) and *n*Bu₄NBr (152 mg, 0.472 mmol, 0.1 equiv.). Purification by silica gel column chromatography (pentane/EtOAc = 2:1) afforded **5.1** (910 mg, 3.82 mmol, 81%) as a yellow solid.

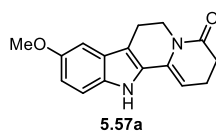
¹H NMR (500 MHz, CDCl₃) δ [ppm] = 7.97 (s, 1H), 7.53–7.51 (m, 1H), 7.34 (dt, *J* = 8.2, 0.9 Hz, 1H), 7.23 (ddd, *J* = 8.2, 7.0, 1.1 Hz, 1H), 7.12 (ddd, *J* = 8.0, 7.1, 1.0 Hz, 1H), 5.49 (t, *J* = 5.0 Hz, 1H), 4.11 (t, *J* = 6.0 Hz, 2H), 2.91 (t, *J* = 6.0 Hz, 2H), 2.70–2.59 (m, 2H), 2.53–2.42 (m, 2H).

¹³C NMR (126 MHz, CDCl₃) δ [ppm] = 169.8, 137.3, 131.4, 128.1, 126.9, 123.6, 120.2, 119.1, 112.0, 111.1, 99.4, 39.3, 31.9, 20.8, 19.6.

HRMS-ESI: calcd. for C₁₅H₁₅N₂O [M + H]⁺: 239.1179; found: 239.1179.

FT-IR: ν [cm⁻¹] = 3287, 2926, 1636, 1436, 1400, 1232, 1214, 742.

9-Methoxy-2,6,7,12-tetrahydroindolo[2,3-*a*]quinolizin-4(3*H*)-one (**5.57a**)



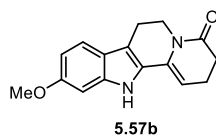
5.57a was prepared according to **General procedure O**, starting from **5.52a** (100 mg, 0.220 mmol, 1.0 equiv.) and POCl₃ (20.1 μ L, 0.220 mmol, 1.0 equiv.) in toluene (3.0 mL). The reaction mixture was subsequently treated with MeOH (3.0 mL), K₂CO₃ (304 mg, 2.20 mmol, 10 equiv.) and *n*Bu₄NBr (7.1 mg, 22.0 μ mol, 0.1 equiv.). Purification by silica gel column chromatography (pentane/EtOAc = 2:1) afforded **5.57a** (45.0 mg, 0.168 mmol, 76%) as a yellow solid.

¹H NMR (500 MHz, CDCl₃) δ [ppm] = 8.15 (s, 1H), 7.22 (dd, *J* = 8.8, 0.6 Hz, 1H), 6.94 (d, *J* = 2.5 Hz, 1H), 6.87 (dd, *J* = 8.8, 2.5 Hz, 1H), 5.51 (t, *J* = 4.9 Hz, 1H), 4.11 (t, *J* = 6.0 Hz, 2H), 3.86 (s, 3H), 2.88 (t, *J* = 6.0 Hz, 2H), 2.63 (t, *J* = 7.8 Hz, 2H), 2.45 (td, *J* = 7.7, 4.9 Hz, 2H).

¹³C NMR (126 MHz, CDCl₃) δ [ppm] = 169.9, 154.5, 132.4, 131.4, 128.9, 127.2, 113.8, 111.9, 111.8, 100.8, 99.2, 56.0, 39.3, 31.9, 20.8, 19.6.

HRMS-ESI: calcd. for C₁₆H₁₆N₂O₂Na [M + Na]⁺: 291.1104; found: 291.1105.

FT-IR: ν [cm⁻¹] = 3308, 2927, 2834, 1665, 1639, 1487, 1396, 1214, 1170, 1025, 801, 753.

10-methoxy-2,6,7,12-tetrahydroindolo[2,3-*a*]quinolizin-4(3*H*)-one (5.57b)

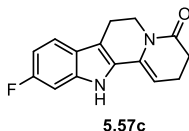
5.57b was prepared according to **General procedure O**, starting from **5.52b** (80.0 mg, 0.176 mmol, 1.0 equiv.) and POCl₃ (16.1 μL, 0.176 mmol, 1.0 equiv.) in toluene (3.0 mL). The reaction mixture was subsequently treated with MeOH (3.0 mL), K₂CO₃ (243 mg, 1.76 mmol, 10 equiv.) and *n*Bu₄NBr (5.7 mg, 18.0 μmol, 0.1 equiv.). Purification by silica gel column chromatography (pentane/EtOAc = 2:1) afforded **5.57b** (40.0 mg, 0.149 mmol, 85%) as a yellow solid.

¹H NMR (500 MHz, CD₂Cl₂) δ [ppm] = 8.12 (s, 1H), 7.37 (d, *J* = 8.6 Hz, 1H), 6.85 (d, *J* = 2.3 Hz, 1H), 6.75 (dd, *J* = 8.6, 2.3 Hz, 1H), 5.45 (t, *J* = 4.9 Hz, 1H), 4.05 (t, *J* = 6.0 Hz, 2H), 3.83 (s, 3H), 2.85 (t, *J* = 6.0 Hz, 2H), 2.57 (t, *J* = 7.7 Hz, 2H), 2.44 (td, *J* = 7.7, 4.9 Hz, 2H).

¹³C NMR (126 MHz, CD₂Cl₂) δ [ppm] = 169.8, 158.0, 138.7, 131.7, 127.6, 121.6, 119.9, 112.2, 110.1, 98.5, 95.0, 55.9, 39.4, 32.3, 21.1, 19.9.

HRMS-ESI: calcd. for C₁₆H₁₇N₂O₂ [M + H]⁺: 269.1284; found: 269.1284.

FT-IR: ν [cm⁻¹] = 3309, 2930, 2835, 1665, 1639, 1487, 1397, 1214, 1170, 1043, 1025, 754.

10-Fluoro-2,6,7,12-tetrahydroindolo[2,3-*a*]quinolizin-4(3*H*)-one (5.57c)

5.57c was prepared according to **General procedure O**, starting from **5.52c** (100 mg, 0.226 mmol, 1.0 equiv.) and POCl₃ (20.6 μL, 0.226 mmol, 1.0 equiv.) in toluene (3.0 mL). The reaction mixture was subsequently treated with MeOH (3.0 mL), K₂CO₃ (313 mg, 2.26 mmol, 10 equiv.) and *n*Bu₄NBr (7.3 mg, 23.0 μmol, 0.1 equiv.). Purification by silica gel column chromatography (pentane/EtOAc = 2:1) afforded **5.57c** (49.0 mg, 0.184 mmol, 81%) as a yellow solid.

¹H NMR (700 MHz, *d*₆-DMSO) δ [ppm] = 11.36 (s, 1H), 7.46 (dd, *J* = 8.6, 5.5 Hz, 1H), 7.09 (dd, *J* = 10.0, 2.3 Hz, 1H), 6.86 (ddd, *J* = 9.8, 8.6, 2.4 Hz, 1H), 5.83 (t, *J* = 4.9 Hz, 1H), 3.93 (t,

$J = 5.9$ Hz, 2H), 2.80 (t, $J = 6.0$ Hz, 2H), 2.48 (t, $J = 8.0$ Hz, 2H), 2.38 (ddd, $J = 8.0, 6.6, 3.2$ Hz, 2H).

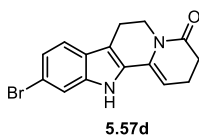
^{13}C NMR (176 MHz, d_6 -DMSO) δ [ppm] = 168.5, 159.6 (d, $J = 235.6$ Hz), 137.2 (d, $J = 12.7$ Hz), 130.7, 129.0, 122.9, 119.7 (d, $J = 10.7$ Hz), 109.9, 107.4 (d, $J = 24.3$ Hz), 100.1, 97.2 (d, $J = 25.8$ Hz), 38.4, 31.2, 20.1, 18.9.

^{19}F NMR (471 MHz, d_6 -DMSO) δ [ppm] = -119.64 (d, $J = 11.5$ Hz).

HRMS-ESI: calcd. for $\text{C}_{15}\text{H}_{13}\text{FN}_2\text{ONa}$ [$\text{M} + \text{Na}$] $^+$: 279.0904; found: 279.0904.

FT-IR: ν [cm^{-1}] = 2954, 2920, 1681, 1457, 1329, 1205, 1174, 1043, 745.

10-Bromo-2,6,7,12-tetrahydroindolo[2,3-*a*]quinolizin-4(3*H*)-one (5.57d)



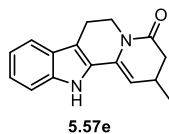
5.57d was prepared according to **General procedure O**, starting from **5.52d** (37.0 mg, 74.0 μmol , 1.0 equiv.) and POCl_3 (6.7 μL , 74.0 μmol , 1.0 equiv.) in toluene (2.0 mL). The reaction mixture was subsequently treated with MeOH (2.0 mL), K_2CO_3 (99.0 mg, 740 μmol , 10 equiv.) and $n\text{Bu}_4\text{NBr}$ (2.4 mg, 7.0 μmol , 0.1 equiv.). Purification by silica gel column chromatography (pentane/EtOAc = 2:1) afforded **5.57d** (20.0 mg, 63.0 μmol , 86%) as a yellow solid.

^1H NMR (700 MHz, d_6 -DMSO) δ [ppm] = 11.42 (s, 1H), 7.48 (dd, $J = 1.8, 0.6$ Hz, 1H), 7.44 (d, $J = 8.4$ Hz, 1H), 7.13 (dd, $J = 8.4, 1.8$ Hz, 1H), 5.87 (t, $J = 4.9$ Hz, 1H), 3.93 (t, $J = 5.9$ Hz, 2H), 2.81 (t, $J = 6.0$ Hz, 2H), 2.48 (d, $J = 7.7$ Hz, 2H), 2.42–2.36 (m, 2H).

^{13}C NMR (176 MHz, d_6 -DMSO) δ [ppm] = 168.4, 138.0, 130.5, 129.2, 125.1, 121.9, 120.3, 115.1, 113.6, 110.0, 100.9, 38.4, 31.1, 20.1, 18.9.

HRMS-ESI: calcd. for $\text{C}_{15}\text{H}_{12}\text{BrN}_2\text{O}$ [$\text{M} - \text{H}$] $^-$: 315.0138; found: 315.0127.

FT-IR: ν [cm^{-1}] = 2961, 2926, 1667, 1652, 1458, 1390, 1213, 1180, 1045, 1180, 1045, 798, 749.

2-Methyl-2,6,7,12-tetrahydroindolo[2,3-*a*]quinolizin-4(3*H*)-one (5.57e)

5.57e was prepared according to **General procedure O**, starting from **5.53a** (150 mg, 0.342 mmol, 1.0 equiv.) and POCl₃ (31.3 μL, 0.342 mmol, 1.0 equiv.) in toluene (4.0 mL). The reaction mixture was subsequently treated with MeOH (4.0 mL), K₂CO₃ (473 mg, 3.42 mmol, 10 equiv.) and *n*Bu₄NBr (11.0 mg, 34.0 μmol, 0.1 equiv.). Purification by silica gel column chromatography (pentane/EtOAc = 2:1) afforded **5.57e** (70.0 mg, 0.258 mmol, 75%) as a yellow solid.

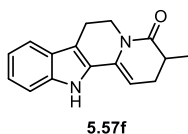
Scale-up reaction starting from **5.53a** (1.00 g, 2.28 mmol, 1.0 equiv.) and POCl₃ (208 μL, 2.28 mmol, 1.0 equiv.) in toluene (30 mL). The reaction mixture was subsequently treated with MeOH (30 mL), K₂CO₃ (3.15 g, 22.8 mmol, 10 equiv.) and *n*Bu₄NBr (73.6 mg, 0.228 mmol, 0.1 equiv.). Purification by silica gel column chromatography (pentane/EtOAc = 2:1) afforded **5.57e** (405 mg, 1.61 mmol, 70%) as a yellow solid.

¹H NMR (500 MHz, CDCl₃) δ [ppm] = 8.43 (s, 1H), 7.51 (d, *J* = 7.9 Hz, 1H), 7.34 (dd, *J* = 8.2, 1.1 Hz, 1H), 7.24–7.19 (m, 1H), 7.15–7.09 (m, 1H), 5.45 (t, *J* = 4.0 Hz, 1H), 4.44–4.38 (m, 1H), 3.84–3.78 (m, 1H), 2.98–2.84 (m, 2H), 2.81–2.65 (m, 2H), 2.39–2.33 (m, 1H), 1.17 (d, *J* = 6.9 Hz, 3H).

¹³C NMR (126 MHz, CDCl₃) δ [ppm] = 169.8, 137.4, 130.1, 128.0, 126.8, 123.6, 120.1, 119.1, 112.1, 111.1, 106.0, 40.0, 39.3, 26.2, 20.8, 20.4.

HRMS-ESI: calcd. for C₁₆H₁₇N₂O [M + H]⁺: 253.1335; found: 253.1335.

FT-IR: ν [cm⁻¹] = 3286, 1638, 1399, 1328, 1303, 1213, 1180, 742.

3-Methyl-2,6,7,12-tetrahydroindolo[2,3-*a*]quinolizin-4(3*H*)-one (5.57f)

5.57f was prepared according to **General procedure O**, starting from **5.53b** (132 mg, 0.301 mmol, 1.0 equiv.) and POCl₃ (27.5 μL, 0.301 mmol, 1.0 equiv.) in toluene (3.5 mL). The

reaction mixture was subsequently treated with MeOH (3.5 mL), K₂CO₃ (416 mg, 3.01 mmol, 10 equiv.) and *n*Bu₄NBr (9.7 mg, 30.0 μmol, 0.1 equiv.). Purification by silica gel column chromatography (pentane/EtOAc = 2:1) afforded **5.57f** (55.0 mg, 0.218 mmol, 72%) as a yellow solid.

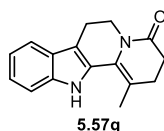
¹H NMR (700 MHz, CD₂Cl₂) δ [ppm] = 8.68 (s, 1H), 7.52–7.51 (m, 1H), 7.36 (dt, *J* = 8.1, 0.9 Hz, 1H), 7.21 (ddd, *J* = 8.2, 7.0, 1.2 Hz, 1H), 7.10 (ddd, *J* = 8.0, 7.0, 1.0 Hz, 1H), 5.61 (dd, *J* = 5.9, 4.0 Hz, 1H), 4.50 (dt, *J* = 12.7, 5.1 Hz, 1H), 3.72–3.68 (m, 1H), 2.95–2.85 (m, 2H), 2.67–2.60 (m, 1H), 2.51 (ddd, *J* = 16.9, 6.6, 5.9 Hz, 1H), 2.24 (ddd, *J* = 16.9, 11.4, 4.1 Hz, 1H), 1.27 (d, *J* = 6.9 Hz, 3H).

¹³C NMR (176 MHz, CD₂Cl₂) δ [ppm] = 173.1, 137.7, 131.3, 128.7, 127.1, 123.6, 120.2, 119.2, 111.8, 111.4, 99.2, 39.9, 36.1, 28.0, 21.1, 16.1.

HRMS-ESI: calcd. for C₁₆H₁₆N₂ONa [M + Na]⁺: 275.1155; found: 275.1161.

FT-IR: ν [cm⁻¹] = 3275, 1638, 1452, 1398, 1328, 1303, 1213, 1180, 742.

1-Methyl-2,6,7,12-tetrahydroindolo[2,3-*a*]quinolizin-4(3*H*)-one (**5.57g**)



5.57g was prepared according to **General procedure O**, starting from **5.53c** (108 mg, 0.247 mmol, 1.0 equiv.) and POCl₃ (22.5 μL, 0.247 mmol, 1.0 equiv.) in toluene (3.0 mL). The reaction mixture was subsequently treated with MeOH (3.0 mL), K₂CO₃ (341 mg, 2.47 mmol, 10 equiv.) and *n*Bu₄NBr (7.9 mg, 25.0 μmol, 0.1 equiv.). Purification by silica gel column chromatography (pentane/EtOAc = 2:1) afforded **5.57g** (40.0 mg, 0.159 mmol, 64%) as a yellow solid.

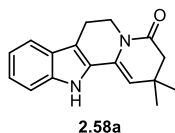
¹H NMR (700 MHz, CD₂Cl₂) δ [ppm] = 8.42 (s, 1H), 7.54–7.52 (m, 1H), 7.41 (dt, *J* = 8.1, 0.9 Hz, 1H), 7.20 (ddd, *J* = 8.2, 7.0, 1.2 Hz, 1H), 7.12 (ddd, *J* = 8.0, 7.0, 1.0 Hz, 1H), 4.05 (t, *J* = 5.9 Hz, 2H), 2.88 (t, *J* = 5.9 Hz, 2H), 2.57–2.48 (m, 2H), 2.47–2.41 (m, 2H), 2.29 (d, *J* = 1.3 Hz, 3H).

¹³C NMR (176 MHz, CD₂Cl₂) δ [ppm] = 169.6, 137.4, 129.4, 126.5, 126.3, 123.3, 120.4, 119.0, 113.1, 112.8, 111.4, 39.7, 32.0, 29.4, 21.4, 19.8.

HRMS-ESI: calcd. for $C_{16}H_{16}N_2ONa$ $[M + Na]^+$: 275.1155; found: 275.1169.

FT-IR: ν [cm^{-1}] = 3356, 1638, 1405, 1356, 1210, 1040, 744.

2,2-Dimethyl-2,6,7,12-tetrahydroindolo[2,3-*a*]quinolizin-4(3*H*)-one (2.58a)



2.58a was prepared according to **General procedure O**, starting from **5.53d** (100 mg, 0.221 mmol, 1.0 equiv.) and $POCl_3$ (20.2 μ L, 0.221 mmol, 1.0 equiv.) in toluene (3.0 mL). The reaction mixture was subsequently treated with MeOH (3.0 mL), K_2CO_3 (306 mg, 2.21 mmol, 10 equiv.) and nBu_4NBr (7.1 mg, 22.0 μ mol, 0.1 equiv.). Purification by silica gel column chromatography (pentane/EtOAc = 2:1) afforded **2.58a** (49.0 mg, 0.184 mmol, 83%) as a yellow solid.

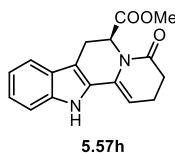
1H NMR (500 MHz, $CDCl_3$) δ [ppm] = 8.63 (s, 1H), 7.53–7.51 (m, 1H), 7.34 (dt, J = 8.2, 0.9 Hz, 1H), 7.23 (ddd, J = 8.2, 7.1, 1.2 Hz, 1H), 7.12 (ddd, J = 8.0, 7.1, 1.0 Hz, 1H), 5.44 (s, 1H), 4.14 (t, J = 6.0 Hz, 2H), 2.93 (t, J = 6.0 Hz, 2H), 2.52 (s, 2H), 1.18 (s, 6H).

^{13}C NMR (126 MHz, $CDCl_3$) δ [ppm] = 169.7, 137.4, 128.9, 128.0, 126.8, 123.5, 120.0, 119.0, 112.1, 111.1, 110.7, 46.5, 39.4, 30.8, 28.2, 20.7.

HRMS-ESI: calcd. for $C_{17}H_{18}N_2ONa$ $[M + Na]^+$: 289.1311; found: 289.1311.

FT-IR: ν [cm^{-1}] = 2930, 1666, 1646, 1395, 1215, 752, 740.

(*S*)-Methyl-4-oxo-2,3,4,6,7,12-hexahydroindolo[2,3-*a*]quinolizine-6-carboxylate (5.57h)



5.57h was prepared according to **General procedure O**, starting from **5.53f** (69 mg, 0.143 mmol, 1.0 equiv.) and $POCl_3$ (13.1 μ L, 0.134 mmol, 1.0 equiv.) in toluene (2.0 mL). The reaction mixture was subsequently treated with MeOH (2.0 mL), K_2CO_3 (198 mg, 1.43 mmol, 10 equiv.) and nBu_4NBr (4.6 mg, 14.0 μ mol, 0.1 equiv.). Purification by silica gel column chromatography (pentane/EtOAc = 1:1) afforded **5.57h** (30.0 mg, 0.101 mmol, 71%) as a

yellow solid.

¹H NMR (700 MHz, CDCl₃) δ [ppm] = 8.02 (s, 1H), 7.53–7.51 (m, 1H), 7.33–7.29 (m, 1H), 7.23–7.20 (m, 1H), 7.12 (ddd, *J* = 8.0, 7.1, 1.0 Hz, 1H), 5.90 (dd, *J* = 6.5, 1.5 Hz, 1H), 5.55 (dt, *J* = 8.0, 3.8 Hz, 1H), 3.60–3.58 (m, 4H), 3.14 (dd, *J* = 16.1, 6.5 Hz, 1H), 2.76–2.71 (m, 1H), 2.67–2.61 (m, 2H), 2.50–2.40 (m, 1H).

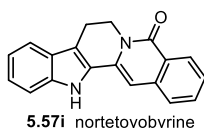
¹³C NMR (176 MHz, CDCl₃) δ [ppm] = 171.3, 170.1, 137.4, 130.2, 127.8, 126.8, 123.8, 120.3, 119.2, 111.1, 109.0, 100.0, 52.8, 50.9, 31.6, 23.1, 19.6.

HRMS-ESI: calcd. for C₁₇H₁₆N₂O₃Na [M + Na]⁺: 319.1053; found: 319.1044.

FT-IR: ν [cm⁻¹] = 2928, 2850, 1736, 1698, 1366, 1331, 1215, 747.

[α]_D²⁶ = +4.6 (*c* = 0.2, CHCl₃).

8,13-Dihydroindolo[2',3':3,4]pyrido[1,2-*b*]isoquinolin-5(7*H*)-one (5.57i)



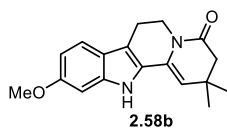
5.57i was prepared according to **General procedure O**, starting from **5.53e** (50.0 mg, 0.106 mmol, 1.0 equiv.) and POCl₃ (9.7 μL, 0.106 mmol, 1.0 equiv.) in toluene (1.5 mL). The reaction mixture was subsequently treated with MeOH (1.5 mL), K₂CO₃ (146 mg, 1.06 mmol, 10 equiv.) and *n*Bu₄NBr (3.4 mg, 11.0 μmol, 0.1 equiv.). Purification by silica gel column chromatography (pentane/EtOAc = 3:1) afforded **5.57i** (25.0 mg, 87.4 μmol, 82%) as a light yellow solid.

¹H NMR (500 MHz, *d*₆-DMSO) δ [ppm] = 11.69 (s, 1H), 8.24 (dd, *J* = 8.0, 1.3 Hz, 1H), 7.71 (td, *J* = 7.5, 1.3 Hz, 1H), 7.61 (dd, *J* = 16.4, 7.8 Hz, 2H), 7.45 (dd, *J* = 18.8, 7.9 Hz, 2H), 7.21 (ddd, *J* = 8.2, 6.9, 1.2 Hz, 1H), 7.10–7.04 (m, 2H), 4.40 (t, *J* = 6.5 Hz, 2H), 3.09 (t, *J* = 6.6 Hz, 2H).

¹³C NMR (126 MHz, *d*₆-DMSO) δ [ppm] = 161.2, 138.0, 136.2, 132.6, 132.4, 128.2, 127.5, 126.1, 126.0, 125.5, 124.5, 123.5, 119.5, 119.1, 112.5, 111.6, 99.0, 40.4, 19.3.

HRMS-ESI: calcd. for C₁₉H₁₃N₂O [M – H]⁻: 285.1033; found: 285.1038.

FT-IR: ν [cm⁻¹] = 2923, 2853, 1738, 1650, 1614, 1595, 1365, 1217, 742.

10-Methoxy-2,2-dimethyl-2,6,7,12-tetrahydroindolo[2,3-*a*]quinolizin-4(3*H*)-one (2.58b).

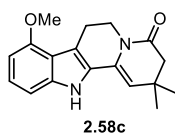
2.58b was prepared according to **General procedure O**, starting from **5.54c** (100 mg, 0.207 mmol, 1.0 equiv.) and POCl₃ (18.9 μL, 0.207 mmol, 1.0 equiv.) in toluene (3.0 mL). The reaction mixture was subsequently treated with MeOH (3.0 mL), K₂CO₃ (287 mg, 2.08 mmol, 10 equiv.) and *n*Bu₄NBr (6.7 mg, 0.021 mmol, 0.1 equiv.). Purification by silica gel column chromatography (pentane/EtOAc = 2:1) afforded **2.58b** (49.0 mg, 0.165 mmol, 85%) as a yellow solid.

¹H NMR (700 MHz, CDCl₃) δ [ppm] = 8.09 (s, 1H), 7.37 (d, *J* = 8.5 Hz, 1H), 6.83 (s, 1H), 6.78 (d, *J* = 8.5 Hz, 1H), 5.27 (s, 1H), 4.09 (t, *J* = 5.9 Hz, 2H), 3.85 (s, 3H), 2.88 (t, *J* = 5.9 Hz, 2H), 2.48 (s, 2H), 1.16 (s, 6H).

¹³C NMR (176 MHz, CDCl₃) δ [ppm] = 169.6, 157.6, 138.3, 128.9, 126.9, 121.3, 119.7, 112.4, 109.7, 109.5, 95.0, 55.8, 46.6, 39.3, 30.8, 28.3, 20.8.

HRMS-EI: calcd. for C₁₈H₂₀N₂O₂ [M]⁺: 296.1519; found: 296.1520.

FT-IR: ν [cm⁻¹] = 2954, 2919, 2850, 1736, 1663, 1628, 1461, 1365, 1230, 12174, 1149.

8-Methoxy-2,2-dimethyl-2,6,7,12-tetrahydroindolo[2,3-*a*]quinolizin-4(3*H*)-one (2.58c)

2.58c was prepared according to **General procedure O**, starting from **5.54a** (100 mg, 0.207 mmol, 1.0 equiv.) and POCl₃ (18.9 μL, 0.207 mmol, 1.0 equiv.) in toluene (3.0 mL). The reaction mixture was subsequently treated with MeOH (3.0 mL), K₂CO₃ (287 mg, 2.08 mmol, 10 equiv.) and *n*Bu₄NBr (6.7 mg, 0.021 mmol, 0.1 equiv.). Purification by silica gel column chromatography (pentane/EtOAc = 2:1) afforded **2.58c** (46.0 mg, 0.155 mmol, 75%) as a yellow solid.

¹H NMR (500 MHz, CDCl₃) δ [ppm] = 8.22 (s, 1H), 7.10 (t, *J* = 8.0 Hz, 1H), 6.92 (dd, *J* = 8.2, 0.6 Hz, 1H), 6.51–6.45 (m, 1H), 5.28 (s, 1H), 4.07 (t, *J* = 6.0 Hz, 2H), 3.90 (s, 3H), 3.14 (t, *J* =

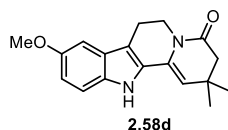
6.0 Hz, 2H), 2.49–2.46 (m, 2H), 1.16 (s, 6H).

^{13}C NMR (126 MHz, CDCl_3) δ [ppm] = 169.6, 155.0, 138.7, 128.9, 126.4, 124.4, 117.2, 112.4, 109.6, 104.4, 100.2, 55.3, 46.6, 39.6, 30.8, 28.3, 22.6.

HRMS-ESI: calcd. for $\text{C}_{18}\text{H}_{19}\text{N}_2\text{O}_2$ $[\text{M} - \text{H}]^-$: 295.1452; found: 295.1452.

FT-IR: ν [cm^{-1}] = 3305, 3286, 2955, 2921, 1662, 1641, 1514, 1397, 1361, 1252, 1106, 742.

9-Methoxy-2,2-dimethyl-2,6,7,12-tetrahydroindolo[2,3-*a*]quinolizin-4(3*H*)-one (2.58d)



2.58d was prepared according to **General procedure O**, starting from **5.54b** (250 mg, 0.519 mmol, 1.0 equiv.) and POCl_3 (47.3 μL , 0.519 mmol, 1.0 equiv.) in toluene (6.0 mL). The reaction mixture was subsequently treated with MeOH (6.0 mL), K_2CO_3 (717 mg, 5.19 mmol, 10 equiv.) and $n\text{Bu}_4\text{NBr}$ (16.7 mg, 0.052 mmol, 0.1 equiv.). Purification by silica gel column chromatography (pentane/EtOAc = 2:1) afforded **2.58d** (118 mg, 0.399 mmol, 77%) as a yellow solid.

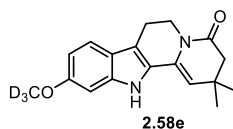
^1H NMR (500 MHz, CDCl_3) δ [ppm] = 7.82 (s, 1H), 7.21 (dd, J = 8.8, 0.7 Hz, 1H), 6.94 (d, J = 2.4 Hz, 1H), 6.90–6.85 (m, 1H), 5.29 (s, 1H), 4.09 (t, J = 6.0 Hz, 2H), 3.86 (s, 3H), 2.89 (t, J = 6.0 Hz, 2H), 2.47 (s, 2H), 1.16 (s, 6H).

^{13}C NMR (176 MHz, CDCl_3) δ [ppm] = 169.6, 154.5, 132.4, 128.9, 128.7, 127.2, 113.7, 112.1, 111.9, 110.4, 100.8, 56.0, 46.6, 39.4, 30.8, 28.3, 20.8.

HRMS-ESI: calcd. for $\text{C}_{18}\text{H}_{21}\text{N}_2\text{O}_2$ $[\text{M} + \text{H}]^+$: 297.1598; found: 297.1611.

FT-IR: ν [cm^{-1}] = 3287, 3272, 2955, 2924, 1663, 1642, 1457, 1289, 1113, 1028, 810, 753.

10-(methoxy- d_3)-2,2-dimethyl-2,6,7,12-tetrahydroindolo[2,3-*a*]quinolizin-4(3*H*)-one (2.58e)



2.58e was prepared according to **General procedure O**, starting from **5.54e** (20 mg, 41 μmol ,

1.0 equiv.) and POCl₃ (6.3 μL, 41 μmol, 1.0 equiv.) in toluene (1.0 mL). The reaction mixture was subsequently treated with MeOH (1.0 mL), K₂CO₃ (57 mg, 0.41 mmol, 10 equiv.) and *n*Bu₄NBr (1.3 mg, 4.1 μmol, 0.1 equiv.). Purification by silica gel column chromatography (pentane/EtOAc = 2:1) afforded **2.58e** (5.0 mg, 17 μmol, 40%) as a yellow solid.

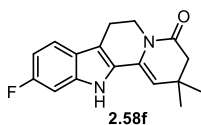
¹H NMR (700 MHz, CDCl₃) δ [ppm] = 8.11 (s, 1H), 7.37 (d, *J* = 8.6 Hz, 1H), 6.81 (d, *J* = 2.1 Hz, 1H), 6.77 (ddd, *J* = 8.6, 2.2, 0.8 Hz, 1H), 5.26 (s, 1H), 4.09 (t, *J* = 6.0 Hz, 2H), 2.87 (t, *J* = 6.0 Hz, 2H), 2.47 (s, 2H), 1.16 (s, 6H).

¹³C NMR (176 MHz, CDCl₃) δ [ppm] = 169.6, 157.6, 138.4, 128.9, 126.9, 121.3, 119.7, 112.4, 109.8, 109.4, 94.9, 55.2–54.7 (m), 46.6, 39.3, 30.8, 28.3, 20.8.

HRMS-EI: calcd. for C₁₈H₁₇D₃N₂O₂Na [M+Na]⁺: 322.1605; found: 322.1612.

FT-IR: ν [cm⁻¹] = 3311, 2955, 2924, 1738, 1662, 1640, 1623, 1557, 1456, 1391, 1364, 1269, 1178, 1110, 753.

10-Fluoro-2,2-dimethyl-2,6,7,12-tetrahydroindolo[2,3-*a*]quinolizin-4(3*H*)-one (**2.58f**)



2.58f was prepared according to **General procedure O**, starting from **5.54f** (80.0 mg, 0.170 mmol, 1.0 equiv.) and POCl₃ (26.1 μL, 0.170 mmol, 1.0 equiv.) in toluene (3.0 mL). The reaction mixture was subsequently treated with MeOH (3.0 mL), K₂CO₃ (235 mg, 1.70 mmol, 10 equiv.) and *n*Bu₄NBr (5.5 mg, 1.7 μmol, 0.1 equiv.). Purification by silica gel column chromatography (pentane/EtOAc = 2:1) afforded **2.58f** (38.5 mg, 0.136 mmol, 80%) as a yellow solid.

¹H NMR (500 MHz, CDCl₃) δ [ppm] = 8.54 (s, 1H), 7.40 (dd, *J* = 8.6, 5.3 Hz, 1H), 7.01 (dd, *J* = 9.5, 2.3 Hz, 1H), 6.91–6.84 (m, 1H), 5.38 (s, 1H), 4.11 (t, *J* = 6.0 Hz, 2H), 2.94–2.87 (m, 2H), 2.49 (s, 2H), 1.17 (s, 6H).

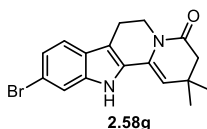
¹³C NMR (126 MHz, CDCl₃) δ [ppm] = 169.7, 160.8 (d, *J* = 239.3 Hz), 137.5 (d, *J* = 12.5 Hz), 128.7, 128.4 (d, *J* = 3.8 Hz), 123.5, 119.8 (d, *J* = 10.3 Hz), 112.1, 110.6, 108.8 (d, *J* = 24.6 Hz), 97.7 (d, *J* = 26.5 Hz), 46.5, 39.3, 30.8, 28.2, 20.7.

¹⁹F NMR (566 MHz, CDCl₃) δ [ppm] = -118.57.

HRMS-ESI: calcd. for $C_{17}H_{17}FN_2ONa$ $[M + Na]^+$: 307.1217; found: 307.1203.

FT-IR: ν [cm^{-1}] = 3294, 2956, 2923, 1663, 1642, 1393, 1360, 1265, 1223, 1134, 796.

10-Bromo-2,2-dimethyl-2,6,7,12-tetrahydroindolo[2,3-*a*]quinolizin-4(3*H*)-one (2.58g)



2.58g was prepared according to **General procedure O**, starting from **5.54g** (80.0 mg, 0.151 mmol, 1.0 equiv.) and $POCl_3$ (23.1 μ L, 0.151 mmol, 1.0 equiv.) in toluene (3.0 mL). The reaction mixture was subsequently treated with MeOH (3.0 mL), K_2CO_3 (209 mg, 1.51 mmol, 10 equiv.) and nBu_4NBr (4.9 mg, 1.5 μ mol, 0.1 equiv.). Purification by silica gel column chromatography (pentane/EtOAc = 2:1) afforded **2.58g** (42.5 mg, 0.123 mmol, 82%) as a yellow solid.

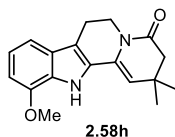
1H NMR (500 MHz, $CDCl_3$) δ [ppm] = 7.93 (s, 1H), 7.49–7.45 (m, 1H), 7.38–7.33 (m, 1H), 7.22 (ddd, J = 8.4, 1.7, 0.8 Hz, 1H), 5.32 (s, 1H), 4.09 (t, J = 6.0 Hz, 2H), 2.89 (t, J = 6.0 Hz, 2H), 2.48 (s, 2H), 1.17 (s, 6H).

^{13}C NMR (126 MHz, $CDCl_3$) δ [ppm] = 169.6, 138.1, 128.6, 128.6, 125.8, 123.4, 120.2, 117.0, 114.0, 112.2, 111.2, 46.4, 39.2, 30.9, 28.2, 20.6.

HRMS-ESI: calcd. for $C_{17}H_{17}N_2OBrNa$ $[M + Na]^+$: 367.0416; found: 367.0423.

FT-IR: ν [cm^{-1}] = 3282, 2955, 1663, 1638, 1452, 1394, 1294, 1233, 1186, 1136, 741.

11-Methoxy-2,2-dimethyl-2,6,7,12-tetrahydroindolo[2,3-*a*]quinolizin-4(3*H*)-one (2.58h)



2.58h was prepared according to **General procedure O**, starting from **5.54d** (100 mg, 0.207 mmol, 1.0 equiv.) and $POCl_3$ (18.9 μ L, 0.207 mmol, 1.0 equiv.) in toluene (3.0 mL). The reaction mixture was subsequently treated with MeOH (3.0 mL), K_2CO_3 (287 mg, 2.08 mmol, 10 equiv.) and nBu_4NBr (6.7 mg, 0.021 mmol, 0.1 equiv.). Purification by silica gel column chromatography (pentane/EtOAc = 2:1) afforded **2.58h** (50.5mg, 0.171 mmol, 82%) as a

yellow solid.

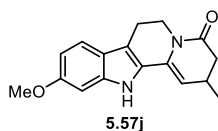
¹H NMR (500 MHz, CDCl₃) δ [ppm] = 8.31 (s, 1H), 7.15–7.11 (m, 1H), 7.04 (t, *J* = 7.8 Hz, 1H), 6.69 (d, *J* = 7.7 Hz, 1H), 5.38 (s, 1H), 4.09 (t, *J* = 6.0 Hz, 2H), 3.97 (s, 3H), 2.90 (d, *J* = 12.0 Hz, 2H), 2.48 (s, 2H), 1.16 (s, 6H).

¹³C NMR (126 MHz, CDCl₃) δ [ppm] = 169.6, 146.0, 128.9, 128.0, 127.6, 120.6, 120.0, 112.7, 111.8, 110.3, 103.6, 55.5, 46.5, 39.3, 30.8, 28.2, 20.9.

HRMS-ESI: calcd. for C₁₈H₂₀N₂O₂K [M + K]⁺: 335.1157; found: 335.1141.

FT-IR: ν [cm⁻¹] = 3312, 2957, 2928, 1662, 1644, 1452, 1394, 1359, 1294, 1233, 1219, 1135, 1040, 743.

10-Methoxy-2-methyl-2,6,7,12-tetrahydroindolo[2,3-*a*]quinolizin-4(3*H*)-one (5.57j)



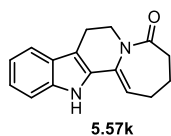
5.57j was prepared according to **General procedure O**, starting from **5.54h** (100 mg, 0.214 mmol, 1.0 equiv.) and POCl₃ (19.5 μL, 0.214 mmol, 1.0 equiv.) in toluene (3.0 mL). The reaction mixture was subsequently treated with MeOH (3.0 mL), K₂CO₃ (295 mg, 2.14 mmol, 10 equiv.) and *n*Bu₄NBr (6.9 mg, 21 μmol, 0.1 equiv.). Purification by silica gel column chromatography (pentane/EtOAc = 2:1) afforded **5.57j** (47.0 mg, 0.167 mmol, 78%) as a yellow solid.

¹H NMR (700 MHz, CD₂Cl₂) δ [ppm] = 8.37 (s, 1H), 7.37 (dt, *J* = 8.6, 0.6 Hz, 1H), 6.85 (dd, *J* = 2.3, 0.5 Hz, 1H), 6.75 (dd, *J* = 8.6, 2.3 Hz, 1H), 5.37 (d, *J* = 4.0 Hz, 1H), 4.34 (dt, *J* = 12.7, 5.3 Hz, 1H), 3.83 (s, 3H), 3.79–3.75 (m, 1H), 2.88–2.83 (m, 2H), 2.79–2.71 (m, 1H), 2.65 (ddd, *J* = 15.4, 5.9, 1.0 Hz, 1H), 2.32 (ddd, *J* = 15.4, 10.3, 0.7 Hz, 1H), 1.15 (d, *J* = 7.0 Hz, 3H).

¹³C NMR (176 MHz, CD₂Cl₂) δ [ppm] = 169.7, 158.0, 138.7, 130.4, 127.4, 121.5, 119.9, 112.4, 110.0, 105.2, 95.0, 55.9, 40.4, 39.4, 26.5, 21.0, 20.5.

HRMS-EI: calcd. for C₁₇H₁₈N₂O₂ [M]⁺: 282.1362; found: 282.1363.

FT-IR: ν [cm⁻¹] 2952, 2931, 1641, 1625, 1454, 1398, 1262, 1159, 1038, 770.

2,3,4,7,8,13-Hexahydro-5H-azepino[1',2':1,2]pyrido[3,4-*b*]indol-5-one (5.57k)

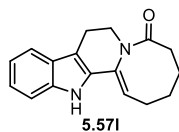
5.57k was prepared according to **General procedure O**, starting from **5.55e** (200 mg, 0.457 mmol, 1.0 equiv.) and POCl₃ (41.7 μL, 0.457 mmol, 1.0 equiv.) in toluene (5.0 mL). The reaction mixture was subsequently treated with MeOH (5.0 mL), K₂CO₃ (631 mg, 4.57 mmol, 10 equiv.) and *n*Bu₄NBr (14.7 mg, 46.0 μmol, 0.1 equiv.). Purification by silica gel column chromatography (pentane/EtOAc = 2:1) afforded **5.57k** (30.0 mg, 0.119 mmol, 26%) as a yellow solid.

¹H NMR (700 MHz, CD₂Cl₂) δ [ppm] = 9.10 (s, 1H), 7.48–7.46 (m, 1H), 7.35 (dt, *J* = 8.1, 0.9 Hz, 1H), 7.18 (ddd, *J* = 8.2, 7.0, 1.2 Hz, 1H), 7.07 (ddd, *J* = 8.0, 7.0, 1.0 Hz, 1H), 6.08 (t, *J* = 7.3 Hz, 1H), 4.07 (t, *J* = 5.9 Hz, 2H), 2.84 (t, *J* = 5.9 Hz, 2H), 2.55 (t, *J* = 7.1 Hz, 2H), 2.37 (q, *J* = 7.5 Hz, 2H), 2.20–2.16 (m, 2H).

¹³C NMR (176 MHz, CD₂Cl₂) δ [ppm] = 175.8, 139.5, 136.6, 131.7, 129.4, 125.3, 122.0, 121.1, 114.1, 114.0, 113.4, 43.4, 37.6, 32.1, 26.1, 23.9.

HRMS-ESI: calcd. for C₁₆H₁₆N₂ONa [M + Na]⁺: 275.1155; found: 275.1152.

FT-IR: ν [cm⁻¹] 2928, 2855, 1713, 1659, 1625, 1442, 1329, 1230, 1170, 745.

2,4,5,8,9,14-Hexahydroazocino[1',2':1,2]pyrido[3,4-*b*]indol-6(3*H*)-one (5.57l)

5.57l was prepared according to **General procedure O**, starting from **5.55f** (200 mg, 0.429 mmol, 1.0 equiv.) and POCl₃ (39.2 μL, 0.429 mmol, 1.0 equiv.) in toluene (5.0 mL). The reaction mixture was subsequently treated with MeOH (5.0 mL), K₂CO₃ (593 mg, 4.29 mmol, 10 equiv.) and *n*Bu₄NBr (13.8 mg, 43.0 μmol, 0.1 equiv.). Purification by silica gel column chromatography (pentane/EtOAc = 2:1) afforded **5.57l** (50.0 mg, 0.168 mmol, 39%) as a yellow solid.

¹H NMR (700 MHz, CD₂Cl₂) δ [ppm] = 8.34 (s, 1H), 7.47–7.46 (m, 1H), 7.34 (dt, *J* = 8.1,

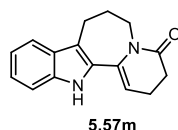
0.9 Hz, 1H), 7.18 (ddd, $J = 8.2, 7.1, 1.2$ Hz, 1H), 7.08 (ddd, $J = 8.0, 7.0, 1.0$ Hz, 1H), 5.77 (t, $J = 8.2$ Hz, 1H), 5.07 (ddd, $J = 12.5, 5.4, 1.2$ Hz, 1H), 3.18–3.14 (m, 1H), 2.97 (ddd, $J = 15.7, 12.4, 5.5$ Hz, 1H), 2.76 (ddd, $J = 15.9, 4.3, 1.2$ Hz, 1H), 2.55 (td, $J = 12.2, 1.6$ Hz, 1H), 2.49–2.39 (m, 2H), 2.10 (dddd, $J = 14.2, 11.9, 8.9, 1.3$ Hz, 1H), 1.99–1.90 (m, 1H), 1.69–1.55 (m, 2H), 1.39–1.28 (m, 1H).

^{13}C NMR (176 MHz, CD_2Cl_2) δ [ppm] = 174.0, 137.3, 133.1, 130.4, 127.6, 123.4, 120.2, 119.1, 116.0, 112.3, 111.3, 42.8, 35.0, 26.6, 25.5, 25.1, 22.1.

HRMS-ESI: calcd. for $\text{C}_{17}\text{H}_{18}\text{N}_2\text{ONa}$ $[\text{M} + \text{Na}]^+$: 289.1311; found: 289.1315.

FT-IR: ν [cm^{-1}] = 3260, 2928, 2854, 1620, 1450, 1406, 1230, 1170, 743 2.

2,3,6,7,8,13-Hexahydro-4H-pyrido[1',2':1,2]azepino[3,4-b]indol-4-one (5.57m)



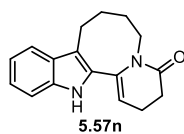
5.57m was prepared according to **General procedure O**, starting from **5.55b** (50.0 mg, 0.114 mmol, 1.0 equiv.) and POCl_3 (10.4 μL , 0.114 mmol, 1.0 equiv.) in toluene (1.5 mL). The reaction mixture was subsequently treated with MeOH (1.5 mL), K_2CO_3 (158 mg, 1.14 mmol, 10 equiv.) and $n\text{Bu}_4\text{NBr}$ (3.7 mg, 11.0 μmol , 0.1 equiv.). Purification by silica gel column chromatography (pentane/EtOAc = 2:1) afforded **5.57m** (15.0 mg, 59.5 μmol , 52%) as a yellow solid.

^1H NMR (700 MHz, CDCl_3) δ [ppm] = 8.00 (s, 1H), 7.55–7.54 (m, 1H), 7.33 (dt, $J = 8.1, 0.9$ Hz, 1H), 7.21 (ddd, $J = 8.2, 7.0, 1.2$ Hz, 1H), 7.13 (ddd, $J = 8.0, 7.0, 1.0$ Hz, 1H), 5.54 (t, $J = 5.1$ Hz, 1H), 3.91–3.83 (m, 2H), 2.93 (t, $J = 7.3$ Hz, 2H), 2.60 (dd, $J = 8.6, 6.7$ Hz, 2H), 2.48–2.39 (m, 2H), 2.10–2.06 (m, 2H).

^{13}C NMR (176 MHz, CDCl_3) δ [ppm] = 170.6, 137.2, 136.0, 129.2, 128.5, 123.2, 120.1, 118.9, 113.3, 110.9, 104.4, 42.2, 31.9, 26.2, 20.1, 19.8.

HRMS-ESI: calcd. for $\text{C}_{16}\text{H}_{16}\text{N}_2\text{ONa}$ $[\text{M} + \text{Na}]^+$: 275.1155; found: 275.1156.

FT-IR: ν [cm^{-1}] 2925, 2858, 1653, 1398, 1328, 1260, 1239, 1171, 745.

2,6,7,8,9,14-Hexahydropyrido[1',2':1,2]azocino[3,4-*b*]indol-4(3*H*)-one (5.57n)

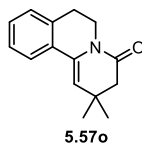
5.57n was prepared according to **General procedure O**, starting from **5.55c** (39.0 mg, 86.0 μmol , 1.0 equiv.) and POCl_3 (7.9 μL , 86.0 μmol , 1.0 equiv.) in toluene (1.5 mL). The reaction mixture was subsequently treated with MeOH (1.5 mL), K_2CO_3 (119 mg, 863 μmol , 10 equiv.) and $n\text{Bu}_4\text{NBr}$ (2.8 mg, 9.0 μmol , 0.1 equiv.). Purification by silica gel column chromatography (pentane/EtOAc = 2:1) afforded **5.57n** (10.0 mg, 37.6 μmol , 43%) as a yellow solid.

^1H NMR (700 MHz, CDCl_3) δ [ppm] = 7.83 (s, 1H), 7.55 (dt, $J = 7.9, 0.9$ Hz, 1H), 7.33 (dt, $J = 8.1, 0.9$ Hz, 1H), 7.22 (ddd, $J = 8.1, 7.0, 1.1$ Hz, 1H), 7.14 (ddd, $J = 8.0, 7.0, 1.0$ Hz, 1H), 5.44 (t, $J = 4.9$ Hz, 1H), 2.92–2.88 (m, 2H), 2.63 (dd, $J = 8.4, 7.3$ Hz, 2H), 2.46–2.42 (m, 2H), 1.93–1.80 (m, 6H).

^{13}C NMR (176 MHz, CDCl_3) δ [ppm] = 170.2, 136.9, 135.2, 128.6, 128.0, 122.9, 119.8, 118.8, 114.9, 110.7, 106.4, 43.3, 31.9, 28.9, 24.1, 23.6, 20.0.

HRMS-ESI: calcd. for $\text{C}_{17}\text{H}_{18}\text{N}_2\text{ONa}$ $[\text{M} + \text{Na}]^+$: 289.1311; found: 289.1388.

FT-IR: ν [cm^{-1}] = 2954, 2922, 2853, 1737, 1661, 1458, 1378, 1217, 1033, 743.

2,2-Dimethyl-2,3,6,7-tetrahydro-4*H*-pyrido[2,1-*a*]isoquinolin-4-one (5.57o)

5.57o was prepared according to **General procedure O**, starting from **5.56d** (138 mg, 0.334 mmol, 1.0 equiv.) and POCl_3 (76.2 μL , 0.835 mmol, 2.5 equiv.) in toluene (4.0 mL). The reaction mixture was subsequently treated with MeOH (4.0 mL), K_2CO_3 (462 mg, 3.34 mmol, 10 equiv.) and $n\text{Bu}_4\text{NBr}$ (10.8 mg, 33.0 μmol , 0.1 equiv.). Purification by neutral aluminium oxide column chromatography (pentane/DCM = 1:1) afforded **5.57o** (25.0 mg, 0.110 mmol, 33%) as a white solid.

^1H NMR (700 MHz, C_6D_6) δ [ppm] = 7.36–7.33 (m, 1H), 7.01–6.95 (m, 2H), 6.76–6.72 (m,

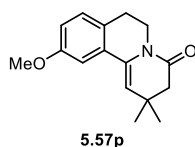
1H), 5.34 (s, 1H), 3.79 (dd, $J = 6.4, 5.4$ Hz, 2H), 2.32 (d, $J = 0.8$ Hz, 2H), 2.31 (td, $J = 5.9, 0.9$ Hz, 2H), 0.92 (s, 6H).

^{13}C NMR (176 MHz, C_6D_6) δ [ppm] = 168.3, 135.1, 134.1, 130.9, 128.4, 128.4, 126.8, 124.3, 112.7, 46.0, 38.3, 30.5, 29.4, 27.9.

HRMS-ESI: calcd. for $\text{C}_{15}\text{H}_{17}\text{NONa}$ $[\text{M} + \text{Na}]^+$: 250.1202; found: 250.1208.

FT-IR: ν [cm^{-1}] = 2948, 2925, 2858, 1974, 1733, 1626, 1492, 1465, 1429, 1320, 1208, 1126, 743.

10-Methoxy-2,2-dimethyl-2,3,6,7-tetrahydro-4H-pyrido[2,1-a]isoquinolin-4-one (5.57p)



5.57p was prepared according to **General procedure O**, starting from **5.56e** (80.0 mg, 0.181 mmol, 1.0 equiv.) and POCl_3 (16.5 μL , 0.181 mmol, 1.0 equiv.) in toluene (3.0 mL). The reaction mixture was subsequently treated with MeOH (3.0 mL), K_2CO_3 (250 mg, 1.81 mmol, 10 equiv.) and $n\text{Bu}_4\text{NBr}$ (5.8 mg, 18 μmol , 0.1 equiv.). Purification by neutral aluminium oxide column chromatography (pentane/DCM = 1:1) afforded **5.57p** (20.0 mg, 77.8 μmol , 43%) as a white solid.

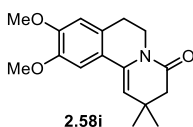
^1H NMR (700 MHz, C_6D_6) δ [ppm] = 6.70 (dd, $J = 8.3, 0.42$ Hz, 1H), 6.66 (dd, $J = 8.3, 2.5$ Hz, 1H), 5.40 (d, $J = 0.9$ Hz, 1H), 3.88–3.82 (m, 2H), 3.32 (s, 3H), 2.35–2.29 (m, 4H), 0.91 (s, 6H). (Due to the solvent peak overlapping, one resonance is missing. But the ABX system could be proved by the coupling constant of the rest two Hs.)

^{13}C NMR (176 MHz, C_6D_6) δ [ppm] = 168.4, 159.1, 134.3, 131.9, 129.4, 127.6, 114.2, 112.9, 109.6, 54.9, 46.0, 38.6, 30.5, 28.7, 27.9.

HRMS-ESI: calcd. for $\text{C}_{16}\text{H}_{19}\text{NO}_2\text{Na}$ $[\text{M} + \text{Na}]^+$: 280.1308; found: 280.1301.

FT-IR: ν [cm^{-1}] = 2926, 2854, 1746, 1655, 1605, 1518, 1466, 1360, 1271, 1232, 1193, 1140, 1109, 1029, 910.

9,10-Dimethoxy-2,2-dimethyl-2,3,6,7-tetrahydro-4H-pyrido[2,1-a]isoquinolin-4-one
(**2.58i**)



2.58i was prepared according to **General procedure O**, starting from **5.56f** (150 mg, 0.317 mmol, 1.0 equiv.) and POCl₃ (28.9 μL, 0.317 mmol, 1.0 equiv.) in toluene (5.0 mL). The reaction mixture was subsequently treated with MeOH (5.0 mL), K₂CO₃ (438 mg, 3.17 mmol, 10 equiv.) and *n*Bu₄NBr (10.2 mg, 32.0 μmol, 0.1 equiv.). Purification by silica gel column chromatography (pentane/EtOAc = 3:1) afforded **2.58i** (80.5 mg, 0.280 mmol, 88%) as a yellow solid.

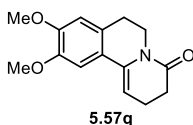
¹H NMR (500 MHz, CDCl₃) δ [ppm] = 7.02 (s, 1H), 6.61 (s, 1H), 5.47 (s, 1H), 3.91–3.89 (m, 5H), 3.88 (s, 3H), 2.77 (t, *J* = 5.9 Hz, 2H), 2.42 (s, 2H), 1.14 (s, 6H).

¹³C NMR (126 MHz, CDCl₃) δ [ppm] = 169.7, 149.3, 148.2, 133.2, 127.6, 122.3, 112.0, 110.8, 106.8, 56.2, 56.1, 46.0, 38.5, 30.5, 28.9, 28.2.

HRMS-ESI: calcd. for C₁₇H₂₁NO₃Na [M + Na]⁺: 310.1413; found: 310.1428.

FT-IR: ν [cm⁻¹] = 2964, 2934, 1775, 1645, 1516, 1388, 1358, 1287, 1263, 1234, 1198, 1109, 937.

9,10-Dimethoxy-2,3,6,7-tetrahydro-4H-pyrido[2,1-a]isoquinolin-4-on (**5.57q**)



5.57q was prepared according to **General procedure O**, starting from **5.56c** (100 mg, 0.225 mmol, 1.0 equiv.) and POCl₃ (20.5 μL, 0.225 mmol, 1.0 equiv.) in toluene (3.0 mL). The reaction mixture was subsequently treated with MeOH (3.0 mL), K₂CO₃ (311 mg, 2.25 mmol, 10 equiv.) and *n*Bu₄NBr (7.2 mg, 22 μmol, 0.1 equiv.). Purification by neutral aluminium oxide column chromatography (pentane/DCM = 1:1) afforded **5.57q** (44.0 mg, 0.170 mmol, 76%) as a yellow solid.

¹H NMR (500 MHz, C₆D₆) δ [ppm] = 6.92 (s, 1H), 6.20 (s, 1H), 5.31 (td, *J* = 5.0, 1.9 Hz, 1H),

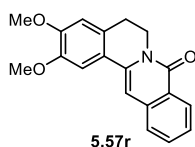
3.93 (td, $J = 5.9, 1.8$ Hz, 2H), 3.46 (s, 3H), 3.36 (s, 3H), 2.41 (td, $J = 7.9, 1.8$ Hz, 2H), 2.38–2.31 (m, 2H), 2.00–1.95 (m, 2H).

^{13}C NMR (126 MHz, C_6D_6) δ [ppm] = 169.0, 150.4, 149.2, 136.4, 127.8, 123.0, 111.6, 108.4, 99.7, 55.9, 55.5, 38.6, 31.6, 29.0, 19.9.

HRMS-ESI: calcd. for $\text{C}_{15}\text{H}_{17}\text{NO}_3\text{Na}$ $[\text{M} + \text{Na}]^+$: 282.1100; found: 282.1106.

FT-IR: ν [cm^{-1}] = 2942, 1682, 1602, 1513, 1465, 1377, 1341, 1272, 1202, 1179, 1162, 752.

2,3-Dimethoxy-5,6-dihydro-8*H*-isoquinolino[3,2-*a*]isoquinolin-8-one (5.57r)



5.57r was prepared according to **General procedure O**, starting from **5.56i** (193 mg, 0.391 mmol, 1.0 equiv.) and POCl_3 (35.7 μL , 0.391 mmol, 1.0 equiv.) in toluene (5.0 mL). The reaction mixture was subsequently treated with MeOH (5.0 mL), K_2CO_3 (541 mg, 3.92 mmol, 10 equiv.) and $n\text{Bu}_4\text{NBr}$ (12.6 mg, 39.0 μmol , 0.1 equiv.). Purification by silica gel column chromatography (pentane/EtOAc = 3:1) afforded **5.57r** (100 mg, 0.326 mmol, 83%) as a yellow solid.

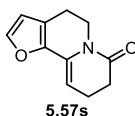
^1H NMR (600 MHz, CDCl_3) δ [ppm] = 8.41 (dt, $J = 8.1, 1.7$ Hz, 1H), 7.62–7.59 (m, 1H), 7.58–7.53 (m, 1H), 7.44–7.40 (m, 1H), 7.26 (d, $J = 2.1$ Hz, 1H), 6.86 (t, $J = 2.1$ Hz, 1H), 6.73 (d, $J = 2.4$ Hz, 1H), 4.39–4.32 (m, 2H), 3.98 (s, 3H), 3.93 (s, 3H), 2.93 (m, 2H).

^{13}C NMR (151 MHz, CDCl_3) δ [ppm] = 162.3, 150.5, 148.6, 137.5, 136.8, 132.4, 128.8, 128.1, 126.3, 126.0, 124.7, 122.4, 110.6, 108.0, 101.5, 56.4, 56.1, 39.8, 28.2.

HRMS-ESI: calcd. for $\text{C}_{19}\text{H}_{17}\text{NO}_3\text{Na}$ $[\text{M} + \text{Na}]^+$: 330.1100 found: 330.1115.

FT-IR: ν [cm^{-1}] = 3001, 2937, 2839, 1644, 1606, 1512, 1466, 1362, 1269, 1234, 1104, 1018, 754.

4,5,8,9-Tetrahydro-7*H*-furo[2,3-*a*]quinolizin-7-one (5.57s)



5.57s was prepared according to **General procedure O**, starting from **5.56j** (43.0 mg,

0.115 mmol, 1.0 equiv.) and POCl₃ (10.5 μL, 0.115 mmol, 1.0 equiv.) in toluene (1.5 mL). The reaction mixture was subsequently treated with MeOH (1.5 mL), K₂CO₃ (158 mg, 1.15 mmol, 10 equiv.) and *n*Bu₄NBr (3.7 mg, 11 μmol, 0.1 equiv.). Purification by neutral aluminium oxide column chromatography (pentane/DCM = 1:1) afforded **5.57s** (18.0 mg, 95.2 μmol, 83%) as a yellow solid.

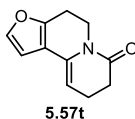
¹H NMR (700 MHz, C₆D₆) δ [ppm] = 6.90 (t, *J* = 1.7 Hz, 1H), 5.80 (t, *J* = 1.7 Hz, 1H), 5.45 (t, *J* = 5.0 Hz, 1H), 3.82 (t, *J* = 6.0 Hz, 2H), 2.30 (t, *J* = 7.7 Hz, 2H), 2.06 (t, *J* = 6.0 Hz, 2H), 1.85 (td, *J* = 7.7, 5.0 Hz, 2H).

¹³C NMR (176 MHz, C₆D₆) δ [ppm] = 168.4, 145.3, 142.6, 130.4, 118.2, 110.8, 98.1, 38.7, 32.0, 21.6, 19.5.

HRMS-ESI: calcd. for C₁₁H₁₁NO₂Na [M + Na]⁺: 212.0682; found: 212.0675.

FT-IR: ν [cm⁻¹] = 2929, 2855, 1725, 1553, 1457, 1380, 1335, 1181, 1019, 742.

4,5,8,9-Tetrahydro-7*H*-furo[3,2-*a*]quinolizin-7-one (**5.57t**)



5.57t was prepared according to **General procedure O**, starting from **5.56k** (40.0 mg, 0.107 mmol, 1.0 equiv.) and POCl₃ (9.7 μL, 0.107 mmol, 1.0 equiv.) in toluene (1.5 mL). The reaction mixture was subsequently treated with MeOH (1.5 mL), K₂CO₃ (147 mg, 1.07 mmol, 10 equiv.) and *n*Bu₄NBr (3.4 mg, 11 μmol, 0.1 equiv.). Purification by neutral aluminium oxide column chromatography (pentane/DCM = 1:1) afforded **5.57t** (10.0 mg, 54.0 μmol, 51%) as a yellow solid.

¹H NMR (700 MHz, C₆D₆) δ [ppm] = 6.90 (dd, *J* = 2.0, 0.7 Hz, 1H), 6.11 (d, *J* = 2.0 Hz, 1H), 4.93 (t, *J* = 4.9 Hz, 1H), 3.81 (t, *J* = 6.1 Hz, 2H), 2.33 (t, *J* = 7.7 Hz, 2H), 2.22–2.18 (m, 2H), 1.87–1.83 (m, 2H).

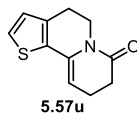
¹³C NMR (176 MHz, C₆D₆) δ [ppm] = 168.7, 150.0, 142.3, 132.5, 115.2, 106.3, 100.0, 38.3, 32.2, 23.0, 19.8.

(Note: as the product owns a vinylogous fragment, which is highly reactive, the NMR shows some impurity, though we used quite mild isolation method.)

HRMS-ESI: calcd. for $C_{11}H_{11}NO_2Na$ $[M + Na]^+$: 212.0682; found: 212.0688.

FT-IR: ν [cm^{-1}] = 2925, 1697, 1368, 1301, 1221, 1168, 1122, 1079, 1041, 746.

4,5,8,9-Tetrahydro-7H-thieno[2,3-a]quinolizin-7-one (5.57u)



5.57u was prepared according to **General procedure O**, starting from **5.56l** (48.0 mg, 0.123 mmol, 1.0 equiv.) and $POCl_3$ (11.2 μ L, 0.123 mmol, 1.0 equiv.) in toluene (1.5 mL). The reaction mixture was subsequently treated with MeOH (1.5 mL), K_2CO_3 (170 mg, 1.23 mmol, 10 equiv.) and nBu_4NBr (4.0 mg, 12 μ mol, 0.1 equiv.). Purification by neutral aluminium oxide column chromatography (pentane/DCM = 1:1) afforded **5.57u** (23.0 mg, 0.112 mmol, 91%) as a yellow solid.

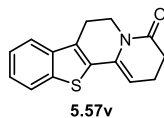
1H NMR (500 MHz, C_6D_6) δ [ppm] = 6.61 (dd, J = 5.1, 2.0 Hz, 1H), 6.31 (dd, J = 5.1, 2.0 Hz, 1H), 5.20 (td, J = 5.0, 2.0 Hz, 1H), 3.83 (td, J = 6.0, 2.0 Hz, 2H), 2.29 (td, J = 7.8, 1.9 Hz, 2H), 2.17 (td, J = 6.0, 2.0 Hz, 2H), 1.79 (tdd, J = 7.5, 4.9, 1.9 Hz, 2H).

^{13}C NMR (126 MHz, C_6D_6) δ [ppm] = 168.9, 136.6, 133.9, 132.4, 128.0, 124.5, 101.1, 39.0, 32.3, 25.6, 20.2.

HRMS-ESI: calcd. for $C_{11}H_{11}NOSNa$ $[M + Na]^+$: 228.0453; found: 228.0453.

FT-IR: ν [cm^{-1}] = 2930, 1681, 1433, 1367, 1331, 1304, 1225, 1171, 1136, 1035, 875, 764.

2,3,6,7-tetrahydro-4H-benzo[4,5]thieno[2,3-a]quinolizin-4-one (5.57v)



5.57v was prepared according to **General procedure O**, starting from **5.56m** (30.0 mg, 68.0 μ mol, 1.0 equiv.) and $POCl_3$ (6.2 μ L, 68 μ mol, 1.0 equiv.) in toluene (1.5 mL). The reaction mixture was subsequently treated with MeOH (1.5 mL), K_2CO_3 (94.0 mg, 0.680 mmol, 10 equiv.) and nBu_4NBr (2.2 mg, 7.0 μ mol, 0.1 equiv.). Purification by neutral aluminium oxide column chromatography (pentane/DCM = 1:1) afforded **5.57v** (15.0 mg, 58.8 μ mol, 86%) as a yellow solid.

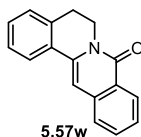
¹H NMR (700 MHz, CD₂Cl₂) δ [ppm] = 7.79 (ddd, *J* = 7.8, 1.3, 0.7 Hz, 1H), 7.63 (ddd, *J* = 7.8, 1.4, 0.7 Hz, 1H), 7.40–7.36 (m, 1H), 7.36–7.33 (m, 1H), 5.66 (t, *J* = 5.0 Hz, 1H), 4.08 (t, *J* = 6.0 Hz, 2H), 2.99–2.90 (m, 2H), 2.58 (t, *J* = 7.8 Hz, 2H), 2.51–2.40 (m, 2H).

¹³C NMR (176 MHz, CD₂Cl₂) δ [ppm] = 169.3, 139.1, 133.5, 131.7, 130.8, 125.8, 125.0, 122.8, 121.9, 104.6, 38.4, 31.9, 23.6, 20.2. (One sp² carbon is missing, probably due to the resonance overlap.)

HRMS-ESI: calcd. for C₁₅H₁₃NOSNa [M + Na]⁺: 278.0610; found: 278.0624.

FT-IR: ν [cm⁻¹] = 2929, 2876, 1652, 1458, 1398, 1382, 1329, 1215, 1045, 745.

5,6-Dihydro-8*H*-isoquinolino[3,2-*a*]isoquinolin-8-one (5.57w)



5.57w was prepared according to **General procedure O**, starting from **5.56h** (217 mg, 0.501 mmol, 1.0 equiv.) and POCl₃ (45.7 μL, 0.501 mmol, 1.0 equiv.) in toluene (6.0 mL). The reaction mixture was subsequently treated with MeOH (6.0 mL), K₂CO₃ (693 mg, 5.01 mmol, 10 equiv.) and *n*Bu₄NBr (16.2 mg, 50.0 μmol, 0.1 equiv.). Purification by silica gel column chromatography (pentane/EtOAc = 5:1) afforded **5.57w** (60 mg, 0.243 mmol, 48%) as a yellow solid.

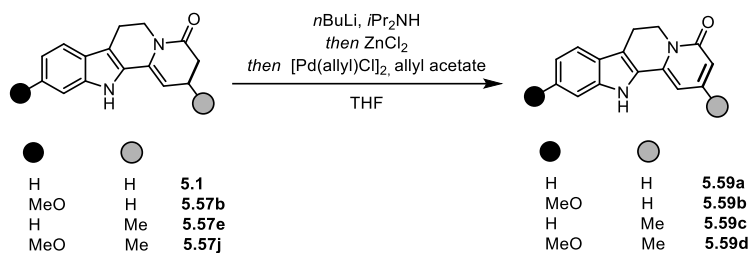
¹H NMR (600 MHz, CD₂Cl₂) δ [ppm] = 8.36 (dd, *J* = 8.1, 1.3 Hz, 1H), 7.90–7.84 (m, 1H), 7.65 (ddd, *J* = 8.2, 6.9, 1.4 Hz, 1H), 7.63–7.60 (m, 1H), 7.46 (ddd, *J* = 8.1, 6.9, 1.4 Hz, 1H), 7.41–7.34 (m, 2H), 7.33–7.27 (m, 1H), 7.05 (s, 1H), 4.37–4.30 (m, 2H), 3.06–2.98 (m, 2H).

¹³C NMR (151 MHz, CD₂Cl₂) δ [ppm] = 162.2, 138.0, 137.0, 136.1, 132.6, 130.7, 129.7, 128.4, 128.1, 127.8, 126.8, 126.7, 125.4, 125.3, 102.8, 40.0, 28.9.

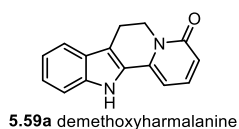
HRMS-ESI: calcd. for C₁₇H₁₃NONa [M + Na]⁺: 270.0889; found: 270.0903.

FT-IR: ν [cm⁻¹] = 2945, 2896, 1647, 1619, 1596, 1491, 1341, 1315, 1166, 766.

7.2.4.3. Oxidative pathway

**General procedure P**^[344a]

To a 0 °C solution of diisopropylamine (10.0 equiv.) in THF was added *n*BuLi (2.5 M in hexane, 10.0 equiv.). The reaction mixture was stirred for 1 h. A solution of enamide (1.0 equiv.) in THF was added dropwise into the resulting mixture. The reaction mixture was stirred for 1 h. ZnCl₂ (1.9 M in 2-Me-THF, 3.5 equiv.) was added and stirred for 1 h. A stock solution of [Pd(allyl)Cl]₂ (2.5 mol%) and allyl acetate (1.2 equiv.) in THF was next added at the same temperature. The reaction mixture was moved into a preheated 60 °C oil bath and stirred for 3 d. The resulting mixture was cooled to room temperature and quenched with NH₄Cl (sat. aq.), diluted with DCM, and the organic phase was separated. The aqueous phase was extracted with DCM and the combined organic layers were washed with brine, dried over MgSO₄, filtered, and concentrated under reduced pressure by rotary evaporation and purified by silica gel column chromatography. (Note: Preparation of [Pd(allyl)Cl]₂, allyl acetate stock solution: [Pd(allyl)Cl]₂ (27 mg, 0.075 mmol) was weighed into a flame dried vial, the vial was evacuated and backfilled with argon (this process was repeated 3 times). Allyl acetate (0.39 mL, 0.36 g, 3.6 mmol) and THF (2.6 mL) were added sequentially and the solution was stirred for 0.5 h.)

7,12-Dihydroindolo[2,3-*a*]quinolizin-4(6*H*)-one (5.59a)

5.59a was prepared according to **General procedure P**, starting from diisopropylamine (0.29 mL, 2.1 mmol, 10.0 equiv.) in THF (5.0 mL) was added *n*BuLi (2.5 M in hexane, 0.84 mL, 2.1 mmol, 10.0 equiv.). A solution of **5.1** (50 mg, 0.21 mmol, 1.0 equiv.) in THF (5.0 mL) was added dropwise into the resulting mixture. Then the reaction mixture was treated with ZnCl₂

(1.9 M in 2-Me-THF, 0.39 mL, 0.73 mmol, 3.5 equiv.). Afterwards a stock solution of [Pd(allyl)Cl]₂ (1.9 mg, 5.1 μmol, 2.5 mol%) and allyl acetate (27 μL, 25 μmol, 1.2 equiv.) in THF (1.0 mL) was next added. Purification by silica gel column chromatography (pentane/EtOAc = 1:2) afforded **5.59a** (38 mg, 0.16 mmol, 76%) as a yellow solid.

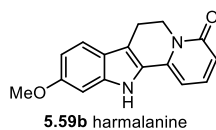
¹H NMR (700 MHz, CD₃OD) δ [ppm] = 8.10 (dt, *J* = 8.0, 1.0 Hz, 1H), 8.06 (dd, *J* = 9.0, 7.1 Hz, 1H), 7.93 (dt, *J* = 8.3, 0.9 Hz, 1H), 7.76 (ddd, *J* = 8.2, 7.0, 1.1 Hz, 1H), 7.61 (ddd, *J* = 8.0, 7.0, 0.9 Hz, 1H), 7.23 (dd, *J* = 7.1, 1.2 Hz, 1H), 6.99 (dd, *J* = 8.9, 1.2 Hz, 1H), 4.95 (t, *J* = 7.0 Hz, 2H), 3.64 (dd, *J* = 7.5, 6.5 Hz, 2H).

¹³C NMR (176 MHz, CD₃OD) δ [ppm] = 165.0, 141.2, 140.3, 140.0, 128.6, 126.9, 125.5, 121.1, 120.4, 117.8, 115.3, 112.8, 102.4, 42.1, 20.3.

HRMS-ESI: calcd. for C₁₅H₁₃N₂O [M + H]⁺: 237.1023; found: 237.1021.

FT-IR: ν [cm⁻¹] = 2927, 2185, 1652, 1568, 1539, 1500, 1452, 1324, 1143, 777, 740.

10-Methoxy-7,12-dihydroindolo[2,3-*a*]quinolizin-4(6*H*)-one (**5.59b**)



5.59b was prepared according to **General procedure P**, starting from diisopropylamine (0.13 mL, 0.93 mmol, 10.0 equiv.) in THF (2.5 mL) was added *n*BuLi (2.5 M in hexane, 0.37 mL, 0.93 mmol, 10.0 equiv.). A solution of **5.57b** (25 mg, 93 μmol, 1.0 equiv.) in THF (2.5 mL) was added dropwise into the resulting mixture. Then the reaction mixture was treated with ZnCl₂ (1.9 M in 2-Me-THF, 0.17 mL, 0.33 mmol, 3.5 equiv.). After that, the stock solution of [Pd(allyl)Cl]₂ (0.85 mg, 2.3 μmol, 2.5 mol%) and allyl acetate (11.2 μL, 0.11 mmol, 1.2 equiv.) in THF (0.5 mL) was next added. Purification by silica gel column chromatography (pentane/EtOAc = 1:2) afforded **5.59b** (15 mg, 56 μmol, 60%) as a yellow solid.

¹H NMR (500 MHz, CDCl₃) δ [ppm] = 8.27 (s, 1H), 7.46 (d, *J* = 8.7 Hz, 1H), 7.33 (dd, *J* = 9.1, 7.0 Hz, 1H), 6.87 (d, *J* = 2.2 Hz, 1H), 6.83 (dd, *J* = 8.7, 2.3 Hz, 1H), 6.48 (dd, *J* = 9.1, 1.2 Hz, 1H), 6.25 (dd, *J* = 7.0, 1.2 Hz, 1H), 4.43 (t, *J* = 6.9 Hz, 2H), 3.87 (s, 3H), 3.06 (t, *J* = 7.0 Hz, 2H).

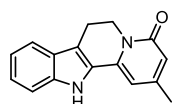
¹³C NMR (126 MHz, CD₃OD) δ [ppm] = 165.0, 159.9, 141.4, 141.2, 140.2, 127.5, 121.3, 121.2,

116.9, 115.8, 111.9, 101.7, 95.3, 55.9, 42.0, 20.4.

HRMS-ESI: calcd. for $C_{16}H_{15}N_2O_2$ $[M + H]^+$: 267.1128; found: 267.1127.

FT-IR: ν [cm^{-1}] = 2922, 2853, 1651, 1567, 1540, 1457, 1375, 1271, 1201, 1161, 1143, 798.

2-Methyl-7,12-dihydroindolo[2,3-*a*]quinolizin-4(6*H*)-one (5.59c)



5.59c demethoxyharmalacine

5.59c was prepared according to **General procedure P**, starting from diisopropylamine (0.17 mL, 1.2 mmol, 10.0 equiv.) in THF (3.0 mL) was added *n*BuLi (2.5 M in hexane, 0.48 mL, 1.2 mmol, 10.0 equiv.). A solution of **5.57e** (30 mg, 0.12 mmol, 1.0 equiv.) in THF (3.0 mL) was added dropwise into the resulting mixture. Then the reaction mixture was treated with $ZnCl_2$ (1.9 M in 2-Me-THF, 0.22 mL, 0.42 mmol, 3.5 equiv.). After that, the stock solution of $[Pd(allyl)Cl]_2$ (1.1 mg, 3.0 μ mol, 2.5 mol%) and allyl acetate (15 μ L, 0.14 mmol, 1.2 equiv.) in THF (0.5 mL) was next added. Purification by silica gel column chromatography (pentane/EtOAc = 1:2) afforded **5.59c** (21 mg, 84 μ mol, 71%) as a yellow solid.

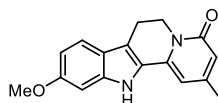
1H NMR (500 MHz, $CDCl_3+CD_3OD$ (v/v = 1:1)) δ [ppm] = 7.82–7.76 (m, 1H), 7.65 (dd, J = 8.3, 1.1 Hz, 1H), 7.48 (ddd, J = 8.2, 7.1, 1.3 Hz, 1H), 7.34 (ddd, J = 8.0, 7.0, 1.1 Hz, 1H), 6.83 (d, J = 1.8 Hz, 1H), 6.59–6.52 (m, 1H), 4.62 (t, J = 7.0 Hz, 2H), 3.34 (t, J = 6.9 Hz, 2H), 2.51 (s, 3H).

^{13}C NMR (126 MHz, $CDCl_3+CD_3OD$ (v/v = 1:1)) δ [ppm] = 163.2, 151.5, 138.4, 137.3, 127.0, 125.2, 123.9, 119.6, 118.9, 115.2, 113.6, 111.4, 103.7, 40.4, 20.5, 19.1.

HRMS-ESI: calcd. for $C_{16}H_{13}N_2O$ $[M - H]^-$: 249.1033; found: 249.1035.

FT-IR: ν [cm^{-1}] = 2924, 1649, 1583, 1568, 1543, 1499, 1364, 1148, 743.

10-Methoxy-2-methyl-7,12-dihydroindolo[2,3-*a*]quinolizin-4(6*H*)-one (5.59d)



5.59d harmalacine

5.59d was prepared according to **General procedure P**, starting from diisopropylamine

(0.35 mL, 2.5 mmol, 15.0 equiv.) in THF (3.0 mL) was added *n*BuLi (2.5 M in hexanes, 1.0 mL, 2.5 mmol, 15.0 equiv.). A solution of **5.57j** (47 mg, 0.17 mmol, 1.0 equiv.) in THF (3.0 mL) was added dropwise into the resulting mixture. Then the reaction mixture was treated with ZnCl₂ (1.9 M in 2-Me-THF, 0.44 mL, 0.83 mmol, 3.5 equiv.). After that, the stock solution of [Pd(allyl)Cl]₂ (0.15 mg, 4.2 μmol, 2.5 mol%) and allyl acetate (22 μL, 0.20 mmol, 1.2 equiv.) in THF (0.5 mL) was next added. Purification by silica gel column chromatography (pentane/EtOAc = 1:2) afforded **5.59d** (36 mg, 0.129 mmol, 77%) as a yellow solid.

¹H NMR (500 MHz, CDCl₃) δ [ppm] = 9.11 (s, 1H), 7.44 (d, *J* = 8.7 Hz, 1H), 6.87 (d, *J* = 2.2 Hz, 1H), 6.82 (dd, *J* = 8.7, 2.3 Hz, 1H), 6.31 (t, *J* = 1.4 Hz, 1H), 6.26 (d, *J* = 1.7 Hz, 1H), 4.41 (t, *J* = 6.9 Hz, 2H), 3.85 (s, 3H), 3.03 (t, *J* = 6.9 Hz, 2H), 2.17 (s, 3H).

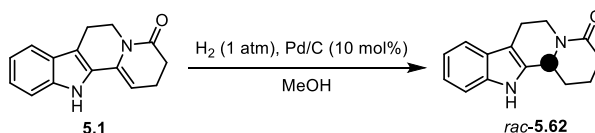
¹³C NMR (126 MHz, CDCl₃) δ [ppm] = 163.2, 158.5, 150.2, 139.6, 137.2, 126.7, 120.5, 120.4, 116.4, 115.2, 111.0, 102.0, 94.9, 55.8, 40.4, 21.5, 19.9.

HRMS-ESI: calcd. for C₁₇H₁₇N₂O₂ [M + H]⁺: 281.1284; found: 281.1284.

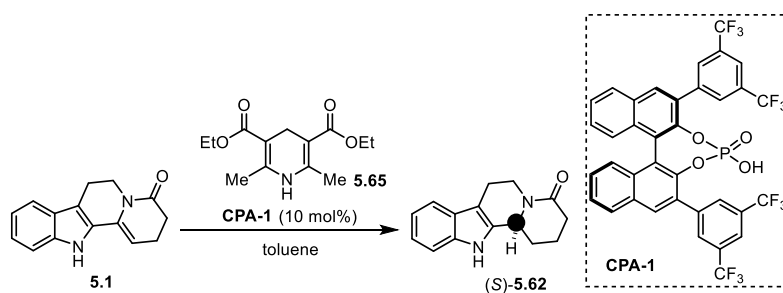
FT-IR: ν [cm⁻¹] = 3184, 2922, 1651, 1626, 1567, 1460, 1374, 1270, 1201, 1139, 1031, 814, 753.

7.2.4.4. Reductive pathway

2,3,6,7,12,12*b*-Hexahydroindolo[2,3-*a*]quinolizin-4(1*H*)-one (*rac*-**5.62**)



To a solution of enamide **5.1** (0.10 g, 0.42 mmol, 1.0 equiv.) in MeOH (10 mL), was added Pd/C (10% Pd on charcoal, 45 mg, 40 μmol, 0.1 equiv.). Then hydrogen was charged to the reaction mixture with a balloon. After the mixture was stirred overnight, it was filtered through Celite[®], and concentrated under reduced pressure. Purification by silica gel column chromatography (pentane/EtOAc = 1:1) afforded *rac*-**5.62** (76 mg, 0.32 mmol, 75%) as a light yellow powder.

2,3,6,7,12,12*b*-hexahydroindolo[2,3-*a*]quinolizin-4(1*H*)-one ((*S*)-5.62)

To a mixture of enamide **5.1** (26 mg, 0.11 mmol, 1.0 equiv.) and Hantzsch ester **5.65** (42 mg, 0.16 mmol, 1.5 equiv.) in toluene (2.5 mL), was added a solution of **CPA-1** (8.4 mg, 10 μ mol, 0.1 equiv.) in toluene (1.0 mL). Then the reaction mixture was immediately moved to a pre-heated 60 °C oil bath. After stirring for 24 h, the resulting mixture was quenched with NaHCO₃ (sat. aq.), diluted with DCM. The organic phase was separated. The aqueous phase was extracted with DCM and the combined organic layers were washed with brine, dried over MgSO₄, filtered, and concentrated under reduced pressure. Purification by silica gel column chromatography (pentane/EtOAc = 1:1) afforded (*S*)-**5.62** (16 mg, 70 μ mol, 61%, 99% (b.r.s.m.), 80% *ee*) as a light yellow powder.

¹H NMR (500 MHz, CDCl₃) δ [ppm] = 8.09 (s, 1H), 7.51 (dd, *J* = 7.8, 1.1 Hz, 1H), 7.34 (dt, *J* = 8.0, 0.9 Hz, 1H), 7.18 (ddd, *J* = 8.2, 7.0, 1.2 Hz, 1H), 7.13 (ddd, *J* = 8.0, 7.0, 1.0 Hz, 1H), 5.23–5.14 (m, 1H), 4.82–4.75 (m, 1H), 2.87 (m, 2H), 2.81–2.73 (m, 1H), 2.62–2.57 (m, 1H), 2.50–2.43 (m, 1H), 2.40 (td, *J* = 11.6, 5.8 Hz, 1H), 2.02–1.93 (m, 1H), 1.92–1.83 (m, 1H), 1.83–1.73 (m, 1H).

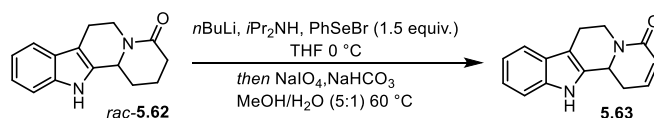
¹³C NMR (126 MHz, CDCl₃) δ [ppm] = 169.5, 136.3, 133.4, 127.0, 122.3, 120.0, 118.6, 111.1, 109.8, 54.6, 40.4, 32.5, 29.2, 21.1, 19.5.

HRMS-EI: calcd. for C₁₅H₁₆N₂O [M]⁺: 240.1257; found: 240.1259.

FT-IR: ν [cm⁻¹] = 3223, 2923, 2853, 1615, 1470, 1445, 1415, 1266, 1235, 741.

$[\alpha]_D^{26} = -191.2$ (*c* = 0.8, CHCl₃); Lit.:^[362] $[\alpha]_D^{25} = -220.2$ (*c* = 0.10 CHCl₃) (94% *ee*).

HPLC: 10% EtOH/Hexane, Chiralpak IA, 1.0 mL/min

6,7,12,12*b*-Tetrahydroindolo[2,3-*a*]quinolizin-4(1*H*)-one (5.63**)^[363]**

Diisopropylamine (234 μL , 1.67 mmol, 10.0 equiv.) was added to dry THF (5.0 mL) at 0 $^{\circ}\text{C}$. *n*BuLi (2.5 M in hexane, 667 μL , 1.67 mmol, 10.0 equiv.) was added and the mixture was stirred for 30 min before cooling to -78°C . A solution of *rac*-**5.62** (40.0 mg, 0.167 mmol, 1.0 equiv.) in THF (2.0 mL) was added dropwise. The reaction was stirred at -78°C for 1 h. A solution of PhSeBr (59.0 mg, 250 μmol , 1.5 equiv.) in THF (2.0 mL) was added dropwise and the reaction mixture was stirred for 24 h. The reaction was quenched with NH_4Cl (sat. aq.) and extracted with DCM. The combined organic phases were washed with brine, dried over MgSO_4 , filtered and concentrated under reduced pressure. The crude selenide was dissolved in methanol (5.0 mL) and water (1.0 mL). NaIO_4 (71.0 mg, 333 μmol , 2.0 equiv.) and NaHCO_3 (16.8 mg, 200 μmol , 1.2 equiv.) were added and the reaction was heated at 60 $^{\circ}\text{C}$ for 24 h. The reaction was quenched with NaHCO_3 (sat. aq.) and extracted with DCM. The combined organic phases were washed with brine, dried over MgSO_4 and concentrated under reduced pressure. The crude product was purified by silica gel column chromatography (pentane/EtOAc = 1:1) to give **5.63** (16.0 mg, 67.2 μmol , 40%) as light yellow powder.

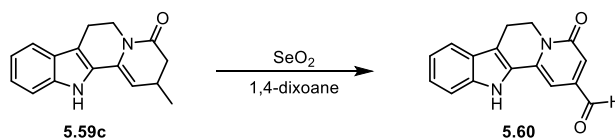
$^1\text{H NMR}$ (500 MHz, d_6 -DMSO) δ [ppm] = 10.96 (s, 1H), 7.44 (dd, $J = 7.9, 1.1$ Hz, 1H), 7.33 (dt, $J = 8.0, 0.9$ Hz, 1H), 7.08 (ddd, $J = 8.2, 7.1, 1.2$ Hz, 1H), 6.99 (ddd, $J = 8.0, 7.1, 1.0$ Hz, 1H), 6.81 (ddd, $J = 9.7, 6.2, 2.1$ Hz, 1H), 5.92 (dd, $J = 9.7, 2.8$ Hz, 1H), 4.91–4.82 (m, 1H), 4.78 (ddd, $J = 13.6, 5.2, 1.9$ Hz, 1H), 3.02 (ddd, $J = 17.7, 6.3, 4.9$ Hz, 1H), 2.88–2.75 (m, 2H), 2.67 (m, 1H), 2.32–2.19 (m, 1H).

$^{13}\text{C NMR}$ (126 MHz, d_6 -DMSO) δ [ppm] = 164.1, 139.4, 136.3, 133.6, 126.1, 124.7, 121.1, 118.6, 117.9, 111.1, 107.0, 51.2, 38.2, 30.3, 20.5.

HRMS-EI: calcd. for $\text{C}_{15}\text{H}_{14}\text{N}_2\text{O}$ $[\text{M}]^+$: 238.1100; found: 238.1099.

FT-IR: ν [cm^{-1}] = 3780, 2918, 2849, 1737, 1655, 1601, 1436, 1324, 1303, 817, 740.

4-Oxo-4,6,7,12-tetrahydroindolo[2,3-*a*]quinolizine-2-carbaldehyde (**5.60**)



To a solution of **5.59c** (30.0 mg, 0.120 mmol, 1.0 equiv.) in 1,4-dioxane (5.0 mL) was added SeO_2 (106 mg, 0.960 mmol, 8.0 equiv.). The mixture was heated to 80 $^{\circ}\text{C}$ and stirred for 2 d.

After cooling to room temperature, the reaction mixture was filtered through Celite[®], concentrated under reduced pressure. The crude product was purified by silica gel column chromatography (pentane/EtOAc = 1:2) afforded **5.60** (5.0 mg, 18,9 μ mol, 16 %) as a yellow solid.

¹H NMR (700 MHz, *d*₆-DMSO) δ [ppm] = 11.86 (s, 1H), 9.92 (s, 1H), 7.61 (dq, *J* = 7.9, 0.8 Hz, 1H), 7.42 (dt, *J* = 8.2, 0.9 Hz, 1H), 7.24 (ddd, *J* = 8.2, 7.0, 1.1 Hz, 1H), 7.08 (ddd, *J* = 7.9, 6.9, 0.9 Hz, 1H), 6.99 (d, *J* = 1.7 Hz, 1H), 6.96 (d, *J* = 1.6 Hz, 1H), 4.35–4.30 (m, 2H), 3.09 (dd, *J* = 7.5, 6.5 Hz, 2H).

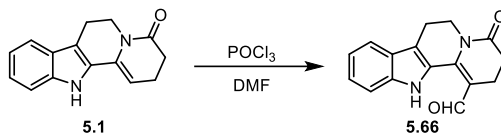
¹³C NMR (176 MHz, *d*₆-DMSO) δ [ppm] = 193.5, 162.0, 144.0, 139.2, 138.4, 127.4, 125.1, 124.3, 122.6, 119.8, 119.6, 114.0, 112.0, 94.1, 54.9, 18.9.

HRMS-ESI: calcd. for C₁₆H₁₂N₂O₂Na [M + Na]⁺: 287.0791 found: 287.0801.

FT-IR: ν [cm⁻¹] = 2951, 2920, 2851, 1704, 1651, 1583, 1568, 1542, 1464, 835, 735.

7.2.4.5. β -formylation

4-Oxo-2,3,4,6,7,12-hexahydroindolo[2,3-*a*]quinolizine-1-carbaldehyde (**5.66**)



POCl₃ (1.28 mL, 2.10 mmol, 5.0 equiv.) was added dropwise to the DMF (3.0 mL) at 0 °C. The mixture was stirred for 1 h. Then a solution of **5.1** (100 mg, 0.420 mmol, 1.0 equiv.) in DMF (2.0 mL) was added to the mixture and stirred for another 3 h. The resulting mixture was quenched with NaHCO₃ (sat. aq.) and extracted with DCM. The combined organic phases were washed with brine, dried over MgSO₄ and concentrated under reduced pressure. The crude product was purified by silica gel column chromatography (pentane/EtOAc = 1:1) to give **5.66** (95.0 mg, 0.357 mmol, 85%) as a yellow powder.

¹H NMR (500 MHz, CDCl₃) δ [ppm] = 12.44 (s, 1H), 9.59 (s, 1H), 7.59–7.57 (m, 1H), 7.50 (dt, *J* = 8.4, 0.9 Hz, 1H), 7.33 (ddd, *J* = 8.3, 6.9, 1.1 Hz, 1H), 7.14 (ddd, *J* = 8.0, 6.9, 1.0 Hz, 1H), 4.27 (t, *J* = 6.2 Hz, 2H), 3.00 (t, *J* = 6.2 Hz, 2H), 2.88–2.78 (m, 2H), 2.74–2.62 (m, 2H).

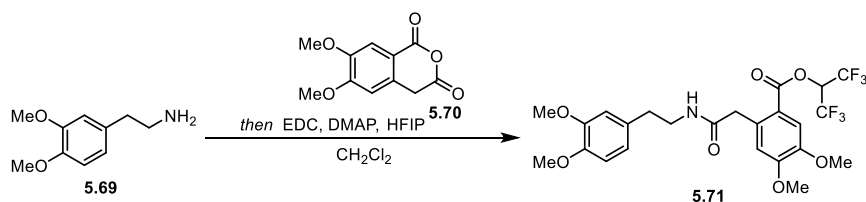
¹³C NMR (126 MHz, CDCl₃) δ [ppm] = 189.8, 170.5, 143.5, 137.3, 126.8, 126.2, 125.1, 120.6, 119.8, 119.5, 112.8, 111.3, 41.1, 31.9, 22.5, 20.8.

HRMS-EI: calcd. for $C_{16}H_{15}N_2O_2$ $[M + H]^+$: 267.1128; found: 267.1136.

FT-IR: ν [cm^{-1}] = 2951, 2918, 2850, 1694, 1649, 1574, 1536, 1393, 1356, 1171, 755.

7.2.4.6. Total synthesis of ilicifoline B

1,1,1,3,3,3-Hexafluoropropan-2-yl 2-(2-((3,4-dimethoxyphenethyl)amino)-2-oxo-ethyl)-4,5-dimethoxybenzoate (5.71)



5.71 was prepared according to **General procedure M**, starting from **5.69** (100 mg, 0.552 mmol, 1.0 equiv.) and **5.70** (123 mg, 0.552 mmol, 1.0 equiv.) in DCM (5.0 mL). The reaction mixture was subsequently treated with EDCI (211 mg, 1.10 mmol, 2.0 equiv.), DMAP (13.5 mg, 0.110 mmol, 0.2 equiv.) and HFIP (292 μ L, 2.76 mmol, 5.0 equiv.). Purification by silica gel column chromatography (pentane/EtOAc = 3:2) afforded **5.71** (190 mg, 0.342 mmol, 62%) as a light yellow solid.

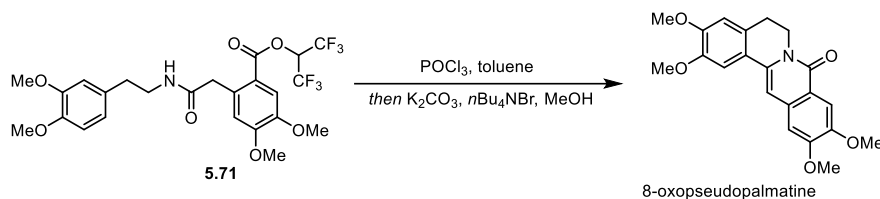
1H NMR (700 MHz, $CDCl_3$) δ [ppm] = 7.46 (s, 1H), 6.91 (s, 1H), 6.71 (d, J = 8.0 Hz, 1H), 6.65 (d, J = 2.0 Hz, 1H), 6.59 (dd, J = 8.1, 2.0 Hz, 1H), 6.08 (s, 1H), 5.93–5.90 (m, 1H), 3.95 (s, 3H), 3.91 (s, 3H), 3.83 (s, 3H), 3.82 (s, 3H), 3.79 (s, 2H), 3.43 (td, J = 7.1, 5.7 Hz, 2H), 2.68 (t, J = 7.1 Hz, 2H).

^{13}C NMR (176 MHz, $CDCl_3$) δ [ppm] = 170.2, 163.4, 154.1, 149.1, 147.9, 147.8, 134.3, 131.3, 120.69 (q, J = 283.7 Hz), 120.65, 116.9, 115.0, 113.5, 112.0, 111.2, 67.3–66.5 (m), 56.4, 56.1, 55.9, 42.0, 40.9, 35.2. (Based on the intensity of the resonance, the peak at δ [ppm] = 55.9 is considered as two methoxy carbons.)

^{19}F NMR (565 MHz, $CDCl_3$) δ [ppm] = -72.98 (d, J = 6.1 Hz).

HRMS-ESI: calcd. for $C_{24}H_{25}F_6NO_7Na$ $[M + Na]^+$: 576.1427; found: 576.1401.

FT-IR: ν [cm^{-1}] 2934, 1749, 1674, 1518, 1263, 1234, 1194, 1110, 768.

2,3,10,11-Tetramethoxy-5,6-dihydro-8*H*-isoquinolino[3,2-*a*]isoquinolin-8-one

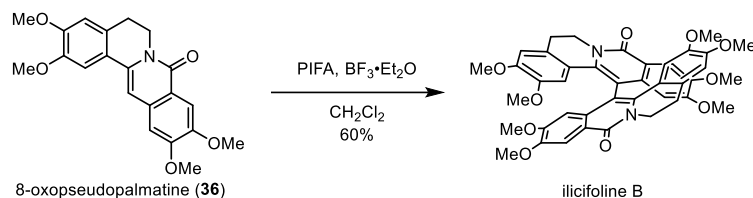
8-Oxopseudopalmatine was prepared according to **General procedure O**, starting from **5.71** (60 mg, 0.11 mmol, 1.0 equiv.) and POCl_3 (9.9 μL , 0.11 mmol, 1.0 equiv.) in toluene (3.0 mL). The reaction mixture was subsequently treated with MeOH (3.0 mL), K_2CO_3 (150 mg, 1.1 mmol, 10 equiv.) and $n\text{Bu}_4\text{NBr}$ (3.5 mg, 0.022 mmol, 0.1 equiv.). Purification by silica gel column chromatography (pentane/EtOAc = 1:1) afforded 8-oxopseudopalmatine (38 mg, 0.104 mmol, 95%) as a yellow solid.

$^1\text{H NMR}$ (700 MHz, CDCl_3) δ [ppm] = 7.81 (s, 1H), 7.25 (s, 1H), 6.94 (s, 1H), 6.83 (s, 1H), 6.74 (s, 1H), 4.39–4.34 (m, 2H), 4.02 (s, 3H), 4.01 (s, 3H), 3.98 (s, 3H), 3.94 (s, 3H), 2.96–2.92 (m, 2H).

$^{13}\text{C NMR}$ (176 MHz, CDCl_3) δ [ppm] = 161.6, 153.7, 150.3, 149.2, 148.6, 136.3, 132.3, 128.6, 122.7, 118.7, 110.7, 108.0, 107.8, 106.1, 101.3, 56.4, 56.4, 56.2, 39.9, 28.3. (Based on the intensity of the resonance, the peak at δ [ppm] = 56.2 is considered as two methoxy carbons.)

HRMS-ESI: calcd. for $\text{C}_{21}\text{H}_{21}\text{NO}_5\text{Na}$ $[\text{M} + \text{Na}]^+$: 390.1312 found: 390.1323.

FT-IR: ν [cm^{-1}] 2929, 1644, 1594, 1509, 1466, 1426, 1255, 1235, 1097, 1027, 747.

2,2',3,3',10,10',11,11'-Octamethoxy-5,5',6,6'-tetrahydro-8*H*,8'*H*-[13,13'-biisoquinolino[3,2-*a*]isoquinoline]-8,8'-dione

A mixture of 8-oxypseudopalmatine (18 mg, 50 μmol , 1.0 equiv.) and PIFA (16 mg, 0.05 mmol, 1.0 equiv.) in DCM (2.0 mL), was added $\text{BF}_3 \cdot \text{Et}_2\text{O}$ (9.7 μL , 0.10 mmol, 2.0 equiv.) at -78°C . The mixture was stirred for 3 h, then quenched with NaHCO_3 (sat. aq.) and diluted with DCM, and the organic phase was separated. The aqueous phase was extracted with DCM and the combined organic layers were washed with brine, dried over MgSO_4 , filtered, and concentrated

under reduced pressure. Purification by silica gel column chromatography (pentane/EtOAc = 1:1 to EtOAc) afforded ilicifoline B (11 mg, 15 μ mol, 60%) as a yellow solid.

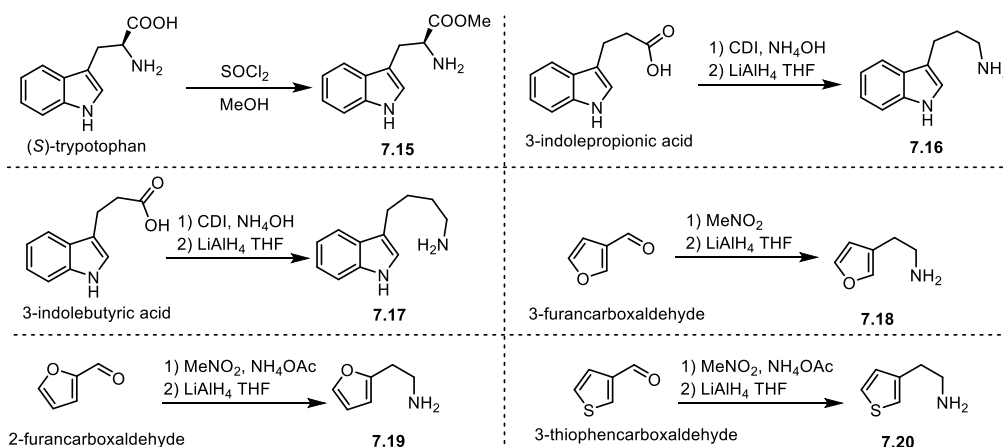
$^1\text{H NMR}$ (700 MHz, CDCl_3) δ [ppm] = 7.95 (s, 2H), 6.76 (s, 2H), 6.43 (s, 2H), 6.34 (s, 2H), 5.05 (dt, J = 13.2, 3.8 Hz, 2H), 4.06 (s, 6H), 3.82 (s, 6H), 3.62 (s, 6H), 3.33 (td, J = 13.2, 3.0 Hz, 2H), 3.03 (s, 6H), 2.52 (dt, J = 15.1, 3.1 Hz, 2H), 2.13 (ddd, J = 14.5, 12.7, 4.2 Hz, 2H).

$^{13}\text{C NMR}$ (176 MHz, CDCl_3) δ [ppm] = 161.0, 153.9, 149.5, 149.2, 146.6, 137.0, 133.6, 131.3, 122.5, 119.0, 111.6, 110.8, 109.2, 108.1, 105.8, 56.4, 56.3, 56.2, 55.2, 41.4, 29.0.

HRMS-EI: calcd. for $\text{C}_{42}\text{H}_{40}\text{N}_2\text{O}_{10}\text{Na}$ $[\text{M} + \text{Na}]^+$: 755.2575; found: 755.2576.

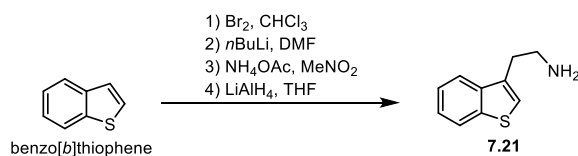
FT-IR: ν [cm^{-1}] 3004, 2928, 1633, 1607, 1587, 1498, 1464, 1440, 1374, 1271, 1226, 1133, 1096, 1008, 876, 749.

7.2.4.7. Preparation of amines for the substrates of the annulation



Scheme 7-8: Noncommercially available amines synthesis by reported methods.

7.15 was prepared from (*S*)-tryptophan by the procedure of Carreira et al.^[364] **7.16** was synthesized from 3-indolepropionic acid according to the procedure of Weinstock et al.^[365] **7.17** was obtained from 3-indolebutyric acid following the procedure of Mewshaw et al.^[366] **7.18** was prepared from 3-furancarboxaldehyde via the procedure of Liotta et al.^[367] **7.19** was prepared from 2-furancarboxaldehyde through the procedure of Huang et al.^[368] **7.20** was prepared from 3-thiophencarboxaldehyde using the procedure of Enzensperger et al.^[369] The spectroscopic data are in agreement with literatures.

2-(Benzo[*b*]thiophen-3-yl)ethan-1-amine (7.21).

Bromination:^[370] Benzo[*b*]thiophene (2.0 g, 15 mmol, 1.0 equiv.) was dissolved in chloroform (30 mL) and cooled by an ice bath. A solution of bromine (0.84 mL, 16 mmol, 1.1 equiv.) in chloroform (10 mL) was slowly added. The reaction mixture was stirred for 1 h and quenched with NaOH (1.0 M aq.) and Na₂S₂O₃ (sat. aq.). The resulting mixture was extracted with DCM. After evaporation of the solvent, the intermediate was dissolved in ethanol and was added dropwise to a solution of KOH (sat. EtOH solution, 20 mL) was added at ice bath. After refluxing for 2 h, H₂O was added and the EtOH was evaporated. The residue was extracted by DCM, washed with brine, dried over MgSO₄, filtered and concentrated under reduced pressure to afford crude 3-bromo-benzo[*b*]thiophene as yellow oil. The crude product was used without purification.

Formylation procedure:^[371] Crude 3-bromo-benzo[*b*]thiophene (3.4 g, 16 mmol, 1.0 equiv.) was dissolved in Et₂O and the solution was cooled to -78 °C. After the dropwise addition *n*BuLi (2.5 M solution in hexane, 6.4 mL, 16 mmol, 1.0 equiv.), the mixture was stirred for 30 min. Following the addition of DMF (1.2 mL, 16 mmol, 1.0 equiv.) at -78 °C, the mixture was allowed to warm to room temperature for 1 h. The reaction mixture was quenched with NH₄Cl (sat. aq.) and extracted with DCM. Combined organic layers were dried over MgSO₄, filtered and concentrated under reduced pressure to afford crude 3-benzo[*b*]thiophene-3-carbaldehyde as yellow oil.

Henry reaction: A flask with NH₄OAc (2.3 g, 30 mmol, 3.0 equiv.) and crude 3-benzo[*b*]thiophene-3-carbaldehyde (1.6 g, 9.9 mmol, 1.0 equiv.) was added MeNO₂ (40 mL) and the reaction mixture was stirred at 115 °C for 2h. After cooled to room temperature, the reaction mixture was diluted with water and DCM, and the organic phase was separated. The aqueous phase was extracted with DCM and the combined organic layers were washed with brine, dried over MgSO₄, filtered and concentrated under reduced pressure to afford the crude 3-(2-nitrovinyl)benzo[*b*]thiophene which could use directly without purification.

Reduction: To a Schlenk flash charged with solid LiAlH₄ (2.2 g, 59 mmol, 6.0 equiv.), was

added THF carefully at 0 °C. Then a solution of crude 3-(2-nitrovinyl)benzo[*b*]thiophene in THF (20 mL) was added dropwise. The resulting reaction mixture was replaced with an oil bath and heated to 65 °C for 3h, then cooled first to room temperature and then to 0 °C. Excess LiAlH₄ was quenched with the drop-wise addition of NaOH (sat. aq.) and H₂O. The suspension was allowed to warm to room temperature overnight and then filtered through a plug of Celite[®]. The organic phase was separated. The aqueous phase was extracted with DCM and the combined organic layers were washed with brine, dried over MgSO₄, filtered, and concentrated under reduced pressure. The crude material was purified by silica gel column chromatography (DCM/MeOH/TEA = 80:20:5) afforded **S38** (300 mg, 1.69 mmol, 11% over 4 steps) as a dark brown solid.

¹H NMR (500 MHz, CD₃OD: CDCl₃ (v/v = 1:1)) δ [ppm] = 7.54 (dt, *J* = 7.9, 1.1 Hz, 1H), 7.46 (dt, *J* = 8.0, 0.9 Hz, 1H), 7.07 (ddd, *J* = 8.0, 7.0, 1.3 Hz, 1H), 7.03 (ddd, *J* = 8.3, 7.3, 1.3 Hz, 1H), 6.92 (s, 1H), 2.75 (s, 4H).

¹³C NMR (126 MHz, CD₃OD: CDCl₃ (v/v = 1:1)) δ [ppm] = 140.2, 138.2, 132.5, 123.9, 123.6, 122.4, 122.3, 121.0, 40.0, 30.1.

HRMS-ESI: calcd. for C₁₀H₁₂NS [M + H]⁺: 178.0685; found: 178.0693.

FT-IR: ν [cm⁻¹] = 3057, 2924, 2864, 1585, 1458, 1427, 1020, 760, 732.

8. Reference

- [1] K. C. Nicolaou, *Proc. R. Soc. A* **2014**, *470*, 20130690.
- [2] I. E. Markó, *Science* **2001**, *294*, 1842–1843.
- [3] K. C. Nicolaou, D. Vourloumis, N. Winssinger, P. S. Baran, *Angew. Chem. Int. Ed.* **2000**, *39*, 44–122.
- [4] F. Wöhler, *Ann. Phys.* **1828**, *88*, 253–256.
- [5] C. Graebe, C. Liebermann, *Ber. Dtsch. Chem. Ges.* **1869**, *2*, 332–334.
- [6] A. Baeyer, *Ber. Dtsch. Chem. Ges.* **1878**, *11*, 1296–1297.
- [7] E. Fischer, *Ber. Dtsch. Chem. Ges.* **1890**, *23*, 799–805.
- [8] R. Robinson, *J. Chem. Soc., Trans.* **1917**, *111*, 762–768.
- [9] H. Fischer, K. Zeile, *Liebigs Ann. Chem.* **1929**, *468*, 98–116.
- [10] E. Fischer, F. Jourdan, *Ber. Dtsch. Chem. Ges.* **1883**, *16*, 2241–2245.
- [11] R. B. Woodward, M. P. Cava, W. D. Ollis, A. Hunger, H. U. Daeniker, K. Schenker, *J. Am. Chem. Soc.* **1954**, *76*, 4749–4751.
- [12] O. Diels, K. Alder, *Liebigs Ann. Chem.* **1928**, *460*, 98–122.
- [13] R. B. Woodward, F. E. Bader, H. Bickel, A. J. Frey, R. W. Kierstead, *Tetrahedron* **1958**, *2*, 1–57.
- [14] R. B. Woodward, *Pure Appl. Chem.* **1973**, *33*, 145–178.
- [15] A. Eschenmoser, C. Wintner, *Science* **1977**, *196*, 1410–1420.
- [16] a) R. Hoffmann, R. B. Woodward, *Acc. Chem. Res.* **1968**, *1*, 17–22; b) R. B. Woodward, R. Hoffmann, *Angew. Chem. Int. Ed.* **1969**, *8*, 781–853.
- [17] a) E. J. Corey, N. M. Weinshenker, T. K. Schaaf, W. Huber, *J. Am. Chem. Soc.* **1969**, *91*, 5675–5677; b) E. J. Corey, T. K. Schaaf, W. Huber, U. Koelliker, N. M. Weinshenker, *J. Am. Chem. Soc.* **1970**, *92*, 397–398.
- [18] a) G. Wittig, U. Schöllkopf, *Chem. Ber.* **1954**, *87*, 1318–1330; b) G. Wittig, W. Haag, *Chem. Ber.* **1955**, *88*, 1654–1666.
- [19] a) L. Horner, H. Hoffmann, H. G. Wippel, *Chem. Ber.* **1958**, *91*, 61–63; b) L. Horner, H. Hoffmann, H. G. Wippel, G. Klahre, *Chem. Ber.* **1959**, *92*, 2499–2505; c) W. S. Wadsworth, W. D. Emmons, *J. Am. Chem. Soc.* **1961**, *83*, 1733–1738.
- [20] A. Baeyer, V. Villiger, *Ber. Dtsch. Chem. Ges.* **1899**, *32*, 3625–3633.
- [21] E. J. Corey, R. K. Bakshi, S. Shibata, C. P. Chen, V. K. Singh, *J. Am. Chem. Soc.* **1987**, *109*, 7925–7926.
- [22] a) J. C. Sheehan, K. R. Henery–Logan, *J. Am. Chem. Soc.* **1957**, *79*, 1262–1263; b) J. C. Sheehan, K. R. Henery–Logan, *J. Am. Chem. Soc.* **1959**, *81*, 3089–3094.
- [23] F. J. Zeelen, *Nat. Prod. Rep.* **1994**, *11*, 607–612.
- [24] W. S. Johnson, *Angew. Chem. Int. Ed.* **1976**, *15*, 9–17.
- [25] G. Stork, R. A. Kretchmer, R. H. Schlessinger, *J. Am. Chem. Soc.* **1968**, *90*, 1647–1648.
- [26] C. A. Grob, W. Baumann, *Helv. Chim. Acta* **1955**, *38*, 594–610.
- [27] W. Dieckmann, *Ber. Dtsch. Chem. Ges.* **1894**, *27*, 102–103.
- [28] a) H. Rupe, C. Frey, *Helv. Chim. Acta* **1944**, *27*, 627–645; b) G. Buchi, W. D. MacLeod, J. Padilla, *J. Am. Chem. Soc.* **1964**, *86*, 4438–4444; c) R. A. Holton, R. R. Juo, H. B. Kim, A. D. Williams, S. Harusawa, R. E. Lowenthal, S. Yogai, *J. Am. Chem. Soc.* **1988**,

- 110, 6558–6560; d) R. A. Holton, H. B. Kim, C. Somoza, F. Liang, R. J. Biediger, P. D. Boatman, M. Shindo, C. C. Smith, S. Kim, *J. Am. Chem. Soc.* **1994**, *116*, 1599–1600; e) R. A. Holton, C. Somoza, H. B. Kim, F. Liang, R. J. Biediger, P. D. Boatman, M. Shindo, C. C. Smith, S. Kim, *J. Am. Chem. Soc.* **1994**, *116*, 1597–1598.
- [29] a) K. C. Nicolaou, C. F. Claiborne, P. G. Nantermet, E. A. Couladouros, E. J. Sorensen, *J. Am. Chem. Soc.* **1994**, *116*, 1591–1592; b) K. C. Nicolaou, Z. Yang, J. J. Liu, H. Ueno, P. G. Nantermet, R. K. Guy, C. F. Claiborne, J. Renaud, E. A. Couladouros, K. Paulvannan, E. J. Sorensen, *Nature* **1994**, *367*, 630–634; c) K. C. Nicolaou, J. J. Liu, Z. Yang, H. Ueno, E. J. Sorensen, C. F. Claiborne, R. K. Guy, C. K. Hwang, M. Nakada, P. G. Nantermet, *J. Am. Chem. Soc.* **1995**, *117*, 634–644; d) K. C. Nicolaou, H. Ueno, J. J. Liu, P. G. Nantermet, Z. Yang, J. Renaud, K. Paulvannan, R. Chadha, *J. Am. Chem. Soc.* **1995**, *117*, 653–659; e) K. C. Nicolaou, Z. Yang, J. J. Liu, P. G. Nantermet, C. F. Claiborne, J. Renaud, R. K. Guy, K. Shibayama, *J. Am. Chem. Soc.* **1995**, *117*, 645–652.
- [30] R. H. Shapiro, M. F. Lipton, K. J. Kolonko, R. L. Buswell, L. A. Capuano, *Tetrahedron Lett.* **1975**, *16*, 1811–1814.
- [31] J. E. McMurry, M. P. Fleming, *J. Am. Chem. Soc.* **1974**, *96*, 4708–4709.
- [32] S. J. Danishefsky, J. J. Masters, W. B. Young, J. T. Link, L. B. Snyder, T. V. Magee, D. K. Jung, R. C. A. Isaacs, W. G. Bornmann, C. A. Alaimo, C. A. Coburn, M. J. Di Grandi, *J. Am. Chem. Soc.* **1996**, *118*, 2843–2859.
- [33] a) M. Tsutomu, M. Kunio, O. Atsumu, *Bull. Chem. Soc. Jpn.* **1971**, *44*, 581–581; b) R. F. Heck, J. P. Nolley, *J. Org. Chem.* **1972**, *37*, 2320–2322.
- [34] a) P. A. Wender, N. F. Badham, S. P. Conway, P. E. Floreancig, T. E. Glass, C. Gränicher, J. B. Houze, J. Jänichen, D. Lee, D. G. Marquess, P. L. McGrane, W. Meng, T. P. Mucciario, M. Mühlebach, M. G. Natchus, H. Paulsen, D. B. Rawlins, J. Satkofsky, A. J. Shuker, J. C. Sutton, R. E. Taylor, K. Tomooka, *J. Am. Chem. Soc.* **1997**, *119*, 2755–2756; b) P. A. Wender, N. F. Badham, S. P. Conway, P. E. Floreancig, T. E. Glass, J. B. Houze, N. E. Krauss, D. Lee, D. G. Marquess, P. L. McGrane, W. Meng, M. G. Natchus, A. J. Shuker, J. C. Sutton, R. E. Taylor, *J. Am. Chem. Soc.* **1997**, *119*, 2757–2758.
- [35] a) K. Morihira, R. Hara, S. Kawahara, T. Nishimori, N. Nakamura, H. Kusama, I. Kuwajima, *J. Am. Chem. Soc.* **1998**, *120*, 12980–12981; b) H. Kusama, R. Hara, S. Kawahara, T. Nishimori, H. Kashima, N. Nakamura, K. Morihira, I. Kuwajima, *J. Am. Chem. Soc.* **2000**, *122*, 3811–3820.
- [36] M. Teruaki, N. Koichi, B. Kazuo, *Chem. Lett.* **1973**, *2*, 1011–1014.
- [37] S. Reformatsky, *Ber. Dtsch. Chem. Ges.* **1887**, *20*, 1210–1211.
- [38] Demselben, *Liebigs Ann. Chem.* **1859**, *110*, 23–45.
- [39] T. Mukaiyama, I. Shiina, H. Iwadare, M. Saitoh, T. Nishimura, N. Ohkawa, H. Sakoh, K. Nishimura, Y.-i. Tani, M. Hasegawa, K. Yamada, K. Saitoh, *Chem. Eur. J.* **1999**, *5*, 121–161.
- [40] a) R. Bharadwaj, H. Yu, *Oncogene* **2004**, *23*, 2016–2027; b) D. A. Brito, Z. Yang, C. L. Rieder, *J. Cell Biol.* **2008**, *182*, 623–629.
- [41] M. H. Crawford, *Science* **1989**, *246*, 34–34.
- [42] a) L. L. Klein, W. W. McWhorter, S. S. Ko, K. P. Pfaff, Y. Kishi, D. Uemura, Y. Hirata, *J. Am. Chem. Soc.* **1982**, *104*, 7362–7364; b) S. S. Ko, J. M. Finan, M. Yonaga, Y. Kishi,

- D. Uemura, Y. Hirata, *J. Am. Chem. Soc.* **1982**, *104*, 7364–7367; c) H. Fujioka, W. J. Christ, J. K. Cha, J. Leder, Y. Kishi, D. Uemura, Y. Hirata, *J. Am. Chem. Soc.* **1982**, *104*, 7367–7369; d) J. K. Cha, W. J. Christ, J. M. Finan, H. Fujioka, Y. Kishi, L. L. Klein, S. S. Ko, J. Leder, W. W. McWhorter, K. P. Pfaff, M. Yonaga, *J. Am. Chem. Soc.* **1982**, *104*, 7369–7371.
- [43] a) R. W. Armstrong, J. M. Beau, S. H. Cheon, W. J. Christ, H. Fujioka, W. H. Ham, L. D. Hawkins, H. Jin, S. H. Kang, *J. Am. Chem. Soc.* **1989**, *111*, 7530–7533; b) Y. Kishi, *Pure Appl. Chem.* **1989**, *61*, 313–324; c) E. M. Suh, Y. Kishi, *J. Am. Chem. Soc.* **1994**, *116*, 11205–11206.
- [44] P. S. Baran, *J. Am. Chem. Soc.* **2018**, *140*, 4751–4755.
- [45] J. Mulzer, *Nat. Prod. Rep.* **2014**, *31*, 595–603.
- [46] Z. Meng, H. Yu, L. Li, W. Tao, H. Chen, M. Wan, P. Yang, D. J. Edmonds, J. Zhong, A. Li, *Nat. Commun.* **2015**, *6*, 6096.
- [47] M. Yang, J. Li, A. Li, *Nat. Commun.* **2015**, *6*, 6445.
- [48] M. Yang, X. Yang, H. Sun, A. Li, *Angew. Chem. Int. Ed.* **2016**, *55*, 2851–2855.
- [49] Z. Lu, Y. Li, J. Deng, A. Li, *Nat. Chem.* **2013**, *5*, 679–684.
- [50] J. Li, P. Yang, M. Yao, J. Deng, A. Li, *J. Am. Chem. Soc.* **2014**, *136*, 16477–16480.
- [51] P. Yang, M. Yao, J. Li, Y. Li, A. Li, *Angew. Chem. Int. Ed.* **2016**, *55*, 6964–6968.
- [52] a) L. Jørgensen, S. J. McKerrall, C. A. Kuttruff, F. Ungeheuer, J. Felding, P. S. Baran, *Science* **2013**, *341*, 878–882; b) S. J. McKerrall, L. Jørgensen, C. A. Kuttruff, F. Ungeheuer, P. S. Baran, *J. Am. Chem. Soc.* **2014**, *136*, 5799–5810; c) Y. Jin, C.–H. Yeh, C. A. Kuttruff, L. Jørgensen, G. Dünstl, J. Felding, S. R. Natarajan, P. S. Baran, *Angew. Chem. Int. Ed.* **2015**, *54*, 14044–14048.
- [53] P. L. Pauson, I. U. Khand, *Ann. N.Y. Acad. Sci.* **1977**, *295*, 2–14.
- [54] M. Schroeder, *Chem. Rev.* **1980**, *80*, 187–213.
- [55] H. L. Riley, J. F. Morley, N. A. C. Friend, *J. Chem. Soc.* **1932**, 1875–1883.
- [56] W. S. Rapson, R. Robinson, *J. Chem. Soc.* **1935**, 1285–1288.
- [57] H. Chu, J. M. Smith, J. Felding, P. S. Baran, *ACS Cent. Sci.* **2017**, *3*, 47–51.
- [58] A. Mendoza, Y. Ishihara, P. S. Baran, *Nat. Chem.* **2012**, *4*, 21–25.
- [59] a) C. Yuan, Y. Jin, N. C. Wilde, P. S. Baran, *Angew. Chem. Int. Ed.* **2016**, *55*, 8280–8284; b) Y. Kanda, Y. Ishihara, N. C. Wilde, P. S. Baran, *J. Org. Chem.* **2020**, *85*, 10293–10320; c) Y. Kanda, H. Nakamura, S. Umemiya, R. K. Puthukanoori, V. R. Murthy Appala, G. K. Gaddamanugu, B. R. Paraselli, P. S. Baran, *J. Am. Chem. Soc.* **2020**, *142*, 10526–10533.
- [60] C. Krishnamurti, S. C. Rao, *Indian J. Anaesth.* **2016**, *60*, 861–862.
- [61] F. Bourgaud, A. Gravot, S. Milesi, E. Gontier, *Plant Sci.* **2001**, *161*, 839–851.
- [62] a) R. B. Rothman, M. H. Baumann, C. M. Dersch, D. V. Romero, K. C. Rice, F. I. Carroll, J. S. Partilla, *Synapse* **2001**, *39*, 32–41; b) C. Pomara, T. Cassano, D. S. Apos, Errico, S. Bello, A. D. Romano, I. Riezzo, G. Serviddio, *Curr. Med. Chem.* **2012**, *19*, 5647–5657.
- [63] R. M. Eglen, *Auton. Autacoid Pharmacol.* **2006**, *26*, 219–233.
- [64] I. P. Singh, P. Shah, *Expert Opin. Ther. Pat.* **2017**, *27*, 17–36.
- [65] M. A. Altinoz, G. Topcu, A. Hacimuftuoglu, A. Ozpinar, A. Ozpinar, E. Hacker, İ. Elmaci, *Neurochem. Res.* **2019**, *44*, 1796–1806.

- [66] J. K. Liu, W. T. Couldwell, *Neurocrit Care* **2005**, *2*, 124–132.
- [67] R. S. Gupta, L. Siminovitch, *Cell* **1977**, *10*, 61–66.
- [68] A. M. Betcher, *Anesth. Analg.* **1977**, *56*.
- [69] L. X. Chen, H. R. Schumacher, *J. Clin. Rheumatol.* **2008**, *14*, S55–S62.
- [70] S. Ferré, *J. Neurochem.* **2008**, *105*, 1067–1079.
- [71] a) R. B. Woodward, W. E. Doering, *J. Am. Chem. Soc.* **1945**, *67*, 860–874; b) J. Gutzwiller, M. Uskokovic, *J. Am. Chem. Soc.* **1970**, *92*, 204–205; c) J. Gutzwiller, M. R. Uskokovic, *J. Am. Chem. Soc.* **1978**, *100*, 576–581; d) G. Stork, D. Niu, A. Fujimoto, E. R. Koft, J. M. Balkovec, J. R. Tata, G. R. Dake, *J. Am. Chem. Soc.* **2001**, *123*, 3239–3242; e) I. T. Raheem, S. N. Goodman, E. N. Jacobsen, *J. Am. Chem. Soc.* **2004**, *126*, 706–707; f) P. Webber, M. J. Krische, *J. Org. Chem.* **2008**, *73*, 9379–9387; g) O. Illa, M. Arshad, A. Ros, E. M. McGarrigle, V. K. Aggarwal, *J. Am. Chem. Soc.* **2010**, *132*, 1828–1830.
- [72] E. Hempelmann, *Parasitol. Res.* **2007**, *100*, 671–676.
- [73] R. N. Chakravarti, D. Chakravarti, *Ind Med Gaz* **1951**, *86*, 96–97.
- [74] S. Patel, *Biomed. Pharmacother.* **2016**, *84*, 1036–1041.
- [75] X. Hui, L. Min, T. Xuan, *Curr. Med. Chem* **2009**, *16*, 327–349.
- [76] D. J. Newman, G. M. Cragg, *J. Nat. Prod.* **2020**, *83*, 770–803.
- [77] a) E. Kellenberger, A. Hofmann, R. J. Quinn, *Nat. Prod. Rep.* **2011**, *28*, 1483–1492; b) M. E. Maier, *Org. Biomol. Chem.* **2015**, *13*, 5302–5343.
- [78] a) A. L. Harvey, *Drug Discov. Today* **2008**, *13*, 894–901; b) N. I. Vasilevich, R. V. Kombarov, D. V. Genis, M. A. Kirpichenok, *J. Med. Chem.* **2012**, *55*, 7003–7009.
- [79] E. J. Corey, K. C. Nicolaou, Y. Machida, C. L. Malmsten, B. Samuelsson, *Proc. Natl. Acad. Sci. U.S.A* **1975**, *72*, 3355–3358.
- [80] K. C. Nicolaou, S. Rigol, *Nat. Prod. Rep.* **2020**, *37*, 1404–1435.
- [81] K. C. Nicolaou, T. Li, M. Nakada, C. W. Hummel, A. Hiatt, W. Wrasidlo, *Angew. Chem. Int. Ed.* **1994**, *33*, 183–186.
- [82] J. Wang, S. M. Soisson, K. Young, W. Shoop, S. Kodali, A. Galgoci, R. Painter, G. Parthasarathy, Y. S. Tang, R. Cummings, S. Ha, K. Dorso, M. Motyl, H. Jayasuriya, J. Ondeyka, K. Herath, C. Zhang, L. Hernandez, J. Allocco, Á. Basilio, J. R. Tormo, O. Genilloud, F. Vicente, F. Pelaez, L. Colwell, S. H. Lee, B. Michael, T. Felcetto, C. Gill, L. L. Silver, J. D. Hermes, K. Bartizal, J. Barrett, D. Schmatz, J. W. Becker, D. Cully, S. B. Singh, *Nature* **2006**, *441*, 358–361.
- [83] K. C. Nicolaou, A. Li, D. J. Edmonds, G. S. Tria, S. P. Ellery, *J. Am. Chem. Soc.* **2009**, *131*, 16905–16918.
- [84] K. C. Nicolaou, Y. Tang, J. Wang, A. F. Stepan, A. Li, A. Montero, *J. Am. Chem. Soc.* **2007**, *129*, 14850–14851.
- [85] K. C. Nicolaou, T. Lister, R. M. Denton, A. Montero, D. J. Edmonds, *Angew. Chem. Int. Ed.* **2007**, *46*, 4712–4714.
- [86] K. C. Nicolaou, A. F. Stepan, T. Lister, A. Li, A. Montero, G. S. Tria, C. I. Turner, Y. Tang, J. Wang, R. M. Denton, D. J. Edmonds, *J. Am. Chem. Soc.* **2008**, *130*, 13110–13119.
- [87] a) G. Mehta, V. Singh, *Chem. Soc. Rev.* **2002**, *31*, 324–334; b) L. F. Tietze, H. P. Bell, S. Chandrasekhar, *Angew. Chem. Int. Ed.* **2003**, *42*, 3996–4028.

- [88] K. C. Morrison, P. J. Hergenrother, *Nat. Prod. Rep.* **2014**, *31*, 6–14.
- [89] R. M. Wilson, S. J. Danishefsky, *J. Org. Chem.* **2006**, *71*, 8329–8351.
- [90] a) P. A. Wender, V. A. Verma, T. J. Paxton, T. H. Pillow, *Acc. Chem. Res.* **2008**, *41*, 40–49; b) P. A. Wender, *Tetrahedron* **2013**, *69*, 7529–7550; c) P. A. Wender, *Nat. Prod. Rep.* **2014**, *31*, 433–440.
- [91] a) M. Kaiser, S. Wetzel, K. Kumar, H. Waldmann, *Cell. Mol. Life Sci.* **2008**, *65*, 1186–1201; b) S. Wetzel, R. S. Bon, K. Kumar, H. Waldmann, *Angew. Chem. Int. Ed.* **2011**, *50*, 10800–10826; c) H. van Hattum, H. Waldmann, *J. Am. Chem. Soc.* **2014**, *136*, 11853–11859.
- [92] H. Shiozawa, T. Kagasaki, T. Kinoshita, H. Haruyama, H. Domon, Y. Utsui, K. Kodama, S. Takahashi, *J. Antibiot.* **1993**, *46*, 1834–1842.
- [93] S. D. Kuduk, F. F. Zheng, L. Sepp–Lorenzino, N. Rosen, S. J. Danishefsky, *Bioorg. Med. Chem. Lett.* **1999**, *9*, 1233–1238.
- [94] E. Llabani, R. W. Hicklin, H. Y. Lee, S. E. Motika, L. A. Crawford, E. Weerapana, P. J. Hergenrother, *Nat. Chem.* **2019**, *11*, 521–532.
- [95] E. Beckmann, *Ber. Dtsch. Chem. Ges.* **1886**, *19*, 988–993.
- [96] L. A. Paquette, P. E. Wiedeman, P. C. Bulman–Page, *J. Org. Chem.* **1988**, *53*, 1441–1450.
- [97] H. Berner, G. Schulz, H. Schneider, *Tetrahedron* **1980**, *36*, 1807–1811.
- [98] A. J. Birch, C. W. Holzapfel, R. W. Rickards, *Tetrahedron* **1966**, *22*, 359–387.
- [99] R. J. Rafferty, R. W. Hicklin, K. A. Maloof, P. J. Hergenrother, *Angew. Chem. Int. Ed.* **2014**, *53*, 220–224.
- [100] R. W. Hicklin, T. L. López Silva, P. J. Hergenrother, *Angew. Chem. Int. Ed.* **2014**, *53*, 9880–9883.
- [101] a) C. Gaul, J. T. Njardarson, S. J. Danishefsky, *J. Am. Chem. Soc.* **2003**, *125*, 6042–6043; b) C. Gaul, J. T. Njardarson, D. Shan, D. C. Dorn, K.–D. Wu, W. P. Tong, X.–Y. Huang, M. A. S. Moore, S. J. Danishefsky, *J. Am. Chem. Soc.* **2004**, *126*, 11326–11337; c) J. T. Njardarson, C. Gaul, D. Shan, X.–Y. Huang, S. J. Danishefsky, *J. Am. Chem. Soc.* **2004**, *126*, 1038–1040; d) D. Shan, L. Chen, J. T. Njardarson, C. Gaul, X. Ma, S. J. Danishefsky, X.–Y. Huang, *Proc. Natl. Acad. Sci. U.S.A* **2005**, *102*, 3772–3776.
- [102] G. R. Pettit, C. L. Herald, D. L. Doubek, D. L. Herald, E. Arnold, J. Clardy, *J. Am. Chem. Soc.* **1982**, *104*, 6846–6848.
- [103] a) P. A. Wender, A. J. Schrier, *J. Am. Chem. Soc.* **2011**, *133*, 9228–9231; b) B. A. DeChristopher, B. A. Loy, M. D. Marsden, A. J. Schrier, J. A. Zack, P. A. Wender, *Nat. Chem.* **2012**, *4*, 705–710; c) B. A. Loy, A. B. Lesser, D. Staveness, K. L. Billingsley, L. Cegelski, P. A. Wender, *J. Am. Chem. Soc.* **2015**, *137*, 3678–3685; d) R. Abdelnabi, D. Staveness, K. E. Near, P. A. Wender, L. Delang, J. Neyts, P. Leyssen, *Biochem. Pharmacol.* **2016**, *120*, 15–21; e) B. J. Albert, A. Niu, R. Ramani, G. R. Marshall, P. A. Wender, R. M. Williams, L. Ratner, A. B. Barnes, G. B. Kyei, *Sci. Rep.* **2017**, *7*, 7456; f) M. D. Marsden, B. A. Loy, X. Wu, C. M. Ramirez, A. J. Schrier, D. Murray, A. Shimizu, S. M. Ryckbosch, K. E. Near, T.–W. Chun, P. A. Wender, J. A. Zack, *PLoS Pathog.* **2017**, *13*, e1006575; g) P. A. Wender, C. T. Hardman, S. Ho, M. S. Jeffreys, J. K. Maclaren, R. V. Quiroz, S. M. Ryckbosch, A. J. Shimizu, J. L. Sloane, M. C. Stevens, *Science* **2017**, *358*, 218–223; h) T. K. Khan, P. A. Wender, D. L. Alkon, *J. Cell. Physiol.*

- 2018, 233, 1523–1534; i) M. D. Marsden, X. Wu, S. M. Navab, B. A. Loy, A. J. Schrier, B. A. DeChristopher, A. J. Shimizu, C. T. Hardman, S. Ho, C. M. Ramirez, P. A. Wender, J. A. Zack, *Virology* **2018**, 520, 83–93; j) C. Ly, A. J. Shimizu, M. V. Vargas, W. C. Duim, P. A. Wender, D. E. Olson, *ACS Chem. Neurosci.* **2020**, 11, 1545–1554; k) P. A. Wender, J. L. Sloane, Q. H. Luu–Nguyen, Y. Ogawa, A. J. Shimizu, S. M. Ryckbosch, J. H. Tyler, C. Hardman, *J. Org. Chem.* **2020**, 85, 15116–15128; l) E. Abramson, C. Hardman, A. J. Shimizu, S. Hwang, L. D. Hester, S. H. Snyder, P. A. Wender, P. M. Kim, M. D. Kornberg, *Cell Chem. Biol.* **2021**, 28, 1–9.
- [104] a) H. M. Wilks, A. Cortes, D. C. Emery, D. J. Halsall, A. R. Clarke, J. J. Holbrook, *Ann. N.Y. Acad. Sci.* **1992**, 672, 80–93; b) R. B. Russell, P. D. Sasiemi, M. J. E. Sternberg, *J. Mol. Biol.* **1998**, 282, 903–918.
- [105] F. J. Dekker, O. Rocks, N. Vartak, S. Menninger, C. Hedberg, R. Balamurugan, S. Wetzel, S. Renner, M. Gerauer, B. Schölermann, M. Rusch, J. W. Kramer, D. Rauh, G. W. Coates, L. Brunsveld, P. I. H. Bastiaens, H. Waldmann, *Nat. Chem. Biol.* **2010**, 6, 449–456.
- [106] J. J. Roach, Y. Sasano, C. L. Schmid, S. Zaidi, V. Katritch, R. C. Stevens, L. M. Bohn, R. A. Shenvi, *ACS Cent. Sci.* **2017**, 3, 1329–1336.
- [107] B. List, *Chem. Rev.* **2007**, 107, 5413–5415.
- [108] a) E. Knoevenagel, *Ber. Dtsch. Chem. Ges.* **1896**, 29, 172–174; b) E. Knoevenagel, *Ber. Dtsch. Chem. Ges.* **1898**, 31, 738–748; c) E. Knoevenagel, *Ber. Dtsch. Chem. Ges.* **1898**, 31, 2585–2595; d) E. Knoevenagel, *Ber. Dtsch. Chem. Ges.* **1898**, 31, 2596–2619.
- [109] a) U. Eder, G. Sauer, R. Wiechert, *Angew. Chem. Int. Ed.* **1971**, 10, 496–497; b) Z. G. Hajos, D. R. Parrish, *J. Org. Chem.* **1974**, 39, 1615–1621.
- [110] C. Agami, F. Meynier, C. Puchot, J. Guilhem, C. Pascard, *Tetrahedron* **1984**, 40, 1031–1038.
- [111] D. Rajagopal, M. S. Moni, S. Subramanian, S. Swaminathan, *Tetrahedron: Asymmetry* **1999**, 10, 1631–1634.
- [112] a) S. Bahmanyar, K. N. Houk, *J. Am. Chem. Soc.* **2001**, 123, 12911–12912; b) S. Bahmanyar, K. N. Houk, *J. Am. Chem. Soc.* **2001**, 123, 11273–11283.
- [113] a) R. B. Woodward, B. W. Au–Yeung, P. Balaram, L. J. Browne, D. E. Ward, B. W. Au–Yeung, P. Balaram, L. J. Browne, P. J. Card, C. H. Chen, *J. Am. Chem. Soc.* **1981**, 103, 3213–3215; b) R. B. Woodward, E. Logusch, K. P. Nambiar, K. Sakan, D. E. Ward, B. W. Au–Yeung, P. Balaram, L. J. Browne, P. J. Card, C. H. Chen, *J. Am. Chem. Soc.* **1981**, 103, 3210–3213; c) R. B. Woodward, E. Logusch, K. P. Nambiar, K. Sakan, D. E. Ward, B. W. Au–Yeung, P. Balaram, L. J. Browne, P. J. Card, C. H. Chen, *J. Am. Chem. Soc.* **1981**, 103, 3215–3217.
- [114] M. Yamaguchi, T. Shiraishi, M. Hirama, *Angew. Chem. Int. Ed.* **1993**, 32, 1176–1178.
- [115] A. Kawara, T. Taguchi, *Tetrahedron Lett.* **1994**, 35, 8805–8808.
- [116] Y. Tu, Z.–X. Wang, Y. Shi, *J. Am. Chem. Soc.* **1996**, 118, 9806–9807.
- [117] S. E. Denmark, Z. Wu, C. M. Crudden, H. Matsuhashi, *J. Org. Chem.* **1997**, 62, 8288–8289.
- [118] D. Yang, Y.–C. Yip, M.–W. Tang, M.–K. Wong, J.–H. Zheng, K.–K. Cheung, *J. Am. Chem. Soc.* **1996**, 118, 491–492.
- [119] M. S. Sigman, E. N. Jacobsen, *J. Am. Chem. Soc.* **1998**, 120, 4901–4902.

- [120] E. J. Corey, M. J. Grogan, *Org. Lett.* **1999**, *1*, 157–160.
- [121] S. J. Miller, G. T. Copeland, N. Papaioannou, T. E. Horstmann, E. M. Ruel, *J. Am. Chem. Soc.* **1998**, *120*, 1629–1630.
- [122] B. List, R. A. Lerner, C. F. Barbas, *J. Am. Chem. Soc.* **2000**, *122*, 2395–2396.
- [123] K. A. Ahrendt, C. J. Borths, D. W. C. MacMillan, *J. Am. Chem. Soc.* **2000**, *122*, 4243–4244.
- [124] a) M. J. Gaunt, C. C. C. Johansson, A. McNally, N. T. Vo, *Drug Discov. Today* **2007**, *12*, 8–27; b) D. W. C. MacMillan, *Nature* **2008**, *455*, 304–308; c) E. N. Jacobsen, D. W. C. MacMillan, *Proc. Natl. Acad. Sci. U.S.A* **2010**, *107*, 20618–20619.
- [125] a) A. Erkkilä, I. Majander, P. M. Pihko, *Chem. Rev.* **2007**, *107*, 5416–5470; b) S. Mukherjee, J. W. Yang, S. Hoffmann, B. List, *Chem. Rev.* **2007**, *107*, 5471–5569.
- [126] P. Melchiorre, *Angew. Chem. Int. Ed.* **2012**, *51*, 9748–9770.
- [127] M. J. Gaunt, C. C. C. Johansson, *Chem. Rev.* **2007**, *107*, 5596–5605.
- [128] T. Hashimoto, K. Maruoka, *Chem. Rev.* **2007**, *107*, 5656–5682.
- [129] D. Enders, O. Niemeier, A. Henseler, *Chem. Rev.* **2007**, *107*, 5606–5655.
- [130] T. Akiyama, J. Itoh, K. Yokota, K. Fuchibe, *Angew. Chem. Int. Ed.* **2004**, *43*, 1566–1568.
- [131] D. Uraguchi, M. Terada, *J. Am. Chem. Soc.* **2004**, *126*, 5356–5357.
- [132] a) D. Parmar, E. Sugiono, S. Raja, M. Rueping, *Chem. Rev.* **2014**, *114*, 9047–9153; b) R. Maji, S. C. Mallojjala, S. E. Wheeler, *Chem. Soc. Rev.* **2018**, *47*, 1142–1158.
- [133] T. Hashimoto, K. Maruoka, *Synthesis* **2008**, *2008*, 3703–3706.
- [134] M. Terada, K. Sorimachi, D. Uraguchi, *Synlett* **2006**, *2006*, 0133–0136.
- [135] a) D. Nakashima, H. Yamamoto, *J. Am. Chem. Soc.* **2006**, *128*, 9626–9627; b) S. Lee, S. Kim, *Tetrahedron Lett.* **2009**, *50*, 3345–3348; c) J.-W. Zhang, Q. Cai, X.-X. Shi, W. Zhang, S.-L. You, *Synlett* **2011**, *2011*, 1239–1242; d) S.-G. Wang, L. Han, M. Zeng, F.-L. Sun, W. Zhang, S.-L. You, *Org. Biomol. Chem.* **2012**, *10*, 3202–3209; e) D. Enders, A. Rembiak, M. Seppelt, *Tetrahedron Lett.* **2013**, *54*, 470–473; f) F. E. Held, D. Grau, S. B. Tsogoeva, *Molecules* **2015**, *20*, 16103–16126; g) H. Wu, Q. Wang, J. Zhu, *Angew. Chem. Int. Ed.* **2017**, *56*, 5858–5861; h) J. Kikuchi, M. Terada, *Angew. Chem. Int. Ed.* **2019**, *58*, 8458–8462; i) H. Wu, Q. Wang, J. Zhu, *J. Am. Chem. Soc.* **2019**, *141*, 11372–11377.
- [136] P. S. J. Kaib, B. List, *Synlett* **2016**, *27*, 156–158.
- [137] A. Berkessel, P. Christ, N. Leconte, J.-M. Neudörfl, M. Schäfer, *Eur. J. Org. Chem.* **2010**, *2010*, 5165–5170.
- [138] a) L. Ratjen, P. García-García, F. Lay, M. E. Beck, B. List, *Angew. Chem. Int. Ed.* **2011**, *50*, 754–758; b) J. Guin, C. Rabalakos, B. List, *Angew. Chem. Int. Ed.* **2012**, *51*, 8859–8863; c) Q. Wang, M. Leutzsch, M. van Gemmeren, B. List, *J. Am. Chem. Soc.* **2013**, *135*, 15334–15337; d) L. Ratjen, M. van Gemmeren, F. Pesciaioli, B. List, *Angew. Chem. Int. Ed.* **2014**, *53*, 8765–8769; e) Q. Wang, M. van Gemmeren, B. List, *Angew. Chem. Int. Ed.* **2014**, *53*, 13592–13595; f) T. James, M. van Gemmeren, B. List, *Chem. Rev.* **2015**, *115*, 9388–9409; g) V. N. Wakchaure, P. S. J. Kaib, M. Leutzsch, B. List, *Angew. Chem. Int. Ed.* **2015**, *54*, 11852–11856; h) V. N. Wakchaure, B. List, *Angew. Chem. Int. Ed.* **2016**, *55*, 15775–15778; i) F. Mandrelli, A. Blond, T. James, H. Kim, B. List, *Angew. Chem. Int. Ed.* **2019**, *58*, 11479–11482; j) V. N. Wakchaure, C. Obradors,

- B. List, *Synlett* **2020**, *31*, 1707–1712.
- [139] T. Gatzemeier, M. van Gemmeren, Y. Xie, D. Höfler, M. Leutzsch, B. List, *Science* **2016**, *351*, 949–952.
- [140] a) I. Čorić, B. List, *Nature* **2012**, *483*, 315–319; b) S. Liao, I. Čorić, Q. Wang, B. List, *J. Am. Chem. Soc.* **2012**, *134*, 10765–10768; c) L. Liu, M. Leutzsch, Y. Zheng, M. W. Alachraf, W. Thiel, B. List, *J. Am. Chem. Soc.* **2015**, *137*, 13268–13271; d) G. C. Tsui, L. Liu, B. List, *Angew. Chem. Int. Ed.* **2015**, *54*, 7703–7706; e) S. Das, L. Liu, Y. Zheng, M. W. Alachraf, W. Thiel, C. K. De, B. List, *J. Am. Chem. Soc.* **2016**, *138*, 9429–9432; f) Y. Xie, G.–J. Cheng, S. Lee, P. S. J. Kaib, W. Thiel, B. List, *J. Am. Chem. Soc.* **2016**, *138*, 14538–14541; g) J. H. Kim, A. Tap, L. Liu, B. List, *Synlett* **2017**, *28*, 333–336; h) Y. Xie, B. List, *Angew. Chem. Int. Ed.* **2017**, *56*, 4936–4940.
- [141] L. Liu, P. S. J. Kaib, A. Tap, B. List, *J. Am. Chem. Soc.* **2016**, *138*, 10822–10825.
- [142] a) P. S. J. Kaib, L. Schreyer, S. Lee, R. Properzi, B. List, *Angew. Chem. Int. Ed.* **2016**, *55*, 13200–13203; b) S. Lee, P. S. J. Kaib, B. List, *J. Am. Chem. Soc.* **2017**, *139*, 2156–2159; c) L. Liu, H. Kim, Y. Xie, C. Farès, P. S. J. Kaib, R. Goddard, B. List, *J. Am. Chem. Soc.* **2017**, *139*, 13656–13659; d) H. Y. Bae, D. Höfler, P. S. J. Kaib, P. Kasaplar, C. K. De, A. Döhring, S. Lee, K. Kaupmees, I. Leito, B. List, *Nat. Chem.* **2018**, *10*, 888–894; e) L. Schreyer, P. S. J. Kaib, V. N. Wakchaure, C. Obradors, R. Properzi, S. Lee, B. List, *Science* **2018**, *362*, 216–219; f) N. Tsuji, J. L. Kennemur, T. Buyck, S. Lee, S. Prévost, P. S. J. Kaib, D. Bykov, C. Farès, B. List, *Science* **2018**, *359*, 1501–1505; g) H. Kim, G. Gerosa, J. Aronow, P. Kasaplar, J. Ouyang, J. B. Lingnau, P. Guerry, C. Farès, B. List, *Nat. Commun.* **2019**, *10*, 770; h) J. Ouyang, J. L. Kennemur, C. K. De, C. Farès, B. List, *J. Am. Chem. Soc.* **2019**, *141*, 3414–3418; i) S. Ghosh, S. Das, C. K. De, D. Yepes, F. Neese, G. Bistoni, M. Leutzsch, B. List, *Angew. Chem. Int. Ed.* **2020**, *59*, 12347–12351; j) R. Properzi, P. S. J. Kaib, M. Leutzsch, G. Pupo, R. Mitra, C. K. De, L. Song, P. R. Schreiner, B. List, *Nat. Chem.* **2020**, *12*, 1174–1179; k) H. Zhou, H. Y. Bae, M. Leutzsch, J. L. Kennemur, D. Bécart, B. List, *J. Am. Chem. Soc.* **2020**, *142*, 13695–13700.
- [143] A. G. Doyle, E. N. Jacobsen, *Chem. Rev.* **2007**, *107*, 5713–5743.
- [144] Y. Takemoto, *Chem. Pharm. Bull.* **2010**, *58*, 593–601.
- [145] T. N. Nguyen, P.–A. Chen, K. Setthakarn, J. A. May, *Molecules* **2018**, *23*, 2317.
- [146] S. Dong, X. Feng, X. Liu, *Chem. Soc. Rev.* **2018**, *47*, 8525–8540.
- [147] J. E. Taylor, S. D. Bull, J. M. J. Williams, *Chem. Soc. Rev.* **2012**, *41*, 2109–2121.
- [148] R. Abdul, T. Cihangir, *Curr. Org. Chem.* **2016**, *20*, 2996–3013.
- [149] G. P. Moss, *Pure Appl. Chem.* **1996**, *68*, 2193–2222.
- [150] S. Kaneko, T. Yoshino, T. Katoh, S. Terashima, *Tetrahedron* **1998**, *54*, 5471–5484.
- [151] J. Carpenter, A. B. Northrup, d. Chung, J. J. M. Wiener, S.–G. Kim, D. W. C. MacMillan, *Angew. Chem. Int. Ed.* **2008**, *47*, 3568–3572.
- [152] S. B. Jones, B. Simmons, A. Mastracchio, D. W. C. MacMillan, *Nature* **2011**, *475*, 183–188.
- [153] R. R. Knowles, J. Carpenter, S. B. Blakey, A. Kayano, I. K. Mangion, C. J. Sinz, D. W. C. MacMillan, *Chem. Sci.* **2011**, *2*, 308–311.
- [154] S. N. Ananchenko, I. V. Torgov, *Tetrahedron Lett.* **1963**, *4*, 1553–1558.
- [155] S. Prévost, N. Dupré, M. Leutzsch, Q. Wang, V. Wakchaure, B. List, *Angew. Chem. Int.*

- Ed.* **2014**, *53*, 8770–8773.
- [156] J.–B. Gualtierotti, D. Pasche, Q. Wang, J. Zhu, *Angew. Chem. Int. Ed.* **2014**, *53*, 9926–9930.
- [157] I. P. Andrews, O. Kwon, *Chem. Sci.* **2012**, *3*, 2510–2514.
- [158] E. M. Phillips, J. M. Roberts, K. A. Scheidt, *Org. Lett.* **2010**, *12*, 2830–2833.
- [159] I. T. Raheem, P. S. Thiara, E. A. Peterson, E. N. Jacobsen, *J. Am. Chem. Soc.* **2007**, *129*, 13404–13405.
- [160] L. M. Schneider, V. M. Schmiedel, T. Pecchioli, D. Lentz, C. Merten, M. Christmann, *Org. Lett.* **2017**, *19*, 2310–2313.
- [161] V. M. Schmiedel, Y. J. Hong, D. Lentz, D. J. Tantillo, M. Christmann, *Angew. Chem. Int. Ed.* **2018**, *57*, 2419–2422.
- [162] S. Su, R. A. Rodriguez, P. S. Baran, *J. Am. Chem. Soc.* **2011**, *133*, 13922–13925.
- [163] R. A. Rodriguez, C.–M. Pan, Y. Yabe, Y. Kawamata, M. D. Eastgate, P. S. Baran, *J. Am. Chem. Soc.* **2014**, *136*, 6908–6911.
- [164] L. W. Hernandez, J. Pospech, U. Klöckner, T. W. Bingham, D. Sarlah, *J. Am. Chem. Soc.* **2017**, *139*, 15656–15659.
- [165] E. H. Southgate, J. Pospech, J. Fu, D. R. Holycross, D. Sarlah, *Nat. Chem.* **2016**, *8*, 922–928.
- [166] S. G. Davies, M. L. H. Green, D. M. P. Mingos, *Tetrahedron* **1978**, *34*, 3047–3077.
- [167] V. VanRheenen, R. C. Kelly, D. Y. Cha, *Tetrahedron Lett.* **1976**, *17*, 1973–1976.
- [168] a) W. H. Brooks, W. C. Guida, K. G. Daniel, *Curr. Top. Med. Chem.* **2011**, *11*, 760–770; b) M. Abram, M. Jakubiec, K. Kamiński, *ChemMedChem* **2019**, *14*, 1744–1761.
- [169] R. Cao, W. Peng, Z. Wang, A. Xu, *Curr. Med. Chem.* **2007**, *14*, 479–500.
- [170] a) D. M. Balitz, J. A. Bush, W. T. Bradner, T. W. Doyle, F. A. Oherron, D. E. Nettleton, *J. Antibiot.* **1982**, *35*, 259–265; b) M. Hassani, W. Cai, K. H. Koelsch, D. C. Holley, A. S. Rose, F. Olang, J. P. Lineswala, W. G. Holloway, J. M. Gerdes, M. Behforouz, H. D. Beall, *J. Med. Chem.* **2008**, *51*, 3104–3115.
- [171] R. Sakai, K. L. Rinehart, Y. Guan, A. H. Wang, *Proc. Natl. Acad. Sci. U.S.A* **1992**, *89*, 11456–11460.
- [172] Y.–s. Zhang, J.–d. Li, C. Yan, *Eur. J. Pharmacol.* **2018**, *819*, 30–34.
- [173] M. Rottmann, C. McNamara, B. K. S. Yeung, M. C. S. Lee, B. Zou, B. Russell, P. Seitz, D. M. Plouffe, N. V. Dharia, J. Tan, S. B. Cohen, K. R. Spencer, G. E. González-Páez, S. B. Lakshminarayana, A. Goh, R. Suwanarusk, T. Jegla, E. K. Schmitt, H.–P. Beck, R. Brun, F. Nosten, L. Renia, V. Dartois, T. H. Keller, D. A. Fidock, E. A. Winzeler, T. T. Diagana, *Science* **2010**, *329*, 1175–1180.
- [174] M. Ozawa, Y. Nakada, K. Sugimachi, F. Yabuuchi, T. Akai, E. Mizuta, S. Kuno, M. Yamaguchi, *Jpn. J. Pharmacol.* **1994**, *64*, 179–188.
- [175] W. Löscher, D. Hönack, *Naunyn–Schmiedeberg's Arch. Pharmacol.* **1992**, *345*, 452–460.
- [176] Y. Ota, T. Chinen, K. Yoshida, S. Kudo, Y. Nagumo, Y. Shiwa, R. Yamada, H. Umihara, K. Iwasaki, H. Masumoto, S. Yokoshima, H. Yoshikawa, T. Fukuyama, J. Kobayashi, T. Usui, *ChemBioChem* **2016**, *17*, 1616–1620.
- [177] Q.–B. Xu, X.–F. Chen, J. Feng, J.–F. Miao, J. Liu, F.–T. Liu, B.–X. Niu, J.–Y. Cai, C. Huang, Y. Zhang, Y. Ling, *Sci. Rep.* **2016**, *6*, 36238.

- [178] J. Stöckigt, A. P. Antonchick, F. Wu, H. Waldmann, *Angew. Chem. Int. Ed.* **2011**, *50*, 8538–8564.
- [179] a) M. Rueffer, N. Nagakura, M. H. Zenk, *Tetrahedron Lett.* **1978**, *19*, 1593–1596; b) N. Nagakura, M. Ruffer, M. H. Zenk, *J. Chem. Soc., Perkin Trans. 1* **1979**, 2308–2312; c) R. T. Brown, J. Leonard, S. K. Sleight, *Phytochemistry* **1978**, *17*, 899–900.
- [180] a) G. N. Smith, *Chem. Commun.* **1968**, 912–914; b) A. R. Battersby, A. R. Burnett, P. G. Parsons, *Chem. Commun.* **1968**, 1280–1281.
- [181] Q. Chen, C. Ji, Y. Song, H. Huang, J. Ma, X. Tian, J. Ju, *Angew. Chem. Int. Ed.* **2013**, *52*, 9980–9984.
- [182] A. Bischler, B. Napieralski, *Ber. Dtsch. Chem. Ges.* **1893**, *26*, 1903–1908.
- [183] A. Pictet, T. Spengler, *Ber. Dtsch. Chem. Ges.* **1911**, *44*, 2030–2036.
- [184] K. C. Nicolaou, C. J. N. Mathison, T. Montagnon, *J. Am. Chem. Soc.* **2004**, *126*, 5192–5201.
- [185] A. Kamal, Y. Tangella, K. L. Manasa, M. Sathish, V. Srinivasulu, J. Chetna, A. Alarifí, *Org. Biomol. Chem.* **2015**, *13*, 8652–8662.
- [186] H. Zhang, R. C. Larock, *J. Org. Chem.* **2002**, *67*, 9318–9330.
- [187] Q. Yan, E. Gin, M. G. Banwell, A. C. Willis, P. D. Carr, *J. Org. Chem.* **2017**, *82*, 4328–4335.
- [188] R. S. Kusurkar, S. K. Goswami, *Tetrahedron* **2004**, *60*, 5315–5318.
- [189] Z.-X. Wang, J.-C. Xiang, Y. Cheng, J.-T. Ma, Y.-D. Wu, A.-X. Wu, *J. Org. Chem.* **2018**, *83*, 12247–12254.
- [190] M. T. Rahman, V. V. N. P. B. Tiruveedhula, J. M. Cook, *Molecules* **2016**, *21*, 1525.
- [191] V. Muñoz, C. Moretti, M. Sauvain, C. Caron, A. Porzel, G. Massiot, B. Richard, L. Le Men–Olivier, *Planta Med.* **1994**, *60*, 455–459.
- [192] J. M. Cook, P. W. Le Quesne, *Phytochemistry* **1971**, *10*, 437–439.
- [193] T. Kishi, M. Hesse, W. Vetter, C. W. Gemenden, W. I. Taylor, H. Schmid, *Helv. Chim. Acta* **1966**, *49*, 946–964.
- [194] a) X. Liao, H. Zhou, X. Z. Wearing, J. Ma, J. M. Cook, *Org. Lett.* **2005**, *7*, 3501–3504; b) D. E. Burke, C. A. DeMarkey, P. W. Le Quesne, J. M. Cook, *J. Chem. Soc., Chem. Commun.* **1972**, 1346–1347; c) G. Buchi, R. E. Manning, S. A. Monti, *J. Am. Chem. Soc.* **1964**, *86*, 4631–4641; d) G. Buchi, R. E. Manning, S. A. Monti, *J. Am. Chem. Soc.* **1963**, *85*, 1893–1894.
- [195] a) R. L. Garnick, P. W. Le Quesne, *J. Am. Chem. Soc.* **1978**, *100*, 4213–4219; b) S. Zhao, X. Liao, T. Wang, J. Flippen–Anderson, J. M. Cook, *J. Org. Chem.* **2003**, *68*, 6279–6295.
- [196] K.-B. Wang, Y.-T. Di, Y. Bao, C.-M. Yuan, G. Chen, D.-H. Li, J. Bai, H.-P. He, X.-J. Hao, Y.-H. Pei, Y.-K. Jing, Z.-L. Li, H.-M. Hua, *Org. Lett.* **2014**, *16*, 4028–4031.
- [197] N. Harada, K. Nakanishi, *Acc. Chem. Res.* **1972**, *5*, 257–263.
- [198] a) A. W. Hofmann, *Ber. Dtsch. Chem. Ges.* **1879**, *12*, 984–990; b) A. W. Hofmann, *Ber. Dtsch. Chem. Ges.* **1881**, *14*, 2725–2736; c) A. W. Hofmann, *Ber. Dtsch. Chem. Ges.* **1885**, *18*, 5–23; d) A. W. Hofmann, *Ber. Dtsch. Chem. Ges.* **1885**, *18*, 109–131; e) K. Löffler, C. Freytag, *Ber. Dtsch. Chem. Ges.* **1909**, *42*, 3427–3431; f) K. Löffler, S. Kober, *Ber. Dtsch. Chem. Ges.* **1909**, *42*, 3431–3438; g) K. Löffler, *Ber. Dtsch. Chem. Ges.* **1910**, *43*, 2035–2048; h) M. E. Wolff, *Chem. Rev.* **1963**, *63*, 55–64.

- [199] J. Pícha, V. Vaněk, M. Buděšínský, J. Mládková, T. A. Garrow, J. Jiráček, *Eur. J. Med. Chem.* **2013**, *65*, 256–275.
- [200] a) F. A. Davis, O. D. Stringer, *J. Org. Chem.* **1982**, *47*, 1774–1775; b) F. A. Davis, B. C. Chen, *Chem. Rev.* **1992**, *92*, 919–934; c) R. W. Clark, T. M. Deaton, Y. Zhang, M. I. Moore, S. L. Wiskur, *Org. Lett.* **2013**, *15*, 6132–6135.
- [201] D. S. Pedersen, T. V. Robinson, D. K. Taylor, E. R. T. Tiekink, *J. Org. Chem.* **2009**, *74*, 4400–4403.
- [202] H. Machleidt, E. Cohnen, R. Tschesche, *Liebigs Ann. Chem.* **1962**, *655*, 70–80.
- [203] R. M. Beesley, C. K. Ingold, J. F. Thorpe, *J. Chem. Soc., Trans.* **1915**, *107*, 1080–1106.
- [204] A. Basha, M. Lipton, S. M. Weinreb, *Tetrahedron Lett.* **1977**, *18*, 4171–4172.
- [205] K. Omura, D. Swern, *Tetrahedron* **1978**, *34*, 1651–1660.
- [206] a) J. N. Brønsted, *Recl. Trav. Chim. Pays-Bas* **1923**, *42*, 718–728; b) T. M. Lowry, *J. Soc. Chem. Ind.* **1923**, *42*, 43–47; c) T. Akiyama, K. Mori, *Chem. Rev.* **2015**, *115*, 9277–9306.
- [207] Q. Xiao, W.-W. Ren, Z.-X. Chen, T.-W. Sun, Y. Li, Q.-D. Ye, J.-X. Gong, F.-K. Meng, L. You, Y.-F. Liu, M.-Z. Zhao, L.-M. Xu, Z.-H. Shan, Y. Shi, Y.-F. Tang, J.-H. Chen, Z. Yang, *Angew. Chem. Int. Ed.* **2011**, *50*, 7373–7377.
- [208] E. J. Corey, C. U. Kim, *J. Am. Chem. Soc.* **1972**, *94*, 7586–7587.
- [209] C. Piemontesi, Q. Wang, J. Zhu, *J. Am. Chem. Soc.* **2016**, *138*, 11148–11151.
- [210] L. S. Liebeskind, J. Srogl, *J. Am. Chem. Soc.* **2000**, *122*, 11260–11261.
- [211] A. de la Torre, D. Kaiser, N. Maulide, *J. Am. Chem. Soc.* **2017**, *139*, 6578–6581.
- [212] D. F. Taber, P. K. Tirunahari, *Tetrahedron* **2011**, *67*, 7195–7210.
- [213] a) H. Hemetsberger, D. Knittel, H. Weidmann, *Monatsh. Chem* **1970**, *101*, 161–165; b) S. Wagaw, B. H. Yang, S. L. Buchwald, *J. Am. Chem. Soc.* **1998**, *120*, 6621–6622.
- [214] a) R. J. Sundberg, T. Yamazaki, *J. Org. Chem.* **1967**, *32*, 290–294; b) R. C. Larock, E. K. Yum, *J. Am. Chem. Soc.* **1991**, *113*, 6689–6690.
- [215] K. Teranishi, S.-i. Nakatsuka, T. Goto, *Synthesis* **1994**, *1994*, 1018–1020.
- [216] M. Inoue, Y. Sumii, N. Shibata, *ACS Omega* **2020**, *5*, 10633–10640.
- [217] T. G. Gant, *J. Med. Chem.* **2014**, *57*, 3595–3611.
- [218] L. S. Bartell, E. A. Roth, C. D. Hollowell, K. Kuchitsu, J. E. Y. Jr., *The Journal of Chemical Physics* **1965**, *42*, 2683–2686.
- [219] a) S.-L. Paiva, C. M. Crews, *Curr. Opin. Chem. Biol.* **2019**, *50*, 111–119; b) H. Gao, X. Sun, Y. Rao, *ACS Medicinal Chemistry Letters* **2020**, *11*, 237–240.
- [220] a) M. Jida, O.-M. Soueidan, B. Deprez, G. Laconde, R. Deprez-Poulain, *Green Chem.* **2012**, *14*, 909–911; b) D. K. Singh, M. Nath, *Org. Biomol. Chem.* **2015**, *13*, 1836–1845.
- [221] a) M. Yamanaka, A. Nishida, M. Nakagawa, *Org. Lett.* **2000**, *2*, 159–161; b) N. Srinivasan, A. Ganesan, *Chem. Commun.* **2003**, 916–917; c) K. Manabe, D. Nobutou, S. Kobayashi, *Biorg. Med. Chem.* **2005**, *13*, 5154–5158; d) S. W. Youn, *J. Org. Chem.* **2006**, *71*, 2521–2523.
- [222] a) Y. Gnas, F. Glorius, *Synthesis* **2006**, *2006*, 1899–1930; b) G. Diaz-Muñoz, I. L. Miranda, S. K. Sartori, D. C. de Rezende, M. Alves Nogueira Diaz, *Chirality* **2019**, *31*, 776–812.
- [223] H. Waldmann, G. Schmidt, M. Jansen, J. Geb, *Tetrahedron* **1994**, *50*, 11865–11884.
- [224] H. Waldmann, G. Schmidt, H. Henke, M. Burkard, *Angew. Chem. Int. Ed.* **1995**, *34*,

- 2402–2403.
- [225] C. Gremmen, B. Willemse, M. J. Wanner, G.–J. Koomen, *Org. Lett.* **2000**, *2*, 1955–1958.
- [226] F. R. Bou–Hamdan, J. L. Leighton, *Angew. Chem. Int. Ed.* **2009**, *48*, 2403–2406.
- [227] J. Seayad, A. M. Seayad, B. List, *J. Am. Chem. Soc.* **2006**, *128*, 1086–1087.
- [228] a) M. J. Wanner, R. N. S. van der Haas, K. R. de Cuba, J. H. van Maarseveen, H. Hiemstra, *Angew. Chem. Int. Ed.* **2007**, *46*, 7485–7487; b) N. V. Sewgobind, M. J. Wanner, S. Ingemann, R. de Gelder, J. H. van Maarseveen, H. Hiemstra, *J. Org. Chem.* **2008**, *73*, 6405–6408; c) D.–J. Cheng, H.–B. Wu, S.–K. Tian, *Org. Lett.* **2011**, *13*, 5636–5639; d) D. Huang, F. Xu, X. Lin, Y. Wang, *Chem. Eur. J.* **2012**, *18*, 3148–3152; e) E. Mons, M. J. Wanner, S. Ingemann, J. H. van Maarseveen, H. Hiemstra, *J. Org. Chem.* **2014**, *79*, 7380–7390.
- [229] a) M. E. Muratore, C. A. Holloway, A. W. Pilling, R. I. Storer, G. Trevitt, D. J. Dixon, *J. Am. Chem. Soc.* **2009**, *131*, 10796–10797; b) C. A. Holloway, M. E. Muratore, R. I. Storer, D. J. Dixon, *Org. Lett.* **2010**, *12*, 4720–4723; c) S. Duce, F. Pesciaioli, L. Gramigna, L. Bernardi, A. Mazzanti, A. Ricci, G. Bartoli, G. Bencivenni, *Adv. Synth. Catal.* **2011**, *353*, 860–864.
- [230] a) C. Carter, S. Fletcher, A. Nelson, *Tetrahedron: Asymmetry* **2003**, *14*, 1995–2004; b) J. Lacour, V. Hebbe–Viton, *Chem. Soc. Rev.* **2003**, *32*, 373–382; c) R. Dorta, L. Shimon, D. Milstein, *J. Organomet. Chem.* **2004**, *689*, 751–758; d) D. B. Llewellyn, B. A. Arndtsen, *Tetrahedron: Asymmetry* **2005**, *16*, 1789–1799; e) N. J. A. Martin, B. List, *J. Am. Chem. Soc.* **2006**, *128*, 13368–13369; f) S. Mayer, B. List, *Angew. Chem. Int. Ed.* **2006**, *45*, 4193–4195; g) M. Mahlau, P. García–García, B. List, *Chem. Eur. J.* **2012**, *18*, 16283–16287; h) M. Mahlau, B. List, *Isr. J. Chem.* **2012**, *52*, 630–638; i) R. J. Phipps, G. L. Hamilton, F. D. Toste, *Nat. Chem.* **2012**, *4*, 603–614; j) K. Brak, E. N. Jacobsen, *Angew. Chem. Int. Ed.* **2013**, *52*, 534–561; k) M. Mahlau, B. List, *Angew. Chem. Int. Ed.* **2013**, *52*, 518–533; l) Z. Zhang, H. Y. Bae, J. Guin, C. Rabalakos, M. van Gemmeren, M. Leutzsch, M. Klussmann, B. List, *Nat. Commun.* **2016**, *7*, 12478.
- [231] a) B. E. Maryanoff, H.–C. Zhang, J. H. Cohen, I. J. Turchi, C. A. Maryanoff, *Chem. Rev.* **2004**, *104*, 1431–1628; b) J. Royer, M. Bonin, L. Micouin, *Chem. Rev.* **2004**, *104*, 2311–2352.
- [232] M. S. Taylor, E. N. Jacobsen, *J. Am. Chem. Soc.* **2004**, *126*, 10558–10559.
- [233] a) R. S. Klausen, E. N. Jacobsen, *Org. Lett.* **2009**, *11*, 887–890; b) Y. Lee, R. S. Klausen, E. N. Jacobsen, *Org. Lett.* **2011**, *13*, 5564–5567.
- [234] R. S. Klausen, C. R. Kennedy, A. M. Hyde, E. N. Jacobsen, *J. Am. Chem. Soc.* **2017**, *139*, 12299–12309.
- [235] N. Mittal, D. X. Sun, D. Seidel, *Org. Lett.* **2014**, *16*, 1012–1015.
- [236] N. Glinsky–Olivier, S. Yang, P. Retailleau, V. Gandon, X. Guinchard, *Org. Lett.* **2019**, *21*, 9446–9451.
- [237] C. Min, N. Mittal, D. X. Sun, D. Seidel, *Angew. Chem. Int. Ed.* **2013**, *52*, 14084–14088.
- [238] C. D. Gheewala, B. E. Collins, T. H. Lambert, *Science* **2016**, *351*, 961–965.
- [239] a) R. F. Salikov, K. P. Trainov, D. N. Platonov, A. Y. Belyy, Y. V. Tomilov, *Eur. J. Org. Chem.* **2018**, *2018*, 5065–5068; b) M. A. Radtke, C. C. Dudley, J. M. O’Leary, T. H. Lambert, *Synthesis* **2019**, *51*, 1135–1138.

- [240] B. Mitschke, M. Turberg, B. List, *Chem* **2020**, *6*, 2515–2532.
- [241] a) A. Borgoo, D. J. Tozer, P. Geerlings, F. De Proft, *Phys. Chem. Chem. Phys.* **2008**, *10*, 1406–1410; b) A. Borgoo, D. J. Tozer, P. Geerlings, F. De Proft, *Phys. Chem. Chem. Phys.* **2009**, *11*, 2862–2868.
- [242] a) L. Schreyer, R. Properzi, B. List, *Angew. Chem. Int. Ed.* **2019**, *58*, 12761–12777; b) M. Rueping, B. J. Nachtsheim, W. Ieawsuwan, I. Atodiresei, *Angew. Chem. Int. Ed.* **2011**, *50*, 6706–6720.
- [243] S. Vellalath, I. Čorić, B. List, *Angew. Chem. Int. Ed.* **2010**, *49*, 9749–9752.
- [244] a) L. F. Tietze, U. Beifuss, *Angew. Chem. Int. Ed.* **1993**, *32*, 131–163; b) A. Padwa, S. K. Bur, *Tetrahedron* **2007**, *63*, 5341–5378.
- [245] K. A. Johnson, *J. Biol. Chem.* **2008**, *283*, 26297–26301.
- [246] M. Mantina, A. C. Chamberlin, R. Valero, C. J. Cramer, D. G. Truhlar, *J. Phys. Chem. A* **2009**, *113*, 5806–5812.
- [247] H. Schiff, *Liebigs Ann. Chem.* **1864**, *131*, 118–119.
- [248] a) H. Mayr, A. R. Ofial, *Tetrahedron Lett.* **1997**, *38*, 3503–3506; b) H. Mayr, B. Kempf, A. R. Ofial, *Acc. Chem. Res.* **2003**, *36*, 66–77; c) L. Kværnø, P.-O. Norrby, D. Tanner, *Org. Biomol. Chem.* **2003**, *1*, 1041–1048; d) R. Appel, H. Mayr, *J. Am. Chem. Soc.* **2011**, *133*, 8240–8251.
- [249] a) H. Böhme, E. Mundlos, O.-E. Herboth, *Chem. Ber.* **1957**, *90*, 2003–2008; b) H. Böhme, H. Ellenberg, *Chem. Ber.* **1959**, *92*, 2976–2981; c) H. Böhme, K. Hartke, *Chem. Ber.* **1960**, *93*, 1305–1309; d) H. Böhme, L. Koch, E. Köhler, *Chem. Ber.* **1962**, *95*, 1849–1858; e) H. Böhme, H. J. Bohn, E. Köhler, J. Roehr, *Liebigs Ann. Chem.* **1963**, *664*, 130–140; f) H. Böhme, K.-H. Mever-Dulheuer, *Liebigs Ann. Chem.* **1965**, *688*, 78–93; g) C. Rochin, O. Babot, J. Dunoguès, F. Duboudin, *Synthesis* **1986**, *1986*, 228–229; h) C. Betschart, B. Schmidt, D. Seebach, *Helv. Chim. Acta* **1988**, *71*, 1999–2021; i) M. J. Earle, R. A. Fairhurst, H. Heaney, G. Papageorgiou, R. F. Wilkins, *Tetrahedron Lett.* **1990**, *31*, 4229–4232; j) D. B. Grotjahn, R. J. Albers, J. Beckman, *Synlett* **2000**, *2000*, 0633–0634.
- [250] N. J. Leonard, A. S. Hay, R. W. Fulmer, V. W. Gash, *J. Am. Chem. Soc.* **1955**, *77*, 439–444.
- [251] H. A. Bates, H. Rapoport, *J. Am. Chem. Soc.* **1979**, *101*, 1259–1265.
- [252] a) C. A. Grob, A. Kaiser, E. Renk, *Helv. Chim. Acta* **1957**, *40*, 2170–2185; b) G. Optiz, A. Griesinger, *Liebigs Ann. Chem.* **1963**, *665*, 101–113; c) G. Stork, A. Brizzolara, H. Landesman, J. Szmuszkovicz, R. Terrell, *J. Am. Chem. Soc.* **1963**, *85*, 207–222; d) G. A. Olah, P. Kreienbuehl, *J. Am. Chem. Soc.* **1967**, *89*, 4756–4759.
- [253] A. Strecker, *Liebigs Ann. Chem.* **1850**, *75*, 27–45.
- [254] J. Wang, X. Liu, X. Feng, *Chem. Rev.* **2011**, *111*, 6947–6983.
- [255] a) C. Mannich, W. Krösche, *Arch. Pharm.* **1912**, *250*, 647–667; b) C. Mannich, *Arch. Pharm.* **1917**, *255*, 261–276.
- [256] O. I. Afanasyev, E. Kuchuk, D. L. Usanov, D. Chusov, *Chem. Rev.* **2019**, *119*, 11857–11911.
- [257] A. Vilsmeier, A. Haack, *Ber. Dtsch. Chem. Ges.* **1927**, *60*, 119–122.
- [258] B. Zhao, X.-Y. Hao, J.-X. Zhang, S. Liu, X.-J. Hao, *Org. Lett.* **2013**, *15*, 528–530.
- [259] L. Leng, X. Zhou, Q. Liao, F. Wang, H. Song, D. Zhang, X.-Y. Liu, Y. Qin, *Angew.*

- Chem. Int. Ed.* **2017**, *56*, 3703–3707.
- [260] B. M. Trost, W. Tang, F. D. Toste, *J. Am. Chem. Soc.* **2005**, *127*, 14785–14803.
- [261] P. D. Bailey, K. M. Morgan, *J. Chem. Soc., Perkin Trans. 1* **2000**, 3578–3583.
- [262] G. W. Gribble, B. Pelcman, *J. Org. Chem.* **1992**, *57*, 3636–3642.
- [263] B. Belleau, *Can. J. Chem.* **1957**, *35*, 651–662.
- [264] a) A. K. Bose, G. Spiegelman, M. S. Manhas, *Tetrahedron Lett.* **1971**, *12*, 3167–3170; b) Y. Yamamoto, T. Nakada, H. Nemoto, *J. Am. Chem. Soc.* **1992**, *114*, 121–125.
- [265] J. B. P. A. Wijnberg, J. J. J. de Boer, W. N. Speckamp, *Recl. Trav. Chim. Pays-Bas* **1978**, *97*, 227–231.
- [266] B. E. Maryanoff, D. F. McComsey, B. A. Duhl–Emswiler, *J. Org. Chem.* **1983**, *48*, 5062–5074.
- [267] a) Z. Xu, Q. Wang, J. Zhu, *J. Am. Chem. Soc.* **2013**, *135*, 19127–19130; b) Z. Xu, Q. Wang, J. Zhu, *J. Am. Chem. Soc.* **2015**, *137*, 6712–6724.
- [268] S. Gao, Y. Q. Tu, X. Hu, S. Wang, R. Hua, Y. Jiang, Y. Zhao, X. Fan, S. Zhang, *Org. Lett.* **2006**, *8*, 2373–2376.
- [269] T. Suto, Y. Yanagita, Y. Nagashima, S. Takikawa, Y. Kurosu, N. Matsuo, T. Sato, N. Chida, *J. Am. Chem. Soc.* **2017**, *139*, 2952–2955.
- [270] H. Liu, J. Yu, X. Li, R. Yan, J.–C. Xiao, R. Hong, *Org. Lett.* **2015**, *17*, 4444–4447.
- [271] a) R. L. Hinman, C. P. Bauman, *J. Org. Chem.* **1964**, *29*, 1206–1215; b) F. Kolundzic, M. N. Noshi, M. Tjandra, M. Movassaghi, S. J. Miller, *J. Am. Chem. Soc.* **2011**, *133*, 9104–9111; c) J. Xu, L. Liang, H. Zheng, Y. R. Chi, R. Tong, *Nat. Commun.* **2019**, *10*, 4754.
- [272] S. V. Ley, J. Norman, W. P. Griffith, S. P. Marsden, *Synthesis* **1994**, *1994*, 639–666.
- [273] a) M. Frigerio, M. Santagostino, *Tetrahedron Lett.* **1994**, *35*, 8019–8022; b) S. De Munari, M. Frigerio, M. Santagostino, *J. Org. Chem.* **1996**, *61*, 9272–9279; c) J. D. More, N. S. Finney, *Org. Lett.* **2002**, *4*, 3001–3003; d) K. C. Nicolaou, C. J. N. Mathison, T. Montagnon, *Angew. Chem. Int. Ed.* **2003**, *42*, 4077–4082.
- [274] A. I. Meyers, M. A. Sturgess, *Tetrahedron Lett.* **1988**, *29*, 5339–5342.
- [275] a) M. Teruaki, M. Jun–ichi, K. Hideo, *Chem. Lett.* **2000**, *29*, 1250–1251; b) M. Teruaki, M. Jun–ichi, Y. Manabu, *Chem. Lett.* **2000**, *29*, 1072–1073.
- [276] X. Zhu, A. Ganesan, *J. Org. Chem.* **2002**, *67*, 2705–2708.
- [277] M. Yamaguchi, R. Hagiwara, K. Gayama, K. Suzuki, Y. Sato, H. Konishi, K. Manabe, *J. Org. Chem.* **2020**, *85*, 10902–10912.
- [278] a) C. Gunanathan, D. Milstein, *Science* **2013**, *341*, 1229712; b) R. H. Crabtree, *Chem. Rev.* **2017**, *117*, 9228–9246; c) T. Irrgang, R. Kempe, *Chem. Rev.* **2019**, *119*, 2524–2549; d) B. G. Reed–Berendt, K. Polidano, L. C. Morrill, *Org. Biomol. Chem.* **2019**, *17*, 1595–1607.
- [279] S. Whitney, R. Grigg, A. Derrick, A. Keep, *Org. Lett.* **2007**, *9*, 3299–3302.
- [280] a) S. M. A. H. Siddiki, K. Kon, K.–i. Shimizu, *Chem. Eur. J.* **2013**, *19*, 14416–14419; b) C. Chaudhari, S. M. A. H. Siddiki, K. Kon, A. Tomita, Y. Tai, K.–i. Shimizu, *Catal. Sci. Technol.* **2014**, *4*, 1064–1069.
- [281] a) S. Imm, S. Bähn, A. Tillack, K. Mevius, L. Neubert, M. Beller, *Chem. Eur. J.* **2010**, *16*, 2705–2709; b) N. Biswas, R. Sharma, D. Srimani, *Adv. Synth. Catal.* **2020**, *362*, 2902–2910.

- [282] N. Lebrasseur, I. Larrosa, *J. Am. Chem. Soc.* **2008**, *130*, 2926–2927.
- [283] a) U. Jana, S. Maiti, S. Biswas, *Tetrahedron Lett.* **2007**, *48*, 7160–7163; b) G. Di Gregorio, M. Mari, F. Bartoccini, G. Piersanti, *J. Org. Chem.* **2017**, *82*, 8769–8775; c) C. Seck, M. D. Mbaye, S. Gaillard, J.–L. Renaud, *Adv. Synth. Catal.* **2018**, *360*, 4640–4645.
- [284] R. Appel, *Angew. Chem. Int. Ed.* **1975**, *14*, 801–811.
- [285] P. Y. Reddy, S. Kondo, T. Toru, Y. Ueno, *J. Org. Chem.* **1997**, *62*, 2652–2654.
- [286] E. Sawatzky, A. Drakopoulos, M. Rölz, C. Sotriffer, B. Engels, M. Decker, *Beilstein J. Org. Chem.* **2016**, *12*, 2280–2292.
- [287] J. L. Simonsen, *J. Chem. Soc., Trans.* **1920**, *117*, 570–578.
- [288] I. Fernández, *Chem. Sci.* **2020**, *11*, 3769–3779.
- [289] I. Hanukoglu, *J. Steroid Biochem. Mol. Biol.* **1992**, *43*, 779–804.
- [290] W. D. Fessner, G. Sedelmeier, P. R. Spurr, G. Rihs, H. Prinzbach, *J. Am. Chem. Soc.* **1987**, *109*, 4626–4642.
- [291] a) J. Kim, H. Kim, S. B. Park, *J. Am. Chem. Soc.* **2014**, *136*, 14629–14638; b) M. Garcia–Castro, S. Zimmermann, M. G. Sankar, K. Kumar, *Angew. Chem. Int. Ed.* **2016**, *55*, 7586–7605.
- [292] E. Sverrisdóttir, T. M. Lund, A. E. Olesen, A. M. Drewes, L. L. Christrup, M. Kreilgaard, *Eur. J. Pharm. Sci.* **2015**, *74*, 45–62.
- [293] J. Wang, C. Xu, Y. K. Wong, Y. Li, F. Liao, T. Jiang, Y. Tu, *Engineering* **2019**, *5*, 32–39.
- [294] H. M. Kantarjian, S. O'Brien, J. Cortes, *Clin. Lymphoma Myeloma Leuk.* **2013**, *13*, 530–533.
- [295] M. A. Jordan, L. Wilson, *Nat. Rev. Cancer* **2004**, *4*, 253–265.
- [296] a) M. J. Towle, K. A. Salvato, J. Budrow, B. F. Wels, G. Kuznetsov, K. K. Aalfs, S. Welsh, W. Zheng, B. M. Seletsky, M. H. Palme, G. J. Habgood, L. A. Singer, L. V. DiPietro, Y. Wang, J. J. Chen, D. A. Quincy, A. Davis, K. Yoshimatsu, Y. Kishi, M. J. Yu, B. A. Littlefield, *Cancer Res.* **2001**, *61*, 1013–1021; b) B. M. Seletsky, Y. Wang, L. D. Hawkins, M. H. Palme, G. J. Habgood, L. V. DiPietro, M. J. Towle, K. A. Salvato, B. F. Wels, K. K. Aalfs, Y. Kishi, B. A. Littlefield, M. J. Yu, *Bioorg. Med. Chem. Lett.* **2004**, *14*, 5547–5550.
- [297] S. L. Scarpace, *Clin. Ther.* **2012**, *34*, 1467–1473.
- [298] a) T. D. Aicher, K. R. Buszek, F. G. Fang, C. J. Forsyth, S. H. Jung, Y. Kishi, M. C. Matelich, P. M. Scola, D. M. Spero, S. K. Yoon, *J. Am. Chem. Soc.* **1992**, *114*, 3162–3164; b) M. J. Yu, W. Zheng, B. M. Seletsky, *Nat. Prod. Rep.* **2013**, *30*, 1158–1164.
- [299] F. Kavanagh, A. Hervey, W. J. Robbins, *Proc. Natl. Acad. Sci. U.S.A* **1951**, *37*, 570–574.
- [300] P. Rasoanaivo, S. Ratsimamanga–Urverg, R. Milijaona, H. Rafatro, A. Rakoto–Ratsimamanga, C. Galeffi, M. Nicoletti, *Planta Med.* **1994**, *60*, 13–16.
- [301] Y. Fukuyama, Y. Asakawa, *J. Chem. Soc., Perkin Trans. 1* **1991**, 2737–2741.
- [302] N. S. Bystrov, B. K. Chernov, V. N. Dobrynin, M. N. Kolosov, *Tetrahedron Lett.* **1975**, *16*, 2791–2794.
- [303] F. Coelho, G. Diaz, *Tetrahedron* **2002**, *58*, 1647–1656.
- [304] Q. Zhang, Y.–T. Di, C.–S. Li, X. Fang, C.–J. Tan, Z. Zhang, Y. Zhang, H.–P. He, S.–L.

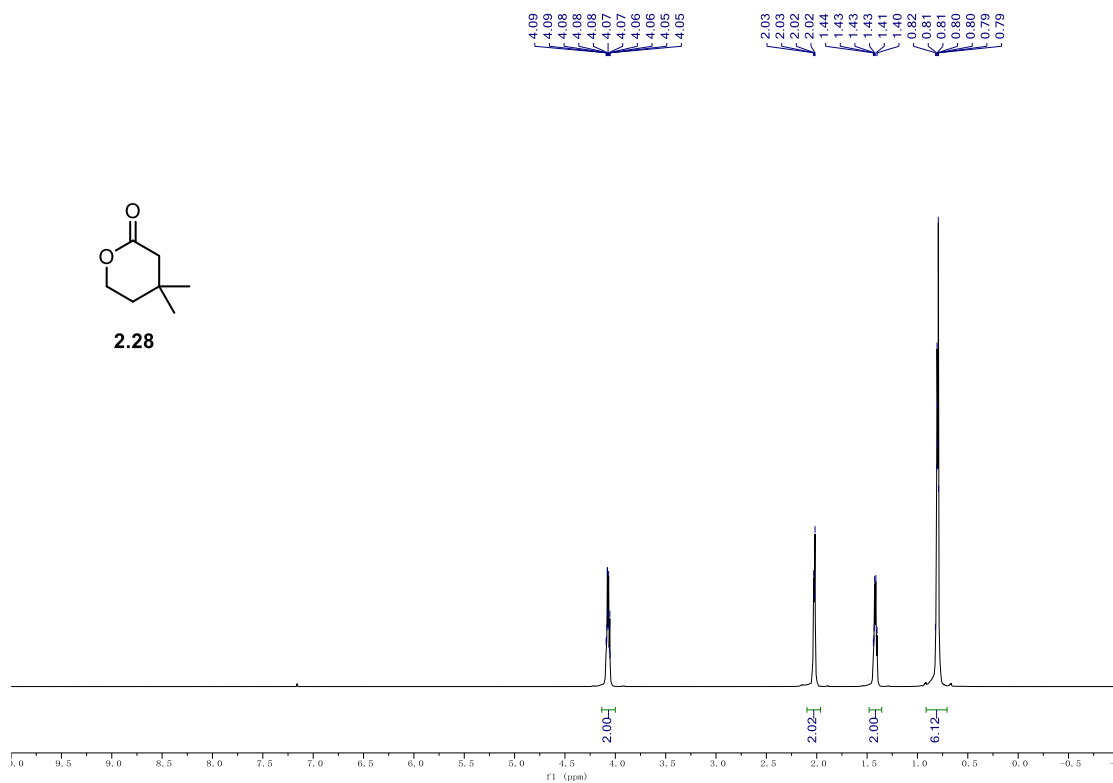
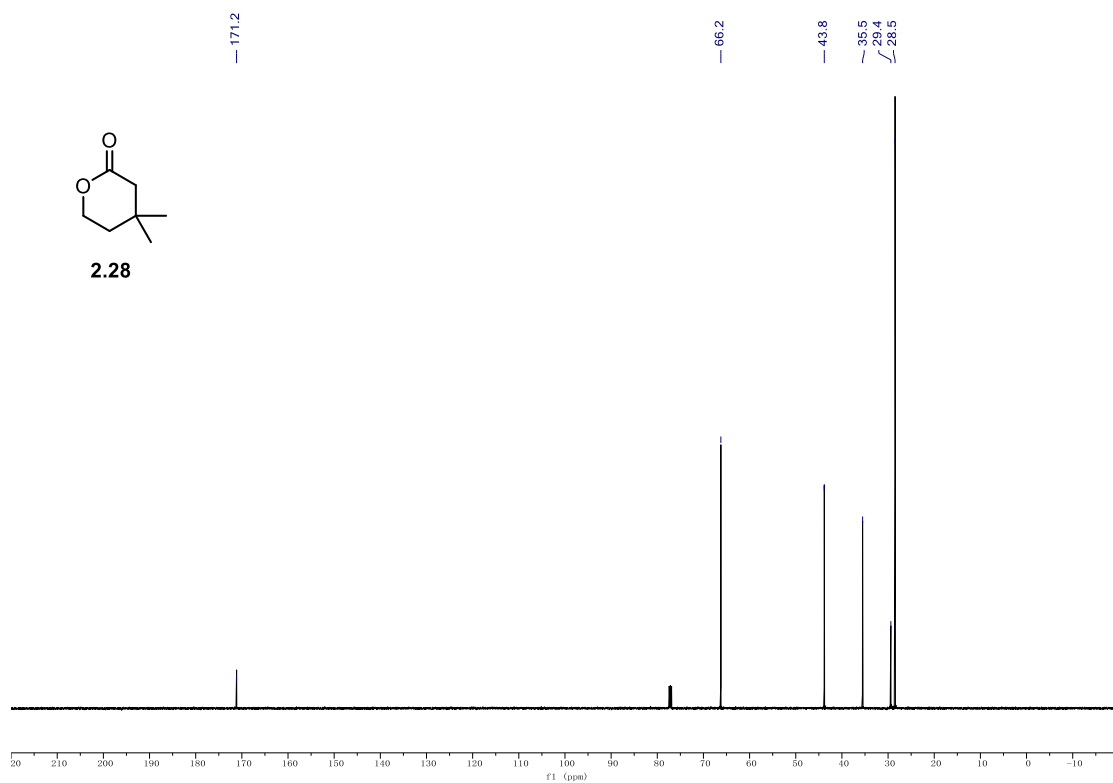
- Li, X.–J. Hao, *Org. Lett.* **2009**, *11*, 2357–2359.
- [305] W.–L. Xiao, L.–M. Yang, N.–B. Gong, L. Wu, R.–R. Wang, J.–X. Pu, X.–L. Li, S.–X. Huang, Y.–T. Zheng, R.–T. Li, Y. Lu, Q.–T. Zheng, H.–D. Sun, *Org. Lett.* **2006**, *8*, 991–994.
- [306] A. Kawamura, M. Kita, H. Kigoshi, *Angew. Chem. Int. Ed.* **2015**, *54*, 7073–7076.
- [307] Y.–N. Wang, G.–Y. Xia, L.–Y. Wang, G.–B. Ge, H.–W. Zhang, J.–F. Zhang, Y.–Z. Wu, S. Lin, *Org. Lett.* **2018**, *20*, 7341–7344.
- [308] J. i. Kobayashi, Y. Hirasawa, N. Yoshida, H. Morita, *Tetrahedron Lett.* **2000**, *41*, 9069–9073.
- [309] M. Tomita, Y. Okamoto, T. Kikuchi, K. Osaki, M. Nishikawa, K. Kamiya, Y. Sasaki, K. Matoba, K. Goto, *Tetrahedron Lett.* **1967**, *8*, 2421–2424.
- [310] S.–M. Zhao, Z. Wang, G.–Z. Zeng, W.–W. Song, X.–Q. Chen, X.–N. Li, N.–H. Tan, *Org. Lett.* **2014**, *16*, 5576–5579.
- [311] F. Abe, T. Yamauchi, *Phytochemistry* **1993**, *35*, 169–171.
- [312] T. P. Lien, C. Kamperdick, T. Van Sung, G. Adam, H. Ripperger, *Phytochemistry* **1998**, *49*, 1797–1799.
- [313] Y.–Y. Lin, M. Risk, S. M. Ray, D. Van Engen, J. Clardy, J. Golik, J. C. James, K. Nakanishi, *J. Am. Chem. Soc.* **1981**, *103*, 6773–6775.
- [314] a) J. Kaneti, A. J. Kirby, A. H. Koedjikov, I. G. Pojarlieff, *Org. Biomol. Chem.* **2004**, *2*, 1098–1103; b) M. E. Jung, G. Piizzi, *Chem. Rev.* **2005**, *105*, 1735–1766; c) M. N. Levine, R. T. Raines, *Chem. Sci.* **2012**, *3*, 2412–2420.
- [315] a) T. van Dijk, J. Chris Slootweg, K. Lammertsma, *Org. Biomol. Chem.* **2017**, *15*, 10134–10144; b) D. Kaiser, A. Bauer, M. Lemmerer, N. Maulide, *Chem. Soc. Rev.* **2018**, *47*, 7899–7925.
- [316] Y. Román–Leshkov, M. E. Davis, *ACS Catalysis* **2011**, *1*, 1566–1580.
- [317] a) J. Chatt, L. A. Duncanson, *J. Chem. Soc.* **1953**, 2939–2947; b) J. Chatt, L. A. Duncanson, L. M. Venanzi, *J. Chem. Soc.* **1955**, 4456–4460.
- [318] T. Curtius, *J. Prakt. Chemie.* **1882**, *26*, 145–208.
- [319] T. Curtius, *Ber. Dtsch. Chem. Ges.* **1902**, *35*, 3226–3228.
- [320] E. Fischer, *Ber. Dtsch. Chem. Ges.* **1905**, *38*, 605–619.
- [321] V. R. Pattabiraman, J. W. Bode, *Nature* **2011**, *480*, 471–479.
- [322] T. M. Schmeing, V. Ramakrishnan, *Nature* **2009**, *461*, 1234–1242.
- [323] S. A. Stalford, C. A. Kilner, A. G. Leach, W. B. Turnbull, *Org. Biomol. Chem.* **2009**, *7*, 4842–4852.
- [324] a) J. L. Hansen, T. M. Schmeing, P. B. Moore, T. A. Steitz, *Proc. Natl. Acad. Sci. U.S.A.* **2002**, *99*, 11670–11675; b) T. Martin Schmeing, K. S. Huang, S. A. Strobel, T. A. Steitz, *Nature* **2005**, *438*, 520–524; c) T. M. Schmeing, K. S. Huang, D. E. Kitchen, S. A. Strobel, T. A. Steitz, *Mol. Cell* **2005**, *20*, 437–448.
- [325] S. De Sarkar, A. Studer, *Org. Lett.* **2010**, *12*, 1992–1995.
- [326] C. Gunanathan, Y. Ben–David, D. Milstein, *Science* **2007**, *317*, 790–792.
- [327] W.–K. Chan, C.–M. Ho, M.–K. Wong, C.–M. Che, *J. Am. Chem. Soc.* **2006**, *128*, 14796–14797.
- [328] H. Sun, J. Zhang, Q. Liu, L. Yu, J. Zhao, *Angew. Chem. Int. Ed.* **2007**, *46*, 6068–6072.
- [329] X. Wu, J. L. Stockdill, P. Wang, S. J. Danishefsky, *J. Am. Chem. Soc.* **2010**, *132*, 4098–

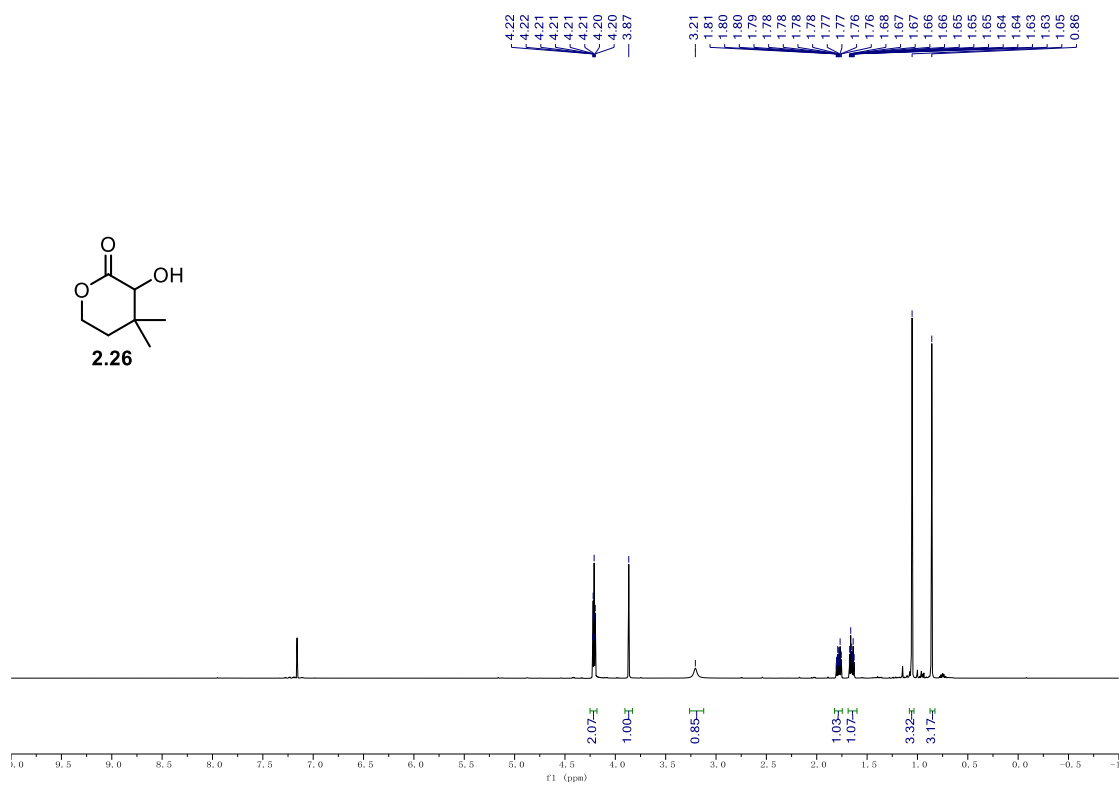
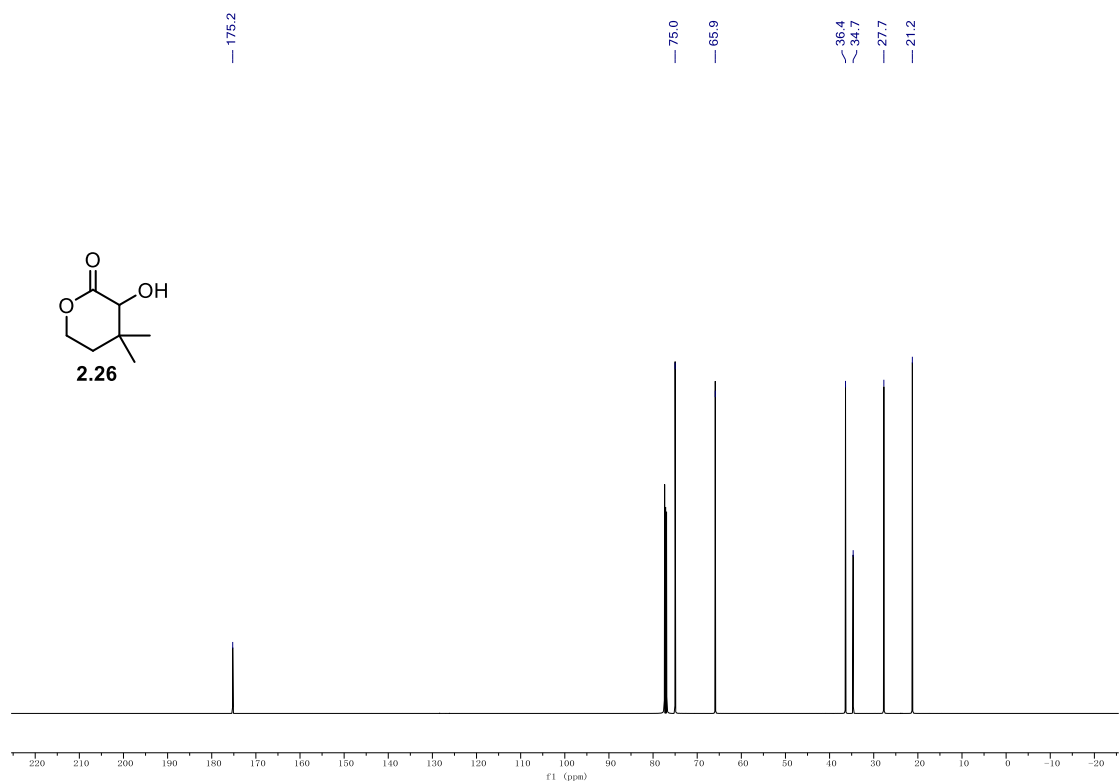
- 4100.
- [330] N. Shangguan, S. Katukojvala, R. Greenberg, L. J. Williams, *J. Am. Chem. Soc.* **2003**, *125*, 7754–7755.
- [331] a) D. Crich, K. Sana, S. Guo, *Org. Lett.* **2007**, *9*, 4423–4426; b) R. S. Talan, A. K. Sanki, S. J. Sucheck, *Carbohydr. Res.* **2009**, *344*, 2048–2050.
- [332] D. Crich, K. Sasaki, *Org. Lett.* **2009**, *11*, 3514–3517.
- [333] A. Das, P. Theato, *Chem. Rev.* **2016**, *116*, 1434–1495.
- [334] a) T. Wieland, W. Schäfer, E. Bokelmann, *Liebigs Ann. Chem.* **1951**, *573*, 99–104; b) J. A. Farrington, P. J. Hextall, G. W. Kenner, J. M. Turner, *J. Chem. Soc.* **1957**, 1407–1413.
- [335] M. Akram, *Cell Biochem. Biophys.* **2014**, *68*, 475–478.
- [336] H. Riezman, *Cell* **2007**, *130*, 587–588.
- [337] R. Schwyzer, B. Iselin, M. Feurer, *Helv. Chim. Acta* **1955**, *38*, 69–79.
- [338] A. El-Faham, F. Albericio, *Chem. Rev.* **2011**, *111*, 6557–6602.
- [339] J. Grundlingh, P. I. Dargan, M. El-Zanfaly, D. M. Wood, *J. Med. Toxicol.* **2011**, *7*, 205.
- [340] a) S. Hatakeyama, *J. Synth. Org. Chem Jpn.* **2006**, *64*, 1132–1138; b) A. Nakano, S. Kawahara, S. Akamatsu, K. Morokuma, M. Nakatani, Y. Iwabuchi, K. Takahashi, J. Ishihara, S. Hatakeyama, *Tetrahedron* **2006**, *62*, 381–389; c) A. Nakano, K. Takahashi, J. Ishihara, S. Hatakeyama, *Org. Lett.* **2006**, *8*, 5357–5360.
- [341] L. Nuhn, I. Overhoff, M. Sperner, K. Kaltenberg, R. Zentel, *Polym. Chem.* **2014**, *5*, 2484–2495.
- [342] D. Walker, J. D. Hiebert, *Chem. Rev.* **1967**, *67*, 153–195.
- [343] a) H. J. Reich, I. L. Reich, J. M. Renga, *J. Am. Chem. Soc.* **1973**, *95*, 5813–5815; b) H. J. Reich, J. M. Renga, I. L. Reich, *J. Am. Chem. Soc.* **1975**, *97*, 5434–5447.
- [344] a) Y. Chen, A. Turlik, T. R. Newhouse, *J. Am. Chem. Soc.* **2016**, *138*, 1166–1169; b) A. Turlik, Y. Chen, T. R. Newhouse, *Synlett* **2016**, *27*, 331–336; c) C. J. Teskey, P. Adler, C. R. Gonçalves, N. Maulide, *Angew. Chem. Int. Ed.* **2019**, *58*, 447–451.
- [345] a) S. Siddiqui, O. Y. Khan, S. Faizi, B. S. Siddiqui, *Heterocycles* **1988**, *27*, 1401–1410; b) S. Siddiqui, O. Y. Khan, S. Faizi, B. S. Siddiqui, *Heterocycles* **1989**, *29*, 521–527.
- [346] K.-B. Wang, D.-H. Li, Y. Bao, F. Cao, W.-J. Wang, C. Lin, W. Bin, J. Bai, Y.-H. Pei, Y.-K. Jing, D. Yang, Z.-L. Li, H.-M. Hua, *J. Nat. Prod.* **2017**, *80*, 551–559.
- [347] a) P. Tang, H. Wang, W. Zhang, F.-E. Chen, *Green Synth. Catal.* **2020**, *1*, 26–41; b) J. Wen, F. Wang, X. Zhang, *Chem. Soc. Rev.* **2021**, *50*, 3211–3237.
- [348] a) I. D. Gridnev, M. Yasutake, N. Higashi, T. Imamoto, *J. Am. Chem. Soc.* **2001**, *123*, 5268–5276; b) T. C. Nugent, M. El-Shazly, *Adv. Synth. Catal.* **2010**, *352*, 753–819; c) K. Murugan, D.-w. Huang, Y.-T. Chien, S.-T. Liu, *Tetrahedron* **2013**, *69*, 268–273; d) X. Li, C. You, H. Yang, J. Che, P. Chen, Y. Yang, H. Lv, X. Zhang, *Adv. Synth. Catal.* **2017**, *359*, 597–602; e) M. R. Friedfeld, H. Zhong, R. T. Ruck, M. Shevlin, P. J. Chirik, *Science* **2018**, *360*, 888–893; f) J. Zhang, C. Liu, X. Wang, J. Chen, Z. Zhang, W. Zhang, *Chem. Commun.* **2018**, *54*, 6024–6027; g) J. Zhang, J. Jia, X. Zeng, Y. Wang, Z. Zhang, I. D. Gridnev, W. Zhang, *Angew. Chem. Int. Ed.* **2019**, *58*, 11505–11512.
- [349] C. Zheng, S.-L. You, *Chem. Soc. Rev.* **2012**, *41*, 2498–2518.
- [350] a) G. Li, Y. Liang, J. C. Antilla, *J. Am. Chem. Soc.* **2007**, *129*, 5830–5831; b) J. Zhou, B. List, *J. Am. Chem. Soc.* **2007**, *129*, 7498–7499; c) L. Simón, J. M. Goodman, *J. Am.*

- Chem. Soc.* **2008**, *130*, 8741–8747; d) Z.–Y. Han, H. Xiao, X.–H. Chen, L.–Z. Gong, *J. Am. Chem. Soc.* **2009**, *131*, 9182–9183; e) G. Li, J. C. Antilla, *Org. Lett.* **2009**, *11*, 1075–1078; f) M. Rueping, C. Brinkmann, A. P. Antonchick, I. Atodiresei, *Org. Lett.* **2010**, *12*, 4604–4607; g) I. A. Khan, A. K. Saxena, *J. Org. Chem.* **2013**, *78*, 11656–11669; h) L. J. Rono, H. G. Yayla, D. Y. Wang, M. F. Armstrong, R. R. Knowles, *J. Am. Chem. Soc.* **2013**, *135*, 17735–17738; i) Y.–L. Du, Y. Hu, Y.–F. Zhu, X.–F. Tu, Z.–Y. Han, L.–Z. Gong, *J. Org. Chem.* **2015**, *80*, 4754–4759; j) D. Y. Park, S. Y. Lee, J. Jeon, C.–H. Cheon, *J. Org. Chem.* **2018**, *83*, 12486–12495; k) W. Xiong, S. Li, B. Fu, J. Wang, Q.–A. Wang, W. Yang, *Org. Lett.* **2019**, *21*, 4173–4176.
- [351] J. M. Hagel, P. J. Facchini, *Plant Cell Physiol.* **2013**, *54*, 647–672.
- [352] D. E. Beck, K. Agama, C. Marchand, A. Chergui, Y. Pommier, M. Cushman, *J. Med. Chem.* **2014**, *57*, 1495–1512.
- [353] J. Yu, Z. Zhang, S. Zhou, W. Zhang, R. Tong, *Org. Chem. Front.* **2018**, *5*, 242–246.
- [354] H. Tohma, M. Iwata, T. Maegawa, Y. Kita, *Tetrahedron Lett.* **2002**, *43*, 9241–9244.
- [355] D. Stubba, G. Lahm, M. Geffe, J. W. Runyon, A. J. Arduengo III, T. Opatz, *Angew. Chem. Int. Ed.* **2015**, *54*, 14187–14189.
- [356] A. Frymarkiewicz, K. Walczyński, *Eur. J. Med. Chem.* **2009**, *44*, 1674–1681.
- [357] P. S. Akula, B.–C. Hong, G.–H. Lee, *Org. Lett.* **2018**, *20*, 7835–7839.
- [358] I. Bonnaventure, A. B. Charette, *J. Org. Chem.* **2008**, *73*, 6330–6340.
- [359] T. J. Clark, J. M. Rodezno, S. B. Clendenning, S. Aouba, P. M. Brodersen, A. J. Lough, H. E. Ruda, I. Manners, *Chem. Eur. J.* **2005**, *11*, 4526–4534.
- [360] M. Inman, C. J. Moody, *Eur. J. Org. Chem.* **2013**, *2013*, 2179–2187.
- [361] O. McCarthy, A. Musso–Buendia, M. Kaiser, R. Brun, L. M. Ruiz–Perez, N. G. Johansson, D. G. Pacanowska, I. H. Gilbert, *Eur. J. Med. Chem.* **2009**, *44*, 678–688.
- [362] P. Mondal, N. P. Argade, *J. Org. Chem.* **2013**, *78*, 6802–6808.
- [363] P. Horrocks, S. Fallon, L. Denman, O. Devine, L. J. Duffy, A. Harper, E.–L. Meredith, S. Hasenkamp, A. Sidaway, D. Monnery, T. R. Phillips, S. M. Allin, *Bioorg. Med. Chem. Lett.* **2012**, *22*, 1770–1773.
- [364] J. Ruchti, E. M. Carreira, *J. Am. Chem. Soc.* **2014**, *136*, 16756–16759.
- [365] S. Zeeli, T. Weill, E. Finkin–Gröner, C. Bejar, M. Melamed, S. Furman, M. Zhenin, A. Nudelman, M. Weinstock, *J. Med. Chem.* **2018**, *61*, 4004–4019.
- [366] R. E. Mewshaw, D. Zhou, P. Zhou, X. Shi, G. Hornby, T. Spangler, R. Scerni, D. Smith, L. E. Schechter, T. H. Andree, *J. Med. Chem.* **2004**, *47*, 3823–3842.
- [367] M. P. Epplin, A. Mohan, L. D. Harris, Z. Zhu, K. L. Strong, J. Bacsá, P. Le, D. S. Menaldino, S. F. Traynelis, D. C. Liotta, *J. Med. Chem.* **2020**, *63*, 7569–7600.
- [368] J. Liu, P. Chakraborty, H. Zhang, L. Zhong, Z.–X. Wang, X. Huang, *ACS Catalysis* **2019**, *9*, 2610–2617.
- [369] M. A. O. Abdel–Fattah, A. H. Abadi, J. Lehmann, P. M. Schweikert, C. Enzensperger, *MedChemComm* **2015**, *6*, 1679–1686.
- [370] S. Fredrich, A. Bonasera, V. Valderrey, S. Hecht, *J. Am. Chem. Soc.* **2018**, *140*, 6432–6440.
- [371] W. Gong, Y. Liu, J. Zhang, Y. Jiao, J. Xue, Y. Li, *Chemistry – An Asian Journal* **2013**, *8*, 546–551.

9. Appendix

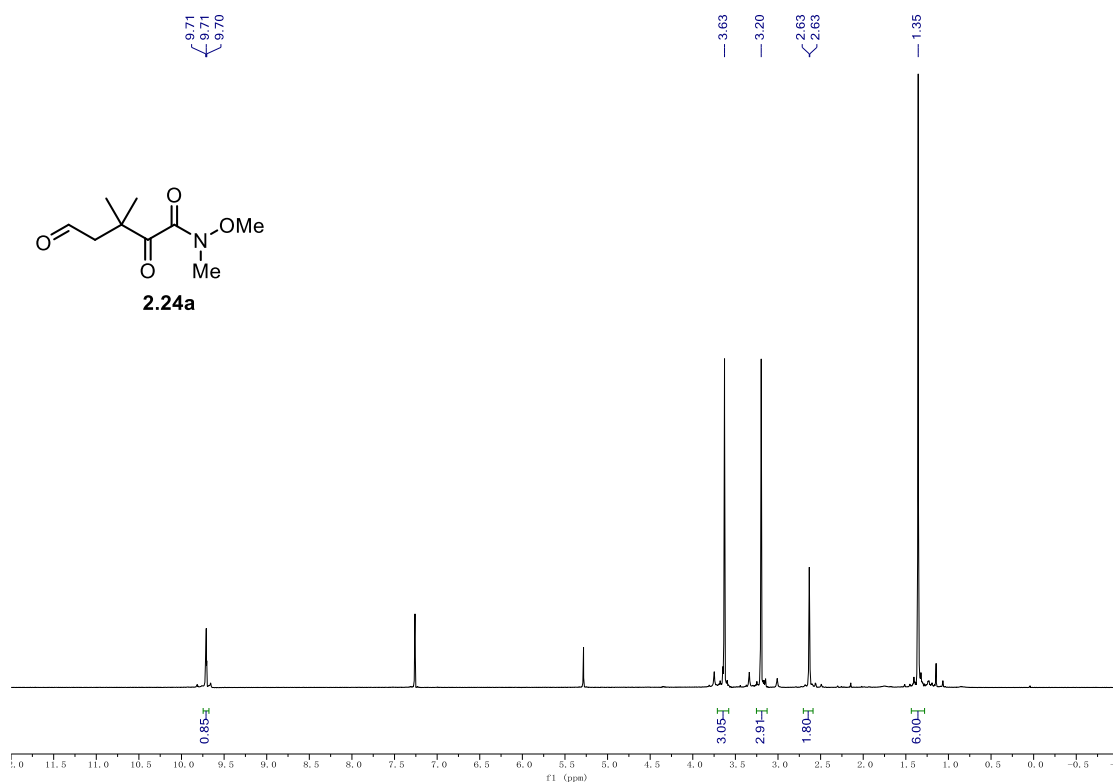
9.1. NMR Spectra

 ^1H NMR (500 MHz, CDCl_3) of **2.28**. ^{13}C NMR (126 MHz, CDCl_3) of **2.28**.

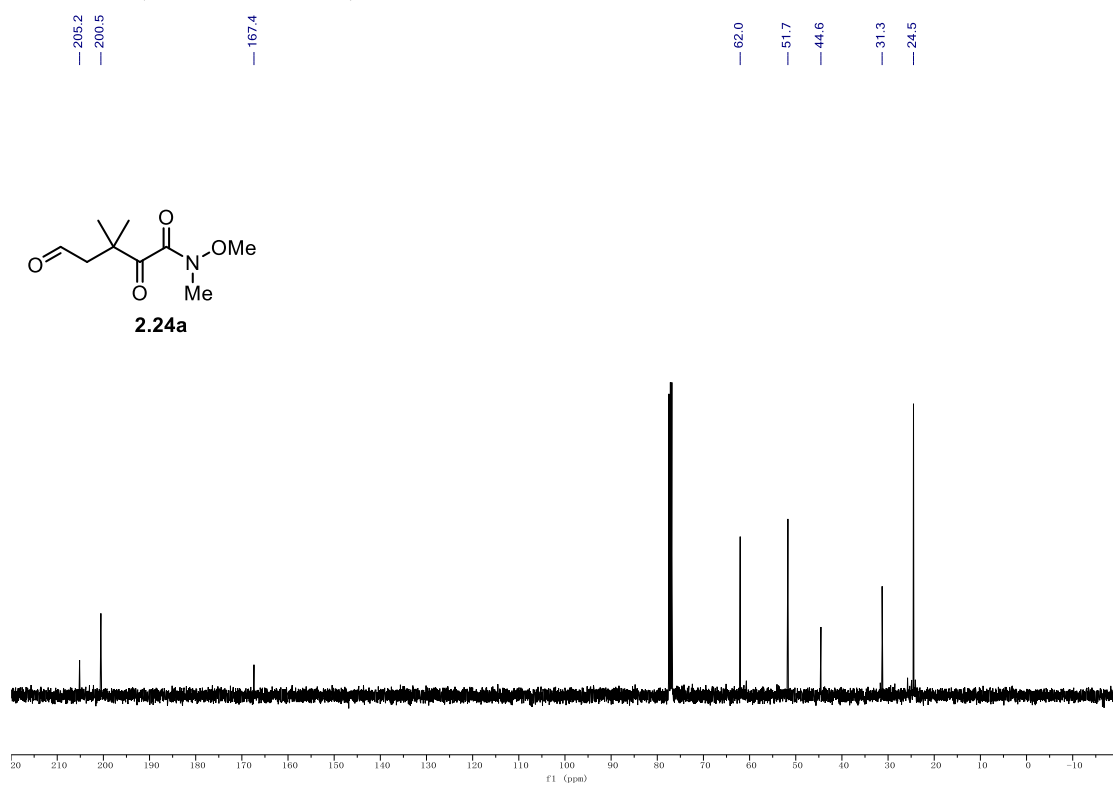
^1H NMR (600 MHz, CDCl_3) of **2.26**. ^{13}C NMR (151 MHz, CDCl_3) of **2.26**.

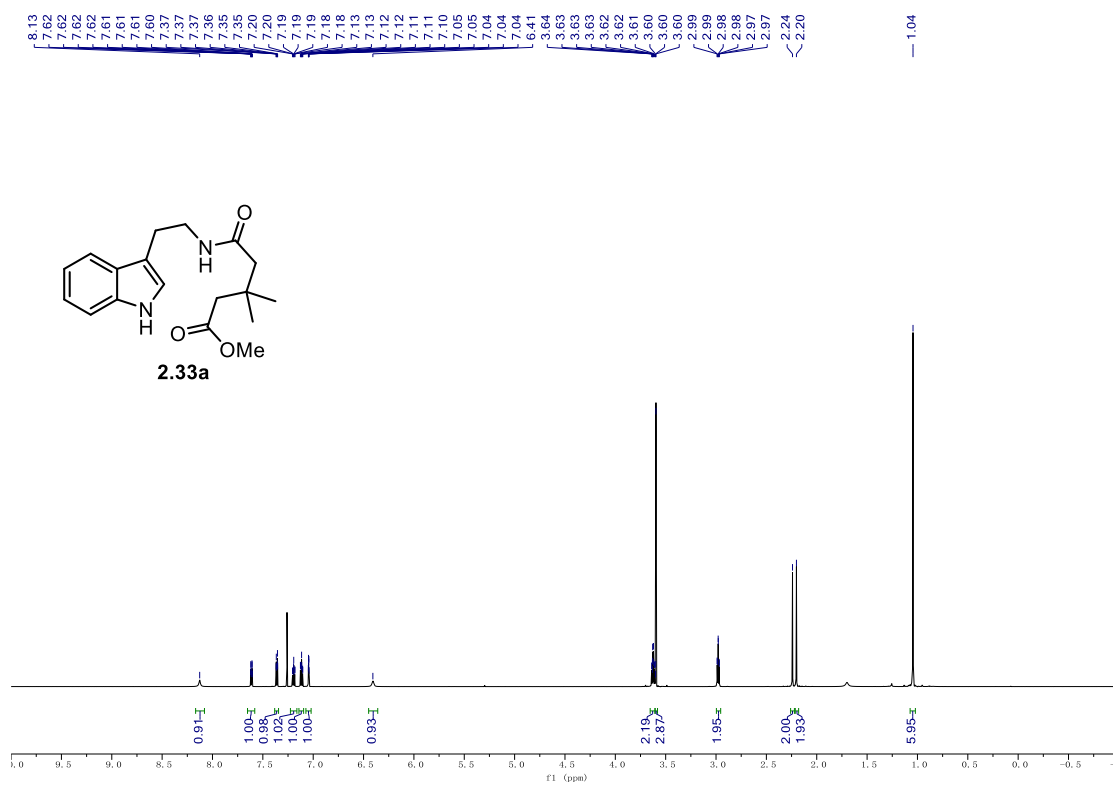
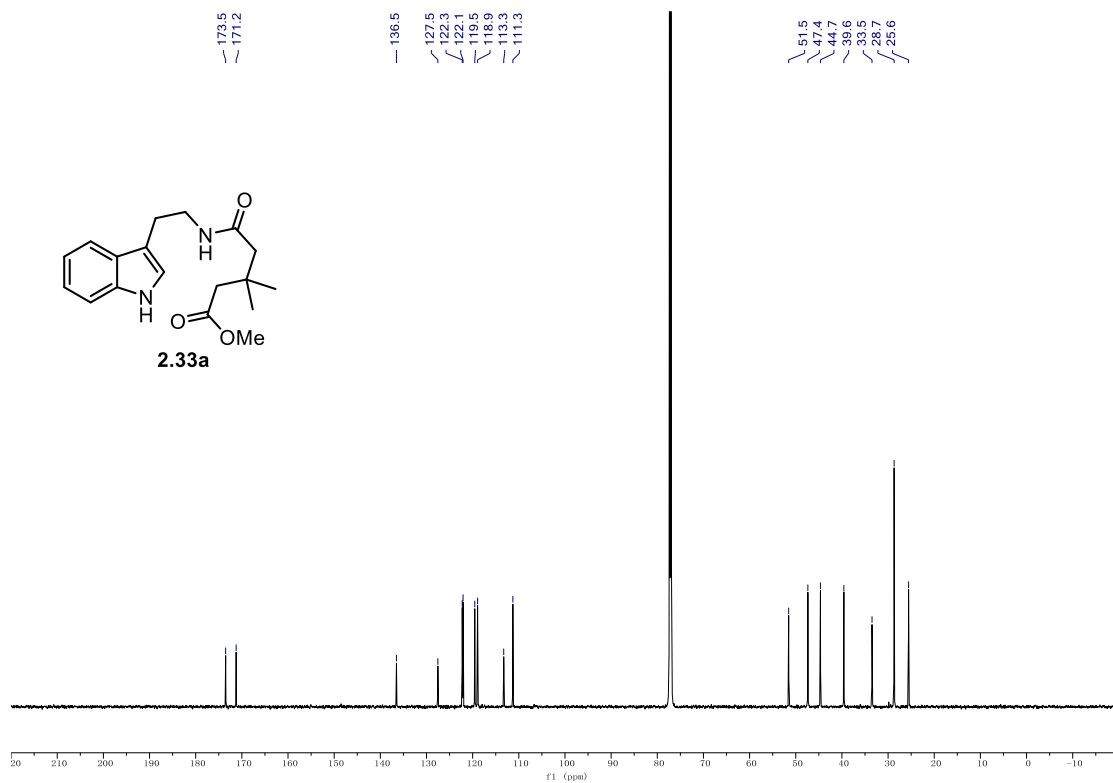
9.1. NMR Spectra

¹H NMR (400 MHz, CDCl₃) of **2.24a**.



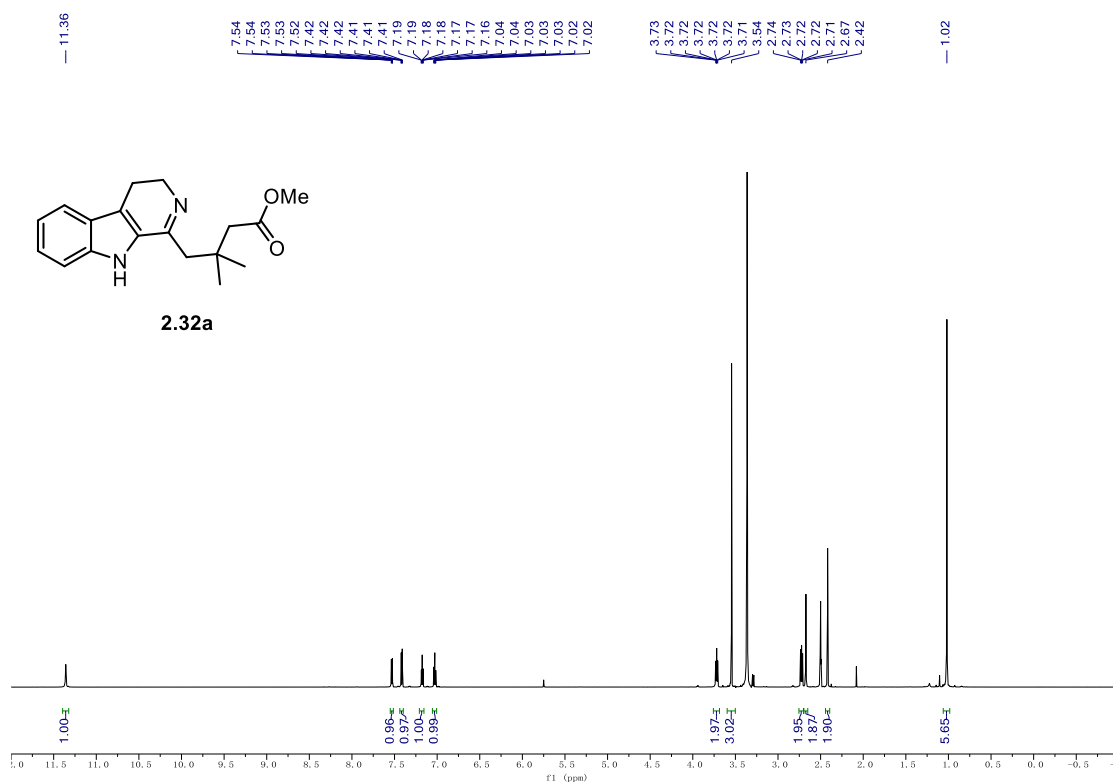
¹³C NMR (101 MHz, CDCl₃) of **2.24a**.



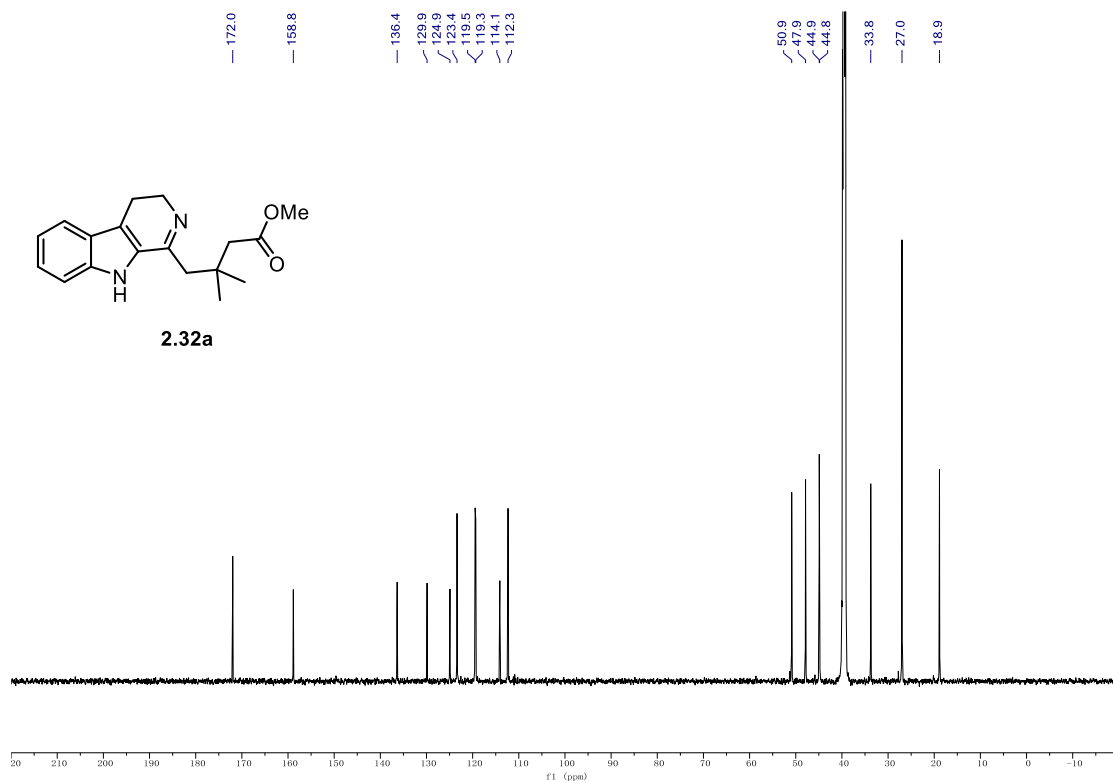
¹H NMR (500 MHz, CDCl₃) of 2.33a.**¹³C NMR (126 MHz, CDCl₃) of 2.33a.**

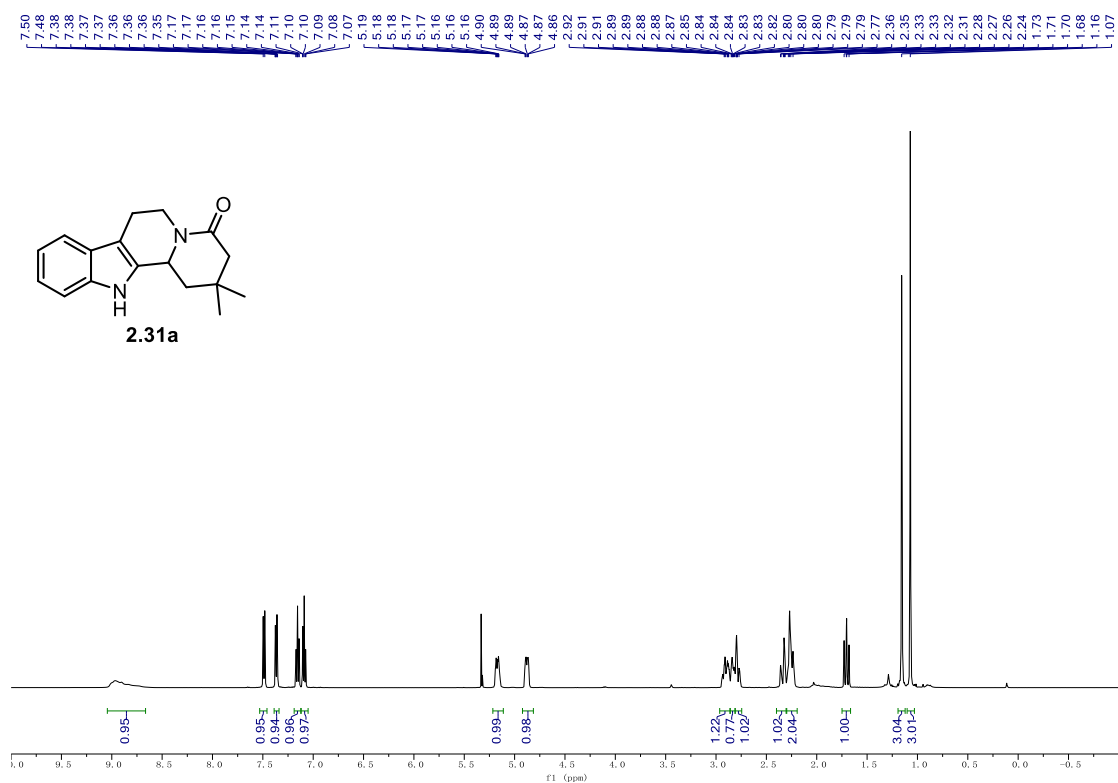
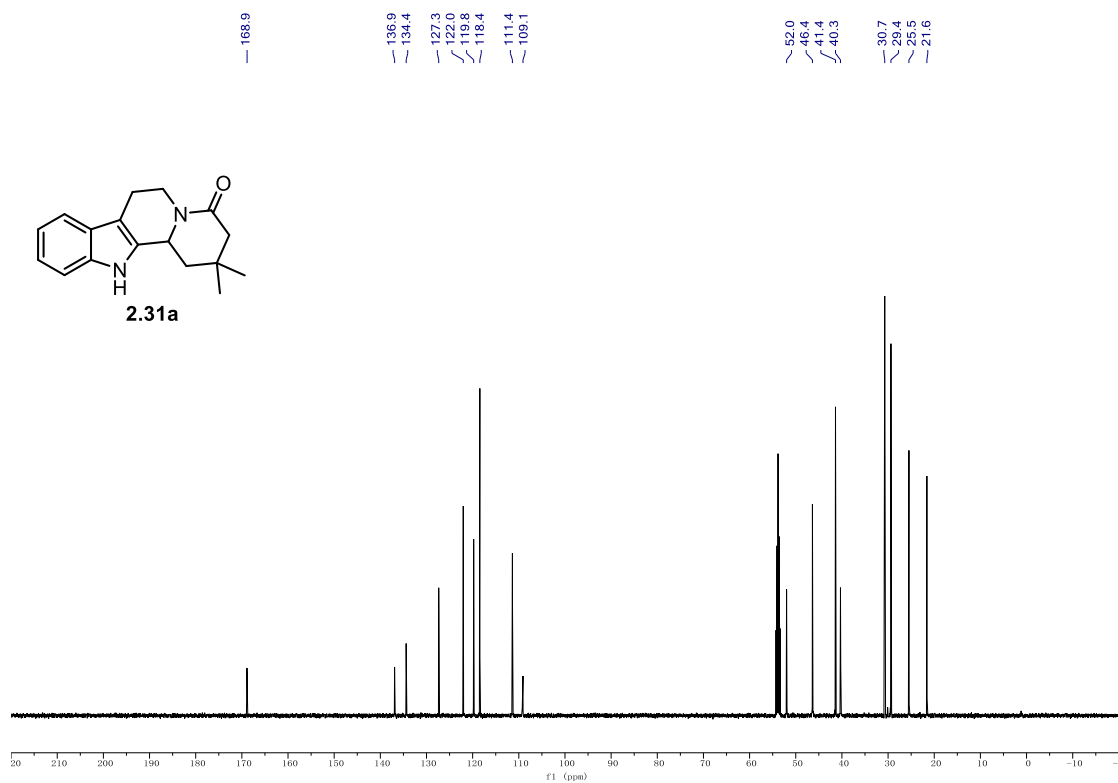
9.1. NMR Spectra

¹H NMR (700 MHz, CDCl₃) of **2.32a**.



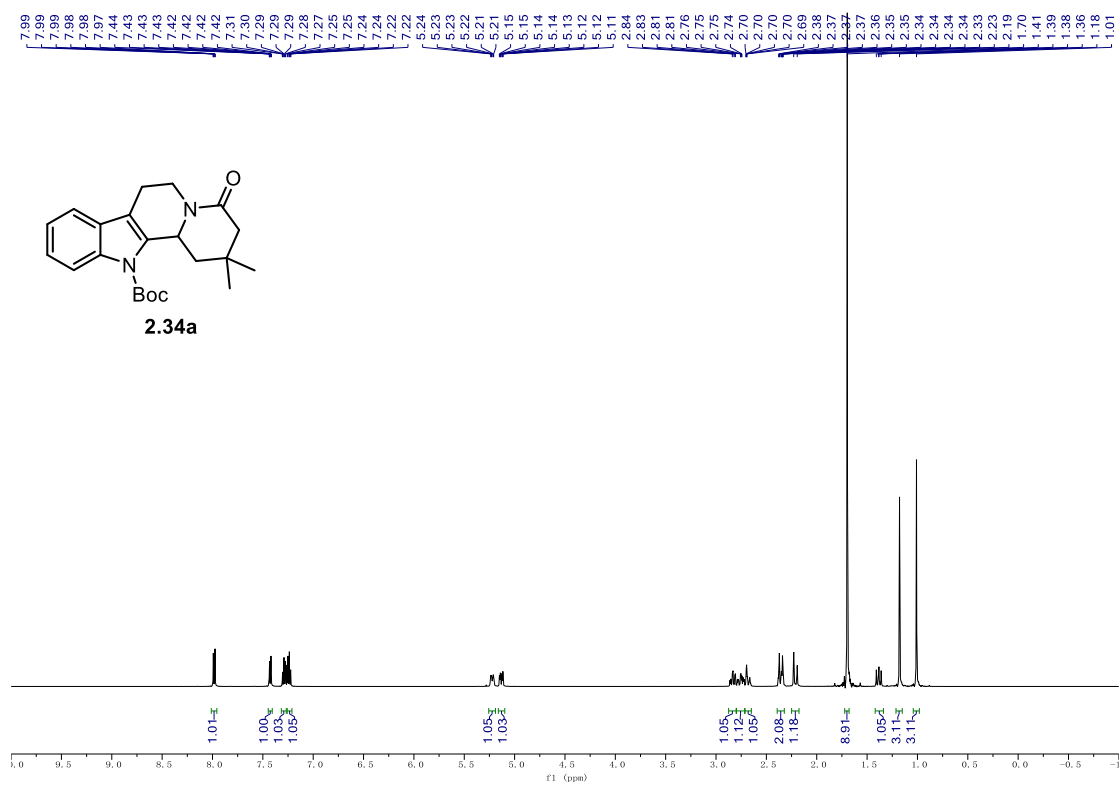
¹³C NMR (176 MHz, CDCl₃) of **2.32a**.



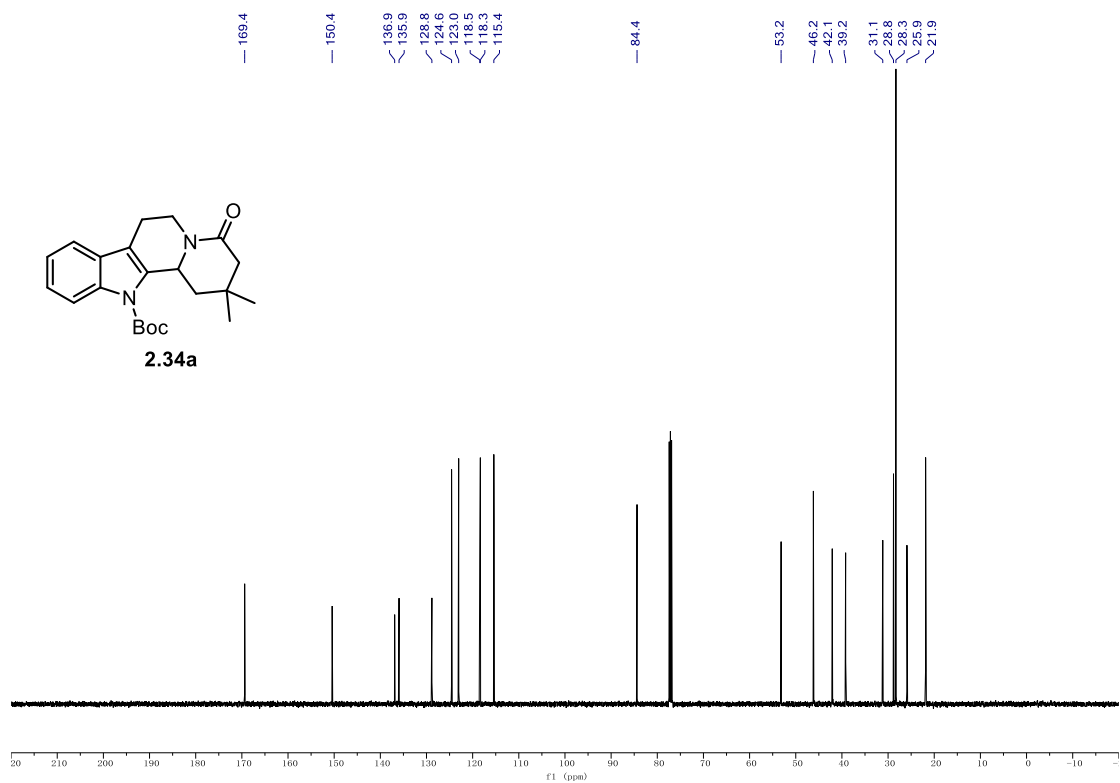
¹H NMR (500 MHz, CD₂Cl₂) of 2.31a.**¹³C NMR (126 MHz, CD₂Cl₂) of 31a.**

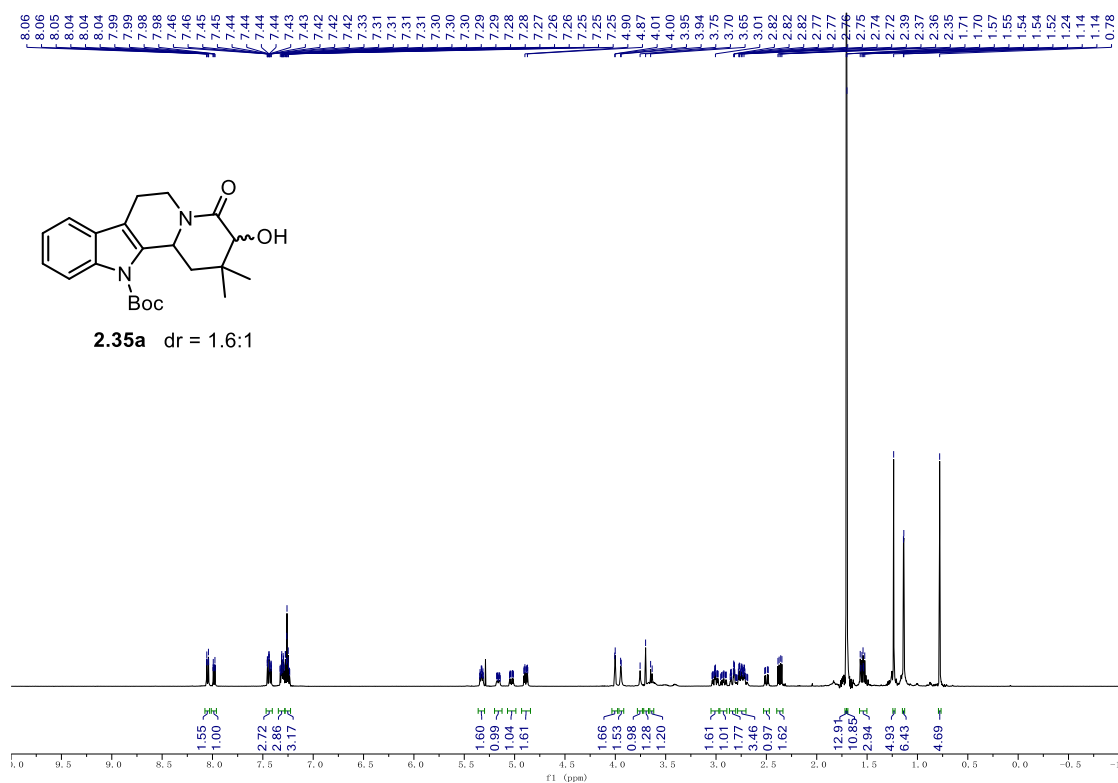
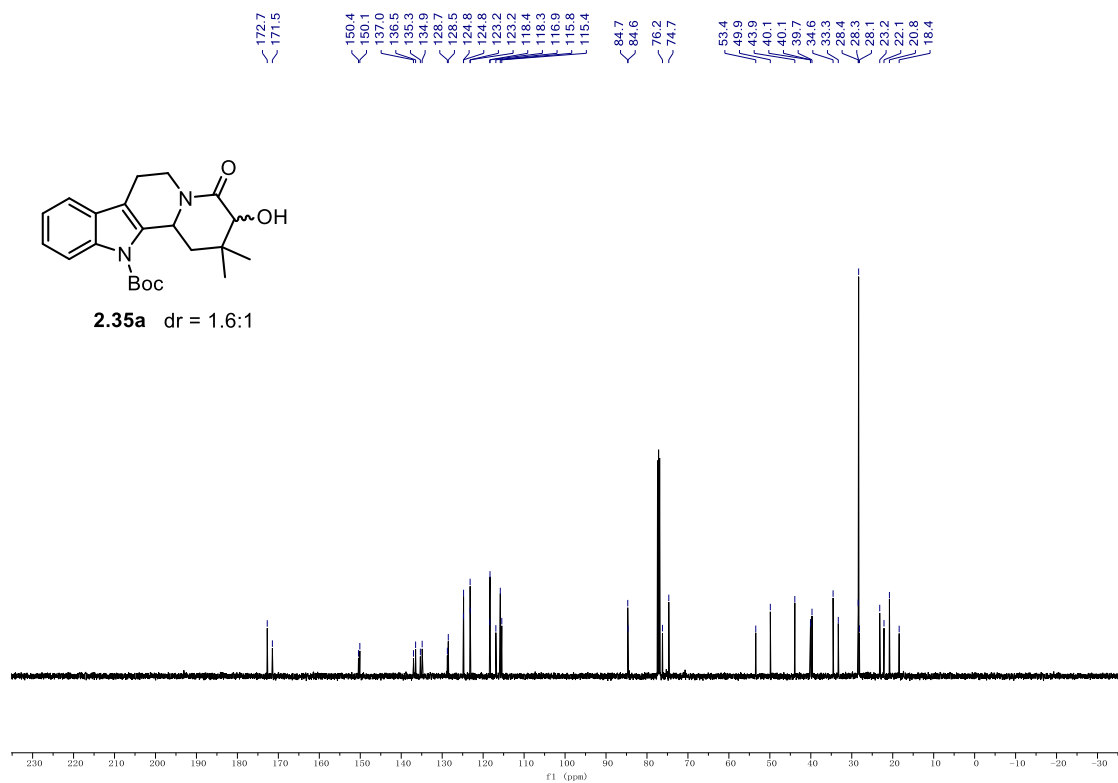
9.1. NMR Spectra

^1H NMR (500 MHz, CDCl_3) of **2.34a**.



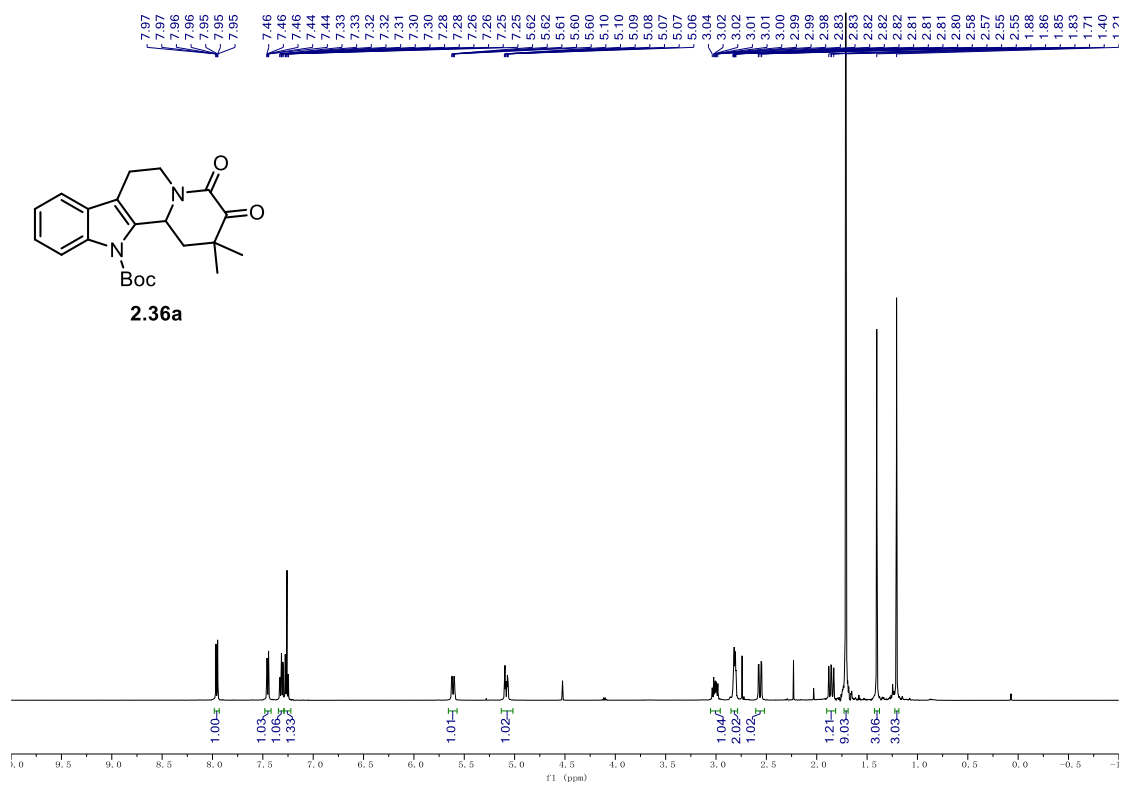
^{13}C NMR (126 MHz, CDCl_3) of **2.34a**.



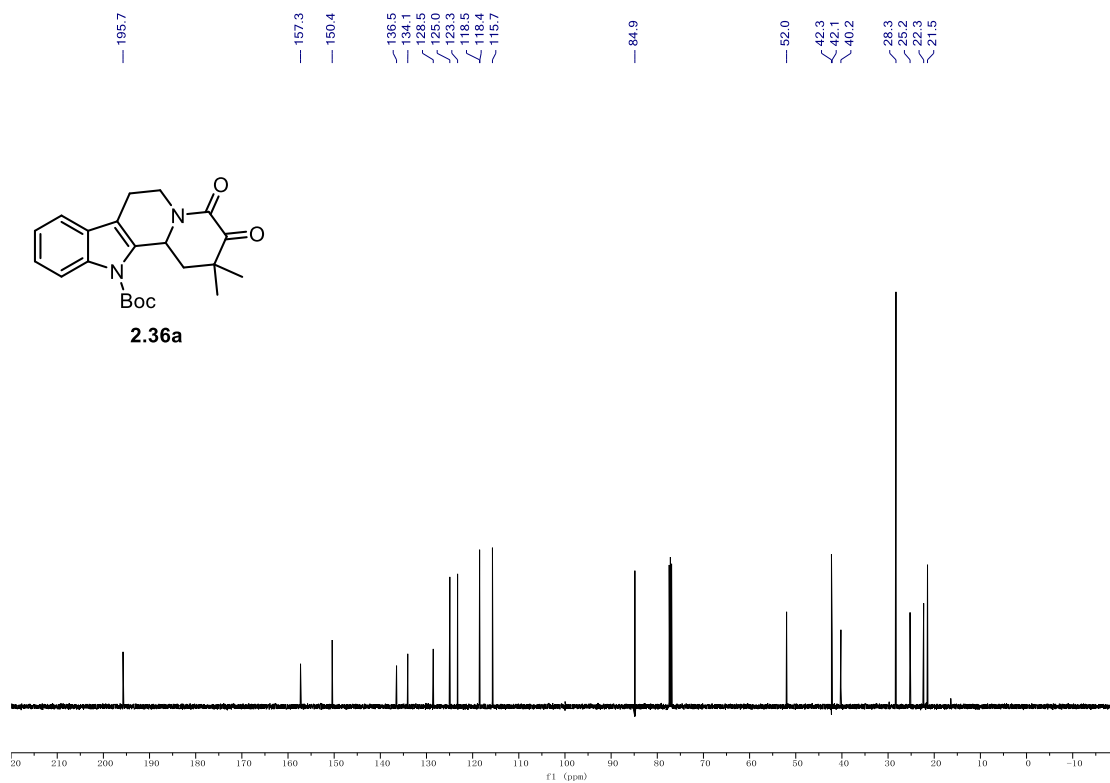
¹H NMR (500 MHz, CDCl₃) of 2.35a.**¹³C NMR (126 MHz, CDCl₃) of 2.35a.**

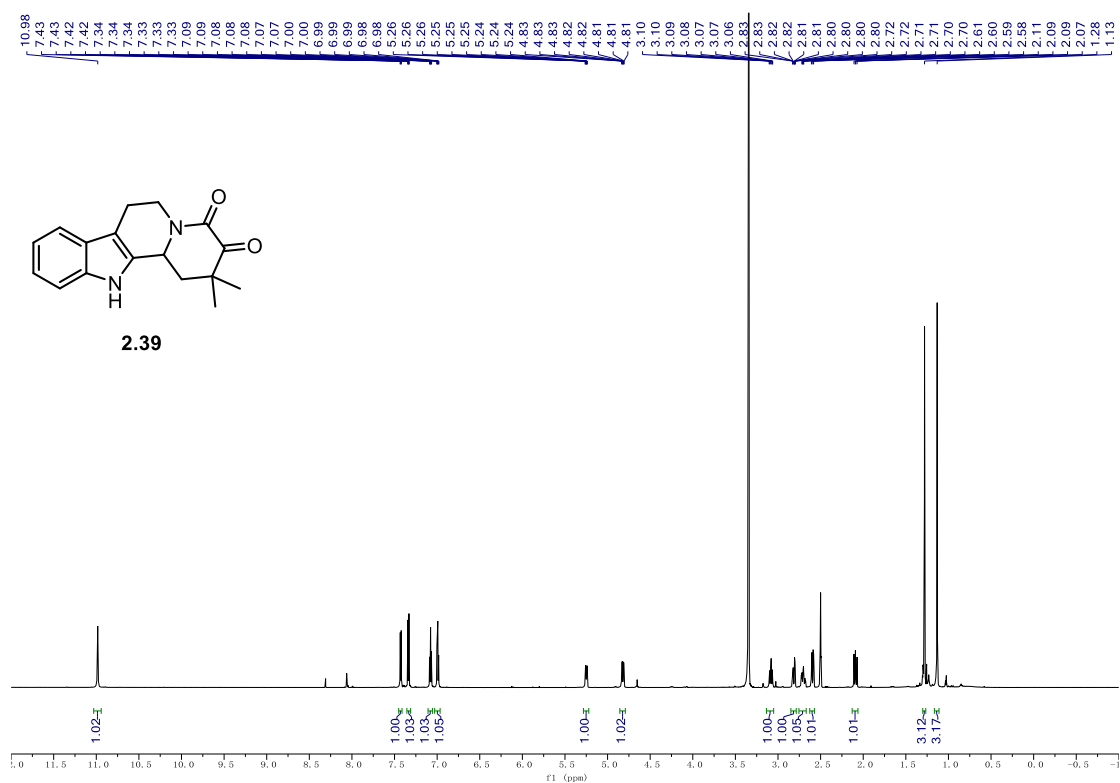
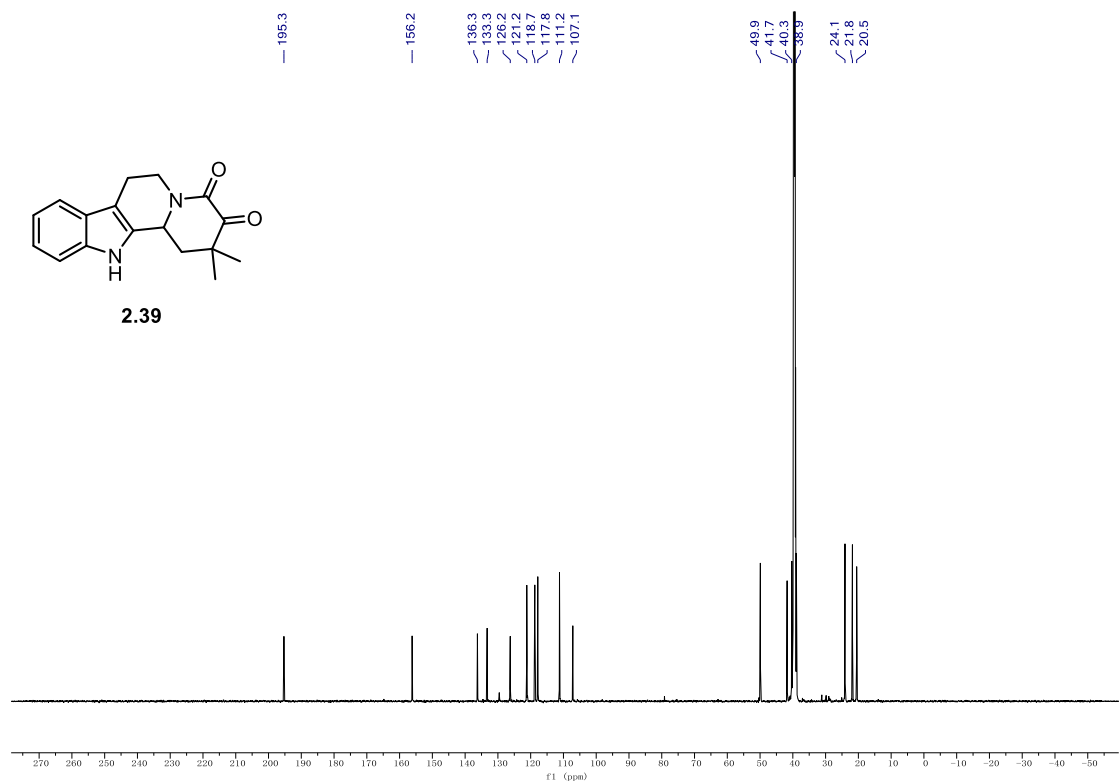
9.1. NMR Spectra

¹H NMR (500 MHz, CDCl₃) of **2.36a**.



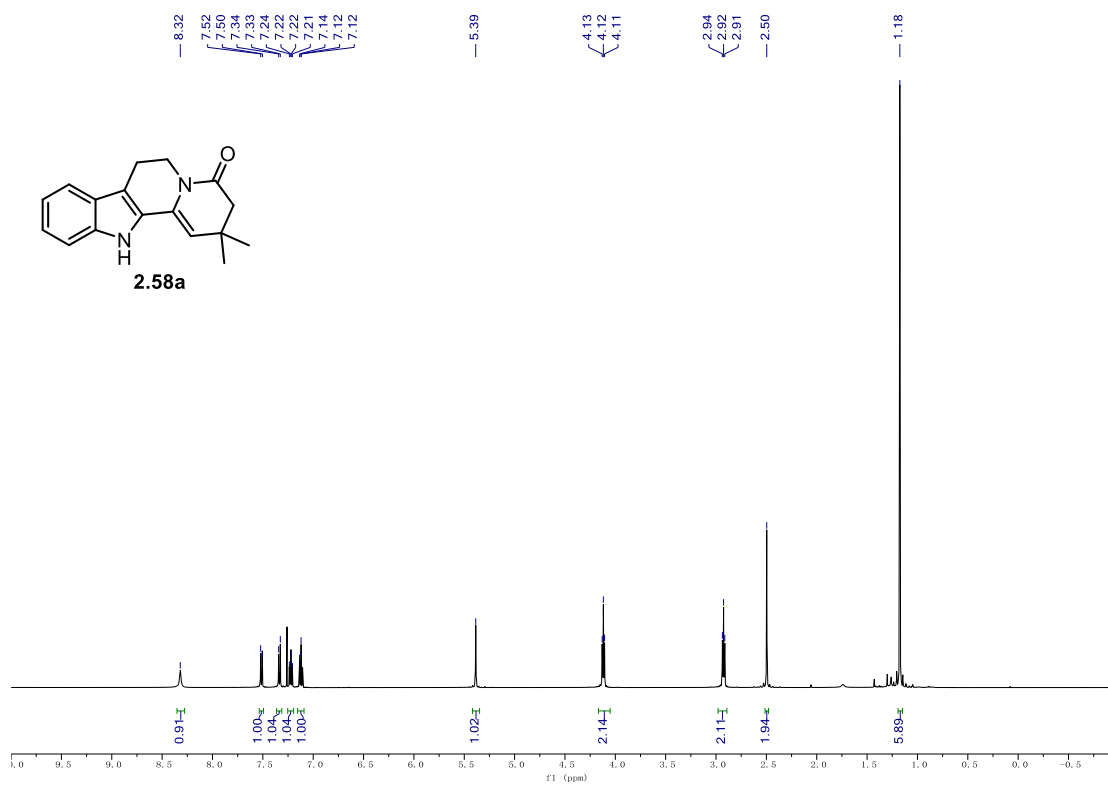
¹³C NMR (126 MHz, CDCl₃) of **2.36a**.



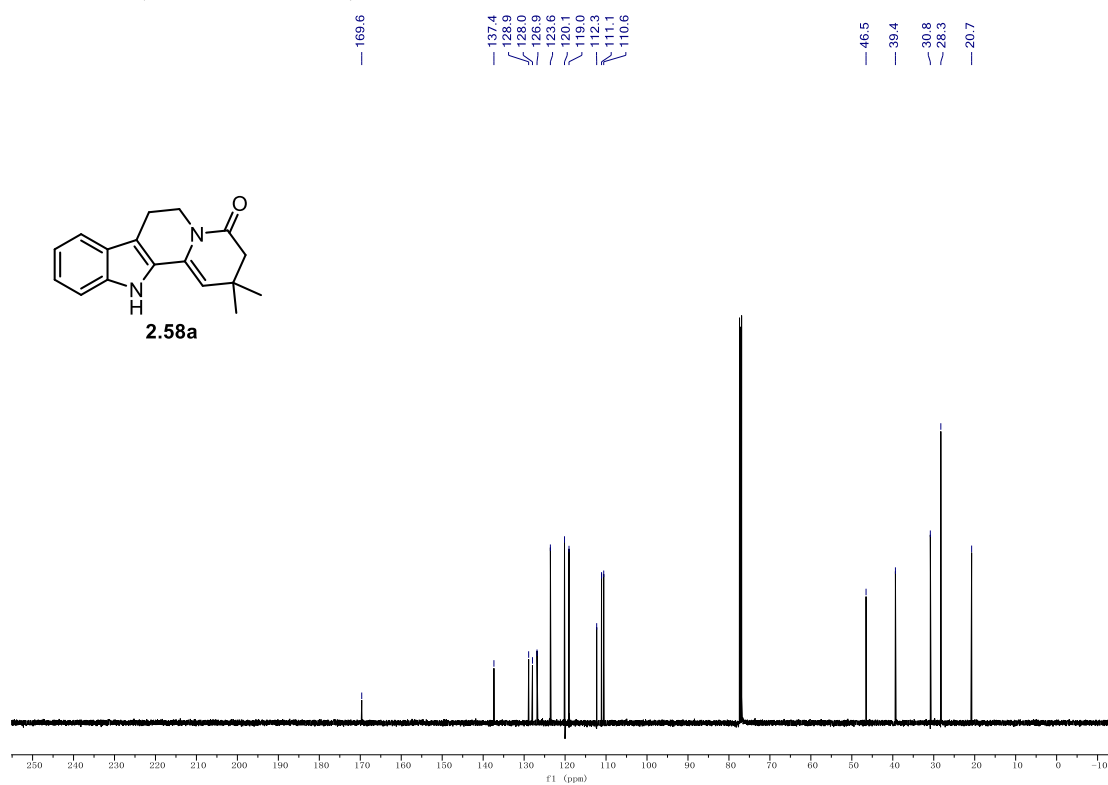
¹H NMR (500 MHz, CDCl₃) of 2.39.**¹³C NMR (126 MHz, CDCl₃) of 2.39.**

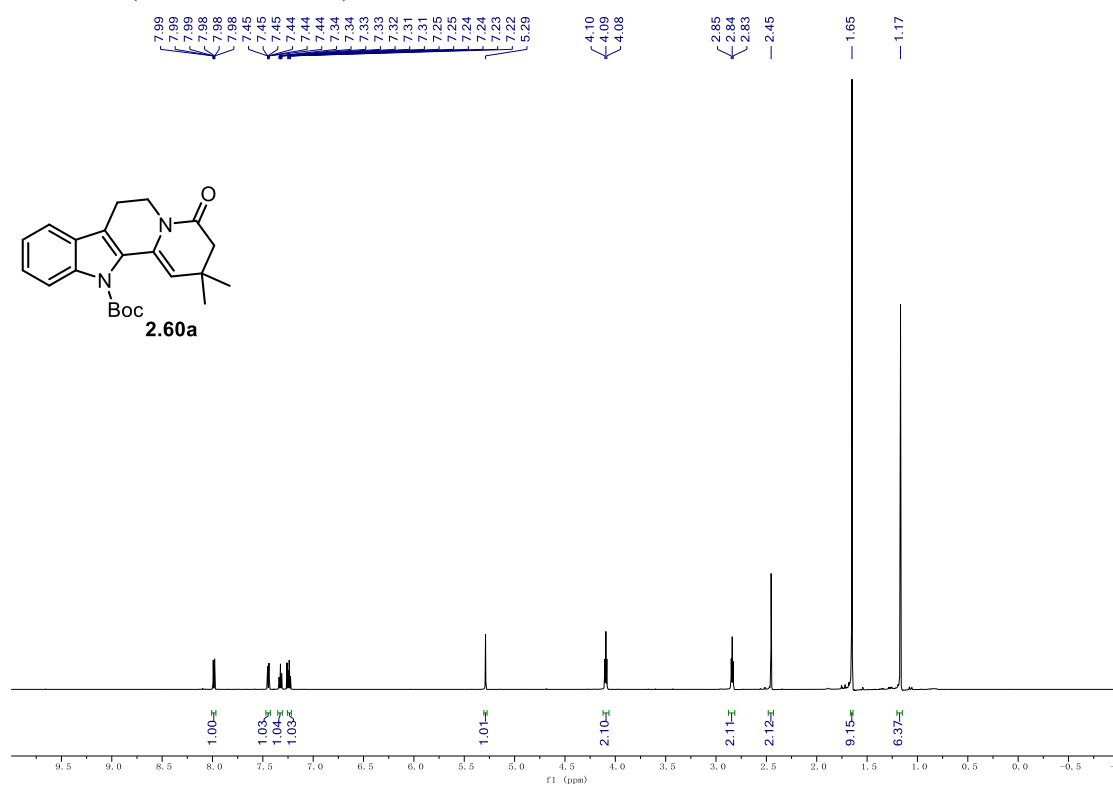
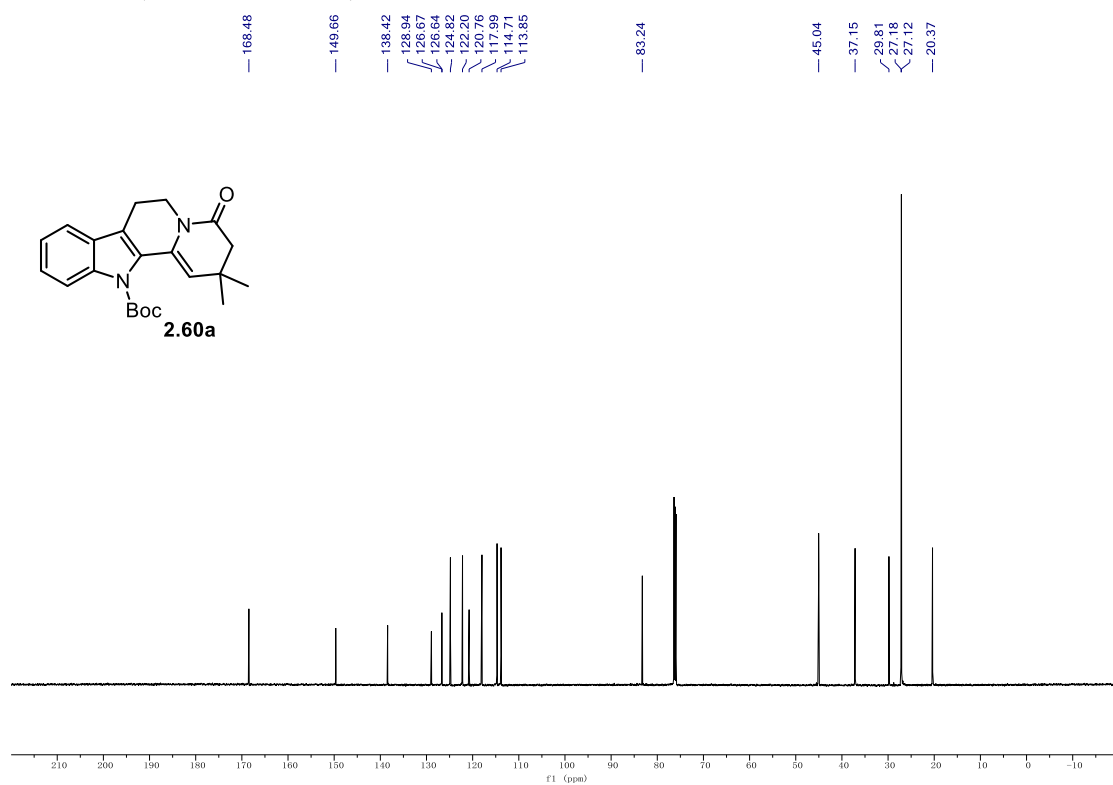
9.1. NMR Spectra

¹H NMR (500 MHz, CDCl₃) of **2.58a**.



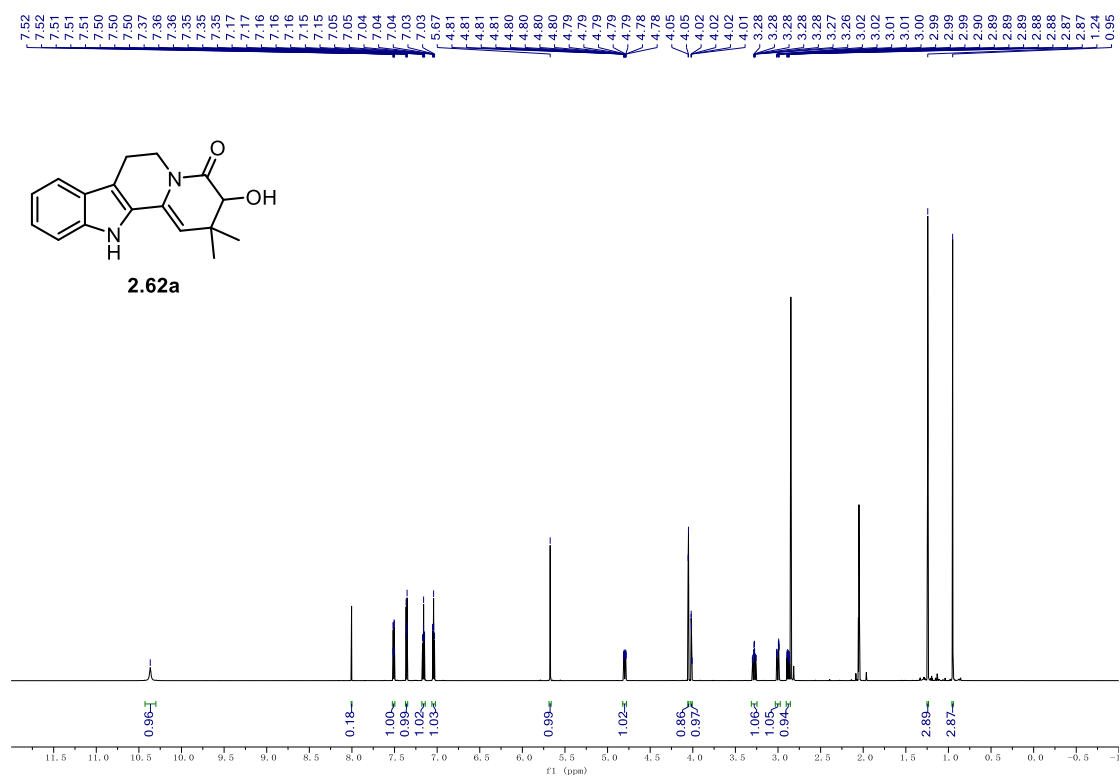
¹³C NMR (126 MHz, CDCl₃) of **2.58a**.



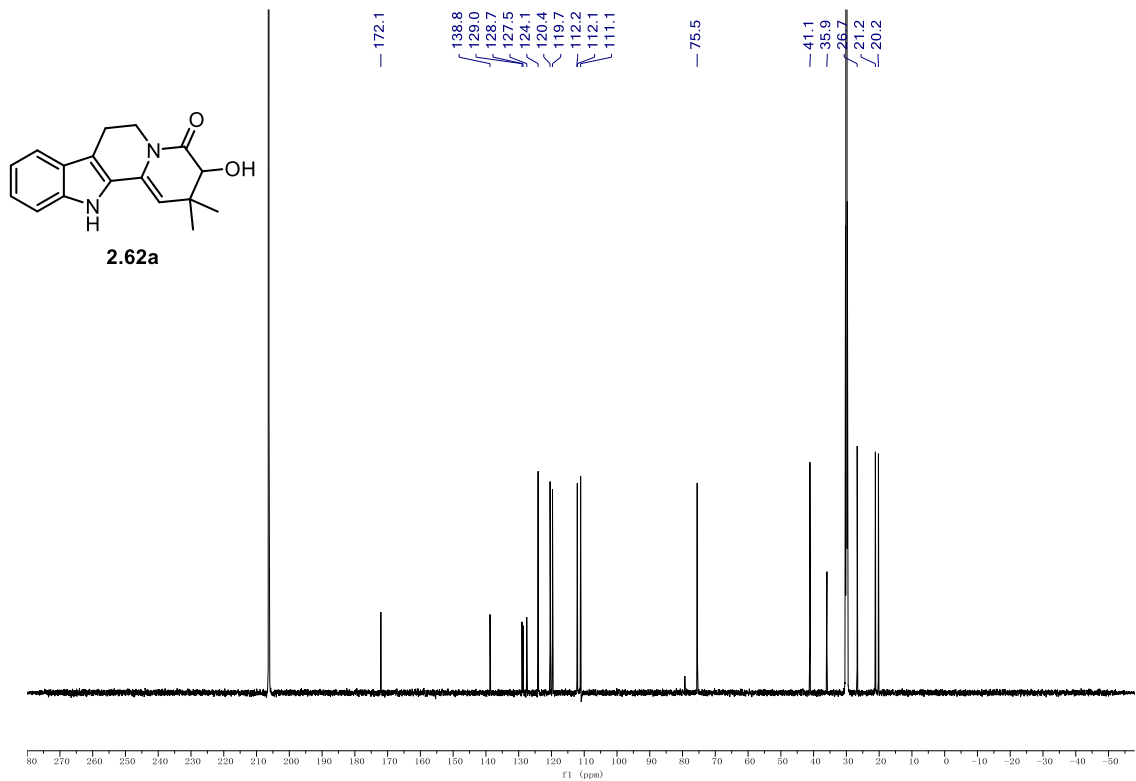
^1H NMR (600 MHz, CDCl_3) of **2.60a**. ^{13}C NMR (151 MHz, CDCl_3) of **2.60a**.

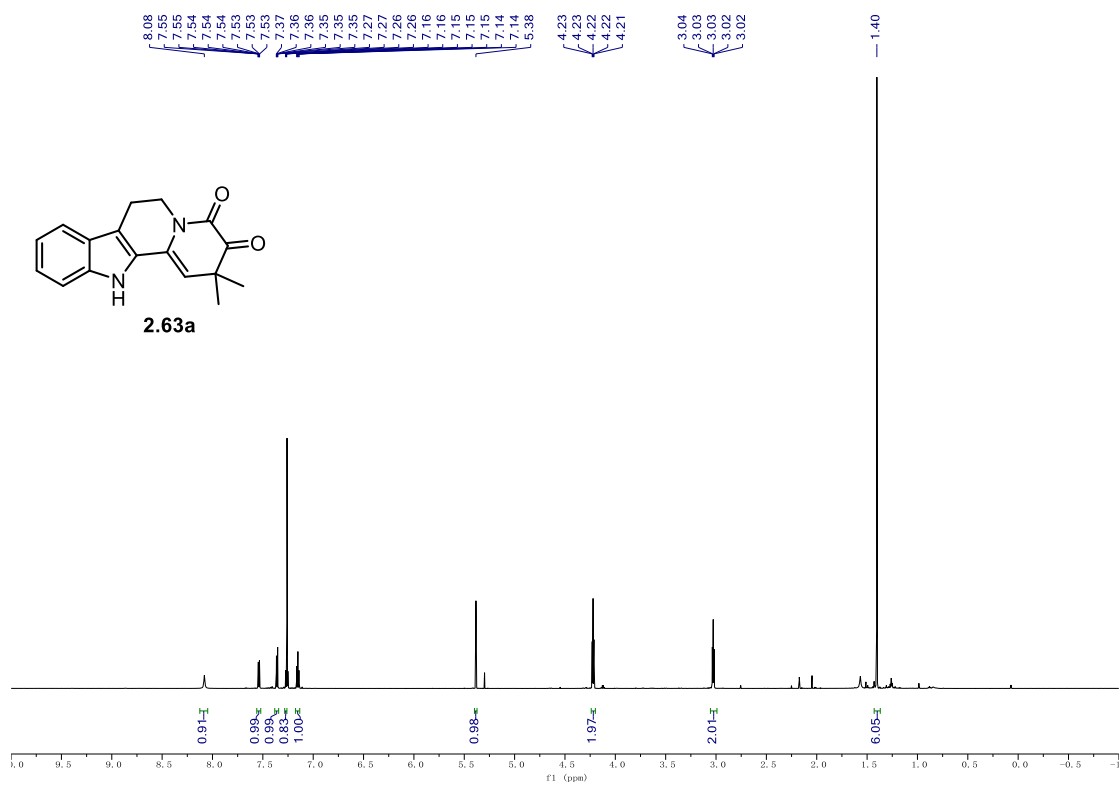
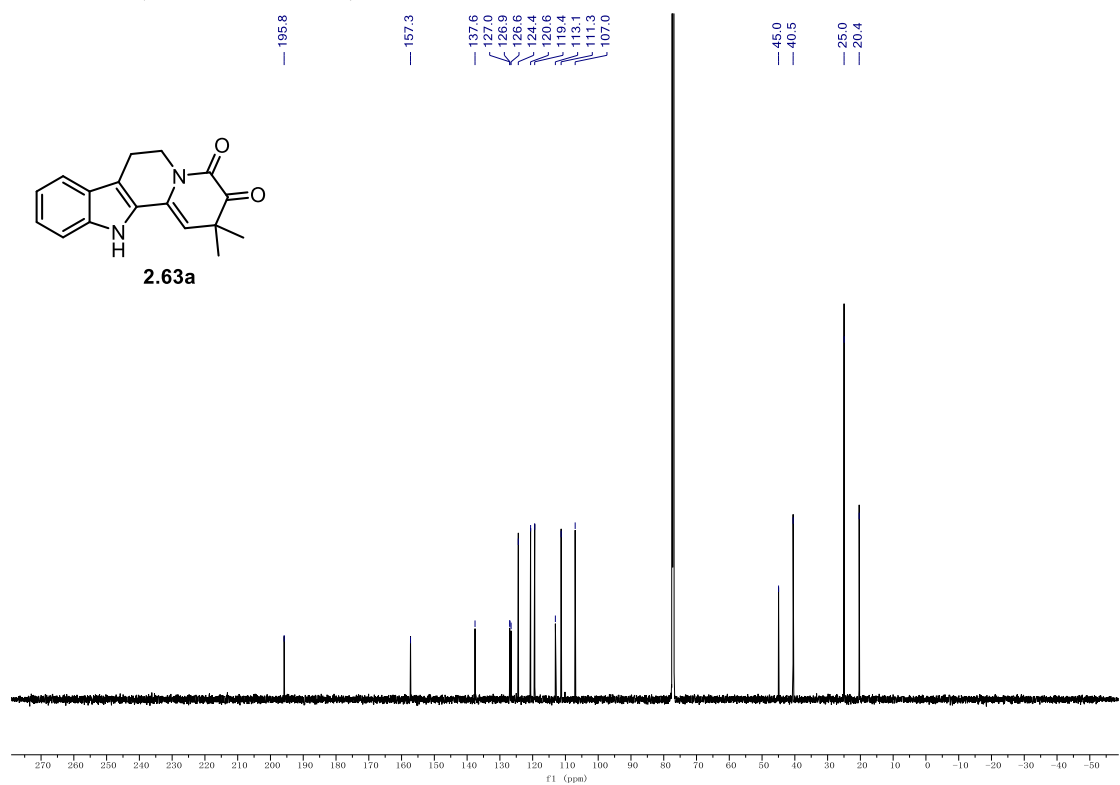
9.1. NMR Spectra

¹H NMR (700 MHz, *d*₆-acetone) of **2.62a**.



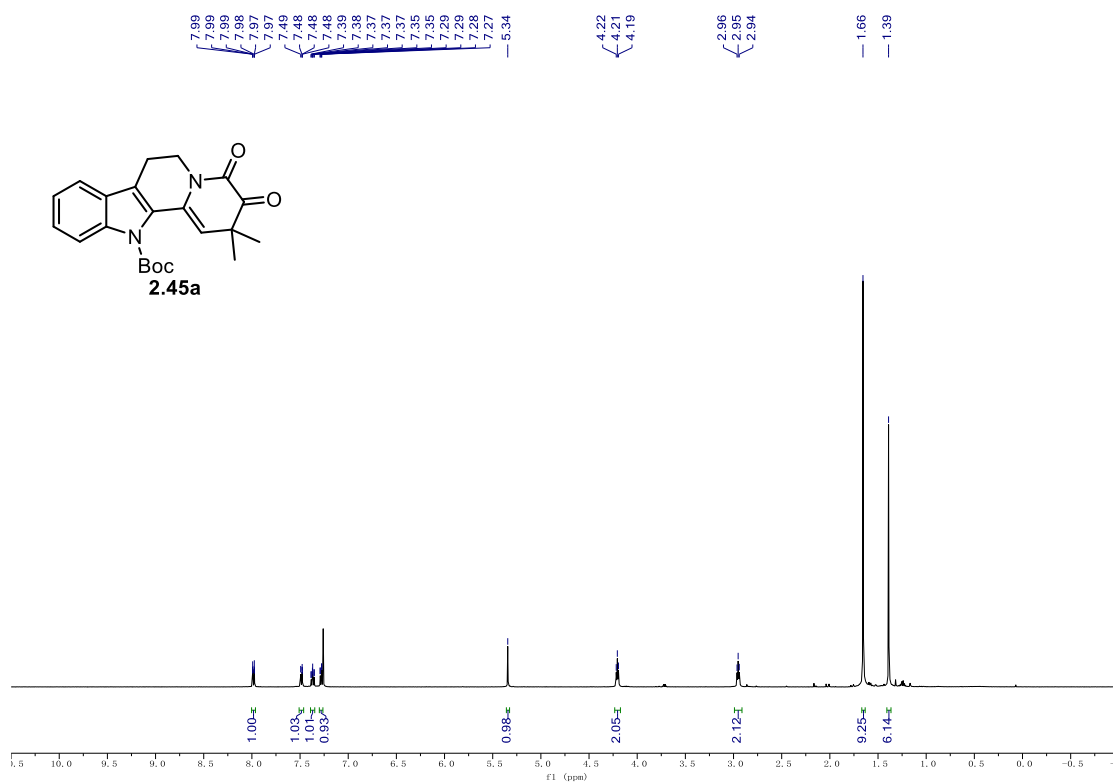
¹³C NMR (176 MHz, *d*₆-acetone) of **2.62a**.



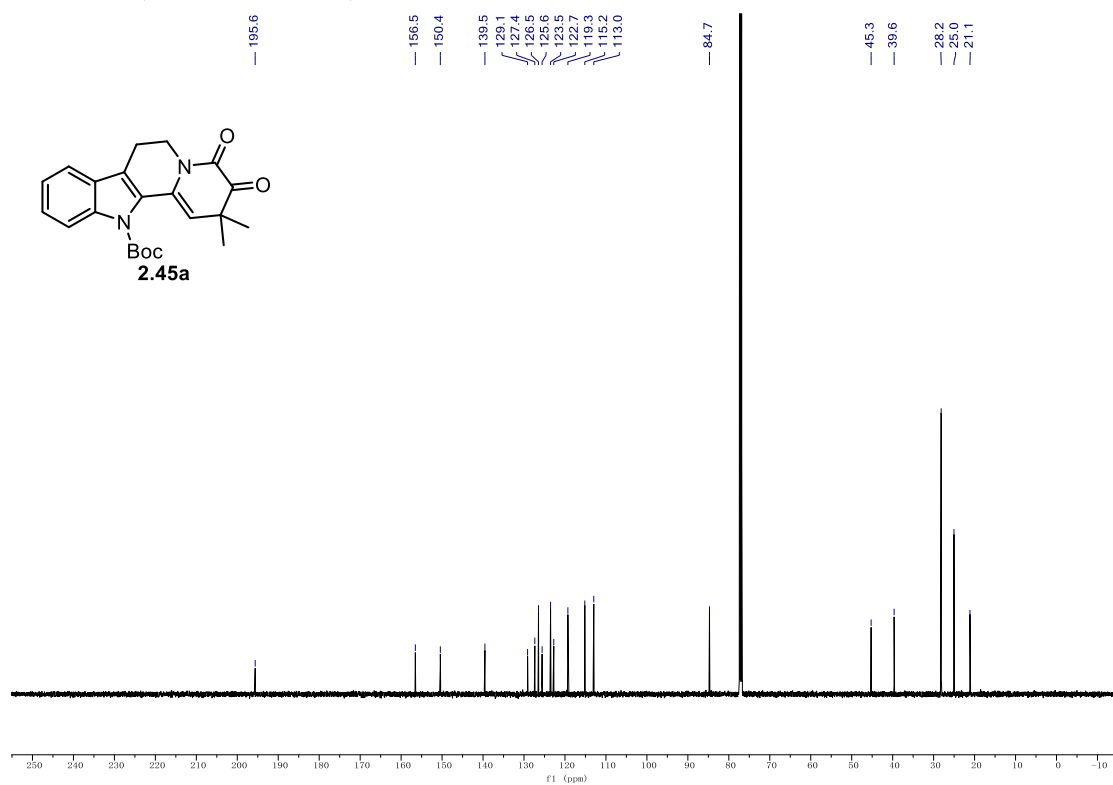
^1H NMR (700 MHz, CDCl_3) of **2.63a.** **^{13}C NMR (176 MHz, CDCl_3) of **2.63a**.**

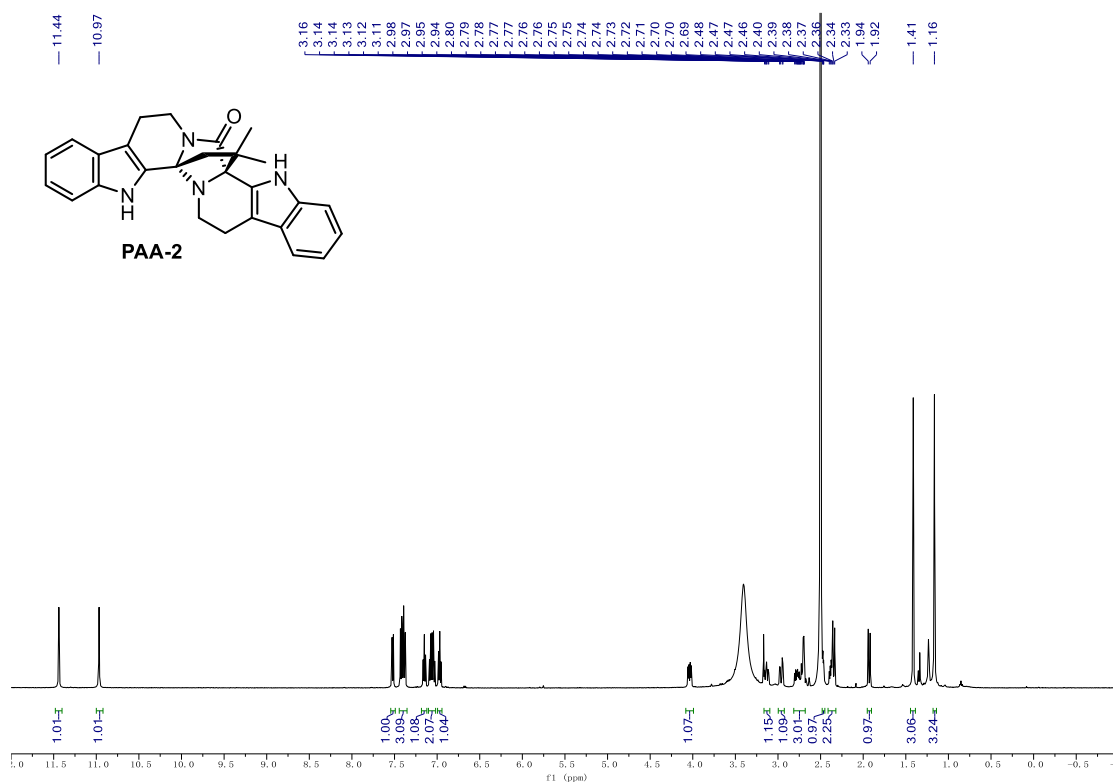
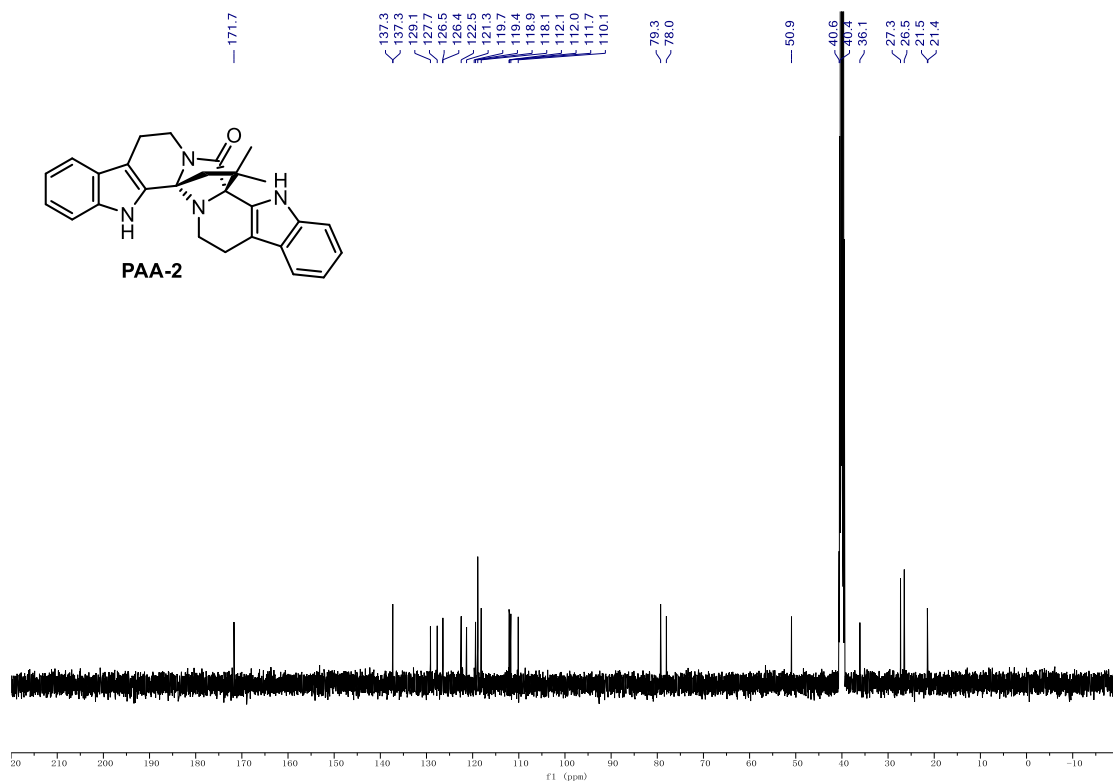
9.1. NMR Spectra

¹H NMR (500 MHz, CDCl₃) of **2.45a**.



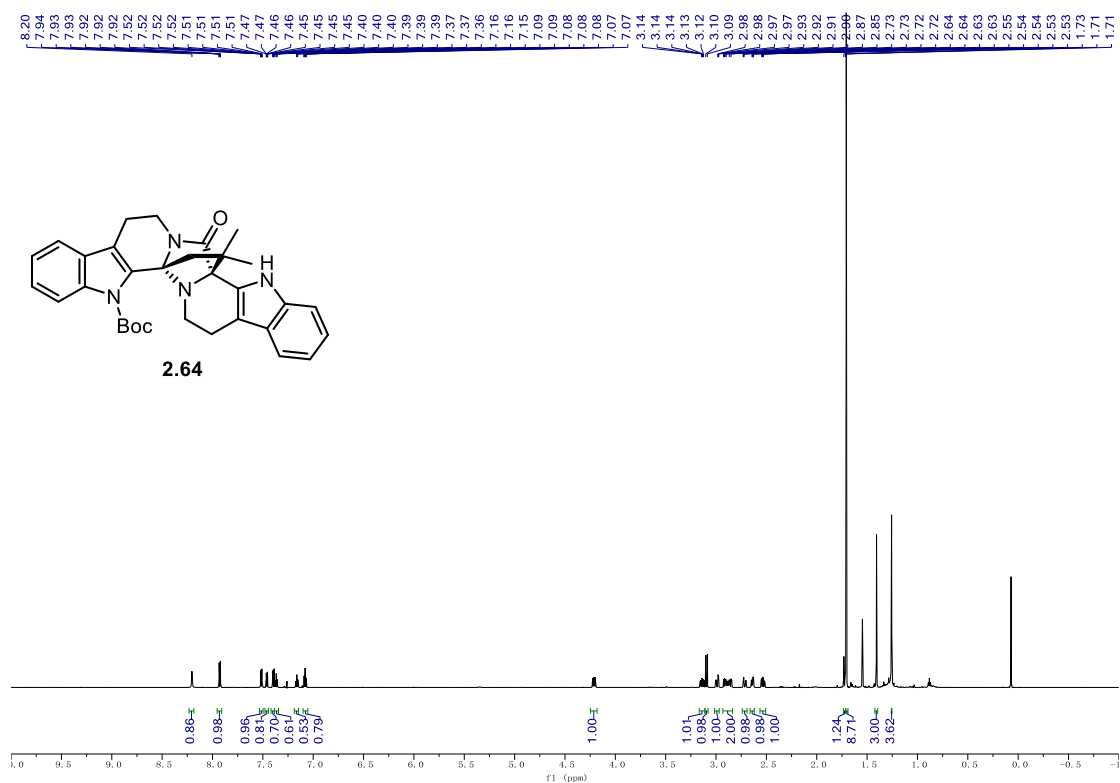
¹³C NMR (126 MHz, CDCl₃) of **2.45a**.



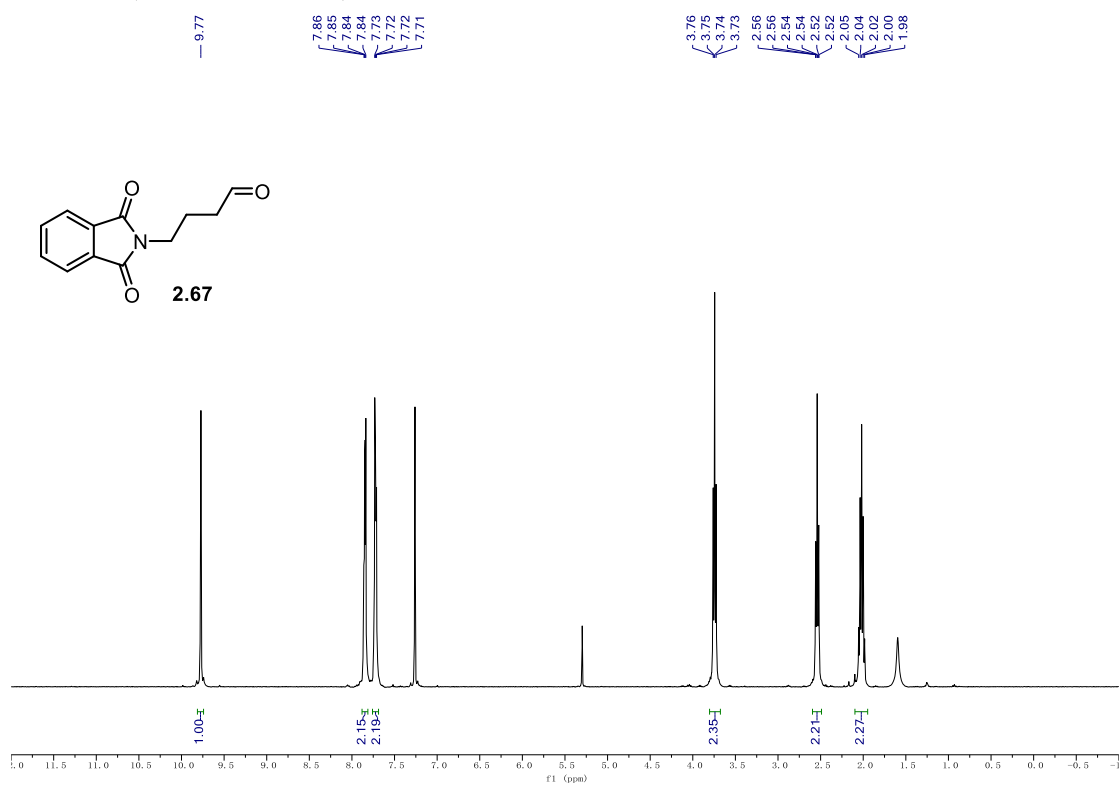
¹H NMR (500 MHz, CDCl₃) of PAA-2.**¹³C NMR (126 MHz, CDCl₃) of PAA-2.**

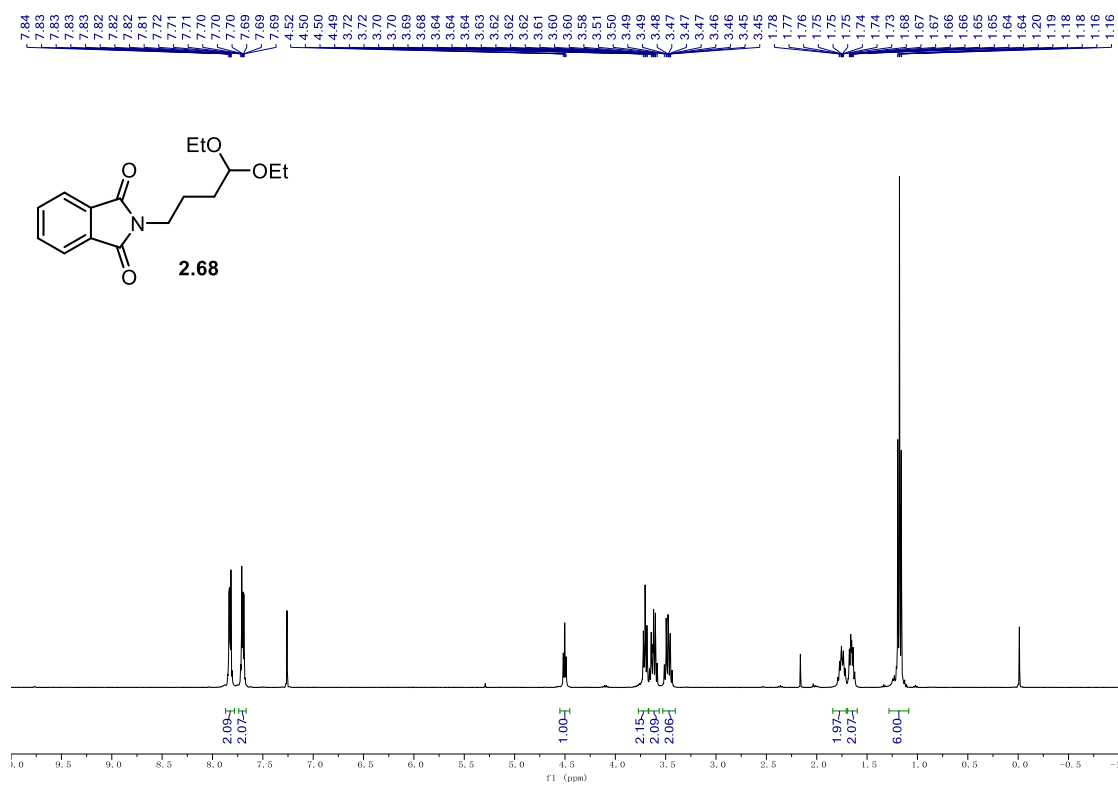
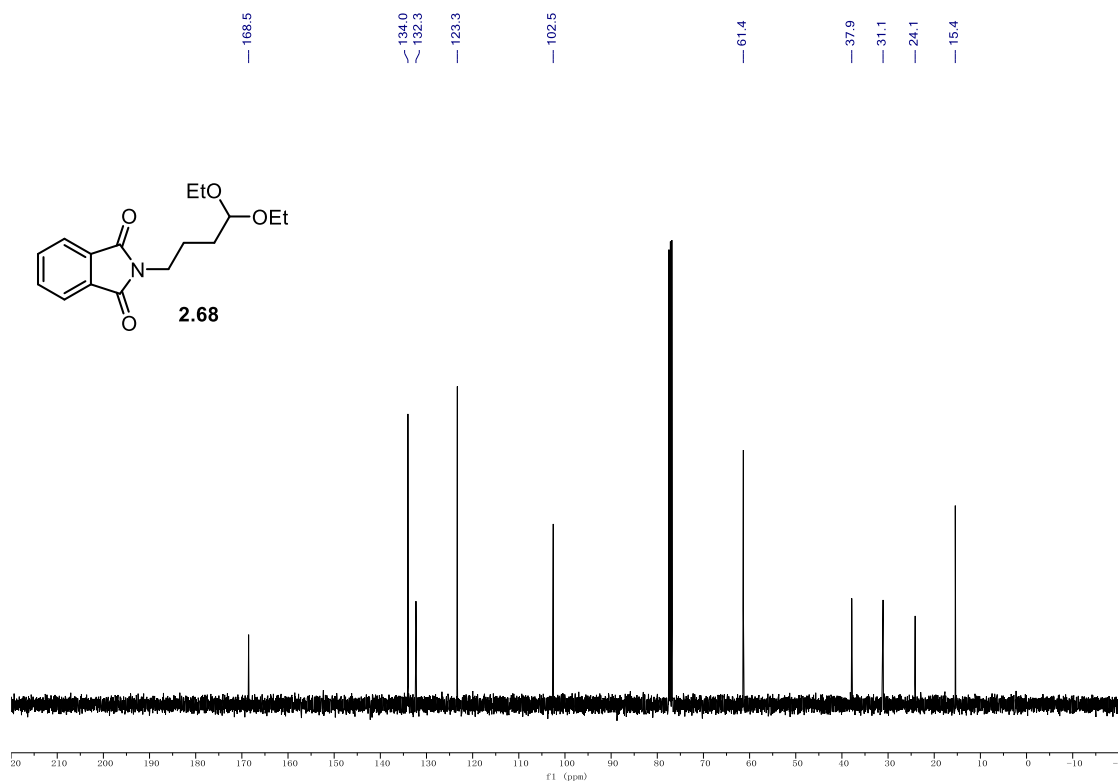
9.1. NMR Spectra

¹H NMR (700 MHz, CDCl₃) of 2.64.



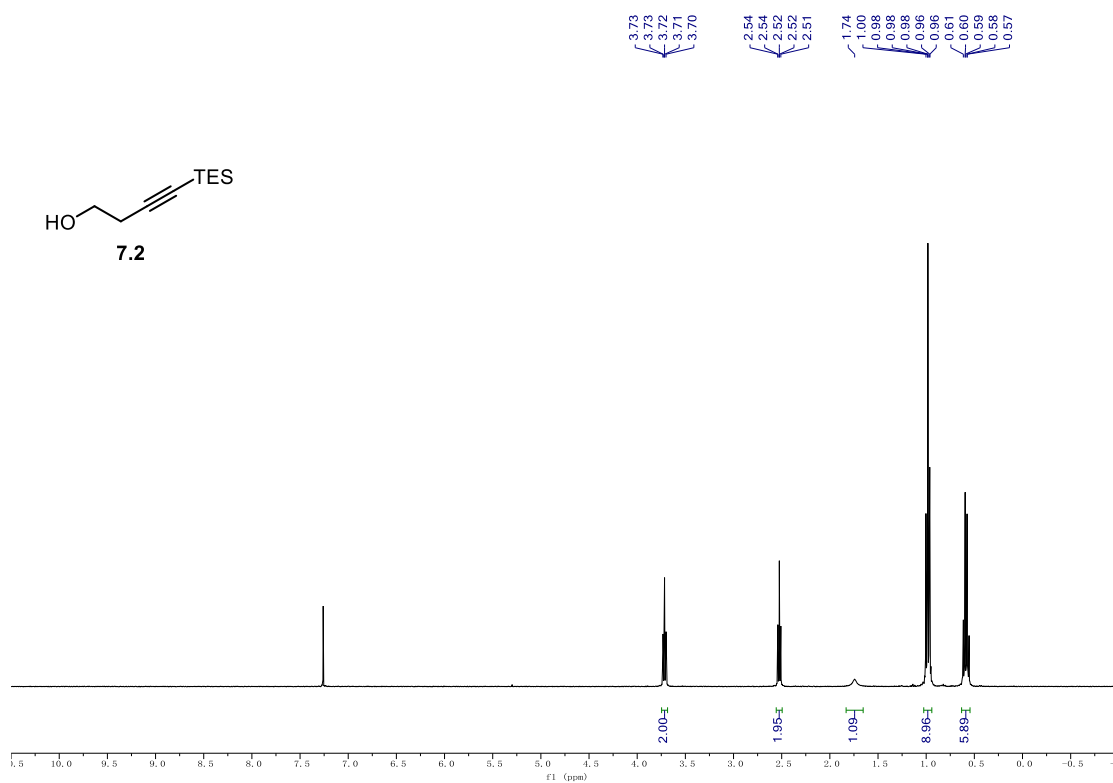
¹H NMR (400 MHz, CDCl₃) of 2.67.



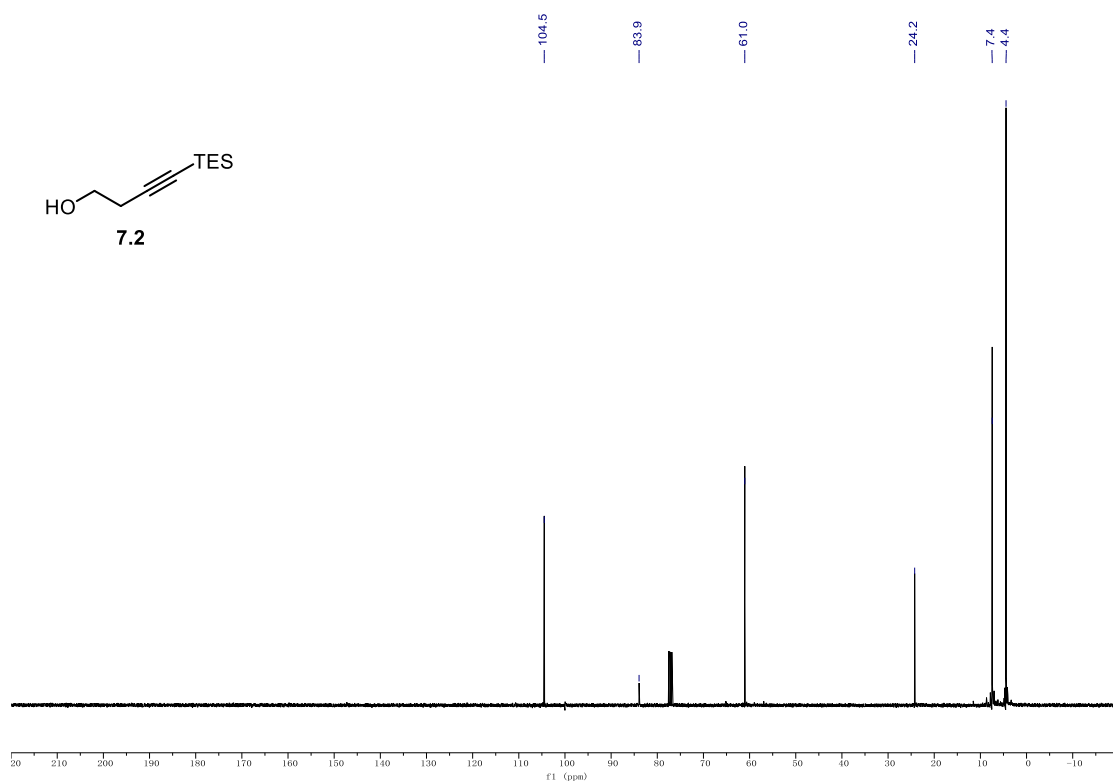
^1H NMR (400 MHz, CDCl_3) of **2.68.** **^{13}C NMR (101 MHz, CDCl_3) of **2.68**.**

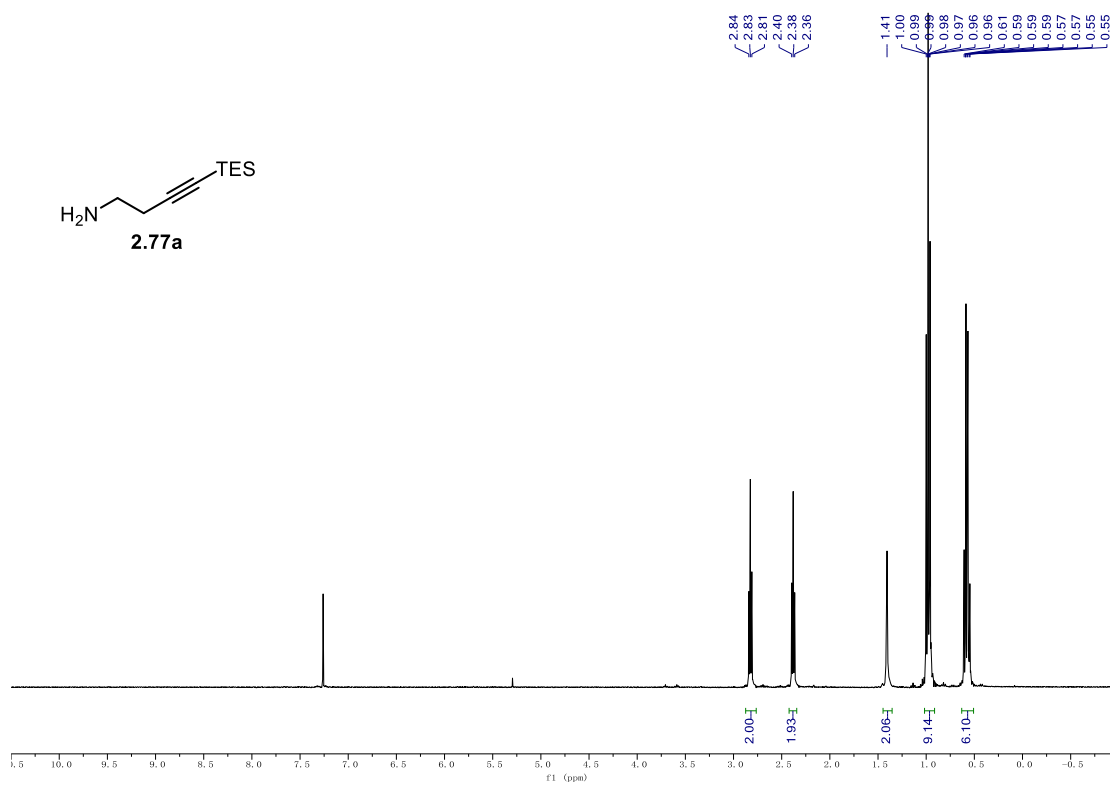
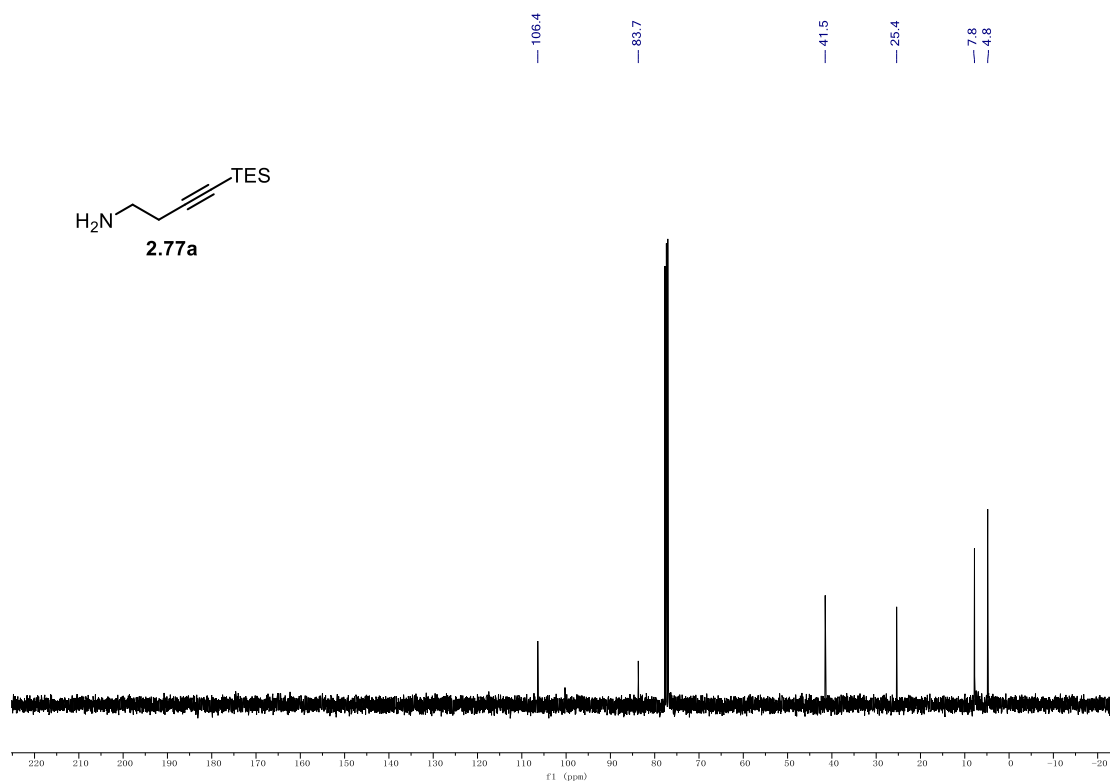
9.1. NMR Spectra

¹H NMR (400 MHz, CDCl₃) of 7.2.



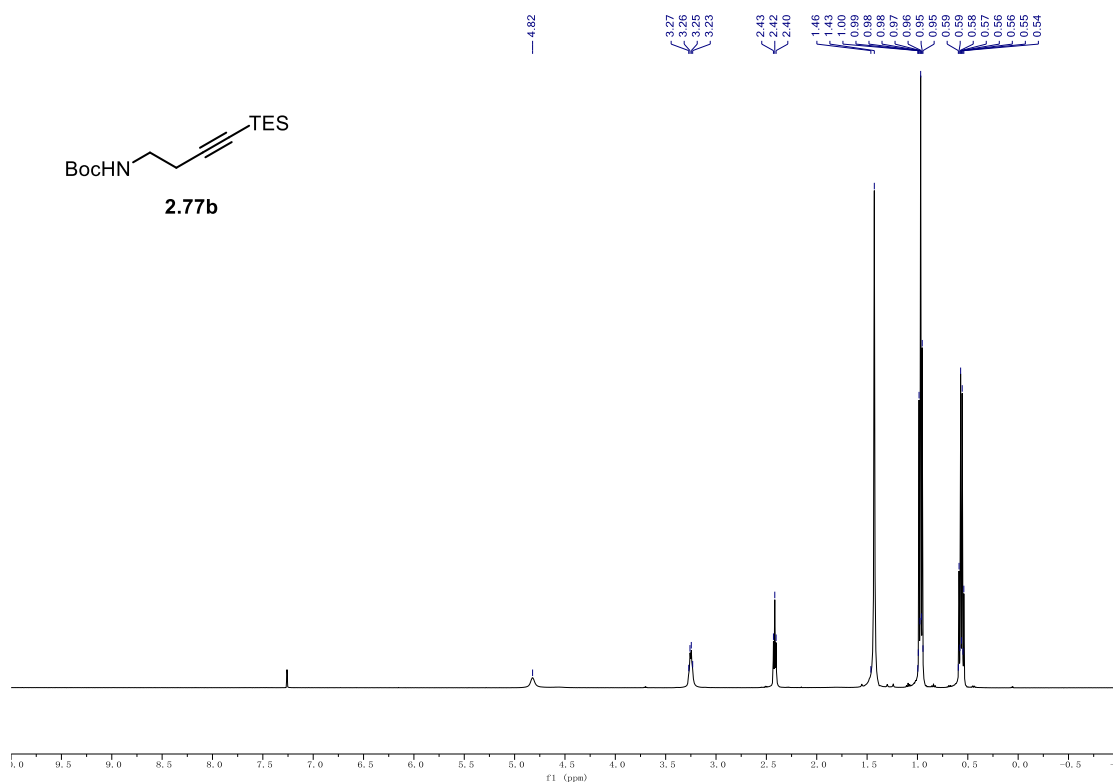
¹³C NMR (101 MHz, CDCl₃) of 7.2.



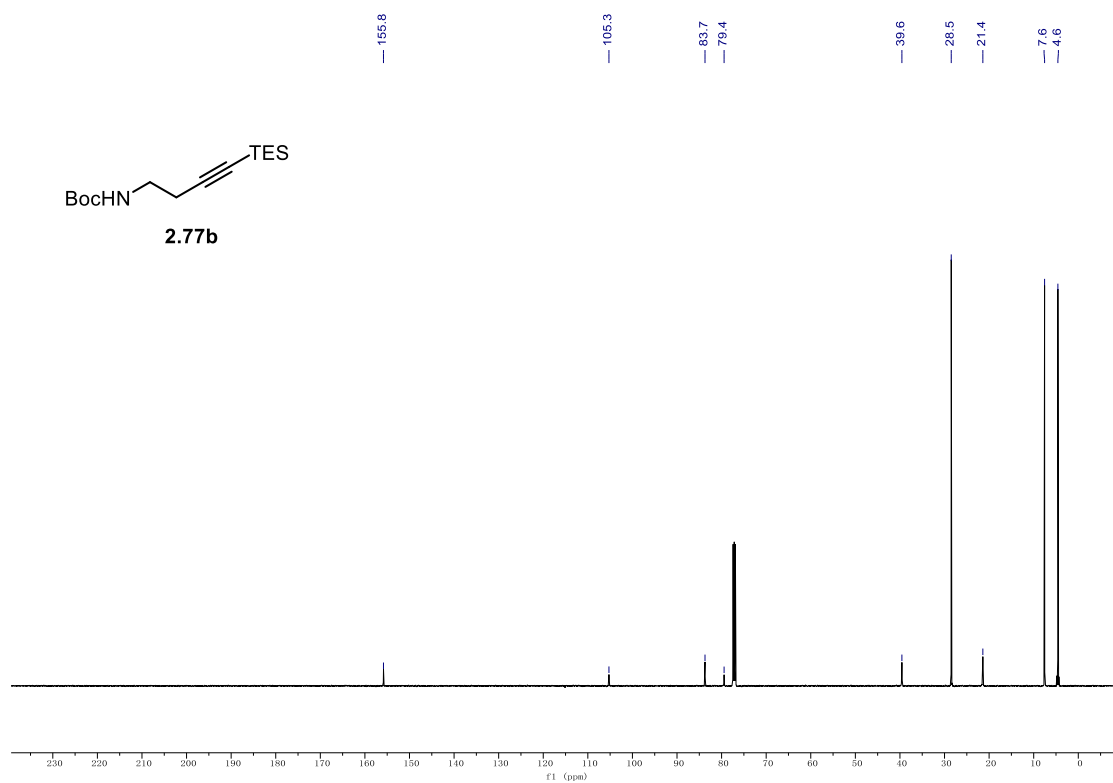
^1H NMR (400 MHz, CDCl_3) of **2.77a**. ^{13}C NMR (101 MHz, CDCl_3) of **2.77a**.

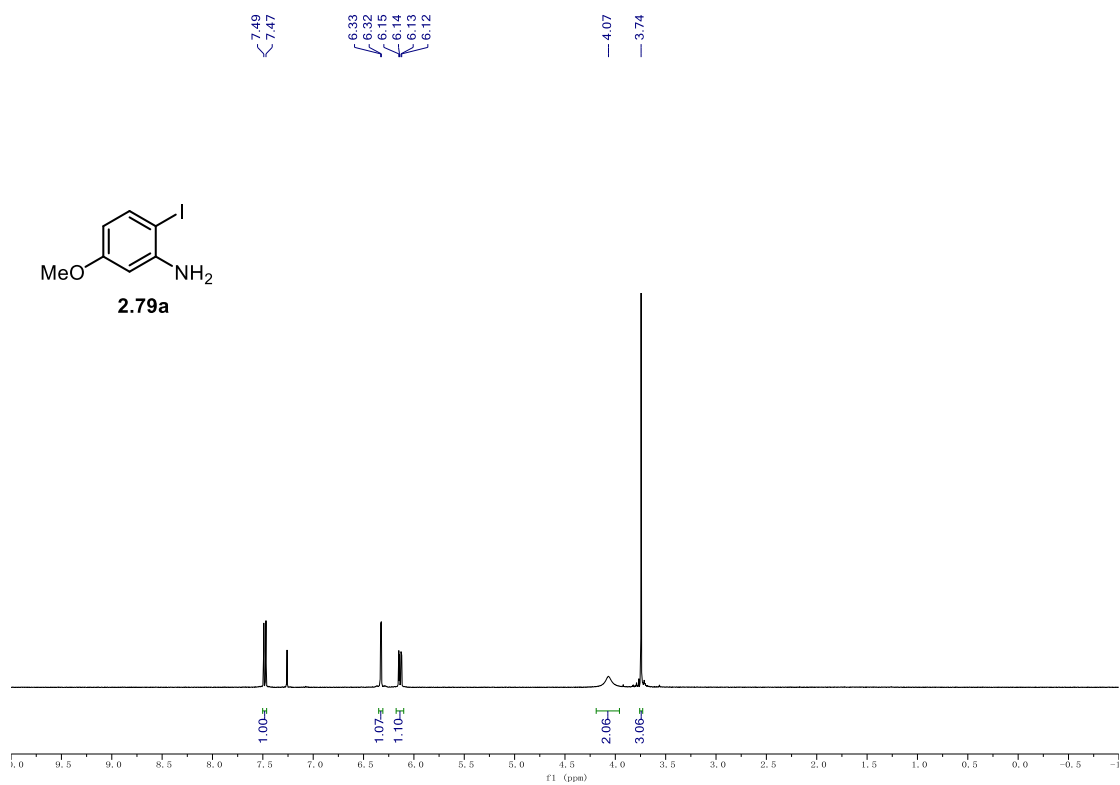
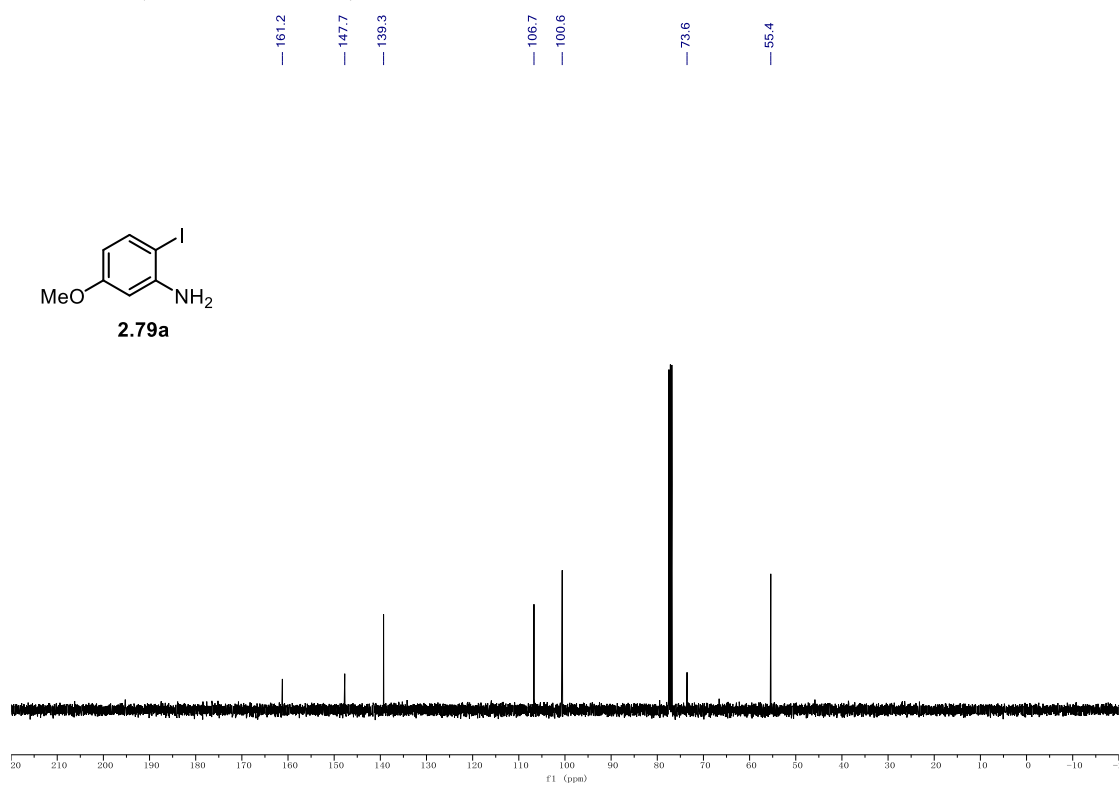
9.1. NMR Spectra

¹H NMR (500 MHz, CDCl₃) of 2.77b.



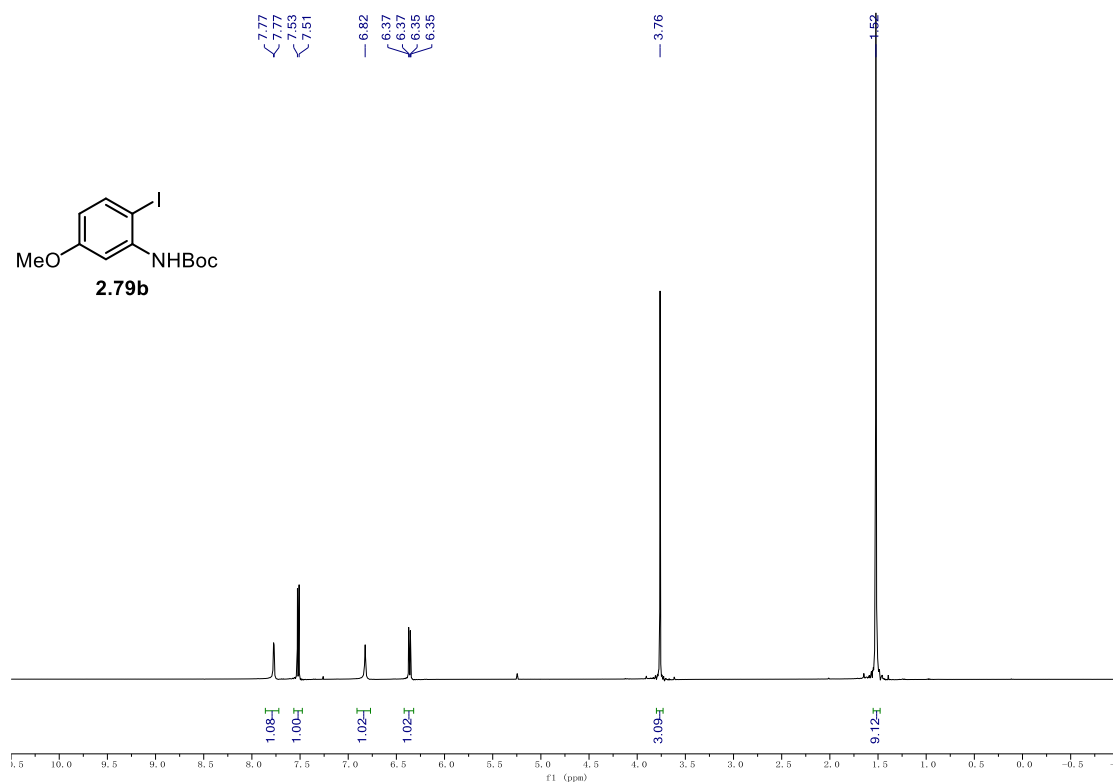
¹³C NMR (126 MHz, CDCl₃) of 2.77b.



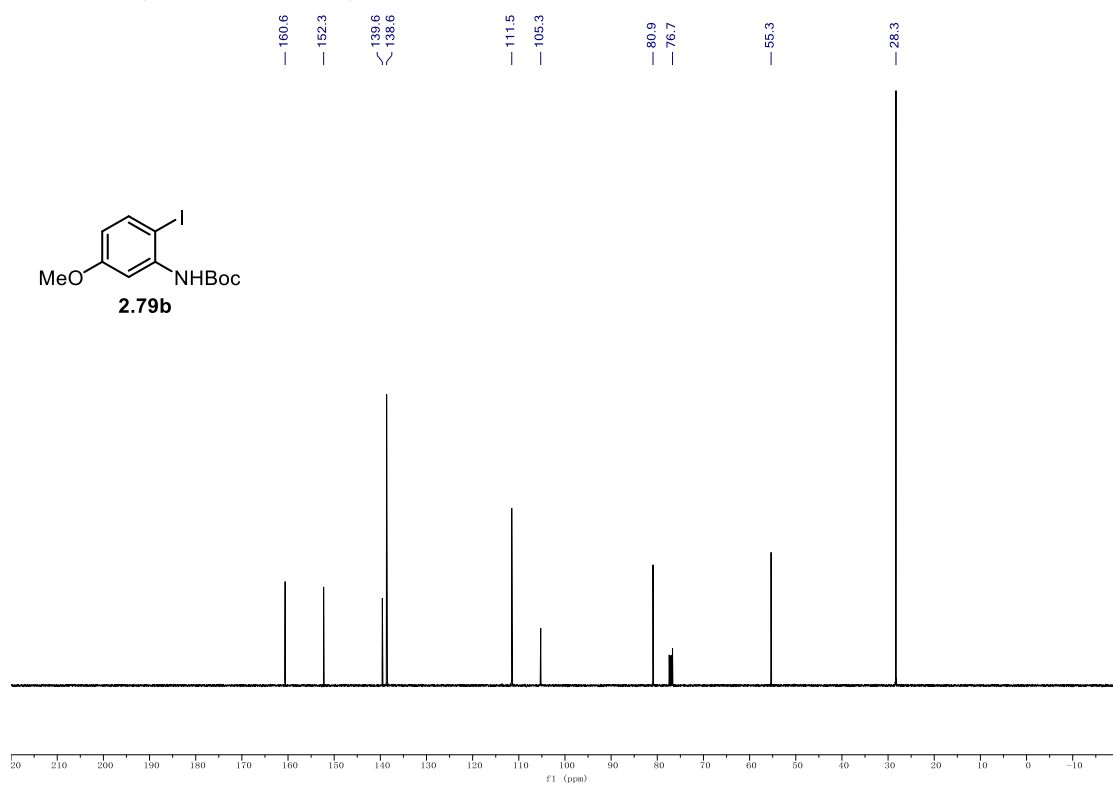
^1H NMR (400 MHz, CDCl_3) of **2.79a.** **^{13}C NMR (101 MHz, CDCl_3) of **2.79a**.**

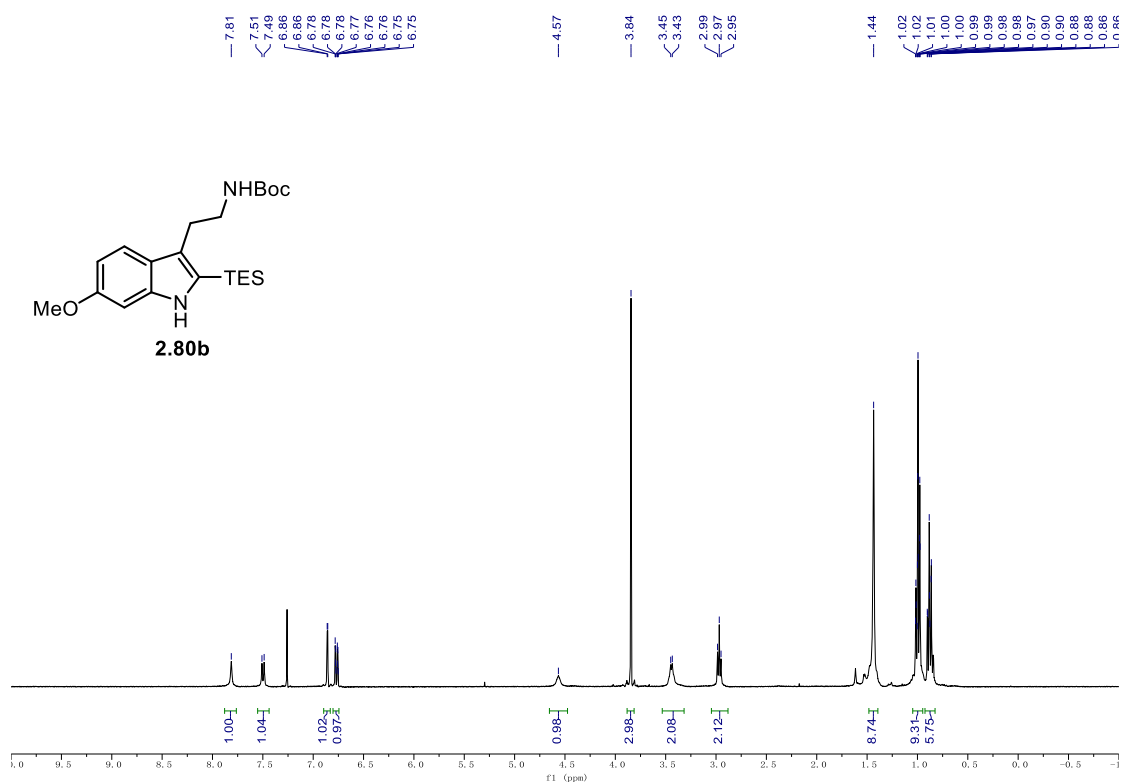
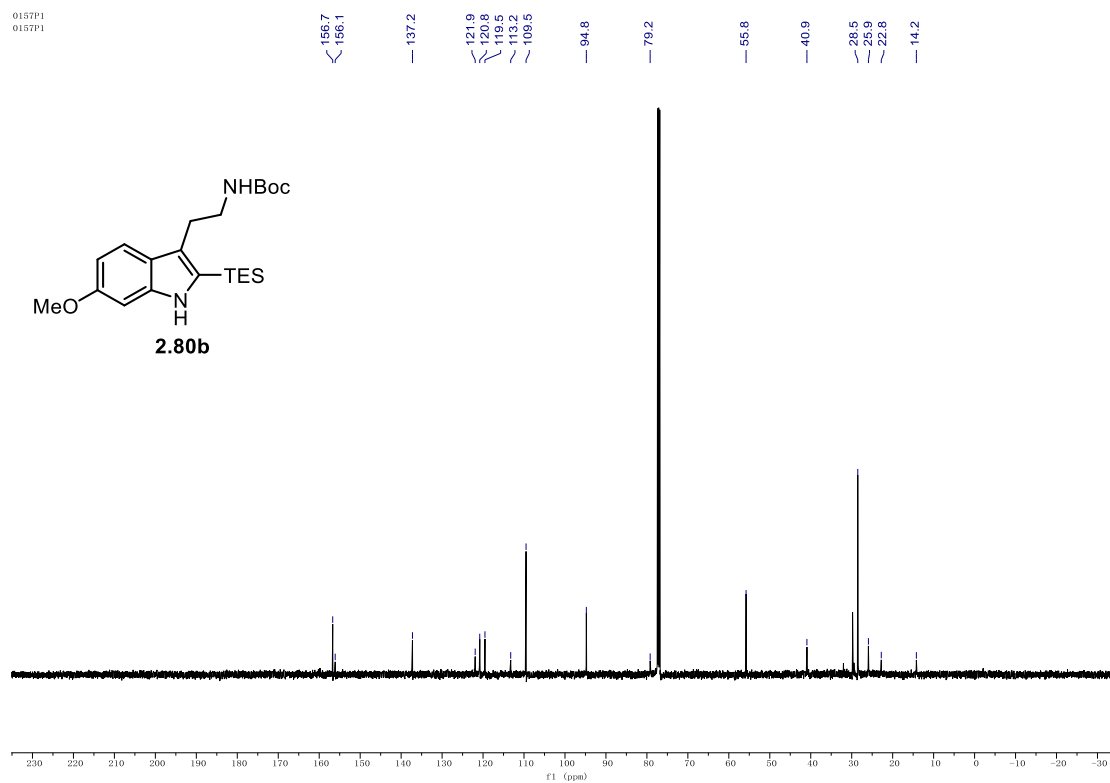
9.1. NMR Spectra

¹H NMR (500 MHz, CDCl₃) of **2.79b**.

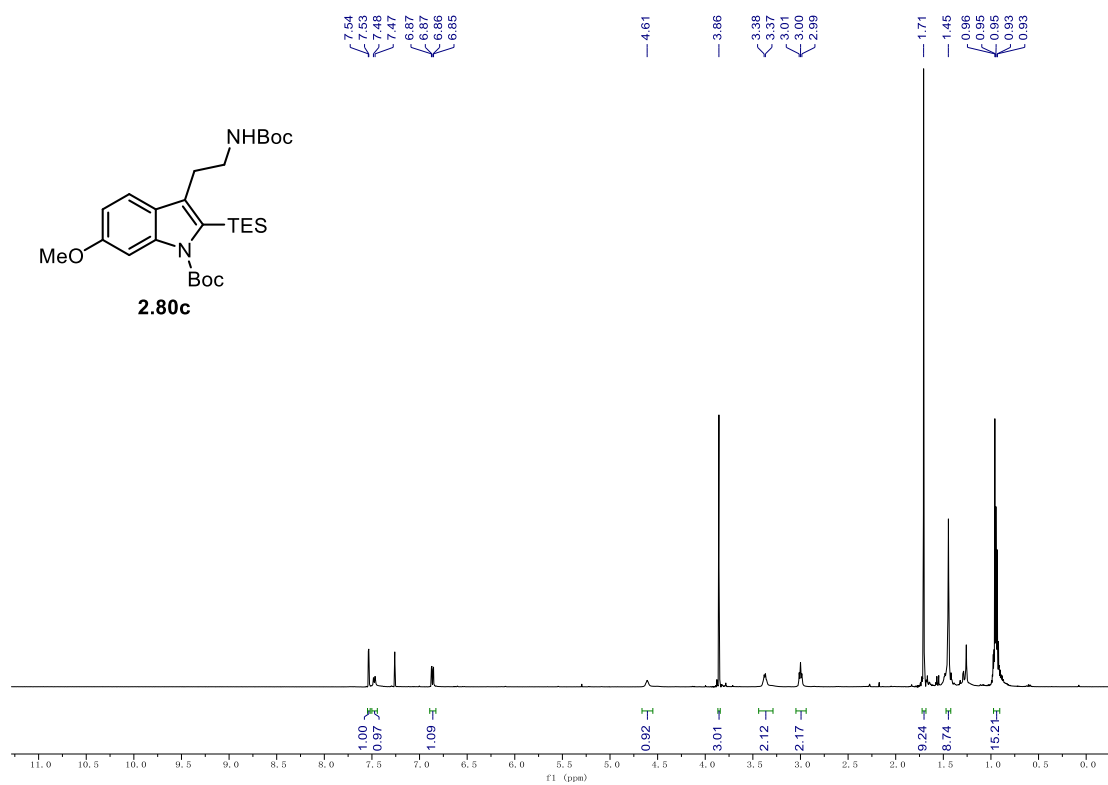
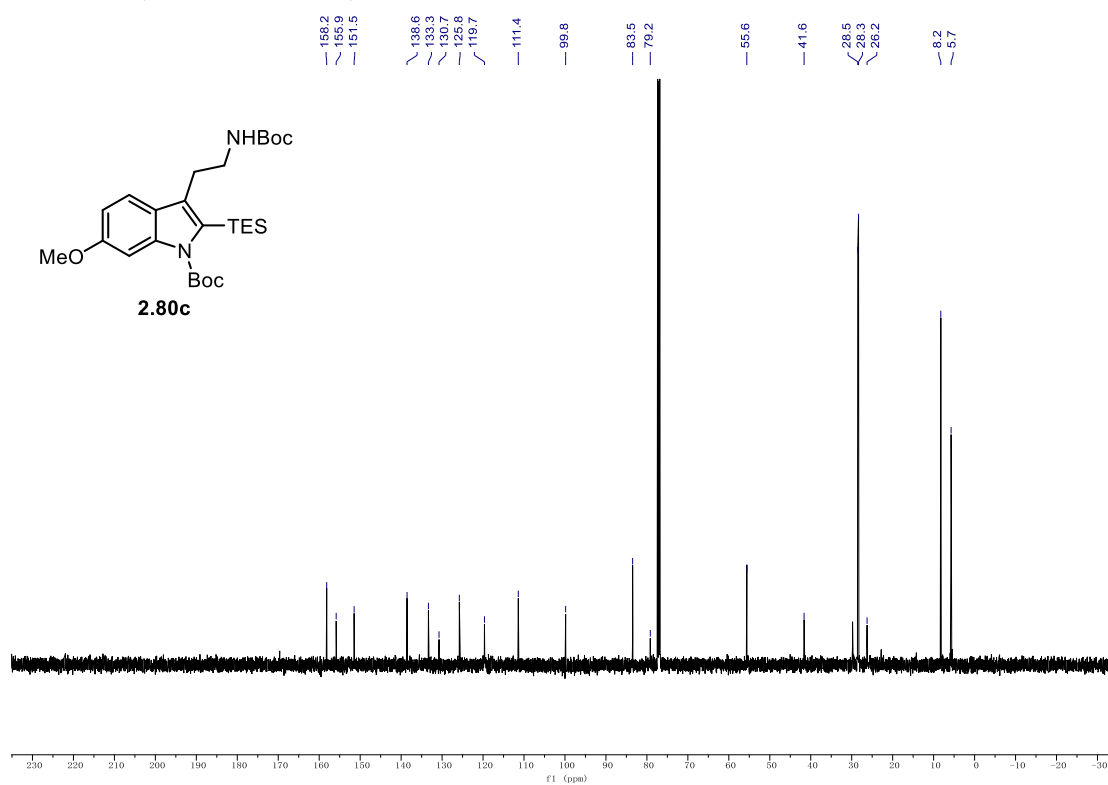


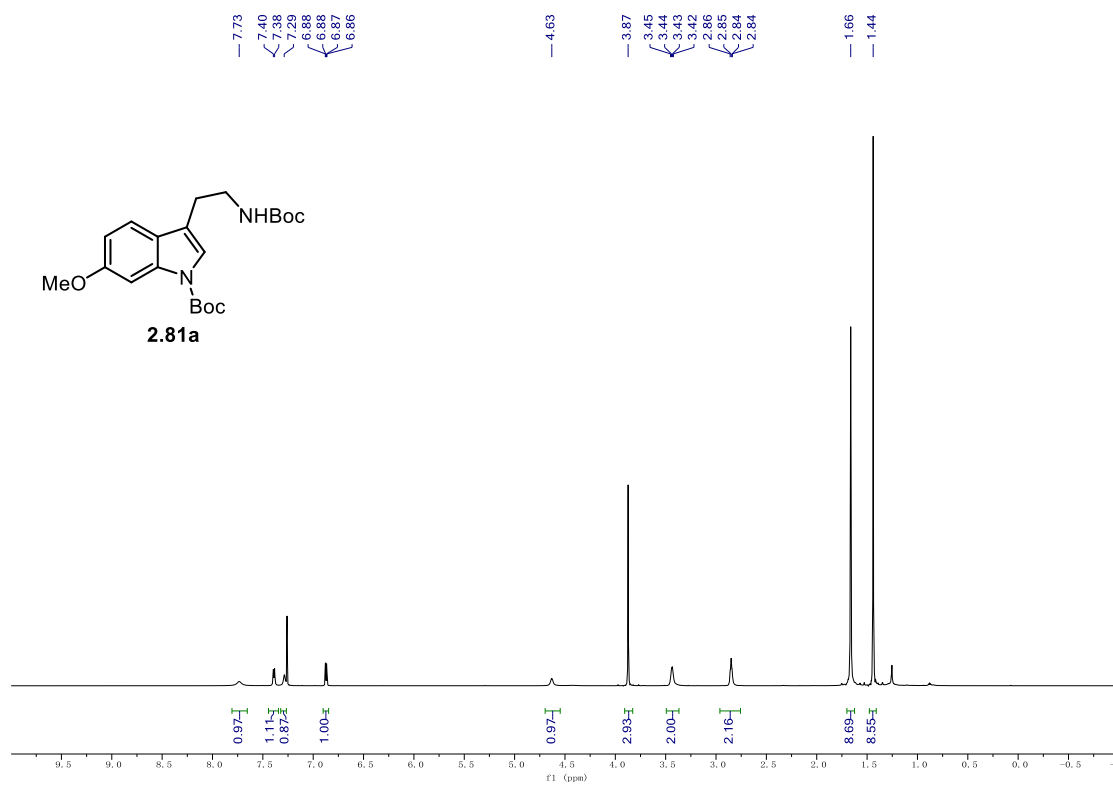
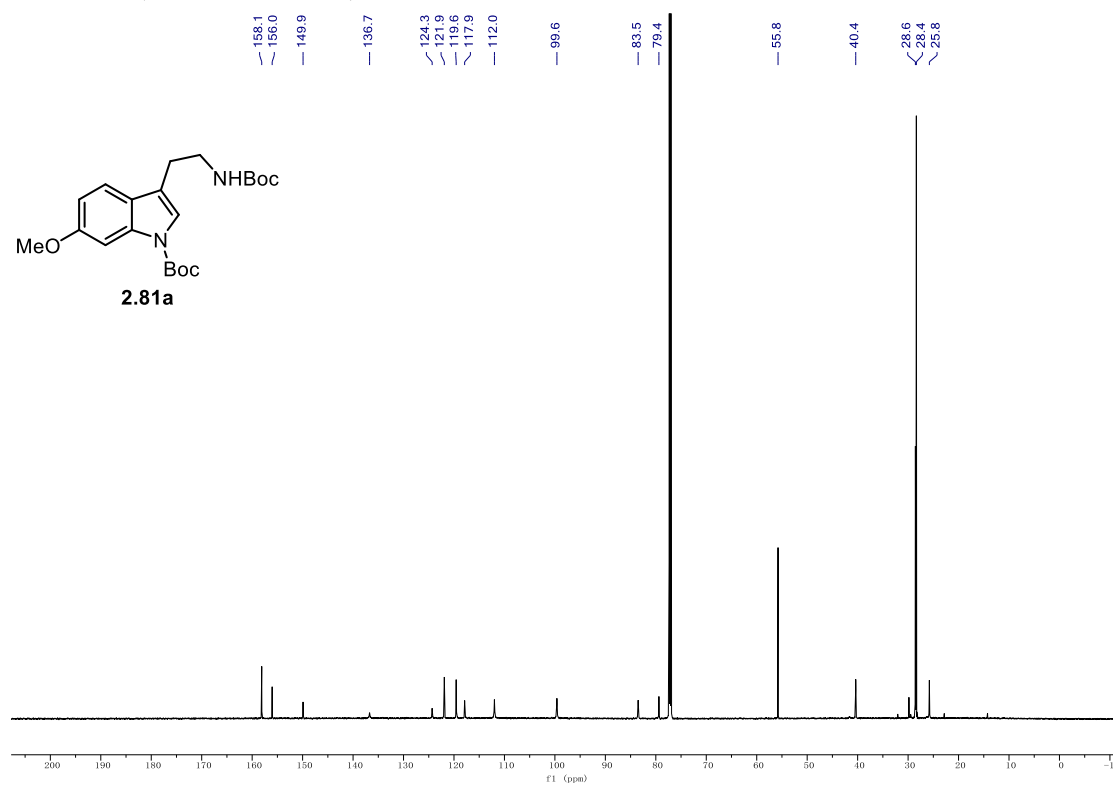
¹³C NMR (126 MHz, CDCl₃) of **2.79b**.



¹H NMR (500 MHz, CDCl₃) of 2.80b.**¹³C NMR (126 MHz, CDCl₃) of 2.80b.**

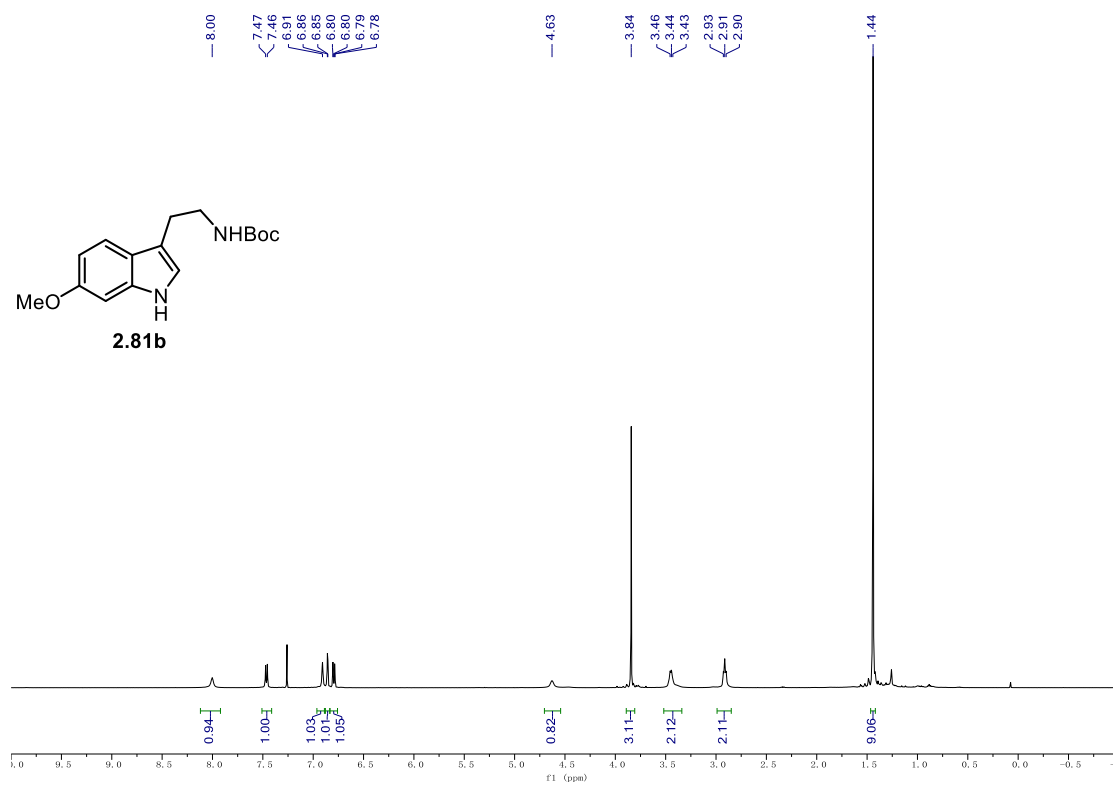
9.1. NMR Spectra

 ^1H NMR (500 MHz, CDCl_3) of **2.80c**. ^{13}C NMR (126 MHz, CDCl_3) of **2.80c**.

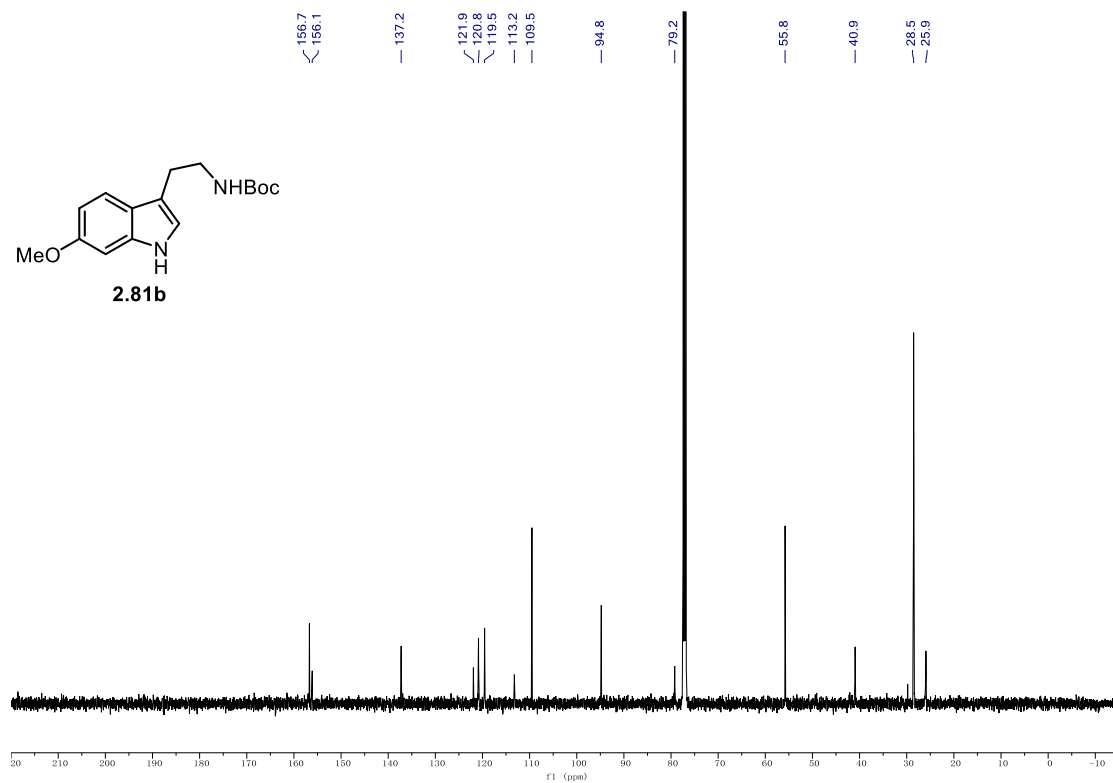
¹H NMR (500 MHz, CDCl₃) of 2.81a.**¹³C NMR (126 MHz, CDCl₃) of 2.81a.**

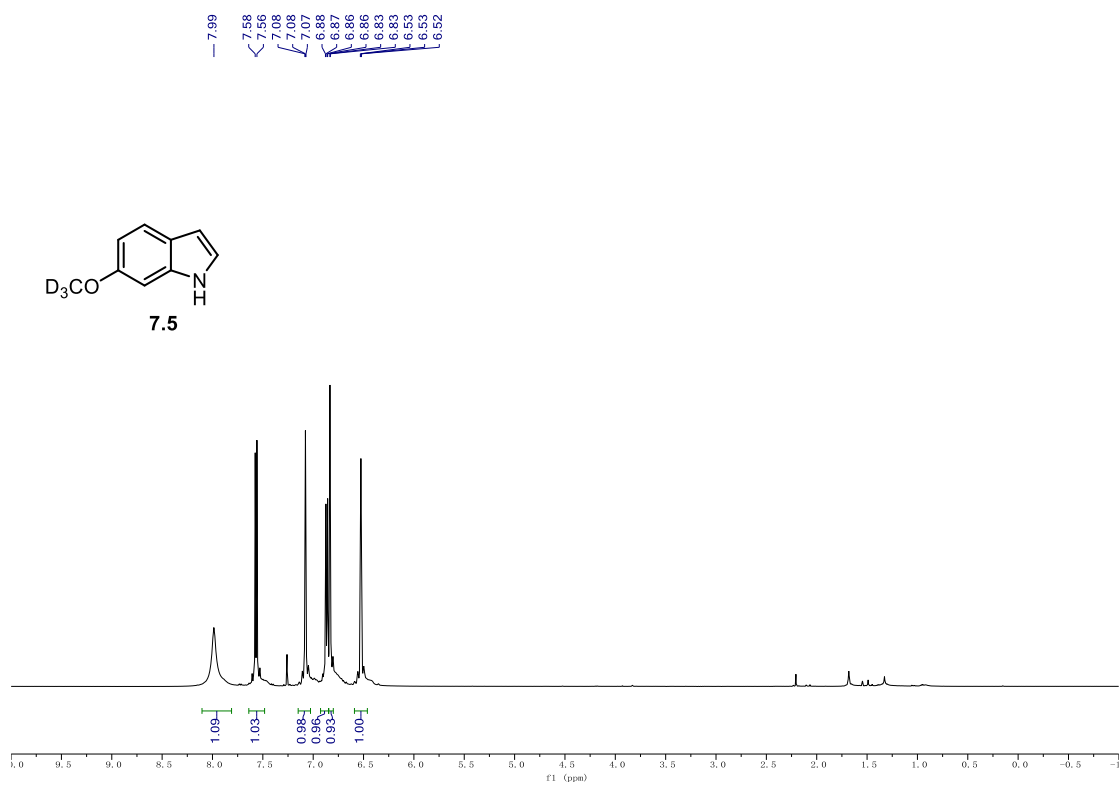
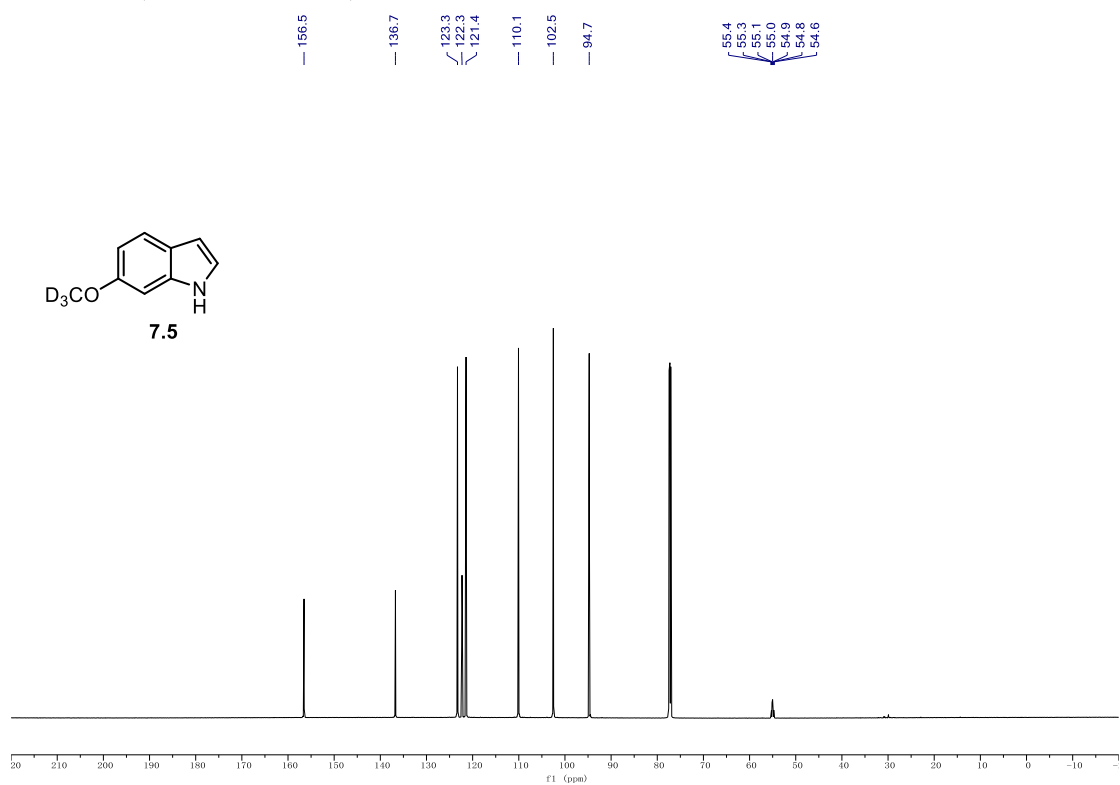
9.1. NMR Spectra

^1H NMR (500 MHz, CDCl_3) of **2.81b**.



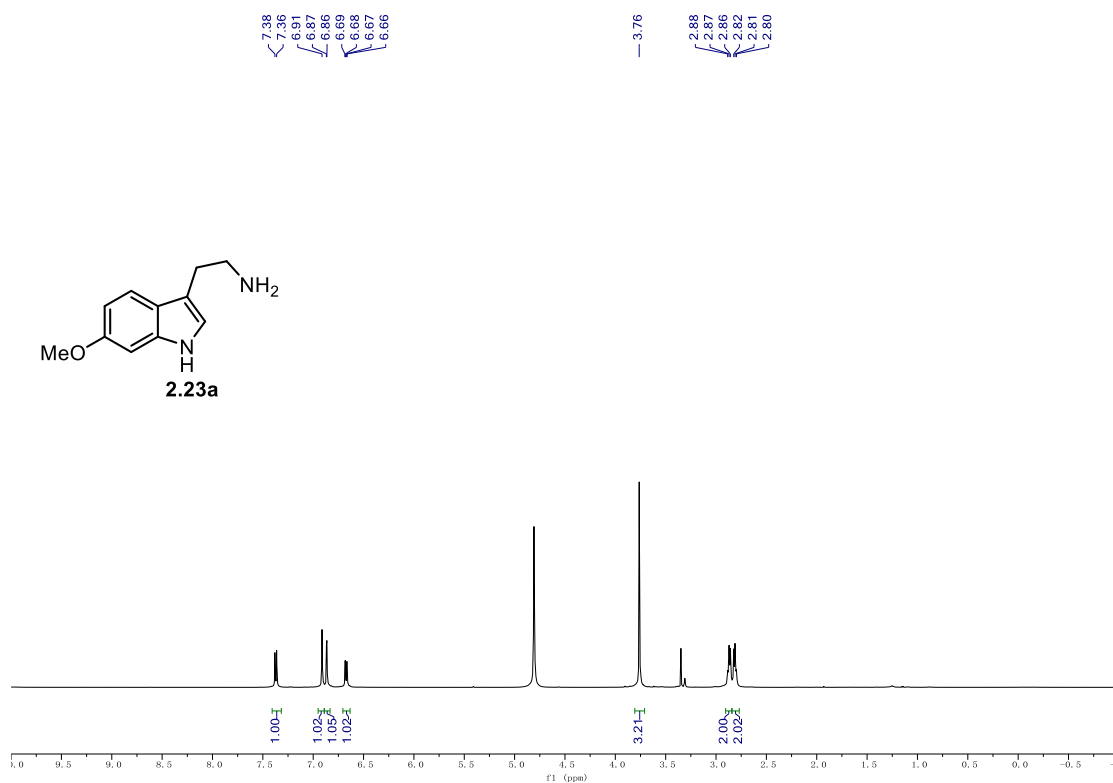
^{13}C NMR (126 MHz, CDCl_3) of **2.81b**.



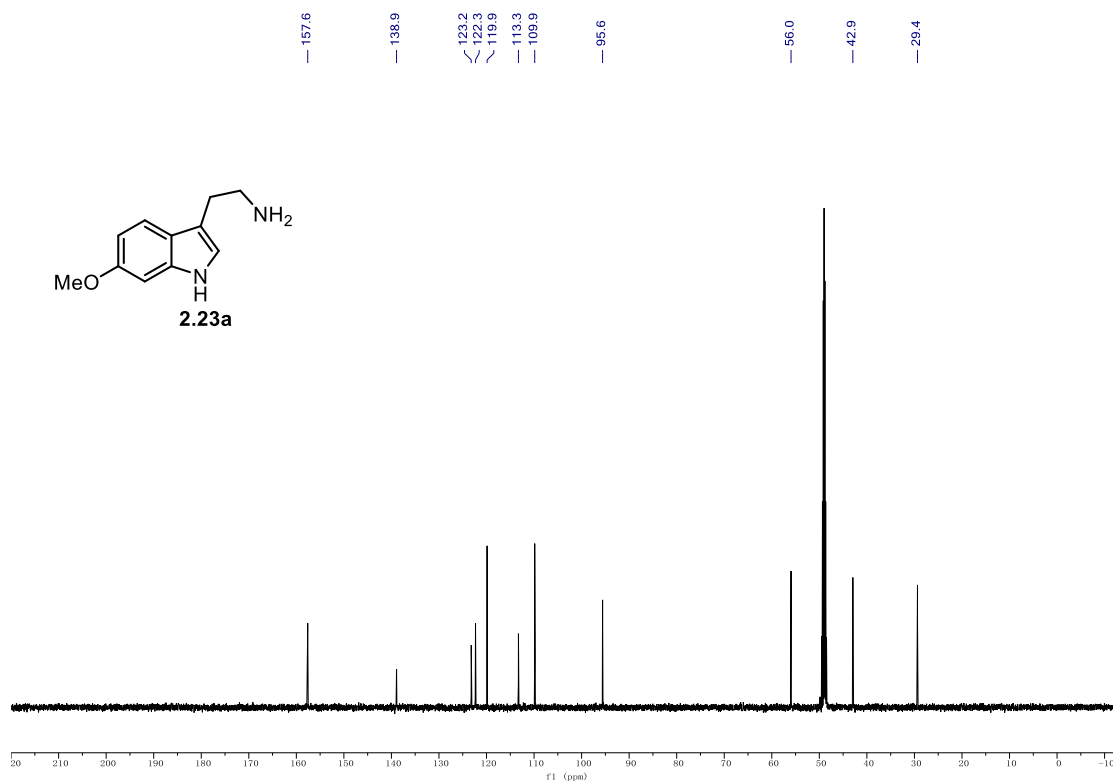
¹H NMR (500 MHz, CDCl₃) of 7.5.**¹³C NMR (176 MHz, CDCl₃) of 7.5.**

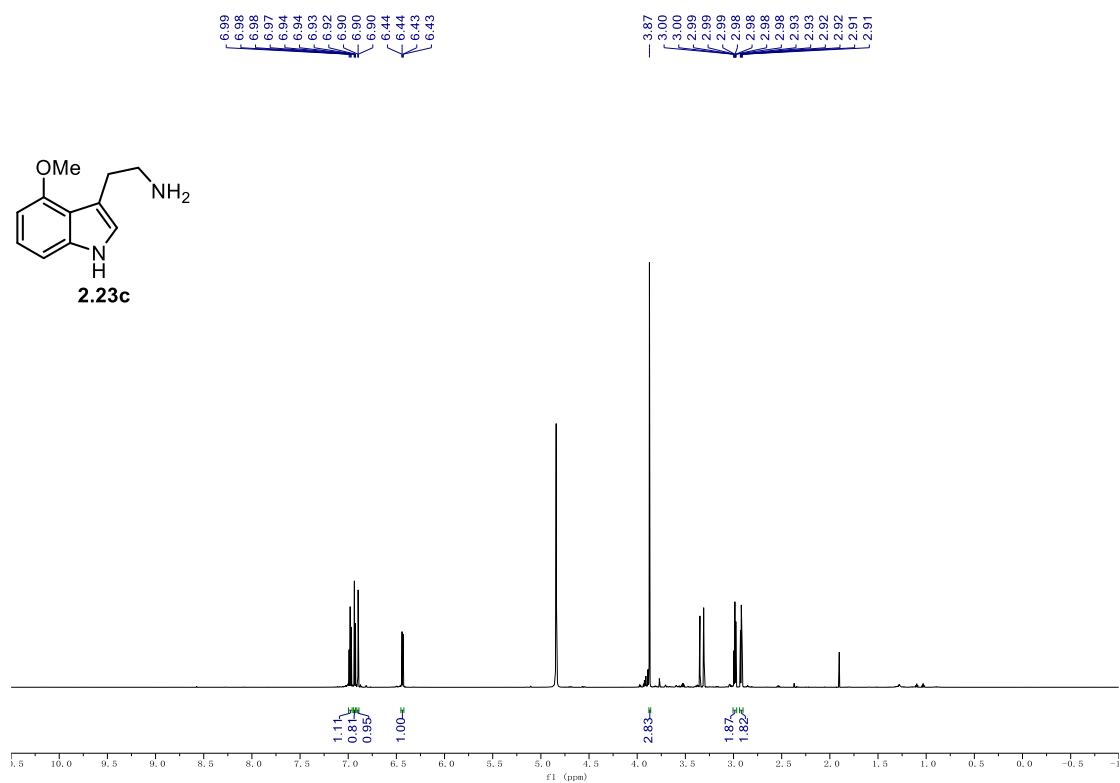
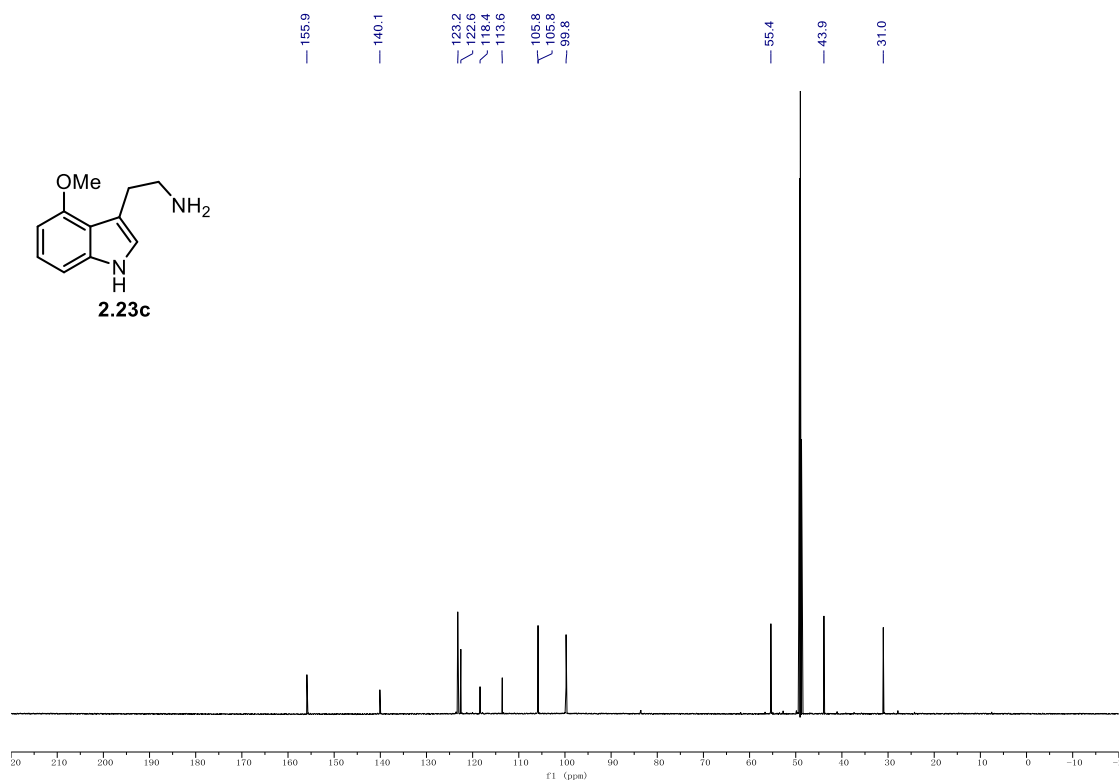
9.1. NMR Spectra

¹H NMR (500 MHz, CD₃OD) of **2.23a**.



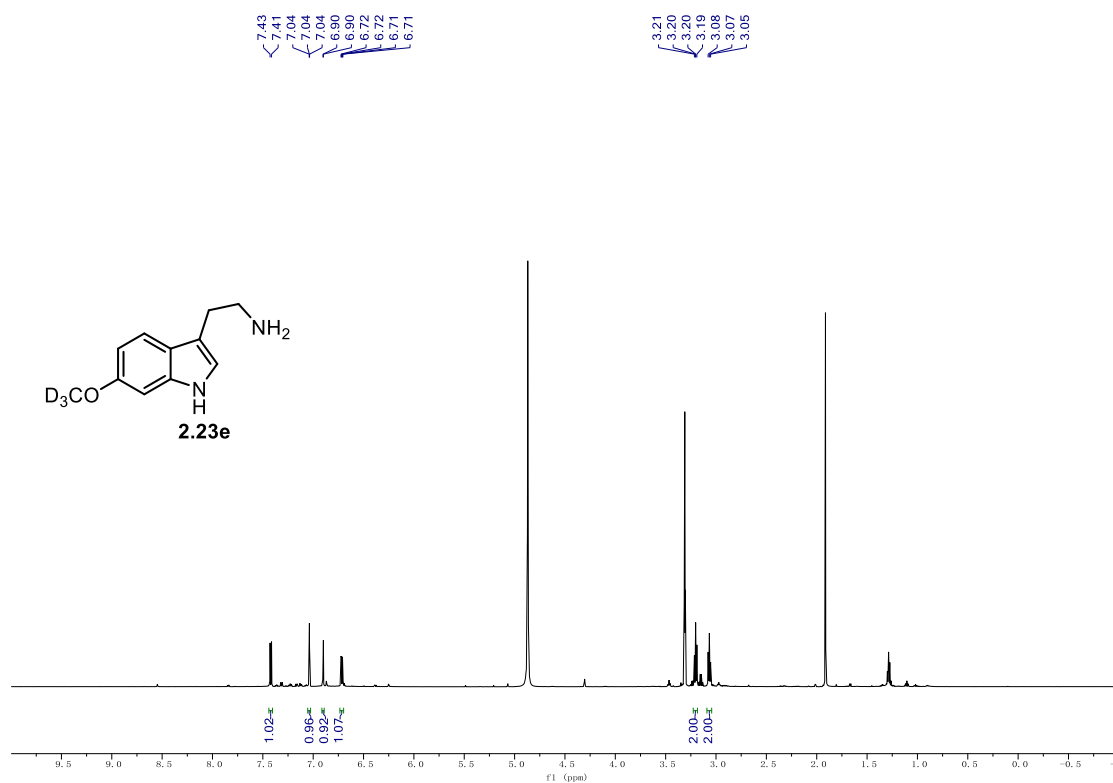
¹³C NMR (126 MHz, CD₃OD) of **2.23a**.



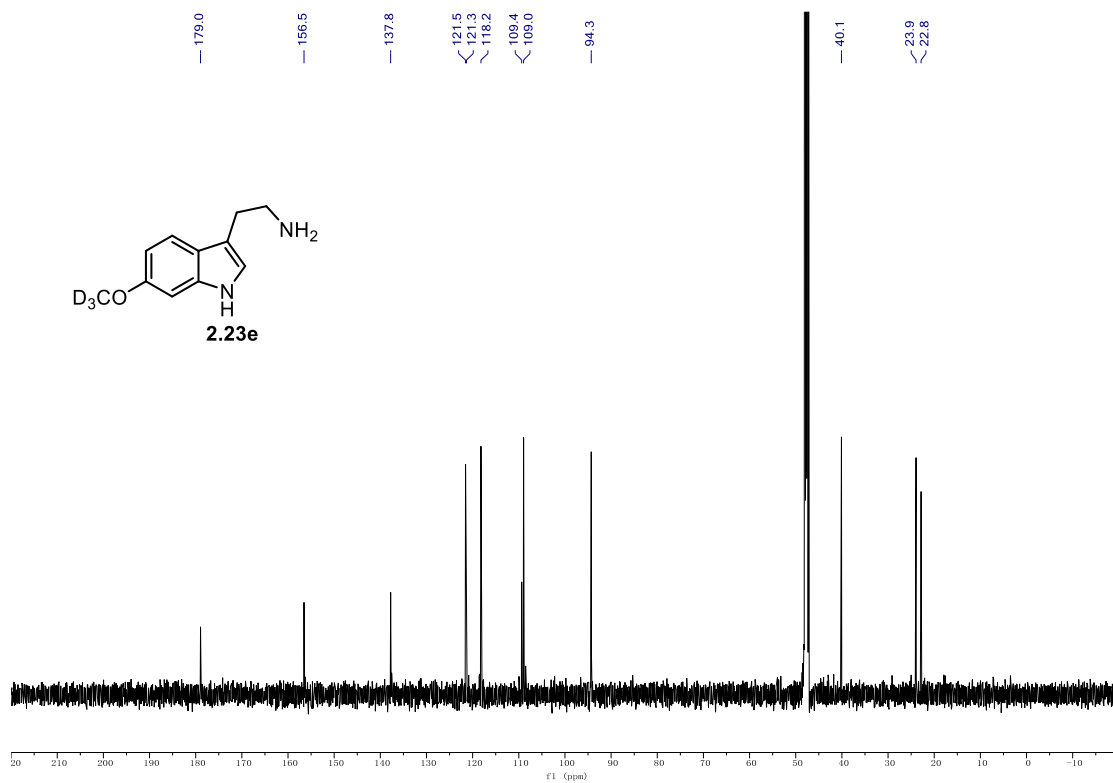
¹H NMR (700 MHz, CD₃OD) of 2.23c.**¹³C NMR (176 MHz, CD₃OD) of 2.23c.**

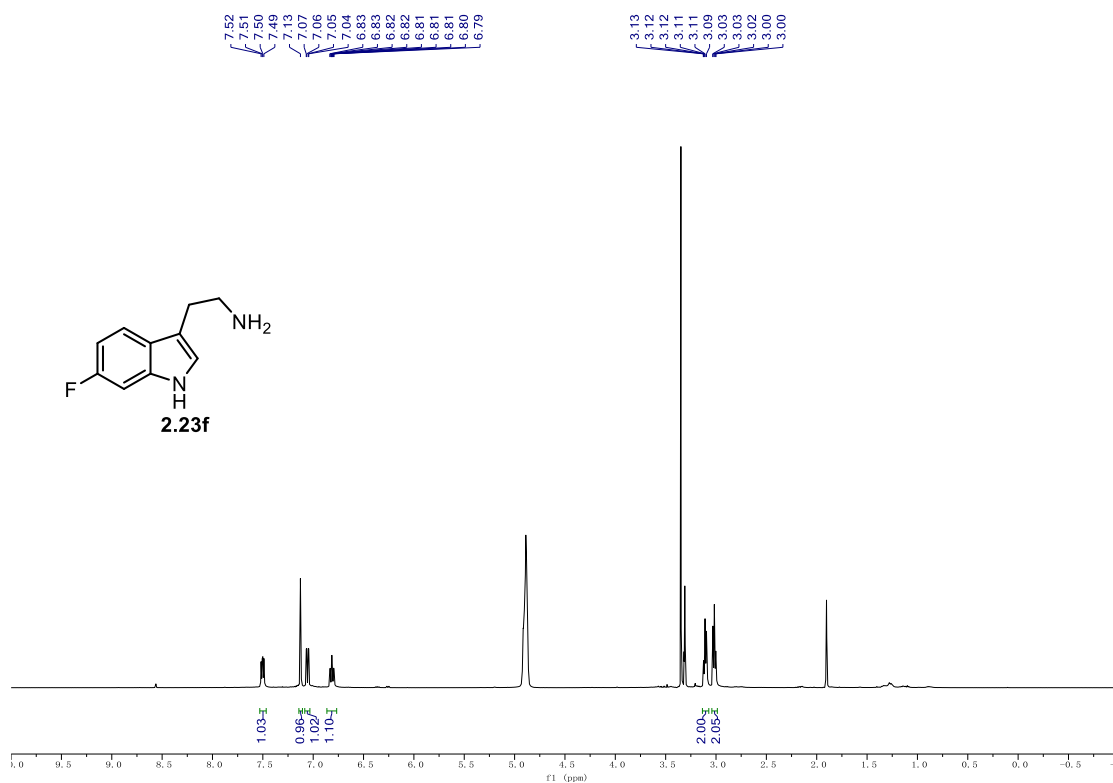
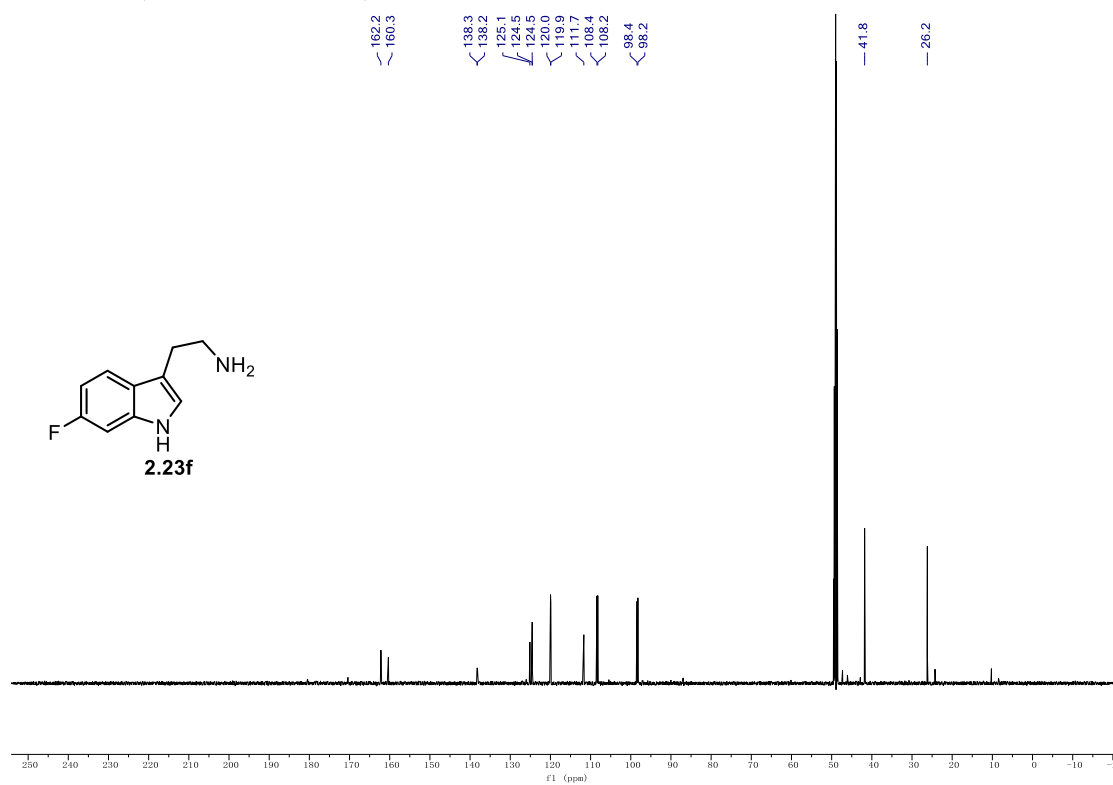
9.1. NMR Spectra

^1H NMR (500 MHz, CD_3OD) of **2.23e**.

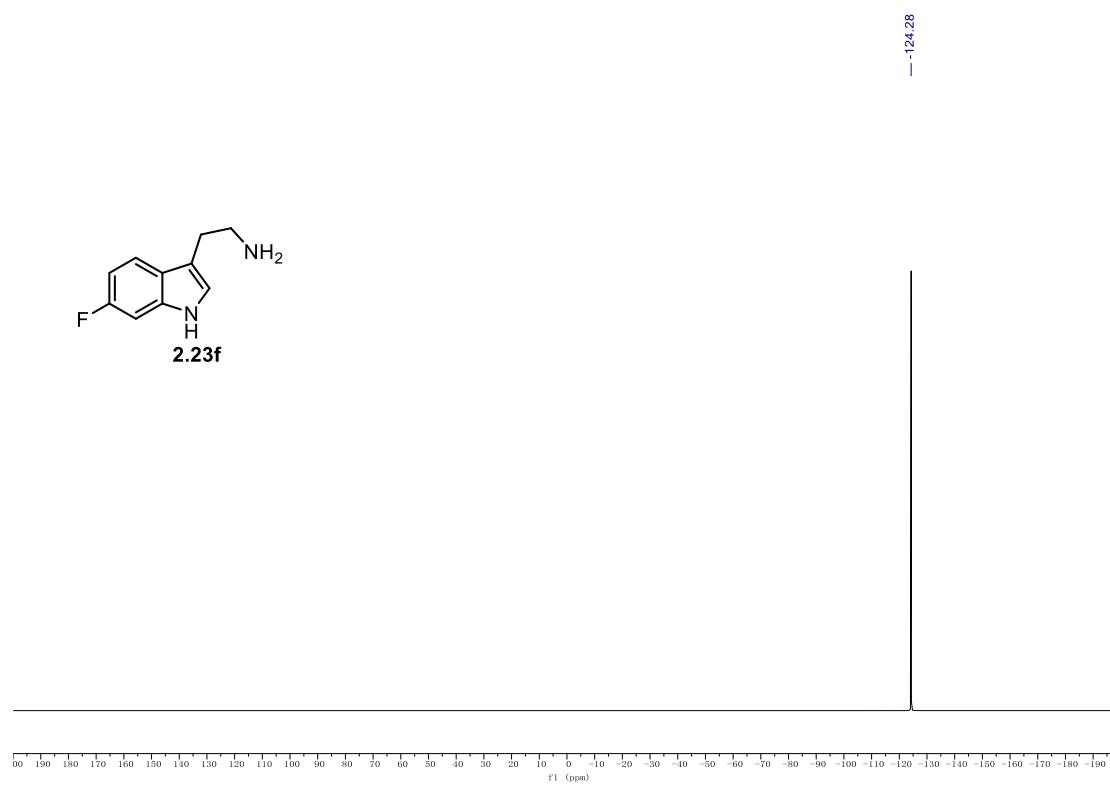


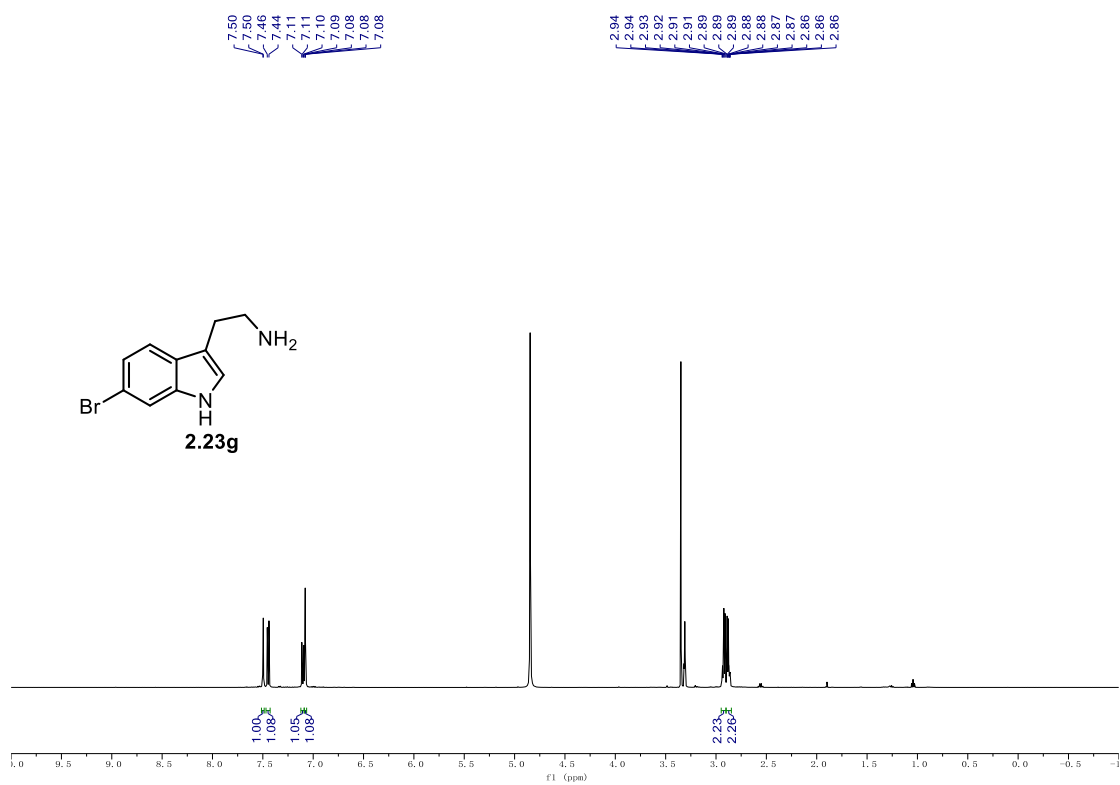
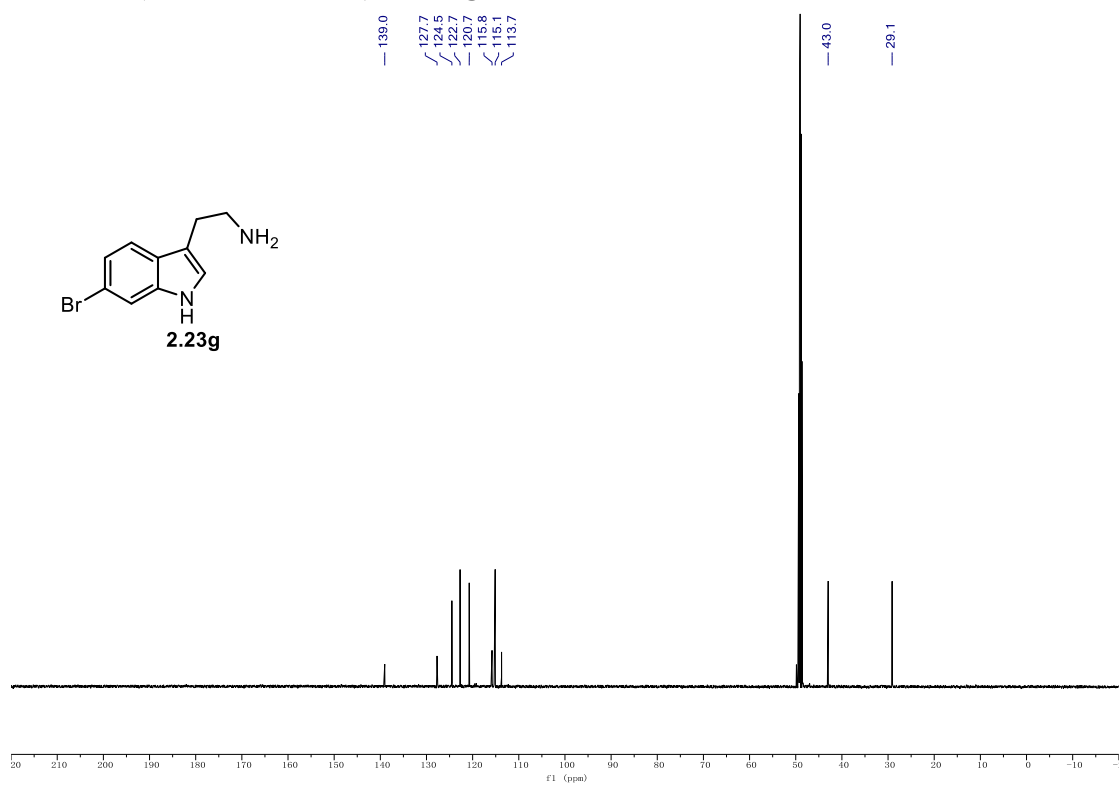
^{13}C NMR (126 MHz, CD_3OD) of **2.23e**.



^1H NMR (500 MHz, CD_3OD) of **2.23f**. ^{13}C NMR (126 MHz, CD_3OD) of **2.23f**.

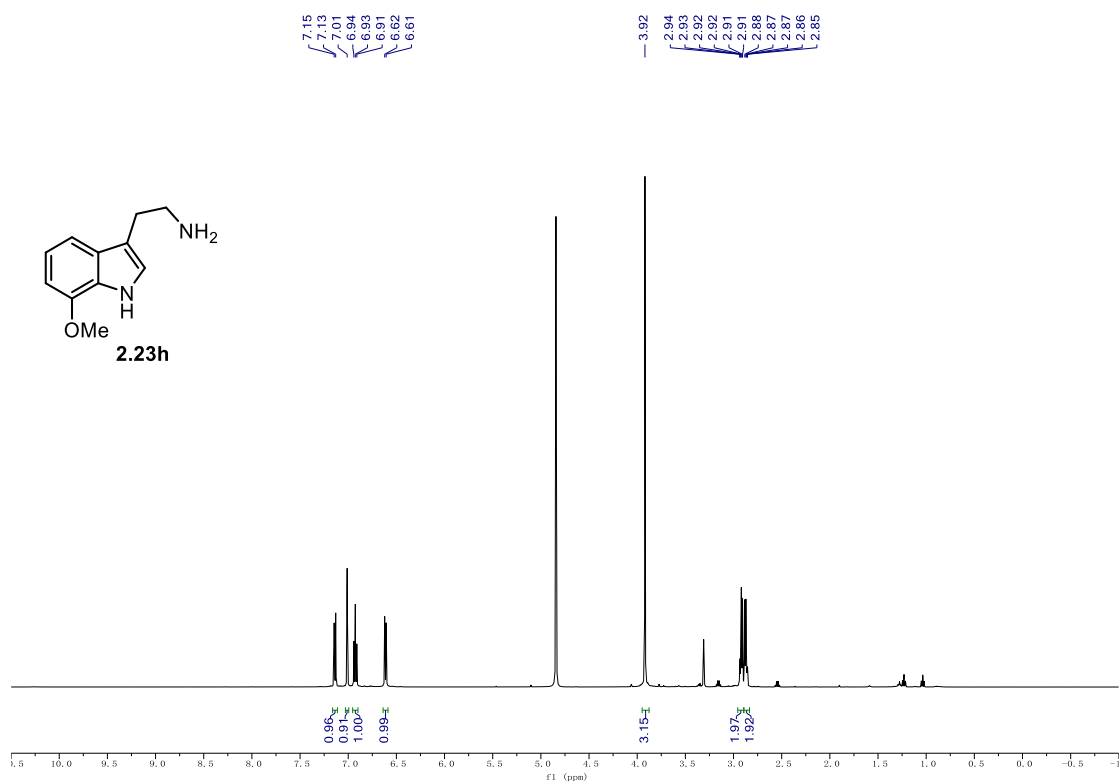
^{19}F NMR (471 MHz, CD_3OD) of 2.23f.



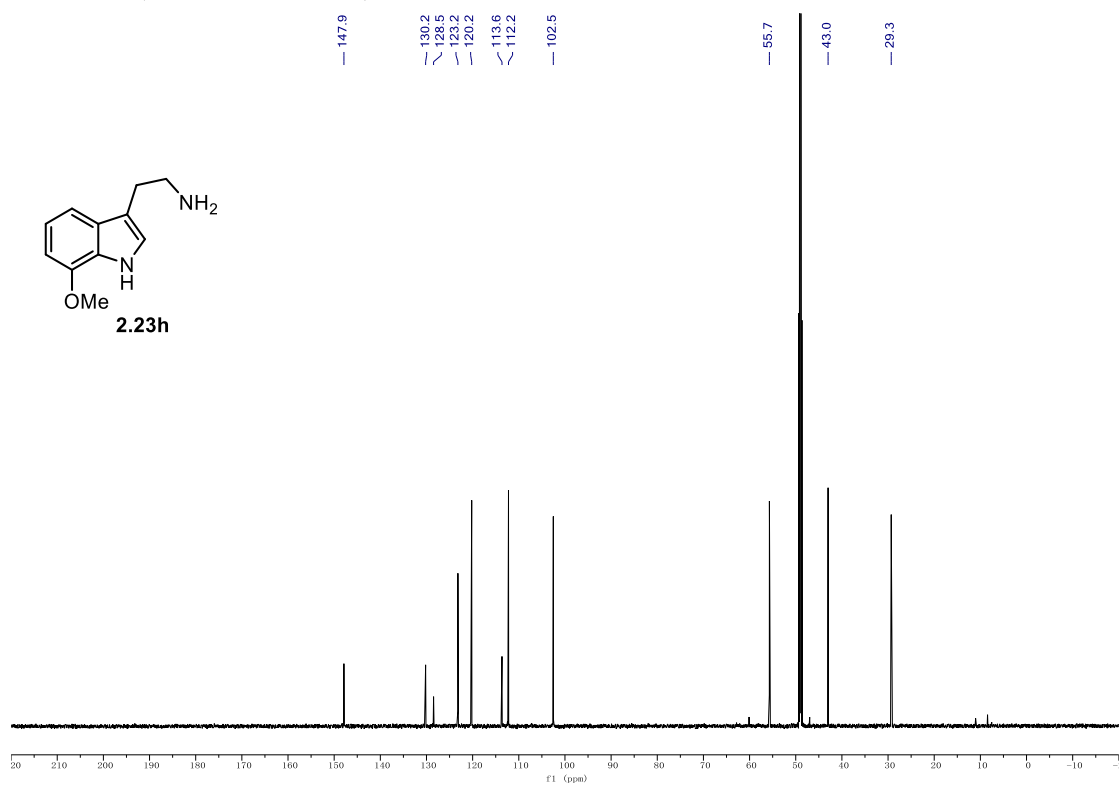
^1H NMR (500 MHz, CD_3OD) of **2.23g**. ^{13}C NMR (126 MHz, CD_3OD) of **2.23g**.

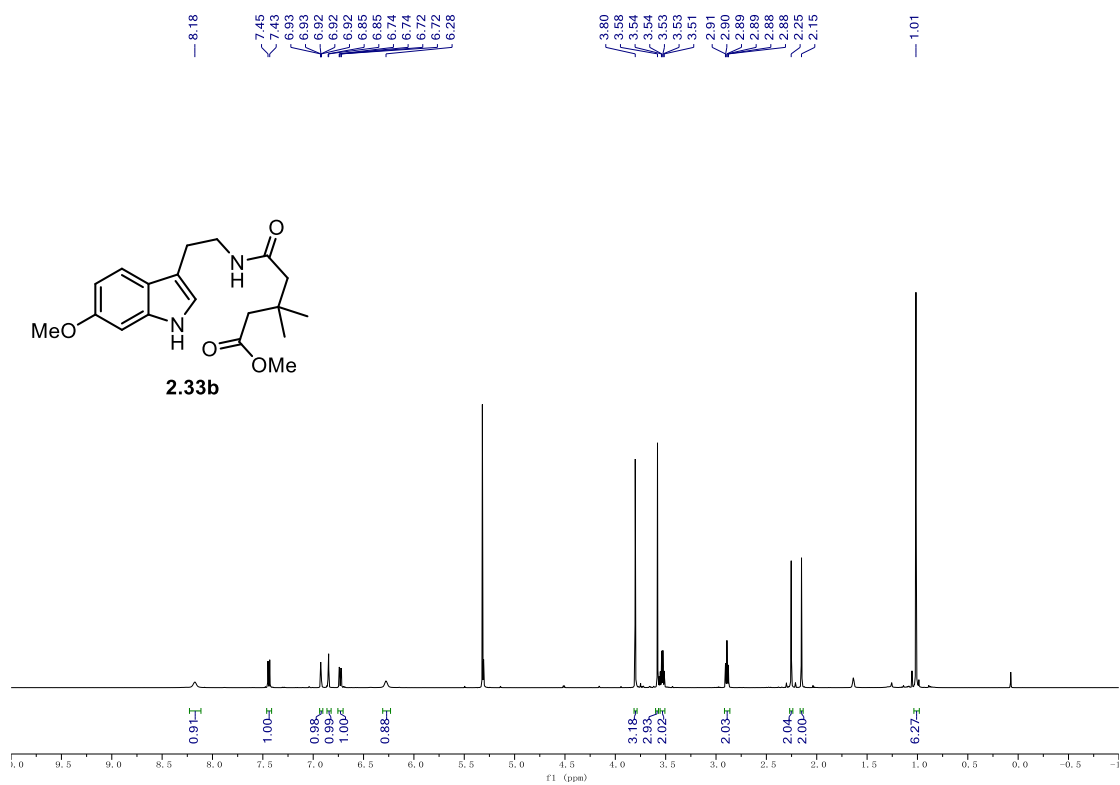
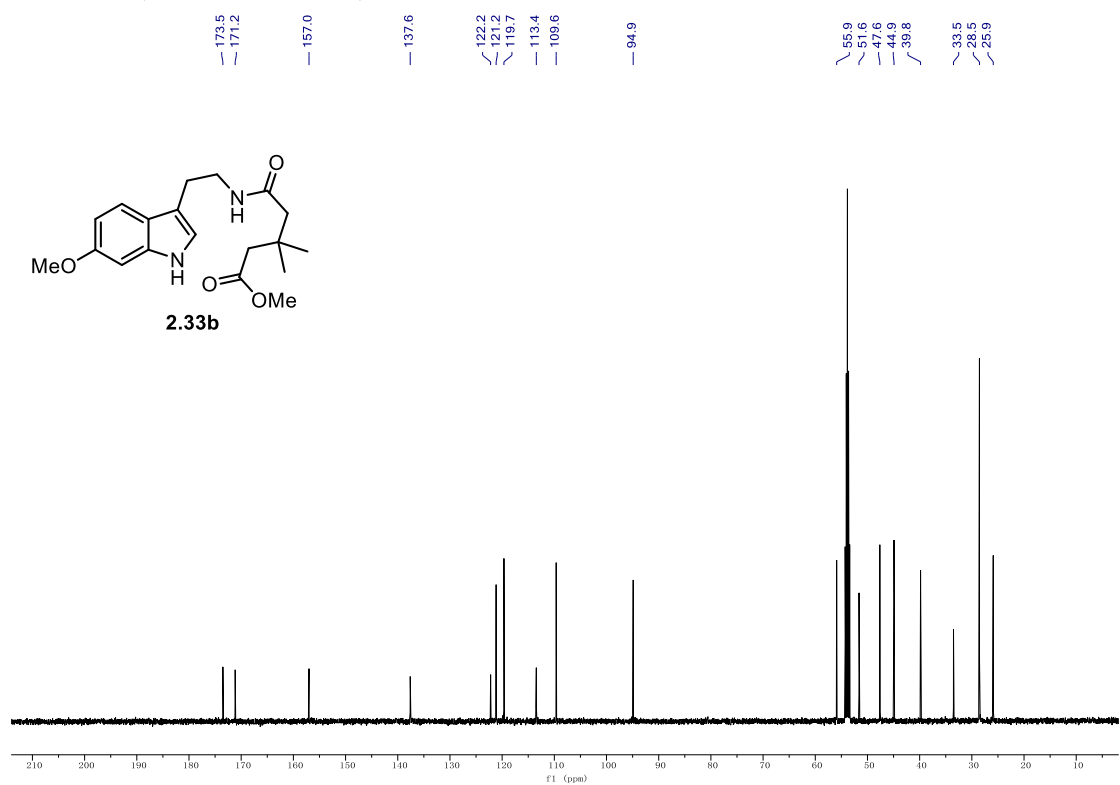
9.1. NMR Spectra

¹H NMR (500 MHz, CD₃OD) of **2.23h**.



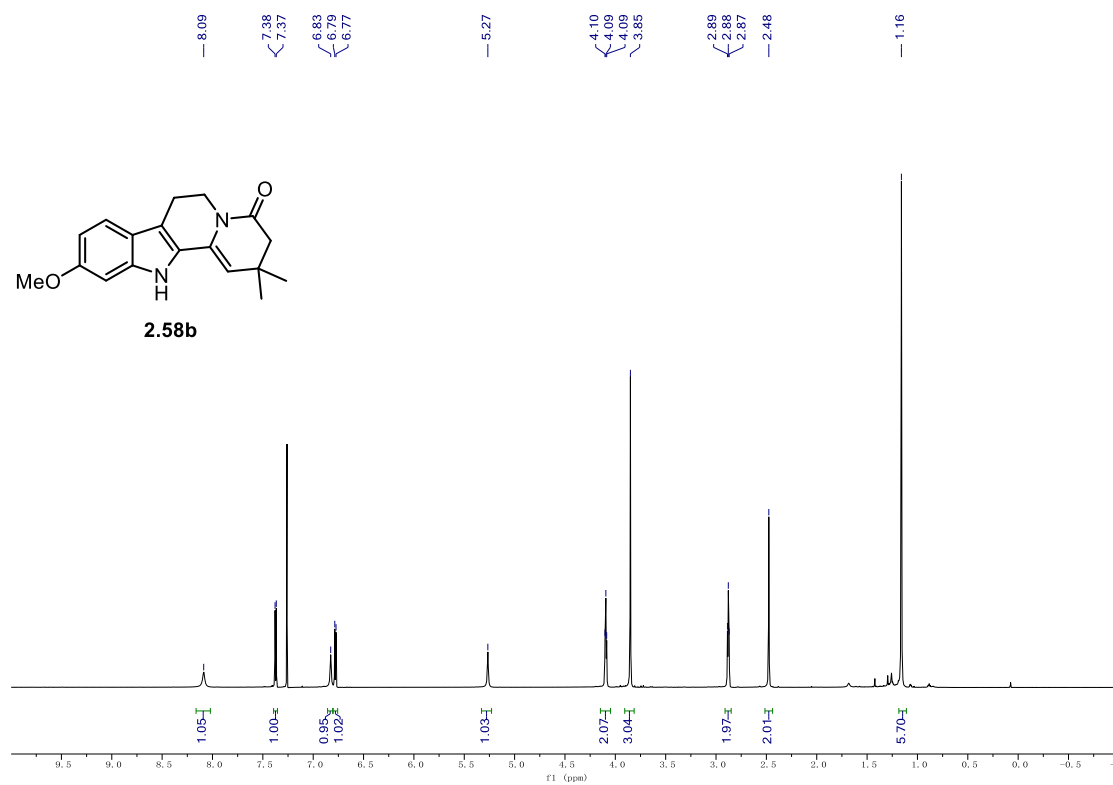
¹³C NMR (126 MHz, CD₃OD) of **2.23h**.



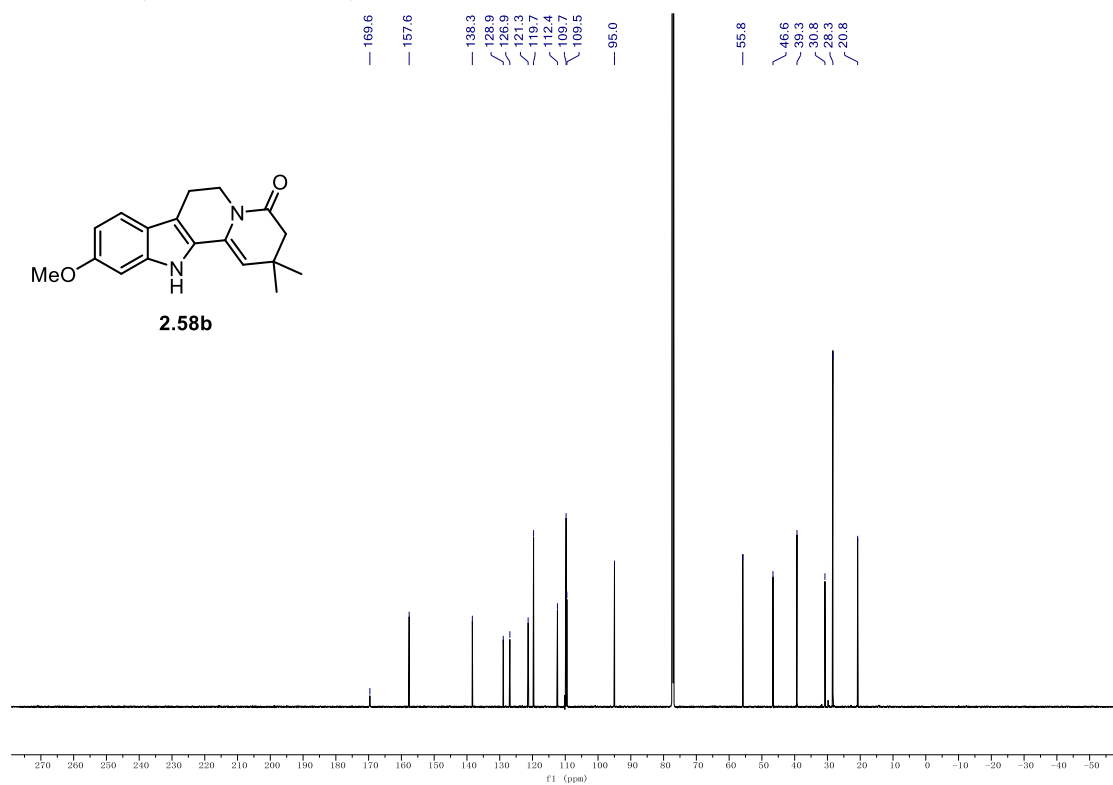
^1H NMR (500 MHz, CD_2Cl_2) of **2.33b**. ^{13}C NMR (126 MHz, CD_2Cl_2) of **2.33b**.

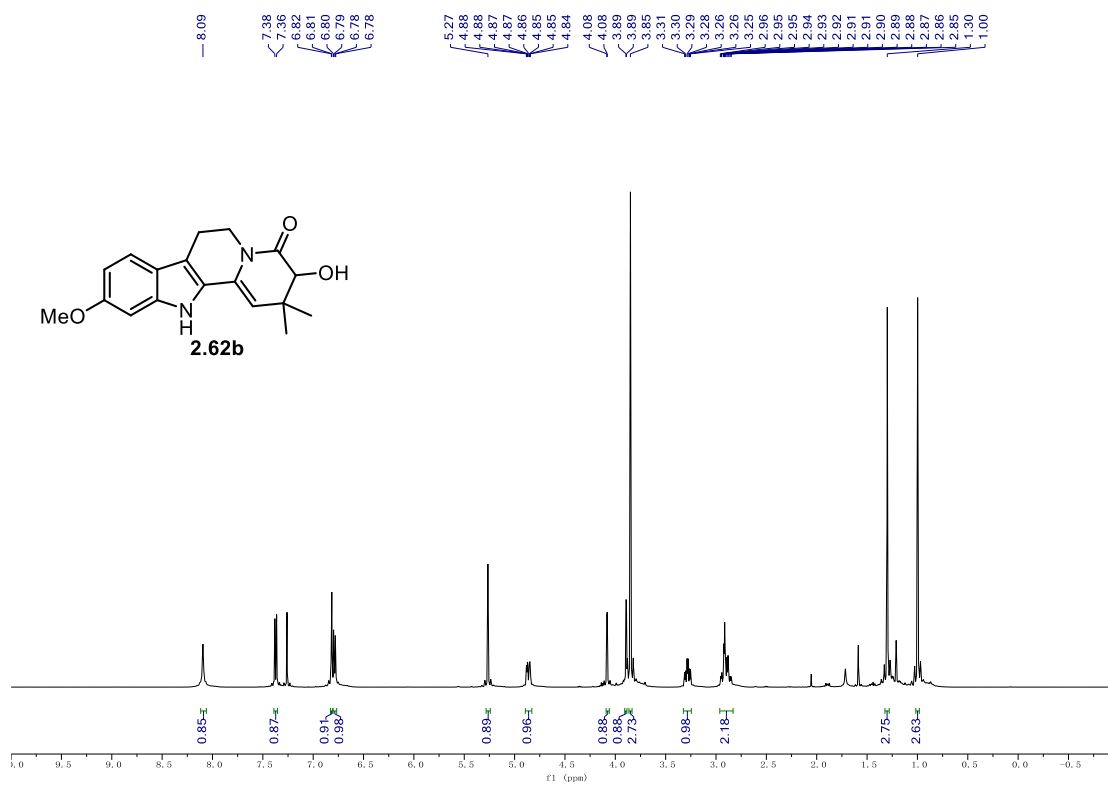
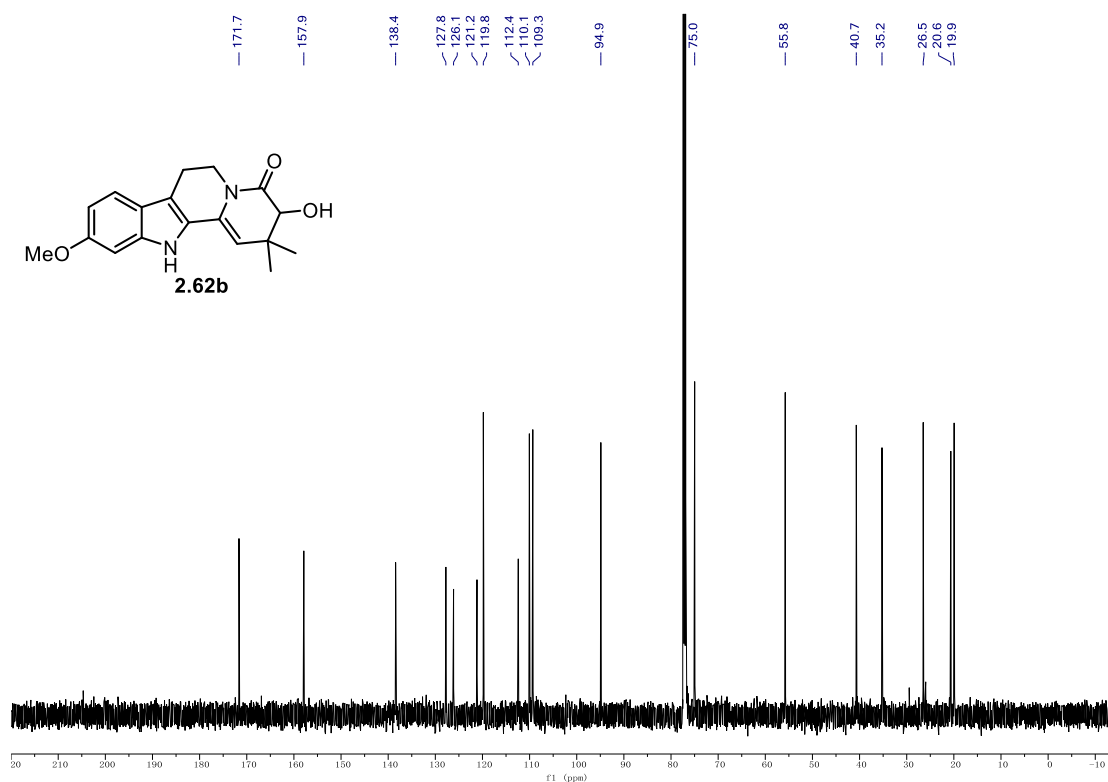
9.1. NMR Spectra

^1H NMR (700 MHz, CDCl_3) of **2.58b**.



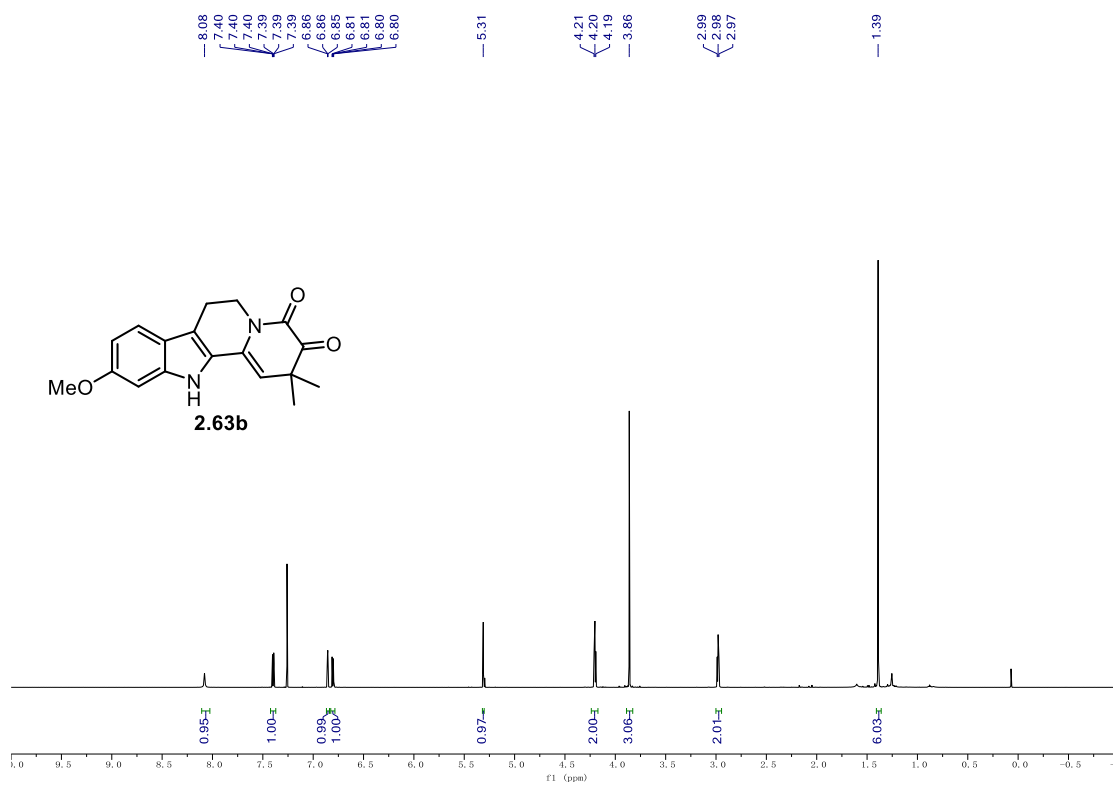
^{13}C NMR (176 MHz, CDCl_3) of **2.58b**.



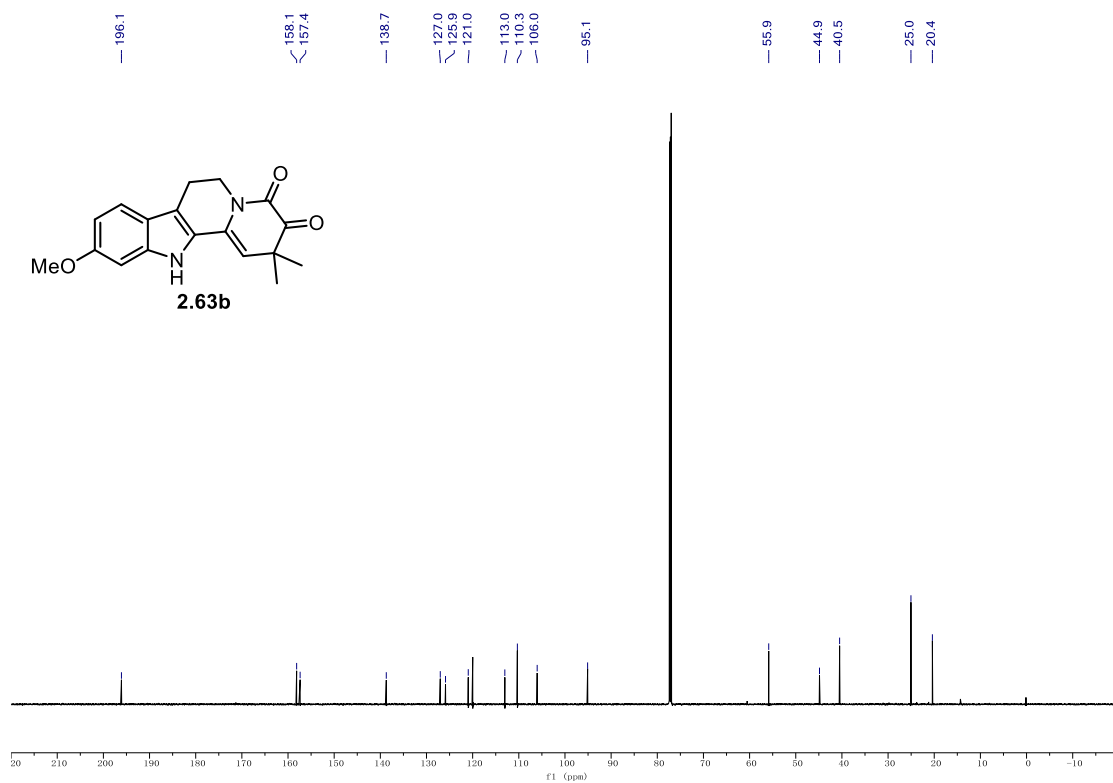
¹H NMR (500 MHz, CDCl₃) of 2.62b.**¹³C NMR (126 MHz, CDCl₃) of 2.62b.**

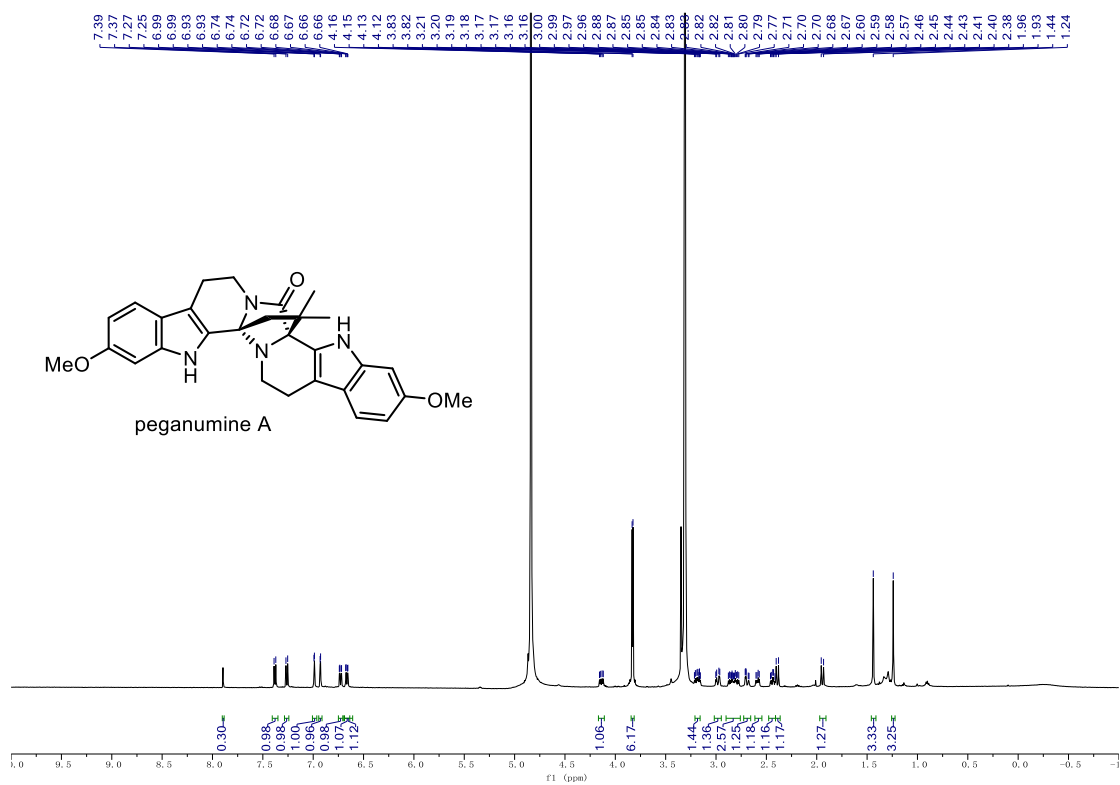
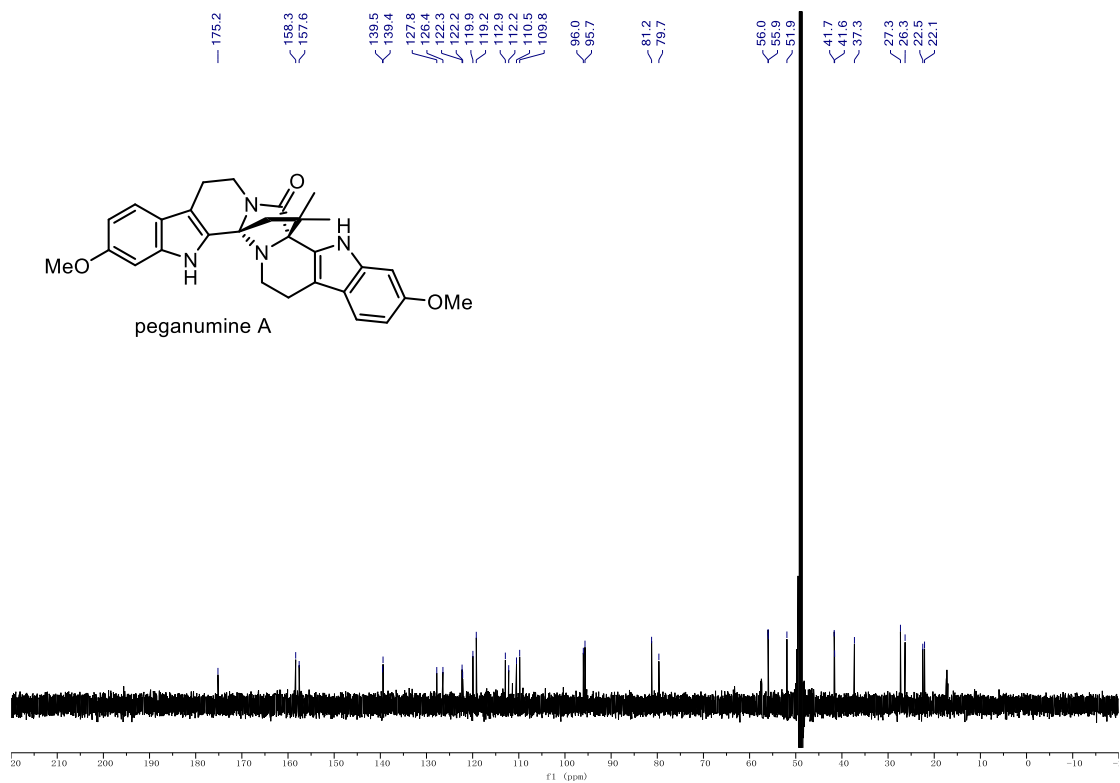
9.1. NMR Spectra

^1H NMR (700 MHz, CDCl_3) of **2.63b**.



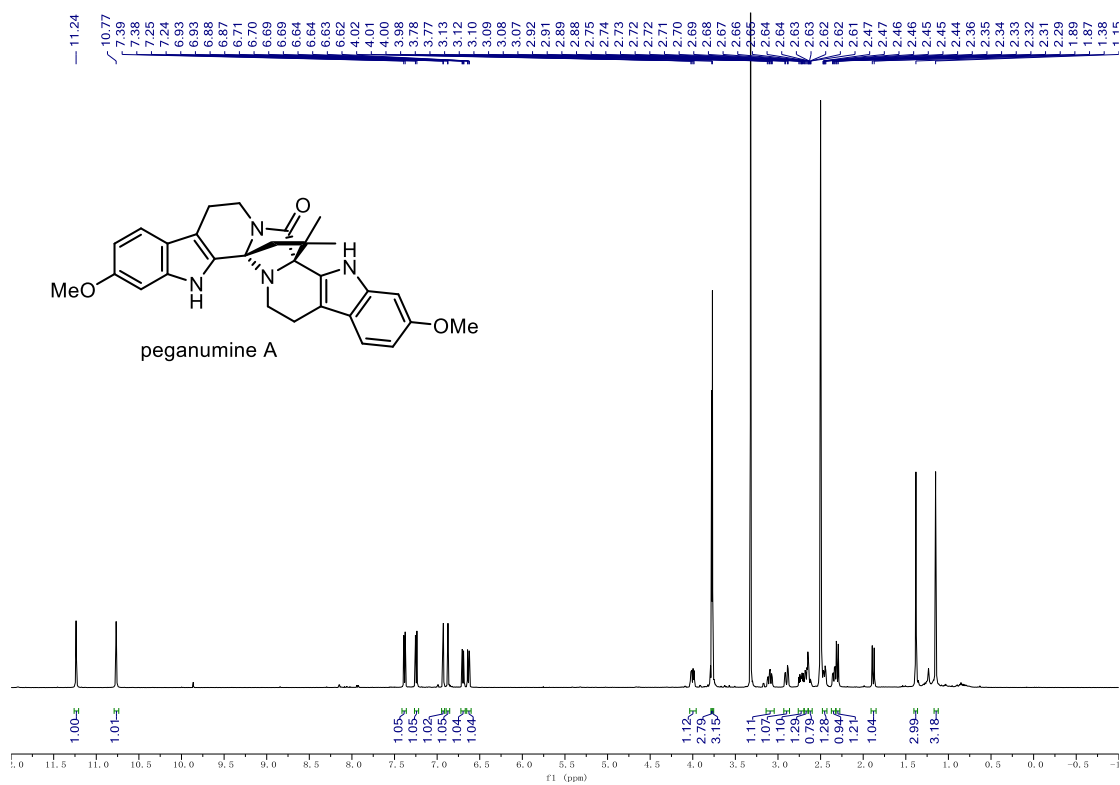
^{13}C NMR (176 MHz, CDCl_3) of **2.63b**.



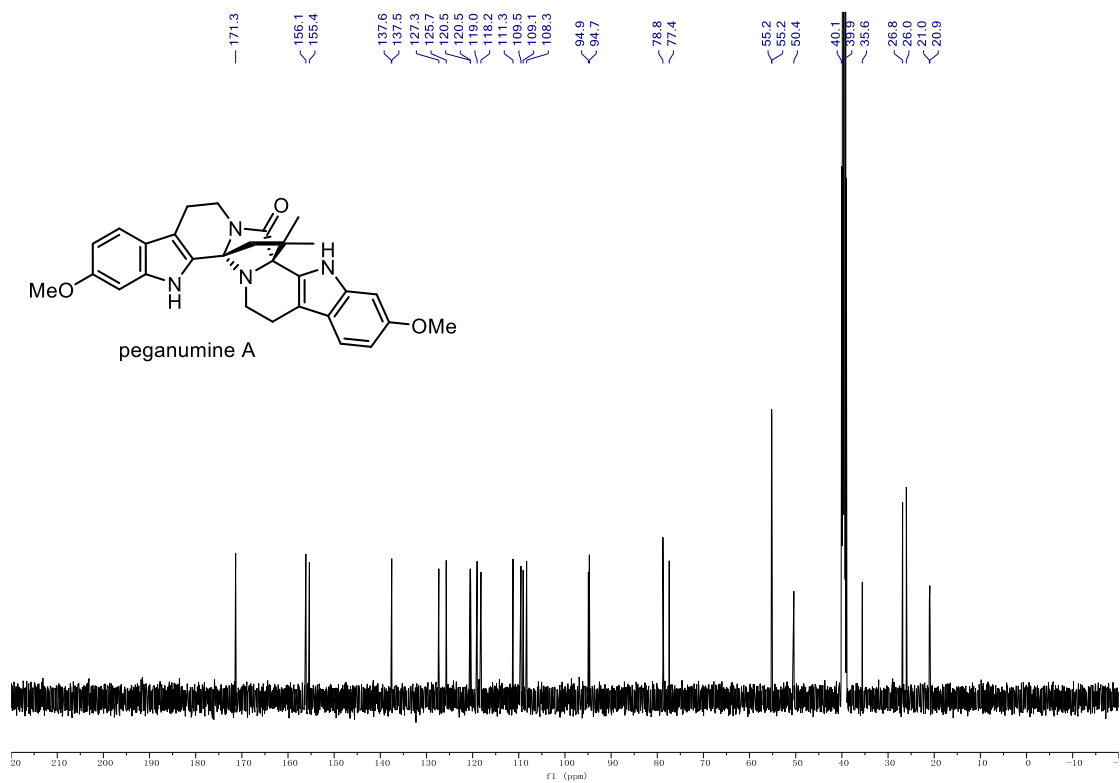
¹H NMR (700 MHz, CD₃OD) of peganumine A.**¹³C NMR (176 MHz, CD₃OD) of peganumine A.**

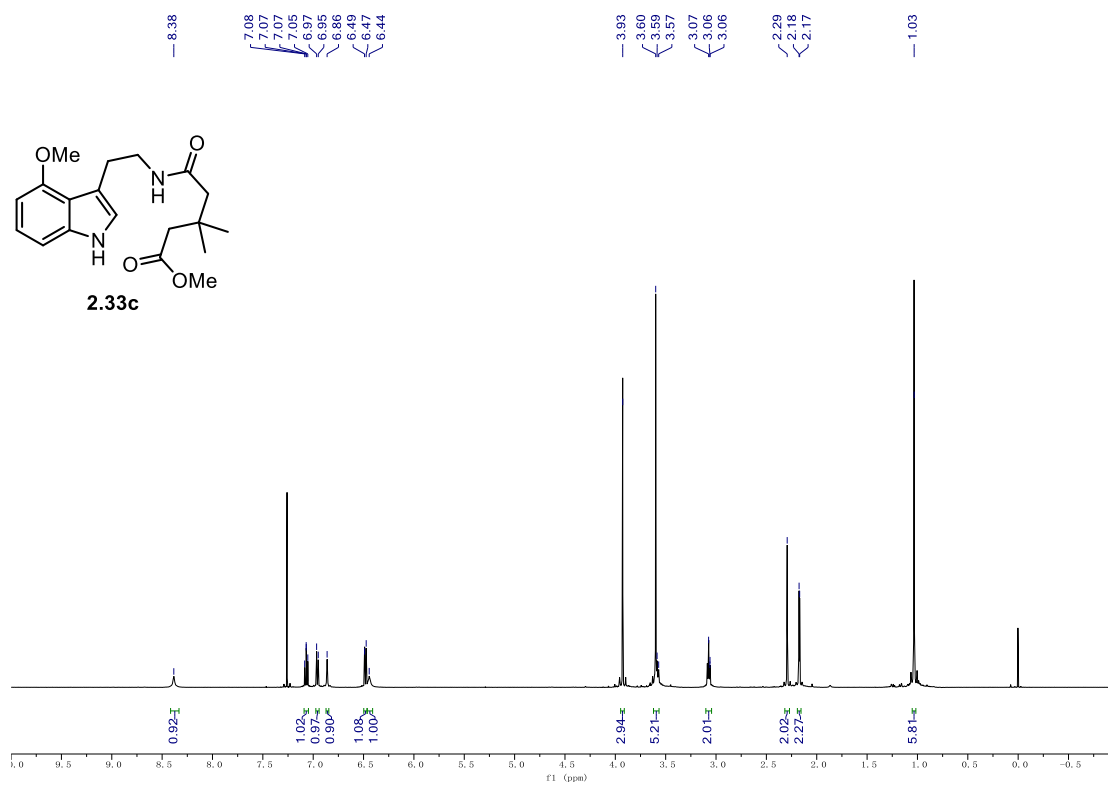
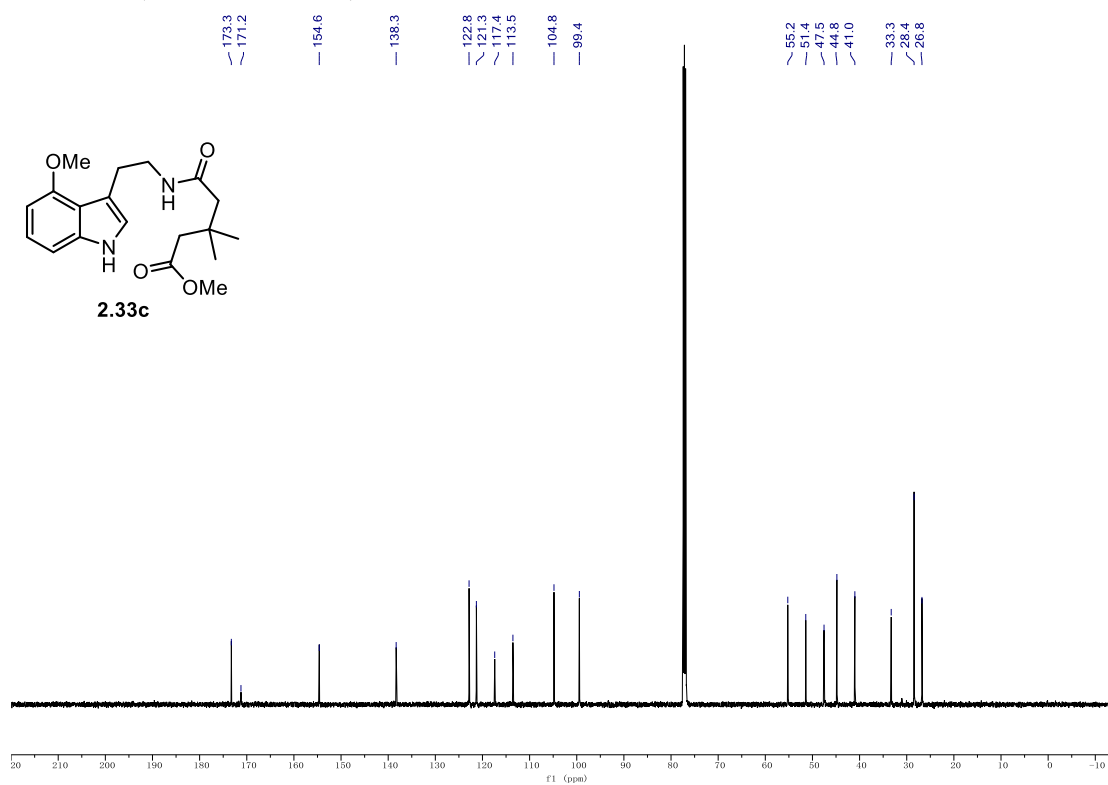
9.1. NMR Spectra

^1H NMR (500 MHz, d_6 -DMSO) of peganumine A.



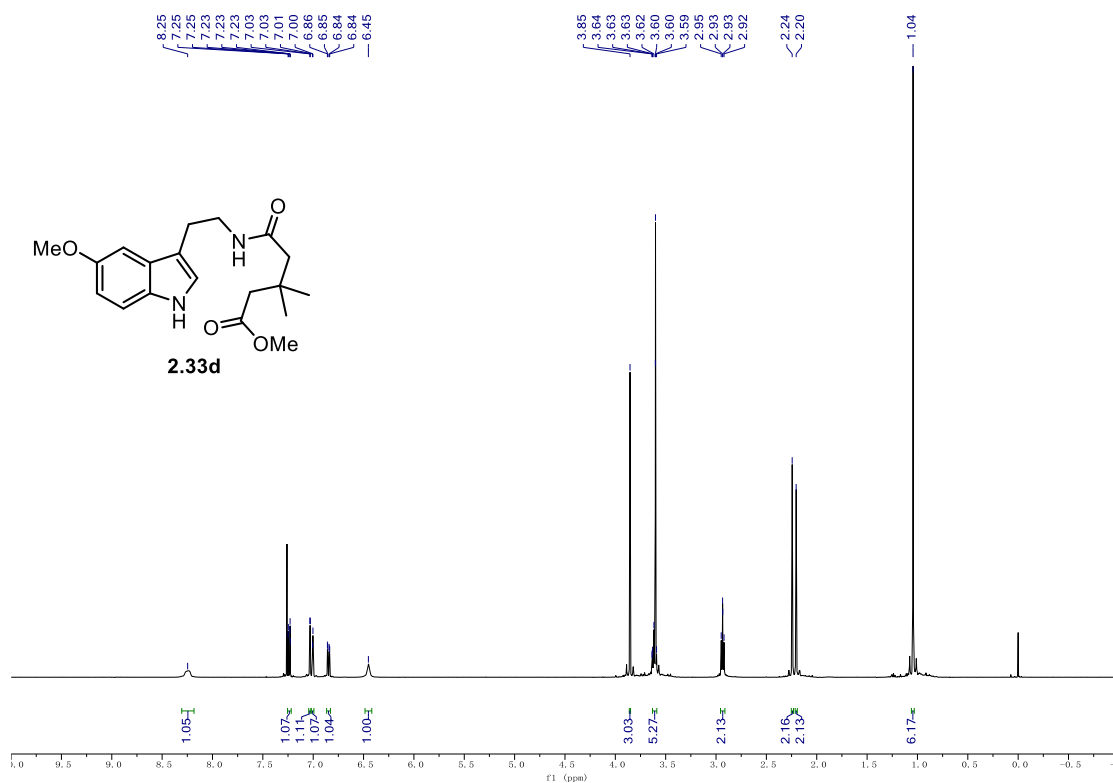
^{13}C NMR (126 MHz, d_6 -DMSO) of peganumine A.



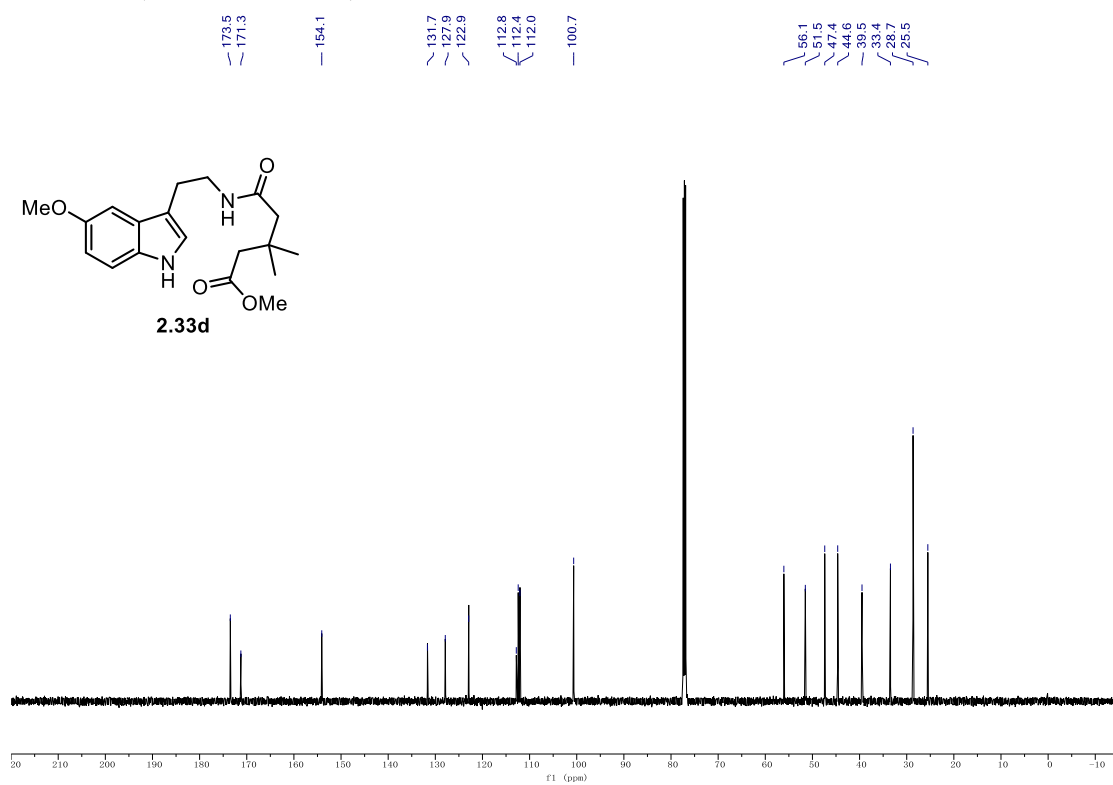
¹H NMR (500 MHz, CDCl₃) of 2.33c.**¹³C NMR (126 MHz, CDCl₃) of 2.33c.**

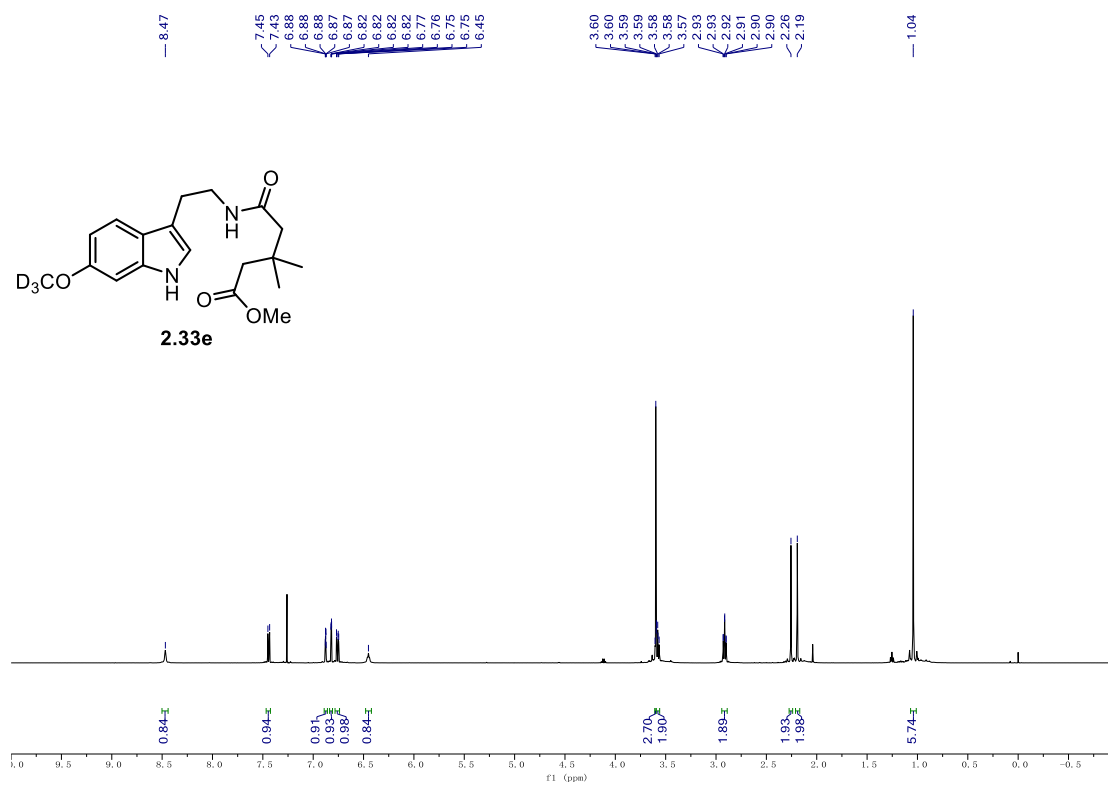
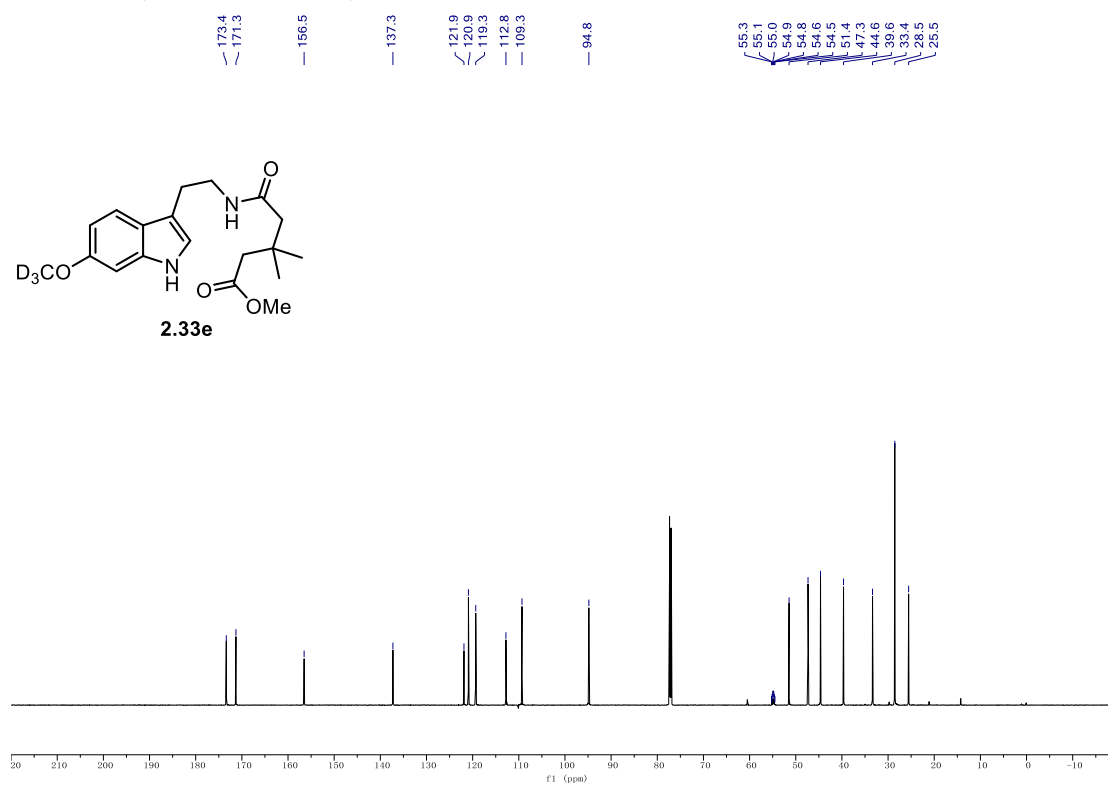
9.1. NMR Spectra

¹H NMR (500 MHz, CDCl₃) of **2.33d**.



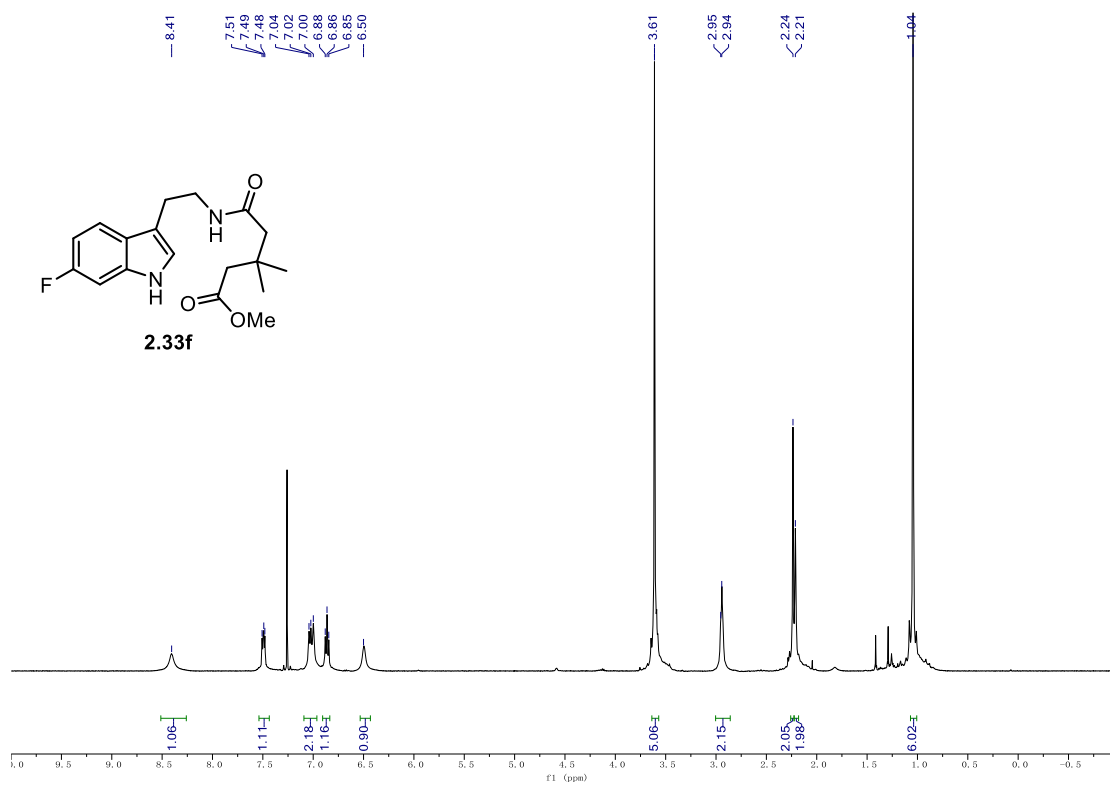
¹³C NMR (126 MHz, CDCl₃) of **2.33d**.



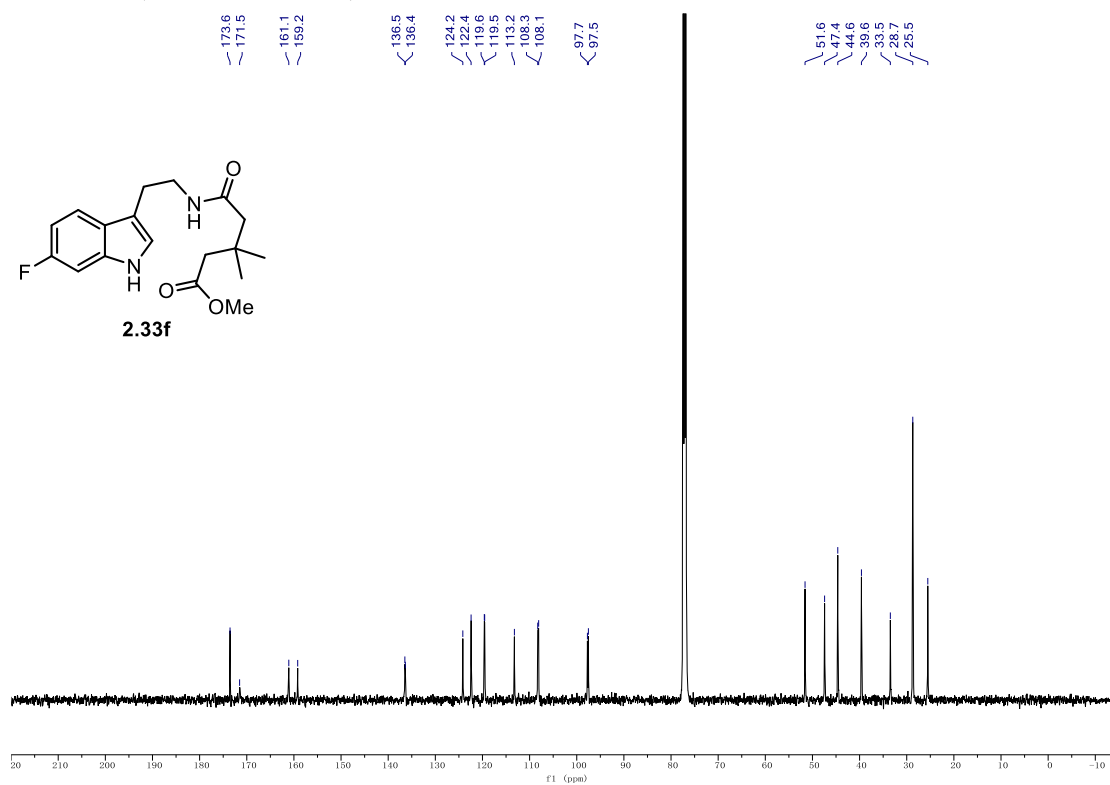
^1H NMR (500 MHz, CDCl_3) of **2.33e**. ^{13}C NMR (126 MHz, CDCl_3) of **2.33e**.

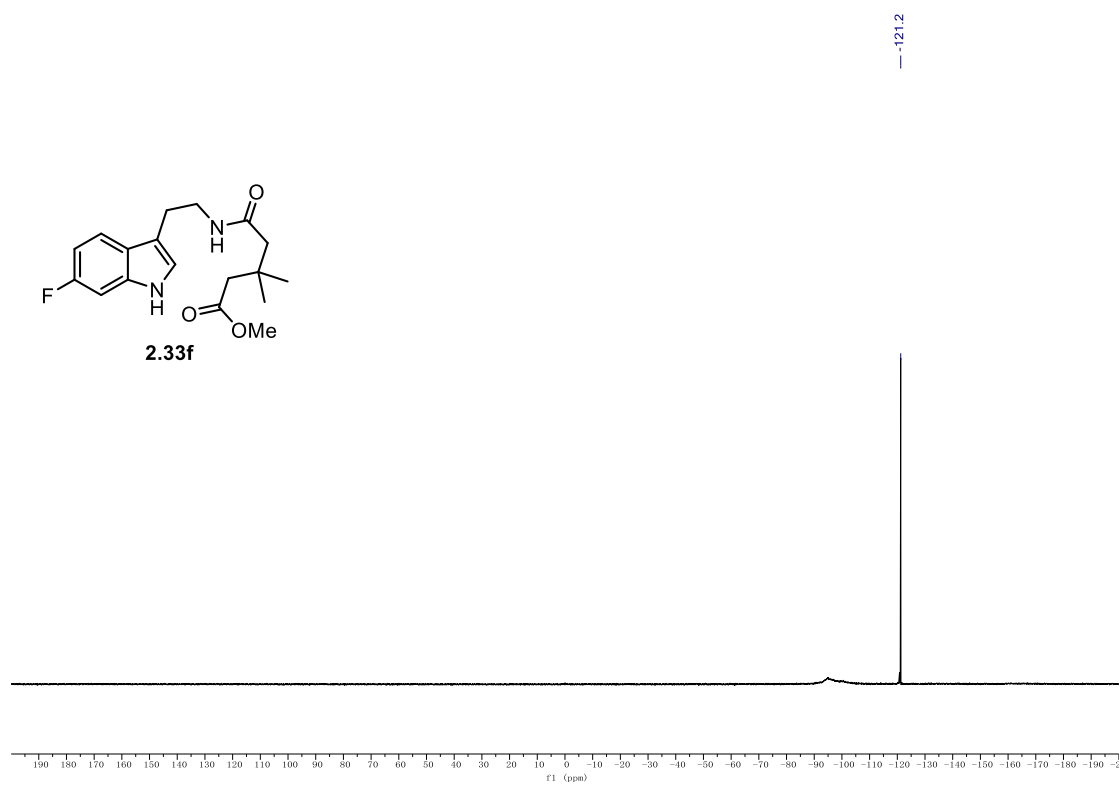
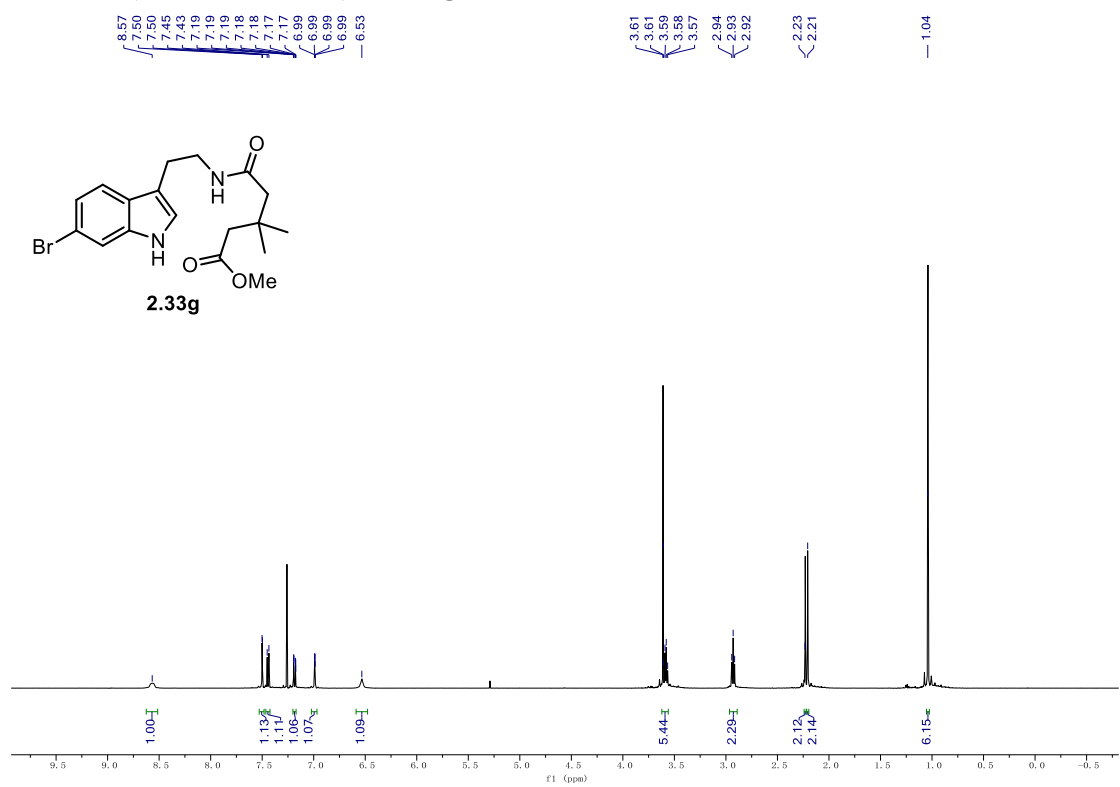
9.1. NMR Spectra

¹H NMR (500 MHz, CDCl₃) of **2.33f**.



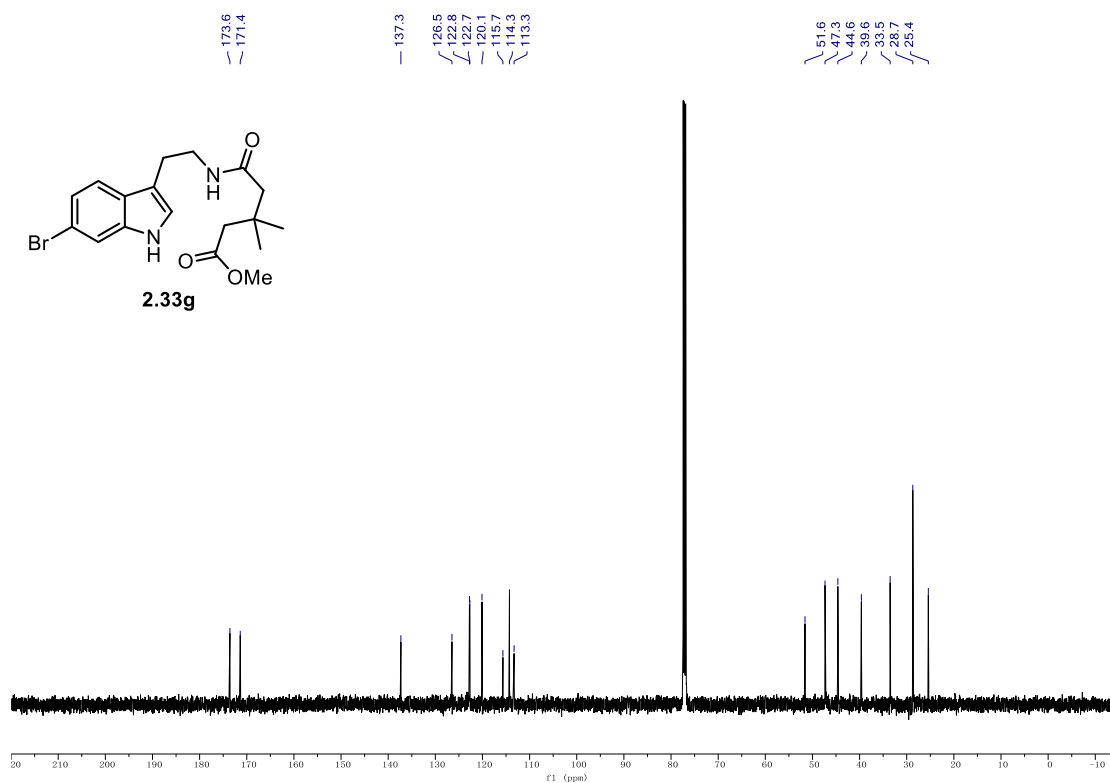
¹³C NMR (126 MHz, CDCl₃) of **2.33f**.



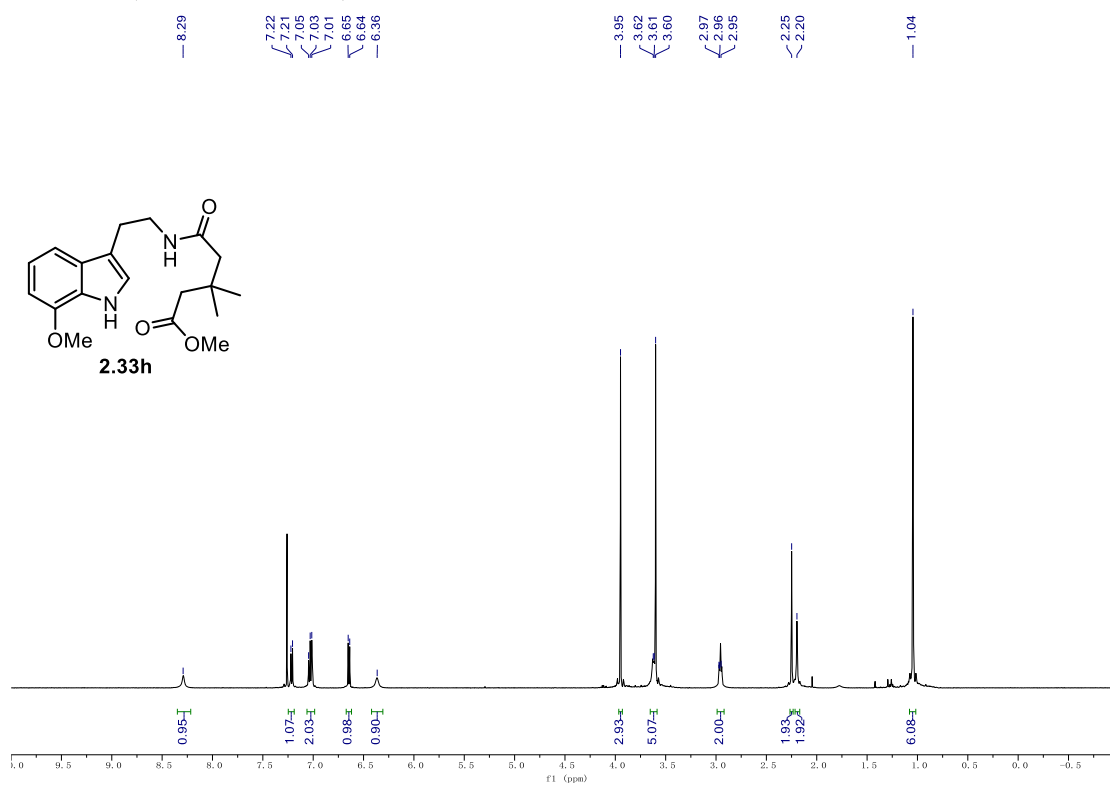
^{19}F NMR (376 MHz, CDCl_3) of **2.33f**. ^1H NMR (500 MHz, CDCl_3) of **2.33g**.

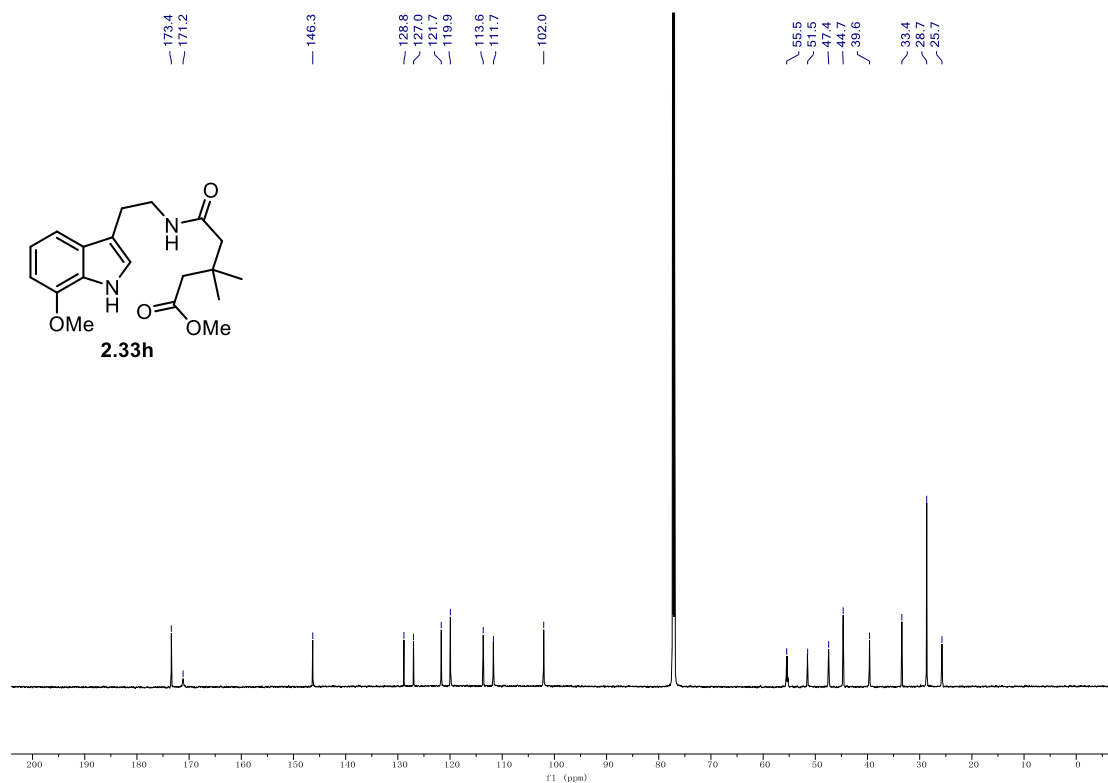
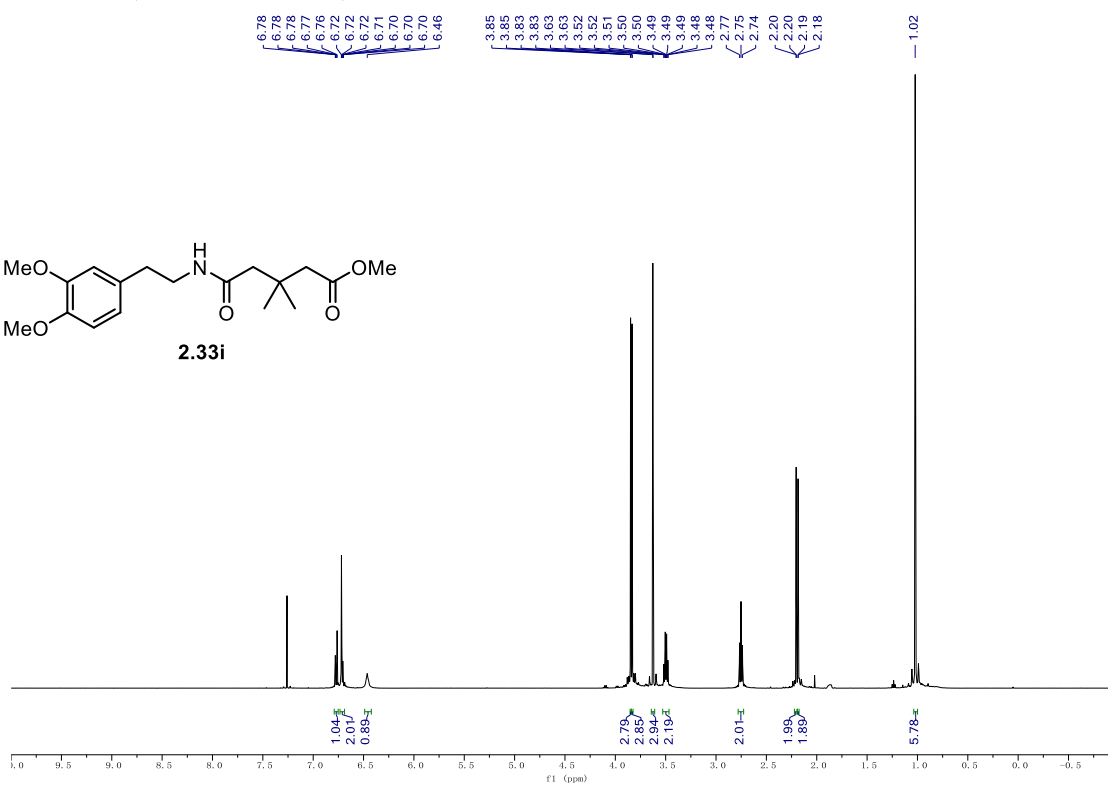
9.1. NMR Spectra

^{13}C NMR (126 MHz, CDCl_3) of **2.33g**.



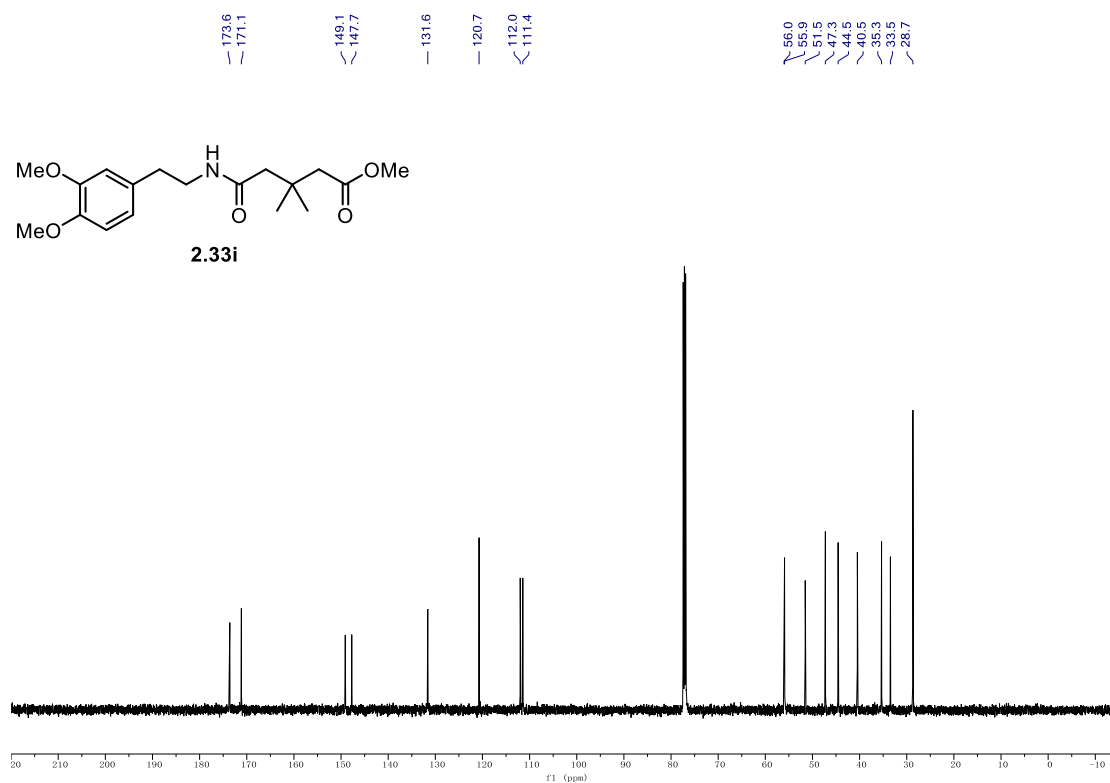
^1H NMR (500 MHz, CDCl_3) of **2.33h**.



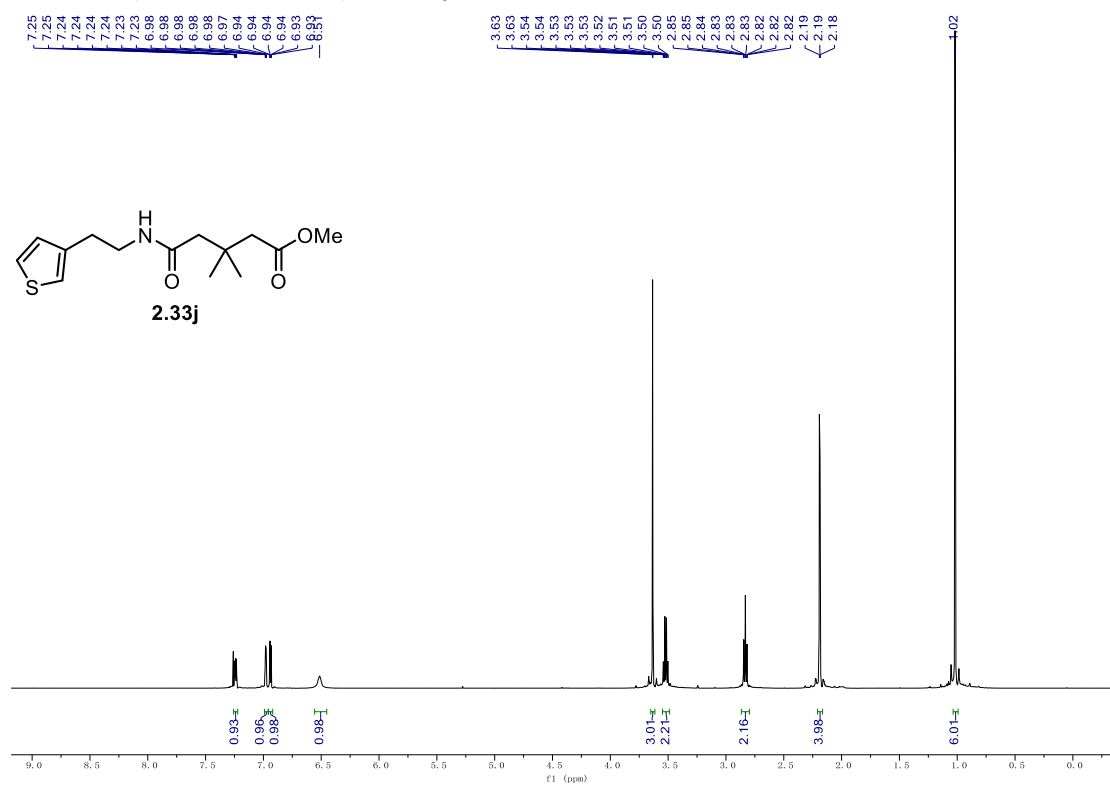
^{13}C NMR (176 MHz, CDCl_3) of **2.33h**. ^1H NMR (500 MHz, CDCl_3) of **2.33i**.

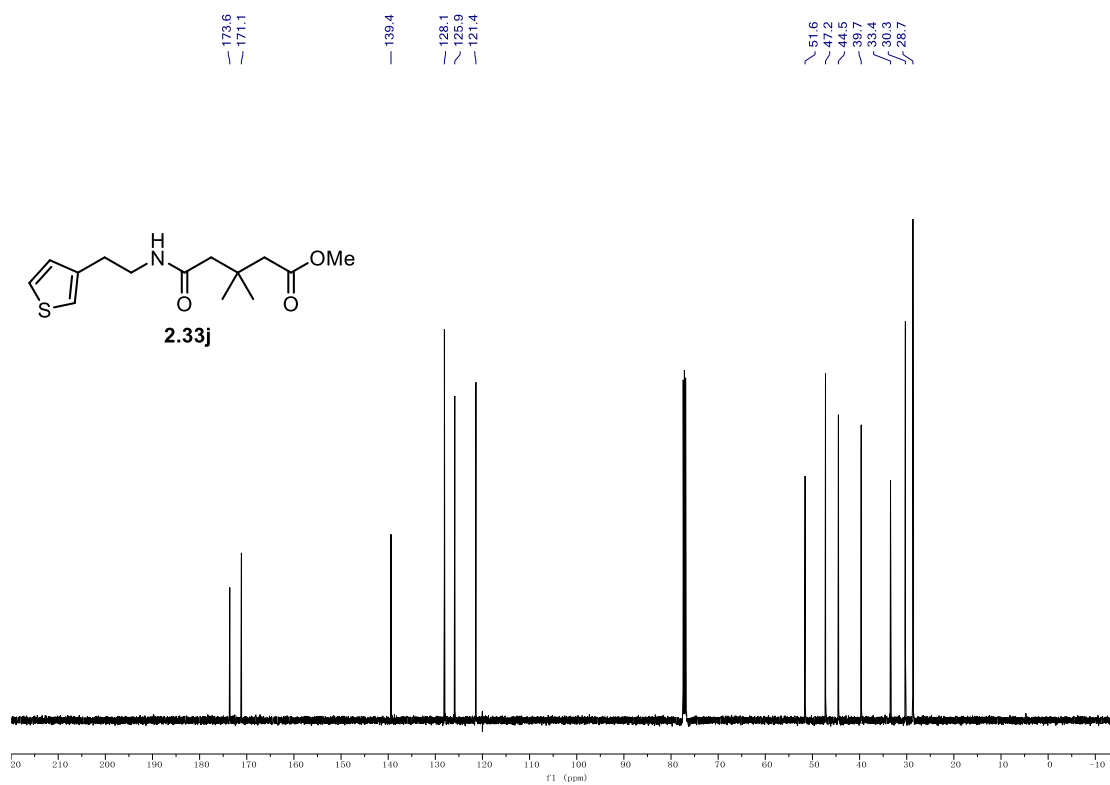
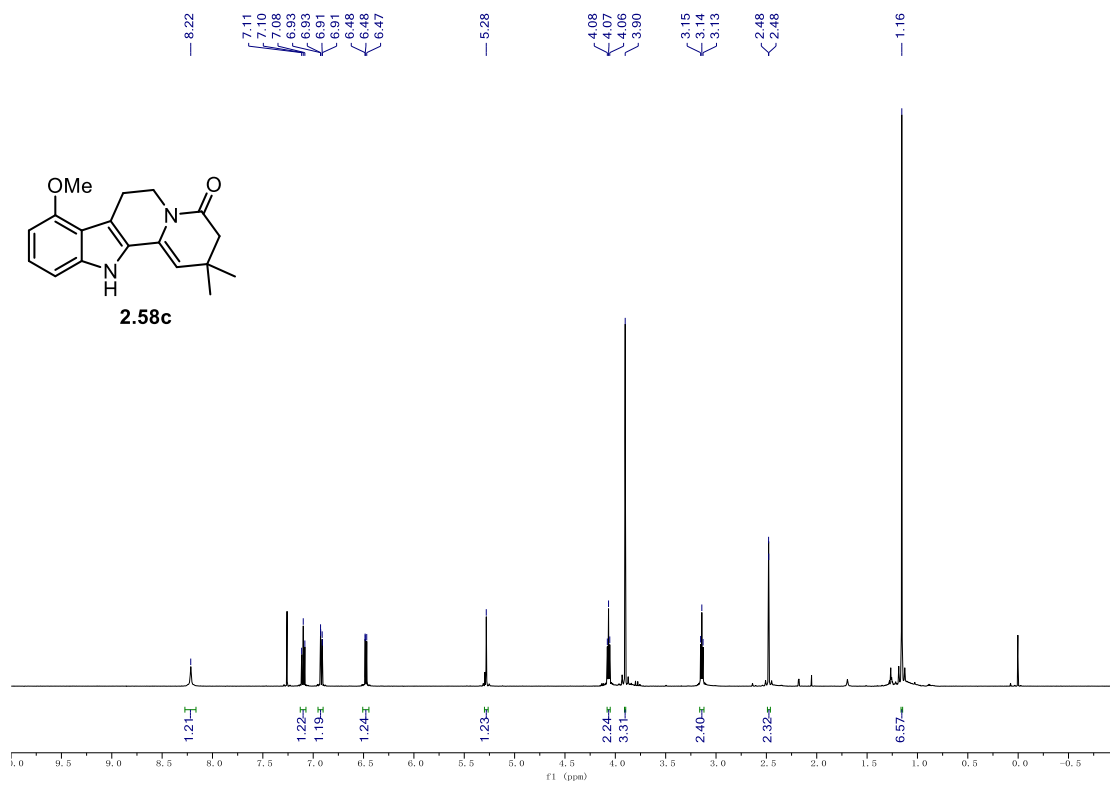
9.1. NMR Spectra

¹³C NMR (126 MHz, CDCl₃) of **2.33i**.



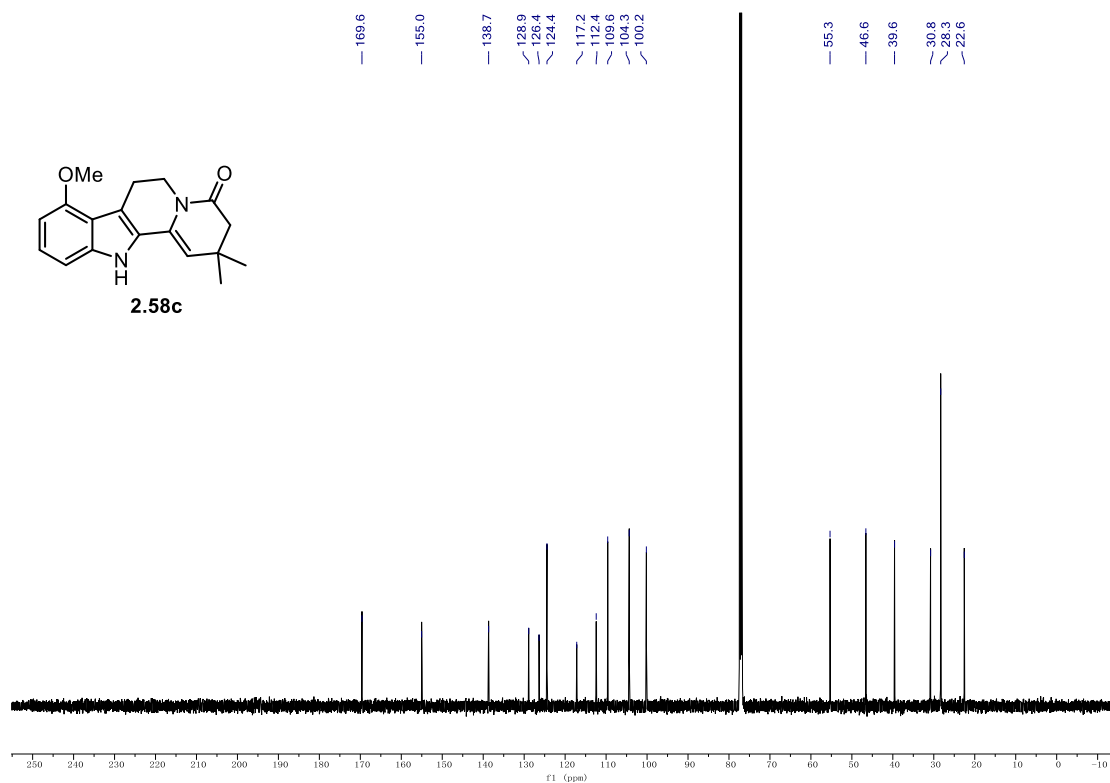
¹H NMR (500 MHz, CDCl₃) of **2.33j**.



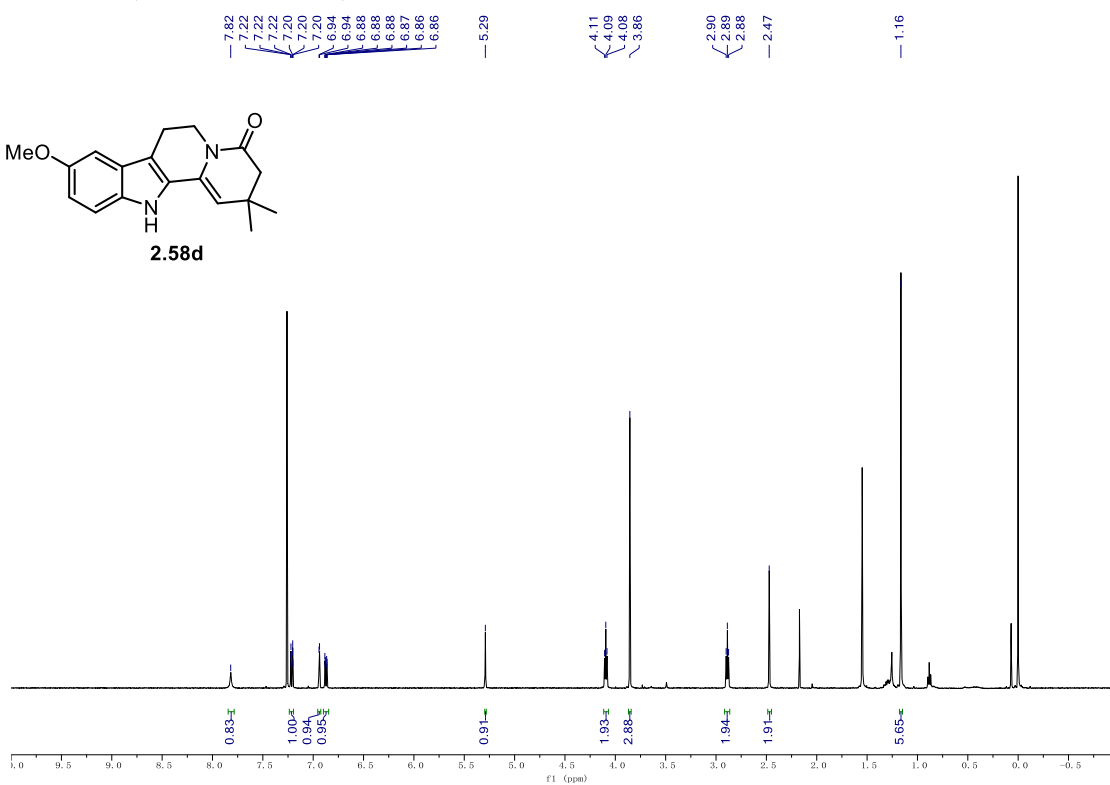
^{13}C NMR (126 MHz, CDCl_3) of **2.33j**. ^1H NMR (500 MHz, CDCl_3) of **2.58c**.

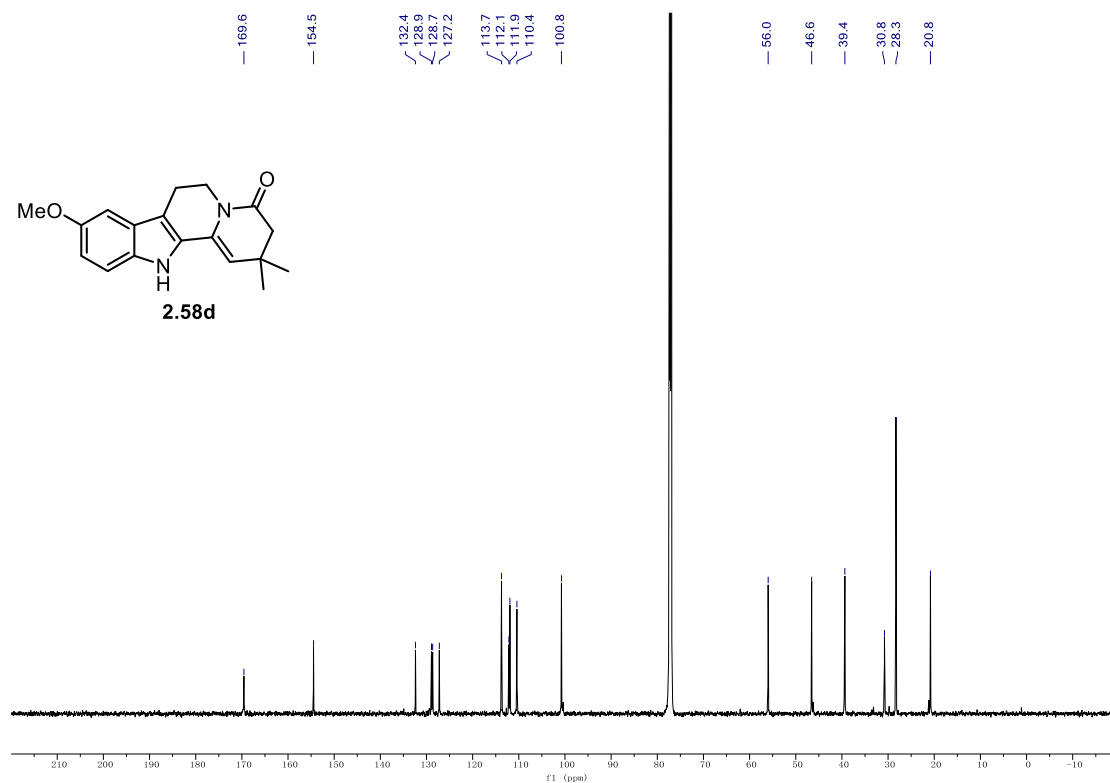
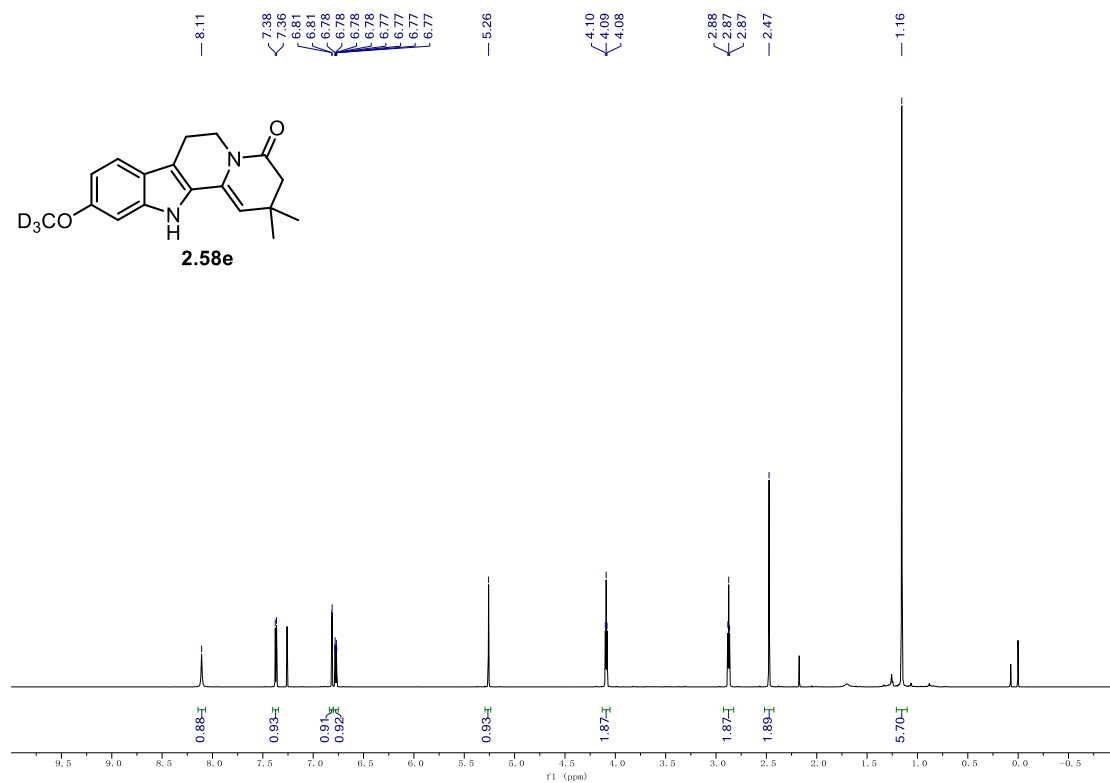
9.1. NMR Spectra

^{13}C NMR (126 MHz, CDCl_3) of **2.58c**.



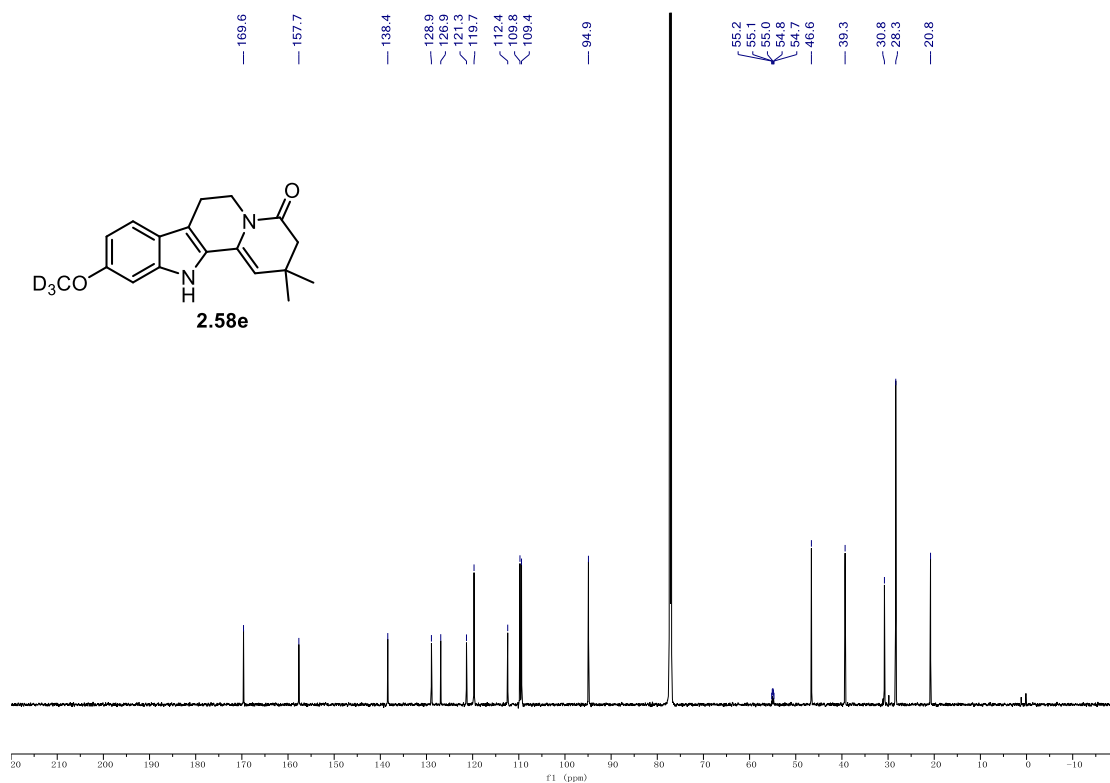
^1H NMR (500 MHz, CDCl_3) of **2.58d**.



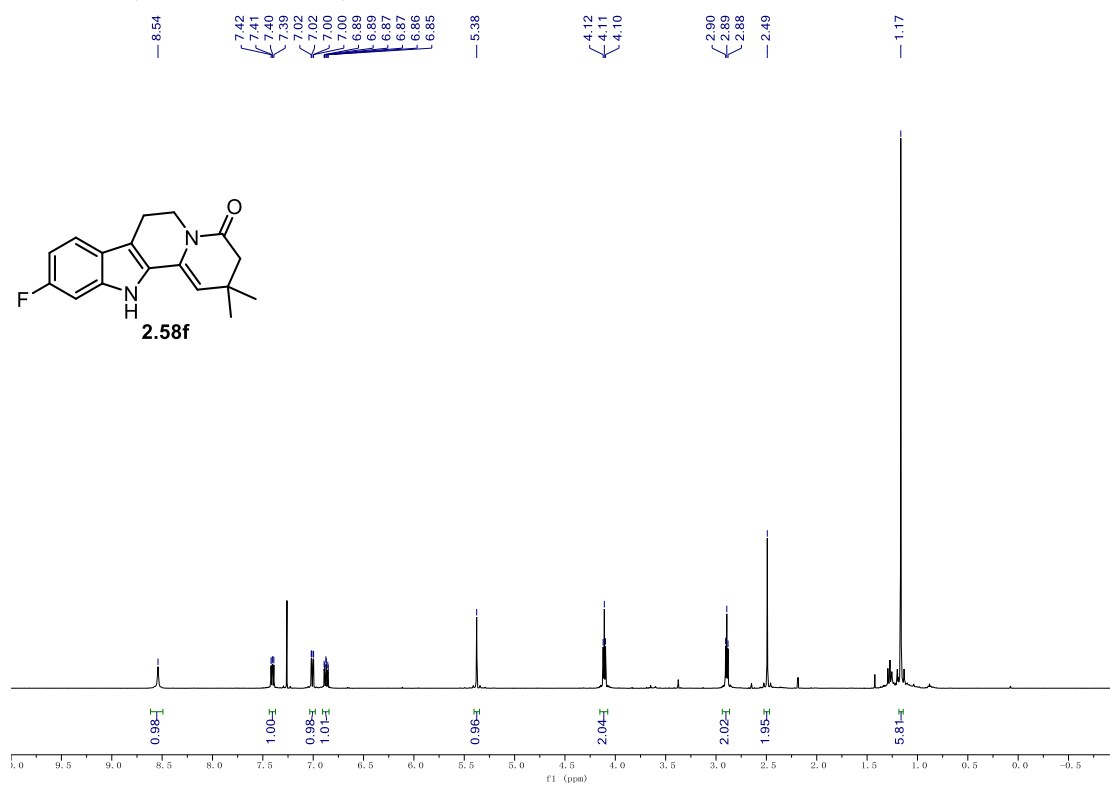
^{13}C NMR (176 MHz, CDCl_3) of **2.58d**. ^1H NMR (500 MHz, CDCl_3) of **2.58e**.

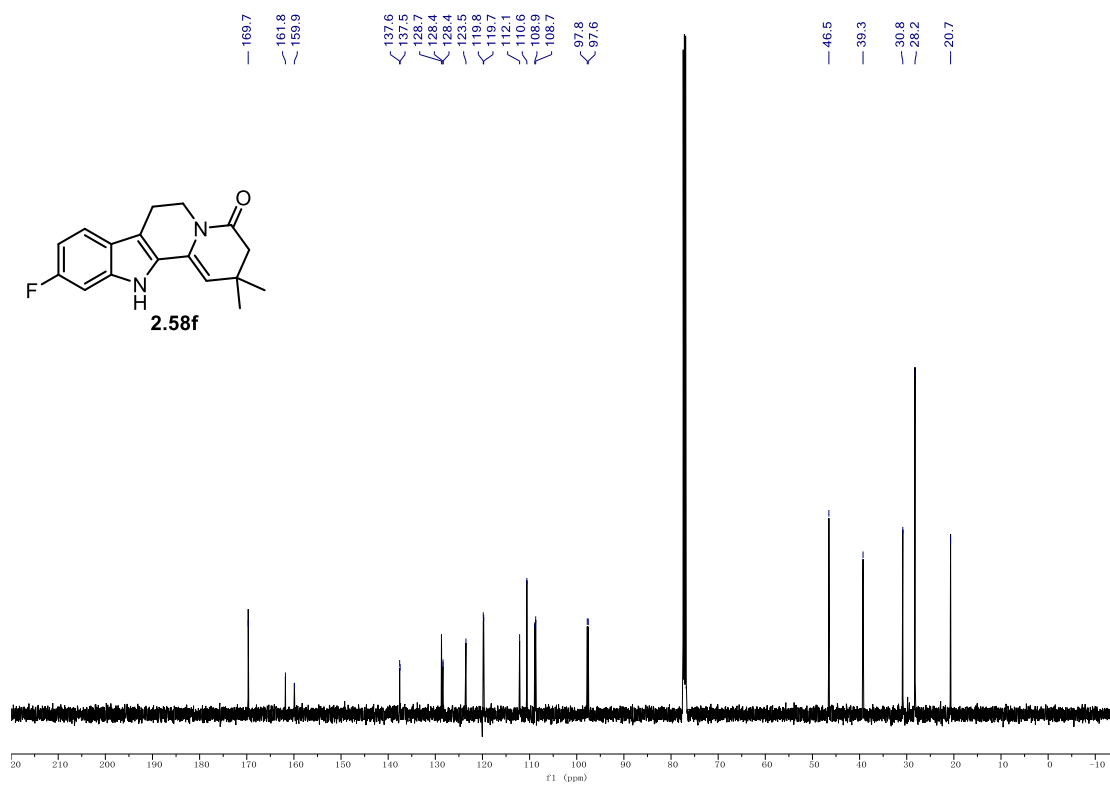
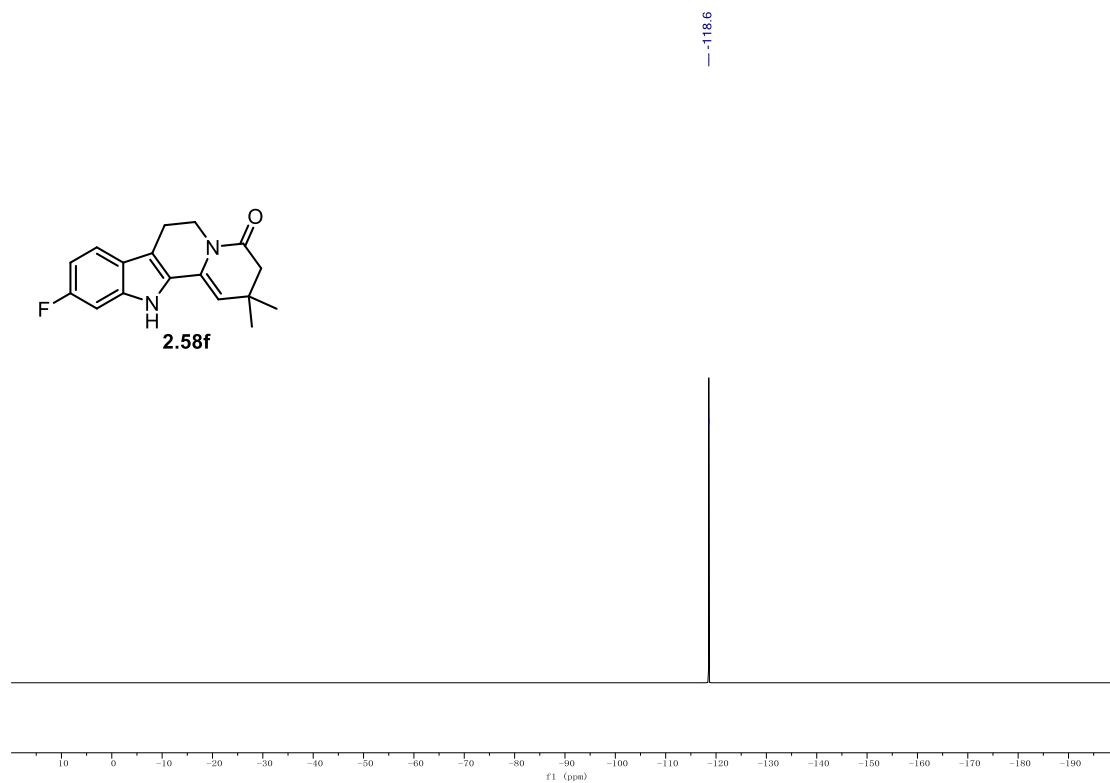
9.1. NMR Spectra

^{13}C NMR (126 MHz, CDCl_3) of **2.58e**.



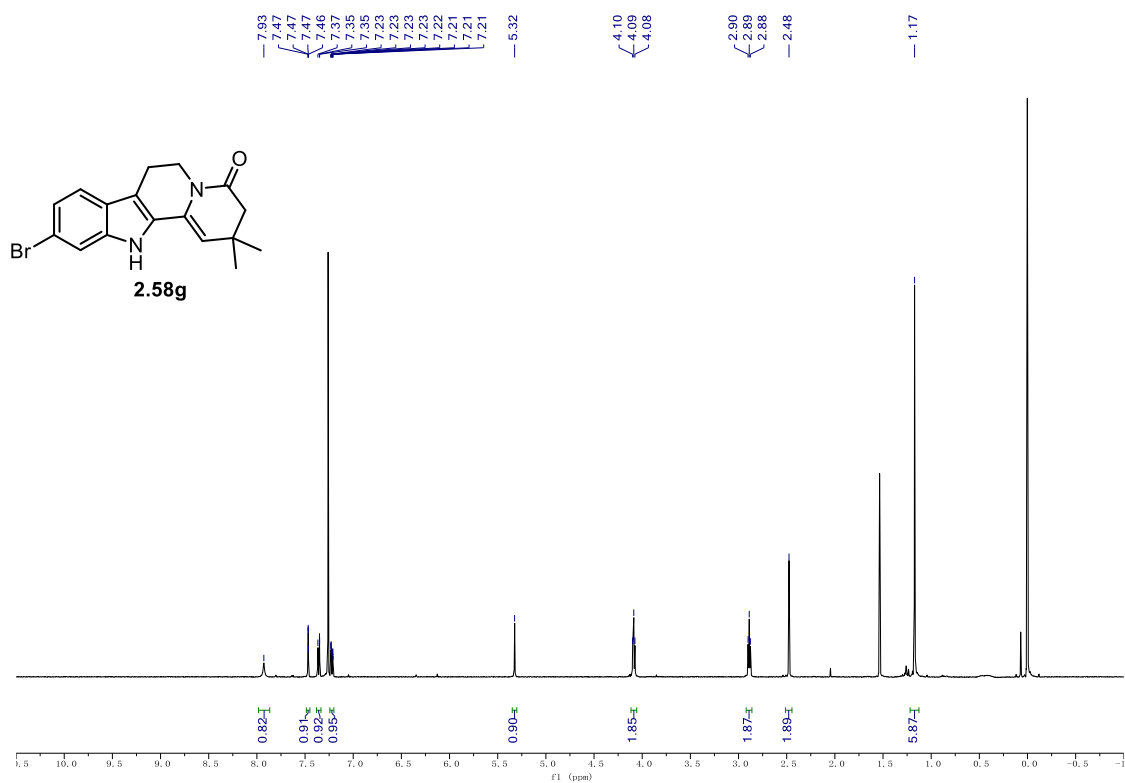
^1H NMR (500 MHz, CDCl_3) of **2.58f**.



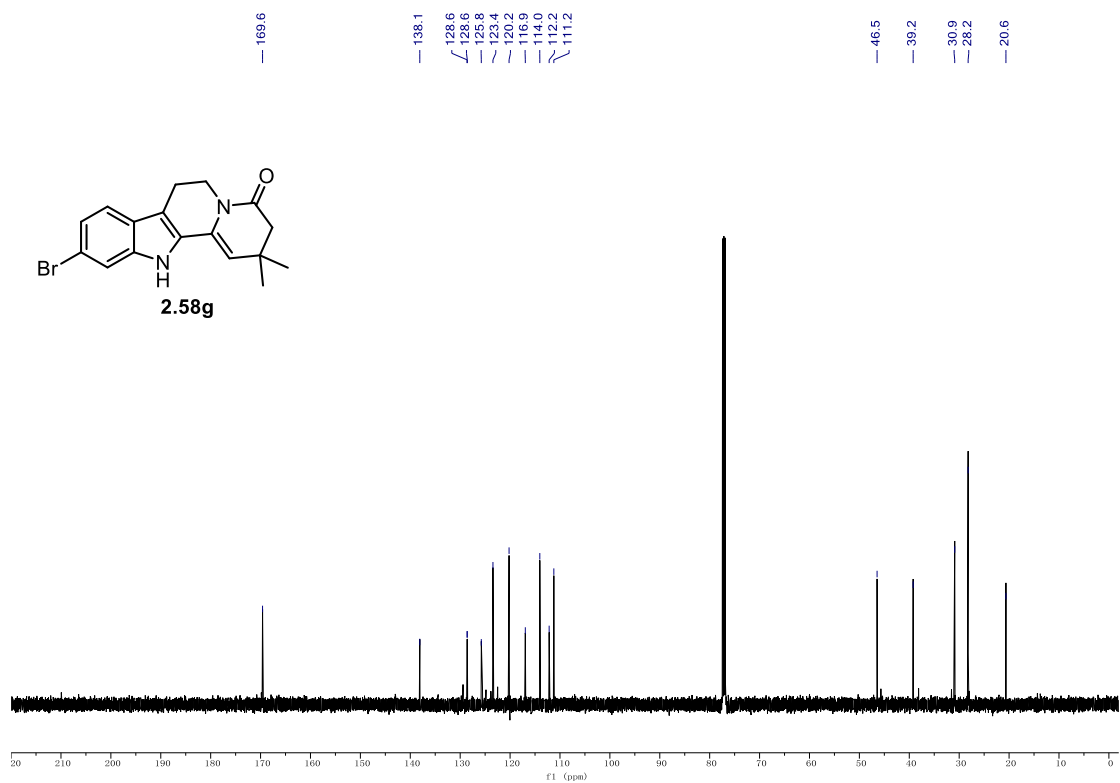
^{13}C NMR (126 MHz, CDCl_3) of **2.58f**. ^{19}F NMR (566 MHz, CDCl_3) of **2.58f**.

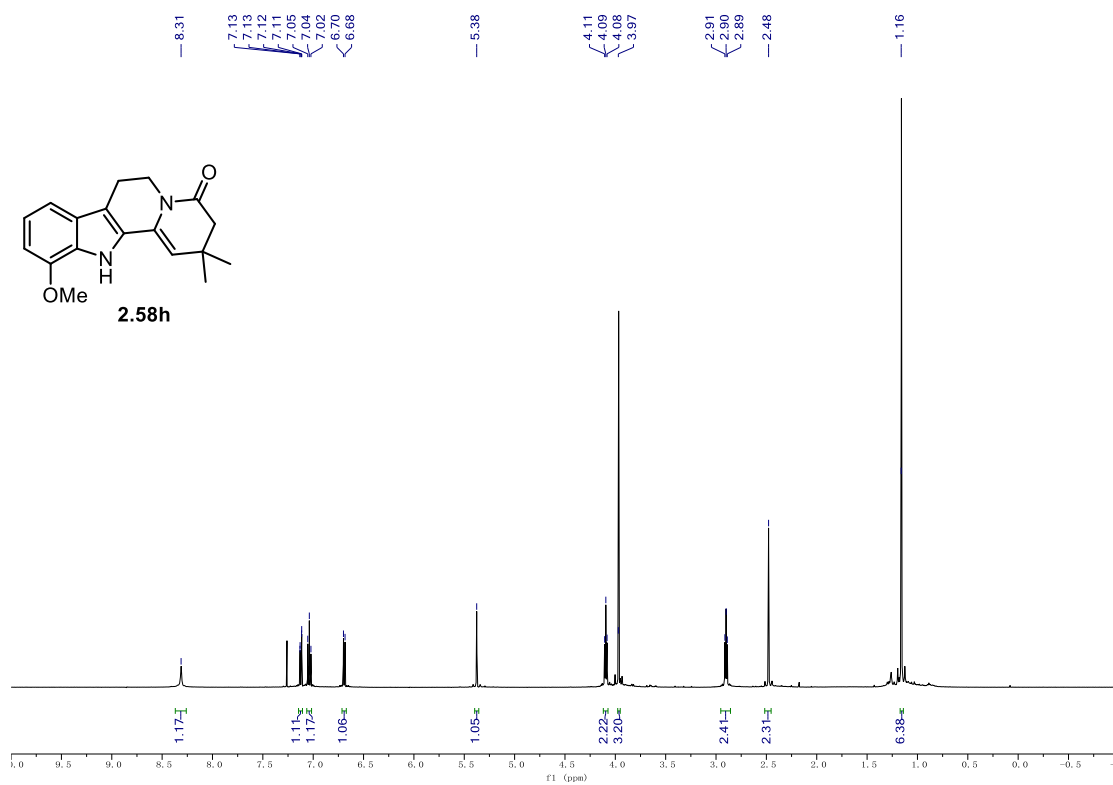
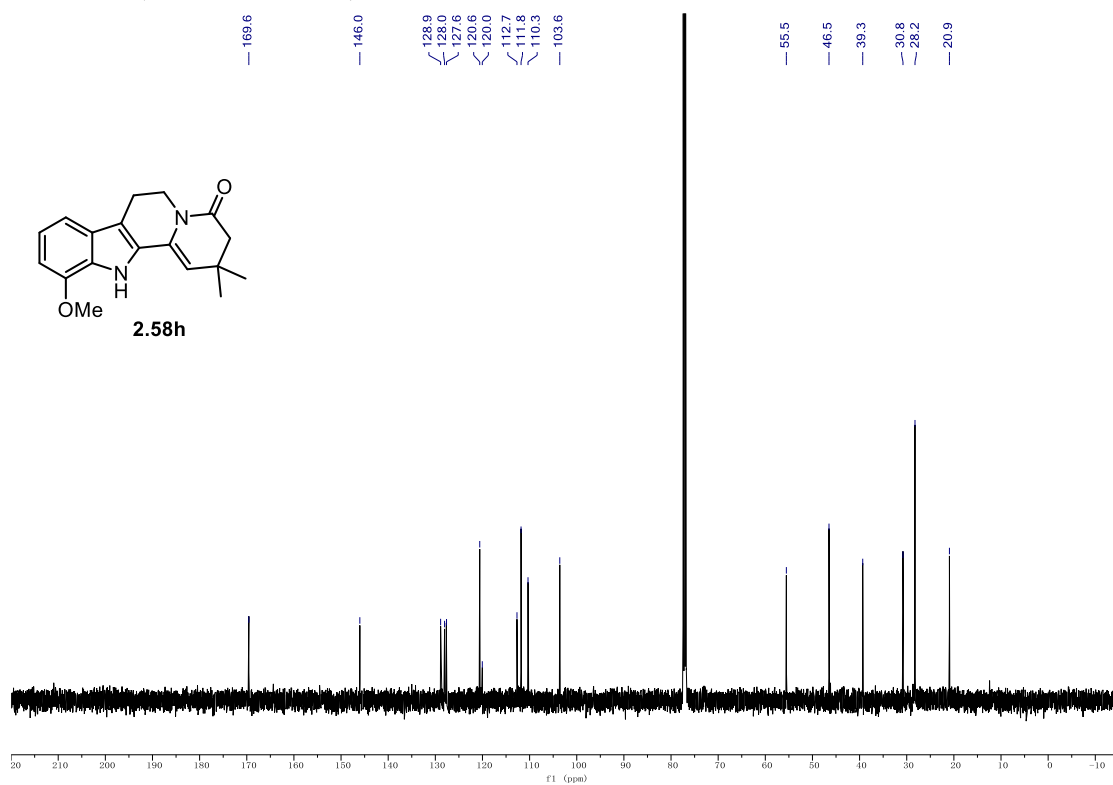
9.1. NMR Spectra

^1H NMR (500 MHz, CDCl_3) of **2.58g**.



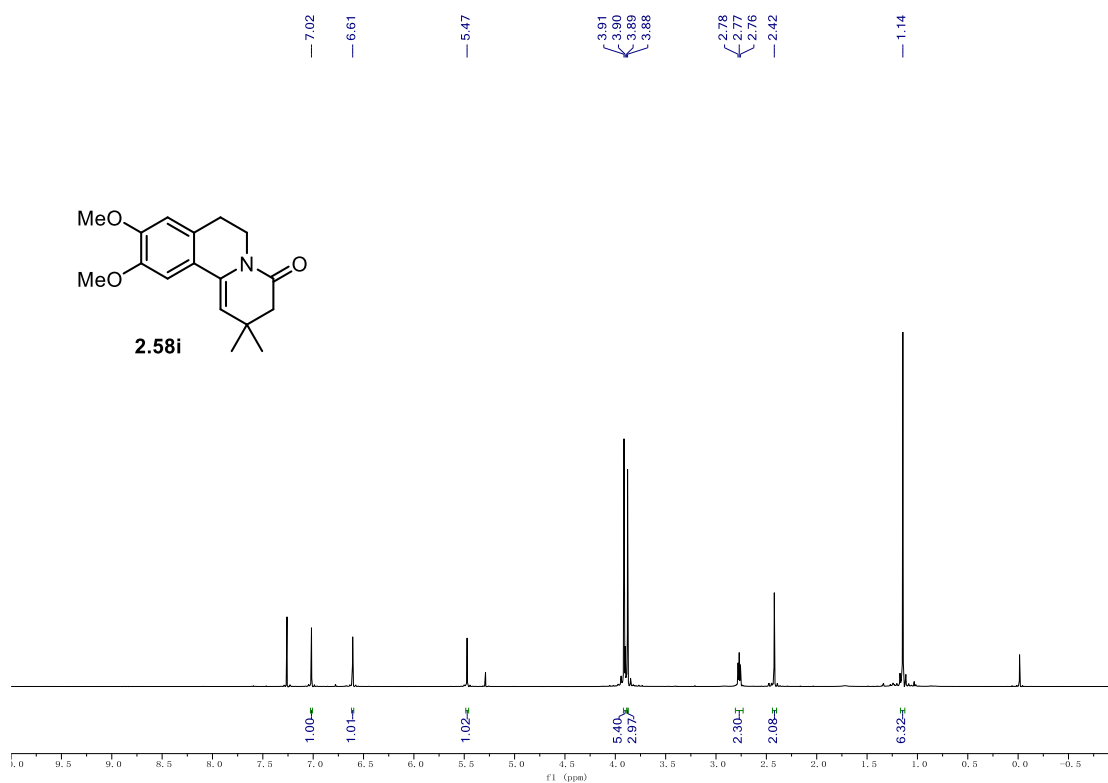
^{13}C NMR (126 MHz, CDCl_3) of **2.58g**.



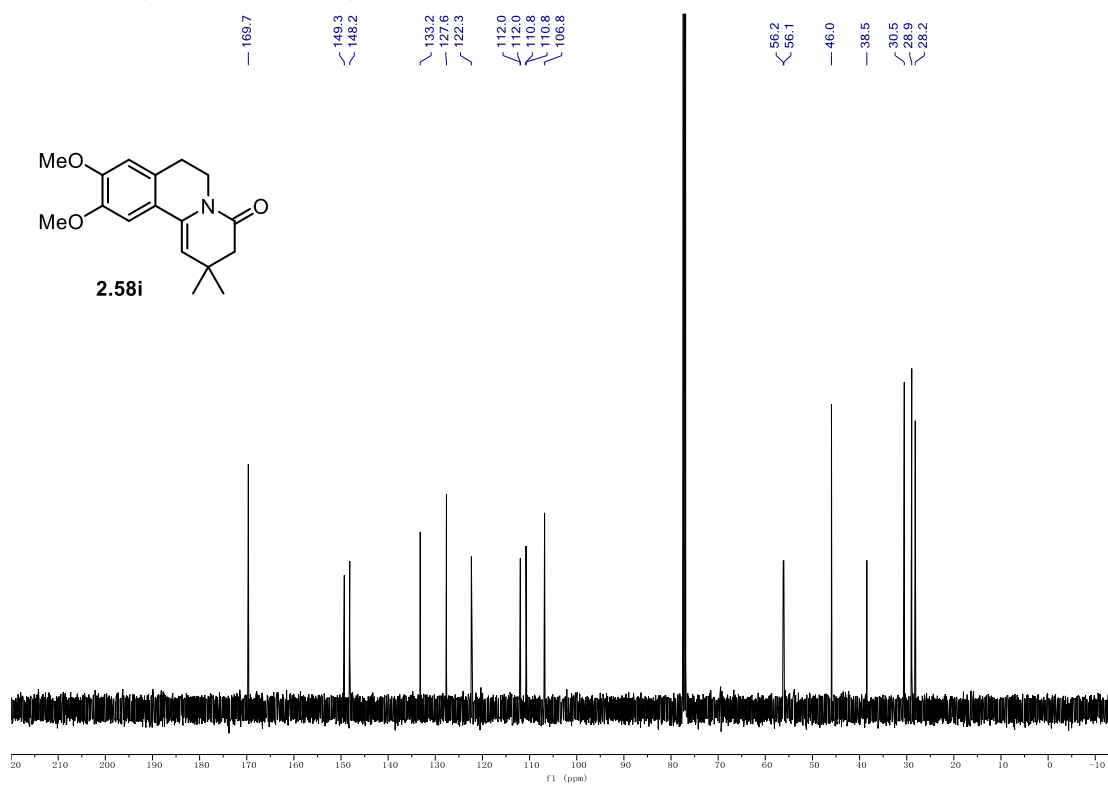
¹H NMR (500 MHz, CDCl₃) of 2.58h.**¹³C NMR (126 MHz, CDCl₃) of 2.58h.**

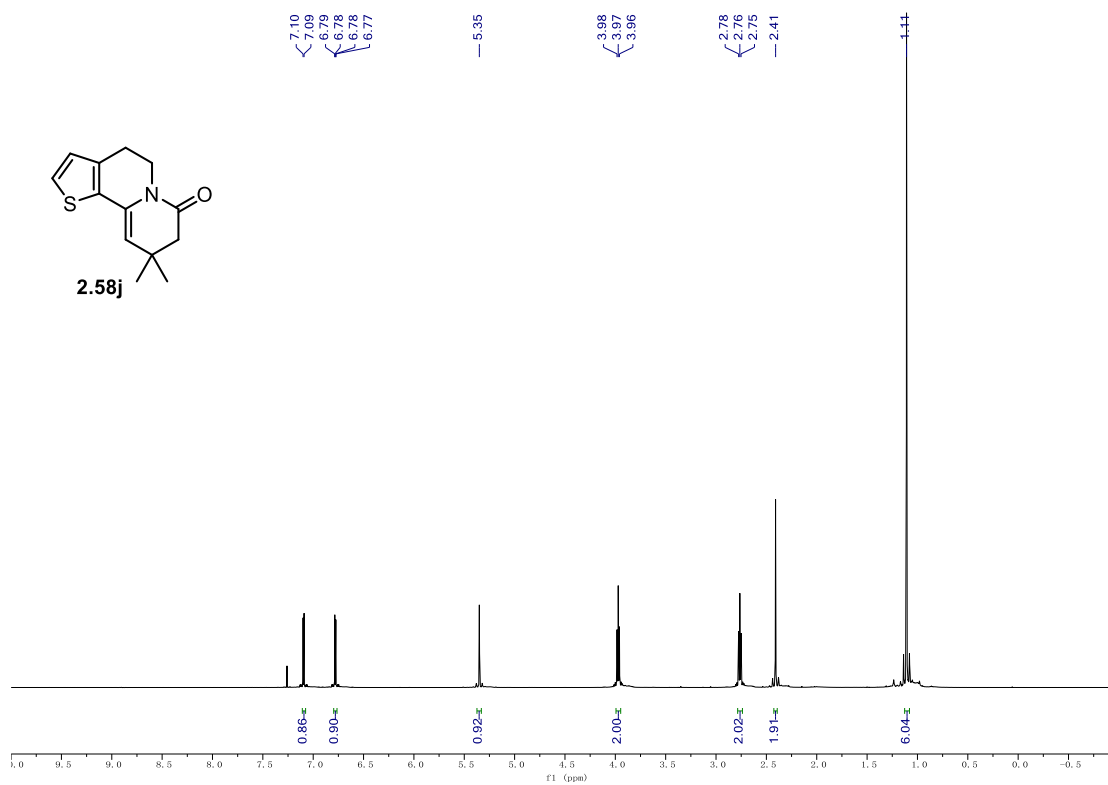
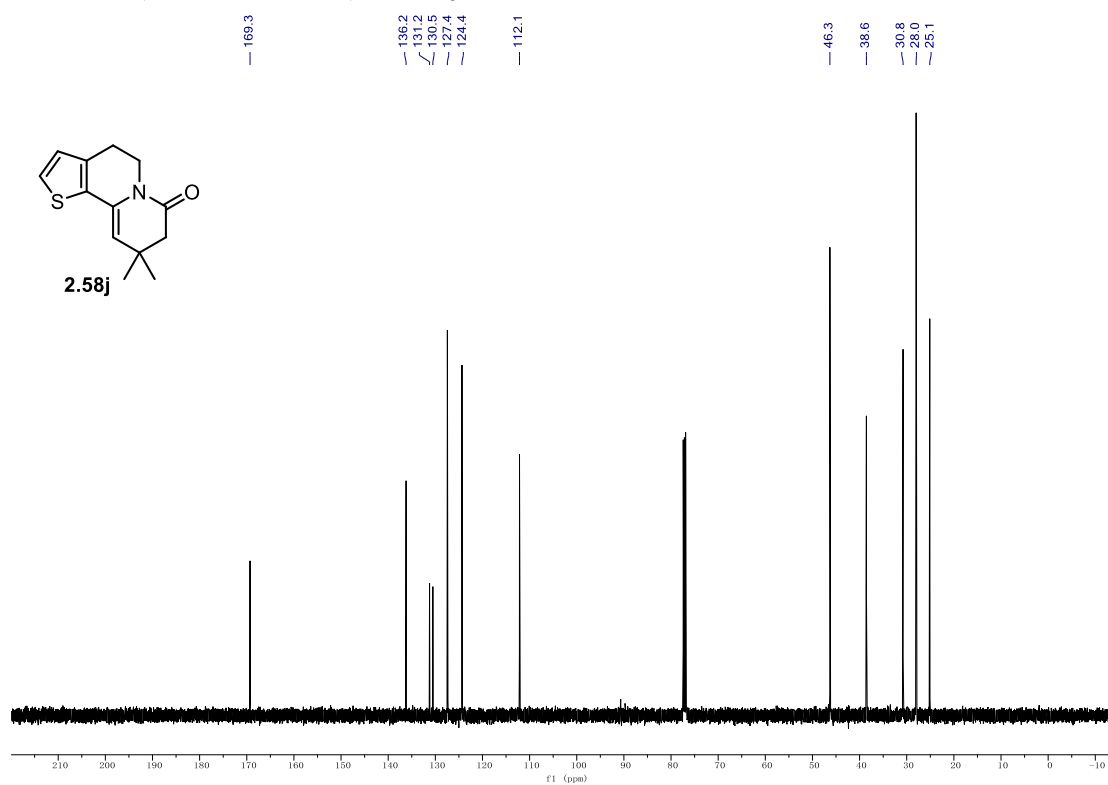
9.1. NMR Spectra

¹H NMR (500 MHz, CDCl₃) of **2.59i**.



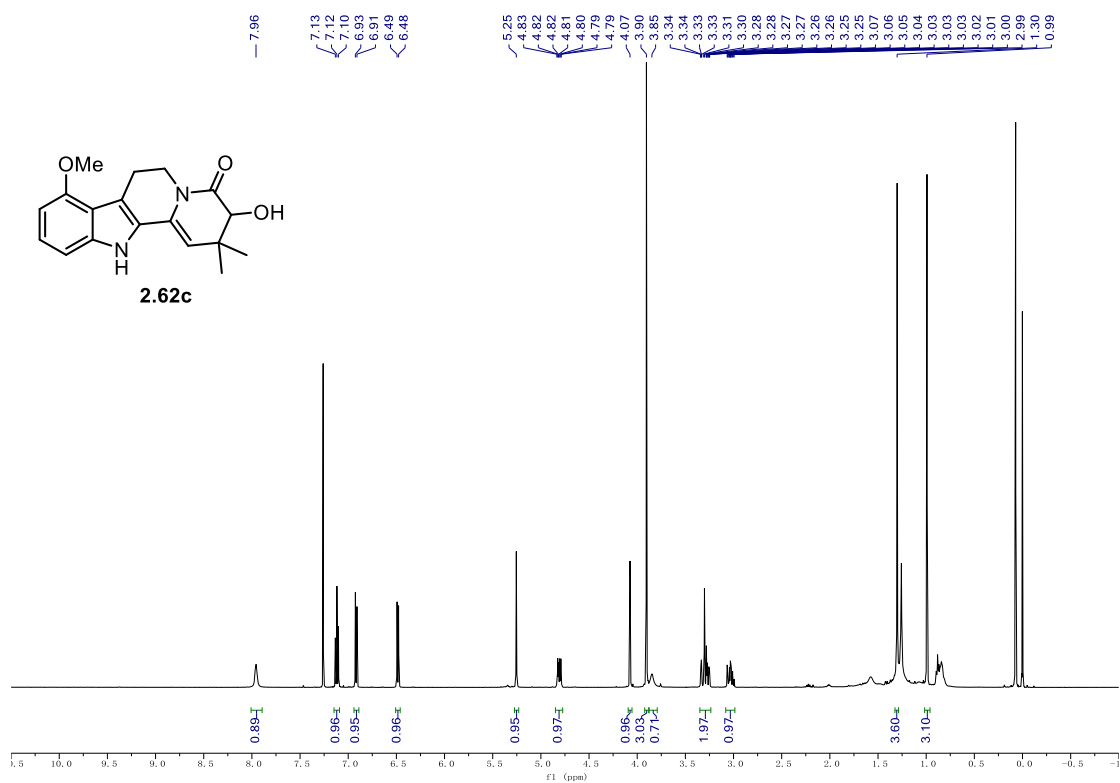
¹³C NMR (126 MHz, CDCl₃) of **2.58i**.



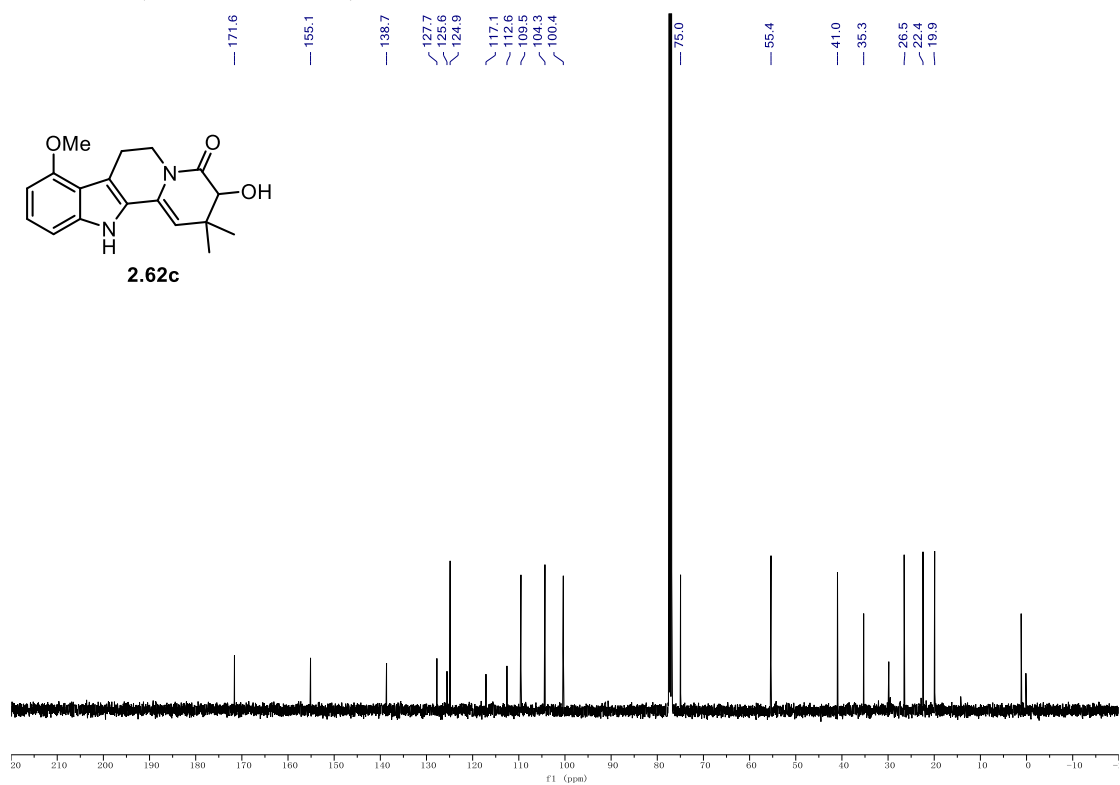
¹H NMR (500 MHz, CDCl₃) of 2.58j.**¹³C NMR (126 MHz, CDCl₃) of 2.58j.**

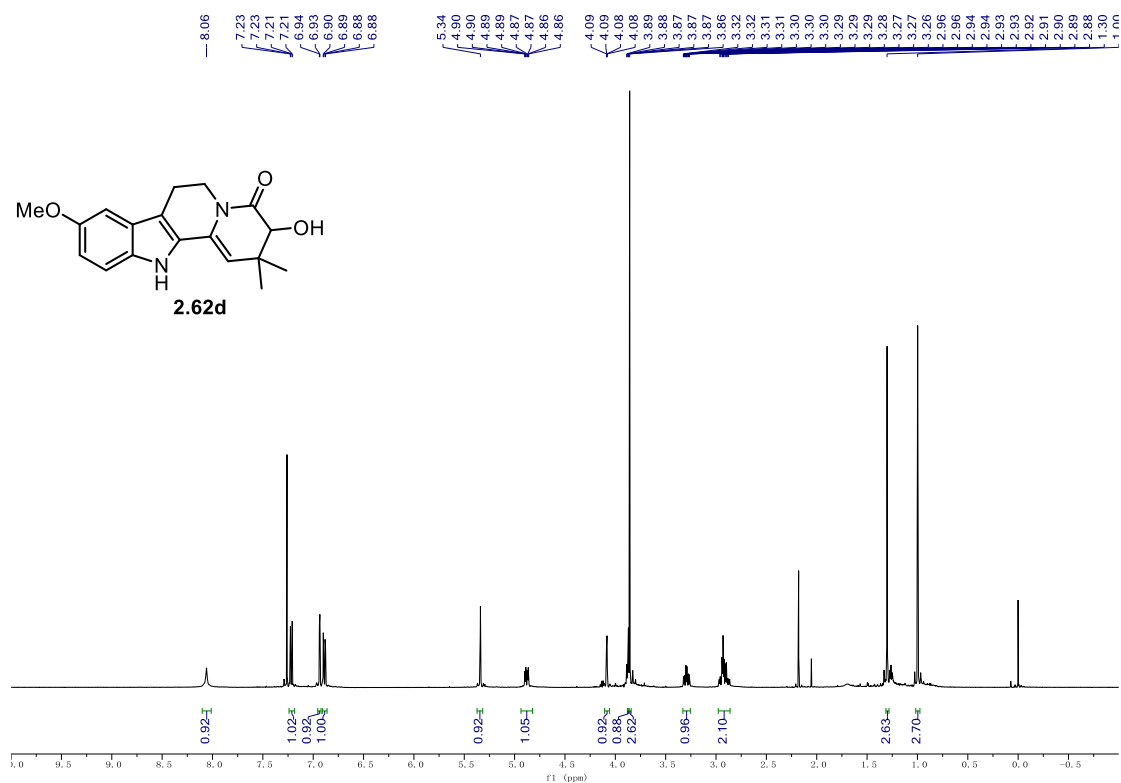
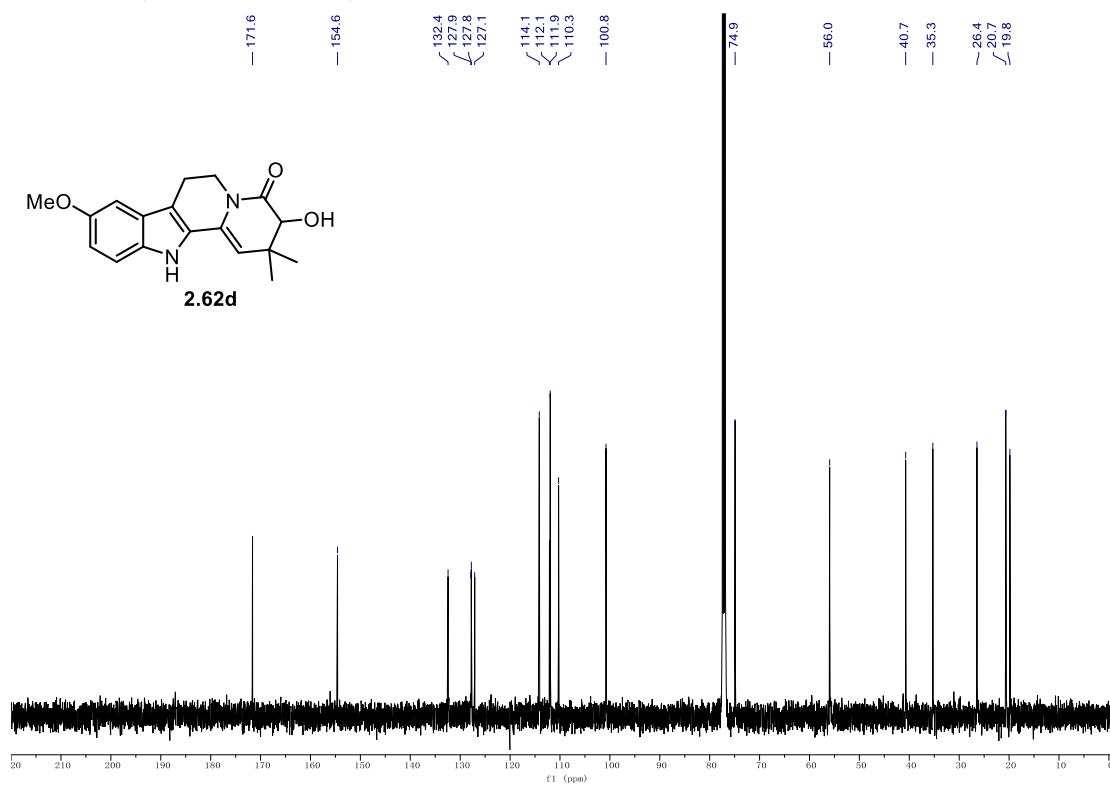
9.1. NMR Spectra

^1H NMR (500 MHz, CDCl_3) of **2.62c**.



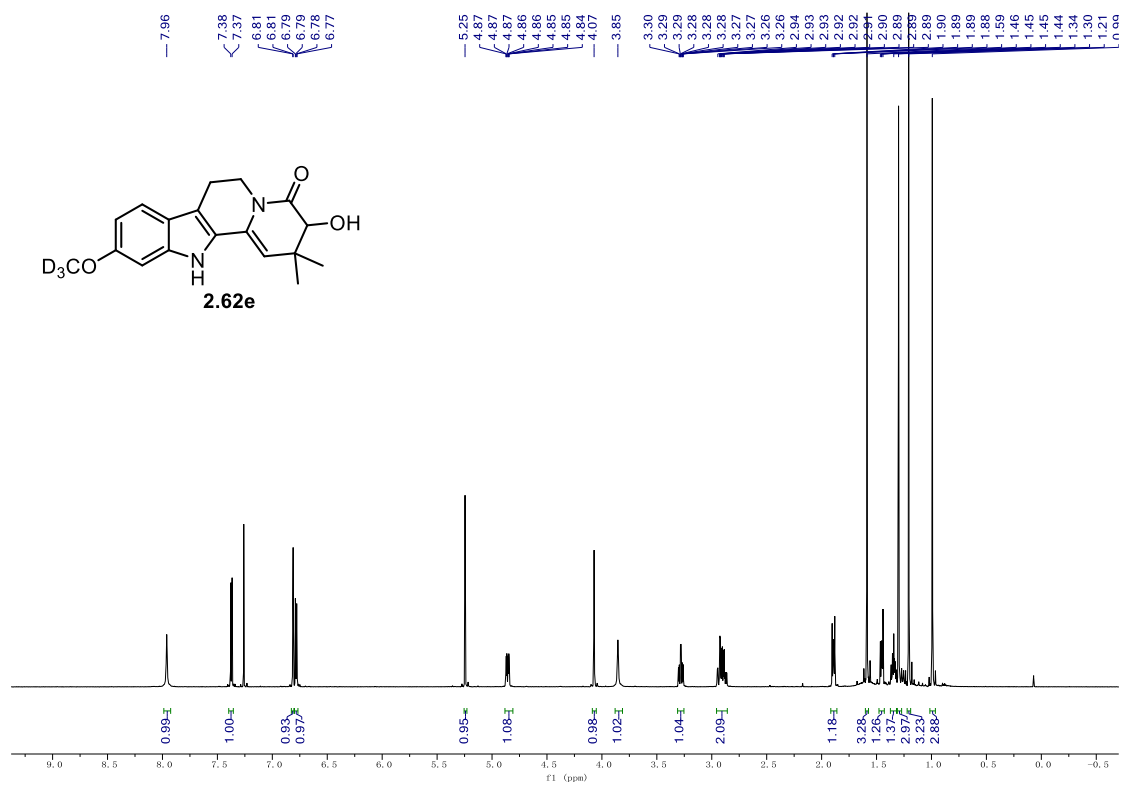
^{13}C NMR (126 MHz, CDCl_3) of **2.62c**.



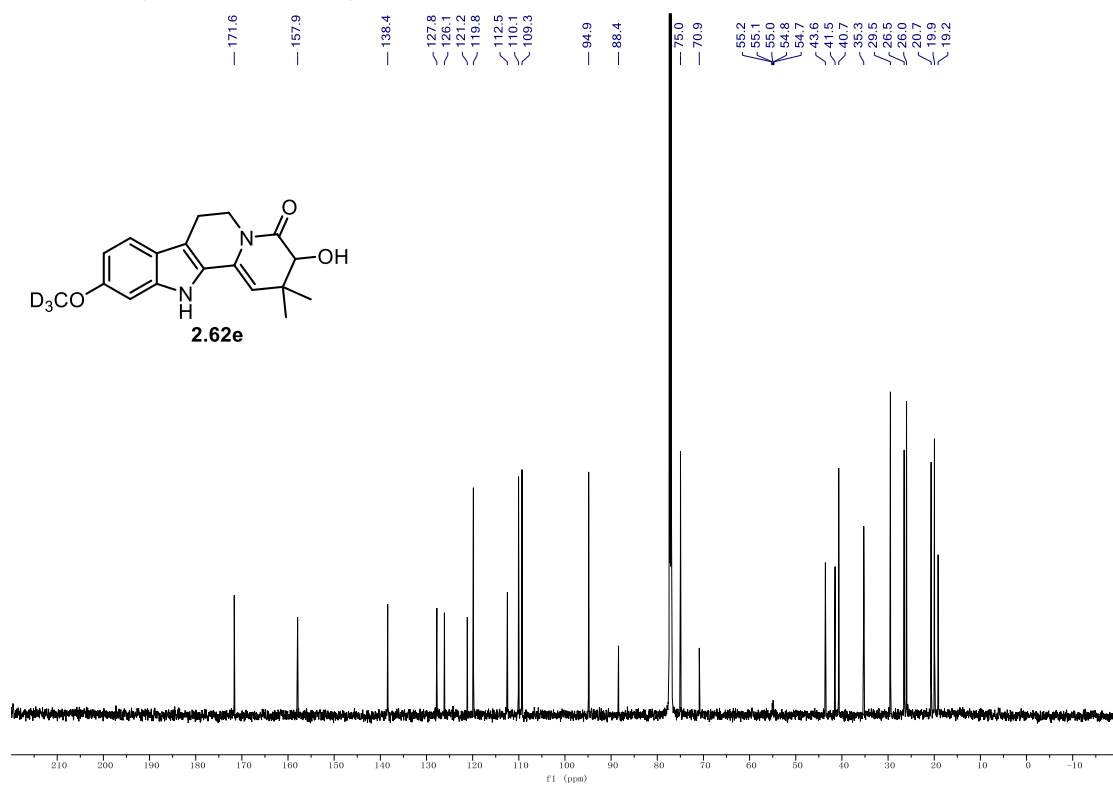
¹H NMR (500 MHz, CDCl₃) of 2.62d.**¹³C NMR (126 MHz, CDCl₃) of 2.62d.**

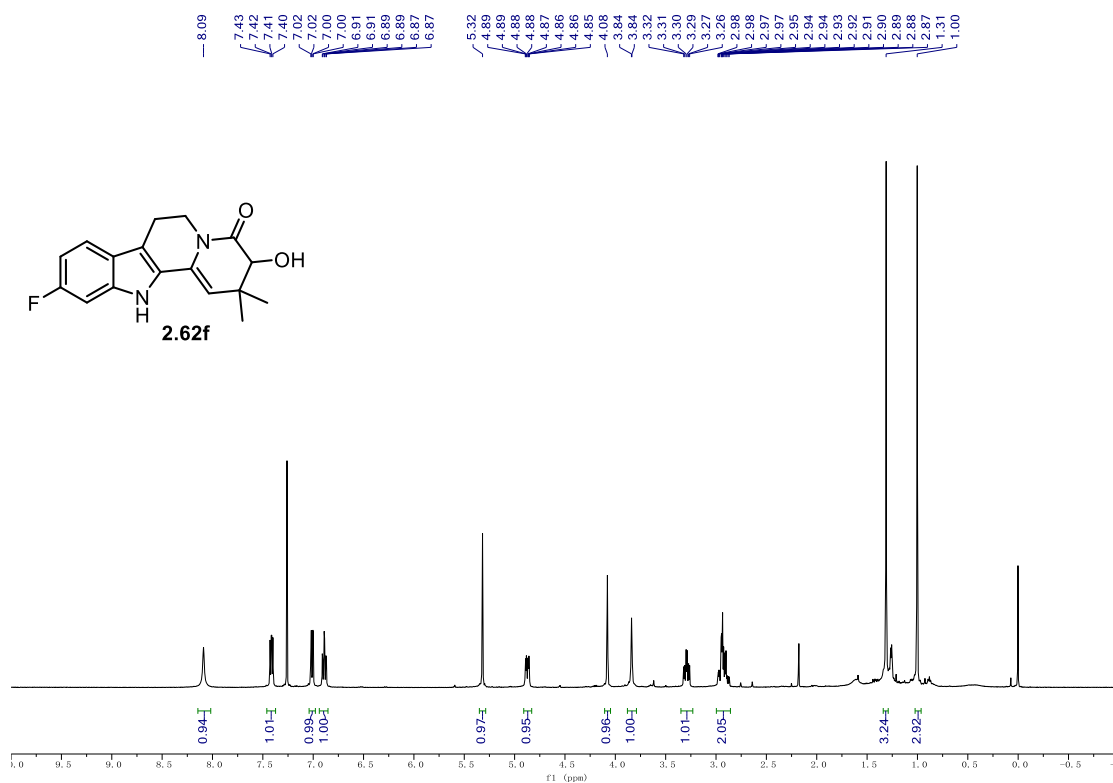
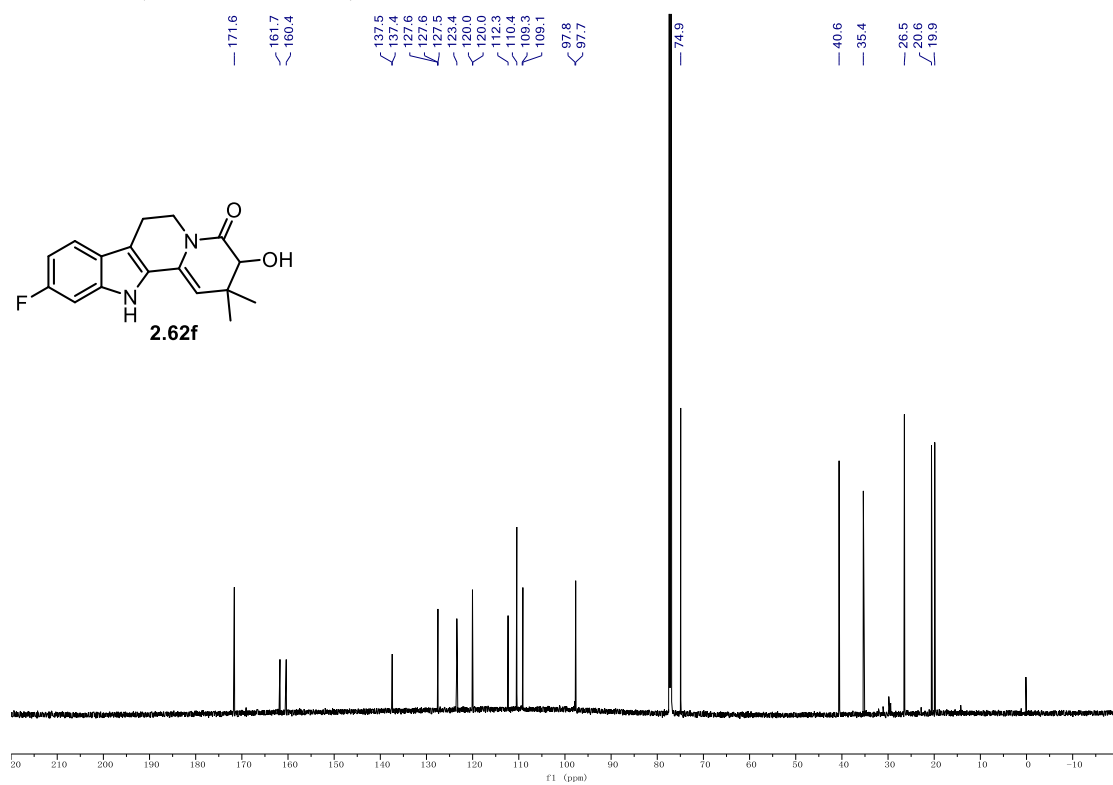
9.1. NMR Spectra

¹H NMR (500 MHz, CDCl₃) of **2.62e**.



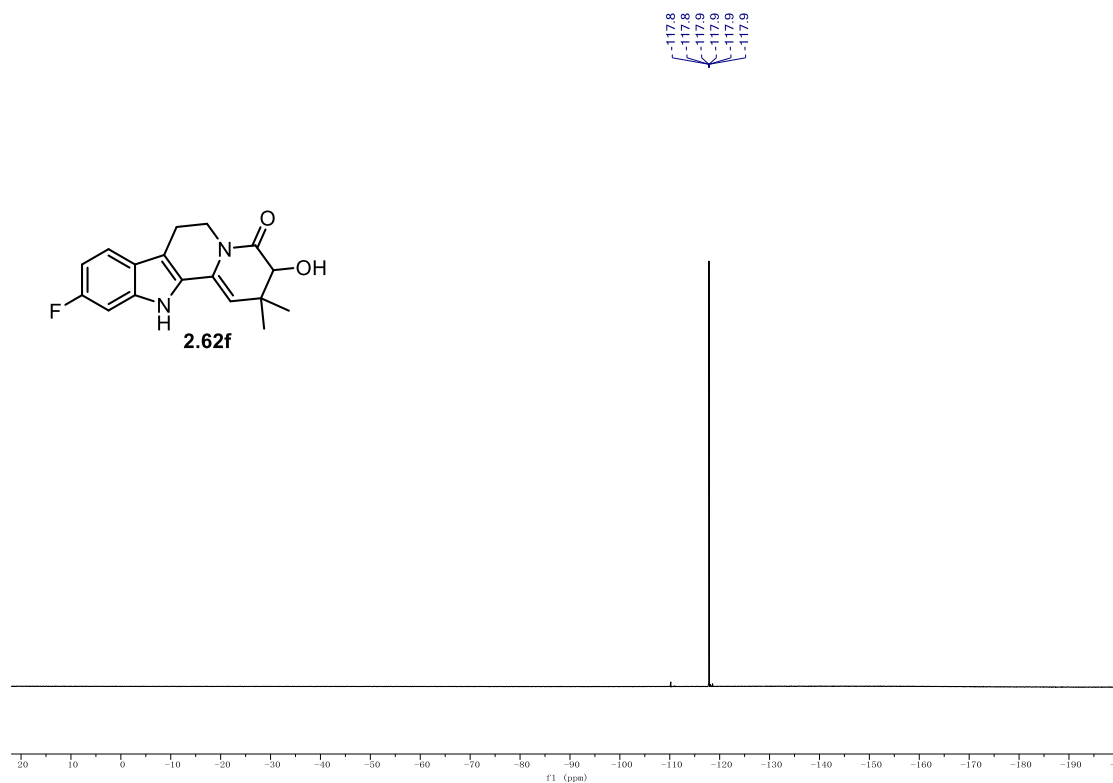
¹³C NMR (126 MHz, CDCl₃) of **2.62e**.



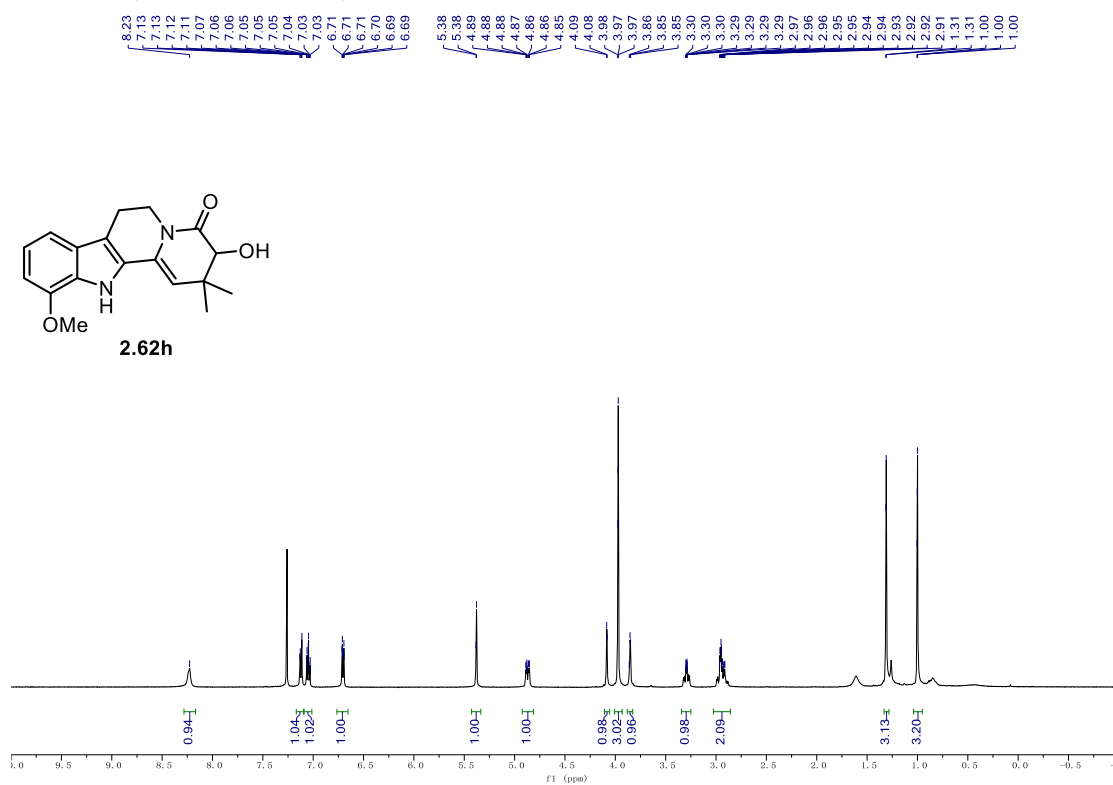
^1H NMR (500 MHz, CDCl_3) of **2.62f.** **^{13}C NMR (176 MHz, CDCl_3) of **2.62f**.**

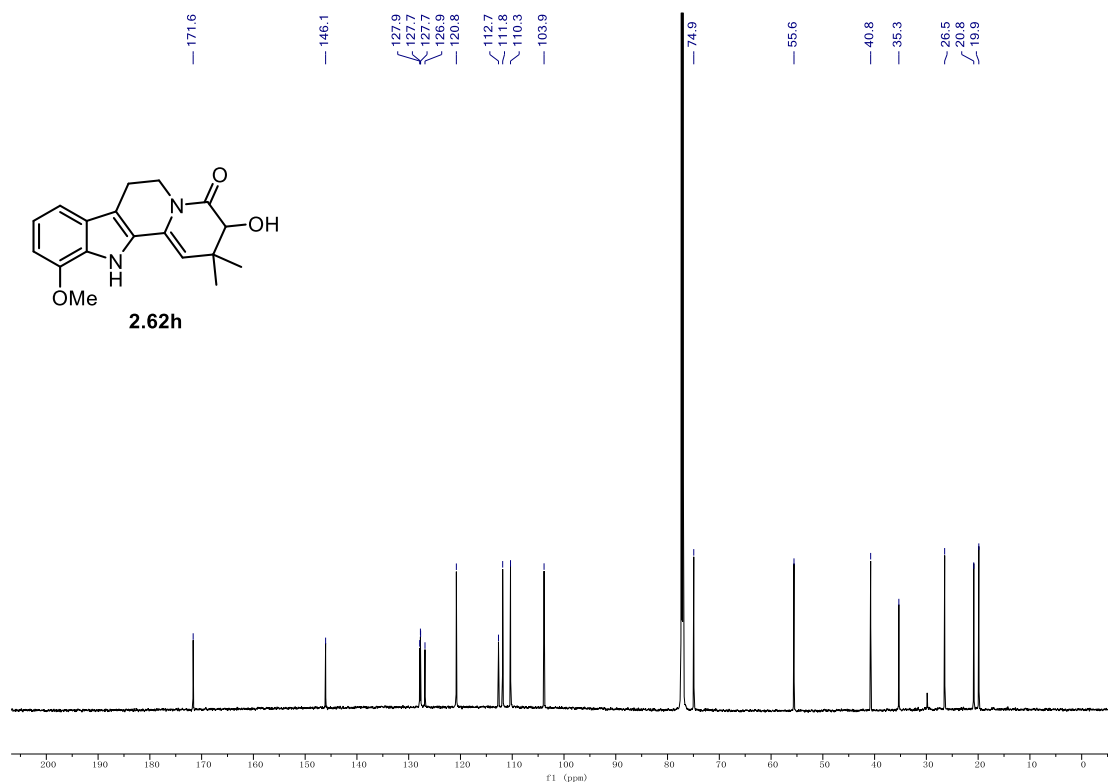
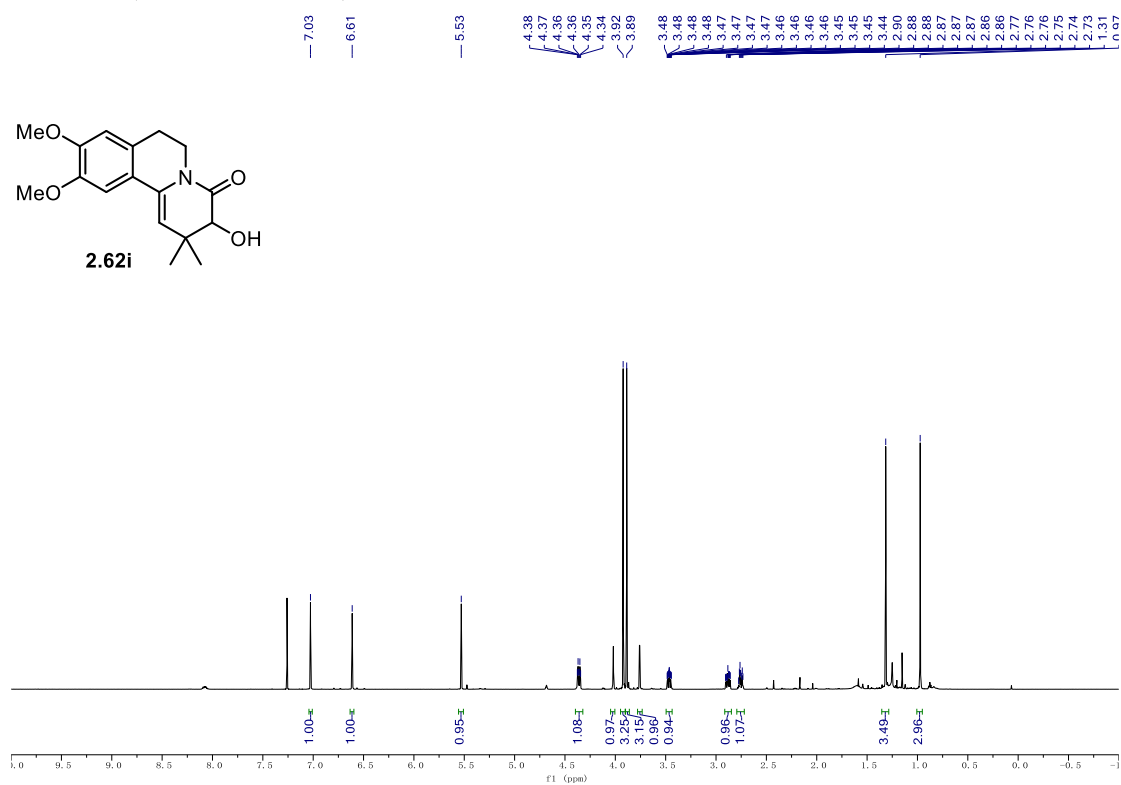
9.1. NMR Spectra

^{19}F NMR (565 MHz, CDCl_3) of **2.62f**.



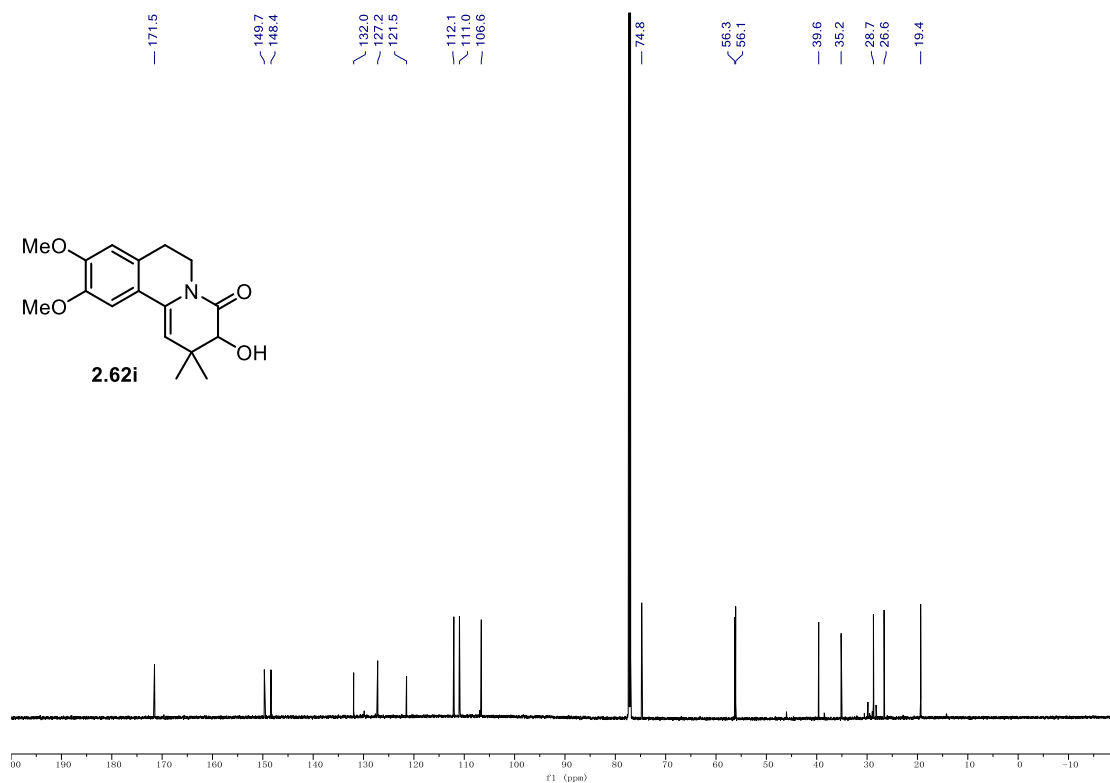
^1H NMR (500 MHz, CDCl_3) of **2.62h**.



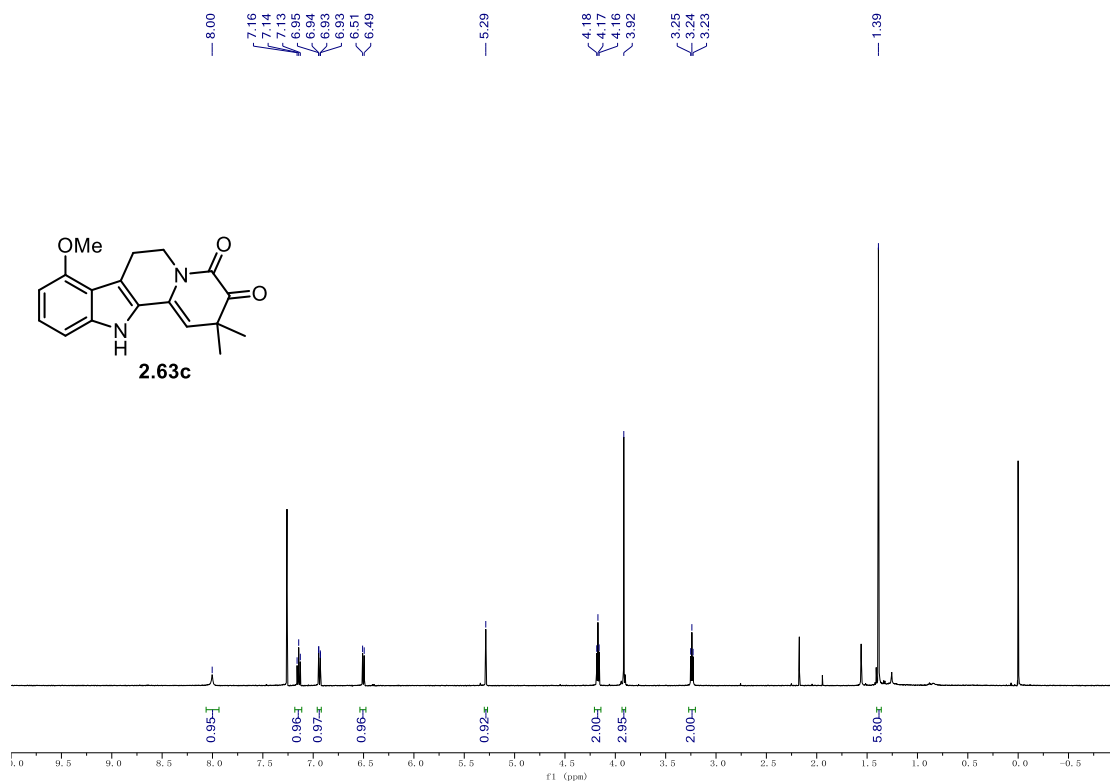
^{13}C NMR (176 MHz, CDCl_3) of **2.62h**. ^1H NMR (500 MHz, CDCl_3) of **2.62i**.

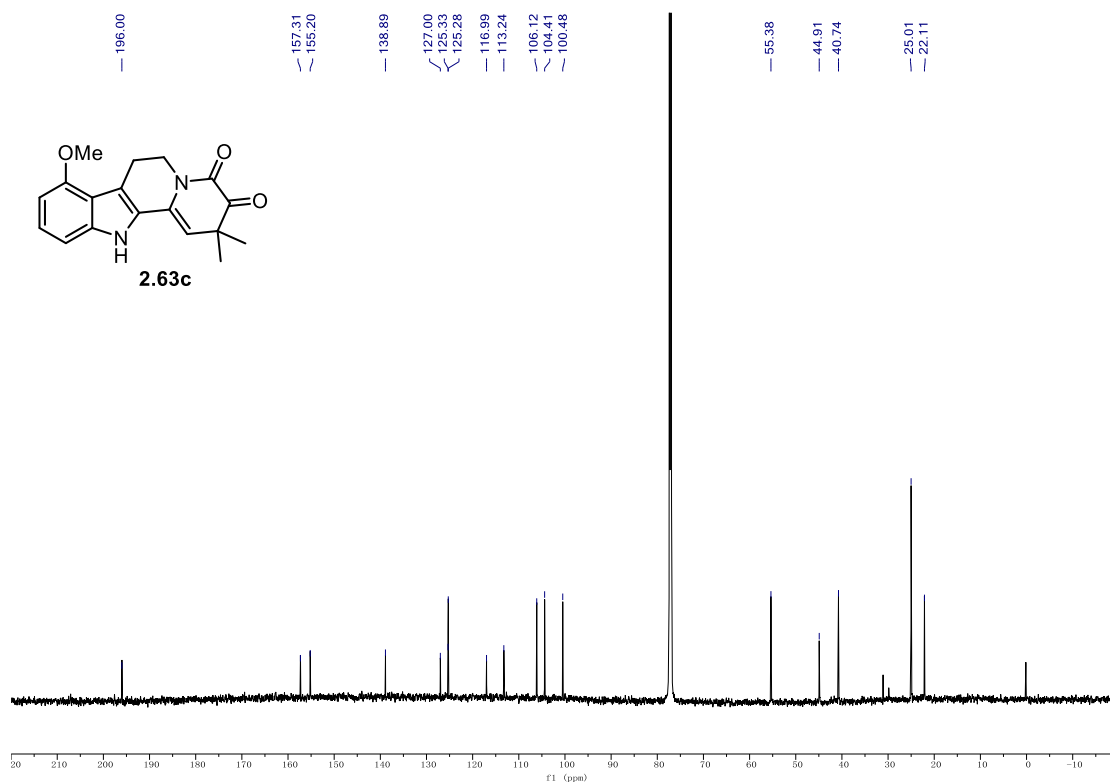
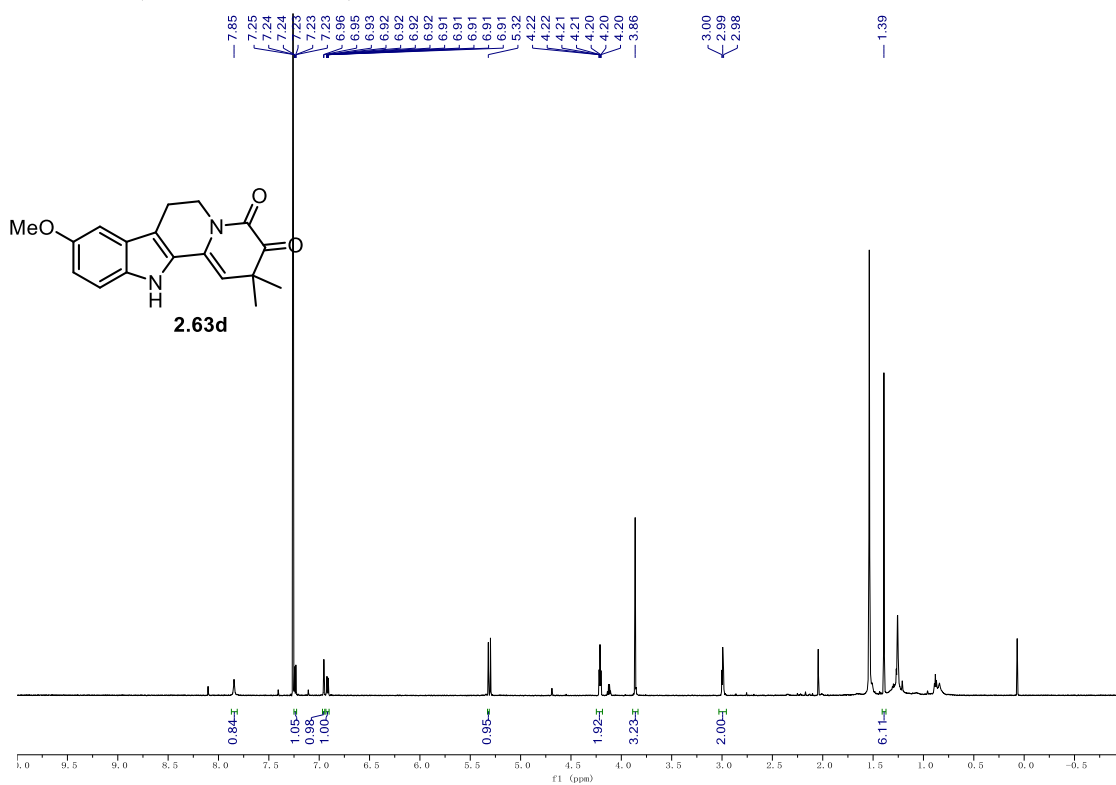
9.1. NMR Spectra

^{13}C NMR (126 MHz, CDCl_3) of **2.62i**.



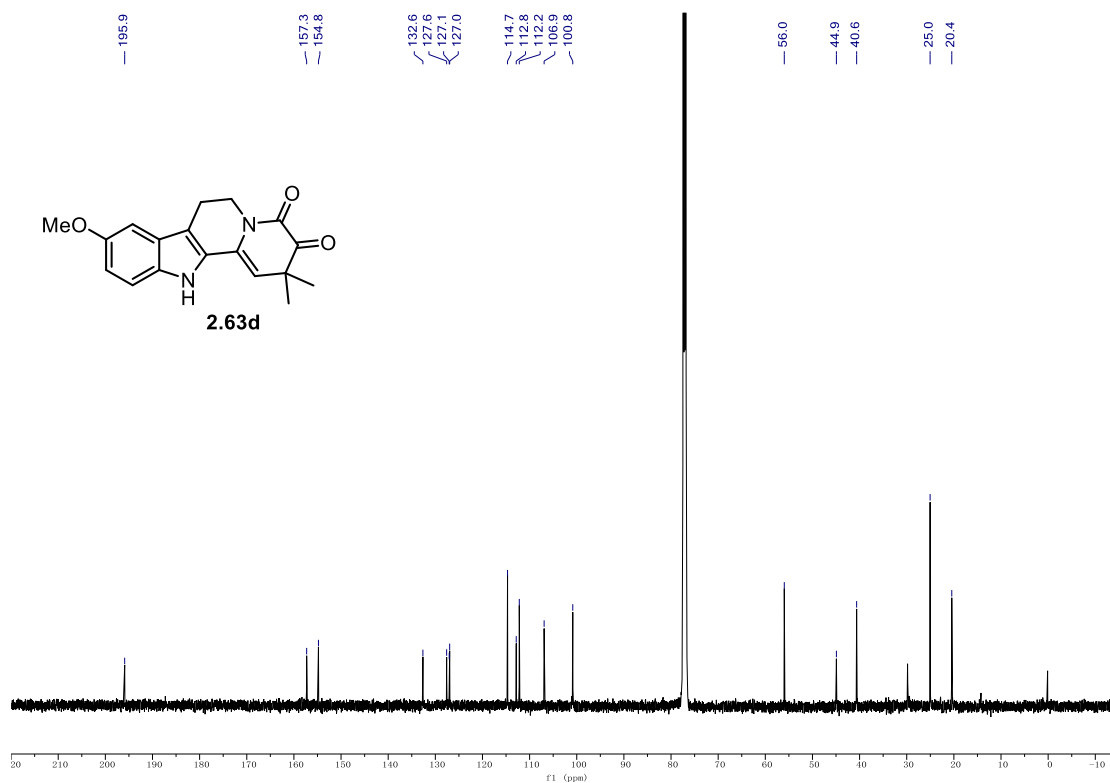
^1H NMR (500 MHz, CDCl_3) of **2.63c**.



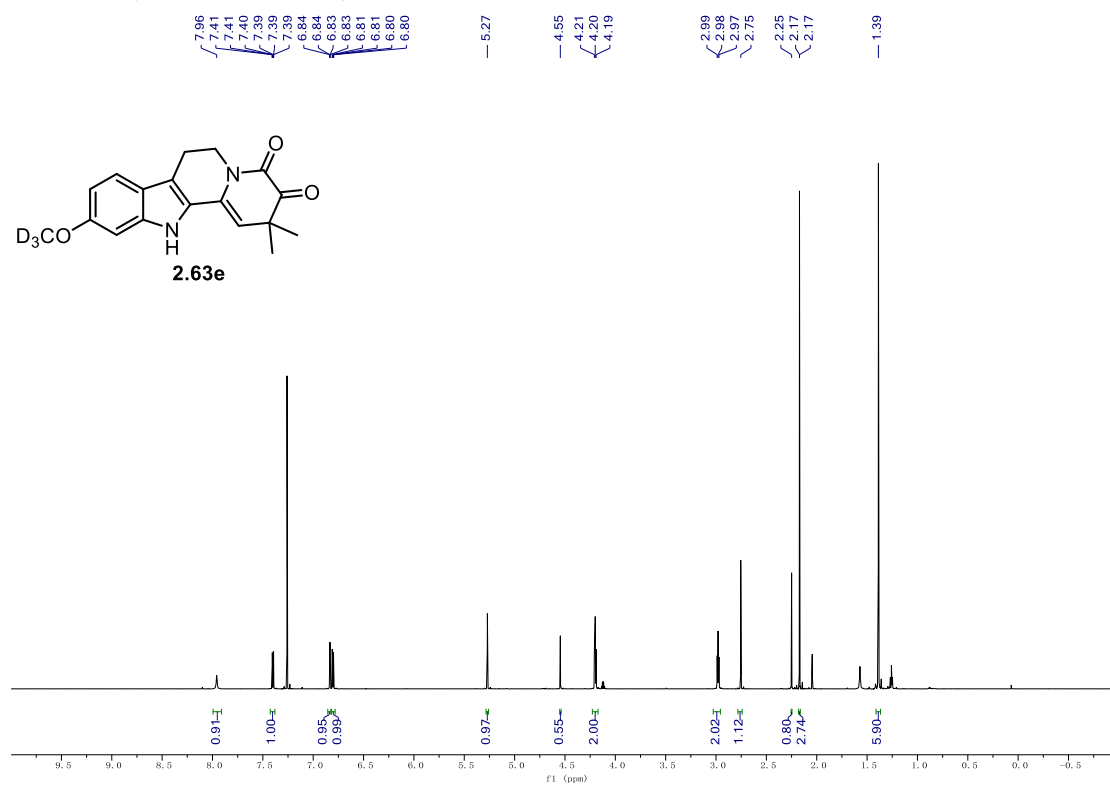
^{13}C NMR (126 MHz, CDCl_3) of **2.63c**. ^1H NMR (700 MHz, CDCl_3) of **2.63d**.

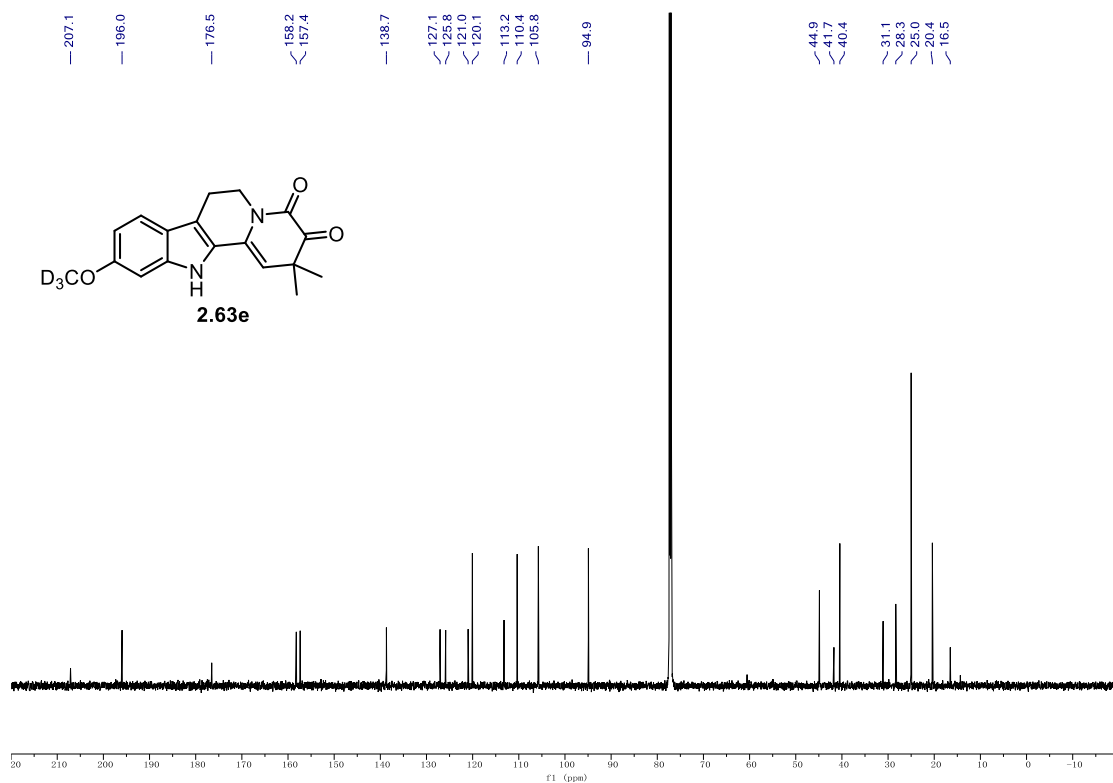
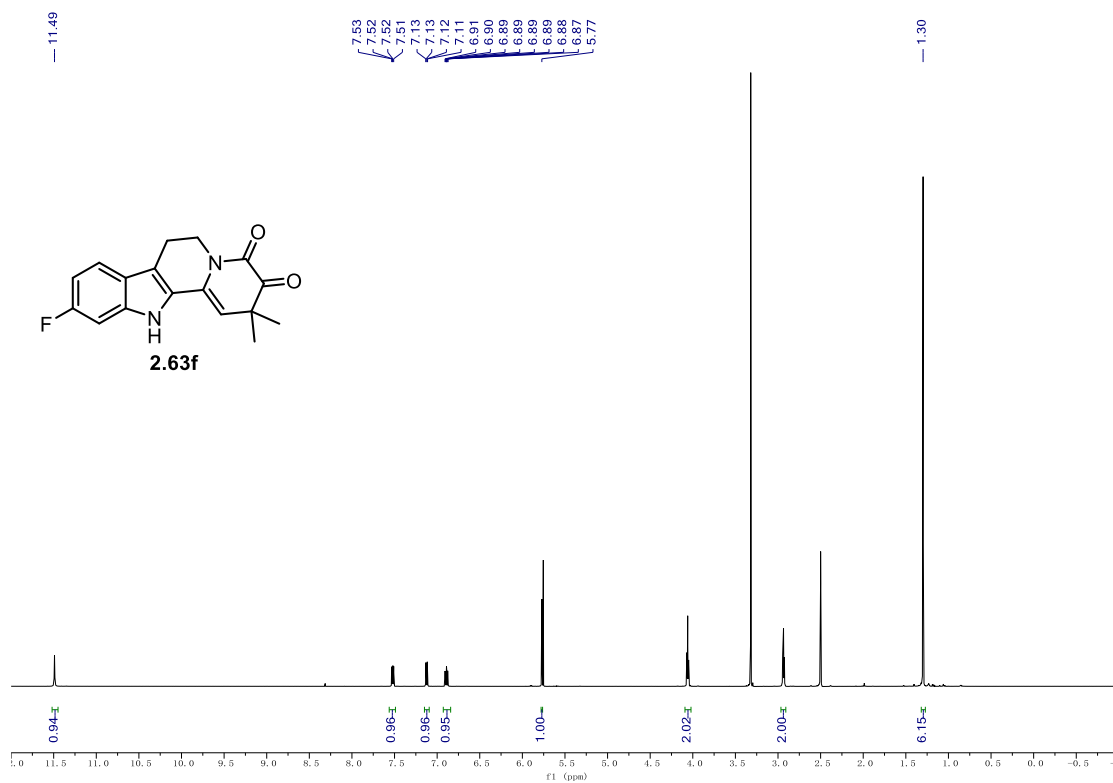
9.1. NMR Spectra

^{13}C NMR (126 MHz, CDCl_3) of **2.63d**.



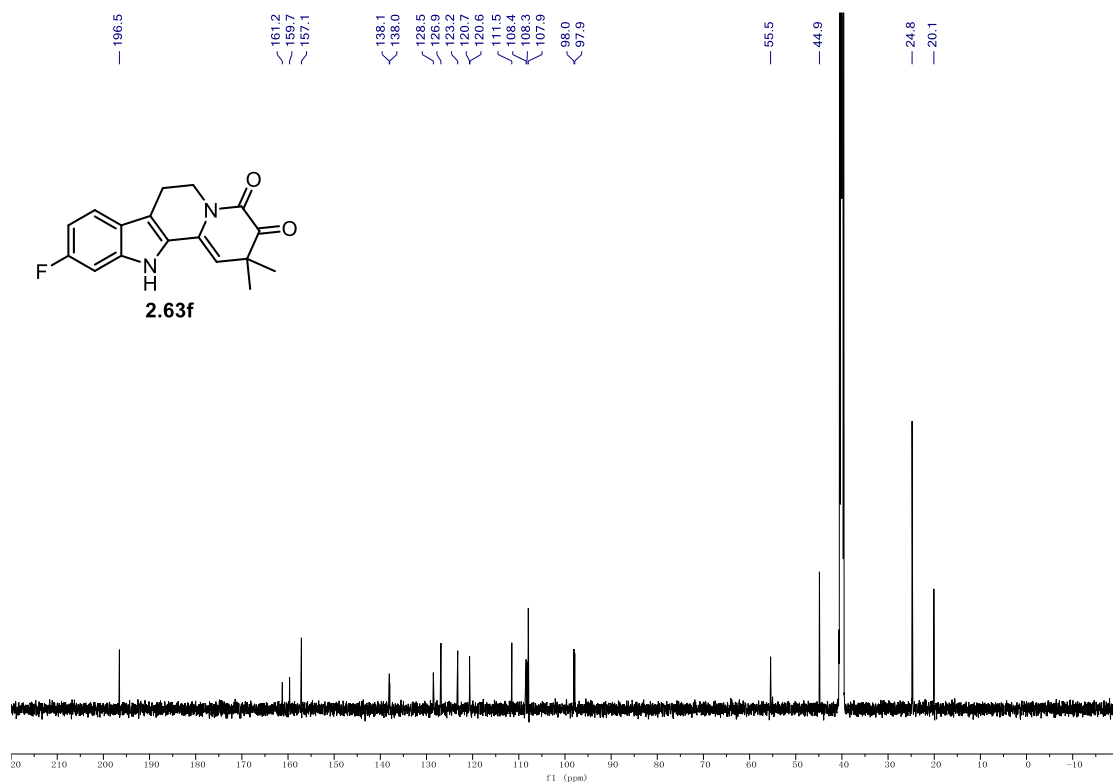
^1H NMR (700 MHz, CDCl_3) of **2.63e**.



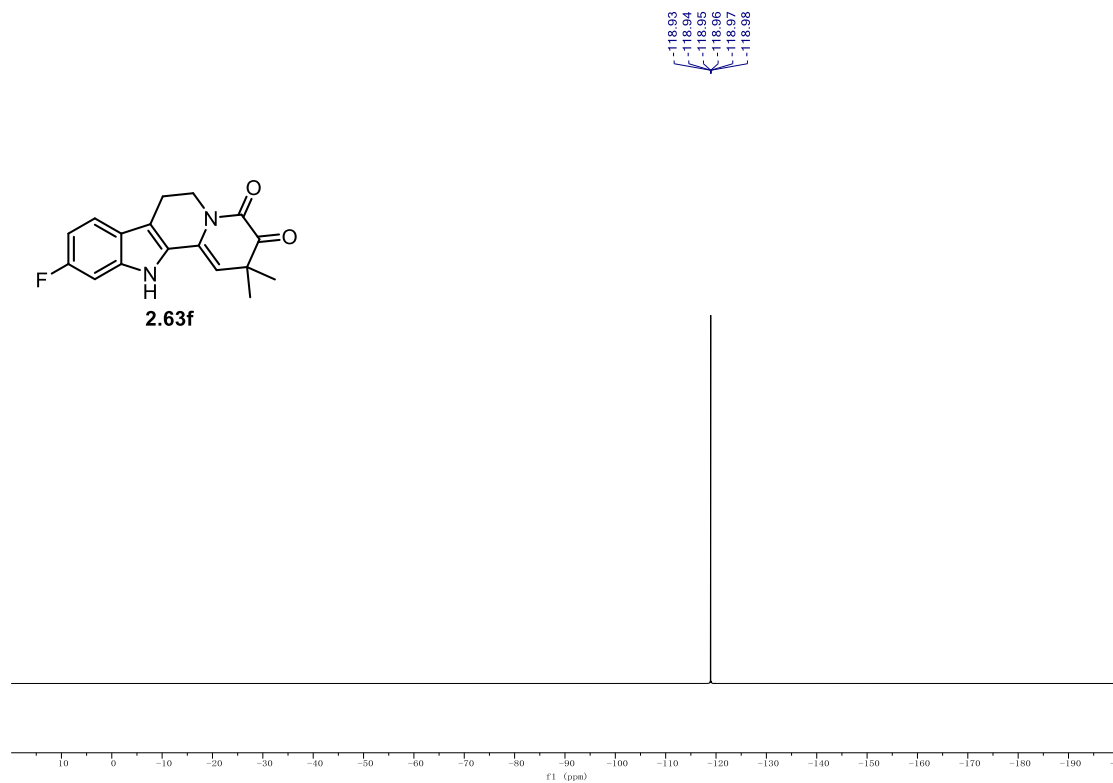
^{13}C NMR (126 MHz, CDCl_3) of **2.63e**. ^1H NMR (600 MHz, d_6 -DMSO) of **2.63f**.

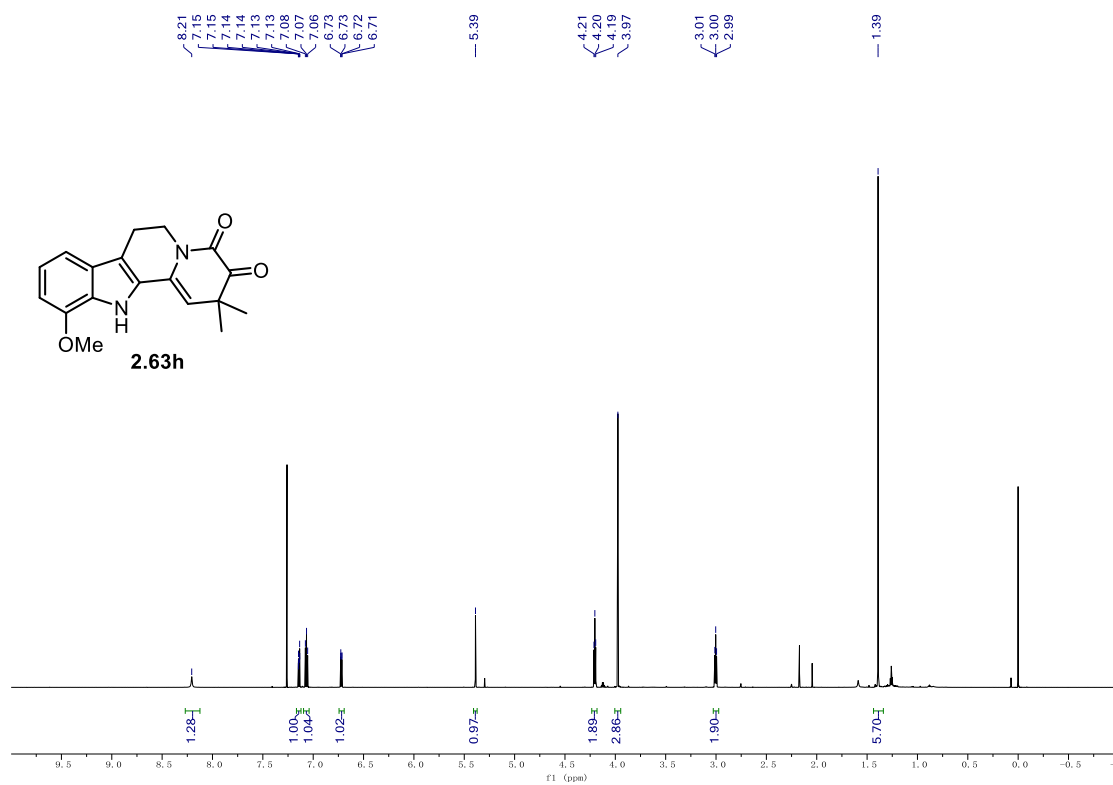
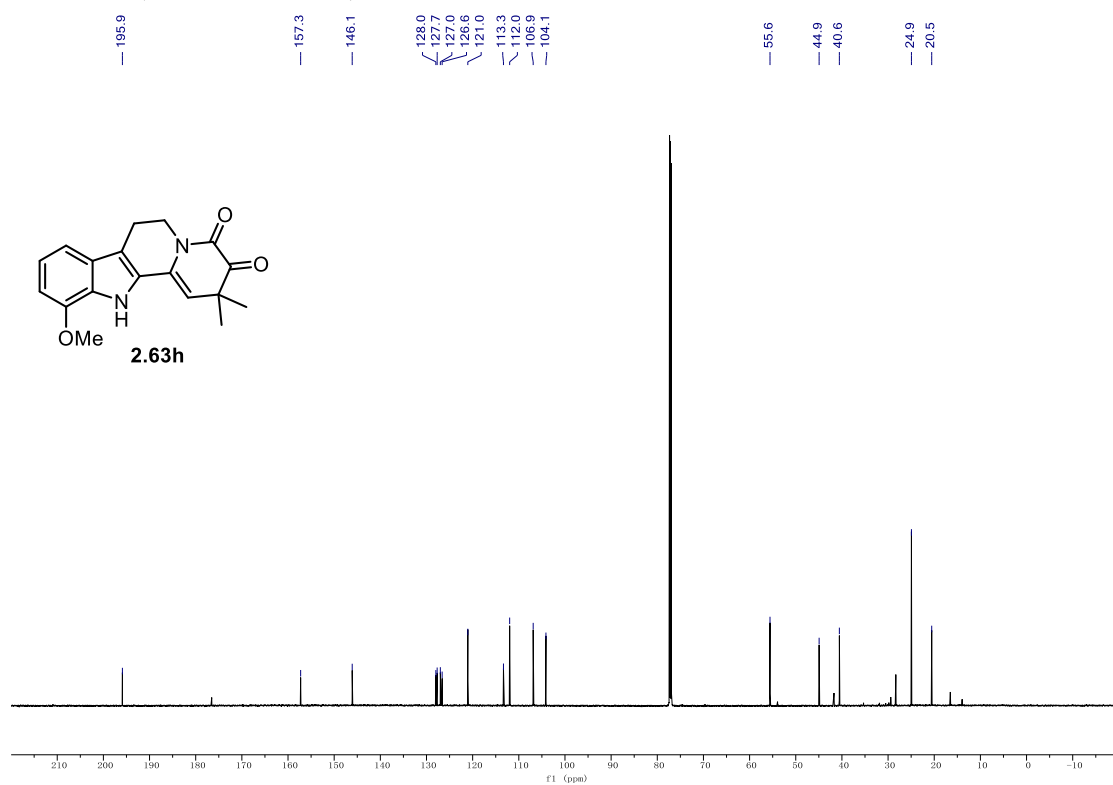
9.1. NMR Spectra

^{13}C NMR (151 MHz, d_6 -DMSO) of **2.63f**.



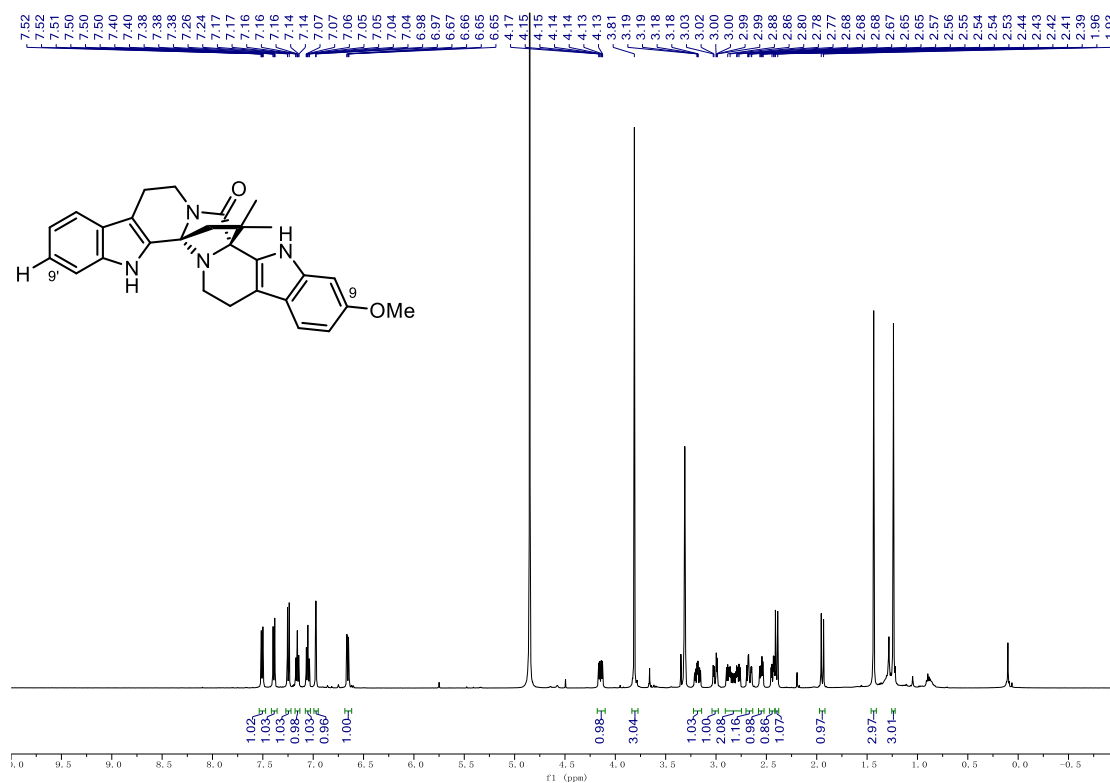
^{19}F NMR (565 MHz, d_6 -DMSO) of **2.63f**.



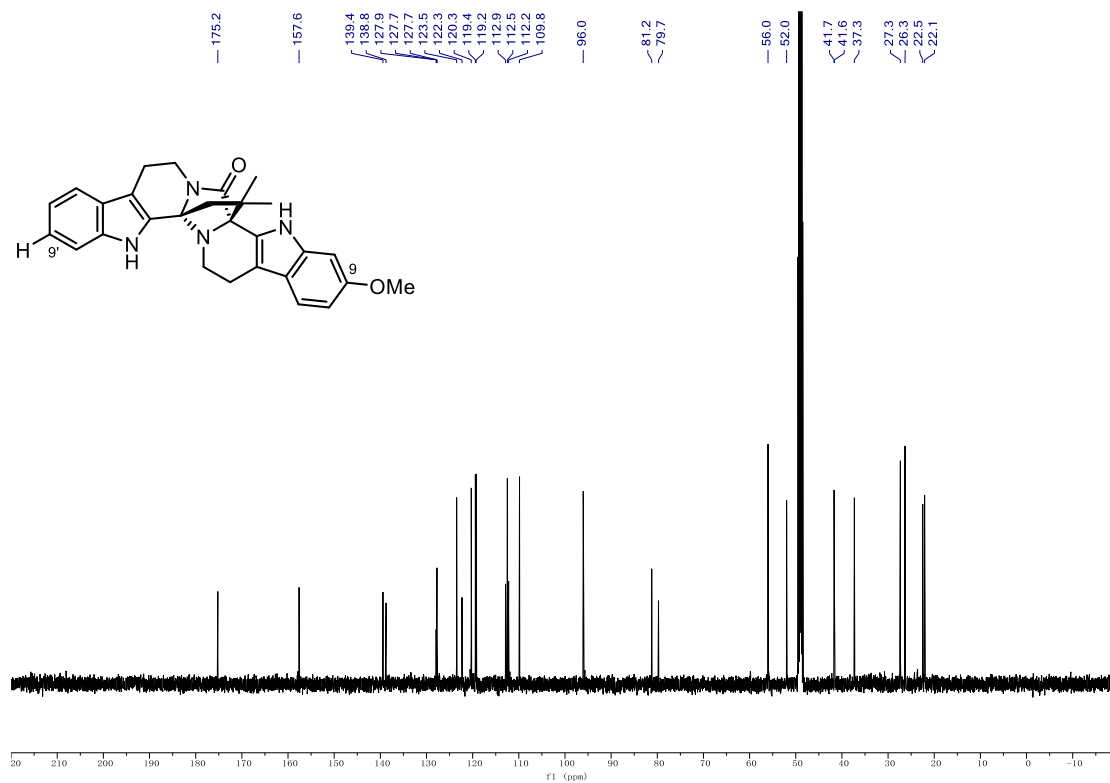
^1H NMR (700 MHz, CDCl_3) of **2.63h.** **^{13}C NMR (176 MHz, CDCl_3) of **2.63h**.**

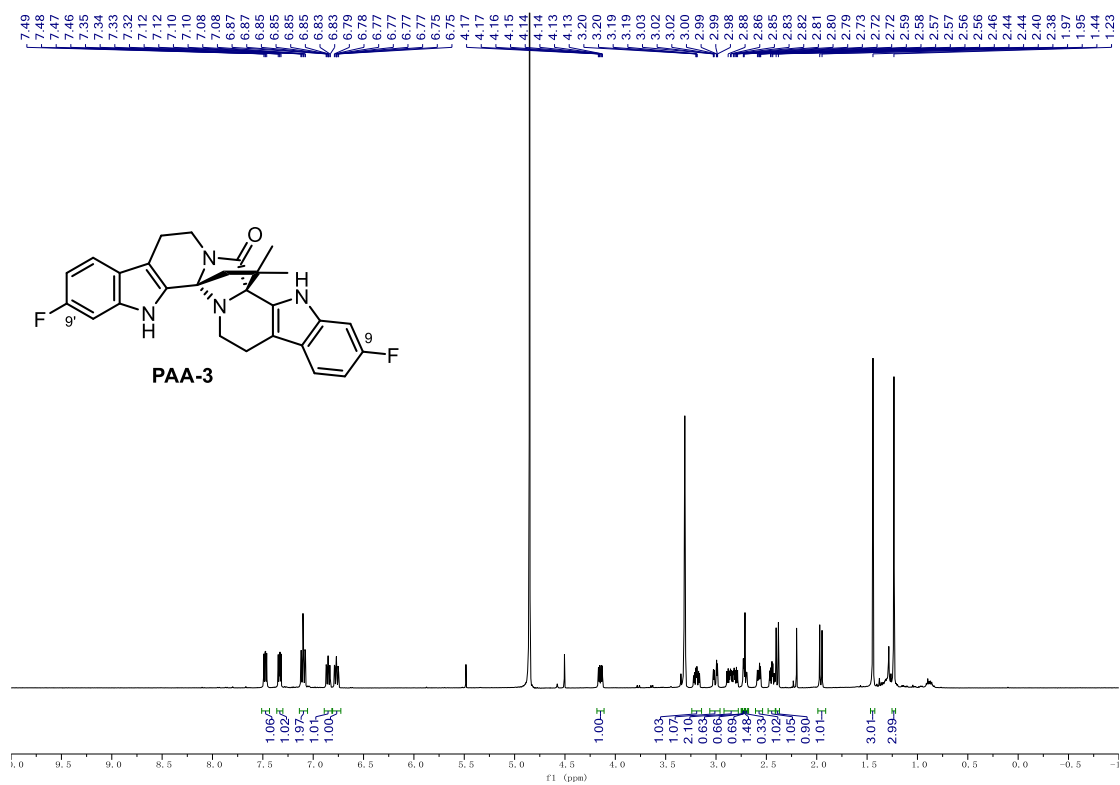
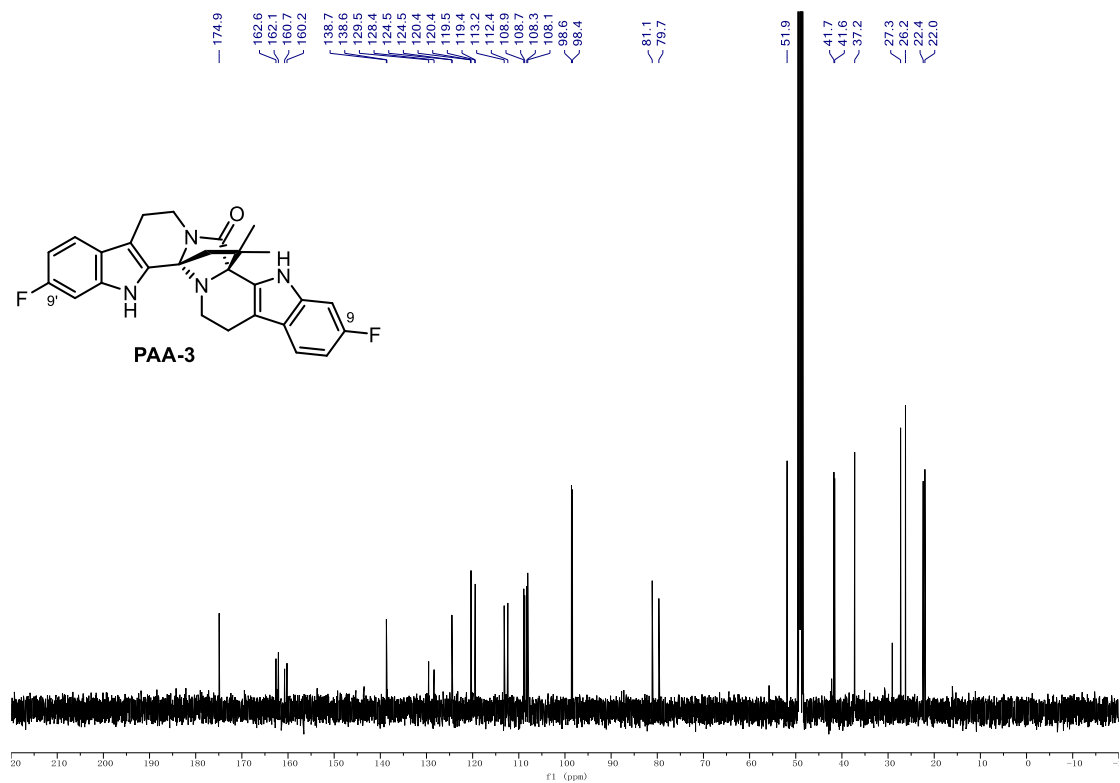
9.1. NMR Spectra

^1H NMR (500 MHz, CD_3OD) of PAA-1.



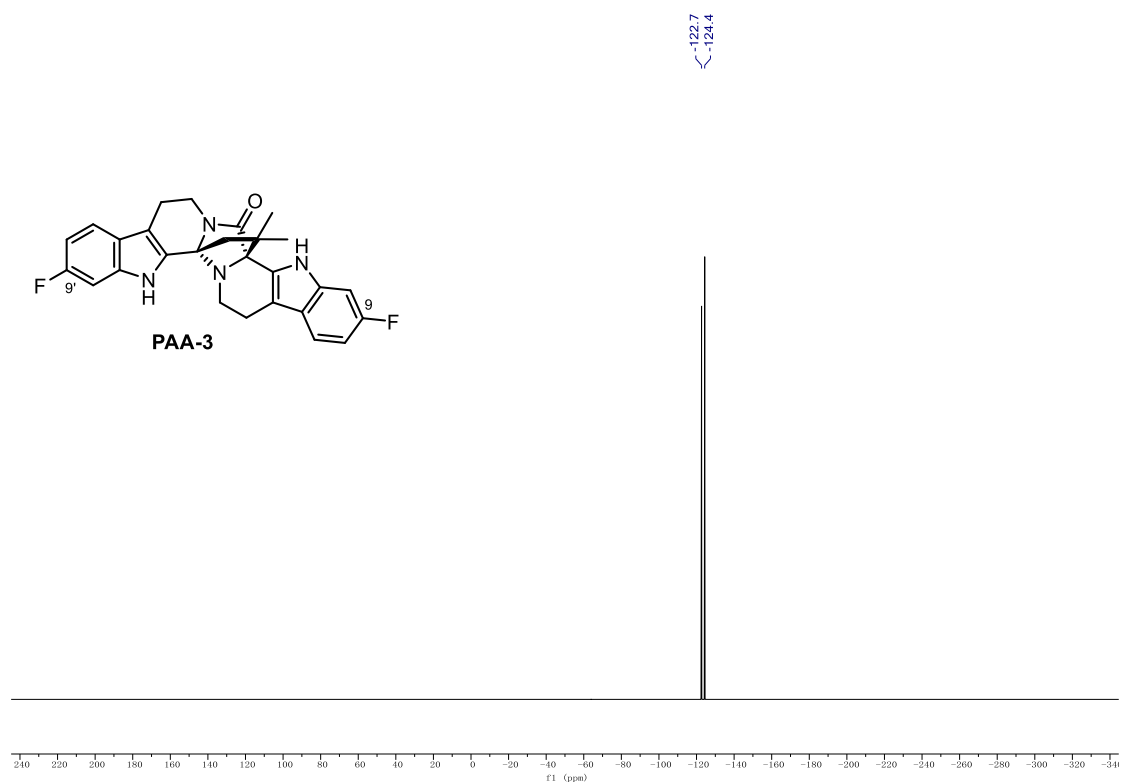
^{13}C NMR (126 MHz, CD_3OD) of PAA-1.



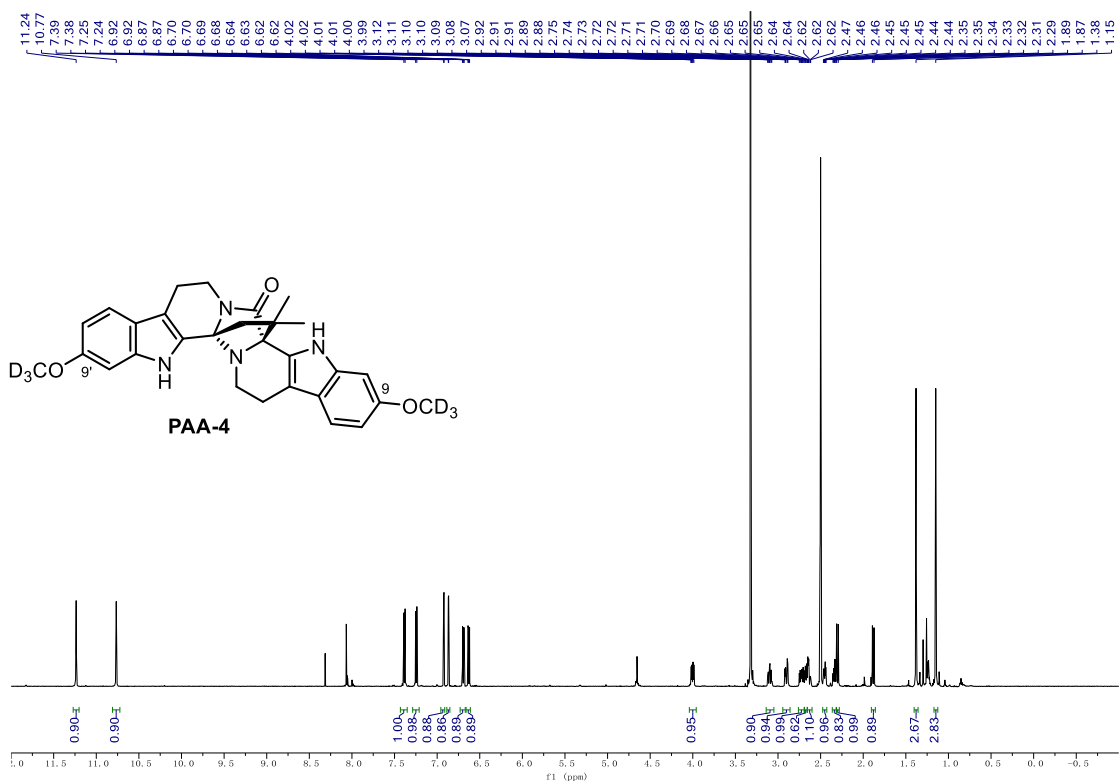
¹H NMR (500 MHz, CD₃OD) of PAA-3.**¹³C NMR (126 MHz, CD₃OD) of PAA-3.**

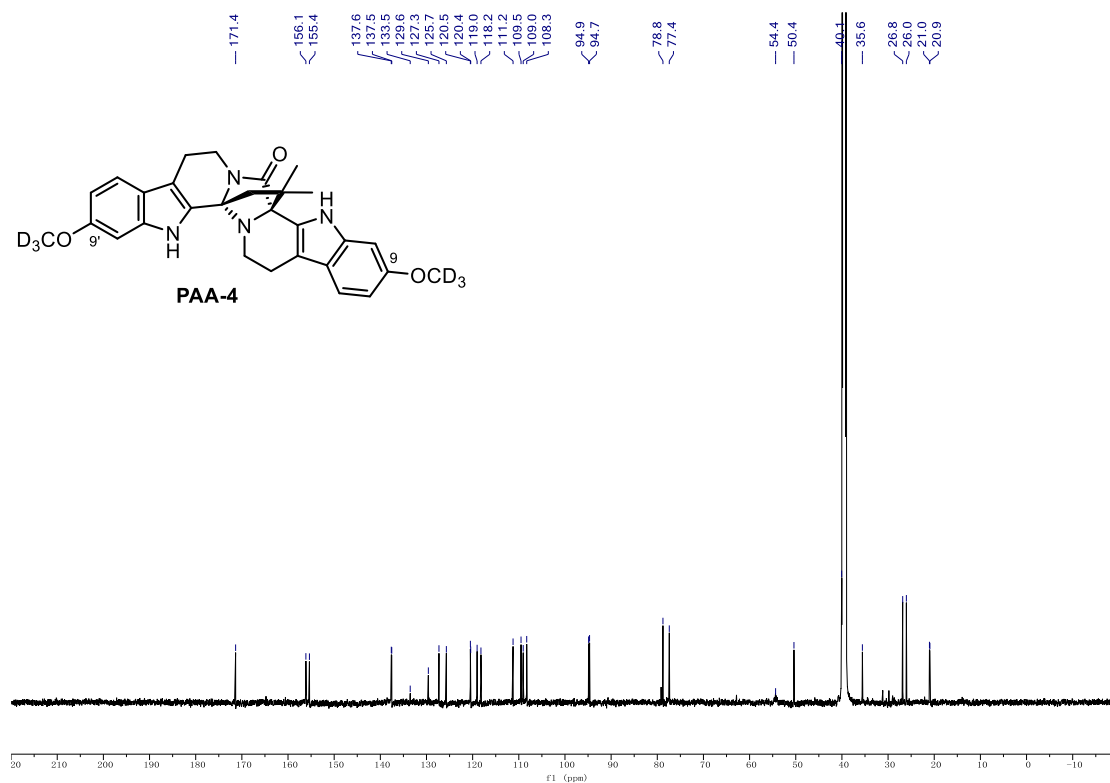
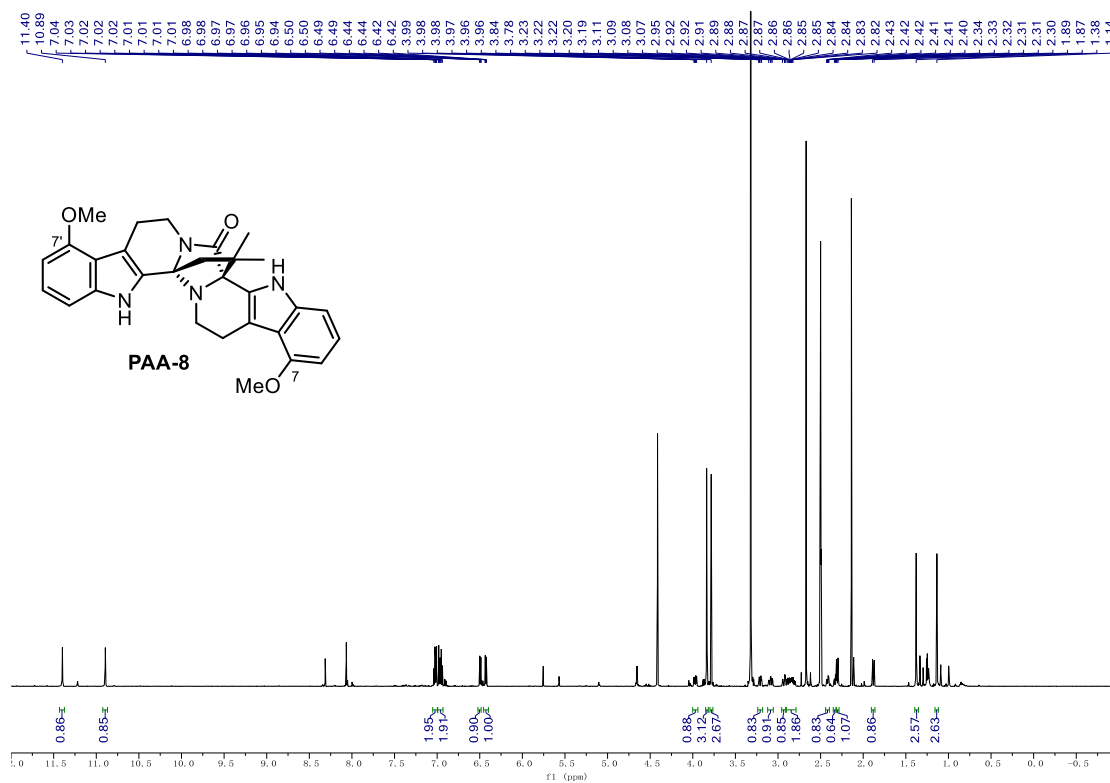
9.1. NMR Spectra

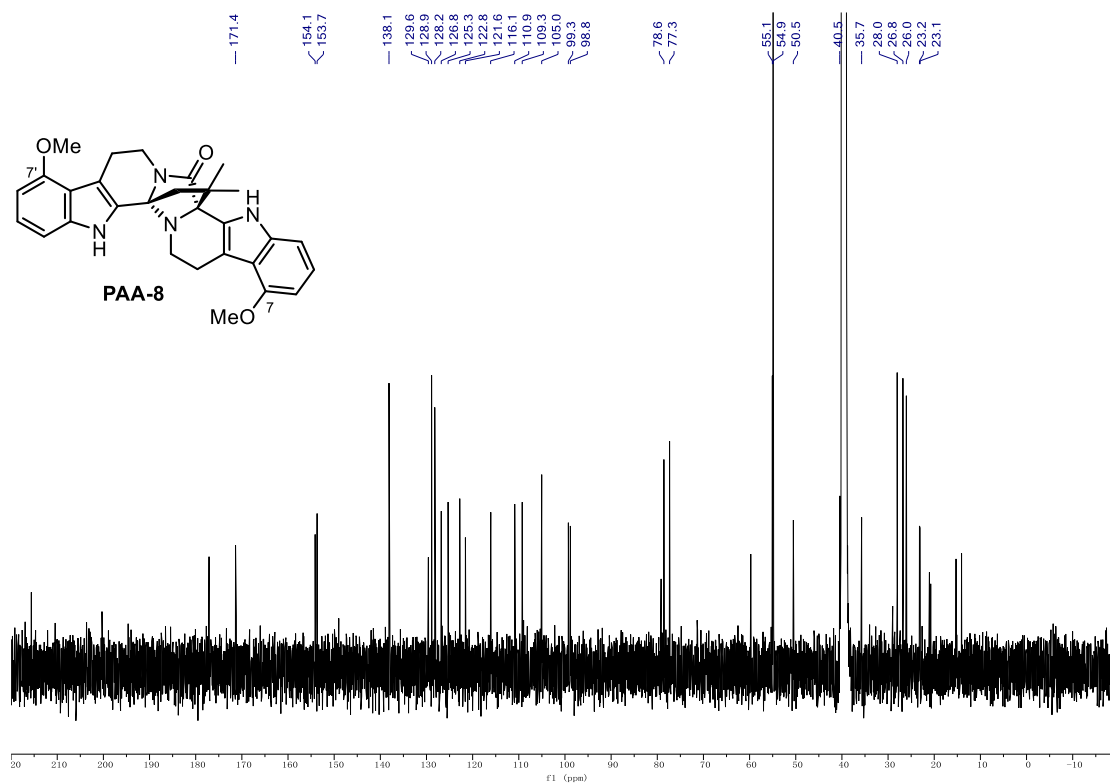
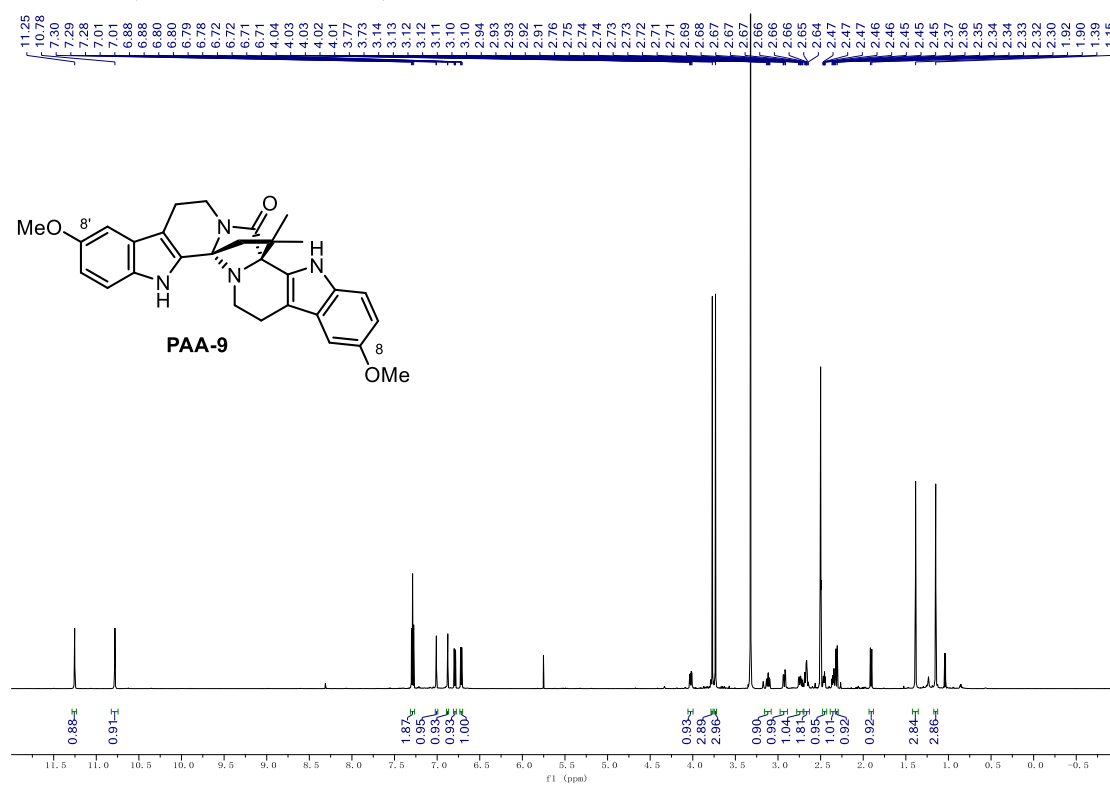
^{19}F NMR (471 MHz, CD_3OD) of PAA-3.



^1H NMR (600 MHz, d_6 -DMSO) of PAA-4.

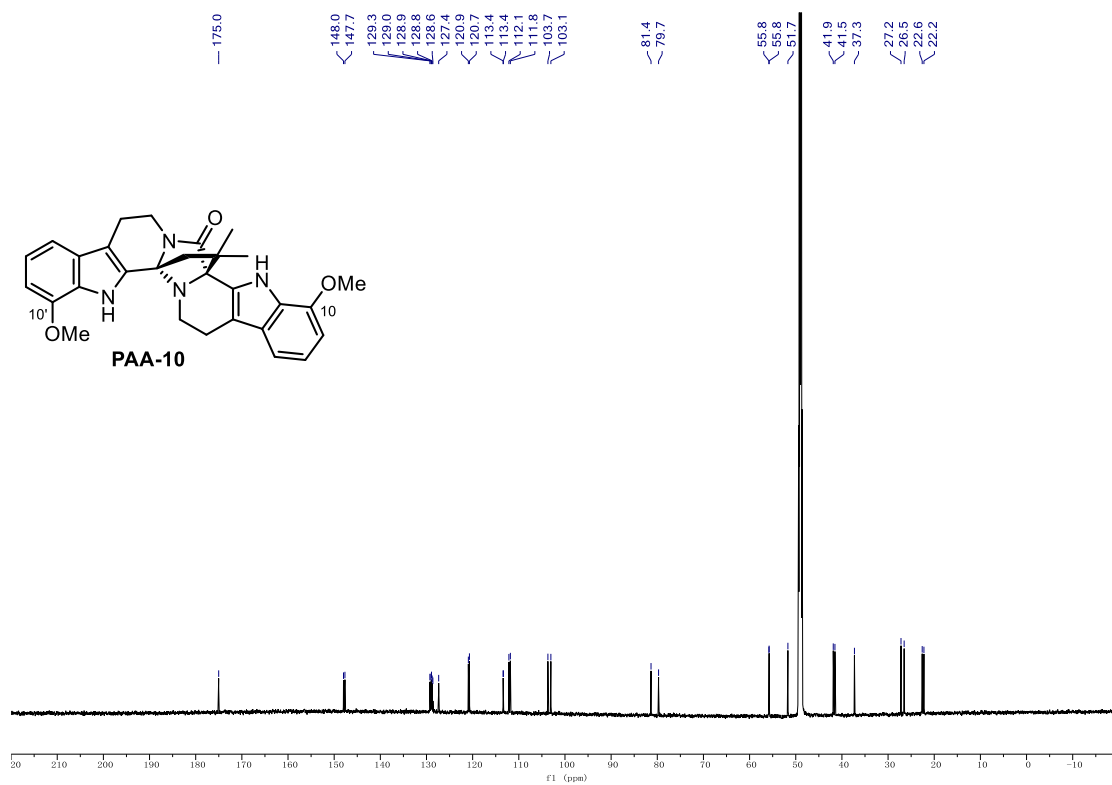


^{13}C NMR (151 MHz, d_6 -DMSO) of PAA-4. ^1H NMR (600 MHz, d_6 -DMSO) of PAA-8.

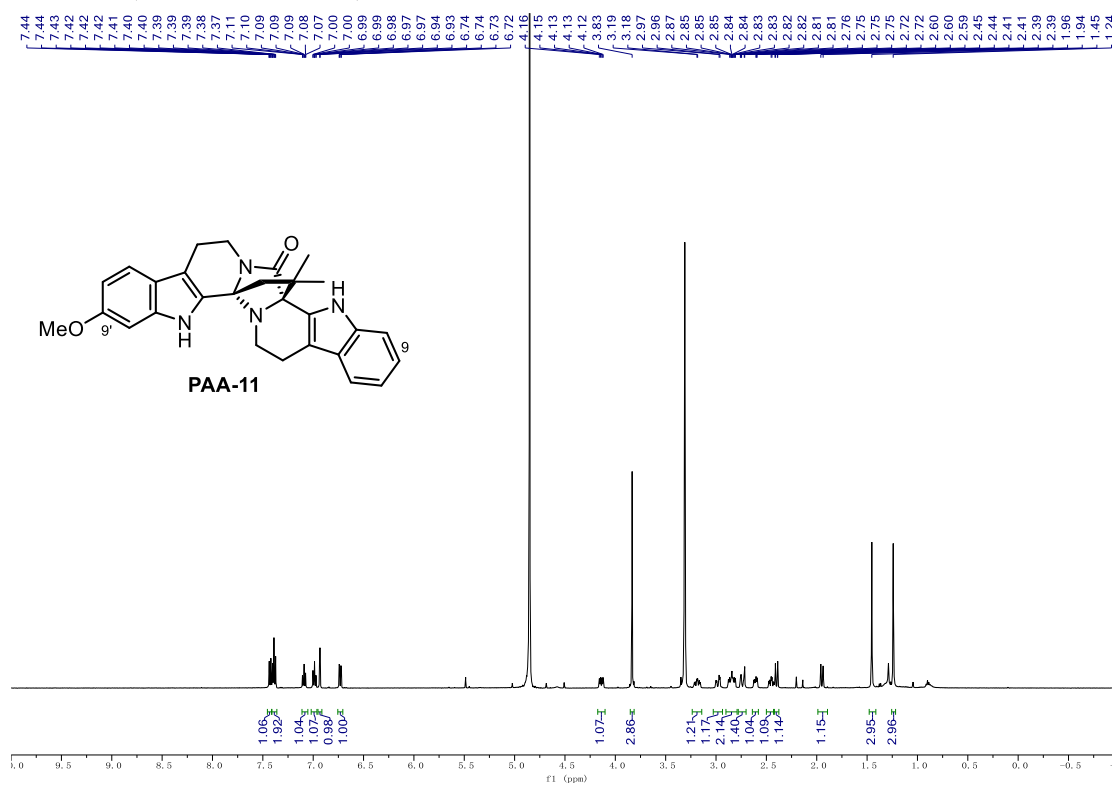
^{13}C NMR (151 MHz, d_6 -DMSO) of PAA-8. ^1H NMR (700 MHz, d_6 -DMSO) of PAA-9.

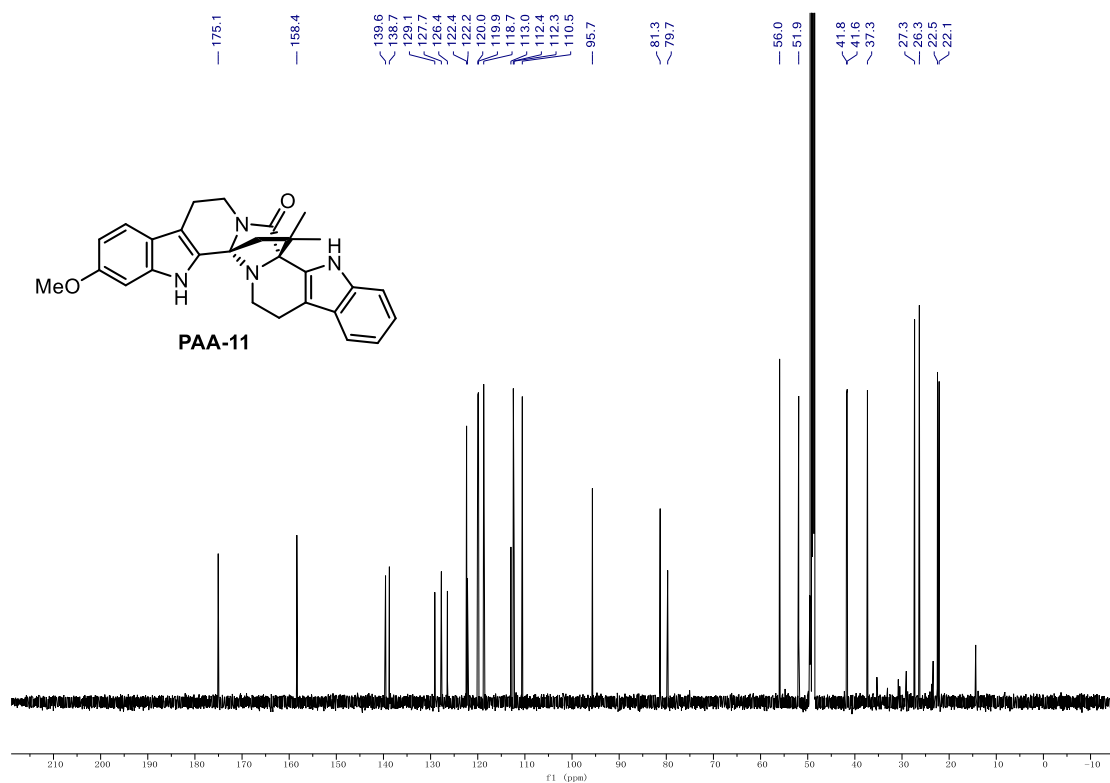
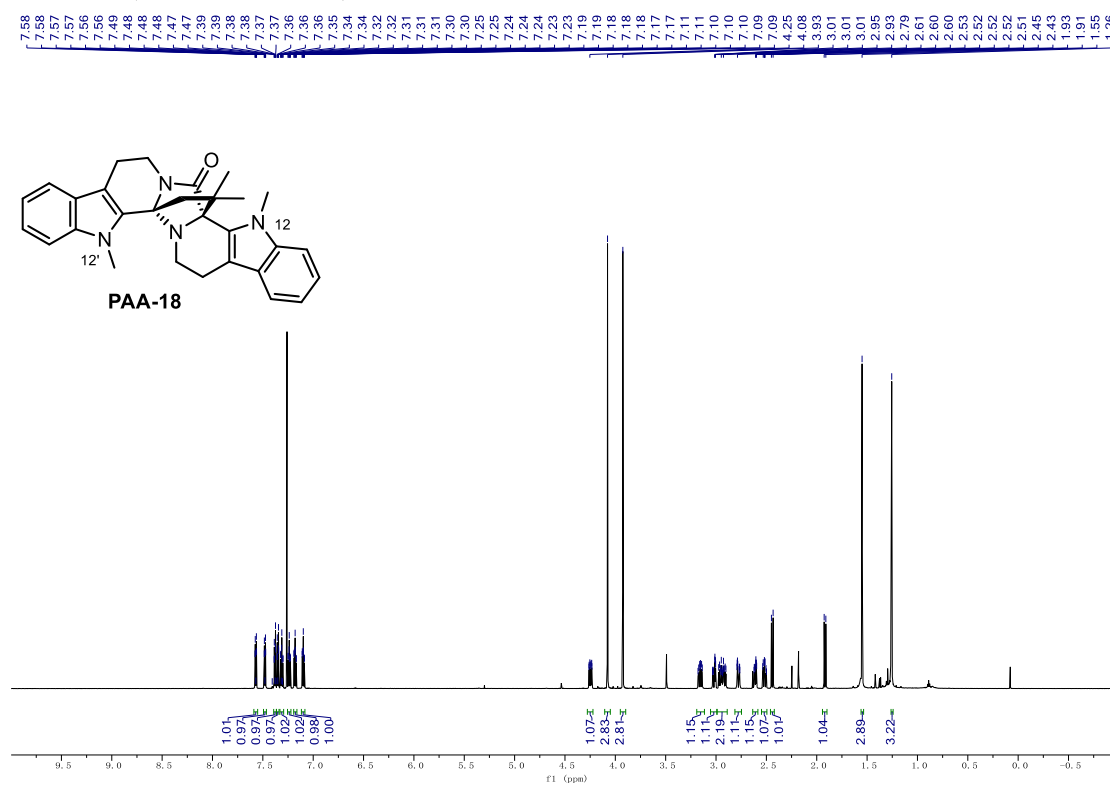
9.1. NMR Spectra

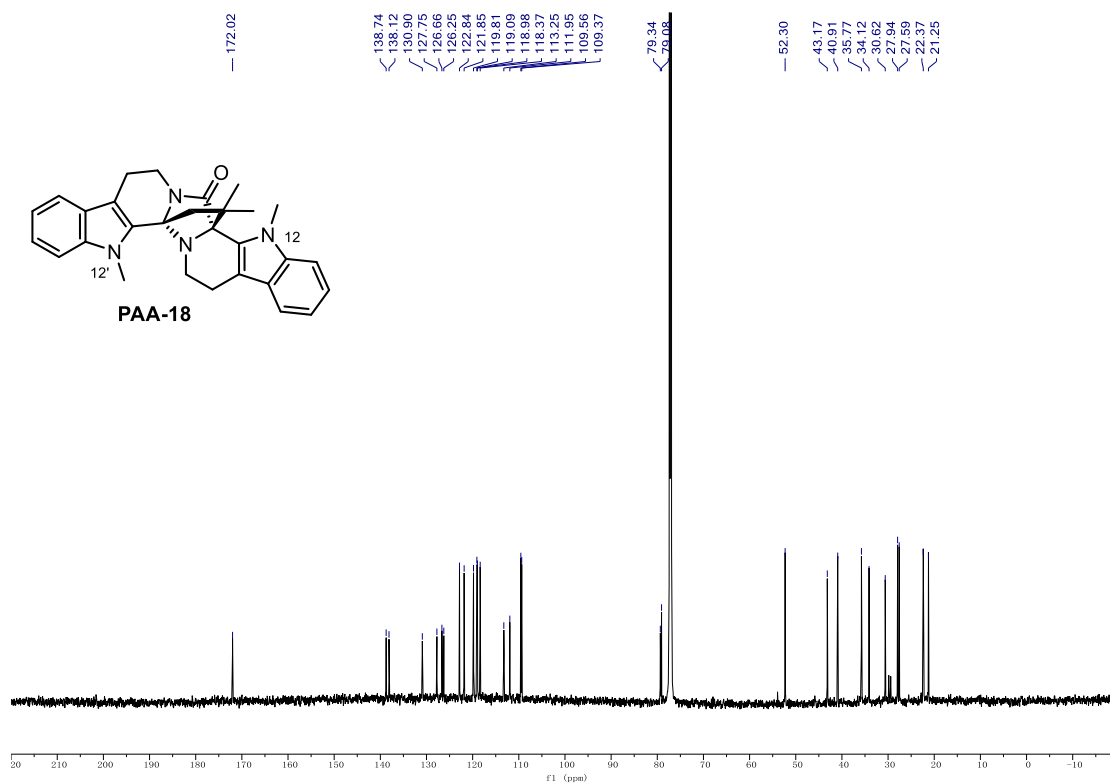
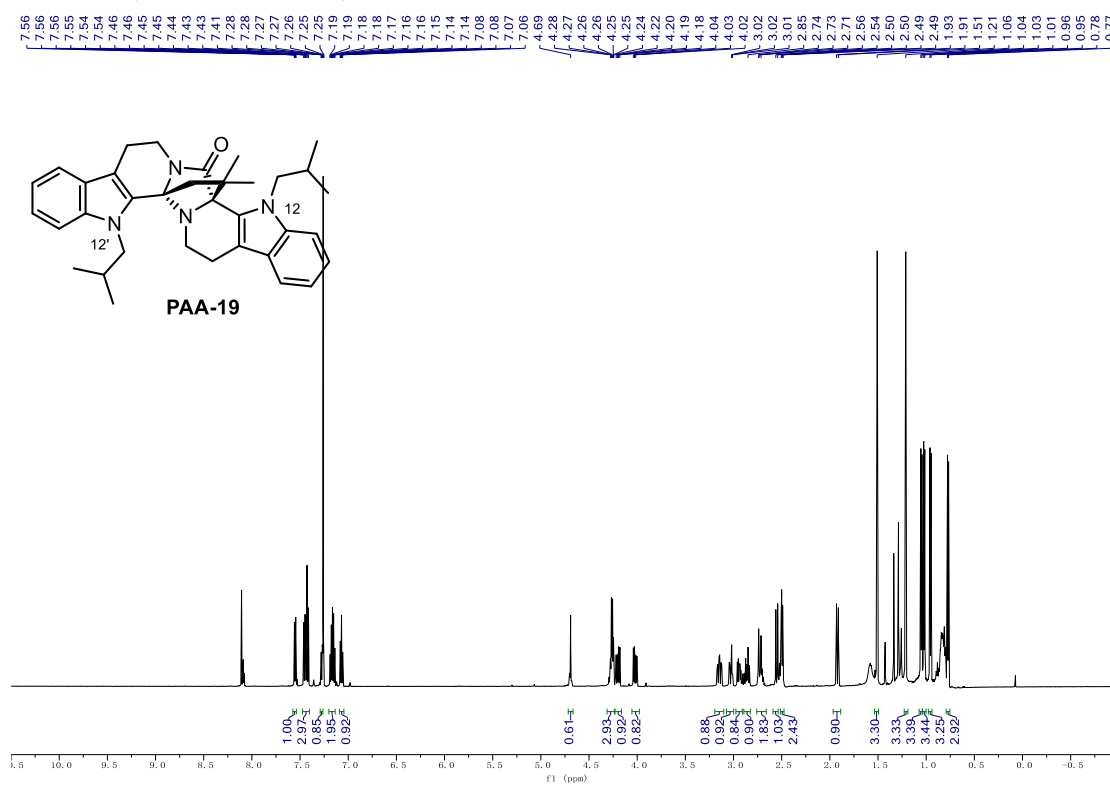
^{13}C NMR (176 MHz, CD_3OD) of PAA-10.

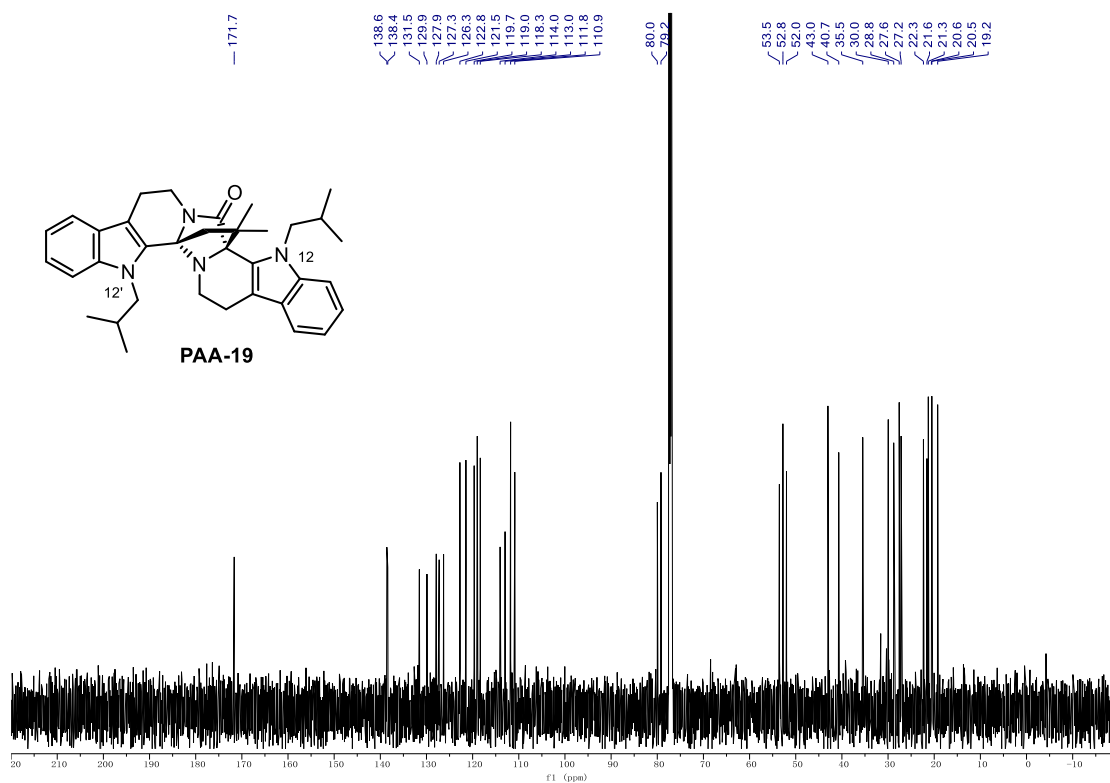
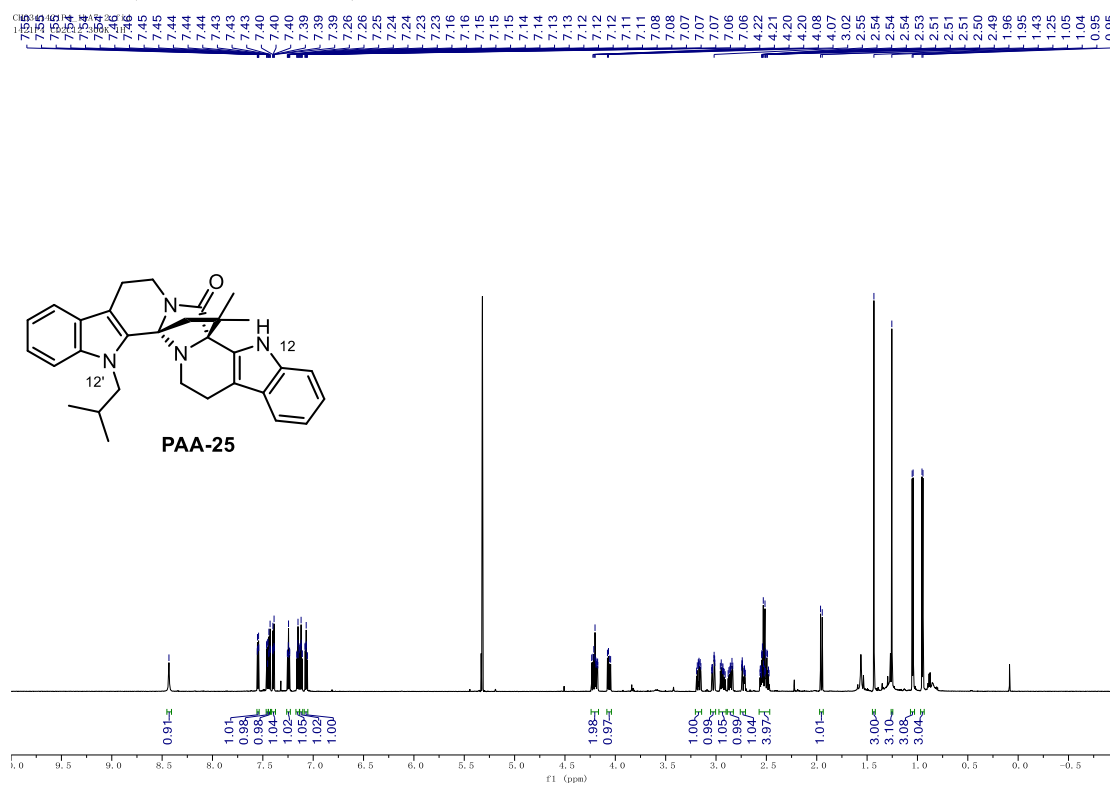


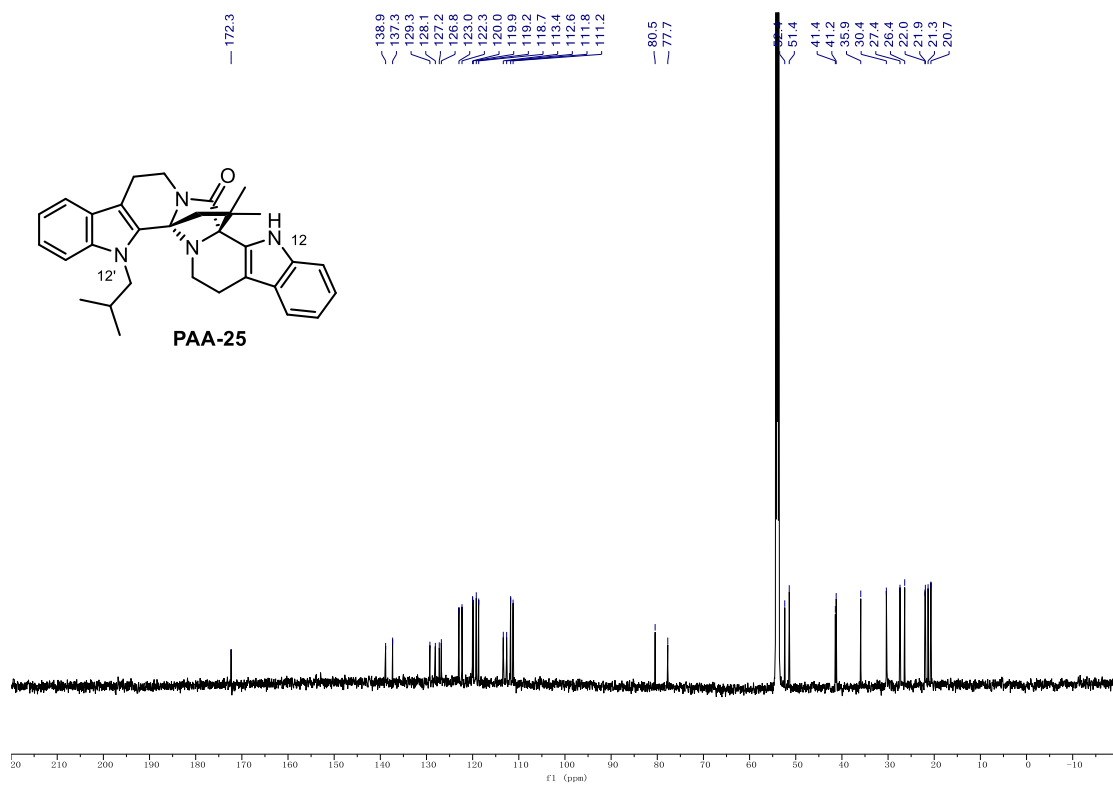
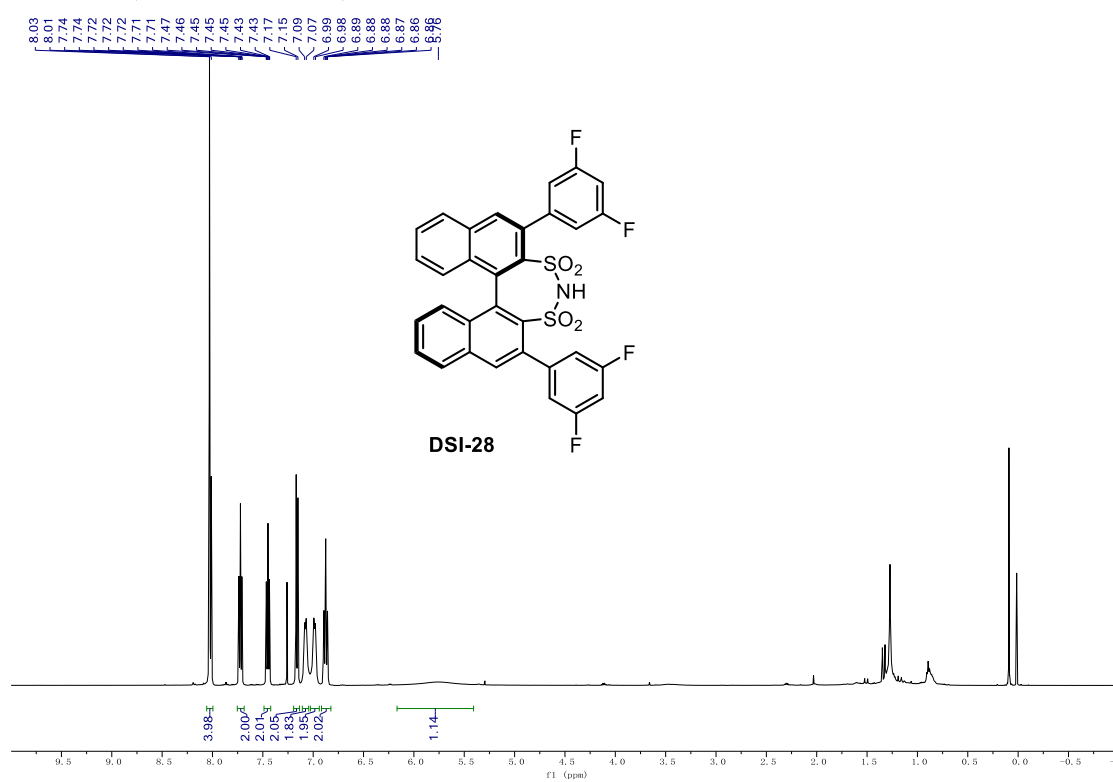
^1H NMR (500 MHz, CD_3OD) of PAA-11.

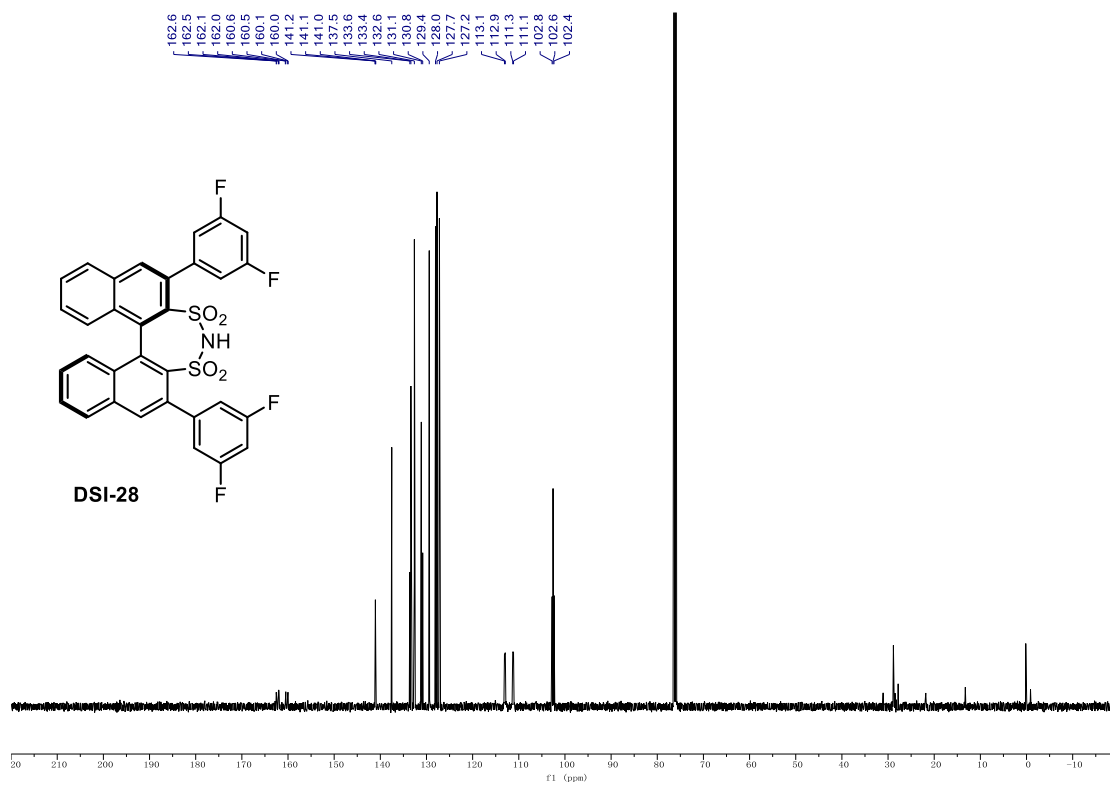
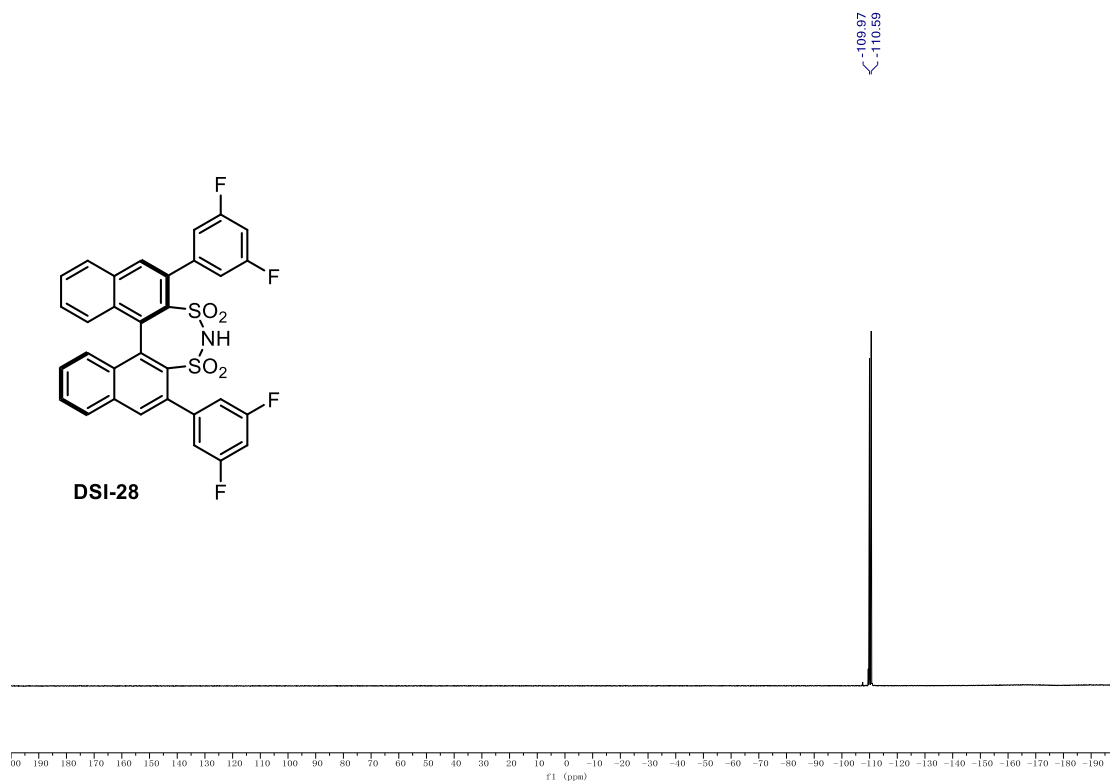


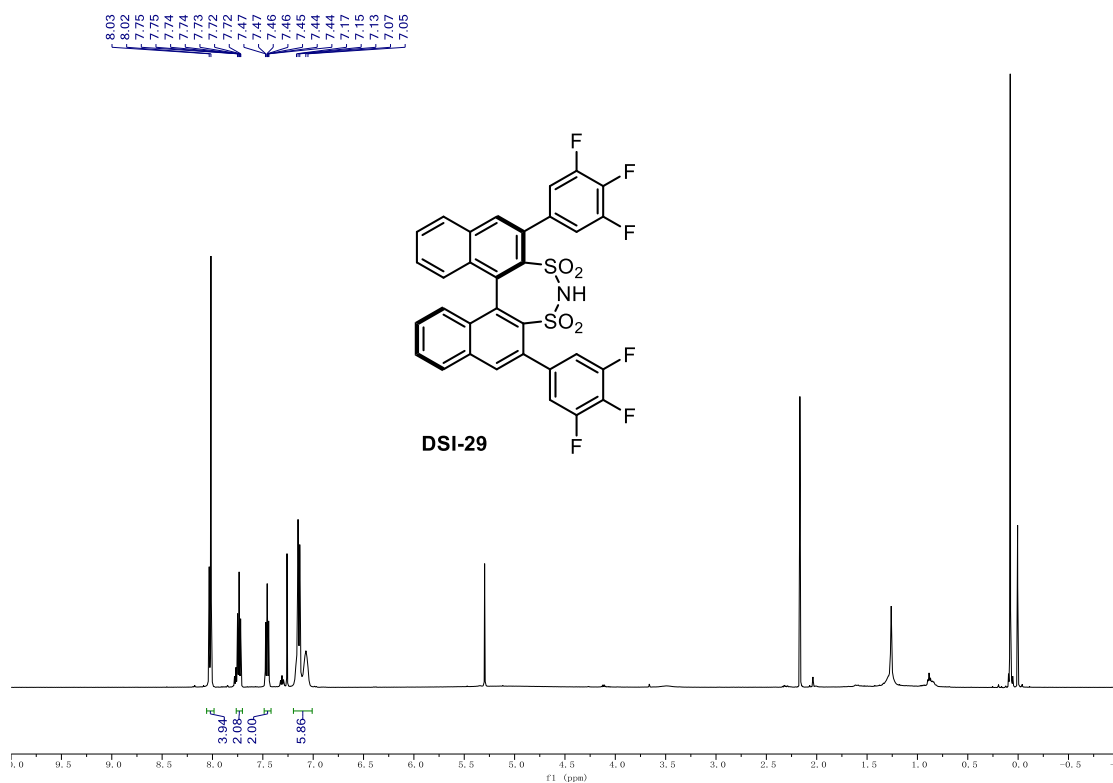
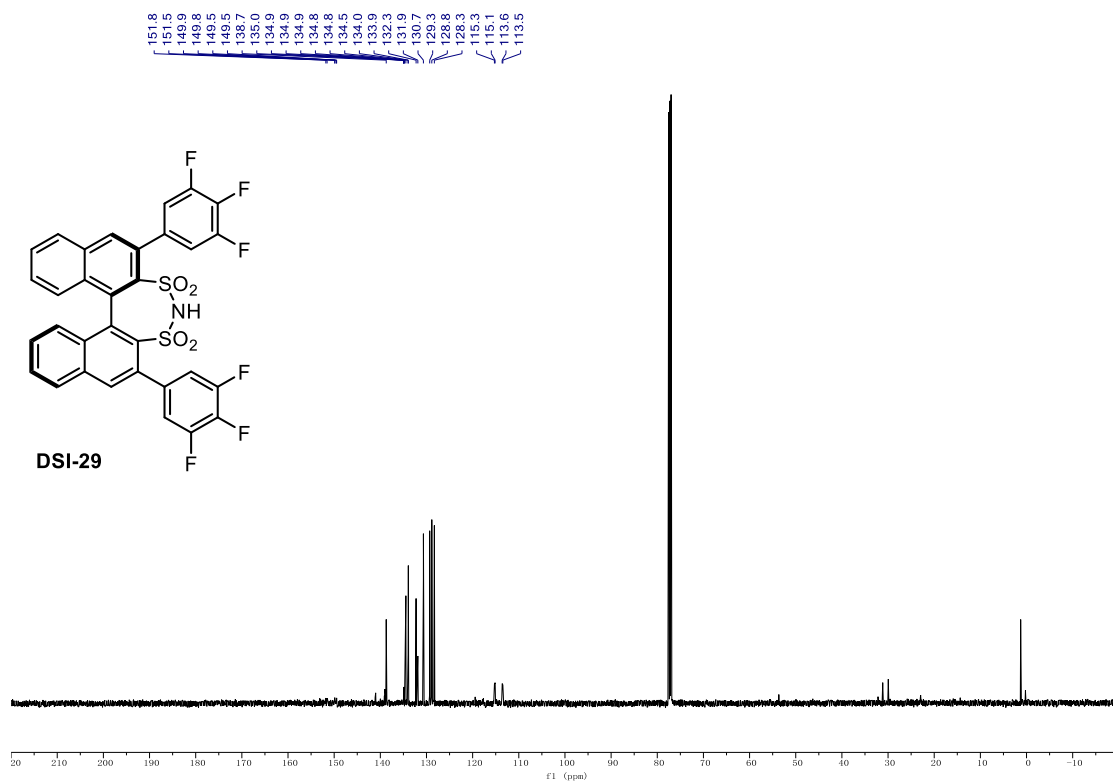
^{13}C NMR (126 MHz, CD_3OD) of PAA-11. ^1H NMR (700 MHz, CDCl_3) of PAA-18.

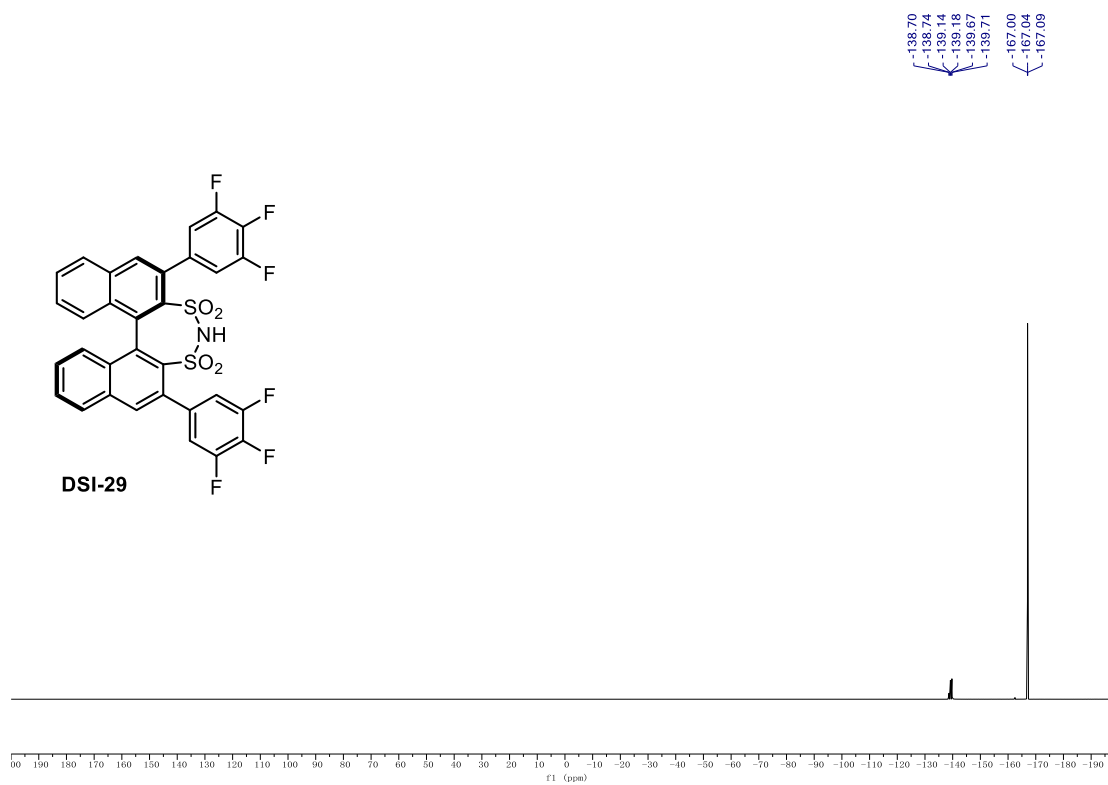
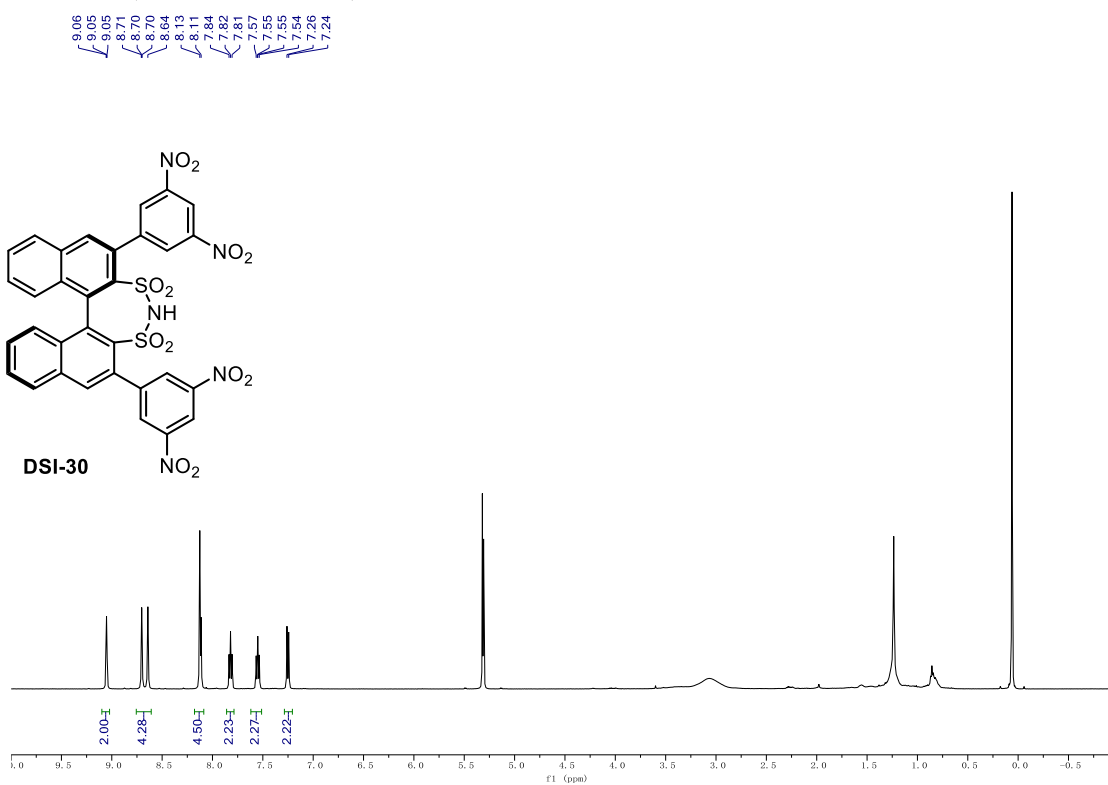
^{13}C NMR (176 MHz, CDCl_3) of PAA-18. **^1H NMR (600 MHz, CDCl_3) of PAA-19.**

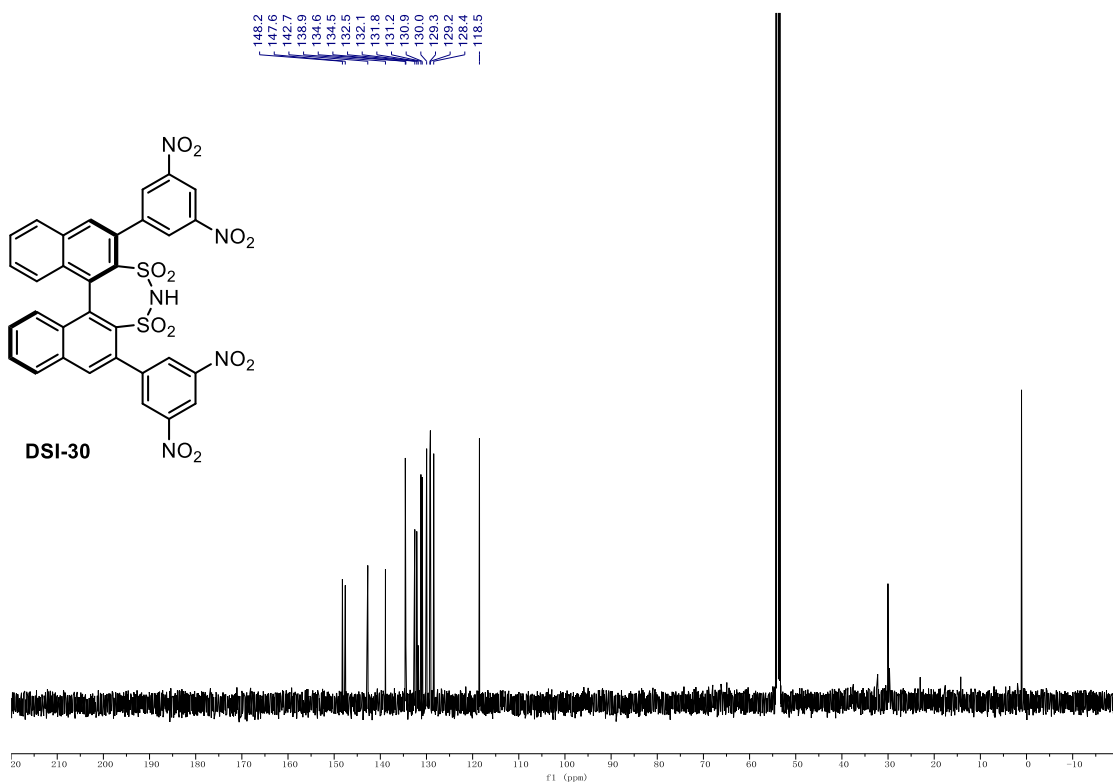
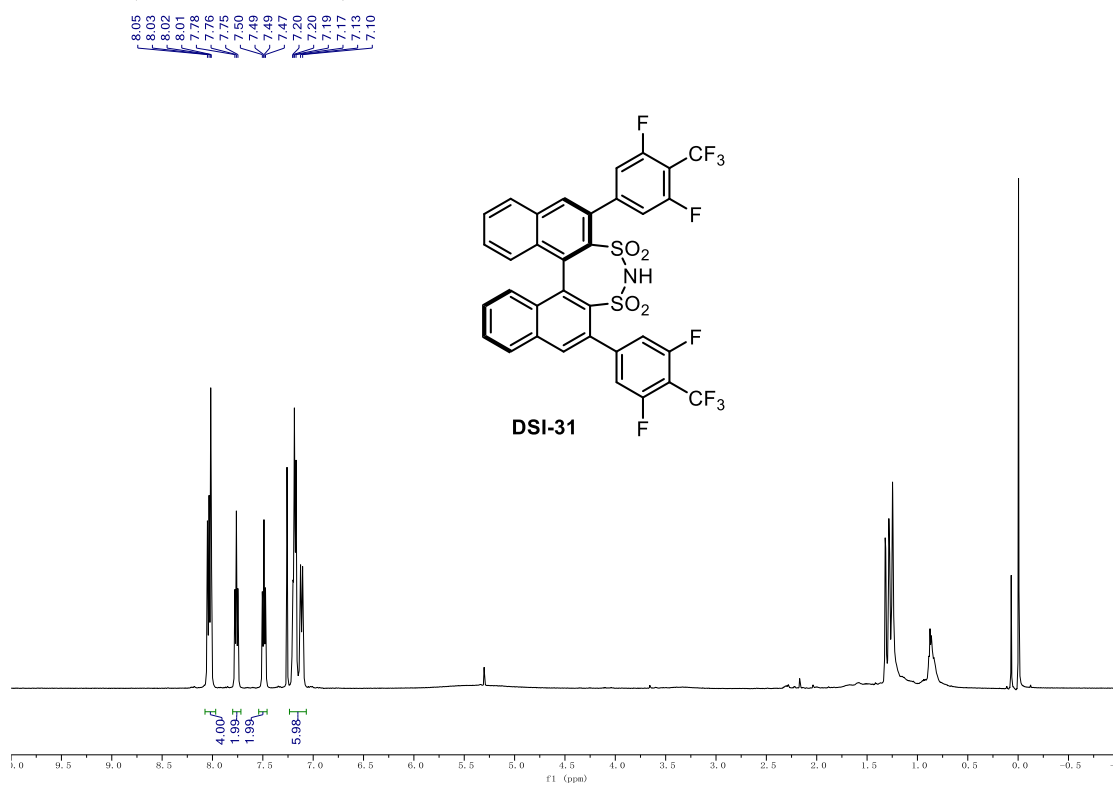
^{13}C NMR (151 MHz, CDCl_3) of PAA-19. ^1H NMR (700 MHz, CD_2Cl_2) of PAA-25.

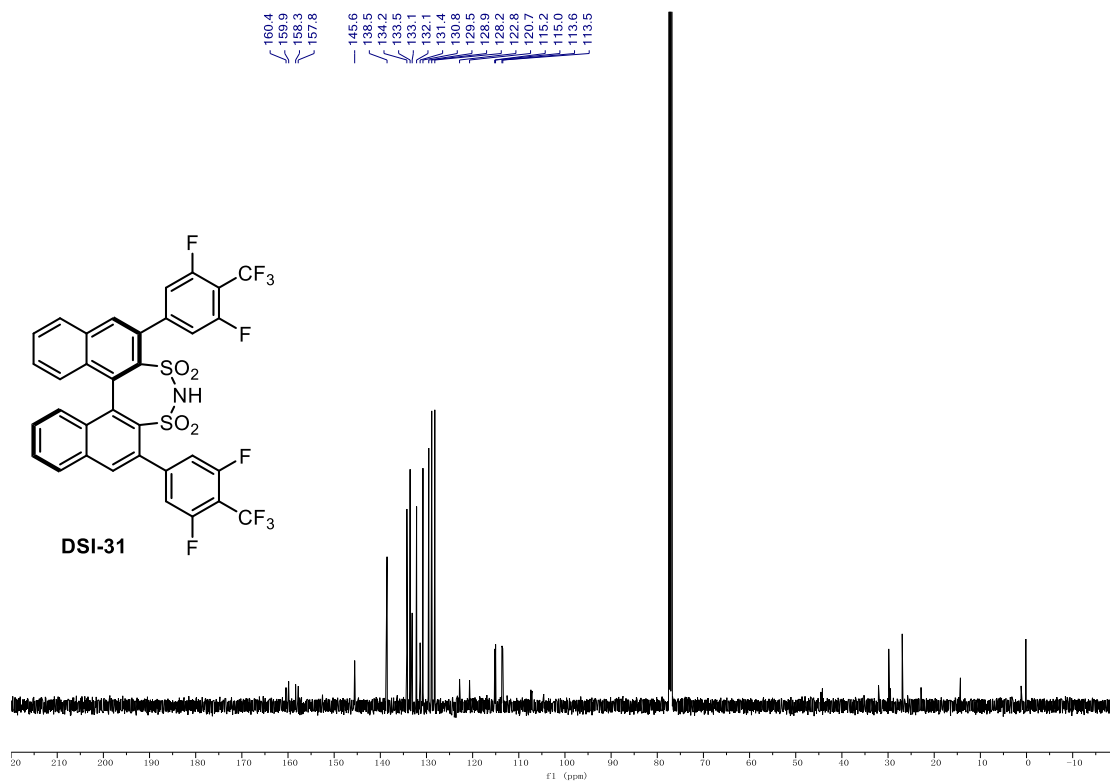
^{13}C NMR (176 MHz, CD_2Cl_2) of PAA-25. ^1H NMR (500 MHz, CDCl_3) of DSI-28.

^{13}C NMR (126 MHz, CDCl_3) of DSI-28. **^{19}F NMR (471 MHz, CDCl_3) of DSI-28.**

¹H NMR (500 MHz, CDCl₃) of DSI-29.**¹³C NMR (126 MHz, CDCl₃) of DSI-29.**

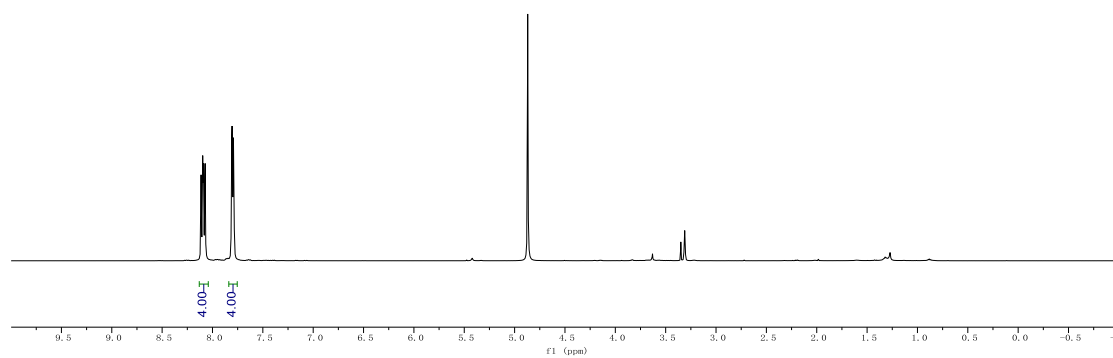
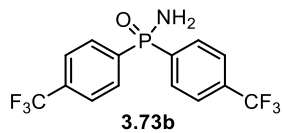
^{19}F NMR (471 MHz, CDCl_3) of DSI-29. ^1H NMR (500 MHz, CD_2Cl_2) of DSI-30.

^{13}C NMR (126 MHz, CD_2Cl_2) of DSI-30. **^1H NMR (500 MHz, CDCl_3) of DSI-31.**

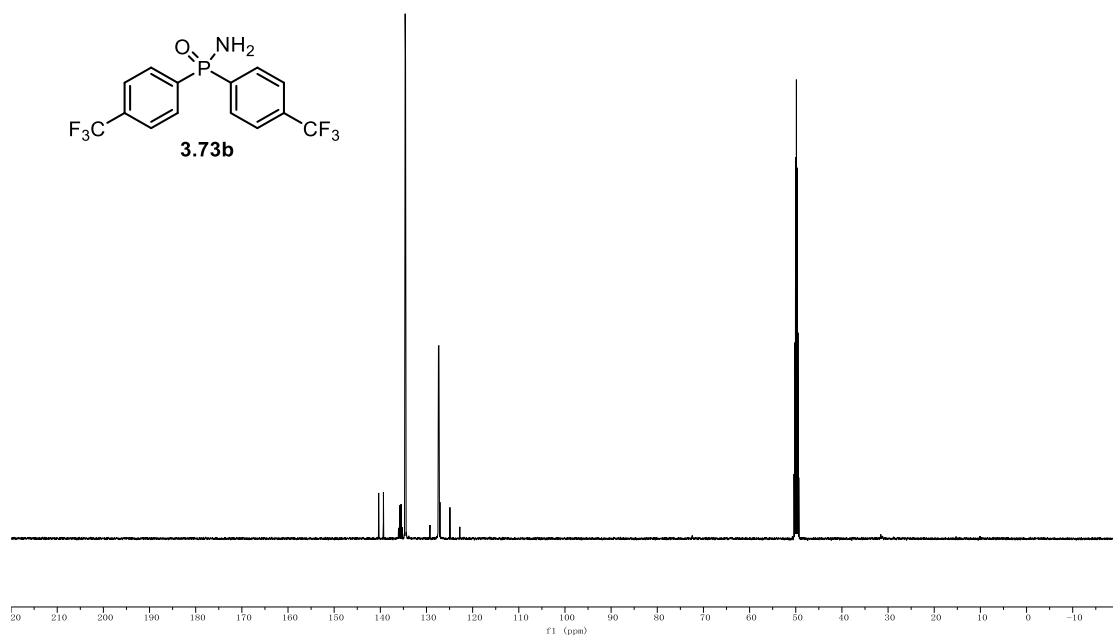
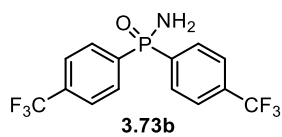
^{13}C NMR (126 MHz, CDCl_3) of DSI-31. ^{19}F NMR (471 MHz, CDCl_3) of DSI-31.

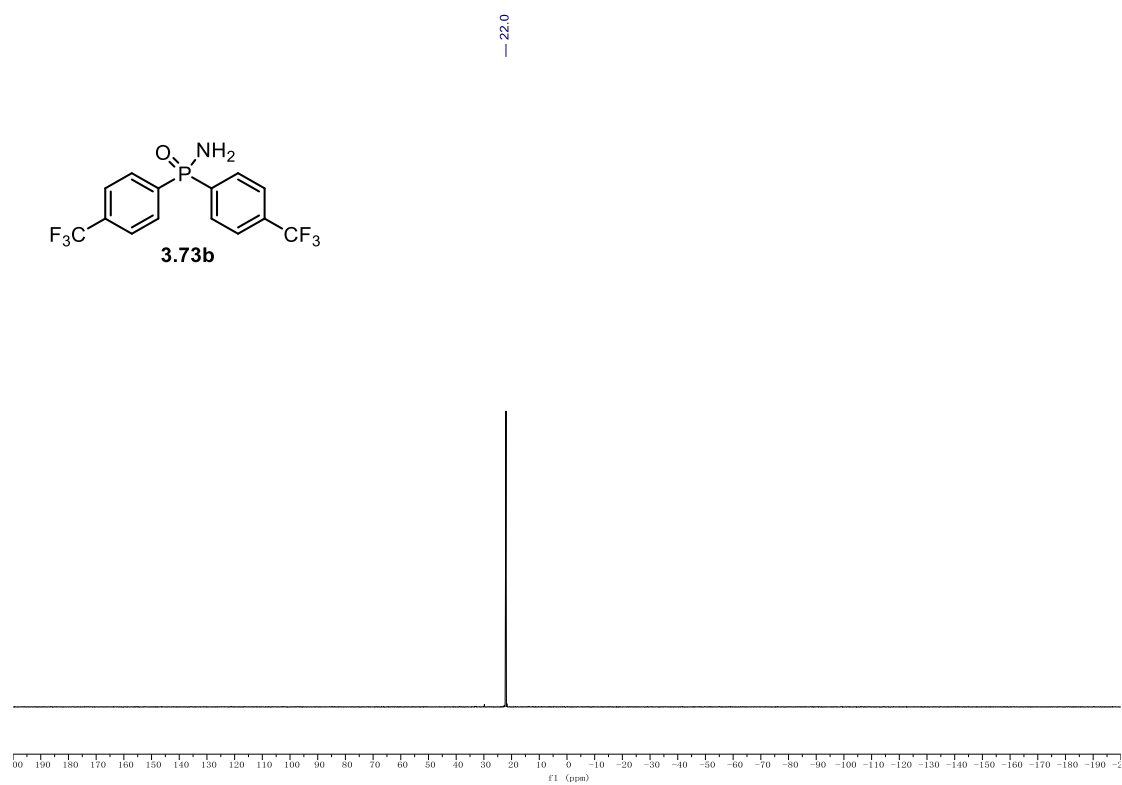
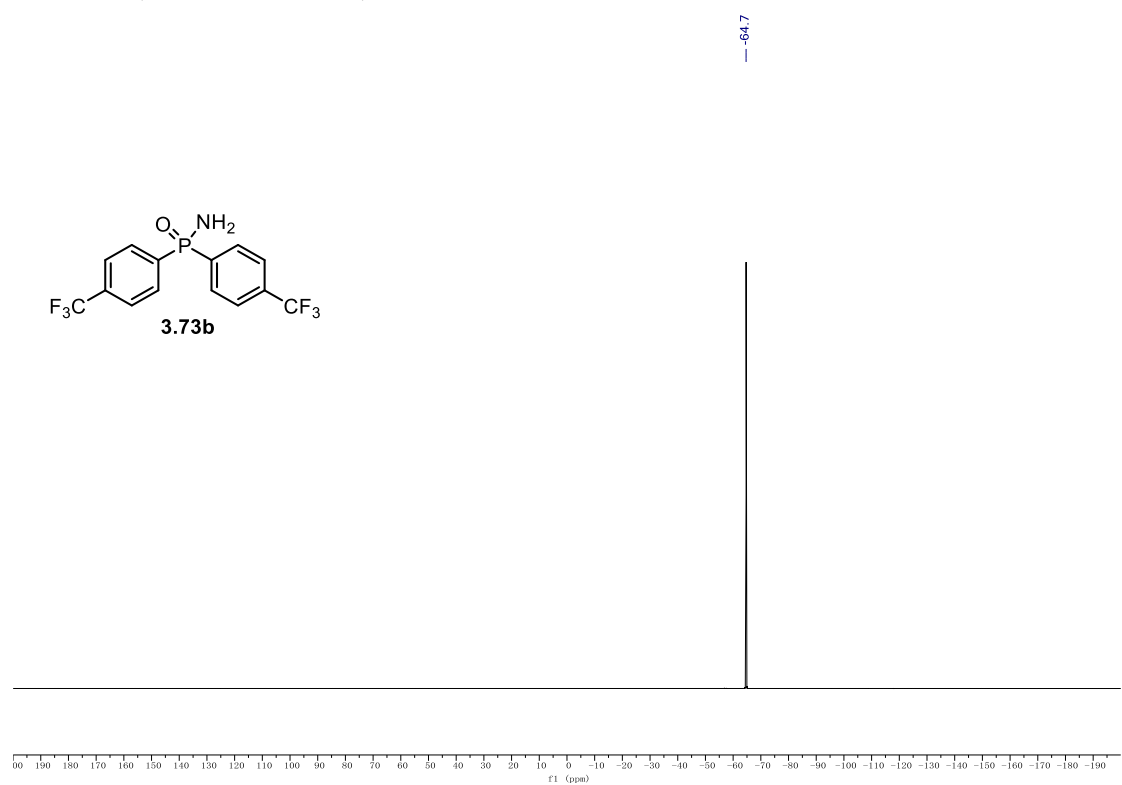
¹H NMR (500 MHz, CD₃OD) of 3.73b.

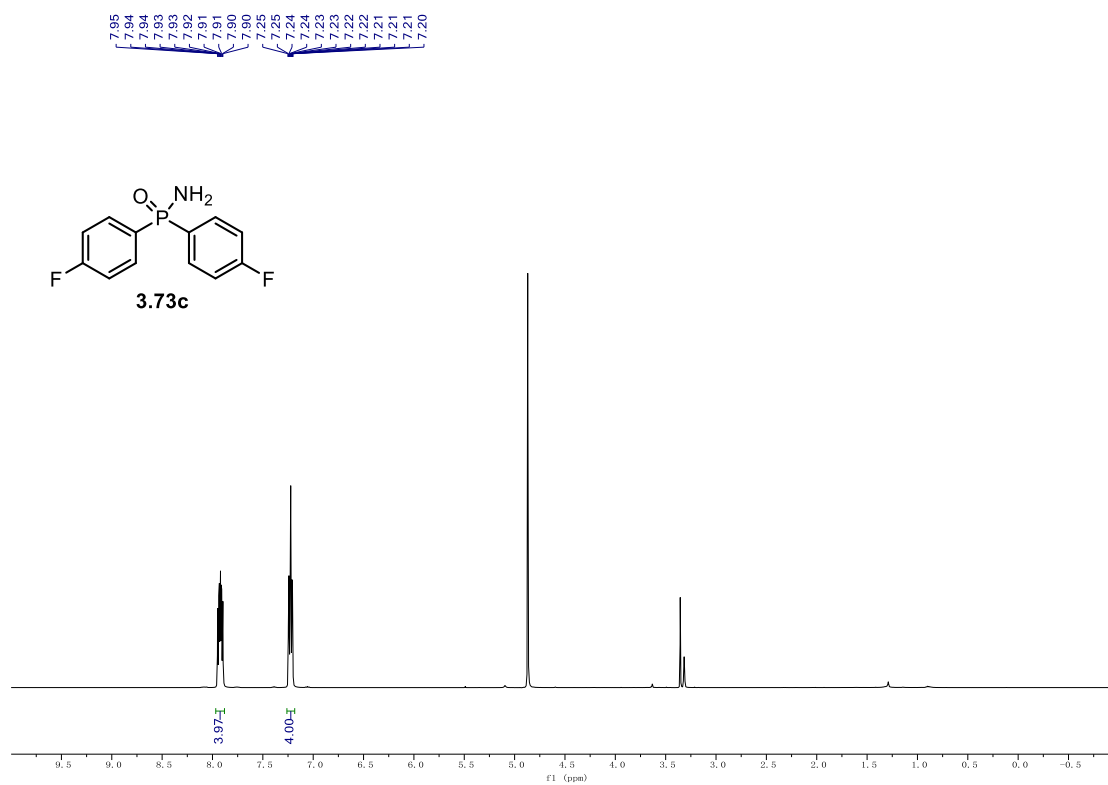
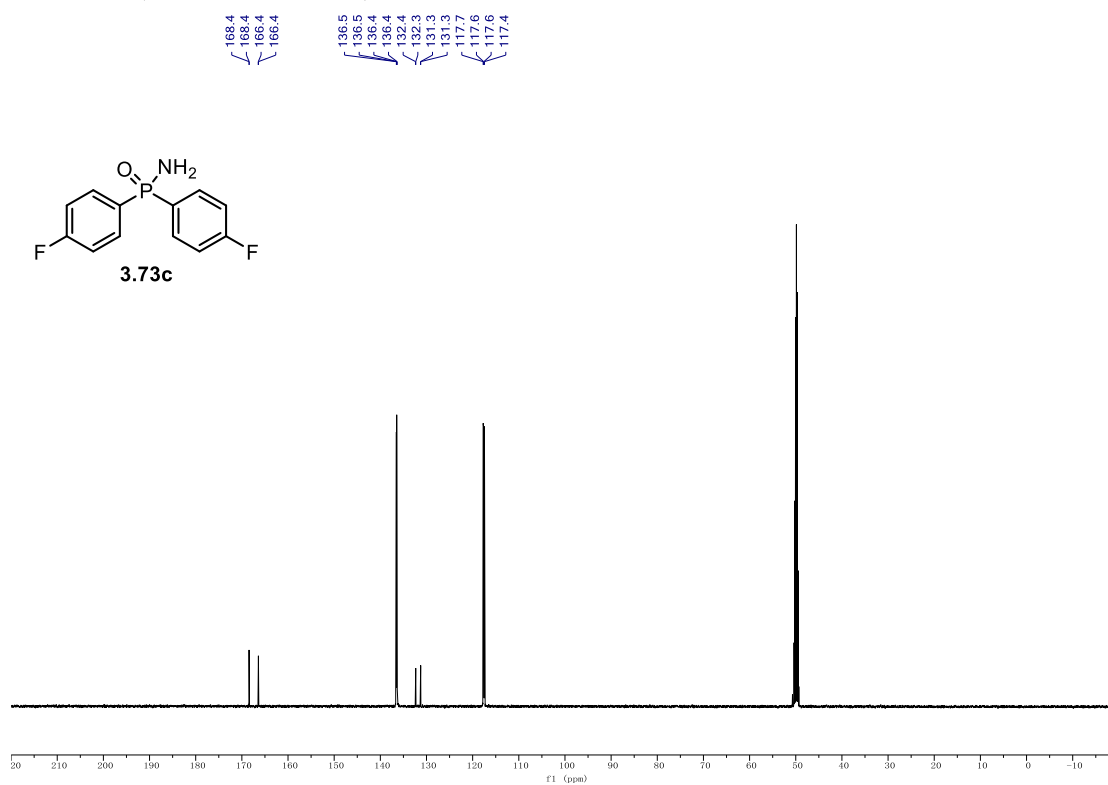
8.11
8.10
8.09
8.07
7.81
7.80
7.79

**¹³C NMR (126 MHz, CD₃OD) of 3.73b.**

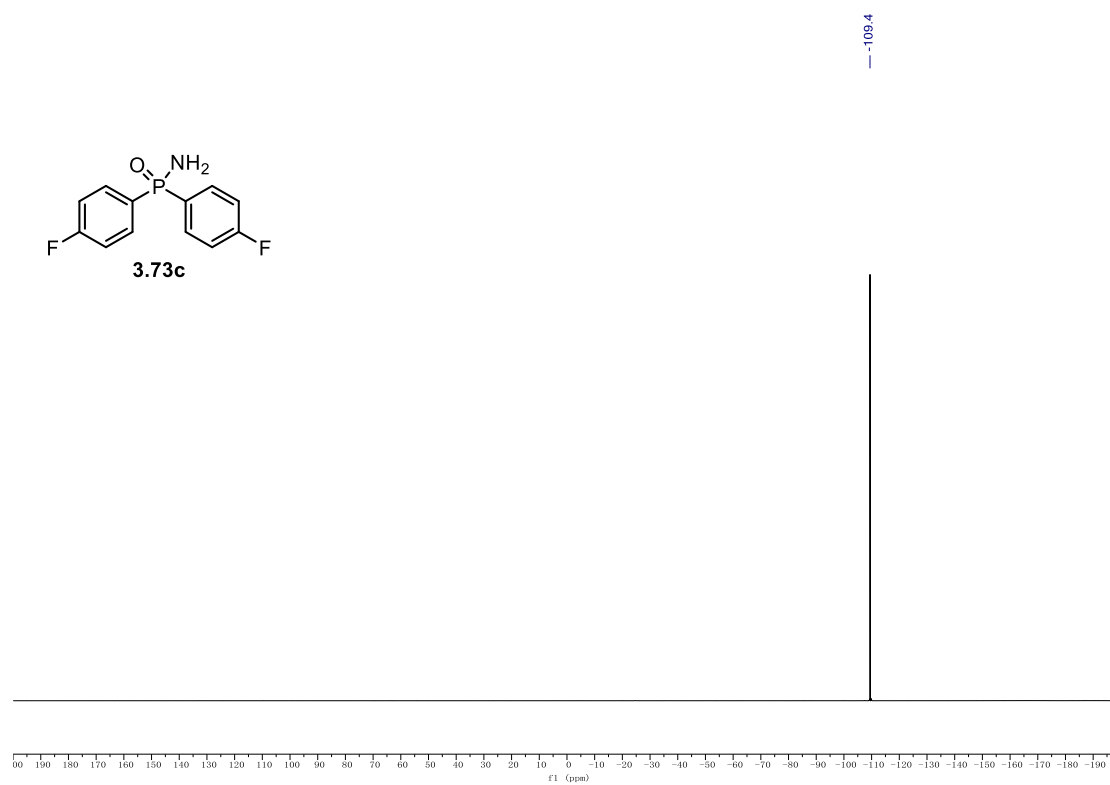
140.4
139.3
136.1
136.0
135.8
134.6
134.5
129.2
127.5
127.4
127.4
127.3
127.3
127.1
124.9
122.8



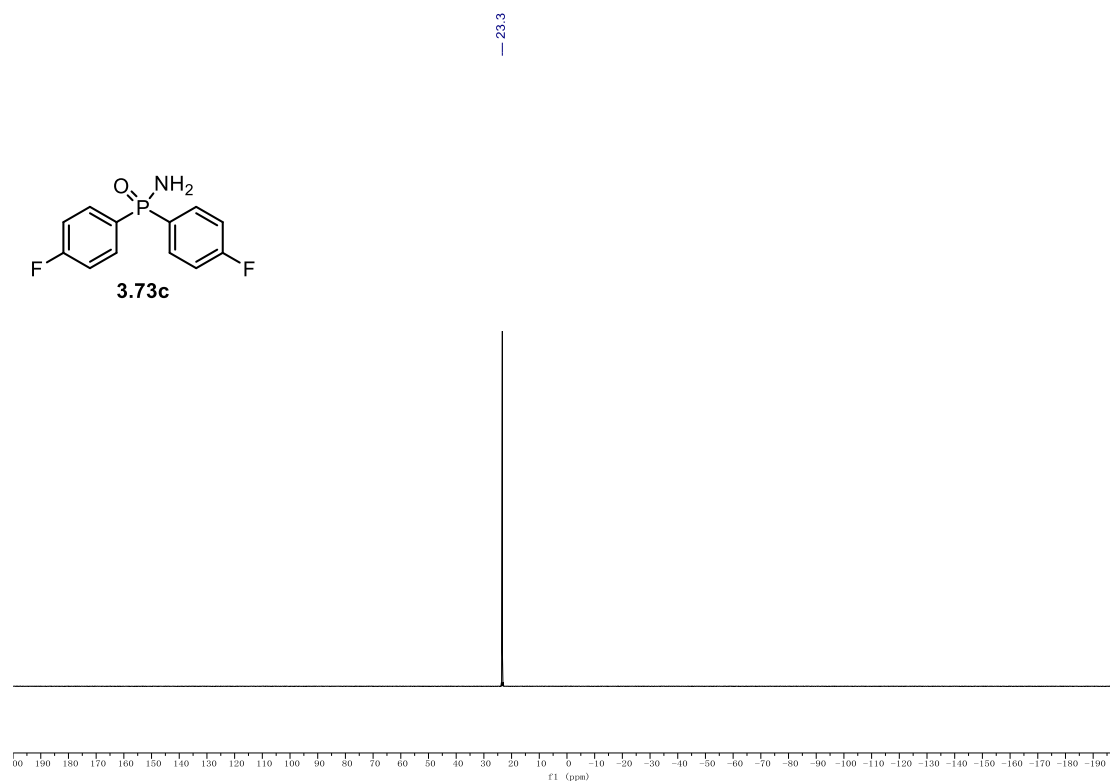
³¹P NMR (203 MHz, CD₃OD) of 3.73b.**¹⁹F NMR (471 MHz, CD₃OD) of 3.73b.**

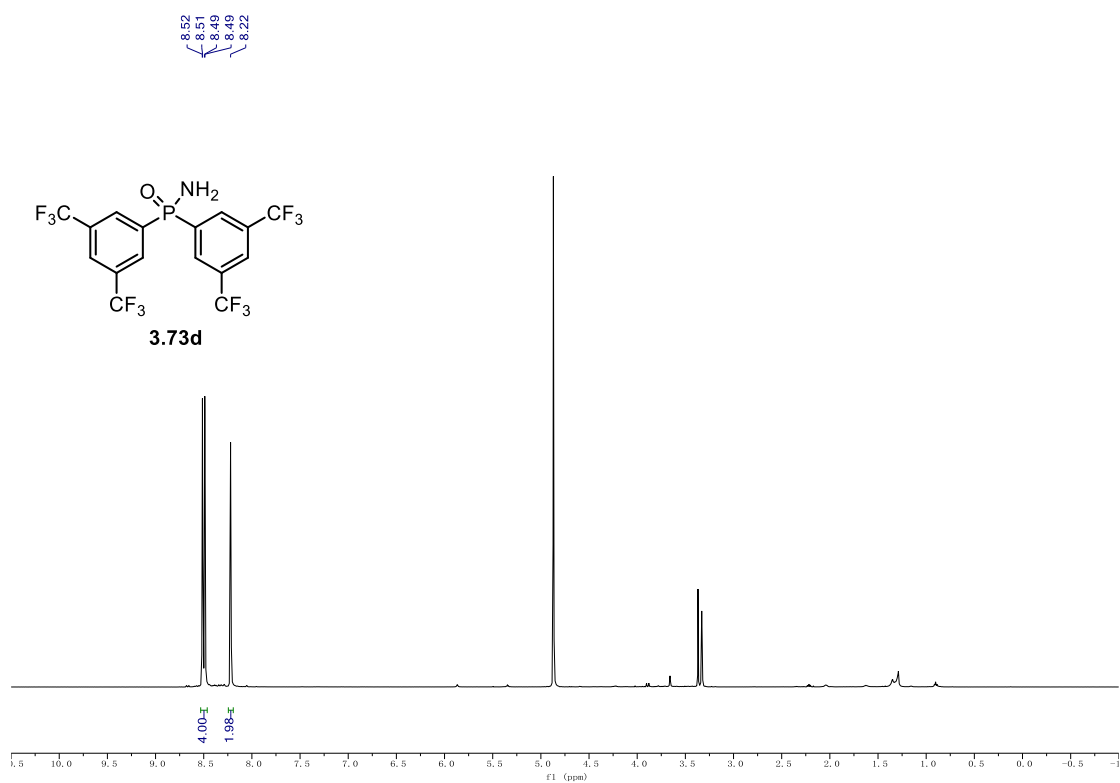
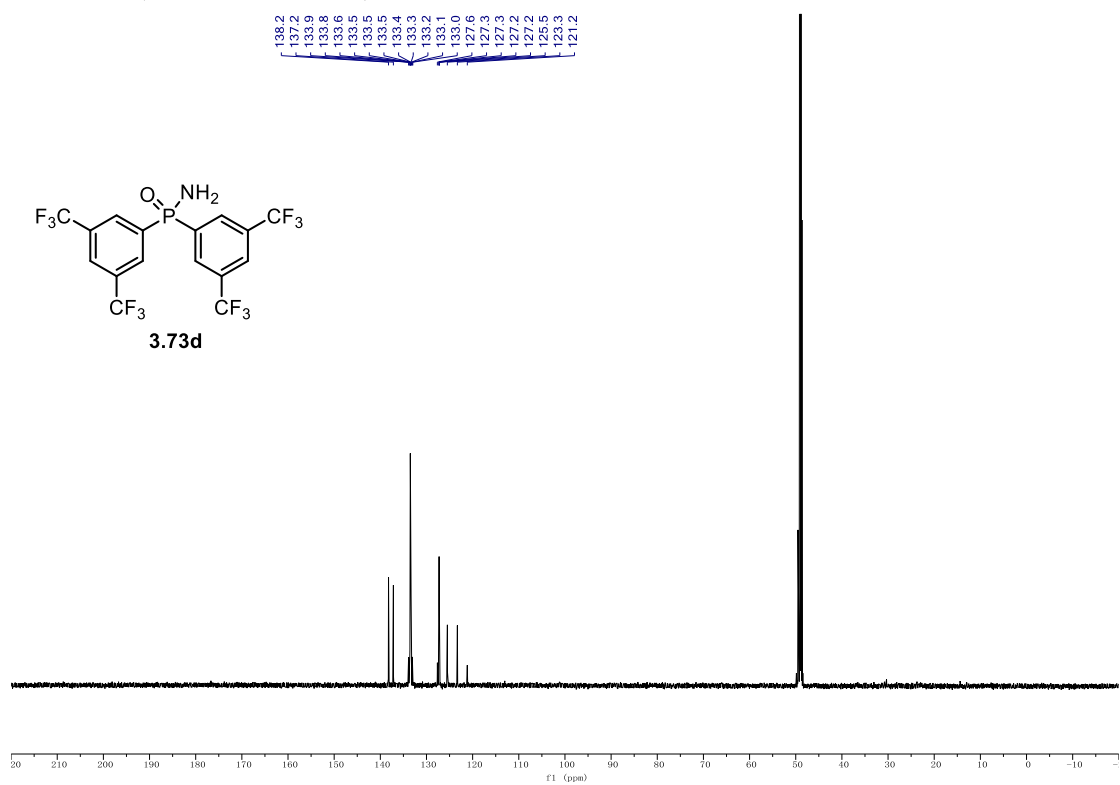
¹H NMR (500 MHz, CD₃OD) of 3.73c.**¹³C NMR (126 MHz, CD₃OD) of 3.73c.**

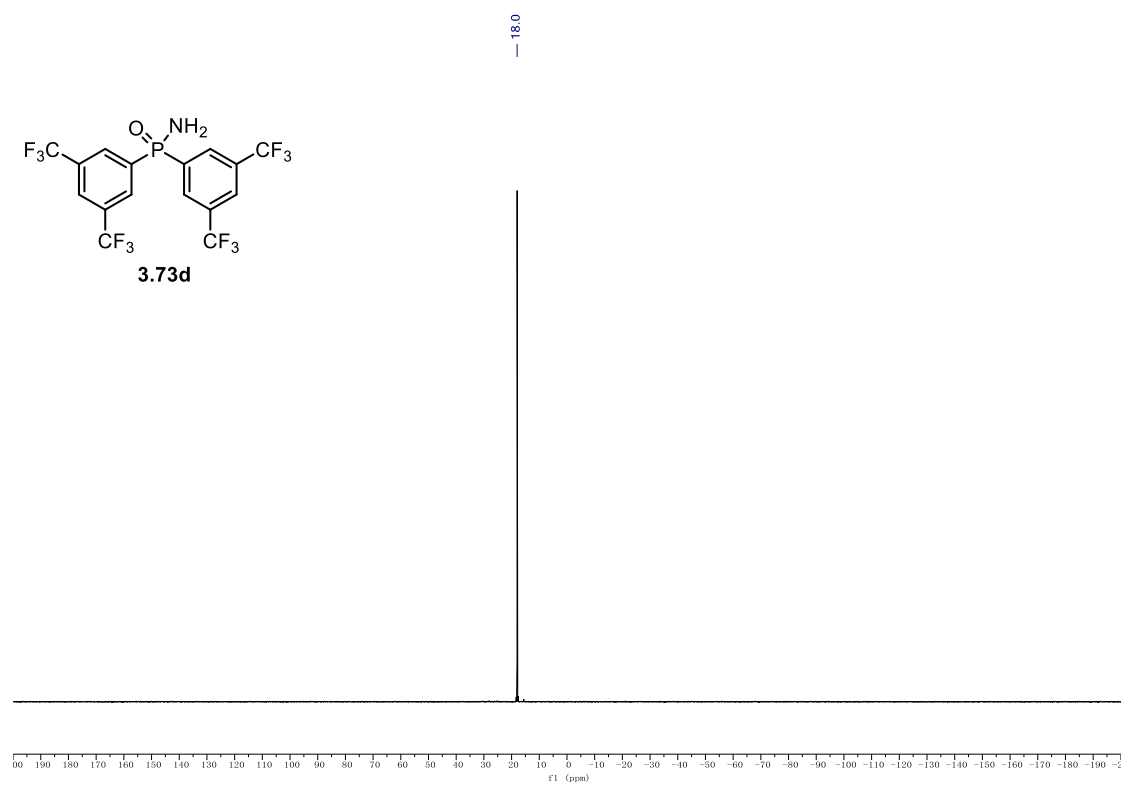
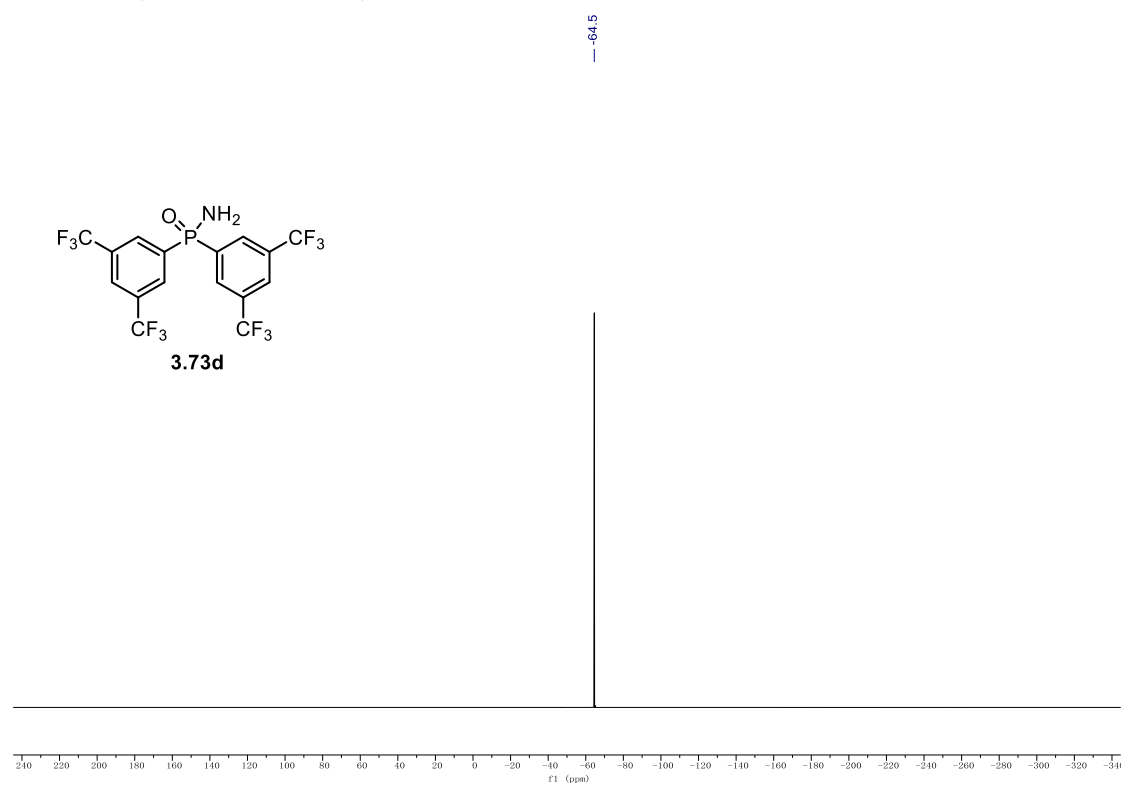
^{31}P NMR (203 MHz, CD_3OD) of **3.73c**.

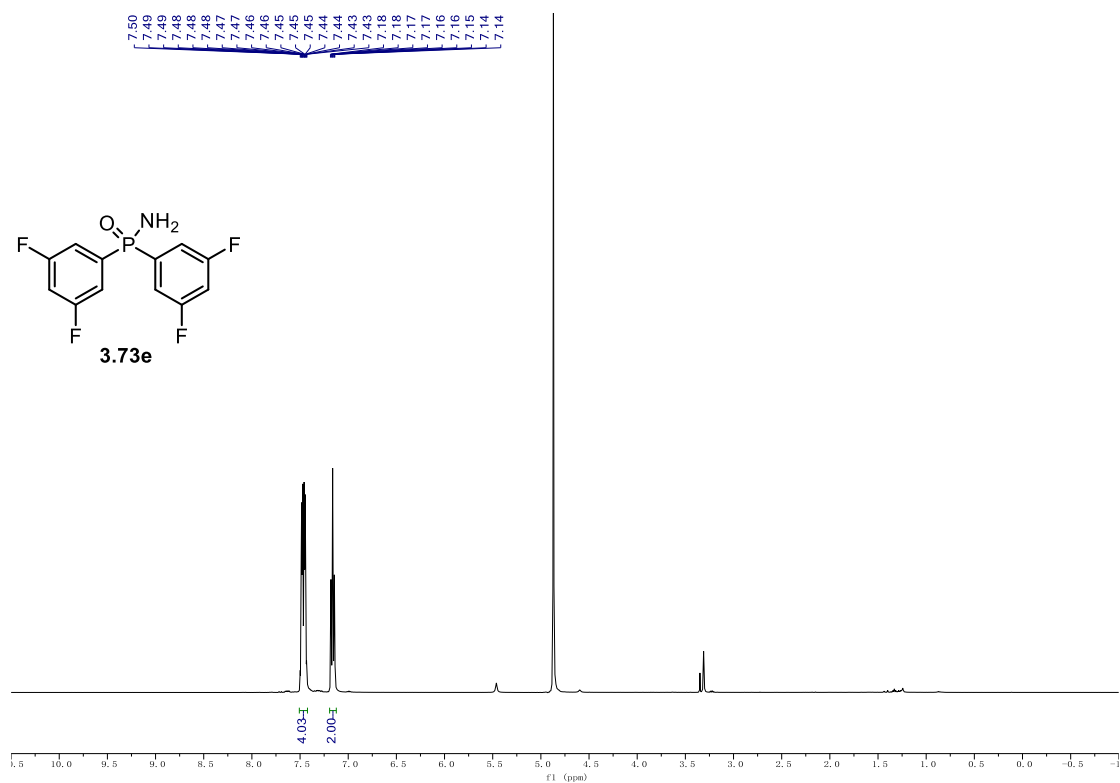
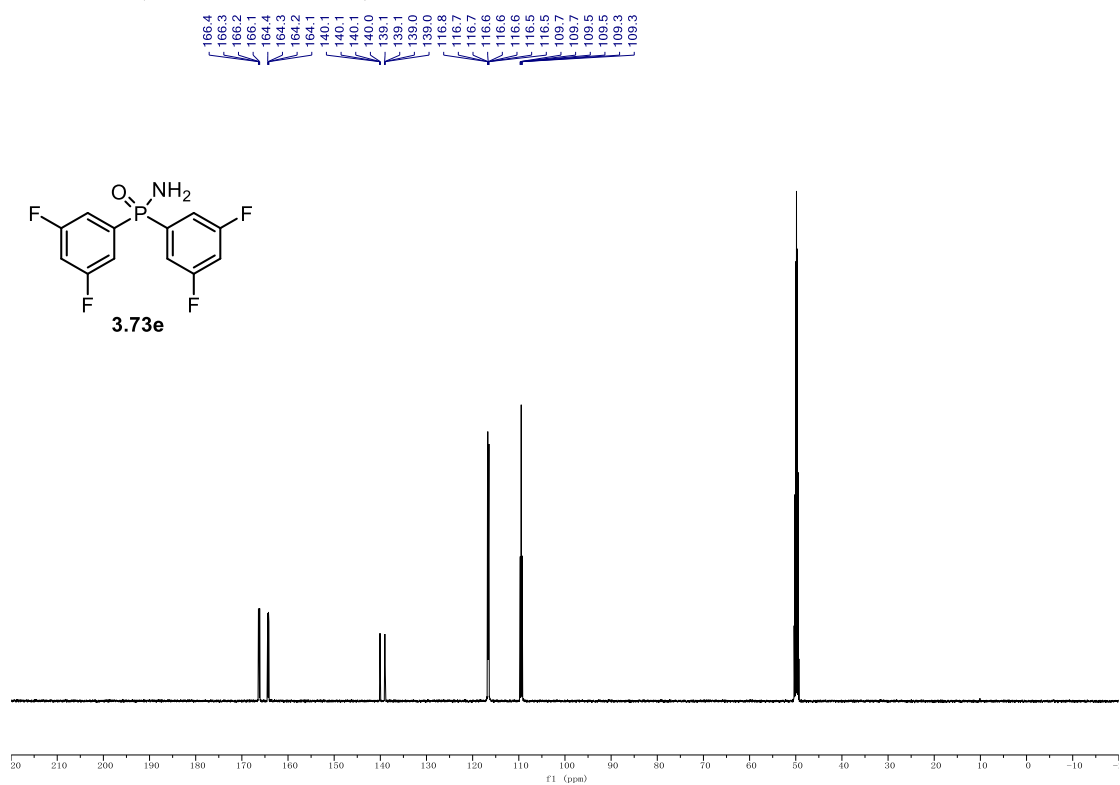


^{19}F NMR (471 MHz, CD_3OD) of **3.73c**.



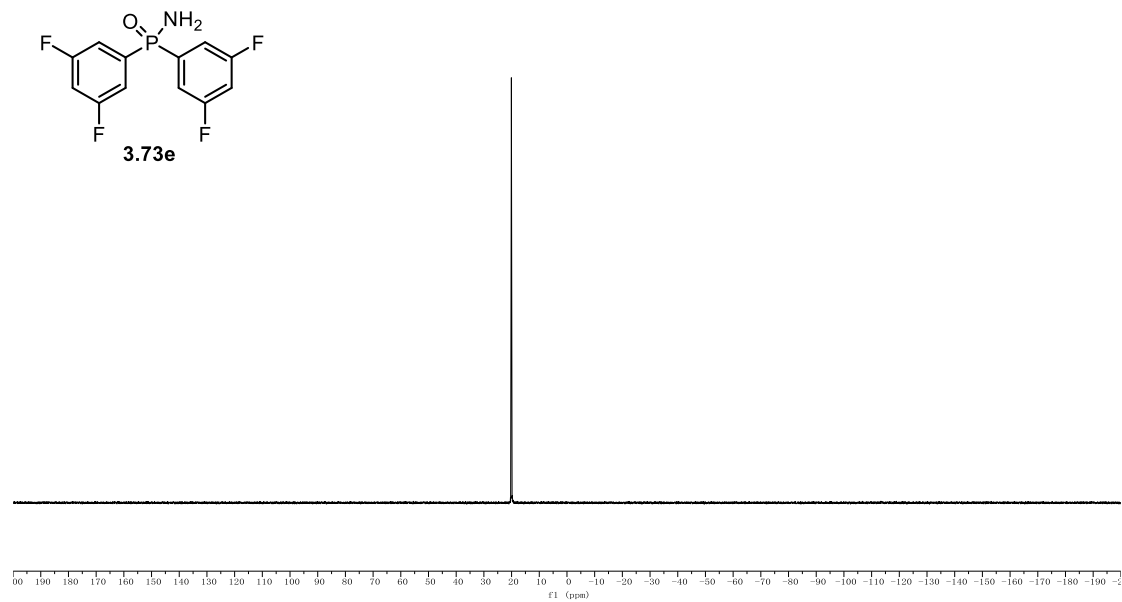
¹H NMR (500 MHz, CD₃OD) of 3.73d.**¹³C NMR (126 MHz, CD₃OD) of 3.73d.**

³¹P NMR (203 MHz, CD₃OD) of 3.73d.**¹⁹F NMR (471 MHz, CD₃OD) of 3.73d.**

¹H NMR (500 MHz, CD₃OD) of 3.73e.**¹³C NMR (126 MHz, CD₃OD) of 3.73e.**

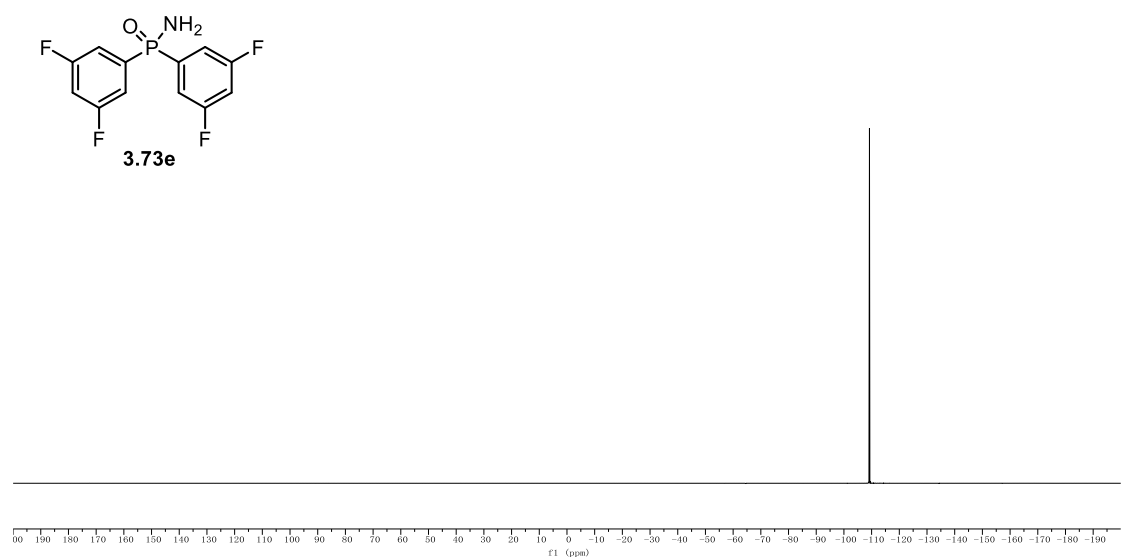
^{31}P NMR (203 MHz, CD_3OD) of **3.73e**.

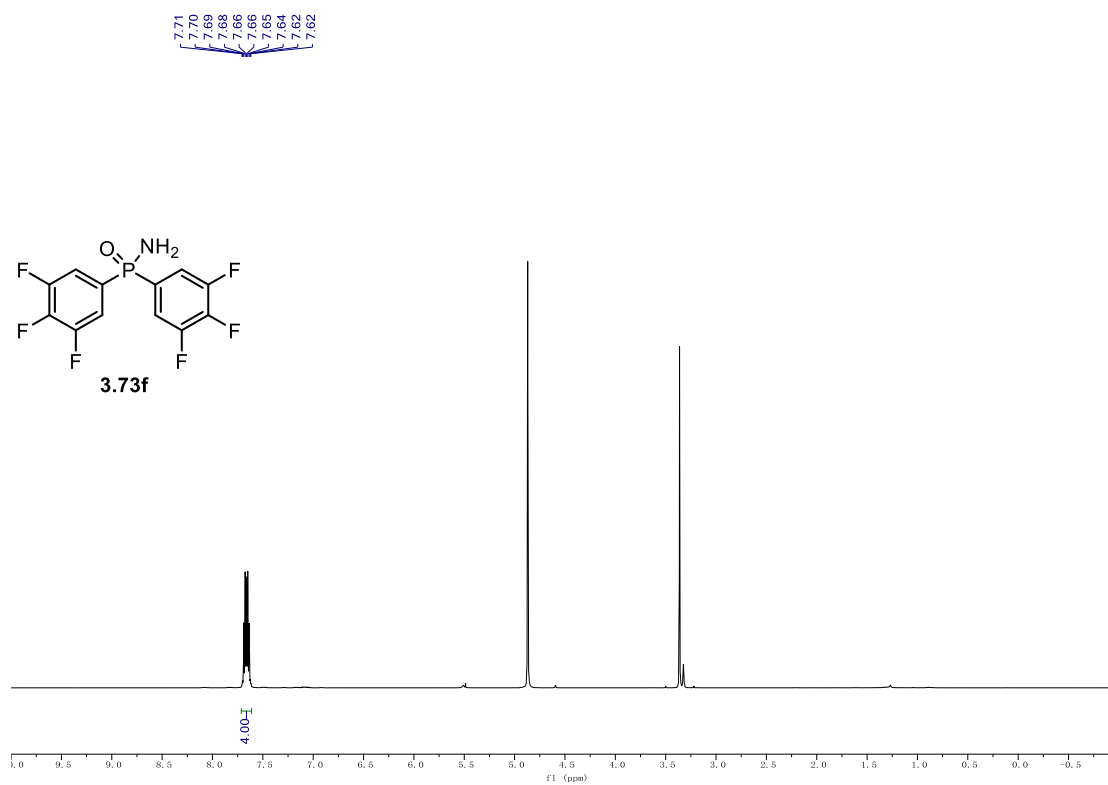
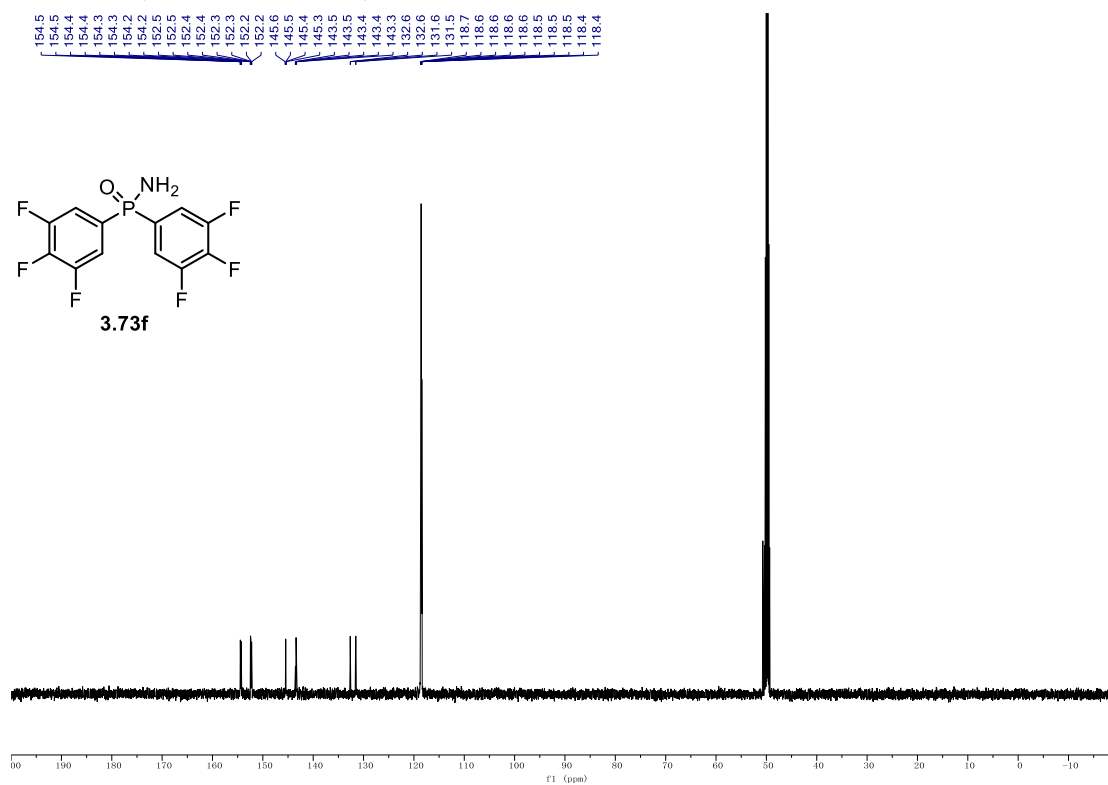
20.1
20.1
20.1
20.1
20.0
20.0

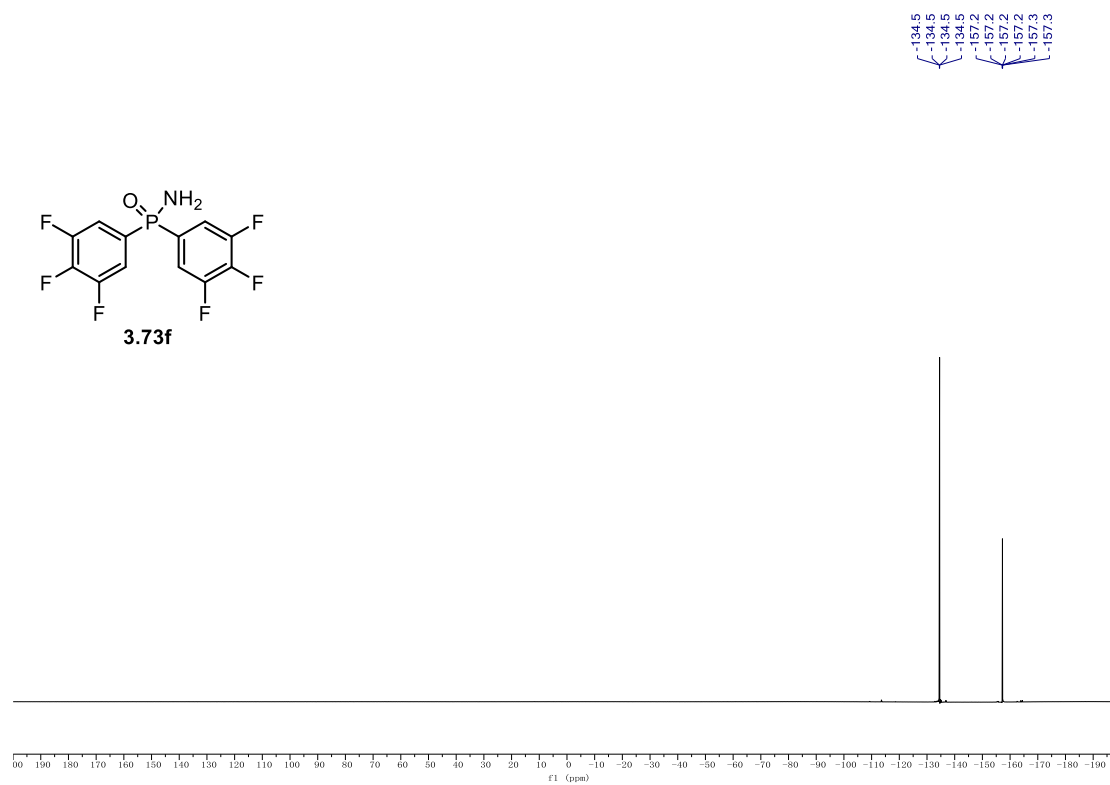
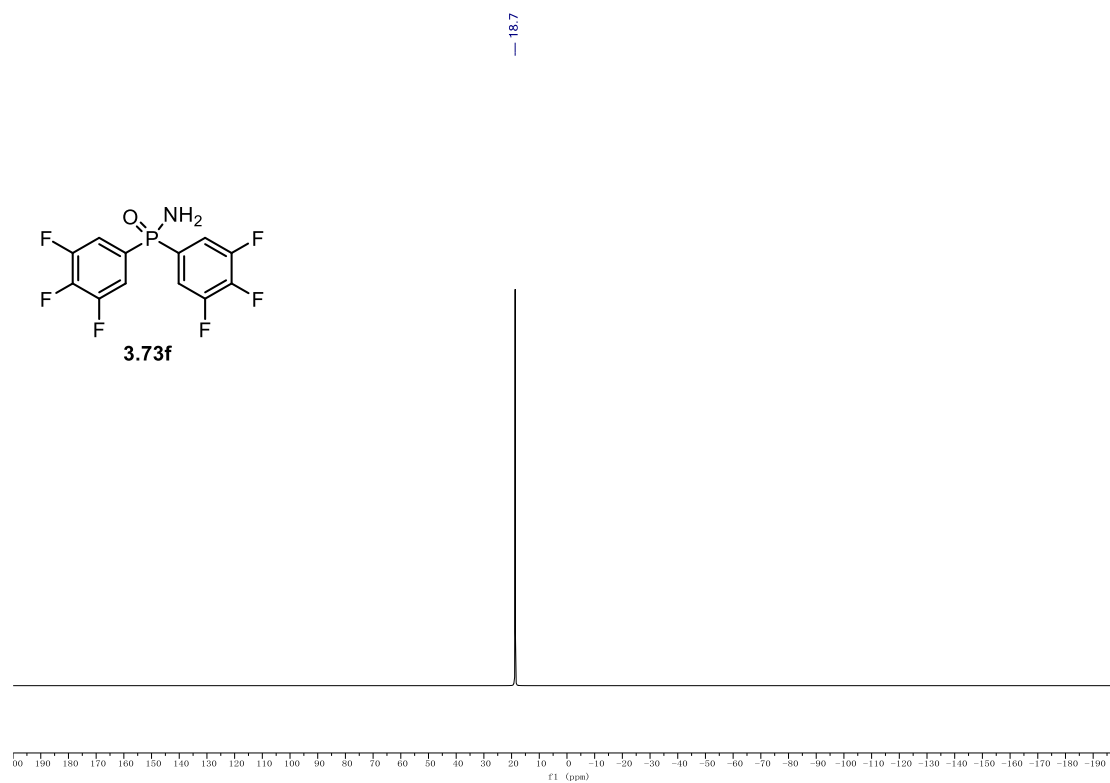


^{19}F NMR (471 MHz, CD_3OD) of **3.73e**.

-109.2
-109.2

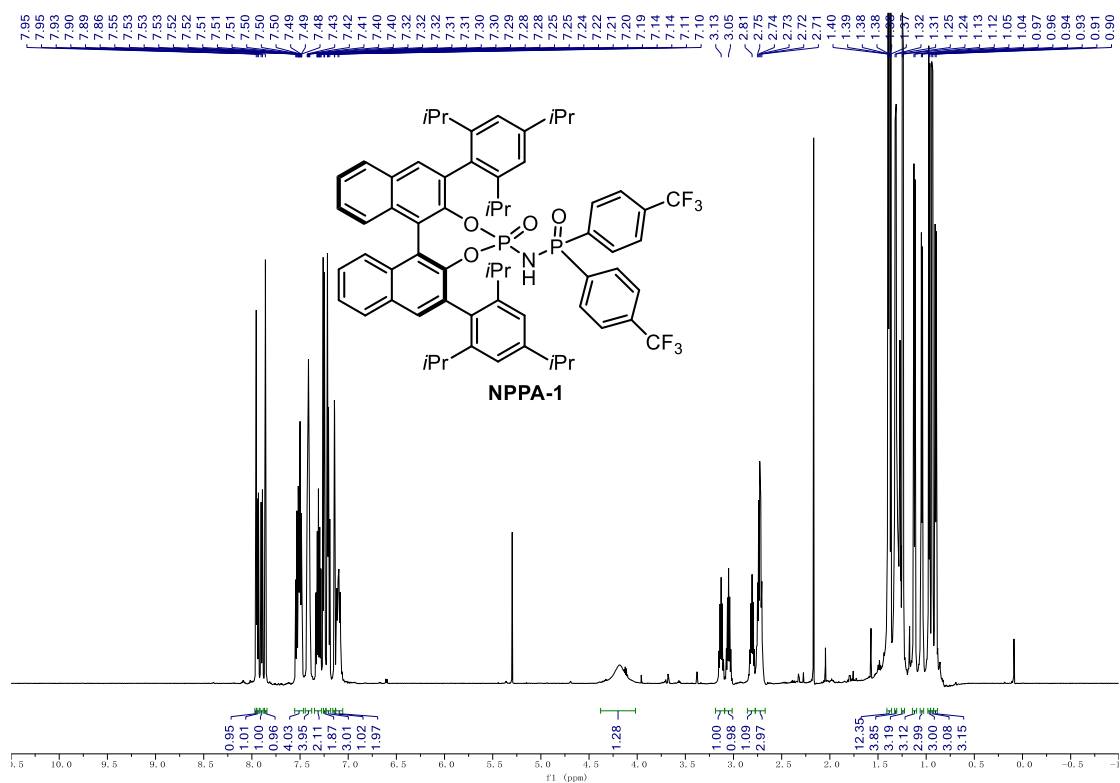


¹H NMR (500 MHz, CD₃OD) of 3.73f**¹³C NMR (126 MHz, CD₃OD) of 3.73f.**

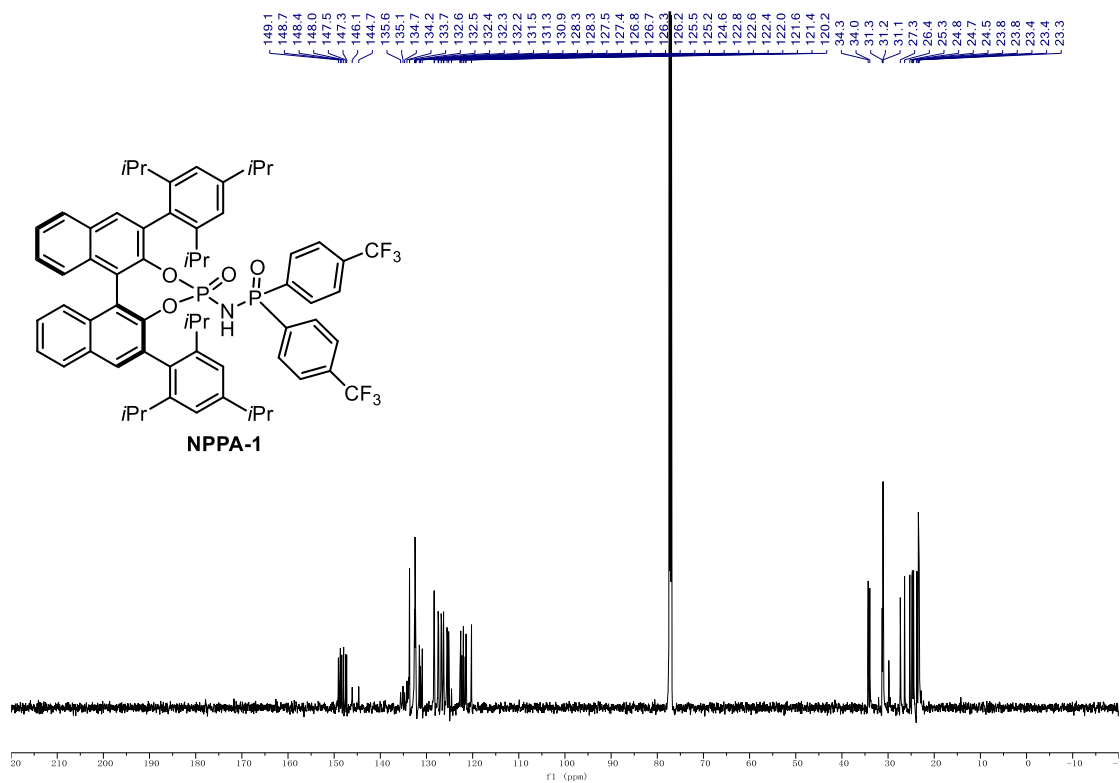
^{31}P NMR (203 MHz, CD_3OD) of **3.73f.** **^{19}F NMR (471 MHz, CD_3OD) of **3.73f**.**

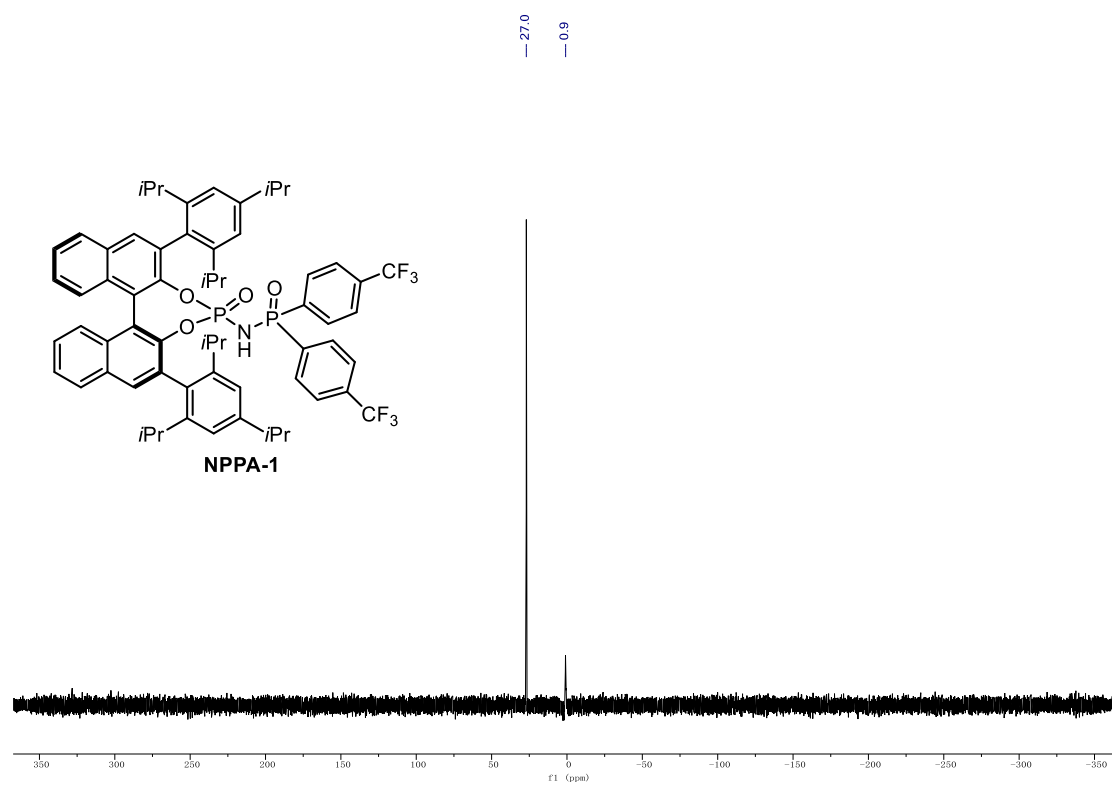
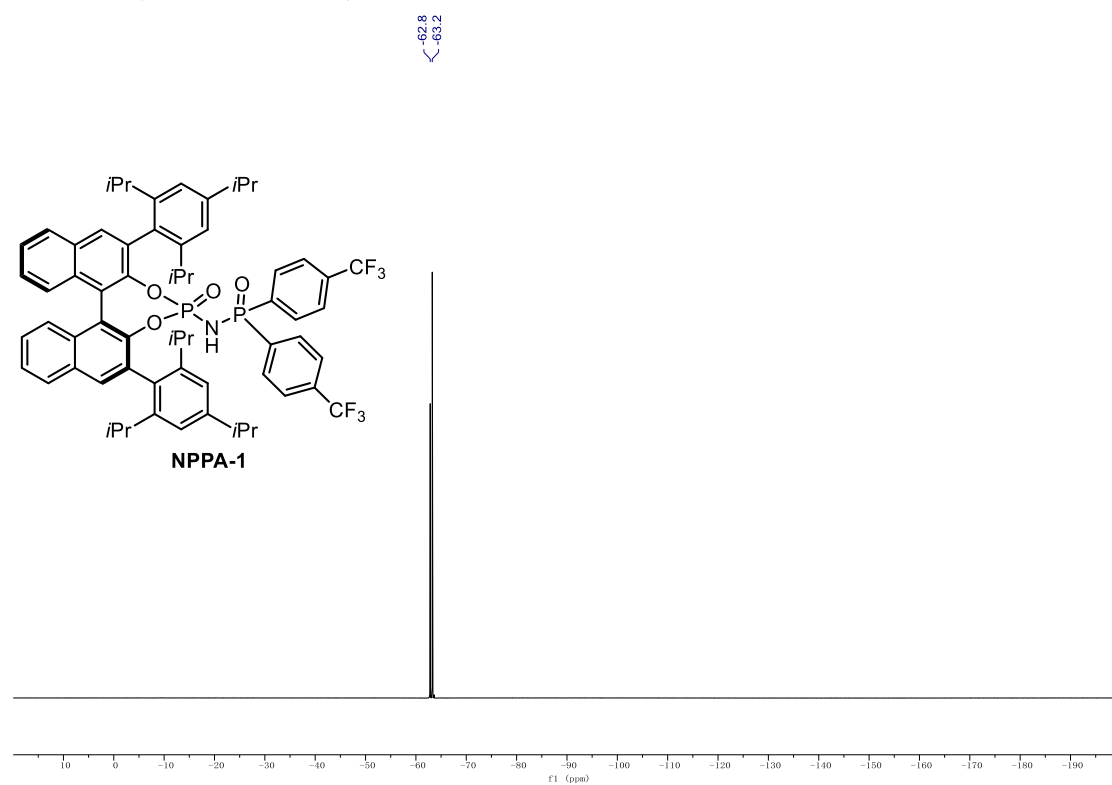
9.1. NMR Spectra

¹H NMR (600 MHz, CDCl₃) of NPPA-1.



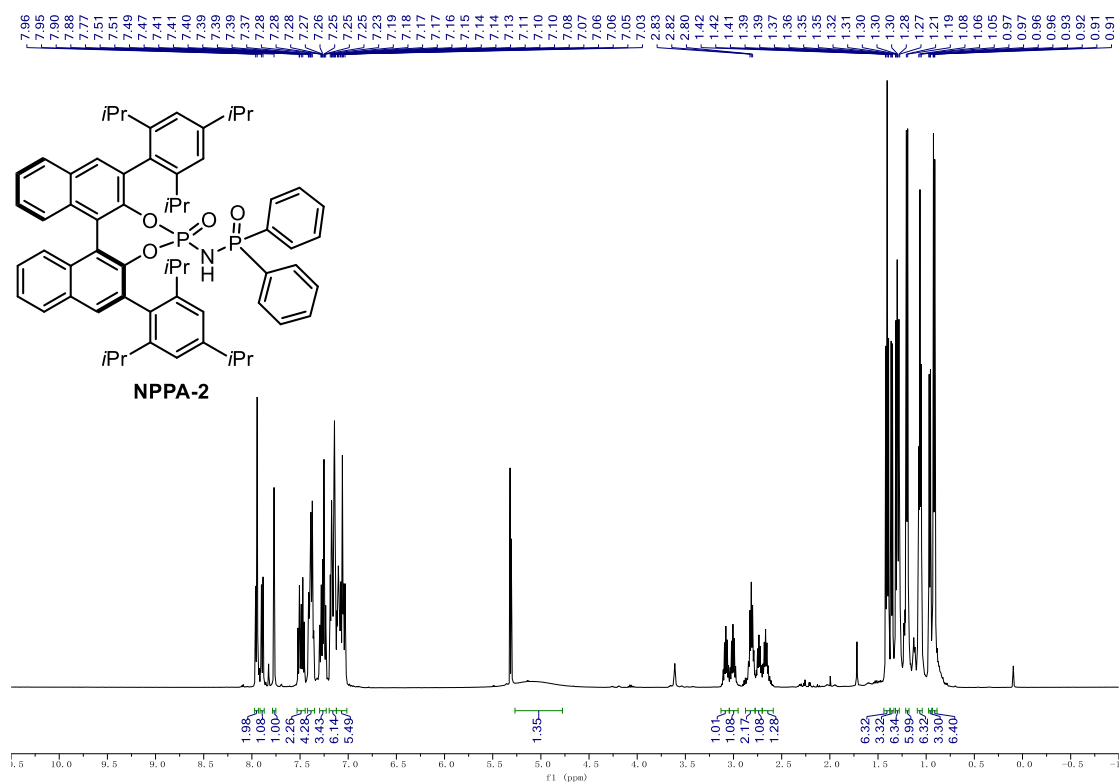
¹³C NMR (151 MHz, CDCl₃) of NPPA-1.



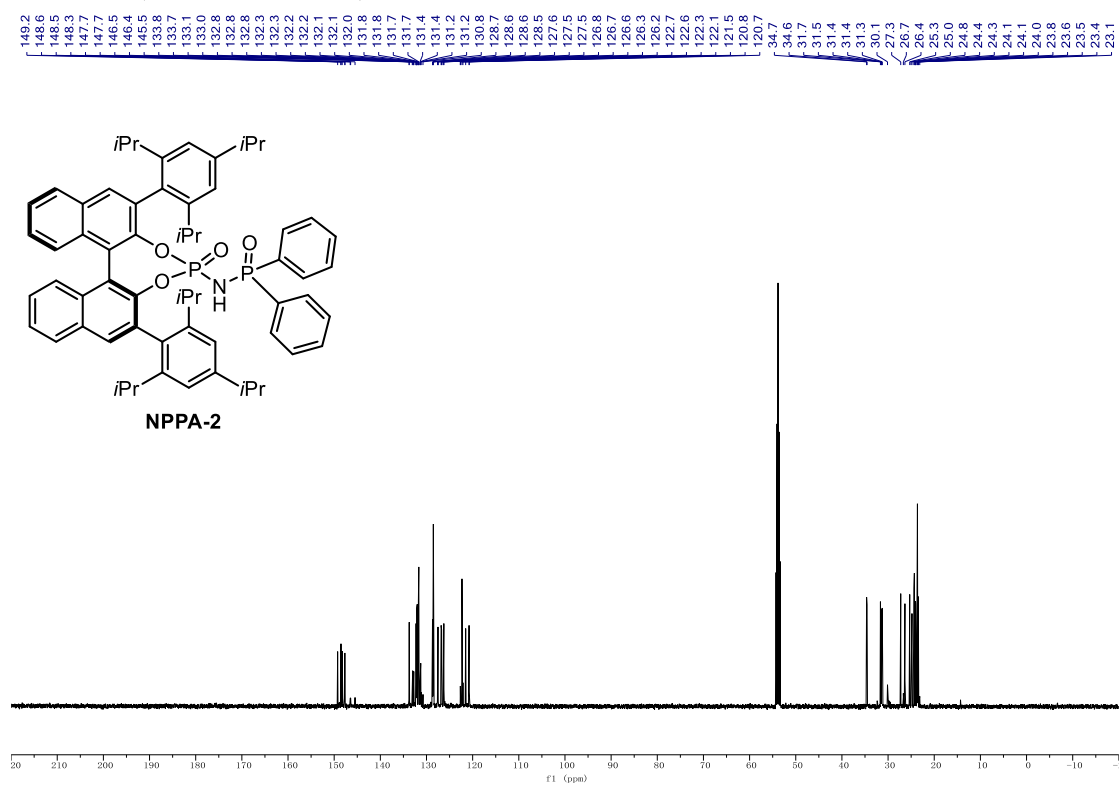
^{31}P NMR (243 MHz, CDCl_3) of NPPA-1. ^{19}F NMR (565 MHz, CDCl_3) of NPPA-1.

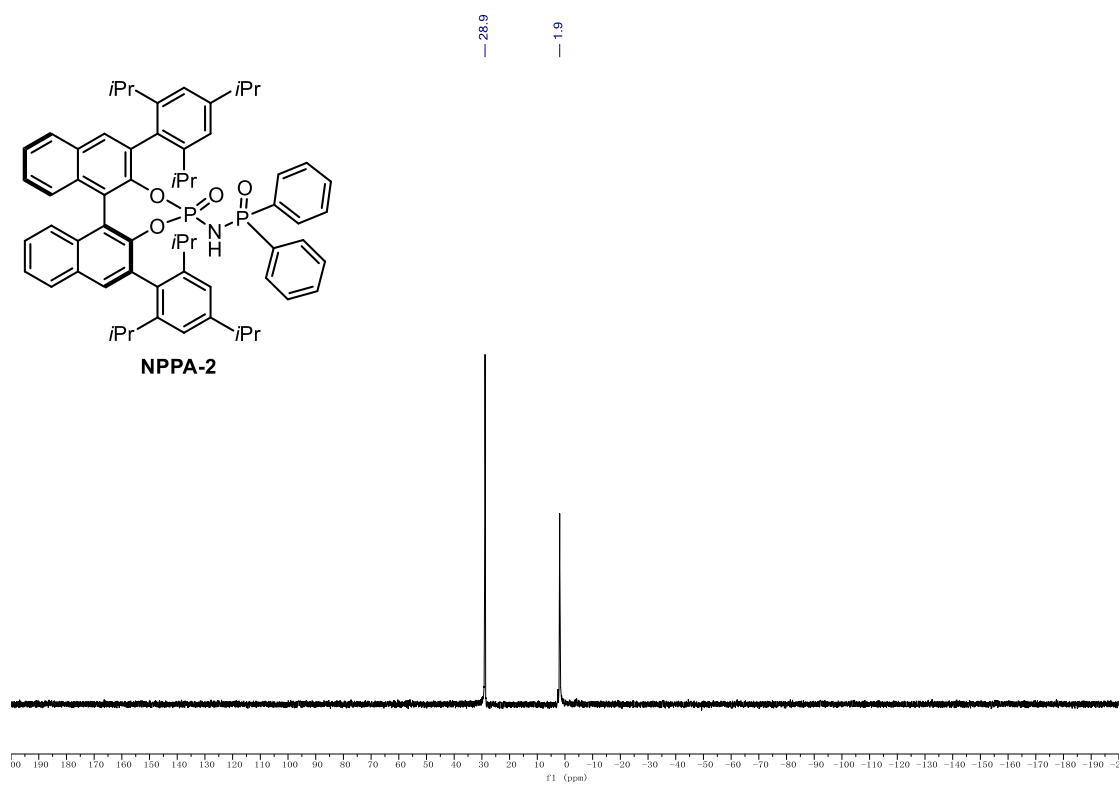
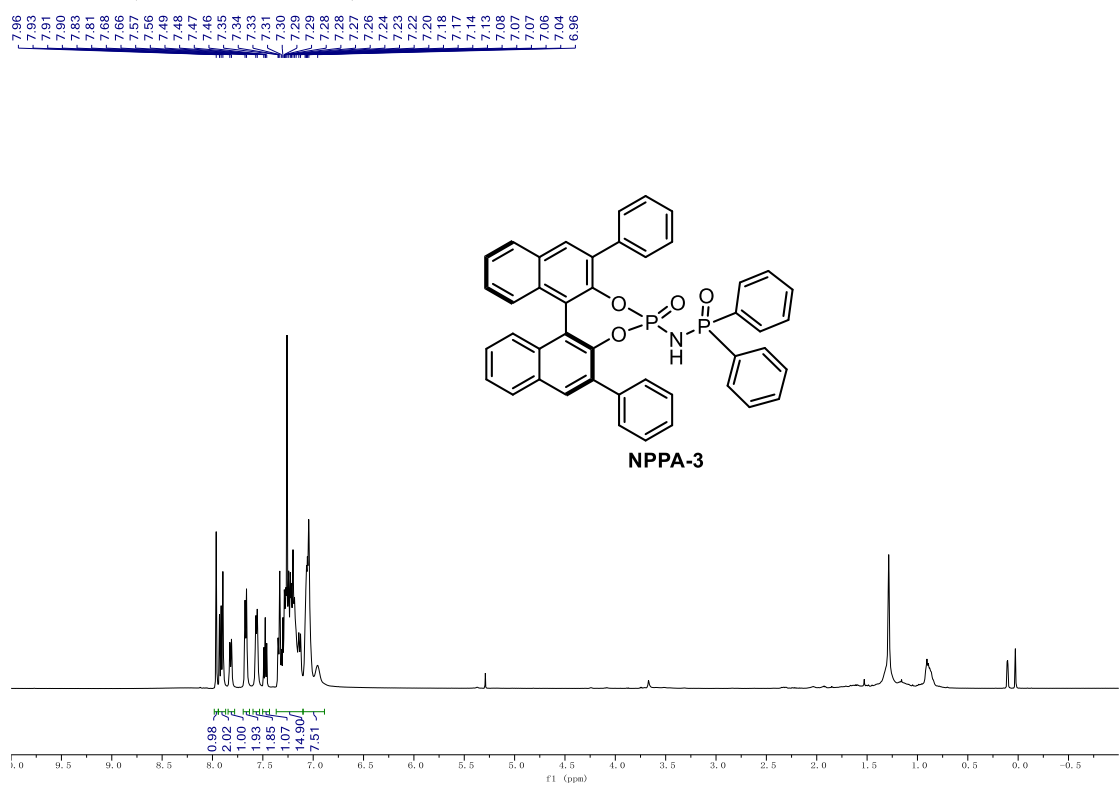
9.1. NMR Spectra

^1H NMR (500 MHz, CD_2Cl_2) of NPPA-2.



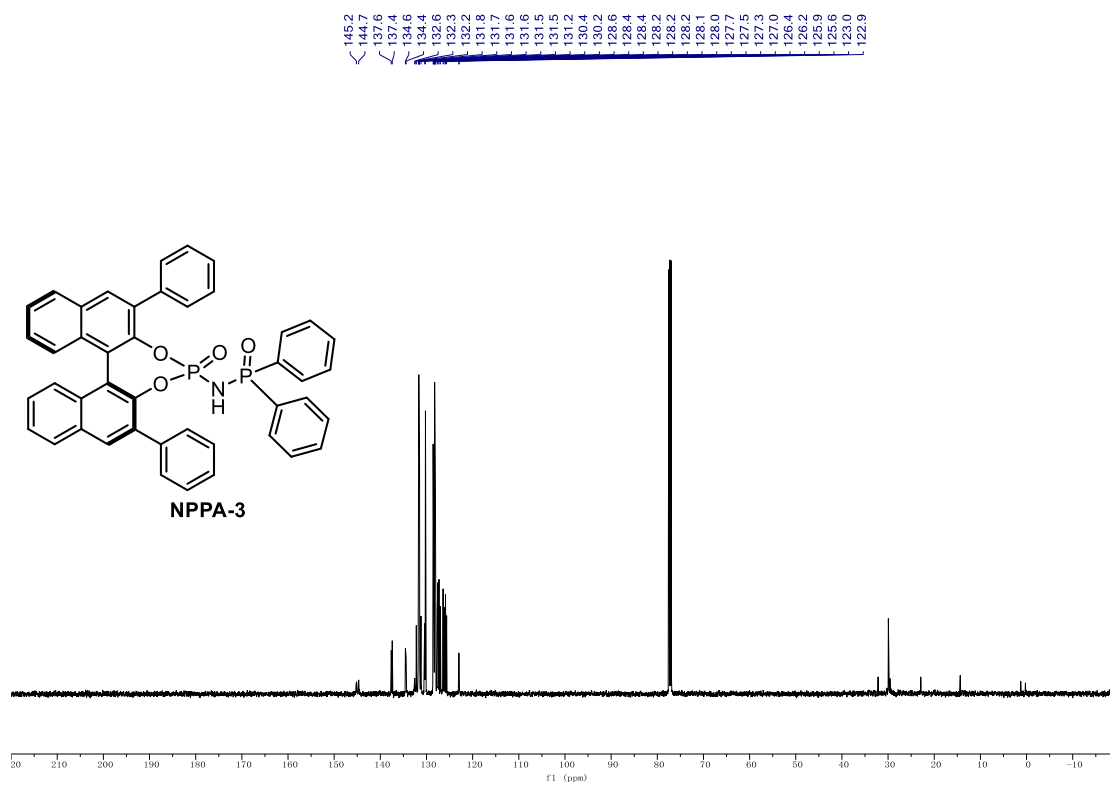
^{13}C NMR (126 MHz, CD_2Cl_2) of NPPA-2.



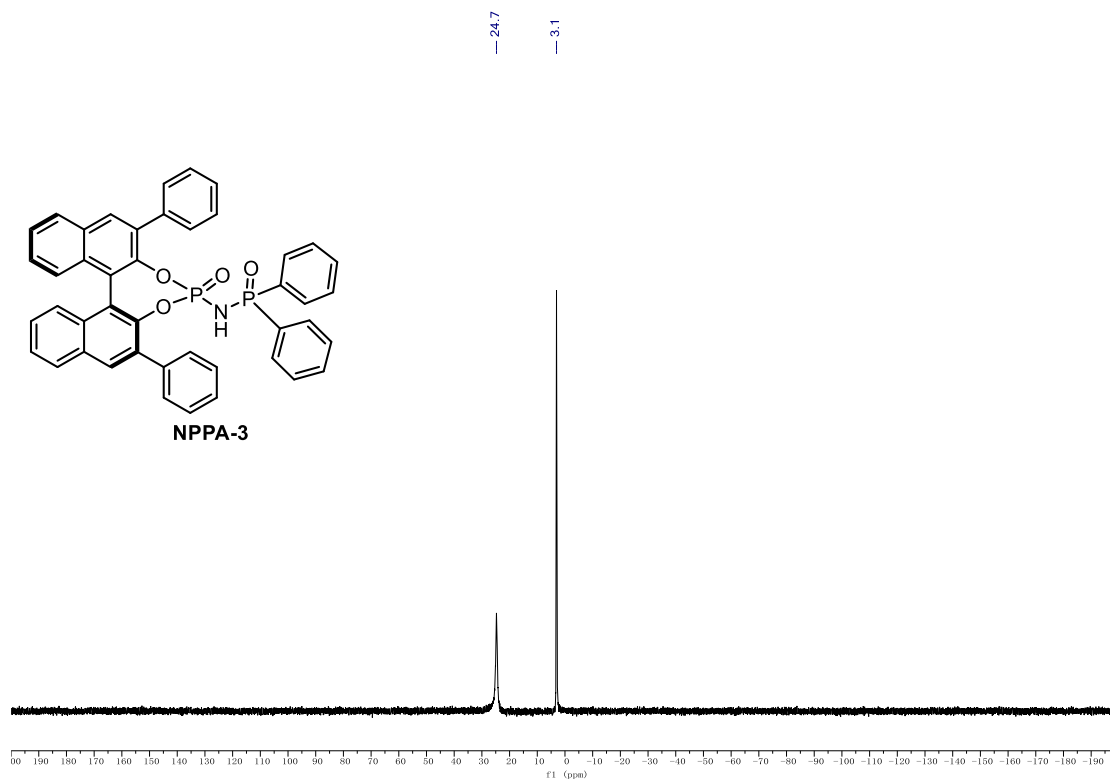
^{31}P NMR (203 MHz, CD_2Cl_2) of NPPA-2. **^1H NMR (500 MHz, CD_2Cl_2) of NPPA-3.**

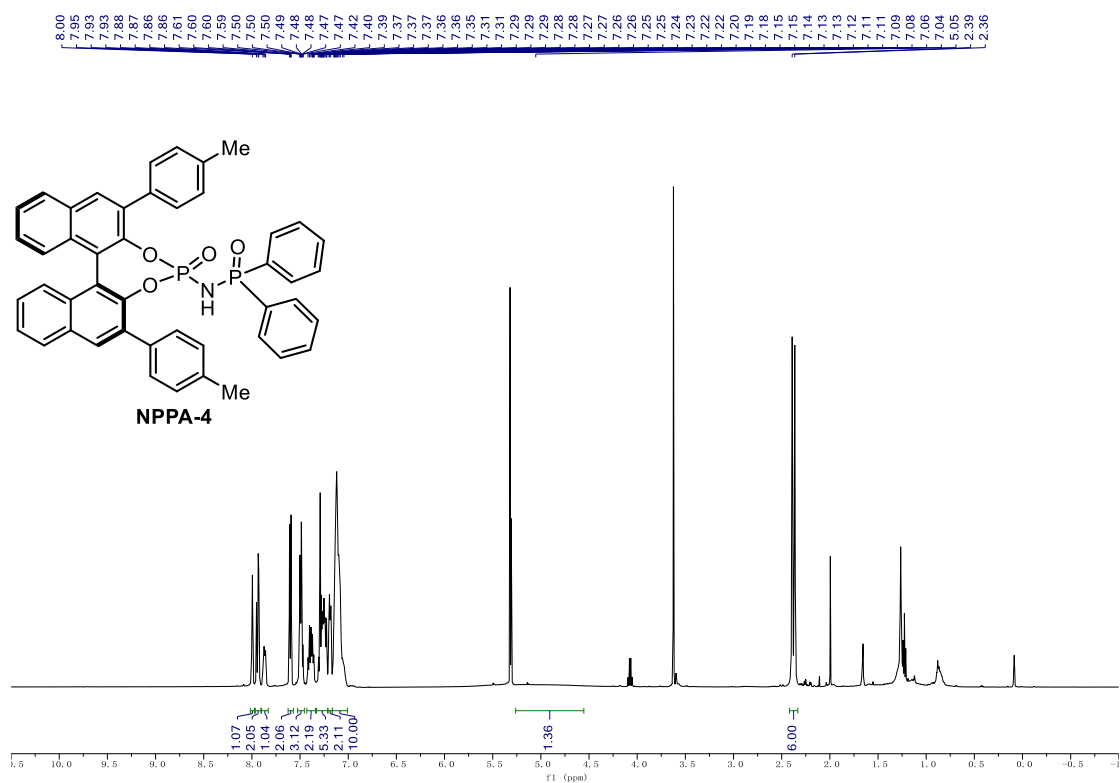
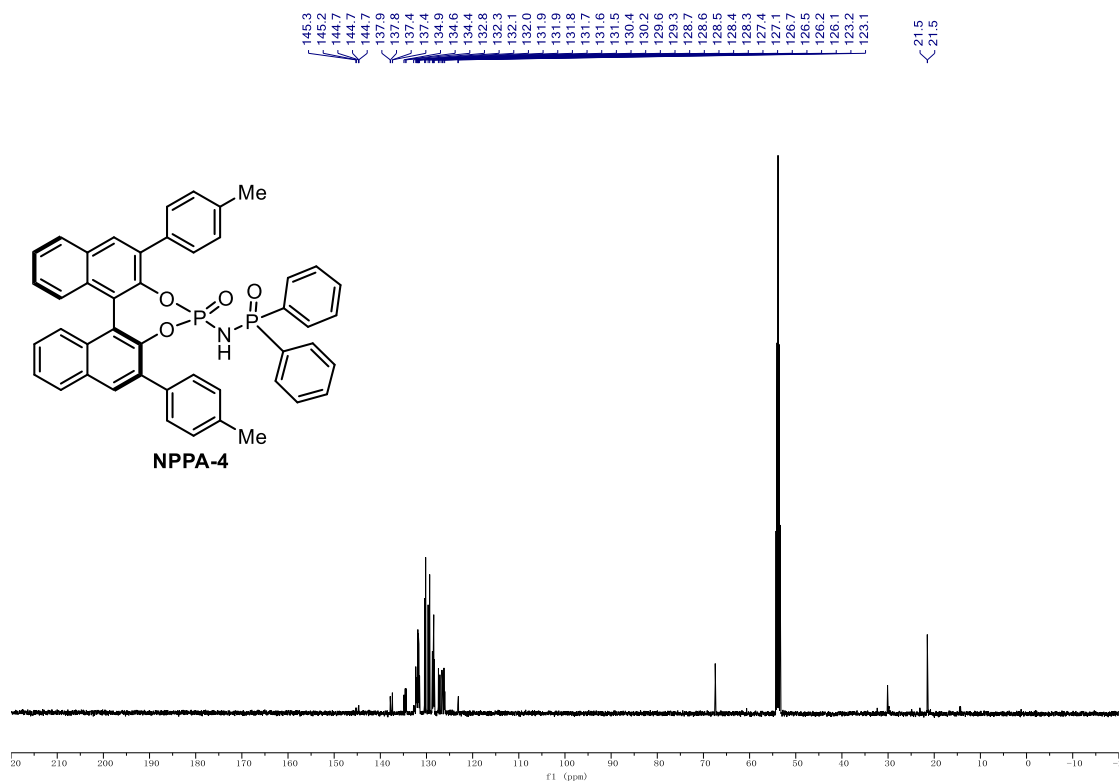
9.1. NMR Spectra

^{13}C NMR (126 MHz, CD_2Cl_2) of NPPA-3.



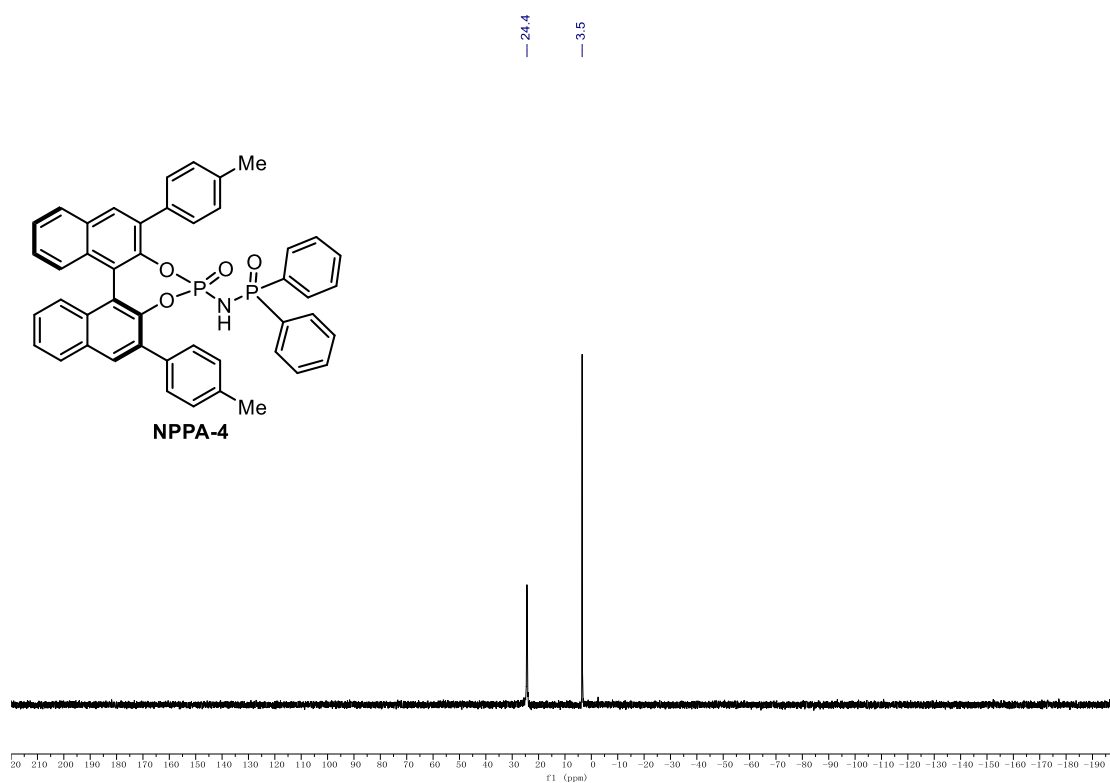
^{31}P NMR (203 MHz, CD_2Cl_2) of NPPA-3.



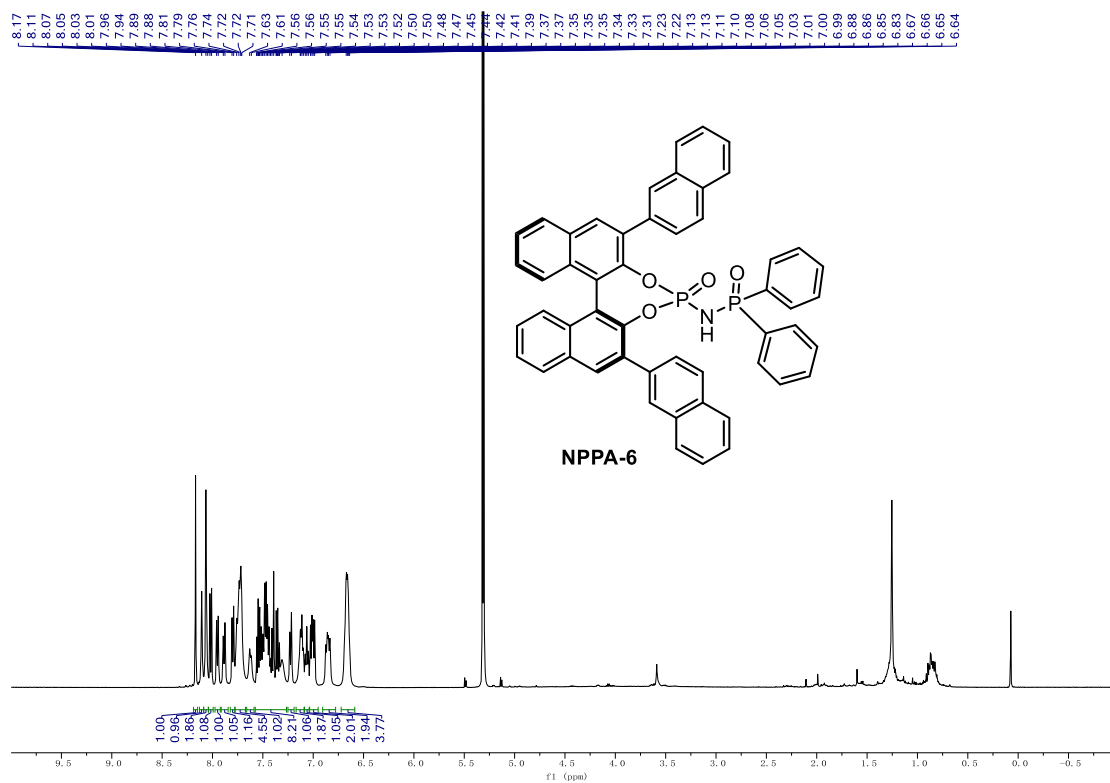
¹H NMR (500 MHz, CD₂Cl₂) of NPPA-4.**¹³C NMR (126 MHz, CD₂Cl₂) of NPPA-4.**

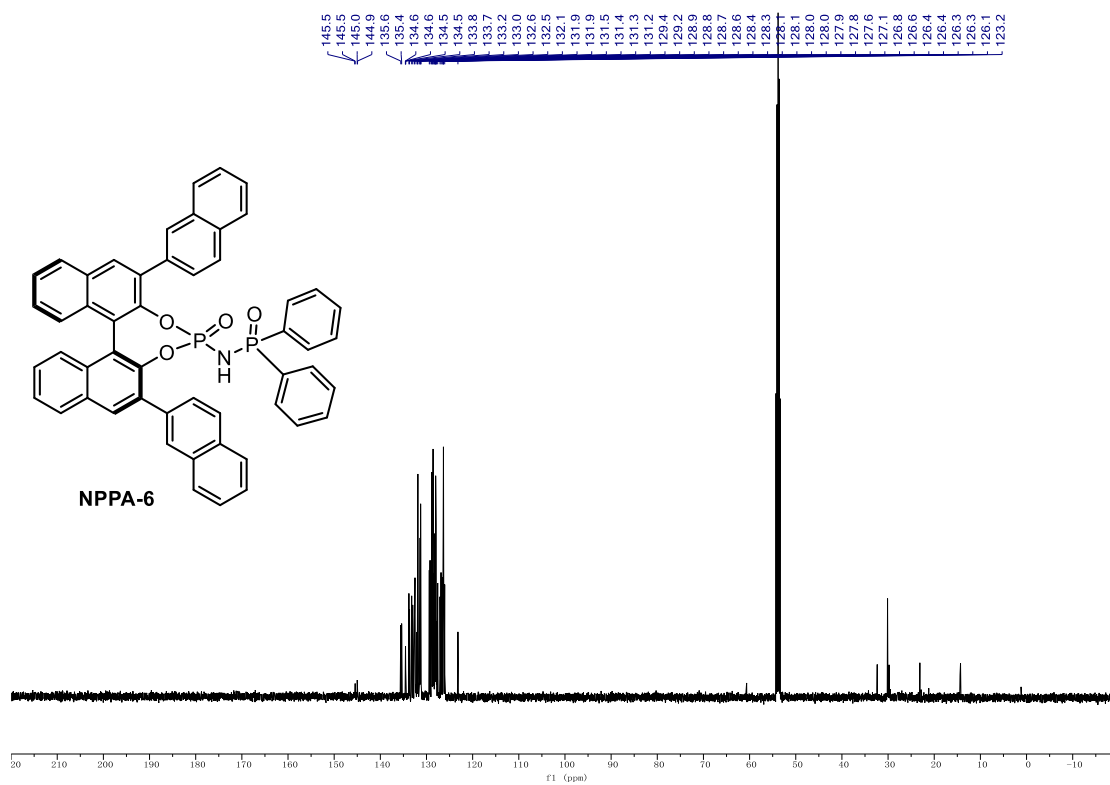
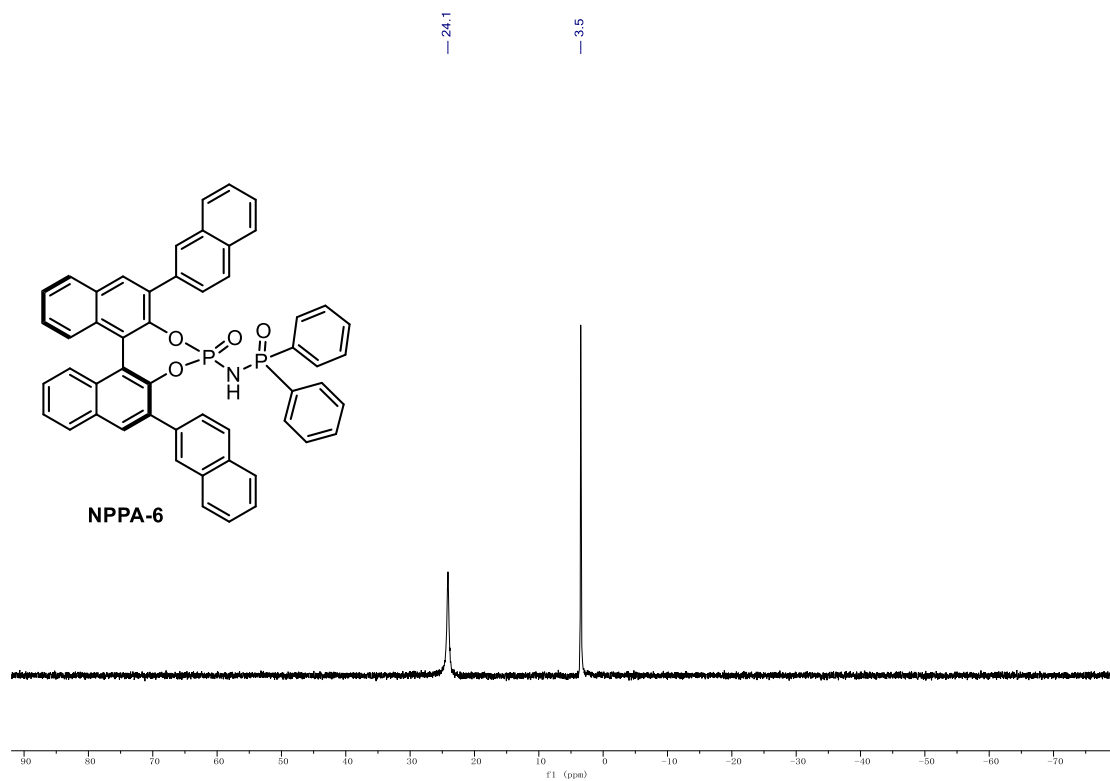
9.1. NMR Spectra

³¹P NMR (203 MHz, CD₂Cl₂) of NPPA-4.



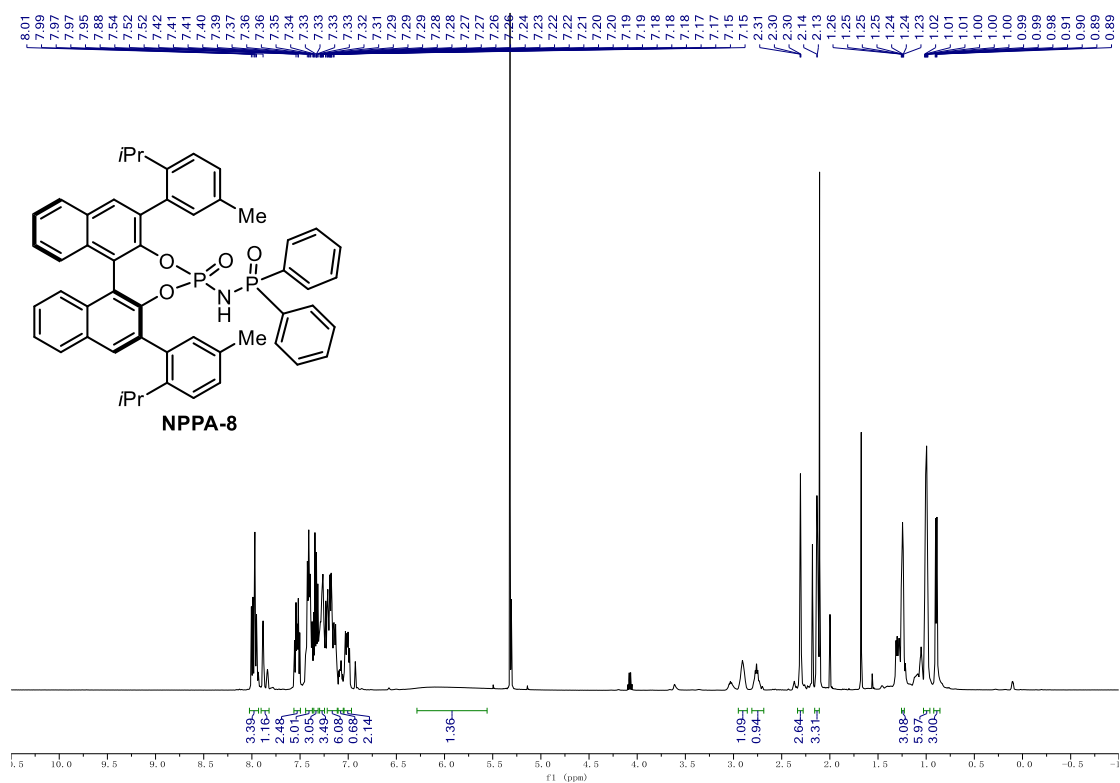
¹H NMR (500 MHz, CD₂Cl₂) of NPPA-6.



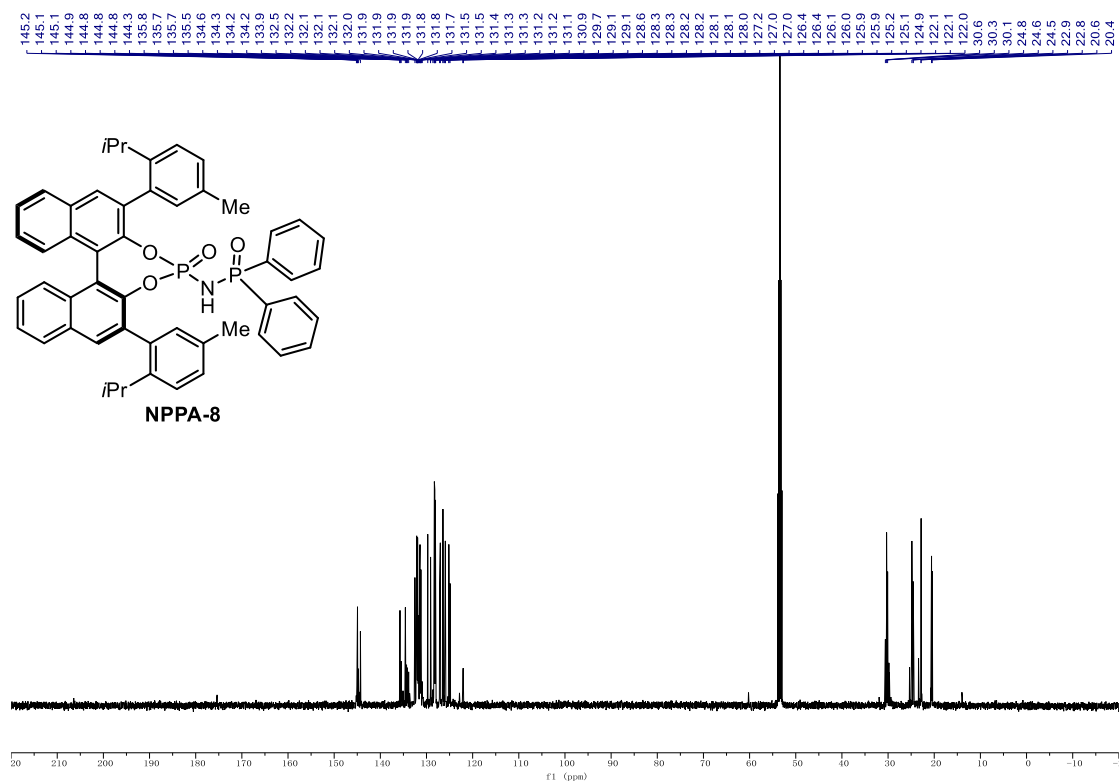
^{13}C NMR (126 MHz, CD_2Cl_2) of NPPA-6. **^{31}P NMR (203 MHz, CD_2Cl_2) of NPPA-6.**

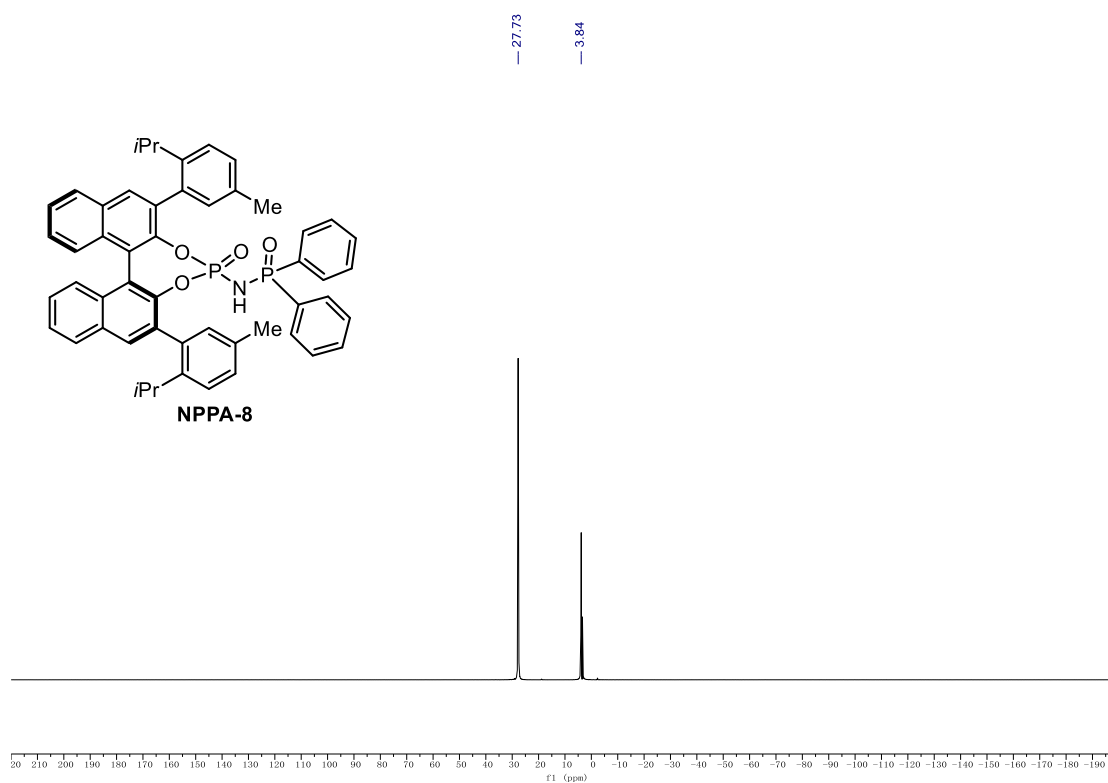
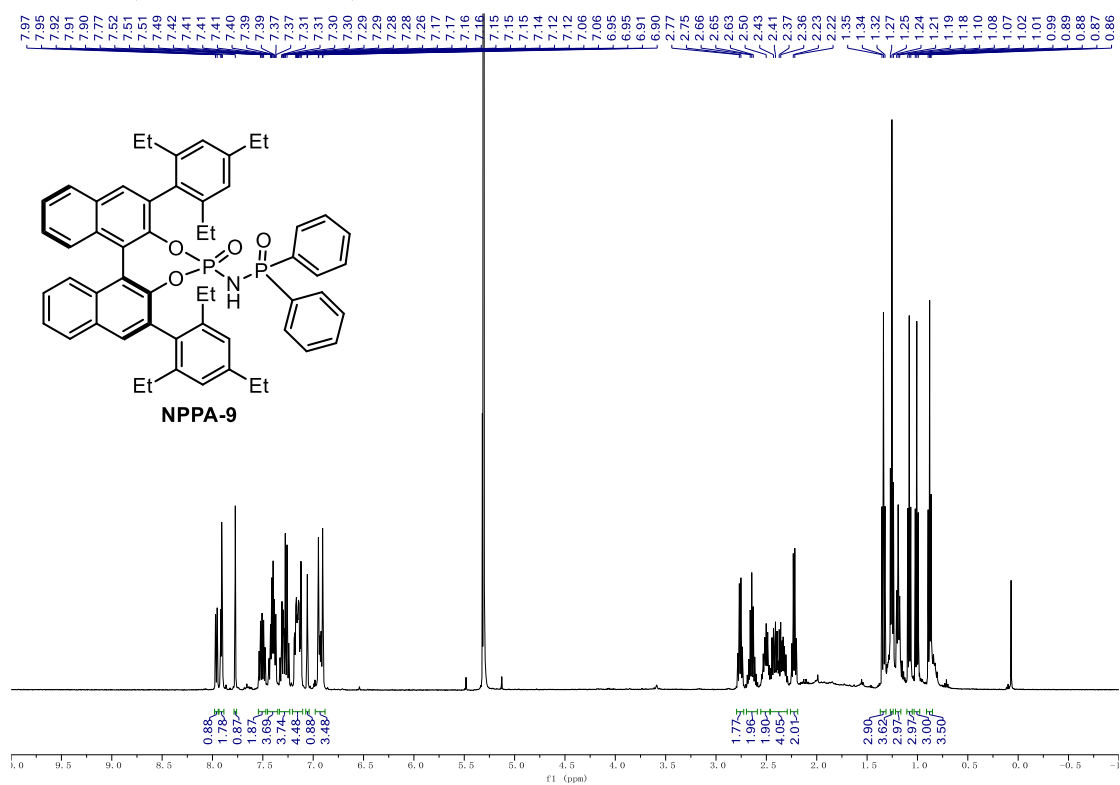
9.1. NMR Spectra

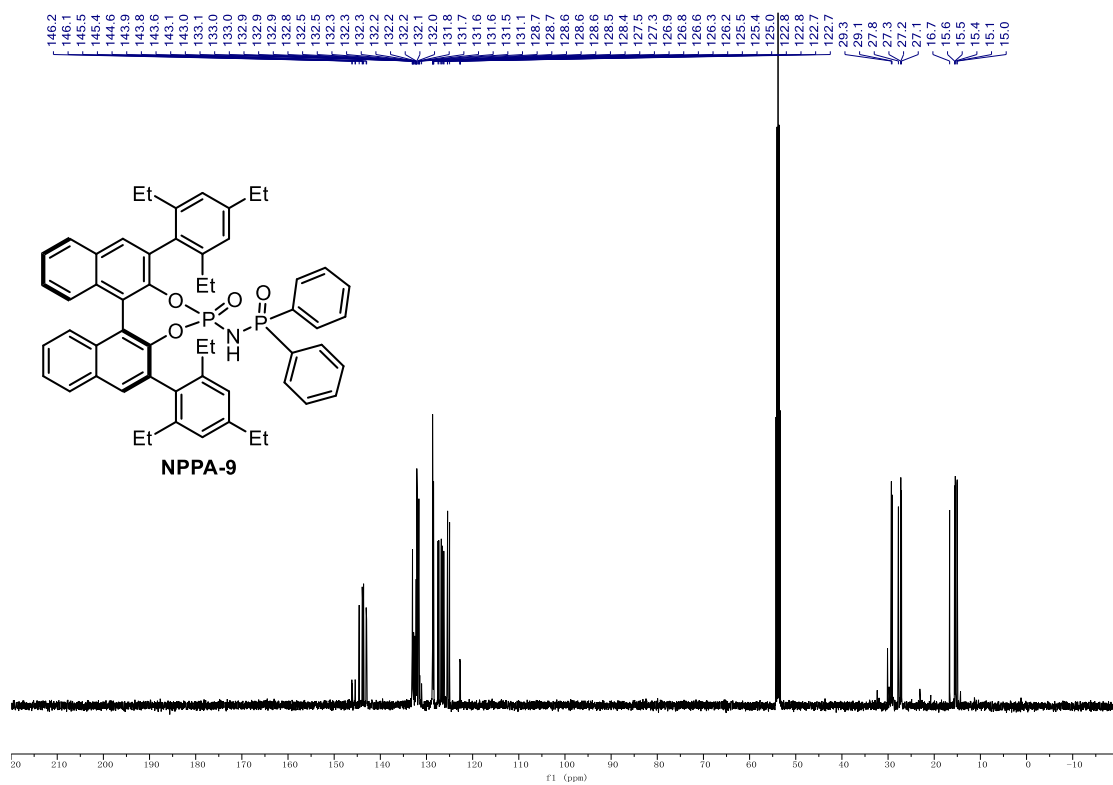
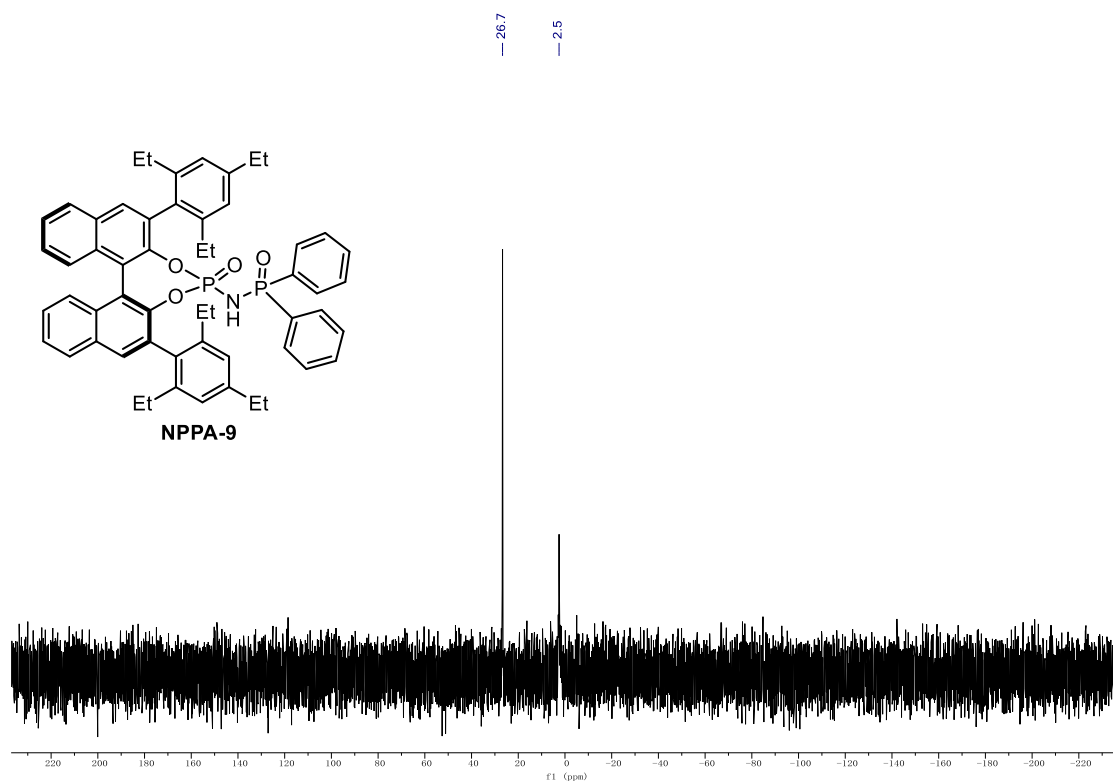
¹H NMR (500 MHz, CD₂Cl₂) of NPPA-8.

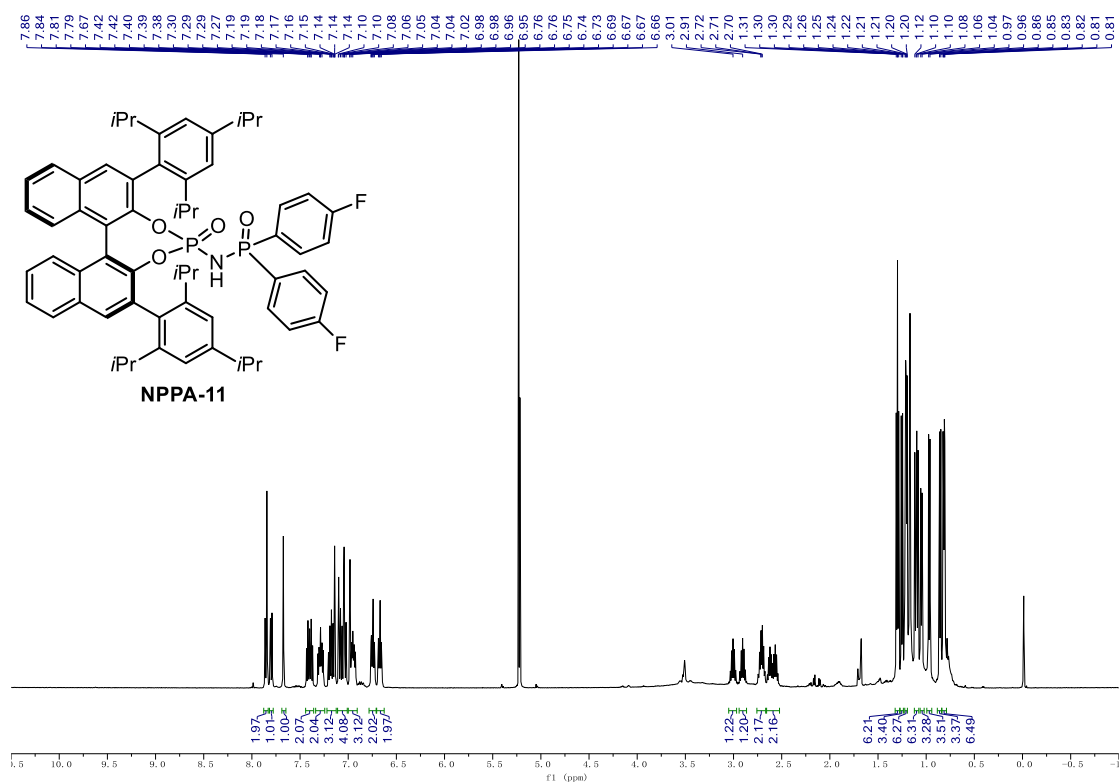
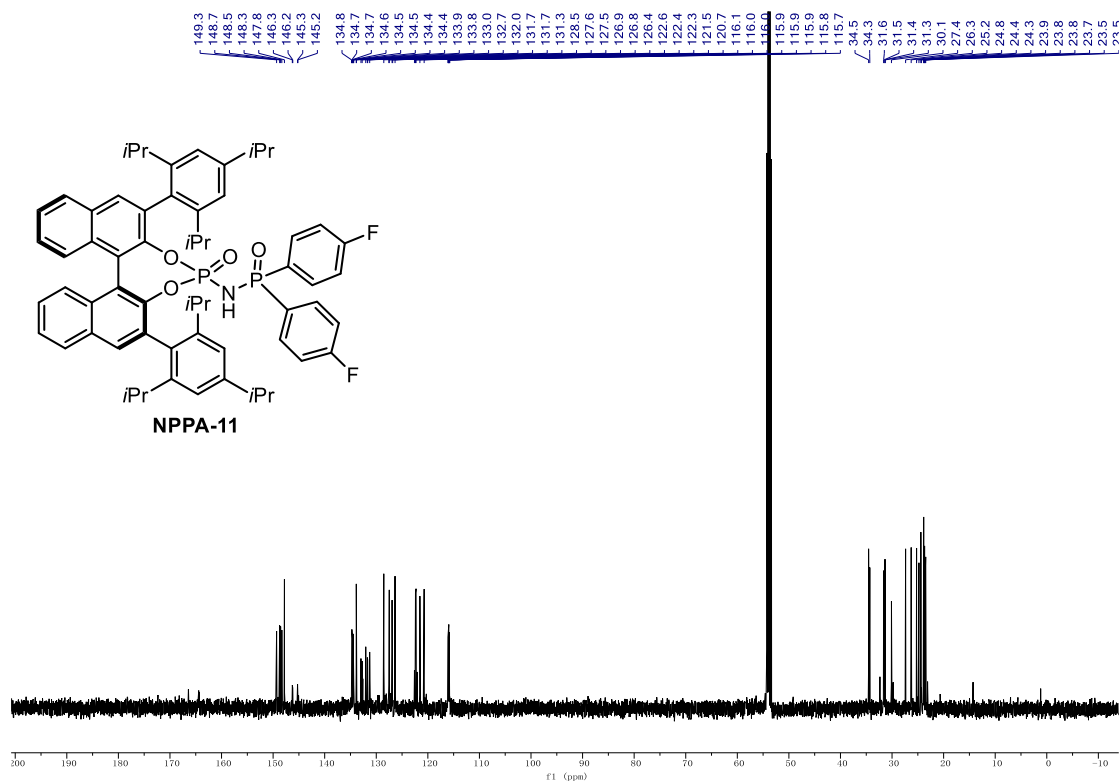


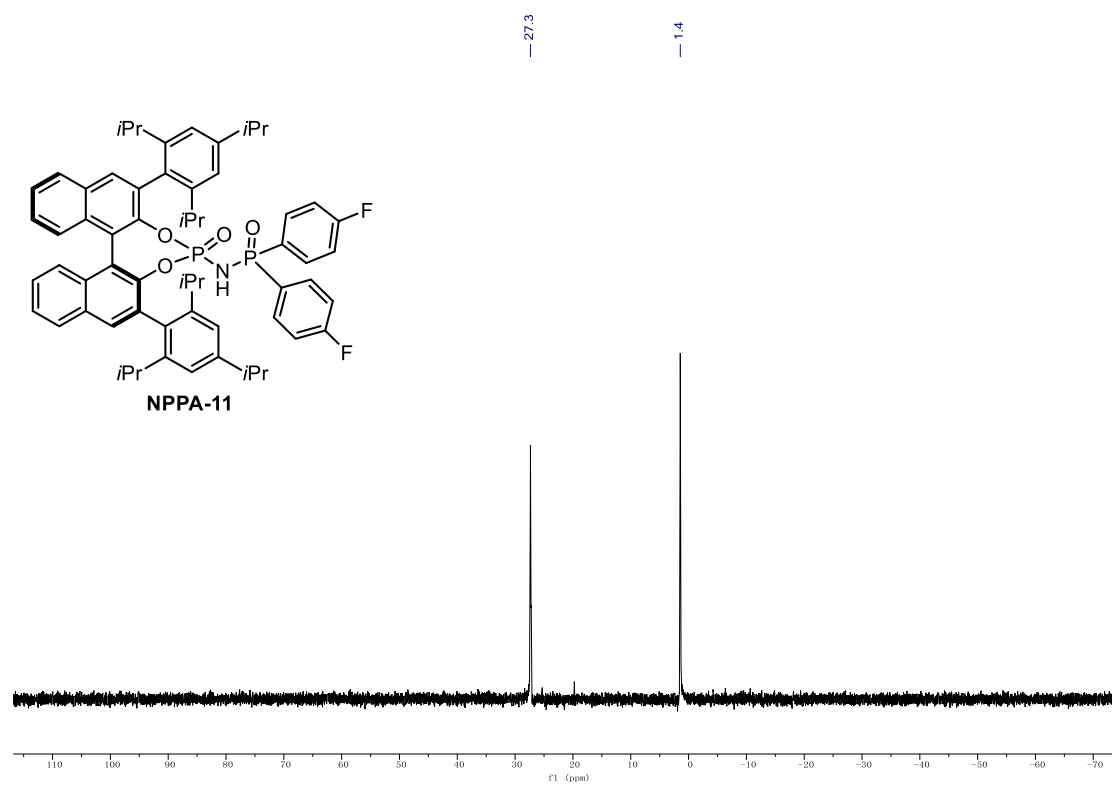
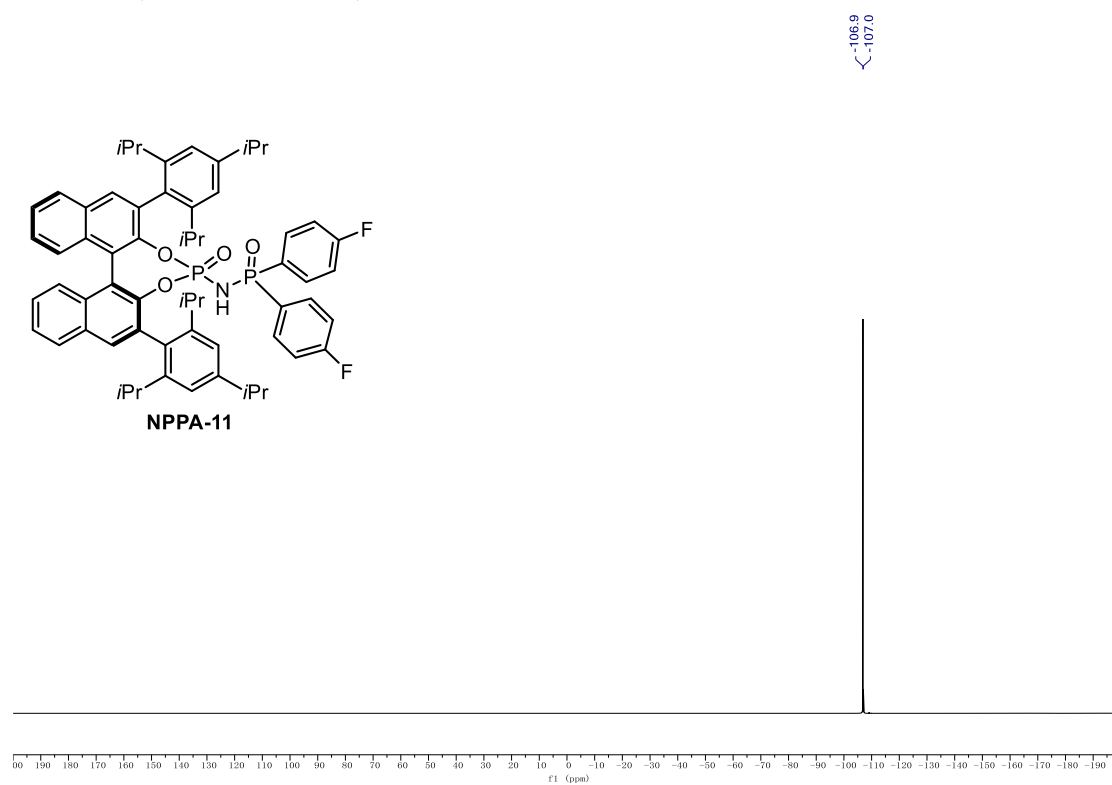
¹³C NMR (126 MHz, CD₂Cl₂) of NPPA-8.

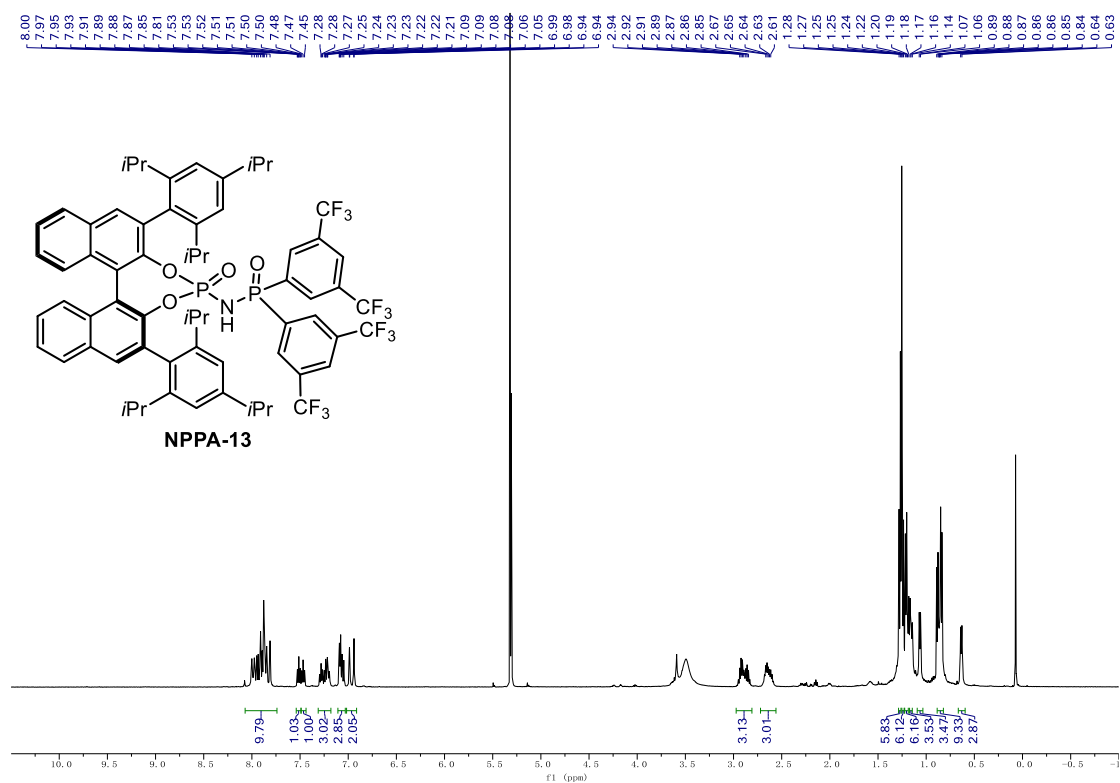
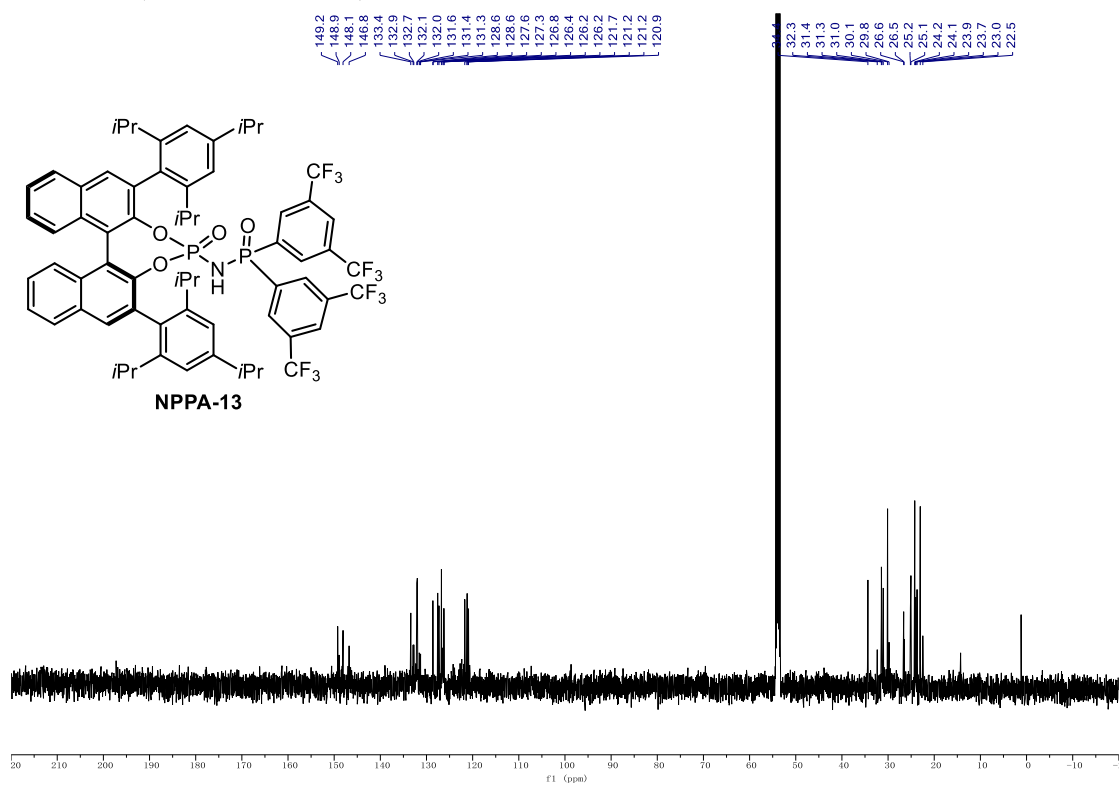


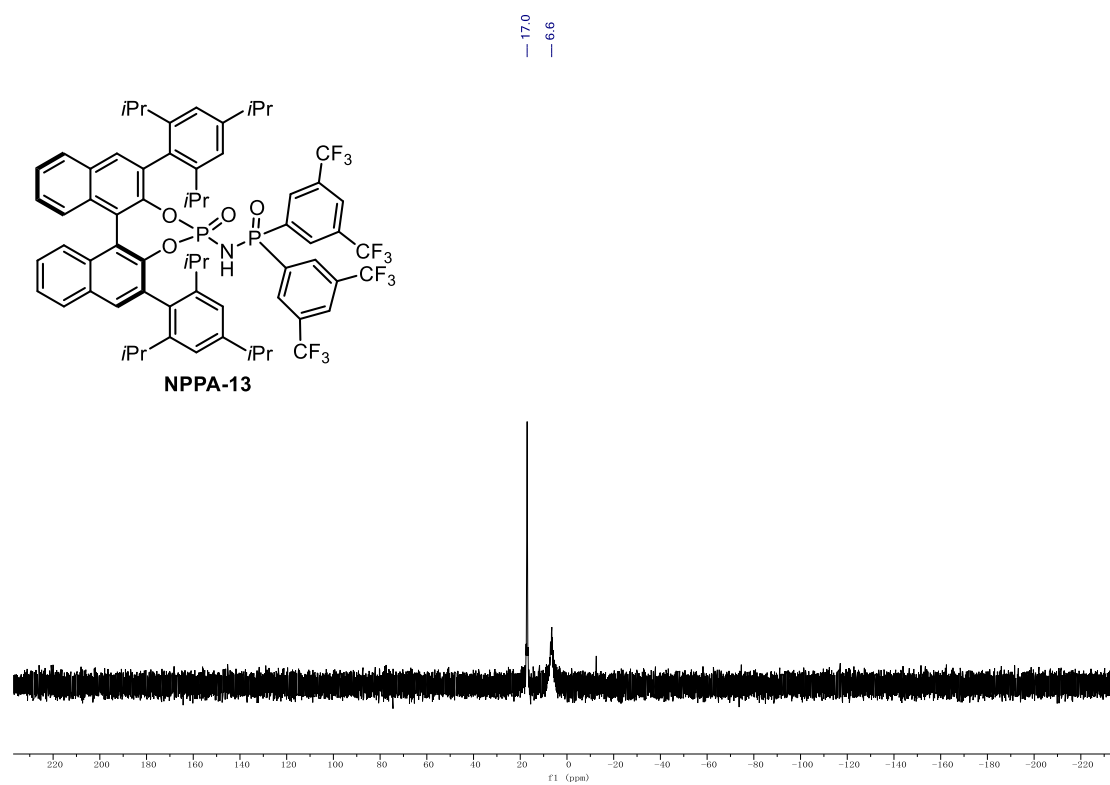
^{31}P NMR (203 MHz, CD_2Cl_2) of NPPA-8. ^1H NMR (500 MHz, CD_2Cl_2) of NPPA-9.

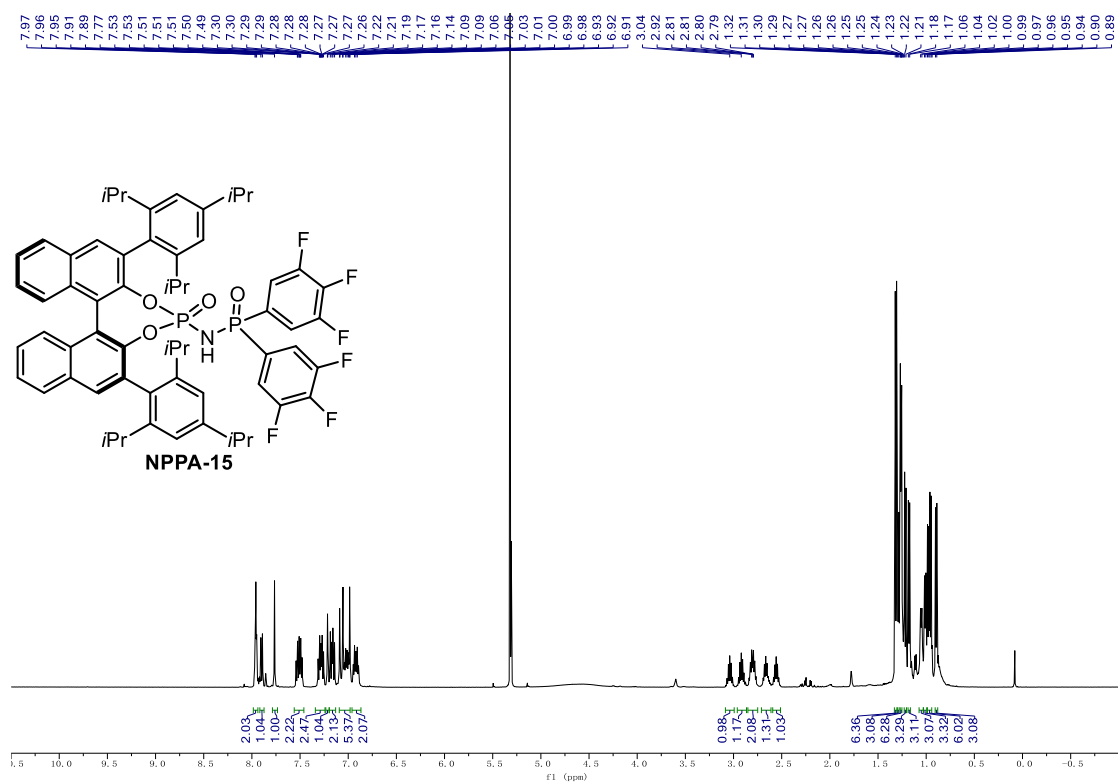
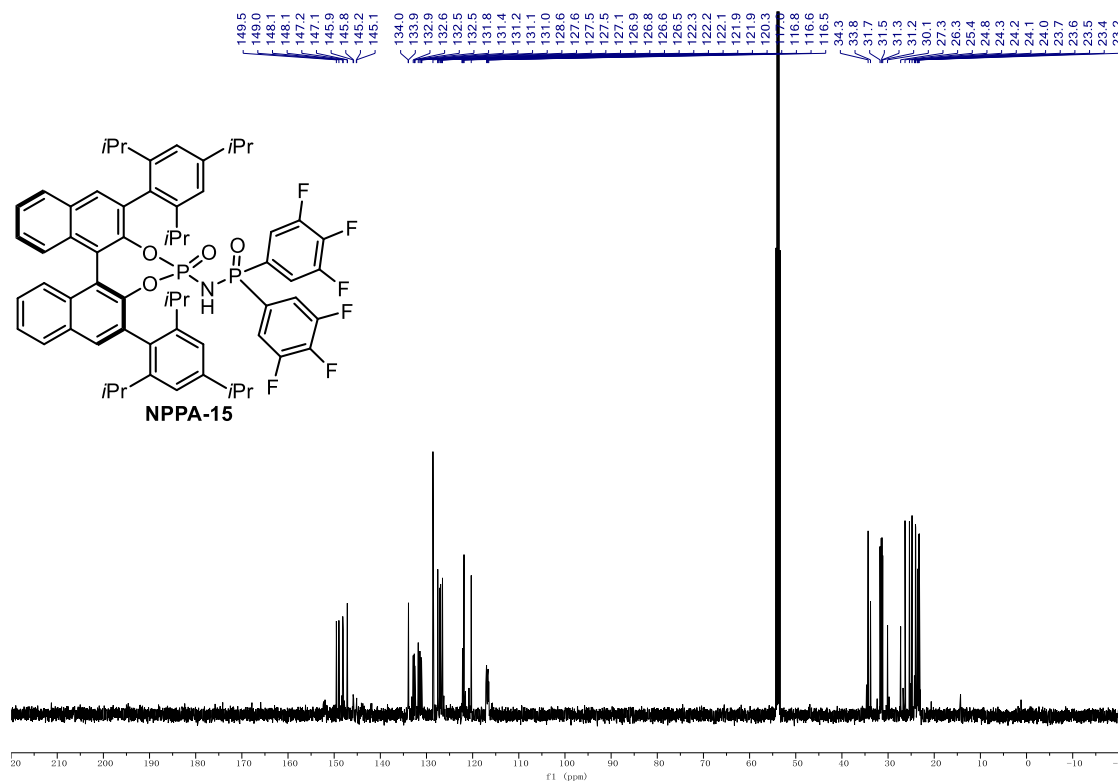
¹³C NMR (126 MHz, CD₂Cl₂) of NPPA-9.**³¹P NMR (203 MHz, CD₂Cl₂) of NPPA-9.**

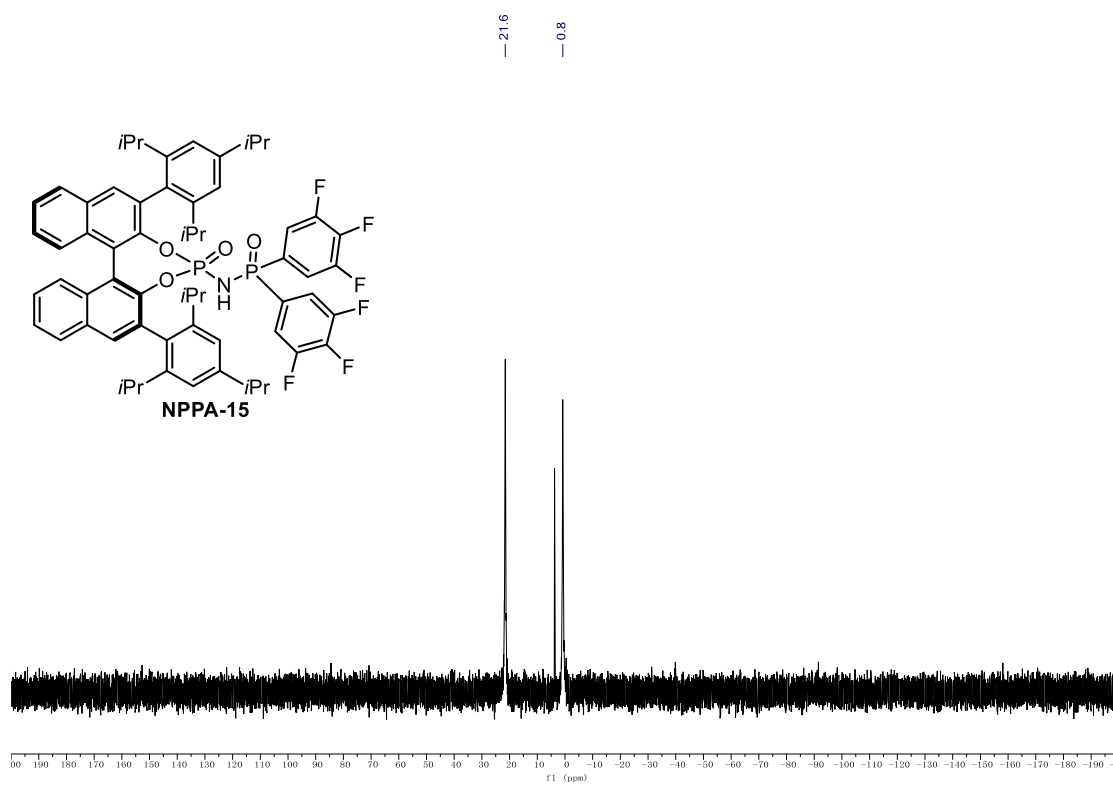
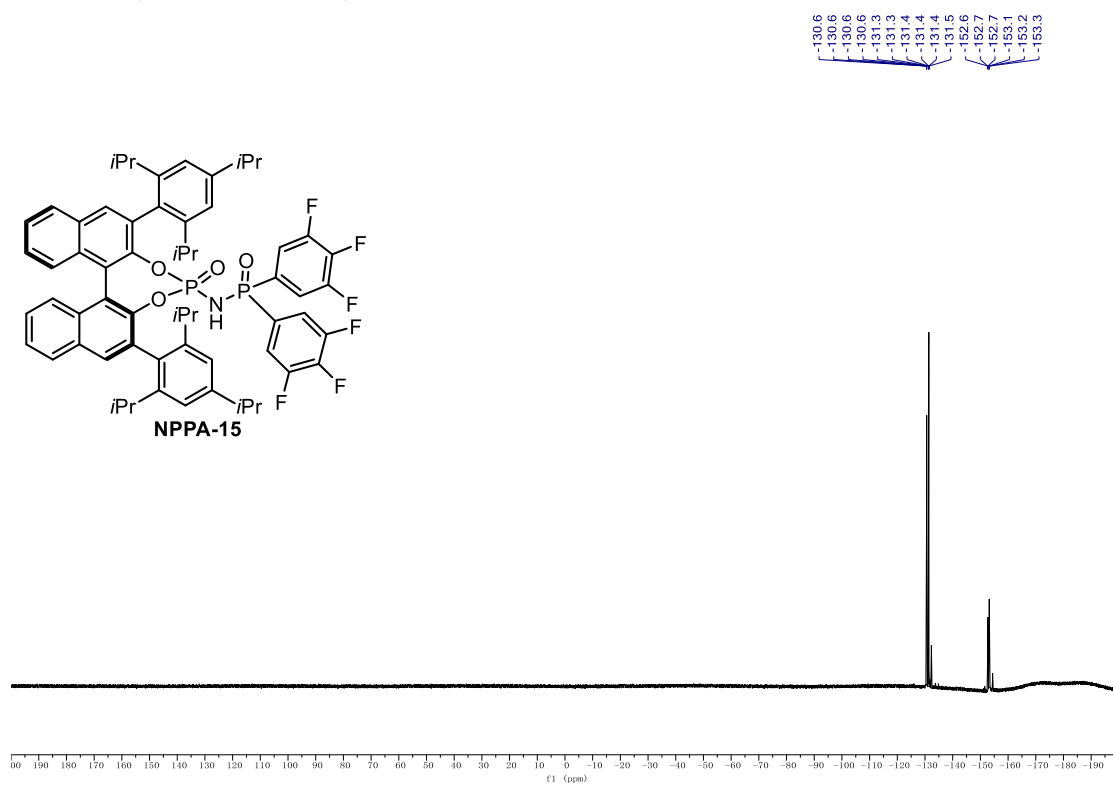
^1H NMR (500 MHz, CD_2Cl_2) of NPPA-11. ^{13}C NMR (126 MHz, CD_2Cl_2) of NPPA-11.

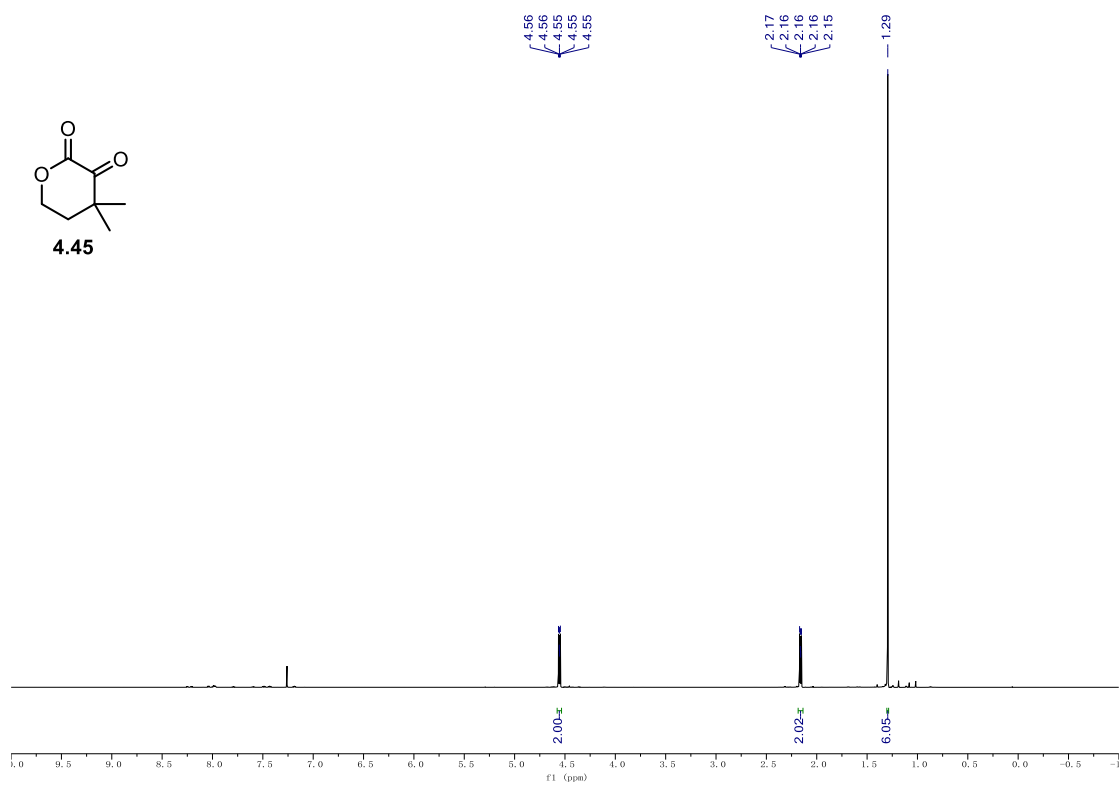
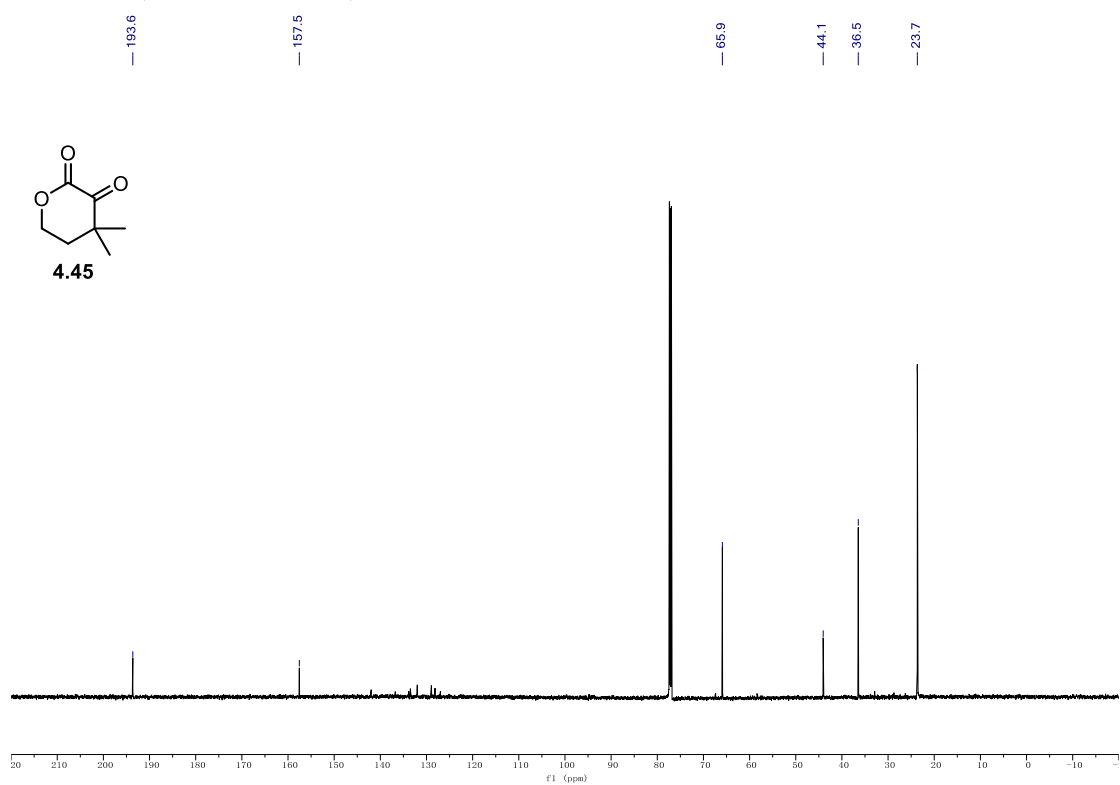
³¹P NMR (203 MHz, CD₂Cl₂) of NPPA-11.**¹⁹F NMR (471 MHz, CD₂Cl₂) of NPPA-11.**

^1H NMR (500 MHz, CD_2Cl_2) of NPPA-13. ^{13}C NMR (126 MHz, CD_2Cl_2) of NPPA-13.

^{31}P NMR (203 MHz, CD_2Cl_2) of NPPA-13. **^{19}F NMR (471 MHz, CD_2Cl_2) of NPPA-13.**

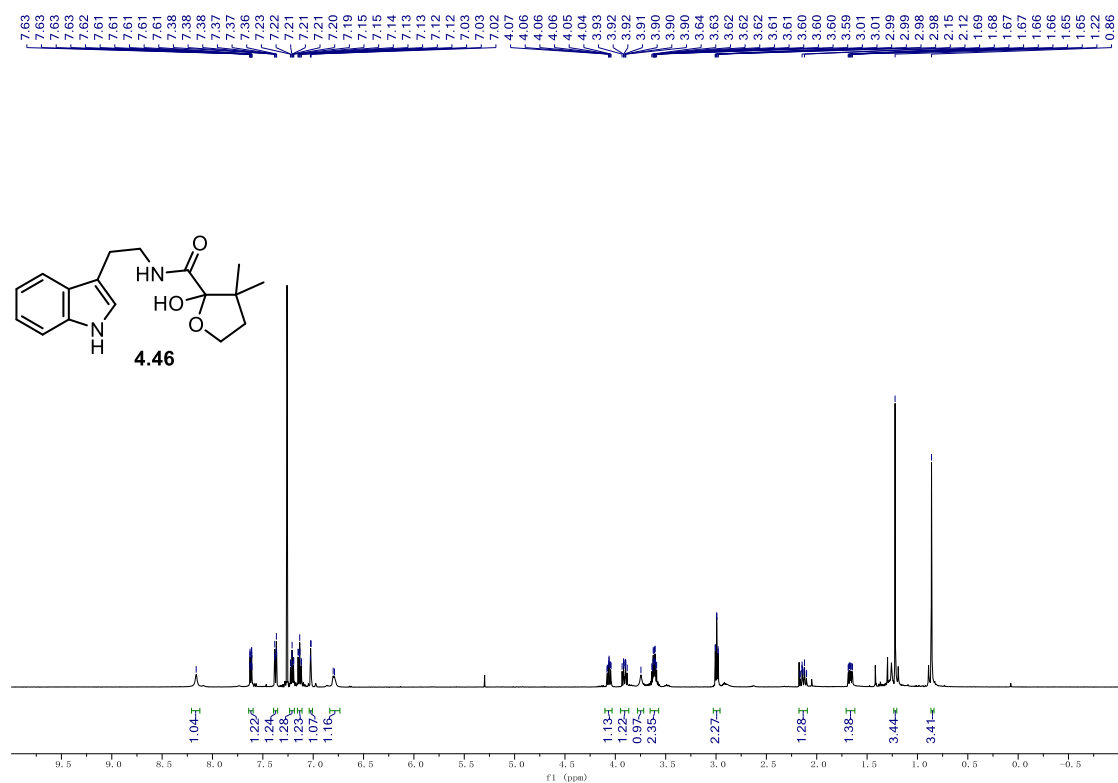
^1H NMR (500 MHz, CDCl_3) of NPPA-15. ^{13}C NMR (126 MHz, CDCl_3) of NPPA-15.

^{31}P NMR (203 MHz, CDCl_3) of NPPA-15. ^{19}F NMR (471 MHz, CDCl_3) of NPPA-15.

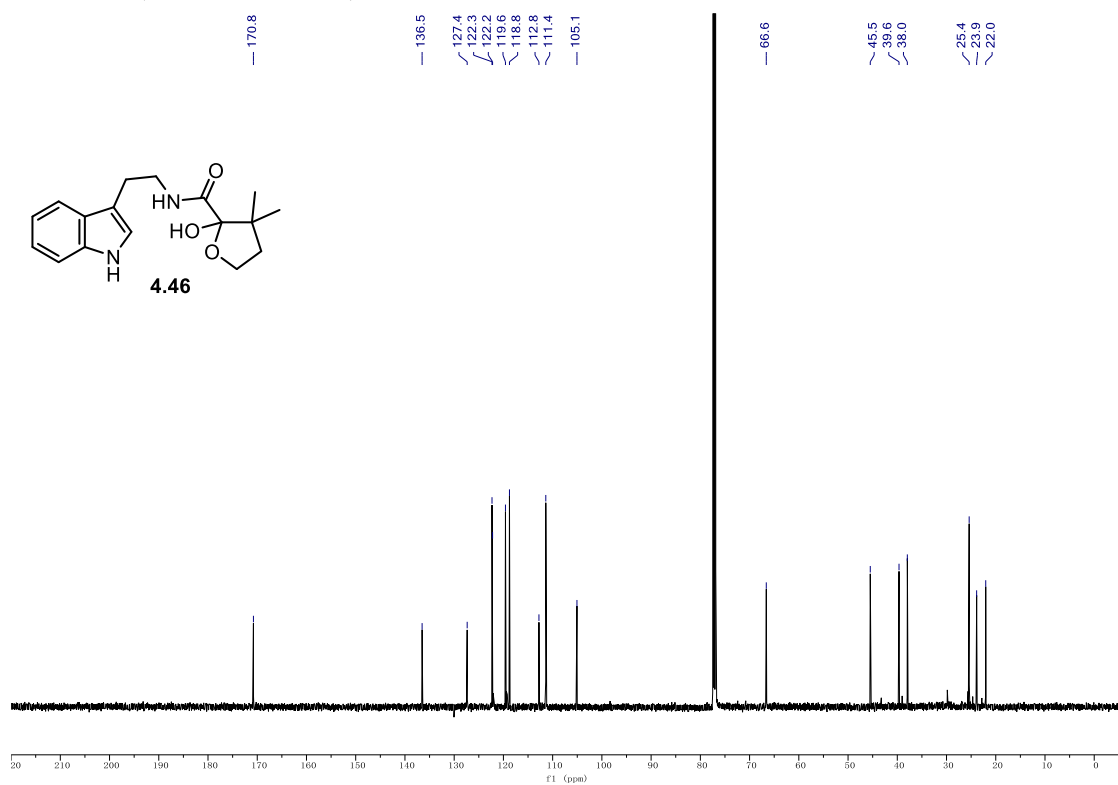
^1H NMR (600 MHz, CDCl_3) of 4.45. **^{13}C NMR (151 MHz, CDCl_3) of 4.45.**

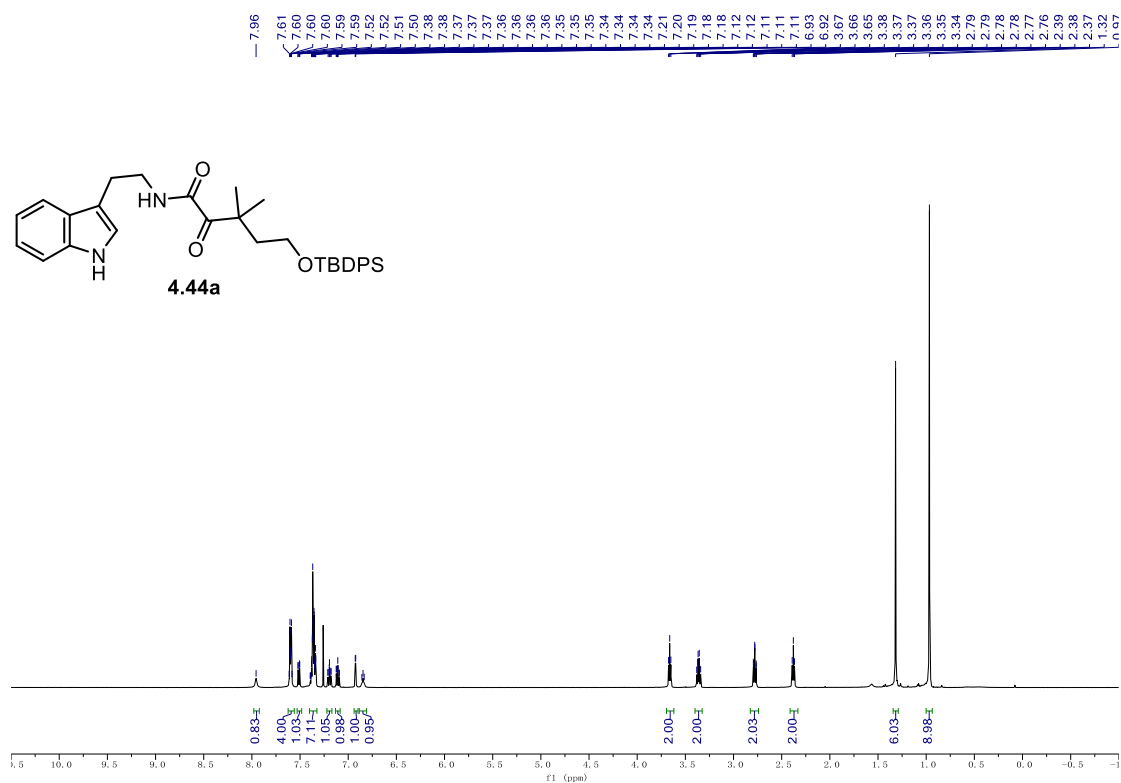
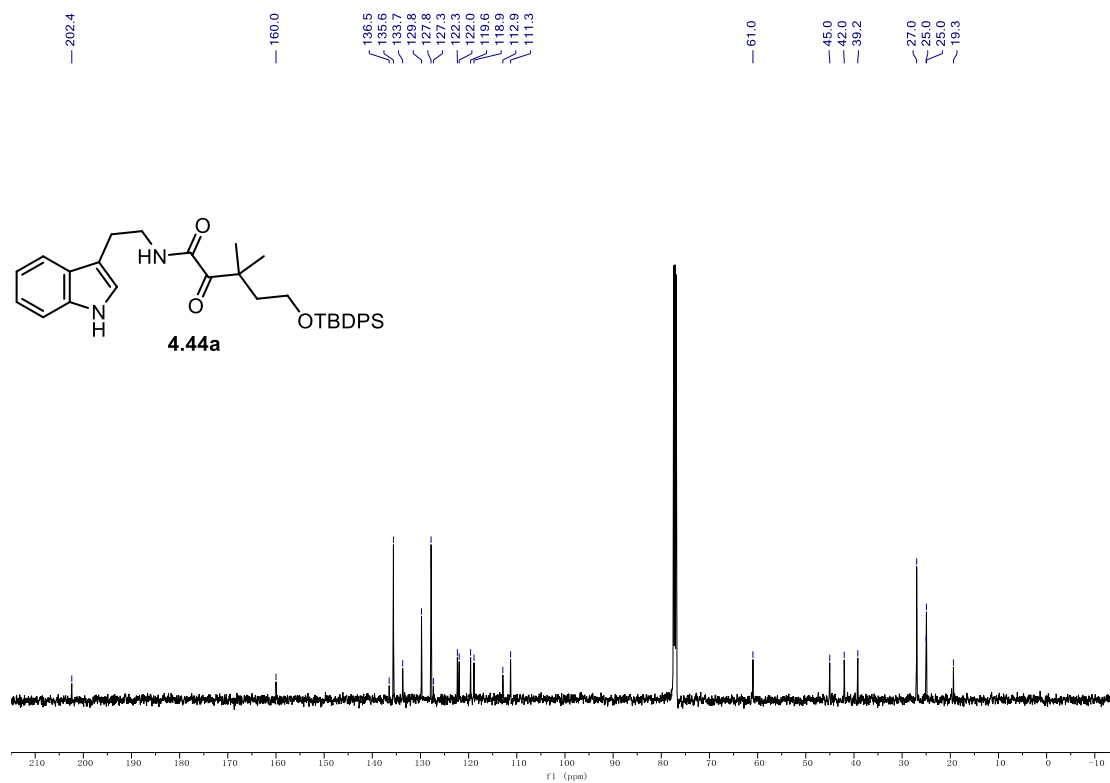
9.1. NMR Spectra

¹H NMR (500 MHz, CDCl₃) of 4.46.



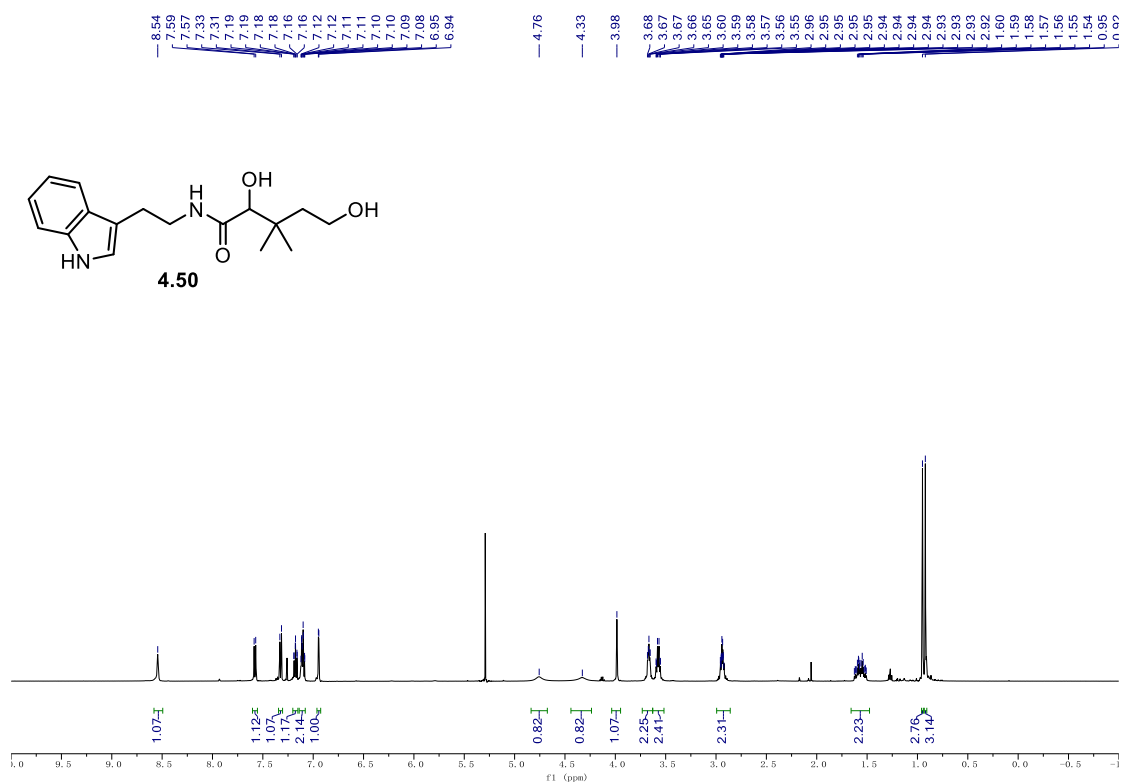
¹³C NMR (126 MHz, CDCl₃) of 4.46.



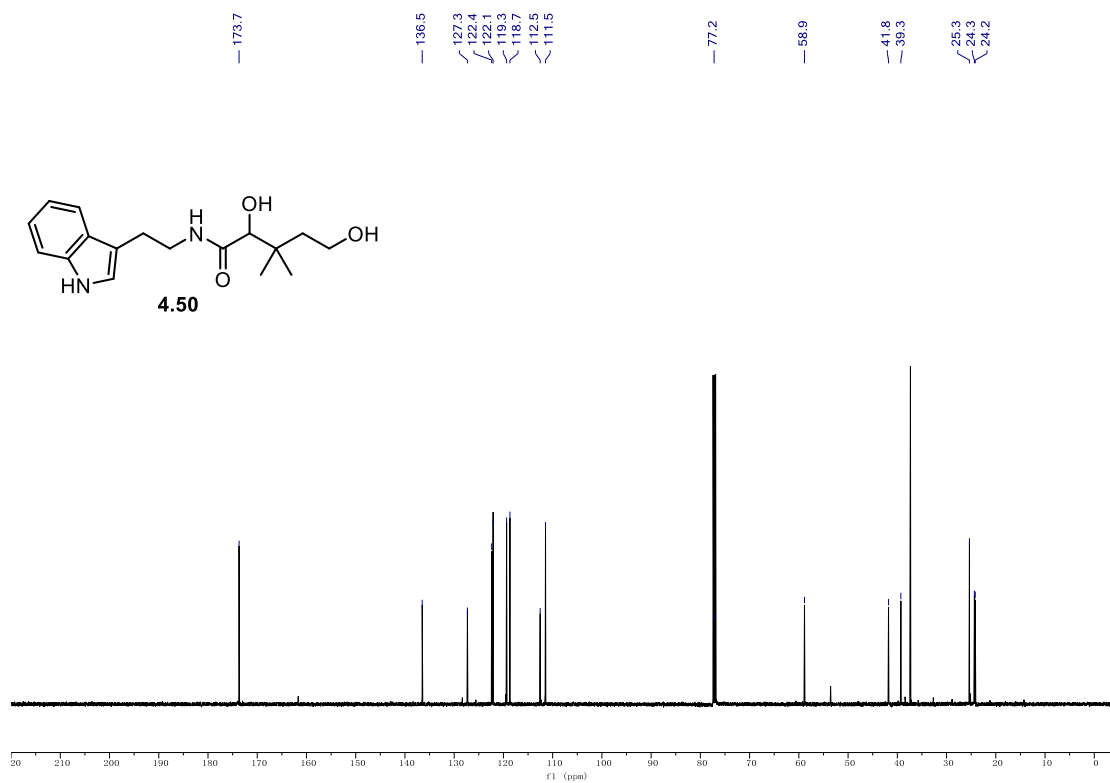
¹H NMR (500 MHz, CDCl₃) of 4.44a.**¹³C NMR (126 MHz, CDCl₃) of 4.44a.**

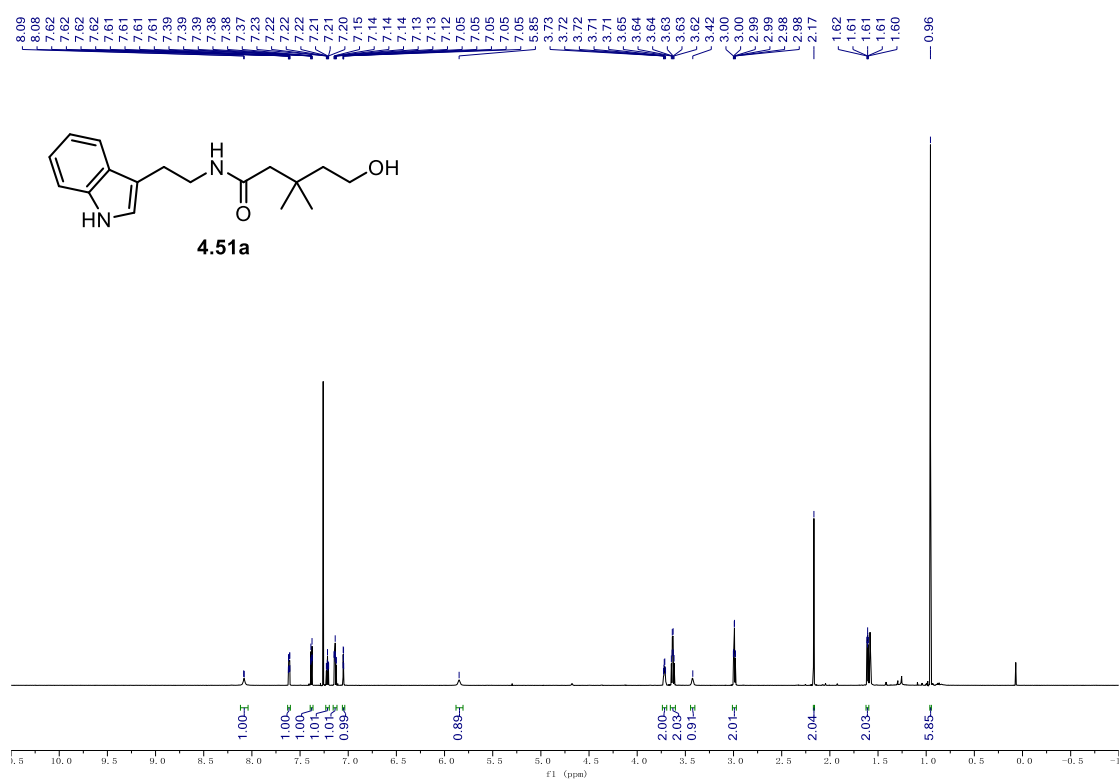
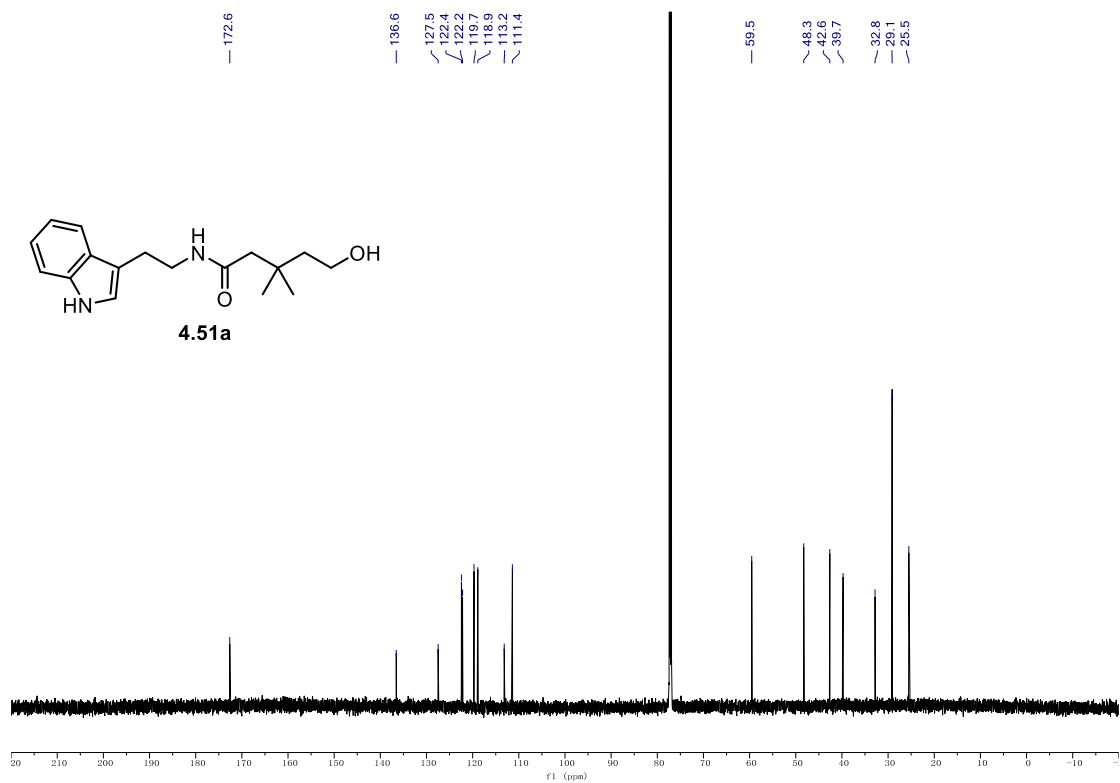
9.1. NMR Spectra

¹H NMR (500 MHz, CDCl₃) of **4.50**.



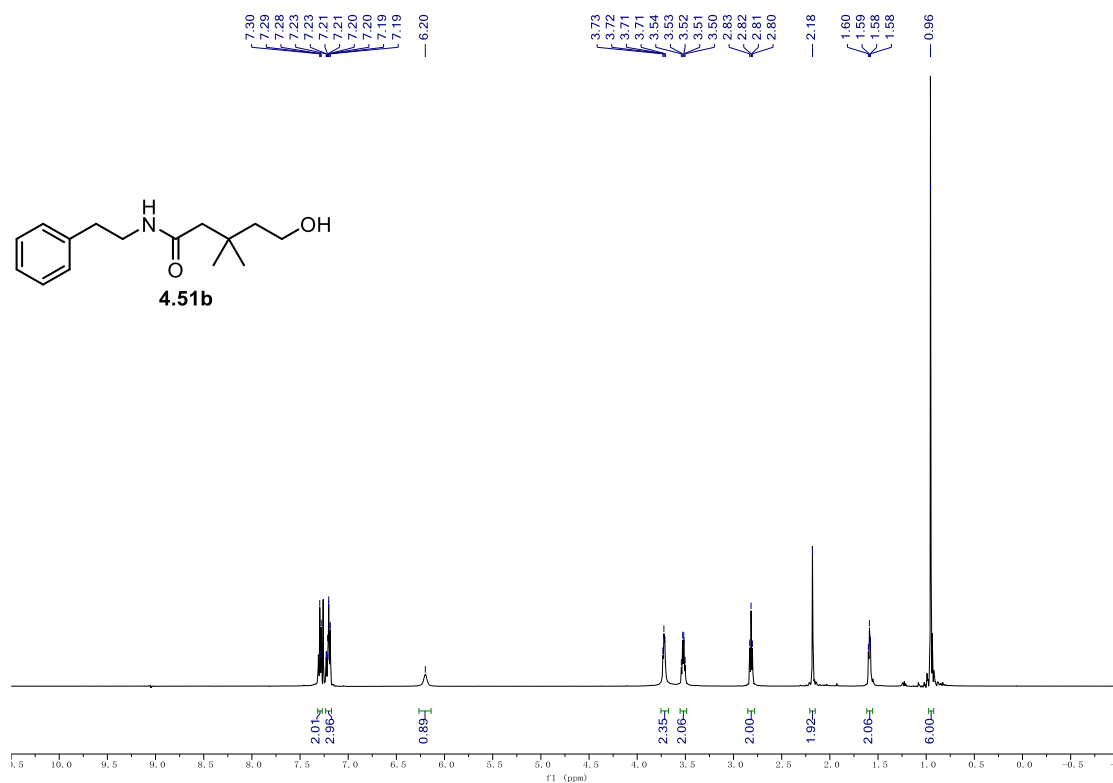
¹³C NMR (126 MHz, CDCl₃) of **4.50**.



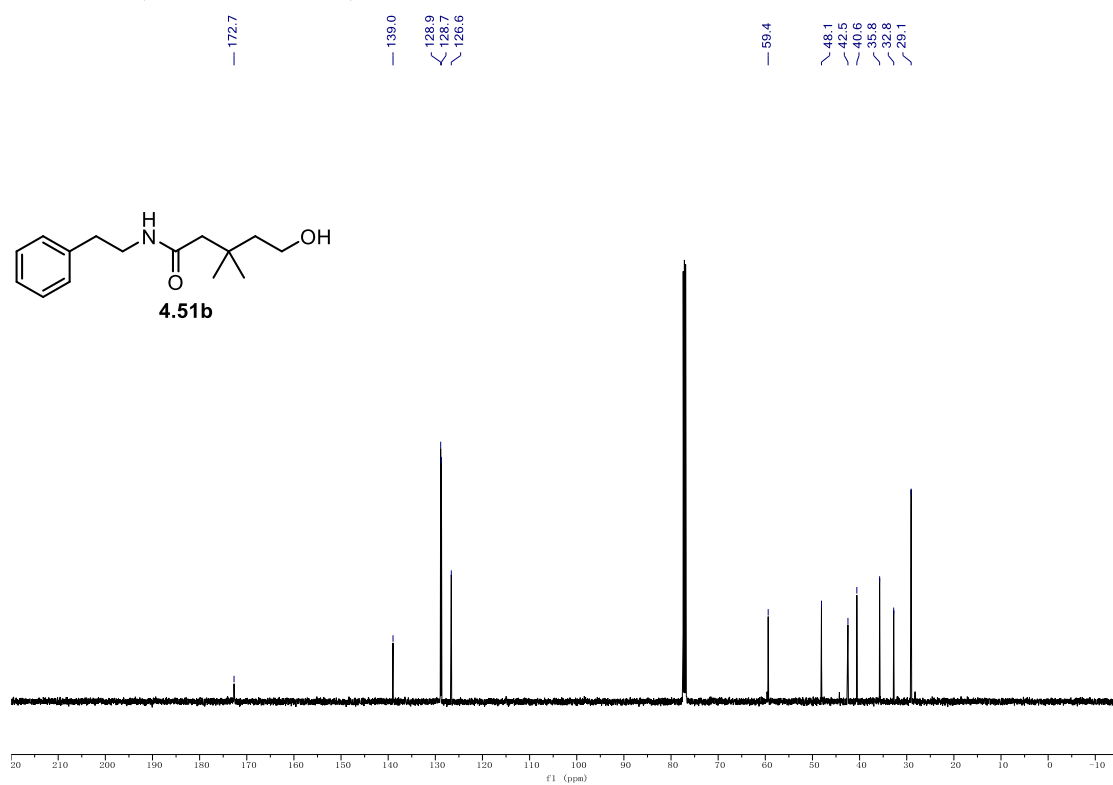
¹H NMR (500 MHz, CDCl₃) of 4.51a.**¹³C NMR (126 MHz, CDCl₃) of 4.51a.**

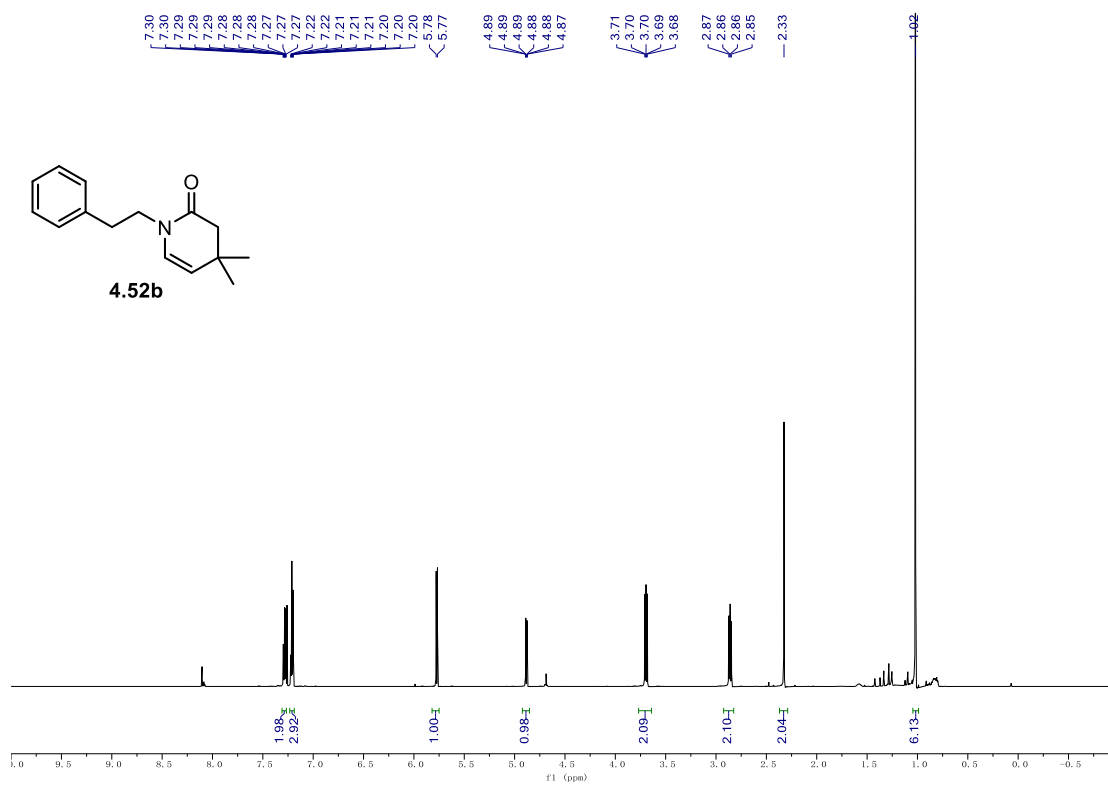
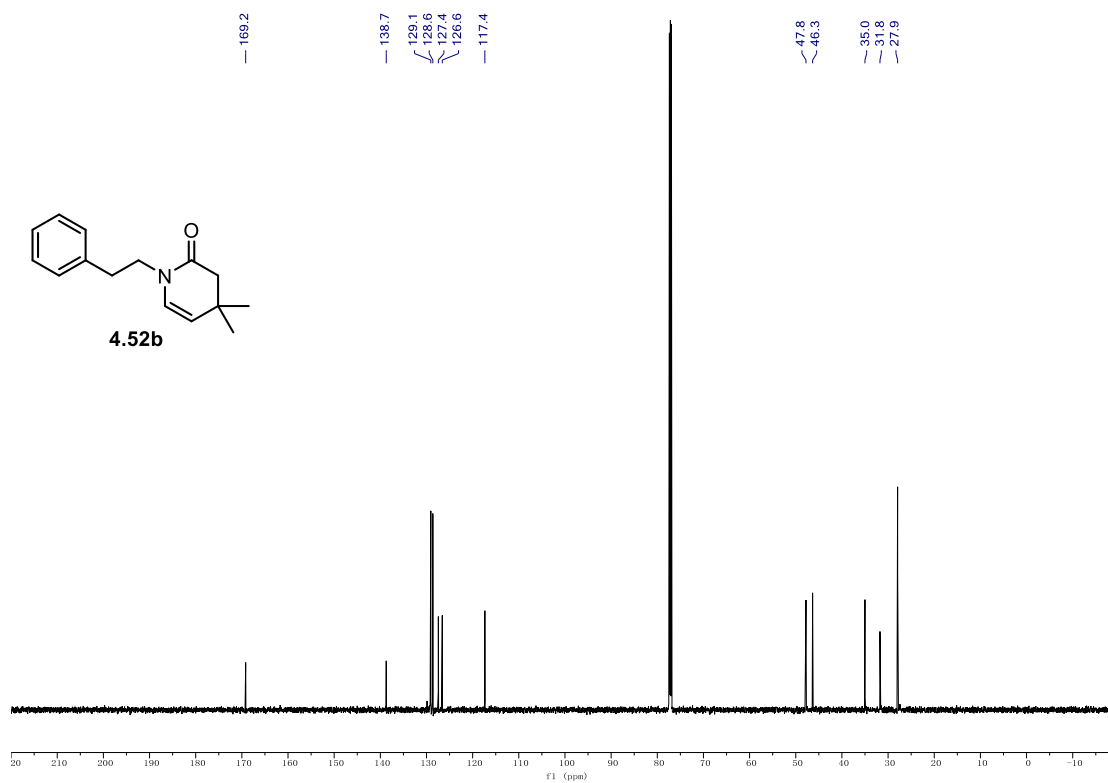
9.1. NMR Spectra

¹H NMR (500 MHz, CDCl₃) of **4.51b**.



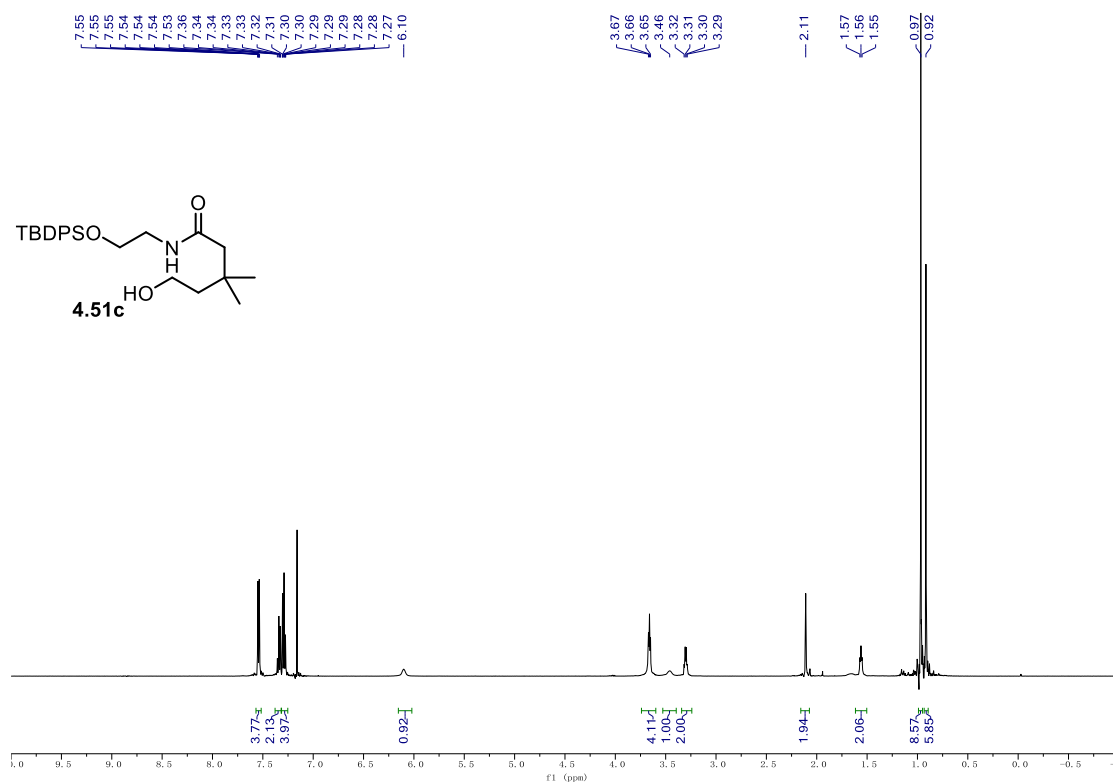
¹³C NMR (126 MHz, CDCl₃) of **4.51b**.



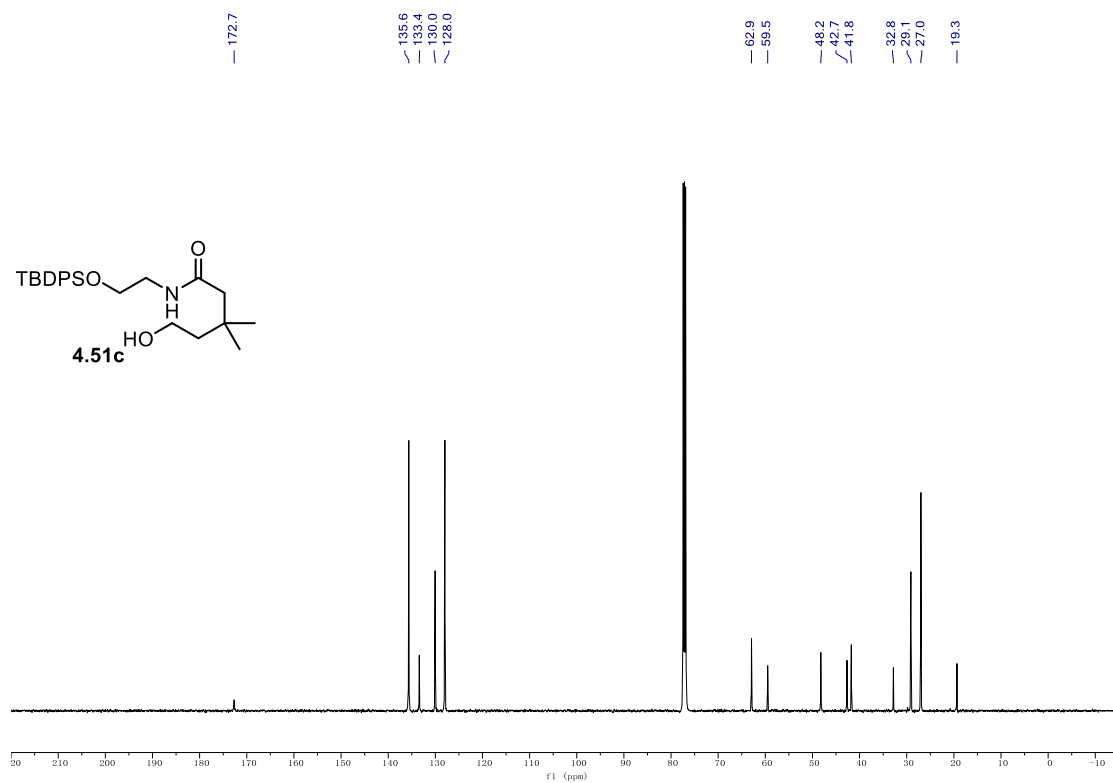
^1H NMR (500 MHz, CDCl_3) of **4.52b**. ^{13}C NMR (126 MHz, CDCl_3) of **4.52b**.

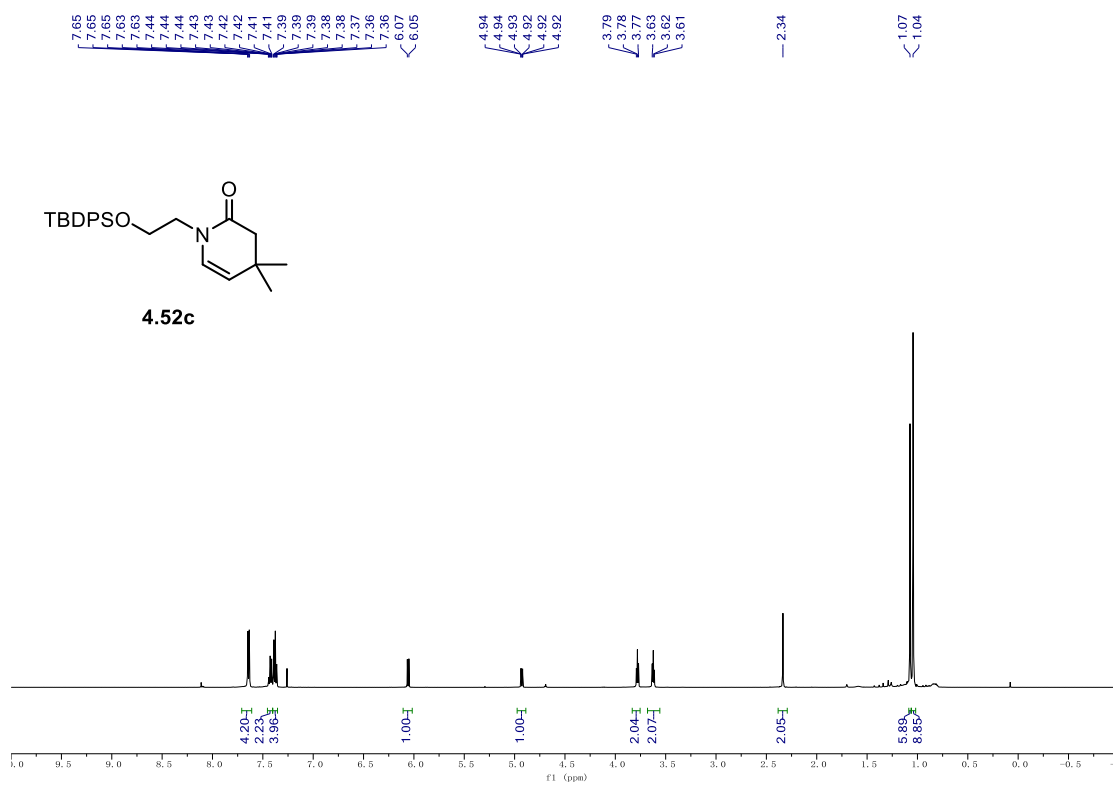
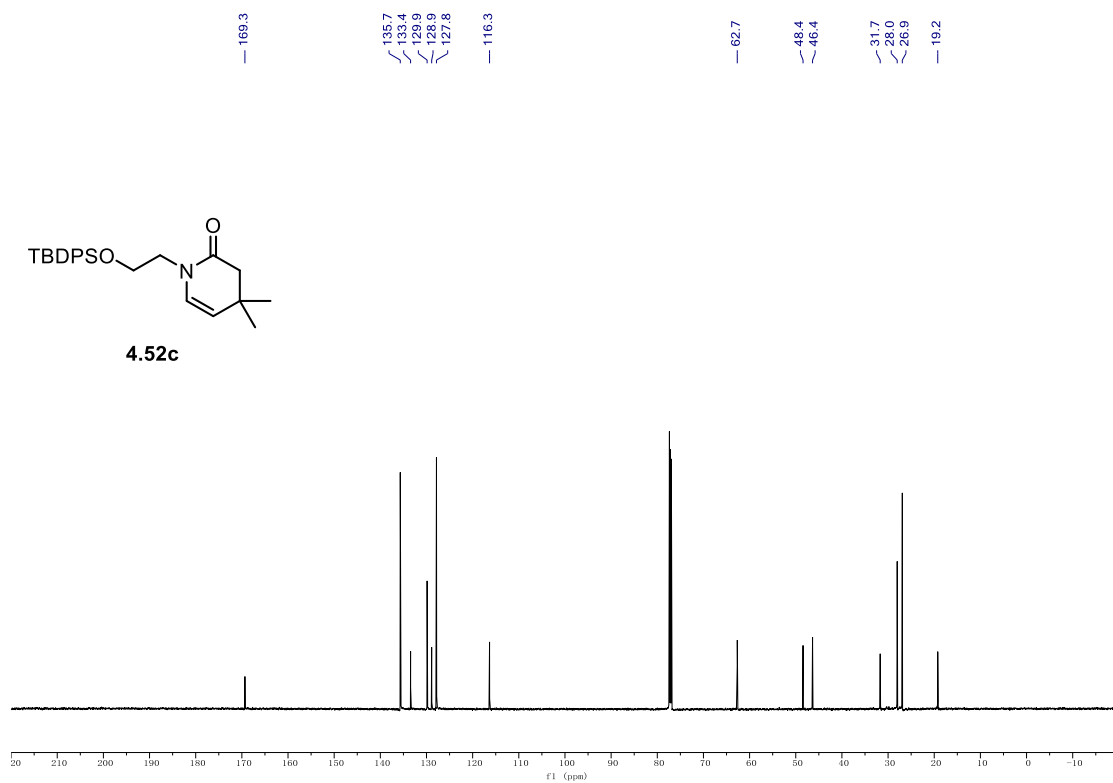
9.1. NMR Spectra

¹H NMR (500 MHz, CDCl₃) of 4.51c.



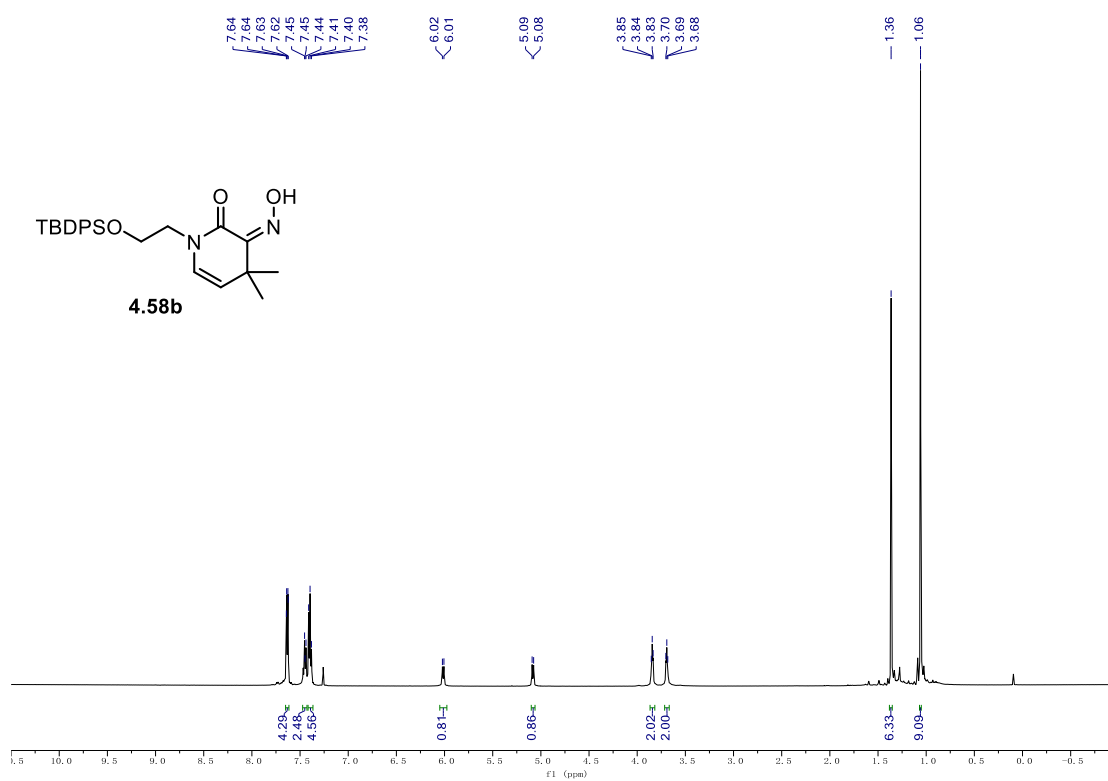
¹³C NMR (126 MHz, CDCl₃) of 4.51c.



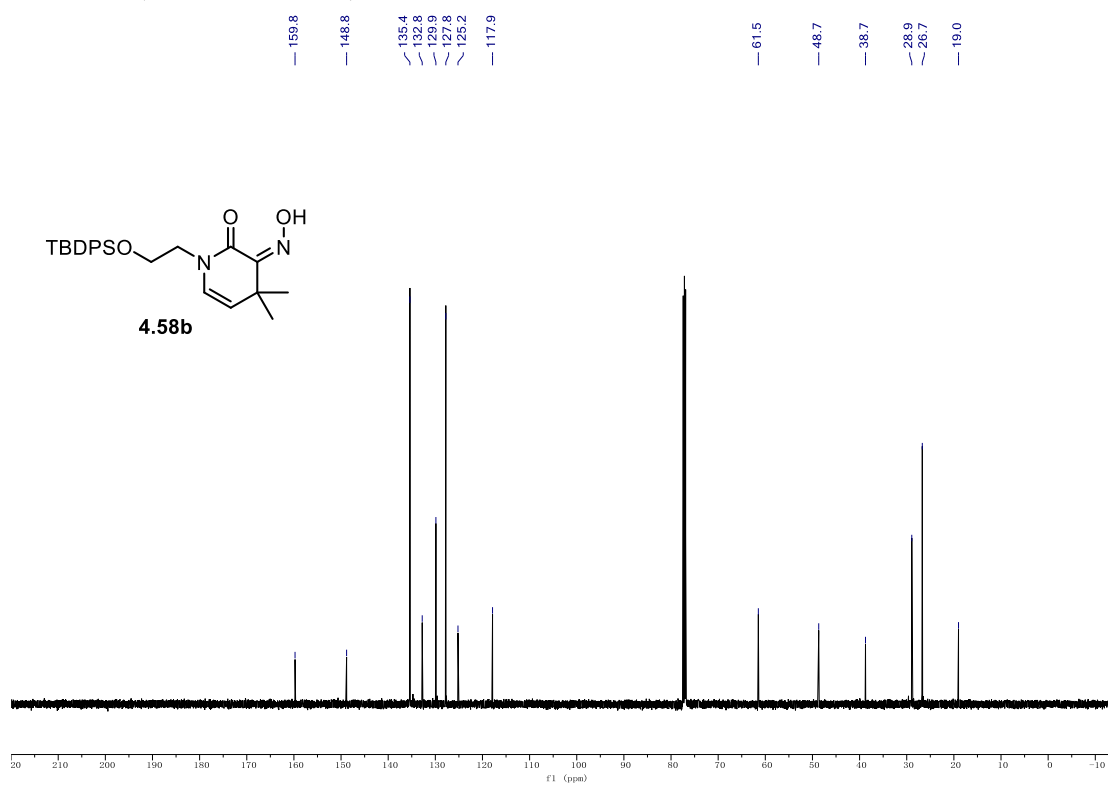
^1H NMR (500 MHz, CDCl_3) of **4.52c**. ^{13}C NMR (151 MHz, CDCl_3) of **4.52c**.

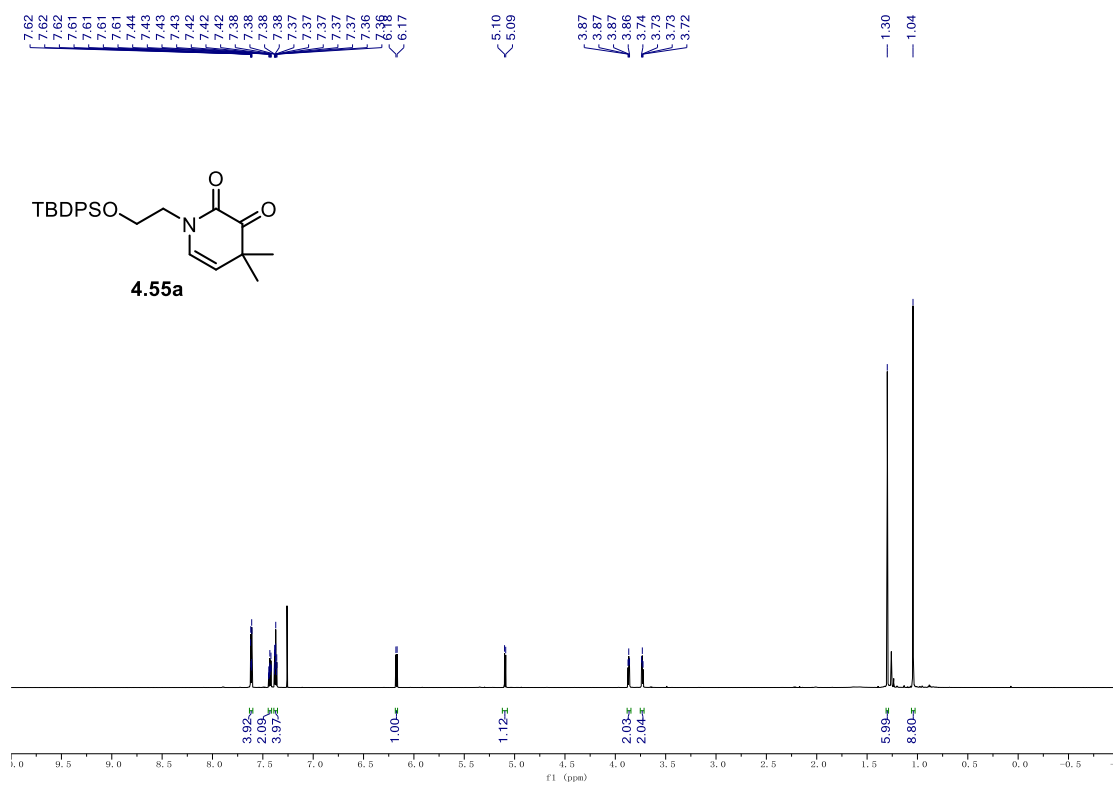
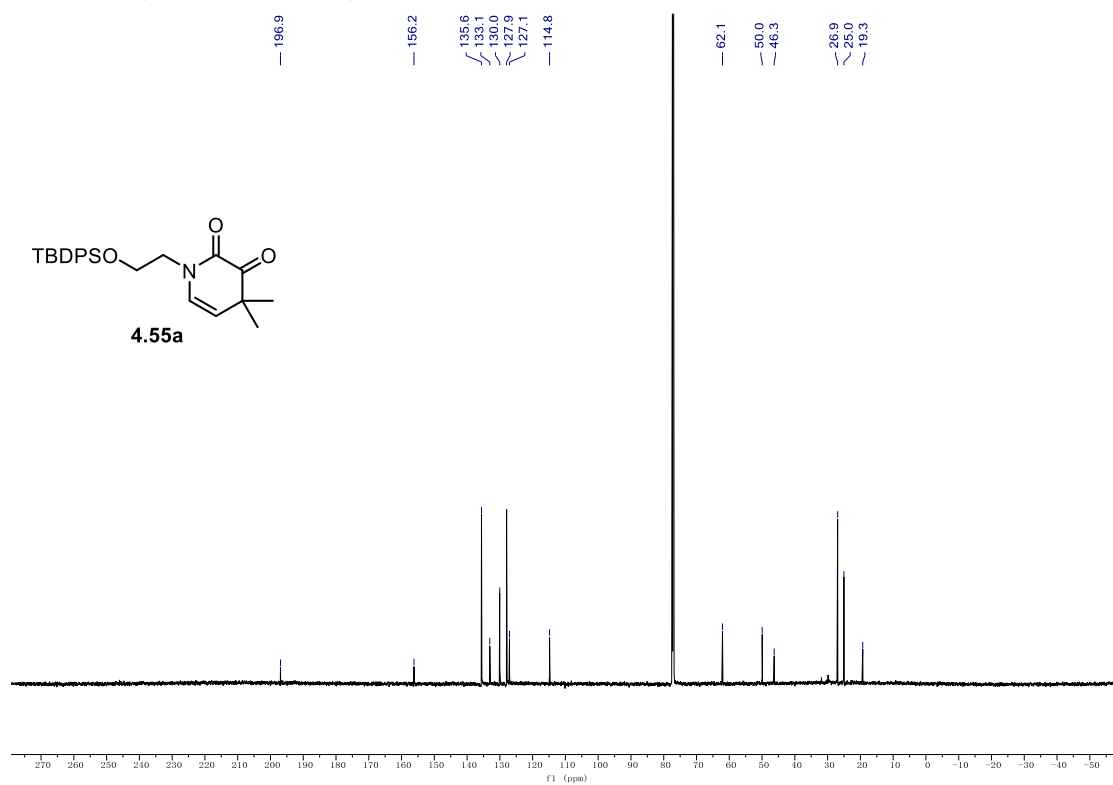
9.1. NMR Spectra

¹H NMR (500 MHz, CDCl₃) of **4.58b**.



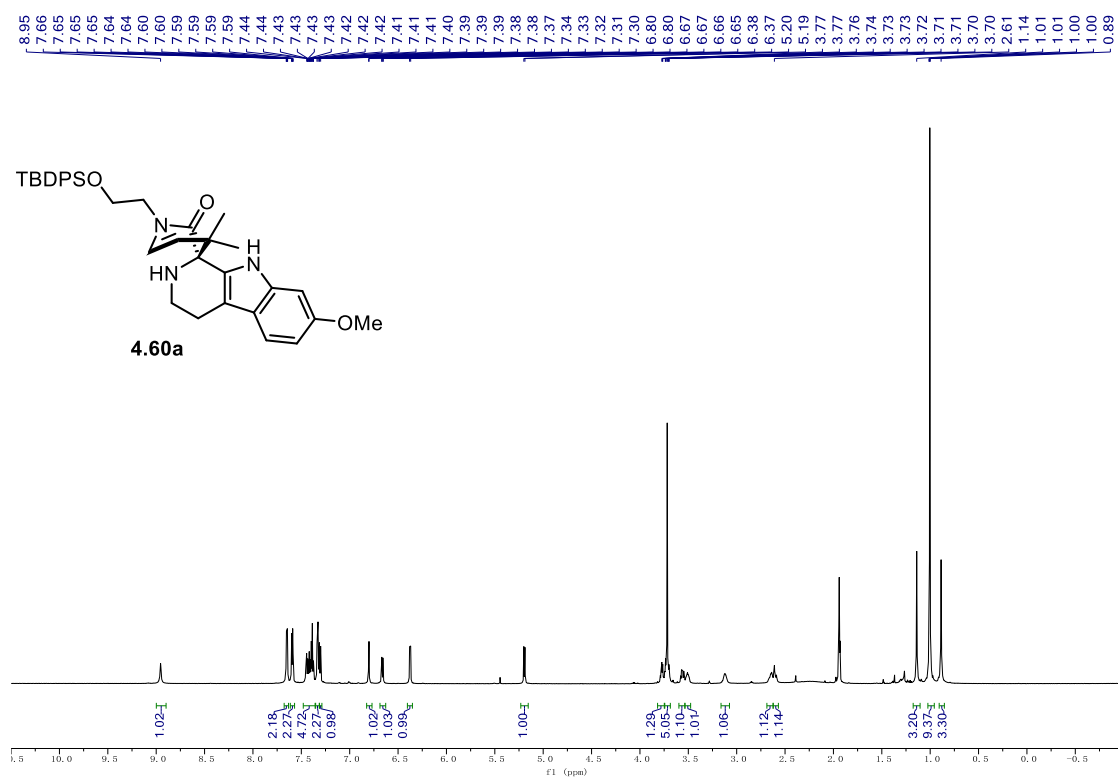
¹³C NMR (126 MHz, CDCl₃) of **4.58b**



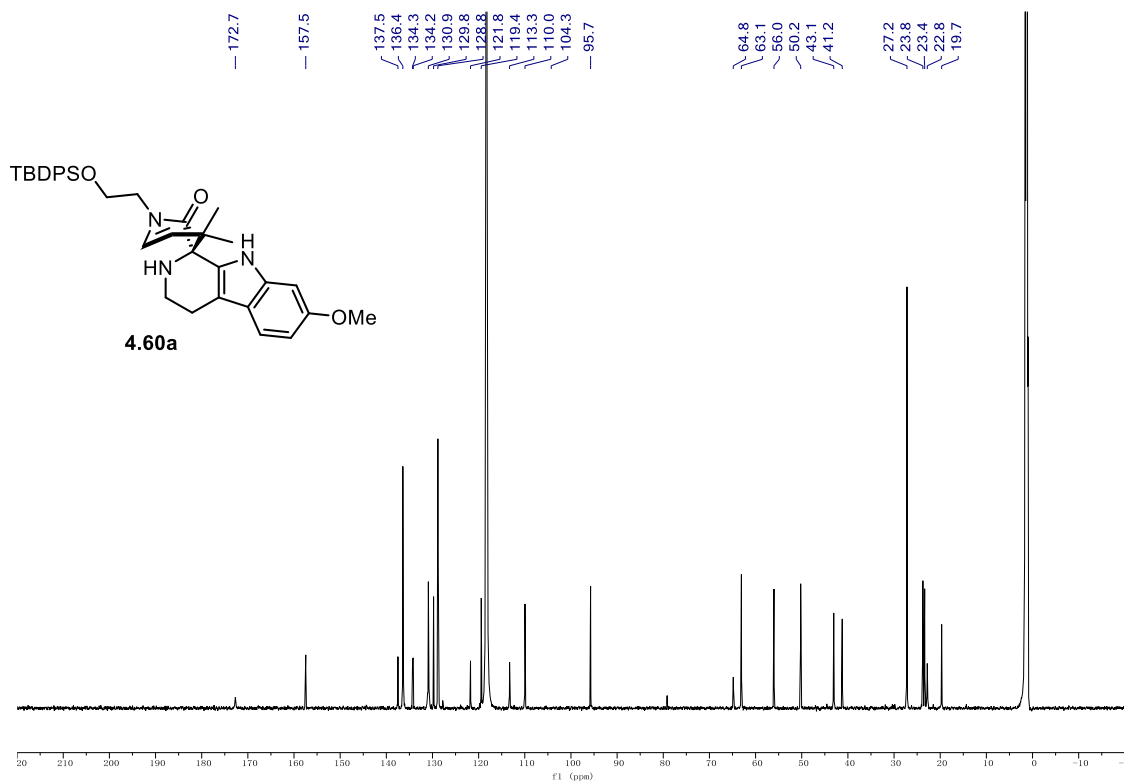
^1H NMR (500 MHz, CDCl_3) of 4.55a. **^{13}C NMR (126 MHz, CDCl_3) of 4.55a.**

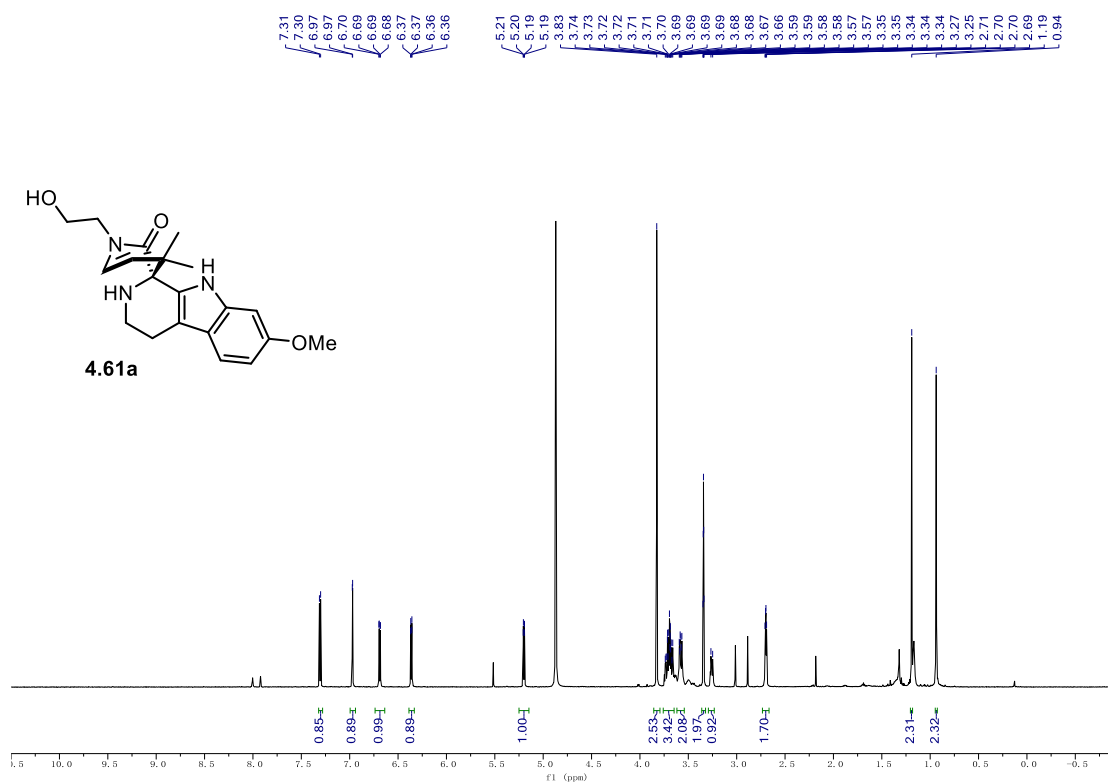
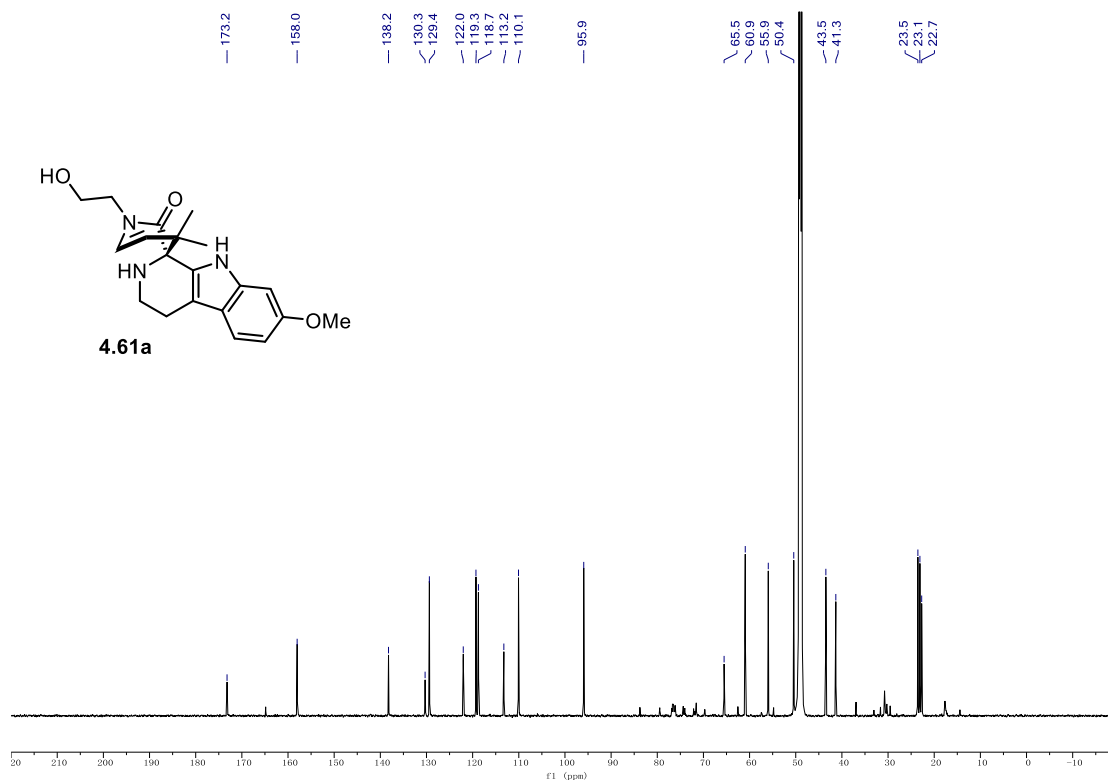
9.1. NMR Spectra

¹H NMR (700 MHz, CD₃CN) of **4.60a**.



¹³C NMR (176 MHz, CD₃CN) of **4.60a**.

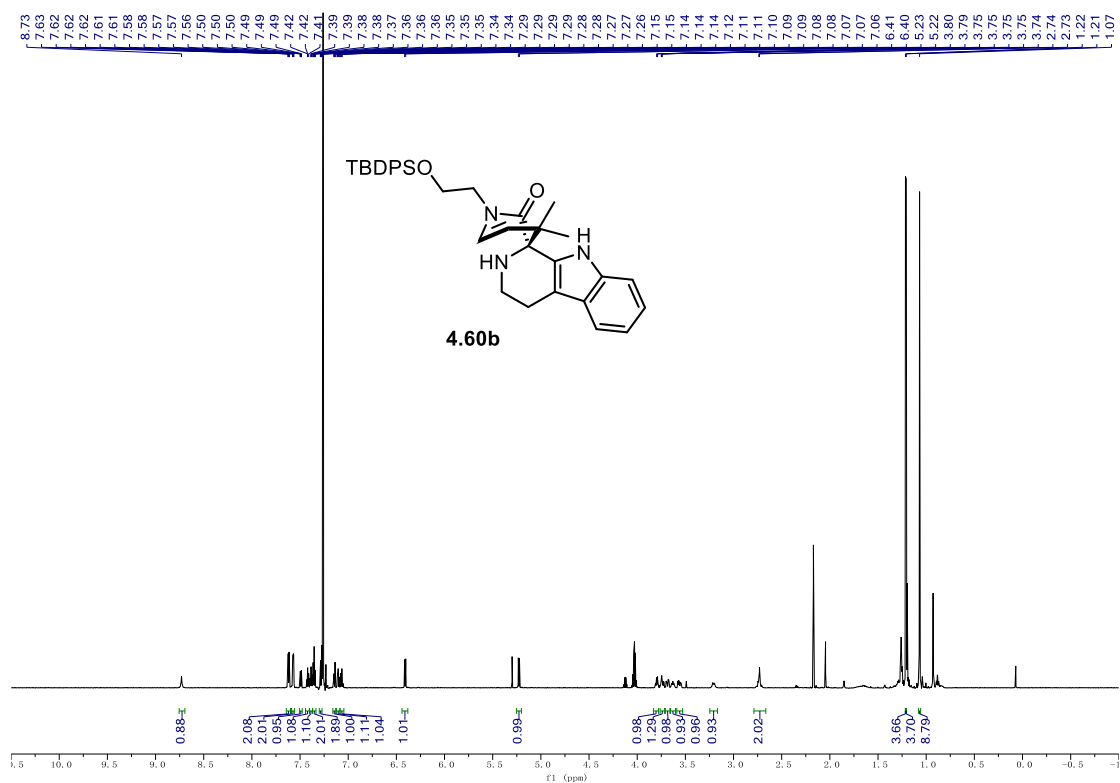


^1H NMR (700 MHz, CD_3OD) of 4.61a. **^{13}C NMR (176 MHz, CD_3OD) of 4.61a.**

(Note: due to the high polarity of this compound, some impurities were showed in the ^{13}C NMR spectra.)

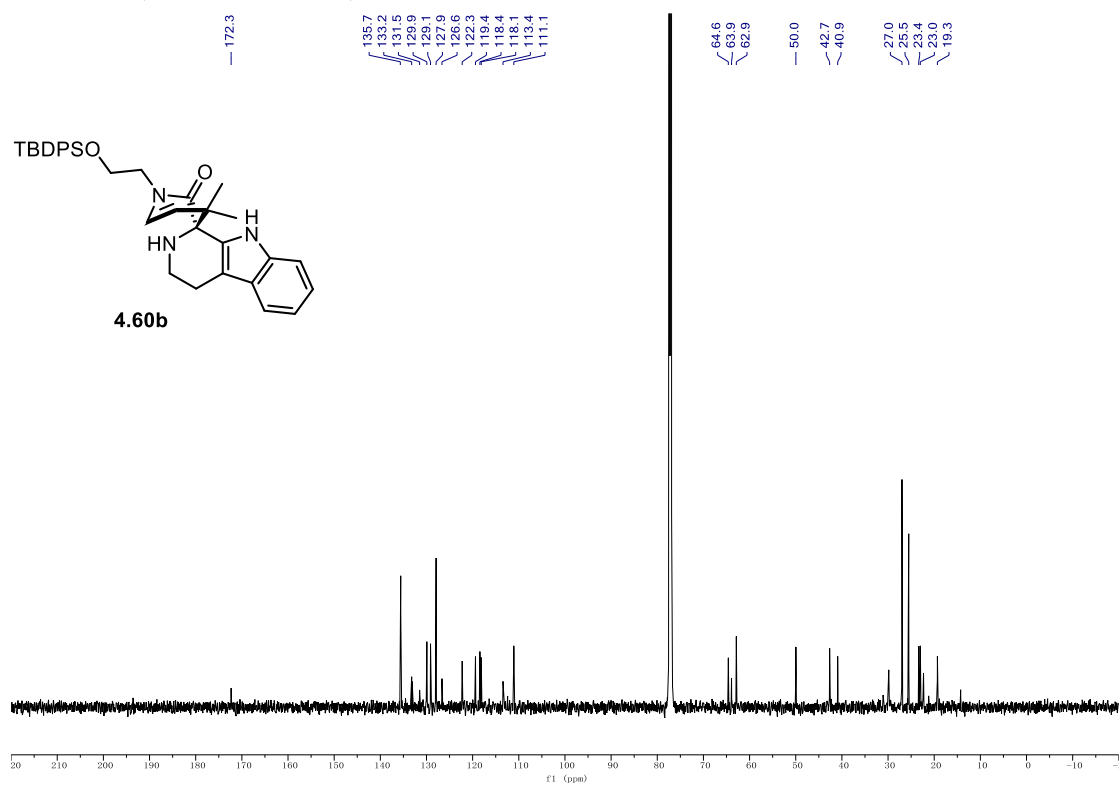
9.1. NMR Spectra

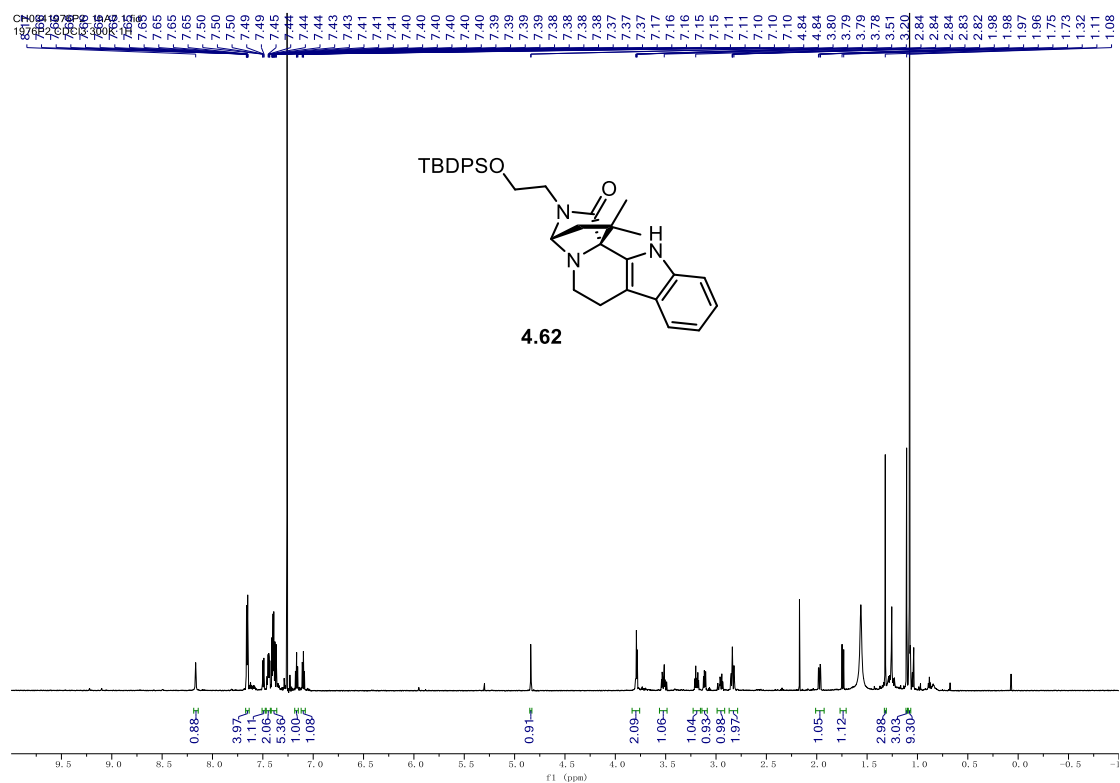
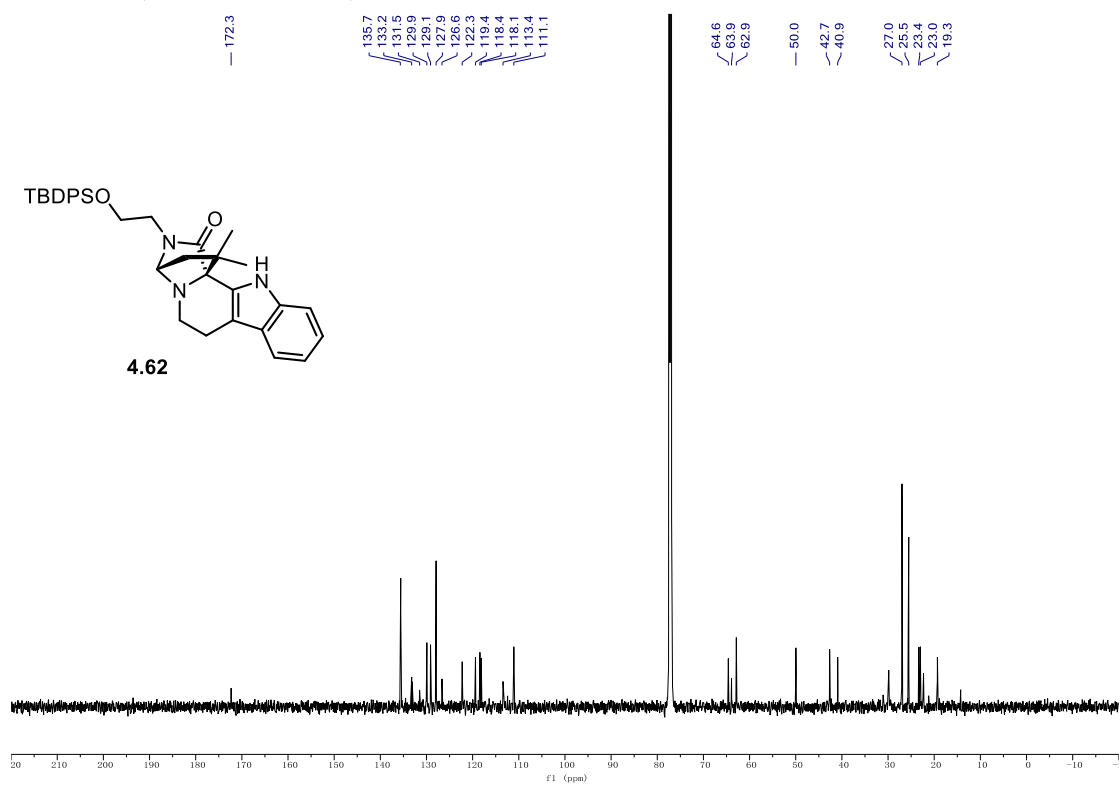
¹H NMR (700 MHz, CDCl₃) of **4.60b**.



(Note: resonance of an impurity at 4.03 ppm)

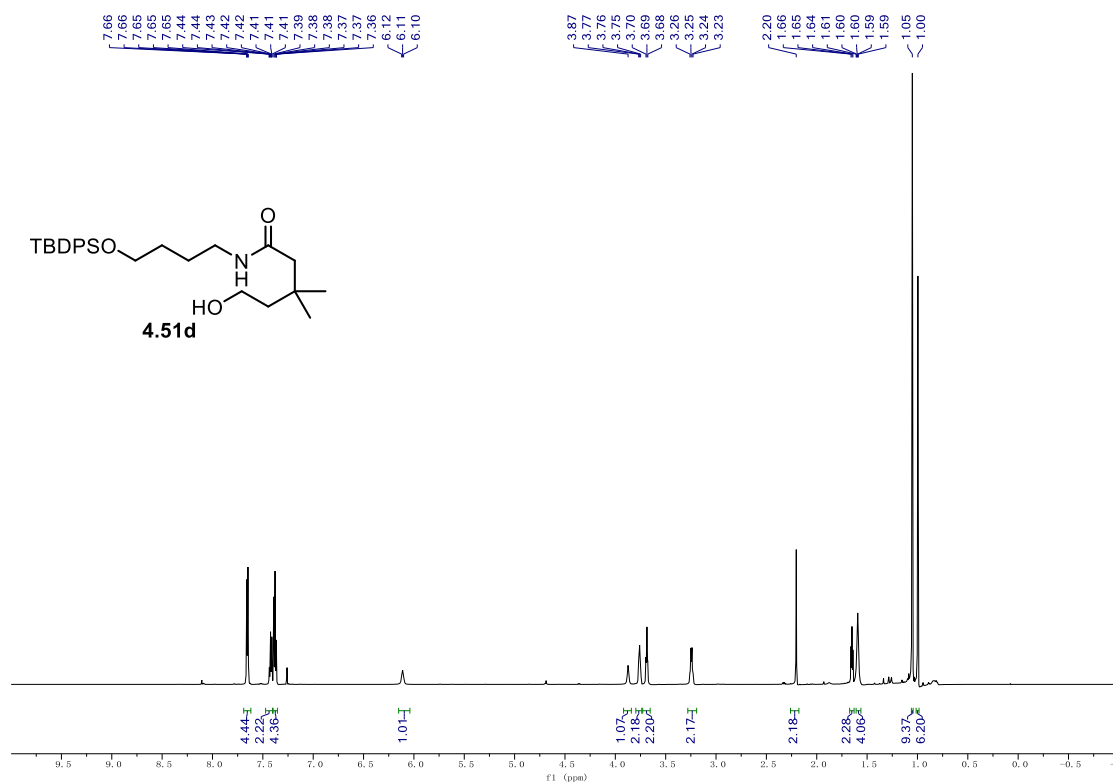
¹³C NMR (176 MHz, CDCl₃) of **4.60b**.



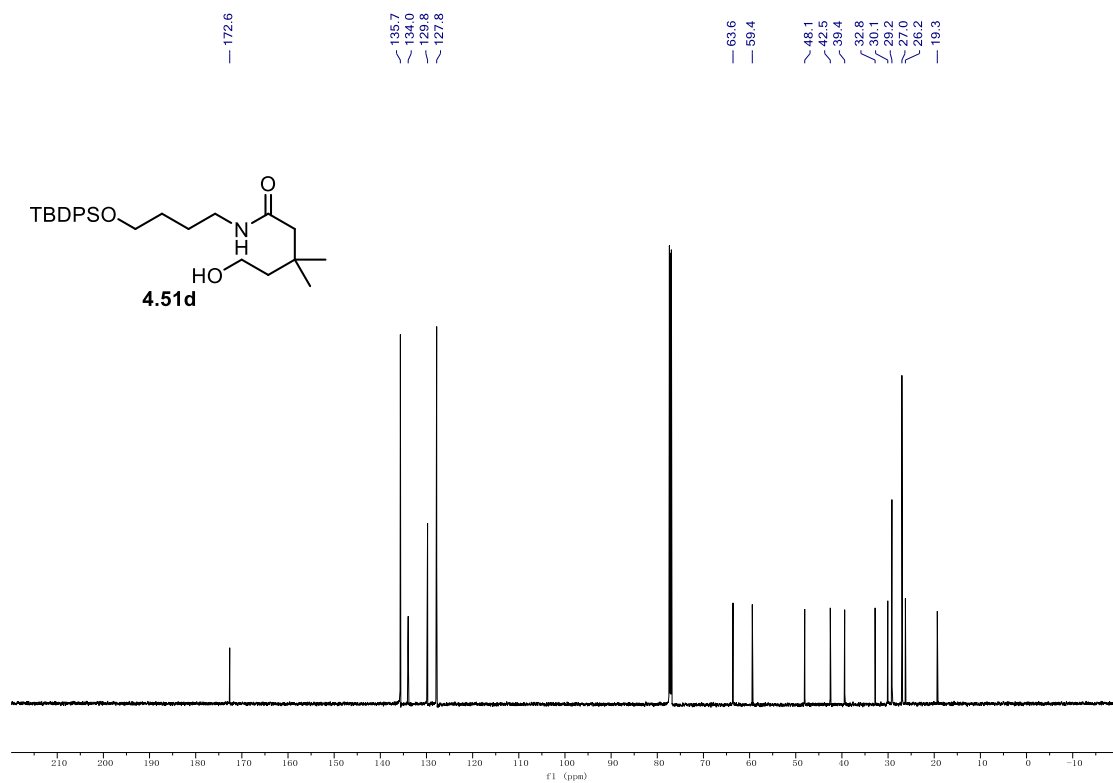
^1H NMR (700 MHz, CDCl_3) of **4.62**. ^{13}C NMR (176 MHz, CDCl_3) of **4.62**.

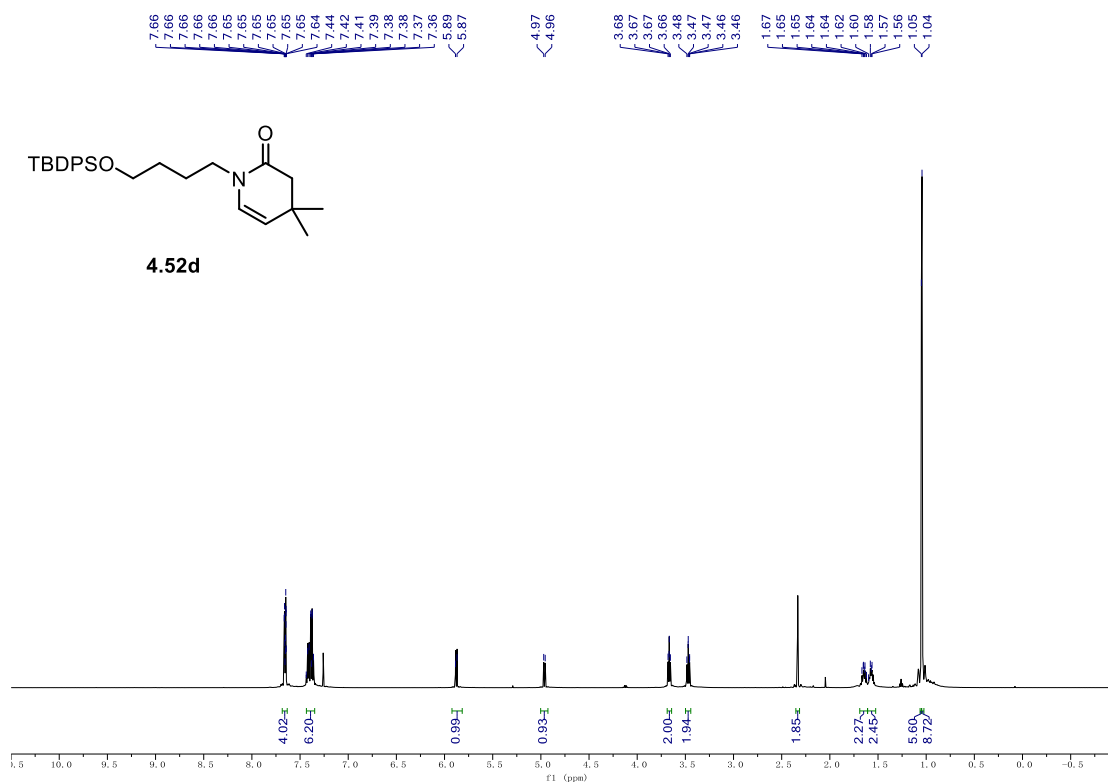
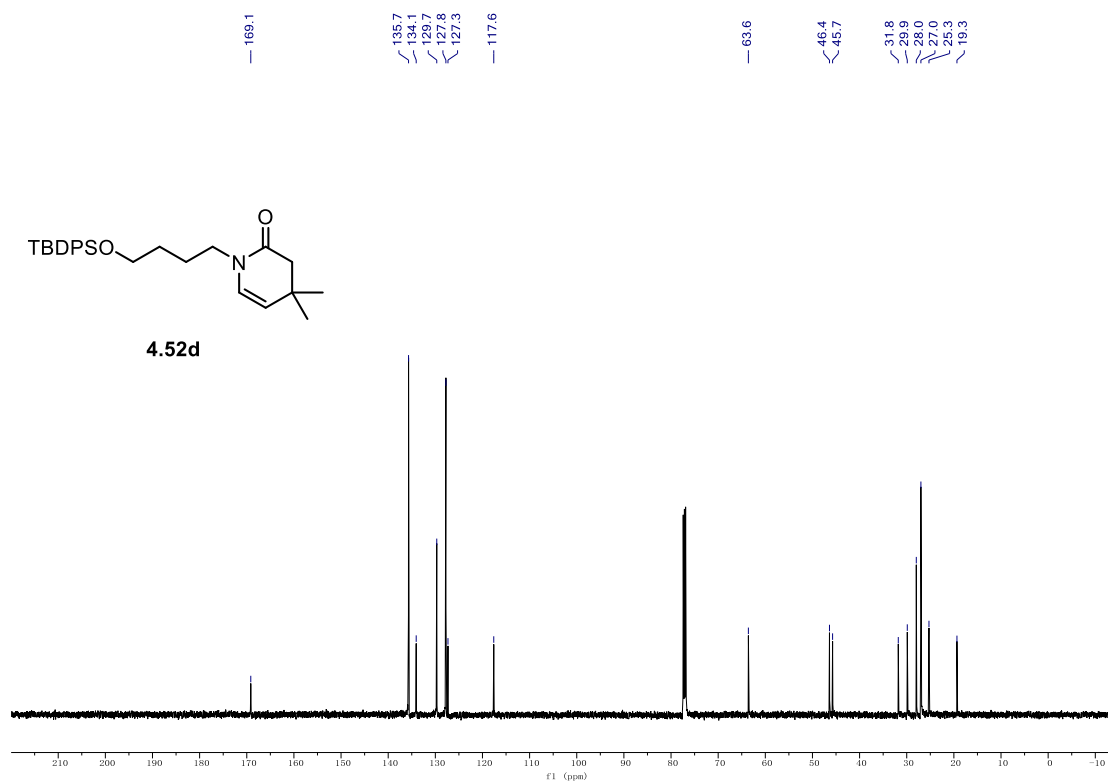
9.1. NMR Spectra

¹H NMR (600 MHz, CDCl₃) of 4.51d.



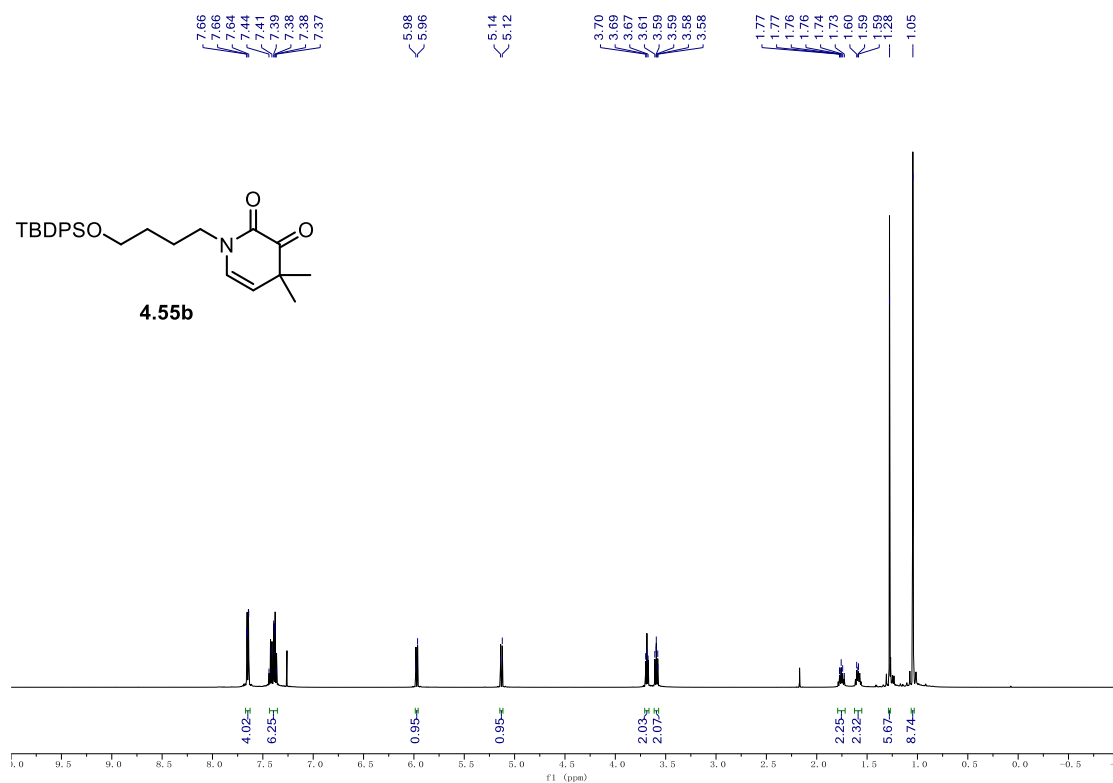
¹³C NMR (151 MHz, CDCl₃) of 4.51d.



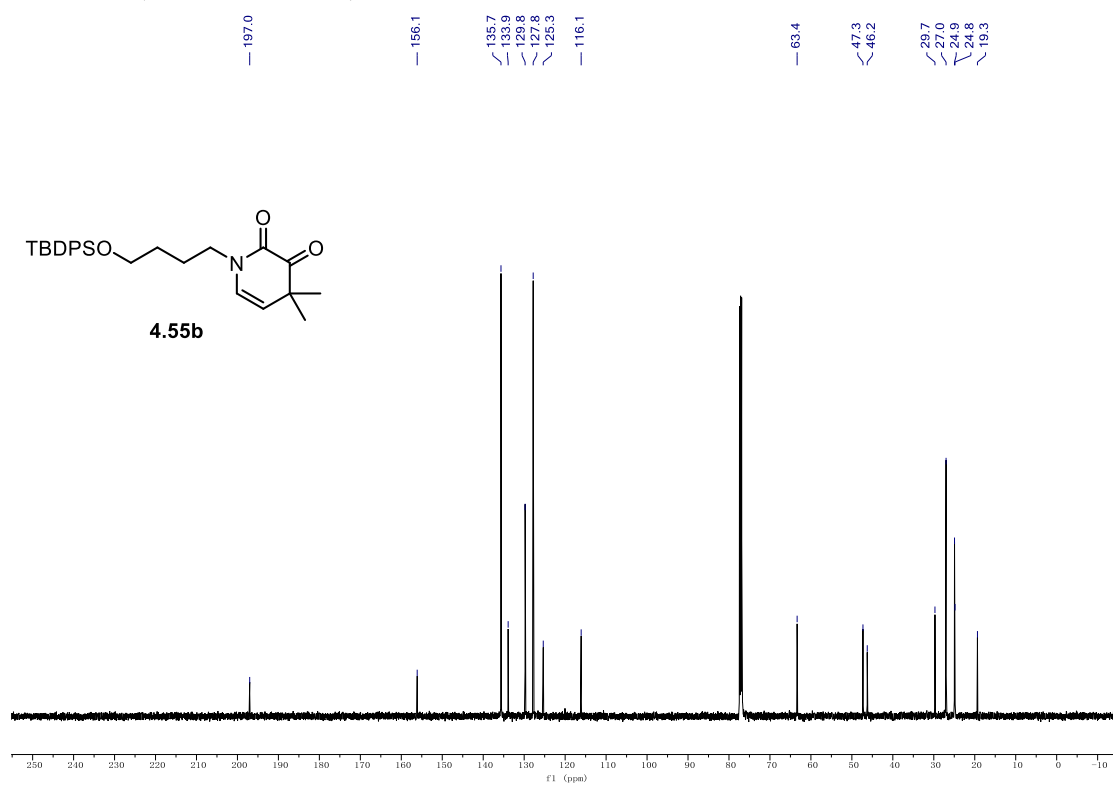
^1H NMR (500 MHz, CDCl_3) of **4.52d**. ^{13}C NMR (126 MHz, CDCl_3) of **4.52d**.

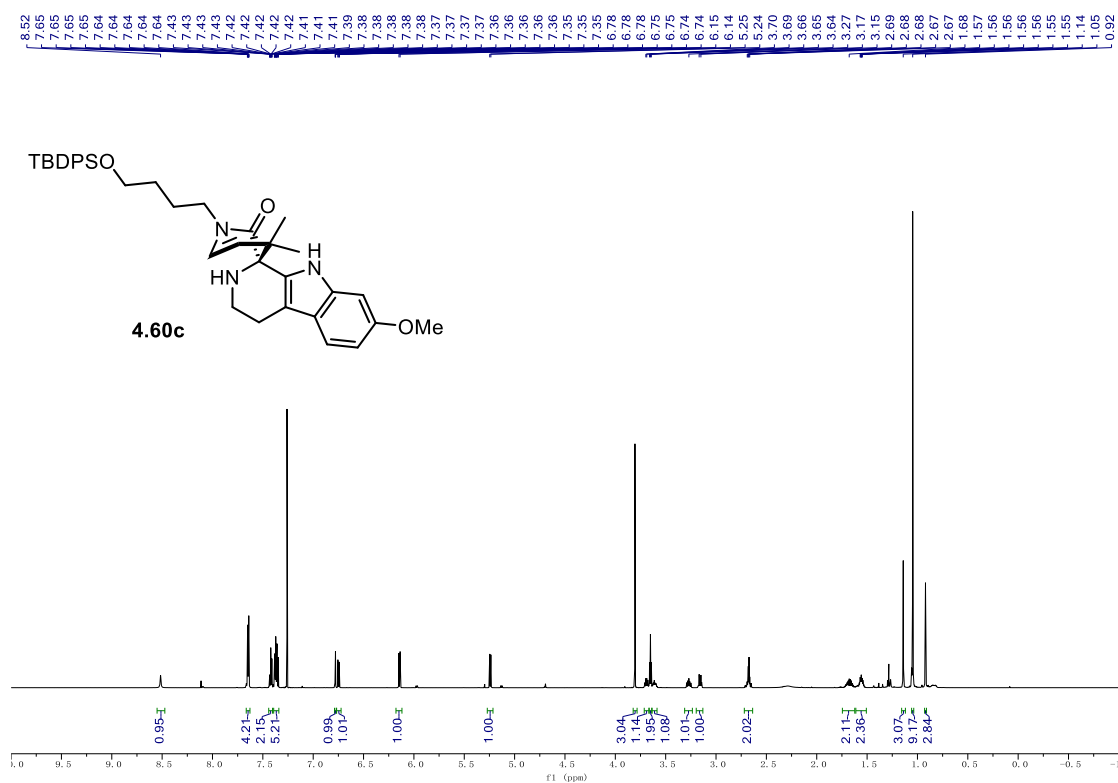
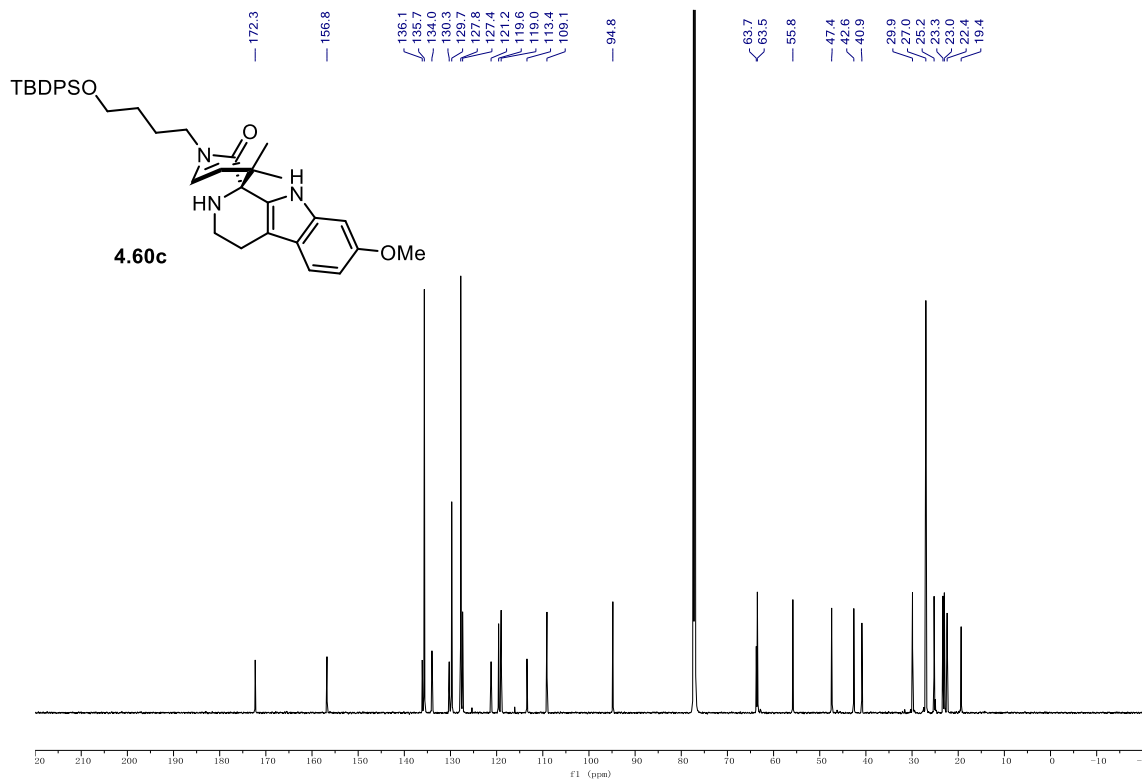
9.1. NMR Spectra

^1H NMR (500 MHz, CDCl_3) of **4.55b**.



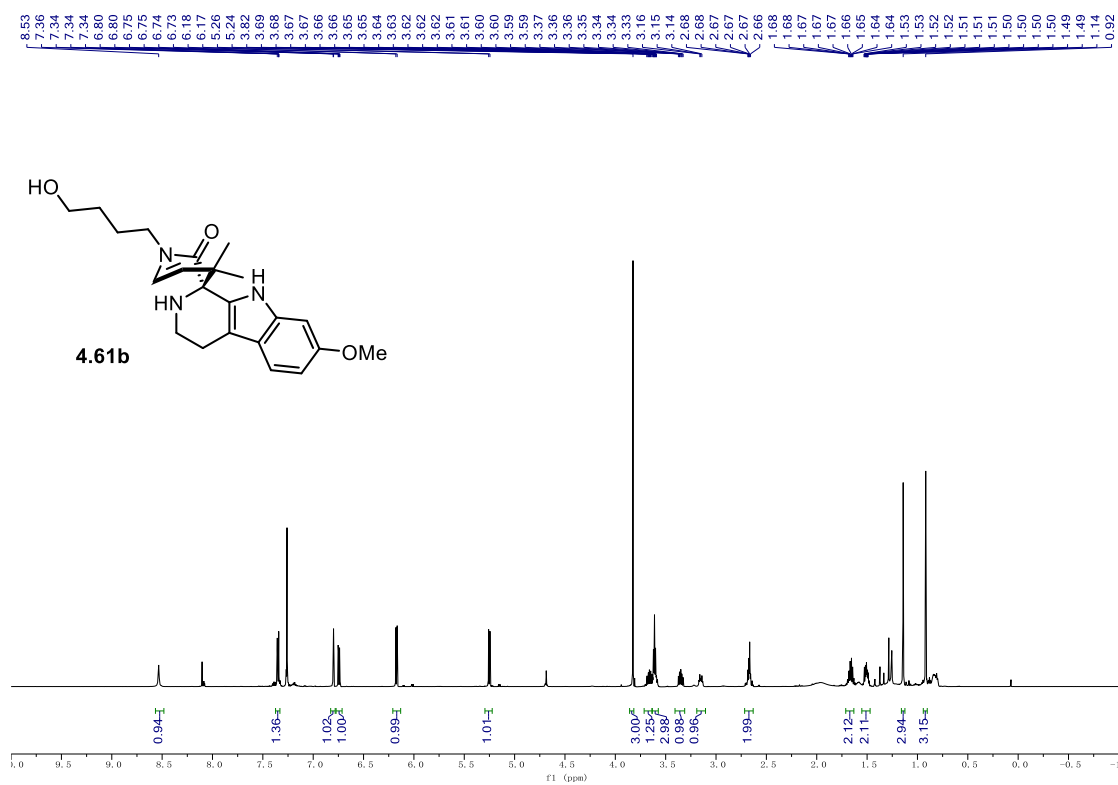
^{13}C NMR (126 MHz, CDCl_3) of **4.55b**.



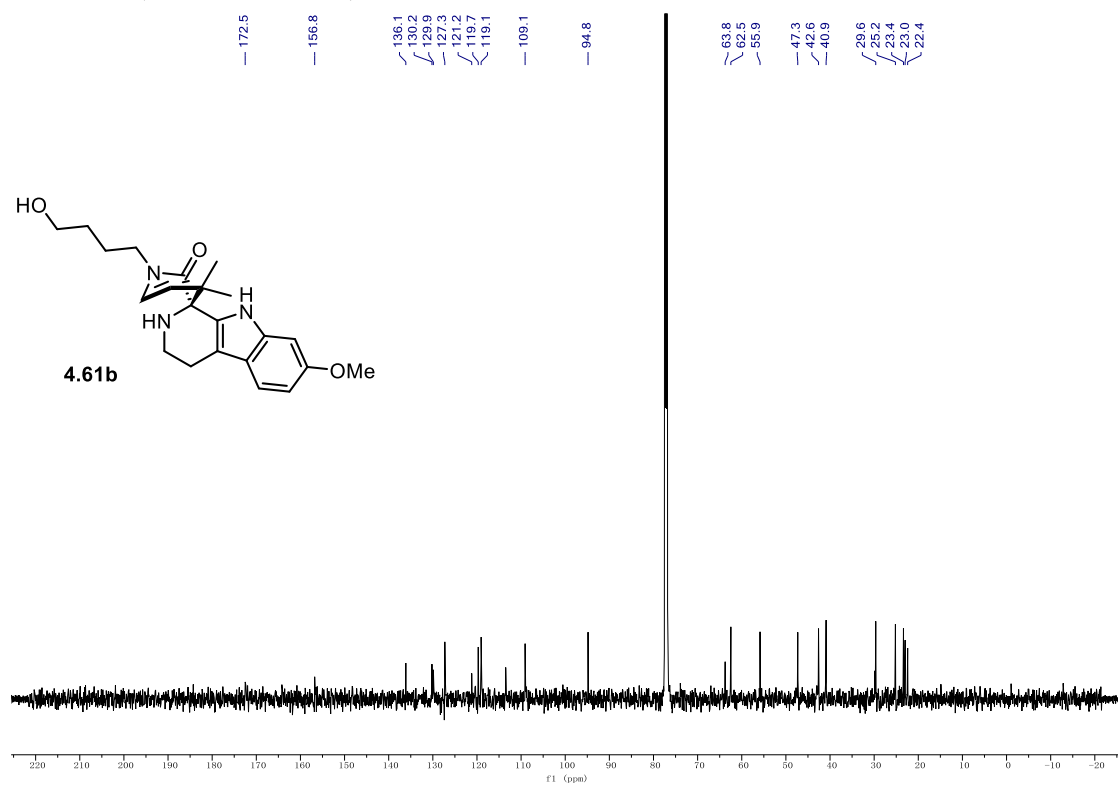
¹H NMR (700 MHz, CDCl₃) of 4.60c.**¹³C NMR (176 MHz, CDCl₃) of 4.60c.**

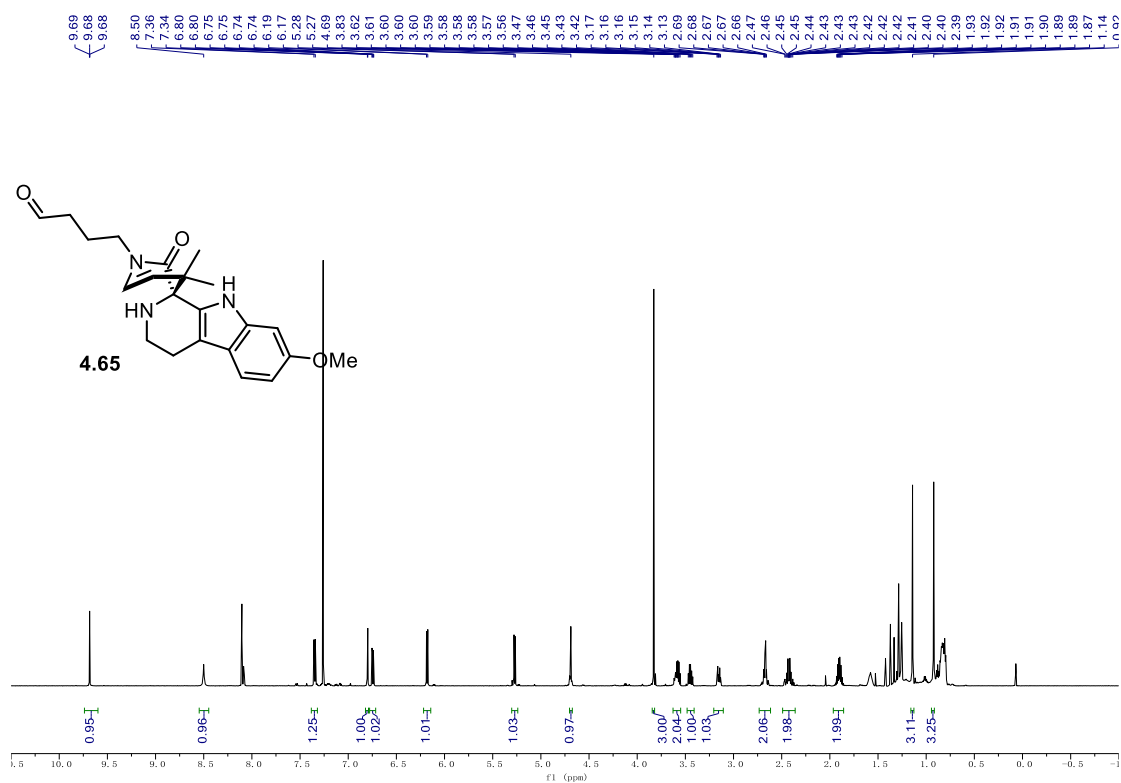
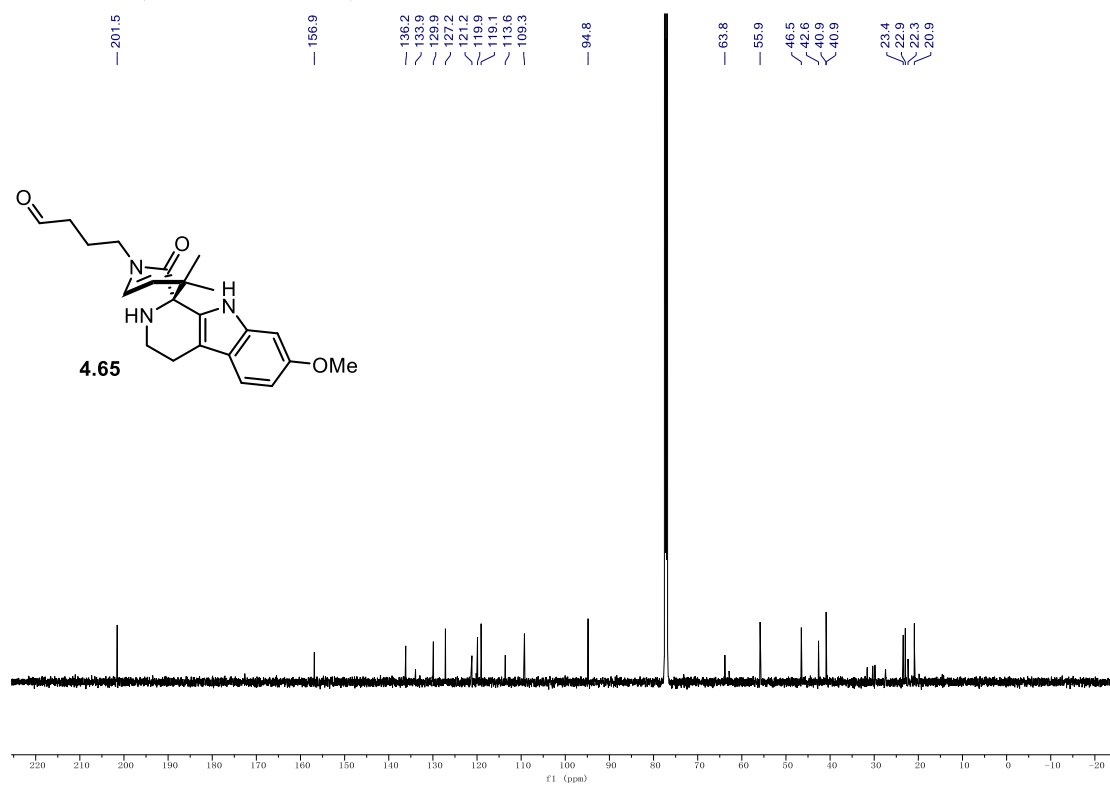
9.1. NMR Spectra

¹H NMR (600 MHz, CDCl₃) of **4.61b**.



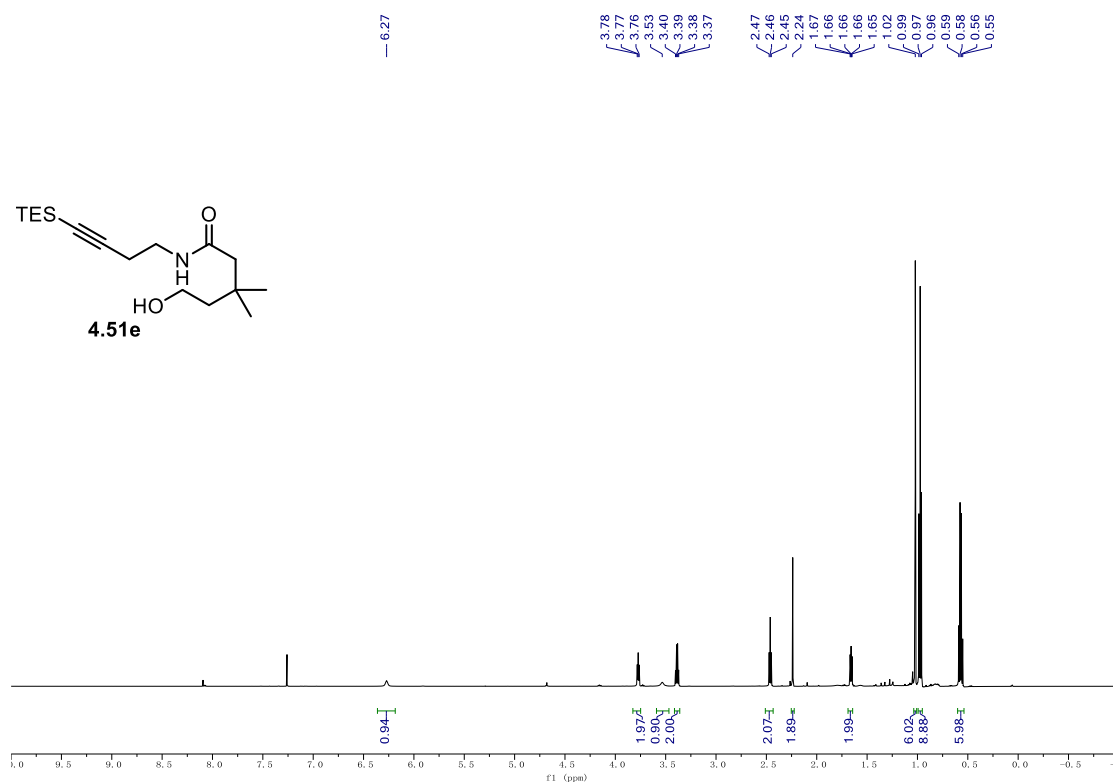
¹³C NMR (151 MHz, CDCl₃) of **4.61b**.



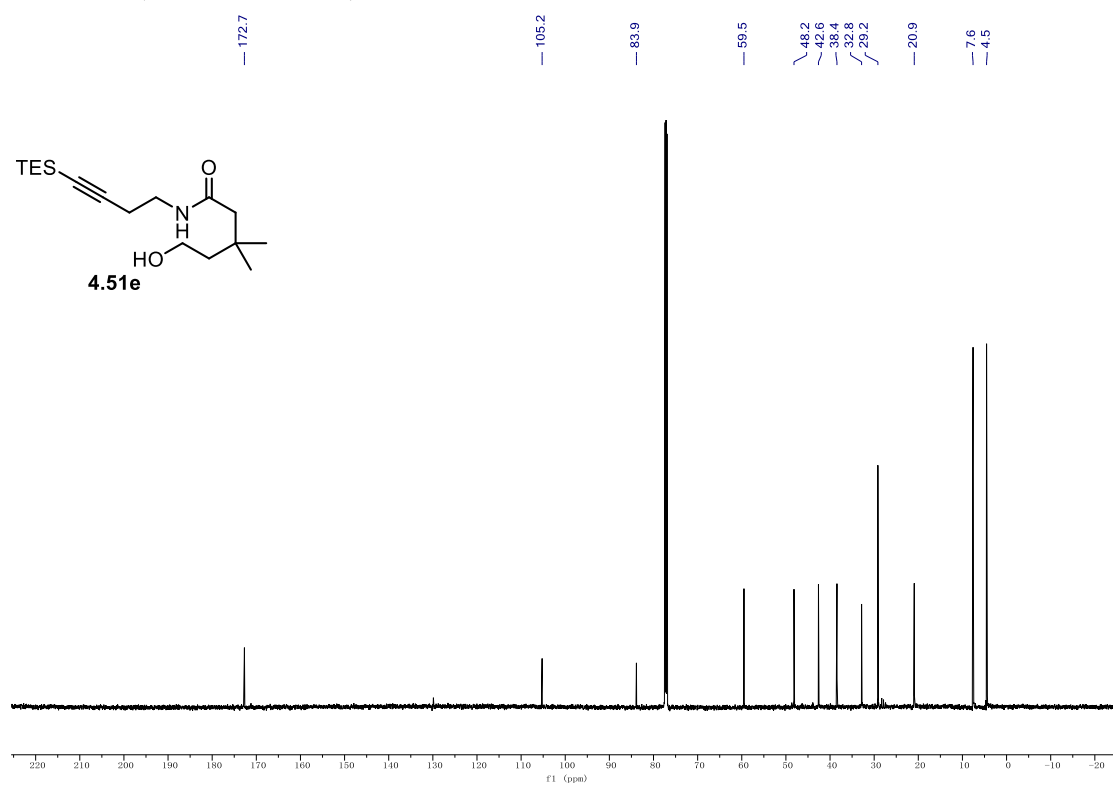
^1H NMR (600 MHz, CDCl_3) of **4.65**. ^{13}C NMR (151 MHz, CDCl_3) of **4.65**.

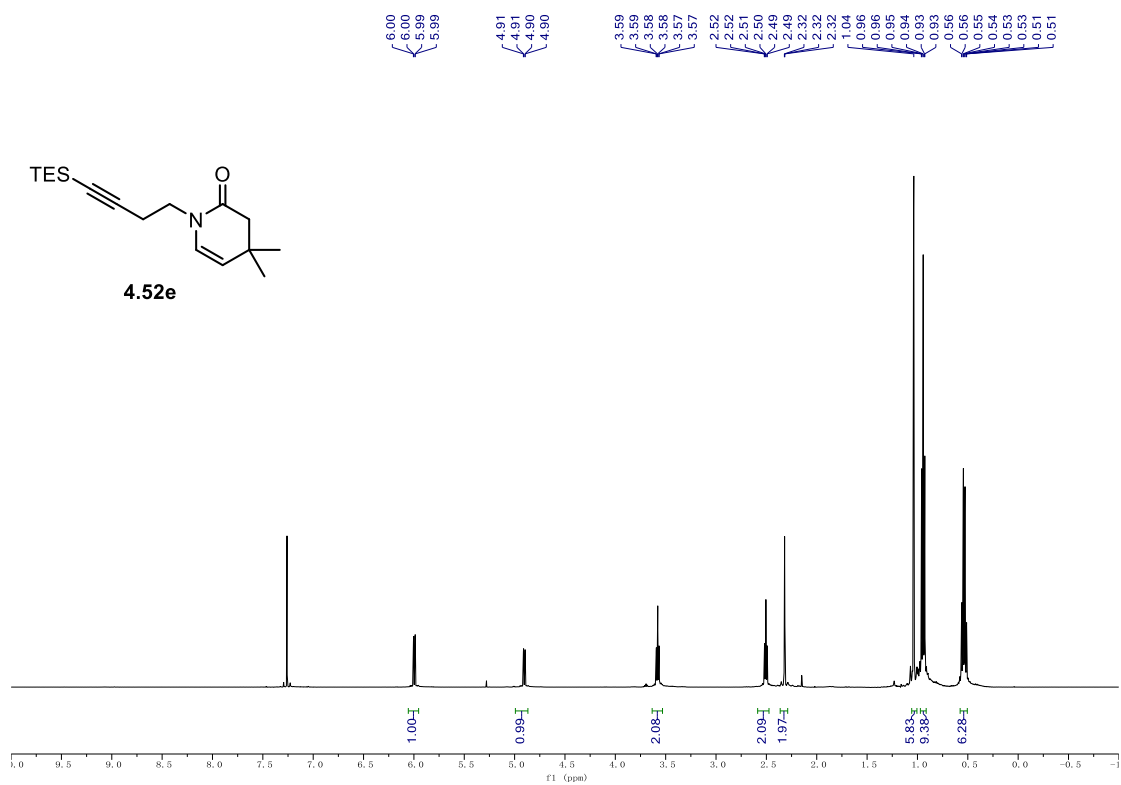
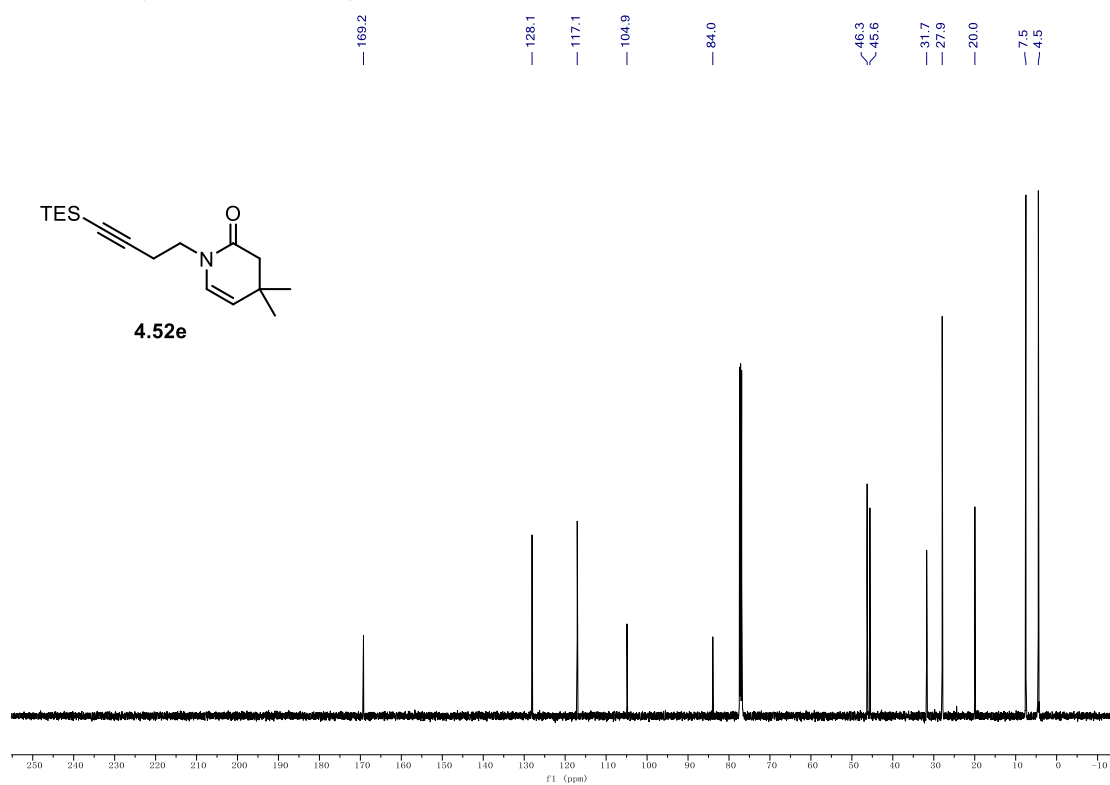
9.1. NMR Spectra

¹H NMR (500 MHz, CDCl₃) of **4.51e**.



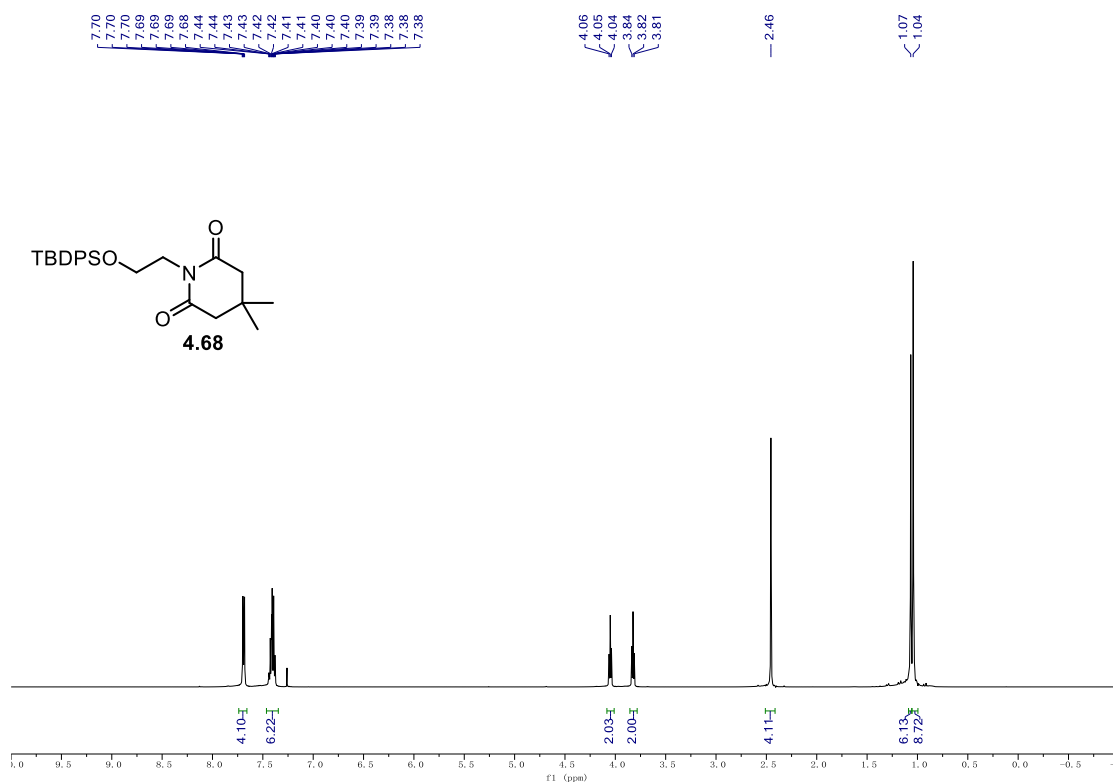
¹³C NMR (126 MHz, CDCl₃) of **4.51e**.



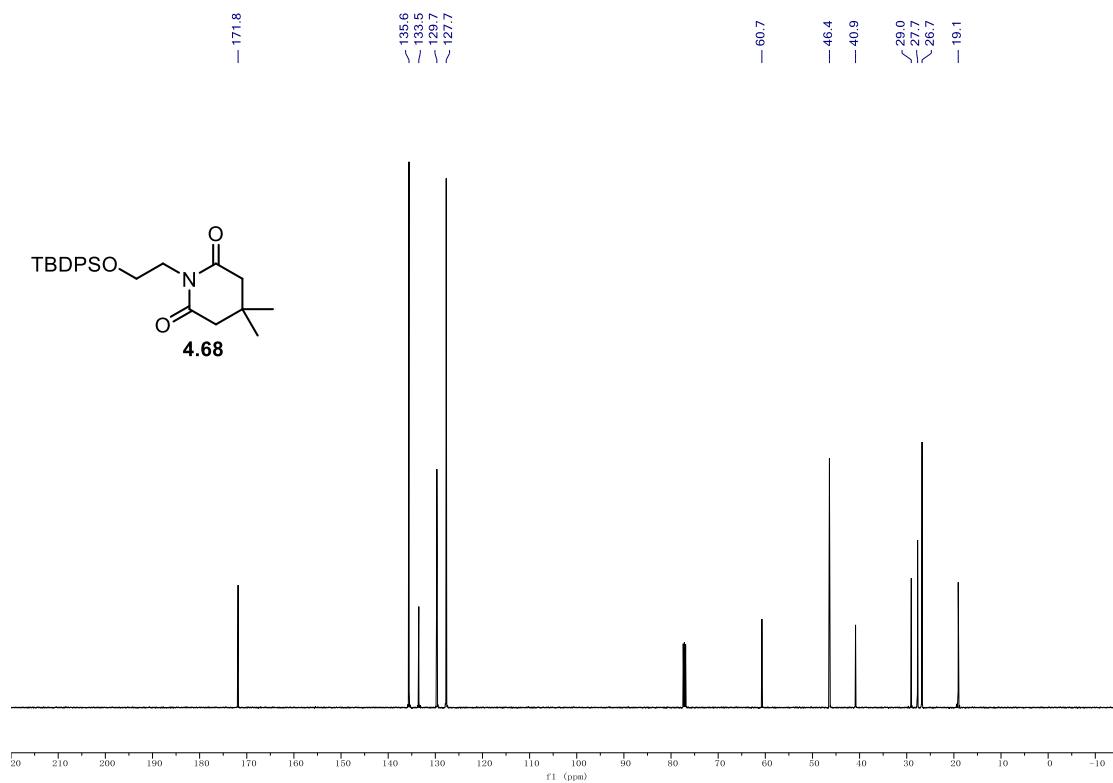
^1H NMR (500 MHz, CDCl_3) of **4.52e**. ^{13}C NMR (126 MHz, CDCl_3) of **4.52e**.

9.1. NMR Spectra

¹H NMR (500 MHz, CDCl₃) of **4.68**.

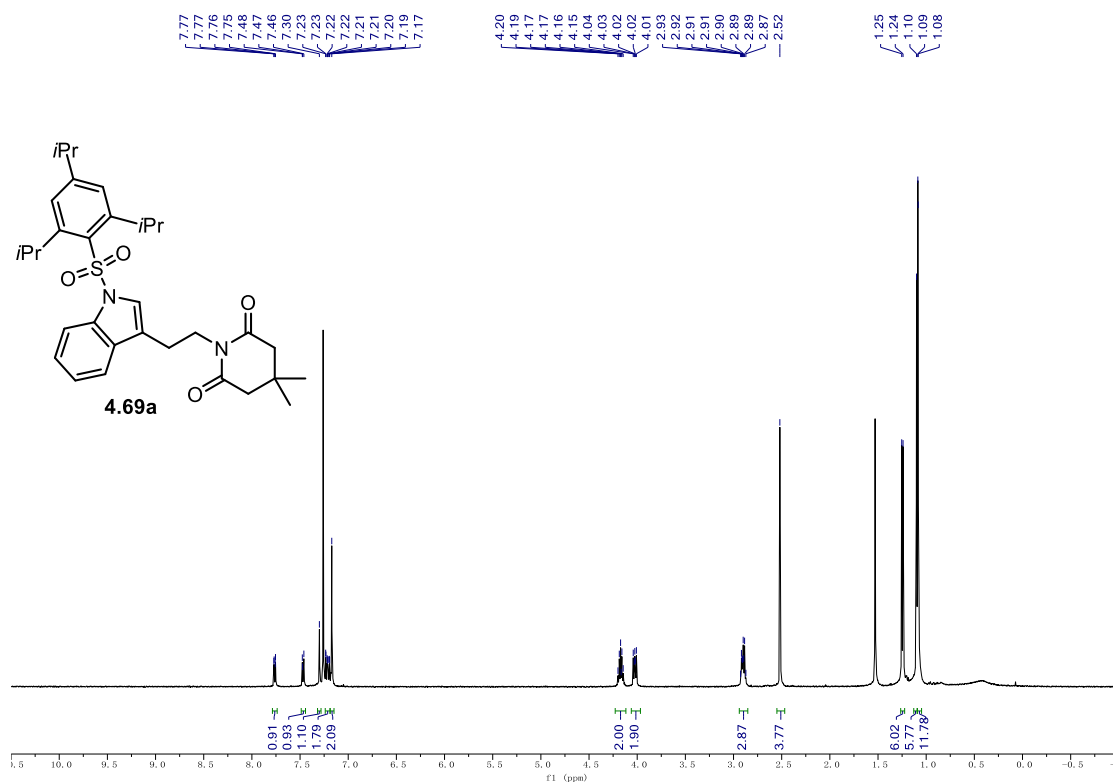


¹³C NMR (126 MHz, CDCl₃) of **4.68**.

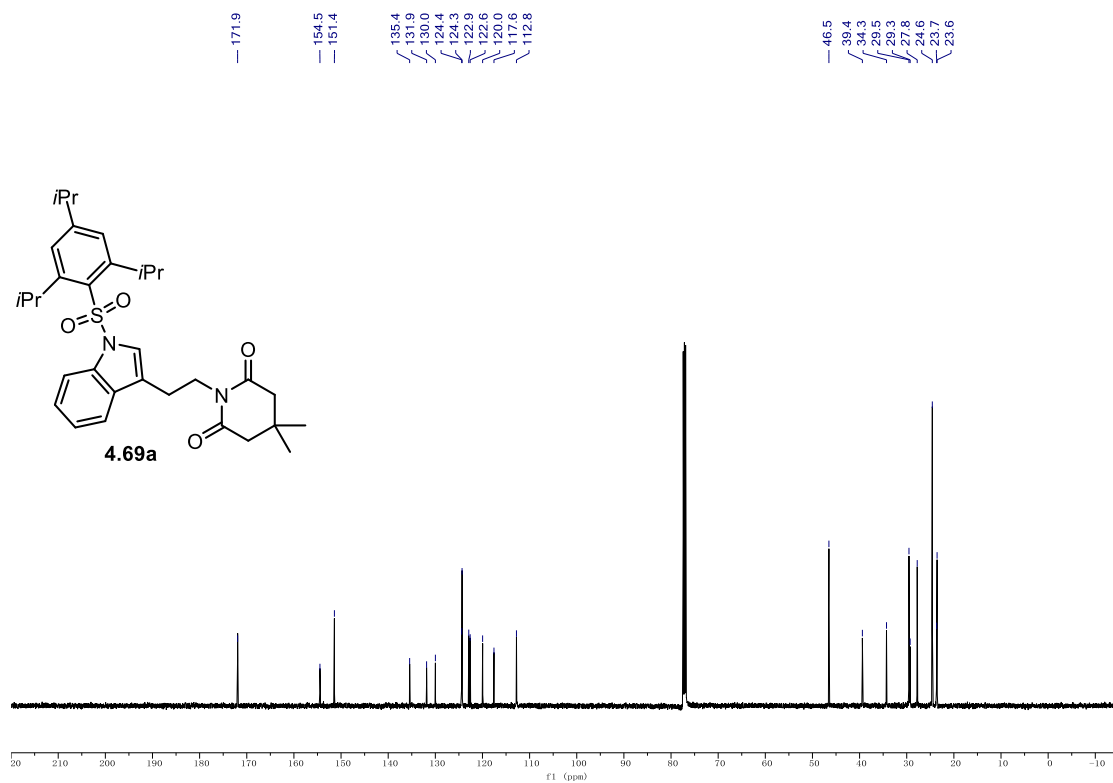


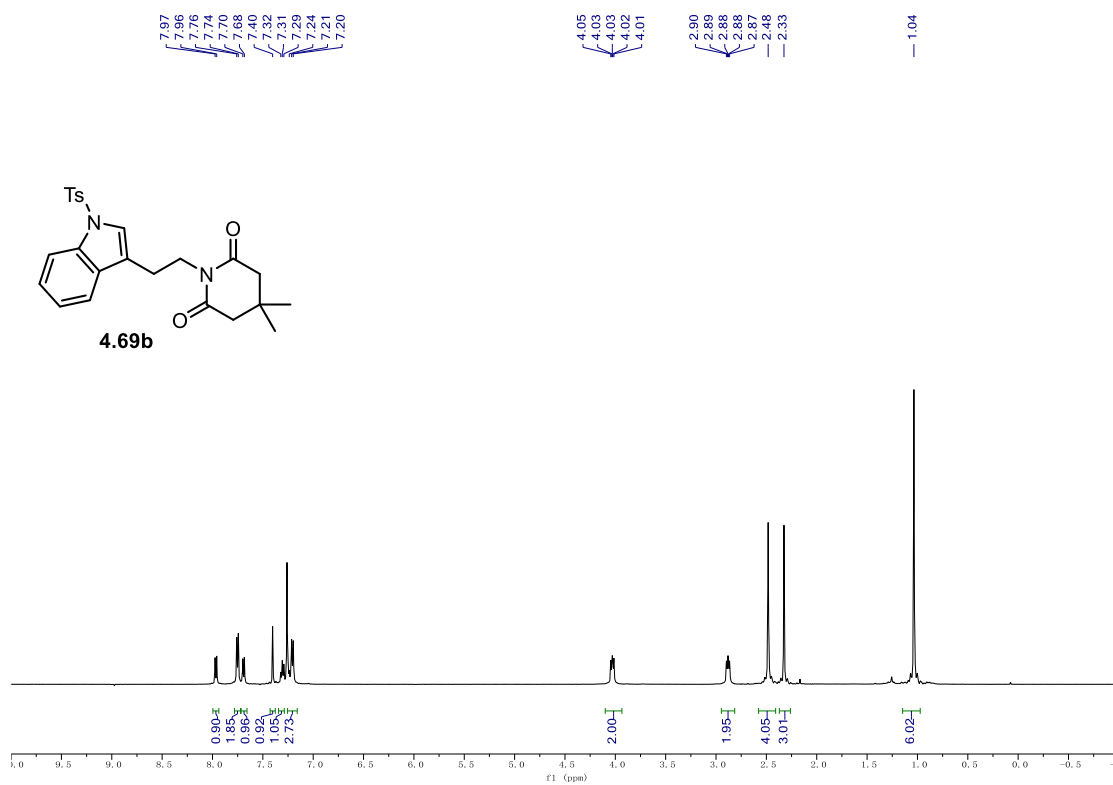
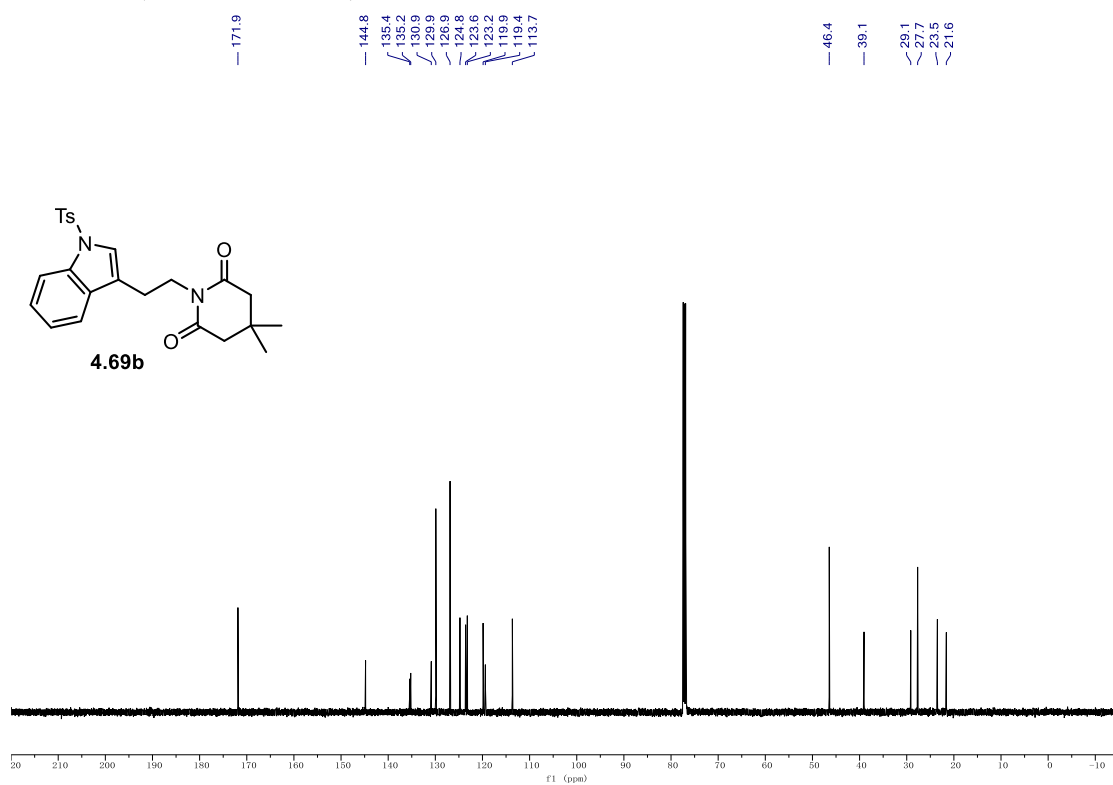
9.1. NMR Spectra

¹H NMR (500 MHz, CDCl₃) of **4.69a**.



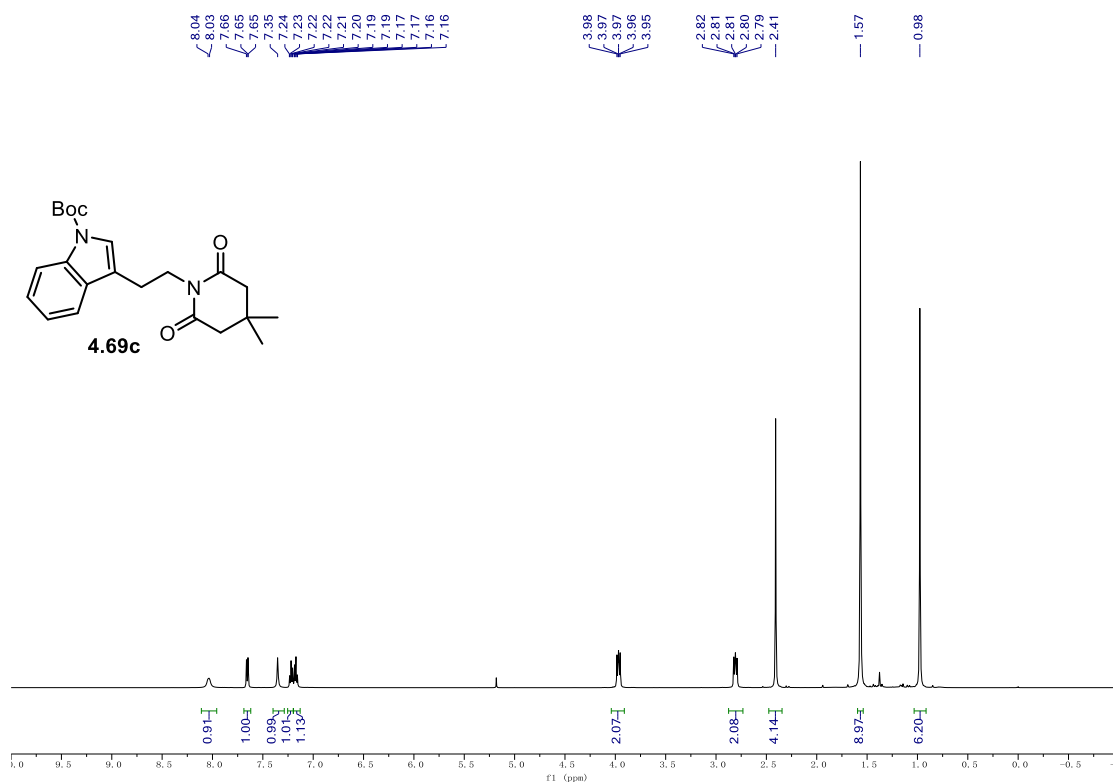
¹³C NMR (126 MHz, CDCl₃) of **4.69a**.



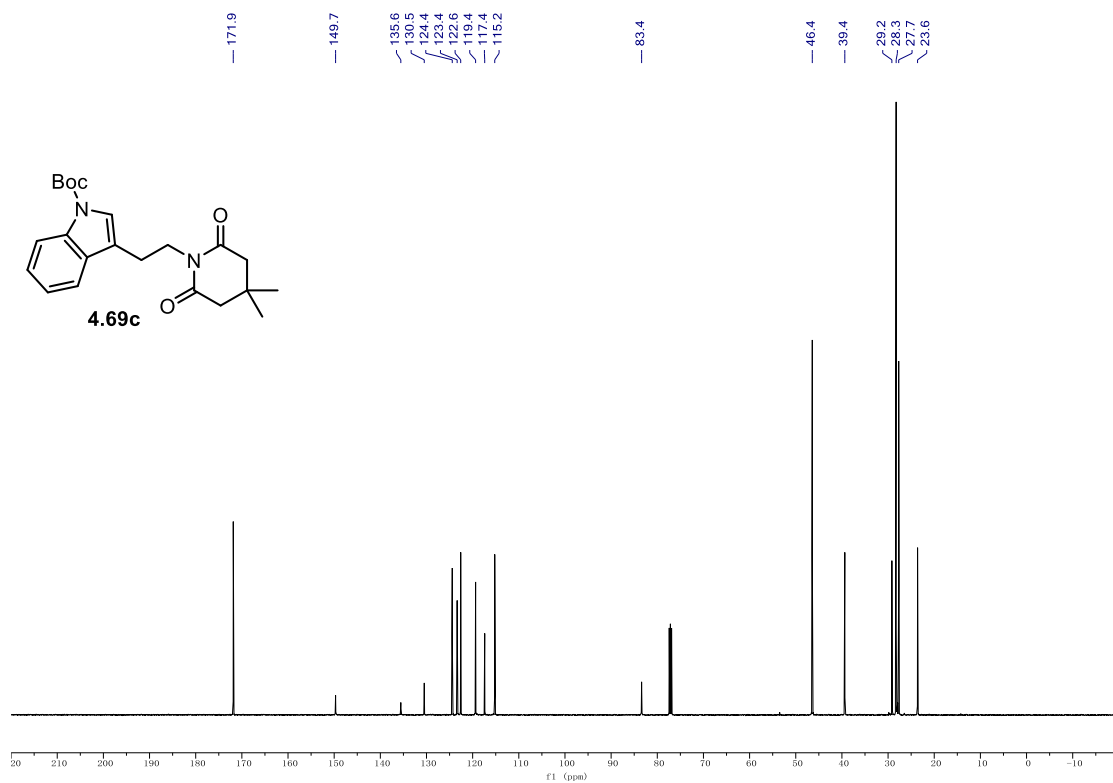
^1H NMR (500 MHz, CDCl_3) of **4.69b**. ^{13}C NMR (126 MHz, CDCl_3) of **4.69b**.

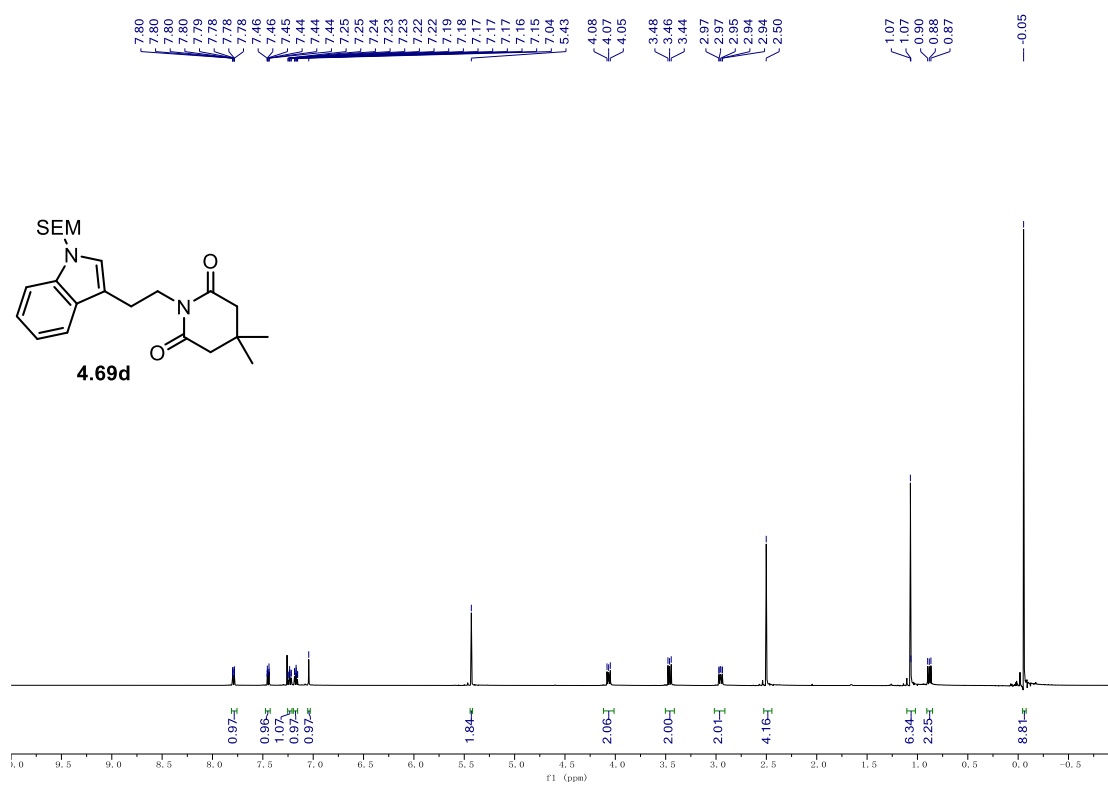
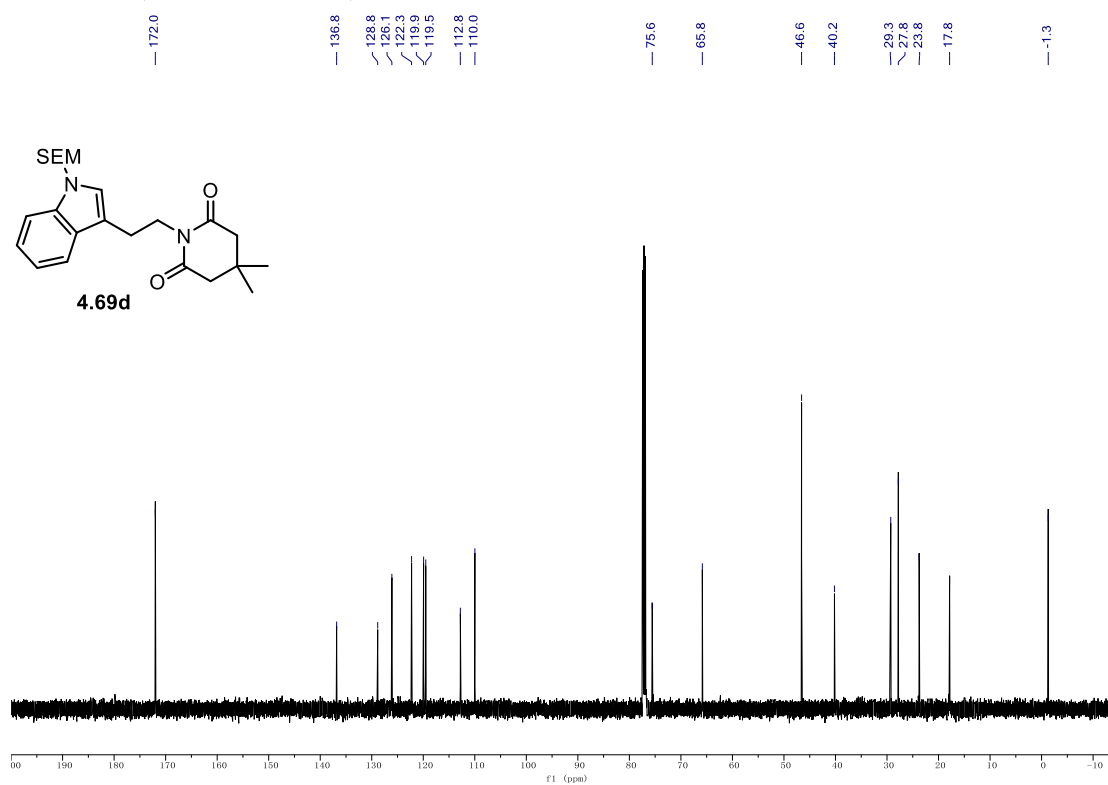
9.1. NMR Spectra

¹H NMR (500 MHz, CDCl₃) of **4.69c**.



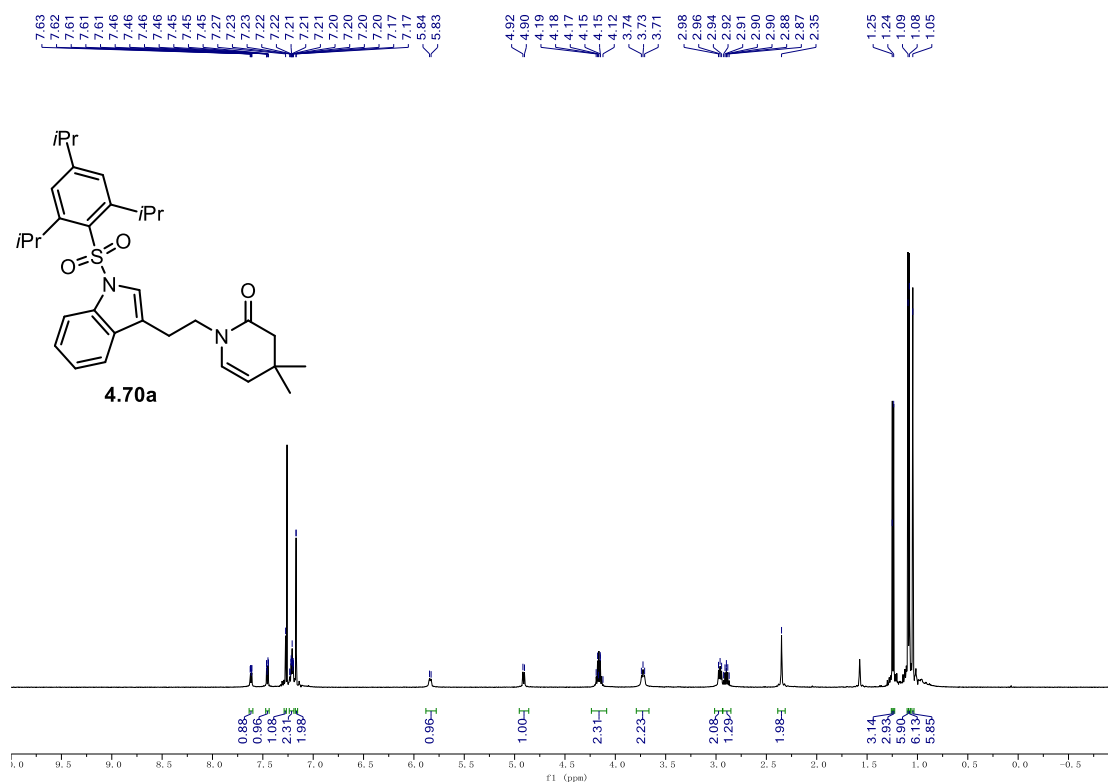
¹³C NMR (126 MHz, CDCl₃) of **4.69c**.



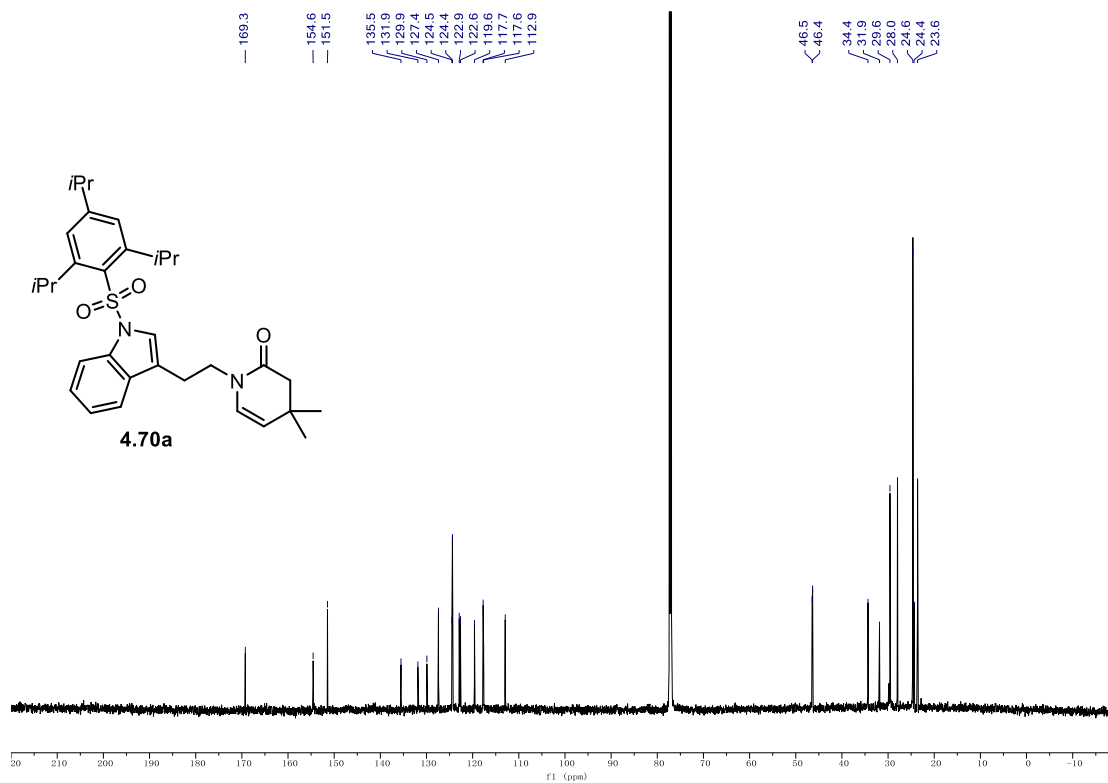
¹H NMR (500 MHz, CDCl₃) of 4.69d.**¹³C NMR (126 MHz, CDCl₃) of 4.69d.**

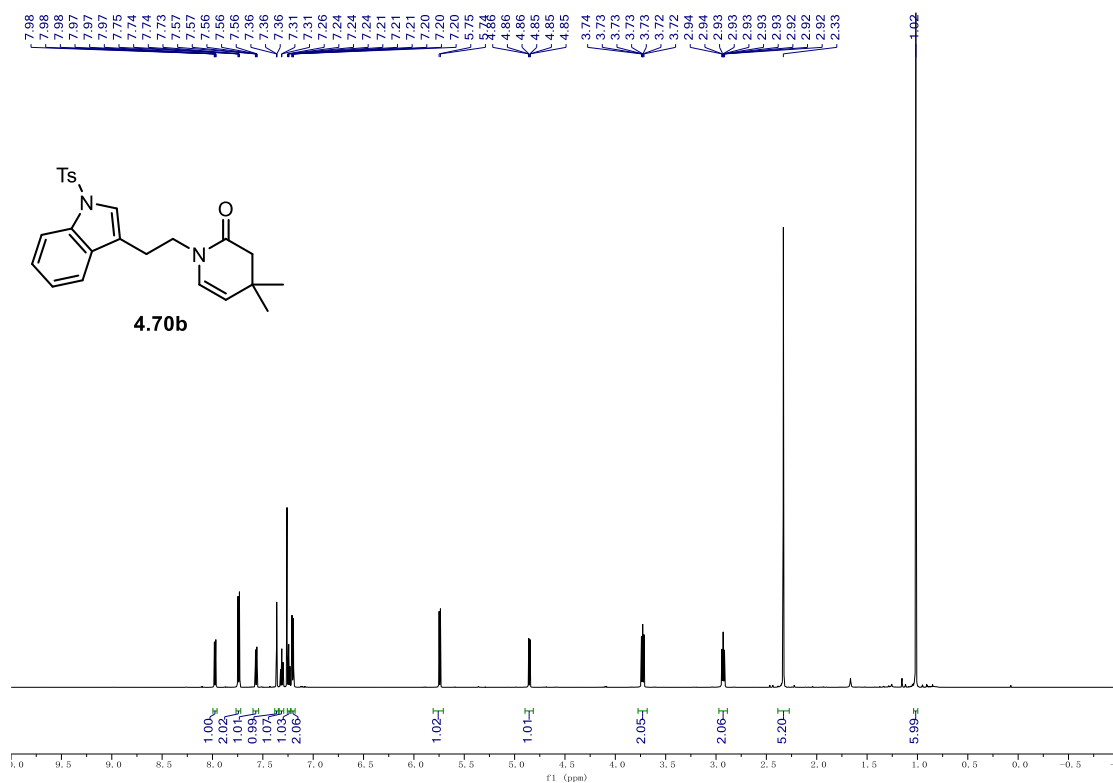
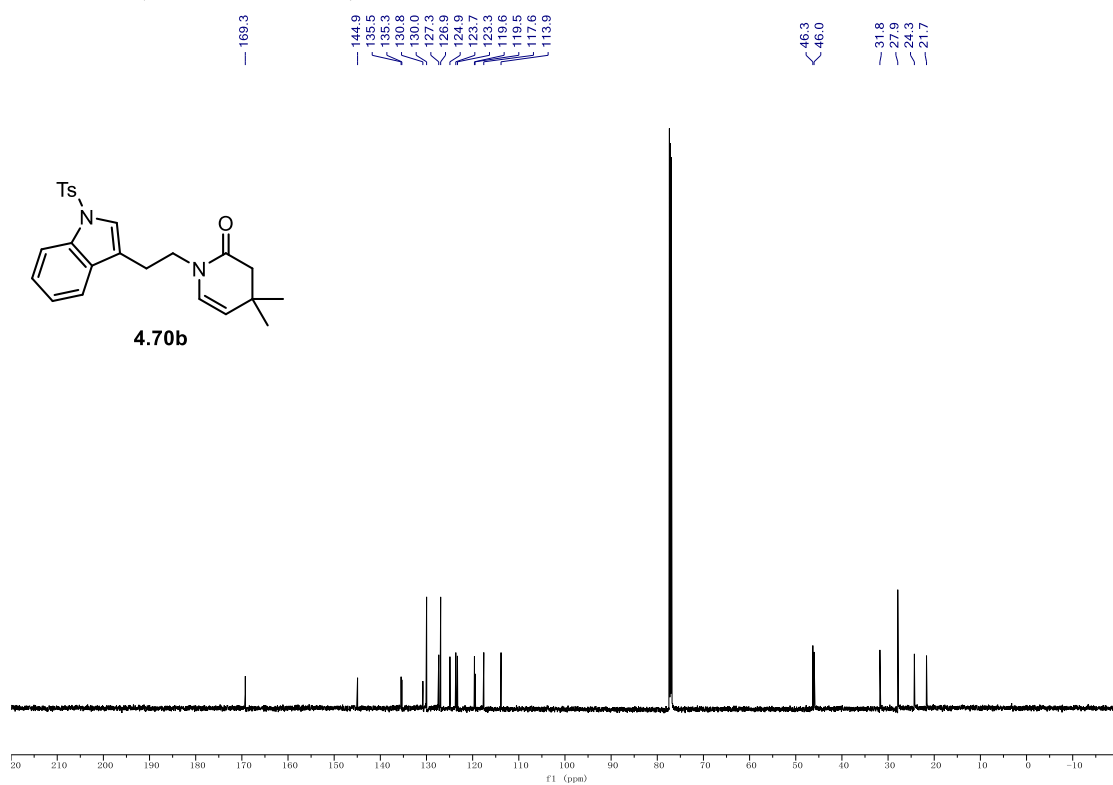
9.1. NMR Spectra

^1H NMR (500 MHz, CDCl_3) of **4.70a**.



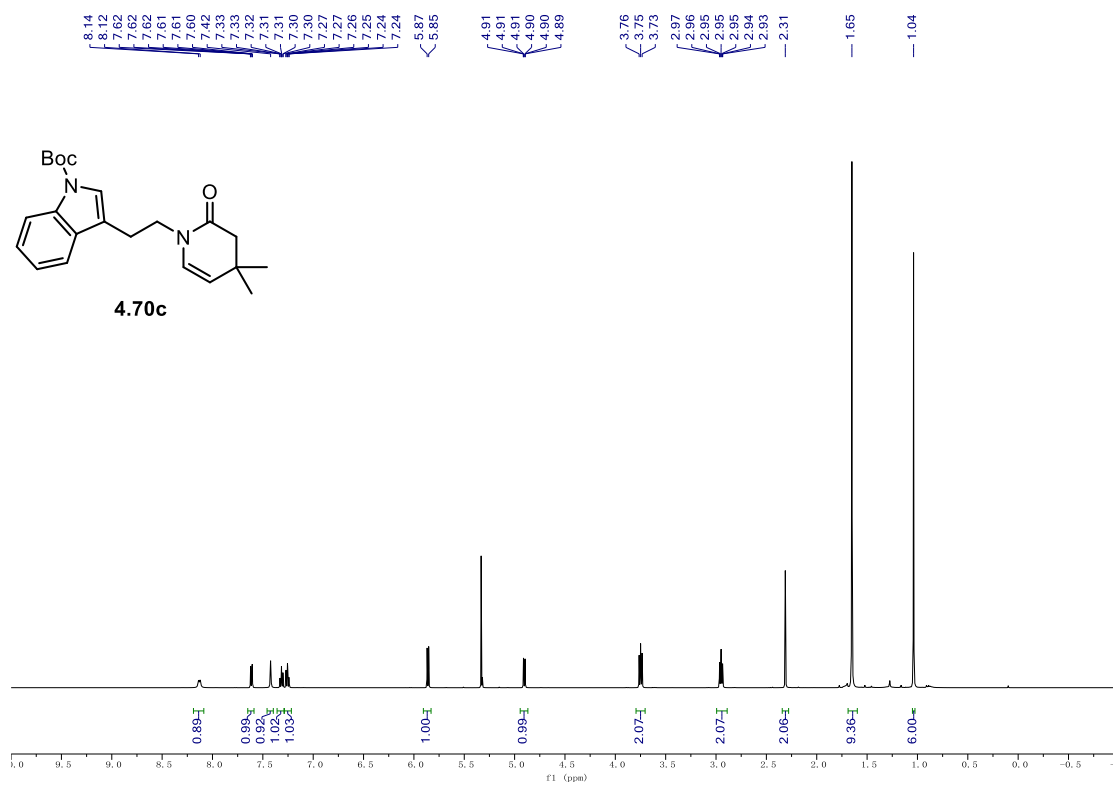
^{13}C NMR (126 MHz, CDCl_3) of **4.70a**.



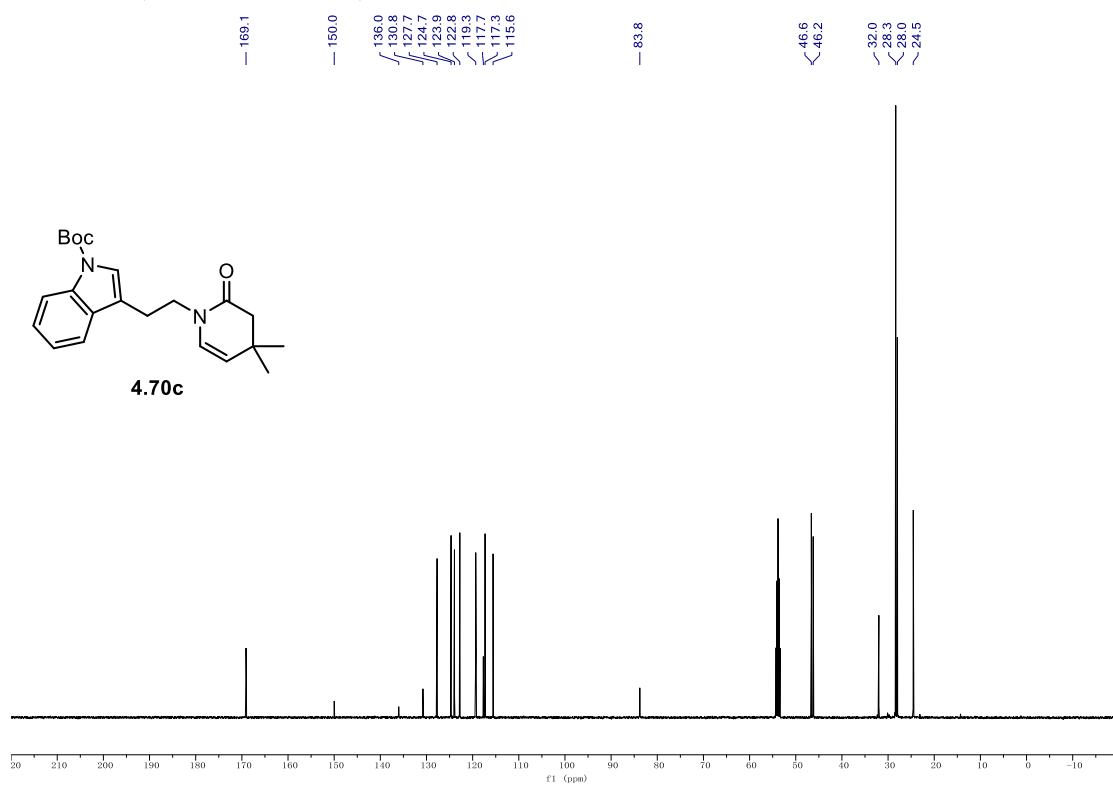
^1H NMR (600 MHz, CDCl_3) of **4.70b**. ^{13}C NMR (151 MHz, CDCl_3) of **4.70b**.

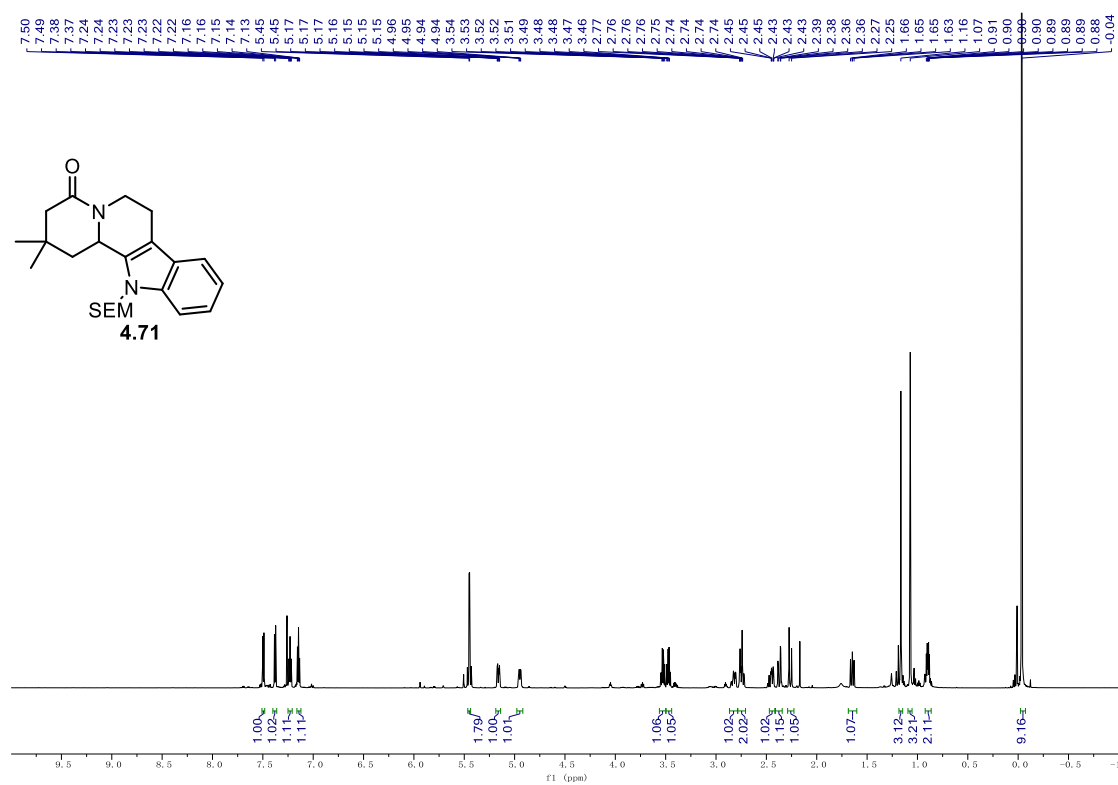
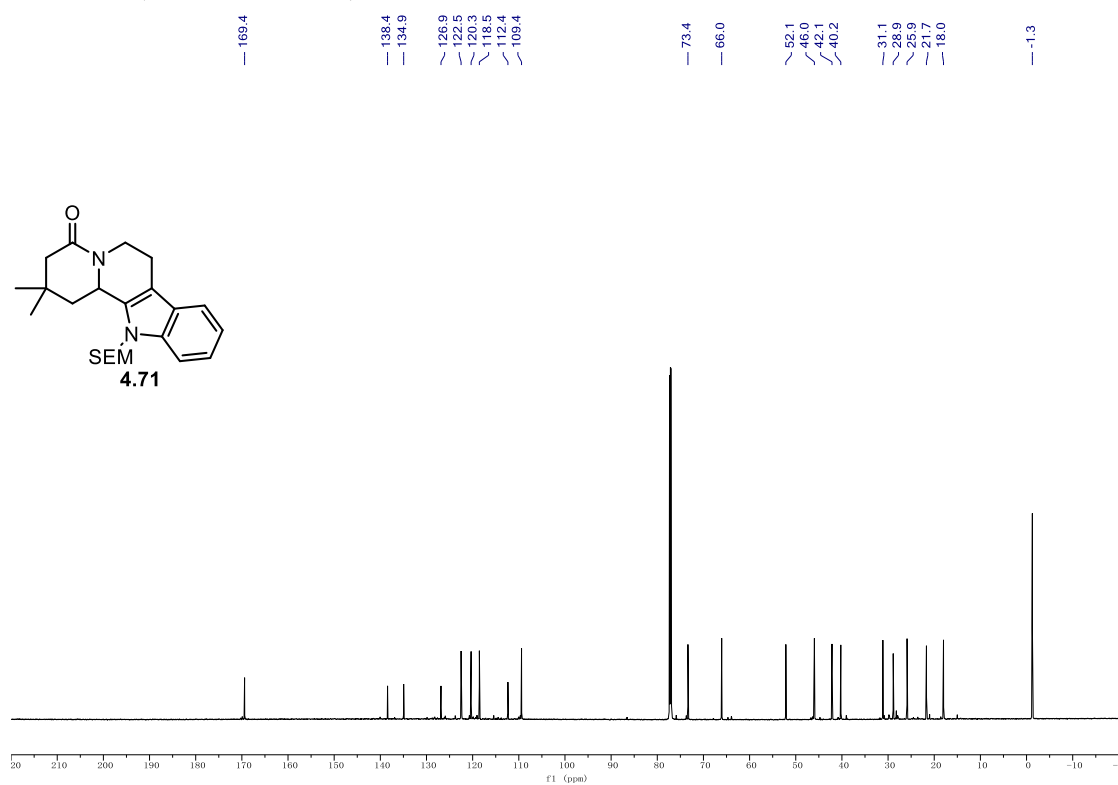
9.1. NMR Spectra

^1H NMR (500 MHz, CD_2Cl_2) of **4.70c**.



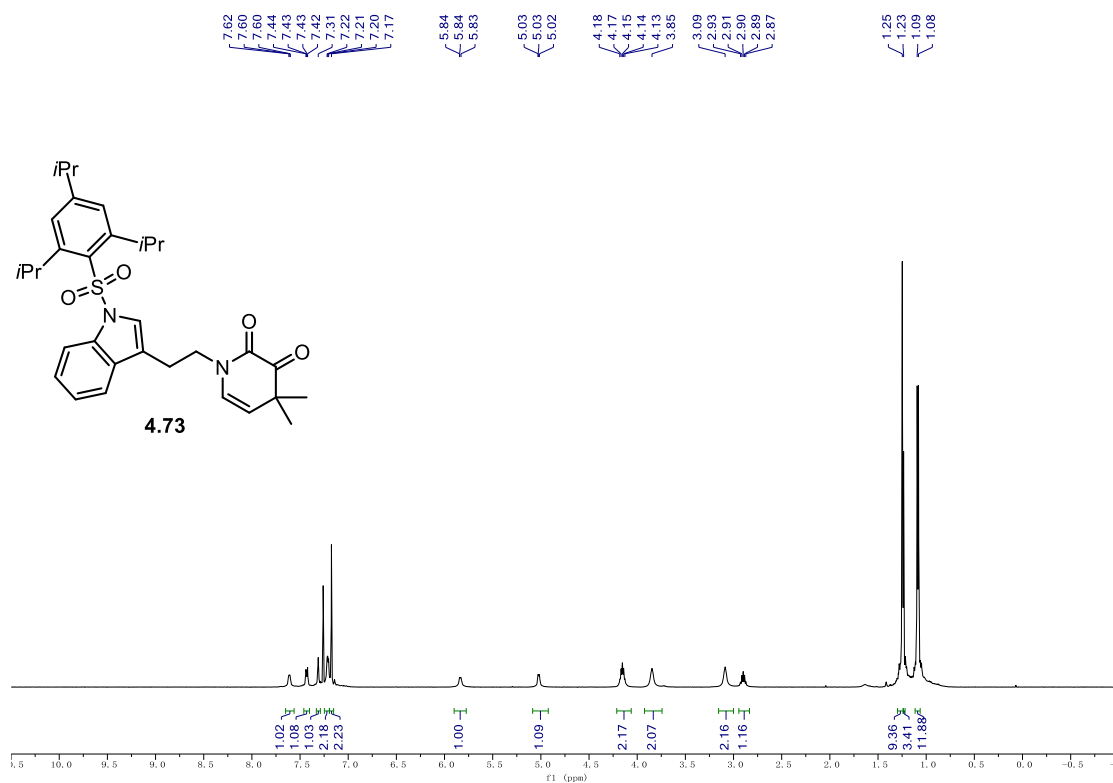
^{13}C NMR (126 MHz, CD_2Cl_2) of **4.70c**.



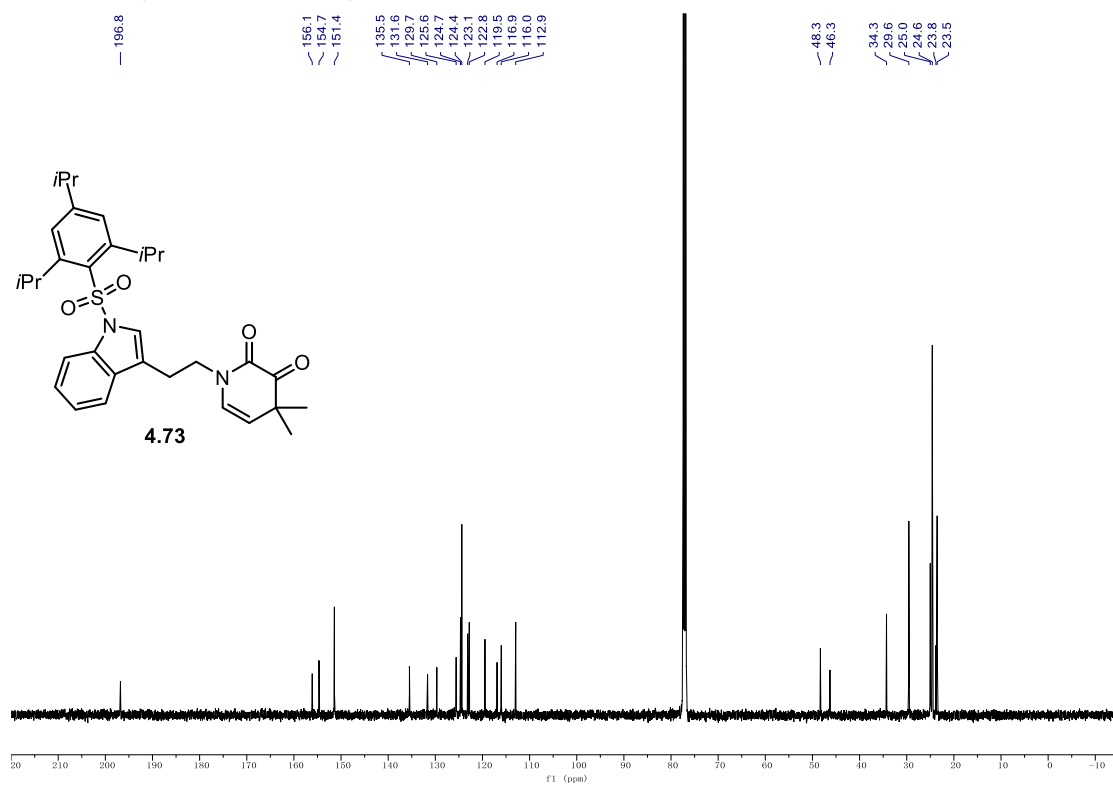
^1H NMR (700 MHz, CDCl_3) of **4.71**. ^{13}C NMR (176 MHz, CDCl_3) of **4.71**.

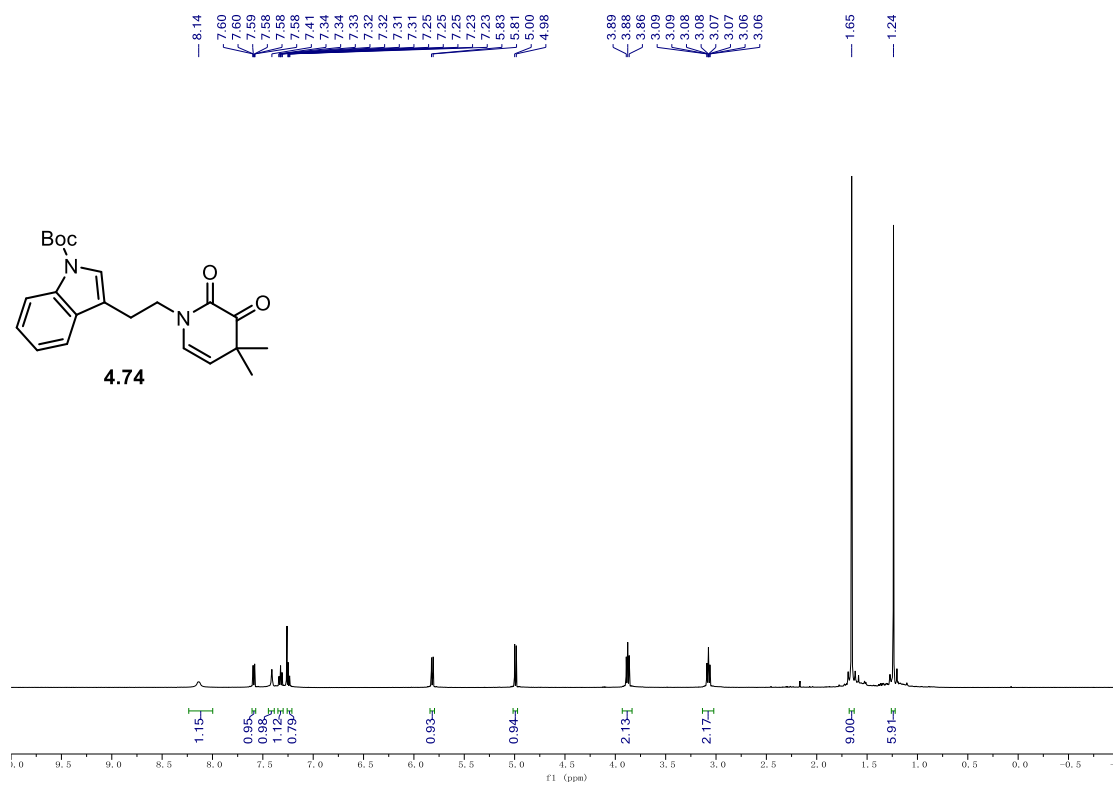
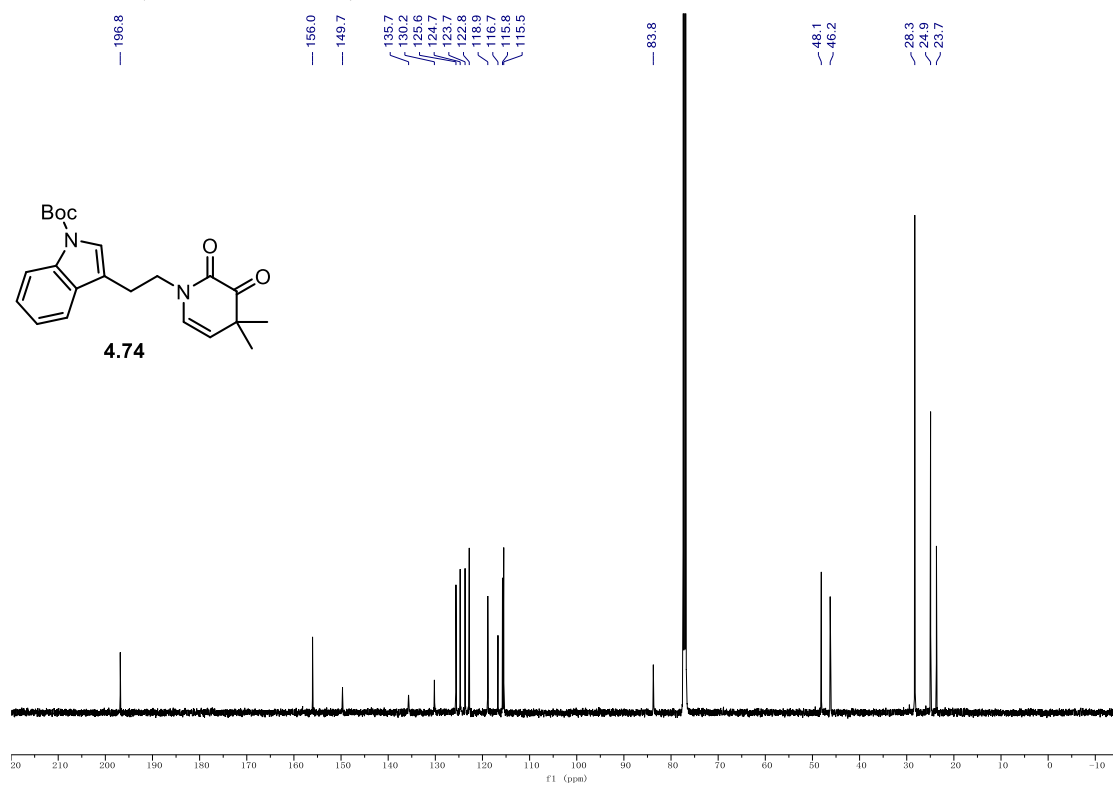
9.1. NMR Spectra

^1H NMR (500 MHz, CDCl_3) of **4.73**.



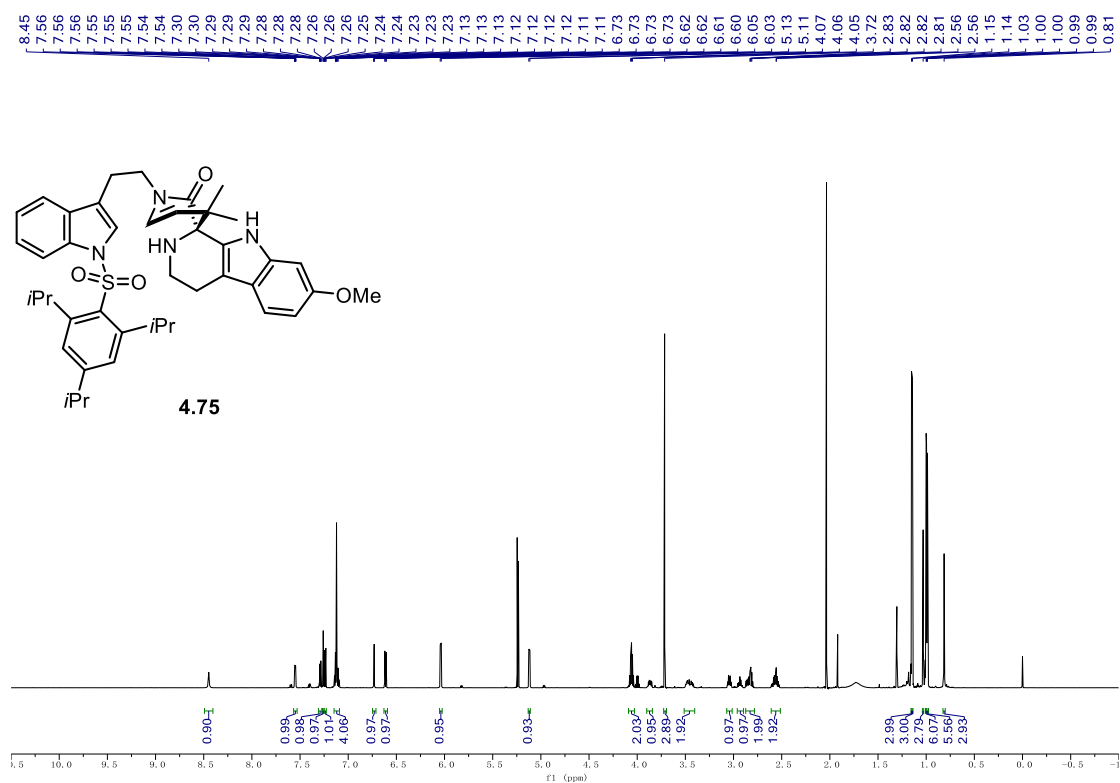
^{13}C NMR (126 MHz, CDCl_3) of **4.73**.



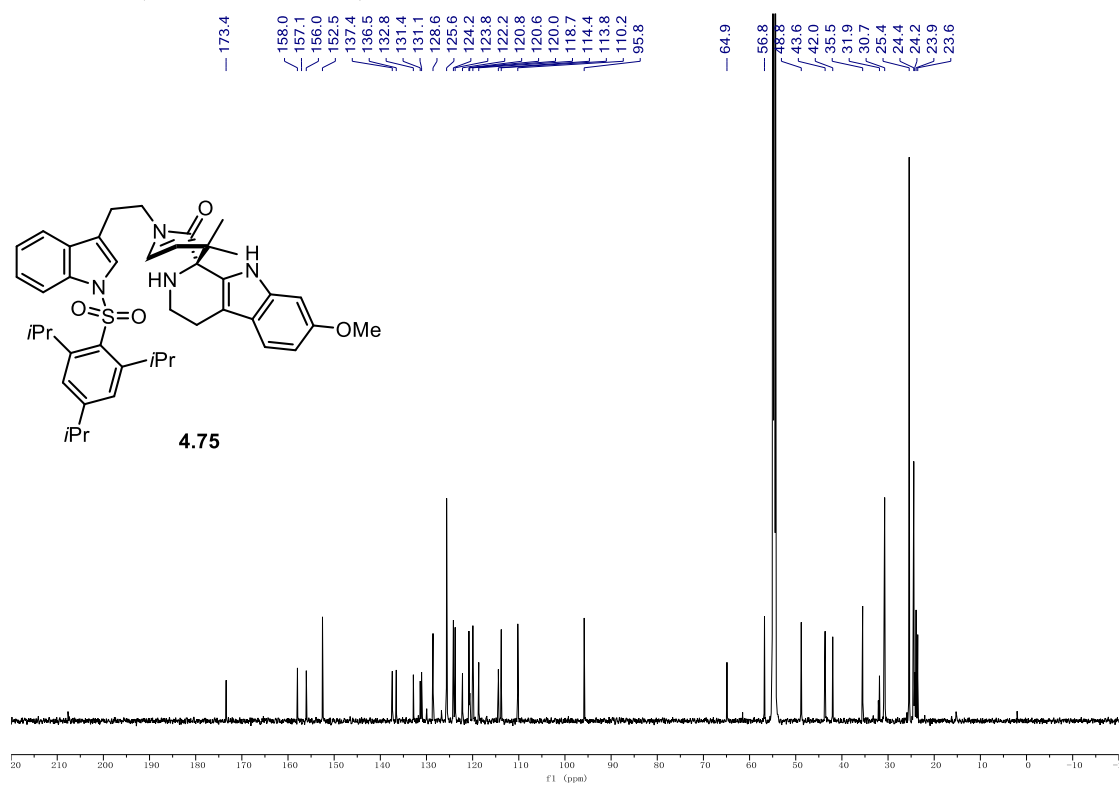
^1H NMR (500 MHz, CDCl_3) of **4.74**. ^{13}C NMR (126 MHz, CDCl_3) of **4.74**.

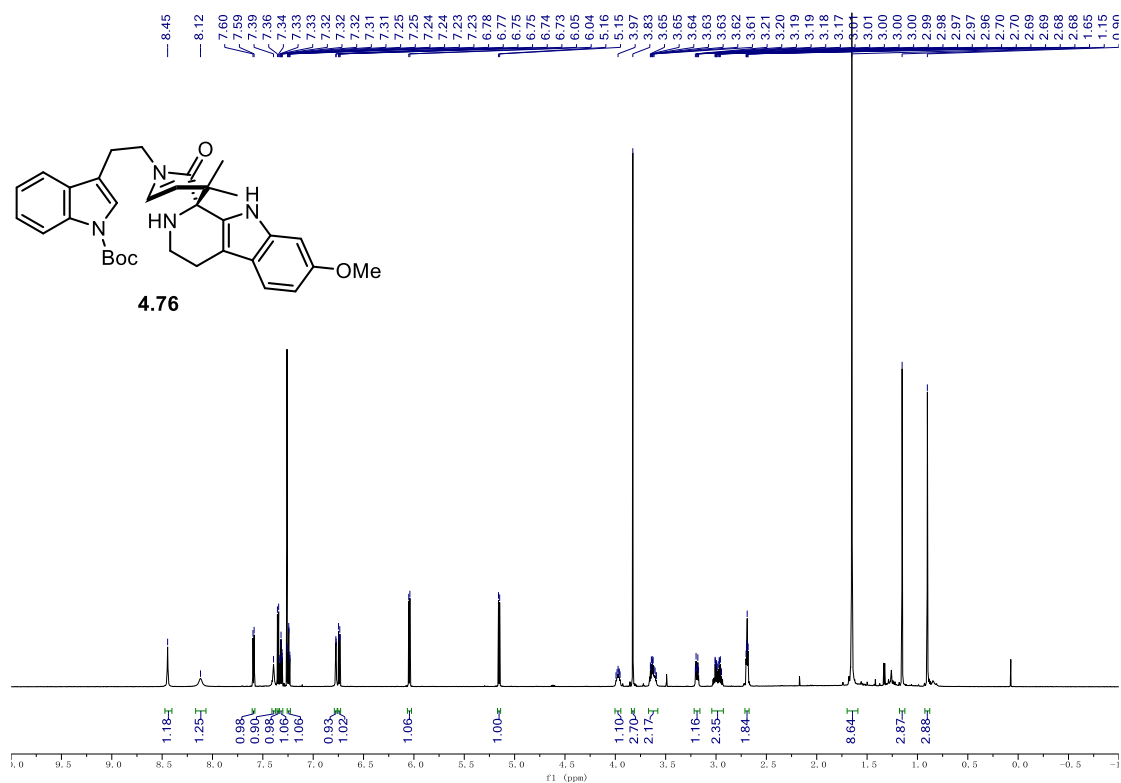
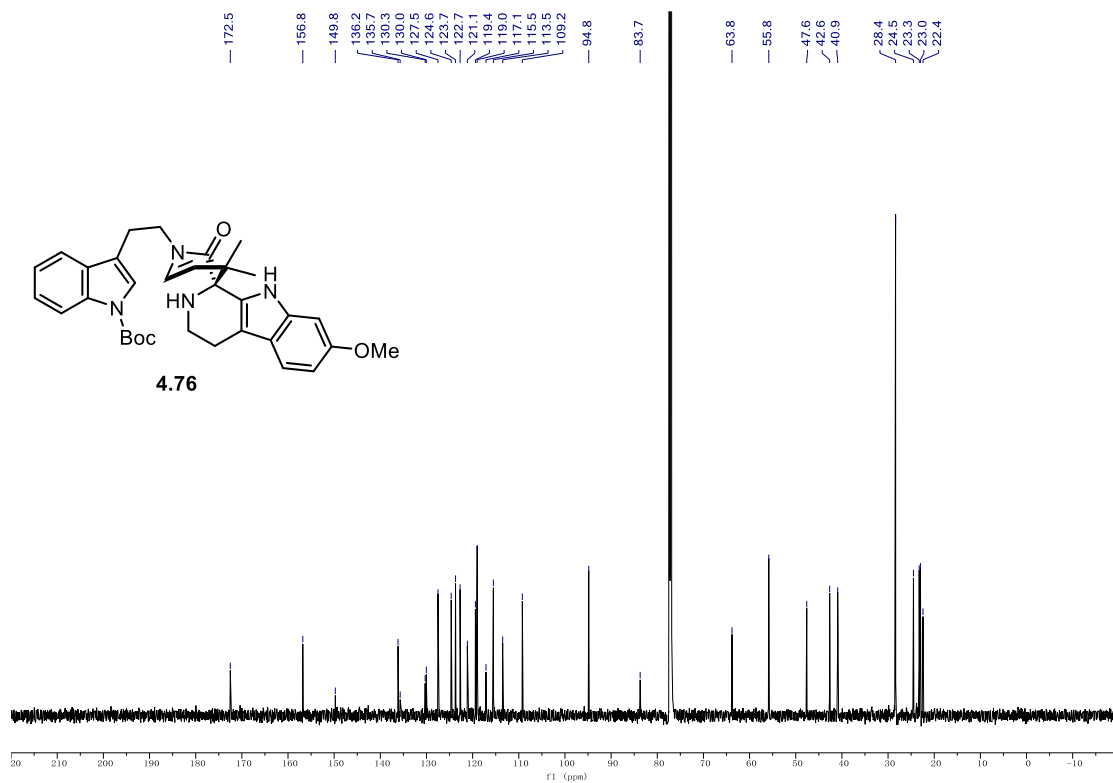
9.1. NMR Spectra

¹H NMR (700 MHz, CD₂Cl₂) of **4.75**.



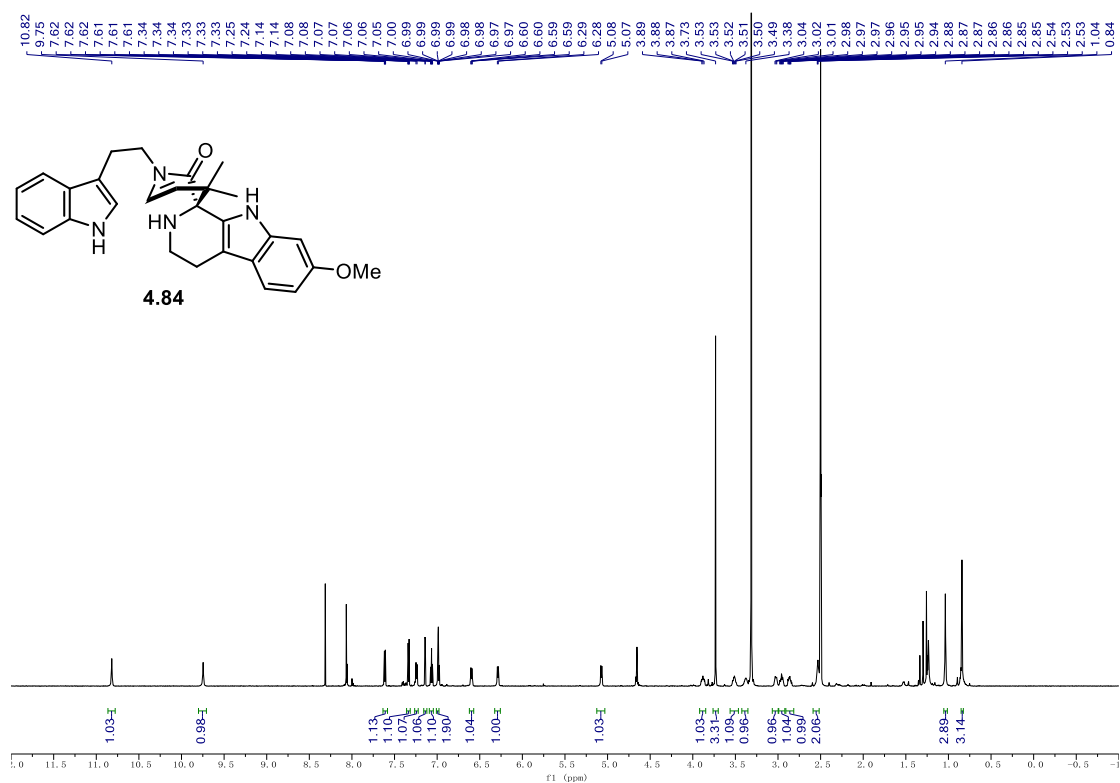
¹³C NMR (176 MHz, CD₂Cl₂) of **4.75**.



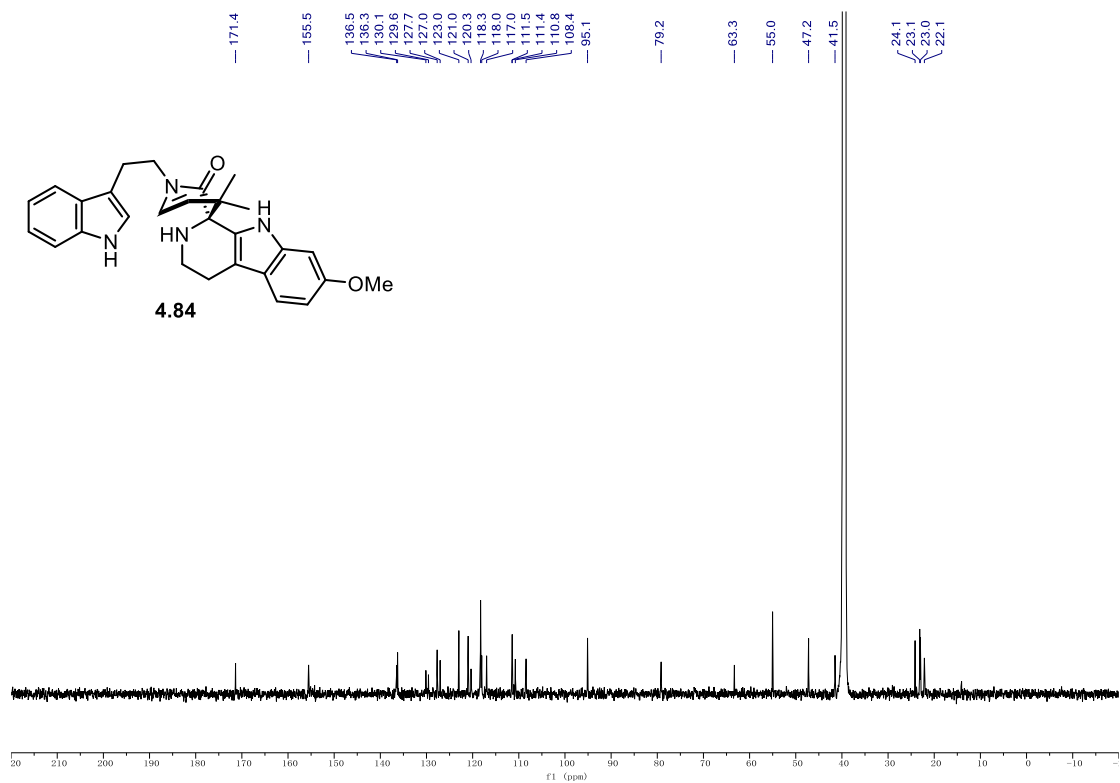
¹H NMR (700 MHz, CDCl₃) of 4.76.**¹³C NMR (176 MHz, CDCl₃) of 4.76.**

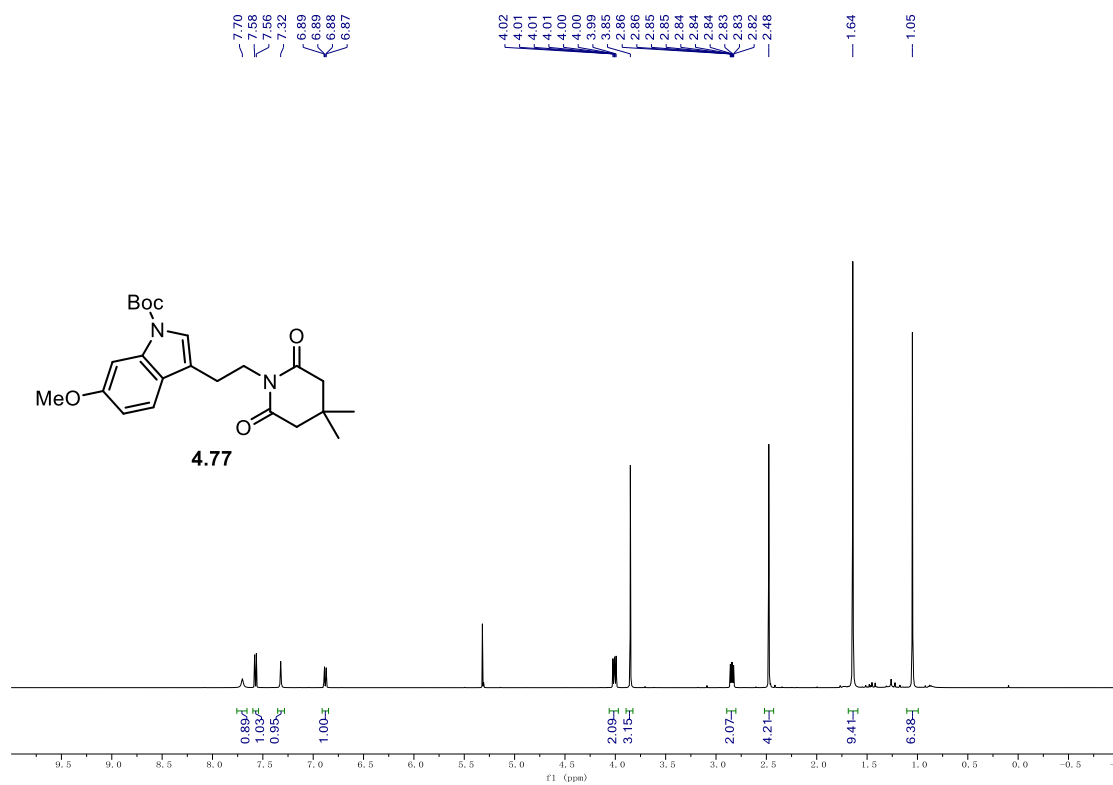
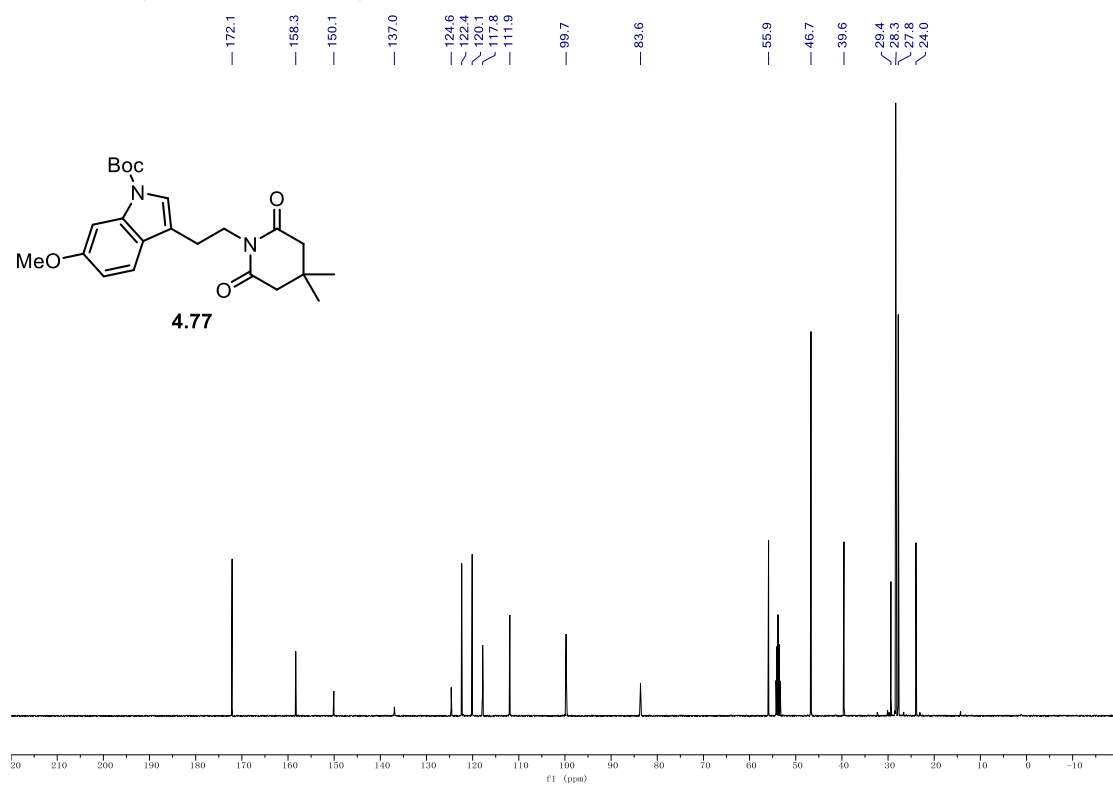
9.1. NMR Spectra

^1H NMR (700 MHz, d_6 -DMSO) of **4.84**.



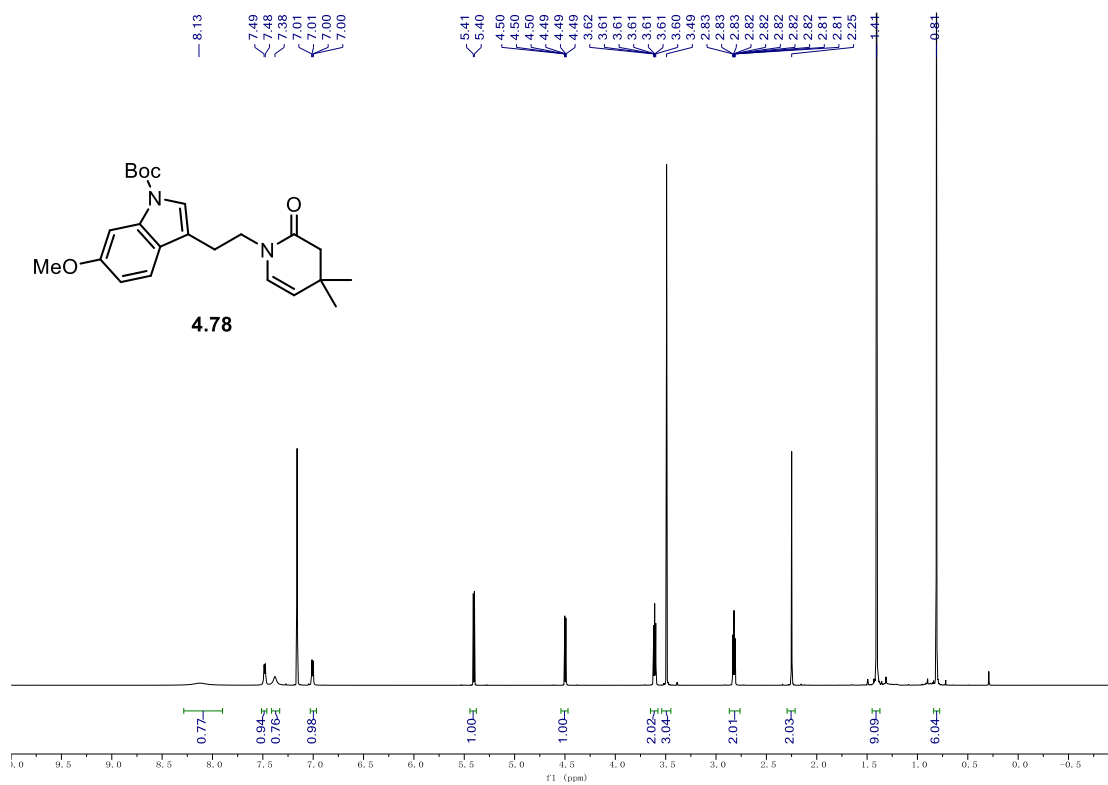
^{13}C NMR (176 MHz, d_6 -DMSO) of **4.84**.



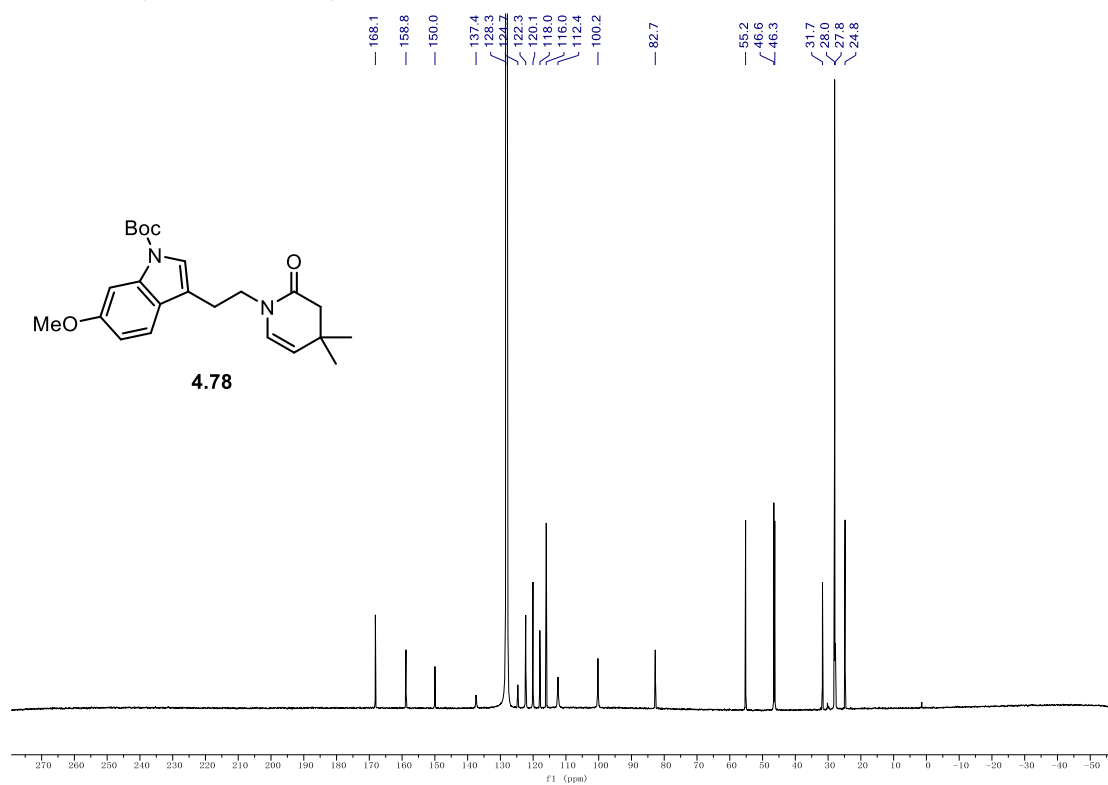
^1H NMR (500 MHz, CD_2Cl_2) of **4.77**. ^{13}C NMR (126 MHz, CD_2Cl_2) of **4.77**.

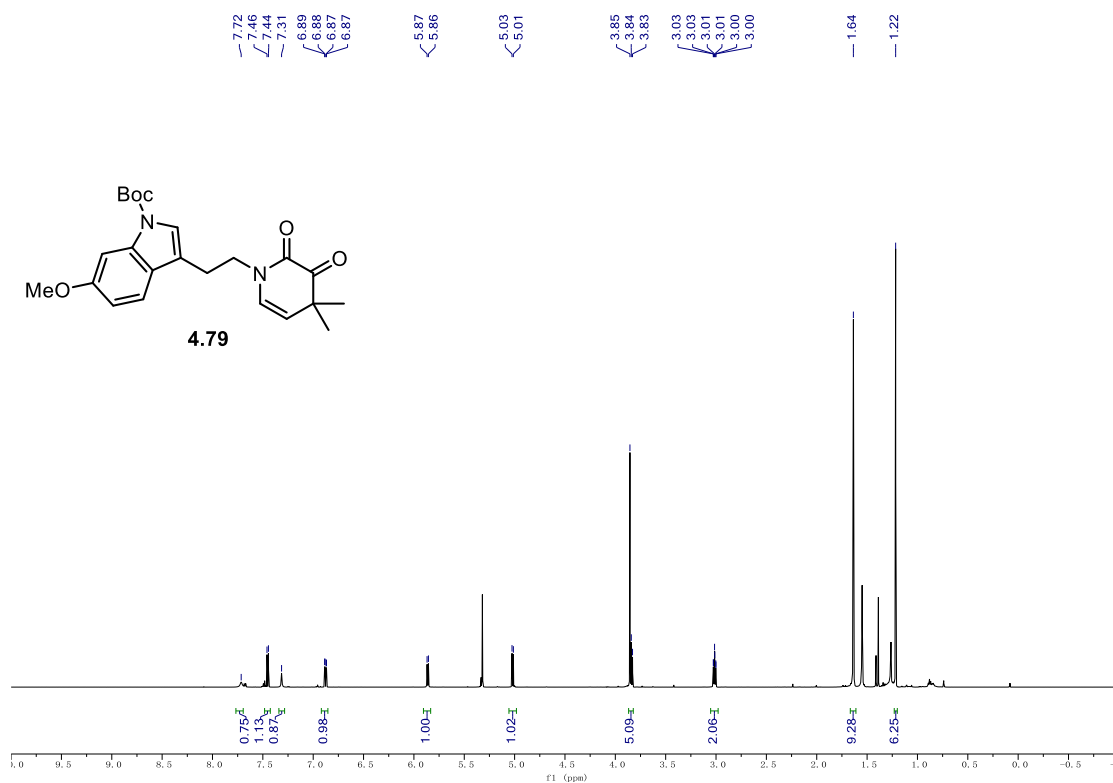
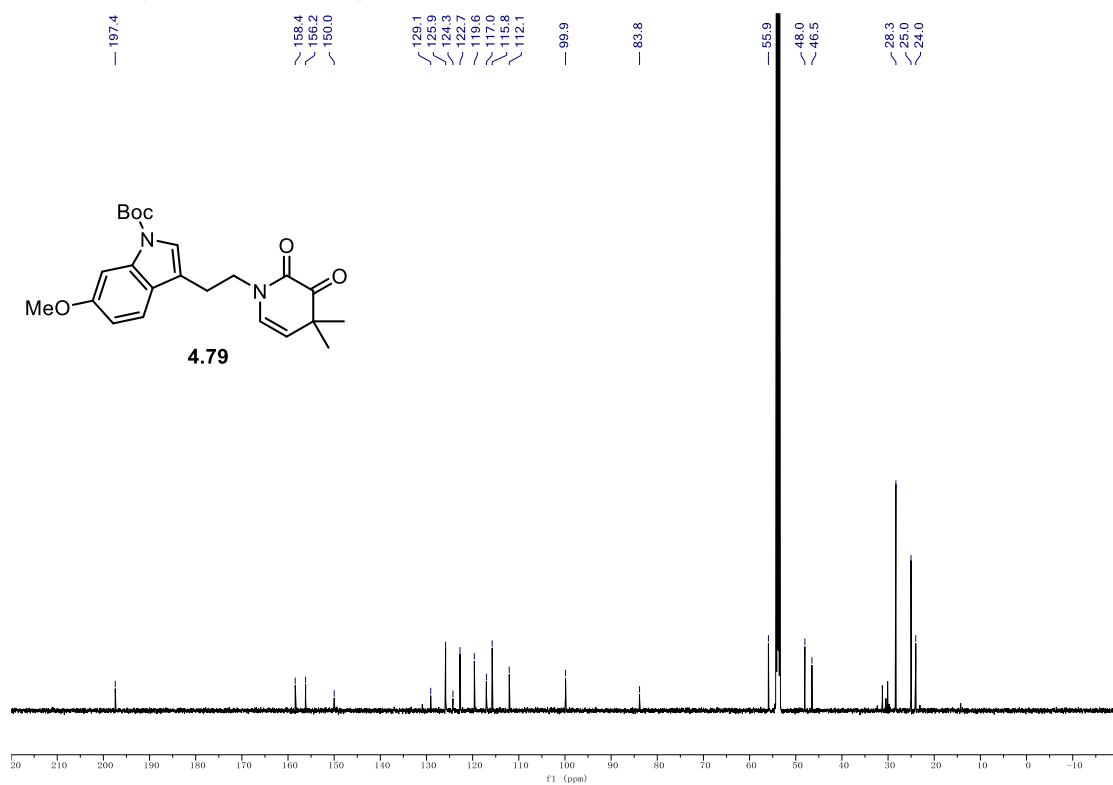
9.1. NMR Spectra

¹H NMR (700 MHz, C₆D₆) of 4.78.



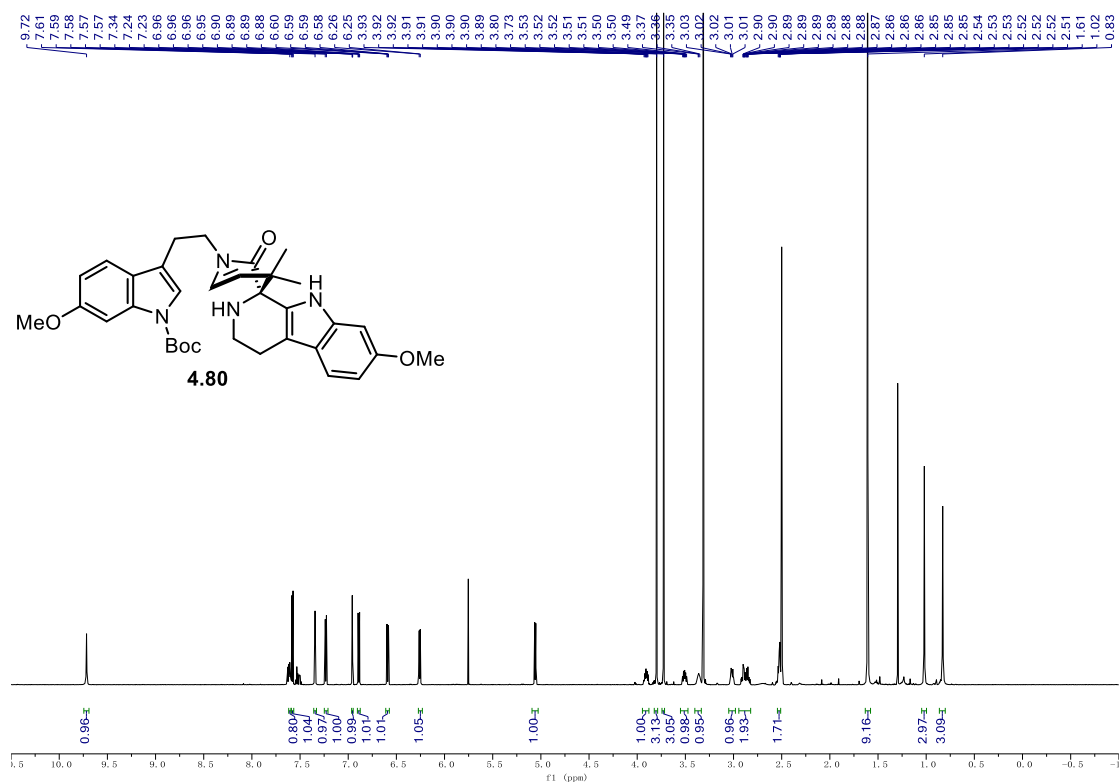
¹³C NMR (176 MHz, C₆D₆) of 4.78.



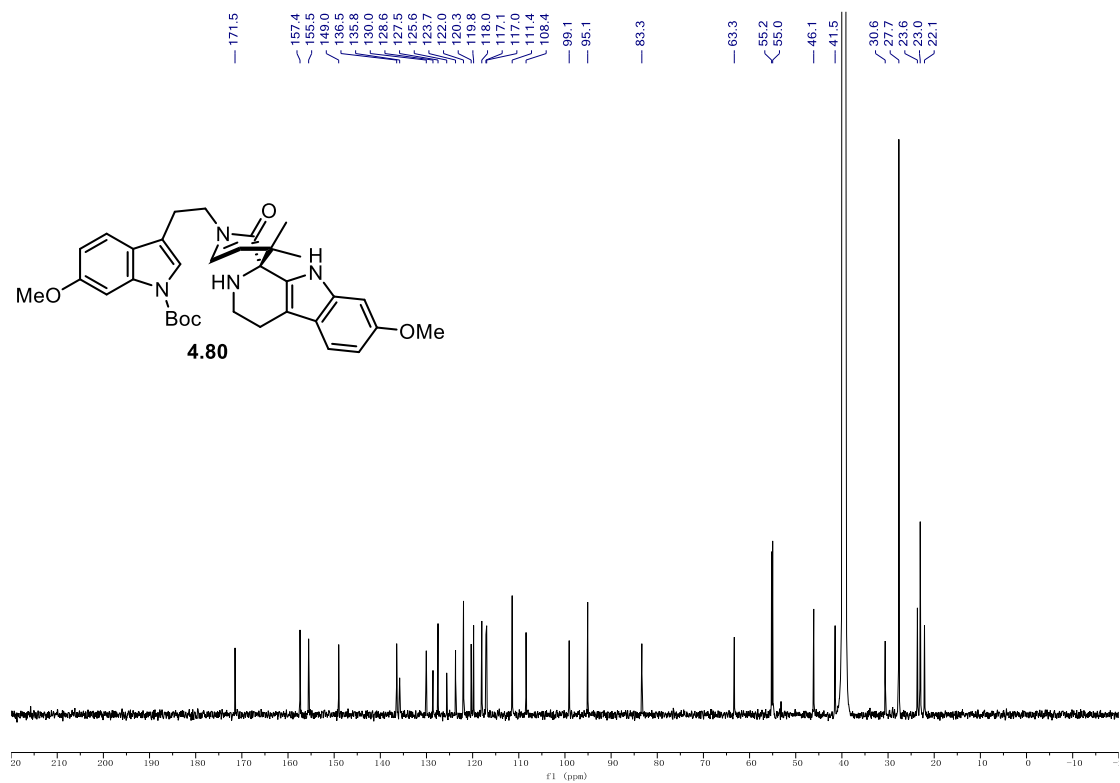
^1H NMR (600 MHz, CD_2Cl_2) of **4.79**. ^{13}C NMR (151 MHz, CD_2Cl_2) of **4.79**.

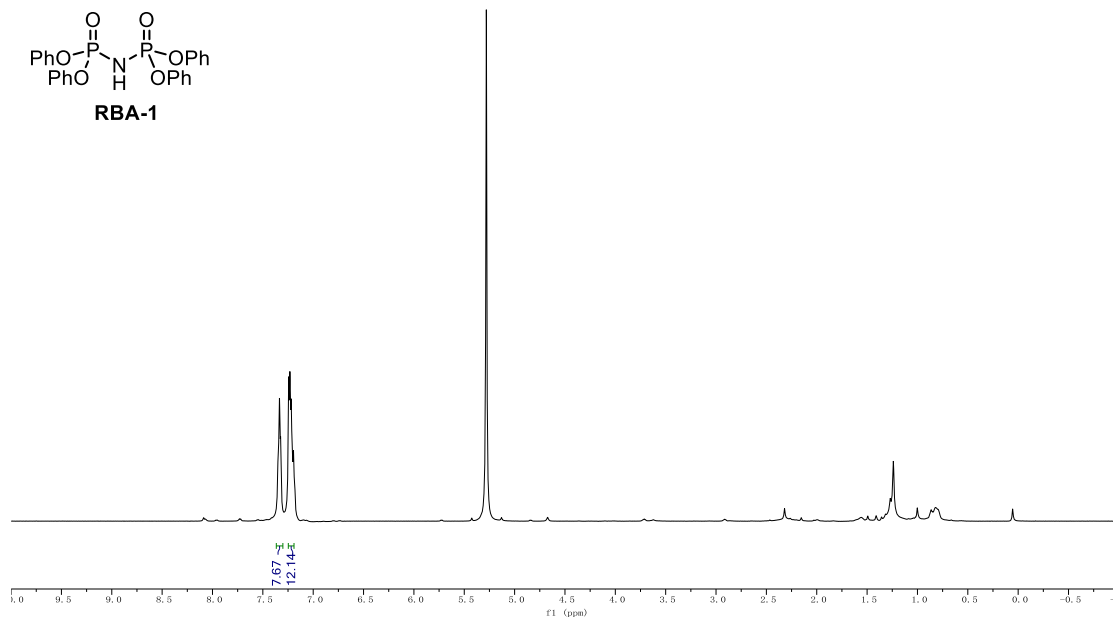
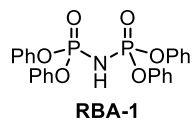
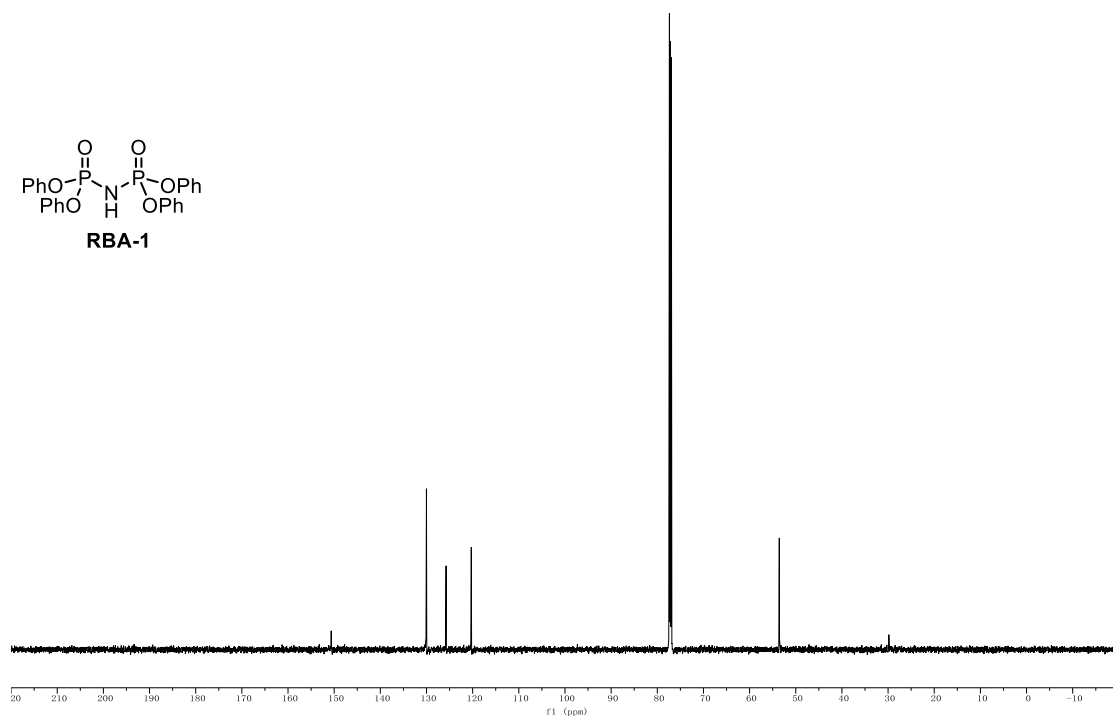
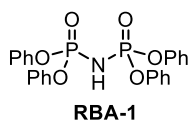
9.1. NMR Spectra

¹H NMR (700 MHz, *d*₆-DMSO) of 4.80.

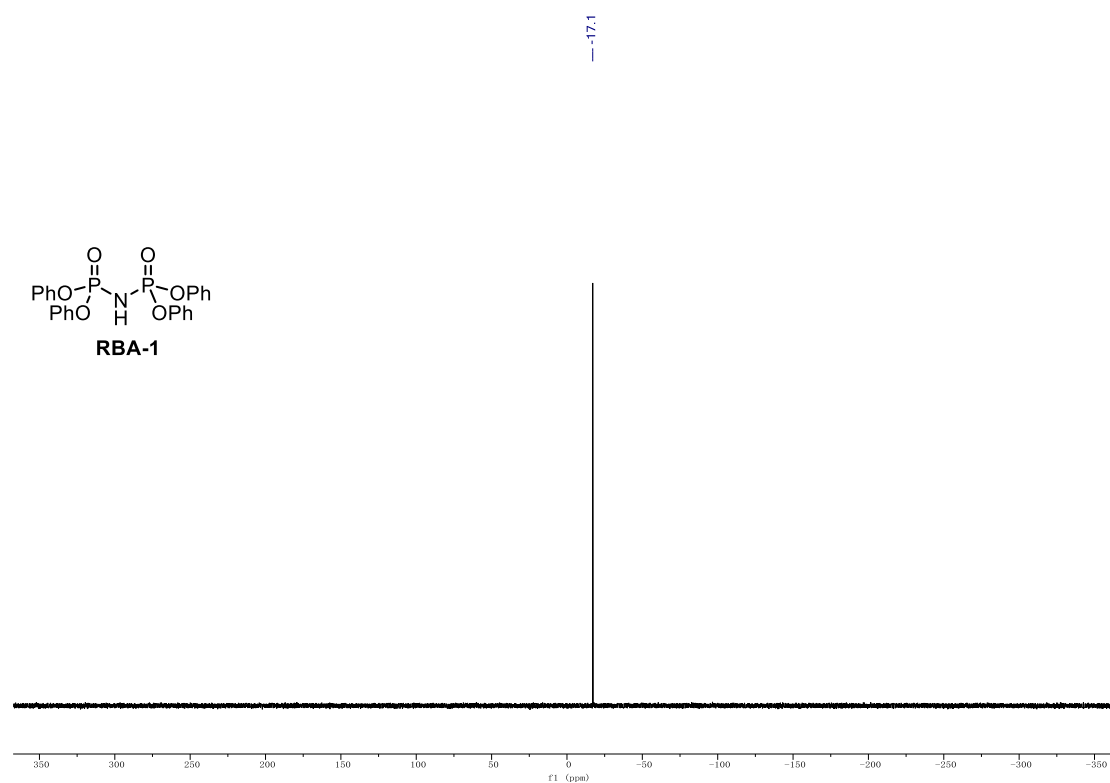


¹³C NMR (176 MHz, *d*₆-DMSO) of 4.80.

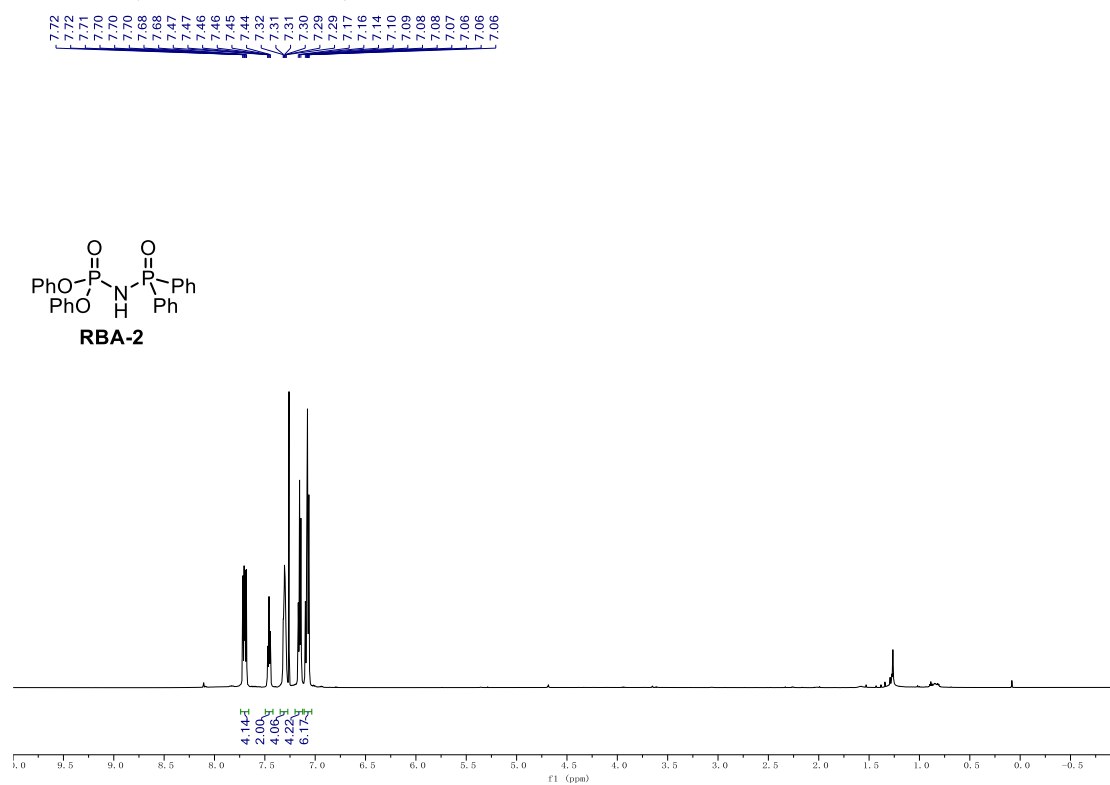


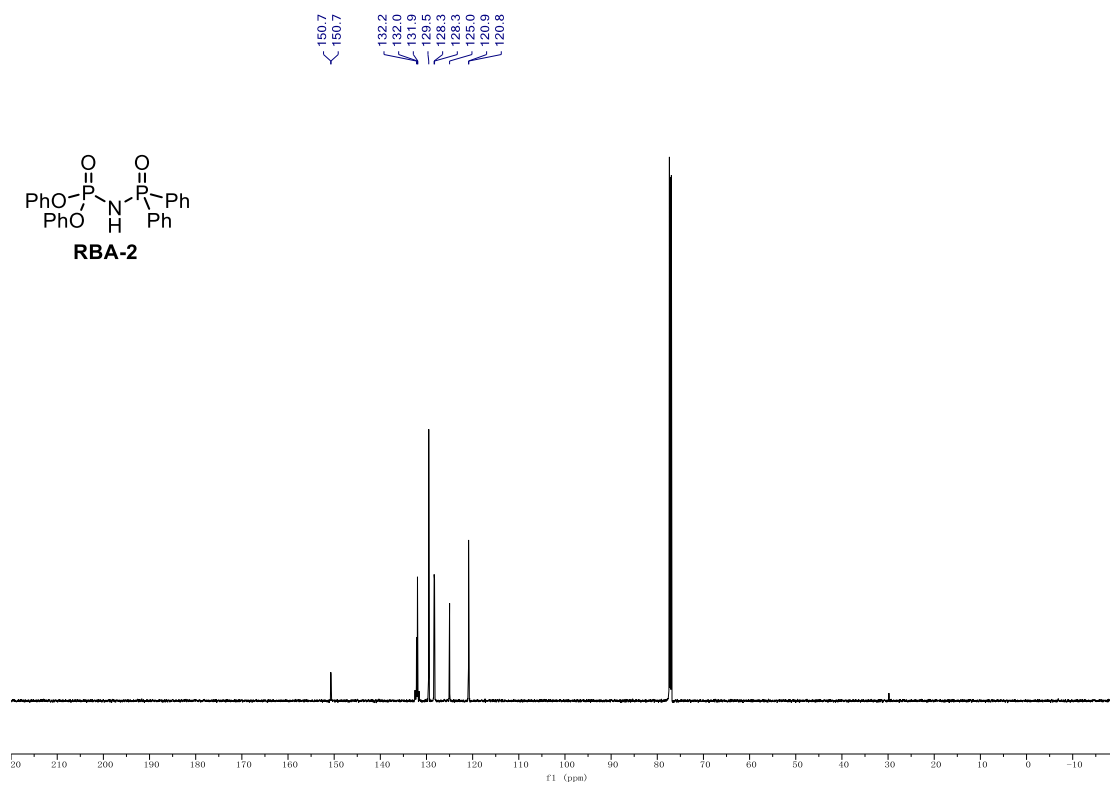
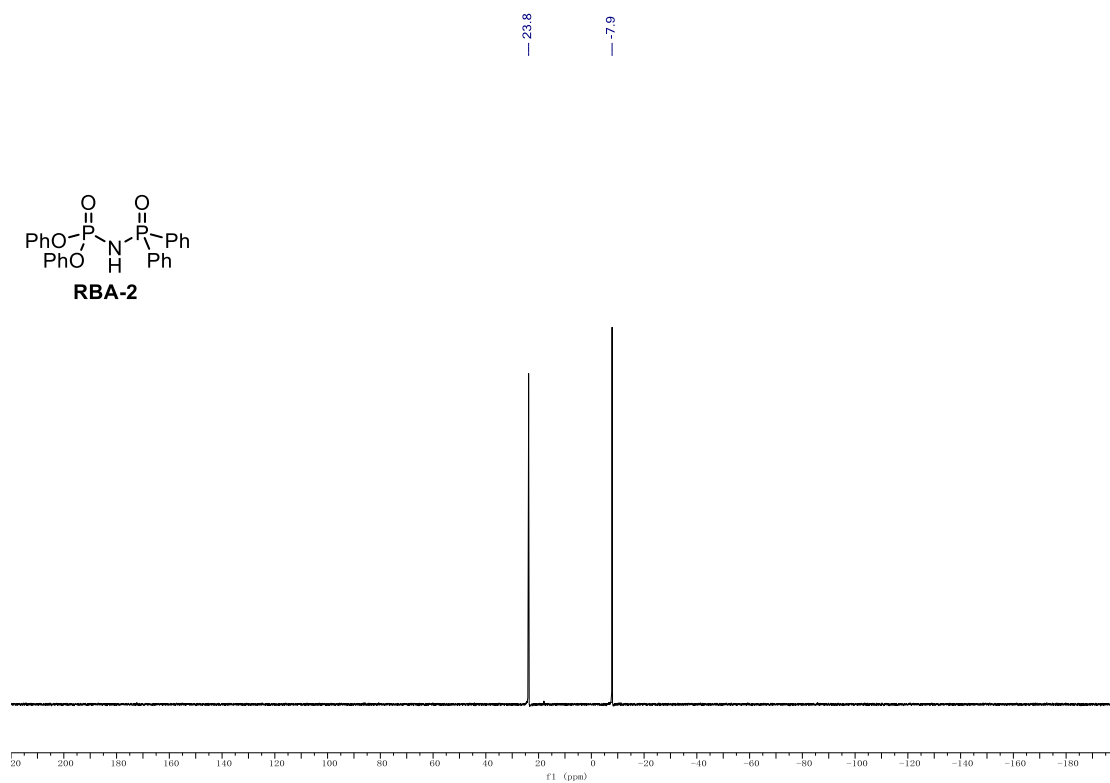
¹H NMR (600 MHz, CDCl₃) of RBA-1.7.35
7.32
7.32
7.24
7.23
7.22
7.21
7.19**¹³C NMR (151 MHz, CDCl₃) of RBA-1.**150.6
130.0
125.8
120.3

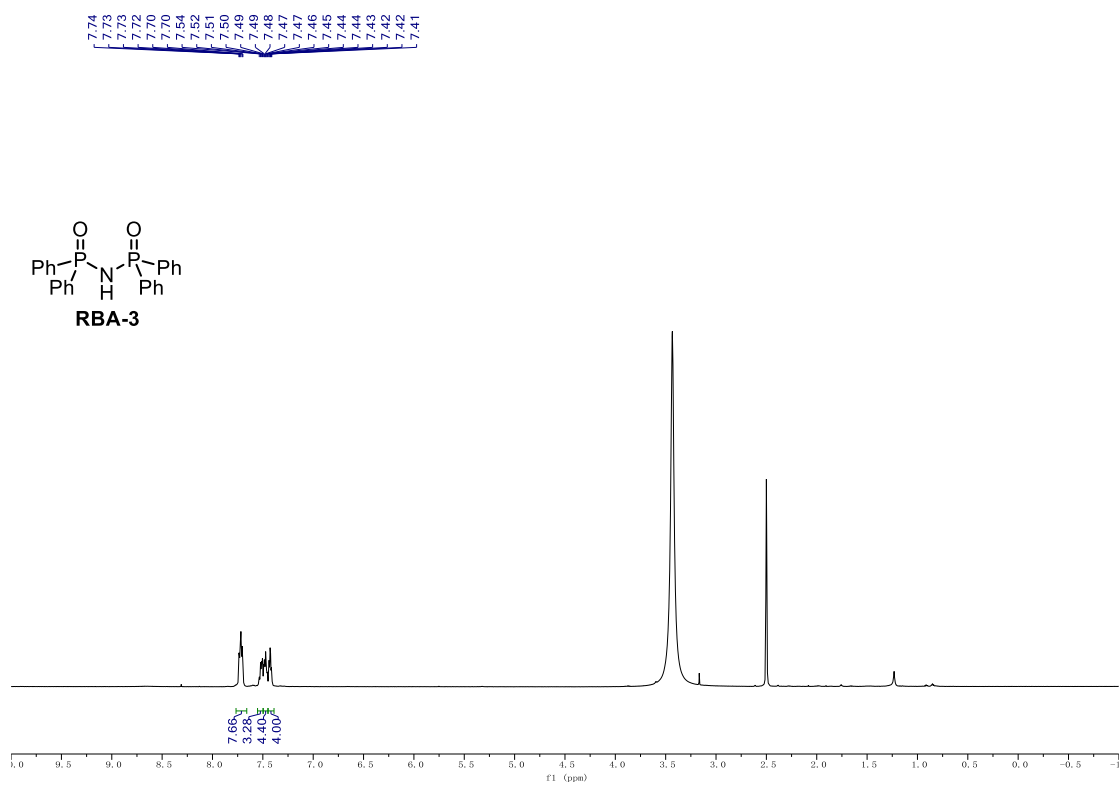
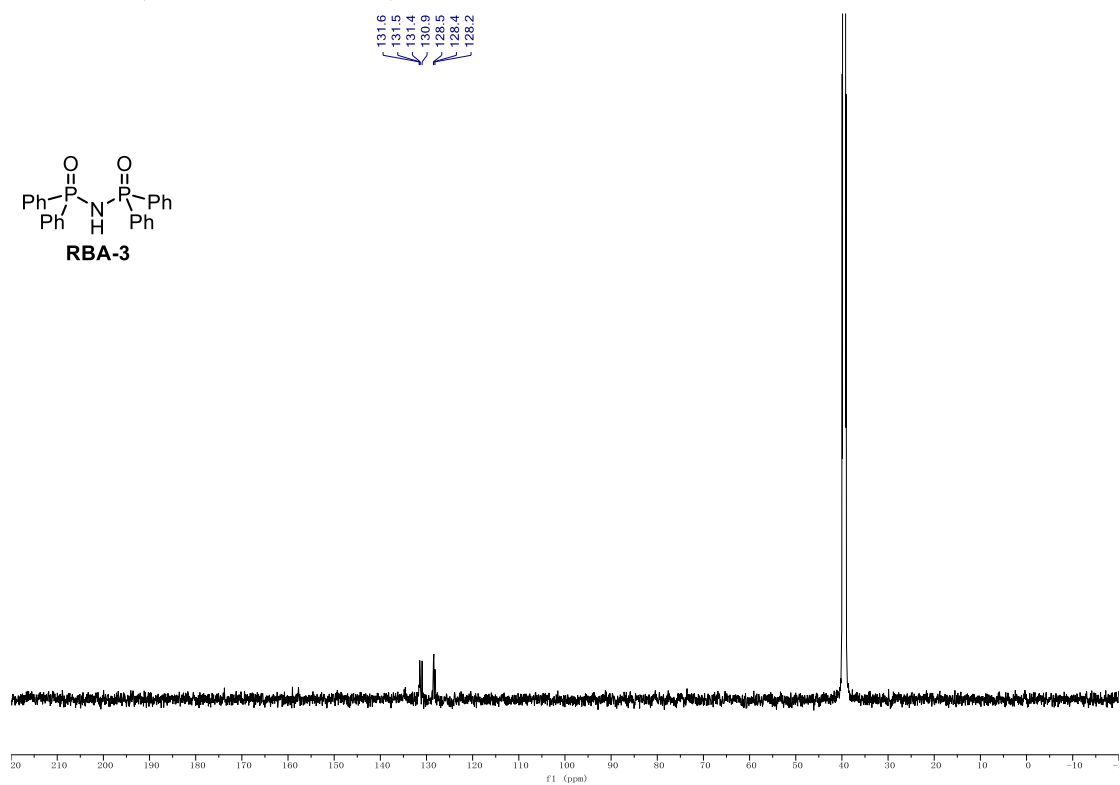
^{31}P NMR (243 MHz, CDCl_3) of **2.28**.

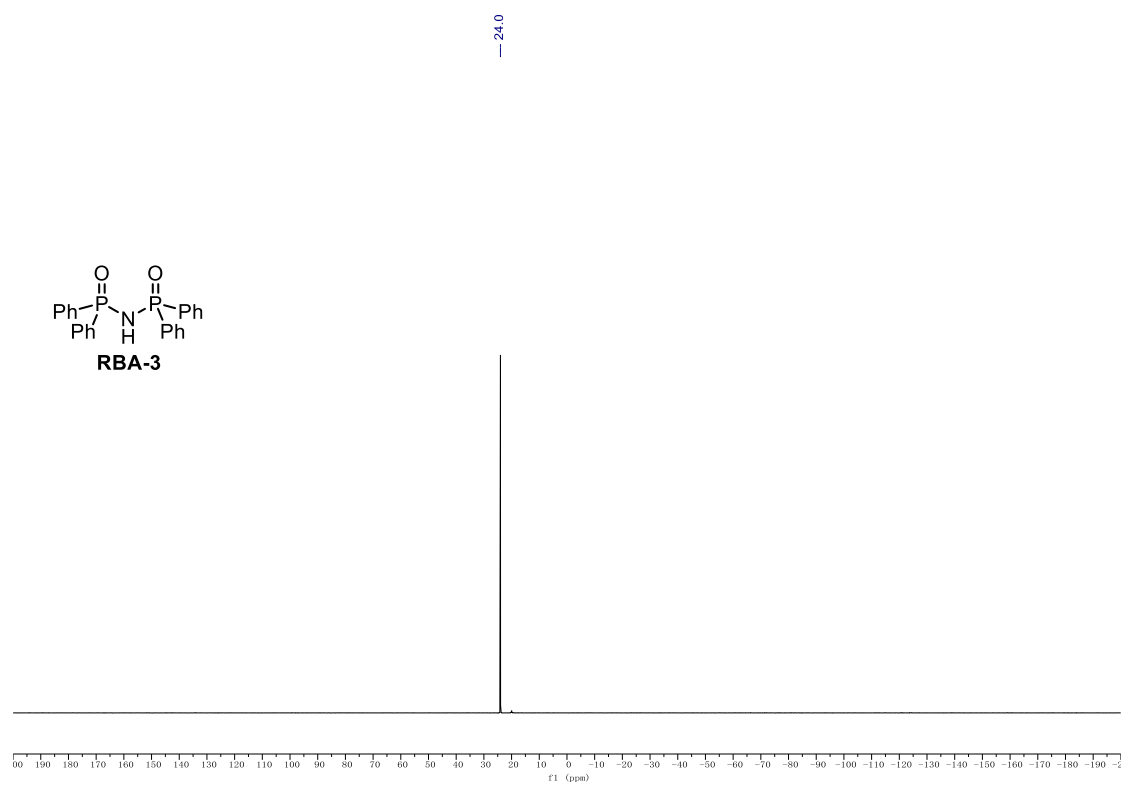
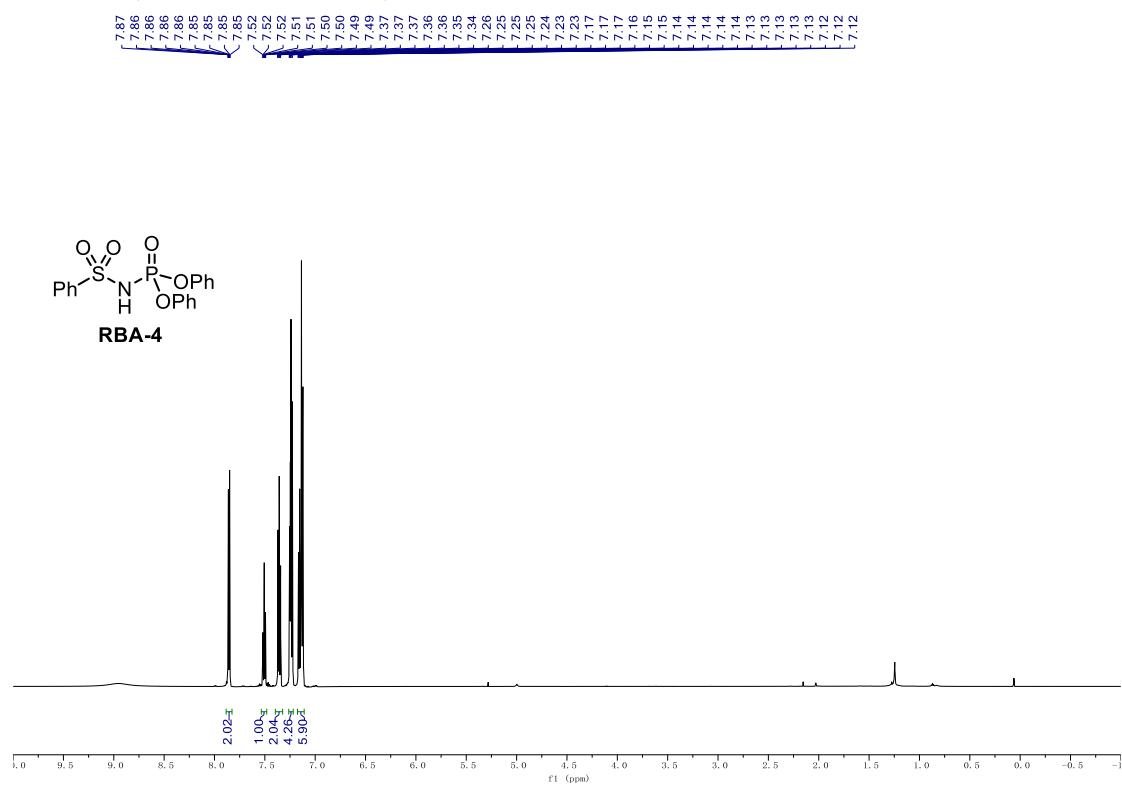


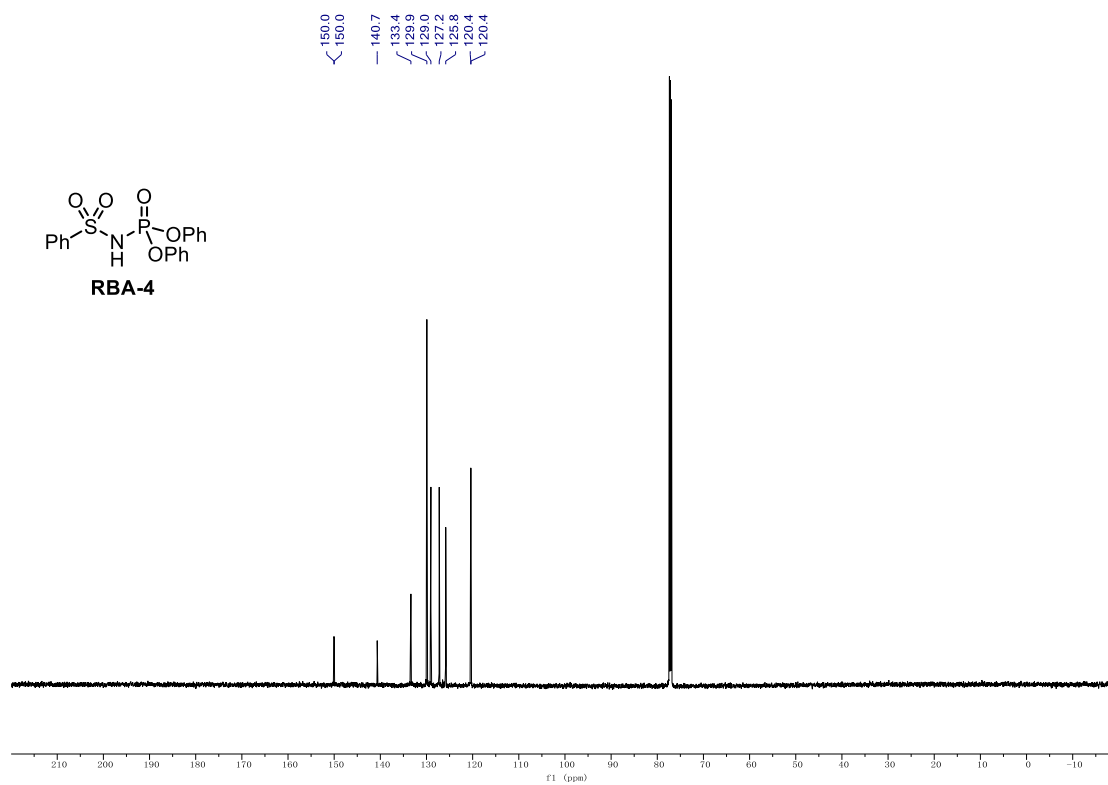
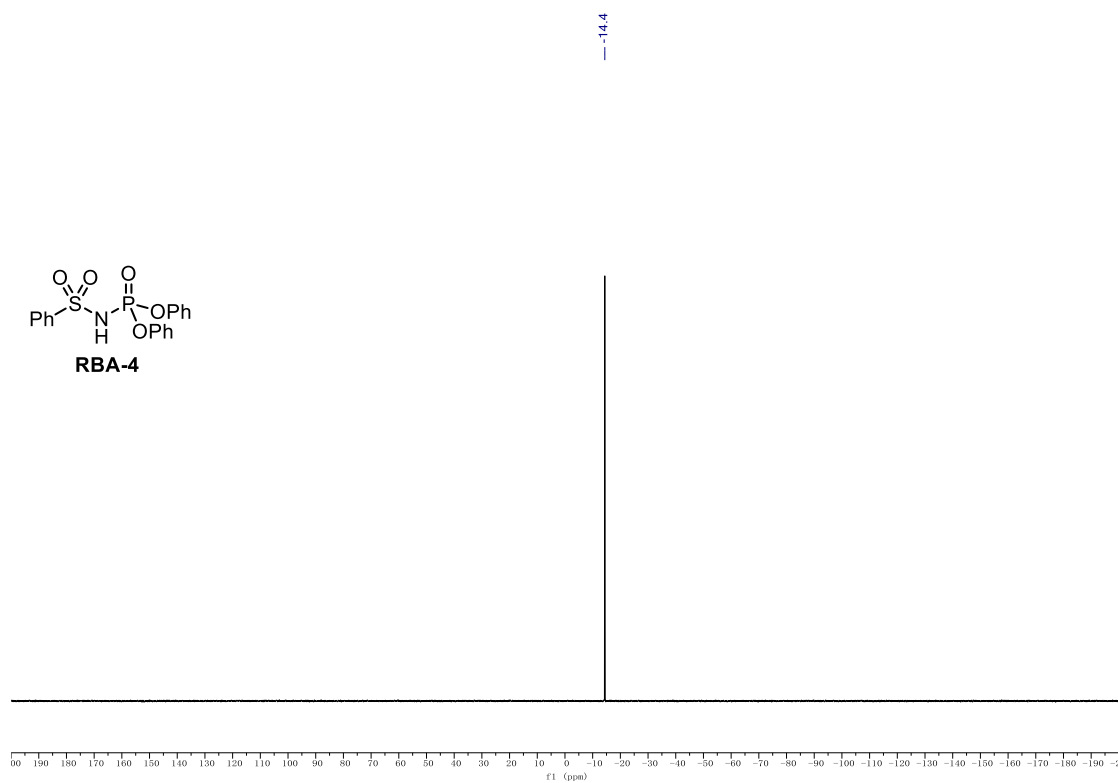
^1H NMR (600 MHz, CDCl_3) of **RBA-2**.



^{13}C NMR (151 MHz, CDCl_3) of RBA-2. **^{31}P NMR (243 MHz, CDCl_3) of RBA-2.**

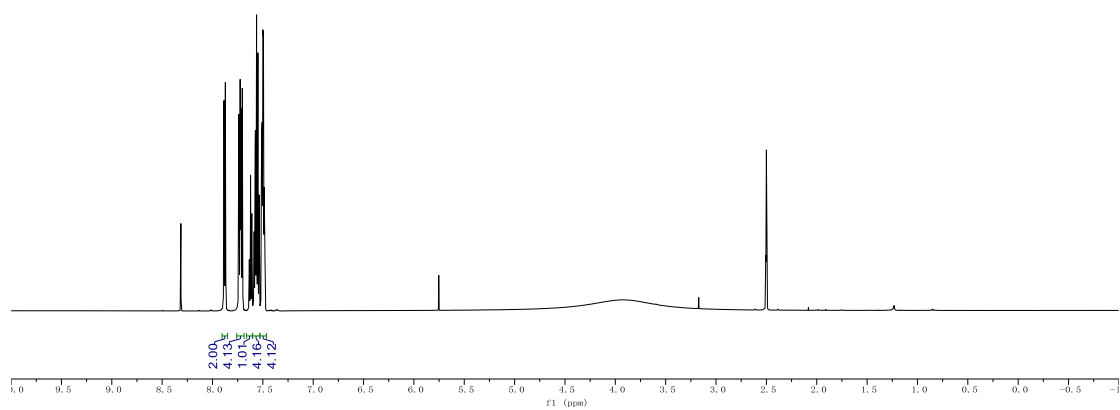
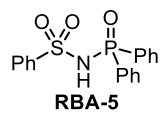
^1H NMR (600 MHz, d_6 -DMSO) of RBA-3. ^{13}C NMR (151 MHz, d_6 -DMSO) of RBA-3.

^{31}P NMR (243 MHz, d_6 -DMSO) of RBA-3. ^1H NMR (600 MHz, d_6 -DMSO) of RBA-4.

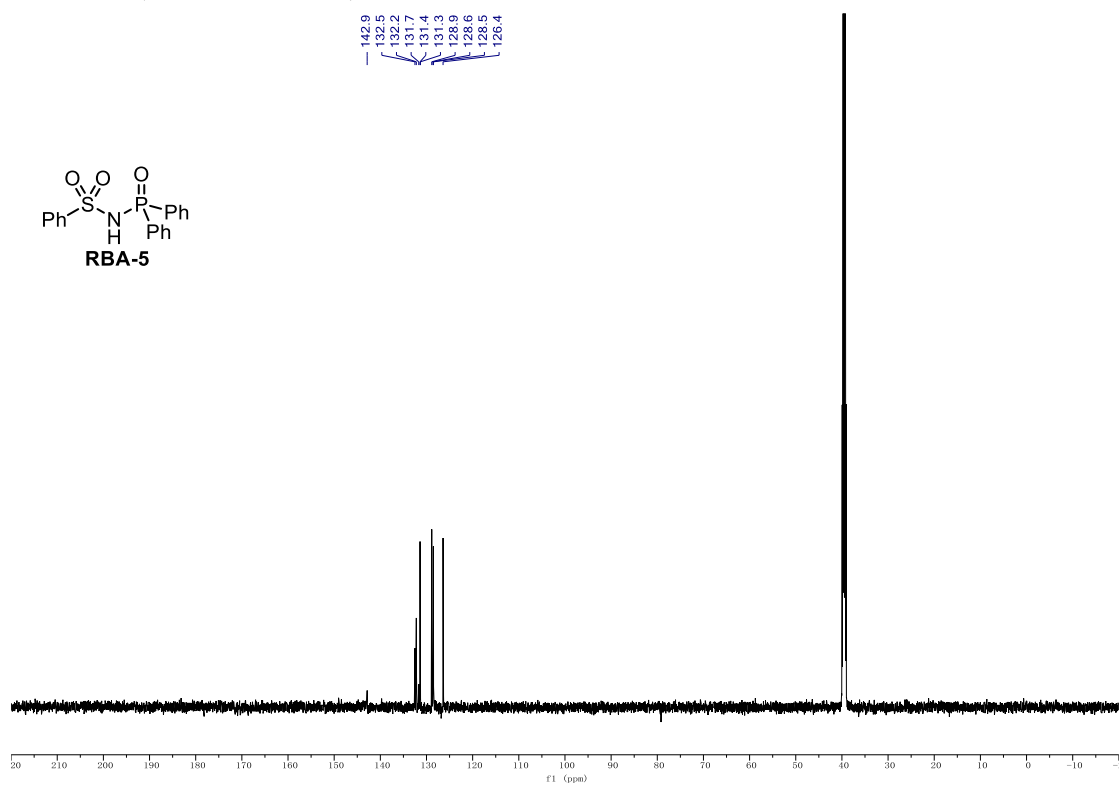
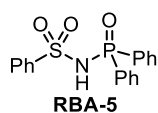
¹³C NMR (151 MHz, *d*₆-DMSO) of RBA-4.**³¹P NMR (243 MHz, *d*₆-DMSO) of RBA-4.**

¹H NMR (500 MHz, CDCl₃) of RBA-5.

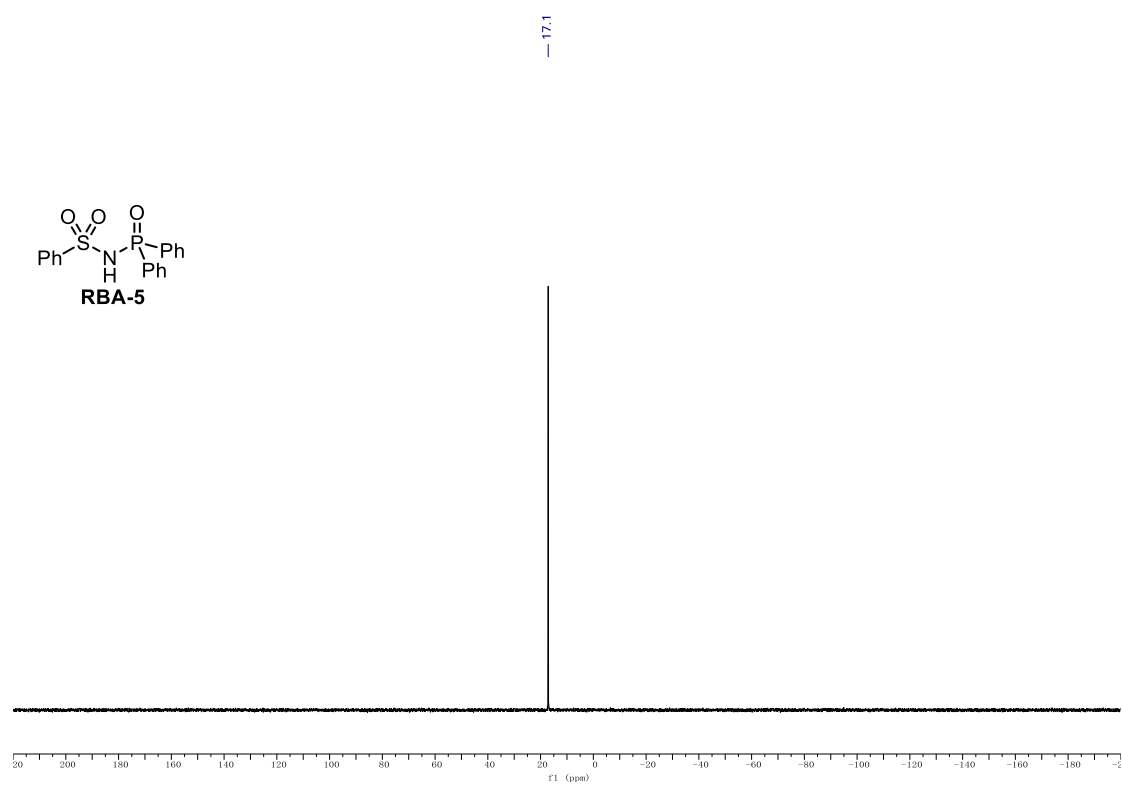
7.89
7.88
7.87
7.87
7.74
7.74
7.73
7.72
7.72
7.72
7.71
7.70
7.70
7.64
7.63
7.63
7.63
7.62
7.61
7.61
7.61
7.59
7.59
7.59
7.58
7.58
7.58
7.57
7.57
7.56
7.56
7.56
7.55
7.55
7.54
7.54
7.53
7.51
7.51
7.50
7.49
7.48
7.48

**¹³C NMR (126 MHz, CDCl₃) of RBA-5.**

142.9
132.5
132.2
131.7
131.4
129.9
128.6
128.5
126.4

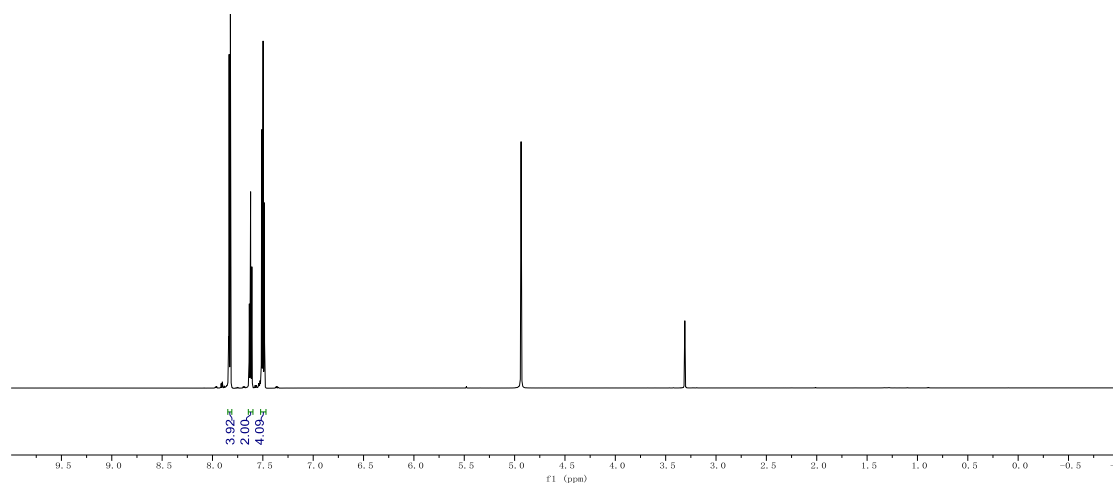
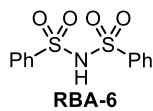


^{31}P NMR (243 MHz, d_6 -DMSO) of **RBA-5**.

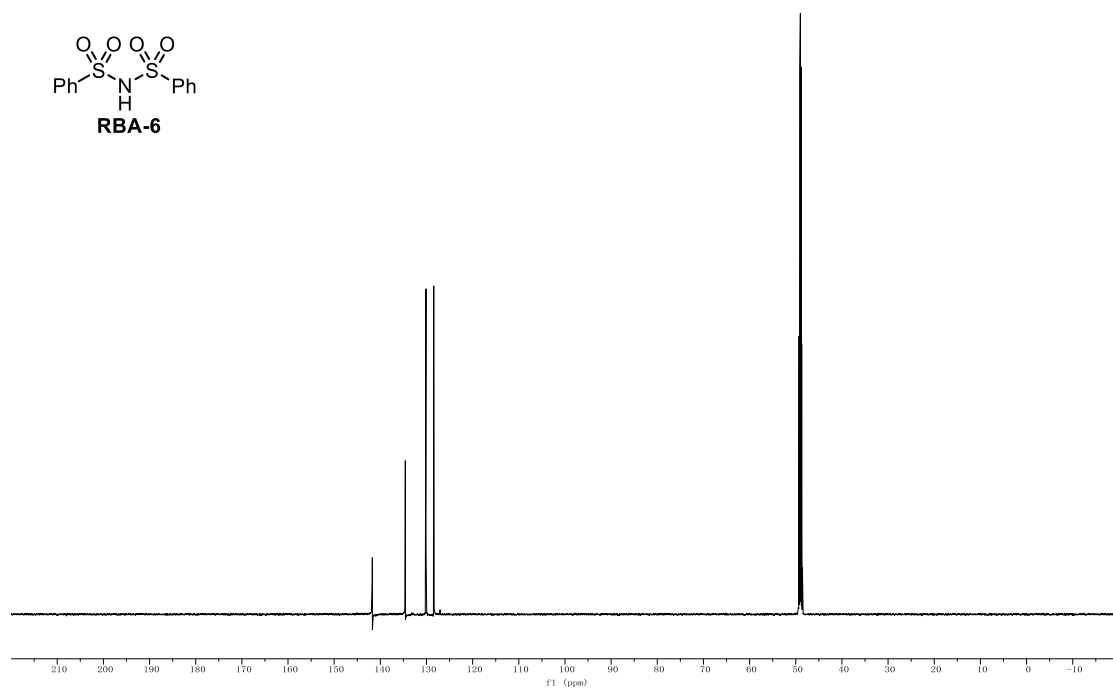


¹H NMR (500 MHz, CDCl₃) of RBA-6.

7.84
7.84
7.83
7.83
7.83
7.82
7.82
7.82
7.64
7.63
7.62
7.62
7.62
7.61
7.61
7.51
7.51
7.51
7.51
7.50
7.50
7.50
7.50
7.49
7.49
7.48
7.48
7.48

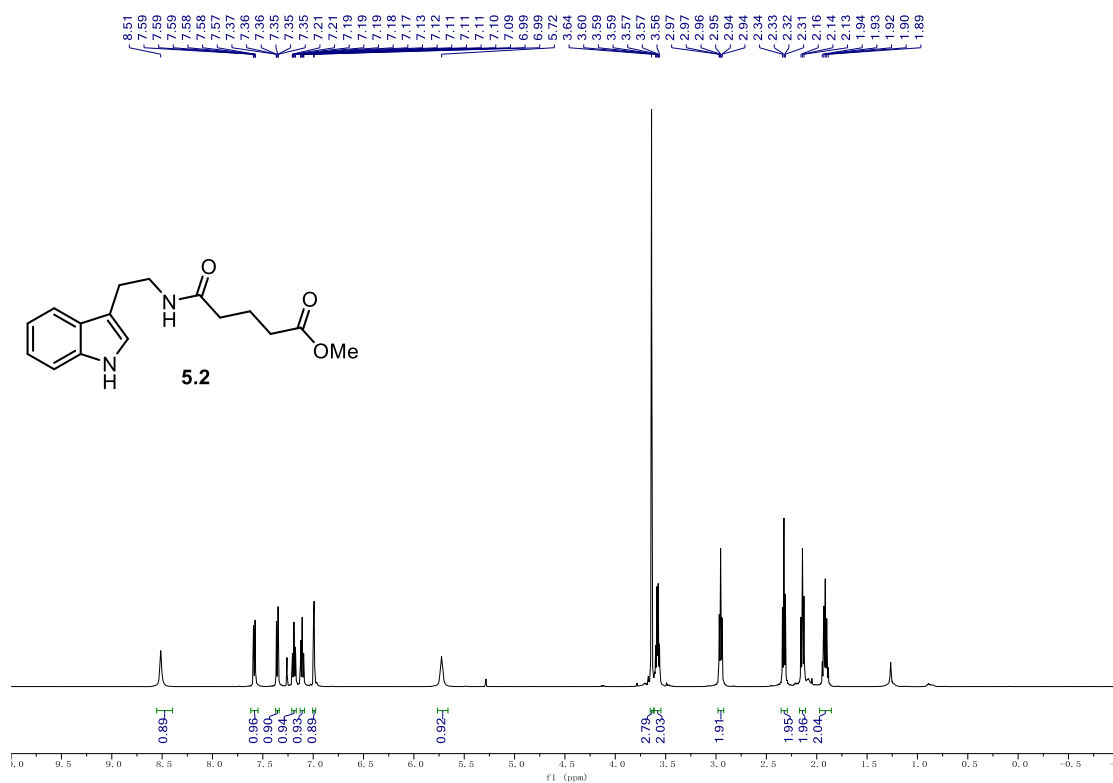
**¹³C NMR (126 MHz, CDCl₃) of RBA-6.**

141.7
134.6
130.1
128.4

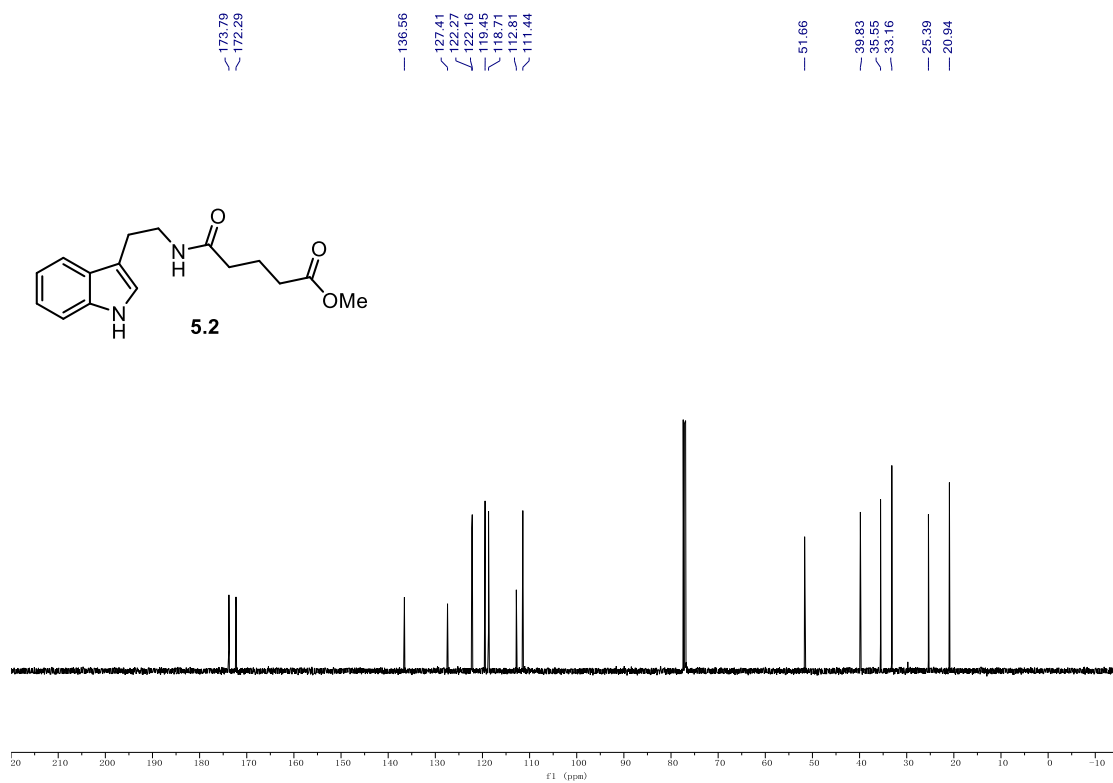


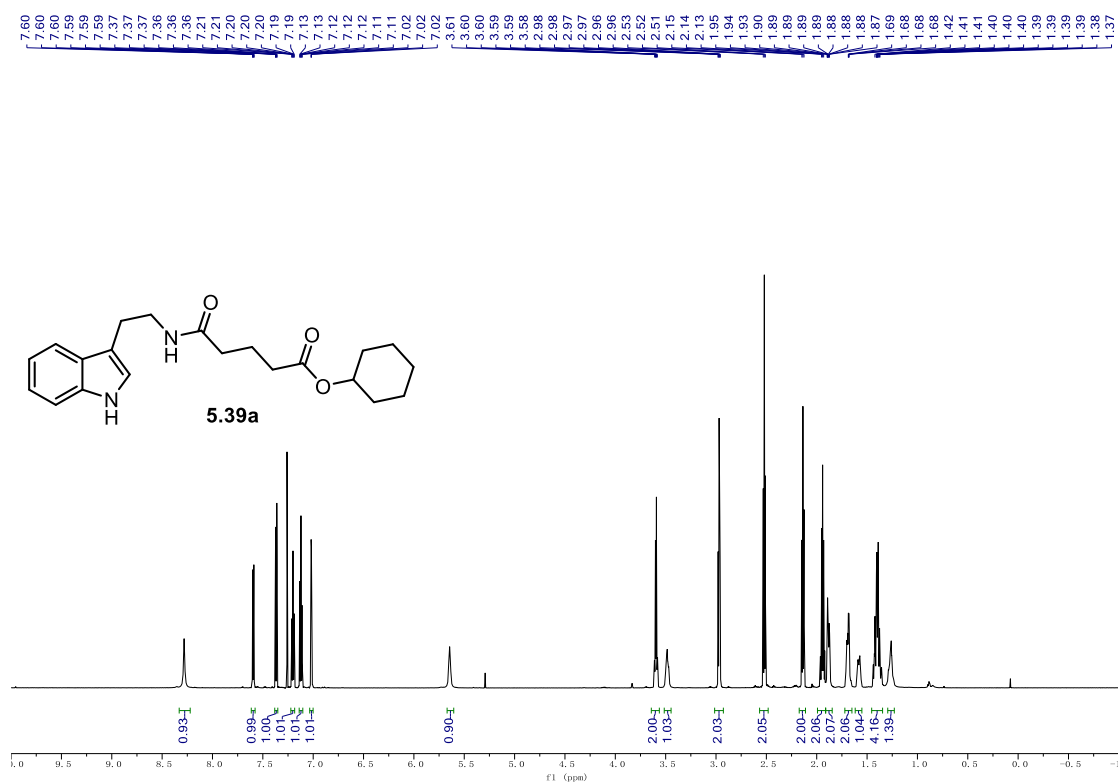
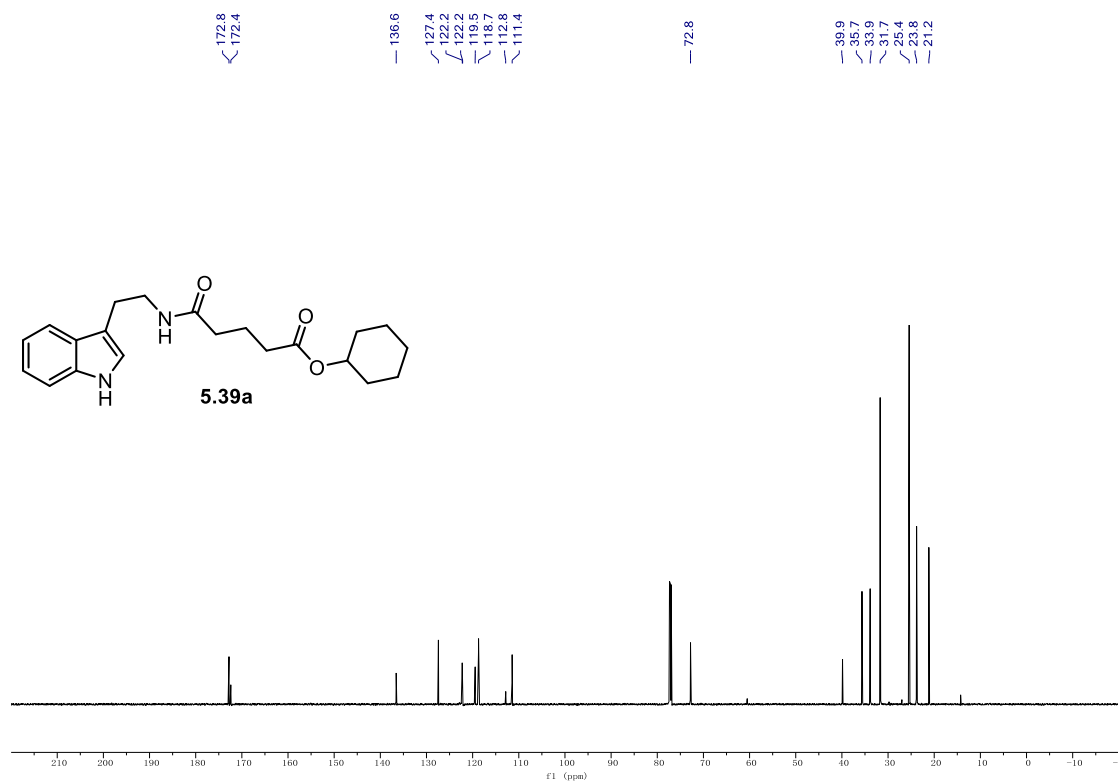
9.1. NMR Spectra

¹H NMR (500 MHz, CDCl₃) of **5.2**.



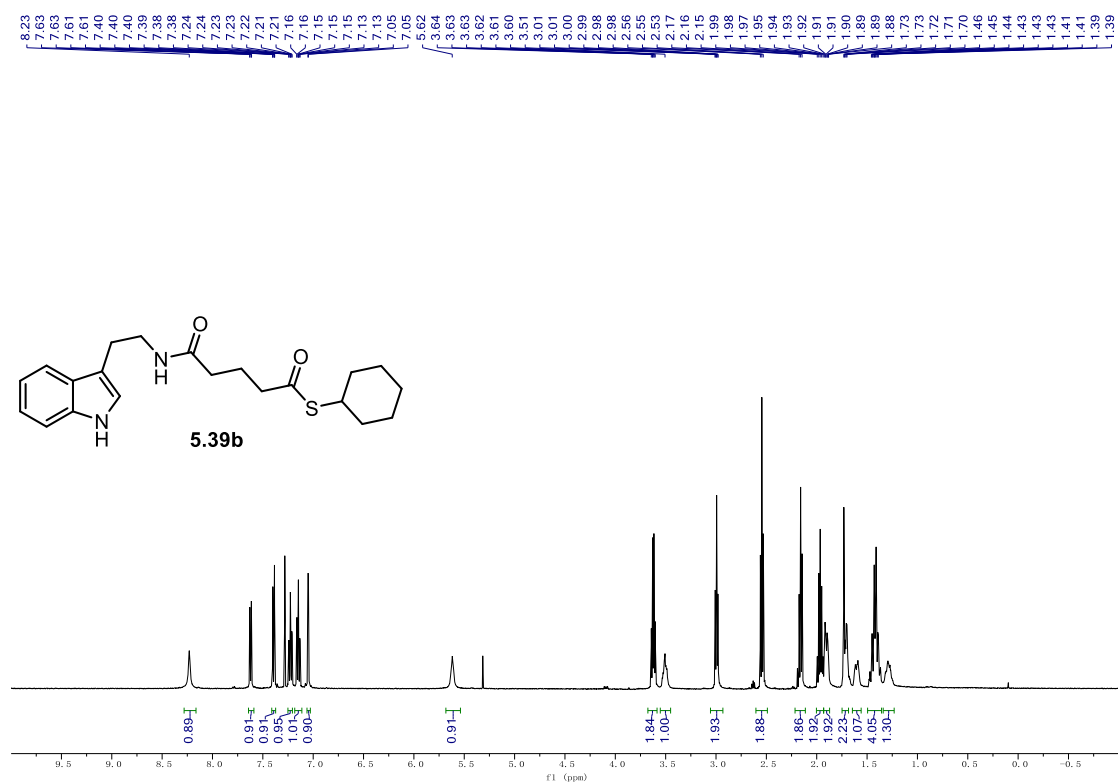
¹³C NMR (126 MHz, CDCl₃) of **5.2**.



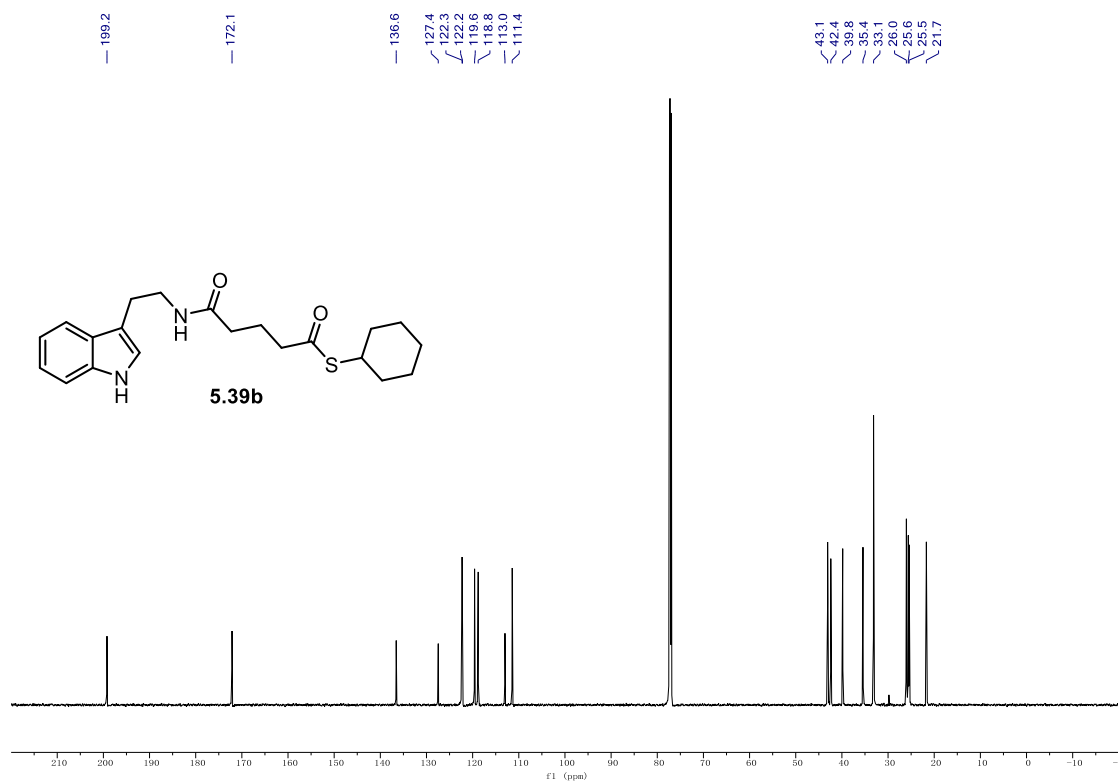
¹H NMR (700 MHz, CDCl₃) 5.39a.**¹³C NMR (126 MHz, CDCl₃) 5.39a.**

9.1. NMR Spectra

^1H NMR (500 MHz, CDCl_3) **5.39b**.

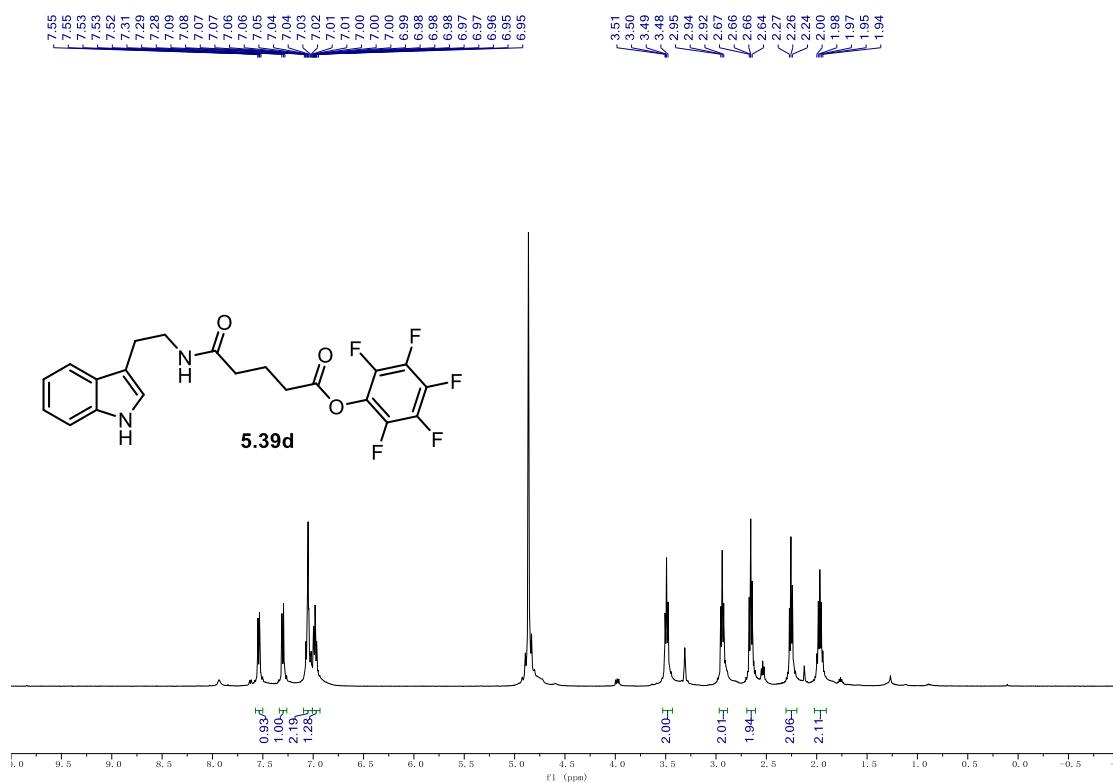


^{13}C NMR (176 MHz, CDCl_3) **5.39b**.

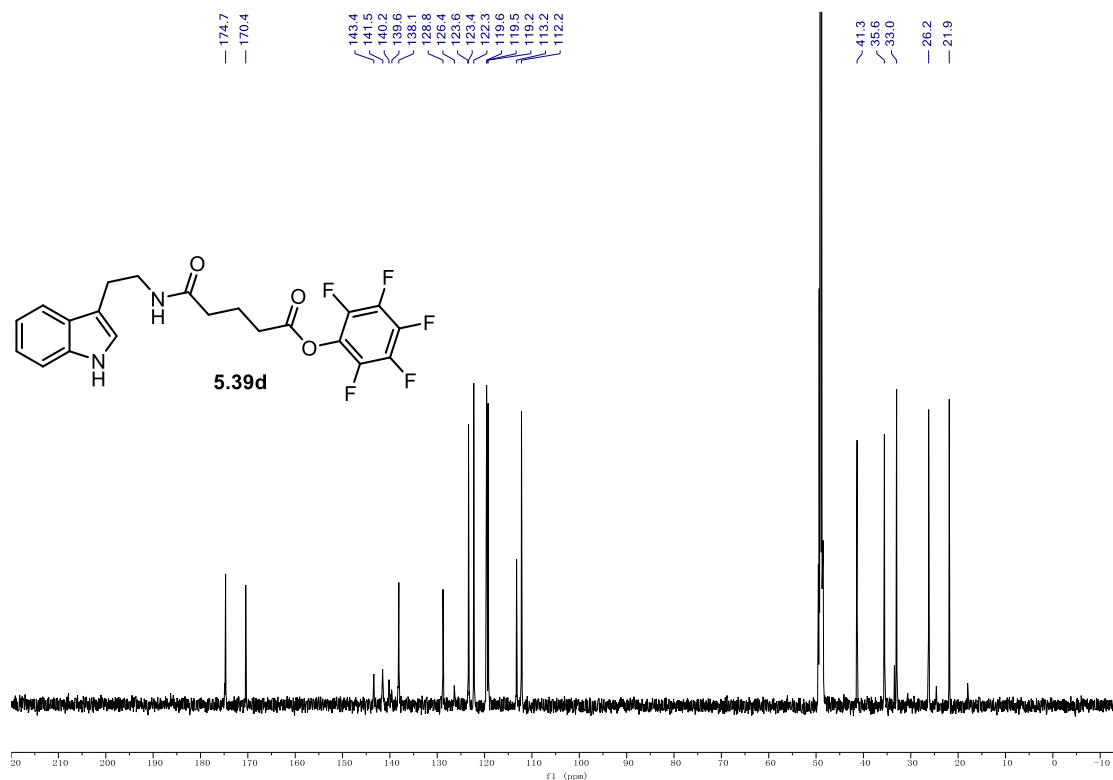


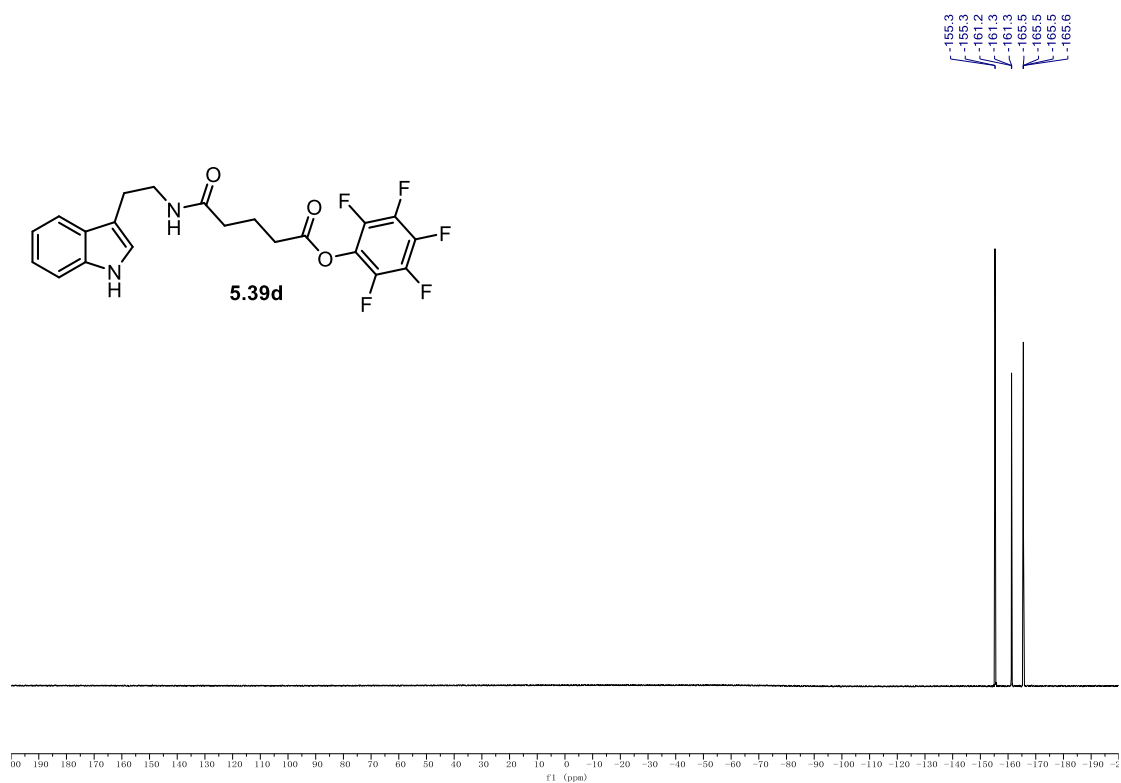
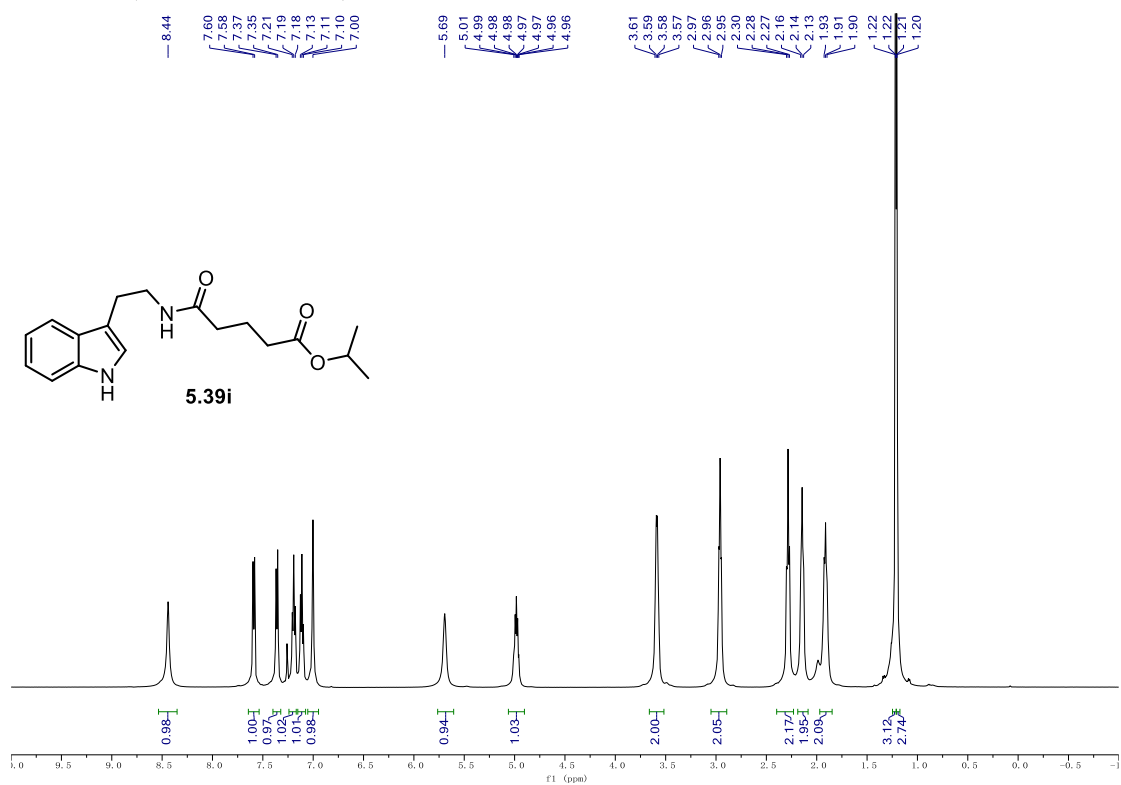
9.1. NMR Spectra

¹H NMR (500 MHz, CD₃OD) **5.39d**.



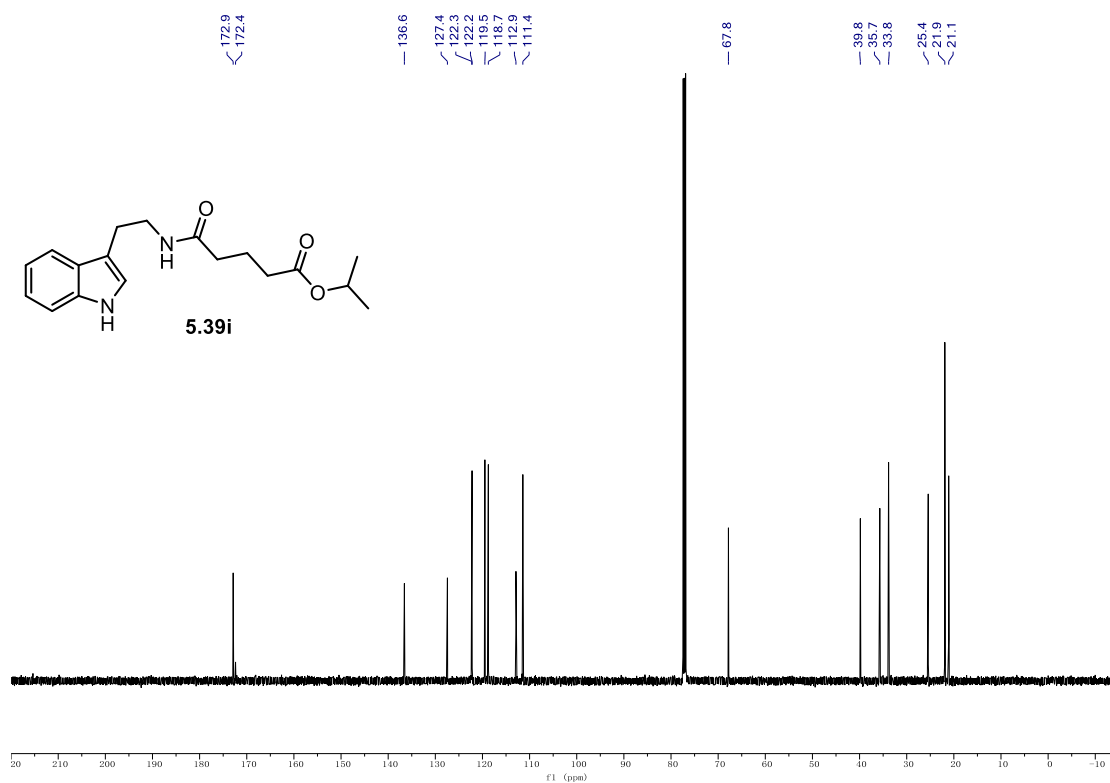
¹³C NMR (126 MHz, CD₃OD) **5.39d**.



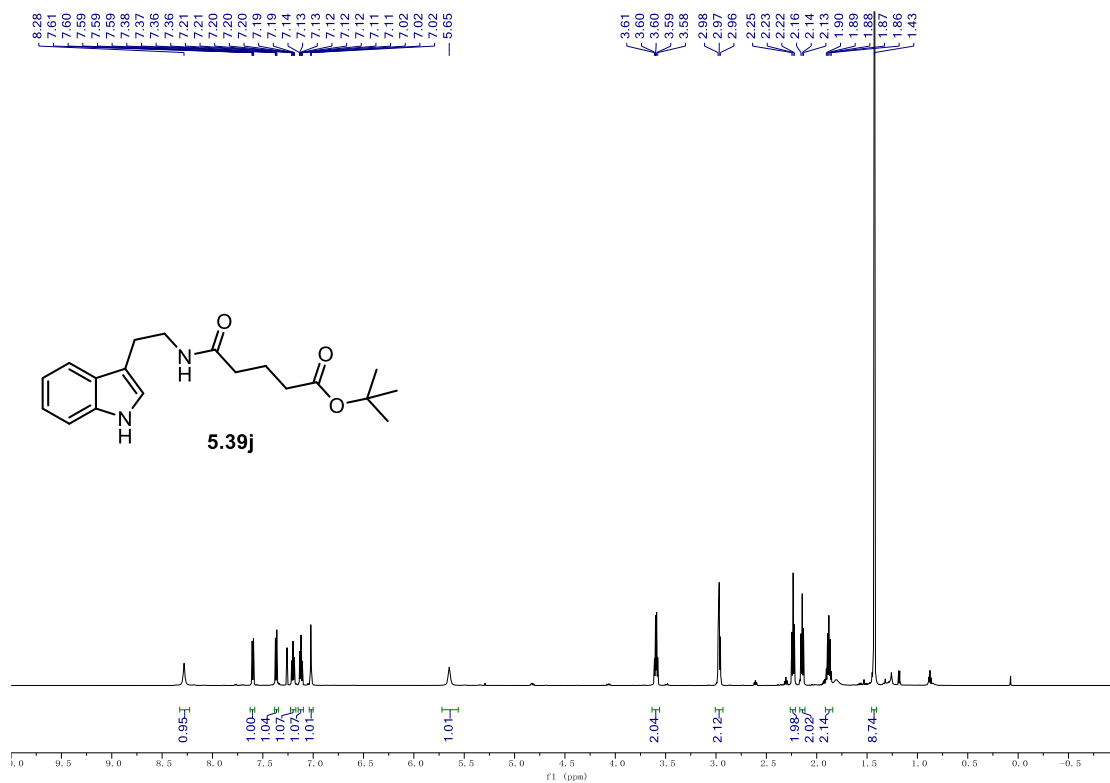
^{19}F NMR (471 MHz, CD_3OD) **5.39d**. ^1H NMR (500 MHz, CDCl_3) of **5.39i**.

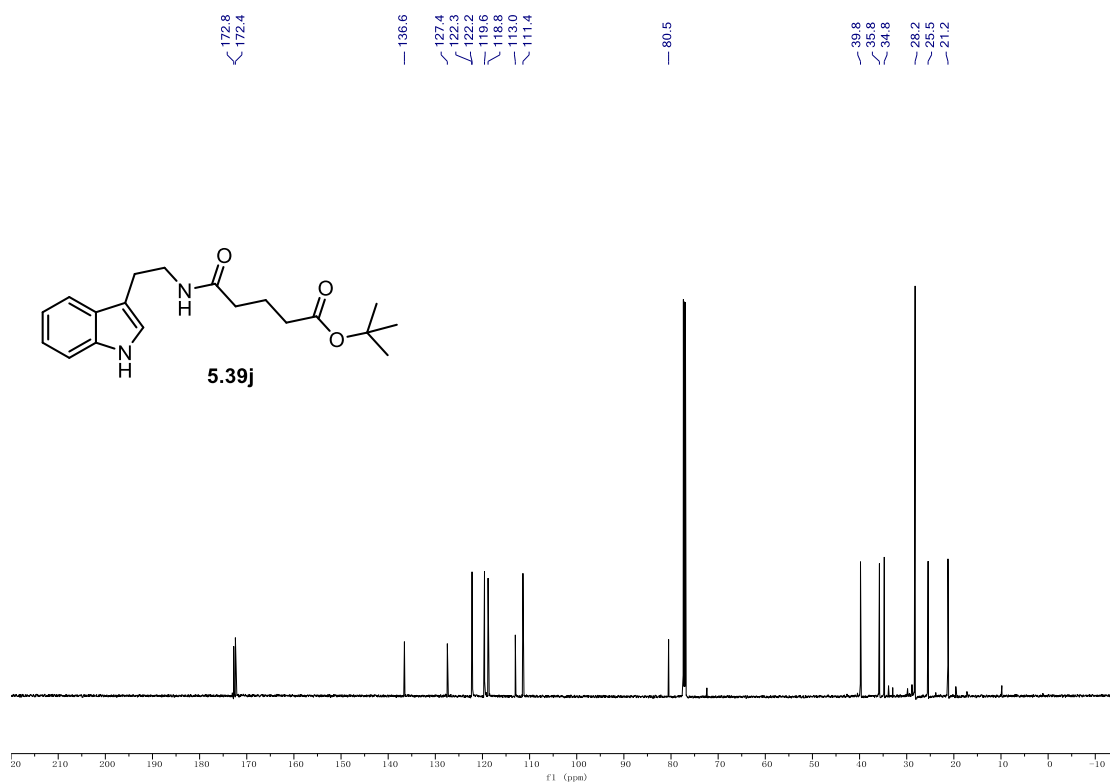
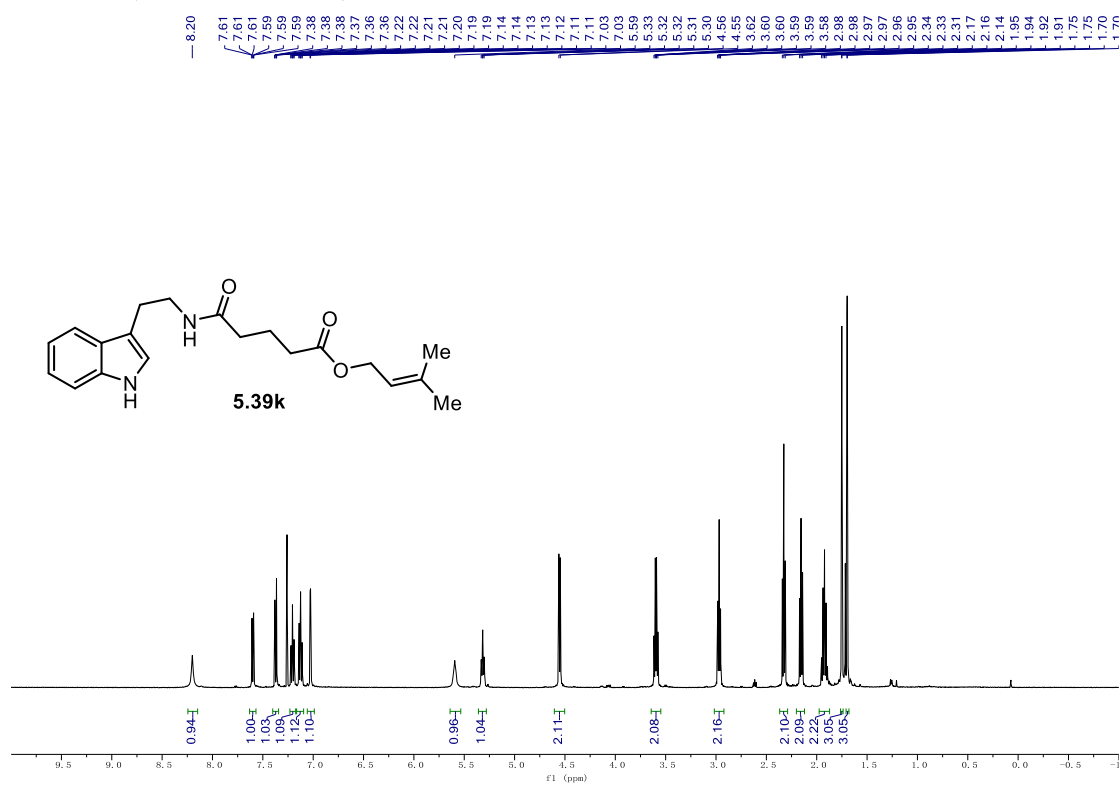
9.1. NMR Spectra

¹³C NMR (126 MHz, CDCl₃) **5.39i**.



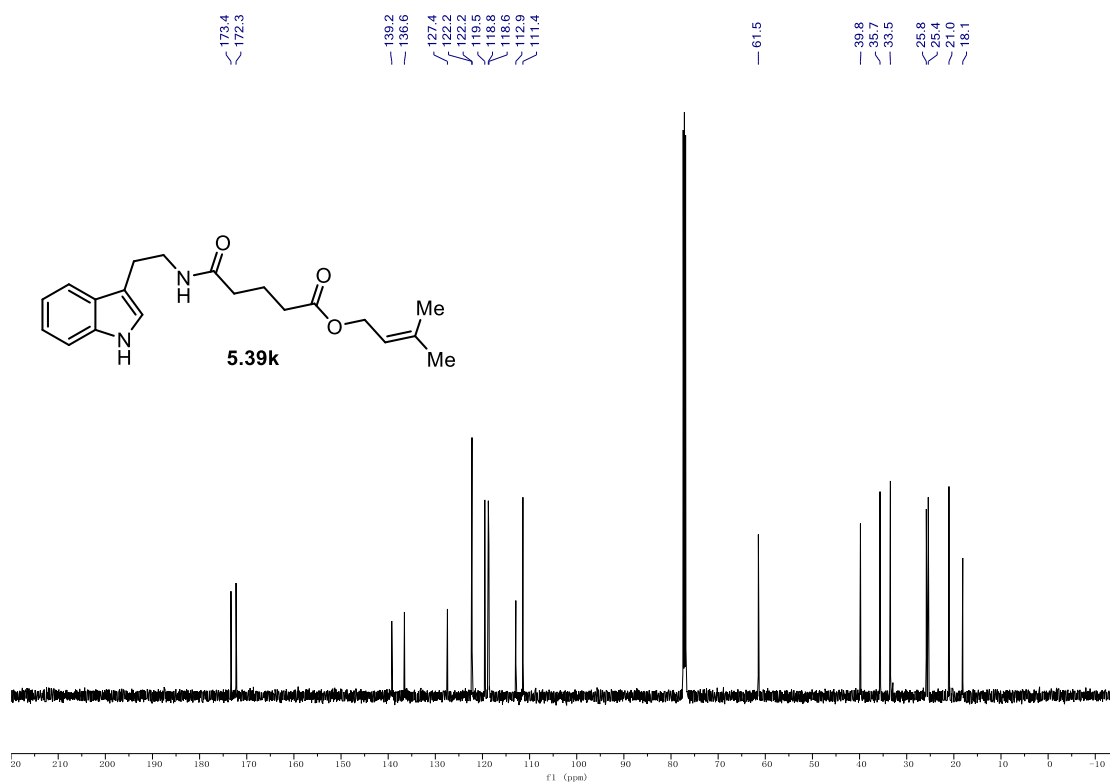
¹H NMR (600 MHz, CDCl₃) **5.39j**.



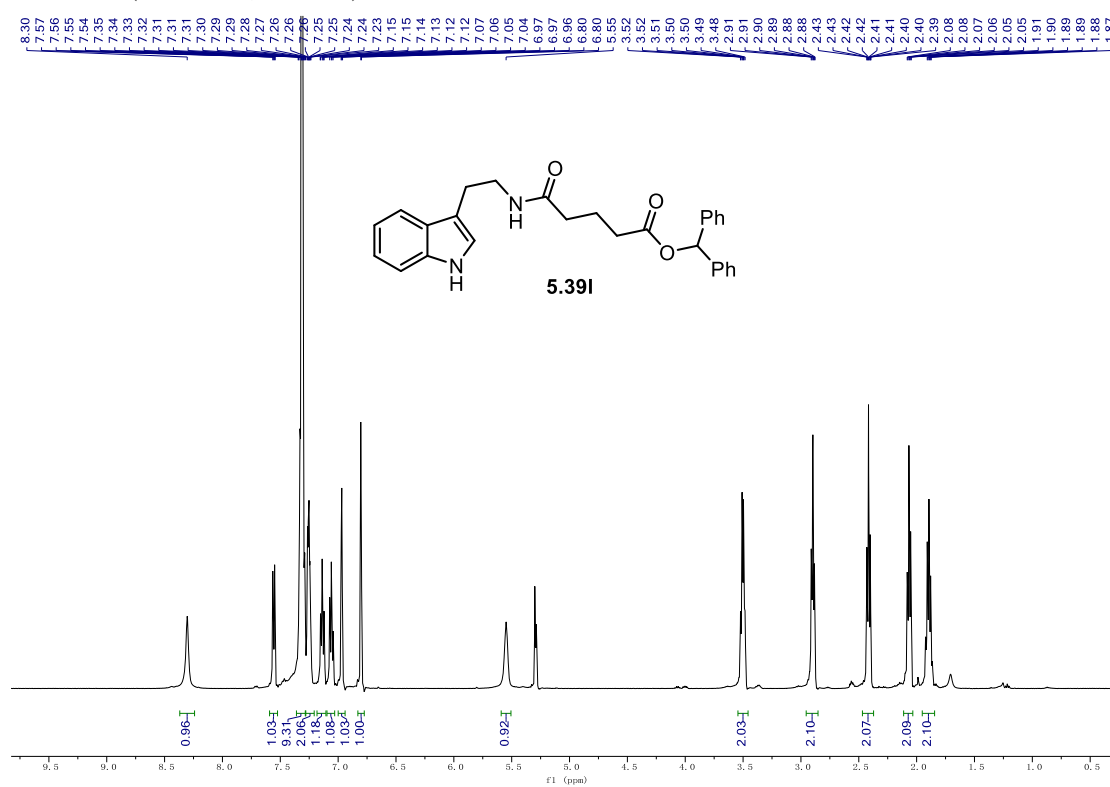
^{13}C NMR (151 MHz, CDCl_3) **5.39j**. ^1H NMR (500 MHz, CDCl_3) **5.39k**.

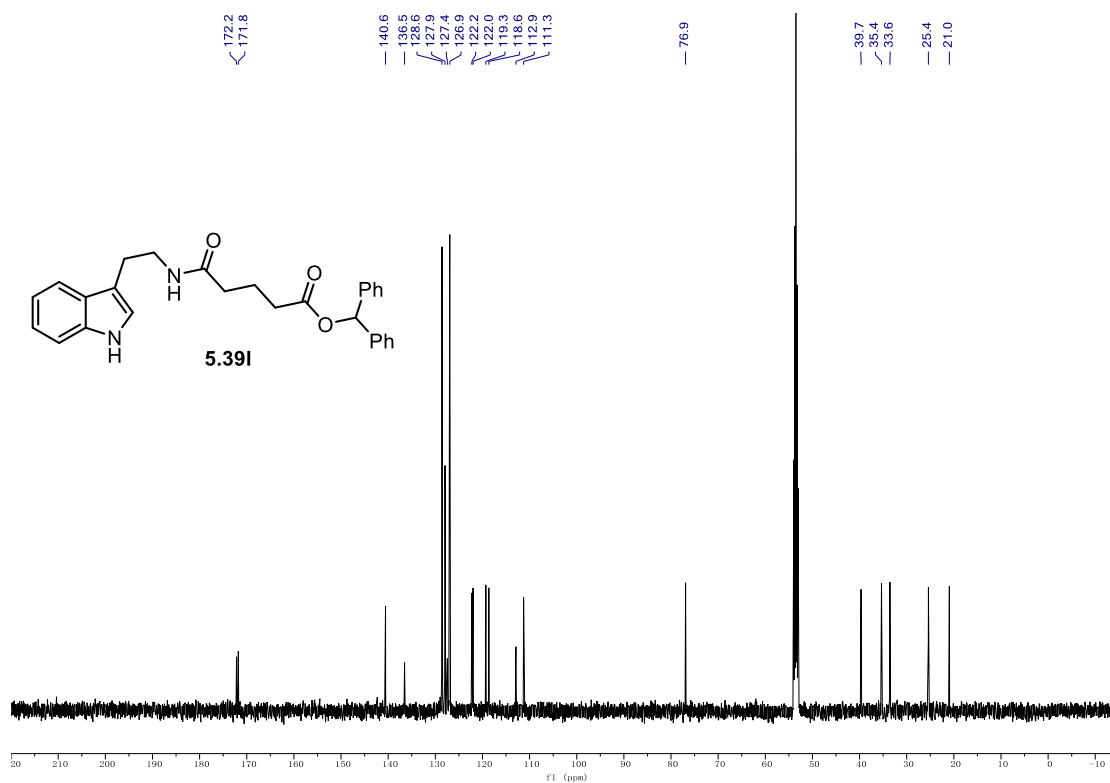
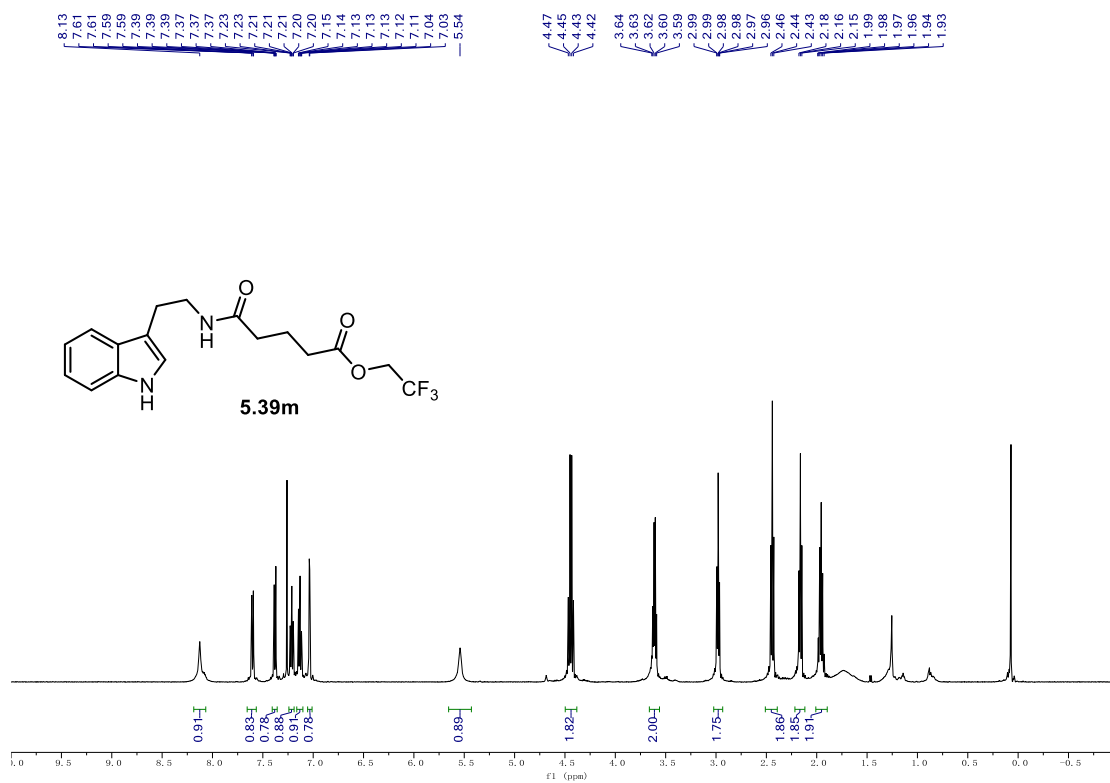
9.1. NMR Spectra

¹³C NMR (126 MHz, CDCl₃) **5.39k**.



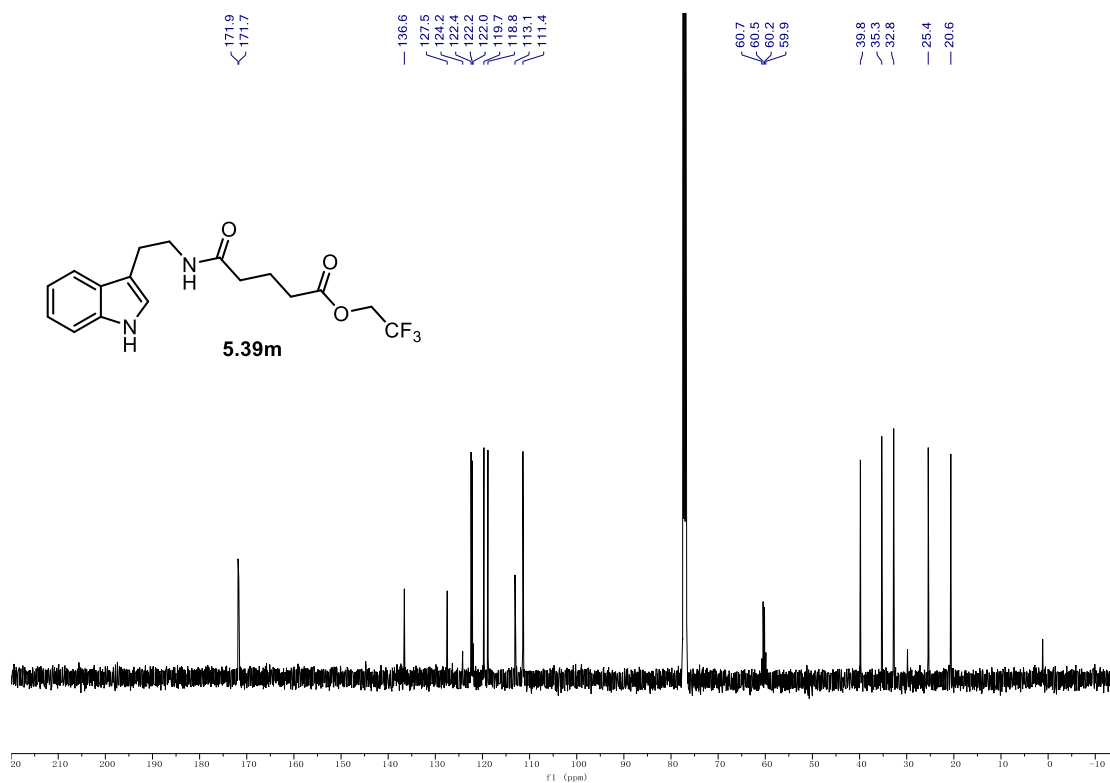
¹H NMR (500 MHz, CD₂Cl₂) **5.39l**.



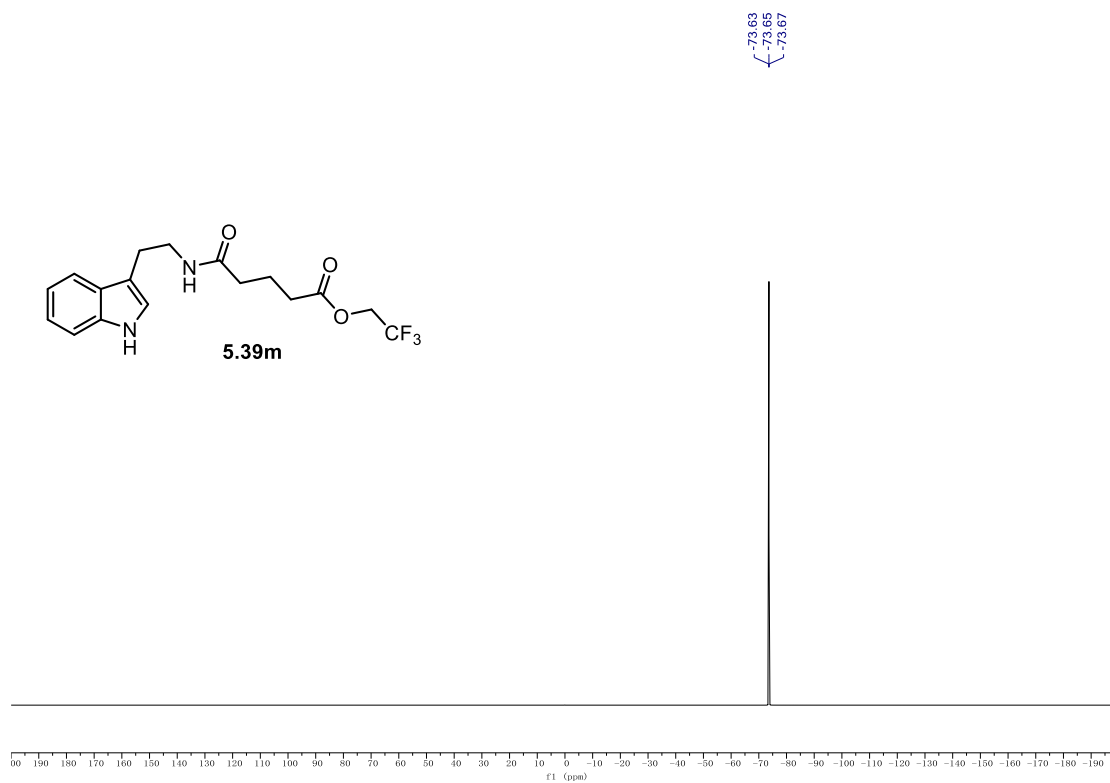
^{13}C NMR (126 MHz, CD_2Cl_2) 5.39l. **^1H NMR (500 MHz, CDCl_3) 5.39m.**

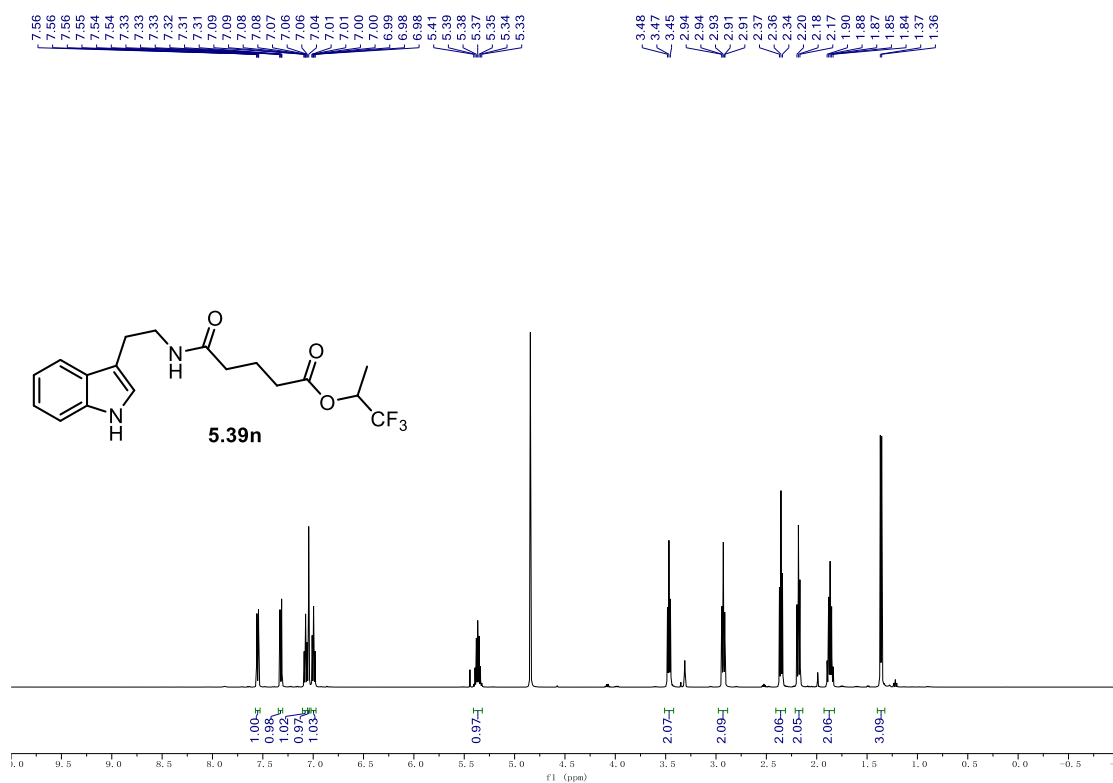
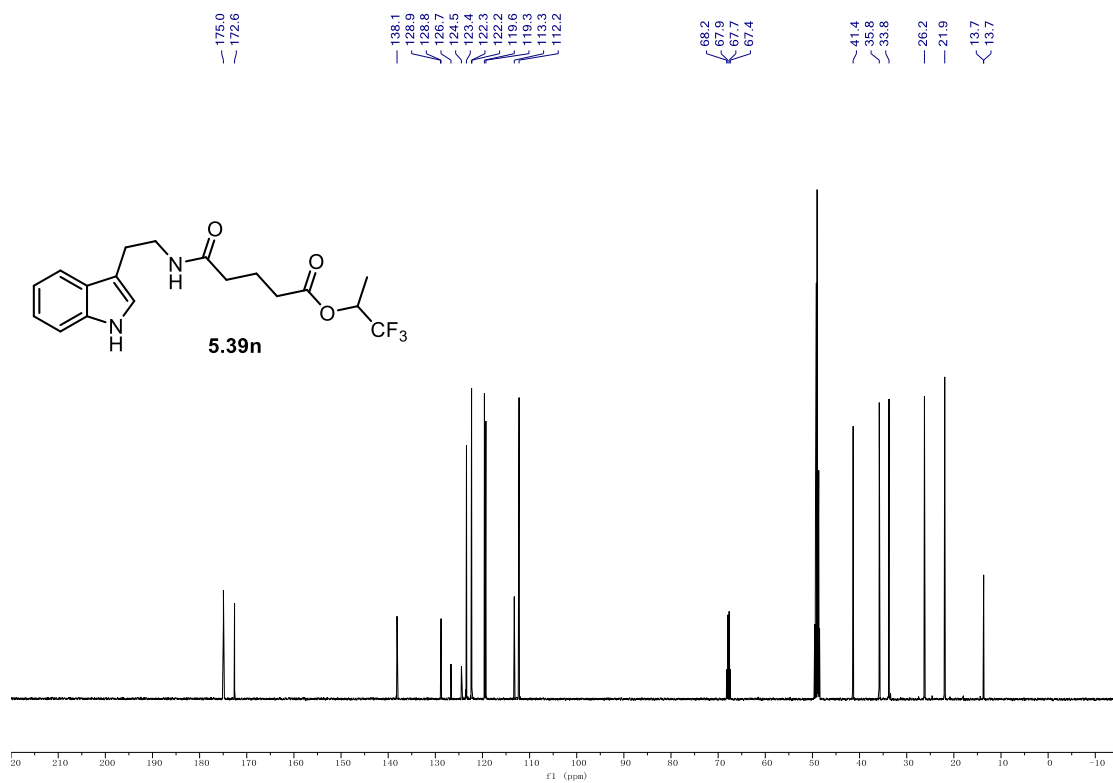
9.1. NMR Spectra

¹³C NMR (126 MHz, CDCl₃) **5.39m**.



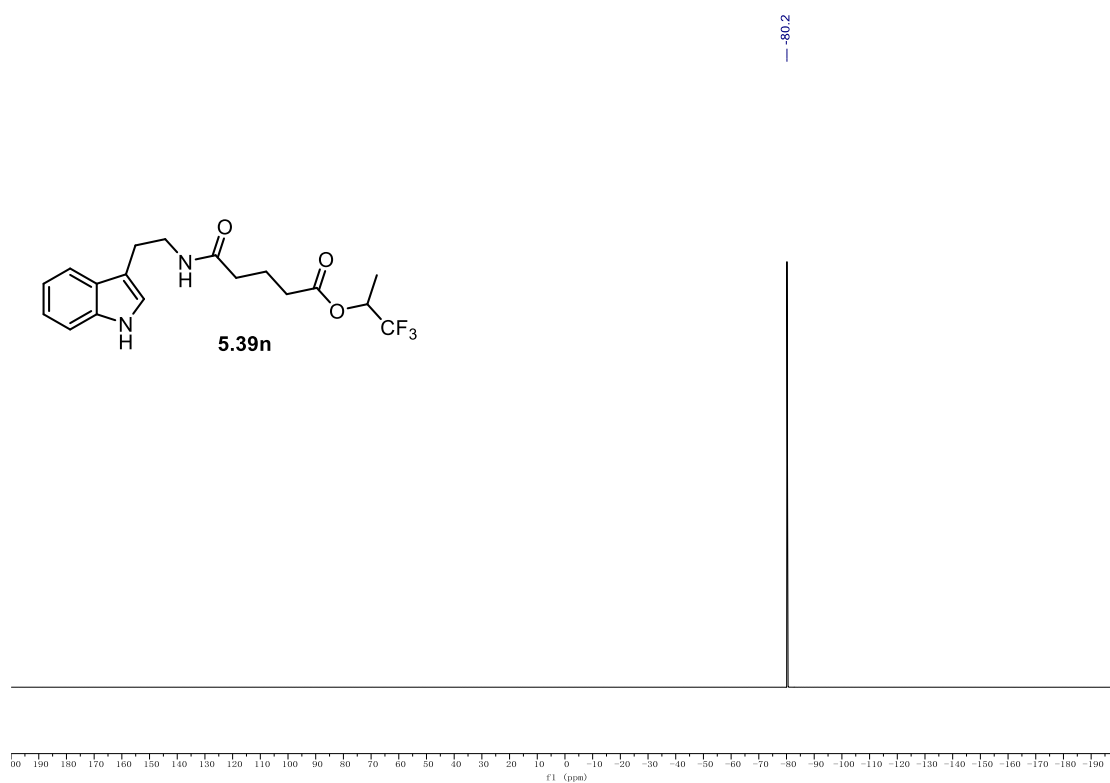
¹⁹F NMR (471 MHz, CDCl₃) **5.39m**.



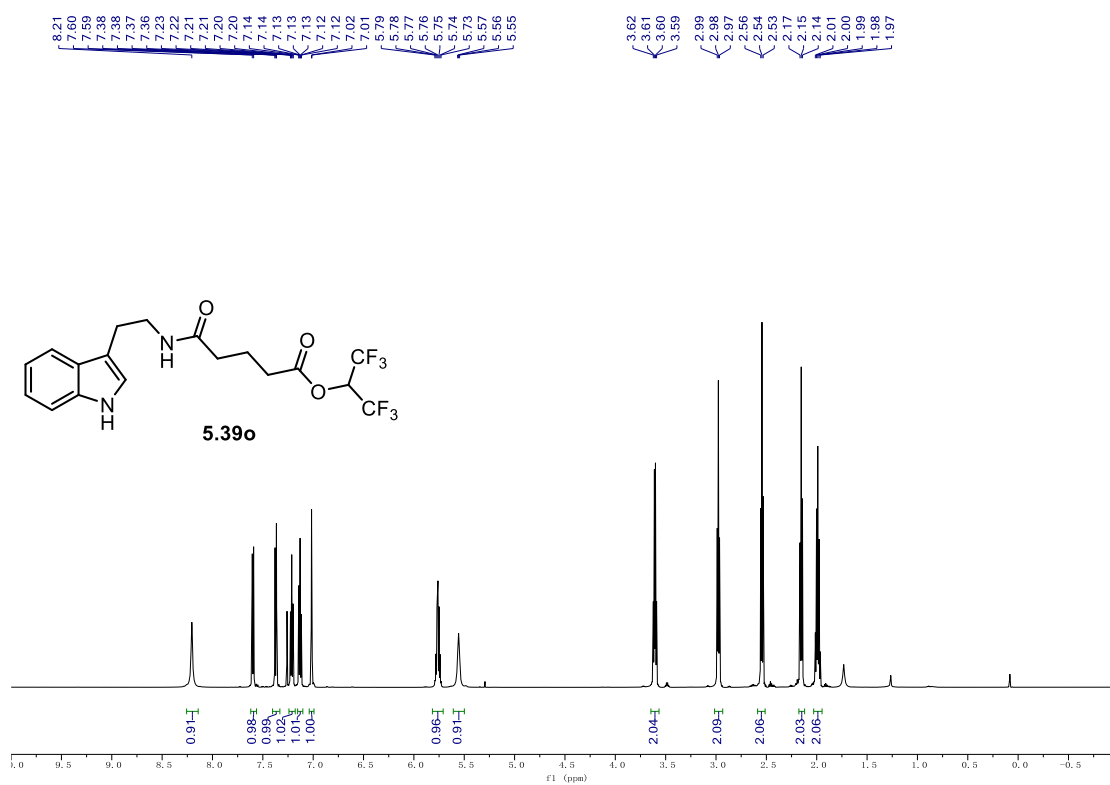
^1H NMR (500 MHz, CD_3OD) 5.39n. **^{13}C NMR (126 MHz, CD_3OD) 5.39n.**

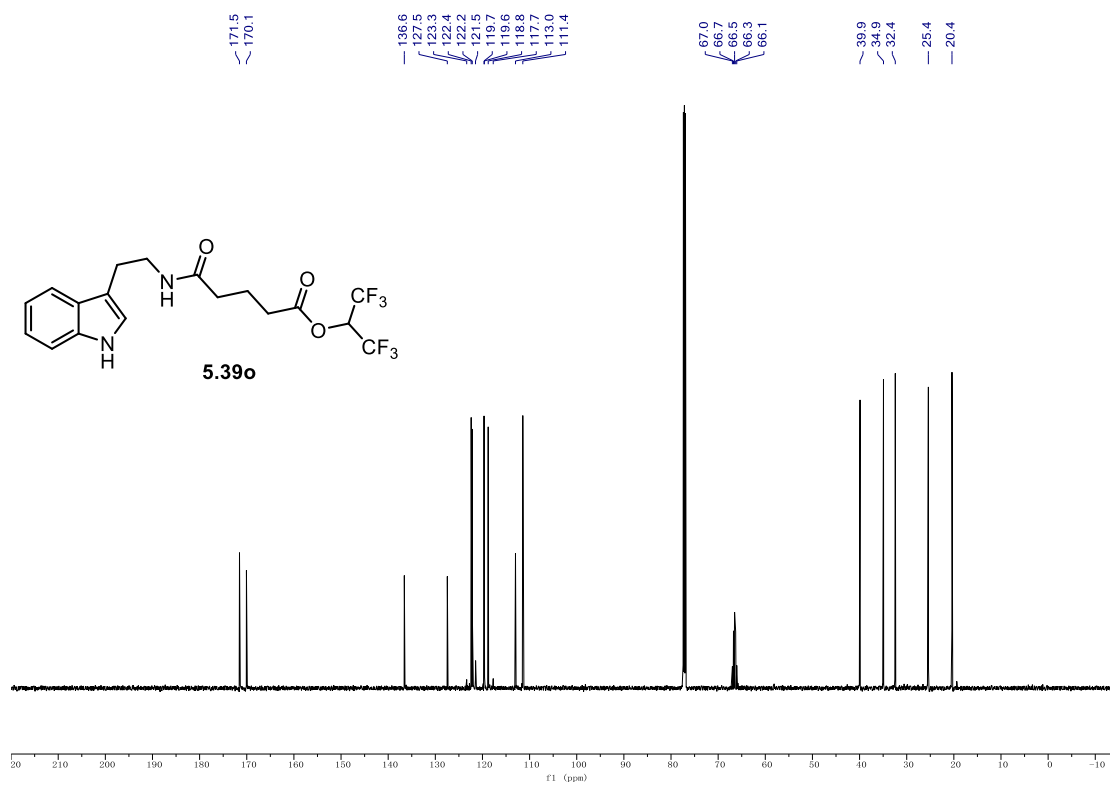
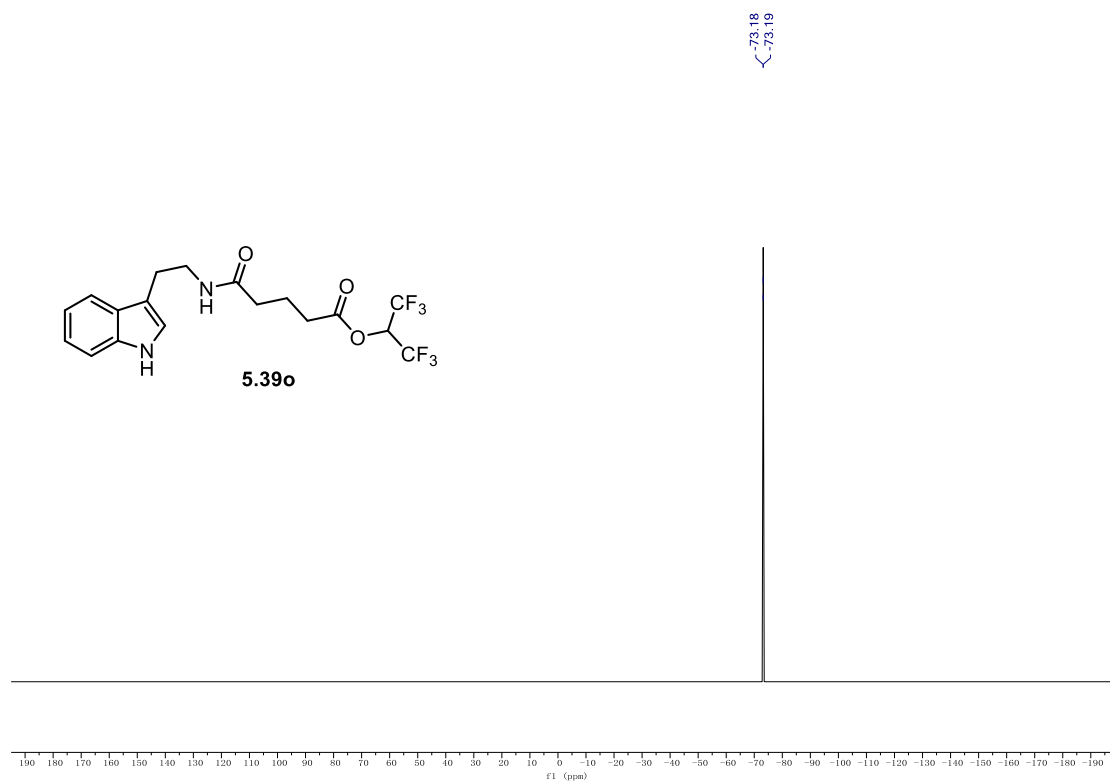
9.1. NMR Spectra

^{19}F NMR (471 MHz, CD_3OD) **5.39n**.



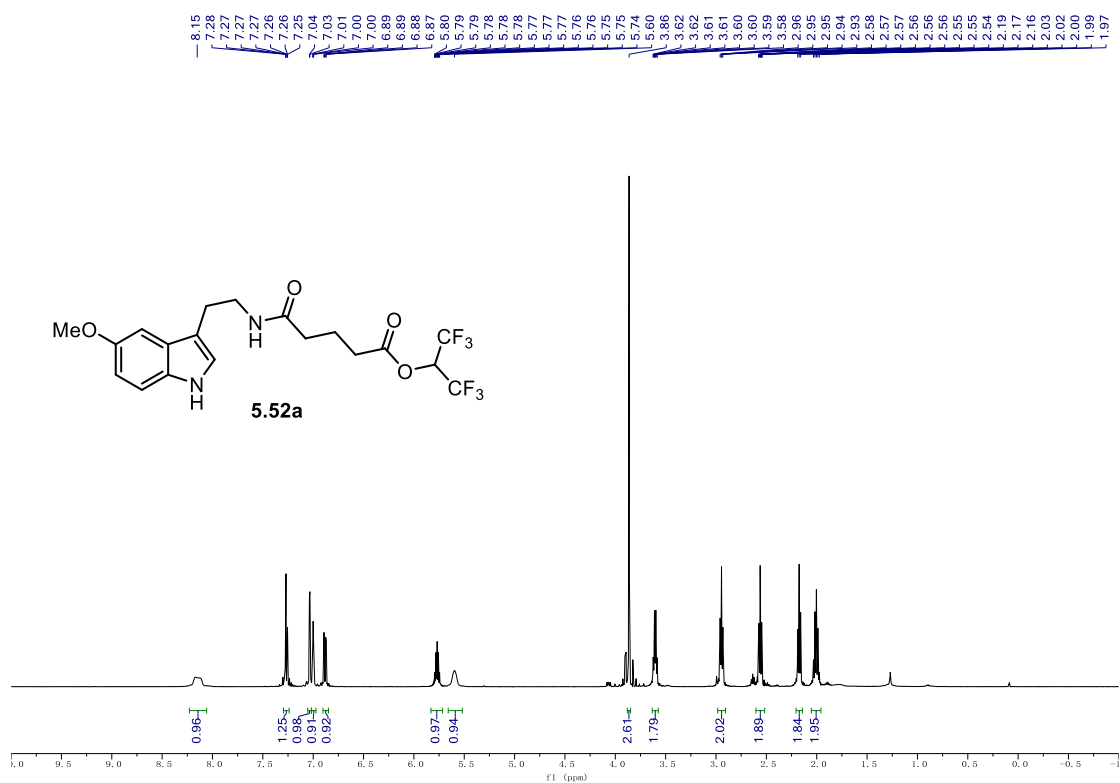
^1H NMR (600 MHz, CDCl_3) **5.39o**.



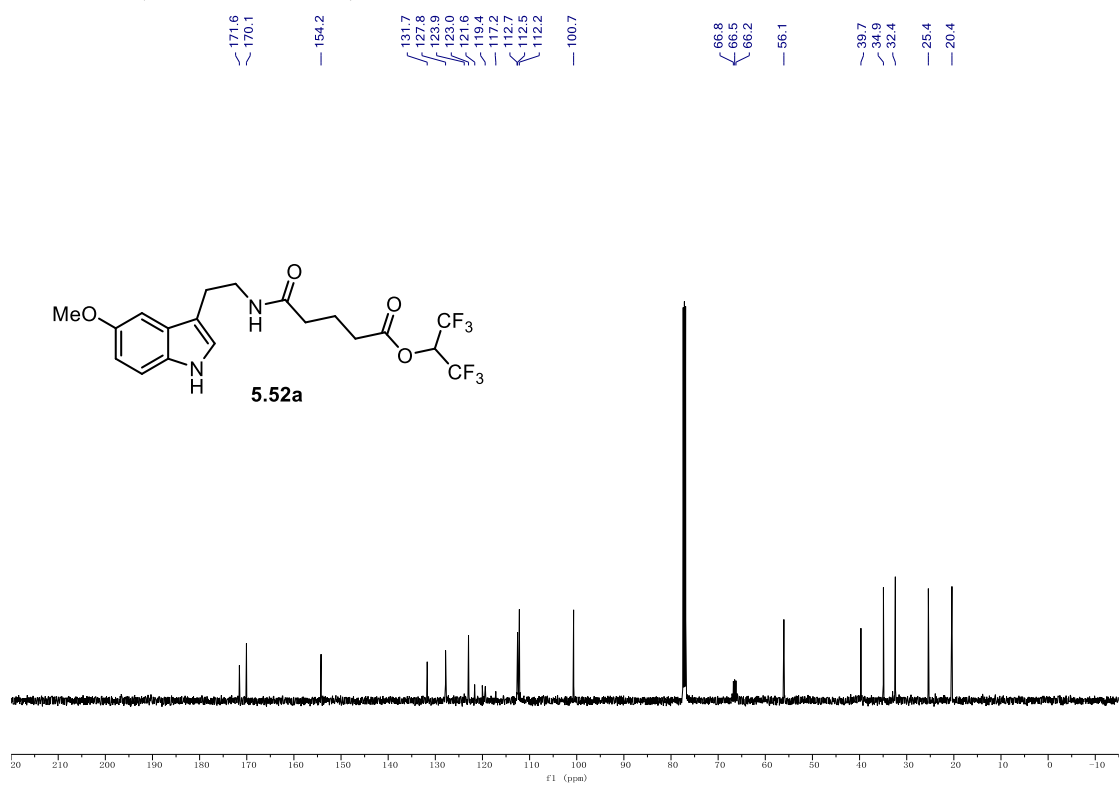
^{13}C NMR (151 MHz, CDCl_3) 5.39o. **^{19}F NMR (565 MHz, CDCl_3) 5.39o.**

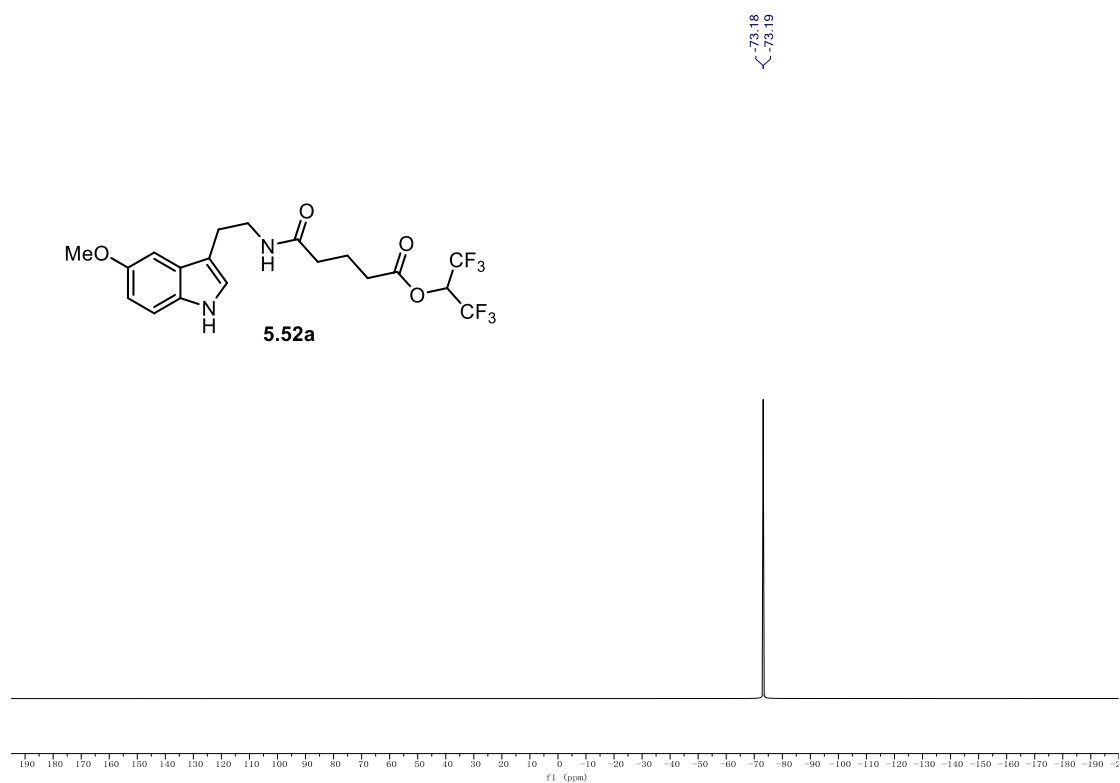
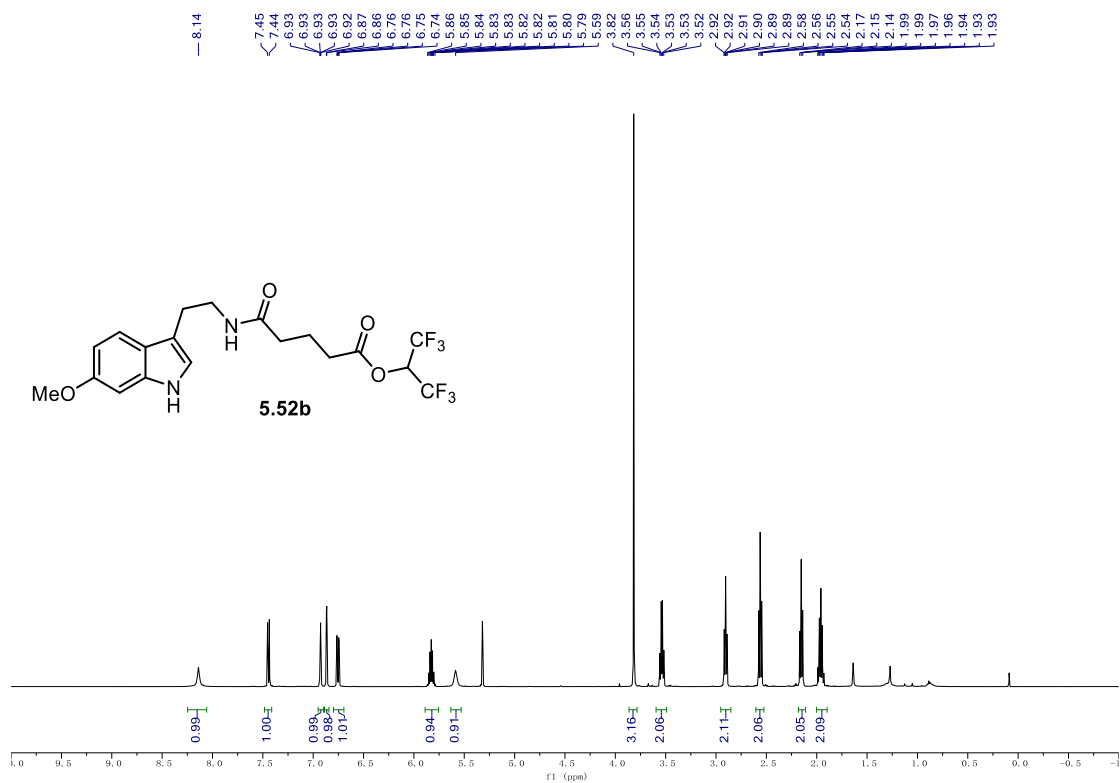
9.1. NMR Spectra

^1H NMR (500 MHz, CDCl_3) **5.52a**.



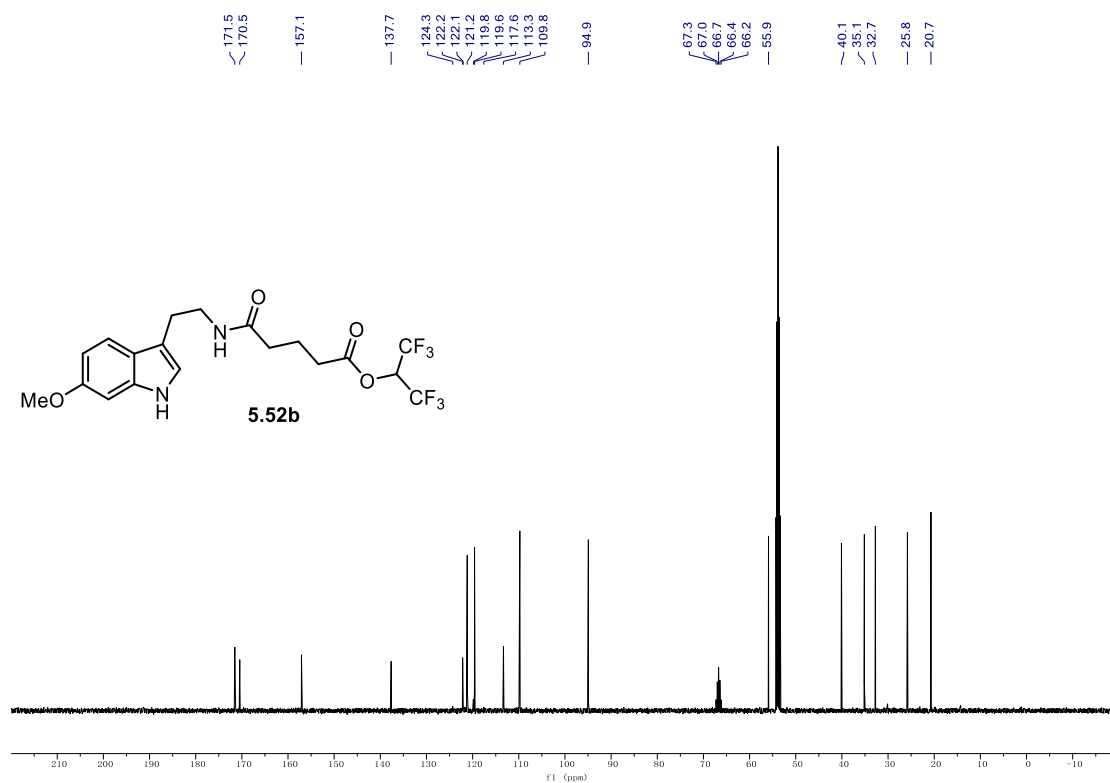
^{13}C NMR (126 MHz, CDCl_3) **5.52a**.



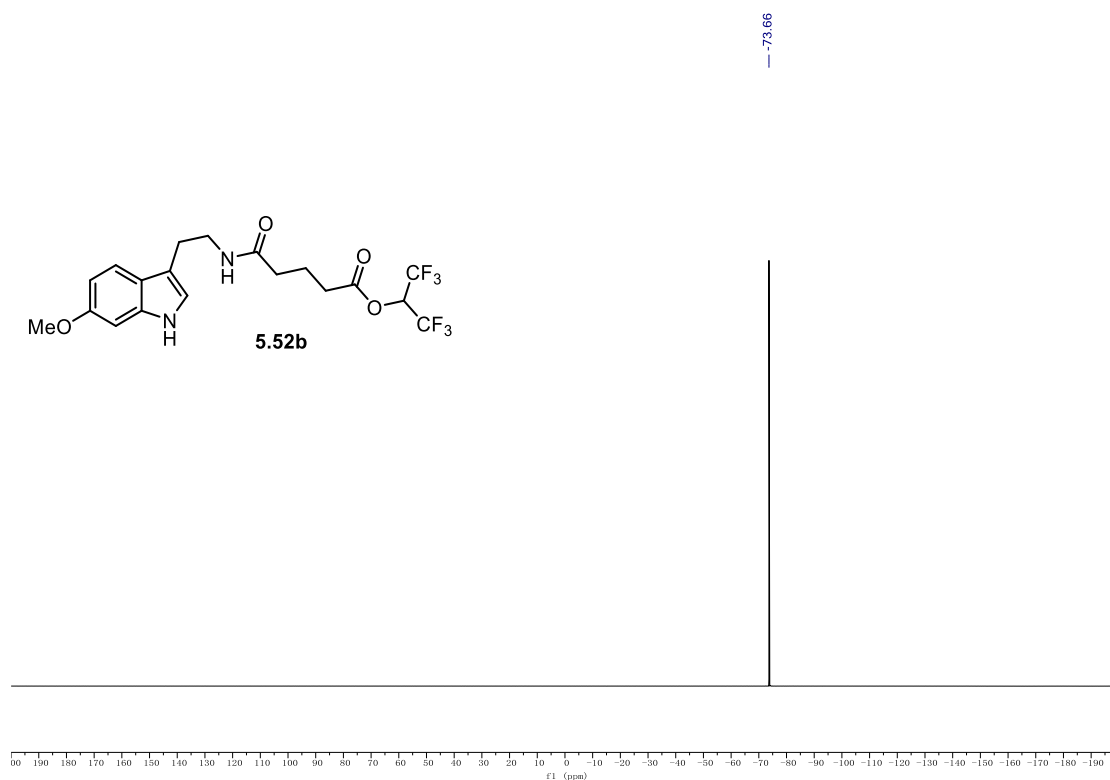
^{19}F NMR (565 MHz, CDCl_3) **5.52a**. ^1H NMR (500 MHz, CD_2Cl_2) **5.52a**.

9.1. NMR Spectra

¹³C NMR (126 MHz, CD₂Cl₂) **5.52a**.

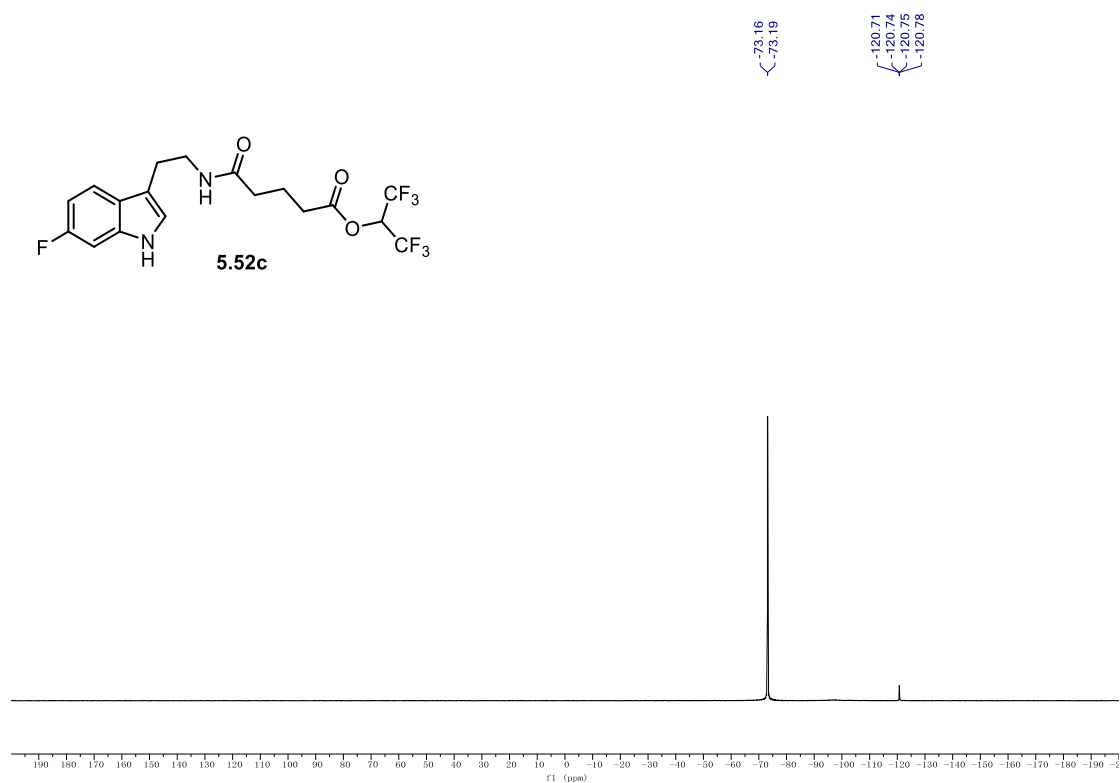


¹⁹F NMR (471 MHz, CD₂Cl₂) **5.52a**.

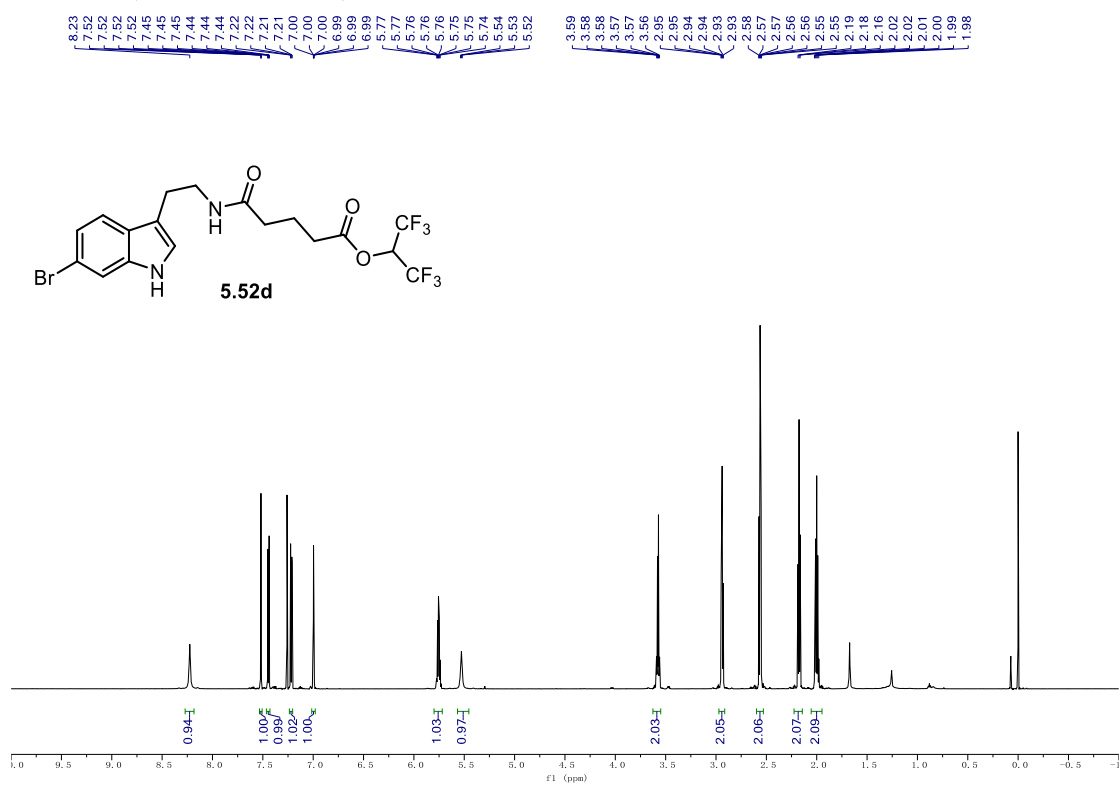


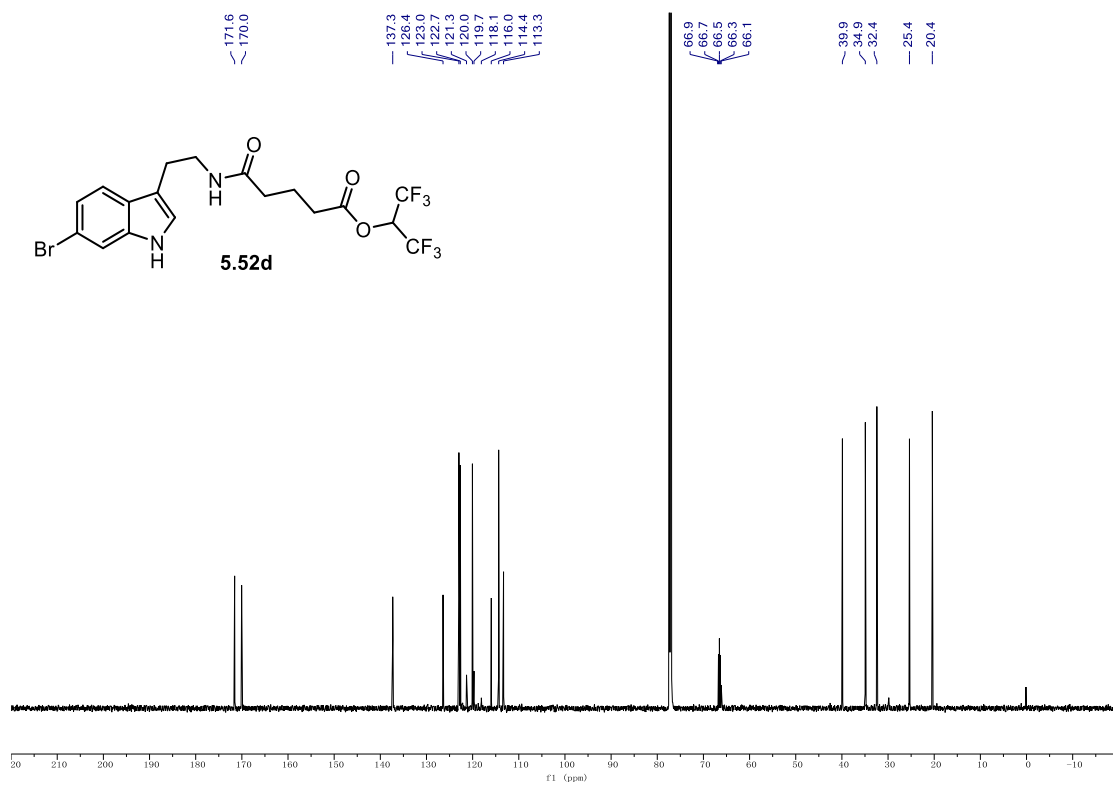
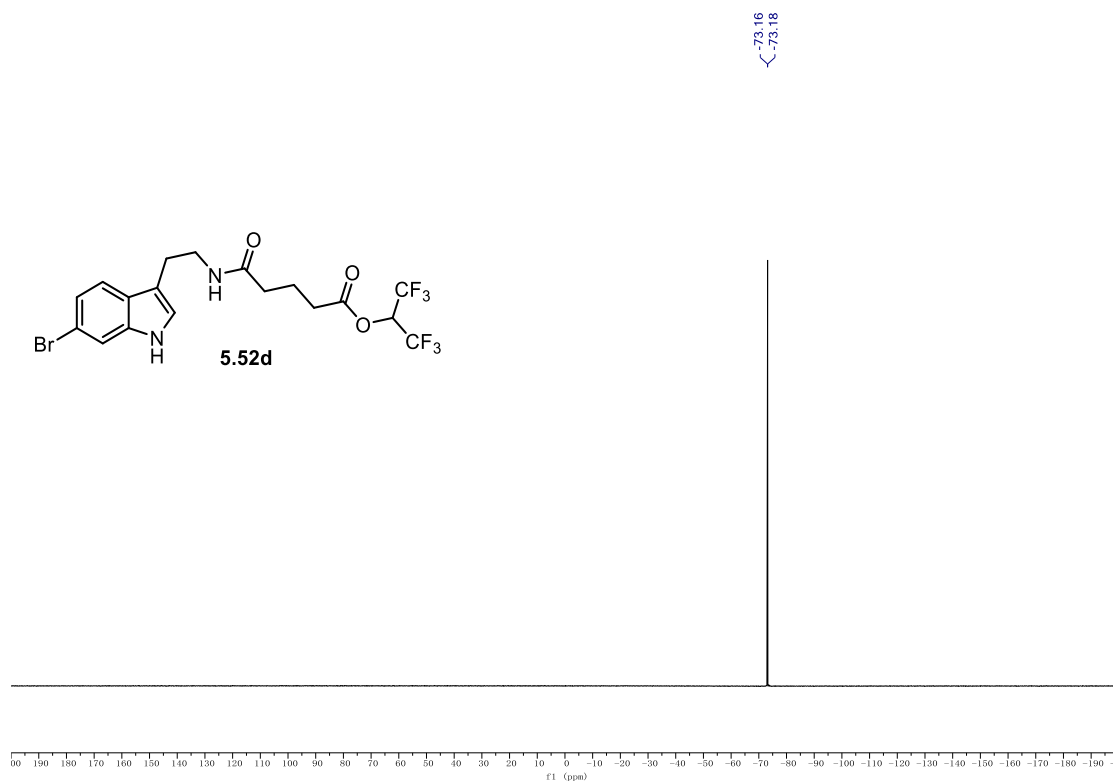
9.1. NMR Spectra

¹⁹F NMR (471 MHz, CDCl₃) 5.52c.



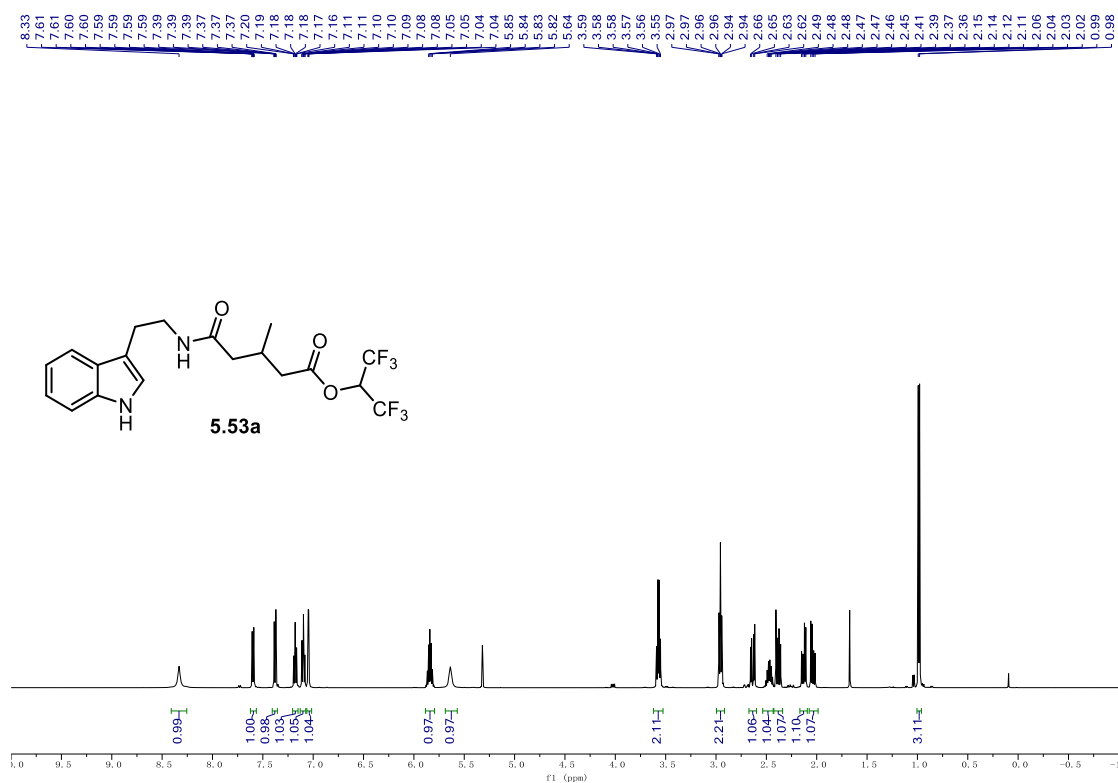
¹H NMR (700 MHz, CDCl₃) 5.52d.



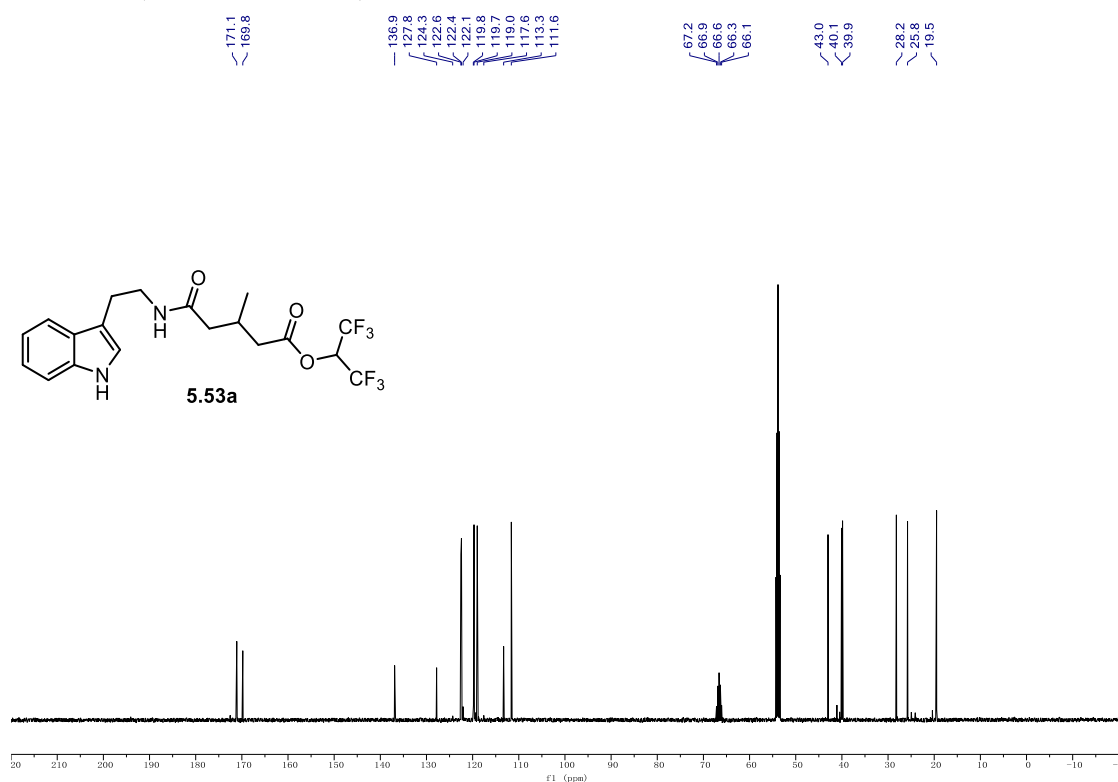
^{13}C NMR (176 MHz, CDCl_3) 5.52d. **^{19}F NMR (471 MHz, CDCl_3) 5.52d.**

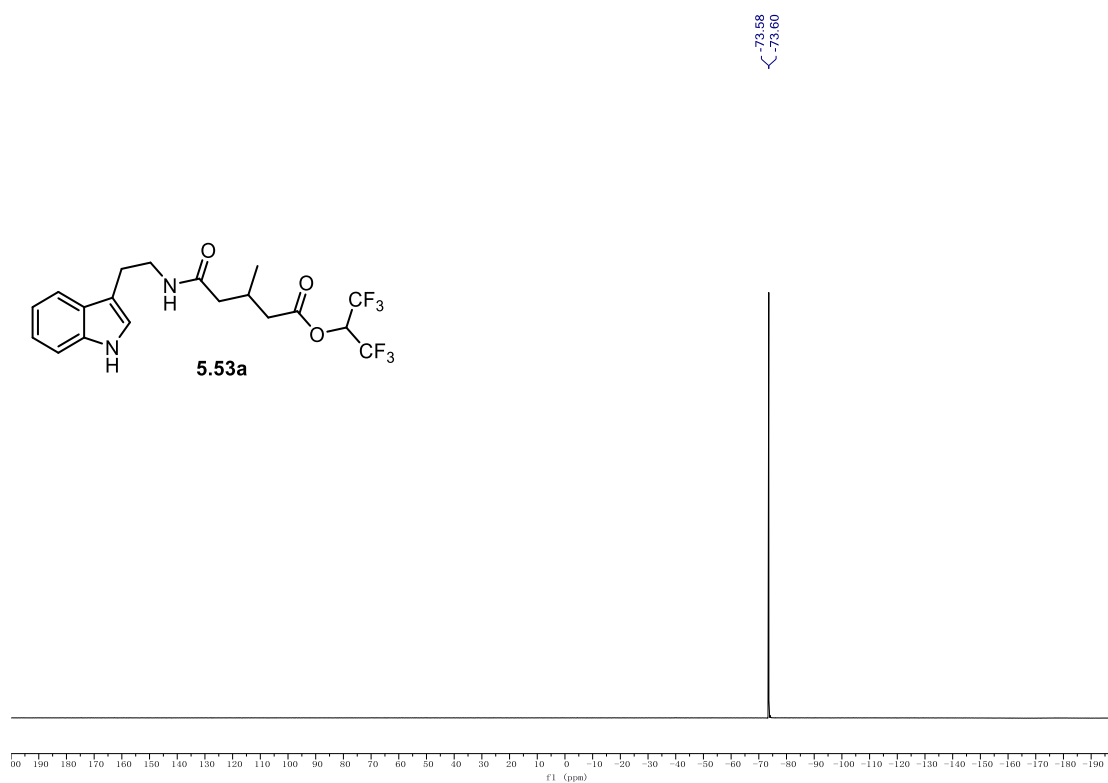
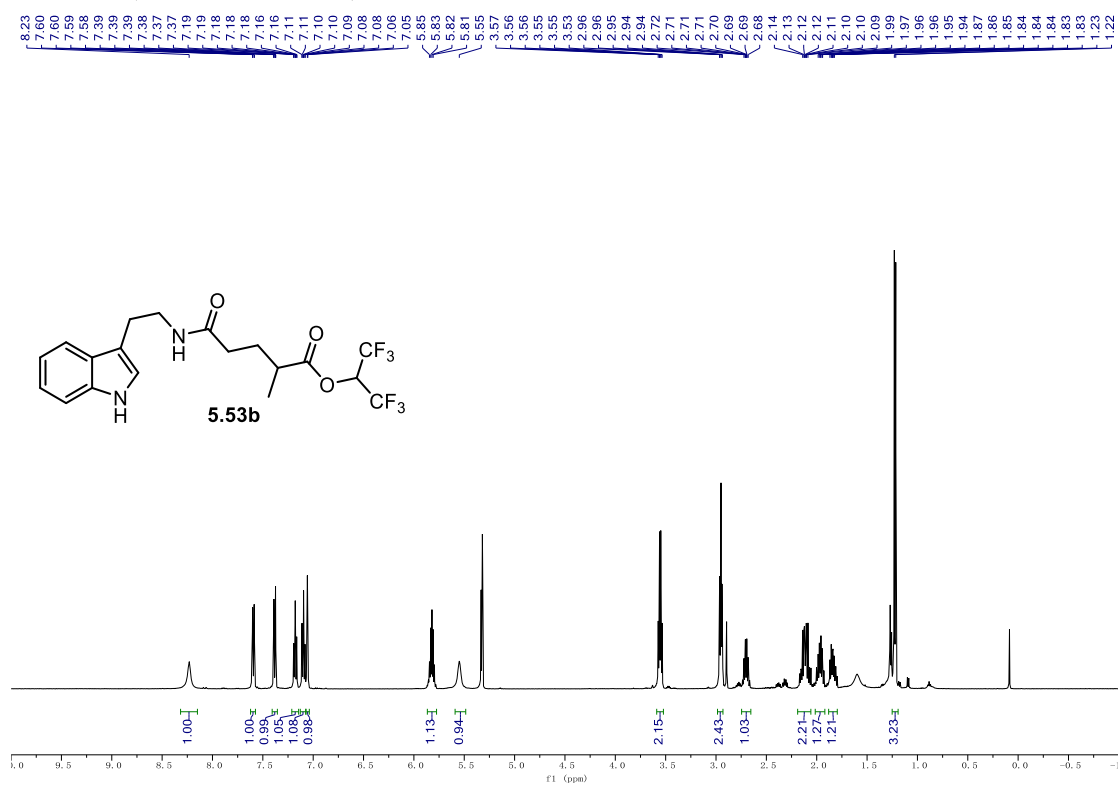
9.1. NMR Spectra

¹H NMR (500 MHz, CD₂Cl₂) **5.53a**.



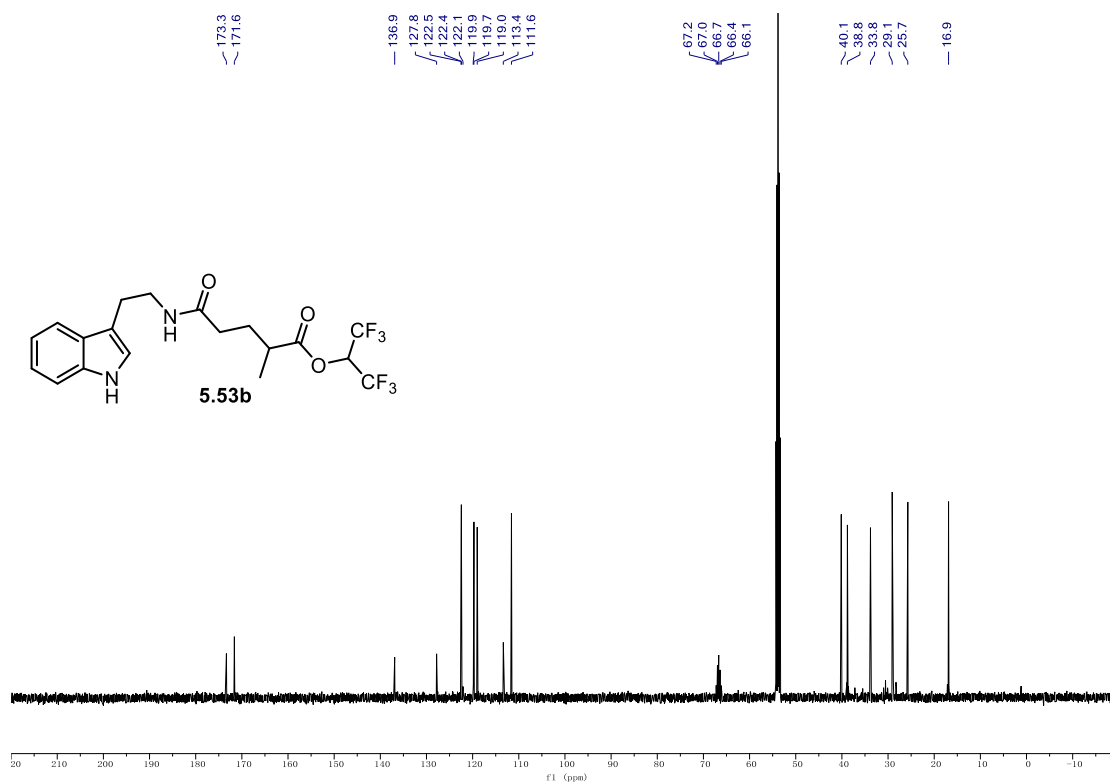
¹³C NMR (126 MHz, CD₂Cl₂) **5.53a**.



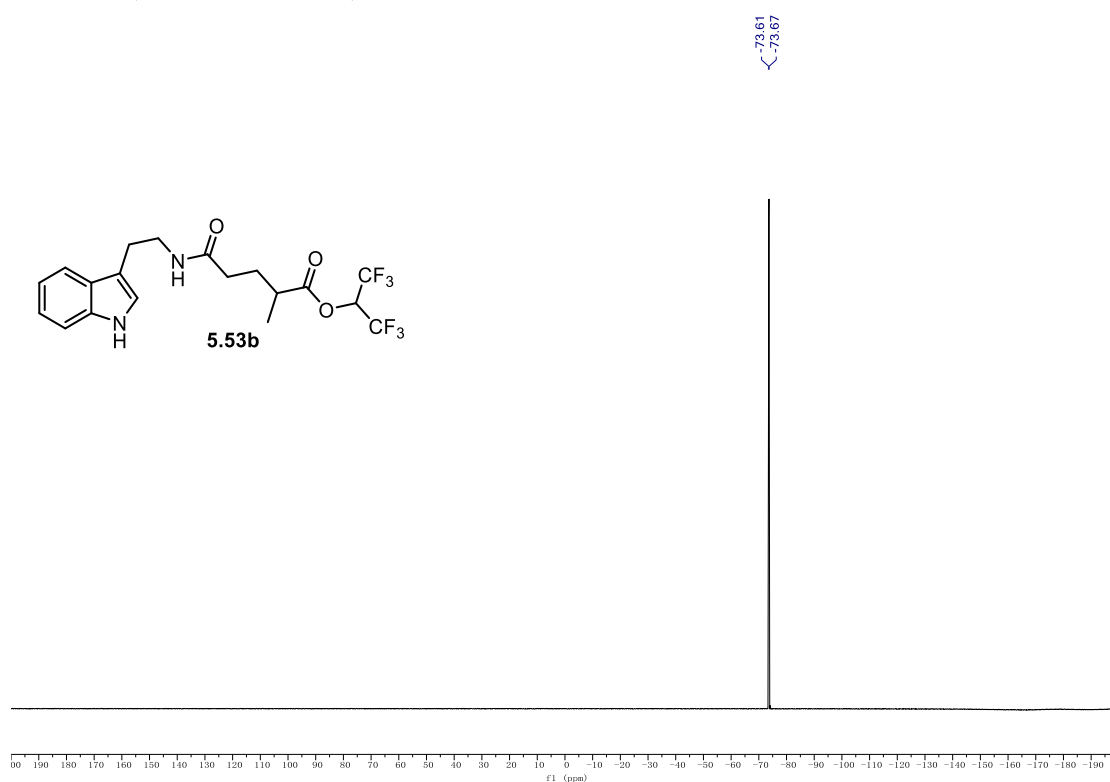
^{19}F NMR (471 MHz, CD_2Cl_2) **5.53a**. ^1H NMR (500 MHz, CD_2Cl_2) **5.53b**.

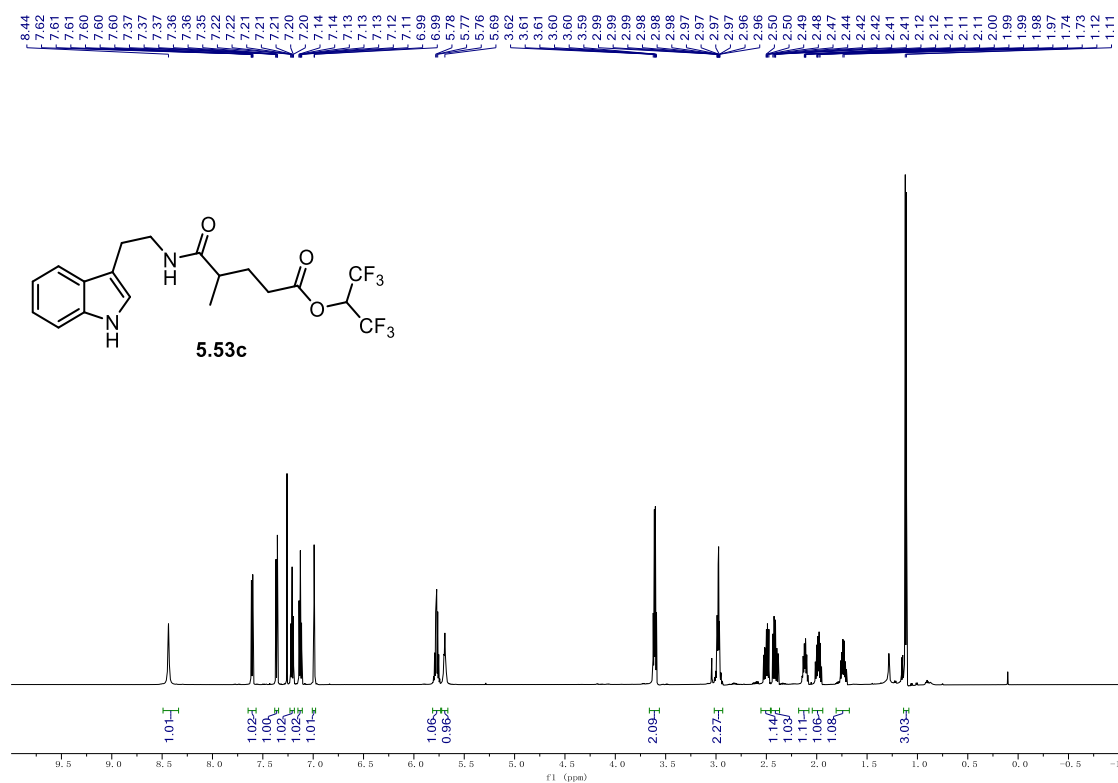
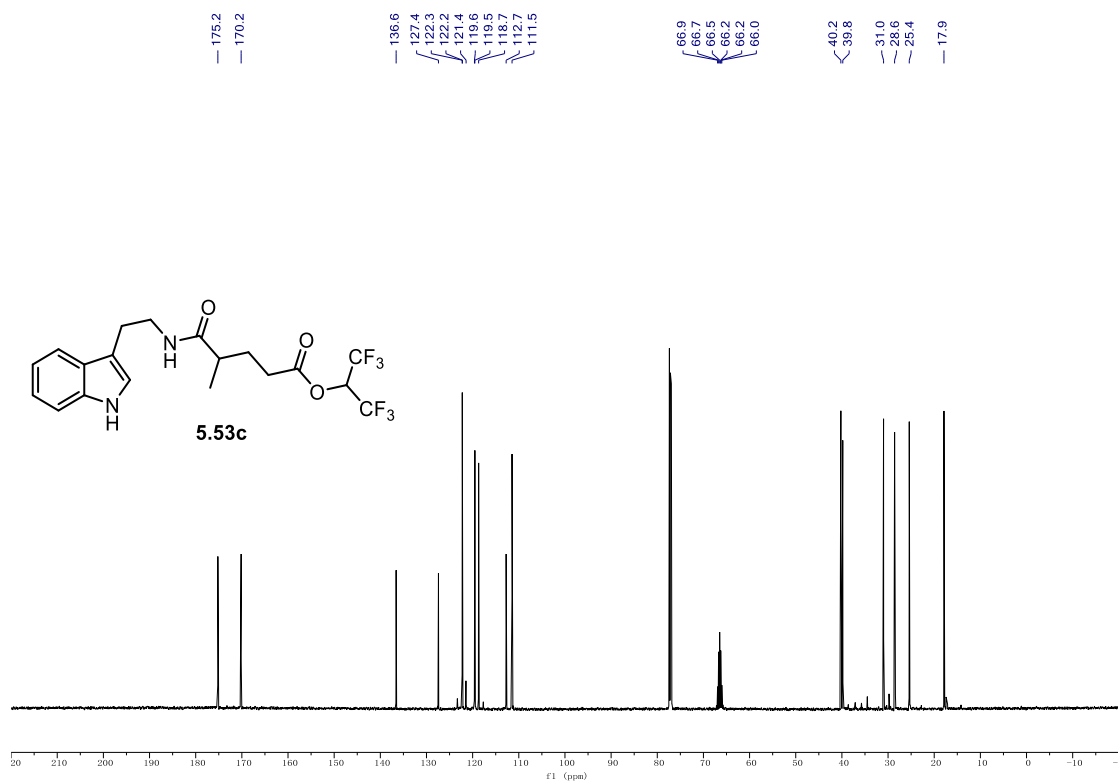
9.1. NMR Spectra

¹H NMR (500 MHz, CD₂Cl₂) **5.53b**.



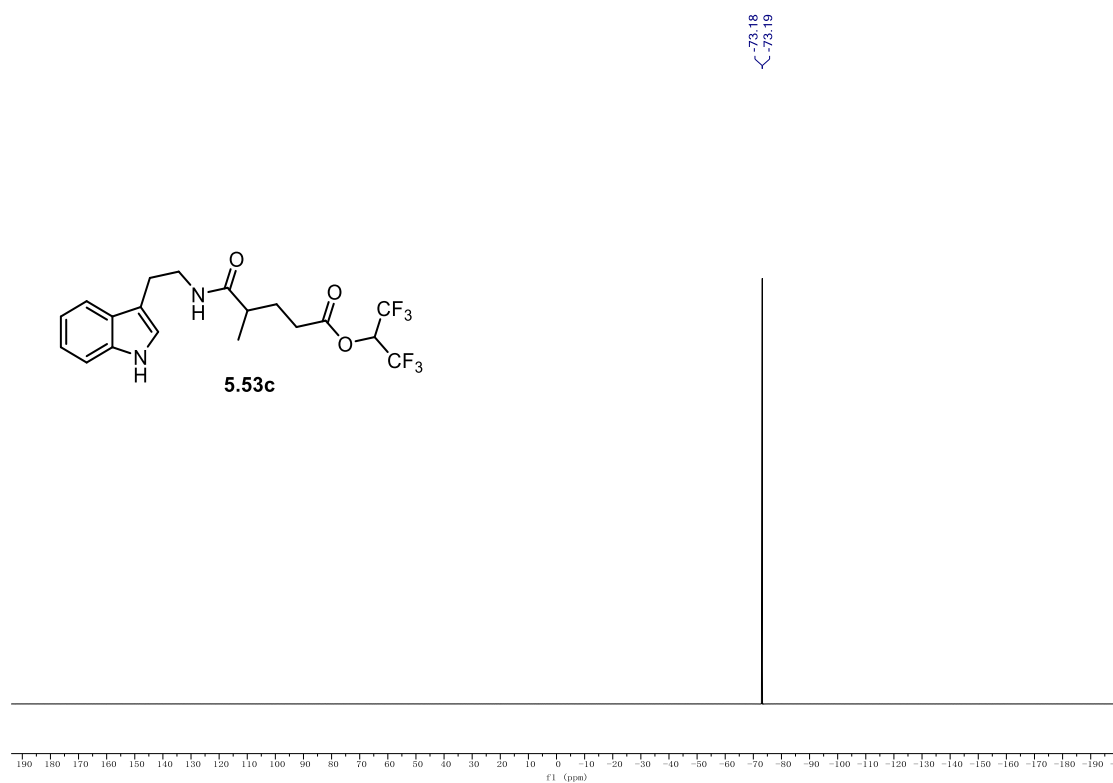
¹H NMR (500 MHz, CD₂Cl₂) **5.53b**.



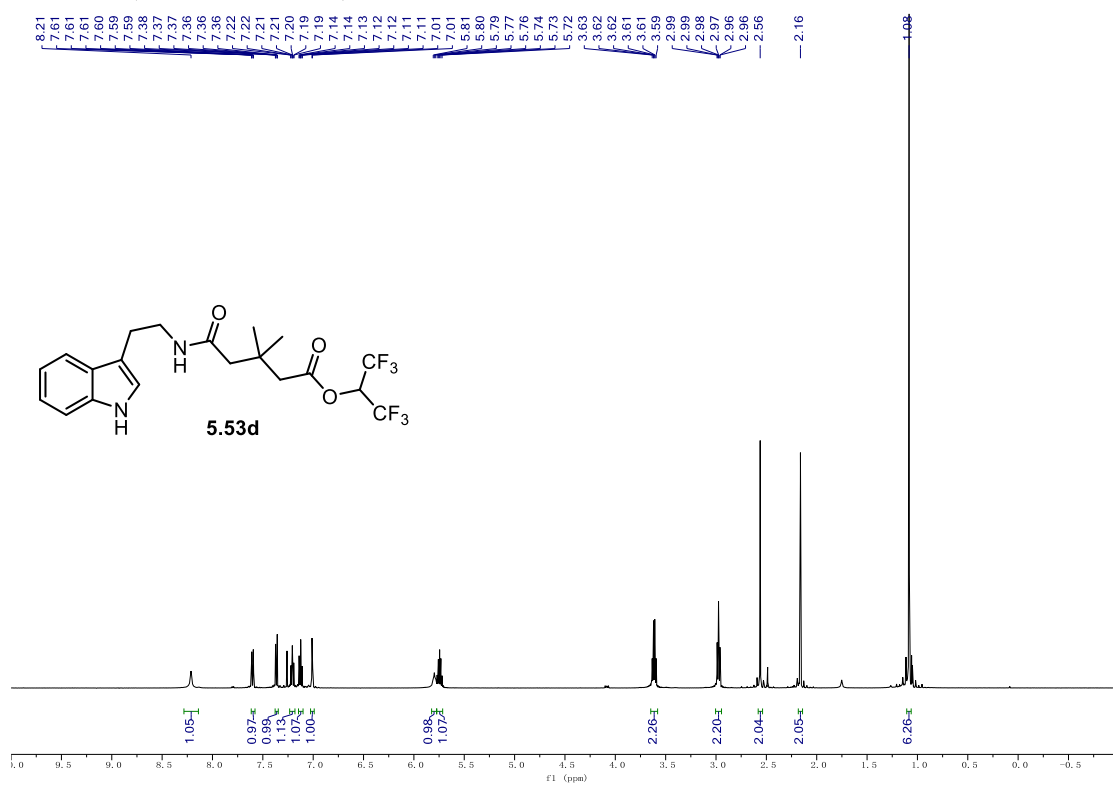
^1H NMR (600 MHz, CDCl_3) **5.53c**. ^{13}C NMR (151 MHz, CDCl_3) **5.53c**.

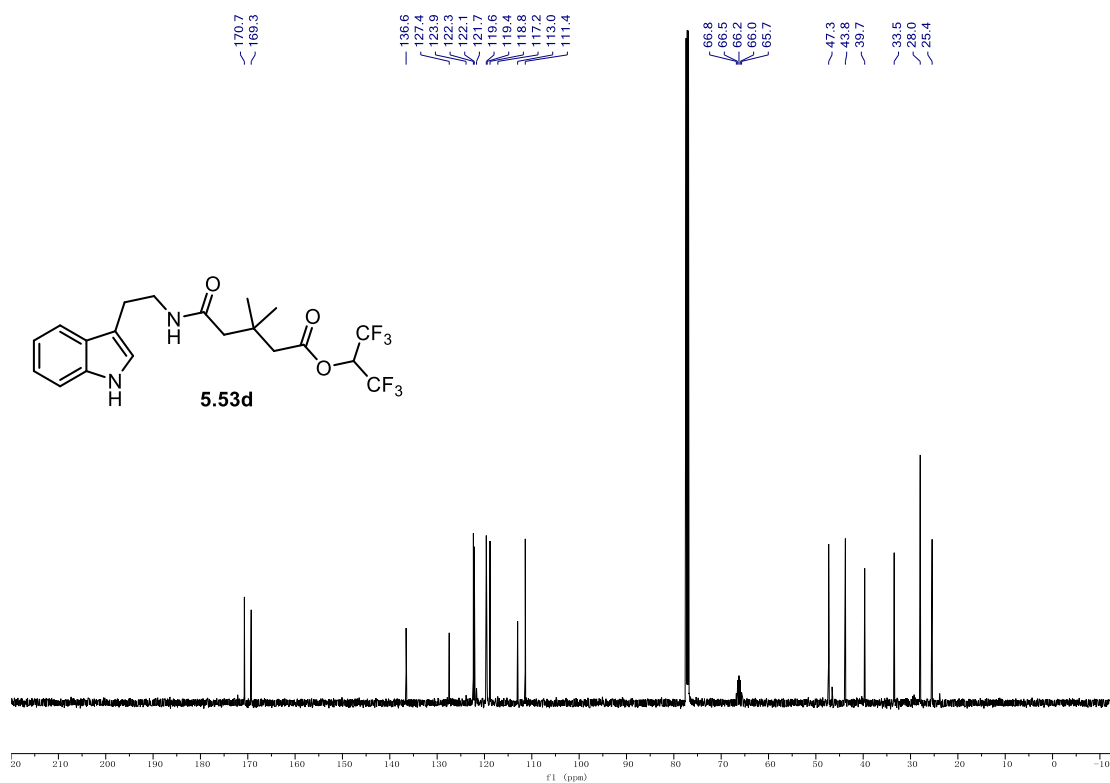
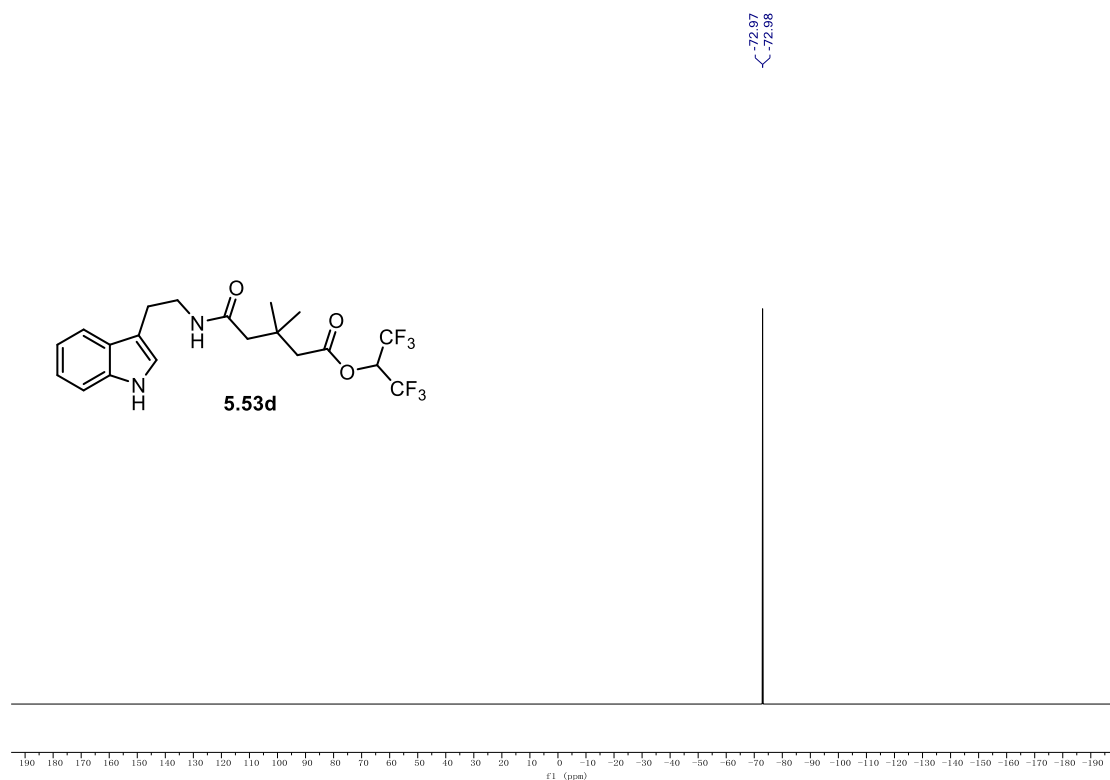
9.1. NMR Spectra

^{19}F NMR (565 MHz, CDCl_3) **5.53c**.



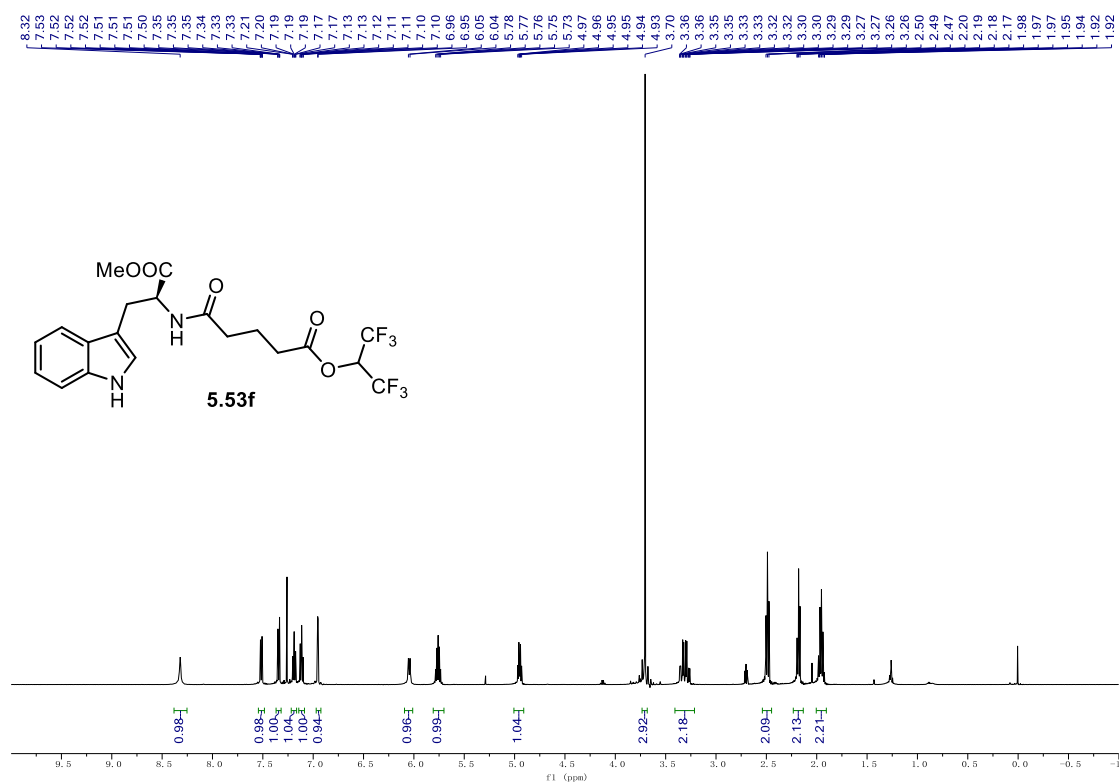
^1H NMR (500 MHz, CDCl_3) **5.53d**.



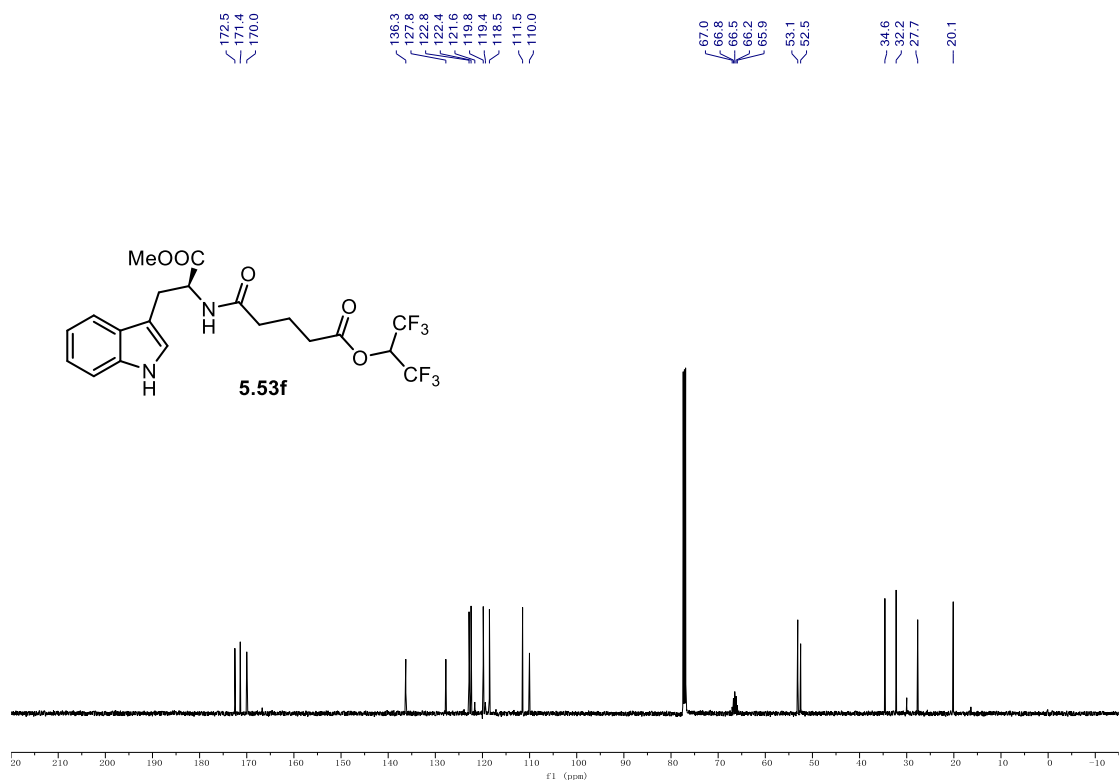
^{13}C NMR (126 MHz, CDCl_3) 5.53d. **^{19}F NMR (565 MHz, CDCl_3) 5.53d.**

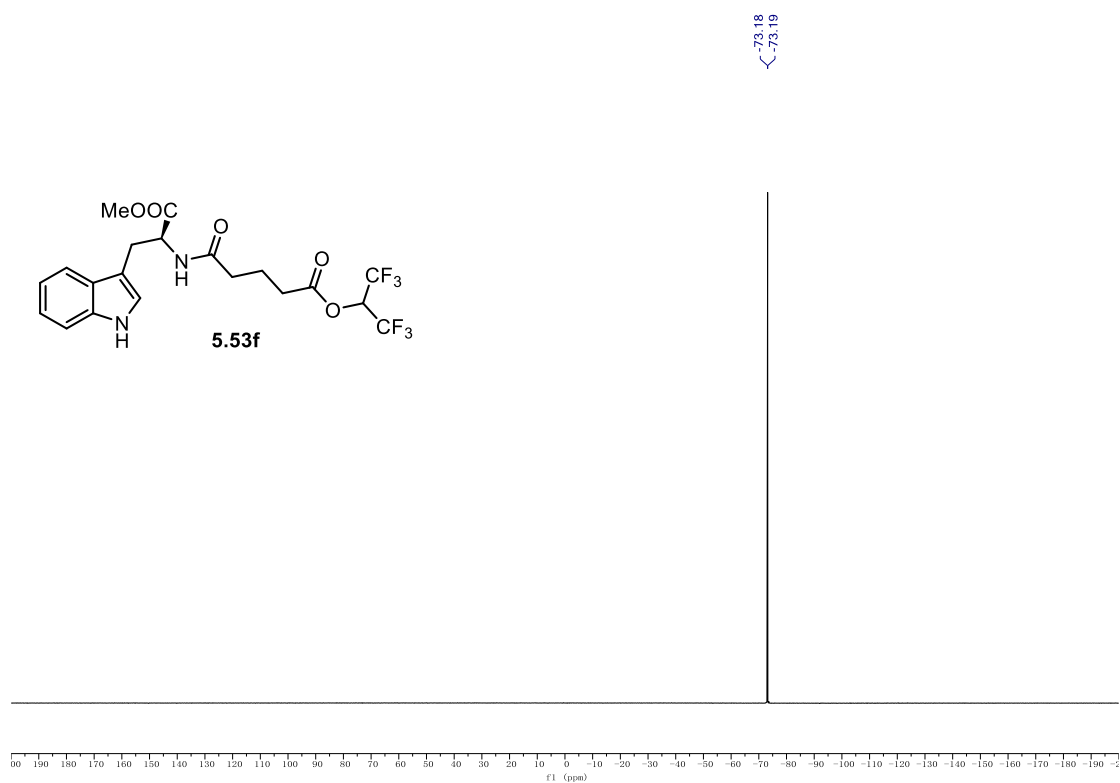
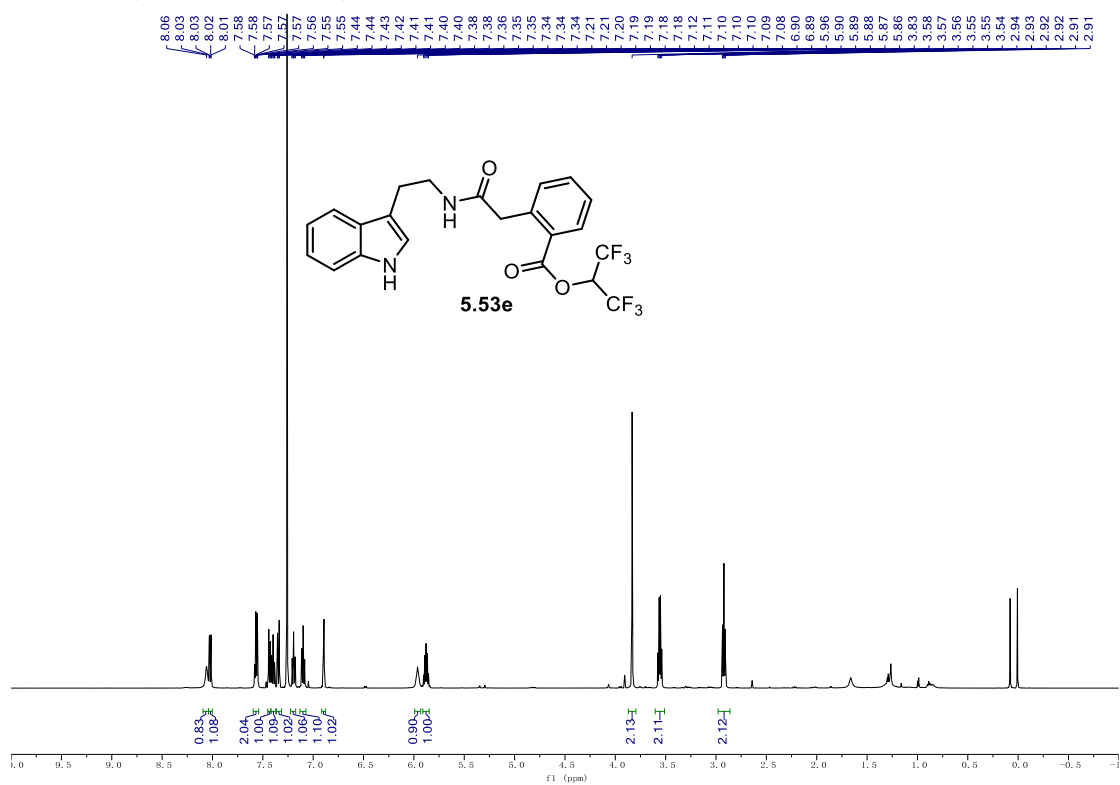
9.1. NMR Spectra

¹H NMR (500 MHz, CDCl₃) **5.53f**.



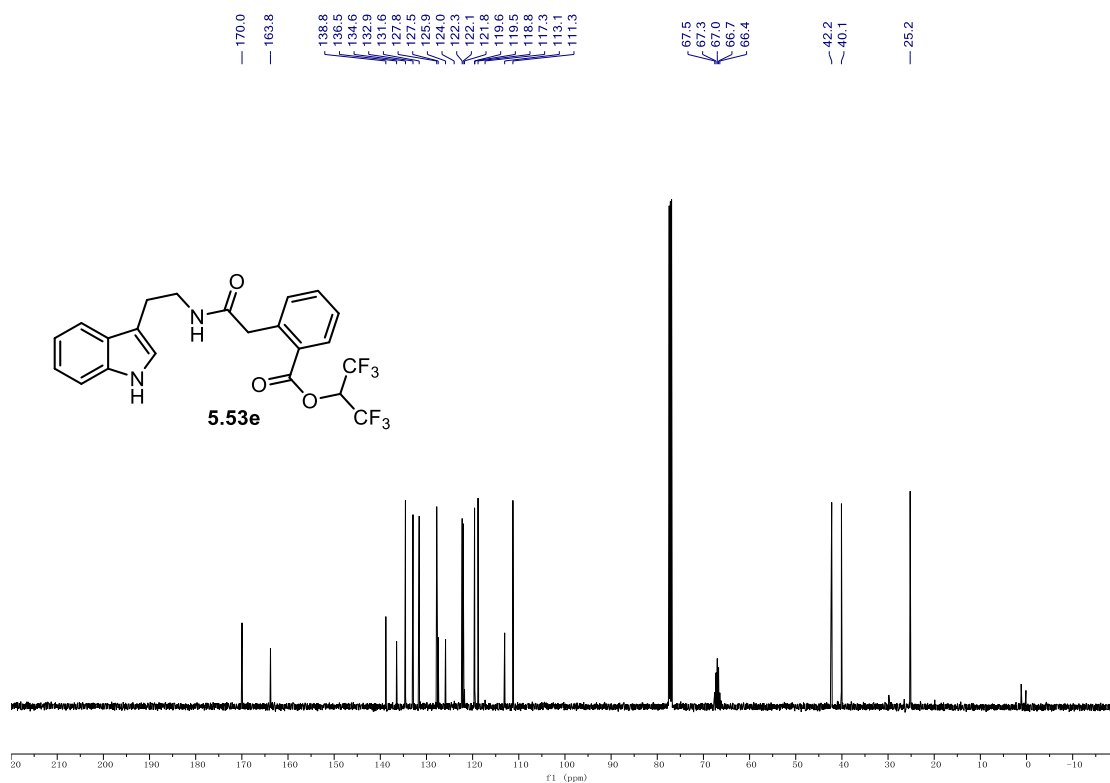
¹³C NMR (126 MHz, CDCl₃) **5.53f**.



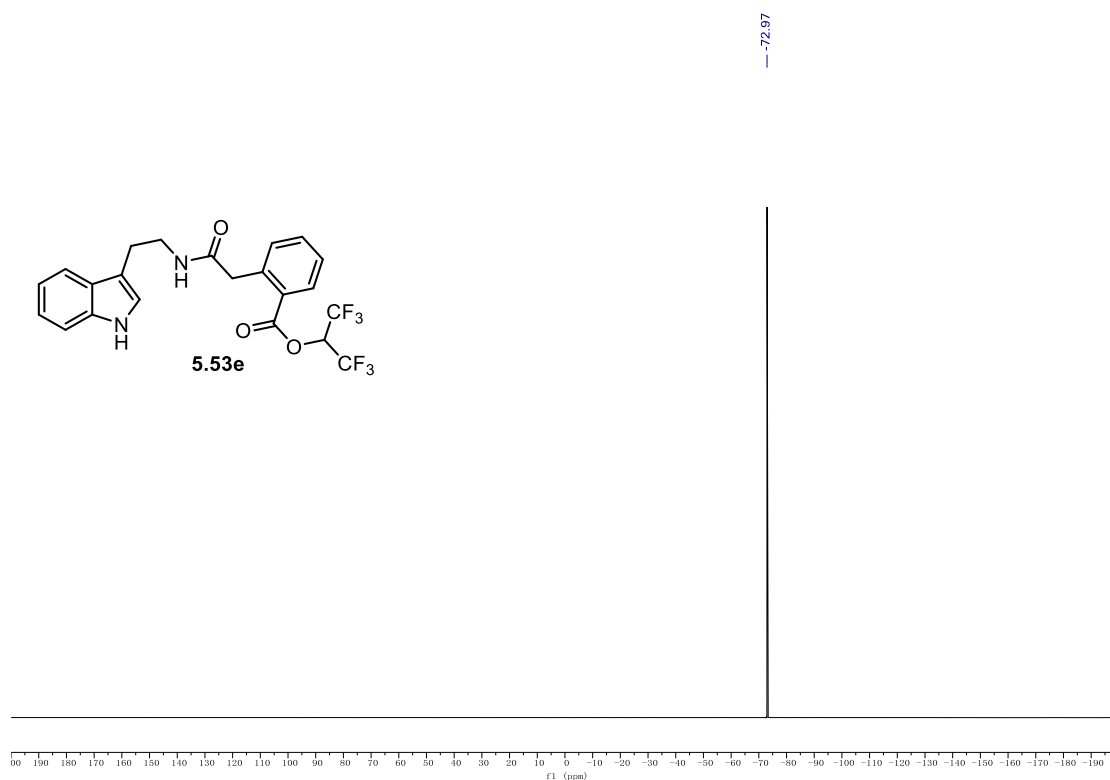
^{19}F NMR (471 MHz, CDCl_3) **5.53f**. ^1H NMR (500 MHz, CDCl_3) **5.53e**.

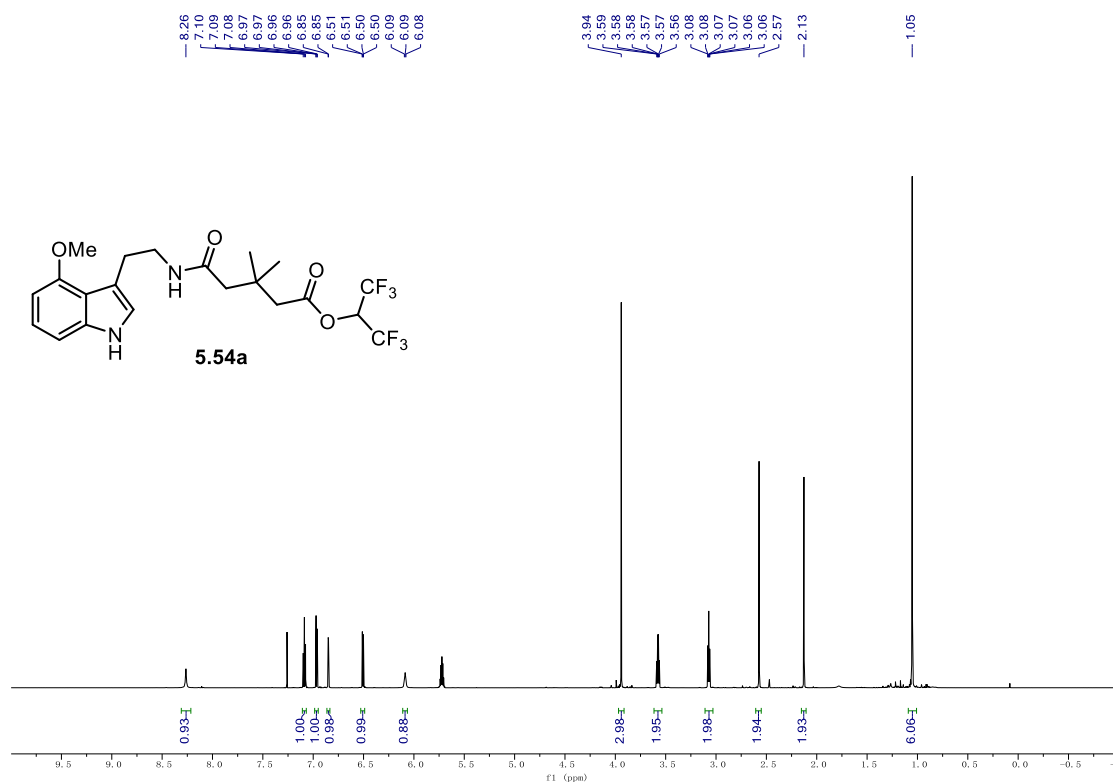
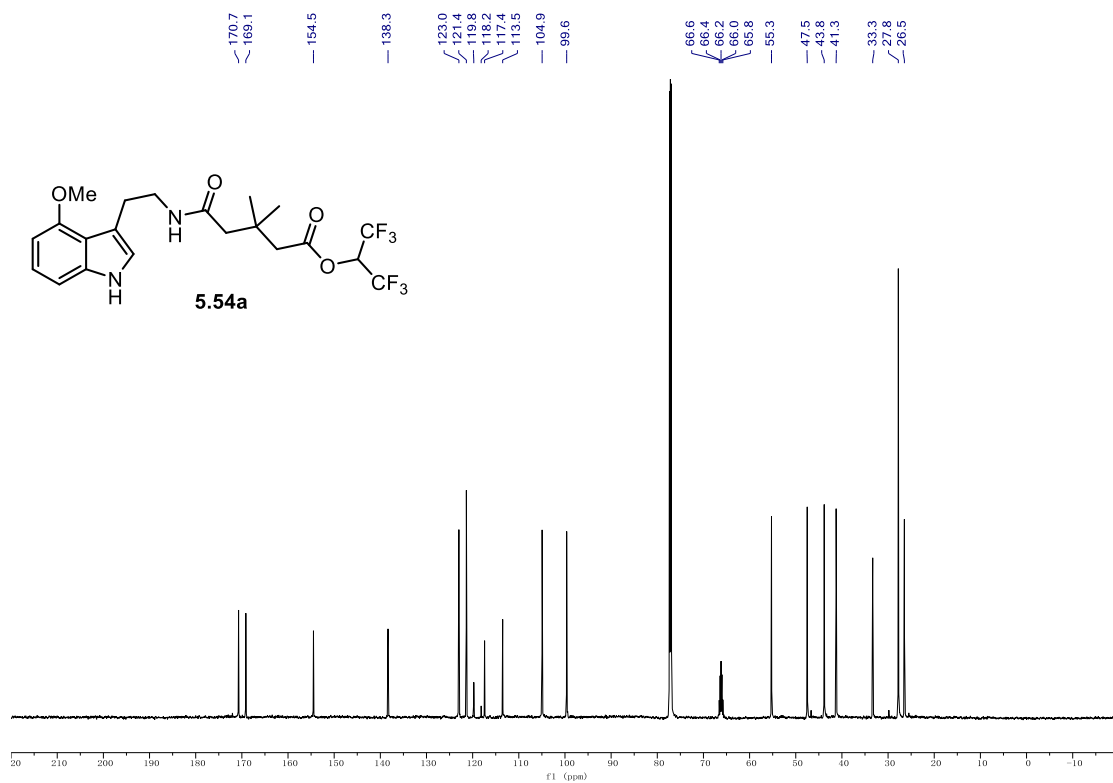
9.1. NMR Spectra

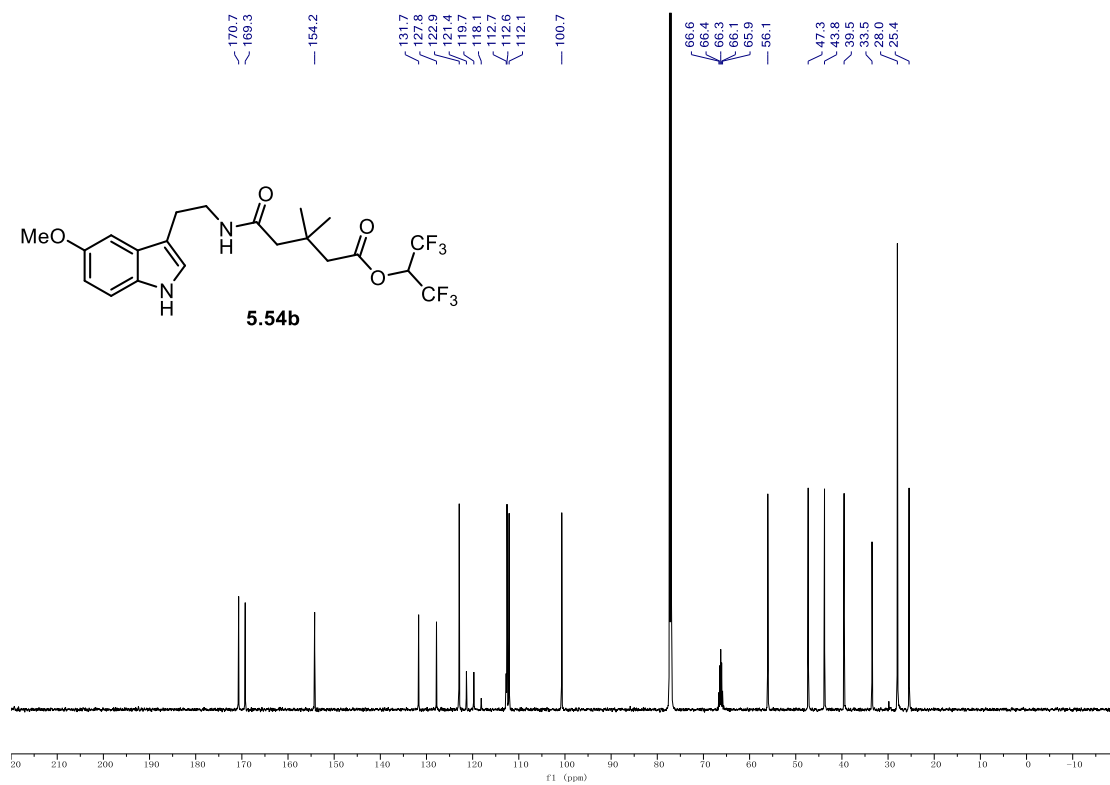
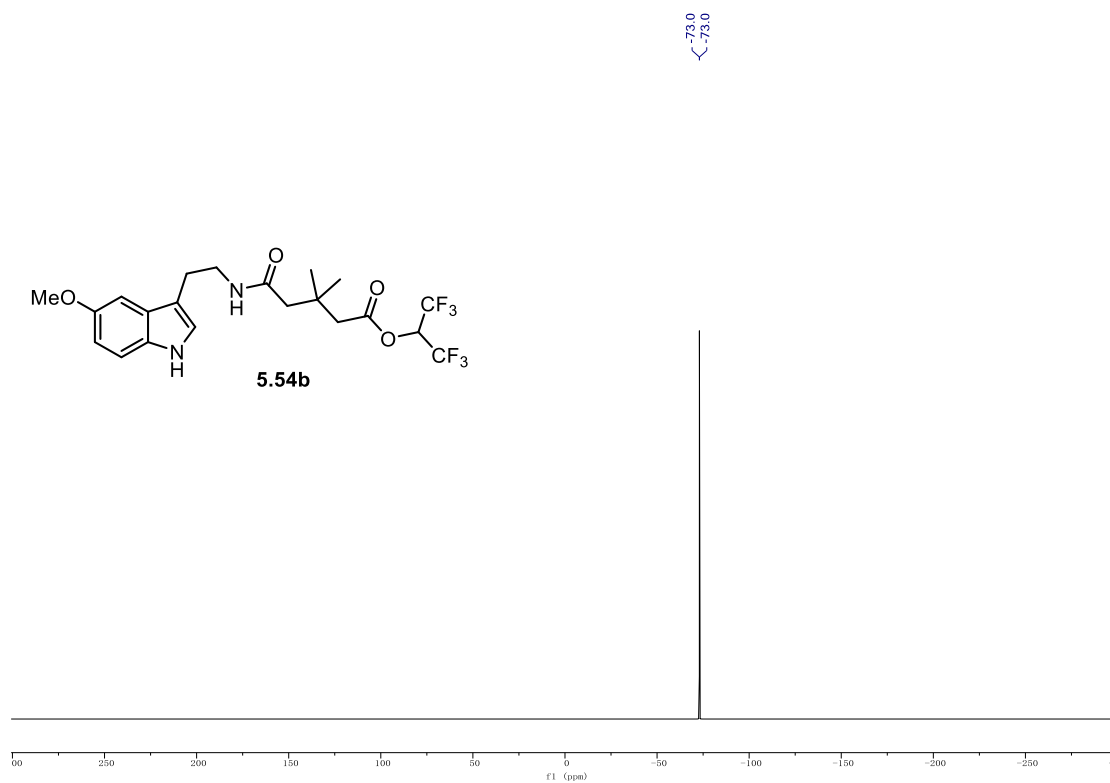
¹³C NMR (126 MHz, CDCl₃) **5.53e**.



¹⁹F NMR (471 MHz, CDCl₃) **5.53e**.

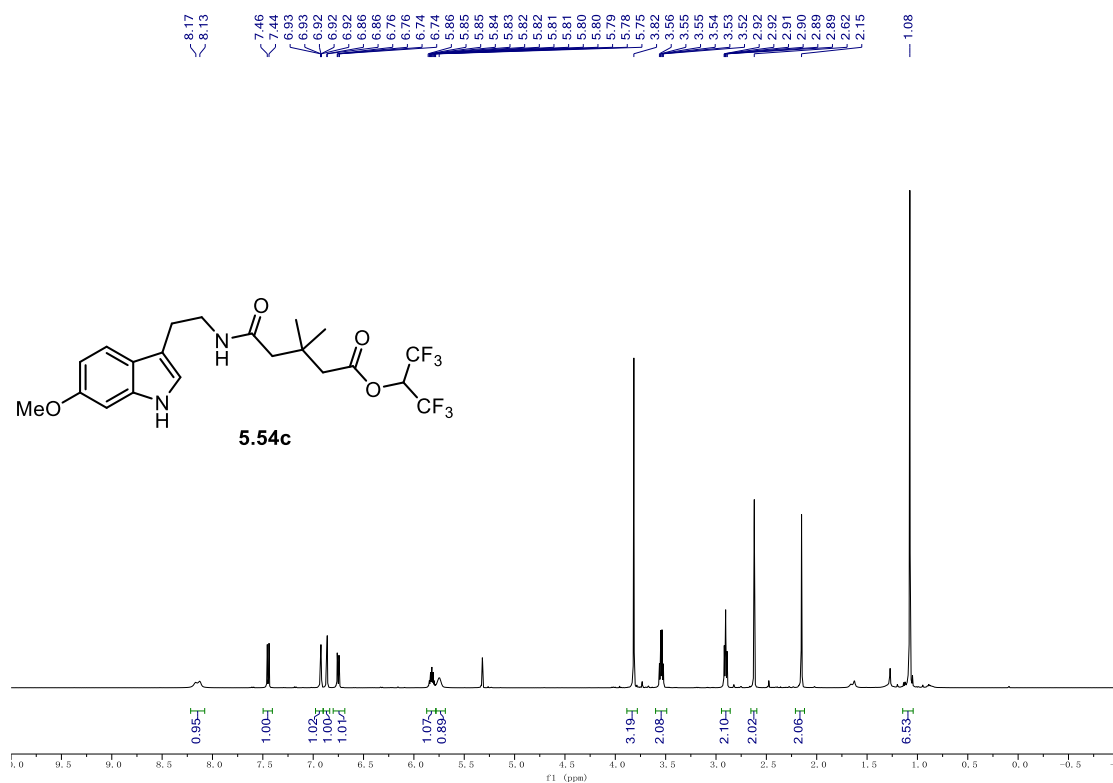


^1H NMR (700 MHz, CDCl_3) 5.54a. **^{13}C NMR (176 MHz, CDCl_3) 5.54a.**

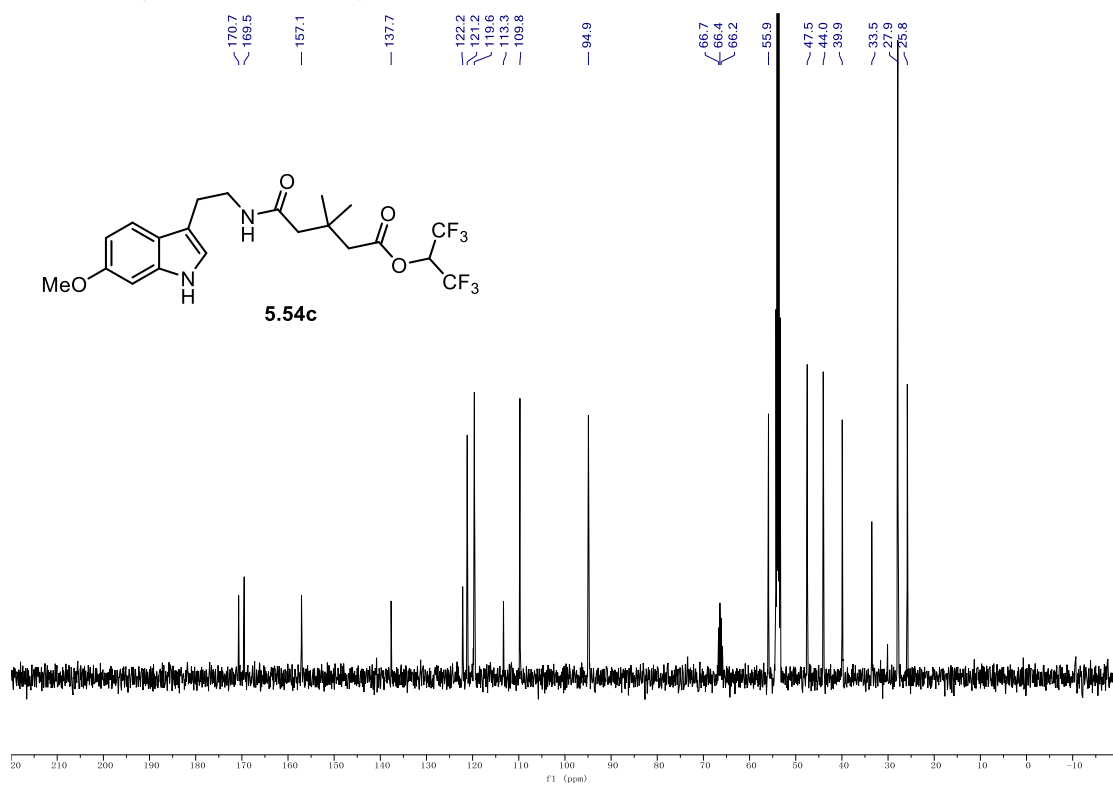
^{13}C NMR (176 MHz, CDCl_3) **5.54b**. ^{19}F NMR (376 MHz, CDCl_3) **5.54b**.

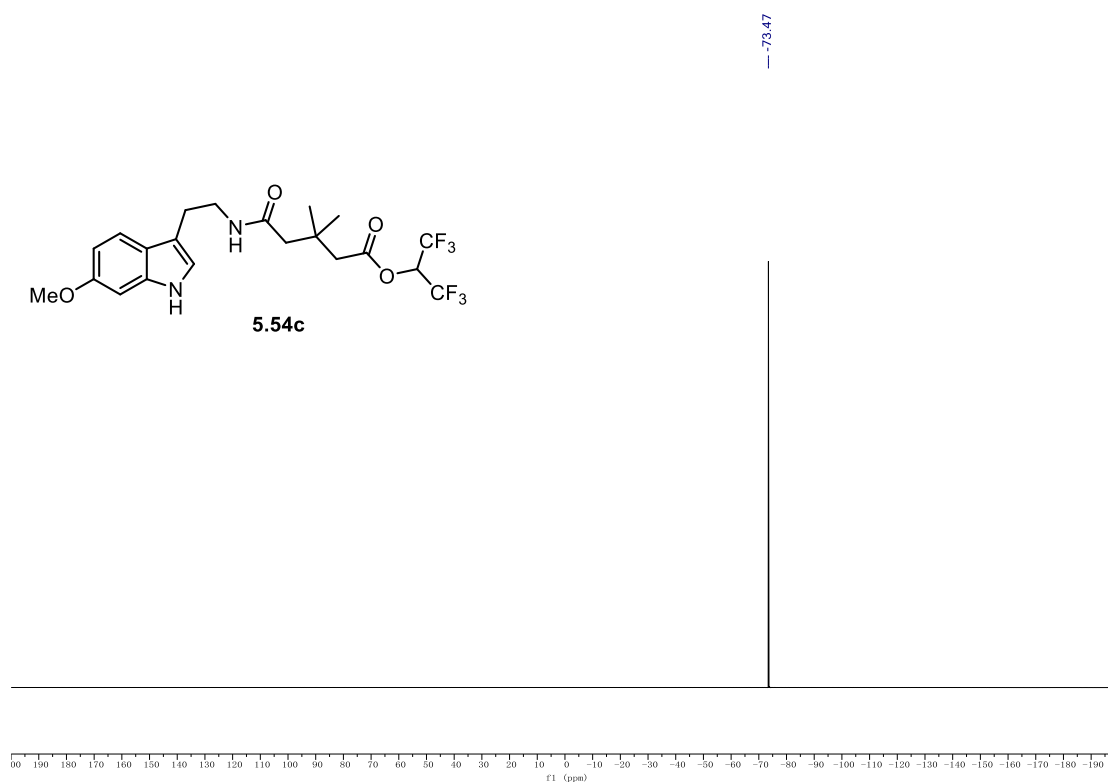
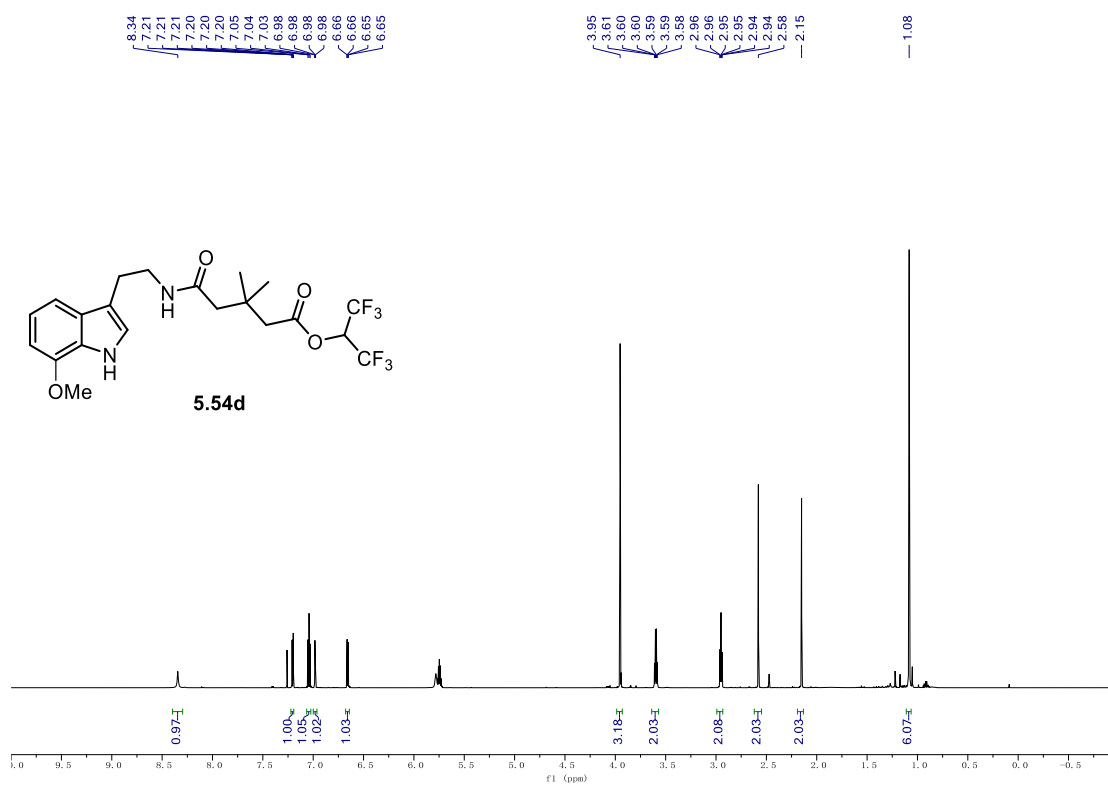
9.1. NMR Spectra

^1H NMR (500 MHz, CD_2Cl_2) of **5.54c**.



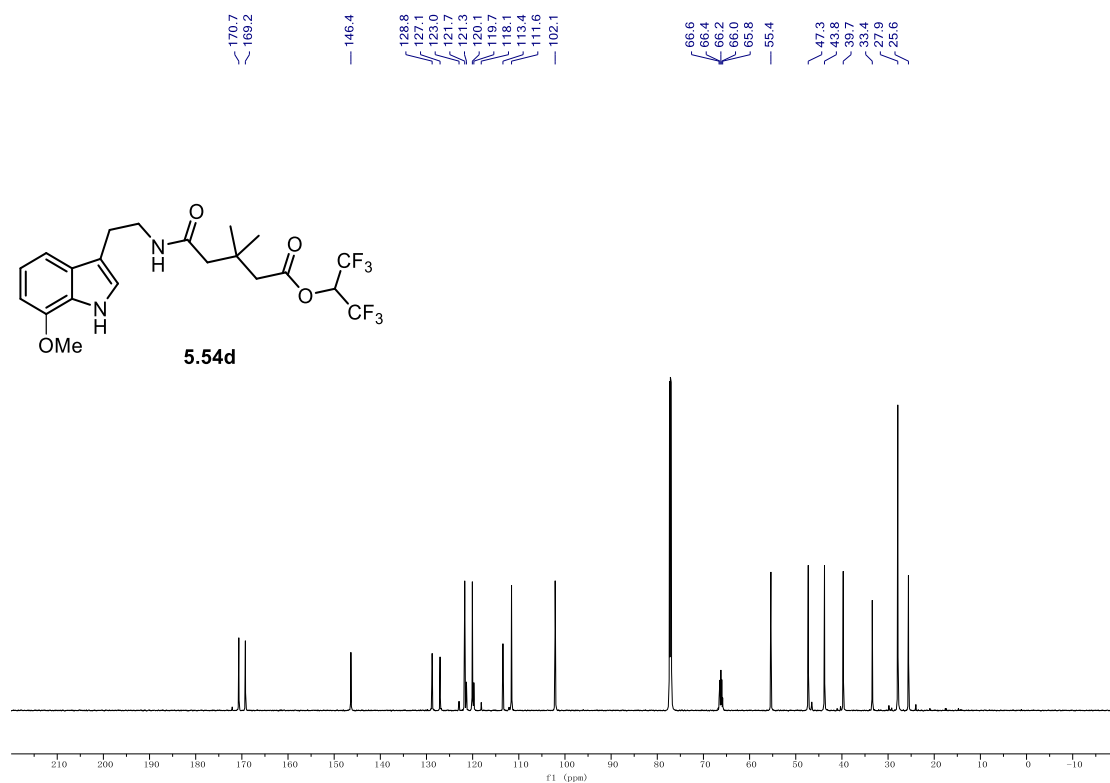
^{13}C NMR (126 MHz, CD_2Cl_2) of **5.54c**.



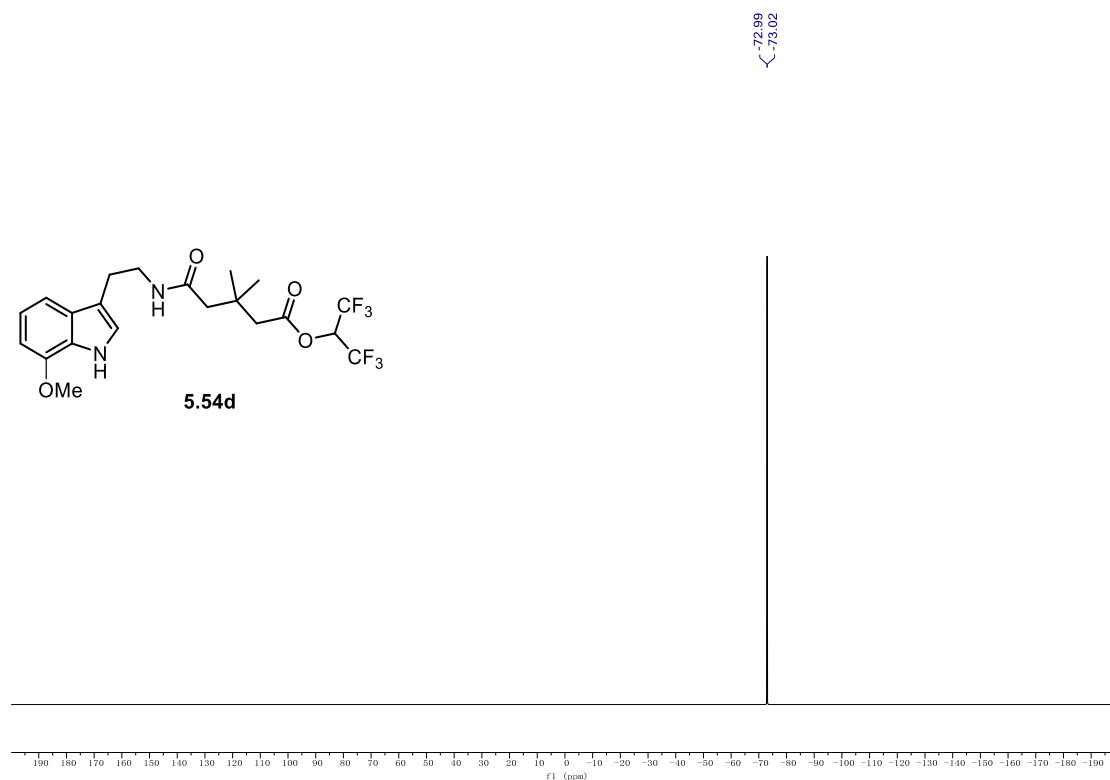
^{19}F NMR (471 MHz, CD_2Cl_2) of **5.54c**. ^1H NMR (700 MHz, CDCl_3) **5.54d**.

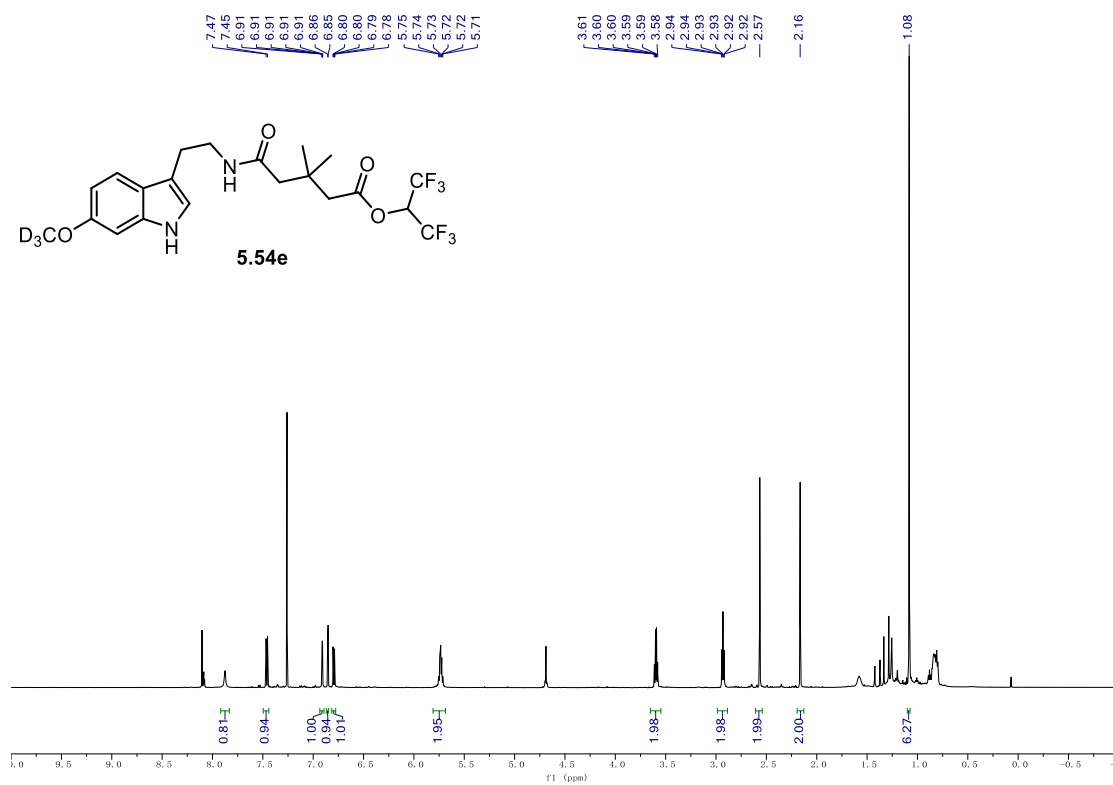
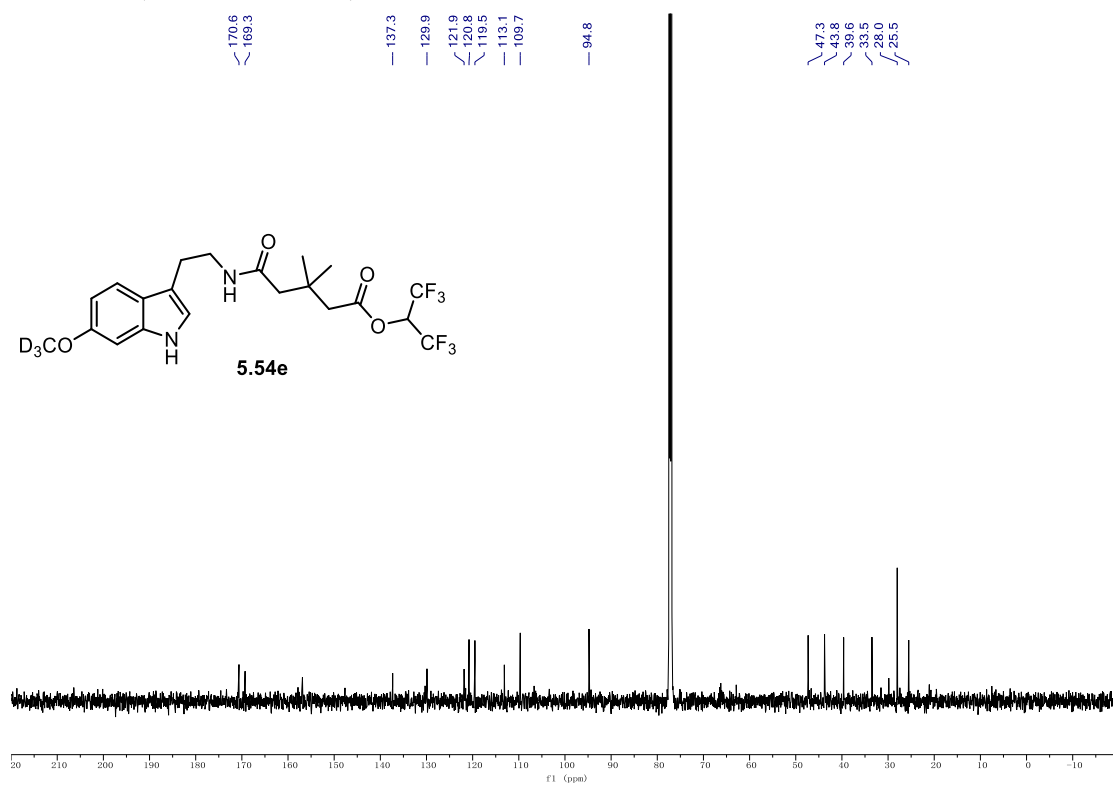
9.1. NMR Spectra

¹³C NMR (176 MHz, CDCl₃) **5.54d**.



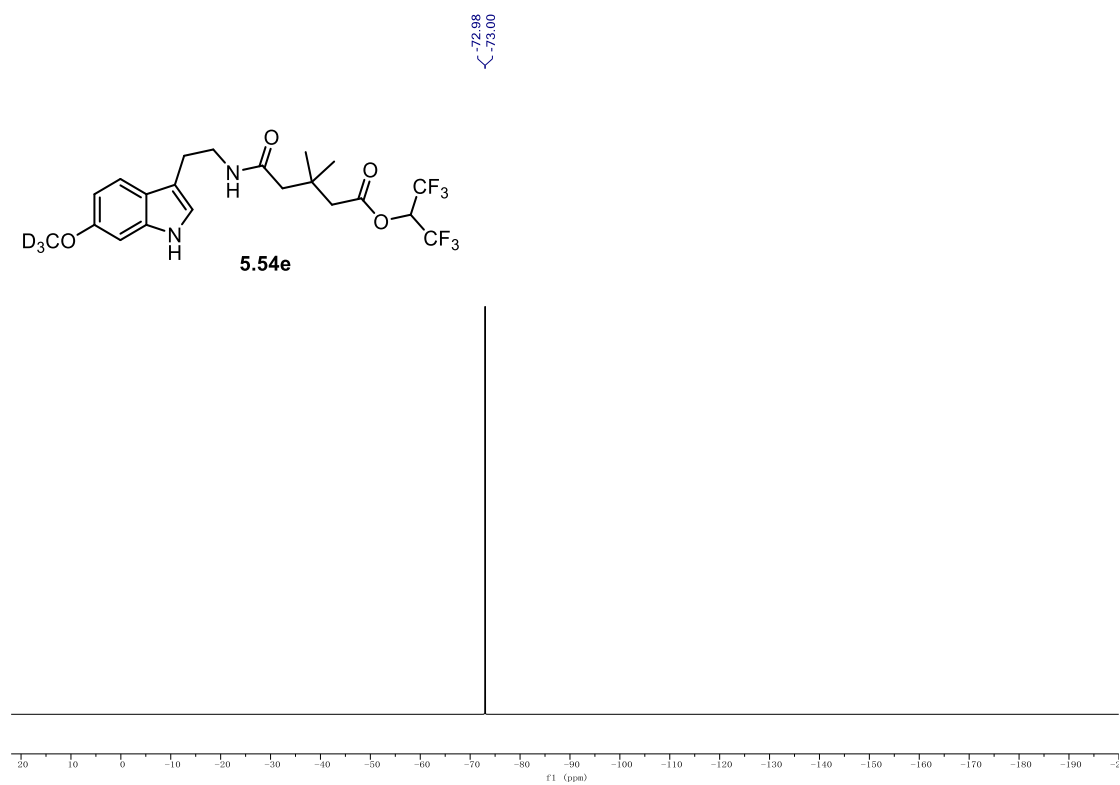
¹⁹F NMR (376 MHz, CDCl₃) of **5.54d**.



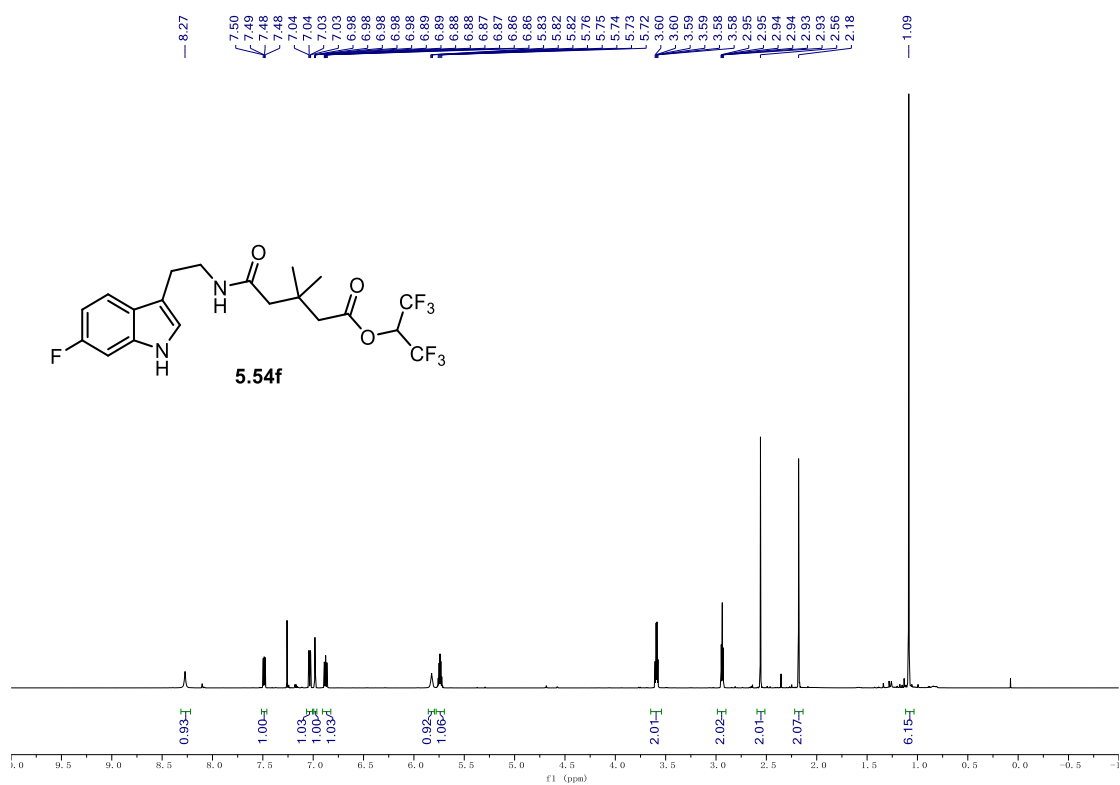
^1H NMR (600 MHz, CDCl_3) **5.54e**. ^{13}C NMR (151 MHz, CDCl_3) **5.54e**.

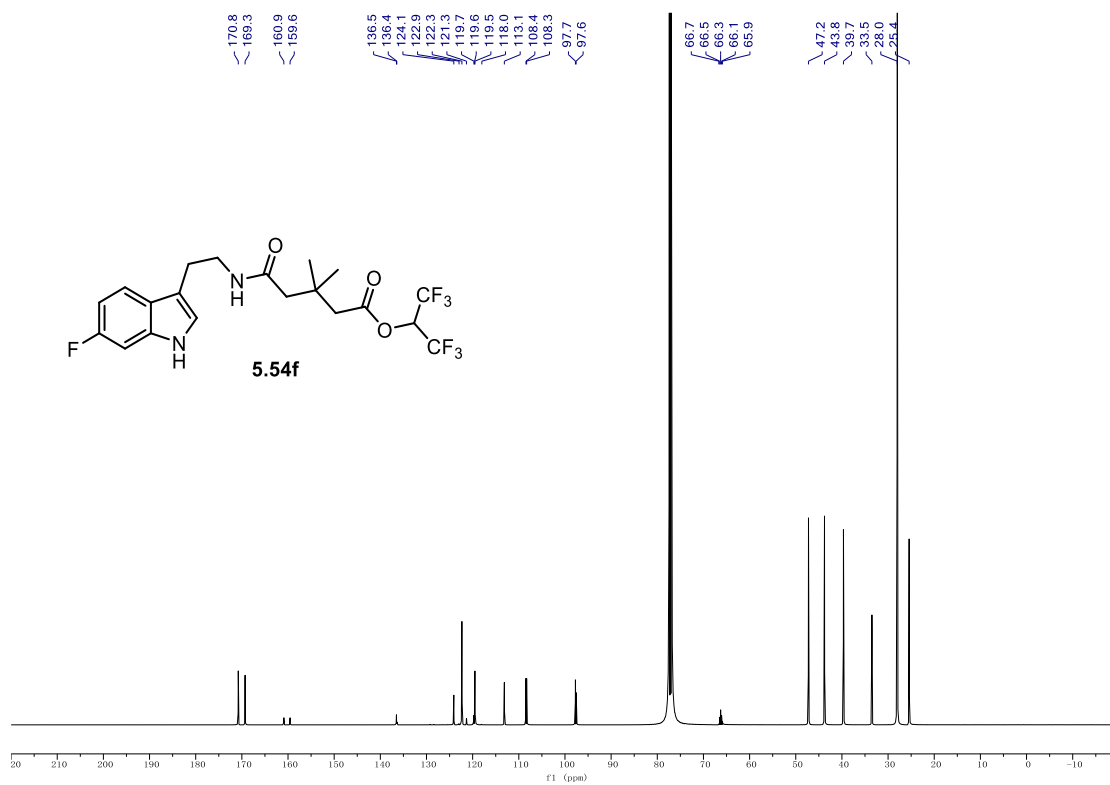
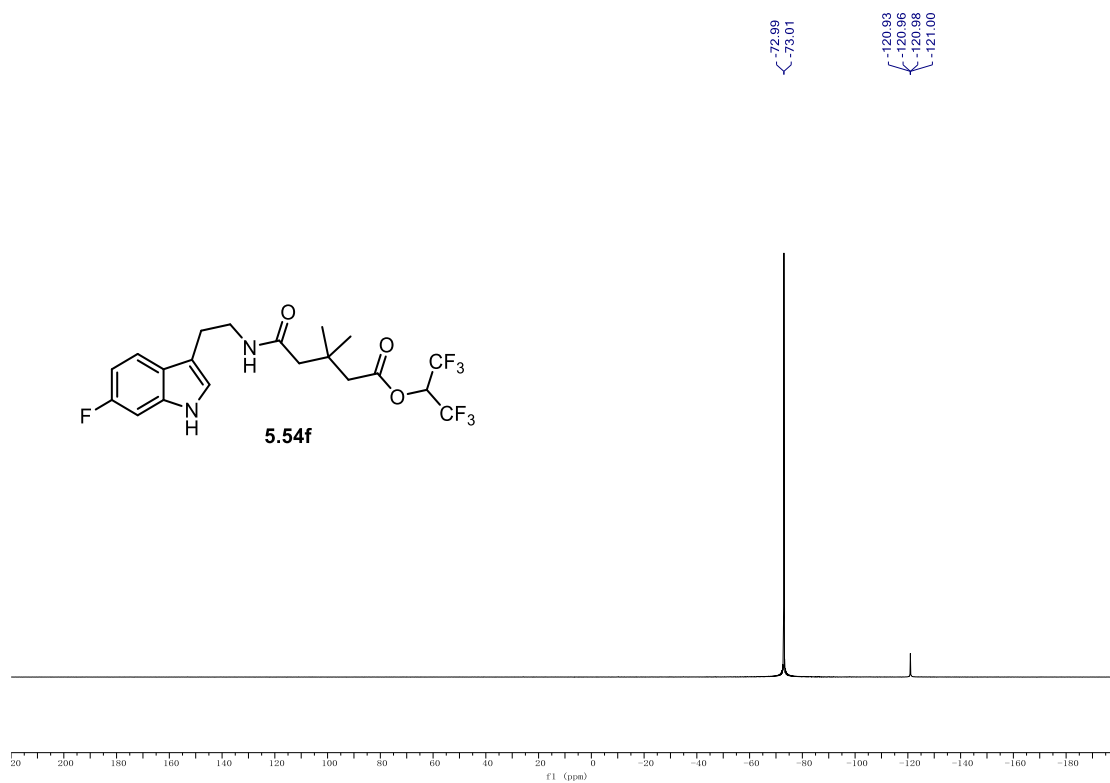
9.1. NMR Spectra

^{19}F NMR (565 MHz, CDCl_3) of **5.54e**.



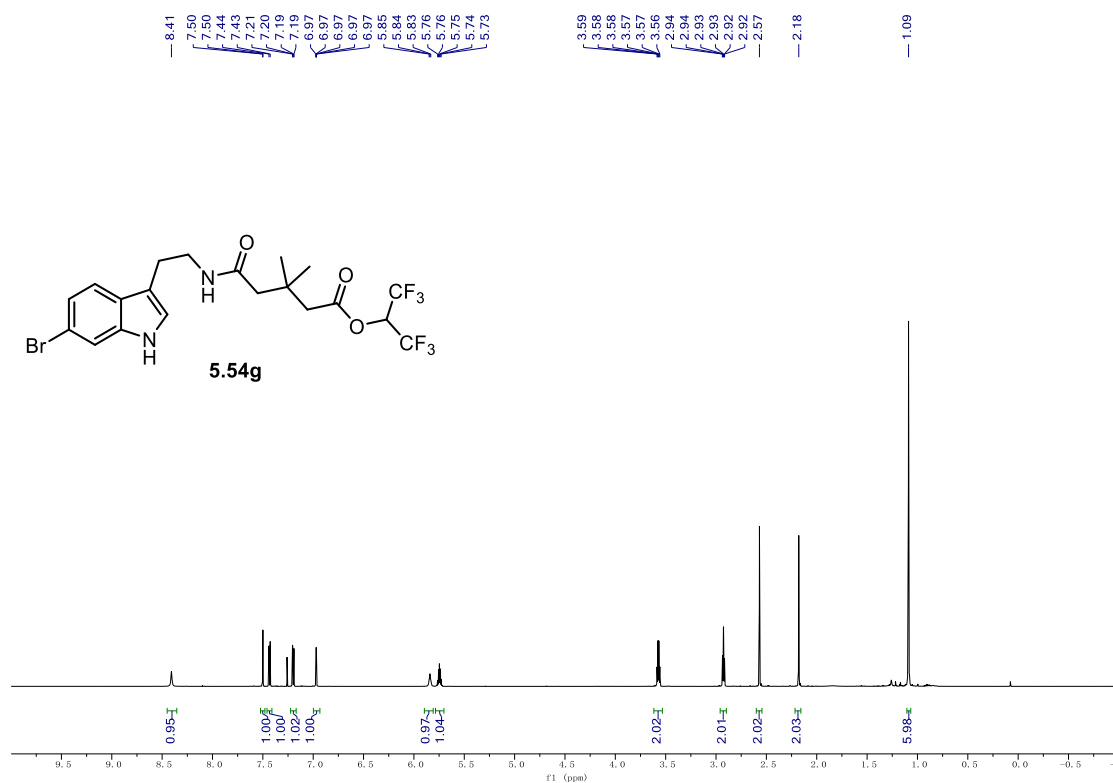
^1H NMR (700 MHz, CDCl_3) **5.54f**.



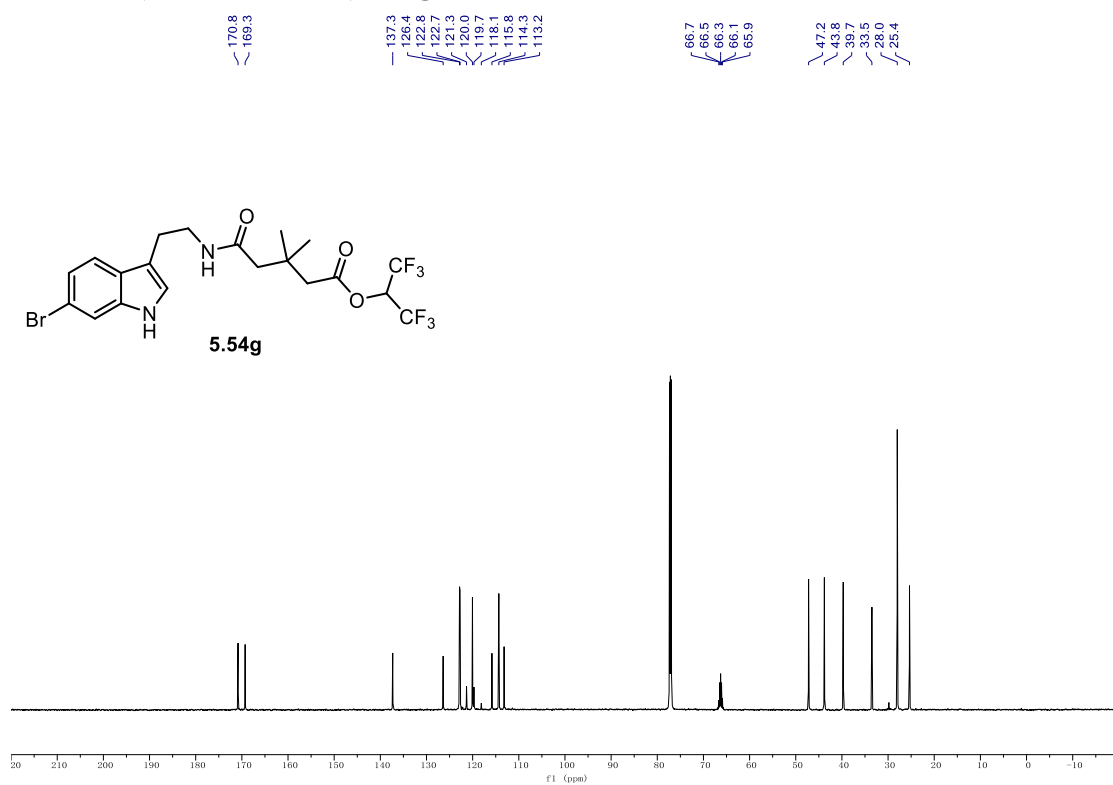
^{13}C NMR (176 MHz, CDCl_3) 5.54f. **^{19}F NMR (376 MHz, CDCl_3) of 5.54f.**

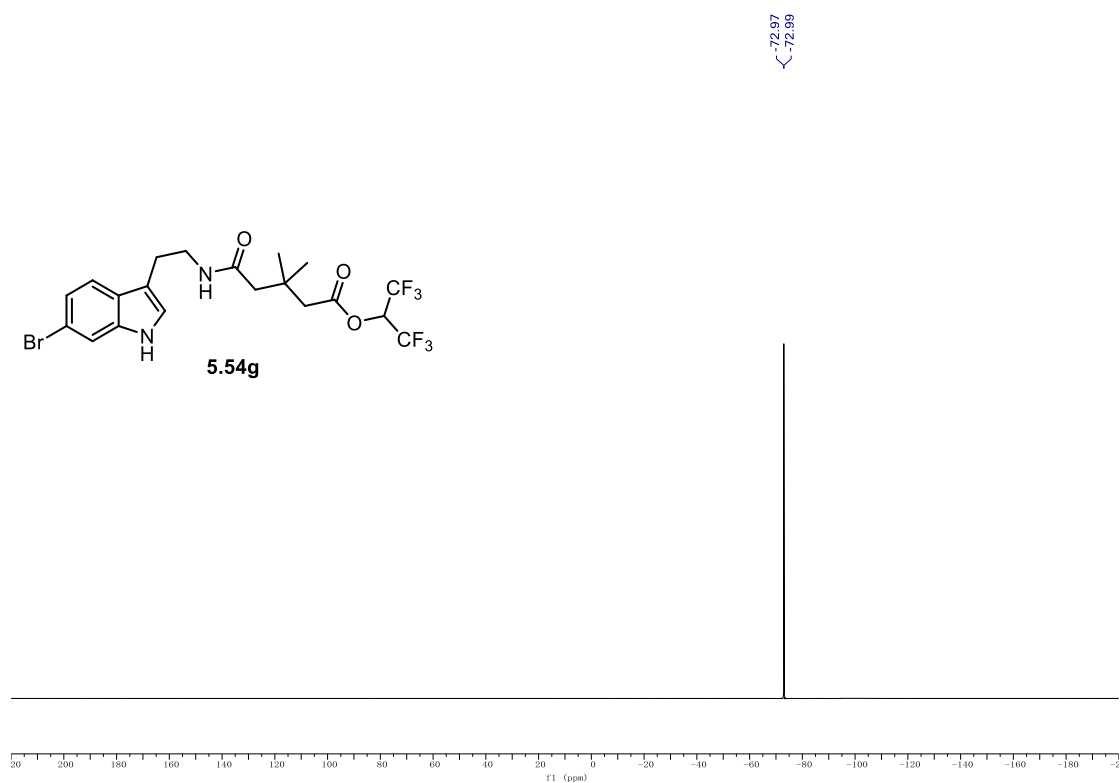
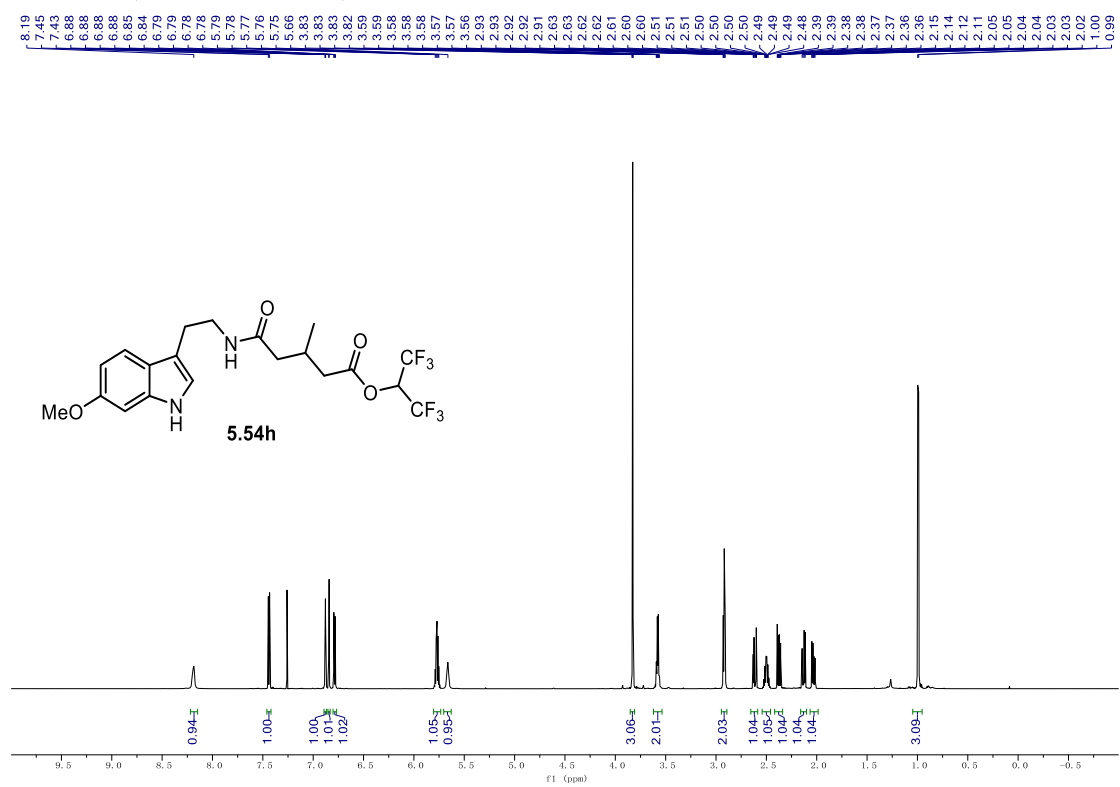
9.1. NMR Spectra

¹H NMR (700 MHz, CDCl₃) **5.54g**.



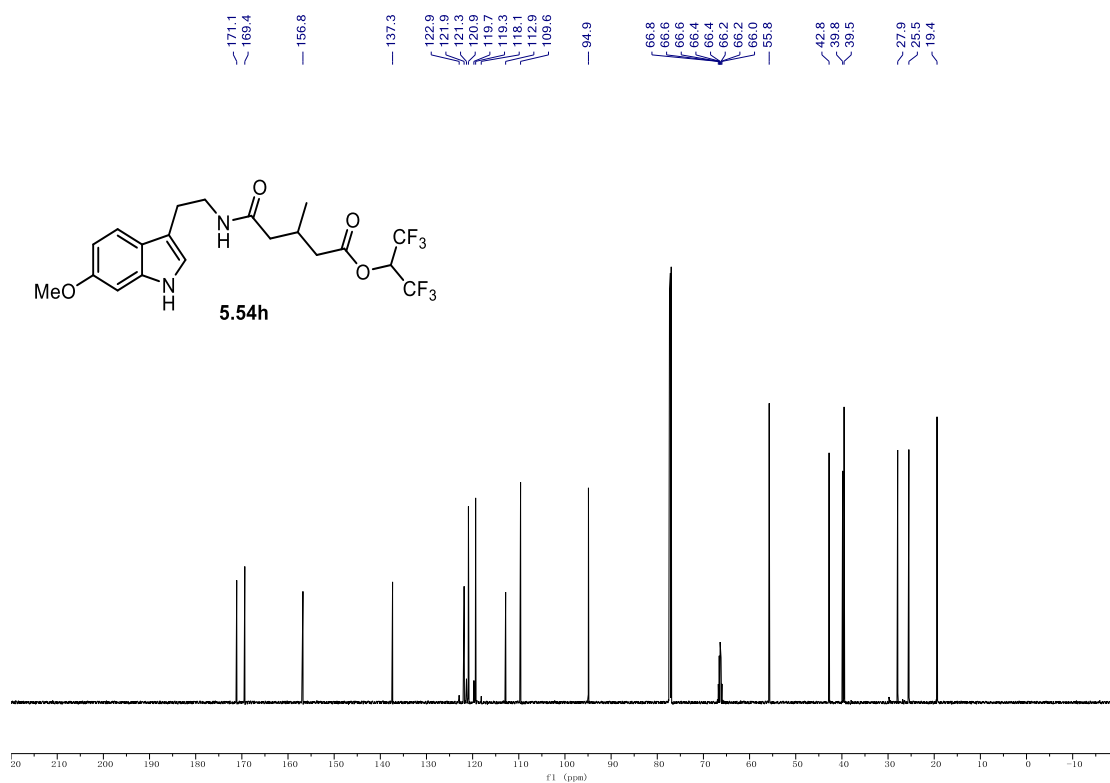
¹³C NMR (176 MHz, CDCl₃) **5.54g**.



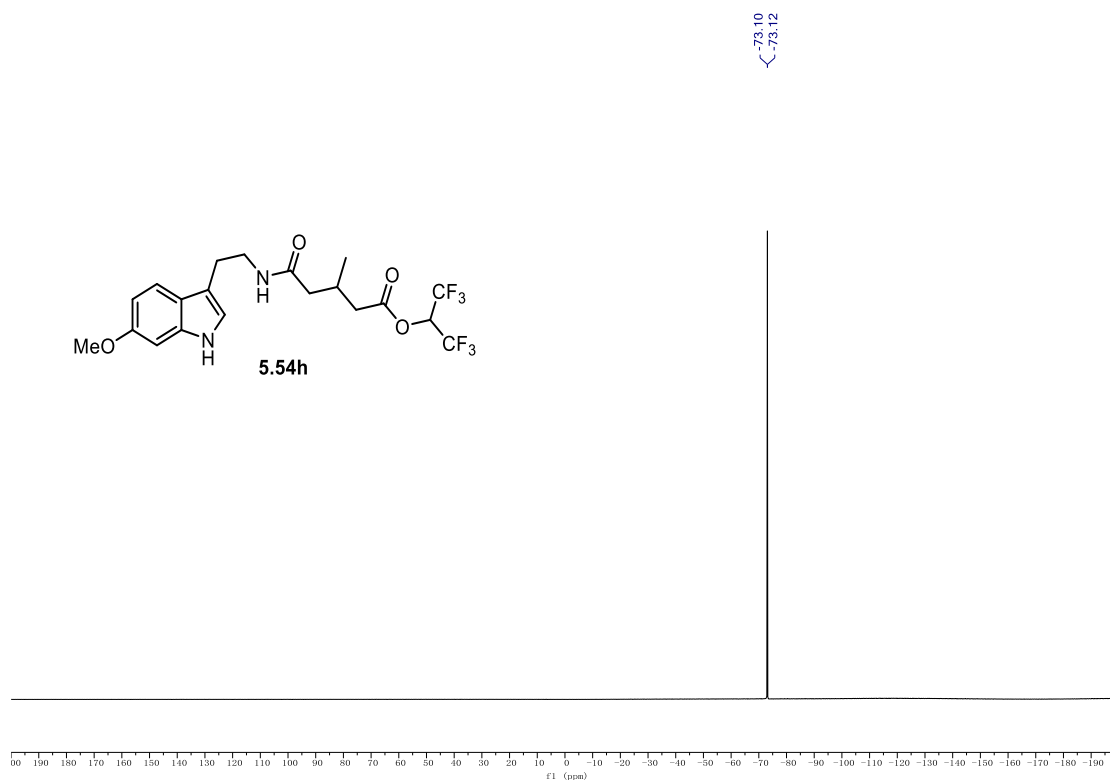
^{19}F NMR (471 MHz, CDCl_3) of **5.54g**. ^1H NMR (700 MHz, CDCl_3) of **5.54h**.

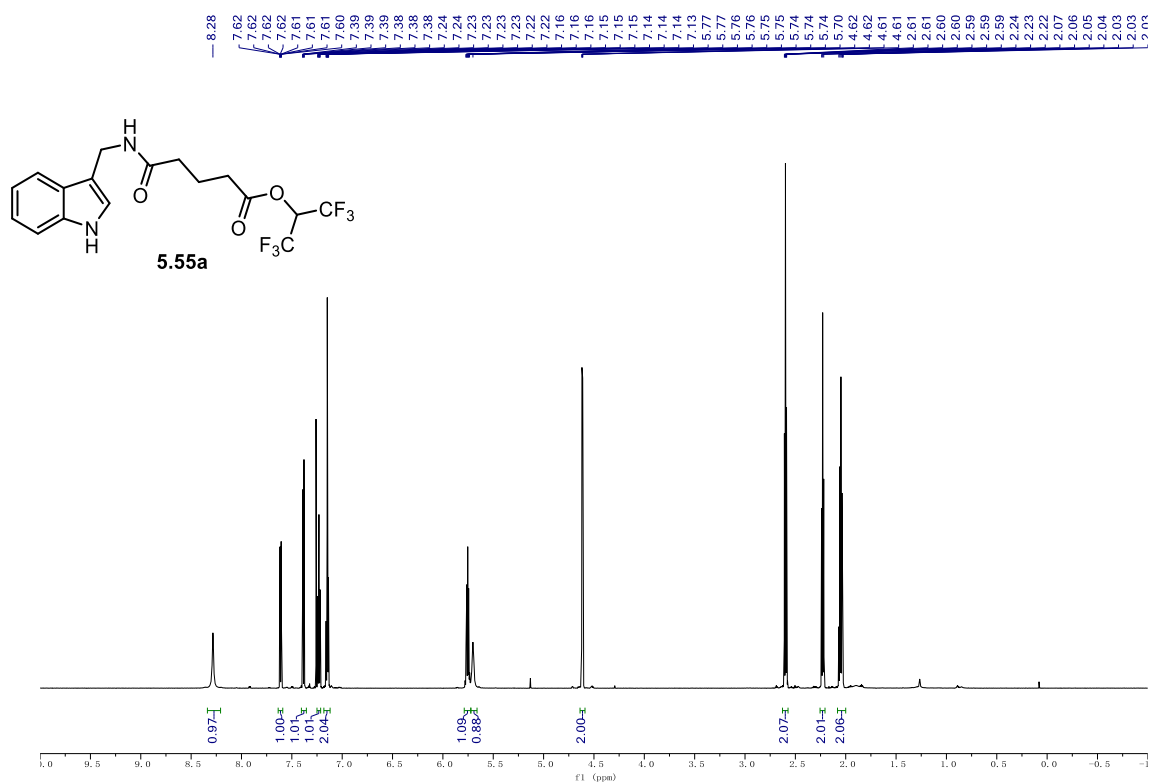
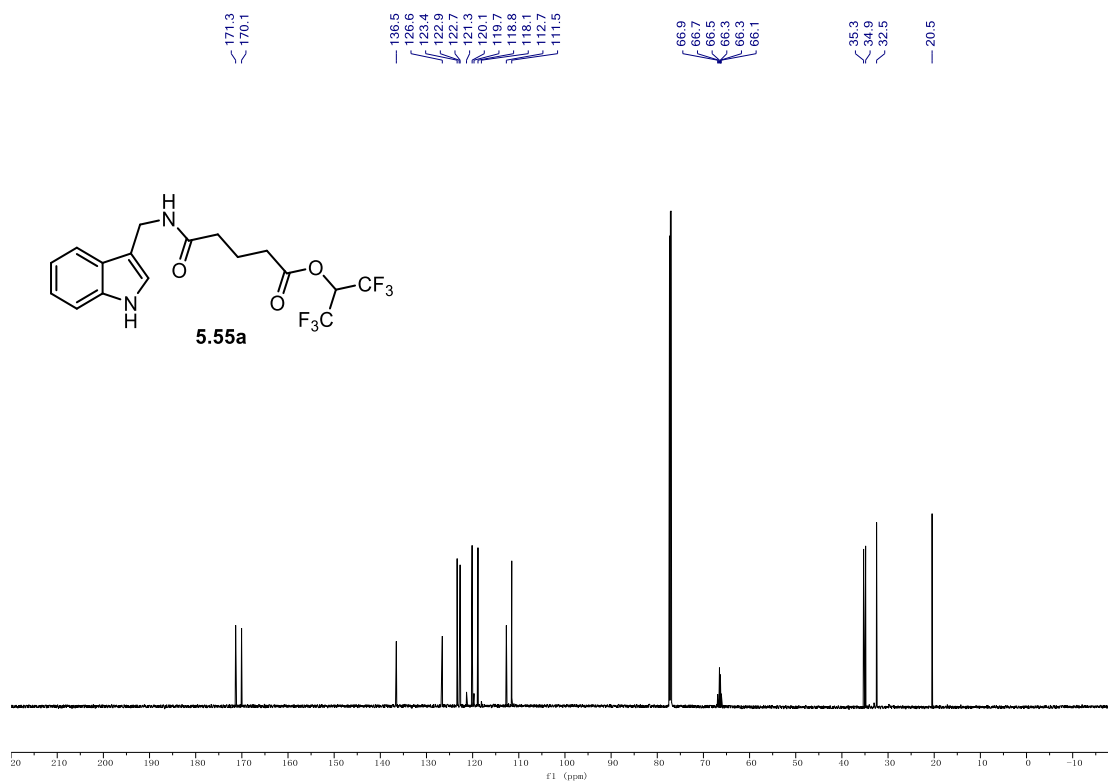
9.1. NMR Spectra

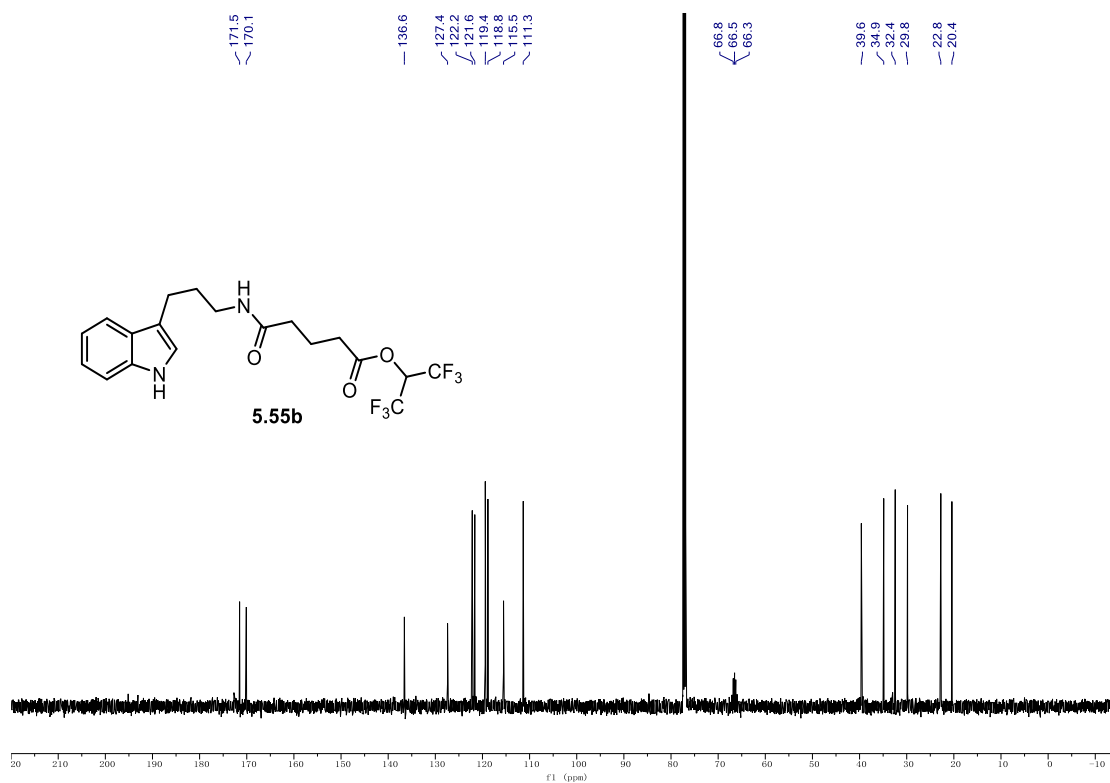
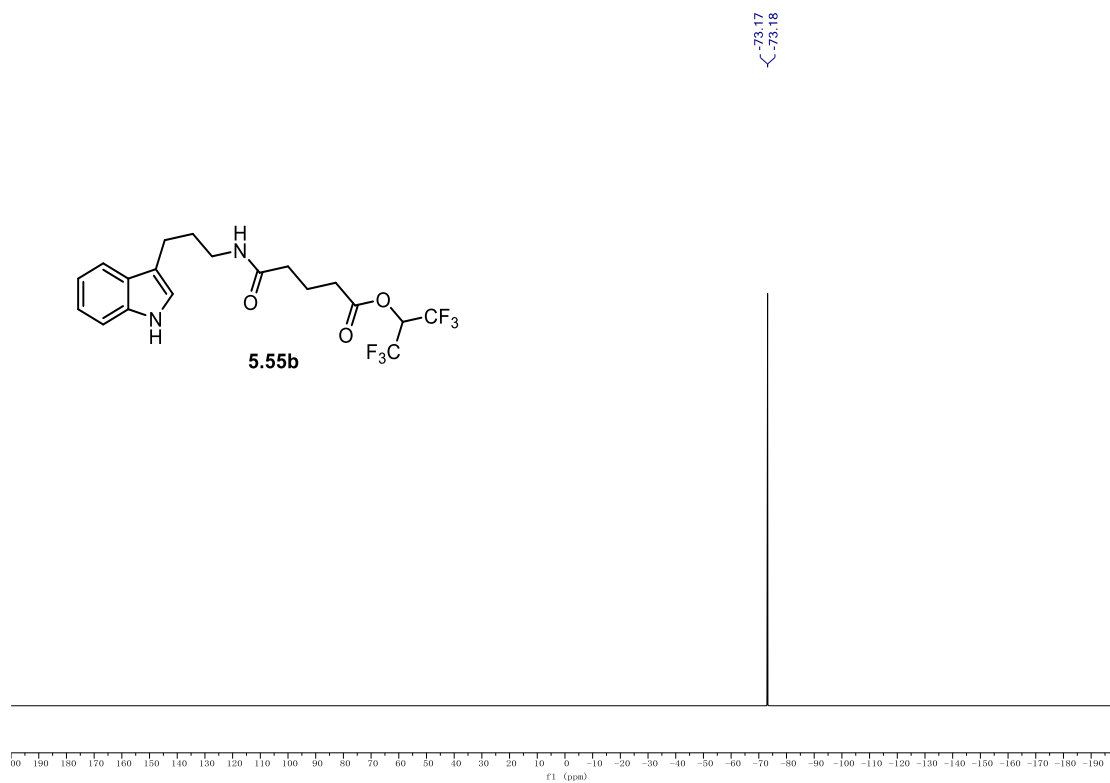
¹³C NMR (176 MHz, CDCl₃) of **5.54h**.



¹⁹F NMR (376 MHz, CDCl₃) of **5.54h**.

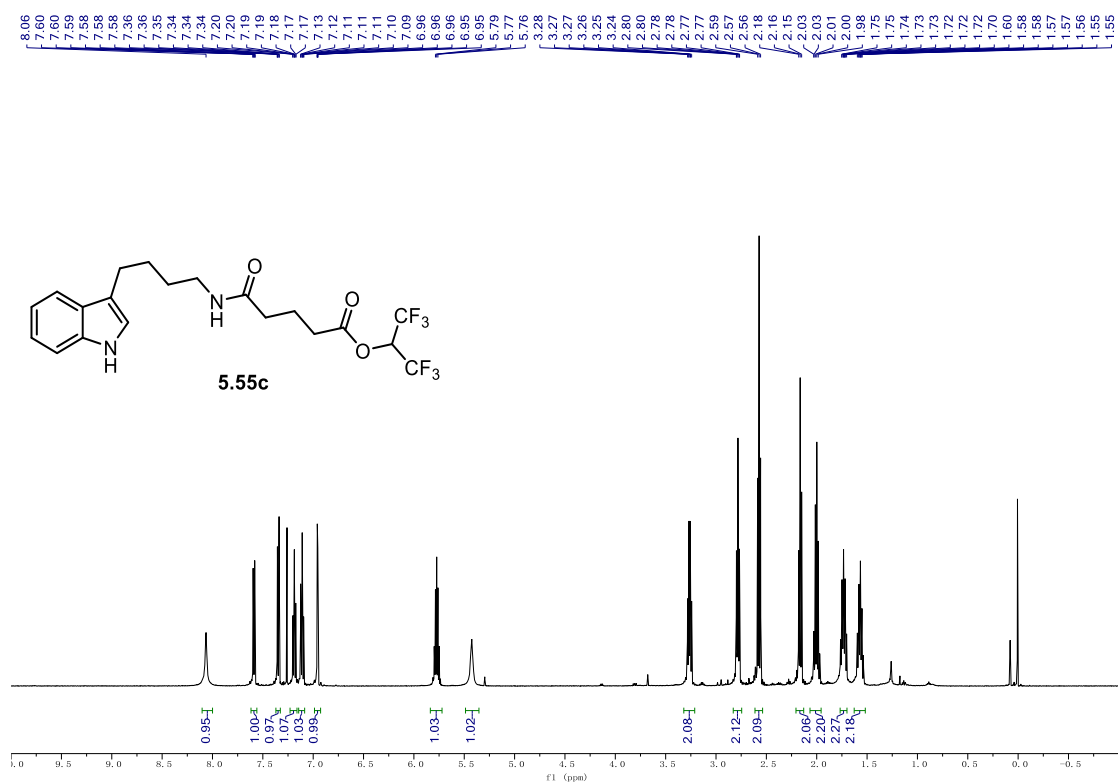


^1H NMR (700 MHz, CDCl_3) of **5.55a**. ^{13}C NMR (176 MHz, CDCl_3) of **5.55a**.

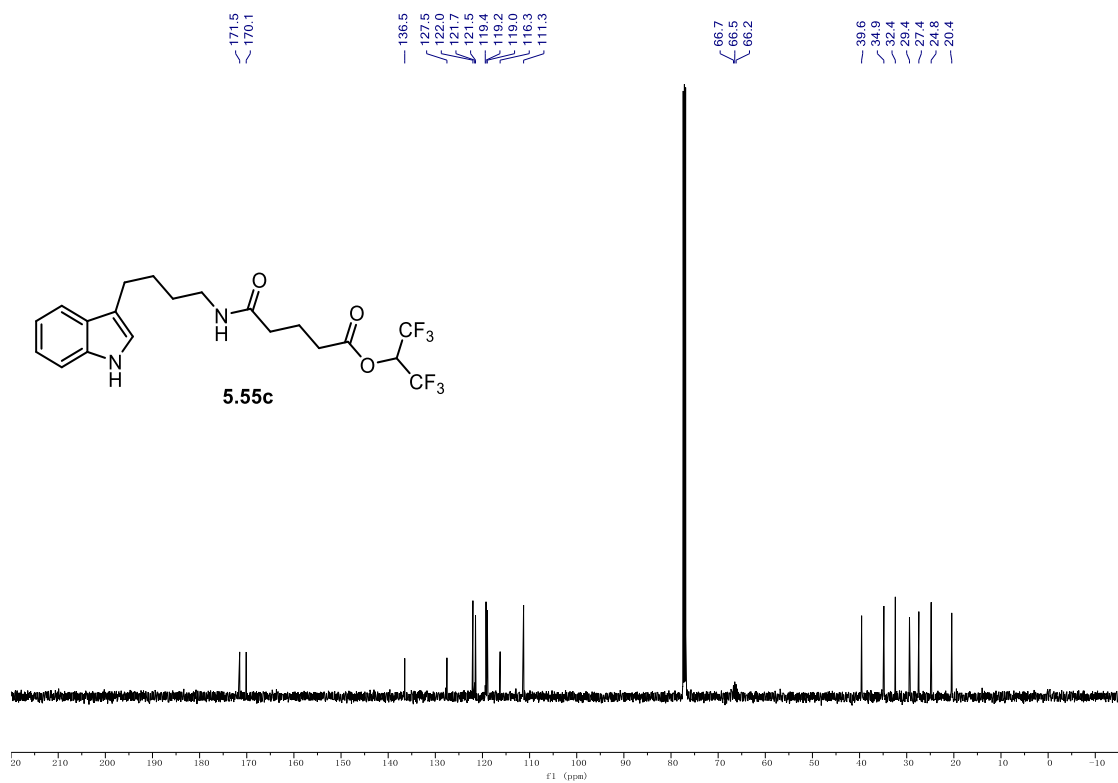
^{13}C NMR (126 MHz, CDCl_3) 5.55b. **^{19}F NMR (471 MHz, CDCl_3) 5.55b.**

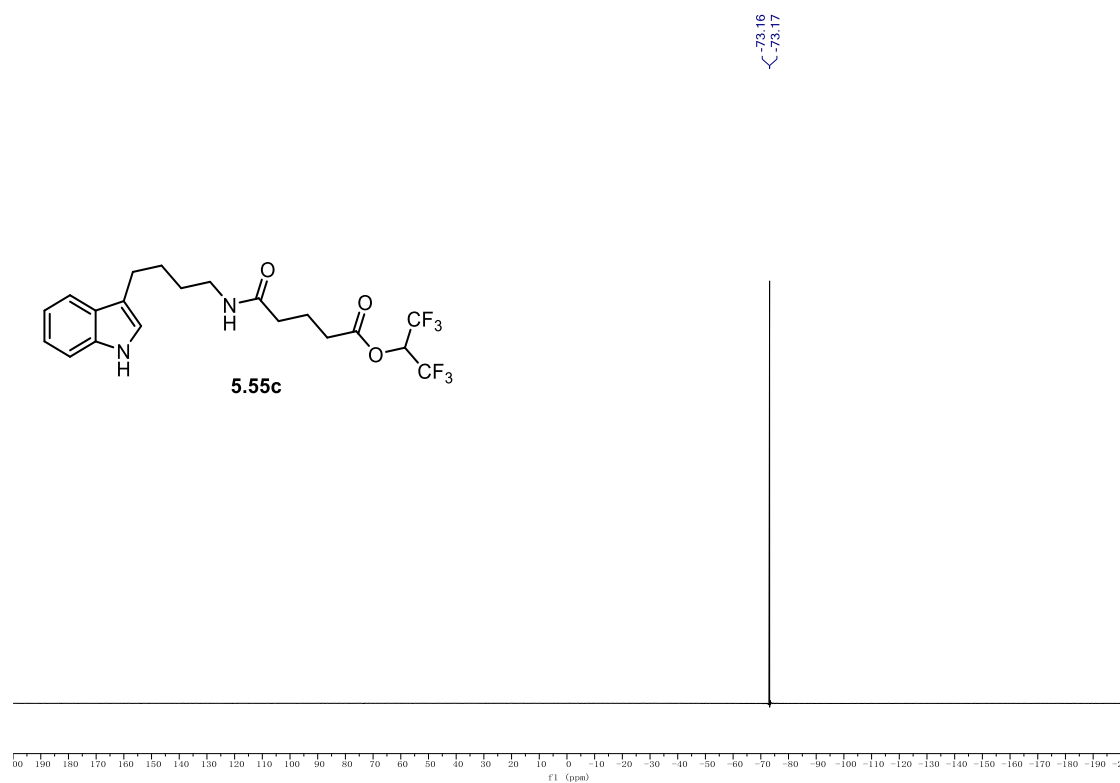
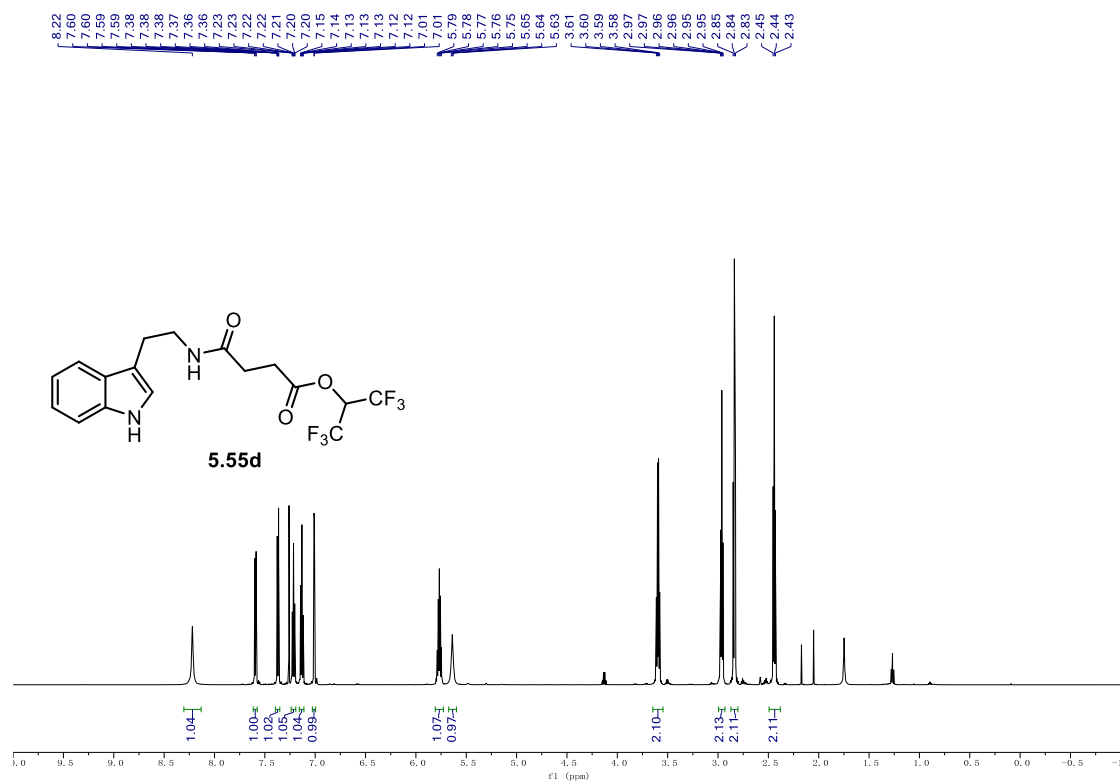
9.1. NMR Spectra

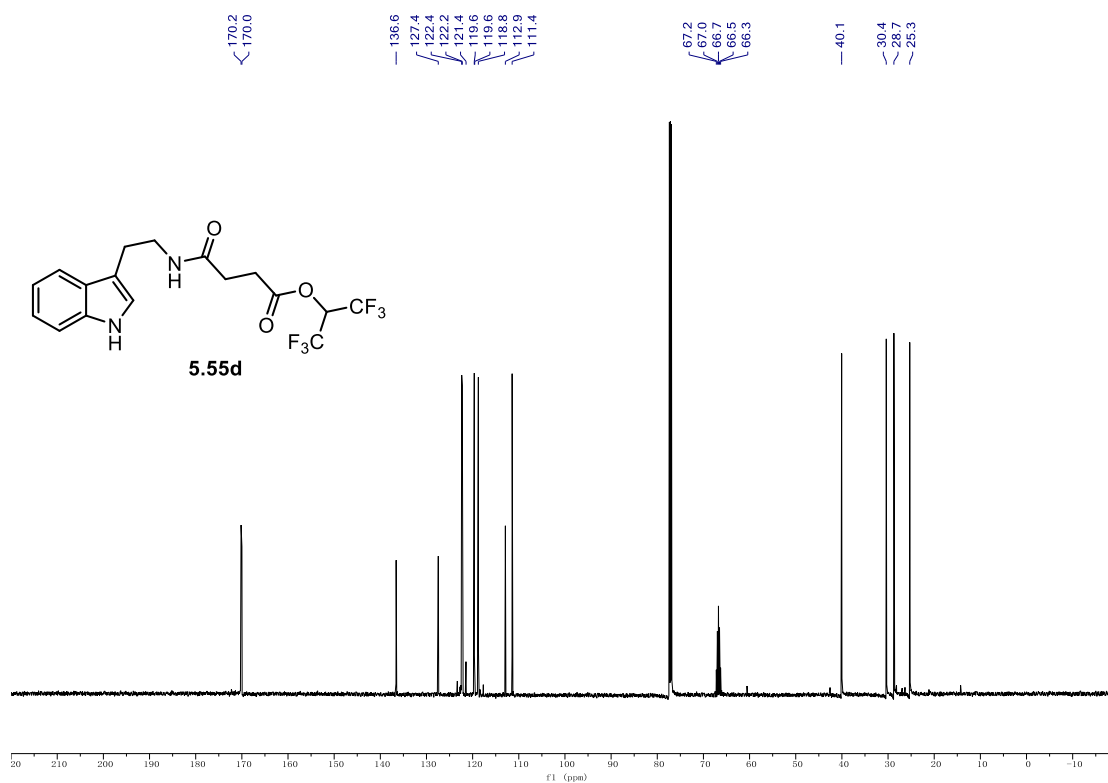
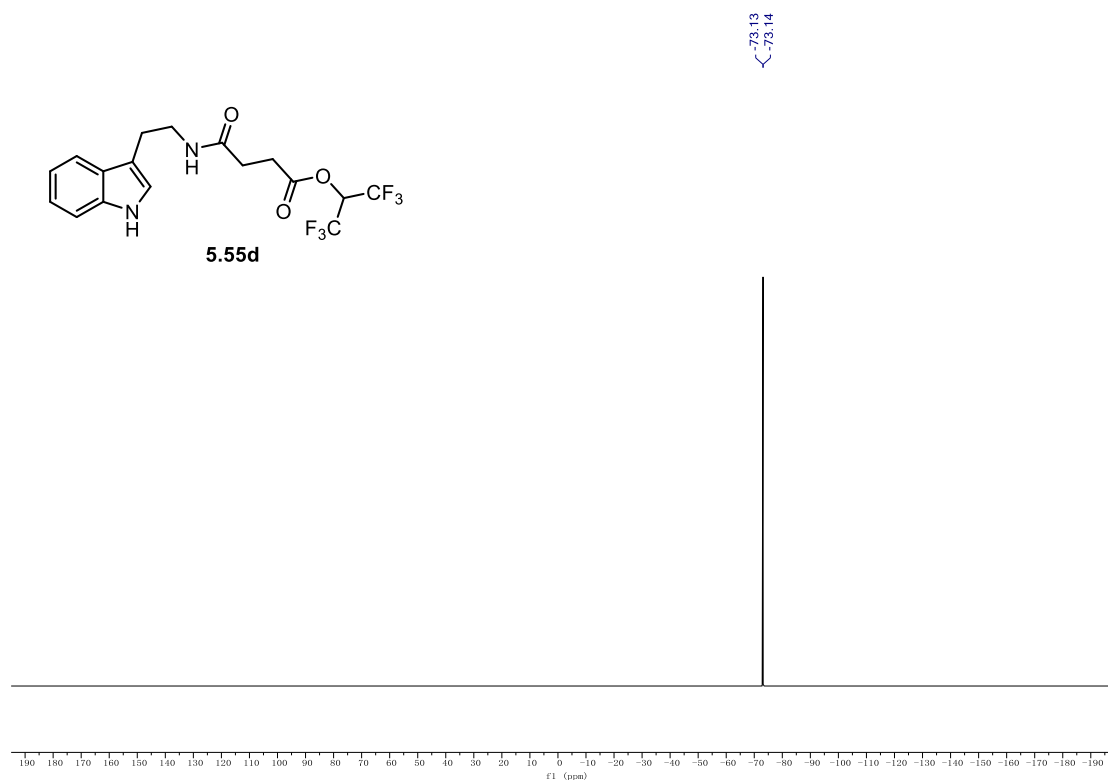
¹H NMR (500 MHz, CDCl₃) **5.55c**.

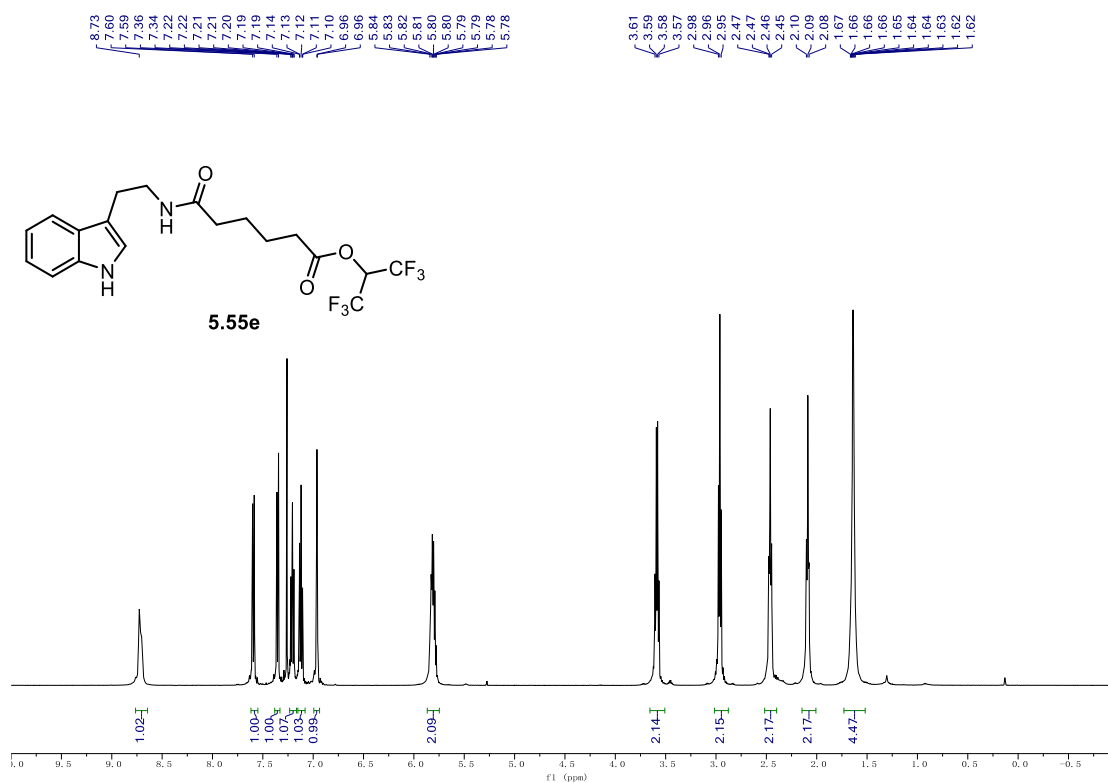
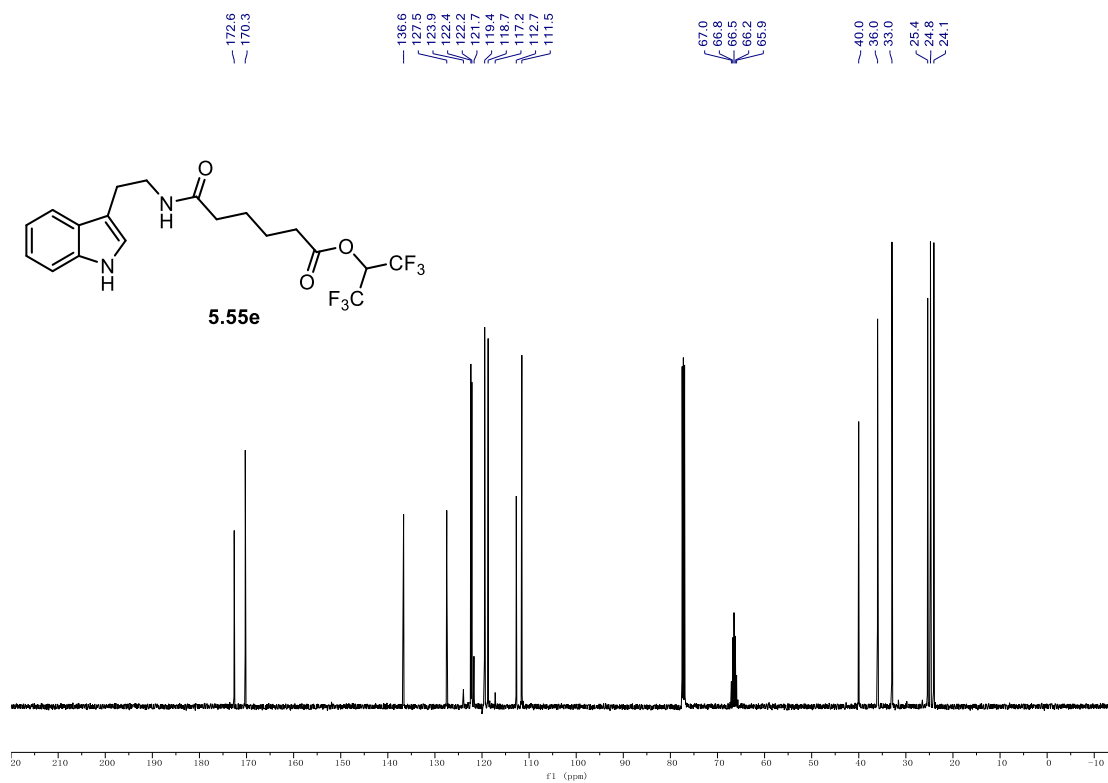


¹³C NMR (126 MHz, CDCl₃) **5.55c**.



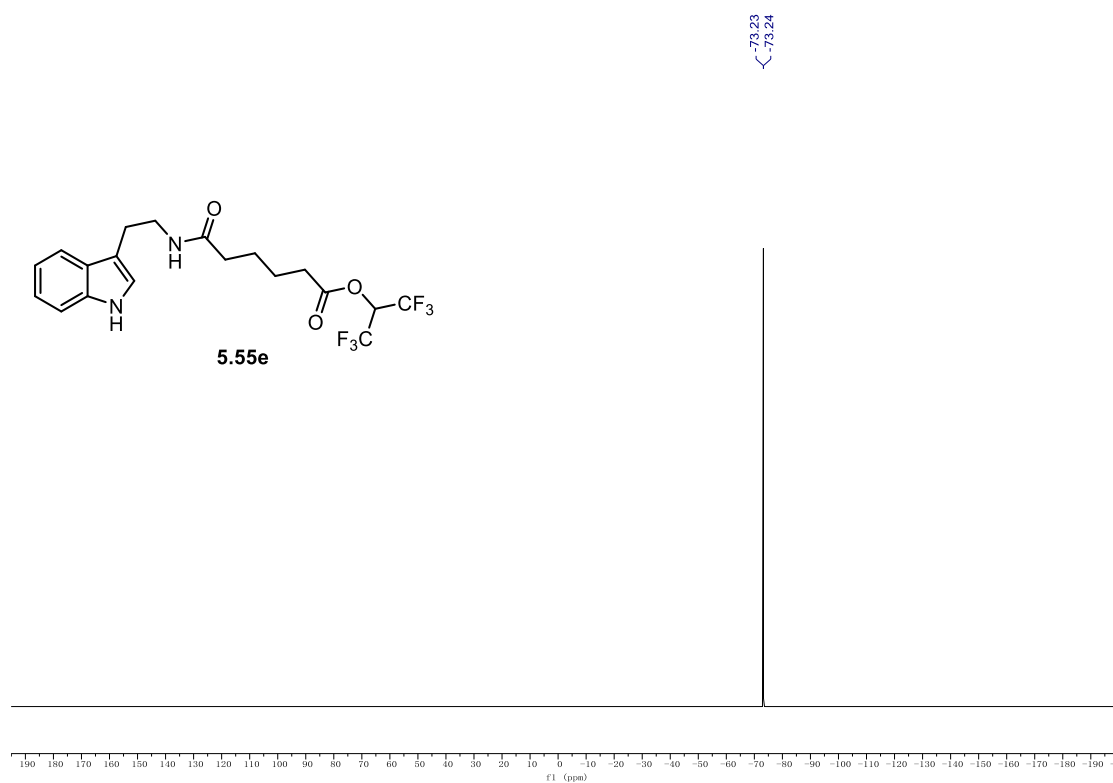
^{19}F NMR (471 MHz, CDCl_3) **5.55c**. ^1H NMR (600 MHz, CDCl_3) of **5.55d**.

^{13}C NMR (151 MHz, CDCl_3) of **5.55d**. ^{19}F NMR (565 MHz, CDCl_3) of **5.55d**.

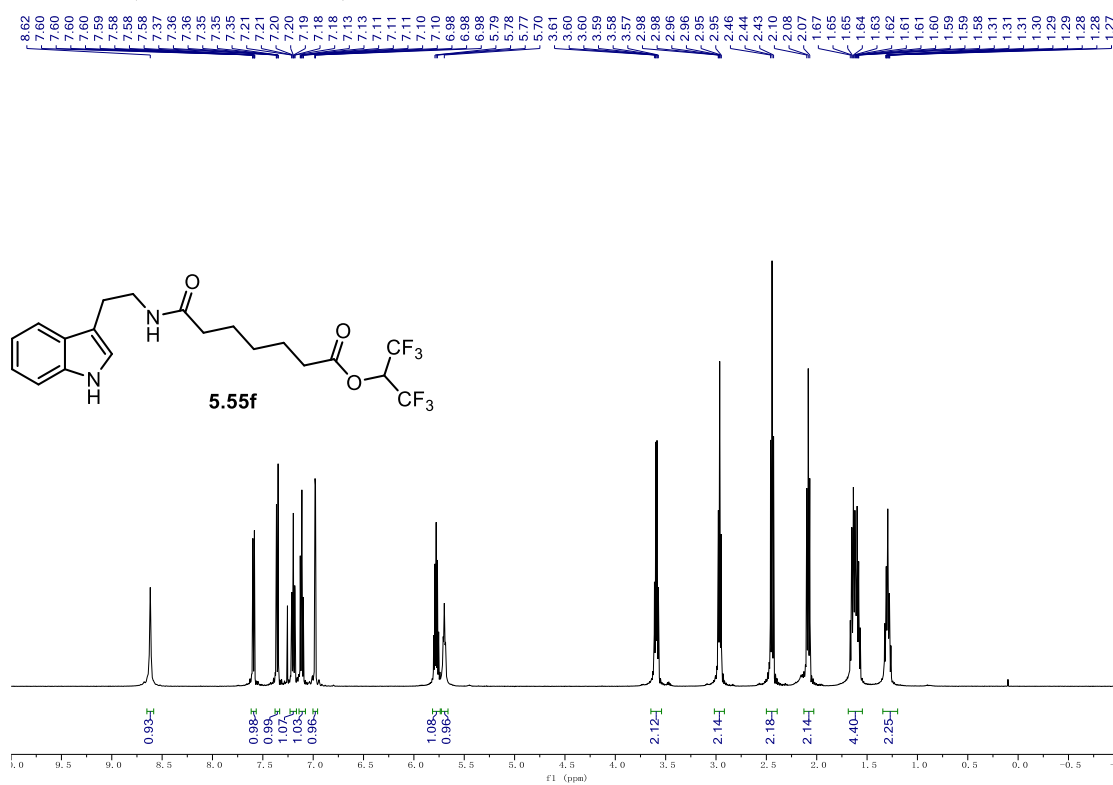
^1H NMR (500 MHz, CDCl_3) 5.55e. **^{13}C NMR (126 MHz, CDCl_3) 5.55e.**

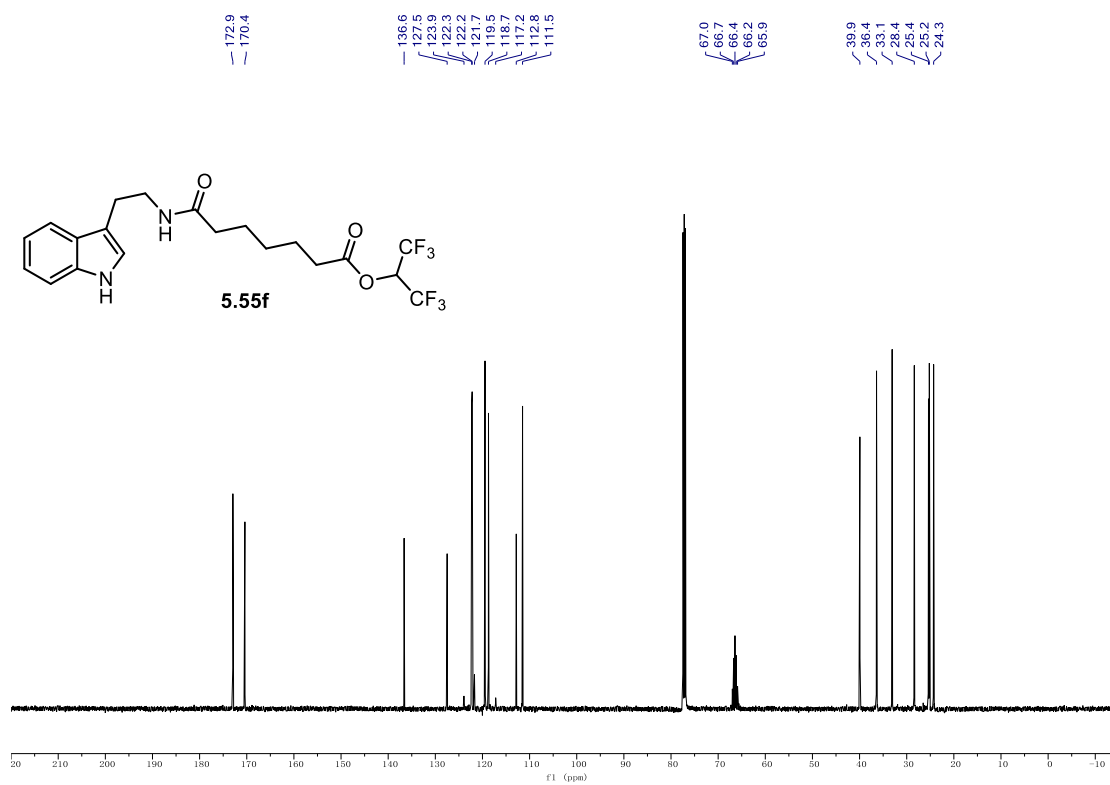
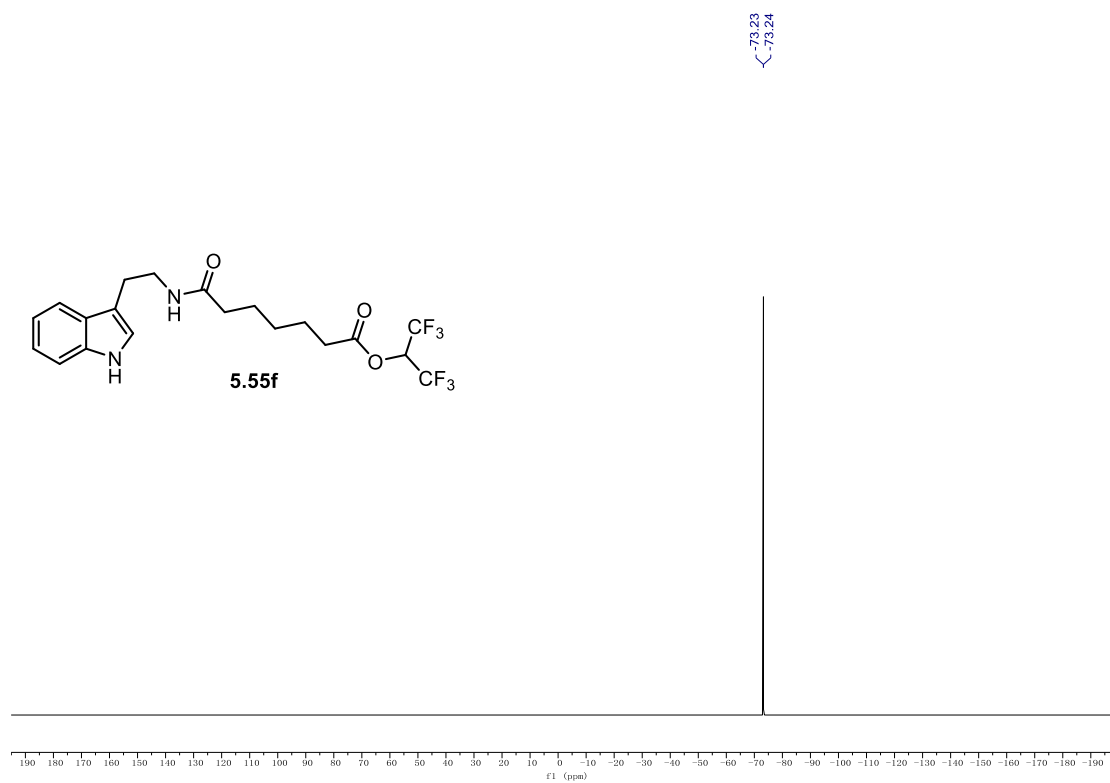
9.1. NMR Spectra

^{19}F NMR (565 MHz, CDCl_3) **5.55e**.



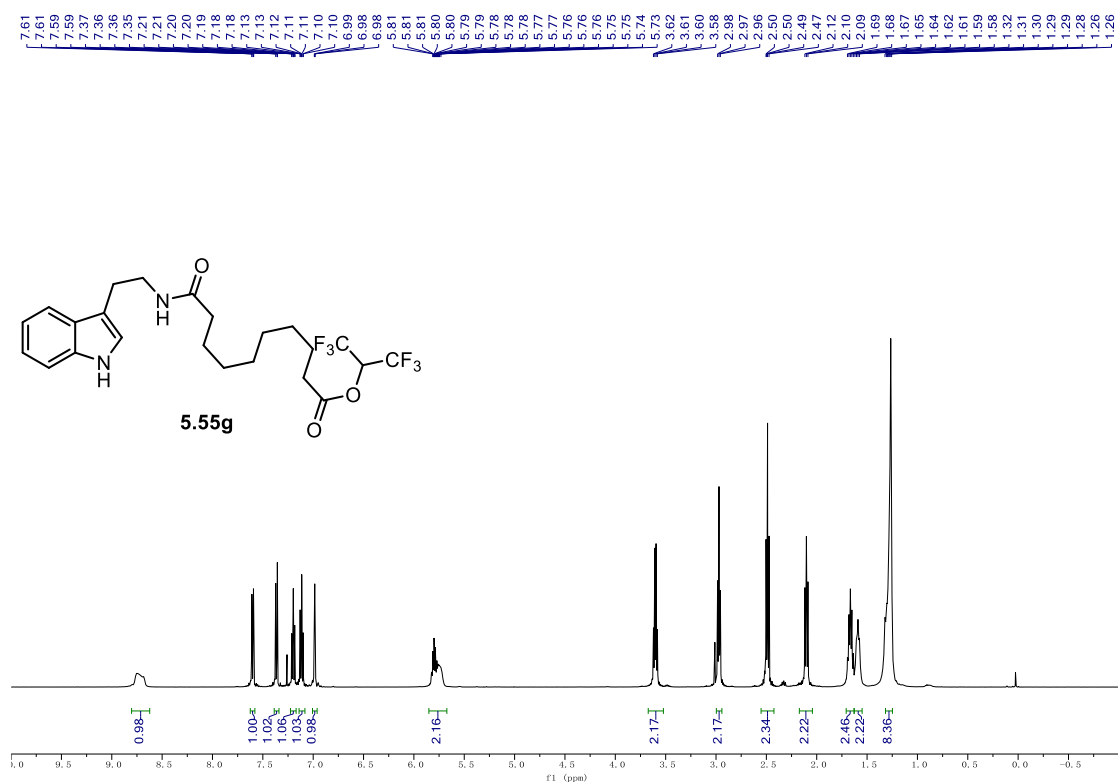
^1H NMR (500 MHz, CDCl_3) **5.55f**.



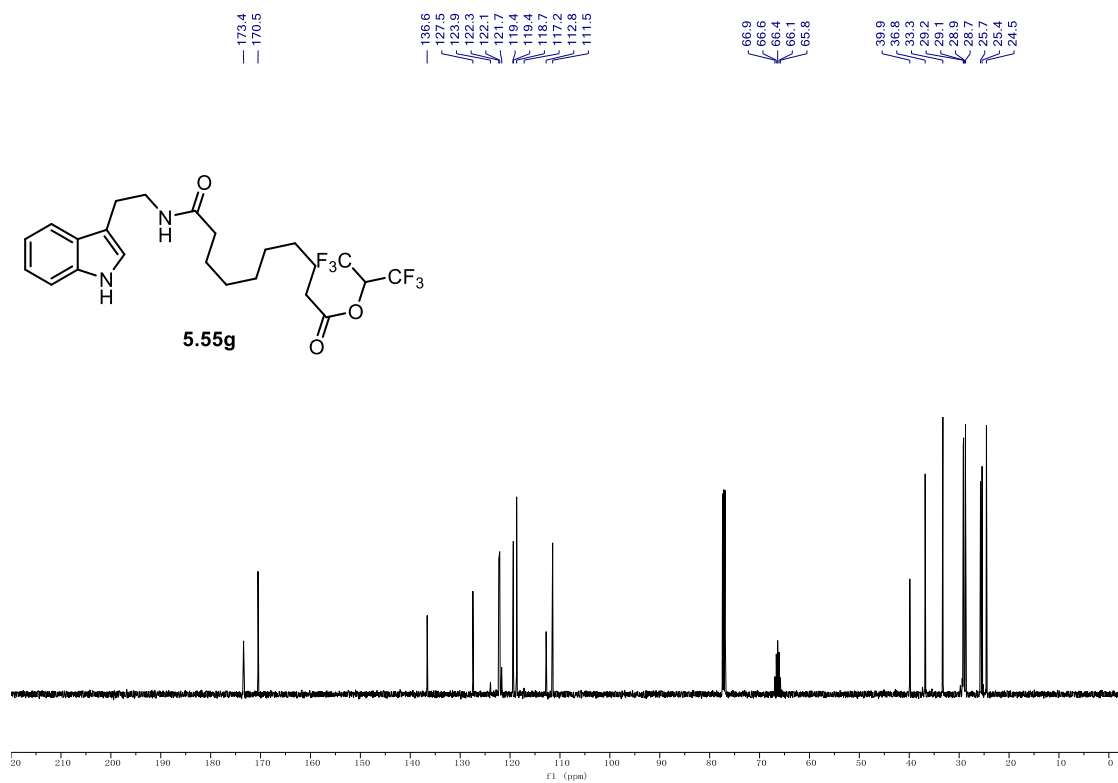
^{13}C NMR (126 MHz, CDCl_3) **5.55f**. ^{19}F NMR (565 MHz, CDCl_3) **5.55f**.

9.1. NMR Spectra

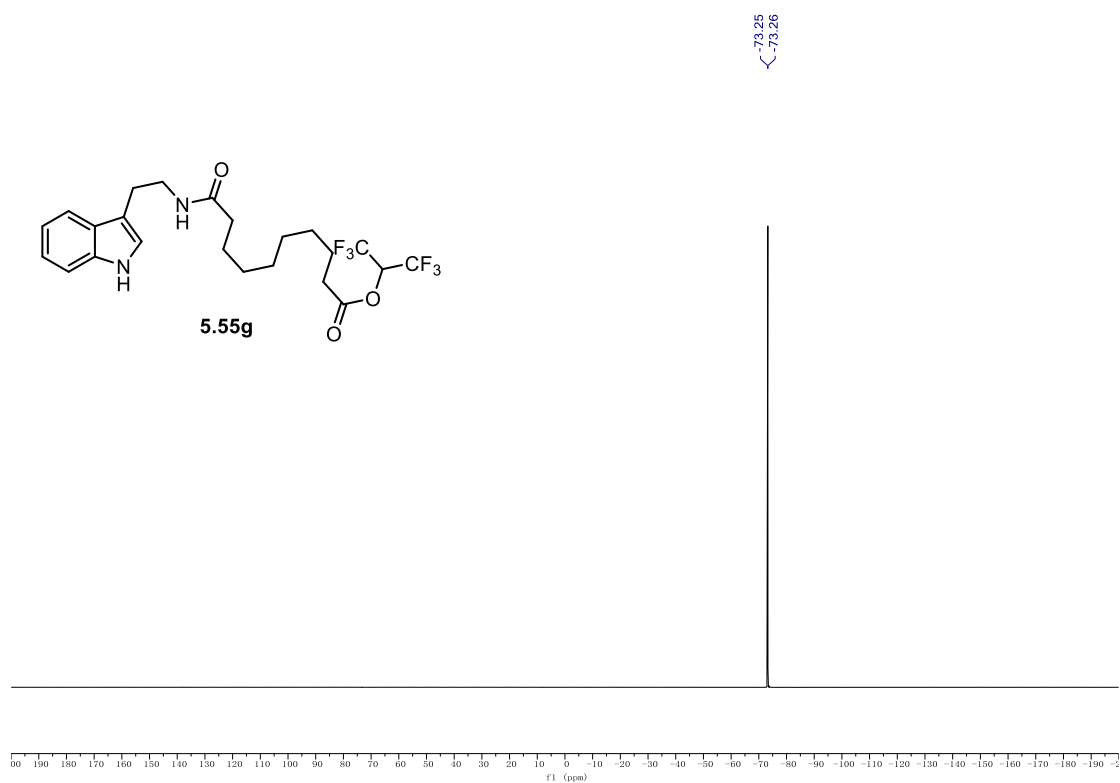
¹H NMR (500 MHz, CDCl₃) of **5.55g**.



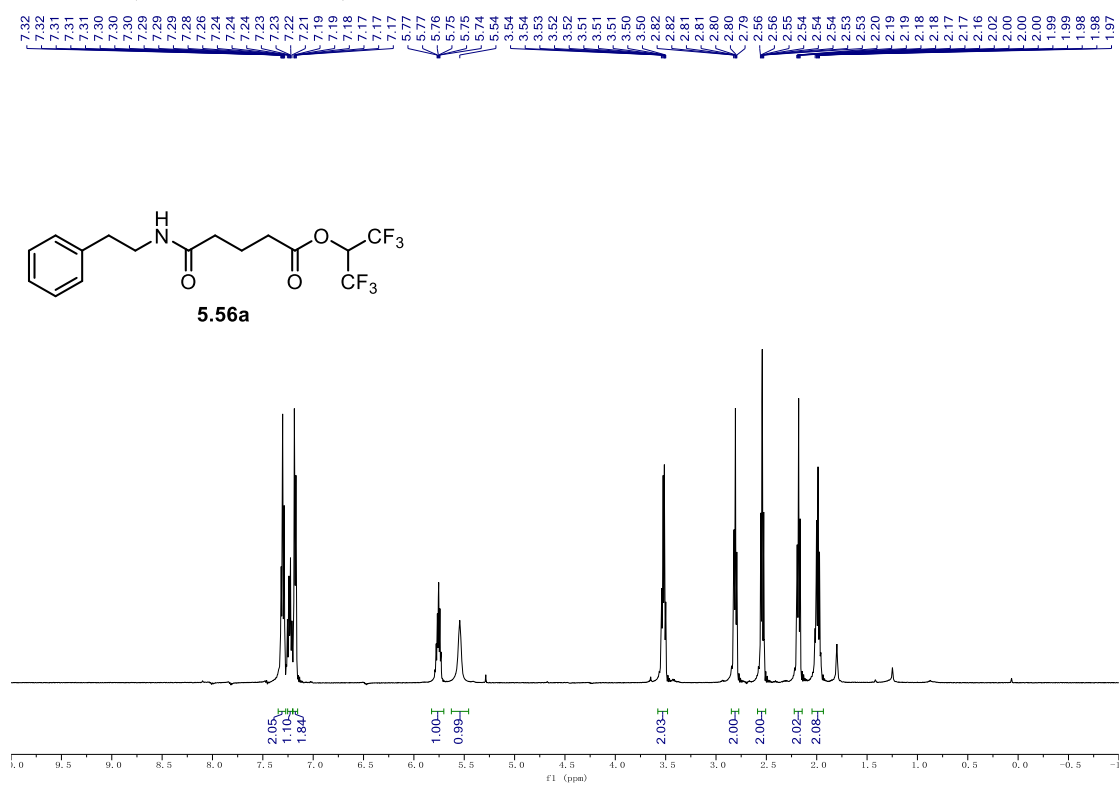
¹³C NMR (126 MHz, CDCl₃) of **5.55g**.



^{19}F NMR (471 MHz, CDCl_3) of **5.55g**.

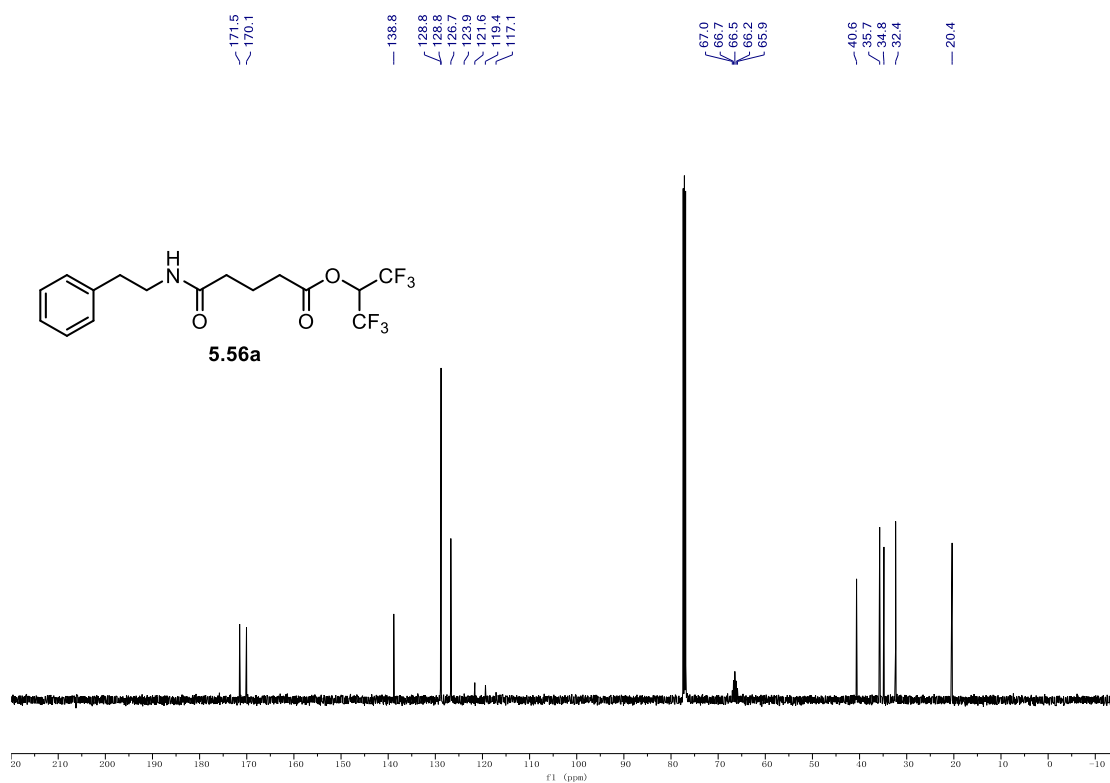


^1H NMR (500 MHz, CDCl_3) of **5.56a**.

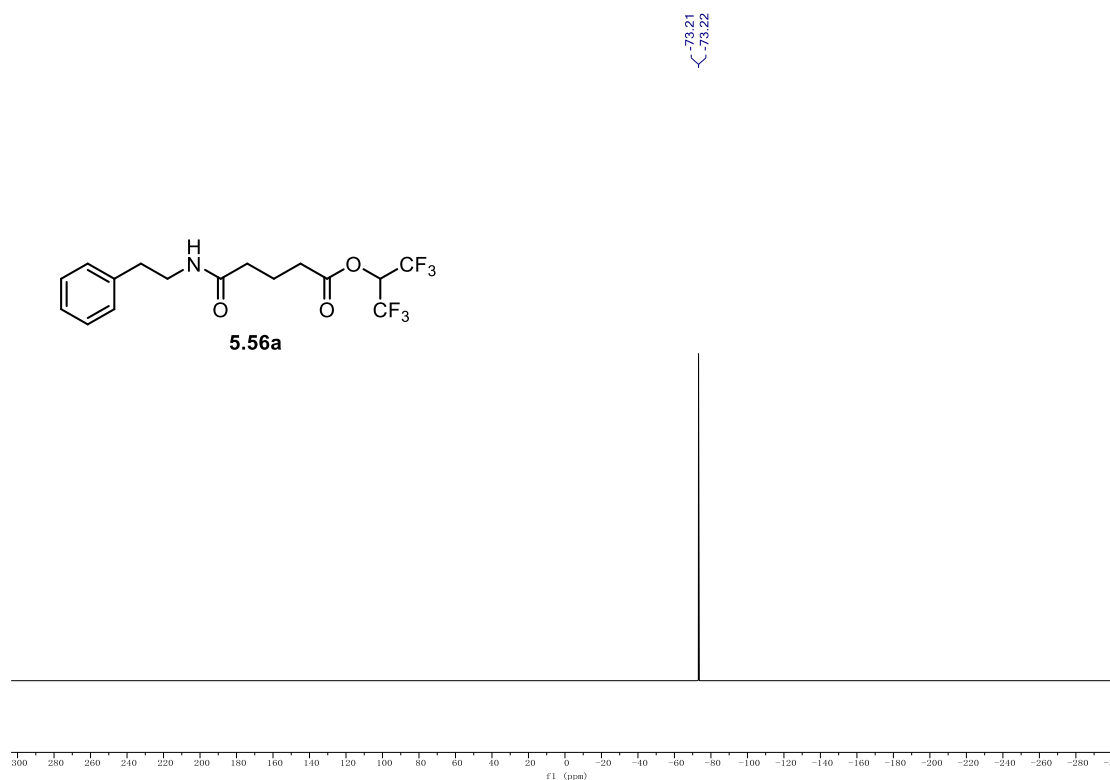


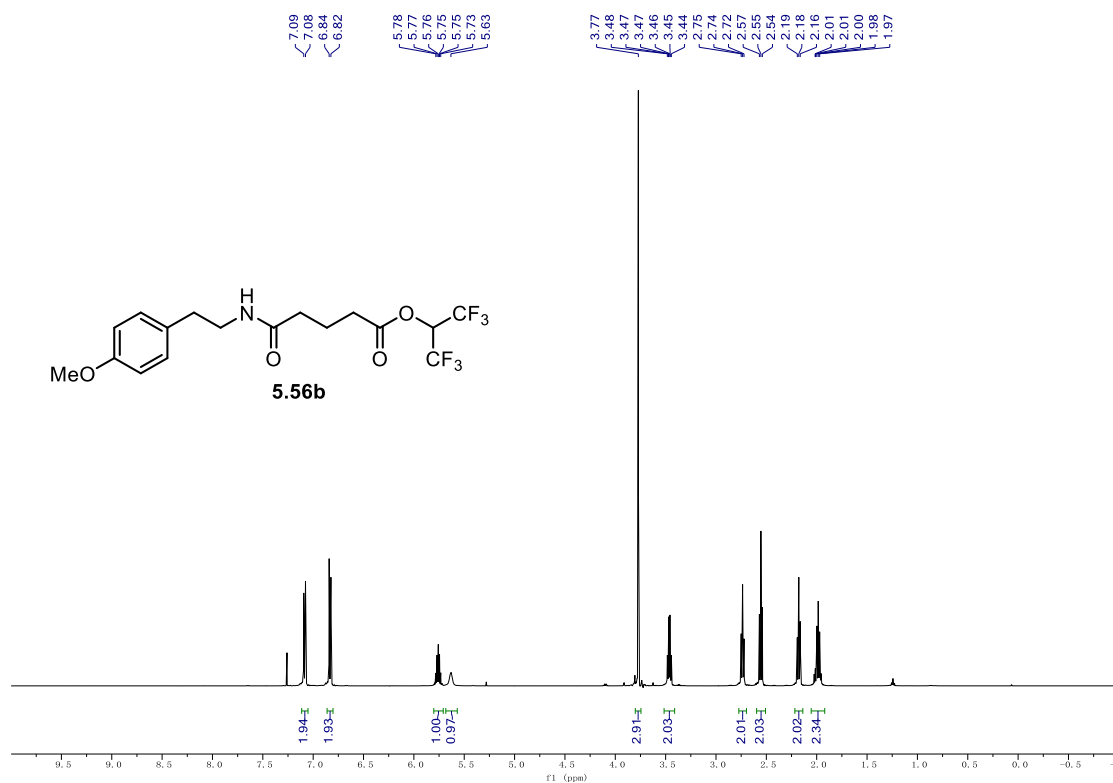
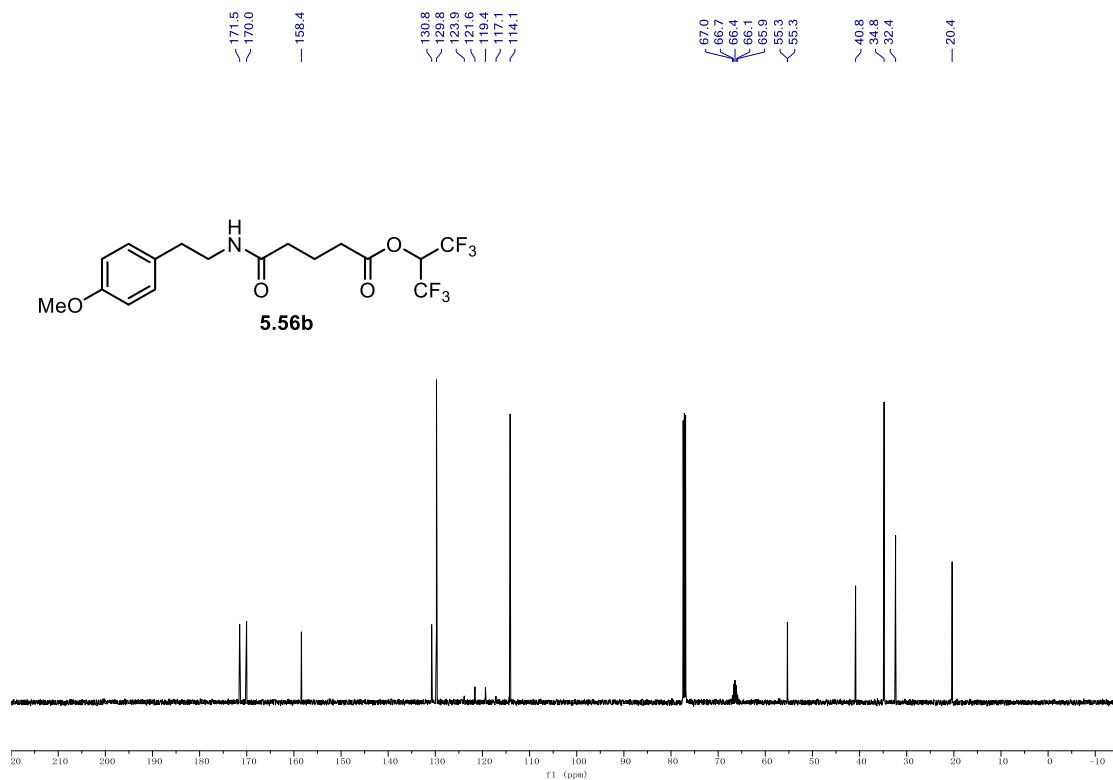
9.1. NMR Spectra

^{13}C NMR (126 MHz, CDCl_3) of **5.56a**.



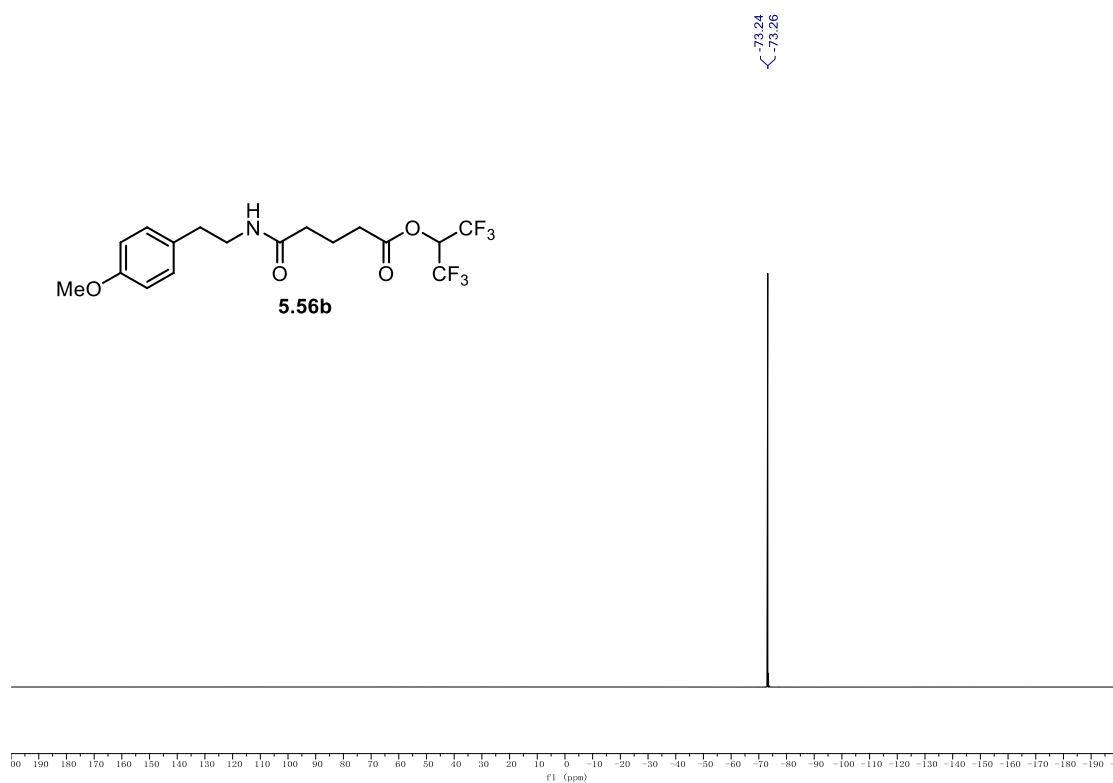
^{19}F NMR (471 MHz, CDCl_3) of **5.56a**.



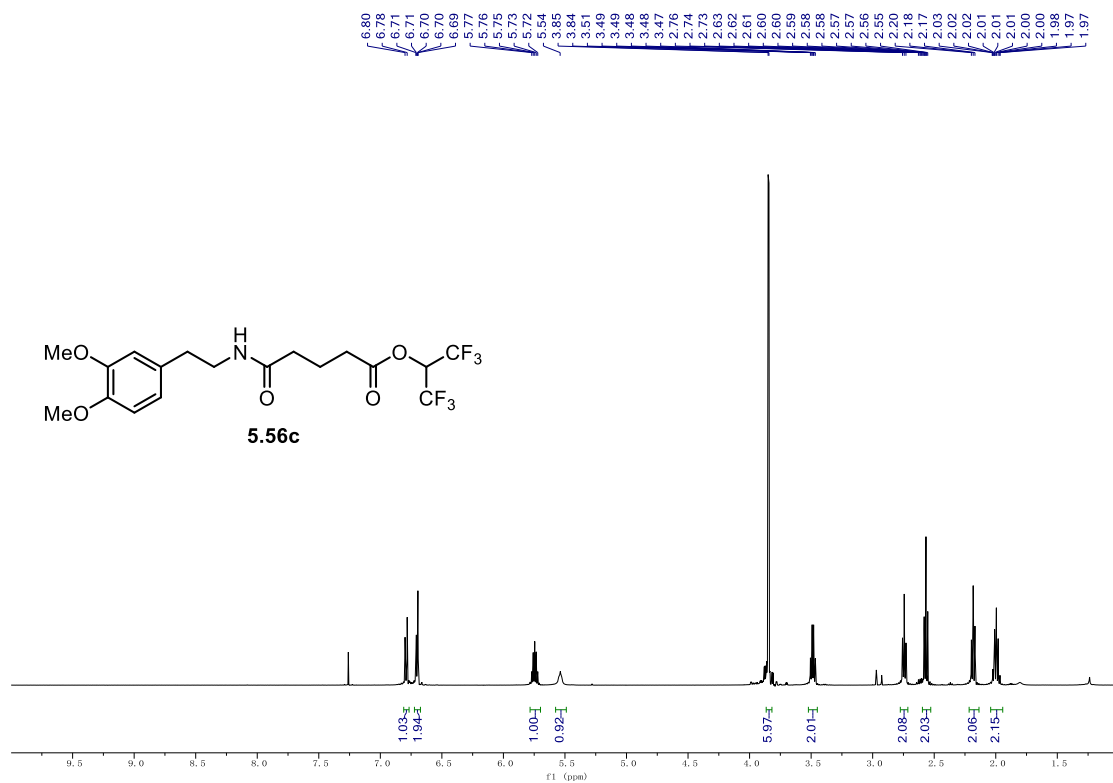
^1H NMR (500 MHz, CDCl_3) of **5.56b**. ^{13}C NMR (126 MHz, CDCl_3) of **5.56b**.

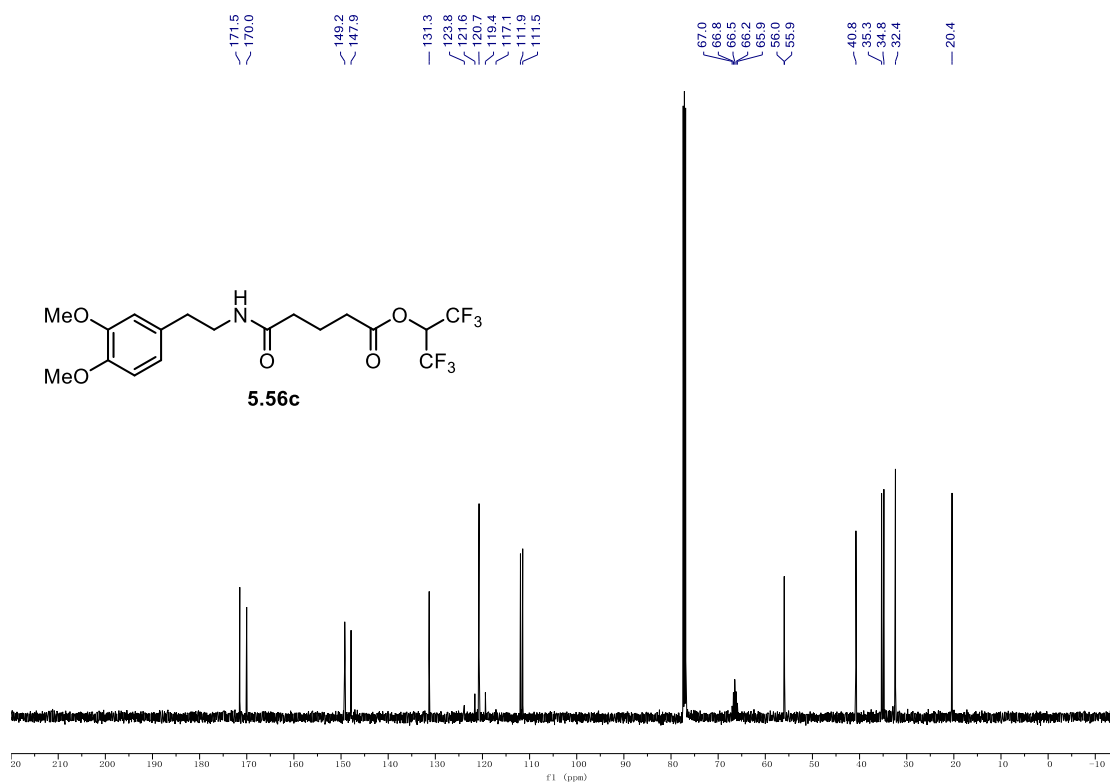
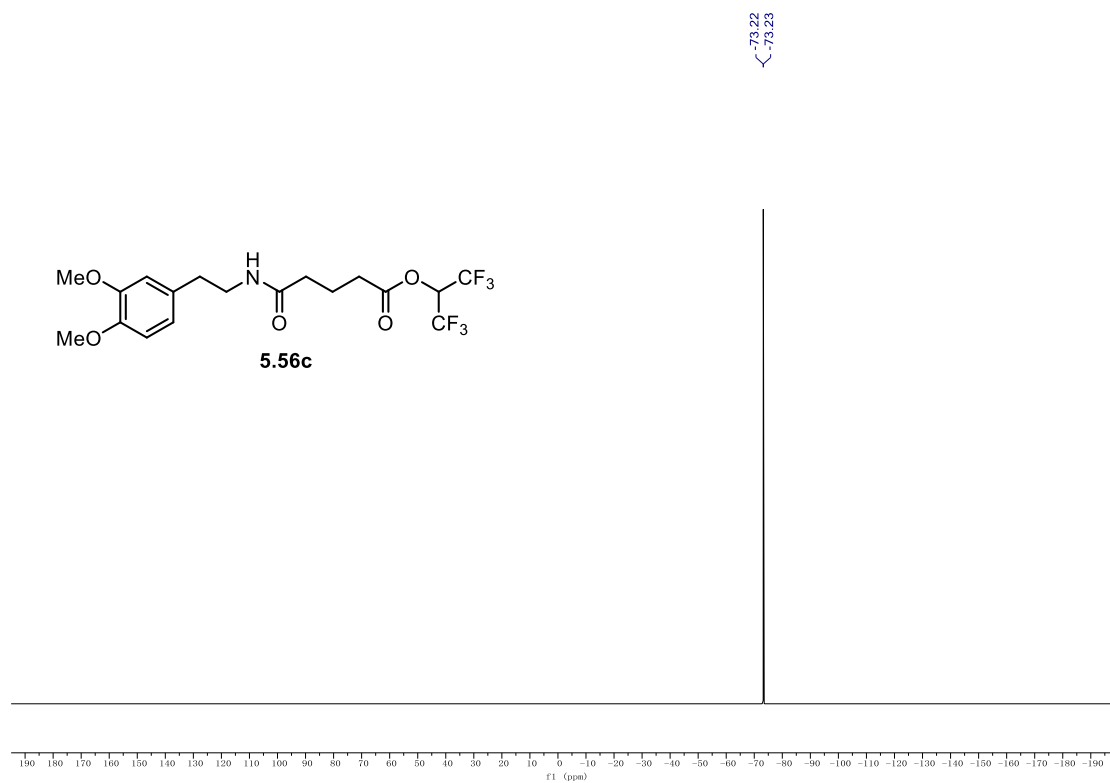
9.1. NMR Spectra

^{19}F NMR (471 MHz, CDCl_3) of **5.56b**.



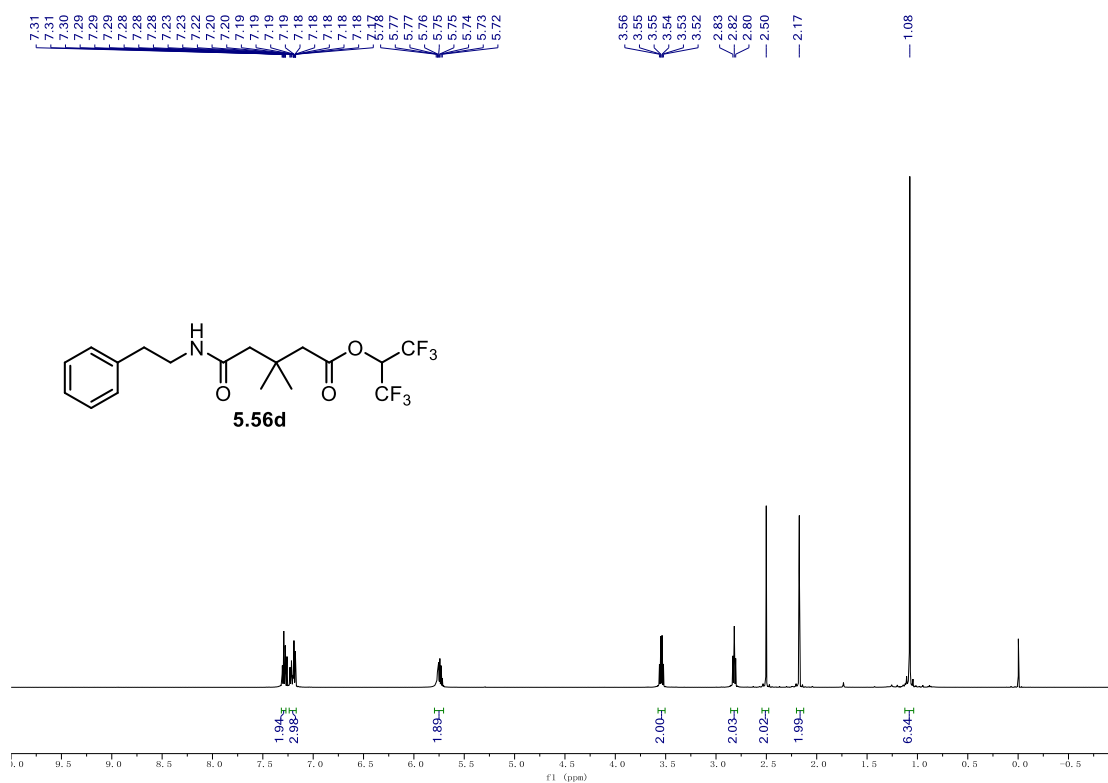
^1H NMR (500 MHz, CDCl_3) **5.56c**.



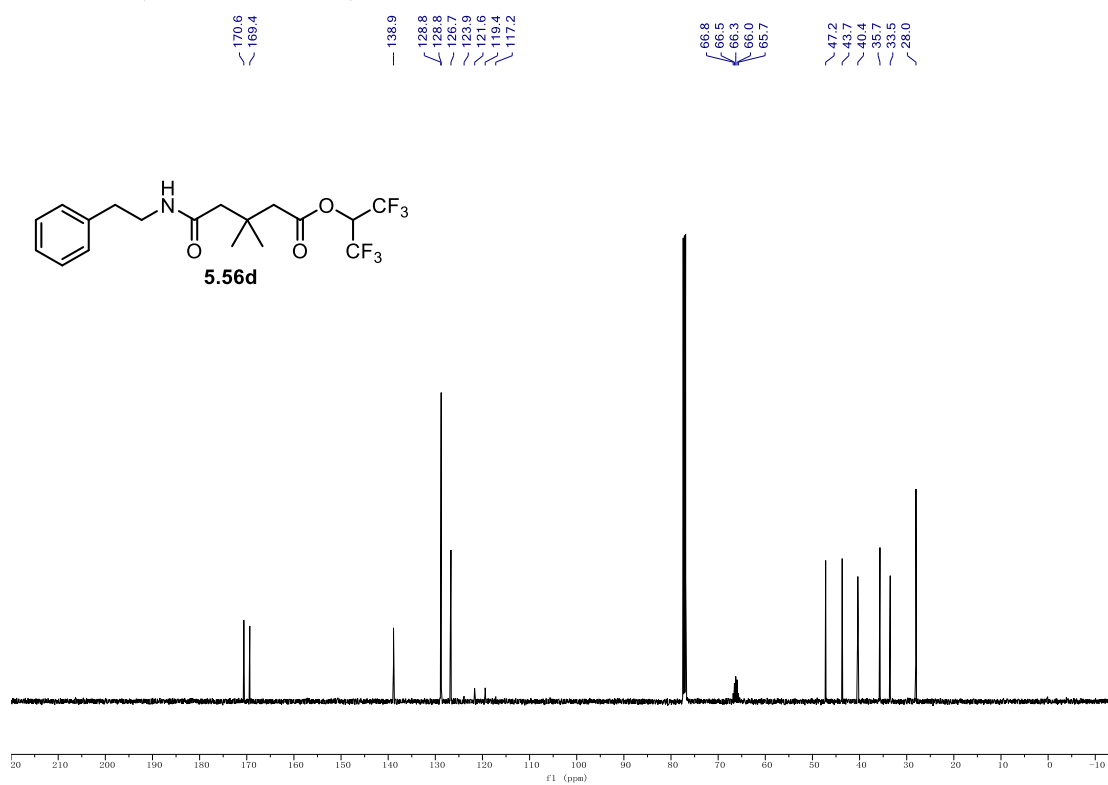
^{13}C NMR (126 MHz, CDCl_3) **5.56c**. ^{19}F NMR (565 MHz, CDCl_3) **5.56c**.

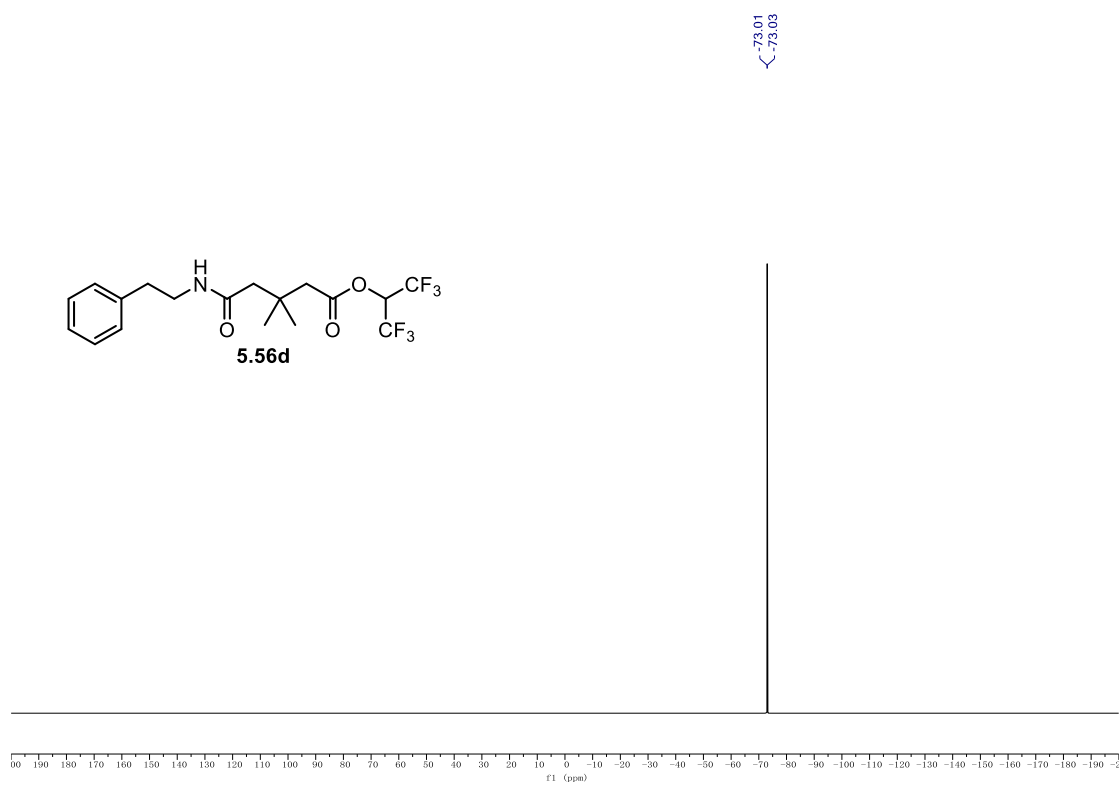
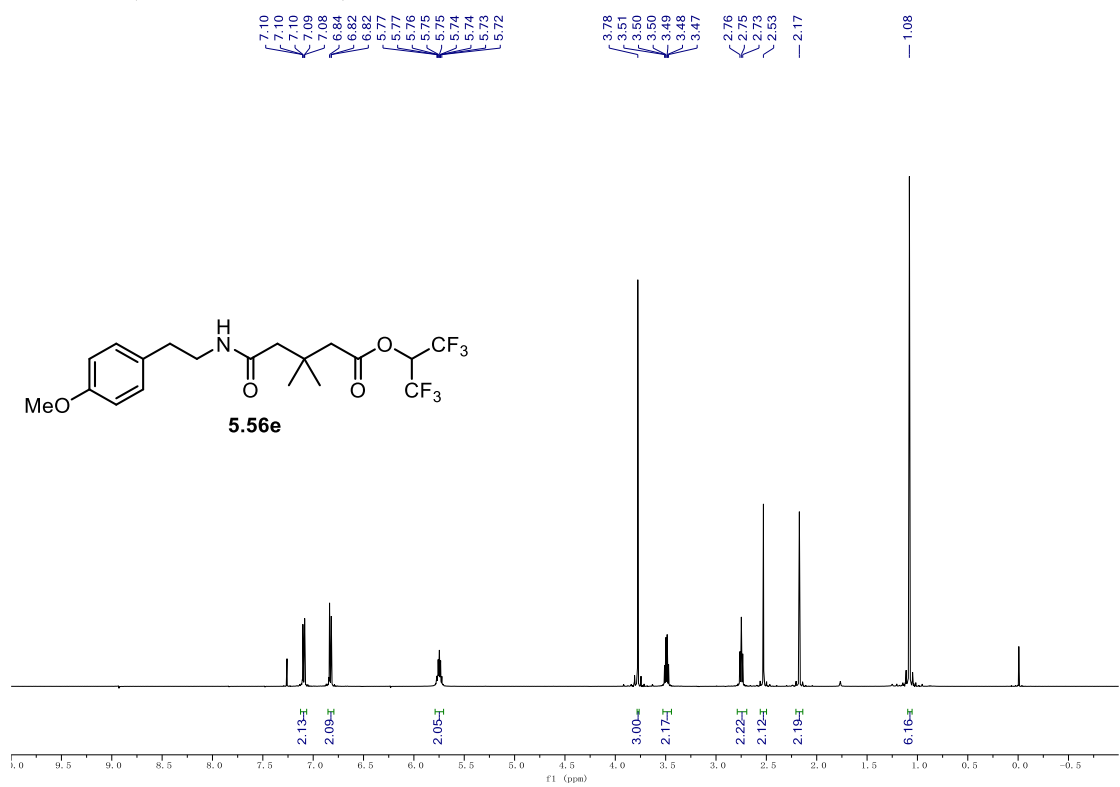
9.1. NMR Spectra

¹H NMR (500 MHz, CDCl₃) **5.56d**.



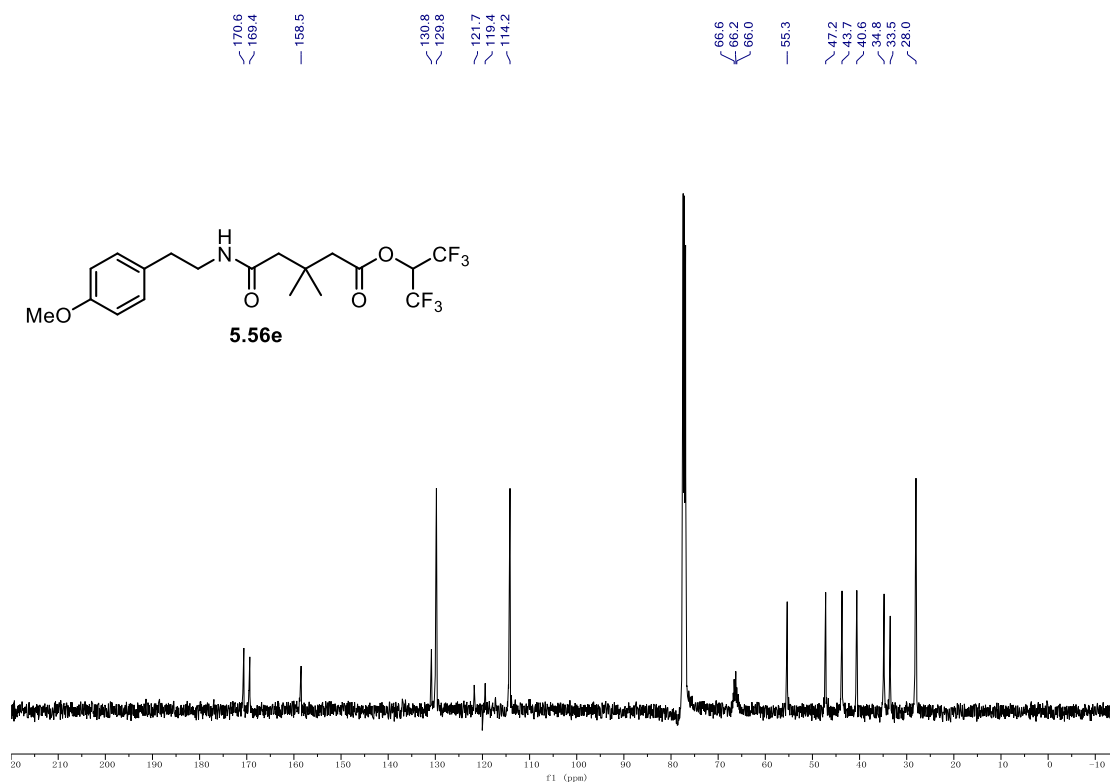
¹³C NMR (126 MHz, CDCl₃) **5.56d**.



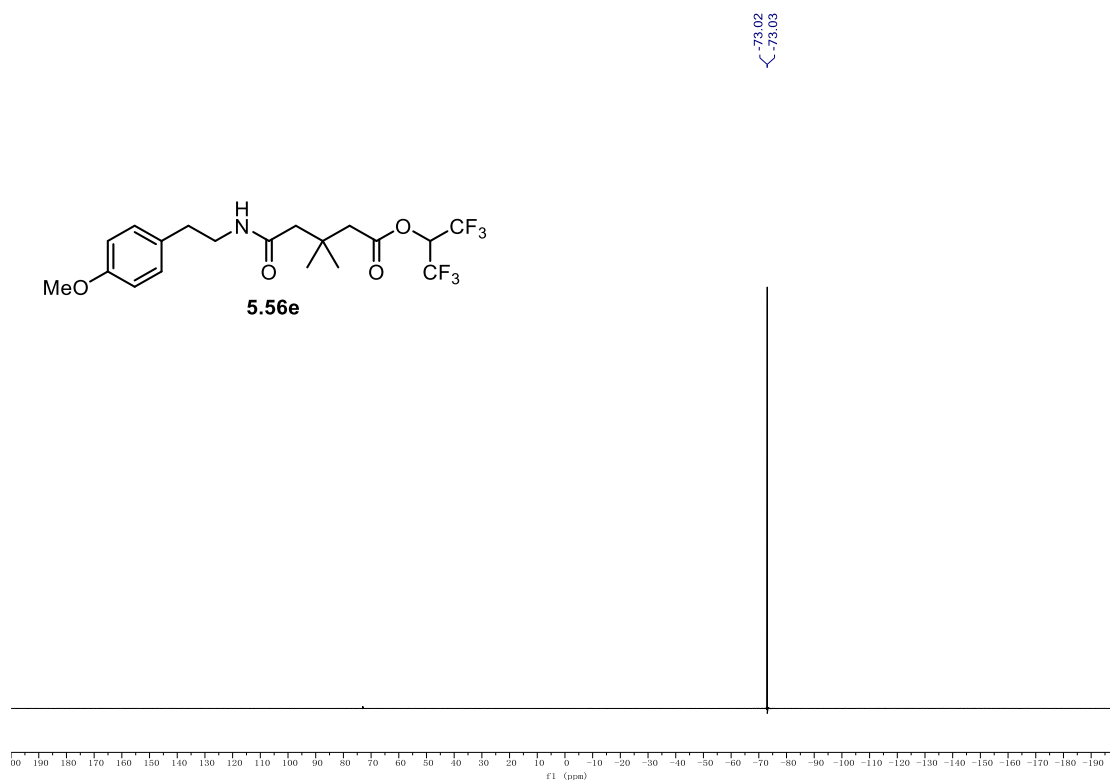
^{19}F NMR (471 MHz, CDCl_3) **5.56d**. ^1H NMR (500 MHz, CDCl_3) **5.56e**.

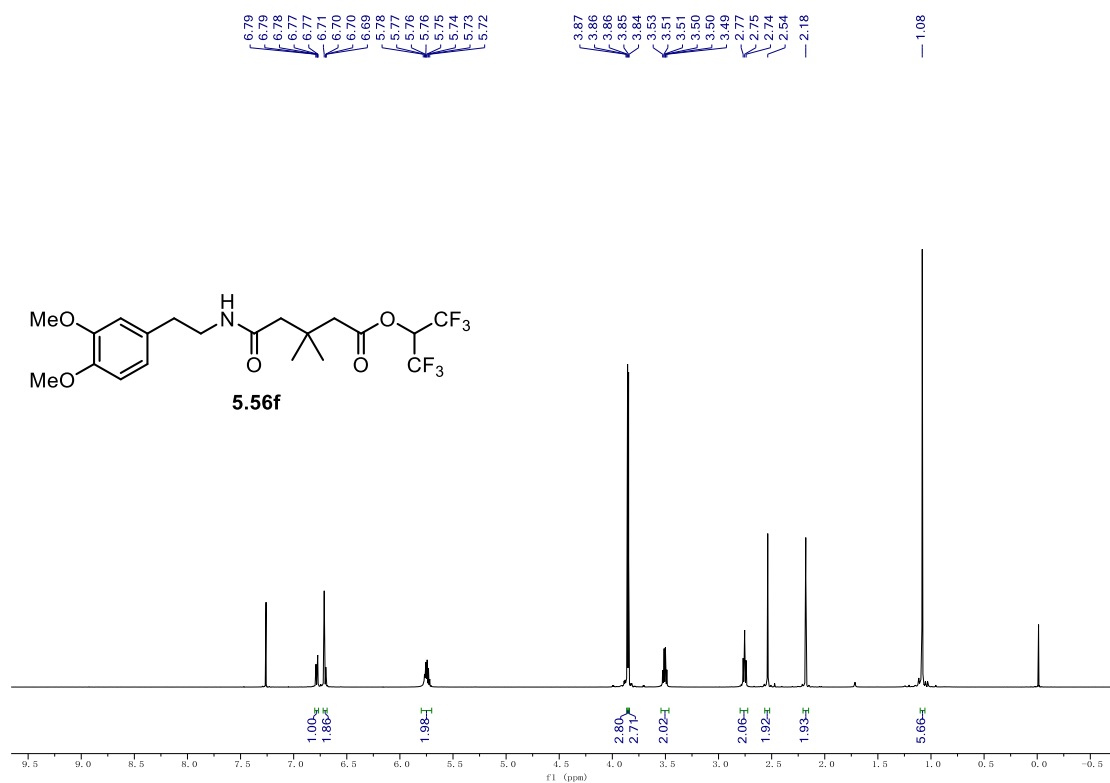
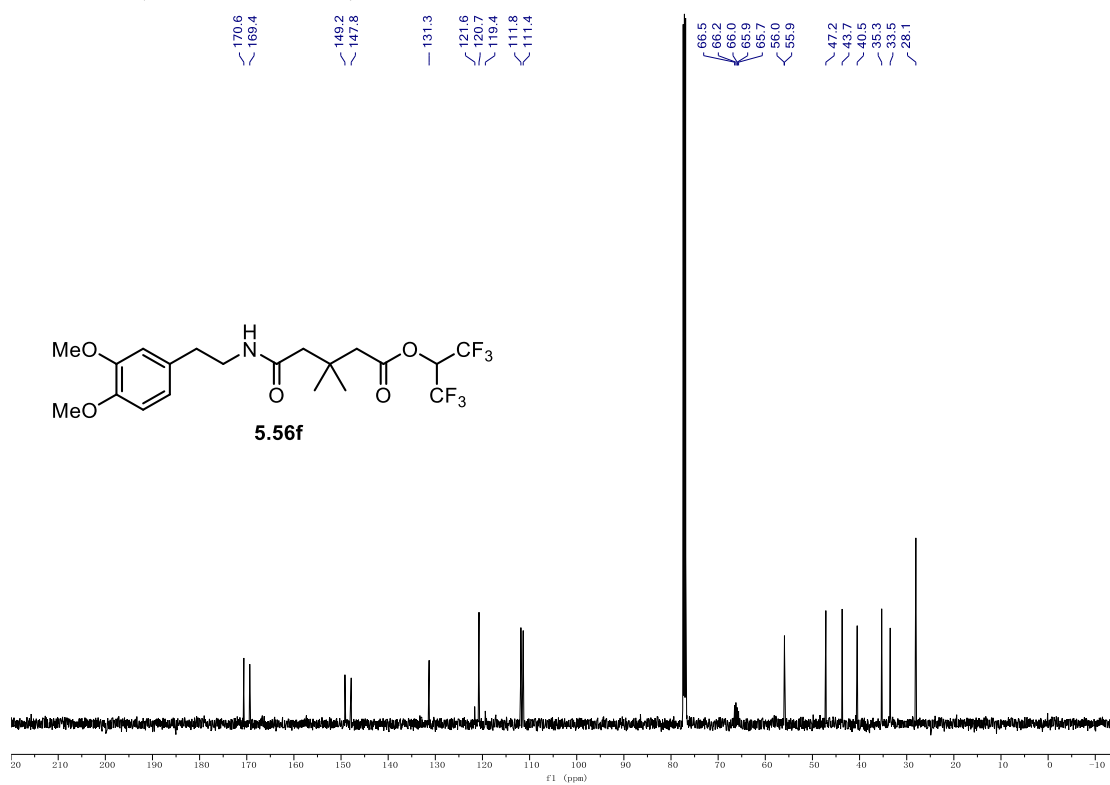
9.1. NMR Spectra

¹³C NMR (126 MHz, CDCl₃) **5.56e**.



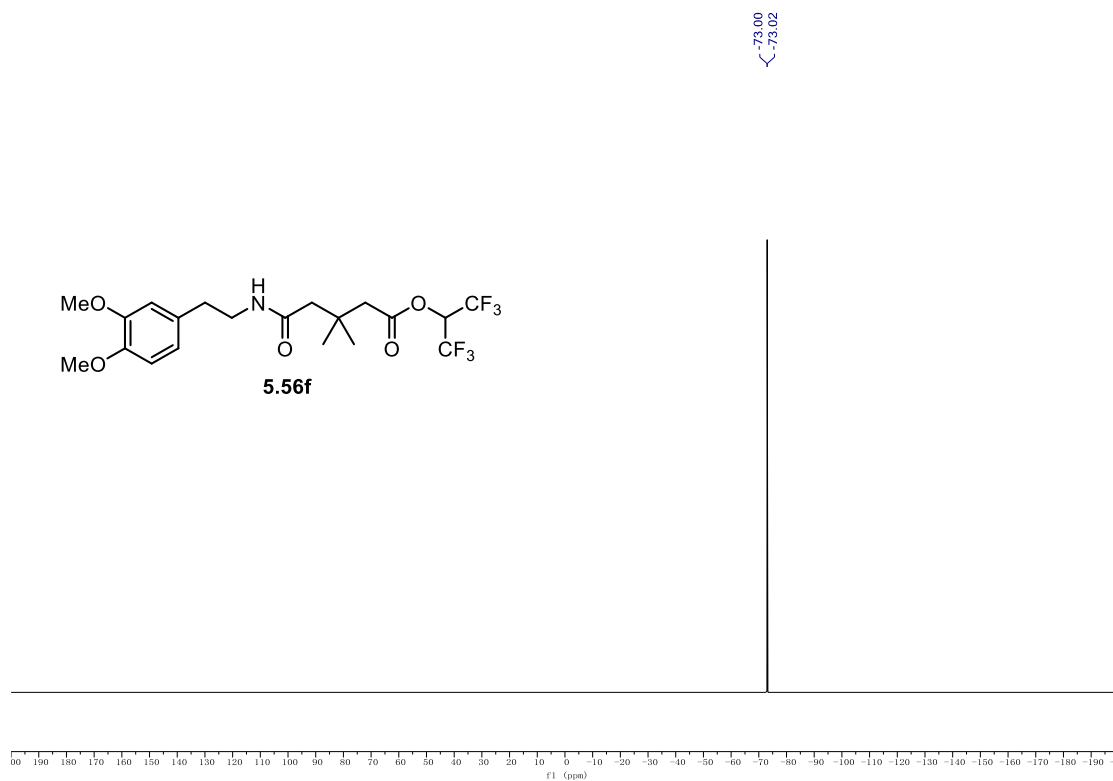
¹⁹F NMR (471 MHz, CDCl₃) **5.56e**.



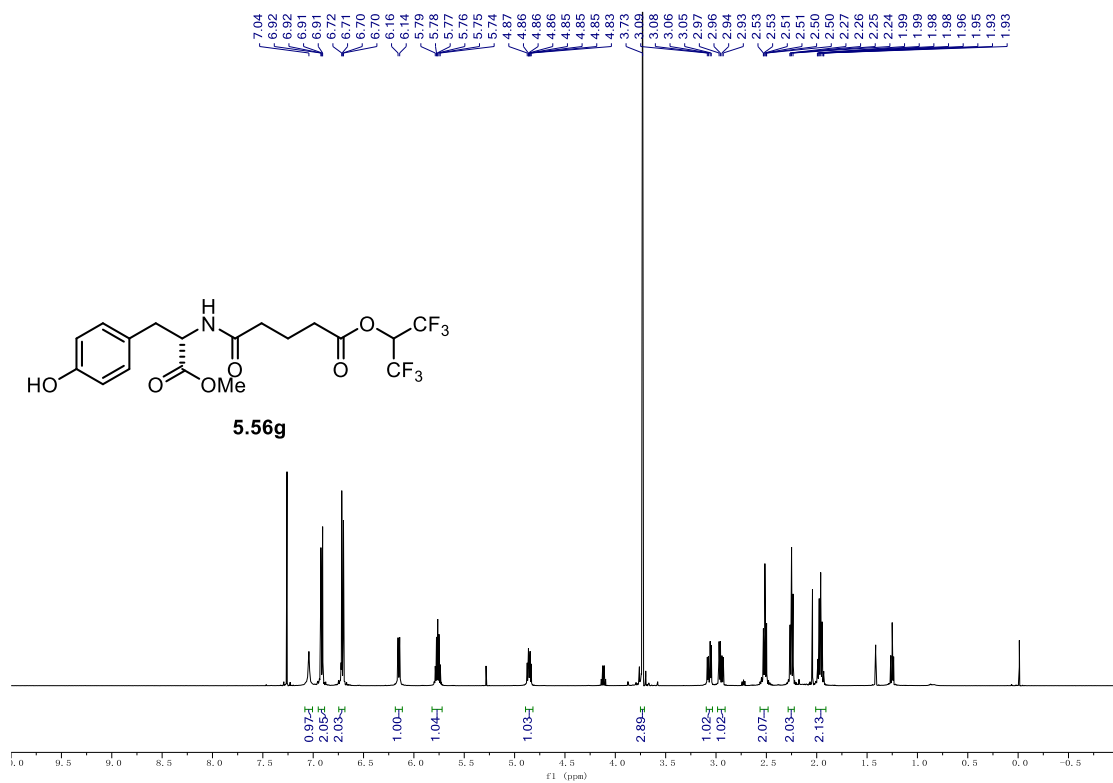
¹H NMR (500 MHz, CDCl₃) 5.56f.**¹³C NMR (126 MHz, CDCl₃) 5.56f.**

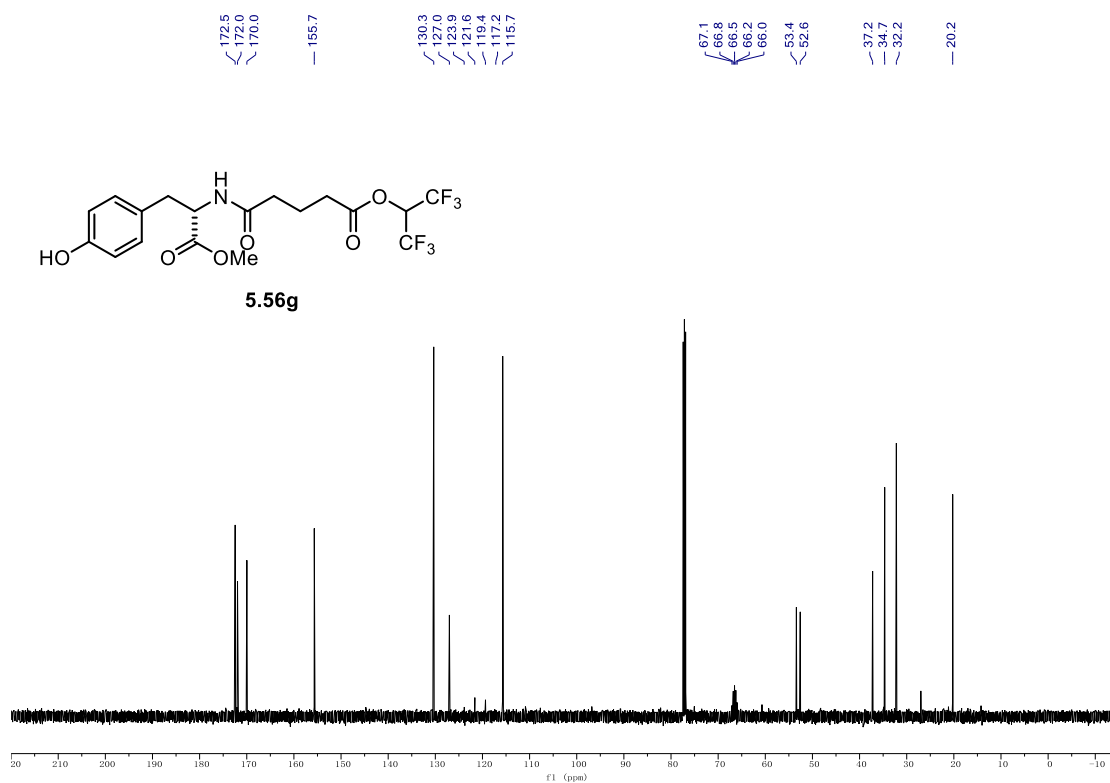
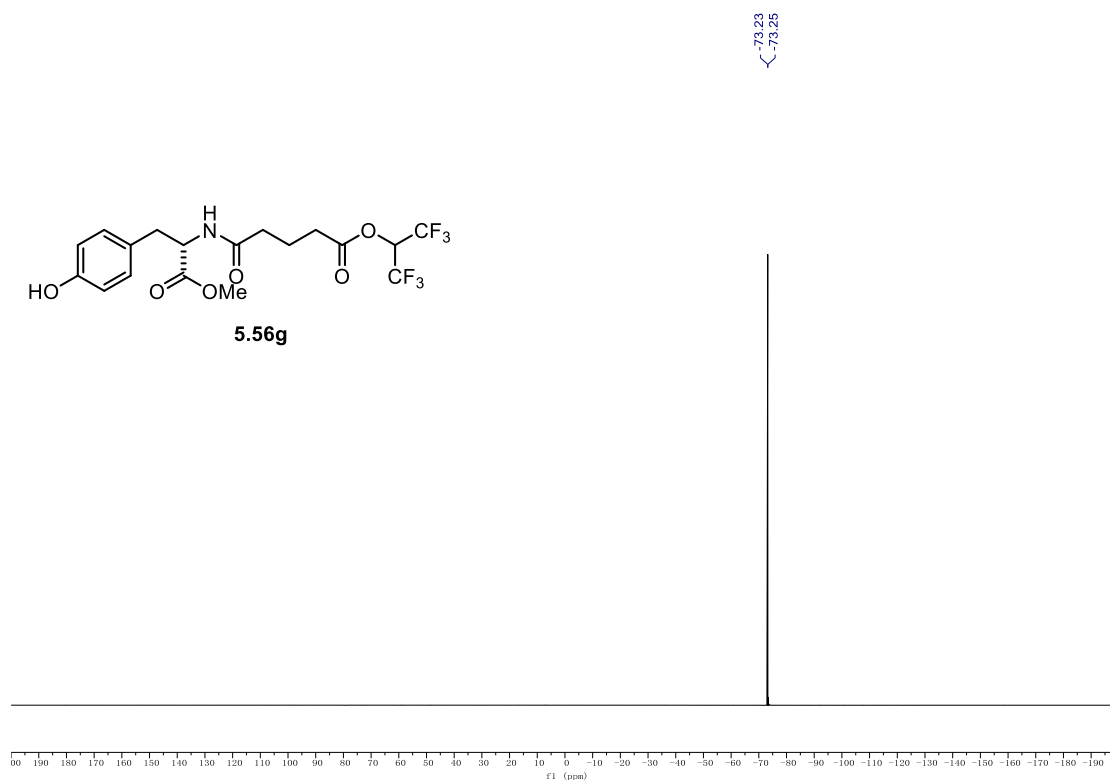
9.1. NMR Spectra

¹⁹F NMR (471 MHz, CDCl₃) 5.56f.



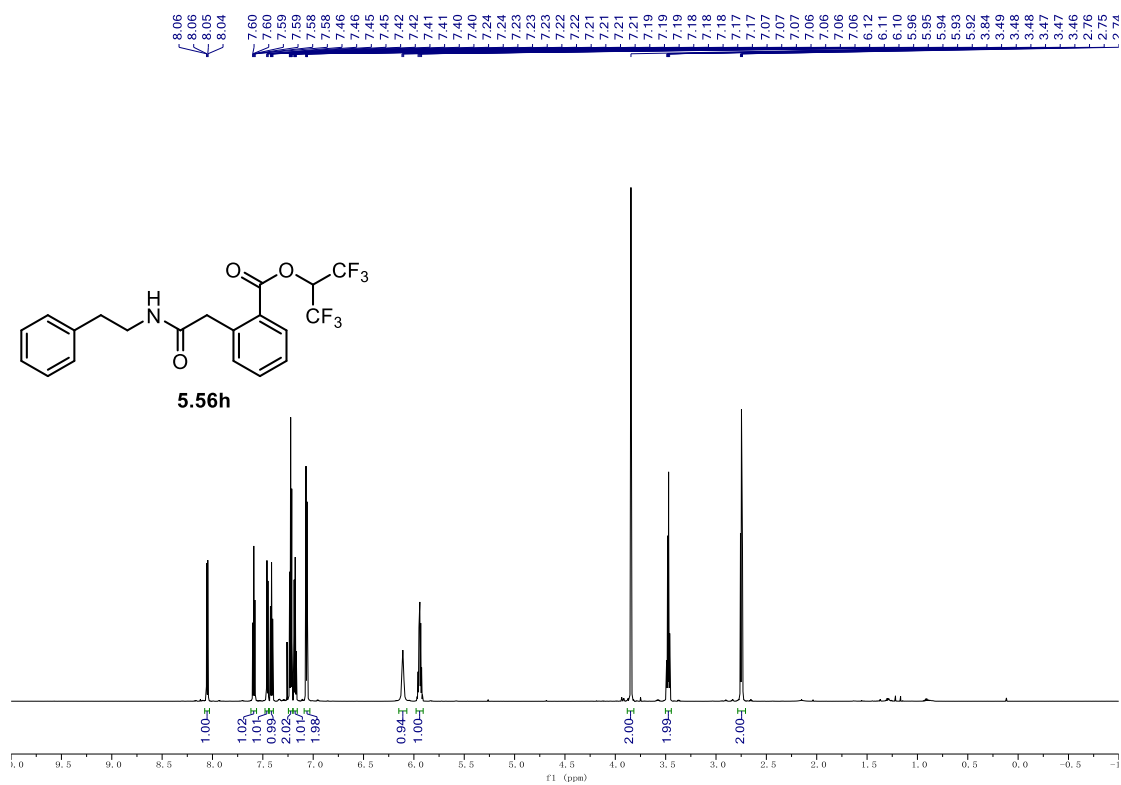
¹H NMR (500 MHz, CDCl₃) of 5.56g.



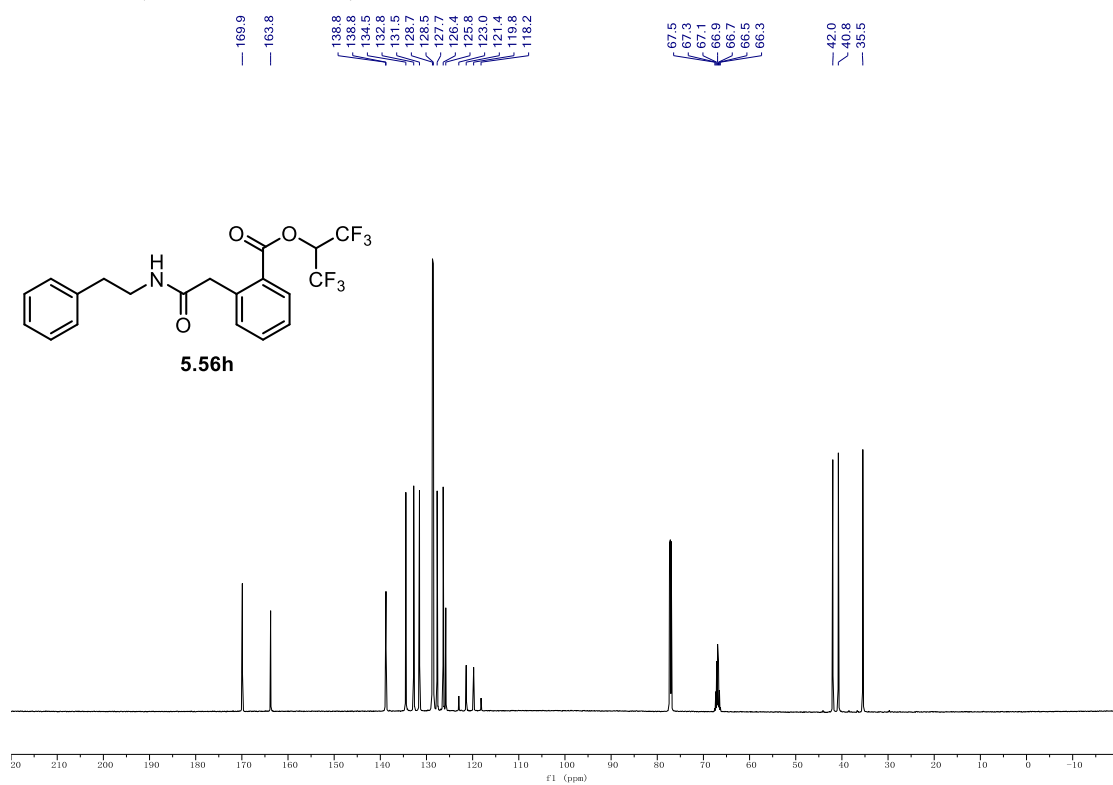
^{13}C NMR (126 MHz, CDCl_3) of **5.56g**. ^{19}F NMR (471 MHz, CDCl_3) of **5.56g**.

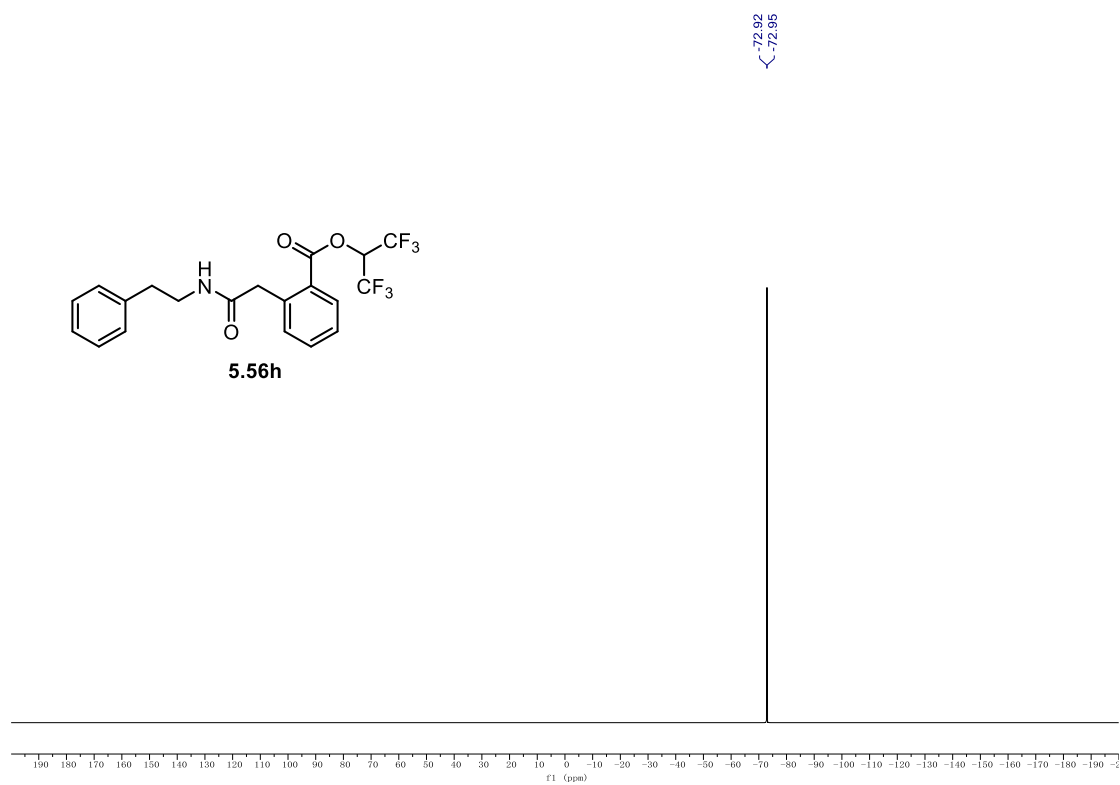
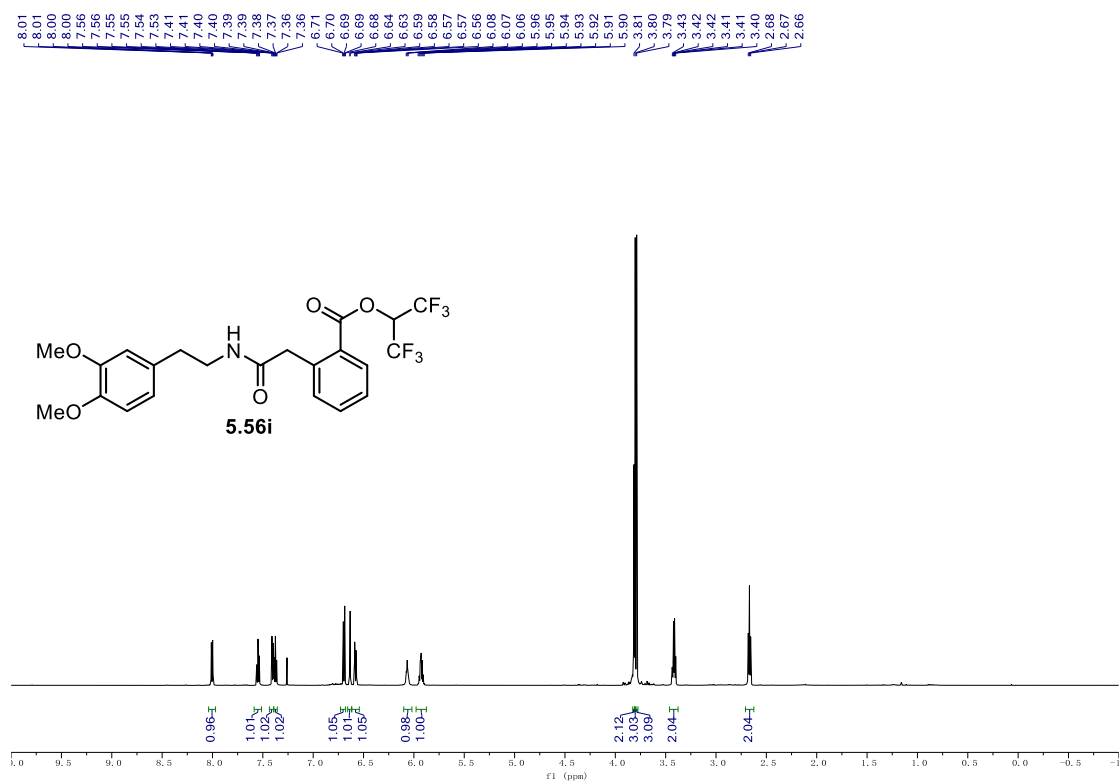
9.1. NMR Spectra

¹H NMR (700 MHz, CDCl₃) **5.56h**.



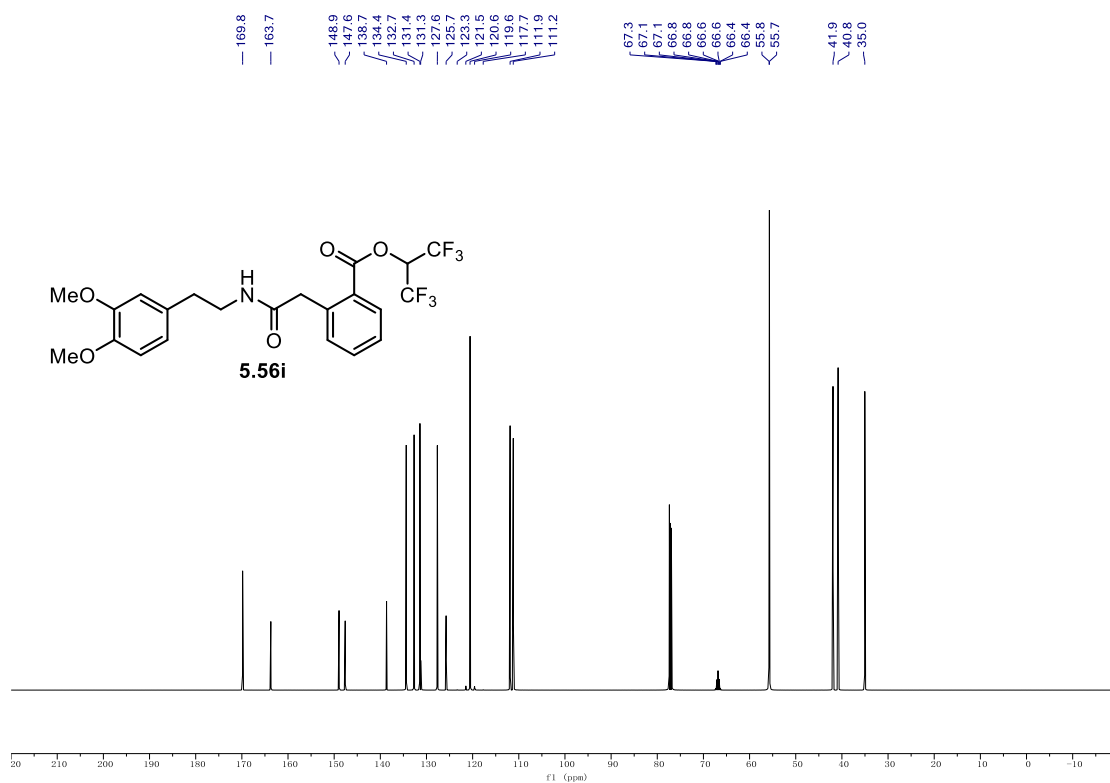
¹³C NMR (176 MHz, CDCl₃) **5.56h**.



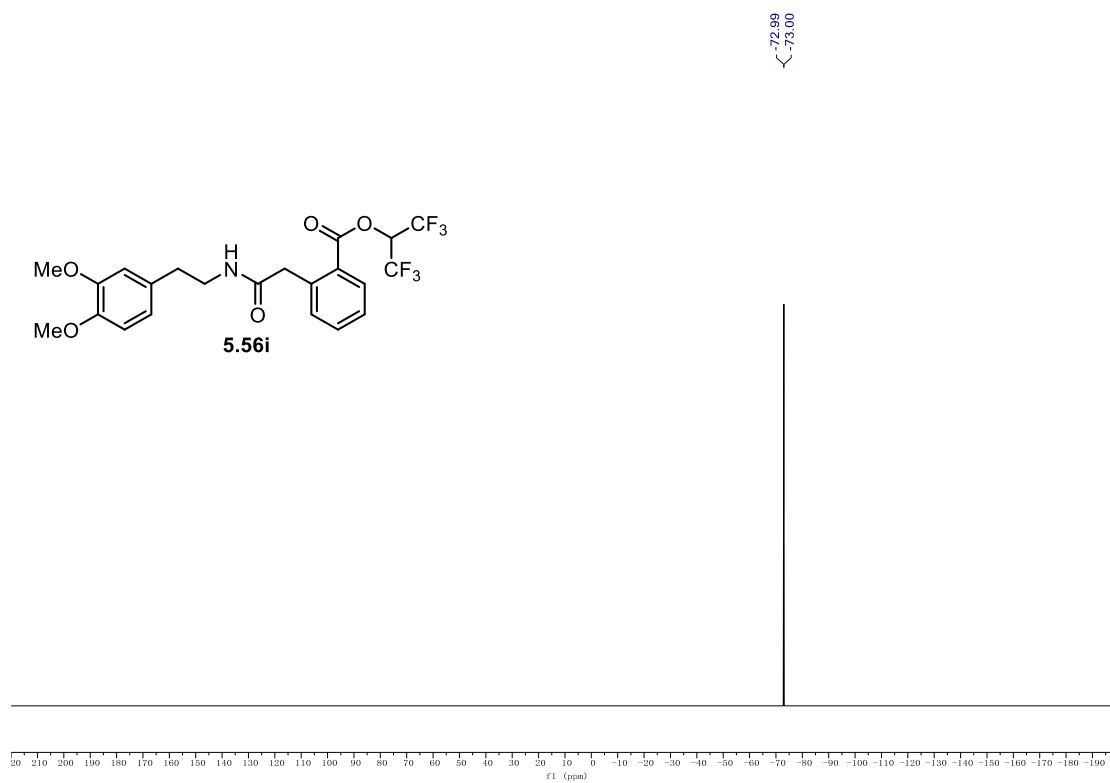
^{19}F NMR (376 MHz, CDCl_3) **5.56h**. ^1H NMR (600 MHz, CDCl_3) **5.56i**.

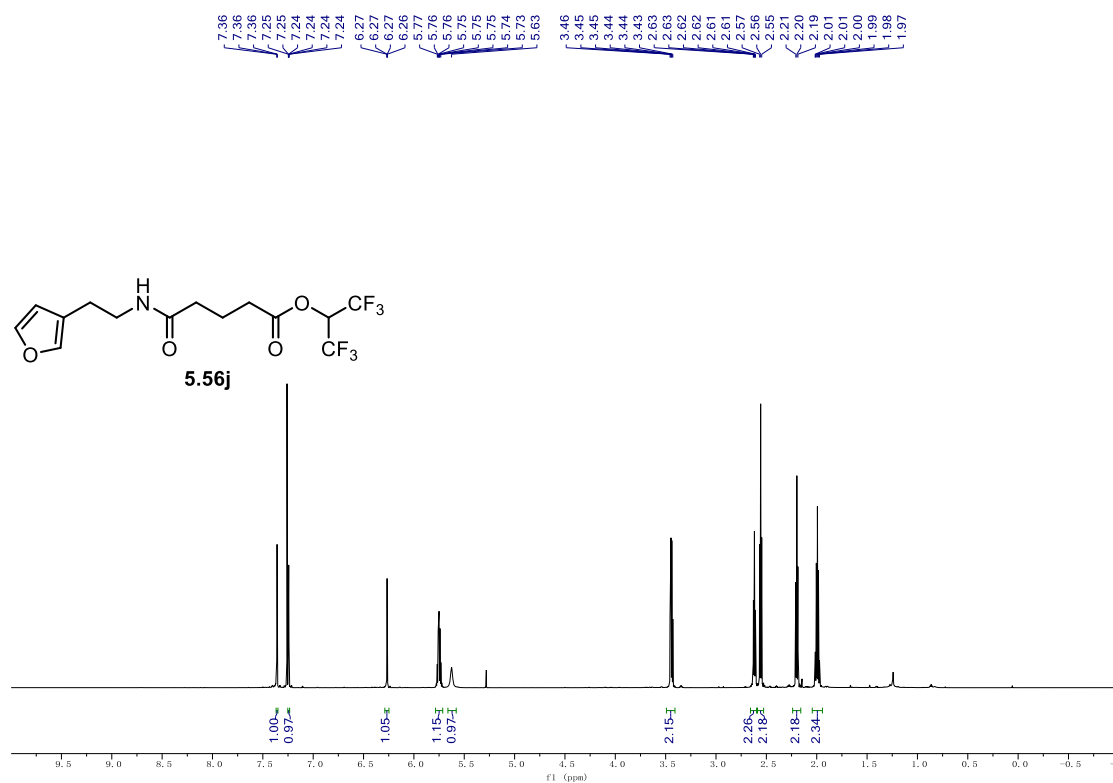
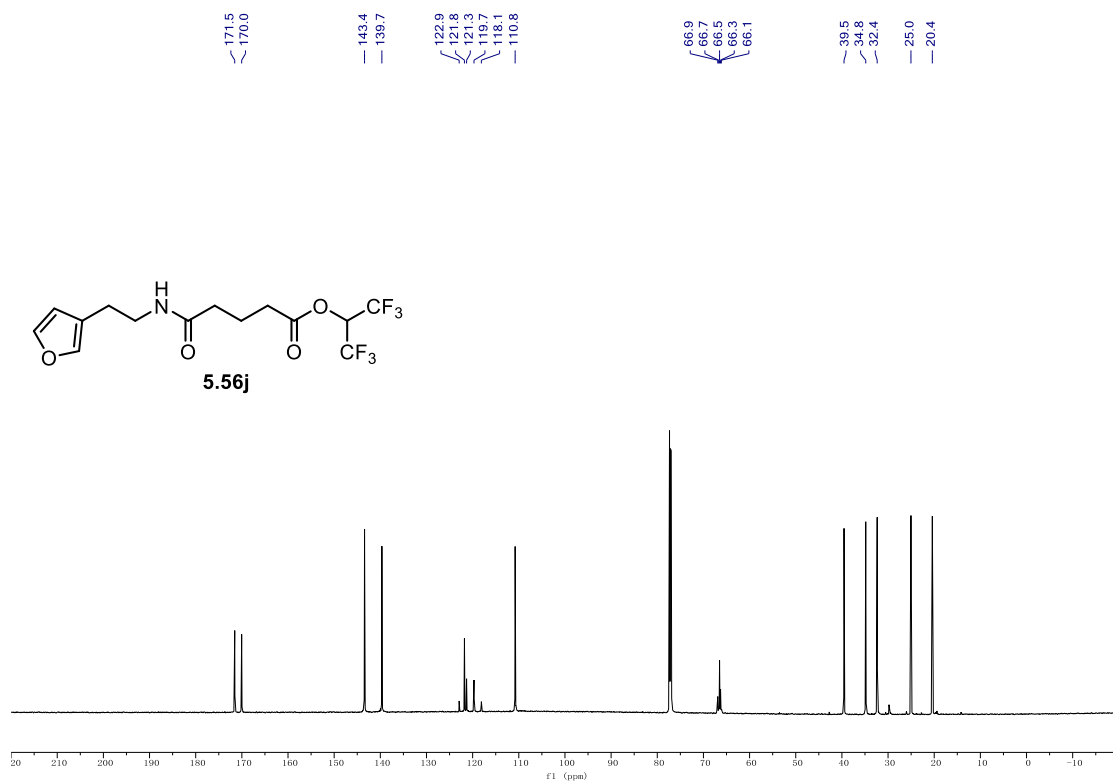
9.1. NMR Spectra

¹³C NMR (151 MHz, CDCl₃) **5.56i**.



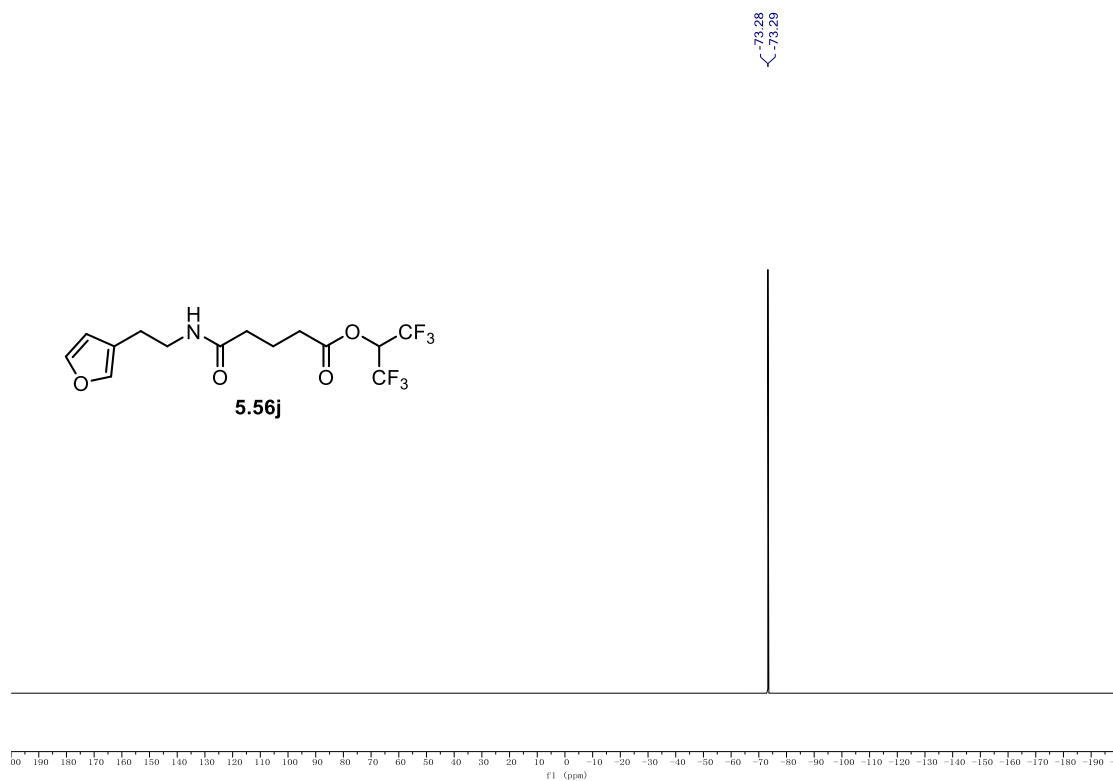
¹⁹F NMR (565 MHz, CDCl₃) **5.56i**.



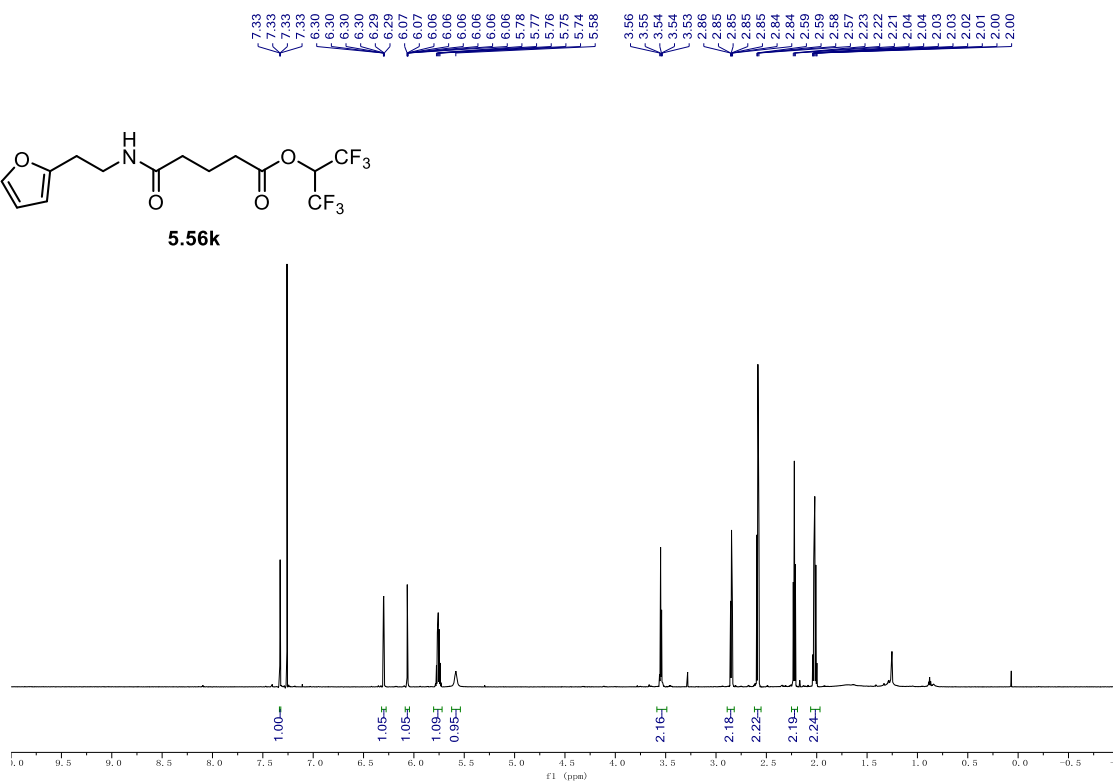
^1H NMR (700 MHz, CDCl_3) 5.56j. **^{13}C NMR (176 MHz, CDCl_3) 5.56j.**

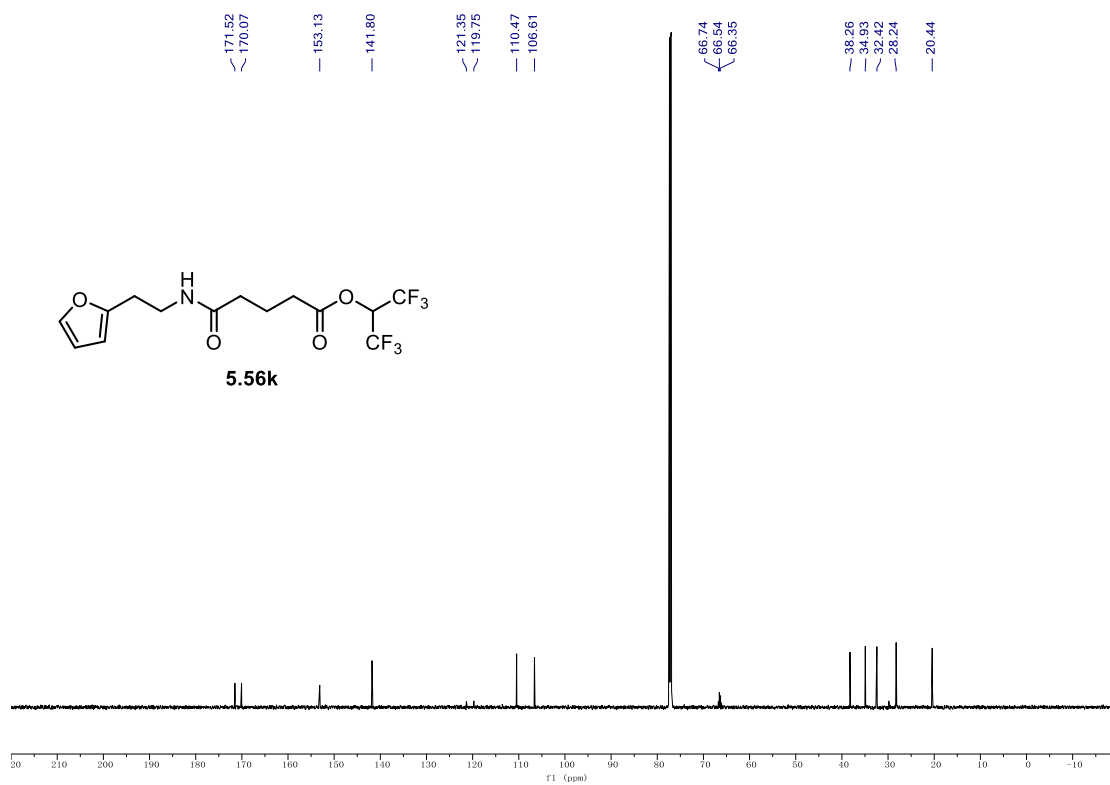
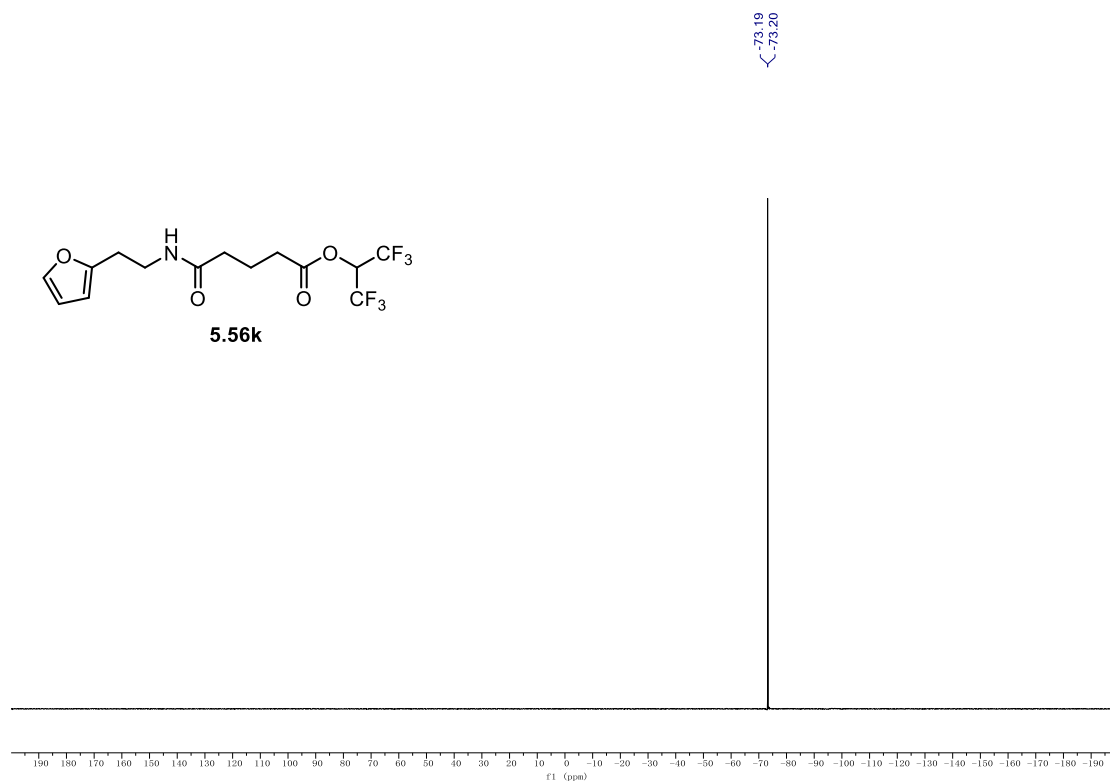
9.1. NMR Spectra

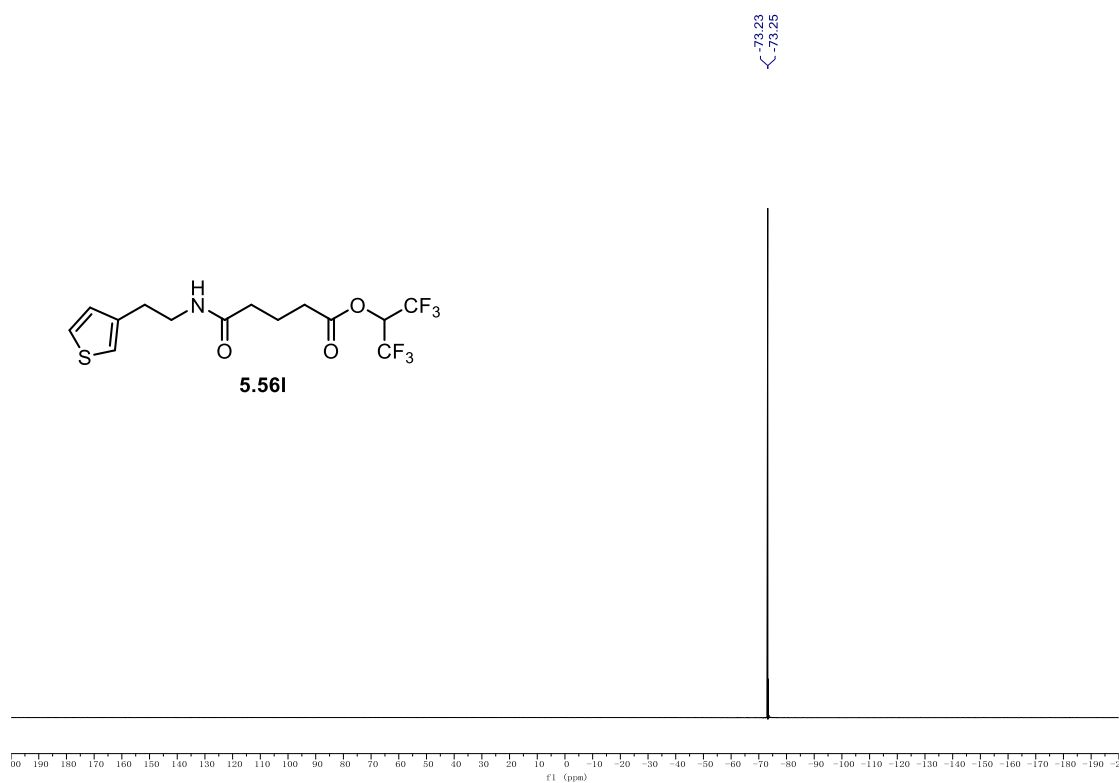
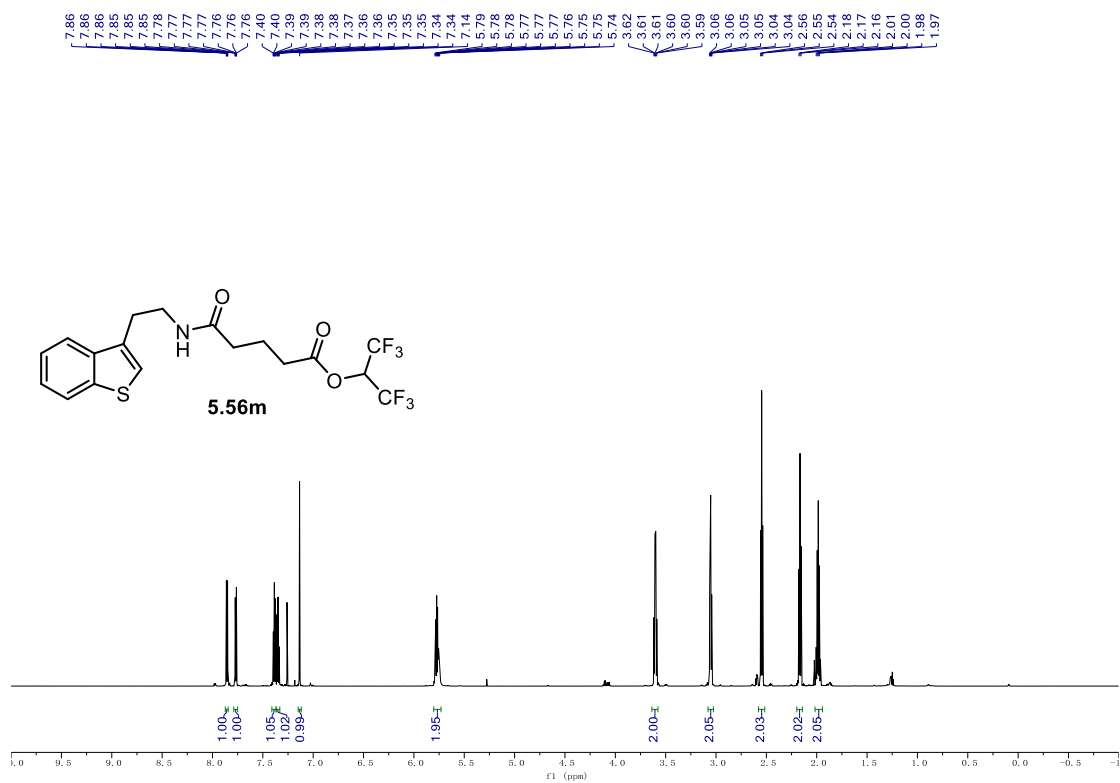
^{19}F NMR (565 MHz, CDCl_3) **5.56j**.



^1H NMR (700 MHz, CDCl_3) **5.56k**.

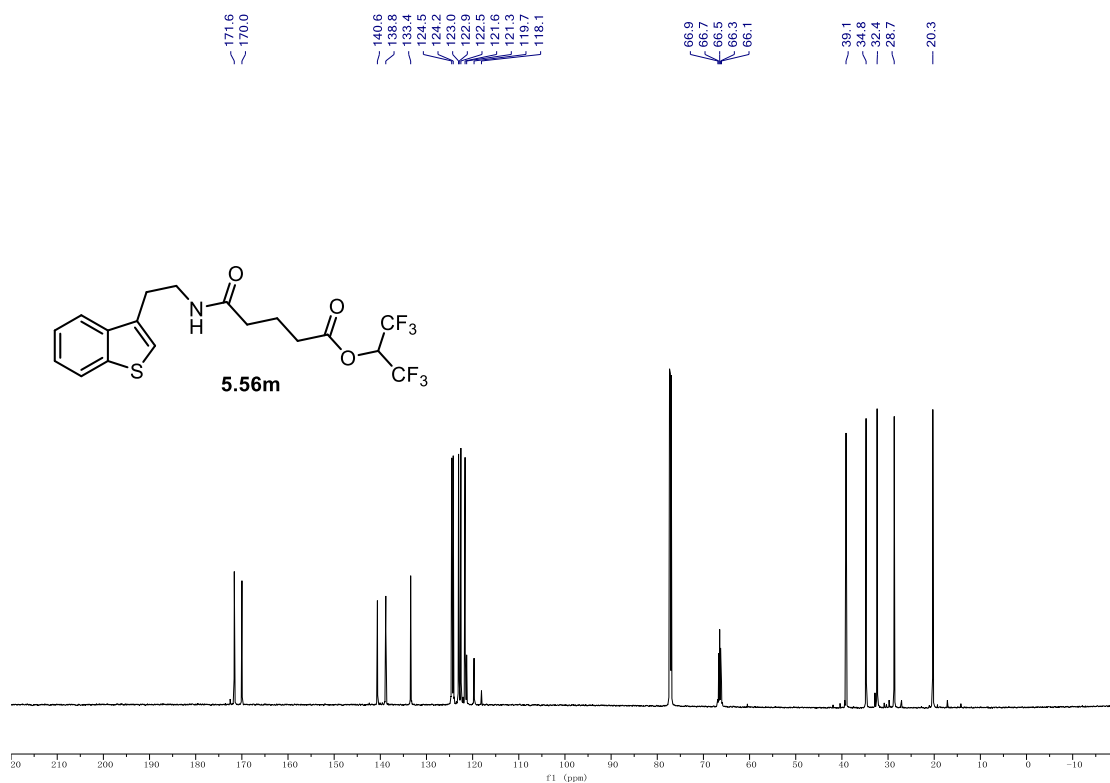


^{13}C NMR (176 MHz, CDCl_3) 5.56k. **^{19}F NMR (376 MHz, CDCl_3) 5.56k.**

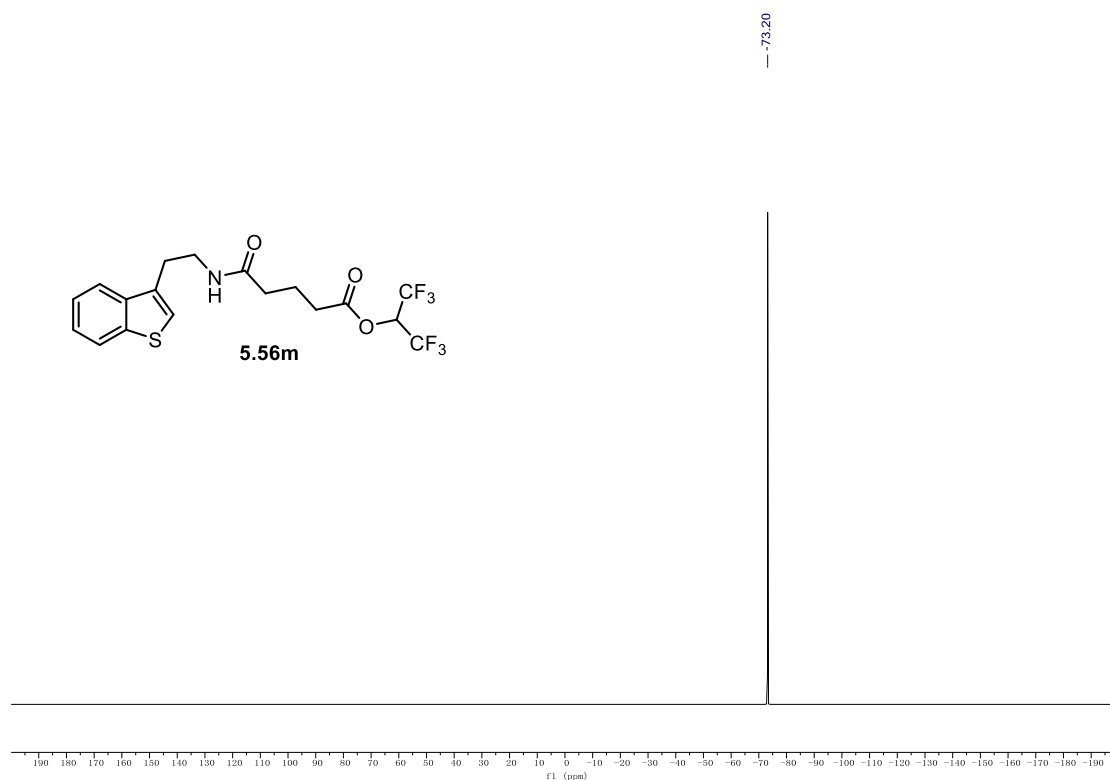
^{19}F NMR (471 MHz, CDCl_3) **5.56l** ^1H NMR (700 MHz, CDCl_3) **5.56m**

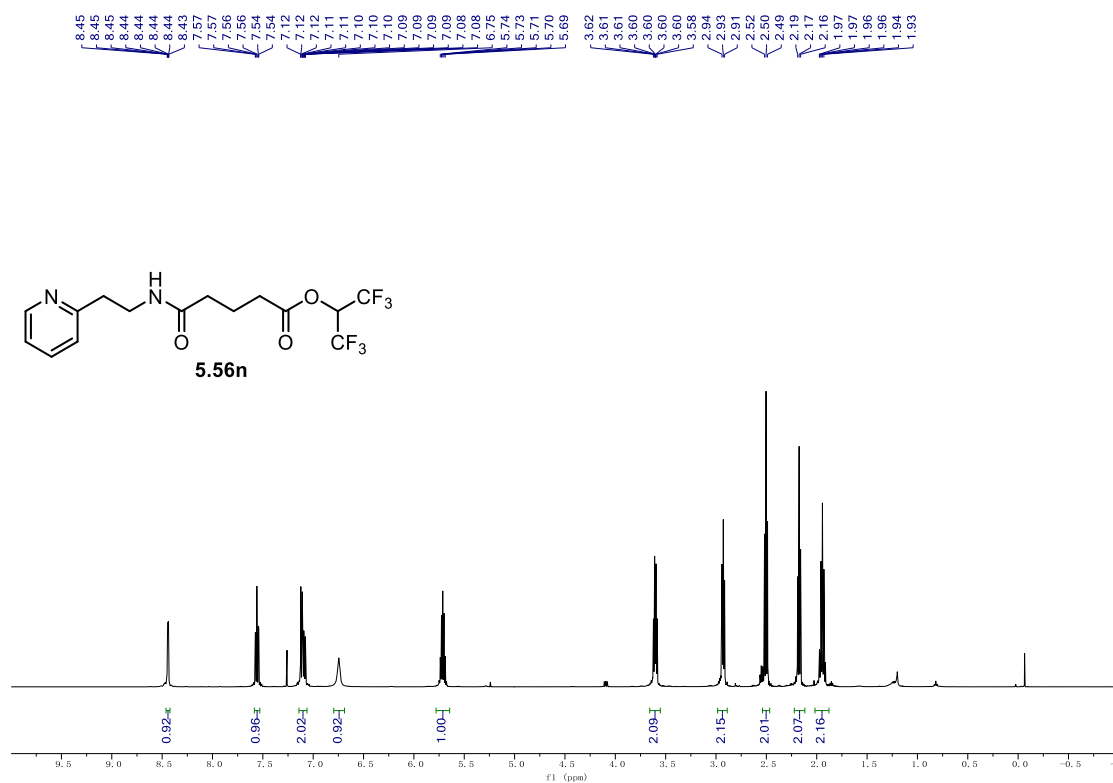
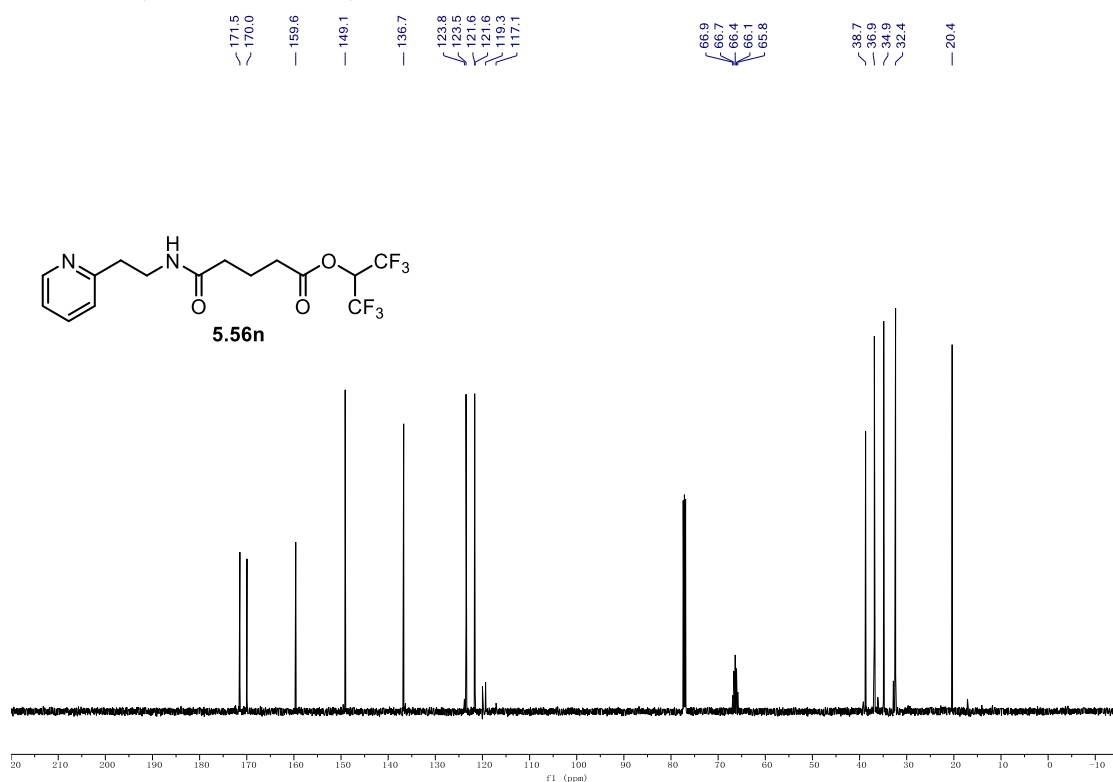
9.1. NMR Spectra

¹³C NMR (176 MHz, CDCl₃) **5.56m**.

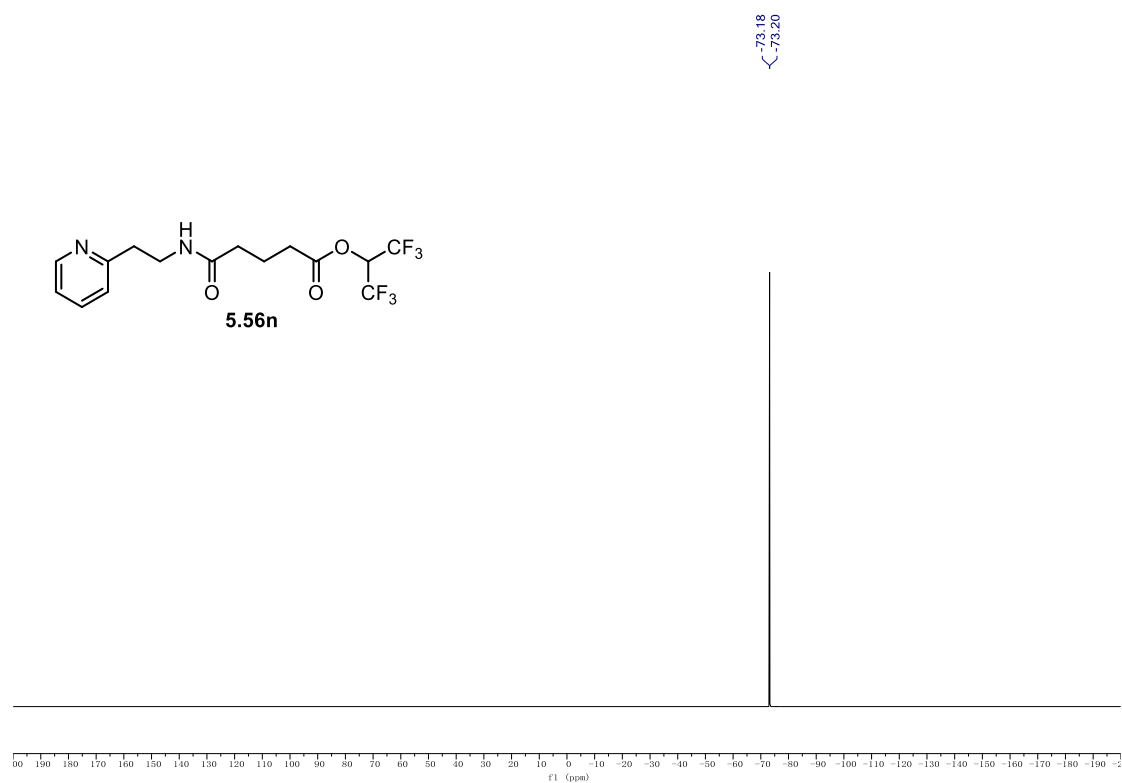


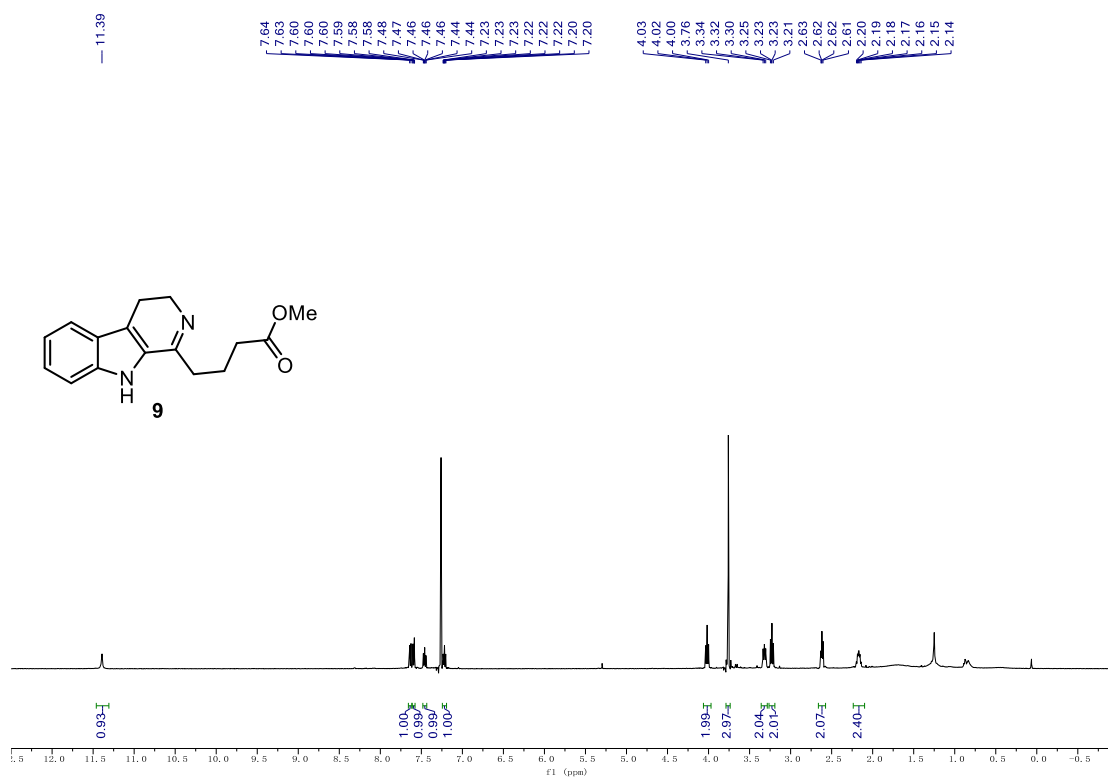
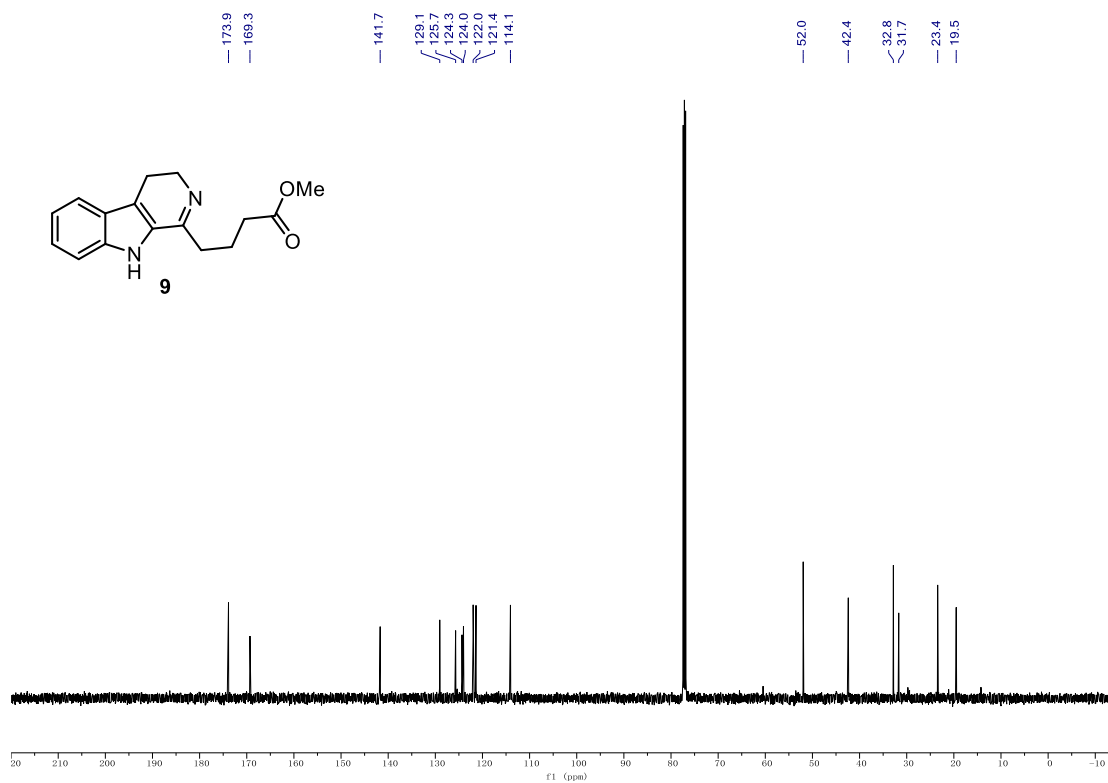
¹⁹F NMR (376 MHz, CDCl₃) **5.56m**.



¹H NMR (500 MHz, CDCl₃) of 5.56n.**¹³C NMR (126 MHz, CDCl₃) of 5.56n.**

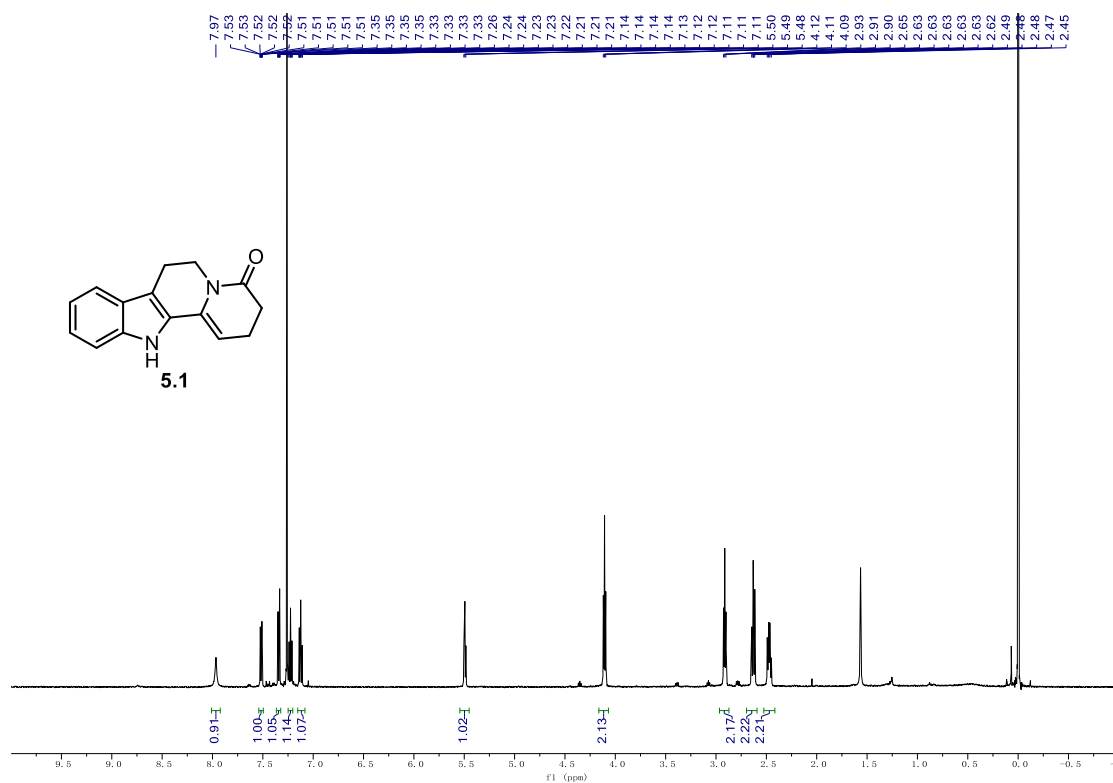
^{19}F NMR (471 MHz, CDCl_3) of **5.56n**.



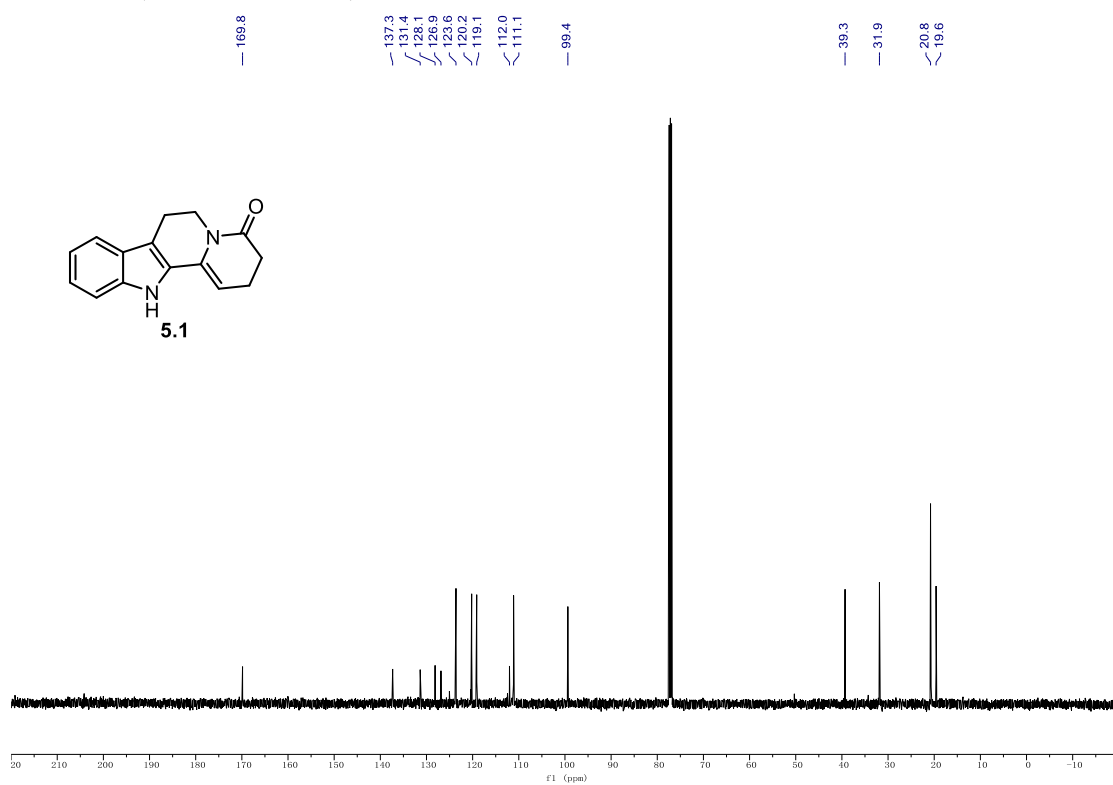
^1H NMR (500 MHz, CDCl_3) of **9**. ^{13}C NMR (126 MHz, CDCl_3) of **9**.

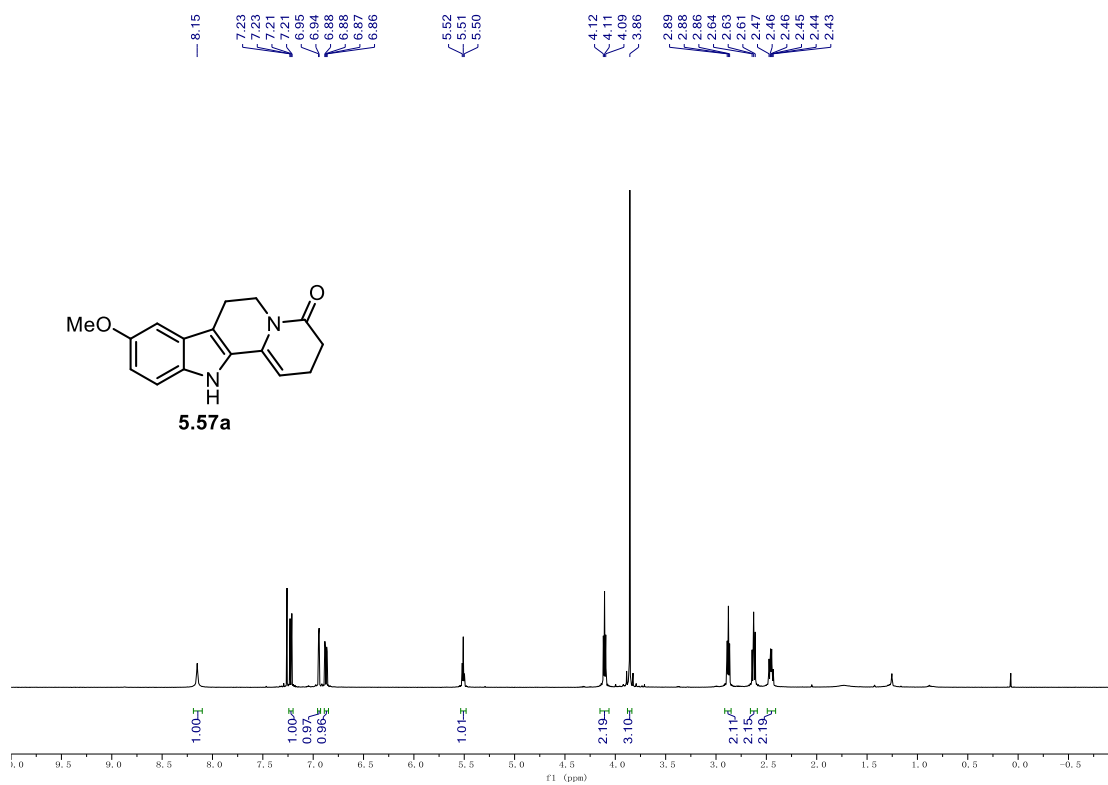
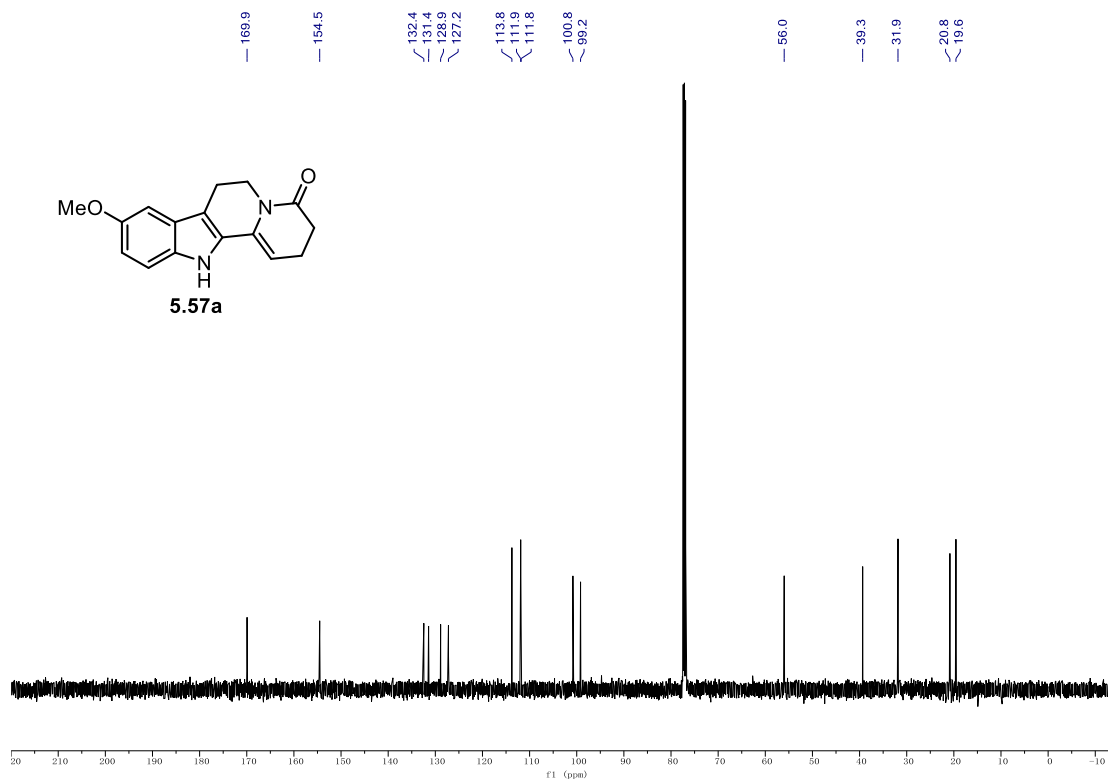
9.1. NMR Spectra

¹H NMR (500 MHz, CDCl₃) of 5.1.



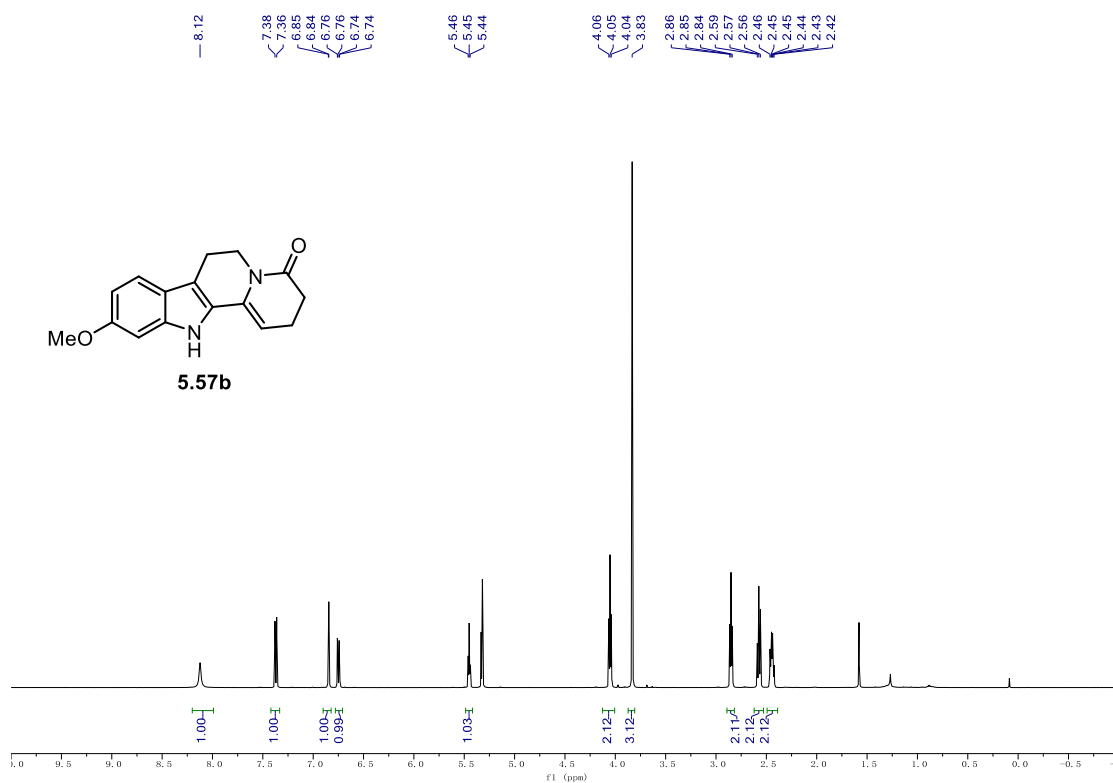
¹³C NMR (126 MHz, CDCl₃) of 5.1.



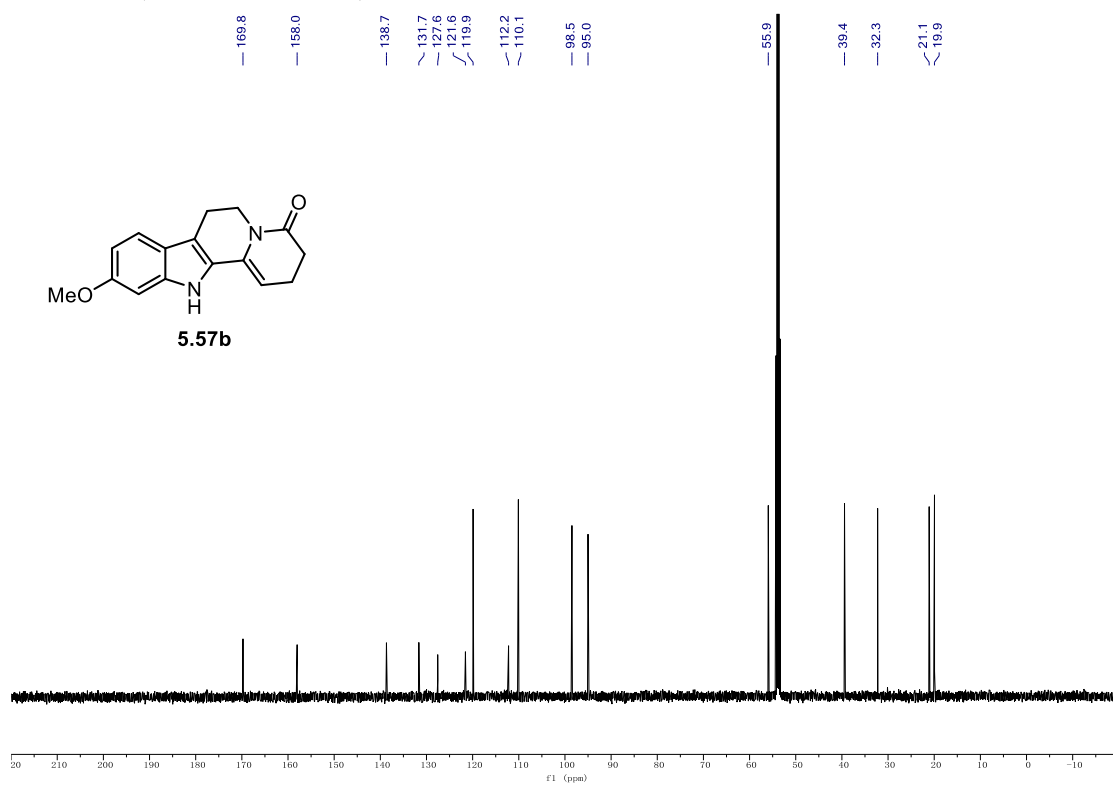
^1H NMR (500 MHz, CDCl_3) of **5.57a**. ^{13}C NMR (126 MHz, CDCl_3) of **5.57a**.

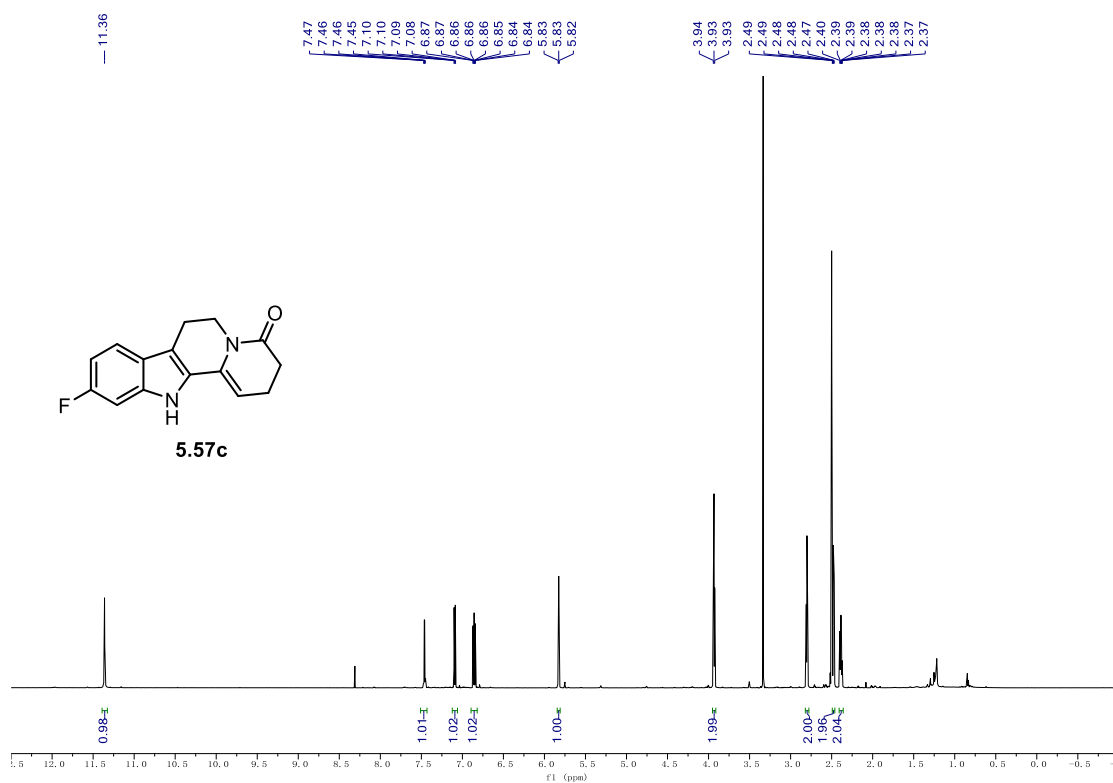
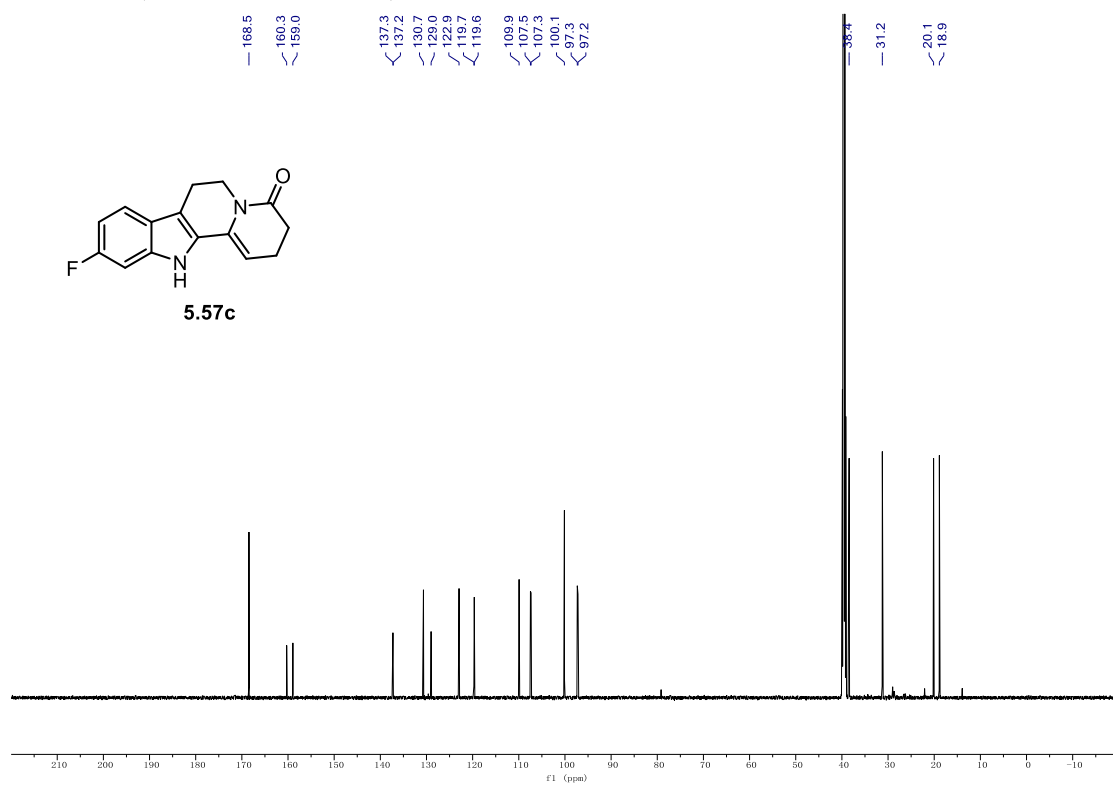
9.1. NMR Spectra

^1H NMR (500 MHz, CD_2Cl_2) of **5.57b**.



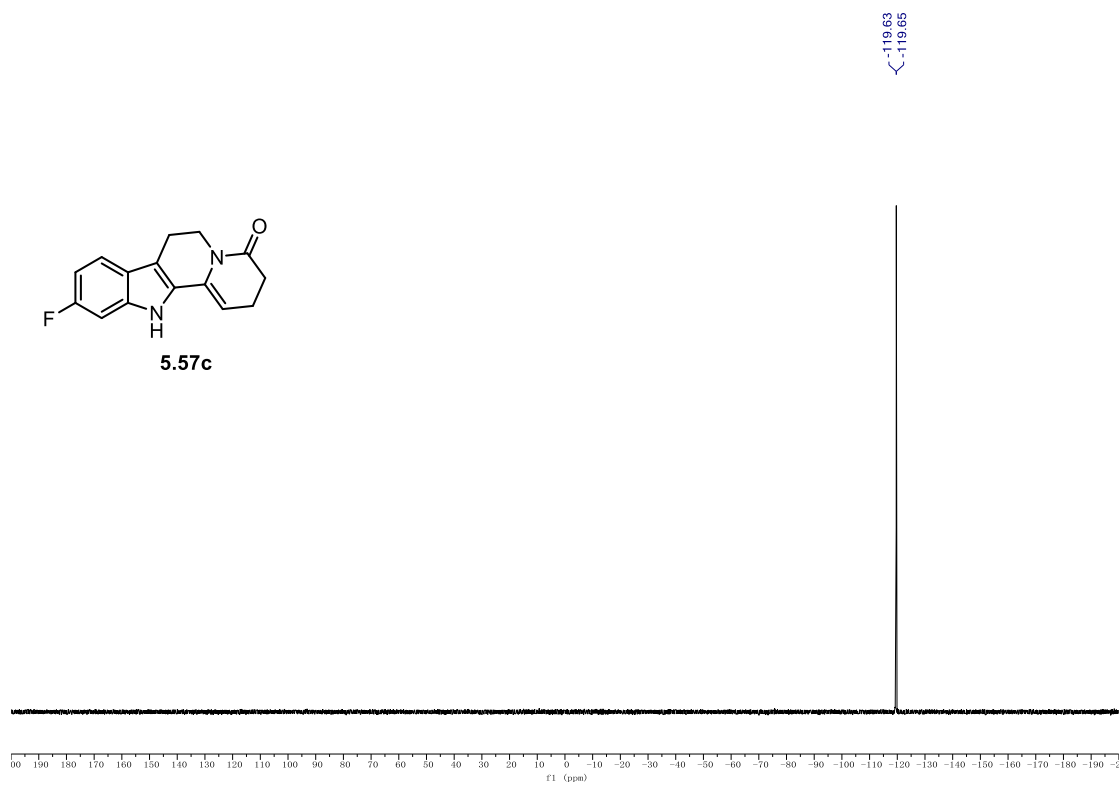
^{13}C NMR (126 MHz, CD_2Cl_2) of **5.57b**.

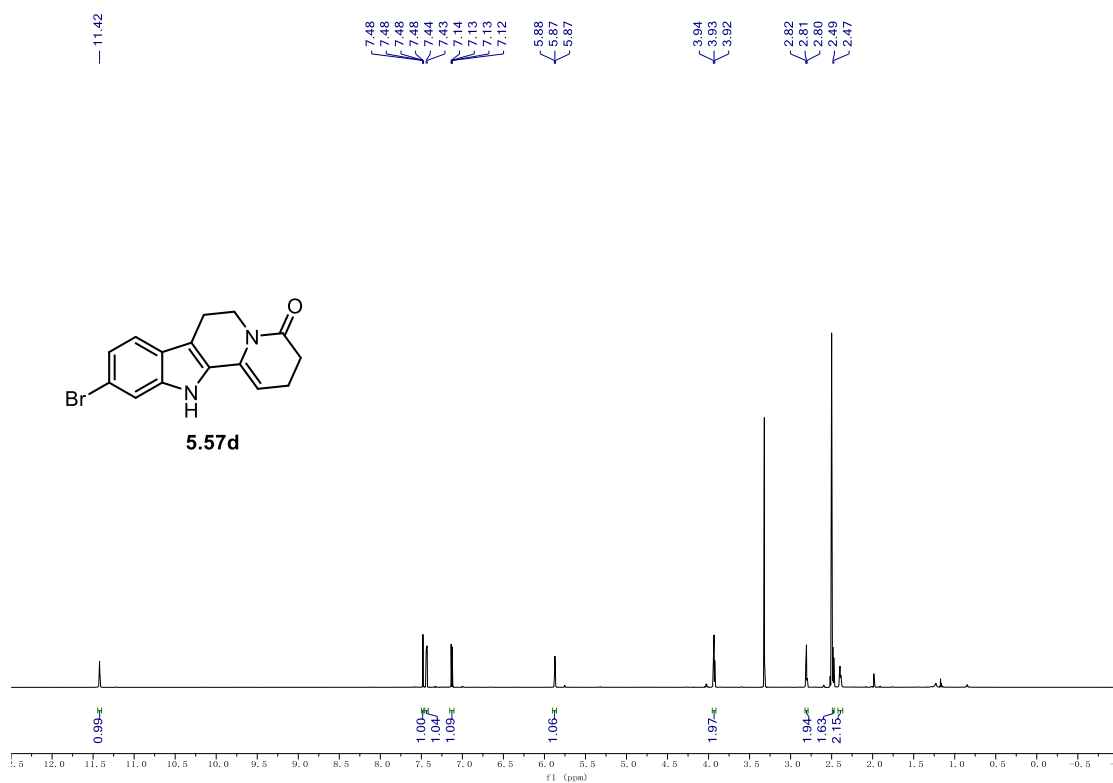
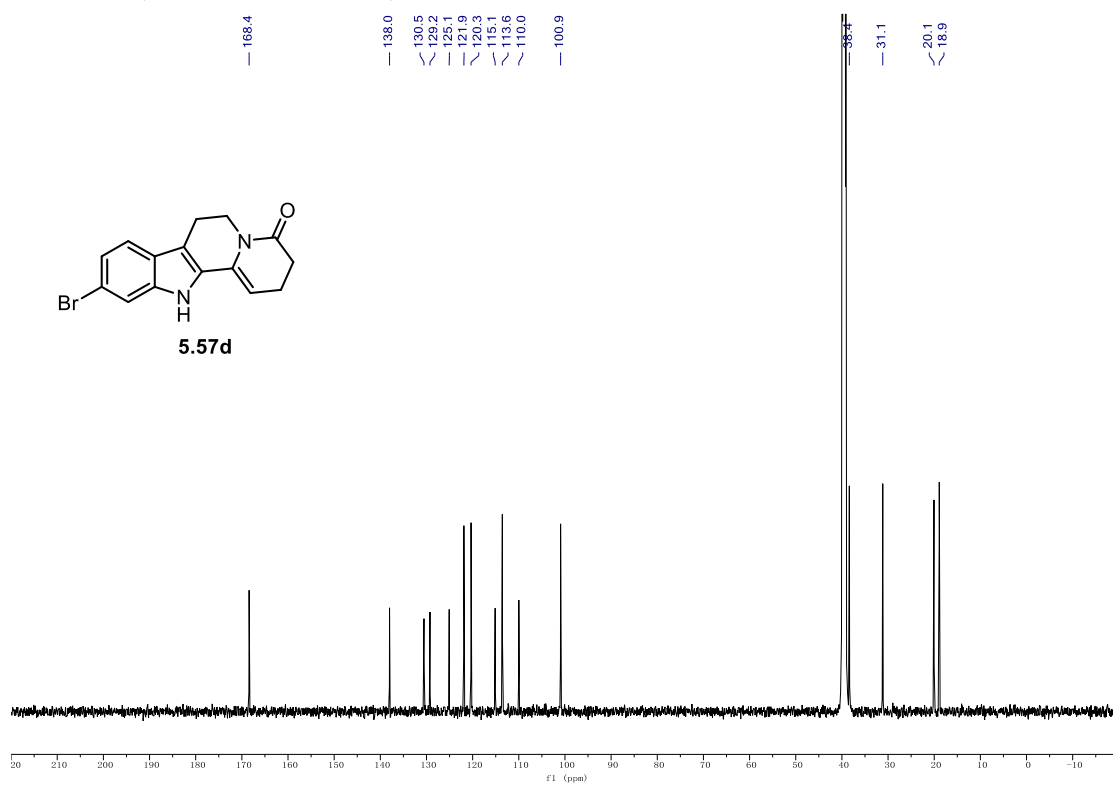


^1H NMR (700 MHz, d_6 -DMSO) of **5.57c**. ^{13}C NMR (176 MHz, d_6 -DMSO) of **5.57c**.

9.1. NMR Spectra

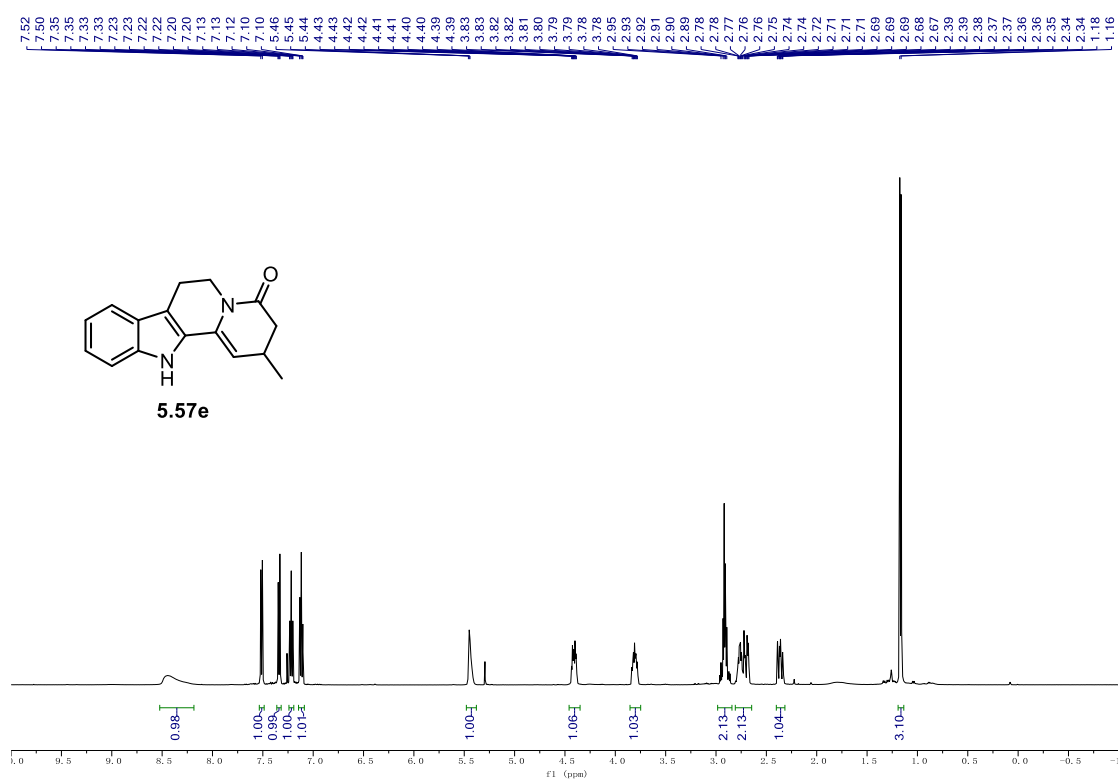
^{19}F NMR (471 MHz, d_6 -DMSO) of **5.57c**.



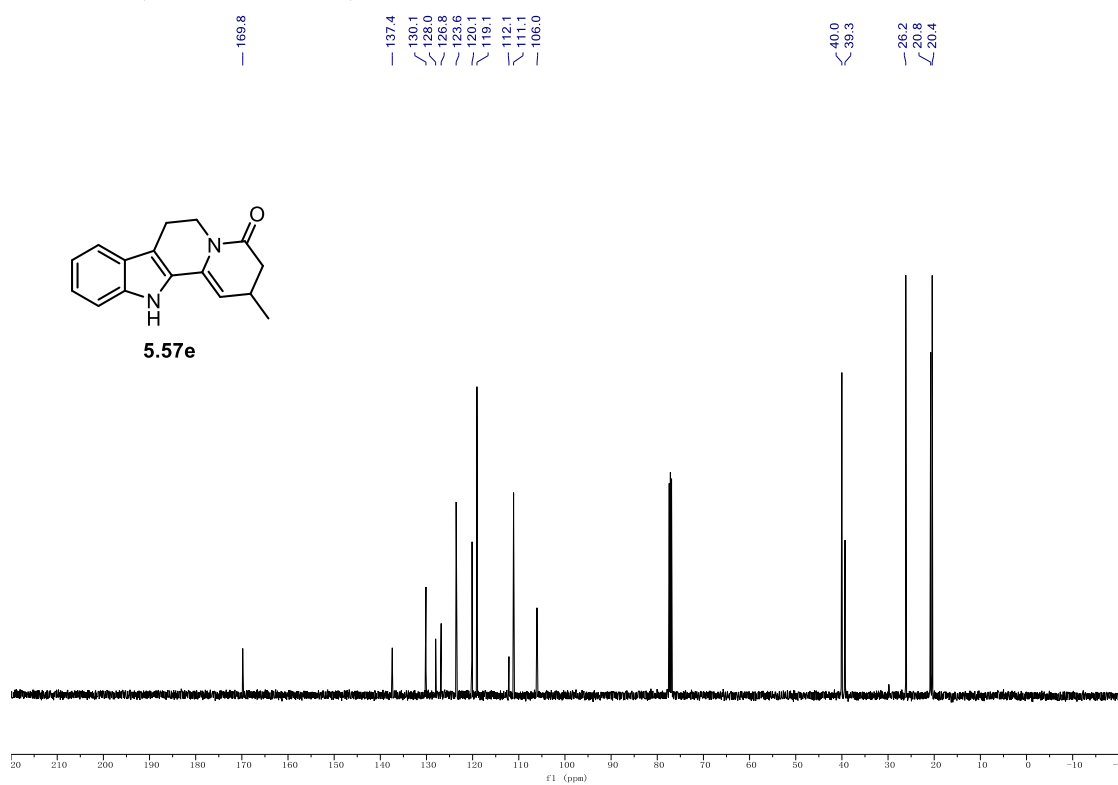
^1H NMR (700 MHz, d_6 -DMSO) of **5.57d**. ^{13}C NMR (176 MHz, d_6 -DMSO) of **5.57d**.

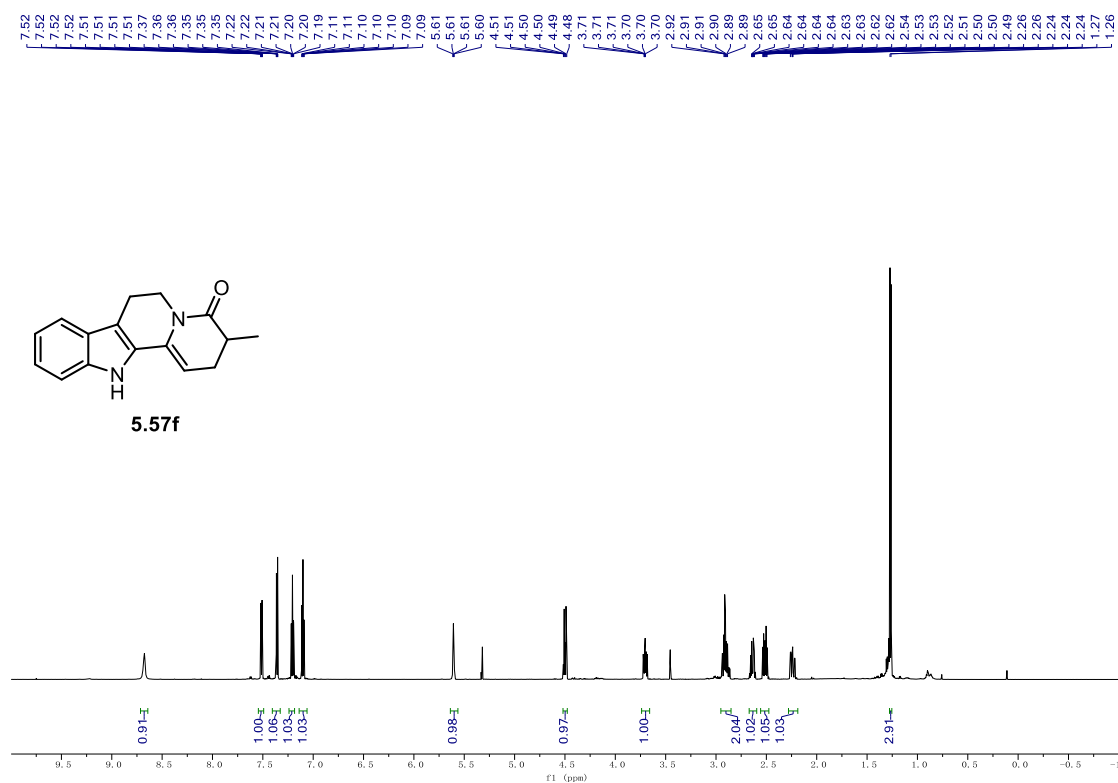
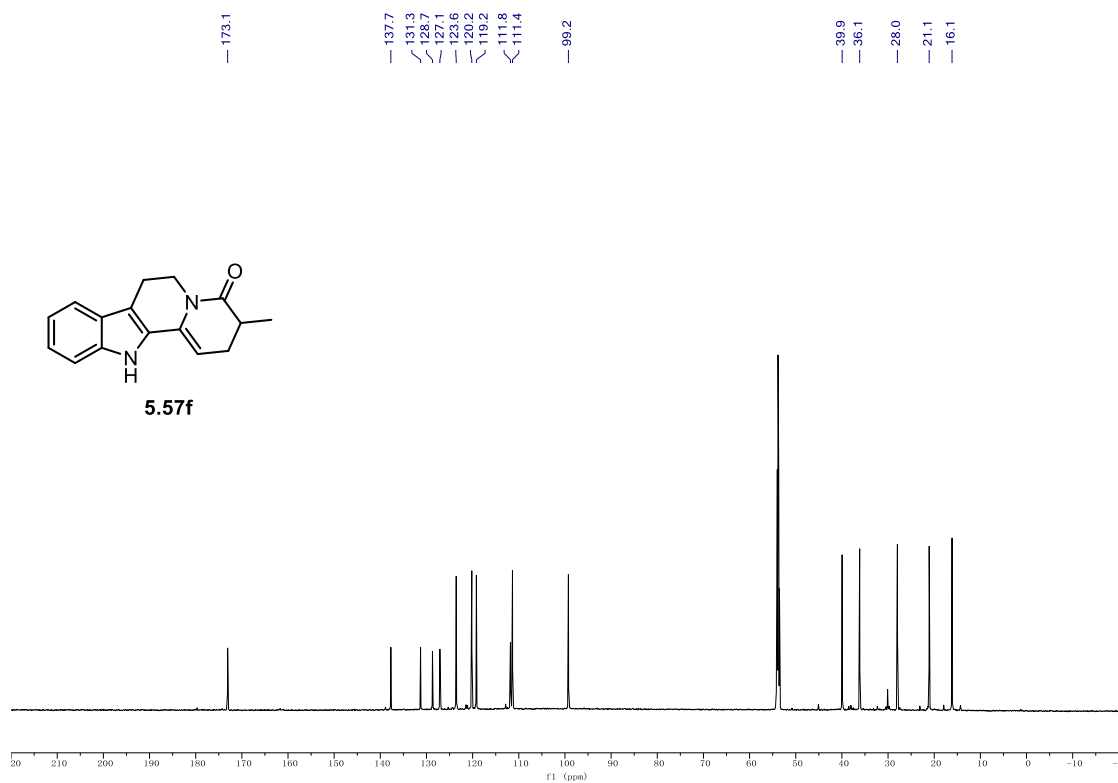
9.1. NMR Spectra

¹H NMR (500 MHz, CDCl₃) of **5.57e**.



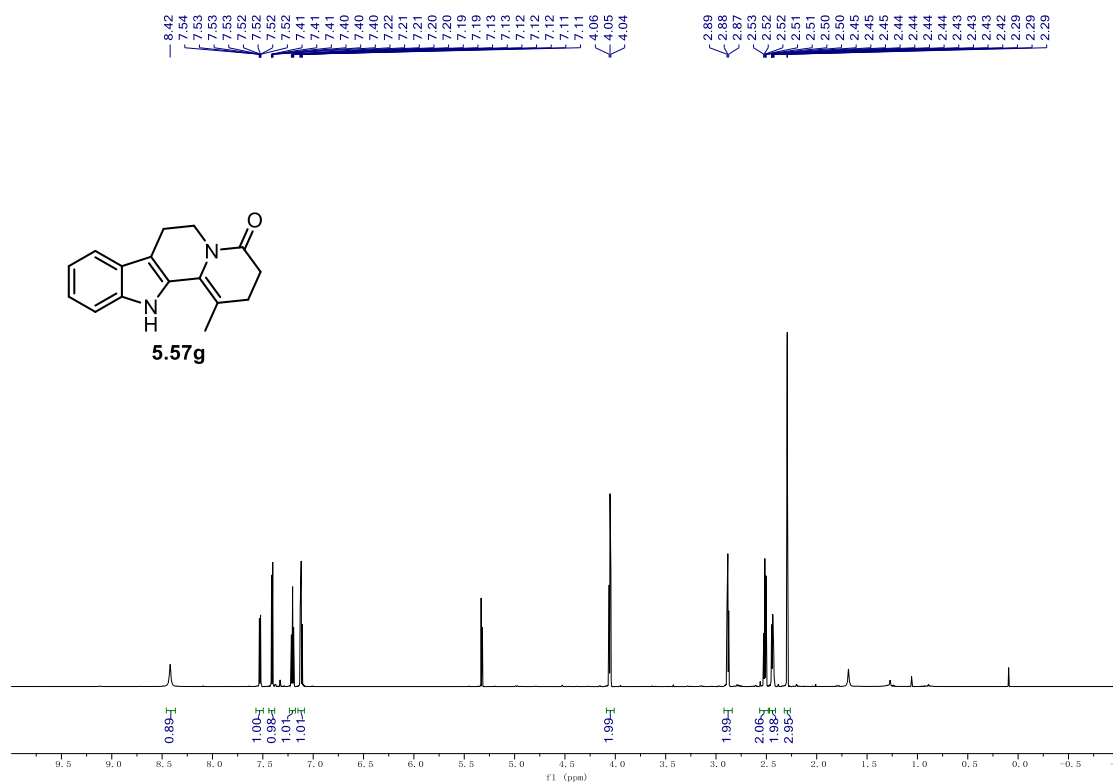
¹³C NMR (126 MHz, CDCl₃) of **5.57e**.



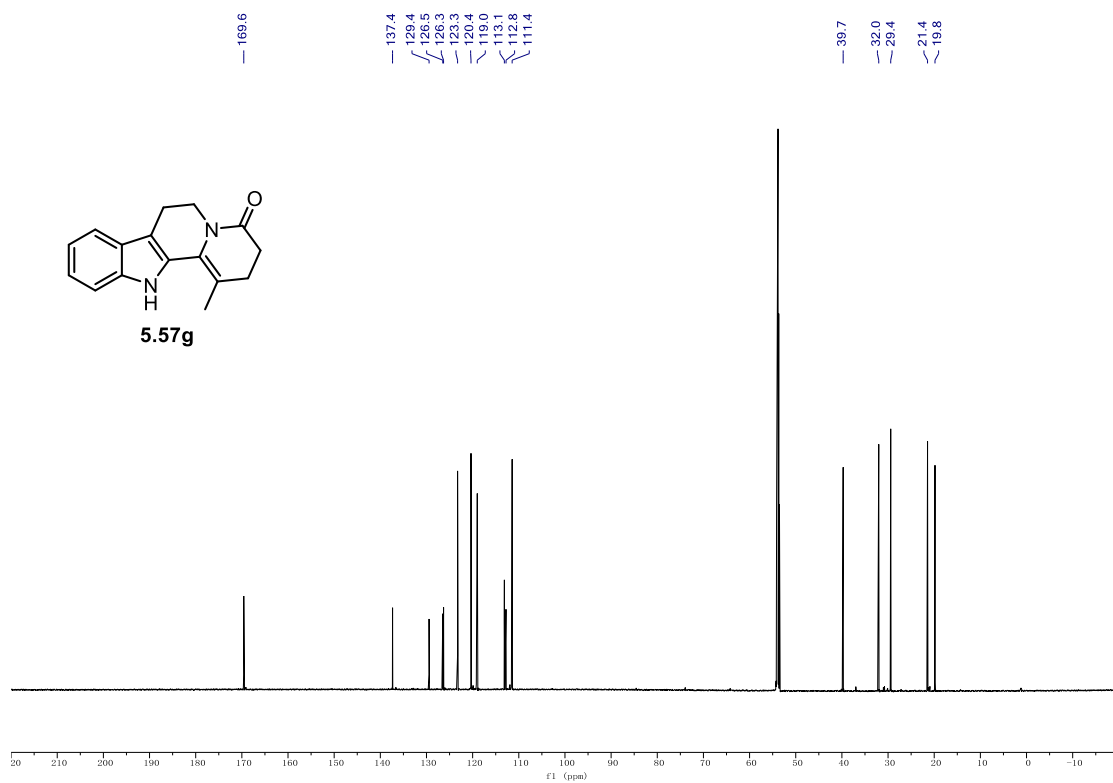
¹H NMR (700 MHz, CD₂Cl₂) of 5.57f.**¹³C NMR (176 MHz, CD₂Cl₂) of 12f.**

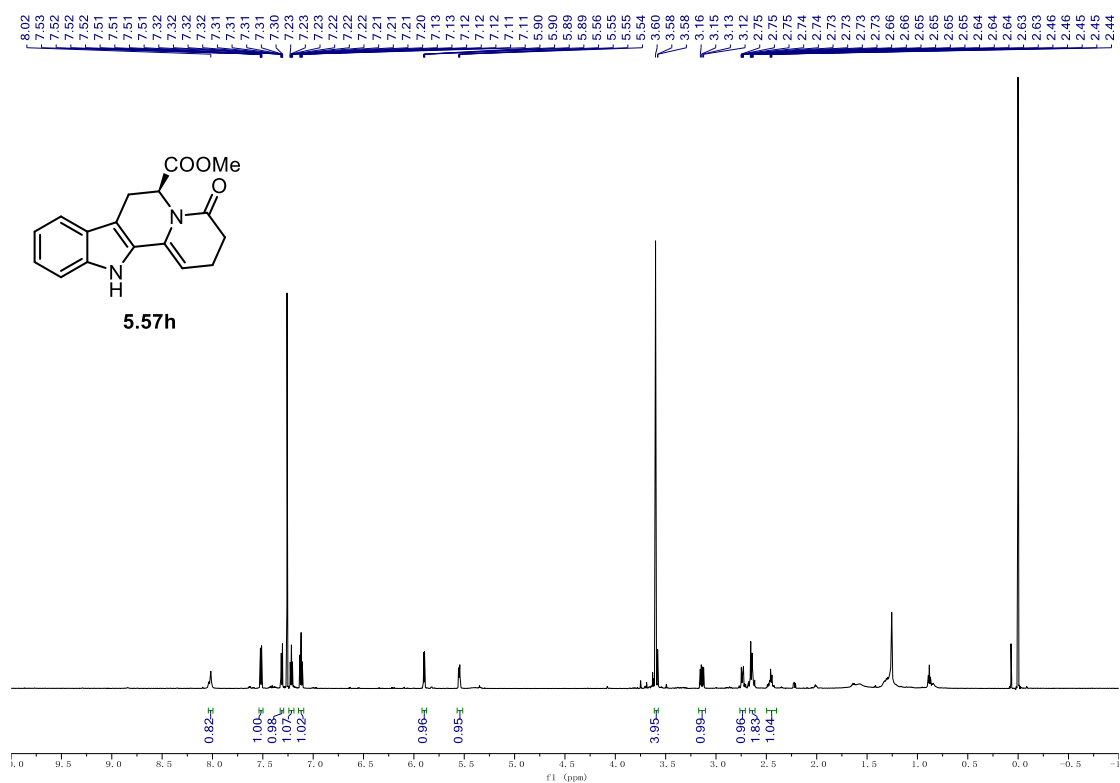
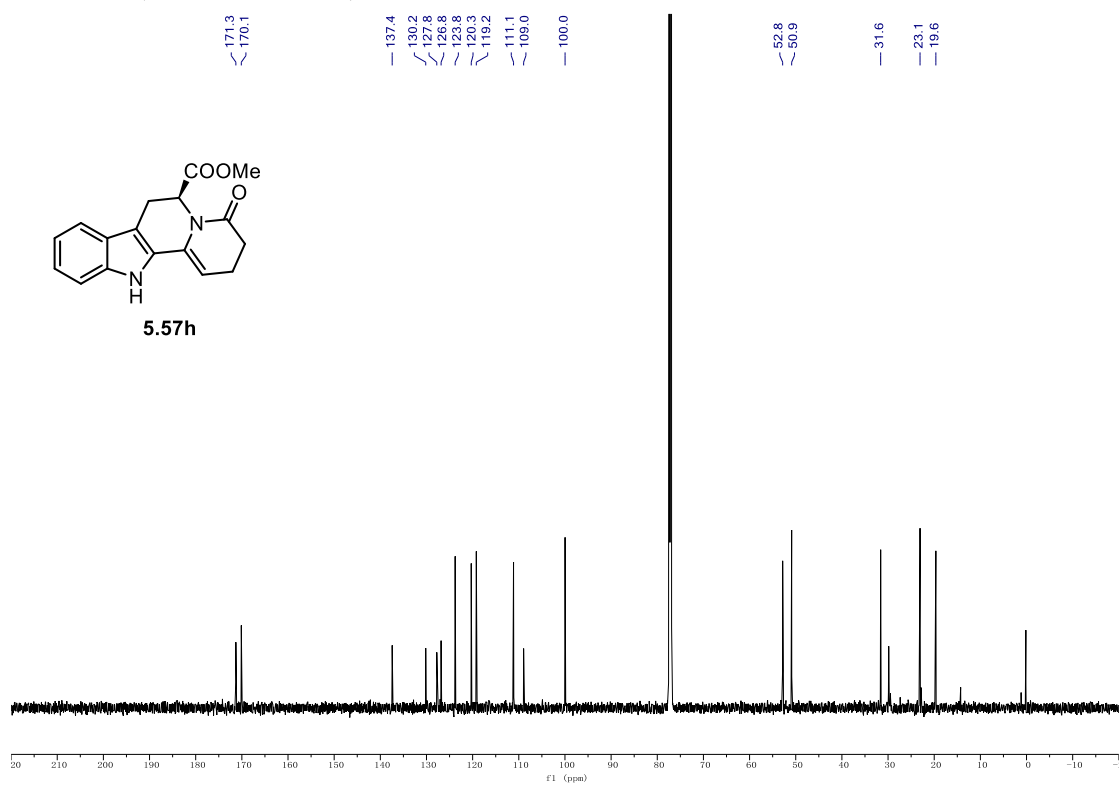
9.1. NMR Spectra

¹H NMR (700 MHz, CD₂Cl₂) of **5.57g**.



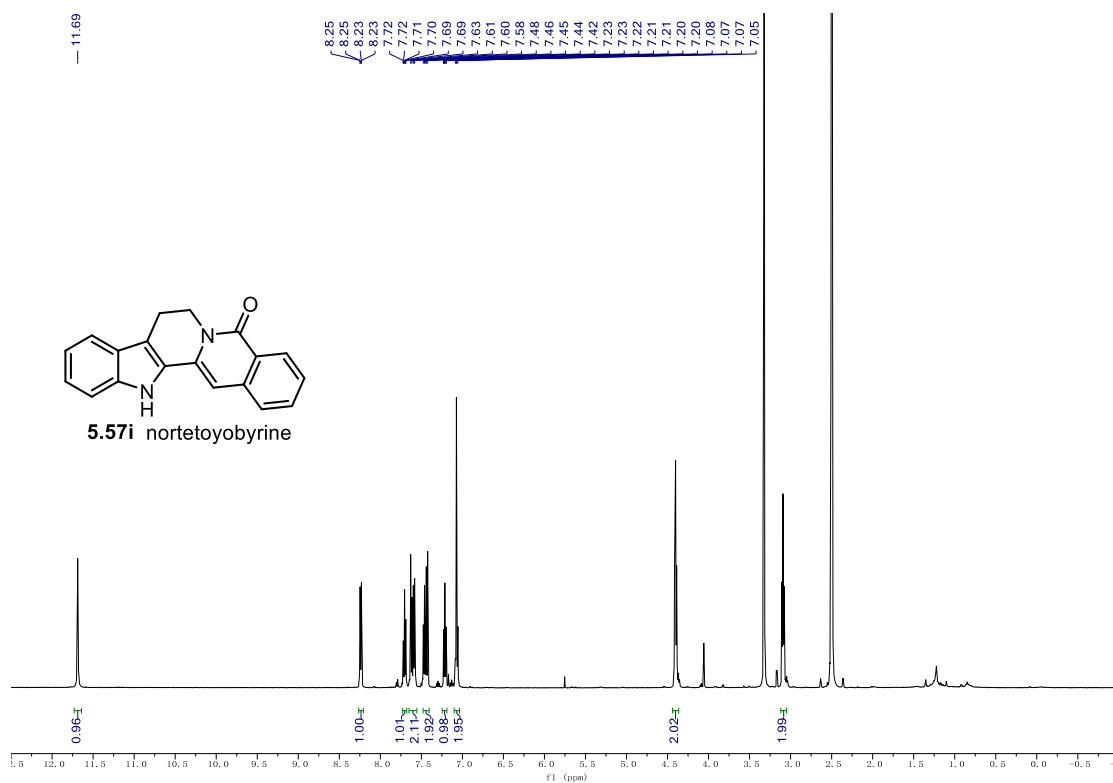
¹³C NMR (176 MHz, CD₂Cl₂) of **5.57g**.



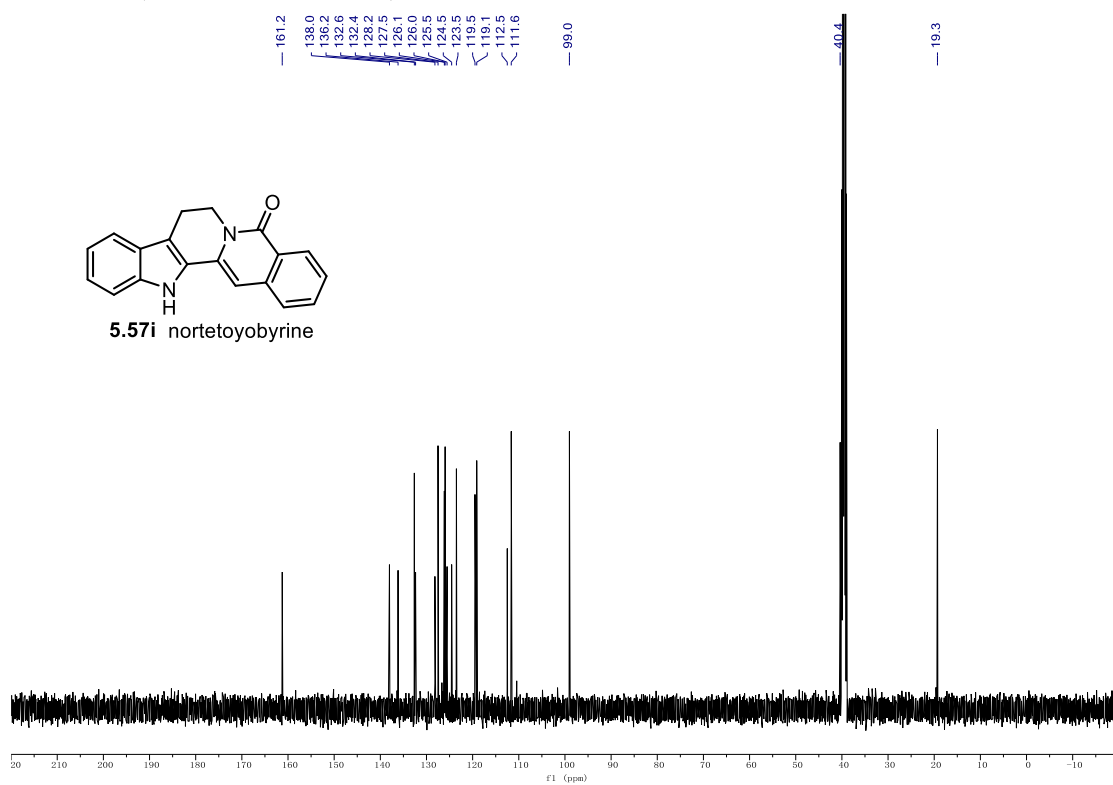
¹H NMR (700 MHz, CDCl₃) of 5.57h.**¹³C NMR (176 MHz, CDCl₃) of 5.57h.**

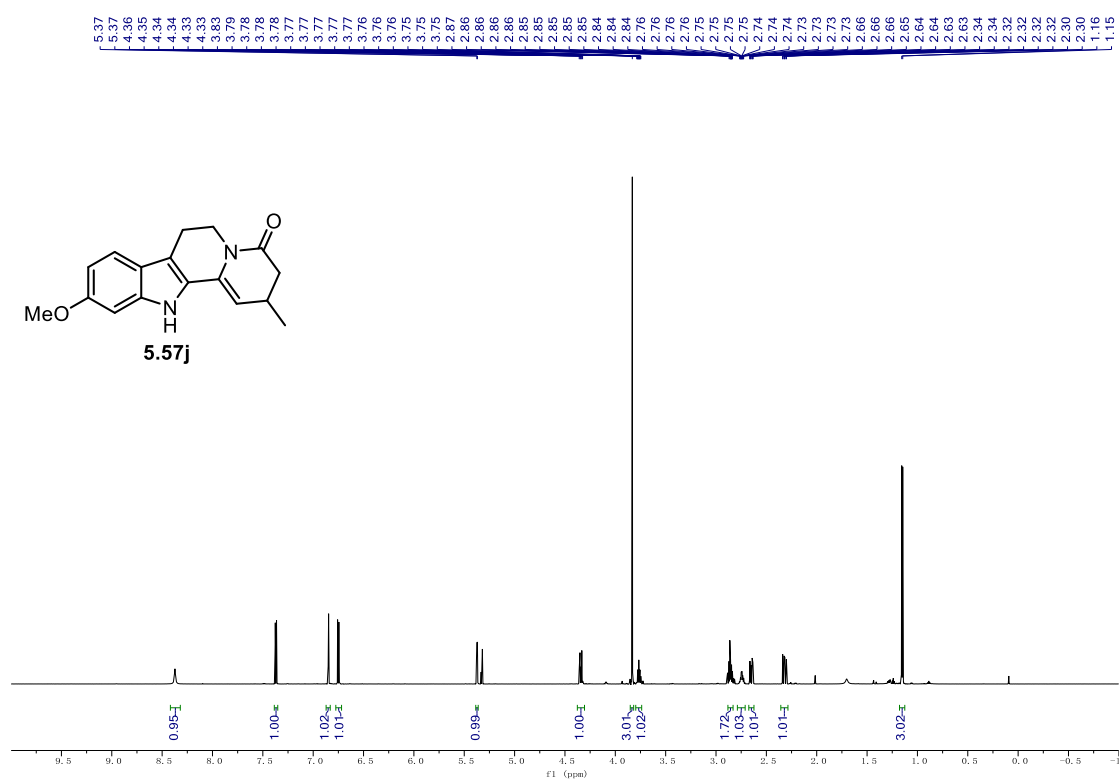
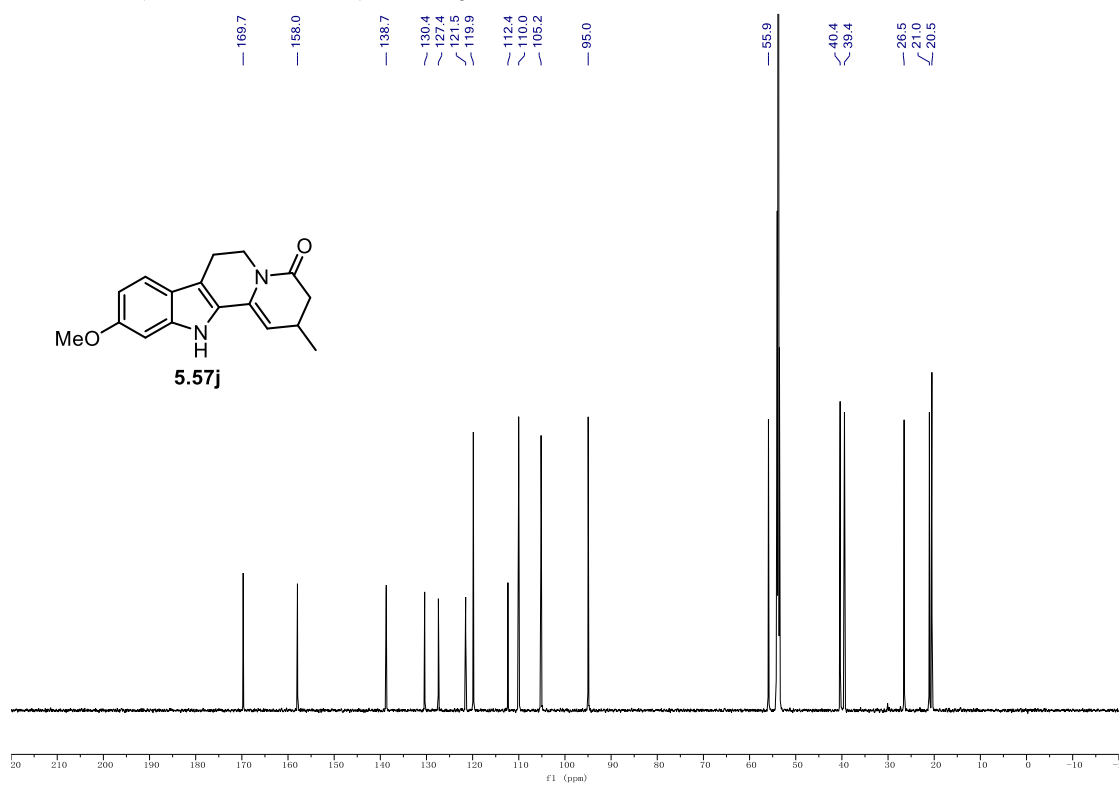
9.1. NMR Spectra

^1H NMR (500 MHz, d_6 -DMSO) of **5.57i**.



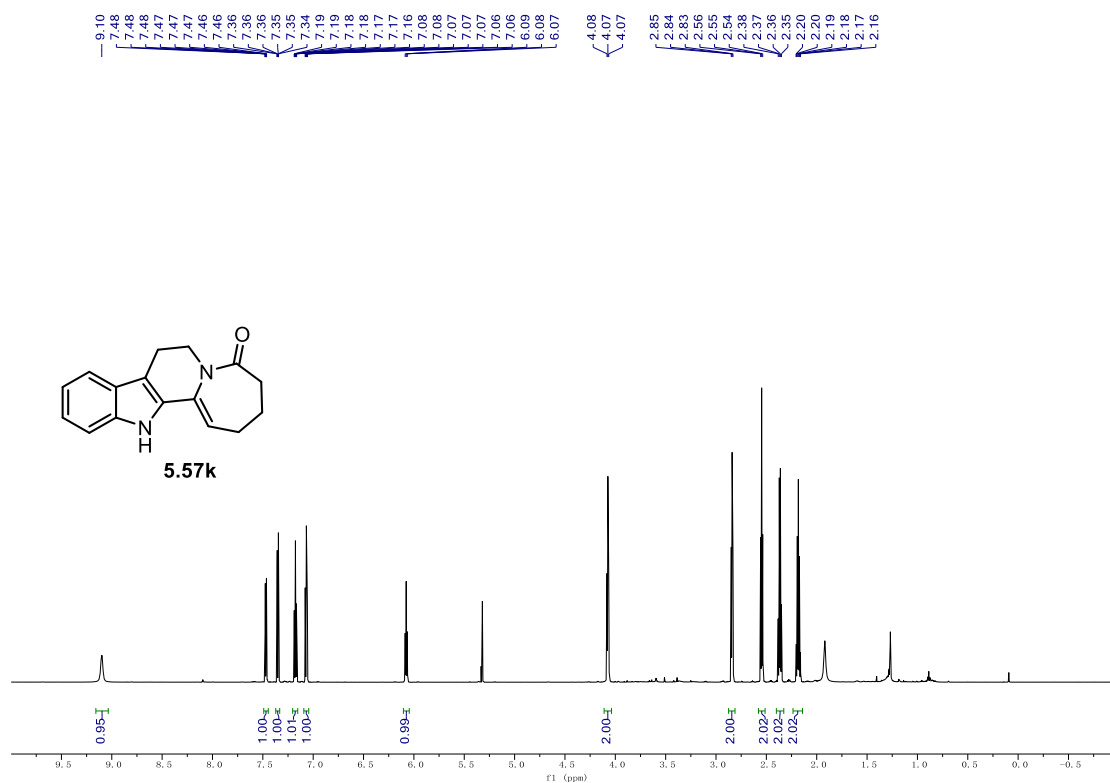
^{13}C NMR (126 MHz, d_6 -DMSO) of **5.57i**.



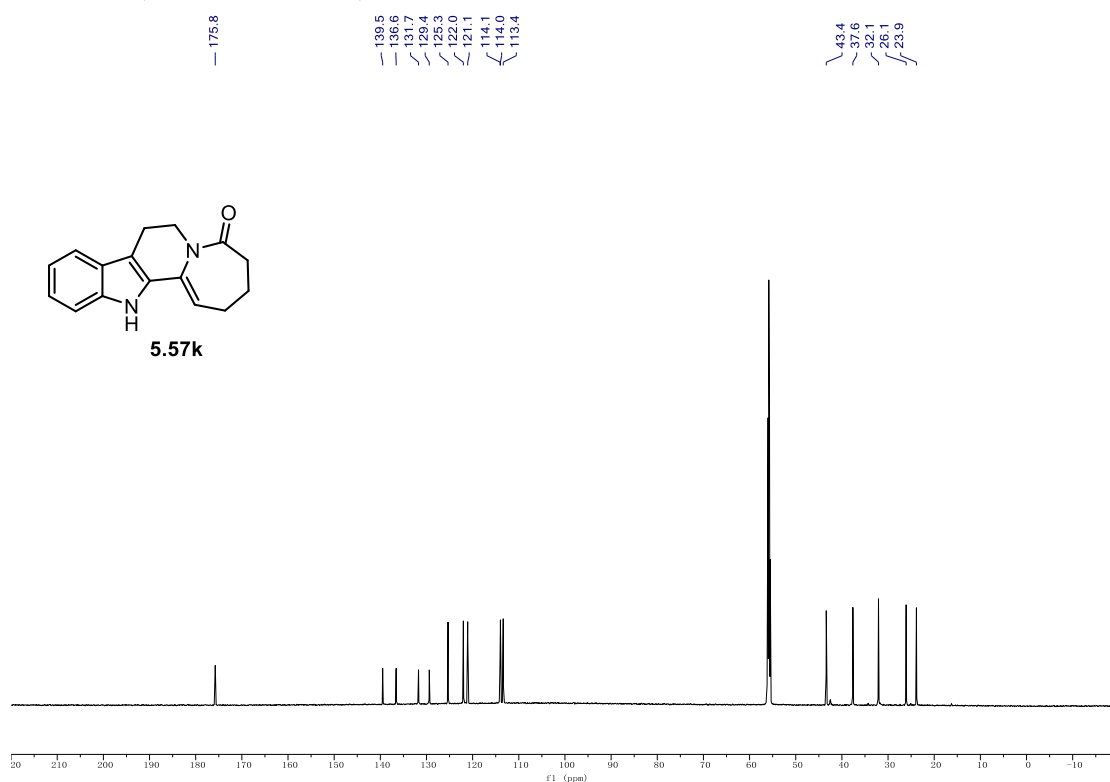
¹H NMR (700 MHz, CD₂Cl₂) of 5.57j.**¹³C NMR (176 MHz, CD₂Cl₂) of 5.57j.**

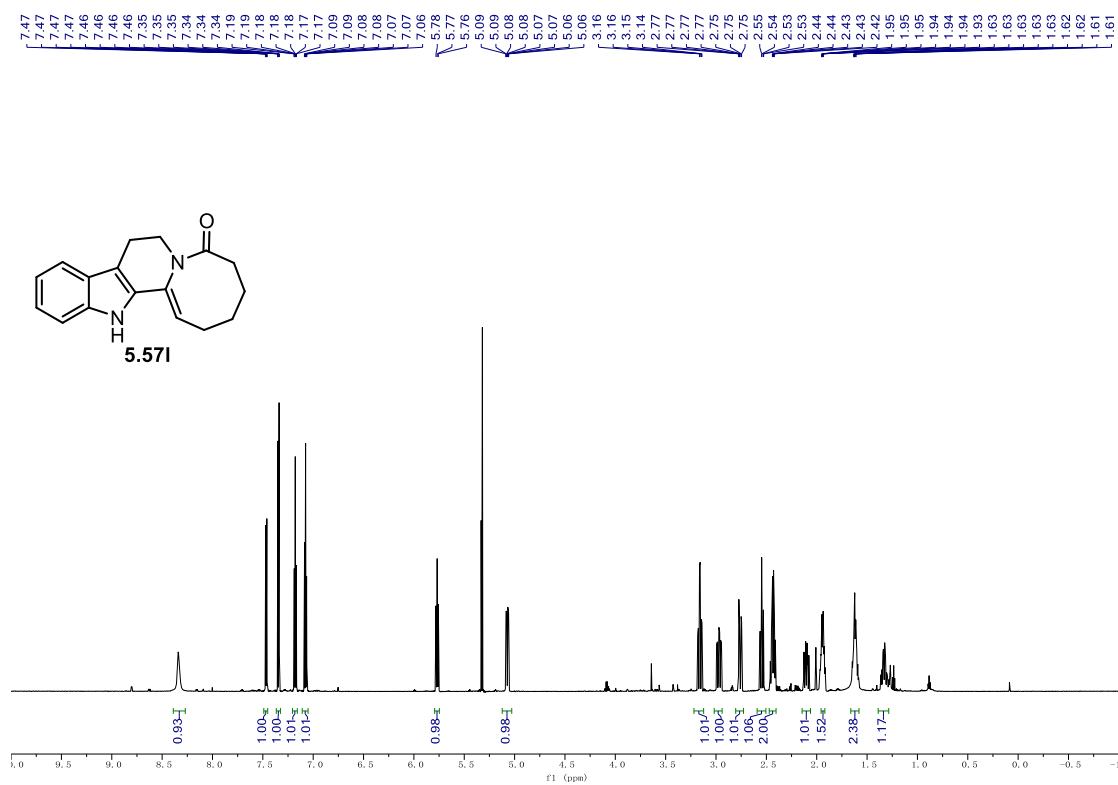
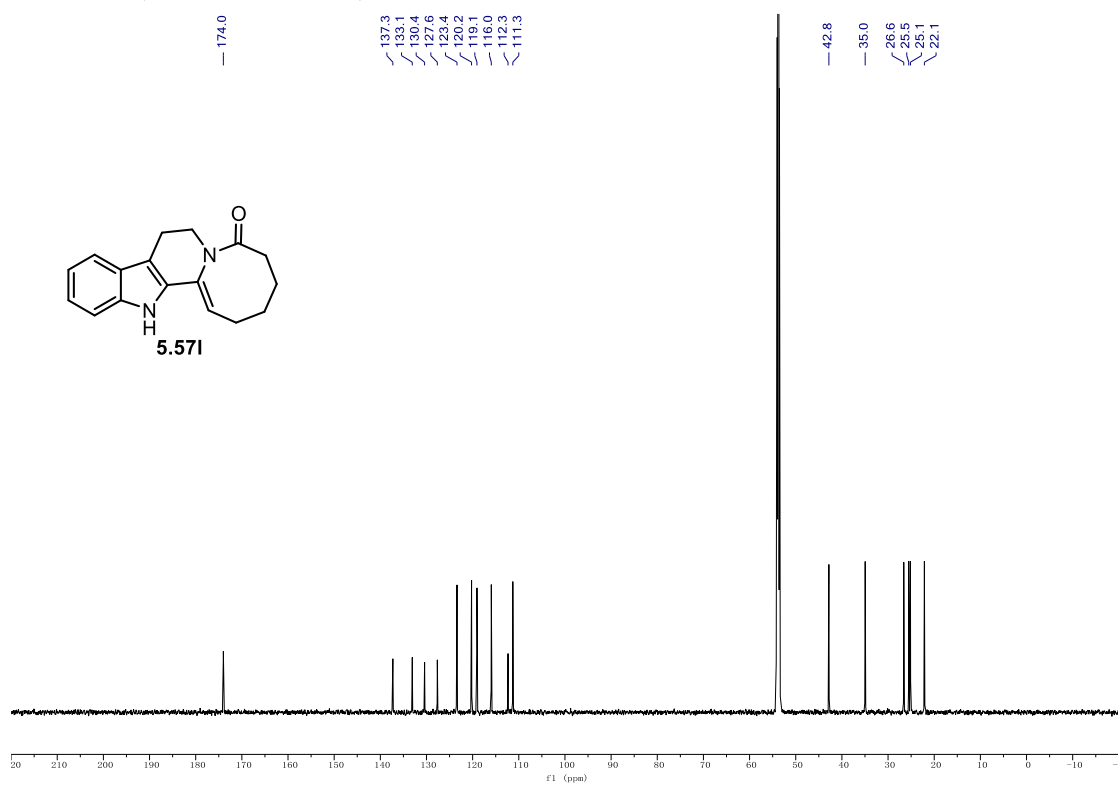
9.1. NMR Spectra

^1H NMR (700 MHz, CD_2Cl_2) of **5.57k**.



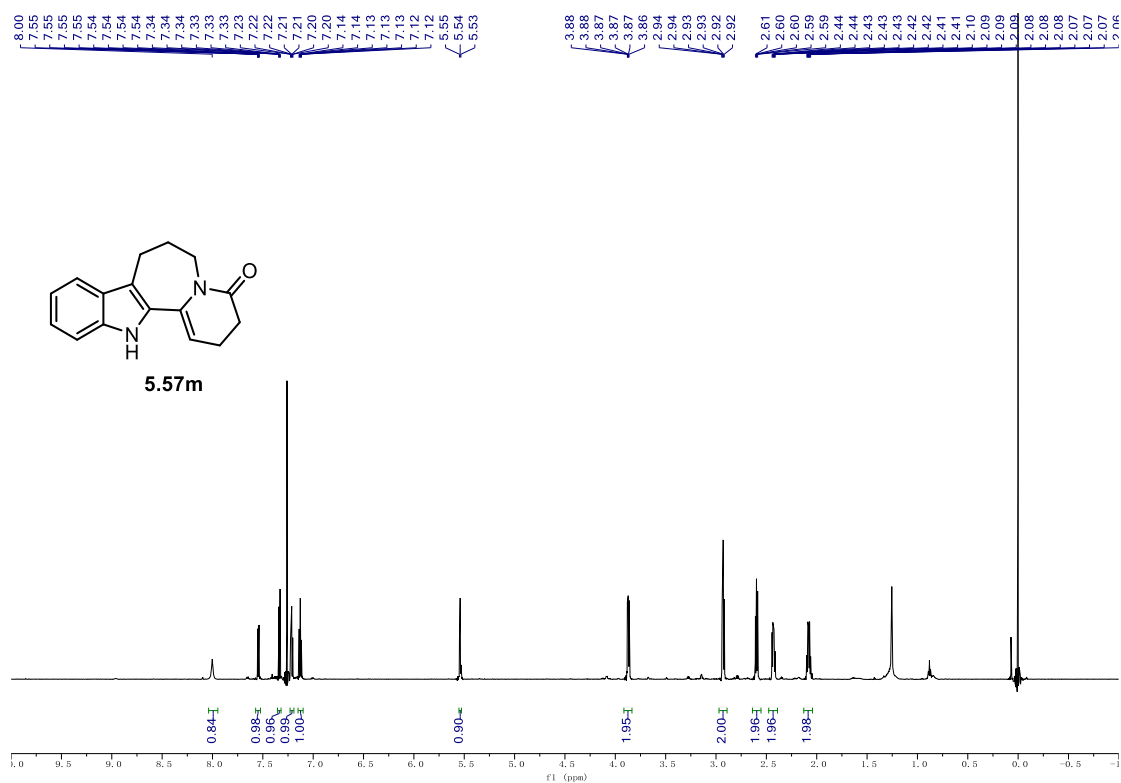
^{13}C NMR (176 MHz, CD_2Cl_2) of **5.57k**.



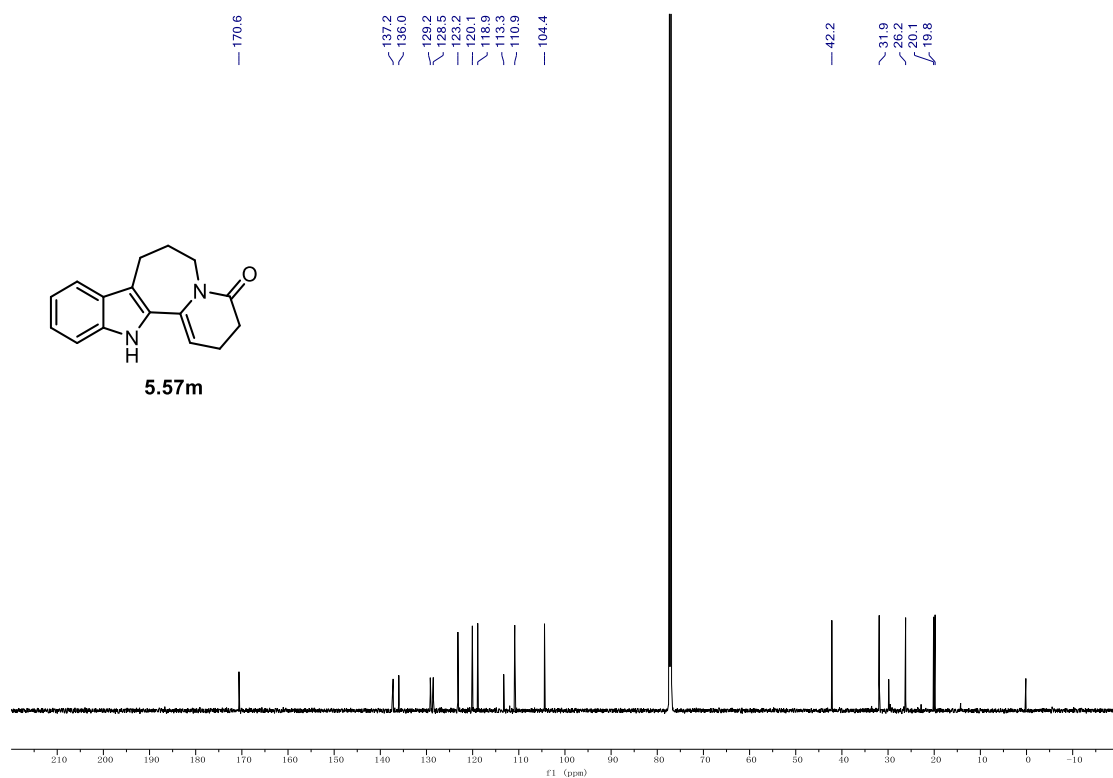
¹H NMR (700 MHz, CD₂Cl₂) of 5.571.**¹³C NMR (176 MHz, CD₂Cl₂) of 5.571.**

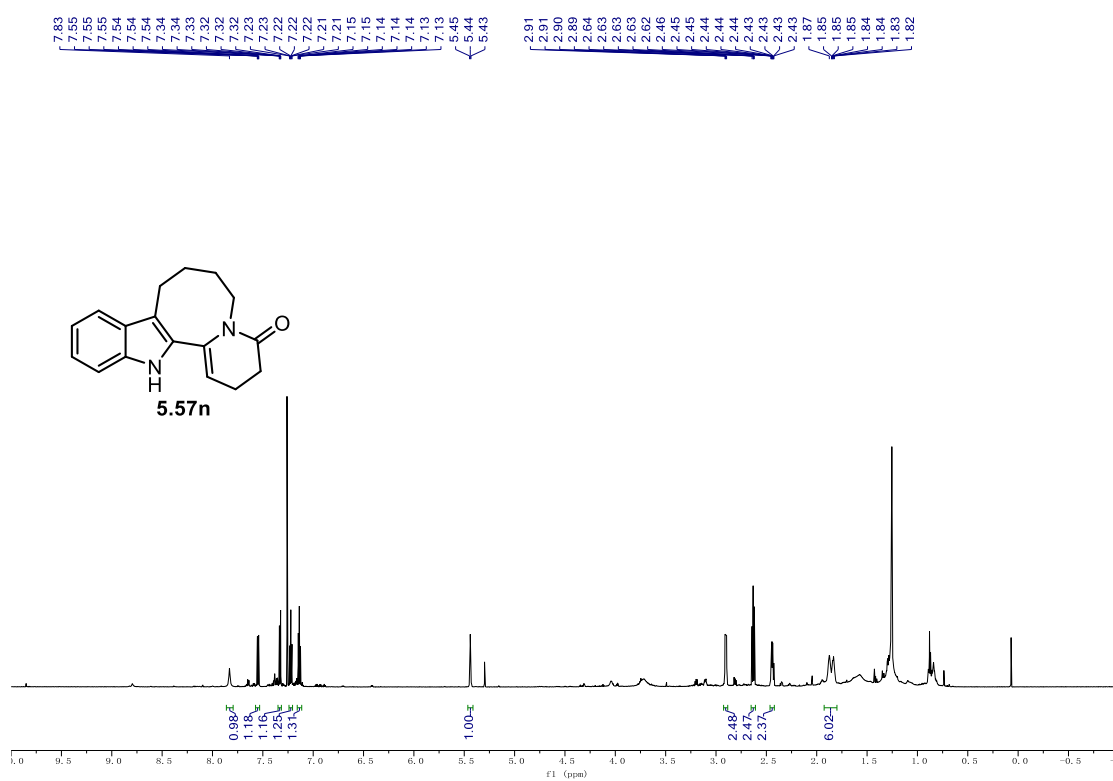
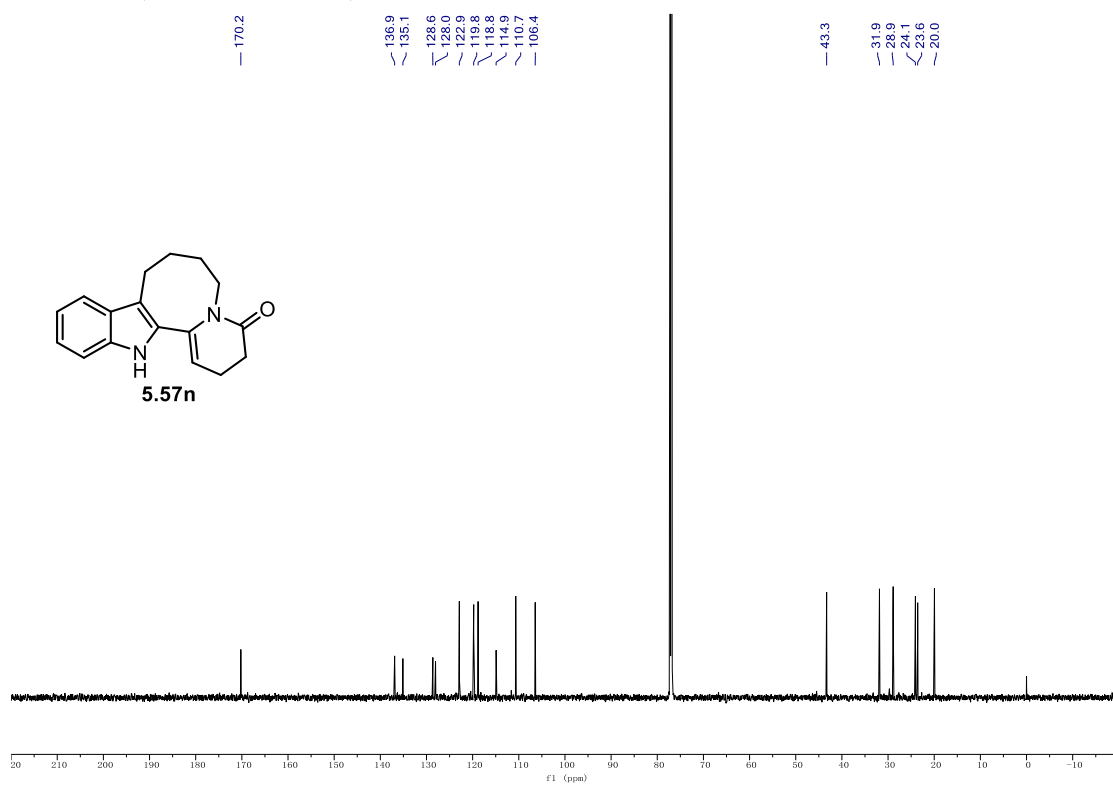
9.1. NMR Spectra

¹H NMR (700 MHz, CDCl₃) of **5.57m**.



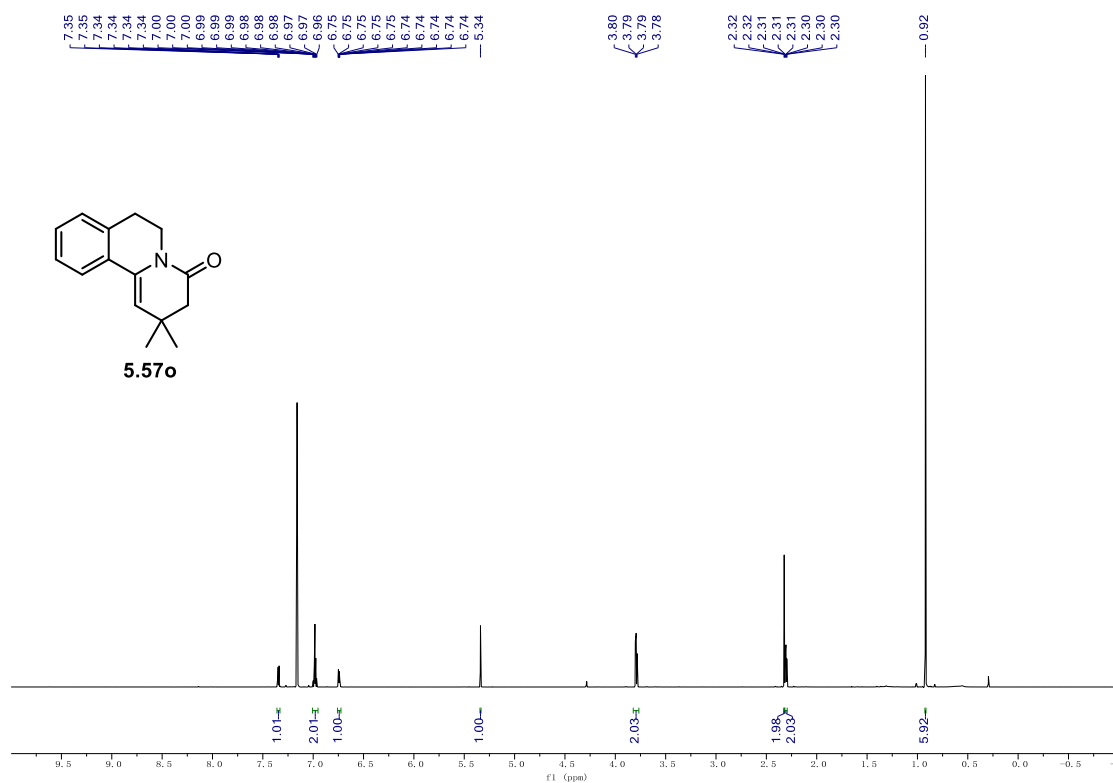
¹³C NMR (176 MHz, CD₂Cl₂) of **5.57m**.



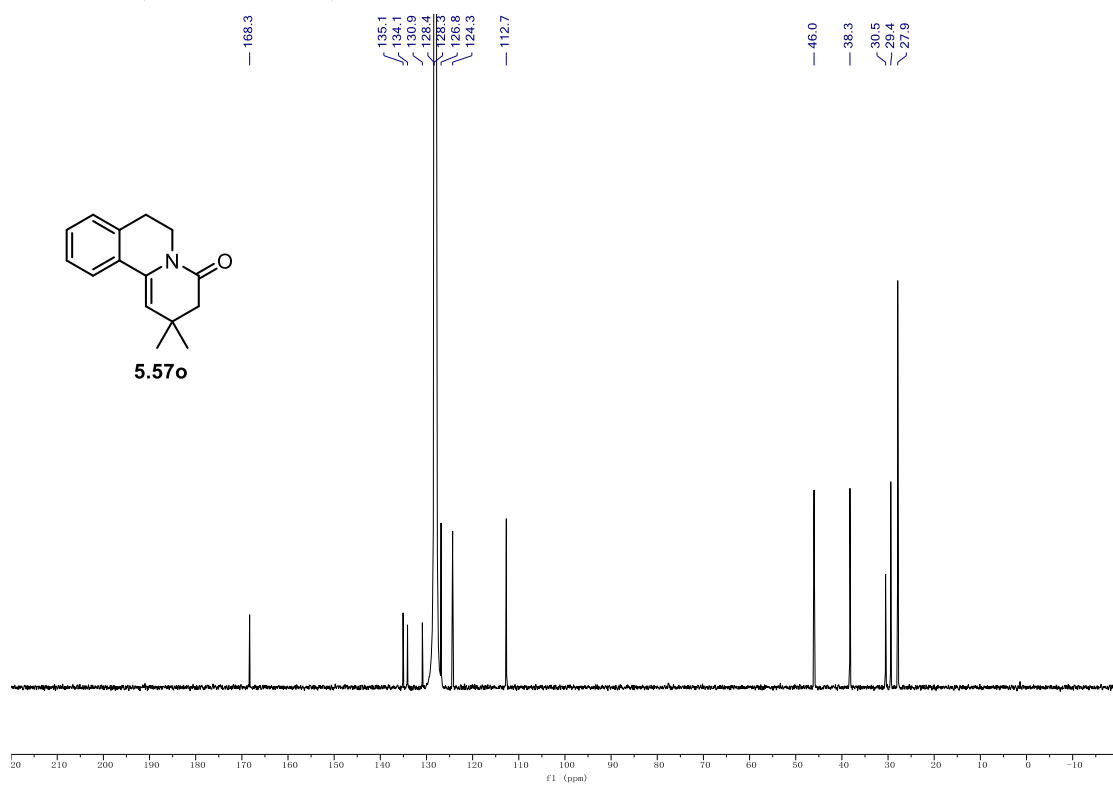
^1H NMR (700 MHz, CDCl_3) of **5.57n**. ^{13}C NMR (176 MHz, CDCl_3) of **5.57n**.

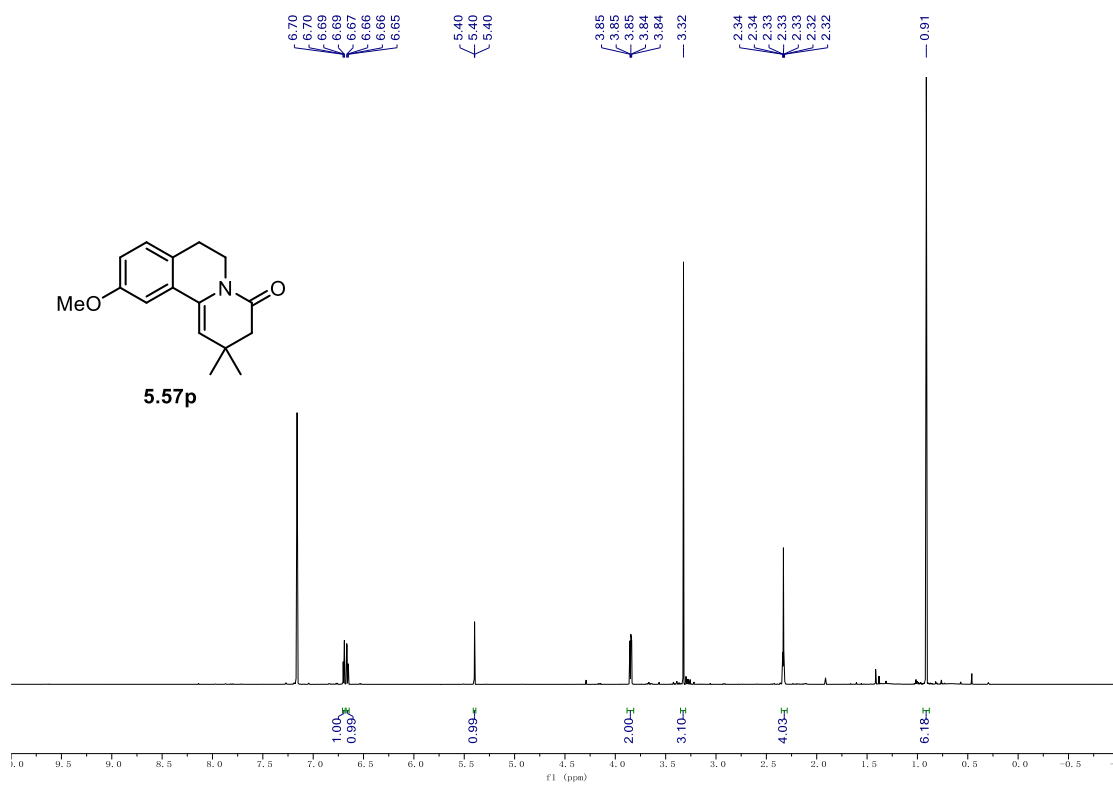
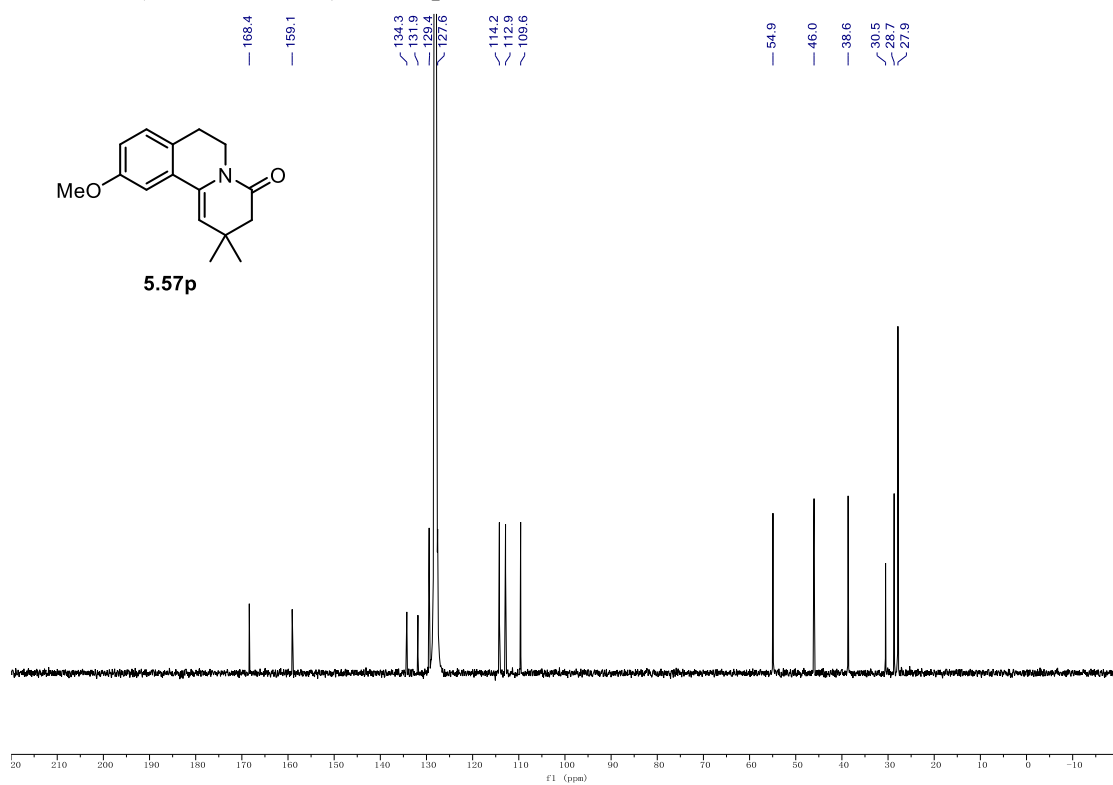
9.1. NMR Spectra

^1H NMR (700 MHz, C_6D_6) of **5.57o**.



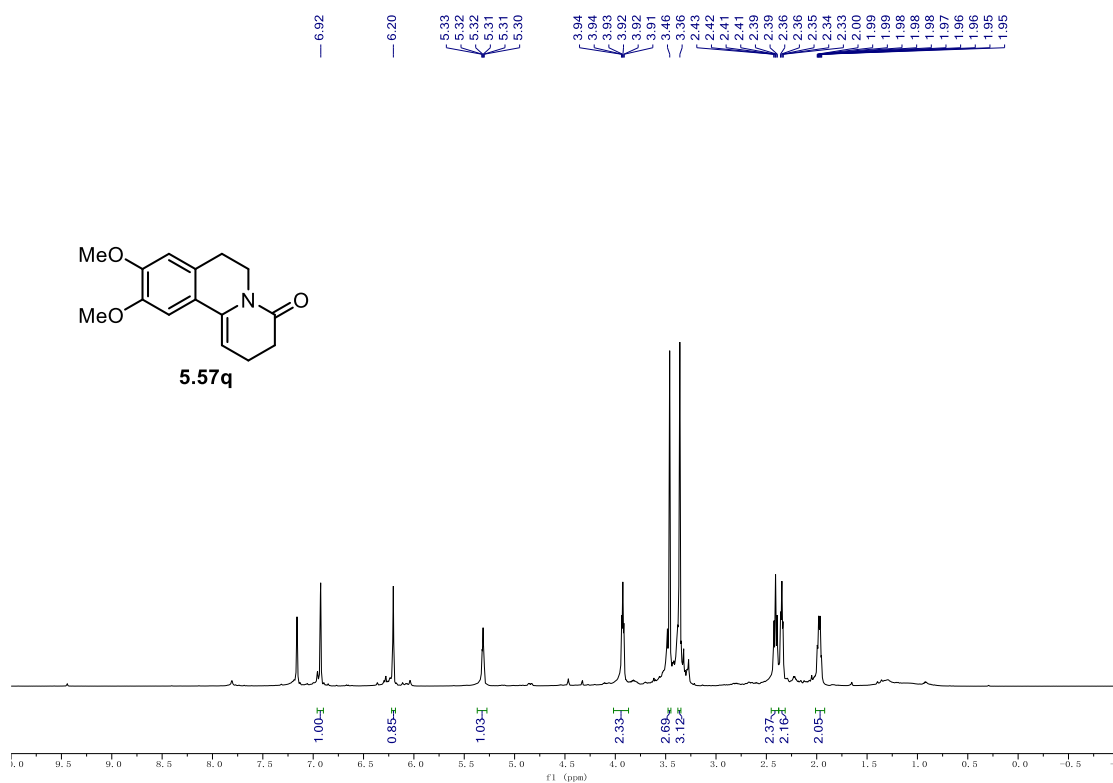
^{13}C NMR (176 MHz, C_6D_6) of **5.57o**.



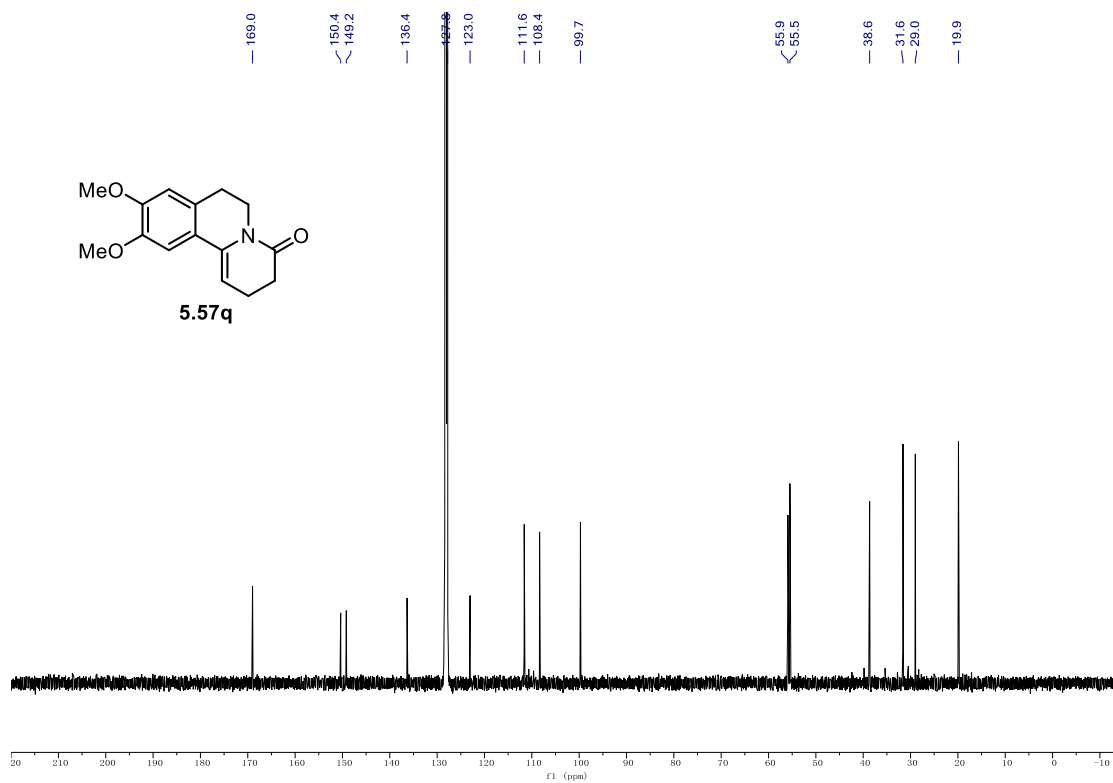
¹H NMR (700 MHz, C₆D₆) of 5.57p.**¹³C NMR (176 MHz, C₆D₆) of 5.57p.**

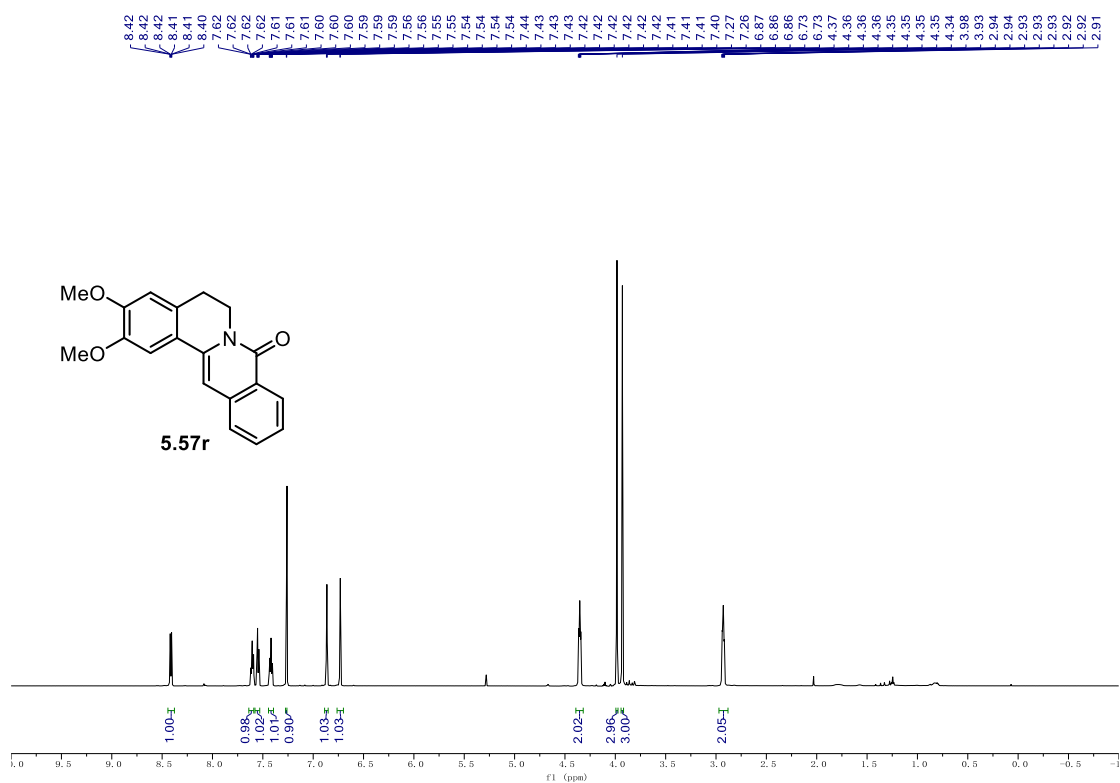
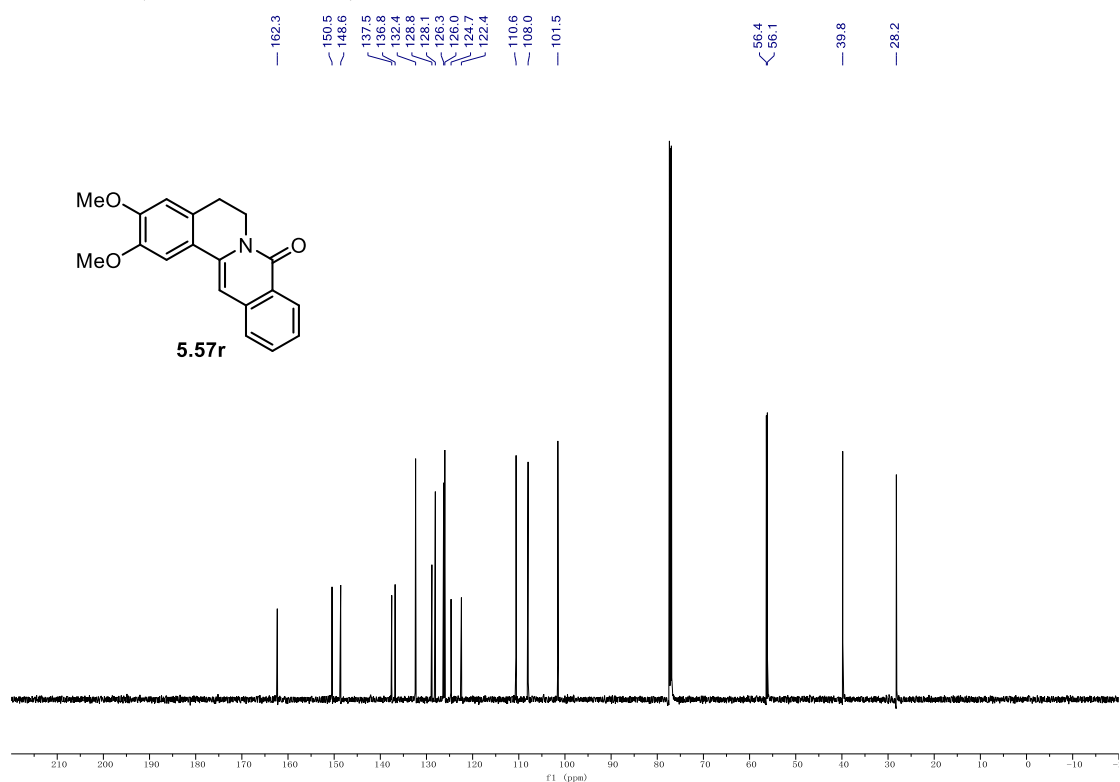
9.1. NMR Spectra

¹H NMR (500 MHz, C₆D₆) of **5.57q**.



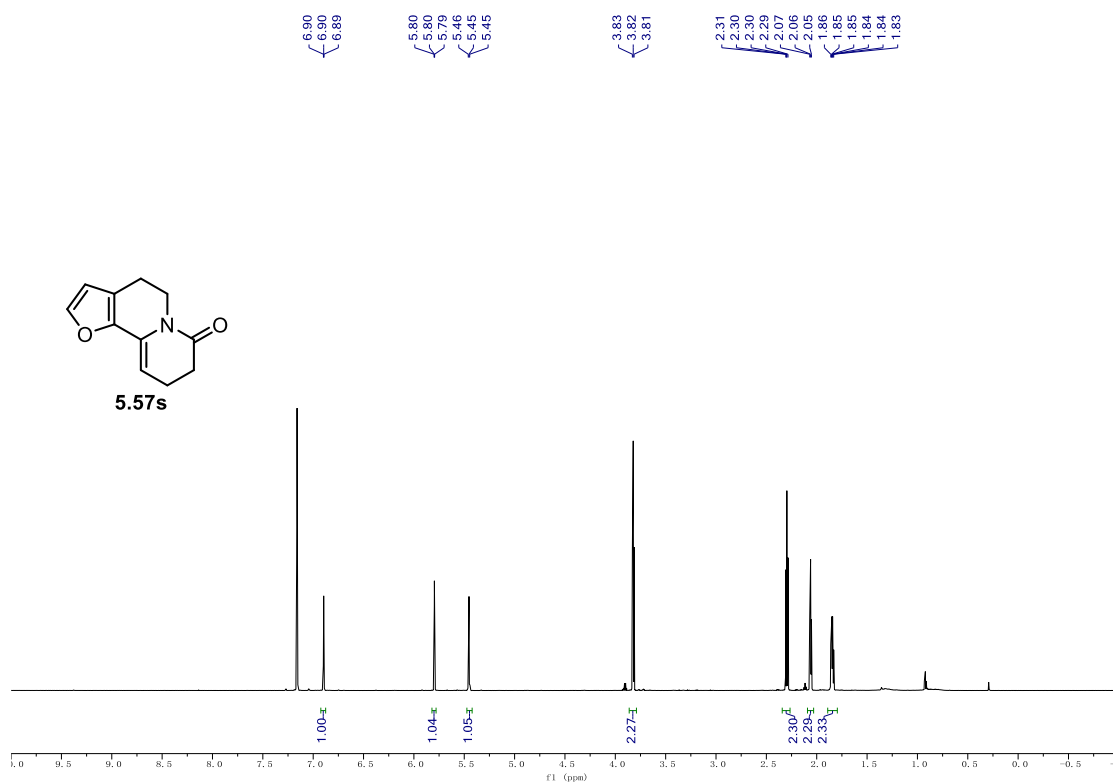
¹³C NMR (126 MHz, C₆D₆) of **5.57q**.



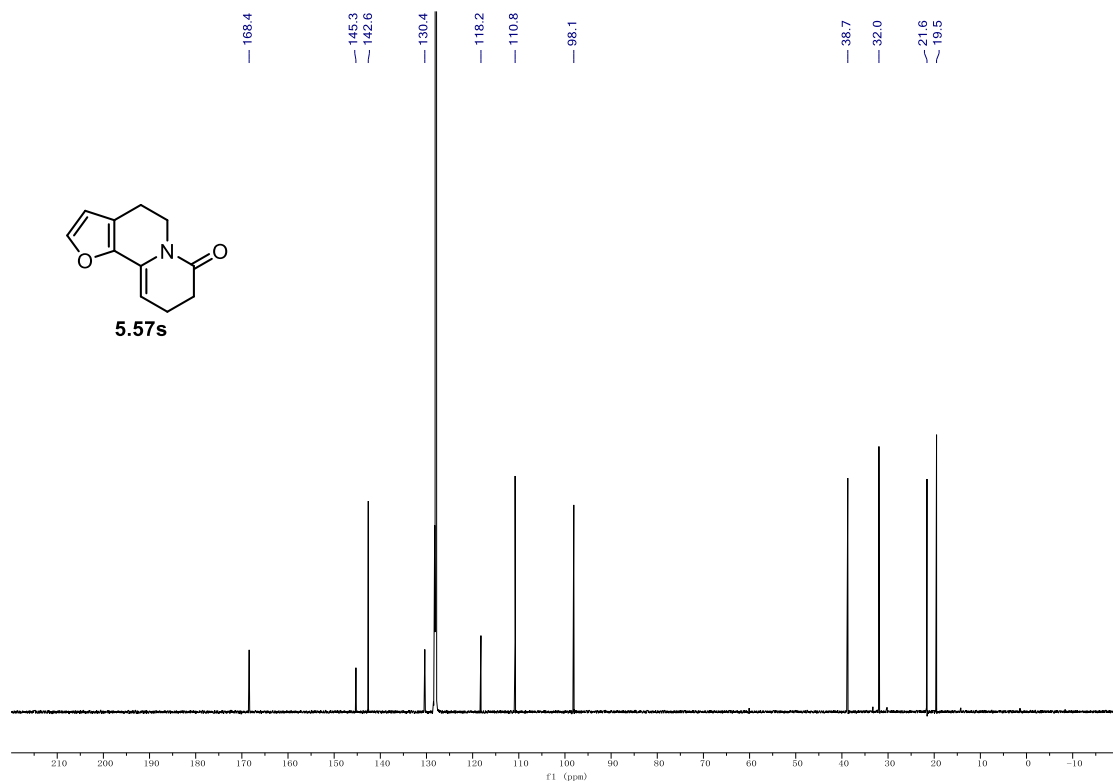
¹H NMR (600 MHz, CDCl₃) of 5.57r.**¹³C NMR (151 MHz, CDCl₃) of 5.57r.**

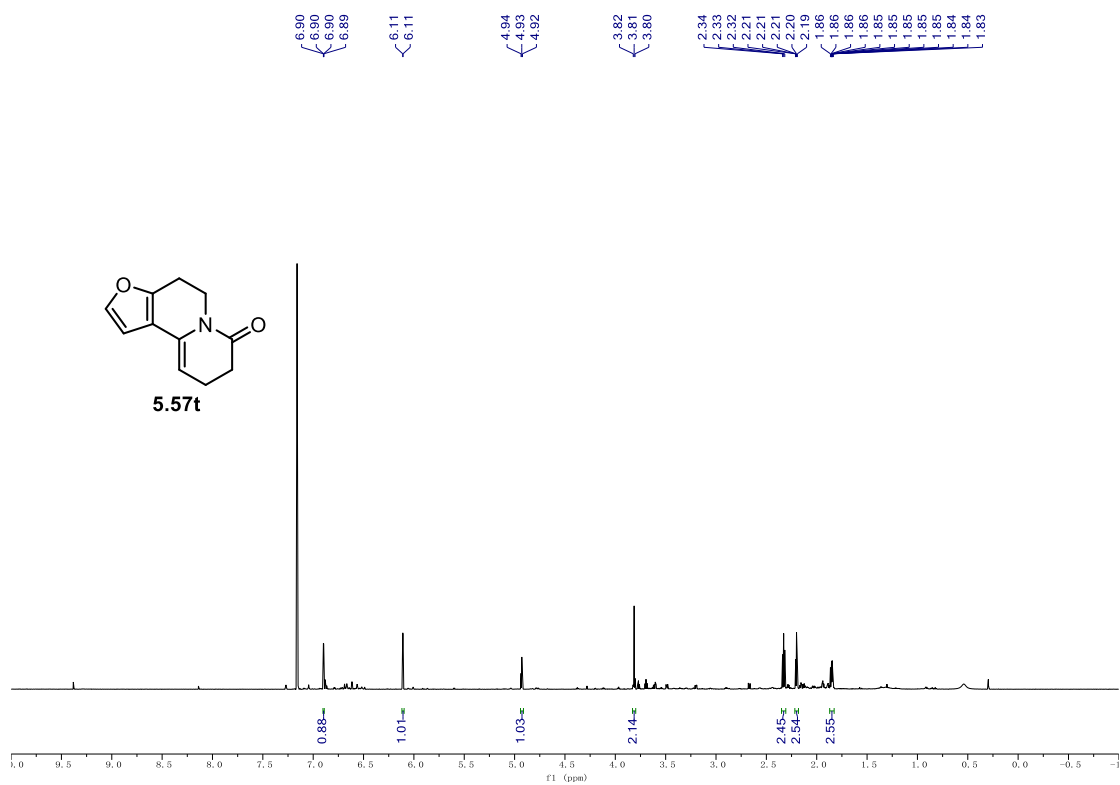
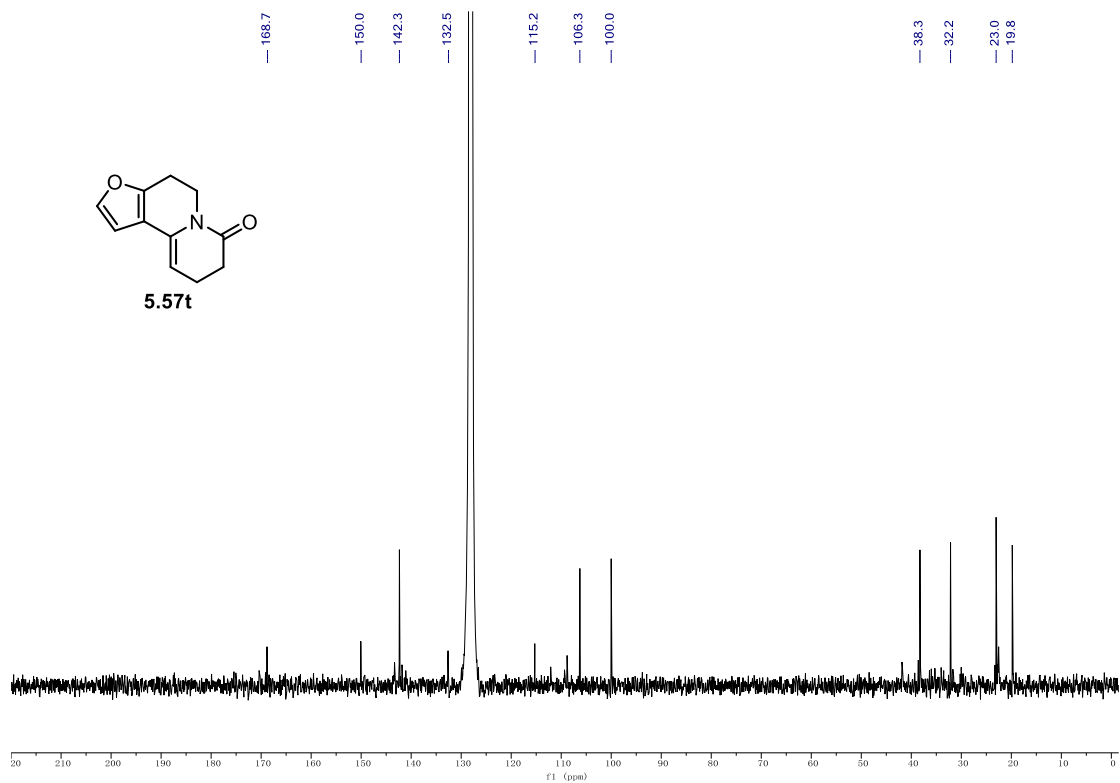
9.1. NMR Spectra

¹H NMR (700 MHz, C₆D₆) of **5.57s**.



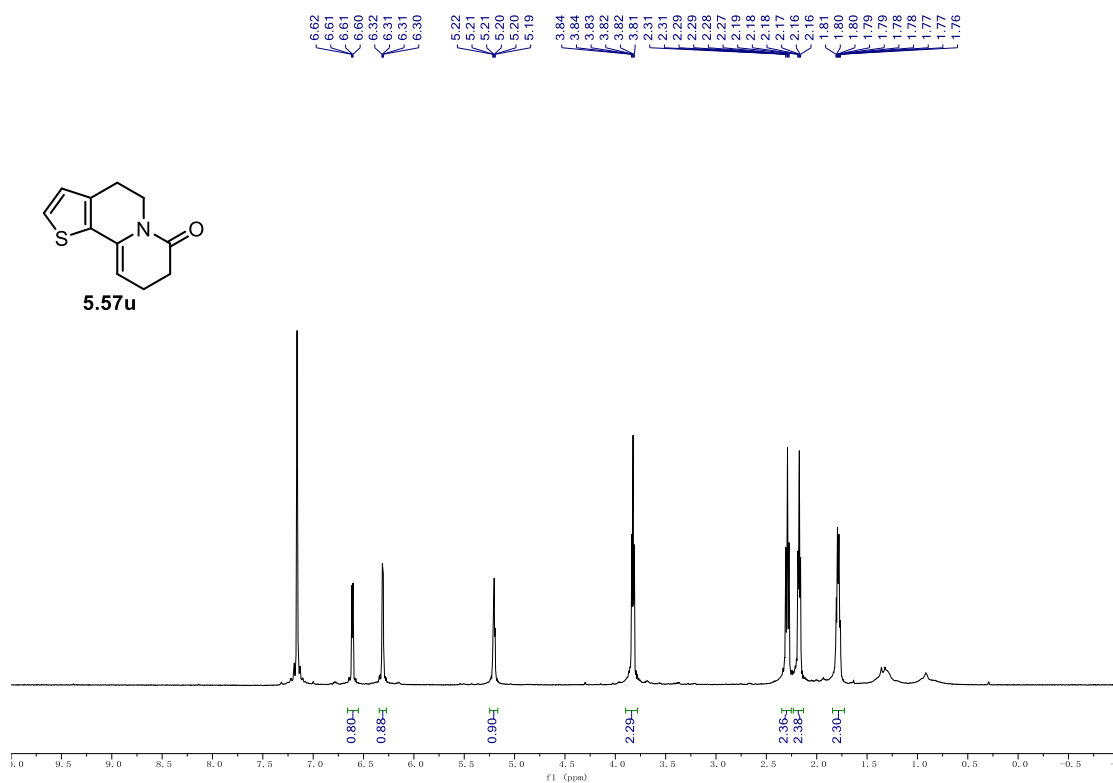
¹³C NMR (176 MHz, C₆D₆) of **5.57s**.



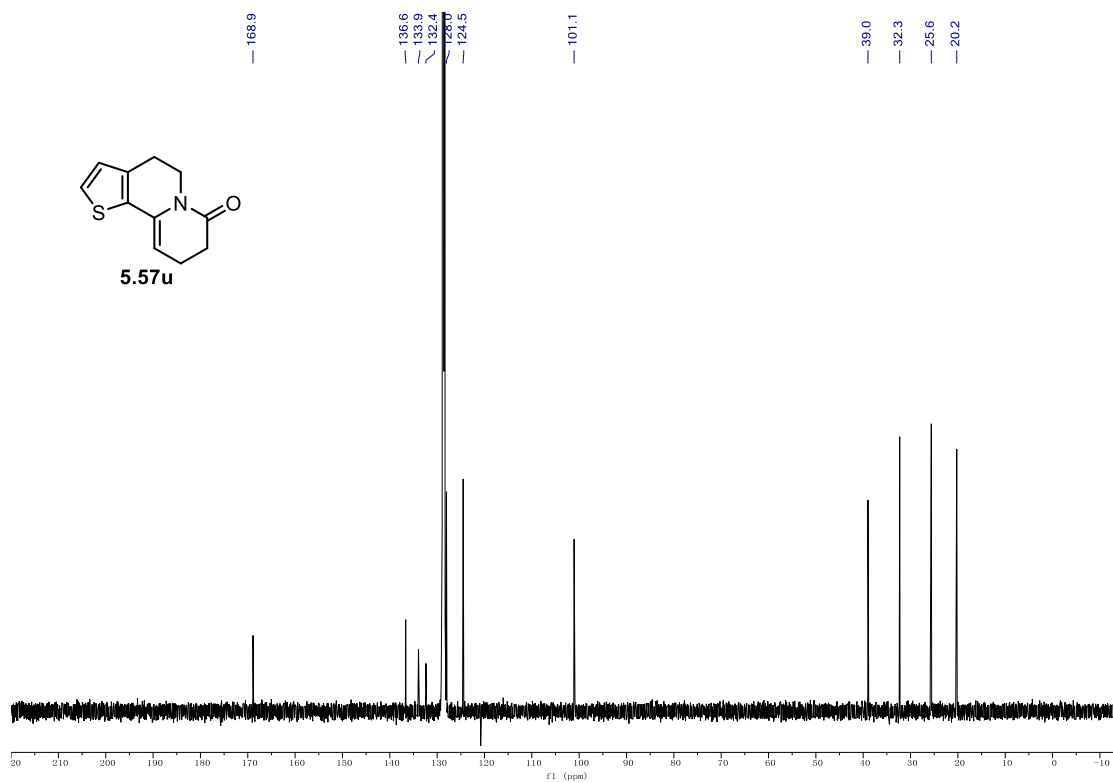
^1H NMR (700 MHz, C_6D_6) of **5.57t**. ^{13}C NMR (176 MHz, C_6D_6) of **5.57t**.

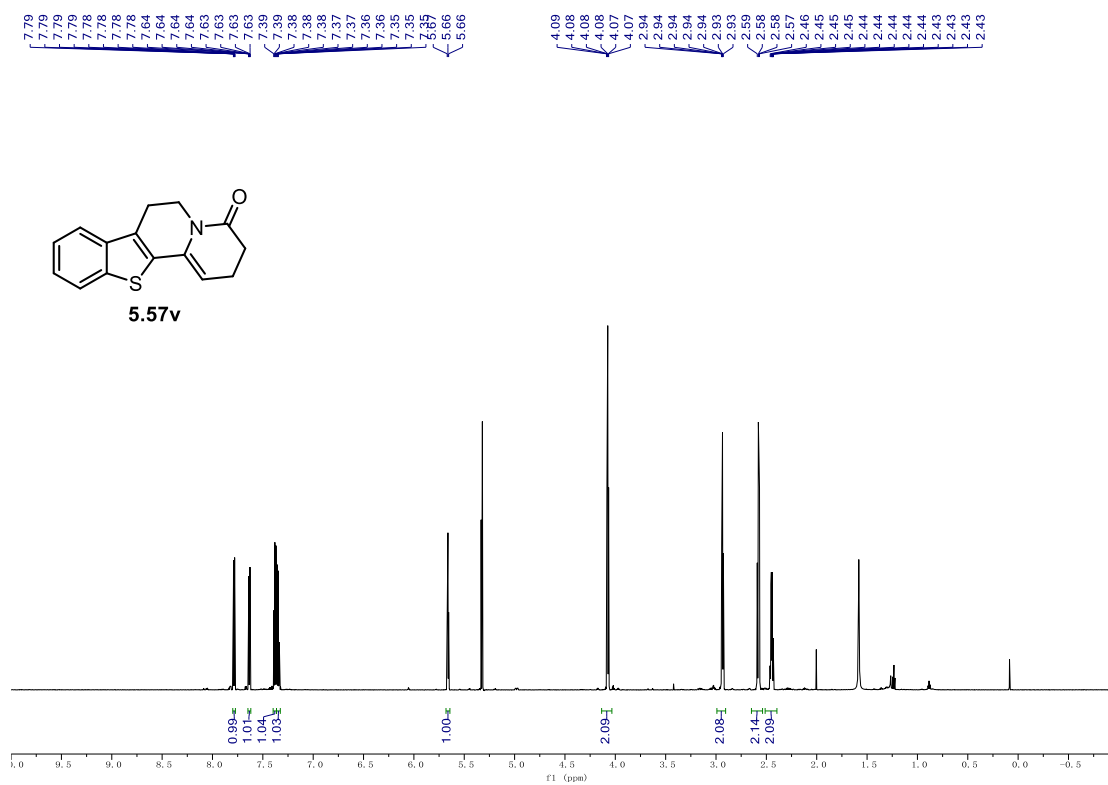
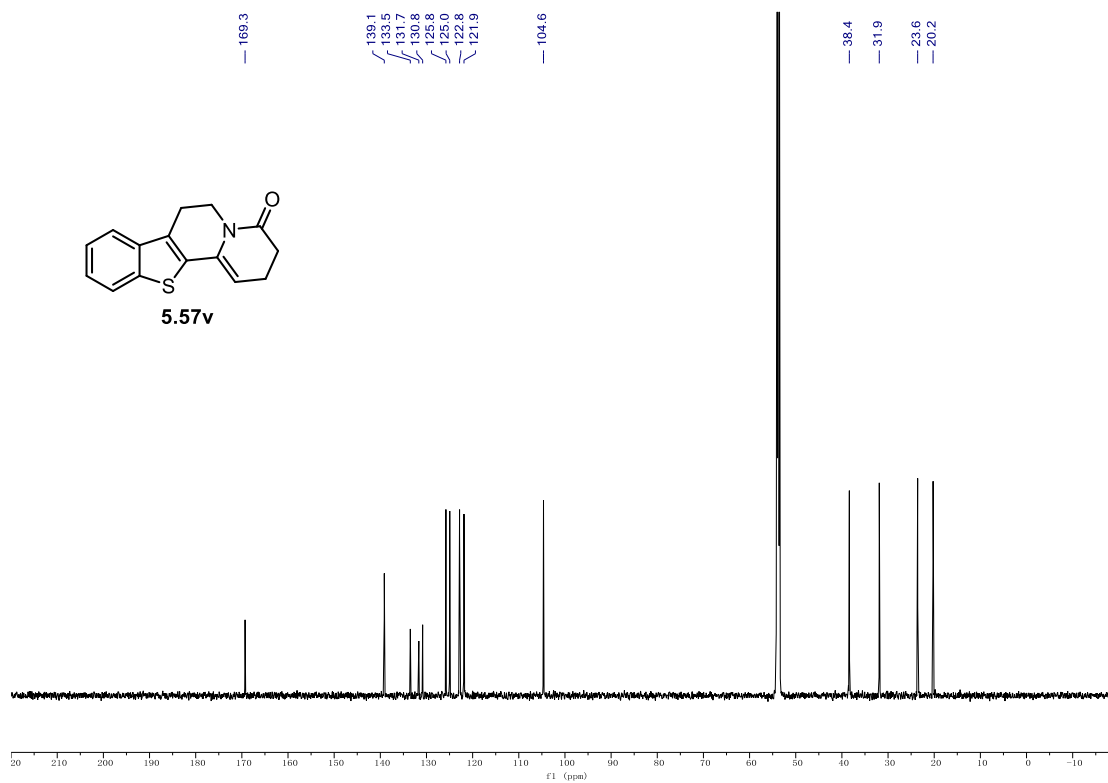
9.1. NMR Spectra

¹H NMR (500 MHz, C₆D₆) of **5.57u**.



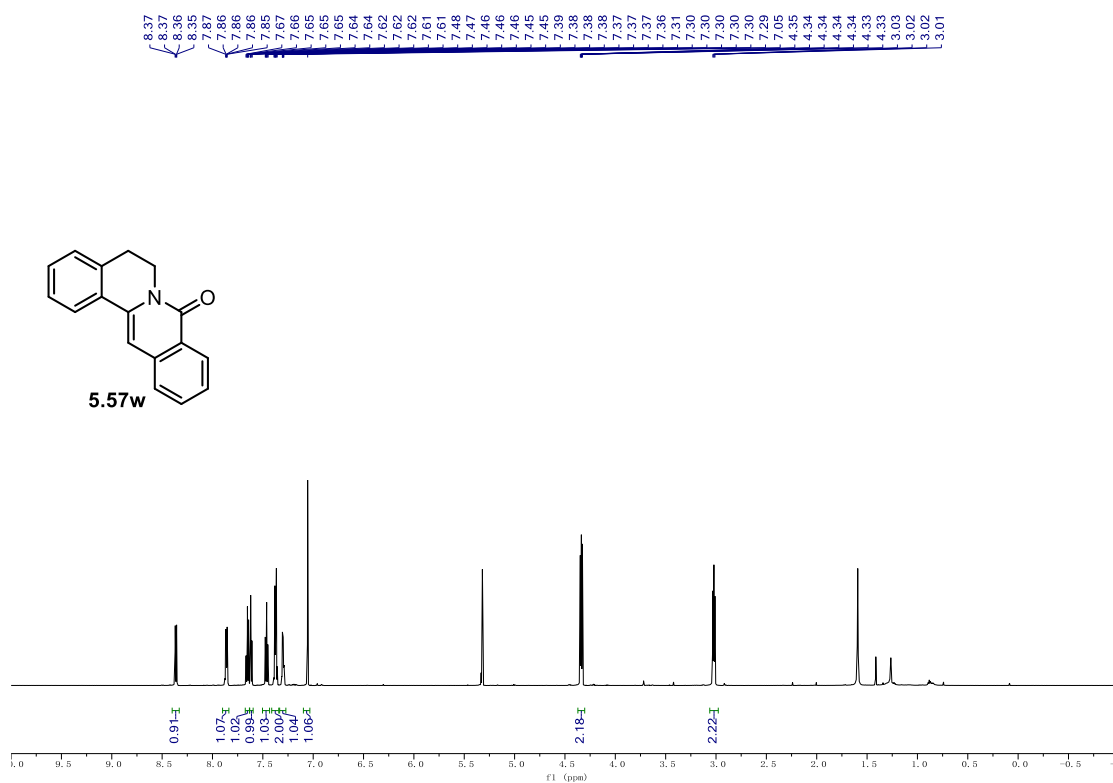
¹³C NMR (126 MHz, C₆D₆) of **5.57u**.



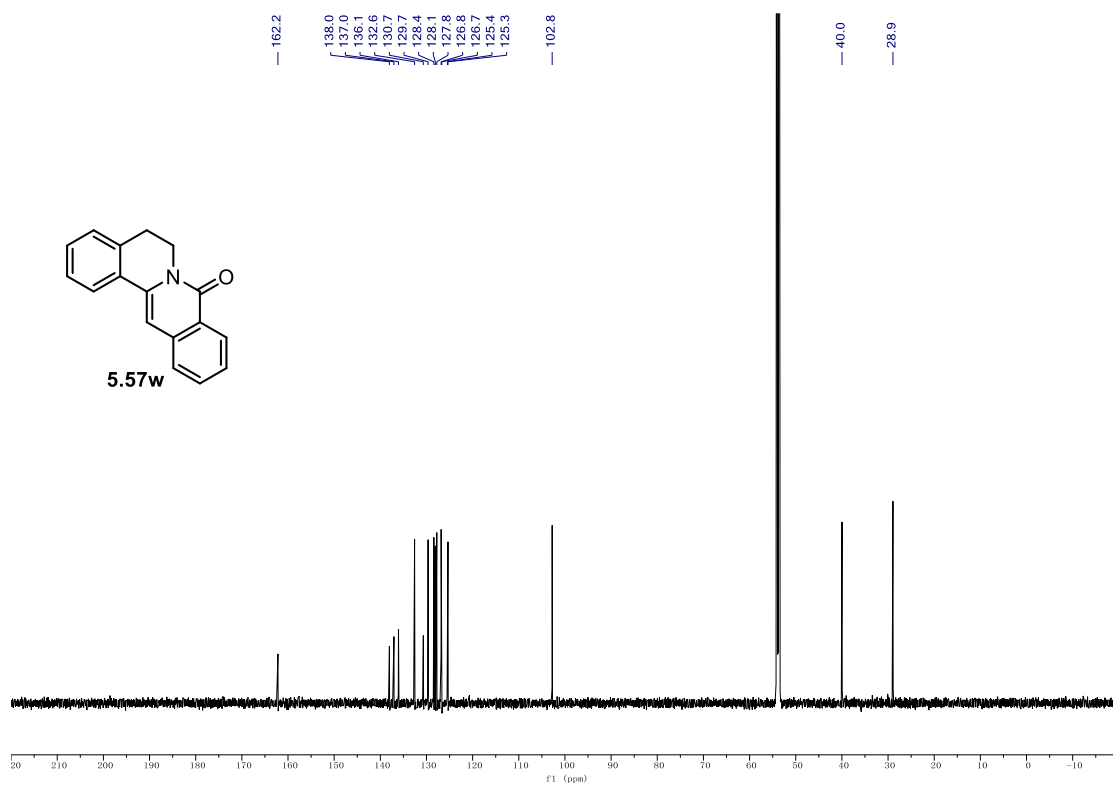
^1H NMR (700 MHz, CD_2Cl_2) of **5.57v**. ^{13}C NMR (176 MHz, CD_2Cl_2) of **5.57v**.

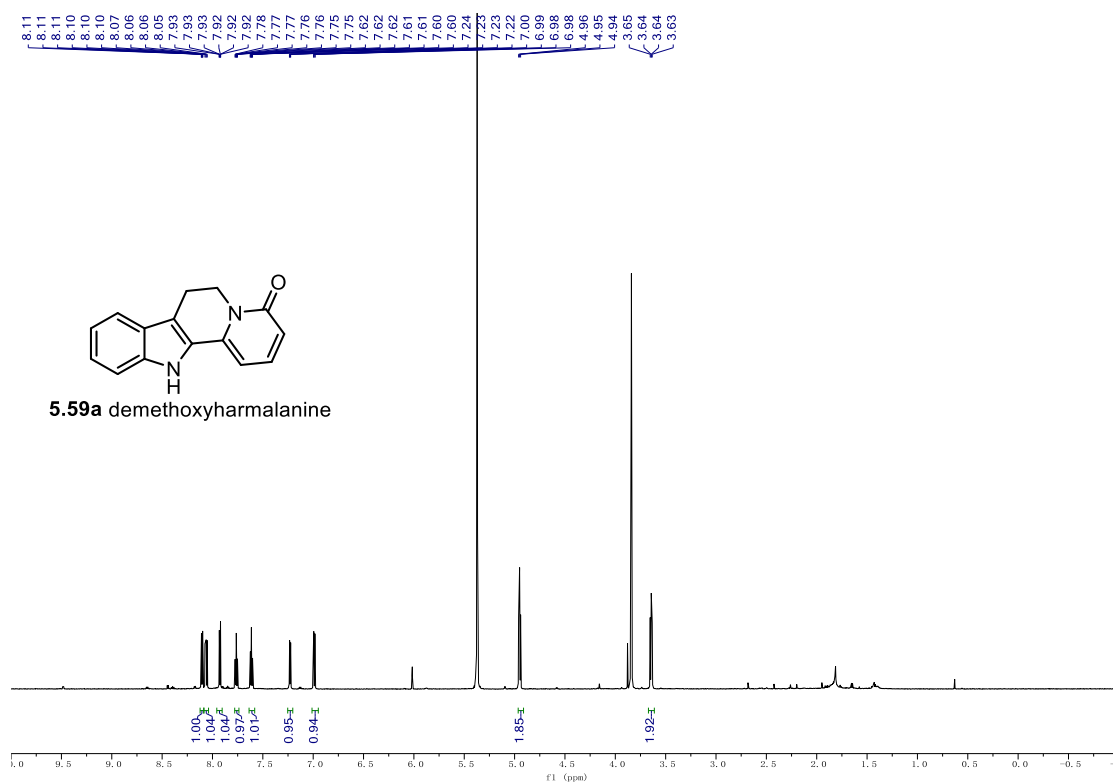
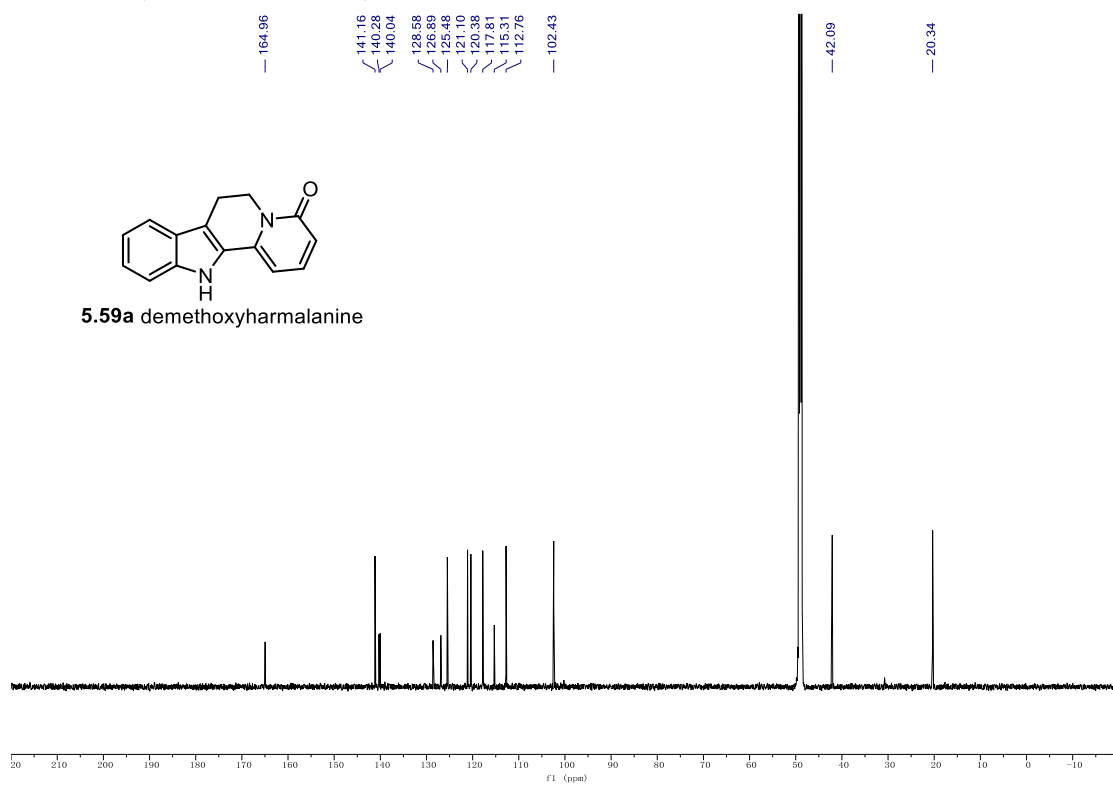
9.1. NMR Spectra

¹H NMR (600 MHz, CD₂Cl₂) of **5.57w**.



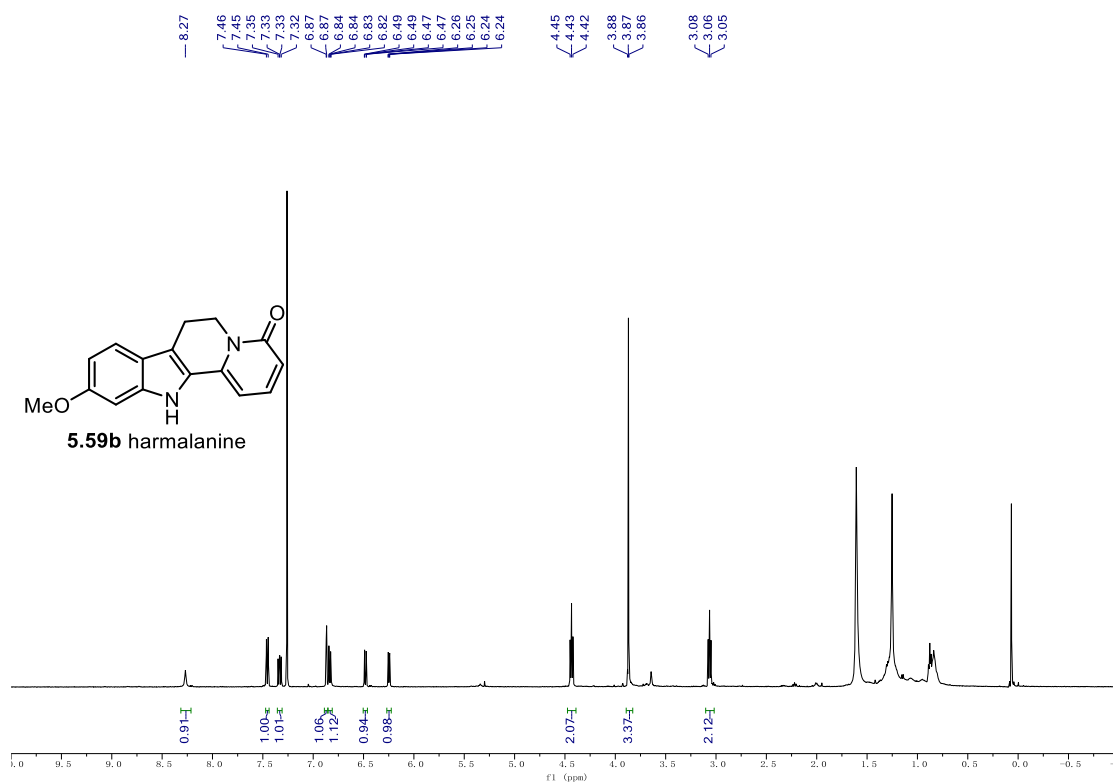
¹³C NMR (151 MHz, CD₂Cl₂) of **5.57w**.



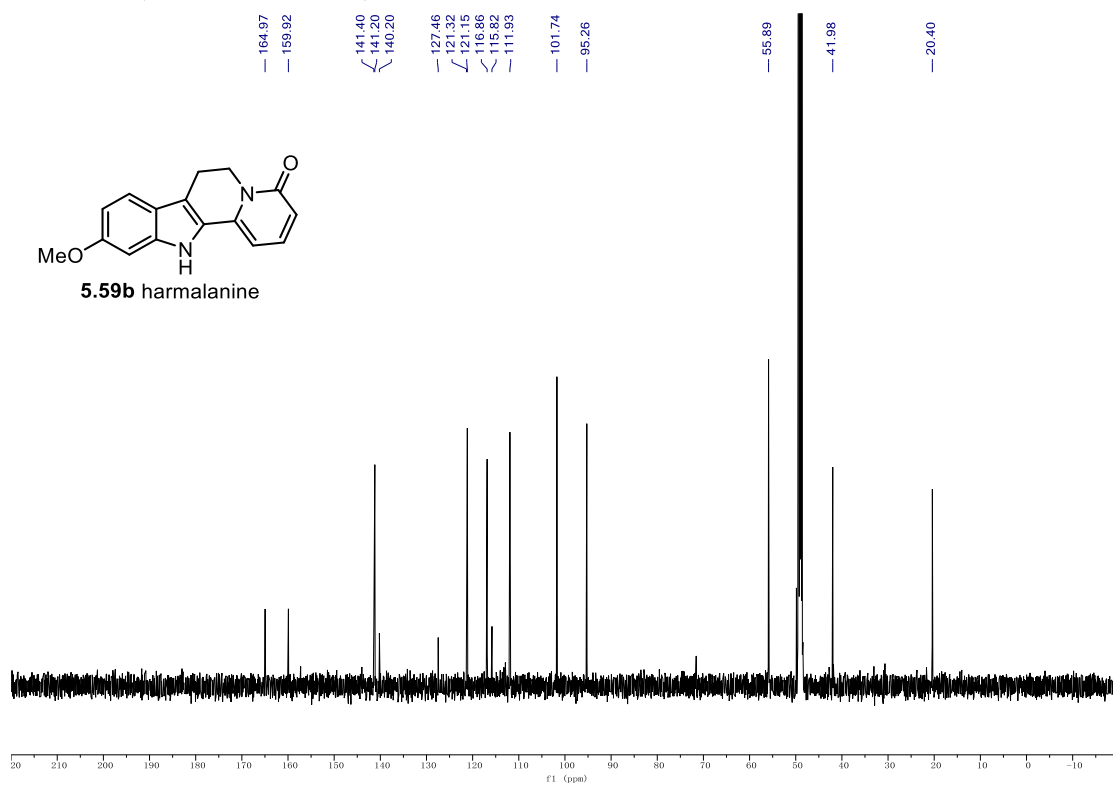
¹H NMR (700 MHz, CD₃OD) of 5.59a.**¹³C NMR (176 MHz, CD₃OD) of 5.59a.**

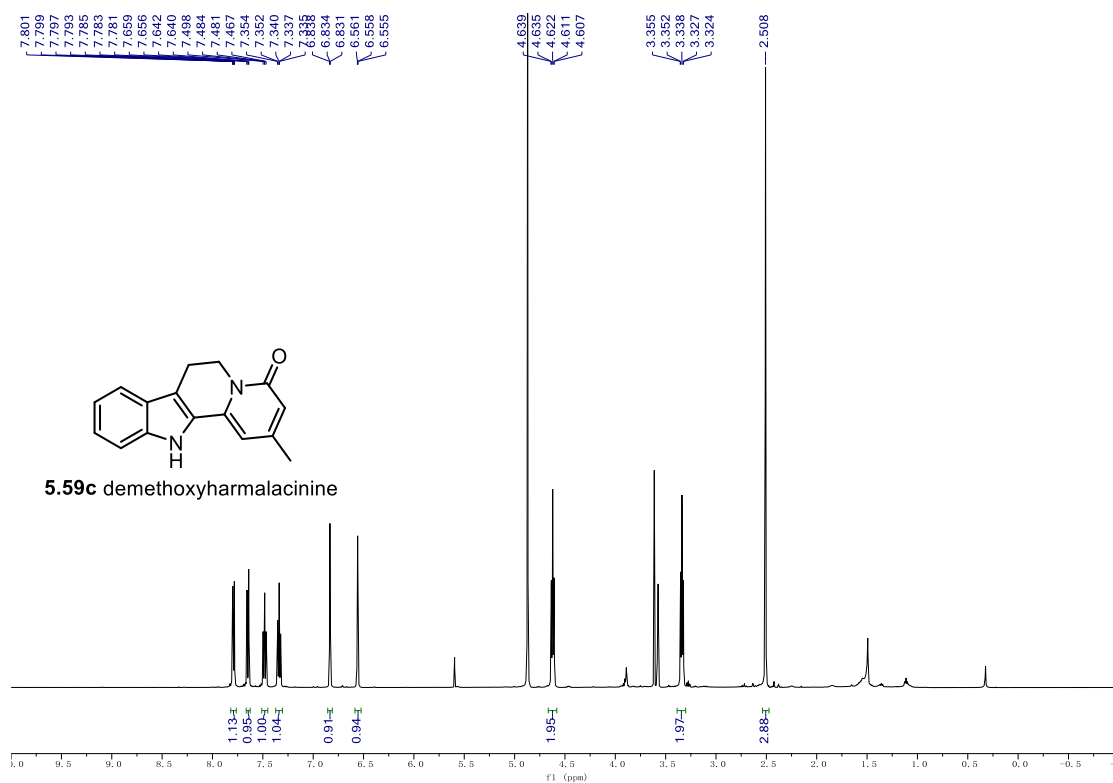
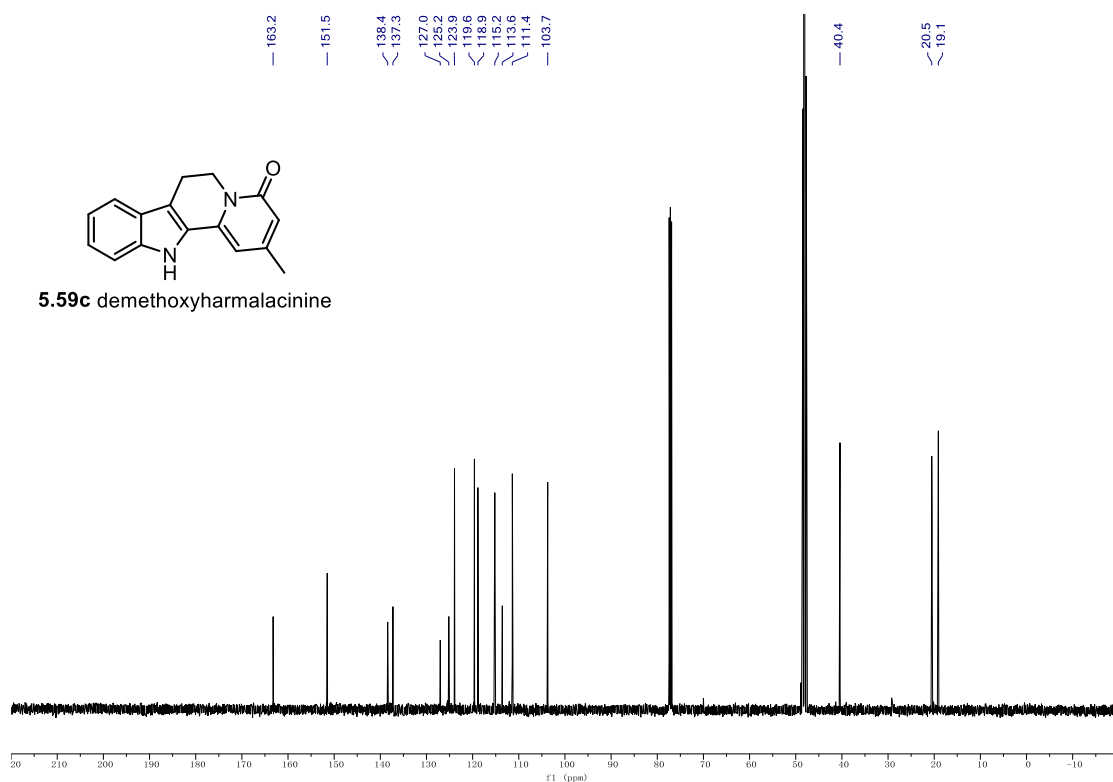
9.1. NMR Spectra

¹H NMR (500 MHz, CDCl₃) of **5.59b**.



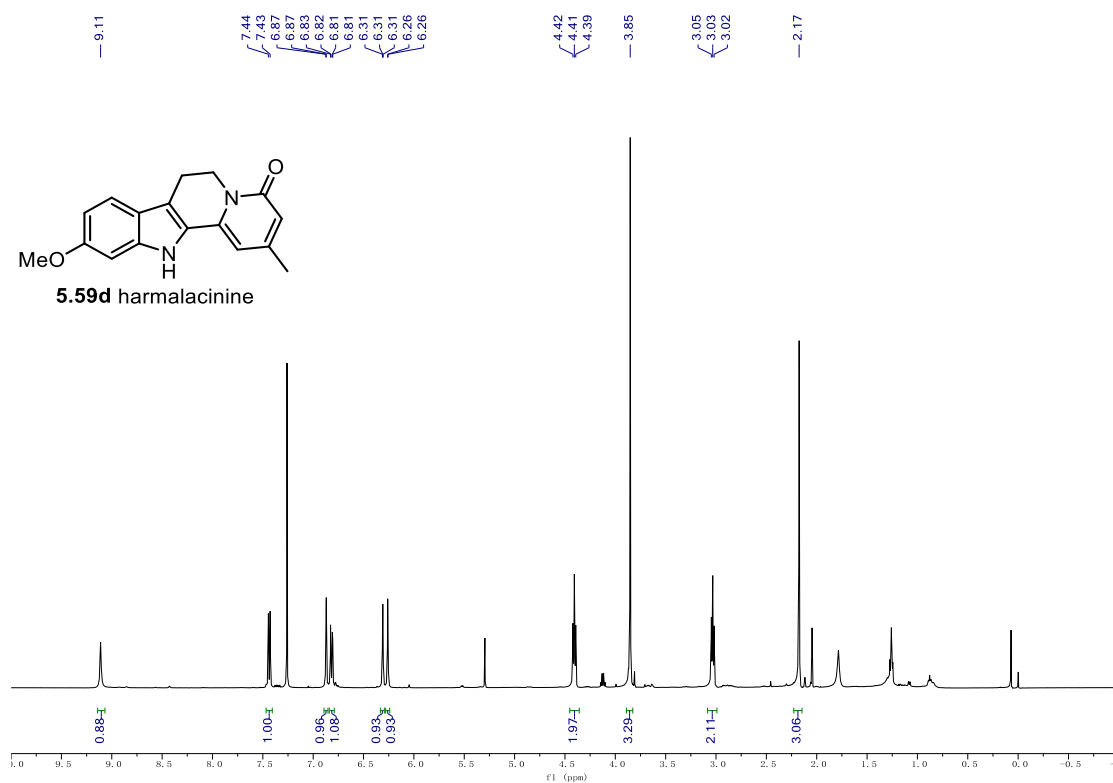
¹³C NMR (126 MHz, CD₃OD) of **5.59b**.



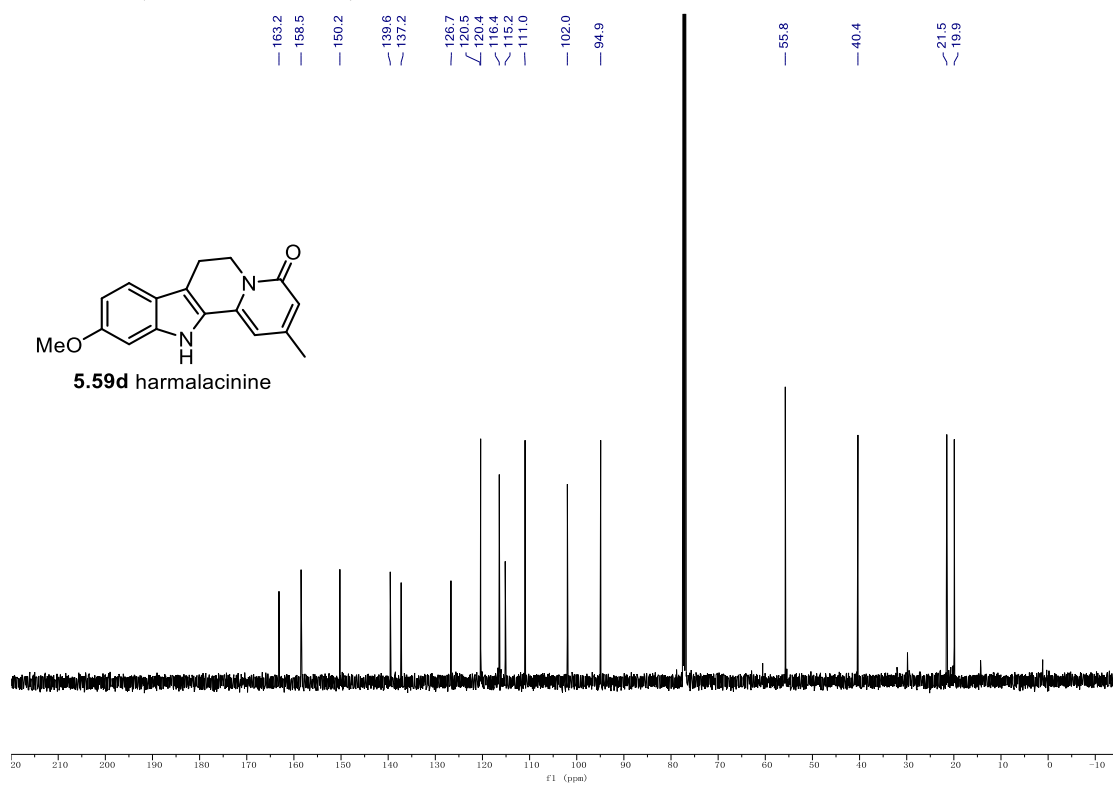
¹H NMR (500 MHz, CDCl₃+CD₃OD (v/v = 1:1)) of 5.59c.**¹³C NMR (126 MHz, CDCl₃+CD₃OD (v/v = 1:1)) of 5.59c.**

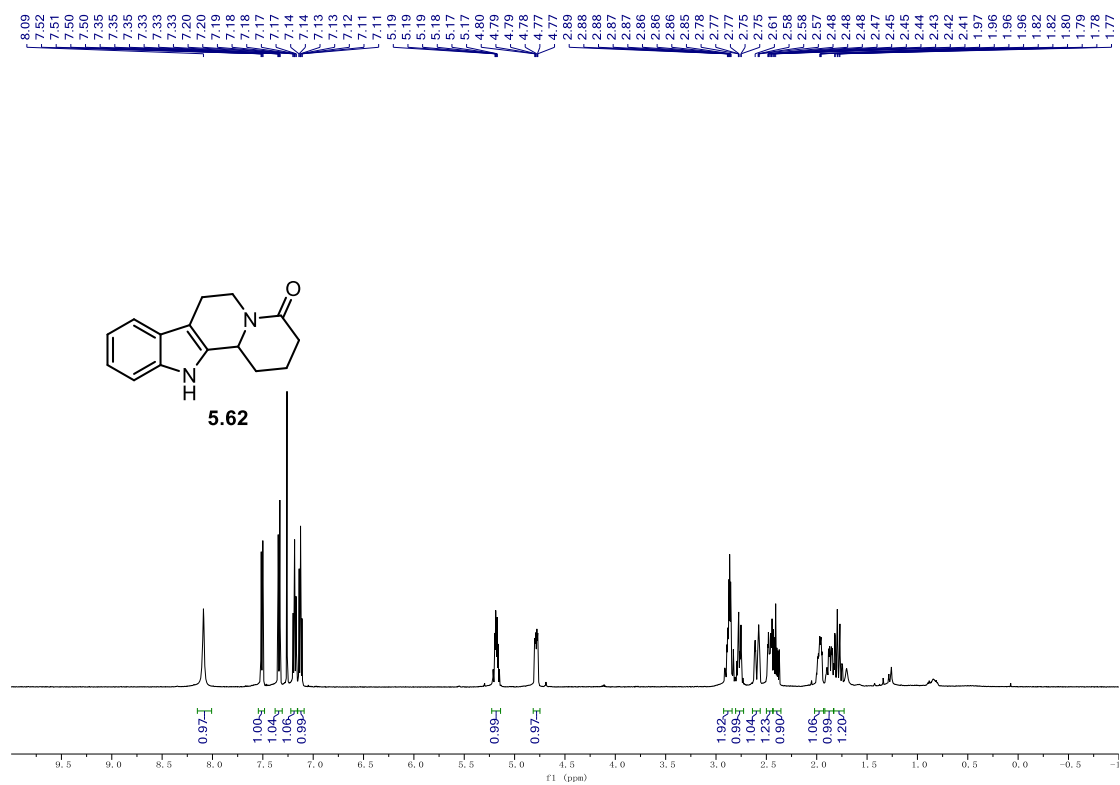
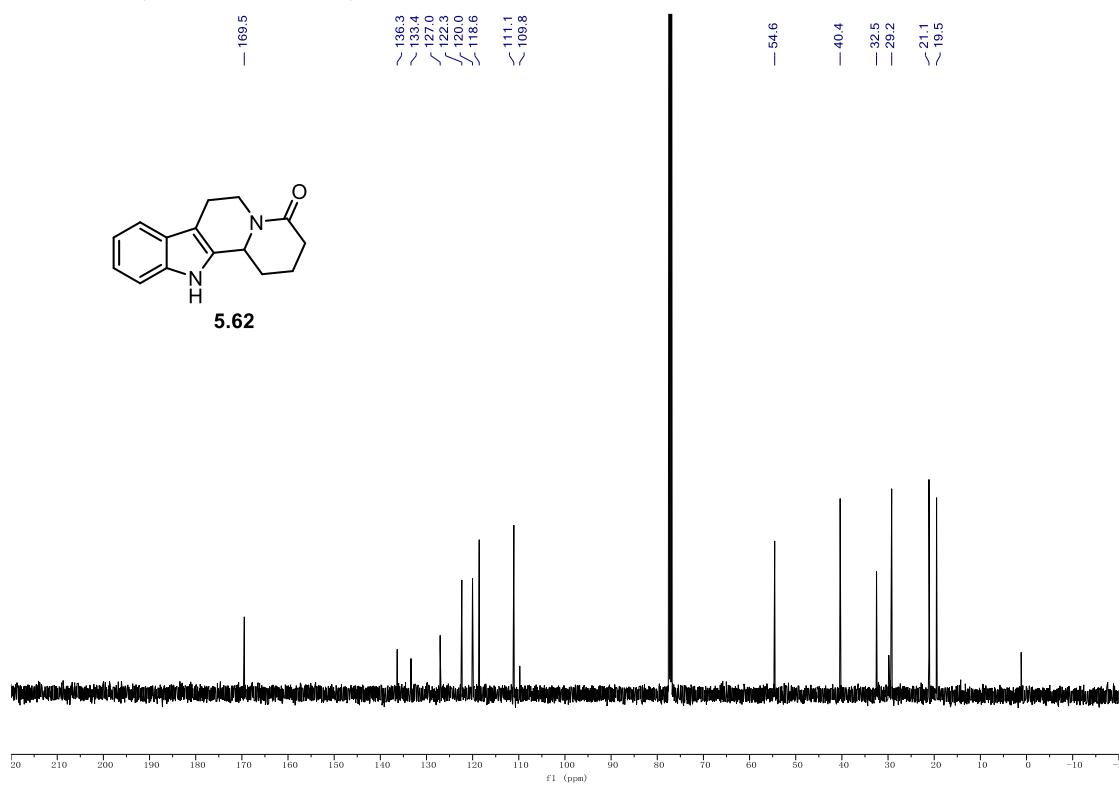
9.1. NMR Spectra

^1H NMR (500 MHz, CDCl_3) of **5.59d**.



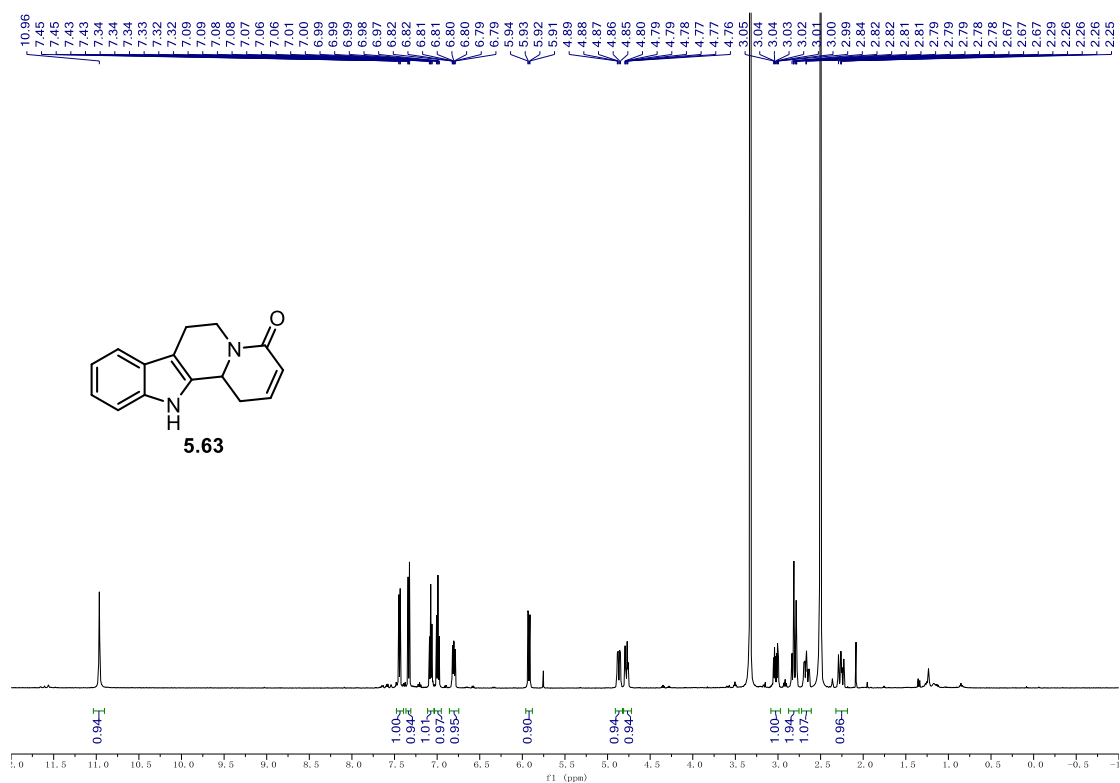
^{13}C NMR (126 MHz, CDCl_3) of **5.59d**.



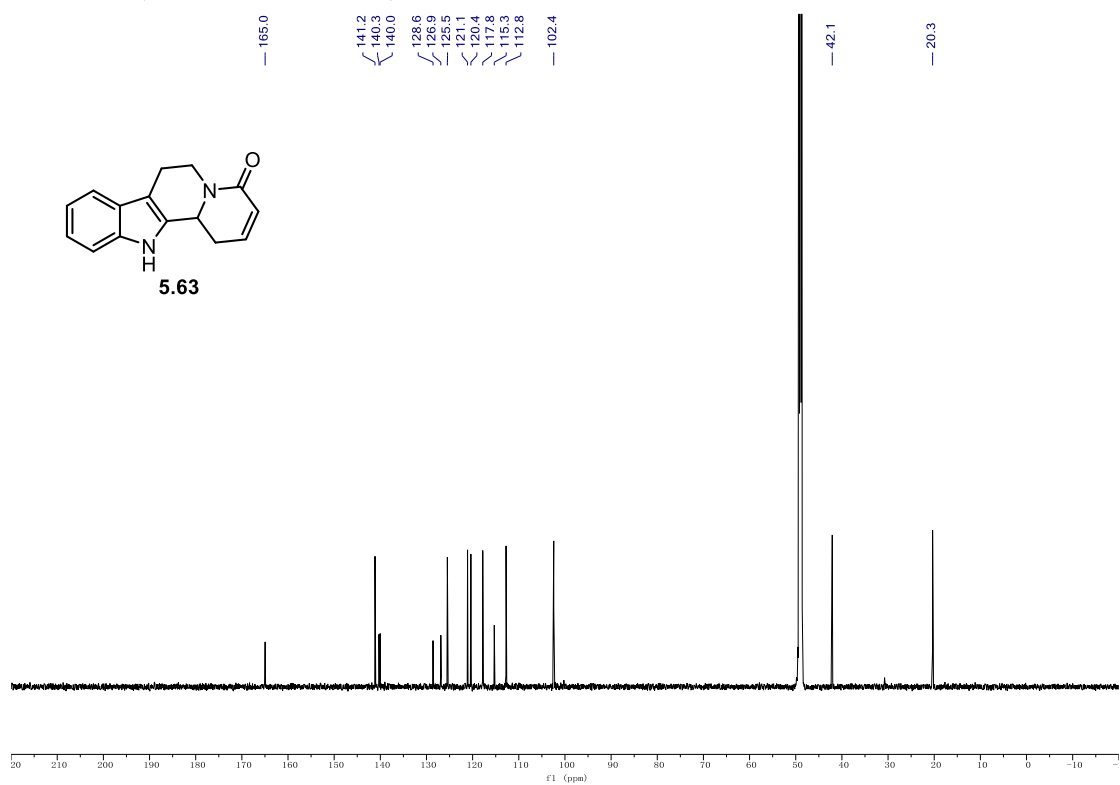
^1H NMR (500 MHz, CDCl_3) of **5.62.** **^{13}C NMR (126 MHz, CDCl_3) of **5.62**.**

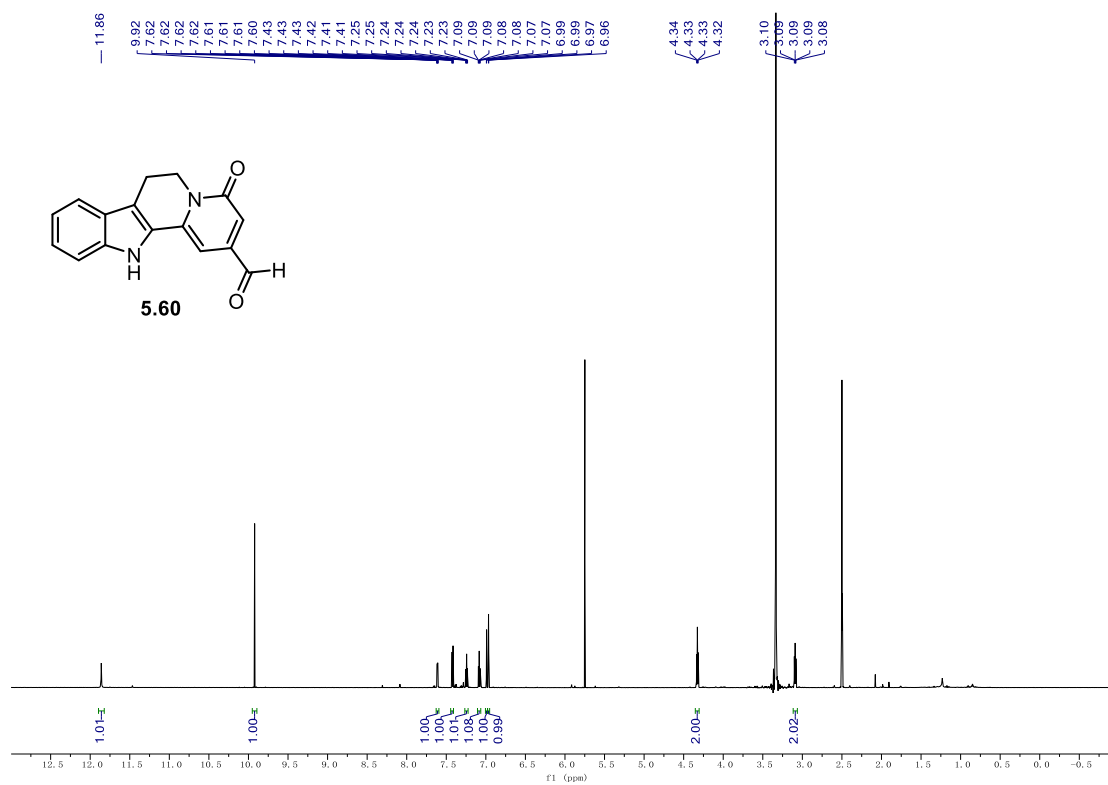
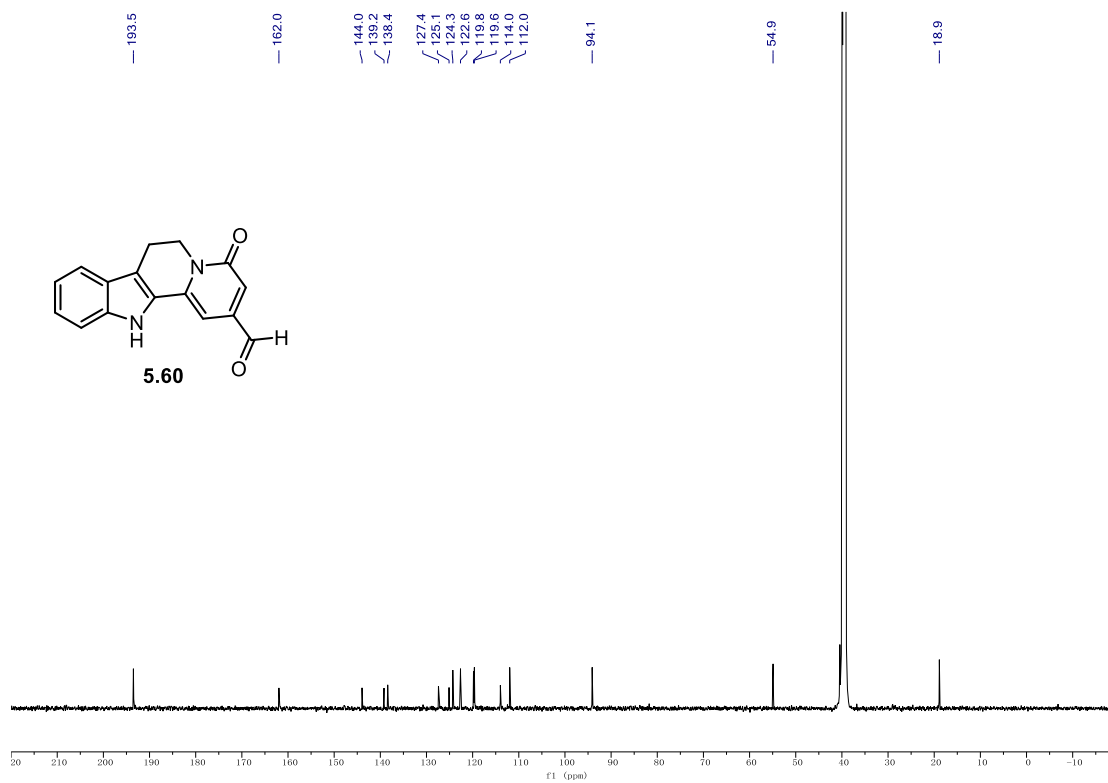
9.1. NMR Spectra

^1H NMR (500 MHz, d_6 -DMSO) of **5.63**.



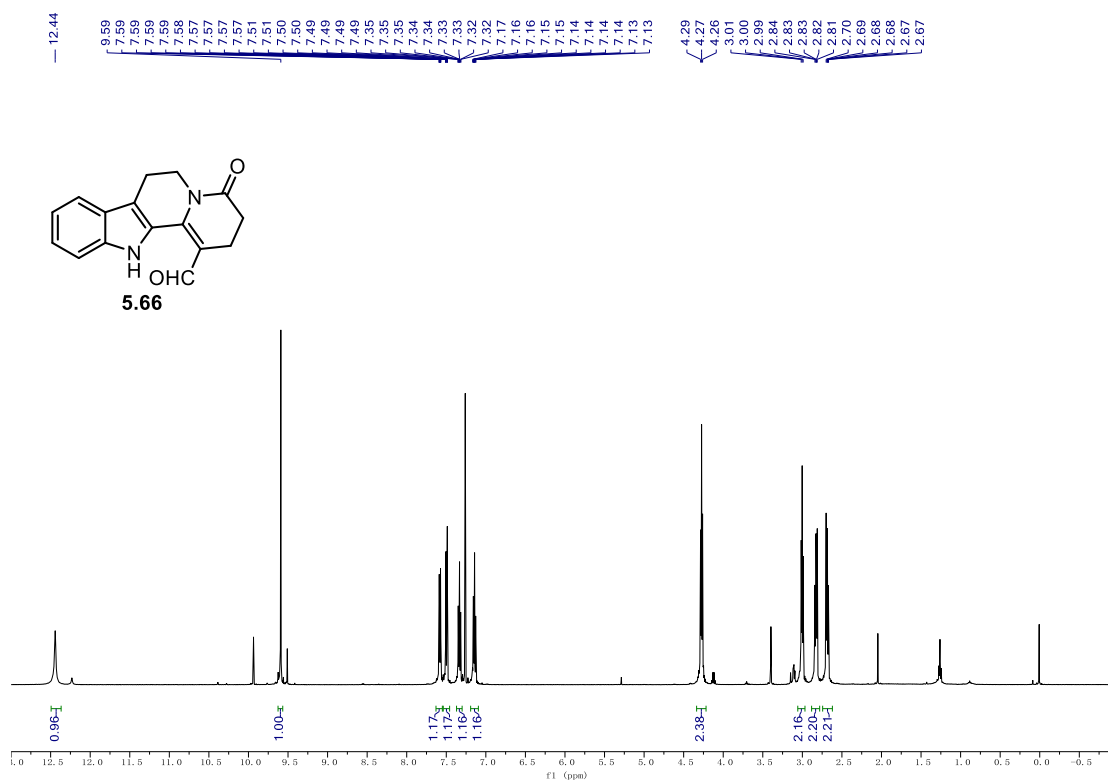
^{13}C NMR (126 MHz, d_6 -DMSO) of **5.63**.



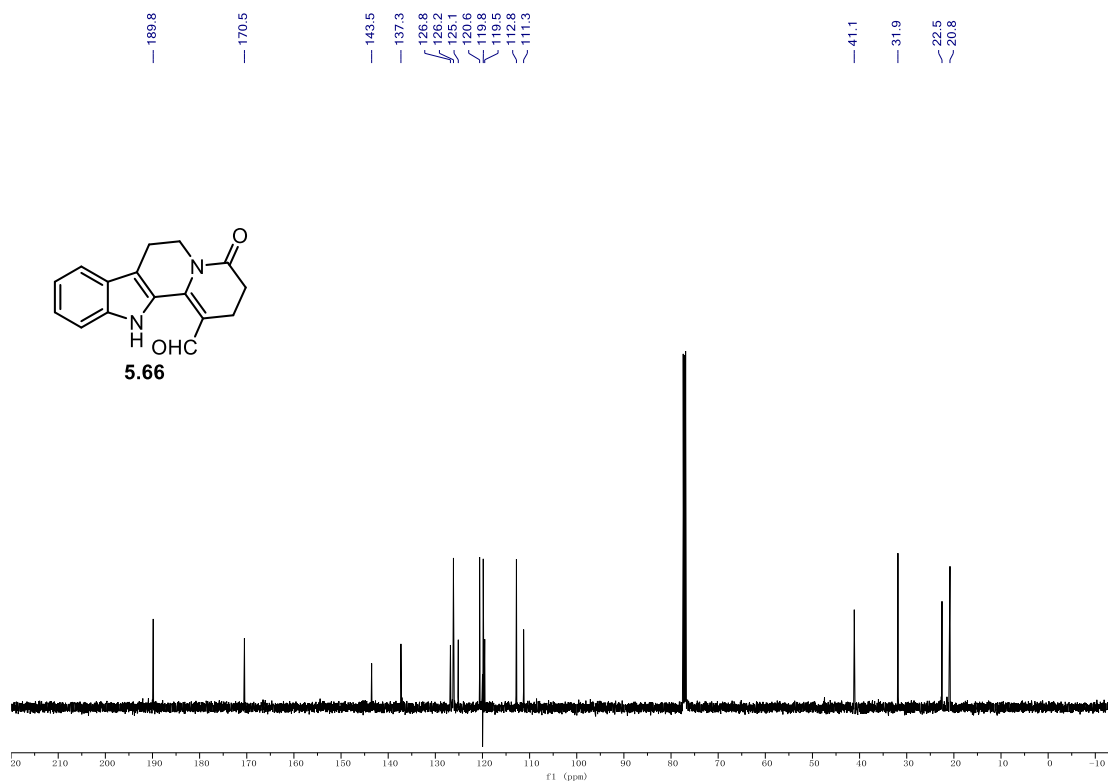
¹H NMR (700 MHz, *d*₆-DMSO) of 5.60.**¹³C NMR (176 MHz, *d*₆-DMSO) of 5.60.**

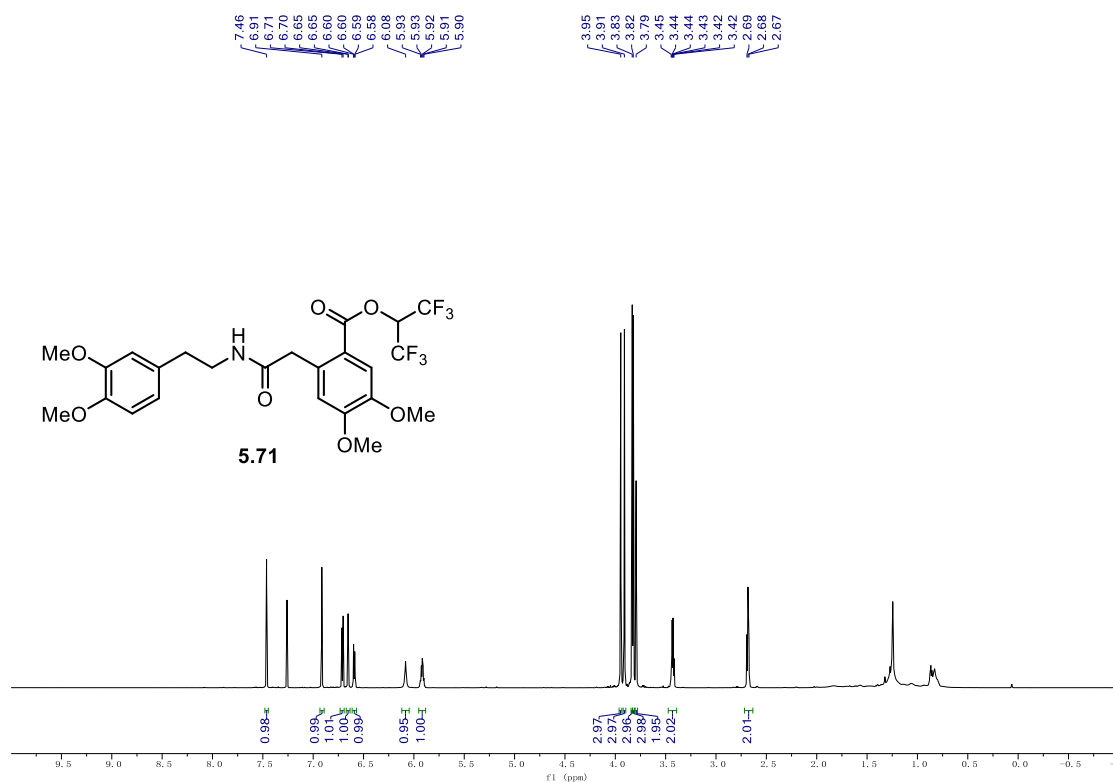
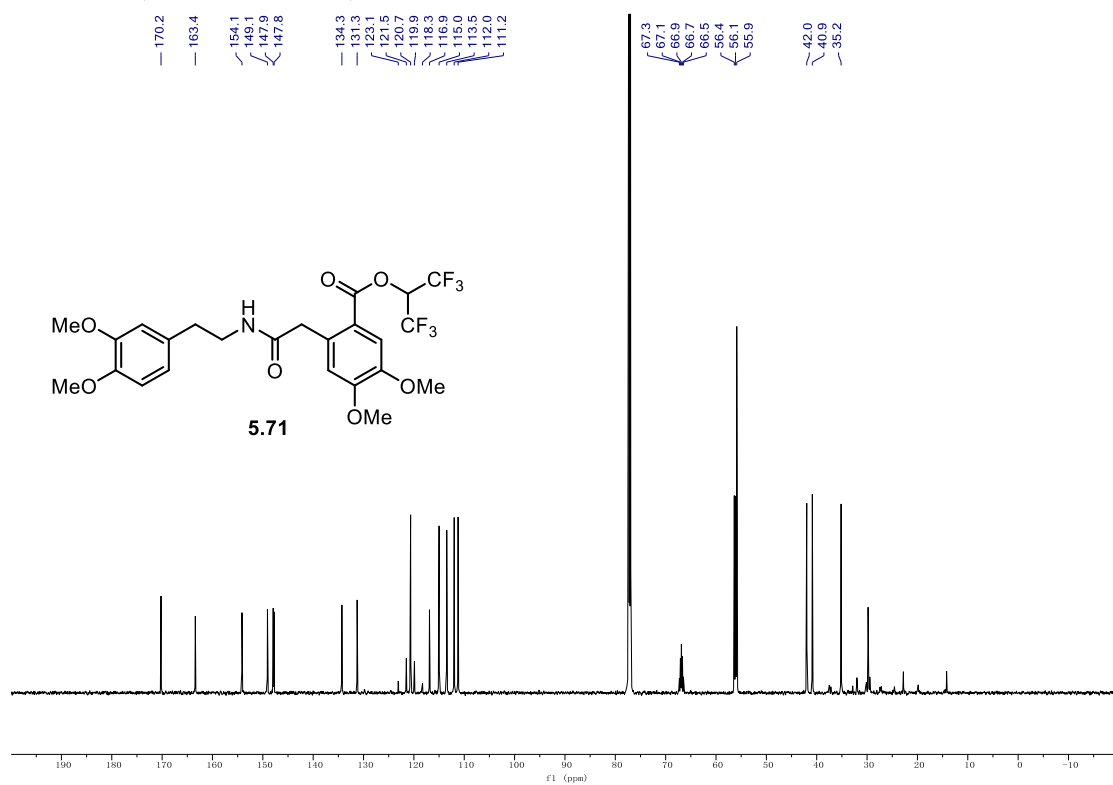
9.1. NMR Spectra

¹H NMR (700 MHz, CDCl₃) of **5.66**.



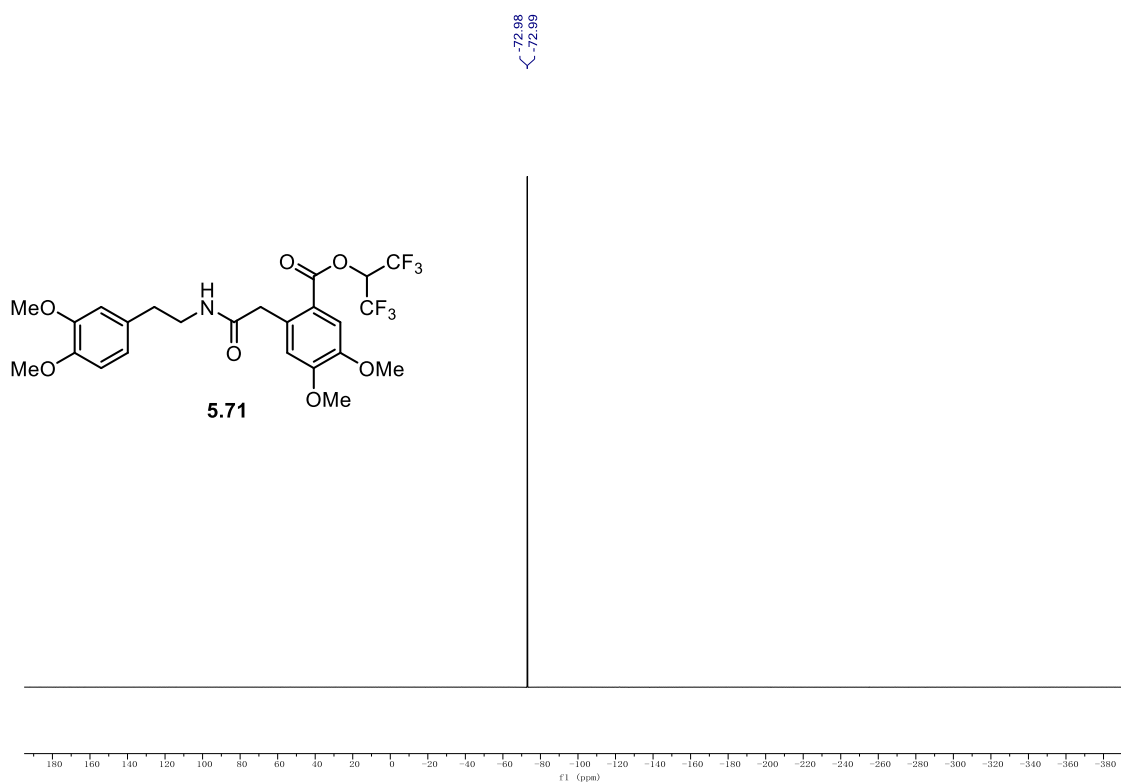
¹³C NMR (176 MHz, CDCl₃) of **5.66**.



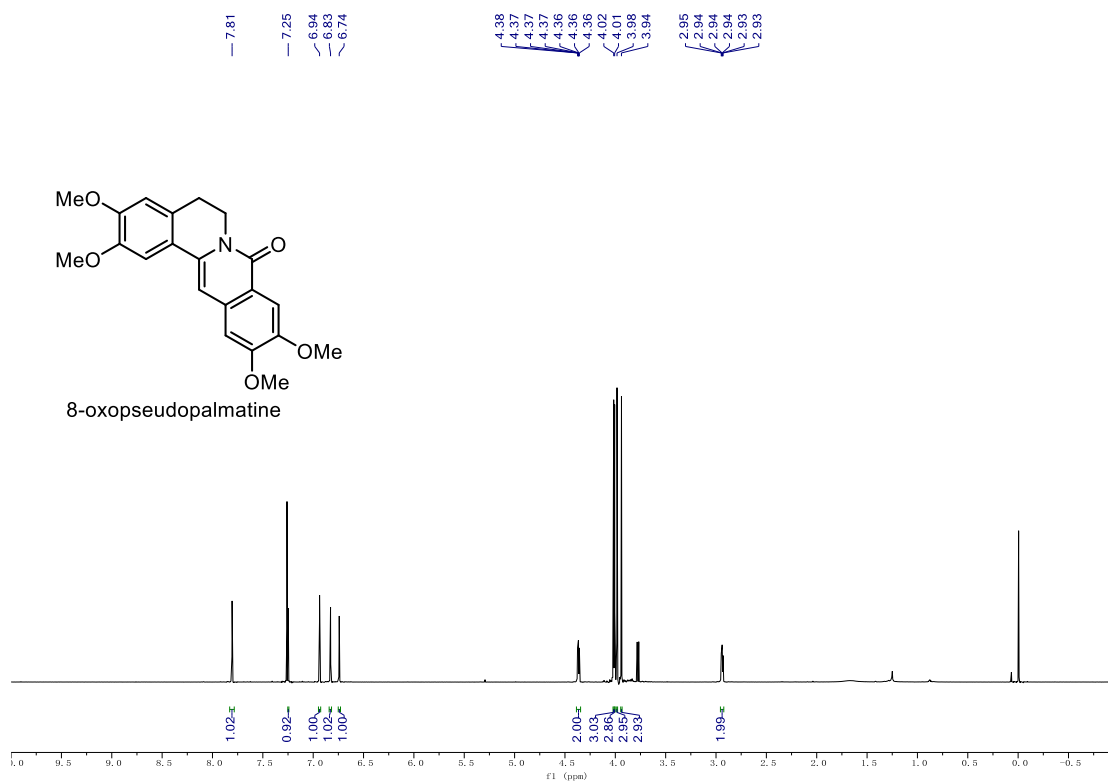
^1H NMR (700 MHz, CDCl_3) of **5.71**. ^{13}C NMR (176 MHz, CDCl_3) of **5.71**.

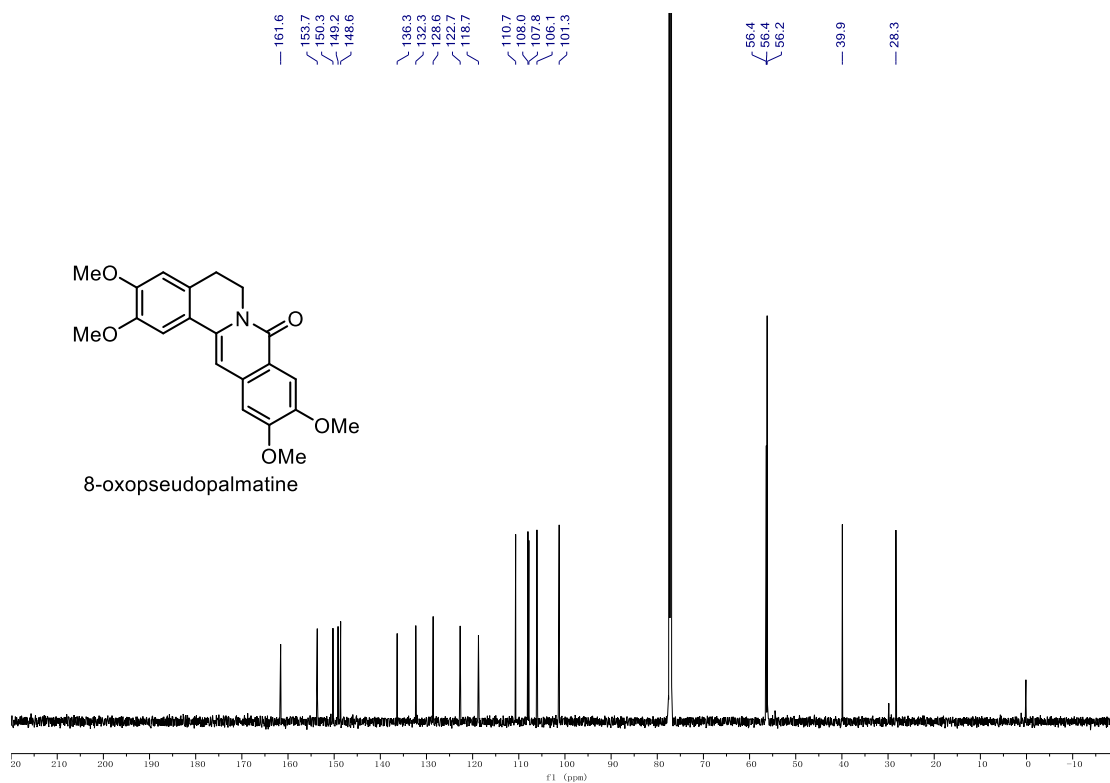
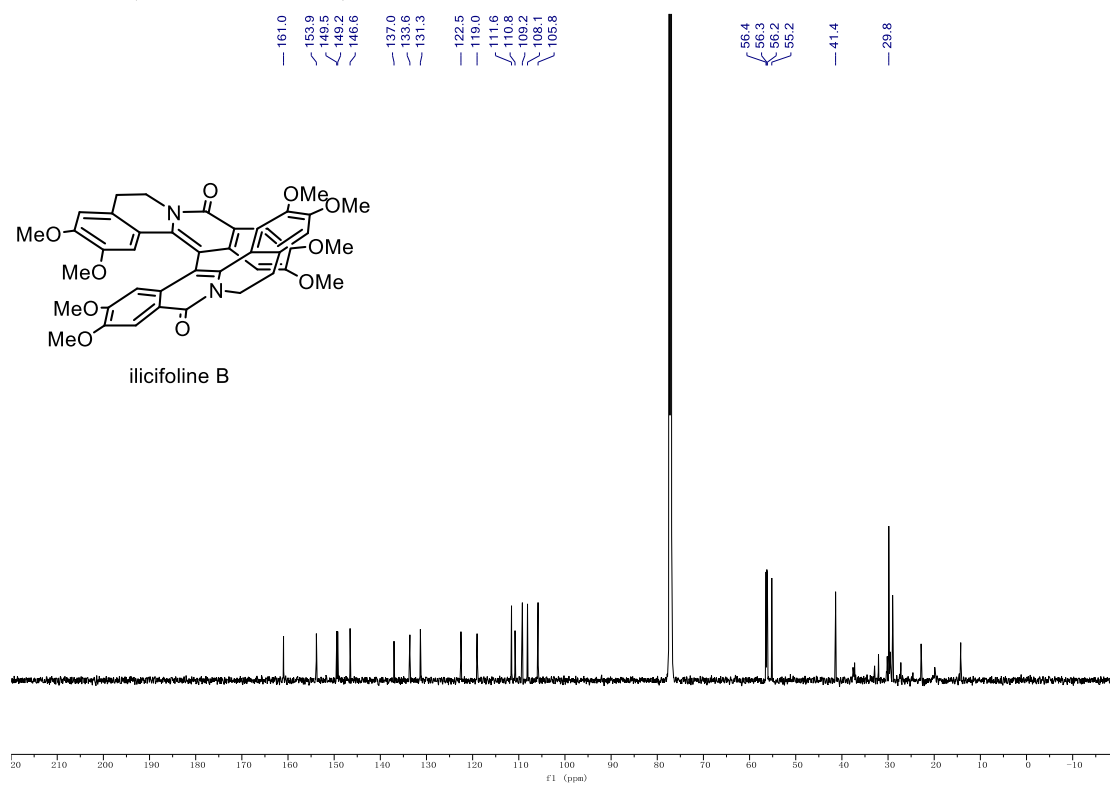
9.1. NMR Spectra

^{19}F NMR (565 MHz, CDCl_3) of **5.71**.



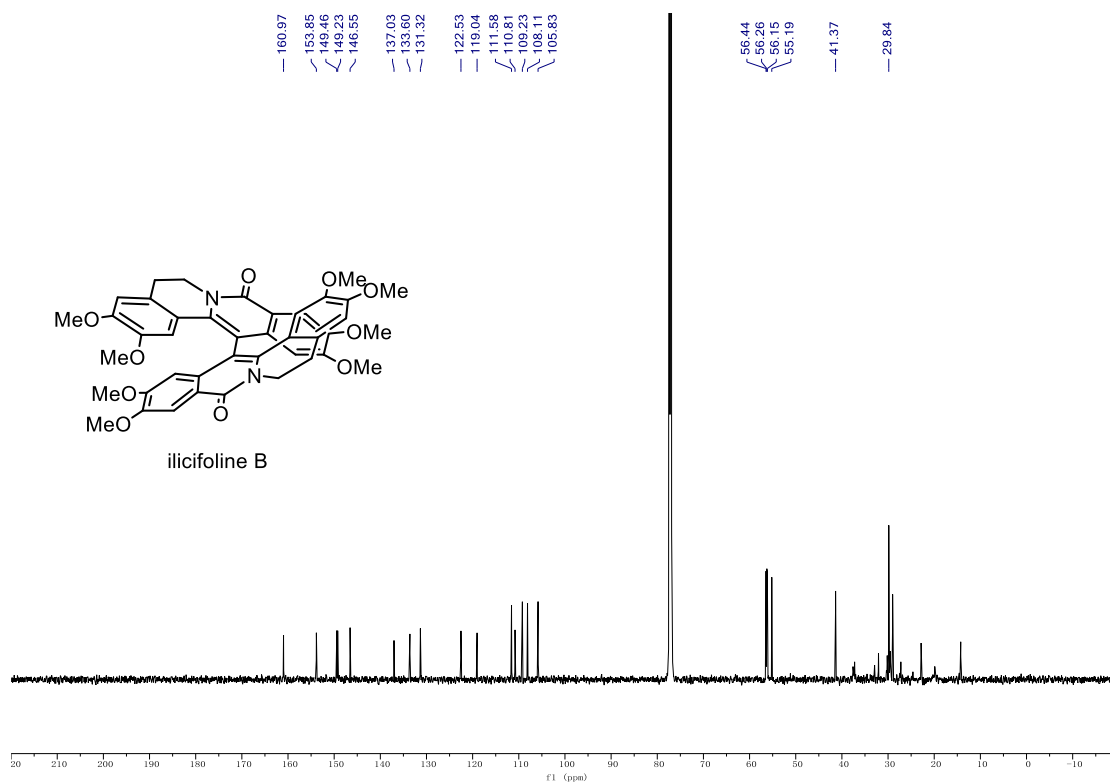
^1H NMR (700 MHz, CDCl_3) of 8-oxopseudopalmatine.



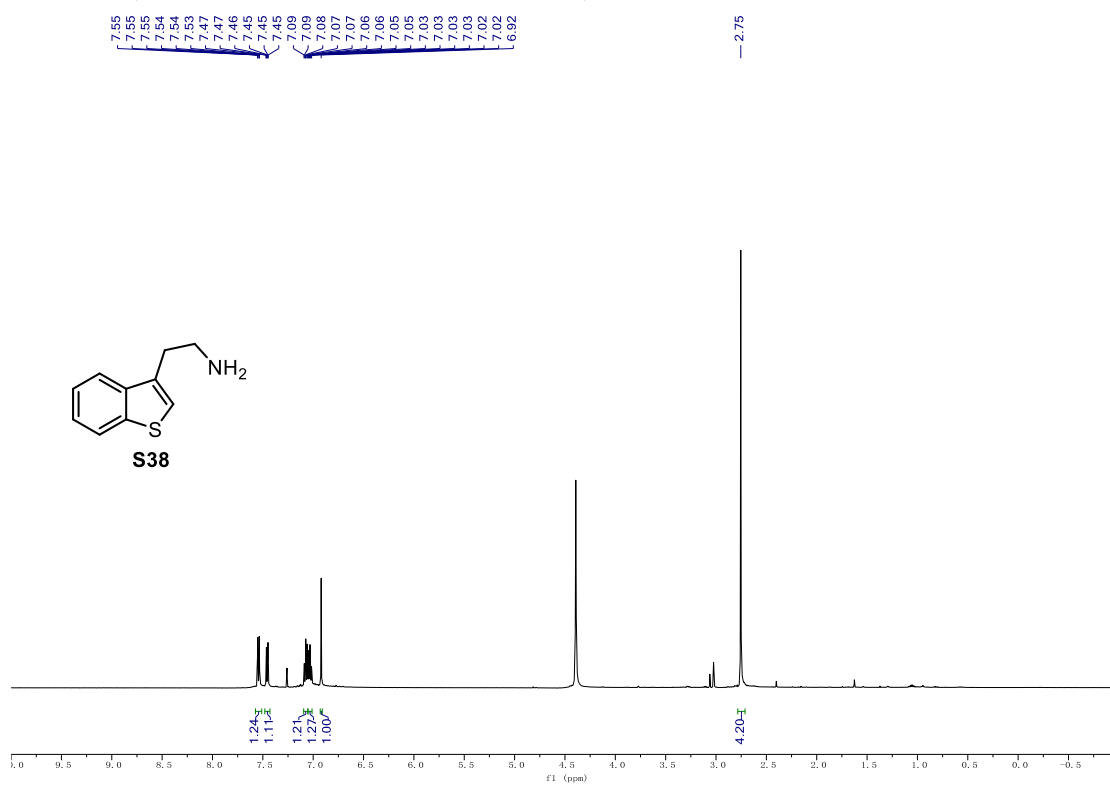
^{13}C NMR (176 MHz, CDCl_3) of 8-oxopseudopalmatine. ^1H NMR (700 MHz, CDCl_3) of ilicifoline B.

9.1. NMR Spectra

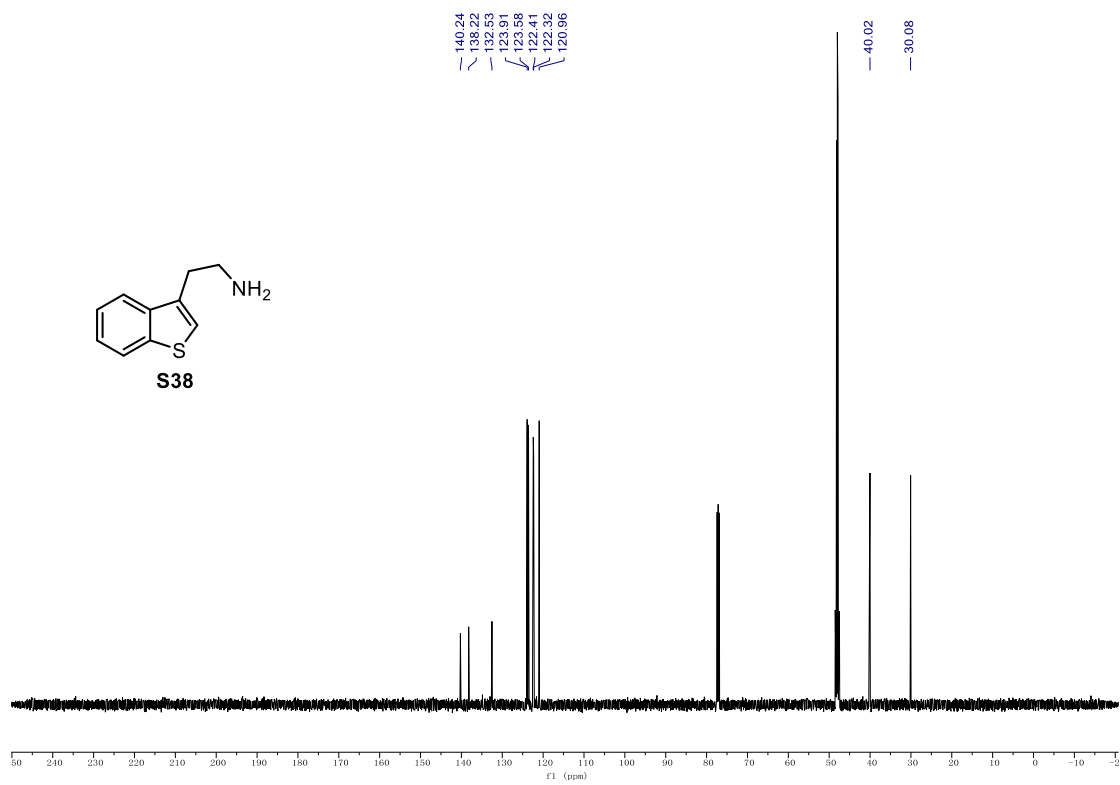
¹³C NMR (176 MHz, CDCl₃) of ilicifoline B.



¹H NMR (500 MHz, CD₃OD: CDCl₃ (v/v = 1:1)) of S38.

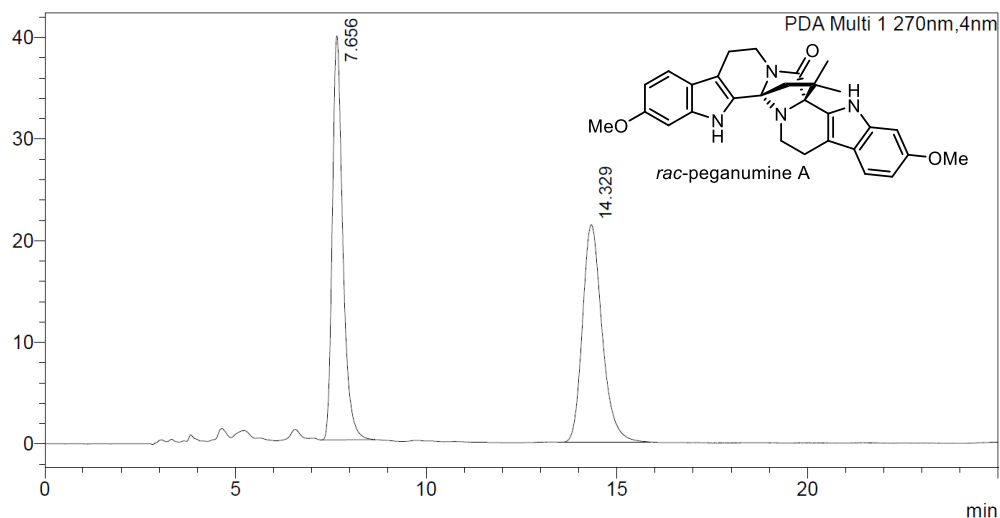


^{13}C NMR (126 MHz, $\text{CD}_3\text{OD}:\text{CDCl}_3$ (v/v = 1:1)) of **S38**.



9.2. HPLC Traces

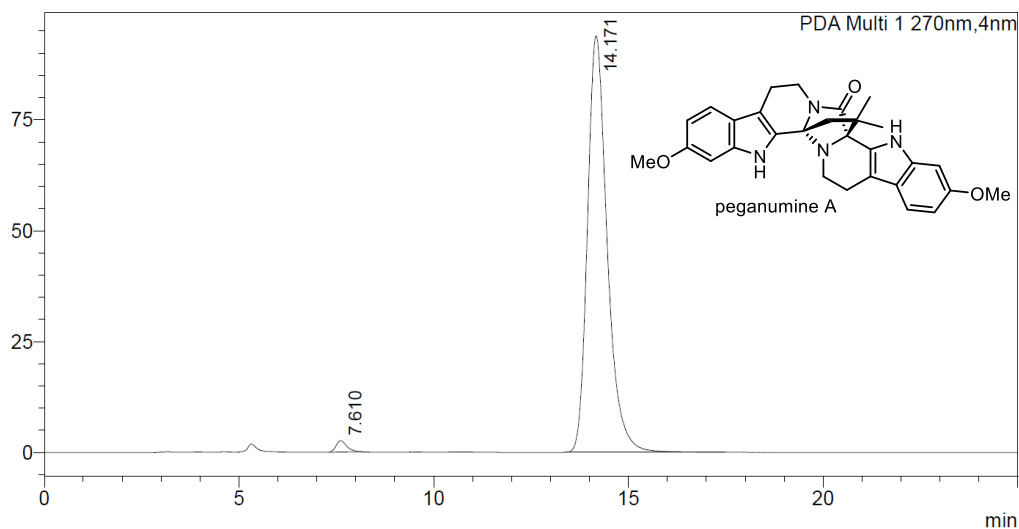
rac-Peganumine A



<Peak Table>

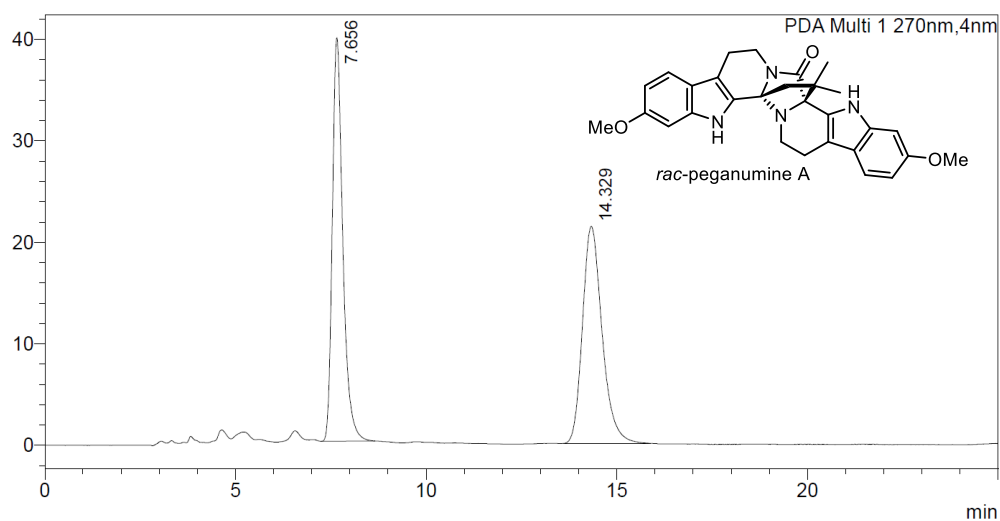
PDA Ch1 270nm					
Peak#	Ret. Time	Area	Area%	Height	Name
1	7.656	759375	49.795	39781	
2	14.329	765637	50.205	21402	
Total		1525012	100.000	61184	

Peganumine A



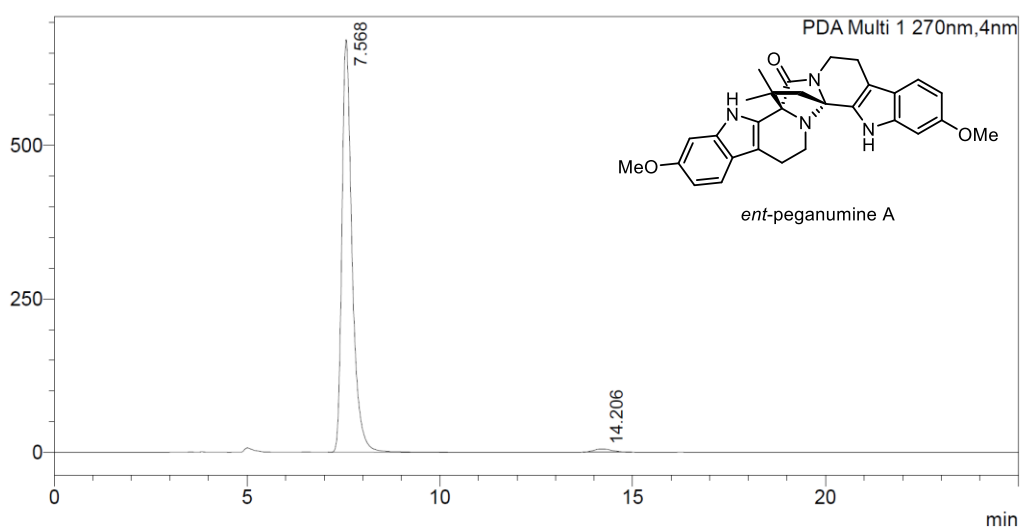
<Peak Table>

PDA Ch1 270nm					
Peak#	Ret. Time	Area	Area%	Height	Name
1	7.610	48338	1.441	2562	
2	14.171	3305614	98.559	93896	
Total		3353952	100.000	96458	

rac-Peganumine A**<Peak Table>**

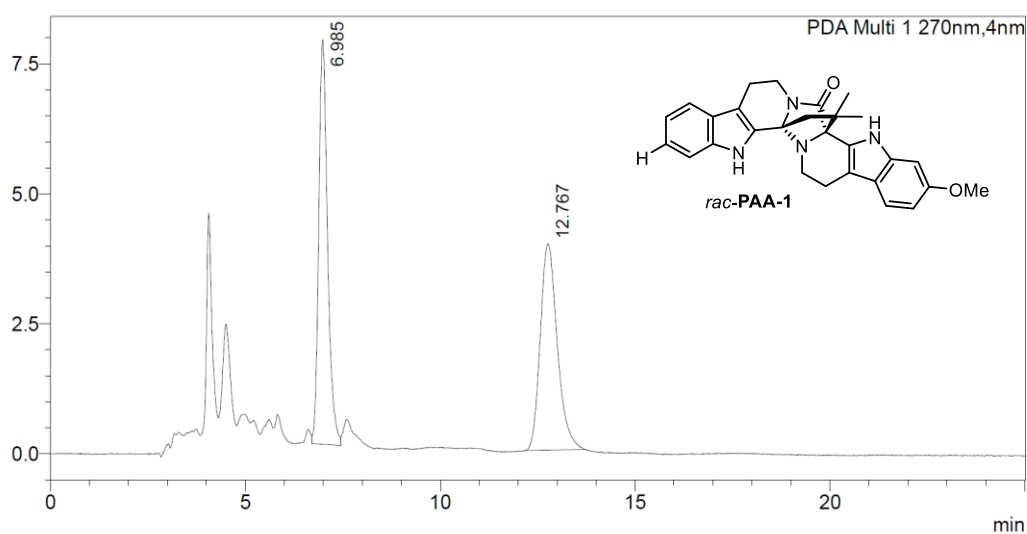
PDA Ch1 270nm

Peak#	Ret. Time	Area	Area%	Height	Name
1	7.656	759375	49.795	39781	
2	14.329	765637	50.205	21402	
Total		1525012	100.000	61184	

ent-Peganumine A**<Peak Table>**

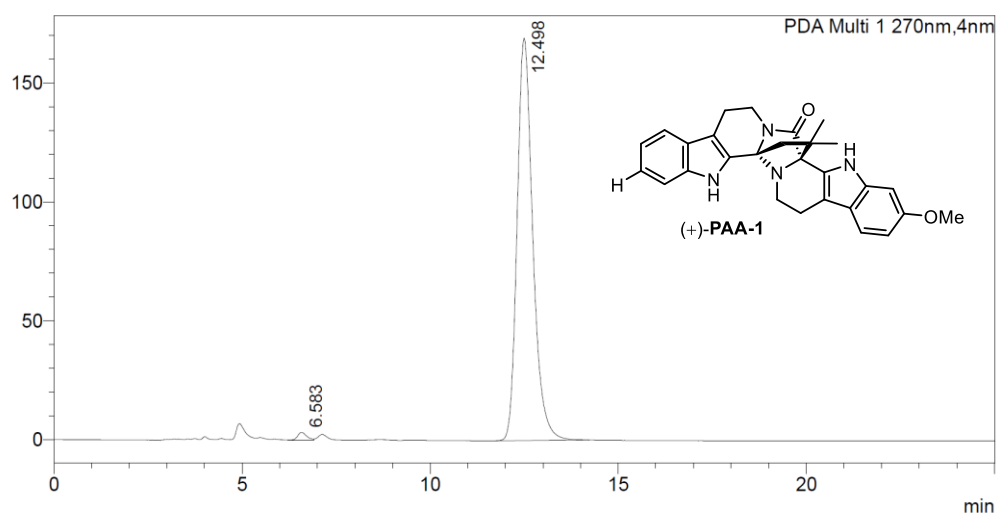
PDA Ch1 270nm

Peak#	Ret. Time	Area	Area%	Height	Name
1	7.568	12333154	98.548	671511	
2	14.206	181749	1.452	5539	
Total		12514902	100.000	677050	

rac-PAA-1**<Peak Table>**

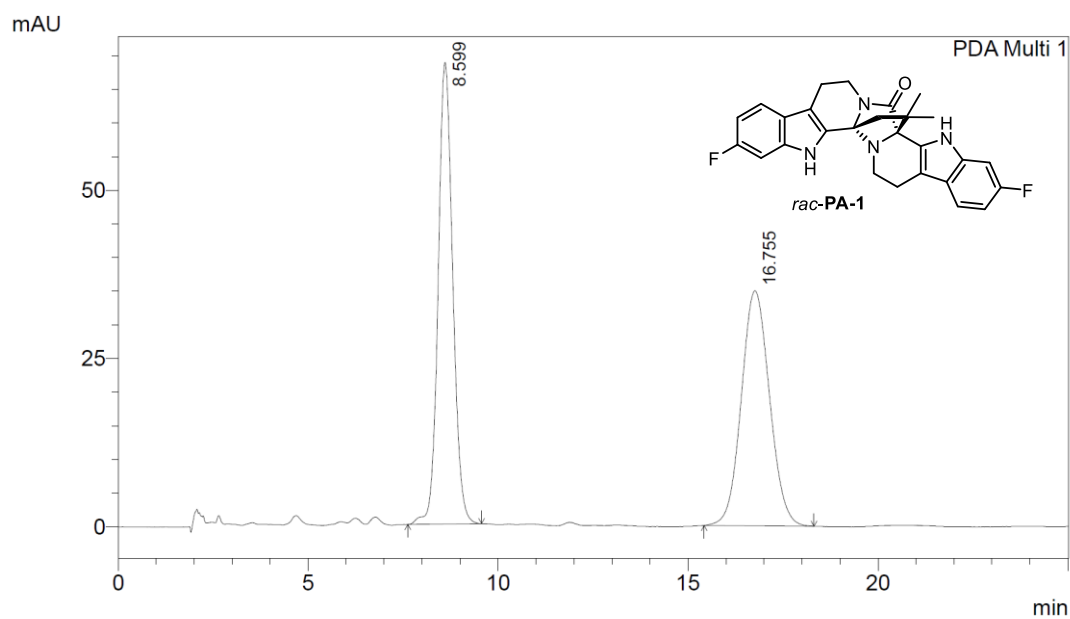
PDA Ch1 270nm

Peak#	Ret. Time	Area	Area%	Height	Name
1	6.985	122385	50.439	7776	
2	12.767	120252	49.561	3967	
Total		242637	100.000	11743	

(+)-PAA-1**<Peak Table>**

PDA Ch1 270nm

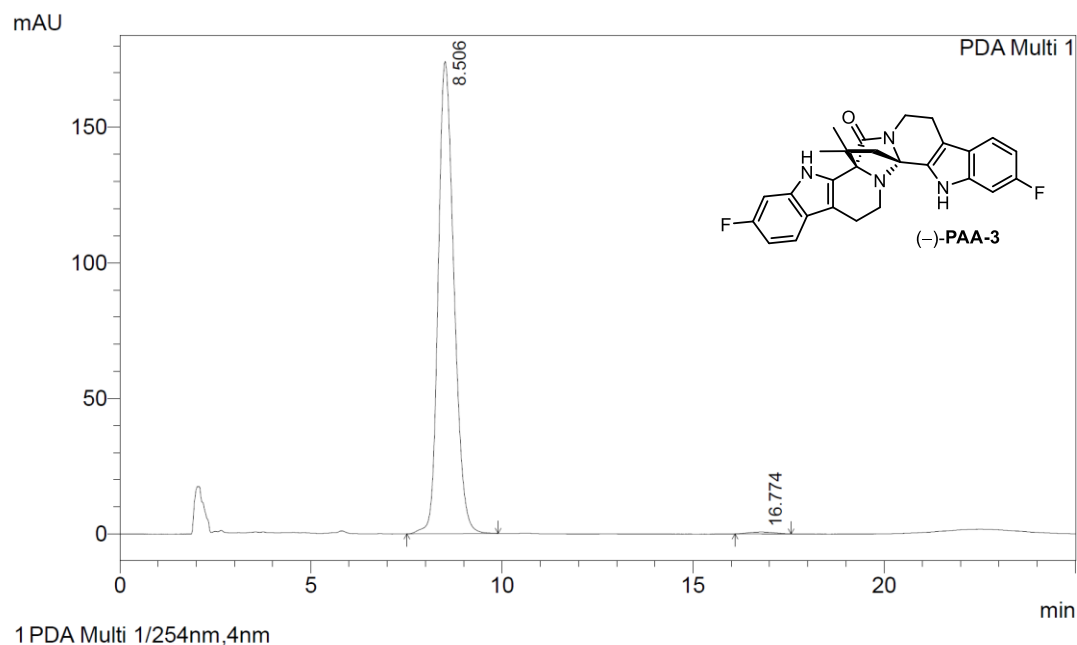
Peak#	Ret. Time	Area	Area%	Height	Name
1	6.583	55528	1.120	3305	
2	12.498	4900408	98.880	169247	
Total		4955937	100.000	172553	

rac-PAA-3

Peak Table

PDA Ch1 270nm

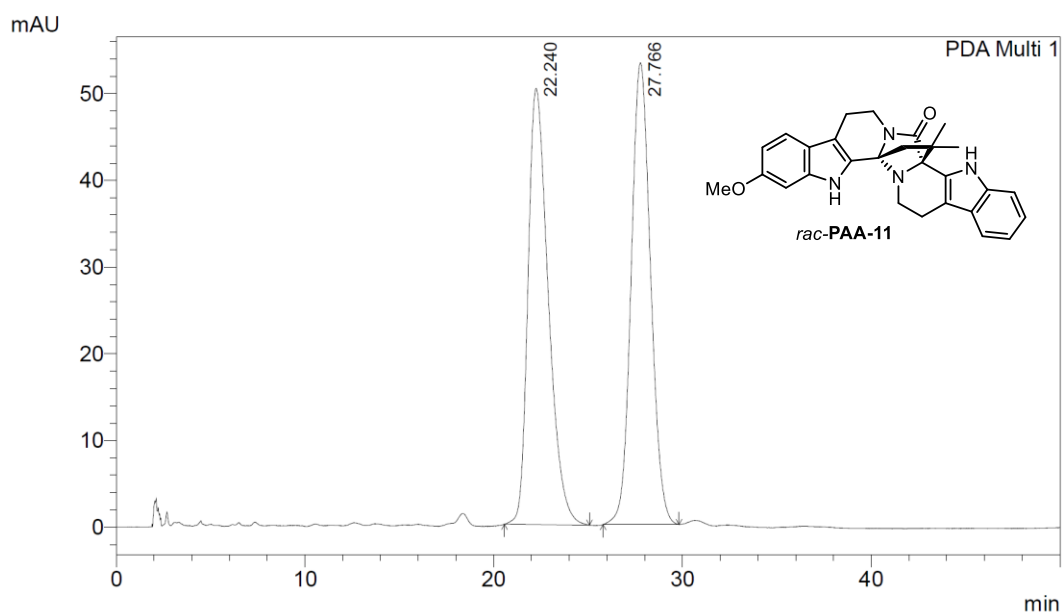
Peak#	Ret. Time	Area	Height	Area%
1	8.599	1843280	68605	50.520
2	16.755	1805315	34941	49.480
Total		3648594	103546	100.000

(-)-PAA-3

Peak Table

PDA Ch1 254nm

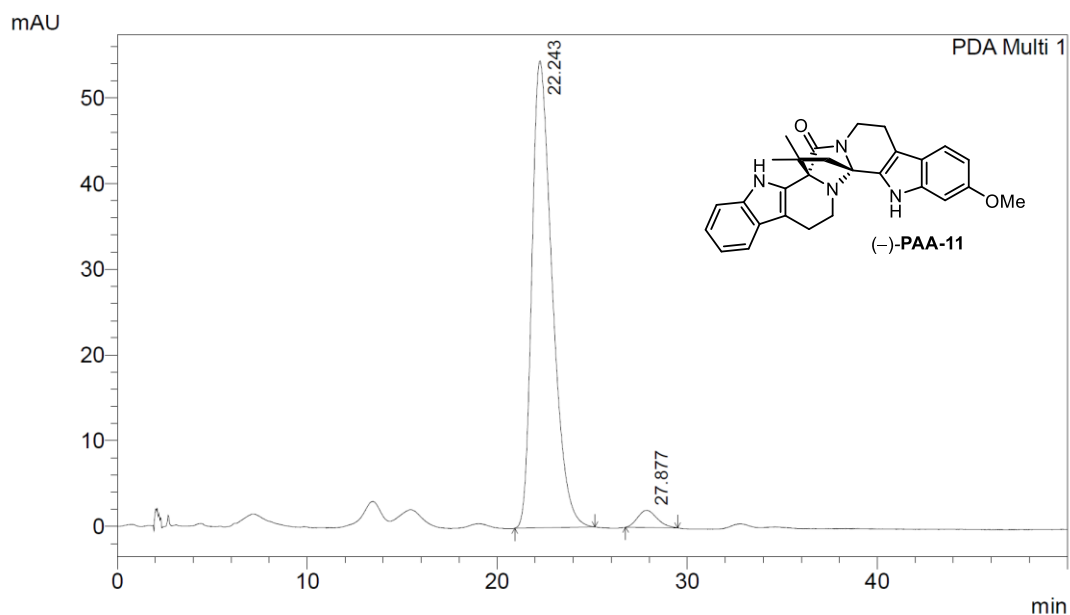
Peak#	Ret. Time	Area	Height	Area%
1	8.506	4993082	174040	99.346
2	16.774	32862	718	0.654
Total		5025945	174758	100.000

rac-PAA-11

Peak Table

PDA Ch1 270nm

Peak#	Ret. Time	Area	Height	Area%
1	22.240	3762577	50294	49.658
2	27.766	3814386	53255	50.342
Total		7576964	103549	100.000

(-)-PAA-11

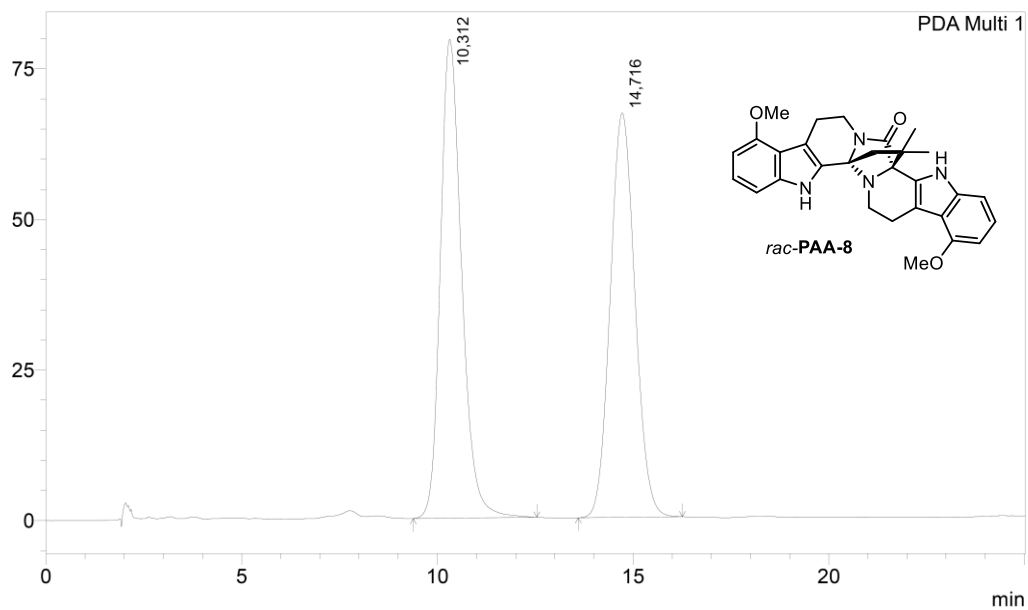
Peak Table

PDA Ch1 270nm

Peak#	Ret. Time	Area	Height	Area%
1	22.243	4048024	54476	96.613
2	27.877	141900	2012	3.387
Total		4189924	56488	100.000

rac-PAA-8

mAU



1 PDA Multi 1/270nm,4nm

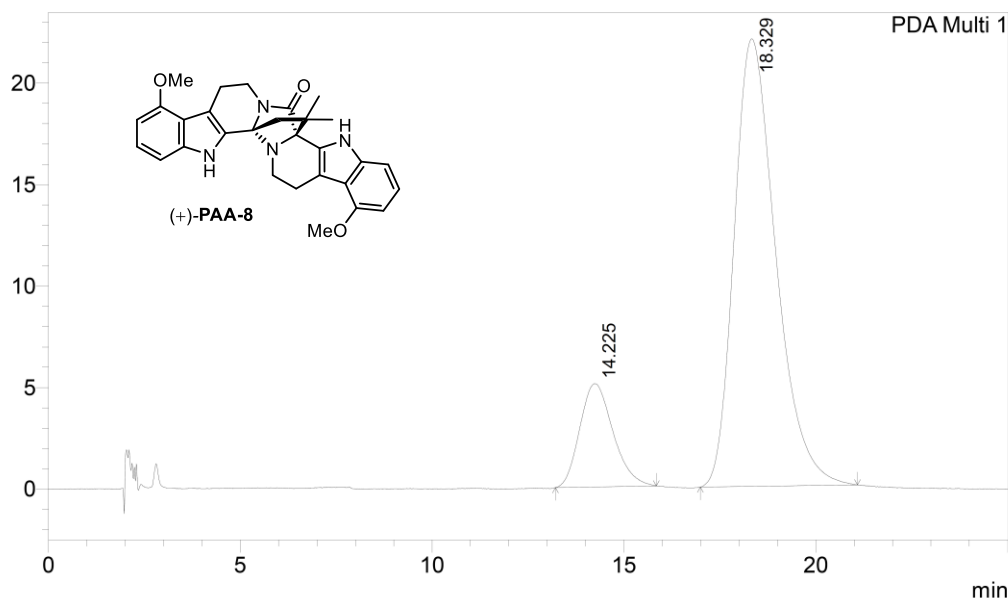
Peak Table

PDA Ch1 270nm

Peak#	Ret. Time	Area	Height	Area%
1	10,312	3005613	79496	50,424
2	14,716	2955039	67148	49,576
Total		5960652	146644	100,000

(+)-PAA-8

mAU

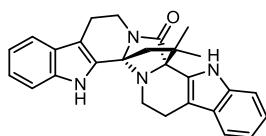


1 PDA Multi 1/270nm,4nm

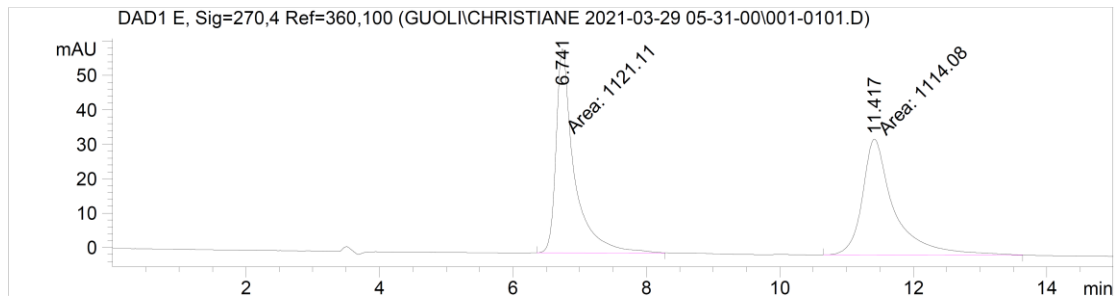
Peak Table

PDA Ch1 270nm

Peak#	Ret. Time	Area	Height	Area%
1	14.225	306276	5097	15.536
2	18.329	1665117	22043	84.464
Total		1971393	27140	100.000

9,9'-Didemethoxy peganumine A

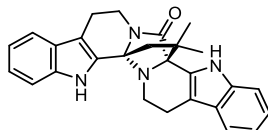
9,9'-didemethoxy peganumine A



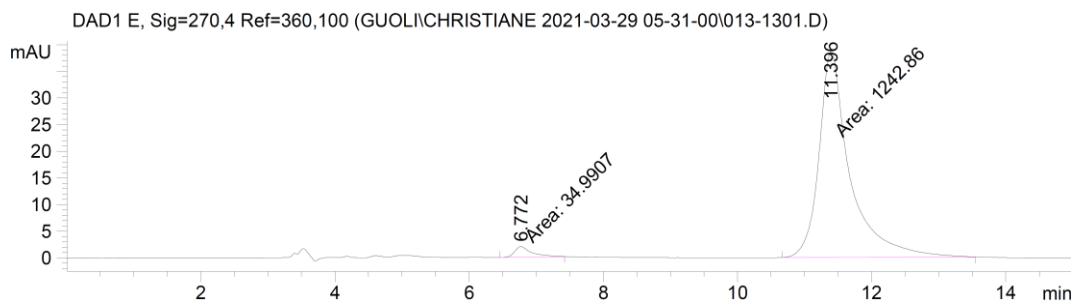
Signal 3: DAD1 E, Sig=270,4 Ref=360,100

Peak #	RetTime [min]	Type	Width [min]	Area [mAU*s]	Height [mAU]	Area %
1	6.741	MM	0.3155	1121.10815	59.22401	50.1572
2	11.417	MM	0.5521	1114.08142	33.63111	49.8428

Totals : 2235.18958 92.85512

(+)-9,9'-Didemethoxy peganumine A

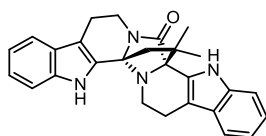
(+)9,9'-didemethoxy peganumine A



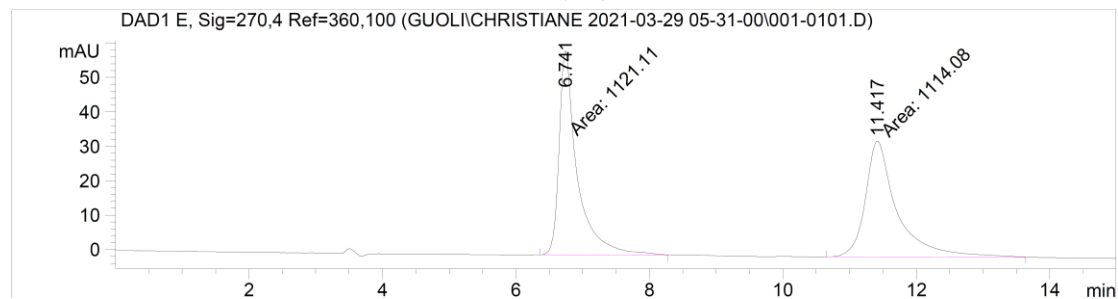
Signal 3: DAD1 E, Sig=270,4 Ref=360,100

Peak #	RetTime [min]	Type	Width [min]	Area [mAU*s]	Height [mAU]	Area %
1	6.772	MM	0.2941	34.99067	1.98298	2.7382
2	11.396	MM	0.5361	1242.86475	38.63677	97.2618

Totals : 1277.85542 40.61975

9,9'-Didemethoxy peganumine A

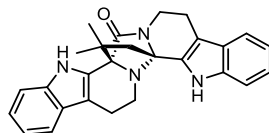
9,9'-didemethoxy peganumine A



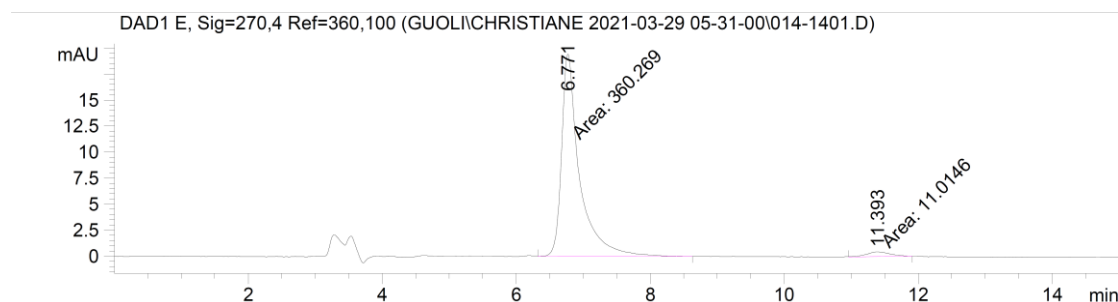
Signal 3: DAD1 E, Sig=270,4 Ref=360,100

Peak #	RetTime [min]	Type	Width [min]	Area [mAU*s]	Height [mAU]	Area %
1	6.741	MM	0.3155	1121.10815	59.22401	50.1572
2	11.417	MM	0.5521	1114.08142	33.63111	49.8428

Totals : 2235.18958 92.85512

(-)-9,9'-Didemethoxy peganumine A

(-)-9,9'-didemethoxy peganumine A



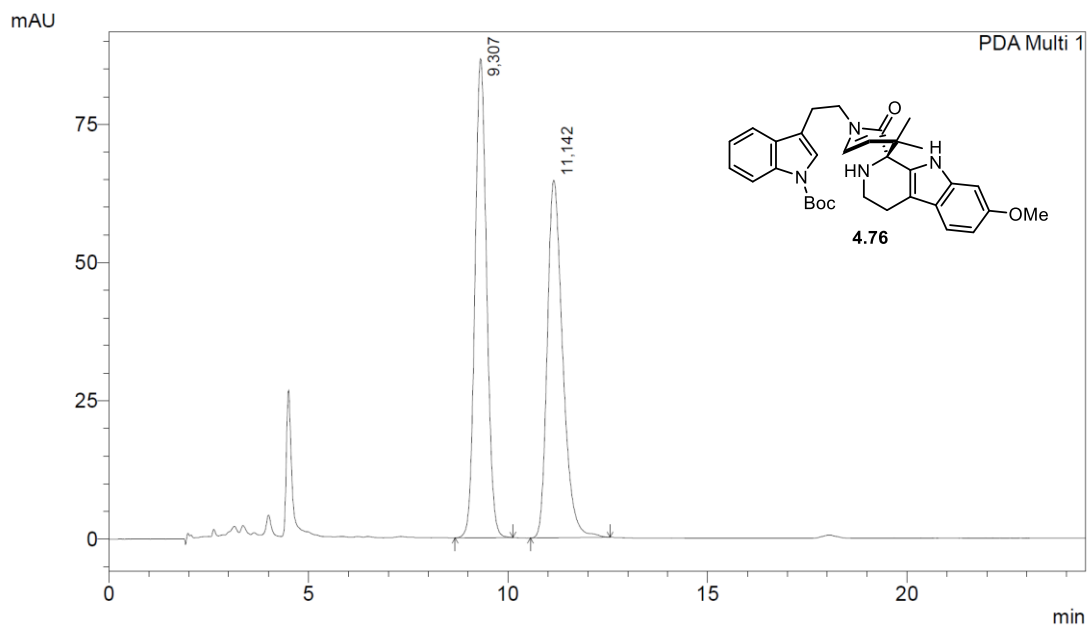
Signal 3: DAD1 E, Sig=270,4 Ref=360,100

Peak #	RetTime [min]	Type	Width [min]	Area [mAU*s]	Height [mAU]	Area %
1	6.771	MM	0.3095	360.26920	19.39791	97.0334
2	11.393	MM	0.4094	11.01460	4.48427e-1	2.9666

Totals : 371.28380 19.84633

9.2. HPLC Traces

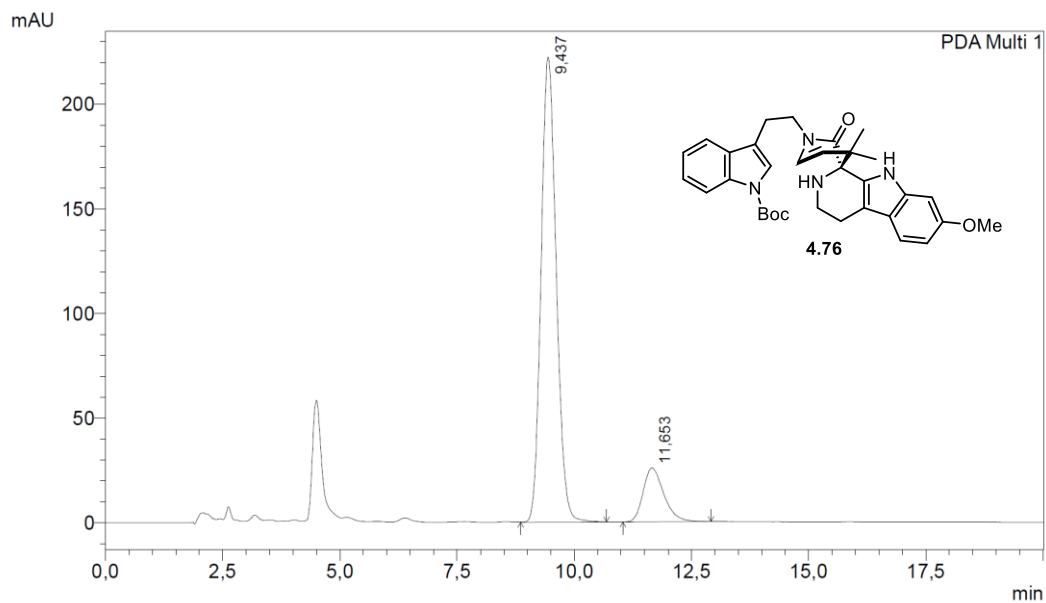
rac-4.76



Peak Table

PDA Ch1 270nm

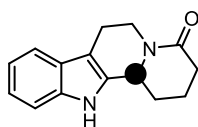
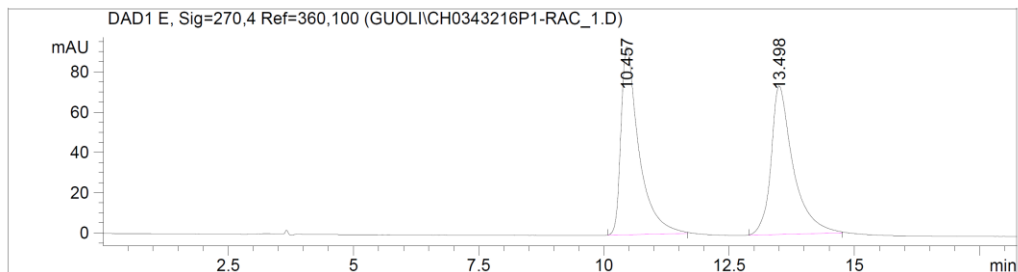
Peak#	Ret. Time	Area	Height	Area%
1	9,307	1760564	86610	50,294
2	11,142	1740009	64681	49,706
Total		3500573	151292	100,000



Peak Table

PDA Ch1 270nm

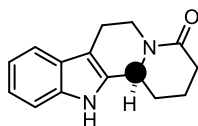
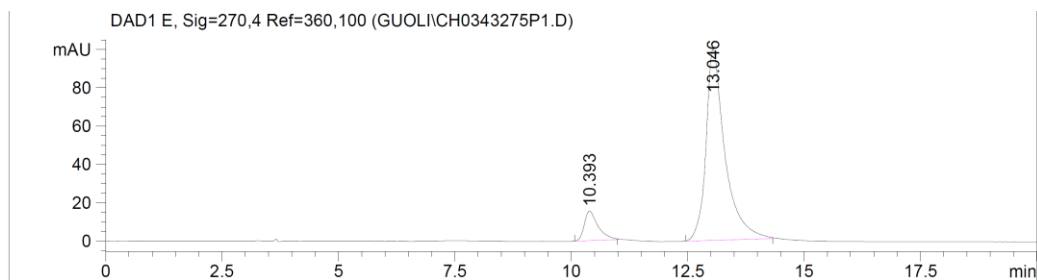
Peak#	Ret. Time	Area	Height	Area%
1	9,437	4991874	222236	86,351
2	11,653	789063	25774	13,649
Total		5780937	248010	100,000

rac-5.62*rac*-5.62

Signal 3: DAD1 E, Sig=270,4 Ref=360,100

Peak #	RetTime [min]	Type	Width [min]	Area [mAU*s]	Height [mAU]	Area %
1	10.457	BB	0.3627	2324.59595	93.30048	50.6335
2	13.498	BB	0.4409	2266.42432	73.67532	49.3665

Totals : 4591.02026 166.97581

(S)-5.62*(S)*-5.62

Signal 3: DAD1 E, Sig=270,4 Ref=360,100

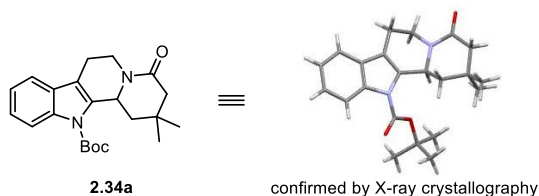
Peak #	RetTime [min]	Type	Width [min]	Area [mAU*s]	Height [mAU]	Area %
1	10.393	BB	0.3036	316.36719	15.40351	10.0180
2	13.046	BB	0.4101	2841.63501	99.83503	89.9820

Totals : 3158.00220 115.23854

9.3. Crystallographic Data

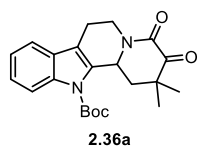
All the samples were provided by Guoli He and the measurements were conducted by Manuela Weber.

Tert-butyl 2,2-dimethyl-4-oxo-1,3,4,6,7,12b-hexahydroindolo[2,3-a]quinolizine-12(2H)-carboxylate (2.34a)



Bond precision:	C–C = 0.0020 Å	Wavelength = 0.71073	
Cell:	a=11.4277(2)	b=13.9121(2)	c=13.0163(2)
	alpha=90	beta=112.4130(6)	gamma=90
Temperature:	100 K		
	Calculated		Reported
Volume	1913.05(5)		1913.05(5)
Space group	P 21/c		P 21/c
Hall group	–P 2ybc		–P 2ybc
Moiety formula	C22 H28 N2 O3		
Sum formula	C22 H28 N2 O3		C22 H28 N2 O3
Mr	368.46		368.46
Dx, g cm ⁻³	1.279		1.279
Z	4		4
Mu (mm ⁻¹)	0.085		0.085
F000	792.0		792.0
F000'	792.34		
h, k, lmax	13, 17, 15		13, 17, 15
Nref	3643		3638
Tmin, Tmax	0.956, 0.974		0.676, 0.801
Tmin'	0.952		
Correction method= # Reported T Limits: Tmin=0.676 Tmax=0.801			
Data completeness=	0.999		Theta(max)= 25.744
R(reflections)=	0.0394(3081)		wR2(reflections)= 0.0954(3638)
S =	1.060		Npar= 249

Tert-butyl 2,2-dimethyl-3,4-dioxo-1,3,4,6,7,12b-hexahydroindolo[2,3-a]quinolizine-12(2H)-carboxylate (2.36a)

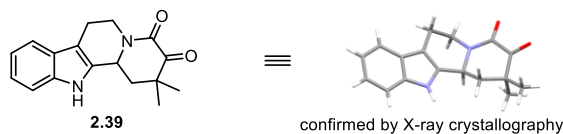


≡

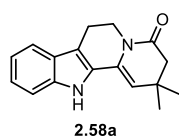


confirmed by X-ray crystallography

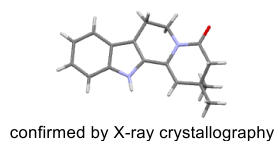
Bond precision:	C–C = 0.0030 Å	Wavelength = 0.71073	
Cell:	a=11.5059(5)	b=13.9501(8)	c=13.0113(7)
	alpha=90	beta=112.686(1)	gamma=90
Temperature:	100 K		
	Calculated		Reported
Volume	1926.85(17)		1926.85(17)
Space group	P 21/c		P 21/c
Hall group	–P 2ybc		–P 2ybc
Moiety formula	C22 H26 N2 O4		
Sum formula	C22 H26 N2 O4		C22 H26 N2 O4
Mr	382.45		382.45
Dx,g cm-3	1.318		1.318
Z	4		4
Mu (mm –1)	0.091		0.091
F000	816.0		816.0
F000'	816.38		
h, k, lmax	13, 16, 15		13, 16, 15
Nref	3406		3385
Tmin,Tmax	0.976, 0.984		0.899, 0.947
Tmin'	0.974		
	Correction method= # Reported T Limits: Tmin=0.899 Tmax=0.947		
	Data completeness= 0.994		Theta(max)= 25.011
	R(reflections)= 0.0428(2527)		wR2(reflections)= 0.0993(3385)
	S = 1.031		Npar= 258

2,2-Dimethyl-1,2,6,7,12,12b-hexahydroindolo[2,3-a]quinolizine-3,4-dione (2.39)

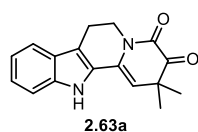
Bond precision:	C–C = 0.0020 Å	Wavelength = 0.71073	
Cell:	a=9.1299(3)	b=12.5352(4)	c=12.7022(4)
	alpha=90	beta=104.052(1)	gamma=90
Temperature:	98 K		
	Calculated		Reported
Volume	1410.20 (8)		1410.20 (8)
Space group	P 21/n		P 21/n
Hall group	–P 2yn		–P 2yn
Moiety formula	C17 H18 N2 O2		
Sum formula	C17 H18 N2 O2		C68 H72 N8 O8
Mr	282.33		1129.33
Dx, g cm ⁻³	1.330		1.330
Z	4		1
Mu (mm ⁻¹)	0.088		0.088
F000	600.0		600.0
F000'	600.25		
h, k, lmax	10, 14, 15		10, 14, 15
Nref	2500		2492
Tmin, Tmax	0.984, 0.994		0.894, 0.958
Tmin'	0.984		
Correction method= # Reported T Limits: Tmin=0.899 Tmax=0.947			
Data completeness= 0.997		Theta(max)= 25.071	
R(reflections)= 0.0382(2026)		wR2(reflections)= 0.0949(2492)	
S = 1.046		Npar= 193	

2,2-Dimethyl-2,6,7,12-tetrahydroindolo[2,3-*a*]quinolizin-4(3*H*)-one (2.58a)

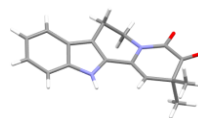
≡



Bond precision:	C–C = 0.0022 Å	Wavelength = 0.71073	
Cell:	a=16.8632(4)	b=13.8539(3)	c=17.8399(4)
	alpha=90	beta=95.1866(8)	gamma=90
Temperature:	100 K		
	Calculated		Reported
Volume	4150.71(16)		4150.71(16)
Space group	P 21/n		P 21/n
Hall group	–P 2yn		–P 2yn
Moiety formula	C17 H18 N2 O		
Sum formula	C17 H18 N2 O		C17 H18 N2 O
Mr	266.33		266.33
Dx, g cm ⁻³	1.279		1.279
Z	12		12
Mu (mm ⁻¹)	0.080		0.080
F000	1704.0		1704.0
F000'	1704.64		
h, k, lmax	20, 16, 21		20, 16, 21
Nref	7386		7346
Tmin, Tmax	0.976, 0.986		0.916, 0.955
Tmin'	0.971		
Correction method= # Reported T Limits: Tmin=0.916 Tmax=0.955			
Data completeness=	0.995		Theta(max)= 25.089
R(reflections)=	0.0448(5498)		wR2(reflections)= 0.1147(7346)
S =	1.026		Npar= 547

2,2-Dimethyl-2,6,7,12-tetrahydroindolo[2,3-a]quinolizine-3,4-dione (2.63a)

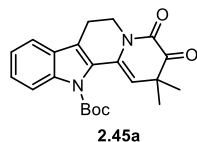
≡



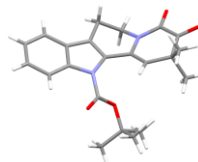
confirmed by X-ray crystallography

Bond precision:	C–C = 0.0031 Å	Wavelength = 1.54178	
Cell:	a=19.6425(9)	b=12.1435(5)	c=14.0884(6)
	alpha=90	beta=106.985(2)	gamma=90
Temperature:	100 K		
	Calculated		Reported
Volume	3213.9(2)		3213.9(2)
Space group	C 2/c		C 2/c
Hall group	–C 2yc		–C 2yc
Moiety formula	C17 H16 N2 O2		
Sum formula	C17 H16 N2 O2		C17 H16 N2 O2
Mr	280.32		280.32
Dx, g cm ⁻³	1.159		1.159
Z	8		8
Mu (mm ⁻¹)	0.620		0.620
F000	1184.0		1184.0
F000'	1187.54		
h, k, lmax	23, 14, 16		23, 14, 16
Nref	2962		2942
Tmin, Tmax	0.928, 0.982		0.648, 0.915
Tmin'	0.766		
Correction method= # Reported T Limits: Tmin=0.648 Tmax=0.915			
Data completeness=	0.993		Theta(max)= 68.580
R(reflections)=	0.0734(2527)		wR2(reflections)= 0.1970(2942)
S =	1.055		Npar= 192

***Tert*-butyl 2,2-dimethyl-3,4-dioxo-3,4,6,7-tetrahydroindolo[2,3-*a*]quinolizine-12(2*H*)-carboxylate (2.45a)**

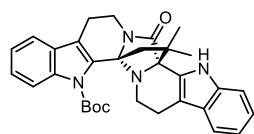


≡

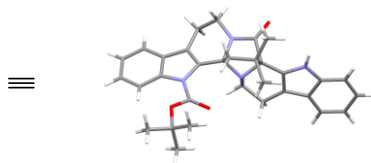


confirmed by X-ray crystallography

Bond precision:	C–C = 0.0030 Å	Wavelength = 0.71073	
Cell:	a=11.3302(3)	b=13.8799(4)	c=13.0726(4)
	alpha=90	beta=111.4166(10)	gamma=90
Temperature:	101 K		
	Calculated		Reported
Volume	1913.87(10)		1913.87(10)
Space group	P 21/c		P 21/c
Hall group	–P 2ybc		–P 2ybc
Moiety formula	C22 H24 N2 O4		
Sum formula	C22 H24 N2 O4		C22 H24 N2 O4
Mr	380.43		380.43
Dx,g cm-3	1.320		1.320
Z	4		4
Mu (mm –1)	0.091		0.091
F000	808.0		808.0
F000'	808.38		
h, k, lmax	13,16,15		13,16,15
Nref	3405		3391
Tmin,Tmax	0.979, 0.986		0.882,0.958
Tmin'	0.979		
	Correction method= # Reported T Limits: Tmin=0.882 Tmax=0.958		
	Data completeness= 0.996		Theta(max)= 25.056
	R(reflections)= 0.0458(2792)		wR2(reflections)= 0.1175(3391)
	S = 1.035		Npar= 258

12'-*tert*-butyl 9,9'-didemethoxy-peganumine A (2.62)

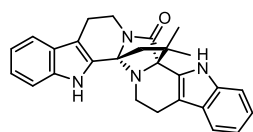
2.62



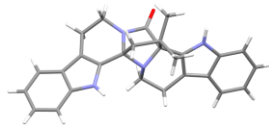
confirmed by X-ray crystallography

Bond precision:	C–C = 0.0040 Å	Wavelength = 0.71073	
Cell:	a=12.5362(3)	b=15.3487(4)	c=16.0461(5)
	alpha=109.5651(9)	beta=94.9391(10)	gamma=94.3915(9)
Temperature:	100 K		
	Calculated		Reported
Volume	2880.10(14)		2880.10(14)
Space group	P –1		P –1
Hall group	–P 1		–P 1
Moiety formula	C32 H34 N4 O3		
Sum formula	C32 H34 N4 O3		C32 H34 N4 O3
Mr	522.63		522.63
Dx,g cm-3	1.205		1.205
Z	4		4
Mu (mm –1)	0.078		0.078
F000	1112.0		1112.0
F000'	1112.44		
h, k, lmax	14, 18, 19		14, 18, 19
Nref	10308		10269
Tmin,Tmax	0.988, 0.997		0.896, 0.958
Tmin'	0.979		
	Correction method= # Reported T Limits: Tmin=0.896 Tmax=0.958		
	Data completeness= 0.996		Theta(max)= 25.144
	R(reflections)= 0.0625(7212)		wR2(reflections)= 0.1741(10269)
	S = 1.024		Npar= 704

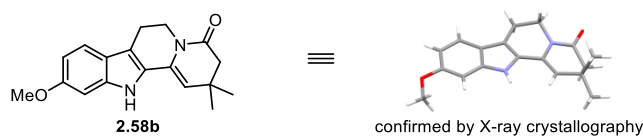
PAA-2



≡



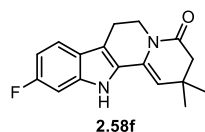
Bond precision:	C–C = 0.0020 Å	Wavelength = 1.54178	
Cell:	a=8.05356(6)	b=10.74589(8)	c=13.49716(10)
	alpha=104.8929(4)	beta=99.6795(3)	gamma=102.5267(3)
Temperature:	100 K		
	Calculated		Reported
Volume	1070.491(14)		1070.490(14)
Space group	P –1		P –1
Hall group	–P 1		–P 1
Moiety formula	C27 H26 N4 O		
Sum formula	C27 H26 N4 O		C27 H26 N4 O
Mr	422.52		422.52
Dx,g cm-3	1.311		1.311
Z	2		2
Mu (mm –1)	0.643		0.643
F000	448.0		448.0
F000'	449.23		
h, k, lmax	9, 13, 16		9, 13, 16
Nref	4063		4031
Tmin,Tmax	0.977, 0.981		0.785,0.958
Tmin'	0.852		
Correction method= # Reported T Limits: Tmin=0.785 Tmax=0.958			
Data completeness=	0.992		Theta(max)= 70.037
R(reflections)=	0.0385(3533)		wR2(reflections)= 0.1006(4031)
S =	1.044		Npar= 291

10-Methoxy-2,2-dimethyl-2,6,7,12-tetrahydroindolo[2,3-*a*]quinolizin-4(3*H*)-one (2.58b)

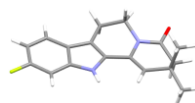
Bond precision:	C–C = 0.0059 Å	Wavelength = 0.71073	
Cell:	a=5.9877(1)	b=24.5424(7)	c=10.7935(3)
	alpha=90	beta=101.725(1)	gamma=90
Temperature:	100 K		
	Calculated		Reported
Volume	1553.04(7)		1553.04(7)
Space group	P 21/c		P 21/c
Hall group	–P 2ybc		–P 2ybc
Moiety formula	C18 H20 N2 O2		
Sum formula	C18 H20 N2 O2		C18 H20 N2 O2
Mr	296.36		296.36
Dx, g cm ⁻³	1.268		1.268
Z	4		4
Mu (mm ⁻¹)	0.083		0.083
F000	632.0		632.0
F000'	632.26		
h, k, lmax	7, 29, 12		7, 29, 12
Nref	2772		2750
Tmin, Tmax	0.973, 0.987		0.913, 0.958
Tmin'	0.973		
Correction method= # Reported T Limits: Tmin=0.913 Tmax=0.958			
Data completeness= 0.992		Theta(max)= 25.134	
R(reflections)= 0.0905(2281)		wR2(reflections)= 0.2100(2750)	
S = 1.081		Npar= 203	

10-Methoxy-2,2-dimethyl-2,6,7,12-tetrahydroindolo[2,3-*a*]quinolizine-3,4-dione (2.63b)

Bond precision:	C–C = 0.0021 Å	Wavelength = 1.54178	
Cell:	a=13.4328(1)	b=14.4122(1)	c=16.2802(1)
	alpha=90	beta=90	gamma=90
Temperature:	100 K		
	Calculated		Reported
Volume	3151.79(4)		3151.78(4)
Space group	P b c a		P b c a
Hall group	–P 2ac 2ab		–P 2ac 2ab
Moiety formula	C18 H18 N2 O3		
Sum formula	C18 H18 N2 O3		C18 H18 N2 O3
Mr	310.34		310.34
Dx, g cm ⁻³	1.308		1.308
Z	8		8
Mu (mm ⁻¹)	0.733		0.733
F000	1312.0		1312.0
F000'	1316.06		
h, k, lmax	16, 17, 19		16, 17, 19
Nref	2895		2889
Tmin, Tmax	0.965, 0.978		0.606, 0.840
Tmin'	0.709		
Correction method= # Reported T Limits: Tmin=0.606 Tmax=0.840			
Data completeness= 0.998		Theta(max)= 68.412	
R(reflections)= 0.0544(2520)		wR2(reflections)= 0.1461(2889)	
S = 1.066		Npar= 211	

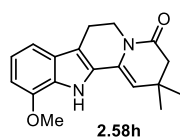
10-Fluoro-2,2-dimethyl-2,6,7,12-tetrahydroindolo[2,3-*a*]quinolizin-4(3*H*)-one (2.58f)

≡

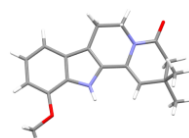


confirmed by X-ray crystallography

Bond precision:	C–C = 0.0025 Å	Wavelength = 0.71073	
Cell:	a=6.0205(2)	b=24.8237(9)	c=10.0119(4)
	alpha=90	beta=101.187(2)	gamma=90
Temperature:	100 K		
	Calculated		Reported
Volume	1467.86(9)		1467.86(9)
Space group	P 21/c		P 21/c
Hall group	–P 2ybc		–P 2ybc
Moiety formula	C17 H17 F N2 O		
Sum formula	C17 H17 F N2 O		C17 H17 F N2 O
Mr	284.33		284.32
Dx, g cm ⁻³	1.287		1.287
Z	4		4
Mu (mm ⁻¹)	0.090		0.733
F000	600.0		600.0
F000'	600.28		
h, k, lmax	7, 29, 11		7, 29, 11
Nref	2603		2588
Tmin, Tmax	0.989, 0.991		0.893, 0.958
Tmin'	0.953		
Correction method= # Reported T Limits: Tmin=0.893 Tmax=0.958			
Data completeness= 0.994		Theta(max)= 25.073	
R(reflections)= 0.0436(2020)		wR2(reflections)= 0.1026(2588)	
S = 1.076		Npar= 192	

11-Methoxy-2,2-dimethyl-2,6,7,12-tetrahydroindolo[2,3-*a*]quinolizin-4(3*H*)-one (2.58h)

≡



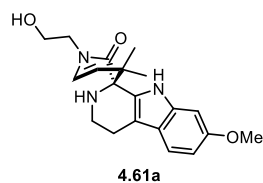
confirmed by X-ray crystallography

Bond precision:	C–C = 0.0040 Å	Wavelength = 1.54178	
Cell:	a=6.24502(5)	b=24.4540(2)	c=10.40942(9)
	alpha=90	beta=105.1280(5)	gamma=90
Temperature:	100 K		
	Calculated		Reported
Volume	1534.59(2)		1534.59(2)
Space group	C c		C c
Hall group	C –2yc		C –2yc
Moiety formula	C18 H20 N2 O2		
Sum formula	C18 H20 N2 O2		C18 H20 N2 O2
Mr	296.36		296.36
Dx, g cm ⁻³	1.283		1.283
Z	4		4
Mu (mm ⁻¹)	0.674		0.674
F000	632.0		632.0
F000'	633.84		
h, k, l _{max}	7, 28, 12		7, 28, 12
N _{ref}	2722 [1368]		2094
T _{min} , T _{max}	0.810, 0.980		0.623, 0.877
T _{min} '	0.700		
	Correction method= # Reported T Limits: T _{min} =0.623 T _{max} =0.877		
	Data completeness= 1.53/0.77		Theta(max)= 66.661
	R(reflections)= 0.0383(2010)		wR2(reflections)= 0.0950(2094)
	S = 1.069		N _{par} = 202

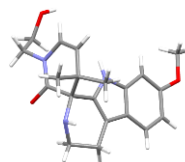
***N*-(2-(1*H*-indol-3-yl)ethyl)-2-hydroxy-3,3-dimethyltetrahydrofuran-2-carboxamide (4.46)**

Bond precision:	C–C = 0.0041 Å	Wavelength = 0.71073	
Cell:	a=7.9072(2)	b=2.7371(5)	c=15.5567(6)
	alpha=90	beta=100.063(1)	gamma=90
Temperature:	100 K		
	Calculated		Reported
Volume	1542.69(9)		1542.69(9)
Space group	P 21/n		P 21/n
Hall group	–P 2yn		–P 2yn
Moiety formula	C17 H22 N2 O3		
Sum formula	C17 H22 N2 O3		C17 H22 N2 O3
Mr	302.37		302.37
Dx, g cm ⁻³	1.302		1.302
Z	4		4
Mu (mm ⁻¹)	0.090		0.090
F000	648.0		648.0
F000'	648.29		
h, k, lmax	9, 15, 18		9, 15, 18
Nref	2943		2938
Tmin, Tmax	0.991, 0.994		0.859, 0.958
Tmin'	0.962		
Correction method= # Reported T Limits: Tmin=0. 859 Tmax=0.958			
Data completeness= 0.998		Theta(max)= 25.702	
R(reflections)= 0.0666(2329)		wR2(reflections)= 0.1726(2938)	
S = 1.066		Npar= 213	

**1-(2-Hydroxyethyl)-7'-methoxy-4,4-dimethyl-1,2',3',4,4',9'-hexahydro-2H-spiro
[pyridine-3,1'-pyrido[3,4-b]indol]-2-one (4.61a)**



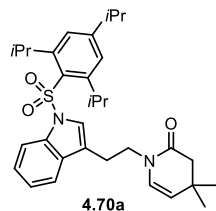
≡



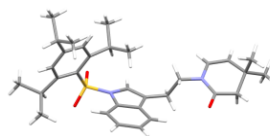
confirmed by X-ray crystallography

Bond precision:	C–C = 0.0020 Å	Wavelength = 0.71073	
Cell:	a=17.6524(3)	b=10.7669(2)	c=19.4362(4)
	alpha=90	beta=90	gamma=90
Temperature:	100 K		
	Calculated		Reported
Volume	3694.08(12)		3694.08(12)
Space group	P b c a		P b c a
Hall group	–P 2ac 2ab		–P 2ac 2ab
Moiety formula	C20 H25 N3 O3		
Sum formula	C20 H25 N3 O3		C20 H25 N3 O3
Mr	355.43		355.43
Dx,g cm-3	1.278		1.278
Z	8		8
Mu (mm –1)	0.087		0.087
F000	1520.0		1520.0
F000'	1520.65		
h, k, lmax	21, 12, 23		21, 12, 23
Nref	3288		3280
Tmin,Tmax	0.975, 0.991		0.930, 0.970
Tmin'	0.952		
	Correction method= # Reported T Limits: Tmin=0.930 Tmax=0.970		
	Data completeness= 0.998		Theta(max)= 25.086
	R(reflections)= 0.0355(2822)		wR2(reflections)= 0.0877(3280)
	S = 1.024		Npar= 251

4,4-Dimethyl-1-(2-(1-((2,4,6-triisopropylphenyl)sulfonyl)-1*H*-indol-3-yl)ethyl)-3,4-dihydropyridin-2(1*H*)-one (4.70a)

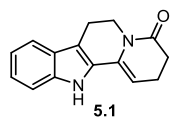


≡

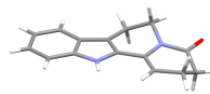


confirmed by X-ray crystallography

Bond precision:	C–C = 0.0087 Å	Wavelength = 0.71073	
Cell:	a=18.7687(8)	b=17.8315(7)	c=11.1194(5)
	alpha=90	beta=126.140(1)	gamma=90
Temperature:	100 K		
	Calculated		Reported
Volume	3005.3(2)		3005.3(2)
Space group	C c		C c
Hall group	C –2yc		C –2yc
Moiety formula	C32 H42 N2 O3 S		
Sum formula	C32 H42 N2 O3 S		C32 H42 N2 O3 S
Mr	534.74		534.74
Dx,g cm ⁻³	1.182		1.182
Z	4		4
Mu (mm ⁻¹)	0.141		0.141
F000	1152.0		1152.0
F000'	1152.94		
h, k, l _{max}	22, 21, 13		22, 21, 13
Nref	5364 [2687]		5103
T _{min} , T _{max}	0.968, 0.989		0.867, 0.970
T _{min} '	0.946		
Correction method= # Reported T Limits: T _{min} =0.867 T _{max} =0.970			
Data completeness=	1.90/0.95		Theta(max)= 25.103
R(reflections)=	0.0540(4377)		wR2(reflections)= 0.1413(5103)
S =	1.042		N _{par} = 351

2,6,7,12-Tetrahydroindolo[2,3-*a*]quinolizin-4(3*H*)-one (5.1)

≡



confirmed by X-ray crystallography

Bond precision:	C–C = 0.0030 Å	Wavelength = 1.54178	
Cell:	a=7.67427(6)	b=17.8315(7)	c=12.89478(10)
	alpha=90	beta=90	gamma=90
Temperature:	100 K		
	Calculated		Reported
Volume	1167.122(16)		1167.122(16)
Space group	P 21 21 21		P 21 21 21
Hall group	P 2ac 2ab		P 2ac 2ab
Moiety formula	C15 H14 N2 O		
Sum formula	C15 H14 N2 O		C15 H14 N2 O
Mr	238.28		238.28
Dx,g cm-3	1.356		1.356
Z	4		4
Mu (mm -1)	0.688		0.688
F000	504.0		504.0
F000'	505.44		
h, k, lmax	9, 14, 15		9, 14, 15
Nref	2055 [1206]		2045
Tmin,Tmax	0.906, 0.953		0.669, 0.915
Tmin'	0.791		
Correction method= # Reported T Limits: Tmin=0.669 Tmax=0.915			
Data completeness=	1.70/1.00	Theta(max)= 66.626	
R(reflections)=	0.0338(1966)	wR2(reflections)= 0.0880(2045)	
S =	1.062	Npar= 164	